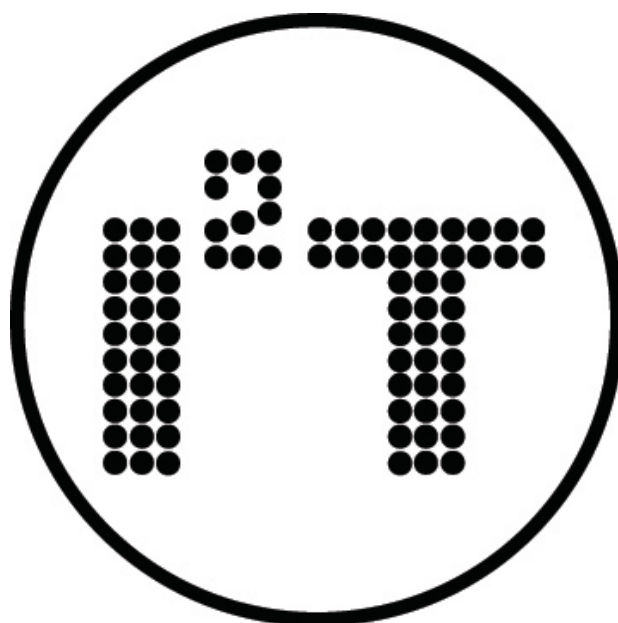


**International Scientific – Practical Conference
«INNOVATIVE INFORMATION
TECHNOLOGIES»**



**PART 2
INNOVATIVE INFORMATION TECHNOLOGIES
IN SCIENCE**

**Prague – 2014
April 21-25**

K 32.97
UDC 681.3; 681.5
I 64

I 64 Innovative Information Technologies: Materials of the International scientific – practical conference. Part 2. /Ed. Uvaysov S. U.–M.: HSE, 2014, 736 p.

ISSN 2303-9728

The materials of The Third International Scientific – Practical Conference is presented below. The Conference reflects the modern state of innovation in education, science, industry and social-economic sphere, from the standpoint of introducing new information technologies.

Digest of Conference materials is presented in 3 parts. It is interesting for a wide range of researchers, teachers, graduate students and professionals in the field of innovation and information technologies.

The editorial board:

A.Abrameshin, S.Aldoshin, A.Bugaev, E.Cheremisina, Yu.Evtushenko, I.Frumin, L.Gamza, J.Halík, I.Ivanov (executive editor), M.Kagan, B.Katalinic, V. Klaban, G.Kuzaev, J.Kokes, V.Maslov(scientific editor) E.Pozhidaev, J.Prachar, G.Savin, L.Schoor, A.Shmid, P.Skalicky, V.Tihomirov, A. Tikhonov(scientific editor), S.Uvaysov(under the general editorship), V.Vasiliev, L.Verbickaya, A.Zhizhchenko

ISSN 2303-9728

LBC 32.97
© The conference organizing committee
© HSE, 2014

Section 2

INNOVATION INFORMATION TECHNOLOGIES IN SCIENCE

APPLICATION OF PARTICLE SWARM OPTIMIZATION ALGORITHM FOR PARAMETRIC RELIABILITY OPTIMIZATION PROBLEM

Anop M., Mikhlichuk V.
IACP FEB RAS, FEFU, Vladivostok

Technical devices and systems optimal parametric synthesis problem taking into account reliability requirements and parameters degradation is to find nominal that provide the maximum probability of acceptability for a predetermined operating time. In this paper we consider a particle swarm optimization algorithm for solving parametric synthesis problem. The applications of the proposed methodology are illustrated through simple case study.

Keywords: parametric reliability, optimization, particle swarm optimization

Introduction

Reliability indicates the probability implementing specific performance or function of products and achieving successfully the objectives within a time schedule under a certain environment. In most of the probabilistic methods of the reliability engineering system, it is assumed that all the probabilities are precise. This means that every probability involved is perfectly determinable. In this case it is usually assumed that there exists some complete probabilistic information about system and component behavior. For the completeness of probabilistic information the following two conditions must be satisfied.

1. All the probabilities or probability distributions are known or perfectly determinable.
2. The system components are independent, i.e., all the random variables, described the component reliability behavior, are independent.

The precise system reliability can be computed theoretically if both the above two conditions are satisfied (it is assumed that the system structure is defined precisely and there exists a function linking the system time to failure as well as the times to failure of the components) [1].

Stochastic reliability optimization problem is either an extension or reformulation of reliability optimization problem with random variations of parameters. Moreover, the resource elements vary and it is reasonable to regard them as stochastic variables. It is also proved that a stochastic programming problem is harder than all other combinatorial optimization problems.

The conventional methods for choosing parameters (parametric synthesis) generally do not take account of parameters field deviations from their design values. As a result the engineering systems designed in such a manner are not optimal in the sense of their gradual failure reliability.

Parametric reliability optimization problem

Suppose that we have a system which depends on a set of n input $x = (x_1, \dots, x_n)^T$. The structure of the system determines the dependence of the output parameters of the internal parameters $Y(x)$. It is considered that the equations $Y(x)$ are described with a model that is given in any form such as analytical equations, algorithmic form or simulation model.

We will say that system is acceptable if $Y(x)$ satisfy the conditions Eq. (1):

$$\mathbf{a} \leq \mathbf{Y}(\mathbf{x}) \leq \mathbf{b}, \quad (1)$$

where \mathbf{Y} , \mathbf{a} and \mathbf{b} are m -vectors of system responses (output parameters) and their specifications, e.g. $Y_1(\mathbf{x})$ – average power, $Y_2(\mathbf{x})$ – delay, $Y_3(\mathbf{x})$ – gain.

The inequalities Eq. (1) define a region D_x in the space of input (system) parameters called the region of acceptability.

$$D_x = \{\mathbf{x} \mid \mathbf{a} \leq \mathbf{Y} \leq \mathbf{b}\} \quad (2)$$

The engineering system parameters are subject to random variations (aging, wear, temperature) and the variations may be considered as stochastic processes:

$$X(t) = \{X_1(t), \dots, X_n(t)\} \quad (3)$$

In general parametric reliability optimization problem (optimal parametric synthesis) can be stated as follows [2].

The equations $\mathbf{Y}(\mathbf{x})$, conditions of acceptability Eq. (1) and a service time T are given. To find such a deterministic vector of parameter ratings (nominal values) $x_{nom} = (x_{1nom}, \dots, x_{nnom})^T$ that the reliability

$$x_{nom} = \arg \max P\{X(x_{nom}, t) \in D_x, x_{nom} \in B_T \cap D_x, \forall t \in [0, T]\} \quad (4)$$

are maximal.

The practical algorithm of the stochastic criterion calculation is based on the conventional Monte Carlo method. In fact the distribution laws of system parameters variations and the characteristics of random parameters degradation processes $X(t)$ are often unknown. The replacement of original stochastic criterion with a certain deterministic one is used in order to reduce computational cost of statistical algorithms or in case of uncertainty conditions allows nearby optimum solutions to be obtained. It is a so-called a “minimal serviceability reserve”, the largest distance from the region margins and e.t.c. [3].

When designing complex analog electronic equipment functions describing the projected system are specified using a simulation model of the “black box” type by applying electrical circuit’s simulation software. The region of acceptability and its borders are not analytically given generally. This condition does not allow obtaining the optimal solution using the classical differential optimization methods. In this case, the problem Eq. (4) can be solved by applying only zero-order optimization methods. It can be formulated as follows

$$\mathbf{x}_{nom} = \arg \max (d(\mathbf{x}_{nom}, \partial D_x), \mathbf{x}_{nom} \in D_x), \quad (5)$$

where $d(\mathbf{x}, \partial D_x)$ is a distance from \mathbf{x} to the boundary ∂D_x . Geometrically the solution of the problem (5) is the center of the inscribed in the region D_x figure with maximum norm.

Particle swarm optimization algorithm

Particle swarm optimization (PSO) algorithm is a population based stochastic optimization technique developed by Eberhart and Kennedy in 1995 [4], inspired by social behavior of bird flocking or fish schooling. The swarm is typically modeled by particles in multidimensional search space that have a position and a velocity where each particle represents a candidate solution to the optimization problem. All the particles have fitness values which are evaluated by the fitness function to be optimized.

Each particle in PSO keeps track of its co-ordinates in the search space which are associated with the best solution it has achieved so far. This value is called *pbest*. Another one is the overall best value tracked by the particle swarm optimizer obtained so far by any particle in the population. The best value is a global best and called *gbest*. Each particle tries to modify its position using the information about their current positions, current velocities, distance between the current position and the *pbest* and also the distance between the current position and the *gbest*. PSO algorithm changes the velocity of each particle towards its *pbest* and *gbest* positions. Acceleration is weighted by a random term with separate random number generated for acceleration towards *pbest* and *gbest* positions.

Let X and V are the particle's position and its velocity in search space respectively. The initial random population is generated as

$$X_i^0 = X_{\min} + rand \cdot (X_{\max} - X_{\min}), \quad (6)$$

where X_i^0 is the initial position of particle i , X_{\min} and X_{\max} are minimum and maximum position of the particle in the search space and $rand$ is the random number between 0 and 1.

At iteration t , each particle i has position X_i^t and velocity V_i^t in search space of n -dimension. Velocity and position of each particle in the next iteration can be calculated for the i -th particle as

$$V_i^{t+1} = W \cdot V_i^t + C_1 \cdot rand_1 \cdot (pbest_i - X_i^t) + C_2 \cdot rand_2 \cdot (gbest - X_i^t), i = 1, 2, \dots, m \quad (7)$$

$$X_i^{t+1} = X_i^t + V_i^{t+1}, \quad \text{If } X_{\min} \leq X_i^{t+1} \leq X_{\max}$$

$$X_i^{t+1} = X_{\min}, \quad \text{If } X_i^{t+1} < X_{\min} \quad (8)$$

$$X_i^{t+1} = X_{\max}, \quad \text{If } X_i^{t+1} > X_{\max}$$

where m is the number of particles in the swarm, t is the pointer of generations (iterations), V_i^t is the velocity of particle i at generation t , W is the weighting factor, C_1 and C_2 are the acceleration factors, $rand_1$ and $rand_2$ are the random numbers between 0 and 1, $pbest_i$ is the personal best of particle i and $gbest$ is the global best of the group.

The convergence speed of each particle could be influenced by the parameters of acceleration factors C_1 and C_2 . The optimization process will modify the position slowly, if the values of acceleration factors are chosen to be very low. On the other hand, the optimization process can become unstable, if the values of C_1 and C_2 are chosen to be very high. In Eq. (7), the first term is the initial velocity of particle which reflects the memory behavior of particle. The second term cognition part which represents the private thinking of the particle itself and the third term is social part which shows the particles behavior from the experience of other particles in the population.

The iteration procedure can be terminated when any one of the following criteria is met, an acceptable solution has been reached or a state with no further improvement in solution has been reached or a predefined number of iterations have been completed.

The optimal reliability planning model formulated as a non-linear optimization problem in Eq. (5) can be solved using the PSO algorithm as follows

- *Step 1:* Initialize the PSO parameters such as population size, maximum number of generations, number of variables: C_1 , C_2 , W .
- *Step 2:* Set the generation counter $t = 0$ and generates m particles randomly using Eq. (6). Similarly generate random initial velocities of all particles.
- *Step 3:* Evaluate the fitness of each particle according to the objective function given in Eq. (4) or Eq. 5 and check the constraint violations Eq. (1) of each particle.
- *Step 4:* Form $pbest$ set from each particle and assign $gbest$ from the $pbest$ set.
- *Step 5:* Update the generation counter $t = t + 1$.
- *Step 6:* Using the global best and the individual best of each particle, the i -th particle velocity in the j -th dimension given by Eq. (7) are updated.
- *Step 7:* Based on the updated velocities, each particle changes its positions as X_i^{t+1} .

If the particle violates its position limits in any dimensions then set its position at the proper limit and do steps 3 and 4.

- *Step 8:* When any of the stopping criteria is satisfied, stop the algorithm or else go to step 5 [5].

Numerical example

As a simple case study it was considered a model of voltage divider (Fig. 1)

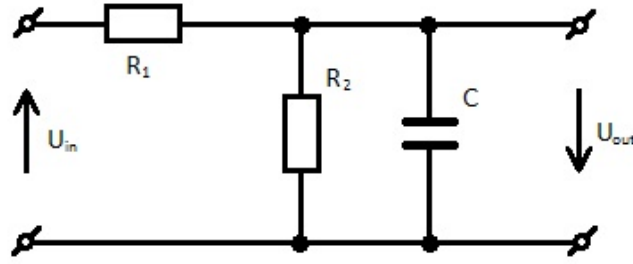


Fig. 1. Schematic circuit diagram of voltage divider.

Nominal capacity $C=1nF$, voltage $U_{in}=10V$, R_1, R_2 is ranged in $[0;1500]\Omega$. The output parameters are follows $Y_1 = \tau < 0.5 \cdot 10^{-6}$ – response speed recharging capacity, $Y_2 = P < 0.1$ – power dissipation, W , $Y_3 = U_{out} \in [4;6]$ – output voltage, V [6].

The region of acceptability and its borders are not analytically given. It is planned to obtain output parameters via electrical circuits simulation software. Besides, there are no appropriate assumptions about parameters variation and the characteristics of its degradation. For fitness evaluation using Eq. (5) its necessary be able calculate function $d(\mathbf{x}, \partial D_x)$. In multidimensional space it's not simple to use standard Euclidean norm. We will compute the distance to the boundary using the dichotomy and values of output parameters. To choose PSO parameters hold a few trial runs of the model (Fig. 2).

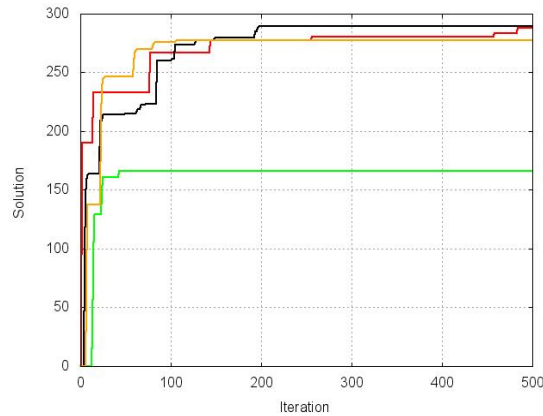


Fig. 2. PSO convergence characteristics with different parameters.

The best parameters obtained in trial experiments follows $W = 0.72$, $C_1 = C_2 = 0.29$. Using these parameters final PSO convergence characteristics are shown in Fig. 3.

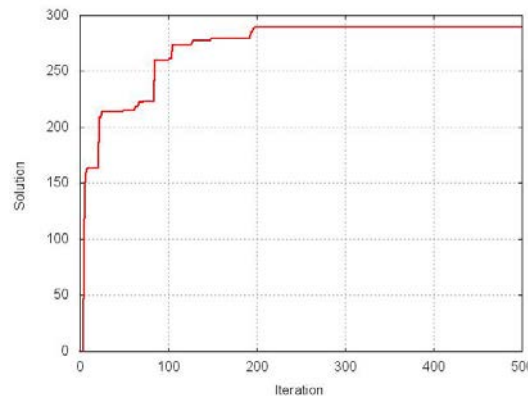


Fig. 3. PSO convergence characteristics.

The effectiveness of this approach is validated by comparing the results obtained with the random search method (Fig. 4).

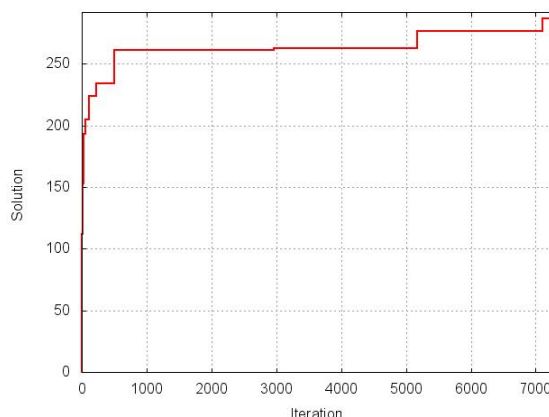


Fig. 4. Random search convergence characteristics.

The proposed algorithm has stronger convergence and stability than standard random search method.

A result of parameters optimization is follows $C=1nF$, $U_{in}=10V$, $R_1=874.99\Omega$, $R_2=874.98\Omega$, $d(\mathbf{x}, \partial D_x)=291.66$.

References

1. Bhunia A.K., Sahoo L., Roy D. Reliability stochastic optimization for a series system with interval component reliability via genetic algorithm. *Applied Mathematics and Computation*, 2010, Vol. 216, 929–939.
2. Abramov O.V., Katueva Y.V. and Nazarov D.A. Construction of acceptability region for parametric reliability optimization. *Reliability & Risk Analysis: Theory & Applications*, 2008, Vol. 10, 20-28.
3. Abramov O.V., Katueva Y.V. and Nazarov D.A. Distributed computing environment for reliability-oriented design. *Reliability & Risk Analysis: Theory & Applications*, 2009, Vol. 12, 39-46.
4. Kennedy J, Eberhart RC. Particle swarm optimization. In: *Proceedings of IEEE international conference on neural networks* Piscataway, NJ, 1995, 1942–8.
5. R. Ashok Bakkiyaraj, N. Kumarappan Optimal reliability planning for a composite electric power system based on Monte Carlo simulation using particle swarm optimization. *Electrical Power and Energy Systems*, 2013, Vol. 47, 109–116.
6. Saushev A.V. Parametric synthesis of technical systems based on the linear approximation of the operational capability range. *Optoelectronics, Instrumentation and Data Processing*, 2013, Vol. 49(1), 51-56.

TERRESTRIAL BIOTIC CARBON SEQUESTRATION: THE EXPERT SYSTEM FOR THE TECHNIFICATION OF THIS PROCESS

Viter, A.V.

Kyiv, M.M.Gryshko National Botanical Garden of the National Academy of Sciences of Ukraine

The terrestrial biotic carbon sequestration facilitates the sink of the greenhouse gases, the regulations of the geochemical and the aqueous runoffs and the climate, the elimination of

the pollutants in the biosphere – these are the ecosystem services, important for the healthing of the environment. However, the potential of this process remains almost unrealized in the many regions of the planet as the respect efficient technologies don't exist. This article presents the project of the expert system, which will be able to encourage the comprehensive fundamental studies and multivariant technification of the mentioned process.

Keywords: environmental healthing, efficacious technologies, project of expert system, sink of greenhouse gases, terrestrial biotic carbon sequestration.

Abbreviations: BOS – biopersistent organic substances; ES – expert system; GHG – greenhouse gases; KB – knowledgebase; NBOS – natural biopersistent organic substances; NPP – net primary productivity; OS – organic substance; OP – operating personnel; PAR – photosynthetically active radiation; PWP – permanent wilting point; SOM – soil organic matter; TBCS – terrestrial biotic carbon sequestration.

The economy of the contemporary humanity follows the opinions, which are behind of the present-day scientific world view. The existing progress in science and engineering is marked by the technologies, which create the environmental problems for the future generations to solve. Such technologies particularly include the generation of isotopes in the new quantities (nuclear power industry), geological, chemical and oceanic carbon sequestration, and so on. Meanwhile, science provides evidence that the possibilities of commodities production increase considerably faster as compared with the possibilities to mitigate adverse anthropogenic impacts on the biosphere [1]. The hydrosphere and the atmosphere serve as the waste sumps to be polluted irresponsibly. The global humanity tends to swell and it will rather choke in own wastes, than will perish from the deficiency of food, energy or something else. Thus, henceforward the science should focus on the invention of the opportunities for the environmental healthing – for the elimination of the adverse anthropogenic effects. The corresponding technologies actually appear to be in shortage today.

We are interested in the technification of the process of the carbon capturing and storing in the earth's crust, particularly in soils, because of the following reasons. The formation of the SOM relates with the range of processes, which are essential for environmental health: (1) the removing of the greenhouse gases (GHG) from the atmosphere [2]; (2) the preserving of the biogenic elements from the migration from the earth's crust into the water and air environments [3, 4]; (3) the buffer functions of the earth in the water and heat exchange (they result in the regulation of the climate and the regime of the watercourses) [5, 6]; (4) the disposal of the OSs, which are unfavorable for biota (it includes the incorporation of these compounds into the humic molecules) [7].

The carbon sequestration in earth's the crust in the form of the organic matter has a drawback. Often it believed to be less efficient economically, than the geological, chemical and oceanic sequestration of carbon. But, all the same, the biotic removal of the carbon from the GHG into the crust more than other way of this element sequestration is based on the natural process, which, certainly, offers the best opportunities for the biosphere healthing.

Today an urgent question must be set: how long-lived and how stable (under alternation of the external factors) are these or those stores of the carbon, removed from the atmosphere. The mechanisms of the carbon sequestration in soils under frigid and humid climate (Canada, and the Russian, European, and USA's northern regions) turn out to be well studied in the light of this question. The modeling promoted the design of the approaches for management of the respective process under these conditions [2]. Evidently, the healthing of the environment should not be associated with the North only, but it must take place in the other biomes as well. Undoubtedly, some other conditions have higher potential for the GHG removal, than the conditions of the North. We mean the geographical belts of the soil-formation processes like chernozems, grey-forest, chestnut and other fertile soils. Still the

comprehension how to manage the phenomenon of the TBCS here remains insufficient. This determines the shortage of technologies (invested with the low level of risk). As a result the TBCS in the biomes of the temperate climate meets the serious constraints in its sense of targeted (man-supported) realization.

The biosphere is not a factory, and natural zones are not factory shops. On the Earth the natural conditions are very diverse and mosaic. Consequently, environmental healthing requires the development of the vast range of the technologies for the carbon capturing and storage depending on the natural conditions (climate, the qualities of parent rock and soil, the topologic and the hydrologic state of the land area) as well as on the anthropogenic factors (labour and technical supply), remoteness from the delivery and outlet markets, the financial status of the firm). We propose the other approach to solving the problem: the design of one or few instant technologies in tandem with the ES. The last is supposed to make the decisions in the form of the technology's models, which is sure to be dissimilar for each of the unique case.

This article is aimed on the determination of the peculiarities of the aforesaid ES. The ES generally consists of two component parts, which are (1) the knowledgebase (KB) about the TBCS in soils; (2) the operating personnel (OP – the specialists, imposed the following tasks: to develop, to manage KB and to involve it in making decisions. They mainly should work as administrators). The first component is to be evolved by means of the updating with the new knowledge, also the perfection and the improvement of the reliability of the existing knowledge. KB is the non-vanishing core of the ES. At the same time the alternation of the OP doesn't principally affect on the operability of the ES. It resembles the situation, under which shake-up in the library doesn't devalue its property and domain in principle.

Below the questions on (1) the main features of the offered KB; (2) the separate research institution as initiator of the development of the thematic knowledge system and its operation are scrutinized.

1. Knowledgebase

1.1 The structure of knowledgebase

It is reasonably to research the problem of the TBCS in several respects: (1) the principles of natural sciences; (2) the engineering; (3) the economics and legislation; (4) the environmentological effects of the designed technologies. Thuswise the KB should be divided into the corresponding categories of the knowledge. The category of natural sciences must be considered to be the core, which serves the base for the rest categories. This part of the KB deserves the very attention. That is why we focus on the designing of the respective direction of the knowledge in this article.

1.2 Introductory remarks

Currently the processes of the carbonic substances formation and accumulation in soils are still understood partially. Thereby the soil scientists discuss the essence of even the fundamental concepts [8]. Arguably the designing of the KB won't be complicated under the arbitrary definitions by the researchers. However, the design of the KB indispensably depends on the set of the following initial ideas about the processes of biotic carbon capturing and sequestration in soils and lithosphere. These ideas should be precise.

1. The photosynthetizing plants generate the flow that provides the removal of the GHG from the atmosphere. (This flow cannot be self-induced – without expenditure of the external energy – in principle.)

2. There is a reverse flow: removed carbon is mineralized and, thus, transferred into the state of the GHG again. (This is self-induced flow – in principle.) The intensity of this flow depends, first, on such a property of the carbonic substances as their metabolizability, secondly, on the conditions, encompassing the carbonic substances.

3. The scale of the metabolizability can be represented: from the substances, which are easily-assimilable by biota, to those, which are hardly-biodegradable. The diverse organic

compounds can occupy the distinct positions on this scale. The intensity of the transition of the carbon into the state of GHG directly depends on the level of the assimilability of the substances. Thus the NBOS is the most reliable storage site for the carbon, which is removed from the GHG.

4. Initially, the plants synthesize easily-assimilable OSs. The last are converted into the NBOS by means of the microbial, plant and fungal metabolism. The process of this conversion is characterized by a) the marginal maximal portion of the substances, which are converted; b) the efficiency; c) the intensity of the conversion. All of the mentioned parameters are determined, firstly, by the genetic properties of the organisms, secondly, by the external environmental factors.

5. In principle, whichever biopersistent the OS may be, there exist the microorganisms, which are able to degrade it [9].

6. Some of the conditions facilitate the availability of the OS for the biodestructors, and the other conditions impede it. Under the last conditions the carbon stays in the state out of GHG for the longer time. The hinderance for the biodestruction can be conditioned, particularly, by the bounding of OSs with the non-organic matter of the earth crust (to be more exact, with the parental rock minerals).

7. The diverse minerals differ in the property of keeping the OSs from the biodestruction.

8. There can be the unequal amount of the minerals, which are able to reinforce the biopersistence of the OSs (in other words to stabilize them), per unit of the earth surface, because of the diversity of the rocks, covering this surface. This depends, firstly, on the rock's chemical (mineral) content, secondly, on the thickness of the rock.

9. The possibility for the stabilization of the OSs is enabled by some factors, which enhance the mixing of the OSs with the rock – the penetration. More specifically this possibility is determined by the rate of the action and the character of these factors. These factors include: (a) the biotic factors; (b) the aqueous regime; (c) the aeolian processes; (d) the anthropogenic impact on the rock/soil.

10. Vice versa the same factors, acting in the unfavorable character and rate, intensify the mineralization and, as a result, accelerate the transition of carbon into the state of the GHG in the atmosphere.

11. The limitations of amount for the accumulation of OSs (especially the stable ones) are the obligatory property of the rocks/soils. In this respect the extensive limitation is associated with the gross amount of substances, storable in the rock/soil, and the intensive limitation – with the amount of substances, accumulable per unit of time.

1.3 The criteria for the knowledge classification in KB

The formulation of the above-mentioned set of initial ideas let us systemically list the primary factors, operating the process of the TBCS in the soils generally in nature, and cluster them into three groups, pertaining: (1) the biotic conversion of the GHG into NBOS (over 25 factors); (2) the degradation of NBOS (about 20 factors); (3) the NBOS-accumulating capacity of the environment (either soil, or parent rock) (about 10 factors).

Conceptually the alternation of any primary factors provides the management of the process. The convenience for the investigation of the factors of the biotic carbon capturing and sequestration as well as for formulation the logical and mathematical relations between these factors becomes possible. Still the most of the factors belong to non-manageable directly. It should be understood, that human can alter only the small number of the parameters and thus impact on the factors. We define such man-altered parameters as the means for management. In the case of the TBCS they are (1) the species (or biological form) of crop (plant); (2a) the combination of natural edaphic factors; (2b) the application of the materials (substances) as the physical and chemical amendments of the soil as well as for the

plant ontogenesis regulation and fertilization; (3) the regime of water supply; (4) the physical treatment of soil; (5) the direct procedures of the plant cultivation; (6) the species composition and the abundance of zoocenosis, soil and epiphytic microbocenosis.

Each of the means for management serves as a certain kind of actuator on the range of the factors. In its turn numerous factors are able to be altered by more than one kind of the means for management. For instance, photosynthetic productivity can be depressed or raised by means of either the choice of plant species, or the fertilization, or the regime of water supply, or the direct practice of crop cultivation (sowing times, formation of plant population density).

The systematization of knowledge is the requisite of any KB. The primary factors and the means for management of the process can be proposed as two keys for the convenient systematization in the case of the TBCS KB. However, these keys fail in comprehension, concerning the making of optimal decisions, particularly technological ones. In order to illustrate the decision making principle we attempted to sketch the algorithm of solving the task of carbon capturing and sequestration in accordance with the set soil and climatic conditions (fig.).

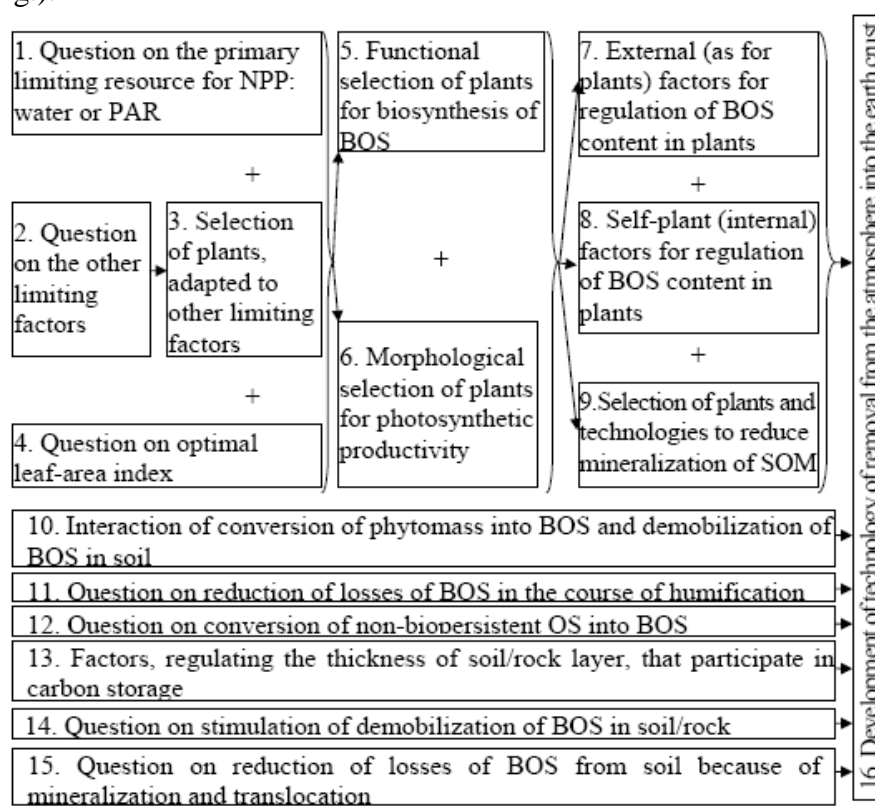


Fig. The algorithm of the researches, required for the development of the technologies for the regulation of the effectiveness of the greenhouse gases sink by means of the terrestrial biotic carbon sequestration.

The questions, presented in the figure, can serve as the additional – auxiliary key for systematization.

1.4 The properties of the knowledge operated by the KB: sophistication and availability

The modern KBs quite often deal with the large scopes of knowledge. In numerous cases it appears to be changeable, as the information can be reversed. In addition the perfection, the correction of existing and the emergence of the principally new knowledge take place permanently. For these reasons the TBCS KB cannot be constant, but rather has a dynamical character.

The knowledge, related to the TBCS can be characterized by two important properties: the sophistication and the availability.

Below we present the scheme for the gradual process of improving of knowledge:

1. Logical guess (the reliable experimental evidence is unavailable).
2. The experimental evidence is available, but it is indirect.
3. The dependence of some factors (parameters) on other ones is underpinned with the experimental evidence, whilst it remains unknown how this dependence is expressed: as linear / non-linear; as direct / inverse / several-phase functionality; as antagonistic / additive / synergistic interaction.
4. The character of this dependence is approximately ascertained, but it isn't mathematically simulated.
5. There exist the singular mathematical models, which are insufficient for the extrapolation on the diversity of the natural objects (e.g. the availability of the simulation for the biome of temperate climate may be available, but still it isn't the sufficient reason for the mathematical extrapolation on the conditions of more frigid and warmer climate zones).
6. There exist the set of the mathematical models, which is sufficient for the mathematical extrapolation.

There is an additional criterion of the perfection of knowledge. The most of the above-listed stages can deal with the knowledge, which is either stated as the unrelated fact, or interpreted in relation to the system of the other phenomena.

It's easy enough to gain some knowledge on the TBCS topic in the some cases, and in the other cases it's difficult to do this. Such an inequality can be illustrated by the following gradation of the knowledge availability. There is some knowledge, that

1. is known for the vast diversity of the objects;
2. is known for the particular objects from their diversity;
3. can be gain by the effort of the (one!) research institution of the agro-biological profile;
4. can be gain by the effort of the national (in our case Ukrainian) science;
5. can be gain in the course of the few-lateral international researches;
6. can be gain by the multi-national researches;
7. is realistic in the technical respect, but is financially unacceptable for the current development of the world science;
8. is non-realistic technically and unacceptable financially for the current world science.

As the matter of fact the comprehension of the last property – the knowledge availability – is indispensable for the making decisions on the disposition of the funds within the discussed topic.

2. The objective of the projected expert system

It is important to mention the following problem: the outlook of the economic system in the world is based on the making super-profits, moreover in the shortest time span. In many cases it's possible due to the conversion of the natural capital into the other form of the capital: financial, technical resources, manufactured production. In fact all this means the exhausting of the biosphere. In contrast the technologies for the environmental healthing are aimed at the restoration of the natural capital. That is why, firstly, these technologies belong to the low-gain ones, and secondly, here the periods of the investment turnover have the same order with the periods of the shifts of human generations. It must be realized, that neither private, nor public business isn't directly interested in the technologies for the environmental healthing, all the more in the scientific studying of the respect problems. Really, scientists can rely only on the episodic financial support of these problems. If so, it must be clearly understood how to spend this money: what research directions will be the most desirable for

filling the gaps in knowledge in the set scientific problem. Unfortunately, the large part of contemporary natural sciences makes no headway (because of the duplication (overlapping) of the previous experiments) instead of directing the scientific force on the investigation of questions, which would enrich the world view. They can be named top-questions.

The priority of spending money for the studying of these or those questions in each particular case must be considered the principle of flexible regulation, depending on the amount of contribution. The solving the question of such a priority belongs to the most important missions of the ES.

So the objective of the work of the ES lies in (1) the prioritizing of the top-questions within the TBCS problem in accordance with the current position of the fundamental science; (2) the coordination of the episodically available financial resources for the investigation of the very top-questions; (3) the coordination of the intelligence of dispersed high-specialized scientists for the same purpose.

3. The extension of knowledge and the management of the process of their development: the potential role of the particular research institution

Conceptually, all steps in the work of the ES are divided into two phases: (1) the modeling of the technologies (in form of the projects) by means of involving some knowledge from the experience of the experiments and the production; (2) the approbation of the designed technologies and their practical adaptation.

The design of each of the technologies covers the decision on the set of questions about: (1) the selection of the plant genus, species, or variety; (2) the place of the selected crop in the rotation scheme as well as the calendar period of cultivation for the annual and few-annual crops; (3) the systems of the primary tillage and the chemical treatments of soil, including manuring; (4) the system of the direct procedures of the plant cultivation; (5) the post-harvesting processing of the plant yield (or of the portion of the yield), intended for the carbon storage; (6) the regulation of microbocenosis and zoocenosis functions in the ecosystem. Most of these questions lie in the competence of the M.M.Gryshko National Botanical Garden of the National Academy of Sciences (NBG of NAS) of Ukraine. Moreover this institution has the following merits, which appears to be desirable, for the participation in the OP of the TBCS ES:

1. The valuable experience, based on the previous original knowledge about such unique questions as the interference in phytocenoses (including the phenomena of allelopathy and plant biolocation); plant acclimatization and domestication; soil engineering.
2. The genebank of the prospective plants.
3. The favourable conditions for the official collaboration with the top Ukrainian and foreign institutions, which conduct the researches in the natural and technological (especially agrarian) sciences.

The listed qualities make it possible for the M.M.Gryshko NBG of NAS of Ukraine to conduct active approbation and adaptation of the modelled technologies, which is the sense of the second phase of the work of the ES.

The purposes of the M.M.Gryshko NBG of NAS of Ukraine go beyond the enabling of the practical application for the designed technologies. Not the least important intention is the invitation of collective intelligence for the efficient work to progress the exploration of the abovementioned scientific problem. This intention appears to be possible by means of the raising of the questions to investigate, coupled with their priority assessment. So in the nearest future we find it necessary to focus our efforts on the matter of the elaboration of the mechanics of TBCS ES. These are the projects of software and the design of the mechanisms of the external scientific communications, mostly international ones.

4. Conclusion remark

The future offers the humanity to rethink the conception of such an activity field as the ecosystem exploitation. This rethinking will necessitate learning how to regulate the numerous processes in the biosphere. The TBCS is one of them. It should be considered that the development of the ES for the TBCS can serve a worth-wile precedent of the scientific-based approaches for the technologization in the area of the environmental healthing.

References

1. Meadows D.H., Randers J., Meadows D. Limits to Growth: The 30-Year Update. – White River Junction, Vermont: Chelsea Green Publishing Co, 2004. – 368 pp.
2. Kudeyarov V.N., Zavarzin G.A., Blagodatskiy S.A. et al. Pools and Flows of Carbon in Terrestrial Ecosystems of Russia / Ed.-in-chief. G.A.Zavarzin – Moscow: Nauka, 2007. – 315 pp. (in Russian)
3. Kerzhentsev A.S. Functional Ecology. – Moscow: Nauka, 2006. – 259 pp. (in Russian)
4. Glazovskaya M.A. Pedolithogenesis and Continental Cycles of Carbon. – Moscow: Librokom Book House, 2009. – 336 pp. (in Russian)
5. Gorshkov V.G. Physical and Biological Principles of Life Stability. – Moscow: VINITI, 1995. – 494 pp. (in Russian)
6. Smagin A.V. Theory and Practice of Soil Engineering. – Moscow: Moscow University Press, 2006. – 544 pp. (in Russian)
7. Tate R.L. Soil Organic Matter: Biological and Ecological Effects. – N. Y. e.a.: John Willey & Sons, 1987. – 291 pp.
8. Morozov A.I. On Soil and Soil Science: A Look from the Outside. – Moscow: GEOS, 2007. – 286 pp. (in Russian)
9. Mishustin Ye.N., Yemtsev V.T. Microbiology: Textbook for universities on agronomy specialties. – Moscow: Agropromizdat All-Union Publ. Co, 1987. – 368 pp. (in Russian)

INTEGRATED APPROACH FOR THE DIAGNOSTICS OF LATENT DEFECTS IN MODERN EQUIPMENT

Dianov, V.N., Luminarskaya, E.S.

Moscow State Industrial University, Russia, Moscow

Considered an integrated approach to the detection of latent defects in the equipment. Informative signs – “amplitude-frequency” in the low-frequency region, electromagnetic radiation – in the field of high frequencies.

I. INTRODUCTION

On the basis of previously discovered properties of passive components of electronic equipment and by analogy with the concept of “infallibility” a new concept of reliability is considered - "non-failure" - which establishes a connection between failure of the equipment, hidden defects in it and its quality. An example of improving the quality of equipment by detecting hidden defects in the security system of the airport is given, a set of informative features is specified and the algorithm for the detection of latent defects in the frequency range up to 4 GHz, depending on the internal and external electromagnetic interference, is offered.

II. INVESTIGATION RESULTS

The development of the set of components, complexity of software for the solution of actual problems and tighter operating conditions of modern equipment (computers, sensors, actuators, optico-television systems, etc.) require the upgrade of existing approaches and the search for new approaches in order to improve reliability. For example, in the process of creating highly reliable instruments a lot of problems arises; in particular, in the process of ensuring high standards of infallibility and durability in the conditions of very low and very high (up to hundreds of degrees) temperatures and high levels of stress. Among the variety of equipment failures the intermittent faults, also known as short-lived, hidden, floating, self-correcting or flicker failures should be considered the most problematic ones from the standpoint of monitoring and diagnostics. Such failures lead to malfunction of equipment and can result not only in significant financial losses, but also in fatal accidents. Failure is described as a self-correcting malfunction of equipment due to short-term impact of external and internal factors on some element (or set of elements).

After the failure the equipment may work normally for a long period of time but the information may be distorted during transfer, storage or processing operations.

Scientists have been studying the problem of equipment malfunction for several decades, starting from the 1960s. But this problem is not fully solved yet. Moreover, it attracts a lot of attention nowadays. For example, one of the most important characteristics of an autonomous navigation system of the International Space Station, which is being created at present, is its fault tolerance, and the priority of ensuring its high reliability by guaranteeing absence of failures ("non-failure") is higher than the priority of tasks of facilities manipulation which were traditionally in the first place by this parameter.

During the process of development of equipment which has a large number (up to several tens of thousands) of potential sources of failure (multiple plugs, contact LSI and VLSI devices, printed guides, communication lines - interface tires, power and grounding tires, etc.), the key problem for ensuring substantial increase of reliability is the diagnostics of failures directly related to the detection and registration of hardware failure sources.

Analysis of research on the subject has shown that there are numerous methods of control which are aimed not at the detection and elimination of sources of failure but at the results of the failure demonstration, and in so doing we eliminate not the cause (in this case the source of failure), but its consequence (i.e. the error caused by the failure), thus leaving the potentiality of existence of latent defects in the equipment.

The specific feature of the proposed method of increasing the equipment reliability sharply by eliminating exposure to failure is the detection of failure sources, in contrast to the previously used approaches to this problem which offered detecting and reporting fault locations. Depending on the principles of formation and obtaining of informative features, the totality of which is used in order to estimate the faulty state of equipment components as a source of failures, there were suggested various methods for detection and registration of failure sources, including those by the "electromagnetic radiation" parameter [1].

The causes of failure in passive elements (PE) of modern electronic equipment (EE) can include various external factors (vibration, power, electric field, temperature and chemical exposure) and numerous hidden defects of equipment leading to its accelerated degradation. The most difficult task is to describe such an important element of apparatus as the connector (electrical contact). The modern theory represents the electrical contact in the form of an oscillatory circuit with elements of R_n , L_n and C_n - resistive, inductive and capacitive resistances of the transition zone (transient resistance) contacts respectively. These parameters defining the resonant vibrations at high frequencies depend on many factors which are difficult to control and, therefore, make the problem of their integrated and operational evaluation urgent.

Theoretical synthesis of process of diagnosing of failures of the REA passive elements at limited information on their technical condition predetermines use of the formal description of PE REA, i.e. their mathematical model of diagnosing. This model has to provide diagnosing of failures and to be suitable for further synthesis and realization of algorithms of diagnosing.

When developing mathematical model of diagnosing of failures of PE REA it is necessary to consider that in PE REA as in object of diagnosing, mechanical, chemical, physical, electric and electromagnetic properties of elements are closely interconnected. At the description of their technical condition it is necessary to use the corresponding ways of formalization of processes (the differential, differential and logical equations, the block diagrams, the focused columns and final machine guns).

Synthesis of the PE EE diverse mathematical models provides their general description as object of diagnosing of failures (latent defects). The most expedient therefore is use of the abstract dynamic system which process of functioning consists in change of a condition of system under the influence of the external and internal reasons. The mathematical model of such system is defined as functionality of a number of variables

$$y = F(T, X, Z, S, S_0, C^*, C, L^*, L)$$

where T – a set of time points of t ; X, Z – sets entrance x and days off of z of signals of system; S – set of conditions of system; S_0 – the closed area of conditions of the system, limiting possible movements in use;

$C^*(T, X, S) = P^*$ and $C(T, X, S) = P$ – the operators of transitions reflecting changes of a condition of system under the influence of external and internal indignations;

$L^*(T, X, S) = Y^*$ and $L(T, X, S) = Y$ – the operators of exits describing formation of an output signal under the influence of internal and external indignations.

For recognition of failures of PE EE as object of diagnosing we will use a set of classes of technical conditions of Ei (where $i = 0, 1, 2, \dots, k; k+1, k+2, \dots, m; m+1, m+2, \dots, N$).

Ei – is a set of technical conditions of the object characterizing set of its possible conditions of si . Entering into this set class Eik ($i = 0, k$) there corresponds to a working order of PE EE, the class Eim ($i = k+1, \dots, m$) – to its failure condition, and class Ein ($i = m+1, \dots, N$) – to its defective condition.

In the experiments on the sustainability of failure mode allows the following: definition of the distribution of contact resistance as a function of steam ON-OFF N ; calculation of statistical characteristics: the expectation of $m^*(R)$ and m^* , the dispersion $D^*(R)$ or D^* ; standard deviation $\sigma^*(R)$ or σ^* ; verification of conformity of distributions obtained experimentally existing theoretical laws of the following criteria: Pearson (χ^2) and A.N. Kolmogorov. Besides solving the problem of experimental determination of the number of series of experiments N , guaranteed to lead to a malfunctioning of contact pairs, and the problem of determining the law of a fault and the validation of the results.

The calculations were carried out by the formulas:

expectation $m^*(R)$

$$m^*(R) = \frac{1}{n} \sum_{i=1}^n R_i$$

dispersion $D^*(R)$

$$D^*(R) = \frac{1}{n-1} \sum_{i=1}^n [R_i - m^*(R)]^2$$

standard deviation $\sigma^*(R)$

$$\sigma^*(R) = \sqrt{D^*(R)}$$

Experimentally, it has been found faulty state in the elements of CEA and received normal distribution parameters and the Poisson law for example, a fault multiple connectors. Change the dynamics of contacts in the simplest case, protect the accelerated depreciation due to a change of on-off switch and observing the change in one of them - the ohmic resistance. Contact pairs test was performed in accordance with the specifications Milliohmmeter method for measuring the contact resistance R and contact pairs by the incident and reflected waves to measure the reflection coefficient.

We shall consider the solution to this problem by example of the airport security system shown in Fig. 1 [2].

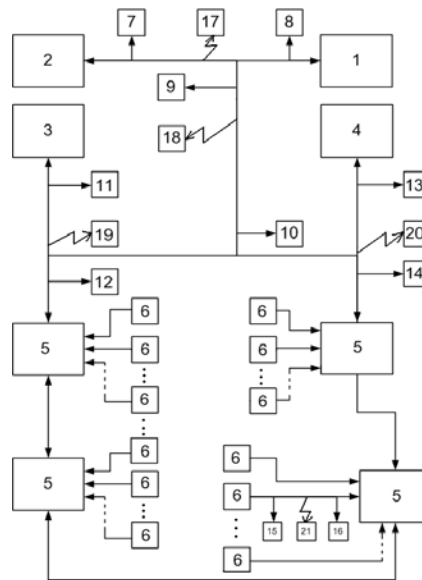


Fig.1. Airport security system of high reliability

The system includes automated workplace (AWP) 1, remote workstation 2, server of the system 3, central controller 4, signal processing unit 5, sensors connected by a sensor line 6 (not shown in Fig. 1), as well as contact failure sensors (CFS) 7-16, contactless failure sensors (CLFS) 17-21.

The contact source of failure is determined by the fact of formation of microcracks and microgaps in communication lines and connectors and a small capacitive component (shares and units of picofarads) in them, followed by a large resistance (up to 10^7 Ohms or higher) in the signal receiver CSF in CMOS structure, for example, with implementation on CMOS-inverters and the appearing effect of signals differentiation. The source of failure is determined in a contactless way by the fact of formation of microresonant circuits and electromagnetic radiation in the result of electrical signal passing in them. In this case, contactless failure sensors can be implemented on passive (L, C - elements) microresonant oscillation circuits.

In the case of two-way electrical signals the CFS is set at the start (end) of the communication line or vice versa. If the signals are unidirectional then the sensors 6 - signal processing unit 5 - CFS is set at the start (by the action of the signal) of communication line - CFS 15 and at its end - CFS 16. Figure 1 shows only one communication line of sensor 6 with unit 5 provided with a contact (15.16 CFS) and contactless (CLFS 21) failure sensors. In a particular case, all lines of communication (if necessary) between blocks 5 and 6 may contain contact and contactless failure sensors. The number of sensors in a single line may be greater than it is shown in Figure 1. The latter circumstance depends on the particular length of the communication line and the size of its discretization where failure fixing is required.

The diagram (Fig. 1) shows contactless failure sensors 17-21, set in immediate proximity to the elements or units being diagnosed. The number of CLFS is chosen on the basis of their sensitivity, length of the communication line and, in general, it can be larger. Figure 1, for simplicity, shows a scheme where only separate communication lines of units 1, 2, 3, 4, 5, 6 are taken. In general, the sensors can be installed on each unit of the above-mentioned communication lines and blocks. Both CFS and CLFS may have both stand-alone and centralized indication (not shown on Figure 1) using blocks 1, 2, 3 and 4.

Failure sensors can be installed, for example, with the help of clips. Simultaneous response of CLFS in different communication lines and non-response of CFS indicates the failure source in the form of external electromagnetic disturbance. Simultaneous response of CLFS and CFS indicates an internal electromagnetic disturbance. The main distinction when including CFS and CLFS into the apparatus is the value of the signal being fixed depending on the distance to the failure source.

Conclusions

A combined approach to detection of latent defects in equipment containing contact or low-frequency components of the defect being detected with amplitude-frequency informative characteristic and non-contact or high-frequency component with an informative "electromagnetic radiation" characteristic is offered.

References

1. 2006 IEEE. Dianov V.N. Active Diagnostics of the Failures in Printed – Circuit – Boards. Moscow State Industrial University, Russia. EMC – Zurich in Singapore 2006. 17th International Zurich Symposium on Electromagnetic Compatibility, 27 February – 3 March 2006, Singapore, Suntec International Convention & Exhibition Centre, pp. 194-197.
2. V.N. Dianov, E.S. Luminarskaya, I.M. Belousov and others. Airport security system with improved reliability. Utility model patent of the Russian Federation No. 123566. Date of publication 27.12.2012. Journal No.36.

TO THE PROBLEM OF THE HANDWRITING CHARACTERS RECOGNITION

Istratov, A.Yu., Fedin, N. A.

Moscow, Higher School of Economics, National Research University

The article discusses development of the segmented characters classifier of the Russian alphabet and of the Arabic numerals on the basis of block neural network structures including the plurality of blocks for each individual character recognition and for the synthesis block decision.

Keywords: pattern recognition, neural network, training of neural networks, base of hand-written characters, recognition of hand-written characters

Introduction

In modern information space a big part is assigned to processes of the exchange of information. In many cases such as processing of hand-written forms, written statements, questioning, organization of an electronic document flow, etc. (i.e. the off-line processing), the need of an automated recognition of the hand-written text (ARHWT) arises. Creation of the full universal implementations of ARHWT systems still remains an open problem as the ARHWT procedure is difficult to formalize and is labor-consuming. It envisages preliminary processing of the image of the hand-written text [1], segmentation of images (setting apart

the isolated characters images) [2], recognition of the segmented images (characters) [4], and orthographic analysis, i.e. solution of tasks which are stubborn in themselves.

One of ARHWT the components is the subsystem of recognition of hand-written single characters (RHWSC). The known attempts at the implementation of similar systems, such as sample, feature and structural classifiers [3, 4], classifiers based on convolution networks [5], ensembles of classifiers [4], etc. [10], – do not allow to receive the satisfactory recognition for practical tasks, or to impose additional restrictions on the presentation of information. Big computing resource intensity, unsatisfactory time of decision-making and bad generalization of the results are also among their shortcomings.

This paper considers development of the handwritten characters classifier of the Russian alphabet and of Arabic numerals in the neural network performance. Unlike previous approaches to implementing the RHWSC systems it is proposed to synthesize in a single set the individual classifiers for every character with the generalizing neural network cascade, which allows to select the winner classifier.

Statement of the Problem

The classifier is input information is a handwritten character image, i.e. the A ($N \times M$) matrix. It is assumed that at the preprocessing step the image was subjected to image binarization operations, zoom, skeletonization and centering within the images [6]. At the same stage, the A matrix is converted into the $\vec{A} = (a_1, a_2, \dots, a_k)^T$ features vector, $k \leq N \times M$. The features vector can be formed as a concatenation of the rows, and by way of more complex transformations [8].

It is required to construct a neural network system (classifier) that performs the reference of the input feature vector (image) to one of the classes of Russian alphabet characters or of digits (32 small letters, 31 capital characters, and 10 handwritten Arabic numerals). The recognition result is the Y scaled system response, characterizing the specific class number.

Development of the classifier

To solve this problem it is proposed to develop a neural network complex comprising the blocks neural network recognition of specific symbols and the synthesis neural network unit. The overall structure of the complex is shown in **Fig. 1**.

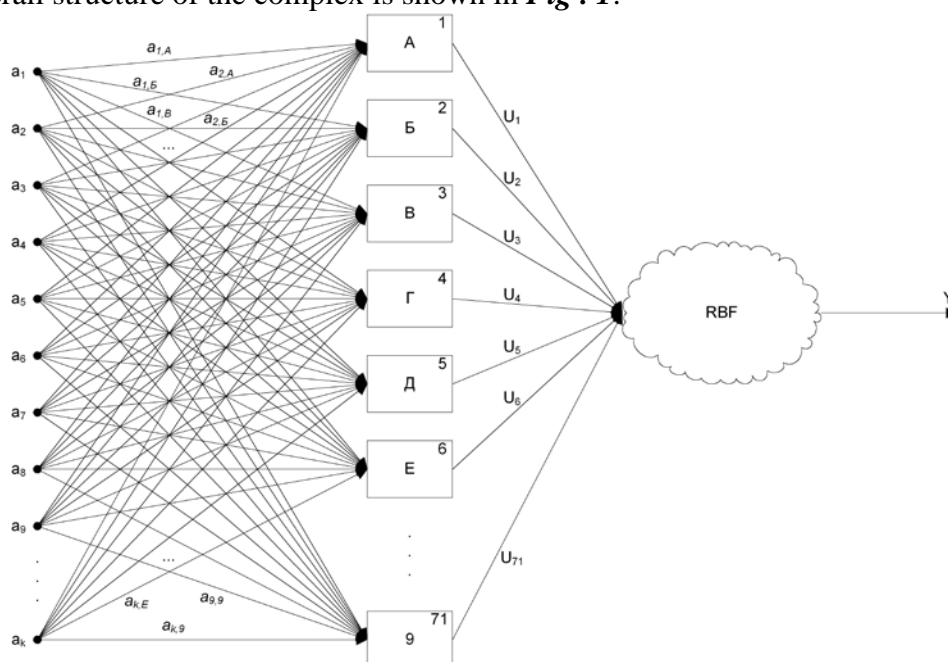


Fig. 1. Structure of the neural network classifier.

Neural network blocks “A, Б, ..., Я, а, б, ..., я, 0, ..., 9” are proposed to be constructed on the basis of two-layer perceptrons (**Fig. 2**) with a sigmoid activation function $f(x) = \frac{1}{1+e^{-x}}$ [7].

Their task is to determine the status of the input vector to the target (its) class , i.e. each unit is trained to recognize only its own class of input vectors:

$$U_1 = \begin{cases} 1, & \text{if the input vector characterizes the "A" character;} \\ 0, & \text{otherwise;} \end{cases}$$

$$U_2 = \begin{cases} 1, & \text{if the input vector characterizes the "А" character;} \\ 0, & \text{otherwise;} \end{cases}$$

$$U_{71} = \begin{cases} 1, & \text{if the input vector characterizes the "9" character;} \\ 0, & \text{otherwise;} \end{cases}$$

where U_p - the p -th block output, $p = 1, 2, \dots, 71$.

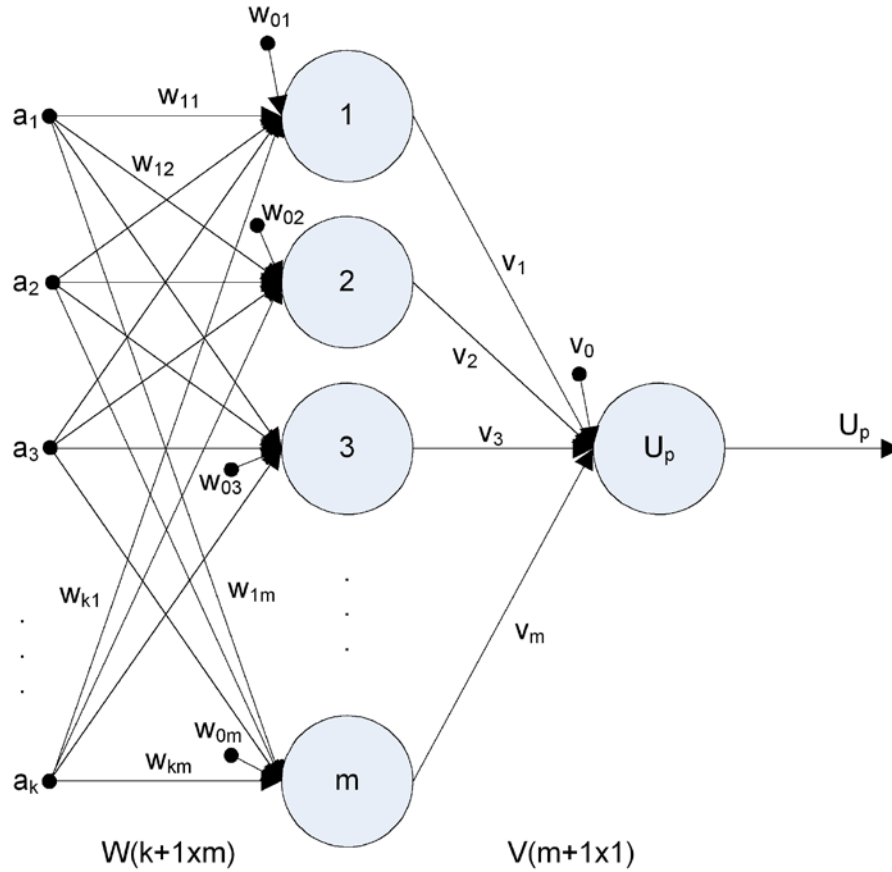


Fig. 2. Structure of a single character classifier (A, Б,..., 9 blocks).

Denote by $W = \{w_{ij}; i = 1, \dots, k+1; j = 1, \dots, m\}$ the matrix of weights for the input layer unit, $\vec{V} = (v_1, v_2, \dots, v_{m+1})^T$ – the output vector of weights layer, (k – dimension of the input vector, m – the number of neurons in the input layer) (**Fig. 2**). Then the output of the p -th determined is given by:

$$U_p = f \left(\sum_{j=1}^m f \left(\sum_{i=1}^k a_i w_{ij} + w_{0j} \right) v_j + v_0 \right). \quad (1)$$

The expert evaluations of individual classifiers (the U_1, U_2, \dots, U_{71} output responses) enter the competitive unit configured on the network-based radial basis functions (RBF) (**Fig. 3**), the output state of which is determined by the expression

$$Y = \sum_{i=1}^z h_i \cdot e^{-\frac{\|\vec{N}_i - \vec{U}\|^2}{b_i^2}} + h_0, \quad (2)$$

where $\vec{U} = (U_1, U_2, \dots, U_{71})^\top$ – the outputs vector of the "A, Б, В, ..., 9", $\vec{N}_i = (\tilde{n}_1^i, \tilde{n}_2^i, \dots, \tilde{n}_{71}^i)^\top$ and b_i the position and width of the i -th hidden layer neuron kernel function respectively, $\|\dots\|$ – the Euclidean norm, $\vec{H} = (h_0, h_1, \dots, h_z)^\top$ – the of the output layer weights vector [7].

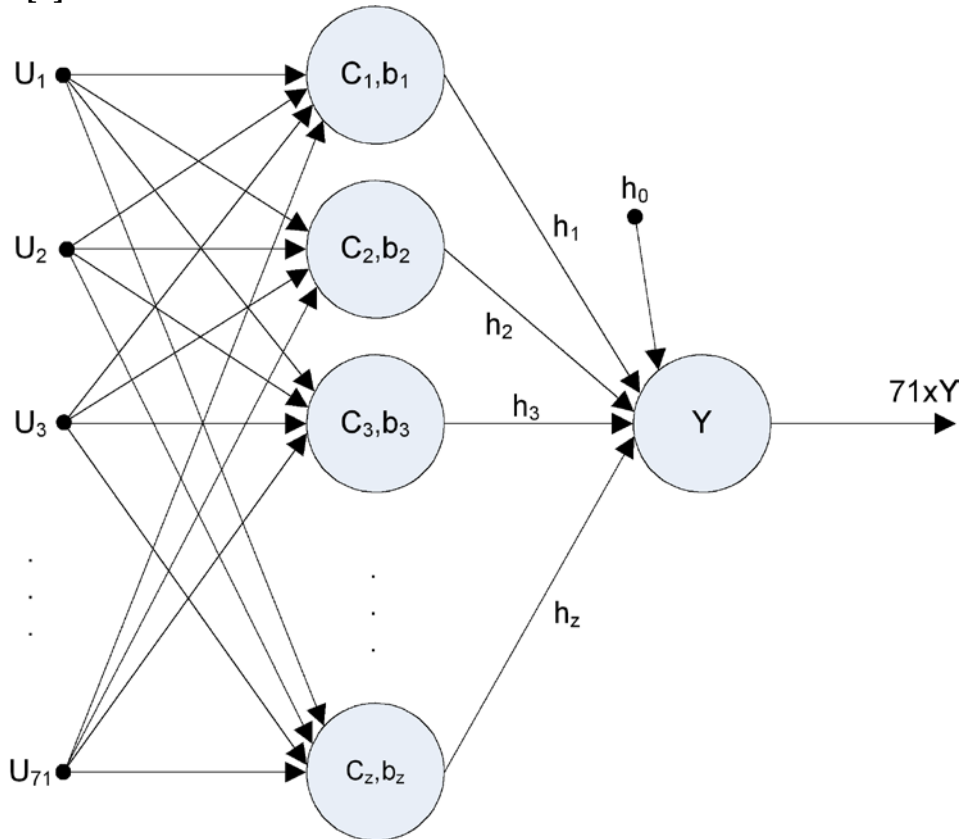


Fig . 3 . Structure of the synthesis classifier (RBF).

Neurons in the hidden RBF network layer perform the assessment of credibility of each expert (the output of the "A, Б, В, ..., 9" blocks) on the basis of comparing their findings. The final recognition result of the \vec{A} input vector is formed in the output RBF network layer.

Through the use of independent classifiers for each character class, is simplified the problem solved by each of the "A, Б, В, ..., 9" blocks, as the classification is made for only two classes: own / alien. At the same time there is a need for further evaluation of the outputs of all discriminators in general. In this paper, this problem is resolved by the RBF-like network.

Training of the Neural Network Complex.

Training of the neural network complex is carried out in two stages. The individual classifiers' training is performed at the first stage, while at the second stage the synthesis classifier is trained. Images for the training are selected from the handwritten characters database [6]. The data used for the training are pre-processed by a uniform mixing of different classes patterns within the sample and by normalization. At this phase of research the input

vector was formed from the input image matrix by concatenating its rows, i.e. $k = NxM$. Initially, the weighting coefficients \mathbf{W} and \vec{V} are given a random value in the interval $(-1, 1)$. For training the "A, Б, В, ..., 9" blocks is used the kind of training with the teacher known as the backpropagation algorithm [7]. The expression for the error is calculated by

$E_p = \frac{1}{2L} \sum_{p=1}^L (U_p - OUT_p)^2$ where OUT_p is the desired output (designation of the teacher), and U_p – the real output of the unit.

Then corrections to the \vec{V} weightings are determined by the equations:

$$\begin{aligned} v'_j &= v_j + \Delta v_j, \quad j = 0, \dots, m \\ \Delta v_0 &= \eta \cdot \delta 2, \quad \Delta v_j = \eta \cdot \delta 2 \cdot OUT_{1j}, \quad j = 1, \dots, m \end{aligned} \quad (3)$$

$$\delta 2 = U_p \cdot (1 - U_p) \cdot (OUT_p - U_p)$$

corrections to the \mathbf{W} coefficients:

$$\begin{aligned} w'_{ij} &= w_{ij} + \Delta w_{ij}, \quad i = 0, 1, \dots, k; \quad j = 1, 2, \dots, m \\ \Delta w_{0j} &= \eta \cdot \delta 1_j, \quad j = 1, 2, \dots, m \\ \Delta w_{ij} &= \eta \cdot \delta 1_j \cdot a_i, \quad i = 1, \dots, k, \quad j = 1, 2, \dots, m \\ \delta 1_j &= OUT_{1j} \cdot (1 - OUT_{1j}) \cdot v'_j \cdot \delta 2, \quad j = 1, 2, \dots, m \end{aligned} \quad (4)$$

where η – the coefficient (intensity) of training, OUT_{1j} ($j = 1, 2, \dots, m$) – the j -th output of the input layer neuron, v'_j – the adjusted (3) vector \vec{V} coefficients, and w'_{ij} – the adjusted (4) matrix \mathbf{W} coefficients.

The process of the RBF network training consists of two parts. First the choice of the number of the hidden layer neurons and the choice of the Gaussian basis functions parameters, then at the given parameters of the hidden layer, the determination of weighting coefficients between the hidden and the output neurons. The input signal of the competitive block is the $\vec{U}_i = (U_1^i, U_2^i, \dots, U_{72}^i)^T$ response vector of units "A, Б, В, ..., 9" on the $\vec{A}_i = (a_1^i, a_2^i, \dots, a_k^i)^T$ input vector.

Determination of the number of neurons in the inner layer is made iteratively. At the first step a hidden layer consists of a single neuron. Its position $\vec{C}_1 = (\tilde{n}_1^1, \tilde{n}_2^1, \dots, \tilde{n}_{71}^1)^T$ coincides with the $\vec{U}_1 = (U_1^1, U_2^1, \dots, U_{72}^1)^T$ first input vector. If the $\vec{U}_i = (U_1^i, U_2^i, \dots, U_{72}^i)^T$ next input vector is remote from the center of existing neurons to a distance greater than a certain α value specified at the start of the training, a new neuron with the center at this point is created. Otherwise the $\vec{C}_i = (\tilde{n}_1^i, \tilde{n}_2^i, \dots, \tilde{n}_{71}^i)^T$ center closest to the given input neuron vector is shifted to $\vec{C}_i' = (\frac{\tilde{n}_1^i + U_1}{2}, \frac{\tilde{n}_2^i + U_2}{2}, \dots, \frac{\tilde{n}_{71}^i + U_{71}}{2})^T$ point. The parameter α is selected from considerations of the nearly equal number of neurons in the inner layer and the number of classes in the training set. Thus the number of neurons in the inner layer and the position of their centers is defined.

The width of the kernel function i -th neuron inner layer of the RBF network is determined by using the *K nearest neighbors* [7,9]. The idea of this method is to take the width of the kernel function of the neuron as equal to twice the average distance to its K nearest neighbors. Thus, the bias will be smaller in those regions of space where the points are dense - here will be well considered the details - and where there are few points, the deviations are larger (and will be interpolated).

Initially to the H weightings coefficients are assigned values from the interval $(-1, 1)$. The further correction of the coefficients is carried out in accordance with the expression:

$$h'_i = h_i + \eta \cdot \text{err} \cdot \frac{h_i}{\sum_{i=1}^z h_i^2}, \quad (5)$$

where – h'_i is the new value of the coefficient at the output of the i -th Gaussian function η – is the intensity of training, err – the difference between the actual and the desired output (indicated by the teacher).

The training process (adjusting the H weights) is terminated when an absolute value of the error reaches the predetermined value.

Experimental Studies

For the classifier training was used the base of the handwritten Russian alphabet characters and of Arabic numerals [6]. The training sample was formed of 56,970 images related to 71 classes (10 classes of digits, 180 examples in the class, 32 classes of small letters, 990 examples in the class, and 29 classes of capital letters, 810 examples in the class). The examples in the training set are uniformly mixed.

For testing was performed a sample of 6330 examples with 20 examples for every digit, with 110 examples of every small letter and with 810 examples for every capital letter.

The training of the "A, Б, В, ..., 9" blocks was effected as follows. The number of neurons m in the input layer was chosen to be k . From the training sample was formed the era – a set of examples (one for each class, i.e., $L = 71$). Further was determined the average total error and the \bar{V} and \bar{W} weights were adjusted according to expressions (3) and (4). Desired output of the "A, Б, В, ..., 9" blocks was encoded by the binary value of $\{0, 1\}$. The training process was stopped when the magnitude of the error did not exceed 0.05.

Further the competitive block was designed on the examples from the training set. Then the H weights were adjusted. The desired output signal Y was selected from the range:

$$\left[\frac{j}{71}, \frac{j+1}{71} \right], \quad j = 0, 1, \dots, 70.$$

The training process was stopped when the err error value did not exceed the value of 0.01.

Conclusion

The obtained results of testing the classifier indicate the possibility to apply the proposed approach to problems of the handwriting recognition. In our experiments the quality of recognition for different characters varied from 85 % to 97 %. This is probably due to the relatively small number of training samples as well as to the fact that the number of training iterations in the experiments was limited by the indicator 300 due to the high time expenditures. In the future, while reducing the dimension of the \bar{A} input features vector, you can optimize the training procedure, greatly simplify the structure of individual classifiers, and increase the number of training examples.

References

1. Sorokin A.I. Razrabotka algoritmov raspoznavaniya rukopisnyh simvolov na osnove analiticheskikh svoystv izobrazheniya [Tekst]: dis. ... kand. tehn. nauk: 05.13.17: Sorokin Andrej Igorevich. – Voronezh, 2010. – 184s. – Bibliogr.: s. 146-153.
2. Goroshkin A.N. Adaptivnoe vydelenie simvolov rukopisnogo teksta. // Vestnik Sibirskogo gosudarstvennogo azerokosmicheskogo universiteta im. akademika M.F. Reshetneva, 2008, № 1, s.15-18.
3. Saljum, S.S. Razrabotka i issledovanie metodov raspoznavaniya rukopisnyh arabskikh tekstov [Tekst]: dis. ... kand. tehn. nauk: 05.13.01: Saljum Said Saleh. – Izhevsk, 2003. – 129s. – Bibliogr.: s.121–127.

4. Jan, D.E. Issledovanie, razvitie i realizacija metodov avtomaticheskogo raspoznavanija rukopisnyh tekstov v komp'yuternyh sistemah [Tekst]: dis. ... kand. fiz.-mat. nauk: 05.13.18: Jan David Evgen'evich – Moskva, 2003. – 179 s.il – Bibliogr.: s. 169-179.
5. La S.T. Metody raspoznavanija rukopisnyh tekstov v sistemah avtomatizacii dokumentooborota na promyshlennyh predpriyatijah [Tekst]: dis. ... kand. tehn. nauk: 05.13.16: La Suan Thang. – Moskva, 2008. – 206 s.il. – Bibliogr.: s. 177-191.
6. Fedin N.A., Istratov A.Ju. Formirovanie bazy segmentirovannyh rukopisnyh simvolov russkogo jazyka.- //Vestnik komp'yuternyh i informacionnyh tehnologij, 2013, №7, s.36-41.Laurene Fausett, “Fundamentals of Neural Networks Architectures, Algorithm, and Applications”, pearson Education 4th edition, 2009.
7. Bagrova I.A., Gricaj A.A., Ponomarjov S.A., Sorokin S.V., Sytnik D.A., Vyor priznakov dlja raspoznavanija pechatnyh kirillicheskih simvolov., OOO "Kompleksnye sistemy", Tver'. Postupila v redakciju 02.06.2010, posle pererabotki 04.06.2010, s. 59-72.
8. Ezhov A.A., Shumskij S.A. Nejrokompyuting i ego primenenija v jekonomike i biznese. Uchebnoe posobie - Moskva: MIFI, 1998.- 224 s.Мозговой А.А. Проблемы существующих методик оптического распознавания рукописного текста.- //Вестник Voronezhского Gosudarstvennogo Tehniceskogo Universiteta, 2012, t. 8, № 7-1, s. 22-25.

GEOINFORMATION TECHNOLOGIES IN COMPLEX MONITORING OF WATER AREAS

Kurakina N. I.

Saint-Petersburg Electrotechnical University “LETI”, Center «GIS technology»

The article deals with the construction questions of estimation coastline condition by the results of investigations and questioning with use of GIS. Suggested the method of varied data metrological supplying. Visual presenting of developed conditions on the map make the understanding of information more easier, give the opportunities of the spatial analysis.

Keywords: complex monitoring, water area, coastal zone, GIS

Currently unified scheme or unified methods for water quality assessment in reservoirs and coastal zones has not been developed. The basis of an offered method is an attempt to combine the information describing condition of water area and the coastal zone from various positions and to lead it to point-based index system, which will allow to estimate current condition of territory based on various sides in uniform normalized scale, and also to create the program for representation of the results of complex estimation, based on a cartographical basis [1, 2]. Ecological cards, created in GIS, form a basis for decision-making in environmental management; they are a result of strict verification of completeness and quality of the ecological information, base for forming a system of monitoring and integrated assessment [3].

The Finnish Gulf is one of the most polluted water systems on the territory of Russia. Ecosystem of the gulf is affected by the strongest polluting load in connection with the realization of large-scale hydraulic engineering works on formation of a sea facade of St.-Petersburg, building of the new bulk-oil port in the Luga Bay, carrying out dredging works, activization of navigation. In order to ensure qualitative life of people, leaving nearby the coastal line of the gulf, it is necessary to conduct ongoing control over a water area condition.

Data of the hydrochemical and hydrobiological analysis has been put in a basis of system for monitoring and a complex estimation of Finnish Gulf” water conditions, taking

into account a hydrology, the analysis of soils on coastal territory, ground adjournment, and also the results of inspections and expertise [4].

The created system is based on the topographical basis having uniform coordinate system, on the databases which keep all the information on analyzed objects, having the uniform organization and structure, on a set of program modules for receiving estimations on earlier developed algorithms. The system of water area monitoring allows to estimate operatively an ecological situation and to represent it on a map, and also to investigate dynamics of pollution in space and time, as well as to receive normalized and integrated estimations.

The data, forming an ecological estimation, has various quality and complexity of definition. Thus there is a problem of combining the diverse data on a uniform metrological basis. In this work method for construction of normalized scales, purposed for combining various estimations, considering characteristics of reliability and degree of participation of each factor, is offered [6, 9].

The proposed method has been tested on the data from long-term observations on coastal territory of the eastern part of the Finnish Gulf. Based on the results of the analysis, thematic maps in ArcGIS ArcInfo were constructed [5].

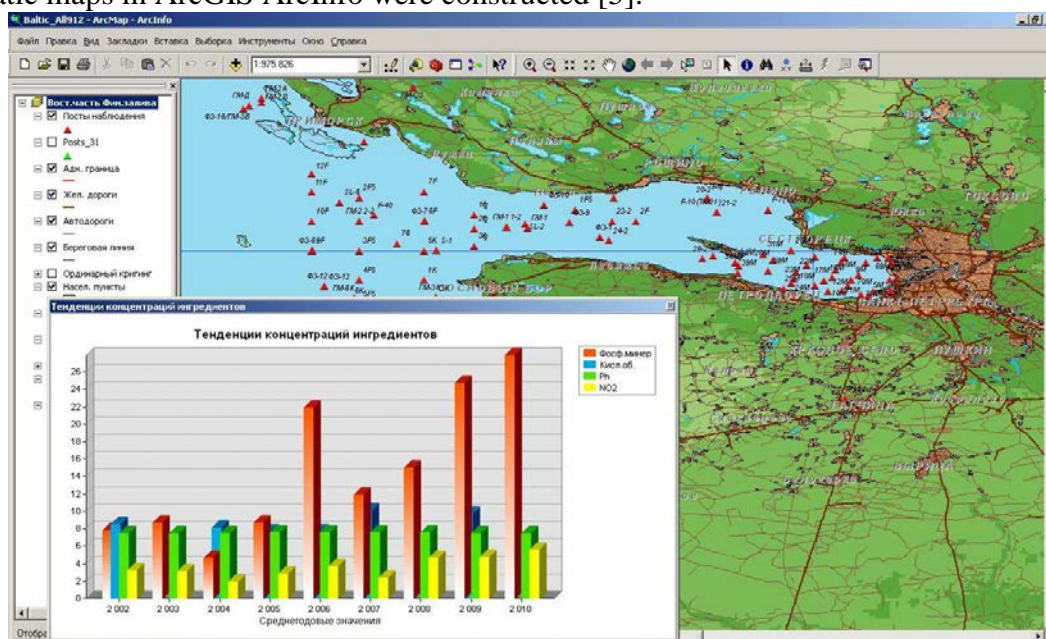


Fig. 1 Pollution dynamics

The developed system has allowed to present a set of estimations and rates in a form of a list of layers in one project, evidently and in an interactive mode to carry out the multiple-factor analysis of water area and coastal territories, to visualize results of the analysis on a map and to provide it to the remote user by the means of Internet in order to support management decisions and recommendations on the environmental management .

References

1. Alekseev V.V., Kurakina Izmeritel'nye sistemy i GIS tekhnologii. SPb. Elmor. 2007. 142 s.
2. Beskid P.P., Kurakina N.I., Orlova N.V. Geoinformatsionnye sistemy i tekhnologii. SPb. RGGMU, 2010, 172 s.
3. Geoinformatika / Ivannikov A. D. [i dr.]. M. : Maks Press, 2001. 349 s.
4. Izrael'. Yu.A. Ekologiya i kontrol' sostoyaniya prirodnoi sredy. Moskva: Gidrometeoizdat, 1984.

5. Gabidinova A.R. Kurakina N. I. Informatsionnaya sreda monitoringa i prostranstvennogo modelirovaniya zagryazneniya vodnykh akvatorii na baze GIS tekhnologii // Izvestiya SPbGETU «LETI». SPb. 2013. № 5. C. 92 – 98.

6. Kurakina N. I., Mikushina V.N. Metodika vedeniya monitoringa vodnykh ob"ektov na baze geoinformatsionnykh tekhnologii// Izvestiya SPbGETU «LETI». SPb. 2010. № 9. C. 85 – 88.

7. Metodicheskie ukazaniya. Metod kompleksnoi otsenki stepeni zagryaznennosti poverkhnostnykh vod po gidrokhimicheskim pokazatelyam. RD 52.24.643-2002. –SPb, Gidrometeoizdat, 2002, 48 s.

8. Kurakina N. I. Modelling of pollution distribution in water areas with usage of geoinformation systems // International Conference «50 Years of Education and Awareness Raising for Shaping the Future of the Oceans and Coasts», St.Petersburg, 2010 г. C. 190-191.

9. Kurakina N.I. River Pollutants Monitored with GIS. Analyzing the Environmental Impact of Water Bodies in Russia // GIS and Science: GIS Best Practices series. Redlands. Esri. 2008. P.39-42.

MODELING IN CPNTOOLS BITRATE MEASUREMENT ALGORITHMS IN THE PACKET-SWITCHED NETWORKS

Mekhanov V.B., Domnin A.L.
Penza, PSU

The article considers the problems of colored timed Petri net apparatus application for modeling the procedures of operative measurement based on algorithms of moving average and exponential smoothing of bitrate in packet switching net channels.

Keywords: flow rate, packet net, quality of service, Petri net, CPN Tools, moving average, exponential smoothing.

Development of modern telecommunication is to a great extent determined by the widespread implementation of quality of service (QoS) methods assurance, which is understood as the ability of a net to provide specific service to the traffic of each application. The necessary service is characterized by such parameters as carrying capacity (pass band), packet delay and its variation (jitter), percent of lost packets [1, 2].

The choice of the most efficient quality of service management methods in corporate networks, development of new QoS methods appear to be a complex problem that may be solved by means of simulation preferably using the instruments of telecommunication net research that are not attached to particular equipment, but based on mathematical models.

The report considers the modeling problems of one of QoS mechanisms – traffic control using the apparatus of hierarchical colored timed Petri nets [3]. The given apparatus features the following advantages:

- Petri net is a universal algorithmic system providing description practically of any algorithms;
- colors enable to describe and model algorithms depending on processed data content;
- hierarchical pattern enables to build complex multicomponent models;
- time property enables to model dynamic characteristics of objects.

CPN Tools is freely distributable packet. It was chosen as a development system, and in order to design network models the authors used a general approach described in [4-6].

Among other QoS mechanisms (traffic marking and classification, queue management, overload management) of great importance are the mechanisms of traffic management that directly determine the packet delay and loss probability thereof, as well as the efficiency of network equipment resource usage. The following are the standard management methods:

- traffic profiling, which is performed at the access level network equipment, and which is to limit user's packet flow rate in accordance with the dedicated bandwidth;
- shaping – smoothing of the traffic pulsation to eliminate bursts leading to the loss of frames and buffer thrashing, and unpredictable delay fluctuations that negatively impact the multimedia applications.

At the present time there is a significant development of various adaptive methods of traffic management and rearrangement of nodal equipment (switches and routers) bandwidth in real time [7].

A mandatory component of any traffic management policy is bitrate measurement. There are the following rate measurement algorithms:

- averaging over adjacent time intervals. The main disadvantage of the said algorithm is the impossibility to estimate bitrate with high burst;
- «sliding window» provides good approximation of the average bitrate by computing the simple moving average (MA), however, requiring considerable computing resources;
- «leaky bucket» and «token bucket» algorithms are easy to realize and therefore extensively used in profiling and shaping, however, practically do not measure the current bitrate, but only the limit thereof.

In order to measure the bitrate in reference [8] it is suggested to use the more easily realizable algorithm of exponential smoothing (EMA), applied in short-term forecasting of time series [9,10].

CPN Tools modeling of traffic rate measurement by algorithms of averaging complementary intervals, «leaky bucket» and «token bucket» is considered in [11,12]. Therefore, further we are to consider the formation principles of colored timed Petri nets for algorithms of bitrate measurement based on EMA and MA algorithms.

EMA algorithm modeling

In the traditional approach the exponential smoothing of the traffic profile directly in the channel for any moment in time $t_j = jTI$, where TI is the bit length, EMA V_j value equals:

$$V_j = \alpha X_j + (1 - \alpha)V_{j-1},$$

where α is smoothing constant ($0 < \alpha < 1$), X_j - instantaneous bitrate at the moment, which may have the value of 0, if at this period of time there is no data transfer in the channel, or the maximum value of physical channel speed V_0 (hereinafter to be considered $V_0 = 1$).

For purposes of traffic management it is necessary to take into account the bitrate not in the random moment of time, but either at the start of frame transfer, or at the end of frame transfer. Besides, the traffic profile represents a time series consisting of zeroes and ones: sequence of ones is determined by the number of bit intervals, during which the frame is transferred, and the sequence of zeroes – by the number of bit intervals, during which there is a pause between frames (fig. 1). Thus, to compute the EMA traffic rate it is possible to use the following recurrence formulas:

$$\begin{cases} VP_i = (1 - \alpha)^{P_i} VL_{i-1} \\ VL_i = 1 - (1 - \alpha)^{L_i} (1 - VP_i) \end{cases} \quad (1)$$

where VP_i , VL_i – average rates respectively at the start and at the end of transfer of i frame; P_i and L_i – length of the interframe pause and transfer time of i frame respectively.

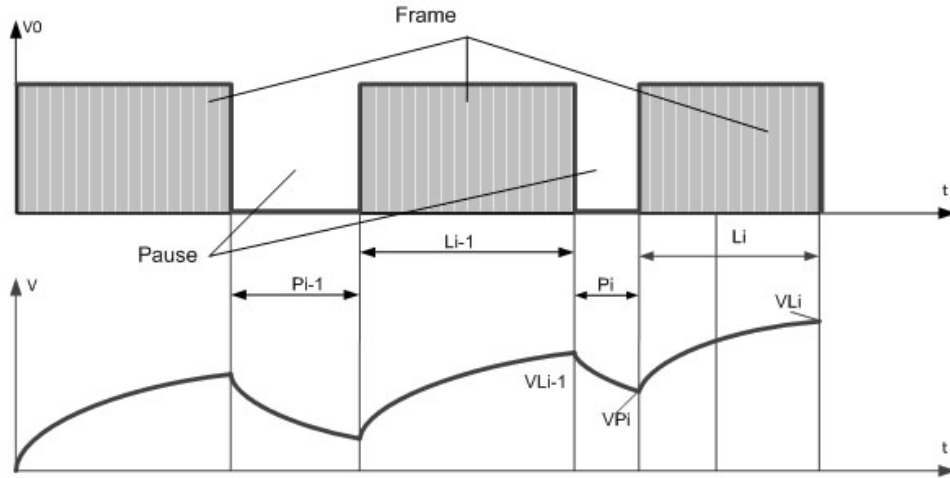


Fig. 1. Timing chart of EMA application

The average rate in the time interval $t \in (t_{i-1}, t_i)$ may be evaluated as follows:
$$V_i = \frac{VP_i P_i + VL_i L_i}{P_i + L_i}$$

In this case to simulate the researched algorithms we form a frame flow, movement of which is determined by the content of the frames, and due to this fact it is important to effectively use the feature of marker coloration. There were introduced two types markers:

- information markers, the movement of which imitates frame processing in a switch marked by a multiset with **frame** color, which may occupied either by transfer of the frame of **frm** color, reflecting the structure of the transferred frame and consisting of sender and receiver addresses **src** and **dst**, **qos** priority control field, **szfrm** size of transferred data and **delay** total delay to compute the delay of frame movement in the net, or by **avail** color (free), that enables to reveal and process the events related to the presence or absence of the frame in position;
- control markers, the colors of which reflect the condition of frame flow processing in the switch.

Petri net simulating the EMA algorithm is shown in fig. 2 and includes the following positions:

- **Traf_input**, that accepts the markers corresponding to the input frame flow;
- **EA_param**, includes the marker with information about the smoothing constant ($= 1/ea_param$);
- **EA_data**, that includes a marker with information about the current value of the computed **ea_data** rate;
- **Data_Collector** – the aggregator of markers with information about the computed rate (count – i marker number, **s_frame_int**, **curTime()+szfrm**, **s0_int**, **s_pause_int**, **szfrm** – computed values of VP_i , VL_i , VL_{i-1} , P_i and L_i respectively).
- **Collector** – output position of the model.

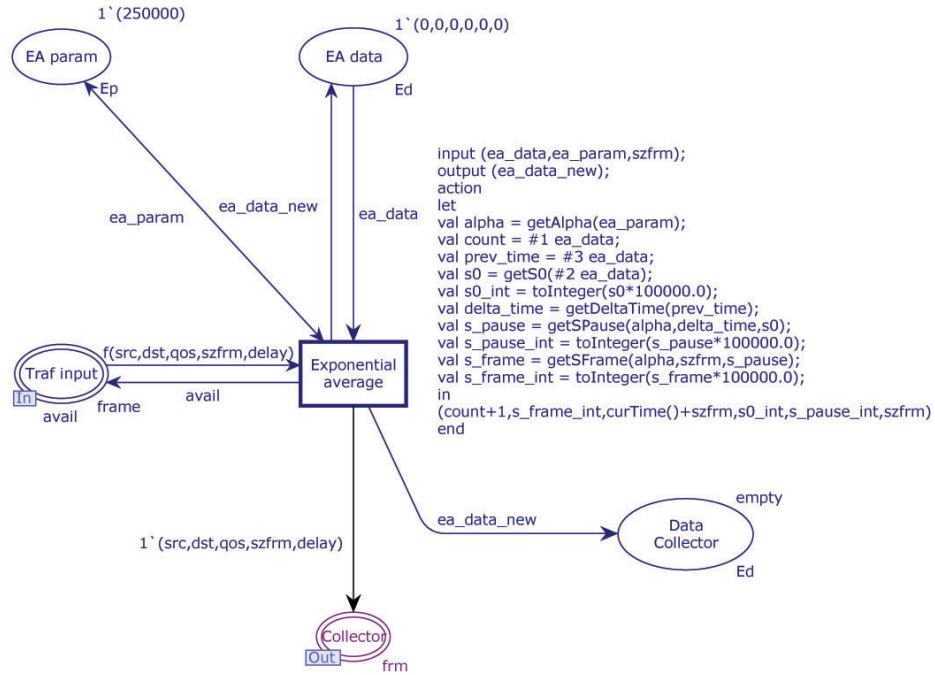


Fig. 2 Petri subnet, modeling the EMA algorithm

In the subnet there is one **Exponential average** transition that realizes traffic profiling according to the algorithm of exponential smoothing by computing next values of VP_i and VL_i rates using CPN ML language procedures. Herewith, the direct computation by formula (1) realizes user **getSPause** and **getSFrame** functions. It should be noted that the use of the above mentioned functions is connected with conversion of the format of variables with floating point in integers, which may lead to an error, the impact of which should be compensated by introduction of scaling.

MA algorithm modeling

Using the traditional approach the simple moving average of traffic in a channel for a random moment of time $t_j = jTI$, V_j will be equal to

$$V_j = \frac{1}{T} \sum_{i=0}^{T-1} X_{j-i} = V_j + \frac{X_j - X_{j-T+1}}{T}, \quad (2)$$

where T – a sliding window of averaging.

Taking into account the fact that the traffic profile represents a time series consisting of zeroes and ones: rate should be computed at the start of frame transfer and at the end of frame transfer, the window will not move along the time axis uninterruptedly, but “by jerks”, as shown in fig. 3. Thus, similarly to EMA, the computation formula for VP_i and VL_i may be represented as follows:

$$\begin{cases} VP_i = VL_{i-1} - \frac{1}{T} \sum_{\tau_1} L_{\tau_1} \\ VL_i = VP_i + \frac{1}{T} L_i - \frac{1}{T} \sum_{\tau_2} L_{\tau_2} \end{cases}, \quad (3)$$

where the sums represent the amount of bits transferred into the channel on time intervals $\tau_1 \in (t_i - P_i - T + 1, t_i - P_i - T)$ and $\tau_2 \in (t_i - P_i - T + 1, t_i - P_i - T)$ respectively, i.e. removed from the window when it moves during i frame arrival and transfer end. The said fact causes certain difficulties in practical realization of the MA algorithm, as it is necessary

not just to retain the frame lengths, caught in the window, but also to retain the length of pauses between them and “split” the last frame, if the rear edge of the window matches the time of the transfer thereof.

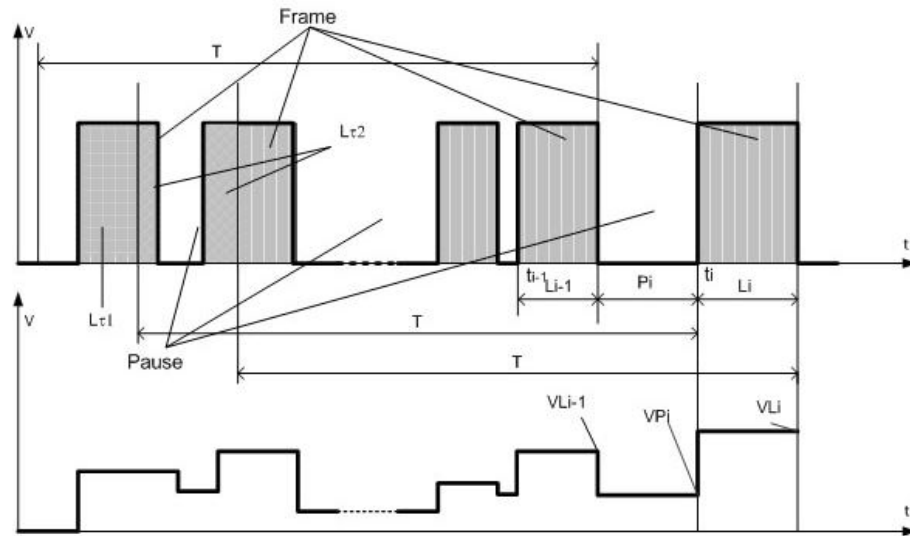


Fig. 3. Time chart of MA application

The variant of Petri net modeling the MA algorithm has been suggested in reference [13], and fig. 4 shows a more compact realization of the subnet including the following positions:

- **Ingress_port**, that accepts the markers describing the frames of the input traffic flow;
- **Forefront, Backfront**, that include time markers representing the start (**Forefront**) and the end (**Backfront**) of frame receiving;
- **SW_param**, contains marker with information about the size of “the sliding window” (fw_param) in bit intervals;
- **Framefront, Frameback**, that contain markers caught in the current position of “the sliding window”, with time markers representing the start (**Framefront**) and the end (**Frameback**) of the respective frame receiving;
- **Cache** – buffer position used for aggregation of two net branches;
- **SW_size**, contains the volume of data caught in “the sliding window” in the current position thereof;
- **Frame_size_cache**, intended for temporary storage of information about the size of the frame added to “the sliding window”;
- **Data_collector2**, contains markers with information about a sequence number of a marker (count2) and volume of data (fw_data_new), caught in “the sliding window” at the moment of the end of the respective frame receiving (current value of channel usage may be computed as a ratio of fw_data_new to fw_param);
- **Packet_counter** – buffer position, calculating marker filling of **Data_collector2** position;
- **Collector** – output port, collecting markers of the processed frames for further processing.

The net operation of MA algorithm modeling is described below.

The next input marker goes to **Ingress_Port** position, after that there takes place **Split_frame** transition actuation. Then **Forefront** position is taken by the marker, containing information about a frame, which will be used for computation of the current position of the

window at the moment of frame appearance (the frame will not be registered in the size of the window), and **Backfront** position – by the time marker increased by the size of the frame.

After that the marker in **Backfront** goes through the transition **No_bf_check** or **Check_backfront**, and marker in **Forefront** – through transition **No_ff_check**, or **Check_forefront**. Transitions **Check_backfront** and **Check_forefront** have the highest priority and are necessary to process the cases, when at appearance of the next frame (**Check_forefront**) or receiving thereof (**Check_backfront**) the back front of “the sliding window” is in the period of time when the receiving of the already arrived frame took place («splitting» of the frame according to formula 3). In such cases the information about the amount of data in “the sliding window” at the current moment should be adjusted. Adjustment values sz_front_new and sz_data_new are computed by the appropriate procedures taking into account the current simulated time obtained using $cT()$ function.

No_bf_check transition or **Check_backfront** transition actuation leads to marker removal from **Back_Front** position, and in case of **No_ff_check** or **Check_forefront** actuation the marker transits to **Cache_buffer** position. Then, there occurs the actuation of **Add_Frame_to_SW** transition that saves information about the processed frame in “the sliding window” (**Frame_front** и **Frame_back**). As the information about the amount of data in the window increases by the size of the appeared frame after receiving thereof, it is necessary to change the values in **SW_size** position after a period of time that equals the size of the frame. The said is realized by **Frame_size_cache** position and **Resize_SW** transition.

Reduce_SW_size transition removes the information about the frames missing the current “sliding window” from **Frame_front**, **Frame_back** and **SW_size** positions.

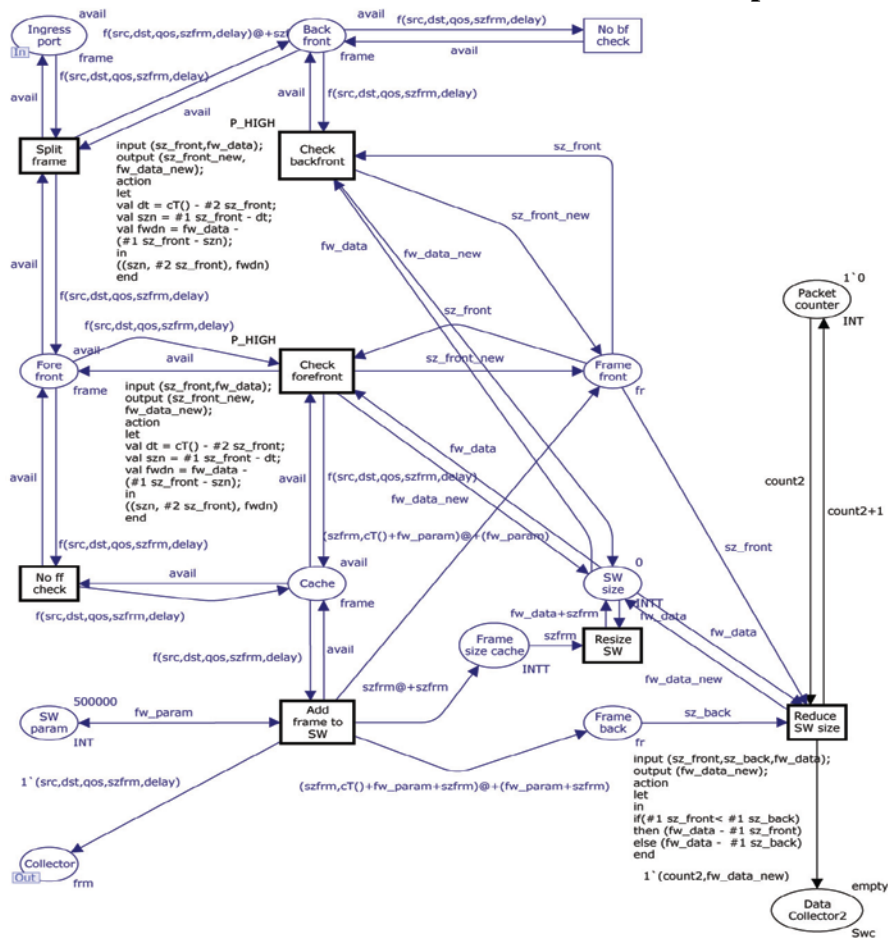


Fig. 4 Petri subnet, modeling the MA algorithm

For the example the created models application, below are the results of modeling of bitrate measurement in the Ethernet switch supporting IEEE 802.1 Q/P. Simulated time is represented in (one cycle corresponds to 100 ns Ethernet or 10 ns for Fast Ethernet). The input traffic was modeled using the special Petri net [14] and represents a combination of two components, merger of which forms the data flow with pronounced bursts:

- Regular, representing a sequence of 100 double-framed packets with the length of 12176, the period of which linearly increases by 5% from 200000.
- Random, with frames, length distribution of which is of pronounced bimodal nature: 25% of all frames have minimal and maximal length (512 and 12176 respectively), the length of others is equally distributed in the remaining range. The frames follow through time intervals, distributed according to the exponential law (technological interval of 160 cycles is also taken into account).

Fig. 5 shows the realization profile of the input traffic with the length of around 11000000 cycles (the amount of frames of the regular composition is 100, average length of the interframe intervals of the random component of the input flow is 2960 cycles), and realization of rate changes through MA ($T=500000$) and EMA ($\alpha=1/250000$) algorithms. The transient process with the length of 500000 bit cycles is not shown. Channel load factor, computed according to the input realization, equals to 0.748.

Both algorithm produce quite similar results and clearly follow the linear trend of implementation concerning the changes in bitrate.

However, the comparison of the Petri nets, presented in figs. 2 and 4, visually shows a clear advantage of EMA algorithm in realization simplicity unlike MA.

Therefore, the presented subnet, modeling MA algorithm, may be implemented not from the point of view of MA feasibility assessment, but as a “sample” model for comparison with new algorithms of bitrate assessment, based on exponential smoothing.

Thus, the modeling results show the effectiveness of the operative measurement of the current bitrates in the telecommunication equipment using EMA algorithm that may be used for evaluation of rate not just of the general flow, but of individual components, corresponding to the introduced QoS classes.

In the engineering realization of EMA algorithm it is possible to decrease the computing complexity via linear approximation of the exponential transfer characteristic, enabling to reduce the number of multiplication in processing of each frame to two.

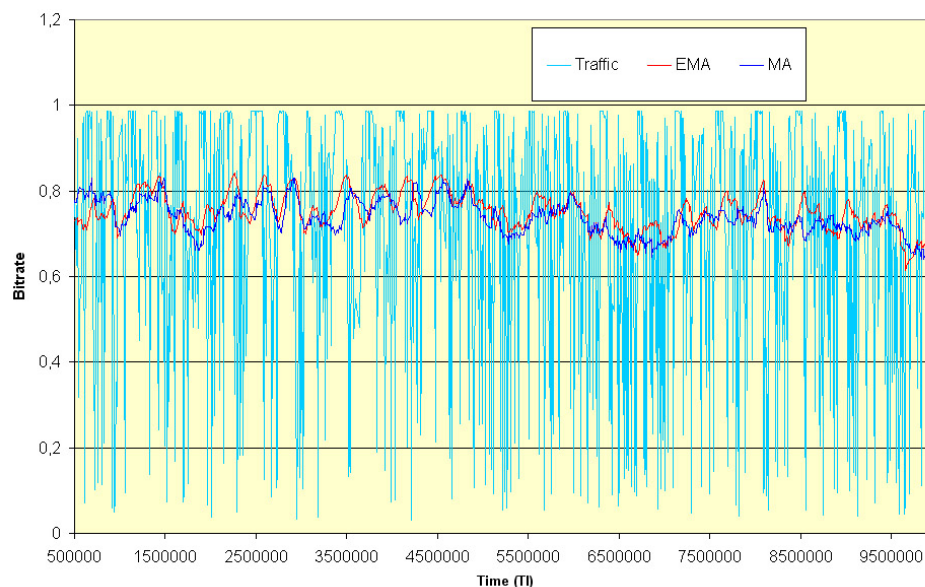


Fig. 5. Results of MA and EMA algorithms modeling

The obtained values of the current rate are easy to use for solution of routine problems of traffic management:

- in the course of profiling during the frame receiving the value V_L is forecasted. This value is compared with the given boundary value, and according to the result of the comparison the frame is either deleted, or marked;
- in the course of shaping of the output traffic in the case, when the forecasted is greater than the boundary value, it is necessary to increase the time of the current pause by a calculated value.

The advantage of the suggested method of bitrate measurement is the possibility of the efficient usage of measurement results for dynamic redistribution of the bandwidth, load balancing and other tasks of net adaptive management. On the basis of the suggested method it is possible to realize EMA of higher orders, modeling of which is performed through cascade connection of several Petri subnets, shown in fig. 2.

The problems of smoothing parameters choice depending on the required accuracy of evaluation of traffic rate and traffic parameters are the subject of the separate research.

References

1. Srinivas Vegesna. IP Quality of Service, Cisco Press, 2001
2. Kucherjavj E.A. Upravlenie trafikom i kachestvo obsluzhivaniya v seti Internet – SPb.: Nauka i tehnika, 2004.
3. K. Jensen and L.M. Kristensen. Coloured Petri Nets -- Modeling and Validation of Concurrent Systems. Springer-Verlag Berlin, 2009
4. Zaitsev D.A. Switched LAN Simulation by Colored Petri Nets // Mathematics and Computers in Simulation. – 2004. – Vol. 65, № 3. – P. 245-249.
5. Mekhanov V.B. Primenenie setej Petri dlja modelirovaniya mehanizmov obespecheniya QoS v komp'yuternyh setjah // Materialy mezhdunarod. simpoziuma «Novye informacionnye tehnologii i menedzhment kachestva (NIT&MQ'2010)» - M.: JeGRI, 2010 - S. 209-214
6. Mekhanov V.B. Primenenie setej Petri dlja modelirovaniya telekommunikacij s podderzhkoj kachestva obsluzhivaniya // Trudy XVII Vserossijskoj nauchno-metodicheskoy konferencii «Telematika'2010», Tom 1. - SPb.: SPbGU ITMO, 2010 - S. 283-284.
7. Muranov A.S. Povyshenie kachestva adaptivnogo upravleniya trafikom paketnyh telekommunikacionnyh setej. Dissertacija na soiskanie nauchnoj stepeni kand. Tehn. nauk – informacionnye tehnologii. – Kiev: NAU, 2010
8. Domnin A.L. Primenenie metoda jeksponencial'nogo sglazhivaniya dlja profilirovaniya i shejpinga setevogo trafika / Materialy mezhdunarodnoj nauchnoj konferencii «Informacionnye tehnologii i sistemy 2013 (ITS 2013)» - Minsk: BGUIR, 2013 - C30-32
9. Greshilov A. A., Stakun V. A., Stakun A. A. Matematicheskie metody postroenija prognozov. — M.: Radio i svjaz', 1997 -112 s
10. Bulashev S.V. Statistika dlja trejderov - M.: Kompanija «Sputnik+», 2003 - 245s
- Domnin A.L., Kizilov E.A., Pushkarev V.A. Modelirovanie mehanizmov QOS v kommutatorah Ethernet cvetnymi setjami Petri / Sb. statej uchastnikov Vserossijskogo konkursa nauchnyh rabot studentov i aspirantov «Telematika '2010: telekommunikacii, veb tehnologii, superkomp'yuting». – SPb.: SPbGU ITMO, 2010 - S. 35-38.
11. Mekhanov V.B., Domnin A.L. Modelirovanie algoritmov upravleniya polosoj propuskaniya cvetnymi setjami Petri // Trudy IX Mezhdunarod. nauchno-tehnicheskoy konferencii «Novye informacionnye tehnologii i sistemy». Ch. 2. - Penza: Izd-vo PGU, 2010. – C 77-82

12. Konnov N.N., Domnin A.S. Razrabotka modeli algoritma «skol'zjashhego» okna cvetnymi vremennymi setjami Petri / Estestvennye i matematicheskie nauki v sovremennom mire. № 9-10. Sbornik statej po materialam IX-X mezhdunarodnoj nauchno-prakticheskoj konferencii. — Novosibirsk: Izd. «SibAK», 2013 - S 76-81

13. Nikishin K.I., Konnov N.N., Domnin A.L. Modelirovanie trafika seti Ethernet cvetnymi setjami Petri / Sb. materialov I Mezhdunar. nauch.-prakt. konf «Sovremennye problemy komp'yuternyh nauk (SPKN-2013)» - Penza : Izd-vo PGU, 2013 - S 120-123

INTELLIGENT SUBJECT SEARCH SUPPORT IN SCIENCE AND EDUCATION

Ivanov V.K., Palyukh B.V., Sotnikov A.N.
Tver, TSTU; Moscow, JSCC RAS

This article presents main results of the pilot study of approaches to the subject information search based on automated semantic processing of mass scientific and technical data. The authors focus on technology of building and qualification of search queries with the following filtering and ranking of search data. Software architecture, specific features of subject search and research results application are considered.

Keywords: genetic algorithm, innovation, data mining, science, education, search query, population, fitness, ranking, relevance, semantic search, filtering, data-warehouse.

Introduction. New efficient scientific knowledge search and synthesis methods (in particular, breakthrough technologies and innovative ideas in economics, science, education) are one of the top research and development targets in the field of information technology. The project Intelligent Distributed Information Management System for Innovations in Science and Education powered by the Russian Foundation of Basic Research (contract No NK13 -07- 00342 \ 13) is to solve this problem. This article presents main results of the pilot study of approaches to the subject information search based on automated semantic processing of mass scientific and technical data.

Specific Features of Subject Search. The major features of subject search tasks which determine the approaches are:

- the required information is often located at the junction of adjacent areas, hence, there is some complexity in the exact wording of the search query.
- along with the information on proper innovation it is desirable to obtain information on applications, risks, specific features, users, authors, producers.
- there is a necessity of available alternatives and different criteria mixing for selecting the most effective practices.
- the information on innovations is fragmentized and heterogeneous; primarily sector-specific character.

In contrast to the search for specific information (facts) on particular aspects of the required content, it is rather difficult to solve a sophisticated problem of searching coordinated information on a target subject. For example, it is required to find the economic performance of mine Rapsadskaya JSCo for the first half of 2013. If we use this phrase as a search query, it is possible to get a relevant answer in the first ten search results of Google. But how can one find the information to analyze scientific, technical, economic and social factors affecting the innovative technical, technological, or financial mechanisms of coal-mining in the eastern regions of Russia?

To solve such search problems users have to employ lots of key concept combinations, clarify them in the course of en-route search on the Web or specialized stores such as patent

databases (DB). It is not obvious that for this purpose any reasonable method would be used without fail. Eventually, a large amount of search results would be at the disposal of a user (tens and hundreds of documents), with the found information being more or less relevant to queries. As is quite common, there would be no opportunity to go into details of all the result data. So, the following questions can arise:

- How can one simultaneously assess the relevance of documents found by different queries? Is the relevance of documents determined correctly?
- Is the data ranking in a certain search system correct from the perspective of a user? Do all the results available for direct assessment meet the user's expectations?
- Are all the results that meet the user's expectations available for direct assessment? Are all the required data (e.g. innovative solutions) found at all?
- How one can filter documents extrinsic to the searched subject?
- Is it possible to find any effective solutions relevant in other application fields, but would be successfully used as an innovation in this domain.
- Is it possible to give a visual assessment to lots of found innovative solutions together with linked objects?

There are no clear-cut ways of solving these problems within trivial solutions. Obviously, we need efficient methods of creating and populating the computer-assisted collections of advanced technologies and ideas which would contain not only their descriptions, but selected, classified and associated data. These data can be used to analyze retrospective and prospects of specific innovations, to search current and likely trends. The project in question is an attempt to offer a number of such innovative approaches.

Problem definition. Thus, a project goal can be summarized as: the exploration of new approaches to innovative solution search methods in the database of a data center and its population with Internet data mining results adapted to visual assessment of selected, classified and associated data. We see three key tasks to attain the goal:

- To develop the technology of building and qualification of search queries with the following filtering and ranking of search data.
- To set up methods of cluster analysis to text documents and multimedia objects in order to use them for tagging the links between search results.
- To create a store of innovative solutions for educational and scientific purposes.

Software Architecture. When developing a general software architecture based on mechanisms of direct automated search of innovative solutions the authors determined view layers, those of services, business logic, data access as well as crosscutting concerns (the UML notations and artifacts were applied). In the behavioral model of a system (Fig.1), in a particular session, we can distinguish two periods of user's activation: query formulation (first step) and visualization of the results including the options of the requested and innovative solutions and linked objects (final step). Interim steps are hidden, off-line run and implement the algorithm of interaction between the system components without active participation of a user.

The main functional components:

- Search module. It involves executing a search query in the Internet search systems and the custom directory of innovative solutions; basic search (query by attributes and full-texts), location, data retrieval and summarizing.
- Query qualification module. Selection and ranking of search results: filtration, subject control, qualification of search query.
- Classification module. Classification of search results: selection of a method, cluster analysis of text documents and multimedia objects, data qualification. As a result we obtain a subset of semantically linked data.

- Link identification module. Link start-up: qualitative classification assessment, selection of the best results, interpretation of results; generating the descriptions of solutions with innovative potential in a given subject segment or for a specified object (article, technology, product).
- Visualization module. It involves mapping of search results, procedures of data processing, classification results including semantic links between objects.
- Data-warehouse (DW) management module involves storage and updating of data search and processing results, parameters, and intermediate data; registry of innovative scientific, technological and educational problems. DW is built on the basis of a vector space model, includes document database access libraries and a data indexer.
- Service module. It involves monitoring and analysis of user access to information resources.

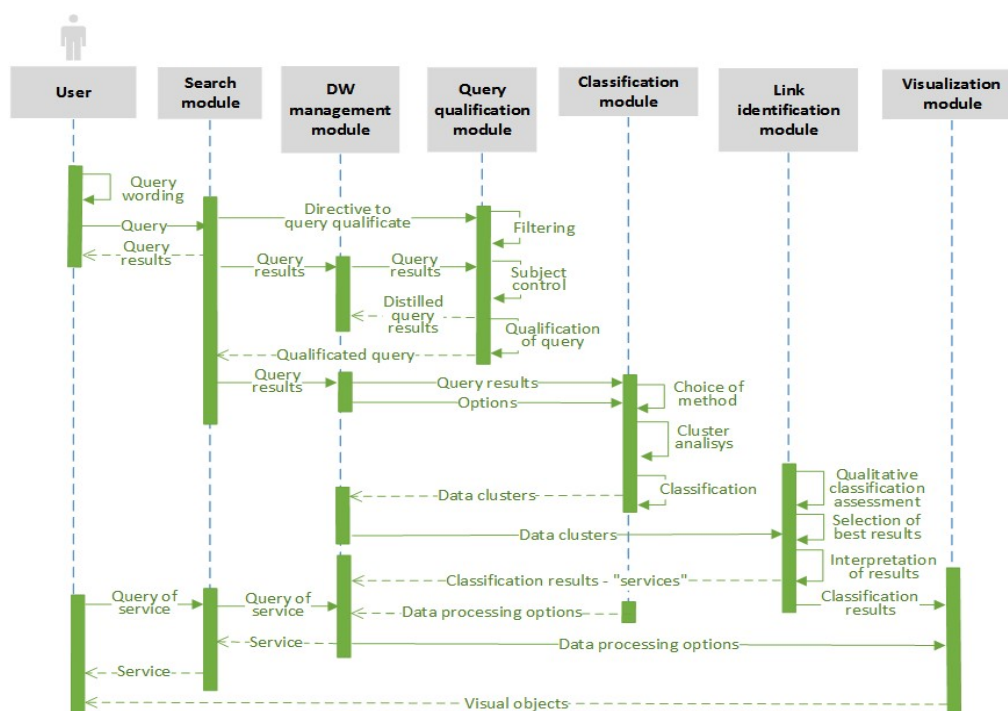


Fig.1. Behaviour of software components

It is particularly remarkable that the developed original object model is oriented to work with any text objects related to the subject of the processing: queries, search results, text documents. Over 30 entity classes specify a document processing environment, a set of documents, methods of calculating the package document similarity measures as well as search functions in document package, types of reports, a collection of document words, lemmatization, a document structure and its specific parts.

The detailed architectural solutions are described in [1].

General Search Algorithm. One of the elements of the presented above architecture is a generalized heuristic algorithm for filtering and rating the search results, which is based on available search engines; the algorithm is supposed to provide a background for search modules and inquiry qualification, as well as for retrieval schedule and search procedures in general.

The algorithm under consideration uses search results of known search engines being in service; it is invariant to them; with various degree of automation; it uses the search engine rating results.

The algorithm instruments a multistep process of sequential filtrations of search results and the analysis of semantic similarity of the found object content to adaptively generated reference texts (k -patterns). For an assessment of quality of ranking executed in compliance with algorithm, a modified DCG measure was used. The ways of generating effective k -patterns were investigated as well.

Let us briefly run through the algorithm operation (Fig.2). The description of a generalized request Q_0 includes the initial set of key concepts of the target document subject.

The generation of the set Q of search queries $q \in Q$, $|Q| = N$ is automated with an adaptive genetic algorithm searching for an effective total pertinence of the resulting document sampling under given evolutionary process depth constraints (see below).

The execution of queries q_{ij} is accompanied with filtering search results R_{qs} rated by a search engine and generating total results R . Filtering provides for the exclusion of some documents which subject area is formally pertinent but should not be the subject of the search for some reasons. It is done by hand or with a classifier which learning set is updated during the analysis of found texts.

The examples of documents being filtered are tutorials, student's papers, training programs, tests and notes, site promotion materials, company's sites, shopping sites, social networking sites; blogs; advertisements; virus-infected resources; nonexistent resources. The generation of k -patterns or reference texts is done simultaneously. They are used for calculating document similarity measures (P_{ka} is a text combination based on the first positions of rated search results, P_{kc} is the most pertinent result, P_{kb} is the text constructed from authority dictionary entries and P_{kd} is a text constructed from Q_0). Further the model of document vector space is used, i.e. each document d (the search results from R and k -patterns) is interpreted as vector $\vec{v}(d) = (w_{1,d}, w_{2,d}, \dots, w_{1,N_r})$, where $w_{t,d}$ is determined with a common metric $tf_{t,d} * idf_{t,d}$. A matrix $M_{N_r \times 4}$ of document semantic similarity from set R with common k -patterns is generated and the rating of documents from R in accordance

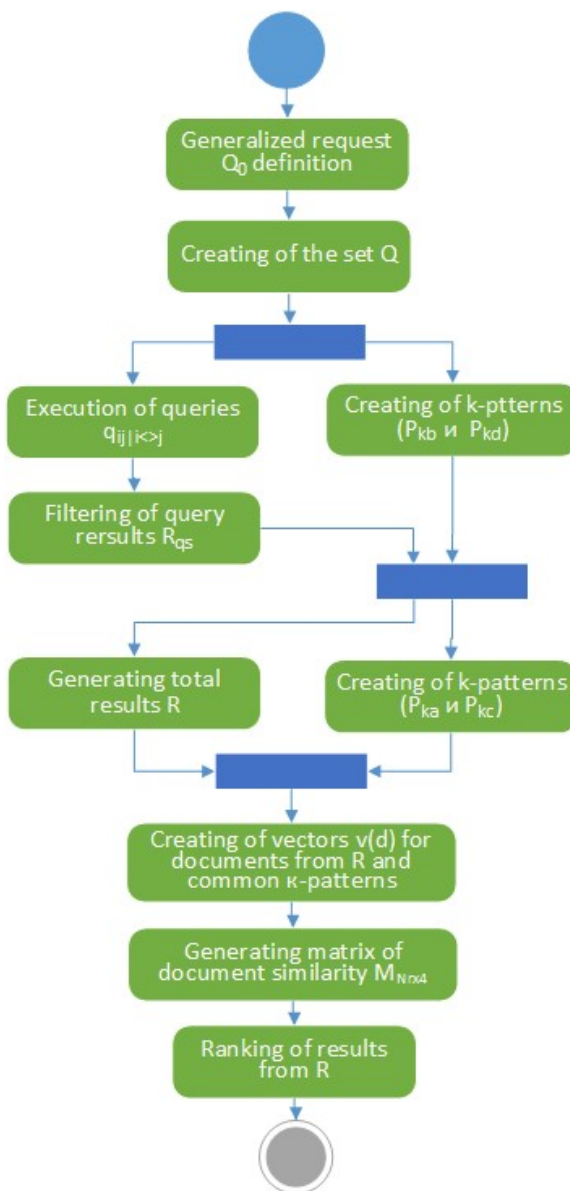


Fig. 2. General pattern of a generalized heuristic algorithm for filtering and rating the search results

with their similarity $Sim(d_1 d_2)$ to k –patterns is done. The algorithm is described in detail in [2].

Note that the project provides for the usage of Internet search engine work results. The proposed search algorithms will be added to authoritative decisions – classical approaches to search result ranking (HITS, PageRank, BrowseRank, MatrixNet) which are based on the combination of document semantic pertinence and authority as well as user's behaviour and experience.

Generation of Search Queries. The project proposes and investigates the approach to search result generation based on a genetic algorithm. The approach is used to specify a semantic kernel of a document desired set and generate sets of effective queries. The problem definition provides for the organization of an evolutionary process generating a stable and effective query population forming a relative search image of a document. A target set of search results is to be formed by such document addresses which are (a) in the first positions of a ranked list constructed by a search engine; (b) present in the result lists of multiple queries; (c) semantically similar to reference texts generated during evolutionary queries; (d) adequate to the environment given to a crawler by a user profile.

The original population from N search queries may be a set of $Q = \{q_i\}$, $|Q| = N$, $N < |Q_0|/2$, $q_i = (k_1, k_2, \dots, k_m)$, where (k_1, k_2, \dots, k_m) is a random combination of key concepts of a search image Q_0 . The value of an objective function must determine the query quality (population individual fitness). For each i -th query result the value may be calculated as $w_i(f, p, s, a)$, where f is determined by a result position in a ranked result list made by a search engine; p is determined by entering the result in the result lists of most queries; s is determined by a semantic similarity to k –patterns formed adaptively during the algorithm execution; a is determined by a user profile as an environment factor (values f, p, s, a are normalized for the range from 0 to 1). The value of a target function for each query is calculated as an averaged weight of query results $\bar{w} = \frac{1}{P} \sum_{i=1}^P w_i$, where w_i is a weight of each result calculated after executing all queries; P is a number of document addresses seen as the query result. The value of a objective function is interpreted as the capability of a search query to generate the results to be in the next population generation.

To choose parent couples the method of genotype outbreeding is proposed. It can provide for the most complete participation of all current queries in generating the next query population (the first parent individual is chosen randomly and the second individual is the "farthest" from the first one, the distance can be calculated as $\Delta \bar{w} = \bar{w}_1 - \bar{w}_2$). The evolutionary operator of crossover is done with discrete recombination which corresponds to the exchange of key words (genes) between queries. The peculiarity of the proposed implementation is that the key word of a parent query is not substituted for the other parent query key word but its synonym. It allows generating considerably more child queries, with properties (semantics) of parent queries being preserved.

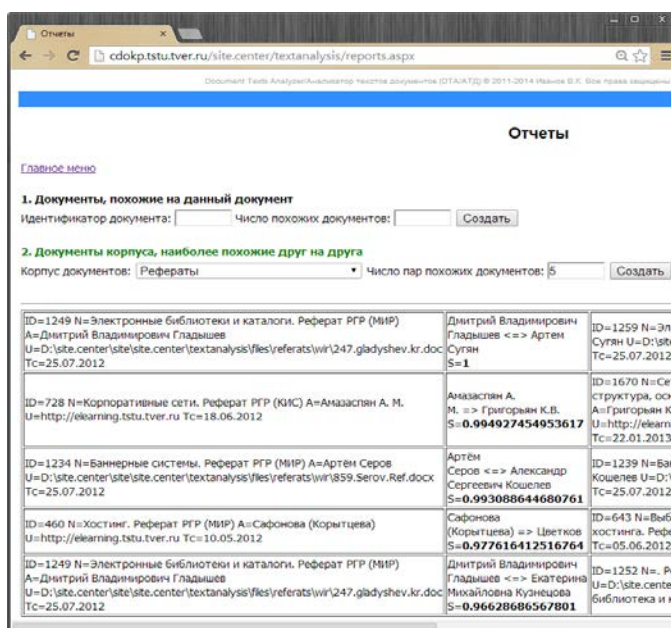
The essence of the most adequate mutation operation of the approach under study is the probabilistic change of a key query word (gene) chosen randomly. The essence of mutation of the approach under study is the change of a key query word (gene) chosen randomly. Since the number of key words in a query $q_i = (k_1, k_2, \dots, k_m)$ is fixed, it is not possible to use such mutation operators as a new gene addition, new gene insertion, gene deletion. Besides, there is no sense in gene place exchange in the context of executing search queries.

To generate a new population an elite selection denying the loss of best solutions is used. An intermediate population is generated. It includes both the parents and their children. N with the best values of a objective function \bar{w} is chosen from all the population members. They will go in the next population. Generally, the condition of terminating the algorithm is

considered to be population stability. For example, when a mean-square deviation of objective function values (query fitness) reaches some threshold specified by an algorithm parameter. The genetic algorithm is described in detail in [3].

The methods of semantic text comparison are used here. They are the computation of key concept weights and the construction of document vectors and not the known approaches (e.g. shingling) based on detecting direct adoptions in the text.

The research of some approaches to data centre different information systematization should be noted. As a result, a multistep algorithm of alternative search in an information catalogue with a target step number to be a base of a desired solution selection is developed [5, 6].



Отчеты			
1. Документы, похожие на данный документ			
Идентификатор документа:	Число похожих документов:	Создать	
2. Документы корпуса, наиболее похожие друг на друга			
Корпус документов:	Число пар похожих документов:	Создать	
ID=1249 N=Электронные библиотеки и каталоги. Реферат РГР (МНП) A=Дмитрий Владимирович Гладышев U=D:\site.center\site\textanalysis\files\referats\wlr\247.gladyshev.kr.doc Tc=25.07.2012	Дмитрий Владимирович Гладышев <=> Артем Сулян S=1	ID=1259 N=Электронные библиотеки и каталоги. Реферат РГР (МНП) A=Дмитрий Владимирович Гладышев U=D:\site.center\site\textanalysis\files\referats\wlr\247.gladyshev.kr.doc Tc=25.07.2012	Дмитрий Владимирович Гладышев <=> Екатерина Михайловна Кузнецова S=0.96628606567801
ID=728 N=Корпоративные сети. Реферат РГР (КНС) A=Амазасян А. М. U=http://elearning.tstu.tver.ru Tc=18.06.2012	Амазасян А. М. => Григорьев К.В. S=0.994927454953617	ID=1670 N=Сети A=Григорьев К.В. U=http://elearning.tstu.tver.ru Tc=22.01.2013	ID=1239 N=Банк A=Сергей Сергеевич Кошелев U=D:\site.center\site\textanalysis\files\referats\wlr\859.Serov.Ref.docx Tc=25.07.2012
ID=1234 N=Банк A=Сергей Сергеевич Кошелев U=D:\site.center\site\textanalysis\files\referats\wlr\859.Serov.Ref.docx Tc=25.07.2012	Артём Серов <=> Александр Сергеевич Кошелев S=0.993088644680761	ID=1239 N=Банк A=Сергей Сергеевич Кошелев U=D:\site.center\site\textanalysis\files\referats\wlr\859.Serov.Ref.docx Tc=25.07.2012	ID=643 N=Выбор A=Сергей Сергеевич Кошелев U=D:\site.center\site\textanalysis\files\referats\wlr\859.Serov.Ref.docx Tc=25.07.2012
ID=460 N=Хостинг. Реферат РГР (МНП) A=Сафонова (Корытцева) U=http://elearning.tstu.tver.ru Tc=10.05.2012	Сафонова (Корытцева) => Цветков S=0.977616412516764	ID=1252 N=Ресурсы A=Дмитрий Владимирович Гладышев U=D:\site.center\site\textanalysis\files\referats\wlr\247.gladyshev.kr.doc Tc=25.07.2012	ID=1252 N=Ресурсы A=Дмитрий Владимирович Гладышев U=D:\site.center\site\textanalysis\files\referats\wlr\247.gladyshev.kr.doc Tc=25.07.2012

Fig. 3. The appearance of one of the reports of experimental software platform DTA

Data Warehouse. The possibilities of Data Warehouse (DW) generation with realizing a document vector space model to use it as a base of a data-centre information support are researched in the project. A software platform Document Text Analyzer (DTA) for semantic document analysis (their metric similarity computation) is developed within DW.

The prototype of the DW was tested successfully when associated technologies of the integral electronic document quality assessment and document pertinence in different contexts analysis were employed [4]. In particular, the debugging of software shell and interface of the TSTU specialized electronic teaching pack database, data centre warehouse components, was done. The database is used to test and apply the project research results. The pioneering technology of the students' work uniqueness assessment (course and design-graphic papers, semester tasks, reports, essays, tests) is put to use.

Application Areas. The list of application areas of the approaches under discussion in the paper, the research results and technologies is given below:

- A competitive analysis and competitive intelligence. A survey of commercial, scientific and technical, social information sources in a target field. A search of business valuable information. A client information acquisition (in CRM systems). A characterization of new fields and directions in business planning. A search of sector innovation decision descriptions.
- Educational technologies. An analysis of students' paper works (graduation, course papers), theses. A selection and expert examination of teaching materials (books, articles, papers, essays, surveys, etc., including web-resources). Scientometrical analytical services.
- The work of competition committees and sponsoring agencies. An expert examination in venture and other investment funds, the work of councils and groups of experts. An analysis of applications, information cards, competition documentation, expert examination rules and conditions. Normalizing and metrological control of technical

documentation. An analysis of project design documentation, standards, norms, rules, regulations, manuals.

- Patenting, novelty expert examination. Materials selection for patent investigations. A documentation analysis of intellectual property objects, license contracts. Technological development forecasting.

- A content analysis of document texts in sociological surveys.
- Staff recruitment at enterprises and in organisations. An analysis of applicants' resumes vacancy descriptions.

- Rubrication of personal digital documents. PC text document (files) classification and grouping.

It should be noted that the project made some patent research which aim was to find analogs of the system designed and establish its novelty. At the moment of the research result report preparation any data of direct project analogs or its components realized are not discovered. The search of the FGBU Federal Institute of Industrial Property's document database did not show any matches of the project results with technologies recorded in official publications of the titles of protection.

Conclusions. One of the R&D management reference models include a competitive analysis and technological development forecasting based on scientometrical analytical services and semantical systems of business valuable information search. A relatively new world trend is evident: an effective use of global knowledge dataflow. Widely-known solutions (illum8, NetBase, Orbit) may be examples. With all the differences of these and similar systems the major search pattern is selecting materials on demand, highlighting key concepts in the desired area and grouping materials respectively, filtering and semantic result processing, generating analytical reports. In this sense, the project tasks the results of which were discussed in the article are timely and urgent, and on the appropriate level of the problem interpretation.

References

1. Ivanov, V.K., Palyukh, B.V., Sotnikov, A.N. Arkhitektura intellektual'noy sistemy informatsionnoy podderzhki innovatsiy v nauke i obrazovanii // Programmnyye produkty i sistemy. – Tver', 2013. – № 4. – P. 197-202.
2. Ivanov, V.K., Vinogradova, N.V. Evristicheskiy algoritm fil'tratsii i semanticheskogo ranzhirovaniya rezul'tatov poiska dokumentov // Vestnik Tverskogo gosudarstvennogo universiteta: nauchnyy zhurnal: Seriya "Prikladnaya matematika" / № 41. - Tver. gos. un - t. –Tver', 2013. – № 3. – P. 97-107.
3. Ivanov, V.K. Osnovnyye shagi geneticheskogo algoritma fil'tratsii rezul'tatov tematicheskogo poiska dokumentov: stat'ya // Innovatsii v nauke. – Novosibirsk, 2013. – № 25. – P. 8-15.
4. Ivanov, V.K., Mironov, V.I. Osobennosti analiza skhodstva dokumentov v razlichnykh kontekstakh zaimstvovaniya pri podgotovke tekstovykh materialov: stat'ya // Otsenka kachestva vysshego professional'nogo obrazovaniya s uchetom trebovaniy FGOS i professional'nykh standartov: materialy dokladov zaoch. nauch.-prakt. konferentsii. – Tver', 2013. – P. 19-26.
5. Palyukh, B.V., Yegereva, I.A. Mnogoshagovaya sistema poiska al'ternativ v informatsionnom kataloge // Programmnyye produkty i sistemy. – Tver', 2013. – № 3. – P. 291-295.
6. Paliukh, B., Egereva, I. Multistep algorithm of alternatives search in an information catalogue // 10th International Conference on Interactive Systems: Problems of Human-Computer Interaction. – Collection of scientific papers. – Ulyanovsk : USTU, 2013. – P. 129-132.

MATHEMATICAL MODELING OF THE HEMISPHERICAL RESONATOR GYROSCOPE

Starostin I.E., *Khalyutina O.S.

*Moscow, Experimental Studio "NaukaSoft"; *Moscow, MIEM HSE*

In this paper mathematical modeling of hemispheric resonant gyroscope with the help of theory of elasticity is considered. The thickness of the hemisphere can be arbitrary. Displays the system of equations with distributed parameters describing the physical processes in gyroscope, and the temperature of the gyroscope is assumed to be constant.

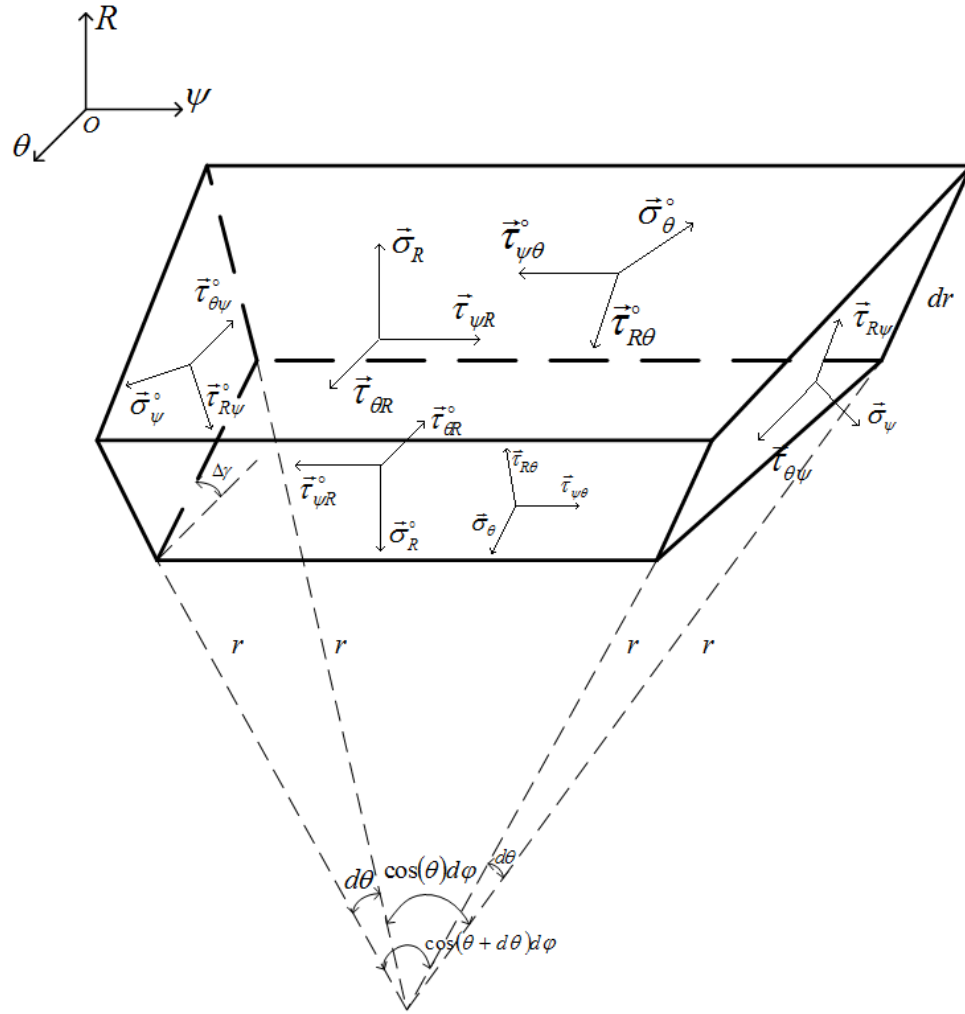
Keywords: hemispherical resonator gyroscope, system of equations in distributed parameters

Currently the sensing elements of navigation systems there are more rigid requirements. It requires constant improvement of processing sensor (for example, gyroscopes) on parameters such as accuracy, resource, weight and size characteristics, cost, etc. In this regard, in domestic and foreign instrument-making along with the improvement of designs and manufacturing technologies of work on creation of devices running on new physical principles. One of the most modern and advanced representatives of devices of this type is hemispherical resonant gyroscope (HRG) principle of operation is based on the inert properties of elastic waves, excited in rotary axisymmetric shells. In the result of the action of the Coriolis happens precession of standing waves from the shell, and in the inertial space [1].

HRG benefits are [1]:

- high accuracy ;
- low sensitivity to linear loads;
- a small start-up time, defined electronics;
- resistance to radiation;
- no moving parts in the design;
- low power consumption;
- the opportunity to work with interruptions in the power supply due to the large time constant.

In the domestic and foreign press published dozens of articles and several monographs devoted to questions of design wave solid-state gyroscopic systems [1-3]. Among other problems, special attention was paid to the methods of mathematical modeling of physical processes in these systems [1-3]. There are currently ring model and shell model of the resonator [1, 2]. However, the models, as can be seen from [1, 2], does not consider the actual wall thickness that does not allow for the distribution of fluctuations along the wall thickness. Therefore, in this paper methods of the theory of elasticity of the developed mathematical model of the distributed coordinates hemispherical resonant gyroscope, which represents a system of partial differential equations. As a gyroscope is a hemispherical shape, a system of ordinary differential equations it is expedient to obtain in spherical coordinates.



$$\begin{aligned}
 \sigma_R &= \sigma_R^\circ + \frac{\partial \sigma_R}{\partial r} dr & \tau_{R\theta} &= \tau_{R\theta}^\circ + \frac{\partial \tau_{R\theta}}{\partial \theta} d\theta & \tau_{R\psi} &= \tau_{R\psi}^\circ + \frac{\partial \tau_{R\psi}}{\partial \varphi} d\varphi \\
 \tau_{\theta R} &= \tau_{\theta R}^\circ + \frac{\partial \tau_{\theta R}}{\partial r} dr & \sigma_\theta &= \sigma_\theta^\circ + \frac{\partial \sigma_\theta}{\partial \theta} d\theta & \tau_{\theta\psi} &= \tau_{\theta\psi}^\circ + \frac{\partial \tau_{\theta\psi}}{\partial \varphi} d\varphi \\
 \tau_{\psi R} &= \tau_{\psi R}^\circ + \frac{\partial \tau_{\psi R}}{\partial r} dr & \tau_{\psi\theta} &= \tau_{\psi\theta}^\circ + \frac{\partial \tau_{\psi\theta}}{\partial \theta} d\theta & \sigma_\psi &= \sigma_\psi^\circ + \frac{\partial \sigma_\psi}{\partial \varphi} d\varphi
 \end{aligned}$$

Figure 1. Infinitely small element of a wave solid-state gyroscopic

Consider the motion of an element of the environment in spherical coordinates (see Fig. 1). The amount of this element is the criterion of Knudsen. In planes perpendicular axes \vec{R} and $\vec{\Theta}$, the point of application of the relevant voltage (normal and tangential) offset from the center in order to indicate not merged. Actually the point of application of these stresses in the centre of the corresponding surfaces.

In accordance with the second law of Newton in the projections on the coordinate axes and after the transition to private spatial derivatives have:

$$\rho \frac{dv_R}{dt} = \rho g_R + \frac{\partial \sigma_R}{\partial r} + \frac{1}{r} \frac{\partial \tau_{R\Theta}}{\partial \theta} + \frac{1}{r \cos(\theta)} \frac{\partial \tau_{R\psi}}{\partial \varphi} + \frac{2\sigma_R - \sigma_\Theta - \sigma_\psi}{r} - \frac{\tau_{R\Theta} \sin(\theta)}{r \cos(\theta)}, \quad (1)$$

$$\rho \frac{dv_{\Theta}}{dt} = \rho g_{\Theta} + \frac{\partial \tau_{\Theta R}}{\partial r} + \frac{1}{r} \frac{\partial \sigma_{\Theta}}{\partial \theta} + \frac{1}{r \cos(\theta)} \frac{\partial \tau_{\Theta \Psi}}{\partial \varphi} + \frac{3\tau_{\Theta R}}{r} + \frac{\sigma_{\Psi}}{r} \sin(\theta) - \frac{\sigma_{\Theta}}{r} \frac{\sin(\theta)}{\cos(\theta)}, \quad (2)$$

$$\rho \frac{dv_{\Psi}}{dt} = \rho g_{\Psi} + \frac{\partial \tau_{\Psi R}}{\partial r} + \frac{1}{r} \frac{\partial \tau_{\Psi \Theta}}{\partial \theta} + \frac{1}{r \cos(\theta)} \frac{\partial \sigma_{\Psi}}{\partial \varphi} + \frac{3\tau_{\Psi R}}{r} - \frac{\tau_{\Psi \Theta} \sin(\theta)}{r \cos(\theta)}, \quad (3)$$

where $v_R, v_{\Theta}, v_{\Psi}$ - projection of the velocity element of the environment on the axis $\vec{R}, \vec{\Theta}, \vec{\Psi}$ accordingly; $g_R, g_{\Theta}, g_{\Psi}$ - projection unit mass forces (including the forces of inertia) on the axis $\vec{R}, \vec{\Theta}, \vec{\Psi}$; ρ - density of the element of the environment. Specific mass inertia forces have the form:

$$g_R = (\omega^2 r \cos(\theta) - 2v_{\Psi} \omega) \cos(\theta) - g \sin(\theta), \quad (4)$$

$$g_{\Theta} = (-\omega^2 r \cos(\theta) + 2\omega v_{\Psi}) \sin(\theta) - g \cos(\theta), \quad (5)$$

$$g_{\Psi} = \frac{d\omega}{dt} r \cos(\theta) + 2\omega(v_R \cos(\theta) - v_{\Theta} \sin(\theta)). \quad (6)$$

Normal and shear stresses are the sum of normal and tangential friction and elasticity:

$$\sigma_R = \sigma_R^y + \sigma_R^{mp}, \quad \sigma_{\Theta} = \sigma_{\Theta}^y + \sigma_{\Theta}^{mp}, \quad \sigma_{\Psi} = \sigma_{\Psi}^y + \sigma_{\Psi}^{mp}, \quad (7)$$

$$\tau_{R\Theta} = \tau_{R\Theta}^y + \tau_{R\Theta}^{mp}, \quad \tau_{R\Psi} = \tau_{R\Psi}^y + \tau_{R\Psi}^{mp}, \quad \tau_{\Psi\Theta} = \tau_{\Psi\Theta}^y + \tau_{\Psi\Theta}^{mp}, \quad (8)$$

$$\tau_{R\Theta} = \tau_{R\Theta}^y + \tau_{R\Theta}^{mp}, \quad \tau_{\Psi R} = \tau_{\Psi R}^y + \tau_{\Psi R}^{mp}, \quad \tau_{\Theta\Psi} = \tau_{\Theta\Psi}^y + \tau_{\Theta\Psi}^{mp}. \quad (9)$$

Hence, by (1) - (9) we have:

$$\begin{aligned} \rho \frac{dv_R}{dt} = & \rho(\omega^2 r \cos(\theta) - 2v_{\Psi} \omega) \cos(\theta) - \rho g \sin(\theta) + \frac{\partial \sigma_R^y}{\partial r} + \frac{\partial \sigma_R^{mp}}{\partial r} + \frac{1}{r} \left(\frac{\partial \tau_{R\Theta}^y}{\partial \theta} + \frac{\partial \tau_{R\Theta}^{mp}}{\partial \theta} \right) + \\ & + \frac{1}{r \cos(\theta)} \left(\frac{\partial \tau_{R\Psi}^y}{\partial \varphi} + \frac{\partial \tau_{R\Psi}^{mp}}{\partial \varphi} \right) + \frac{2\sigma_R^y - \sigma_{\Theta}^y - \sigma_{\Psi}^y}{r} + \frac{2\sigma_R^{mp} - \sigma_{\Theta}^{mp} - \sigma_{\Psi}^{mp}}{r} - \frac{(\tau_{R\Theta}^y + \tau_{R\Theta}^{mp}) \sin(\theta)}{r \cos(\theta)}, \end{aligned} \quad (7)$$

$$\begin{aligned} \rho \frac{dv_{\Theta}}{dt} = & \rho(-\omega^2 r \cos(\theta) + 2\omega v_{\Psi}) \sin(\theta) - \rho g \cos(\theta) + \frac{\partial \tau_{\Theta R}^y}{\partial r} + \frac{\partial \tau_{\Theta R}^{mp}}{\partial r} + \frac{1}{r} \left(\frac{\partial \sigma_{\Theta}^y}{\partial \theta} + \frac{\partial \sigma_{\Theta}^{mp}}{\partial \theta} \right) + \\ & + \frac{1}{r \cos(\theta)} \left(\frac{\partial \tau_{\Theta\Psi}^y}{\partial \varphi} + \frac{\partial \tau_{\Theta\Psi}^{mp}}{\partial \varphi} \right) + \frac{3\tau_{\Theta R}^y}{r} + \frac{3\tau_{\Theta R}^{mp}}{r} + \left(\frac{\sigma_{\Psi}^y}{r} + \frac{\sigma_{\Psi}^{mp}}{r} \right) \sin(\theta) - \left(\frac{\sigma_{\Theta}^y}{r} + \frac{\sigma_{\Theta}^{mp}}{r} \right) \frac{\sin(\theta)}{\cos(\theta)}, \end{aligned} \quad (8)$$

$$\begin{aligned} \rho \frac{dv_{\Psi}}{dt} = & \rho \left(\frac{d\omega}{dt} r \cos(\theta) + 2\omega(v_R \cos(\theta) - v_{\Theta} \sin(\theta)) \right) + \frac{3(\tau_{\Psi R}^y + \tau_{\Psi R}^{mp})}{r} - \frac{(\tau_{\Psi\Theta}^y + \tau_{\Psi\Theta}^{mp}) \sin(\theta)}{r \cos(\theta)} + \\ & + \frac{\partial \tau_{\Psi R}^y}{\partial r} + \frac{\partial \tau_{\Psi R}^{mp}}{\partial r} + \frac{1}{r} \left(\frac{\partial \tau_{\Psi\Theta}^y}{\partial \theta} + \frac{\partial \tau_{\Psi\Theta}^{mp}}{\partial \theta} \right) + \frac{1}{r \cos(\theta)} \left(\frac{\partial \sigma_{\Psi}^y}{\partial \varphi} + \frac{\partial \sigma_{\Psi}^{mp}}{\partial \varphi} \right). \end{aligned} \quad (9)$$

For tensions and their components is the law of pairs of tangential tensions:

$$\tau_{R\Psi}^y = \tau_{\Psi R}^y, \quad \tau_{\Theta\Psi}^y = \tau_{\Psi\Theta}^y, \quad \tau_{R\Theta}^y = \tau_{\Theta R}^y, \quad (10)$$

$$\tau_{R\Psi}^{mp} = \tau_{\Psi R}^{mp}, \quad \tau_{\Theta\Psi}^{mp} = \tau_{\Psi\Theta}^{mp}, \quad \tau_{R\Theta}^{mp} = \tau_{\Theta R}^{mp}. \quad (11)$$

The relationship between the displacements element of the environment and speeds element has the form:

$$v_R = \frac{dS_R}{dt}, \quad v_{\Theta} = \frac{dS_{\Theta}}{dt}, \quad v_{\Psi} = \frac{dS_{\Psi}}{dt}, \quad (12)$$

where $S_R, S_{\Theta}, S_{\Psi}$ - проекции смещения элемента среды на оси $\vec{R}, \vec{\Theta}, \vec{\Psi}$ соответственно.

Consider now the laws of elasticity and friction. Components of elasticity are determined by the displacements. In the general case of anisotropic these components take the form [4]:

$$\sigma_R^y = E_R^n (\varepsilon_R + \mu_{R,\Theta} \varepsilon_\Theta + \mu_{R,\Psi} \varepsilon_\Psi) + E_{R,R\Theta}^\gamma \gamma_{R\Theta} + E_{R,R\Psi}^\gamma \gamma_{R\Psi} + E_{R,\Psi\Theta}^\gamma \gamma_{\Psi\Theta}, \quad (13)$$

$$\sigma_\Theta^y = E_\Theta^n (\mu_{\Theta,R} \varepsilon_R + \varepsilon_\Theta + \mu_{\Theta,\Psi} \varepsilon_\Psi) + E_{\Theta,R\Theta}^\gamma \gamma_{R\Theta} + E_{\Theta,R\Psi}^\gamma \gamma_{R\Psi} + E_{\Theta,\Psi\Theta}^\gamma \gamma_{\Psi\Theta}, \quad (14)$$

$$\sigma_\Psi^y = E_\Psi^n (\mu_{\Psi,R} \varepsilon_R + \mu_{\Psi,\Theta} \varepsilon_\Theta + \varepsilon_\Psi) + E_{\Psi,R\Theta}^\gamma \gamma_{R\Theta} + E_{\Psi,R\Psi}^\gamma \gamma_{R\Psi} + E_{\Psi,\Psi\Theta}^\gamma \gamma_{\Psi\Theta}, \quad (15)$$

$$\tau_{R\Theta}^y = E_{R\Theta,R}^\varepsilon \varepsilon_R + E_{R\Theta,\Theta}^\varepsilon \varepsilon_\Theta + E_{R\Theta,\Psi}^\varepsilon \varepsilon_\Psi + E_{R\Theta}^\tau \gamma_{R\Theta} + E_{R\Theta,R\Psi}^\gamma \gamma_{R\Psi} + E_{R\Theta,\Psi\Theta}^\gamma \gamma_{\Psi\Theta}, \quad (16)$$

$$\tau_{R\Psi}^y = E_{R\Psi,R}^\varepsilon \varepsilon_R + E_{R\Psi,\Theta}^\varepsilon \varepsilon_\Theta + E_{R\Psi,\Psi}^\varepsilon \varepsilon_\Psi + E_{R\Psi,R\Theta}^\gamma \gamma_{R\Theta} + E_{R\Psi}^\tau \gamma_{R\Psi} + E_{R\Psi,\Psi\Theta}^\gamma \gamma_{\Psi\Theta}, \quad (17)$$

$$\tau_{\Psi\Theta}^y = E_{\Psi\Theta,R}^\varepsilon \varepsilon_R + E_{\Psi\Theta,\Theta}^\varepsilon \varepsilon_\Theta + E_{\Psi\Theta,\Psi}^\varepsilon \varepsilon_\Psi + E_{\Psi\Theta,R\Theta}^\gamma \gamma_{R\Theta} + E_{\Psi\Theta,R\Psi}^\gamma \gamma_{R\Psi} + E_{\Psi\Theta}^\tau \gamma_{\Psi\Theta}, \quad (18)$$

where ε_R , ε_Θ , ε_Ψ - deformation of stretching/compression along the axes \vec{R} , $\vec{\Theta}$, $\vec{\Psi}$ accordingly; $\gamma_{R\Theta}$, $\gamma_{R\Psi}$, $\gamma_{\Psi\Theta}$ - angular deformation in planes $\vec{R}\vec{\Theta}$, $\vec{R}\vec{\Psi}$, $\vec{\Psi}\vec{\Theta}$ accordingly; E_R^n , E_Θ^n , E_Ψ^n - Young's moduls of tension/compression along the axes \vec{R} , $\vec{\Theta}$, $\vec{\Psi}$ accordingly; $\mu_{R,\Theta}$, $\mu_{R,\Psi}$, $\mu_{\Theta,R}$, $\mu_{\Theta,\Psi}$, $\mu_{\Psi,R}$, $\mu_{\Psi,\Theta}$ - Poisson's ratios supply appropriate tensions on the corresponding deformation of stretching/compression; $E_{R,R\Theta}^\gamma$, $E_{R,R\Psi}^\gamma$, $E_{R,\Psi\Theta}^\gamma$, $E_{\Theta,R\Theta}^\gamma$, $E_{\Theta,R\Psi}^\gamma$, $E_{\Theta,\Psi\Theta}^\gamma$, $E_{\Psi,R\Theta}^\gamma$, $E_{\Psi,R\Psi}^\gamma$, $E_{\Psi,\Psi\Theta}^\gamma$ - Young's moduls of relevant normal tension component in respect of the corresponding angular deformations; $E_{R\Theta}^\tau$, $E_{R\Psi}^\tau$, $E_{\Psi\Theta}^\tau$ - modules shift in planes $\vec{R}\vec{\Theta}$, $\vec{R}\vec{\Psi}$, $\vec{\Psi}\vec{\Theta}$ accordingly; the rest E are modules shift relevant tangential stresses on the corresponding angular and linear deformations. Deformation of stretching/compression and shear deformation have the form [4]:

$$\varepsilon_R = \frac{\partial S_R}{\partial r}, \quad \varepsilon_\Theta = \frac{1}{r} \frac{\partial S_\Theta}{\partial \theta}, \quad \varepsilon_\Psi = \frac{1}{r \cos(\theta)} \frac{\partial S_\Psi}{\partial \varphi}, \quad (19)$$

$$\gamma_{R\Theta} = \frac{1}{r} \frac{\partial S_R}{\partial \theta} + \frac{\partial S_\Theta}{\partial r}, \quad \gamma_{R\Psi} = \frac{1}{r \cos(\theta)} \frac{\partial S_R}{\partial \varphi} + \frac{\partial S_\Psi}{\partial r}, \quad \gamma_{\Psi\Theta} = \frac{1}{r} \frac{\partial S_\Psi}{\partial \theta} + \frac{1}{r \cos(\theta)} \frac{\partial S_\Theta}{\partial \varphi}. \quad (20)$$

According to (19), (20) the system of equations (13) - (18) takes the form:

$$\begin{aligned} \sigma_R^y = & E_R^n \left(\frac{\partial S_R}{\partial r} + \mu_{R,\Theta} \frac{1}{r} \frac{\partial S_\Theta}{\partial \theta} + \mu_{R,\Psi} \frac{1}{r \cos(\theta)} \frac{\partial S_\Psi}{\partial \varphi} \right) + E_{R,R\Theta}^\gamma \left(\frac{1}{r} \frac{\partial S_R}{\partial \theta} + \frac{\partial S_\Theta}{\partial r} \right) + \\ & + E_{R,R\Psi}^\gamma \left(\frac{1}{r \cos(\theta)} \frac{\partial S_R}{\partial \varphi} + \frac{\partial S_\Psi}{\partial r} \right) + E_{R,\Psi\Theta}^\gamma \left(\frac{1}{r} \frac{\partial S_\Psi}{\partial \theta} + \frac{1}{r \cos(\theta)} \frac{\partial S_\Theta}{\partial \varphi} \right), \end{aligned} \quad (21)$$

$$\begin{aligned} \sigma_\Theta^y = & E_\Theta^n \left(\mu_{\Theta,R} \frac{\partial S_R}{\partial r} + \frac{1}{r} \frac{\partial S_\Theta}{\partial \theta} + \mu_{\Theta,\Psi} \frac{1}{r \cos(\theta)} \frac{\partial S_\Psi}{\partial \varphi} \right) + E_{\Theta,R\Theta}^\gamma \left(\frac{1}{r} \frac{\partial S_R}{\partial \theta} + \frac{\partial S_\Theta}{\partial r} \right) + \\ & + E_{\Theta,R\Psi}^\gamma \left(\frac{1}{r \cos(\theta)} \frac{\partial S_R}{\partial \varphi} + \frac{\partial S_\Psi}{\partial r} \right) + E_{\Theta,\Psi\Theta}^\gamma \left(\frac{1}{r} \frac{\partial S_\Psi}{\partial \theta} + \frac{1}{r \cos(\theta)} \frac{\partial S_\Theta}{\partial \varphi} \right), \end{aligned} \quad (22)$$

$$\begin{aligned} \sigma_\Psi^y = & E_\Psi^n \left(\mu_{\Psi,R} \frac{\partial S_R}{\partial r} + \mu_{\Psi,\Theta} \frac{1}{r} \frac{\partial S_\Theta}{\partial \theta} + \frac{1}{r \cos(\theta)} \frac{\partial S_\Psi}{\partial \varphi} \right) + E_{\Psi,R\Theta}^\gamma \left(\frac{1}{r} \frac{\partial S_R}{\partial \theta} + \frac{\partial S_\Theta}{\partial r} \right) + \\ & + E_{\Psi,R\Psi}^\gamma \left(\frac{1}{r \cos(\theta)} \frac{\partial S_R}{\partial \varphi} + \frac{\partial S_\Psi}{\partial r} \right) + E_{\Psi,\Psi\Theta}^\gamma \left(\frac{1}{r} \frac{\partial S_\Psi}{\partial \theta} + \frac{1}{r \cos(\theta)} \frac{\partial S_\Theta}{\partial \varphi} \right), \end{aligned} \quad (23)$$

$$\begin{aligned}
 \tau_{R\Theta}^y &= E_{R\Theta,R}^\varepsilon \frac{\partial S_R}{\partial r} + E_{R\Theta,\Theta}^\varepsilon \frac{1}{r} \frac{\partial S_\Theta}{\partial \theta} + E_{R\Theta,\Psi}^\varepsilon \frac{1}{r \cos(\theta)} \frac{\partial S_\Psi}{\partial \varphi} + E_{R\Theta}^\tau \left(\frac{1}{r} \frac{\partial S_R}{\partial \theta} + \frac{\partial S_\Theta}{\partial r} \right) + \\
 &+ E_{R\Theta,R\Psi}^\gamma \left(\frac{1}{r \cos(\theta)} \frac{\partial S_R}{\partial \varphi} + \frac{\partial S_\Psi}{\partial r} \right) + E_{R\Theta,\Psi\Theta}^\gamma \left(\frac{1}{r} \frac{\partial S_\Psi}{\partial \theta} + \frac{1}{r \cos(\theta)} \frac{\partial S_\Theta}{\partial \varphi} \right), \\
 \tau_{R\Psi}^y &= E_{R\Psi,R}^\varepsilon \frac{\partial S_R}{\partial r} + E_{R\Psi,\Theta}^\varepsilon \frac{1}{r} \frac{\partial S_\Theta}{\partial \theta} + E_{R\Psi,\Psi}^\varepsilon \frac{1}{r \cos(\theta)} \frac{\partial S_\Psi}{\partial \varphi} + E_{R\Psi,R\Theta}^\gamma \left(\frac{1}{r} \frac{\partial S_R}{\partial \theta} + \frac{\partial S_\Theta}{\partial r} \right) + \\
 &+ E_{R\Psi}^\tau \left(\frac{1}{r \cos(\theta)} \frac{\partial S_R}{\partial \varphi} + \frac{\partial S_\Psi}{\partial r} \right) + E_{R\Psi,\Psi\Theta}^\gamma \left(\frac{1}{r} \frac{\partial S_\Psi}{\partial \theta} + \frac{1}{r \cos(\theta)} \frac{\partial S_\Theta}{\partial \varphi} \right),
 \end{aligned} \tag{24}$$

$$\begin{aligned}
 \tau_{\Psi\Theta}^y &= E_{\Psi\Theta,R}^\varepsilon \frac{\partial S_R}{\partial r} + E_{\Psi\Theta,\Theta}^\varepsilon \frac{1}{r} \frac{\partial S_\Theta}{\partial \theta} + E_{\Psi\Theta,\Psi}^\varepsilon \frac{1}{r \cos(\theta)} \frac{\partial S_\Psi}{\partial \varphi} + E_{\Psi\Theta,R\Theta}^\gamma \left(\frac{1}{r} \frac{\partial S_R}{\partial \theta} + \frac{\partial S_\Theta}{\partial r} \right) + \\
 &+ E_{\Psi\Theta,R\Psi}^\gamma \left(\frac{1}{r \cos(\theta)} \frac{\partial S_R}{\partial \varphi} + \frac{\partial S_\Psi}{\partial r} \right) + E_{\Psi\Theta}^\tau \left(\frac{1}{r} \frac{\partial S_\Psi}{\partial \theta} + \frac{1}{r \cos(\theta)} \frac{\partial S_\Theta}{\partial \varphi} \right).
 \end{aligned} \tag{26}$$

In the case of an isotropic medium, by

$$E_R^n = E_\Theta^n = E_\Psi^n = E^n, \quad E_{R\Theta}^\tau = E_{R\Psi}^\tau = E_{\Psi\Theta}^\tau = E^\tau,$$

$$\mu_{R,\Theta} = \mu_{R,\Psi} = \mu_{\Theta,R} = \mu_{\Theta,\Psi} = \mu_{\Psi,R} = \mu_{\Psi,\Theta} = \mu$$

and the remaining coefficients equal to zero for an isotropic medium, we have according to (21) - (26):

$$\sigma_R^y = E^n \left(\frac{\partial S_R}{\partial r} + \mu \left(\frac{1}{r} \frac{\partial S_\Theta}{\partial \theta} + \frac{1}{r \cos(\theta)} \frac{\partial S_\Psi}{\partial \varphi} \right) \right), \tag{27}$$

$$\sigma_\Theta^y = E^n \left(\frac{1}{r} \frac{\partial S_\Theta}{\partial \theta} + \mu \left(\frac{\partial S_R}{\partial r} + \frac{1}{r \cos(\theta)} \frac{\partial S_\Psi}{\partial \varphi} \right) \right), \tag{28}$$

$$\sigma_\Psi^y = E^n \left(\frac{1}{r \cos(\theta)} \frac{\partial S_\Psi}{\partial \varphi} + \mu \left(\frac{\partial S_R}{\partial r} + \frac{1}{r} \frac{\partial S_\Theta}{\partial \theta} \right) \right), \tag{29}$$

$$\tau_{R\Theta}^y = E^\tau \left(\frac{1}{r} \frac{\partial S_R}{\partial \theta} + \frac{\partial S_\Theta}{\partial r} \right), \tag{30}$$

$$\tau_{R\Psi}^y = E^\tau \left(\frac{1}{r \cos(\theta)} \frac{\partial S_R}{\partial \varphi} + \frac{\partial S_\Psi}{\partial r} \right), \tag{31}$$

$$\tau_{\Psi\Theta}^y = E^\tau \left(\frac{1}{r} \frac{\partial S_\Psi}{\partial \theta} + \frac{1}{r \cos(\theta)} \frac{\partial S_\Theta}{\partial \varphi} \right). \tag{32}$$

Similarly (21) - (26) we obtain for the components of the friction in the general case of an anisotropic medium:

$$\begin{aligned}
 \sigma_R^{mp} &= G_R^n \left(\frac{\partial v_R}{\partial r} + \mu_{R,\Theta}^* \frac{1}{r} \frac{\partial v_\Theta}{\partial \theta} + \mu_{R,\Psi}^* \frac{1}{r \cos(\theta)} \frac{\partial v_\Psi}{\partial \varphi} \right) + \\
 &+ G_{R,R\Theta}^\gamma \left(\frac{1}{r} \frac{\partial v_R}{\partial \theta} + \frac{\partial v_\Theta}{\partial r} \right) + G_{R,R\Psi}^\gamma \left(\frac{1}{r \cos(\theta)} \frac{\partial v_R}{\partial \varphi} + \frac{\partial v_\Psi}{\partial r} \right) + G_{R,\Psi\Theta}^\gamma \left(\frac{1}{r} \frac{\partial v_\Psi}{\partial \theta} + \frac{1}{r \cos(\theta)} \frac{\partial v_\Theta}{\partial \varphi} \right),
 \end{aligned} \tag{33}$$

$$\begin{aligned}\sigma_{\Theta}^{mp} = & G_{\Theta}^n \left(\mu_{\Theta,R}^* \frac{\partial v_R}{\partial r} + \frac{1}{r} \frac{\partial v_{\Theta}}{\partial \theta} + \mu_{\Theta,\Psi}^* \frac{1}{r \cos(\theta)} \frac{\partial v_{\Psi}}{\partial \varphi} \right) + \\ & + G_{\Theta,R\Theta}^{\gamma} \left(\frac{1}{r} \frac{\partial v_R}{\partial \theta} + \frac{\partial v_{\Theta}}{\partial r} \right) + G_{\Theta,R\Psi}^{\gamma} \left(\frac{1}{r \cos(\theta)} \frac{\partial v_R}{\partial \varphi} + \frac{\partial v_{\Psi}}{\partial r} \right) + G_{\Theta,\Psi\Theta}^{\gamma} \left(\frac{1}{r} \frac{\partial v_{\Psi}}{\partial \theta} + \frac{1}{r \cos(\theta)} \frac{\partial v_{\Theta}}{\partial \varphi} \right),\end{aligned}\quad (34)$$

$$\begin{aligned}\sigma_{\Psi}^{mp} = & G_{\Psi}^n \left(\mu_{\Psi,R}^* \frac{\partial v_R}{\partial r} + \mu_{\Psi,\Theta}^* \frac{1}{r} \frac{\partial v_{\Theta}}{\partial \theta} + \frac{1}{r \cos(\theta)} \frac{\partial v_{\Psi}}{\partial \varphi} \right) + \\ & + G_{\Psi,R\Theta}^{\gamma} \left(\frac{1}{r} \frac{\partial v_R}{\partial \theta} + \frac{\partial v_{\Theta}}{\partial r} \right) + G_{\Psi,R\Psi}^{\gamma} \left(\frac{1}{r \cos(\theta)} \frac{\partial v_R}{\partial \varphi} + \frac{\partial v_{\Psi}}{\partial r} \right) + G_{\Psi,\Psi\Theta}^{\gamma} \left(\frac{1}{r} \frac{\partial v_{\Psi}}{\partial \theta} + \frac{1}{r \cos(\theta)} \frac{\partial v_{\Theta}}{\partial \varphi} \right),\end{aligned}\quad (35)$$

$$\begin{aligned}\tau_{R\Theta}^{mp} = & G_{R\Theta,R}^{\varepsilon} \frac{\partial v_R}{\partial r} + G_{R\Theta,\Theta}^{\varepsilon} \frac{1}{r} \frac{\partial v_{\Theta}}{\partial \theta} + G_{R\Theta,\Psi}^{\varepsilon} \frac{1}{r \cos(\theta)} \frac{\partial v_{\Psi}}{\partial \varphi} + \\ & + G_{R\Theta}^{\tau} \left(\frac{1}{r} \frac{\partial v_R}{\partial \theta} + \frac{\partial v_{\Theta}}{\partial r} \right) + G_{R\Theta,R\Psi}^{\gamma} \left(\frac{1}{r \cos(\theta)} \frac{\partial v_R}{\partial \varphi} + \frac{\partial v_{\Psi}}{\partial r} \right) + G_{R\Theta,\Psi\Theta}^{\gamma} \left(\frac{1}{r} \frac{\partial v_{\Psi}}{\partial \theta} + \frac{1}{r \cos(\theta)} \frac{\partial v_{\Theta}}{\partial \varphi} \right),\end{aligned}\quad (36)$$

$$\begin{aligned}\tau_{R\Psi}^{mp} = & G_{R\Psi,R}^{\varepsilon} \frac{\partial v_R}{\partial r} + G_{R\Psi,\Theta}^{\varepsilon} \frac{1}{r} \frac{\partial v_{\Theta}}{\partial \theta} + G_{R\Psi,\Psi}^{\varepsilon} \frac{1}{r \cos(\theta)} \frac{\partial v_{\Psi}}{\partial \varphi} + \\ & + G_{R\Psi,R\Theta}^{\gamma} \left(\frac{1}{r} \frac{\partial v_R}{\partial \theta} + \frac{\partial v_{\Theta}}{\partial r} \right) + G_{R\Psi}^{\tau} \left(\frac{1}{r \cos(\theta)} \frac{\partial v_R}{\partial \varphi} + \frac{\partial v_{\Psi}}{\partial r} \right) + G_{R\Psi,\Psi\Theta}^{\gamma} \left(\frac{1}{r} \frac{\partial v_{\Psi}}{\partial \theta} + \frac{1}{r \cos(\theta)} \frac{\partial v_{\Theta}}{\partial \varphi} \right),\end{aligned}\quad (37)$$

$$\begin{aligned}\tau_{\Psi\Theta}^{mp} = & G_{\Psi\Theta,R}^{\varepsilon} \frac{\partial v_R}{\partial r} + G_{\Psi\Theta,\Theta}^{\varepsilon} \frac{1}{r} \frac{\partial v_{\Theta}}{\partial \theta} + G_{\Psi\Theta,\Psi}^{\varepsilon} \frac{1}{r \cos(\theta)} \frac{\partial v_{\Psi}}{\partial \varphi} + \\ & + G_{\Psi\Theta,R\Theta}^{\gamma} \left(\frac{1}{r} \frac{\partial v_R}{\partial \theta} + \frac{\partial v_{\Theta}}{\partial r} \right) + G_{\Psi\Theta,R\Psi}^{\gamma} \left(\frac{1}{r \cos(\theta)} \frac{\partial v_R}{\partial \varphi} + \frac{\partial v_{\Psi}}{\partial r} \right) + G_{\Psi\Theta}^{\tau} \left(\frac{1}{r} \frac{\partial v_{\Psi}}{\partial \theta} + \frac{1}{r \cos(\theta)} \frac{\partial v_{\Theta}}{\partial \varphi} \right);\end{aligned}\quad (38)$$

and similarly for an isotropic medium (27) - (32):

$$\sigma_R^{mp} = G^n \left(\frac{\partial v_R}{\partial r} + \mu^* \left(\frac{1}{r} \frac{\partial v_{\Theta}}{\partial \theta} + \frac{1}{r \cos(\theta)} \frac{\partial v_{\Psi}}{\partial \varphi} \right) \right),\quad (39)$$

$$\sigma_{\Theta}^{mp} = G^n \left(\frac{1}{r} \frac{\partial v_{\Theta}}{\partial \theta} + \mu^* \left(\frac{\partial v_R}{\partial r} + \frac{1}{r \cos(\theta)} \frac{\partial v_{\Psi}}{\partial \varphi} \right) \right),\quad (40)$$

$$\sigma_{\Psi}^{mp} = G^n \left(\frac{1}{r \cos(\theta)} \frac{\partial v_{\Psi}}{\partial \varphi} + \mu^* \left(\frac{\partial v_R}{\partial r} + \frac{1}{r} \frac{\partial v_{\Theta}}{\partial \theta} \right) \right),\quad (41)$$

$$\tau_{R\Theta}^{mp} = G^{\tau} \left(\frac{1}{r} \frac{\partial v_R}{\partial \theta} + \frac{\partial v_{\Theta}}{\partial r} \right),\quad (42)$$

$$\tau_{R\Psi}^{mp} = G^{\tau} \left(\frac{1}{r \cos(\theta)} \frac{\partial v_R}{\partial \varphi} + \frac{\partial v_{\Psi}}{\partial r} \right),\quad (43)$$

$$\tau_{\Psi\Theta}^{mp} = G^{\tau} \left(\frac{1}{r} \frac{\partial v_{\Psi}}{\partial \theta} + \frac{1}{r \cos(\theta)} \frac{\partial v_{\Theta}}{\partial \varphi} \right).\quad (44)$$

Consider the boundary conditions. No tension inside the sphere (air friction disregarded), so entering the inner radius of the sphere $R_{\text{внутр}}$ (and outer, respectively $R_{\text{внеш}}$) can be written as:

$$\text{with } r = R_{\text{внутр}} \quad \sigma_R^y + \sigma_R^{mp} = 0, \quad \tau_{\Theta R}^y + \tau_{\Theta R}^{mp} = 0, \quad \tau_{\Psi R}^y + \tau_{\Psi R}^{mp} = 0.\quad (45)$$

tensions on the rim either, hence we have:

$$\text{with } \theta = 0 \quad \sigma_{\Theta}^y + \sigma_{\Theta}^{mp} = 0, \quad \tau_{R\Theta}^y + \tau_{R\Theta}^{mp} = 0, \quad \tau_{\Psi\Theta}^y + \tau_{\Psi\Theta}^{mp} = 0. \quad (46)$$

Consider now the outer surface of the hemisphere. On this surface affect external excitation pulses $\vec{p}_{\text{вонеш}}$ (Fig. 5). And at the point where there are glasses with leg tensions support legs σ_h , balancing gravity glasses, as well as shear tensions $\tau_h(\theta)$ perpendicular to the radius, creating a glass angular acceleration, angular velocity of glasses if changing (see Fig. 5). Hence, for the stimuli:

$$r = R_{\text{внеш}}, \quad -\theta_{\text{вонеш}} \leq \theta \leq 0, \quad \varphi \in \phi_{\text{внут}} \quad \sigma_R^y + \sigma_R^{mp} = p_{\text{вонеш}}(t), \quad \tau_{\Theta R}^y + \tau_{\Theta R}^{mp} = 0, \quad \tau_{\Psi R}^y + \tau_{\Psi R}^{mp} = 0; \quad (47)$$

$$r = R_{\text{внеш}}, \quad -\theta_{\text{вонеш}} \leq \theta \leq 0, \quad \varphi \notin \phi_{\text{внут}} \quad \sigma_R^y + \sigma_R^{mp} = 0, \quad \tau_{\Theta R}^y + \tau_{\Theta R}^{mp} = 0, \quad \tau_{\Psi R}^y + \tau_{\Psi R}^{mp} = 0; \quad (48)$$

$$r = R_{\text{внеш}}, \quad -\theta_h < \theta < -\theta_{\text{вонеш}} \quad \sigma_R^y + \sigma_R^{mp} = 0, \quad \tau_{\Theta R}^y + \tau_{\Theta R}^{mp} = 0, \quad \tau_{\Psi R}^y + \tau_{\Psi R}^{mp} = 0; \quad (49)$$

$$r = R_{\text{внеш}}, \quad \theta < -\theta_h \quad \sigma_R^y + \sigma_R^{mp} = \sigma_h, \quad \tau_{\Theta R}^y + \tau_{\Theta R}^{mp} = 0, \quad \tau_{\Psi R}^y + \tau_{\Psi R}^{mp} = \tau_h(\theta). \quad (50)$$

Let define the tension σ_h . This tension, as noted above, the force of gravity balances the gyroscope. Hence:

$$\sigma_h = \frac{m_g g}{S_h}, \quad (51)$$

where S_h - area of support legs, a m_g - mass of "glasses". We now consider the tangential tension $\tau_h(\theta)$. Let Δr - the distance from the legs to the point under consideration to the attachment surface to stem glasses, and Δr_h - radius of leg. Then the shear tension is determined in accordance with:

$$\tau_h(\Delta r) = \frac{\tau_h(\Delta r_h)}{\Delta r_h} \Delta r. \quad (52)$$

Let define M_h , - the torque produced by tangential tensions:

$$M_h = \int_0^{\Delta r_h} \tau_h(\Delta r) \cdot 2\pi \Delta r \cdot d\Delta r \cdot \Delta r = 2\pi \int_0^{\Delta r_h} \tau_h(\Delta r) \cdot (\Delta r)^2 \cdot d\Delta r;$$

hence, by (52) we have:

$$M_h = 2\pi \frac{\tau_h(\Delta r_h)}{\Delta r_h} \int_0^{\Delta r_h} (\Delta r)^3 \cdot d\Delta r = \frac{1}{2} \pi \tau_h(\Delta r_h) \cdot (\Delta r_h)^3;$$

hence by (52) we have:

$$\tau_h(\Delta r) = \frac{2M_h}{\pi \cdot (\Delta r_h)^4} \Delta r; \quad (53)$$

considering that

$$S_h = \pi \cdot (\Delta r_h)^2,$$

we have:

$$\tau_h(\Delta r) = \frac{2\pi M_h}{S_h^2} \Delta r. \quad (54)$$

According to Newton's second law for rotational motion, we have:

$$M_h = J \frac{d\omega}{dt};$$

Hence by (54) we have:

$$\tau_h(\Delta r) = \frac{2\pi J}{S_h^2} \frac{d\omega}{dt} \Delta r;$$

hence, taking into account that

$$\Delta r = R_{\text{внел}} \cos(\theta),$$

we have:

$$\tau_{\text{н}}(\theta) = \frac{2\pi J}{S_{\text{н}}^2} \frac{d\omega}{dt} R_{\text{внел}} \cos(\theta). \quad (55)$$

According to (173), (51), (55) have one of the boundary conditions completely:

$$r = R_{\text{внел}}, \theta < -\theta_{\text{н}} \quad \sigma_R^y + \sigma_R^{mp} = \frac{m_z g}{S_{\text{н}}}, \tau_{\Theta R}^y + \tau_{\Theta R}^{mp} = 0, \tau_{\Psi R}^y + \tau_{\Psi R}^{mp} = \frac{2\pi J}{S_{\text{н}}^2} \frac{d\omega}{dt} R_{\text{внел}} \cos(\theta). \quad (56)$$

Equations (7) - (12), (21) - (49), (56) are closed system of equations describing the dynamics of the hemispherical resonant gyroscope. In the specified initial conditions, external influences $p_{\text{возб}}(t)$, mass gyro, square feet, the geometric sizes of a gyroscope, modules, young's modulus, shear, similar modules for friction, the angular speed of rotation of a gyroscope system (7) - (12), (21) - (49), (56) provides the ability to predict the dynamics of fluctuations of the medium.

So, we have a closed system of equations hemispherical resonant gyroscope. In [1], the solution of system of equations in partial derivatives in the approximation of wall thickness proposed analytical techniques, with the use of atomic functions. The above system of equations can be written for a nonlinear medium. Therefore, in General case it must be solved numerically. For the numerical solution of this system you must choose a break is shown in Fig. 2. The size of an element is selected from a good approximation of conditions within this element density, elasticity modulus, friction linear dependence on the spatial coordinates. On Fig. 2A. shows the environment in the hemisphere (the final element of the environment in the General case is not necessarily equal to the thickness of the wall), and in Fig. 2B - view this split at the top.

For the numerical solution of systems of equations in partial derivatives there are two methods: the method of finite differences and finite elements method [5, 6]. Finite difference method is finite difference approximation of derivatives by space and time and intelligence thereby system of partial differential equations to the system of algebraic equations (in the case of the linearity of the system - linear system of algebraic equations) [5]. Finite element method involves the use of piecewise-analytic approximation solution [6]. For the problems of mechanics at present finite element method is used [6].

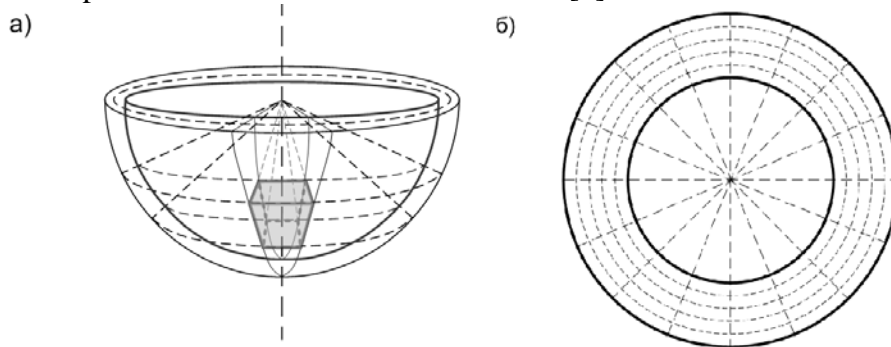


Figure 2. Split into finite elements

Indeed, for the correct solution of the system simulating the hemispherical resonatory gyroscope, the finite difference method you must select the environment, the volume of which takes the value determined by the criterion of Knudsen. Given that the gyroscope is made of quartz, mechanical properties of which are given in the table. 1, and that in this volume is the number of particles N_q about 105, define this volume ΔV , in compliance with:

$$\Delta V = \frac{MN_q}{\rho N_A}, \quad (57)$$

where N_A - Avogadro number ($N_A = 6,022 \cdot 10^{23} \text{ моль}^{-1}$); ρ - mass density; M - molar mass.

Table 1. Mechanical properties of quartz

Mass density, g/sm ³	Molar mass, g/mole
2,63	60

Hence, according to (57) and Table. 1, we have: $\Delta V = 3,788 \cdot 10^{-18} \text{ см}^3$. The volume of the region of integration V_{umm} determined, with the inner $R_{внутр}$ and outer $R_{внеш}$ gyroscope radius, according to:

$$V_{umm} = \frac{2}{3} \pi (R_{внеш}^3 - R_{внутр}^3). \quad (58)$$

Using data from the gyroscope in Table 2, we have according to (58) $V_{umm} = 33,2315 \text{ см}^3$.

Table 2. Geometrical dimensions of the hemispherical resonator gyroscope

inner radius, см	outer radius, см
3	3,5

Hence, integrating gyroscope considered finite difference methods, it is necessary to solve a system of equations, written for the number of elements $N_{эл}$, equal:

$$N_{эл} = \frac{V_{umm}}{\Delta V} = \frac{33,2315 \text{ см}^3}{3,788 \cdot 10^{-18} \text{ см}^3} = 8,773 \cdot 10^{18}.$$

I.e. must solve the system of algebraic equations about $1019 \div 1020$. Therefore, it is necessary to achieve the intended purpose finite element method [6], which was done in [1] using atomic functions. In this case the item is selected in medium suitable dimensions such that the density and Young's modulus in the range element of the medium are well approximated by a linear dependence on the spatial coordinates, and using the analytical dependence up to the unknown coefficients that change over time, we obtain a system of differential - algebraic equations for each element of the medium. This method was used in [1] using atomic functions.

References

1. Bassarab M.A., V.F. Kravchenko, Matveev, V.A. Matematicheskoe modelirovanie fizicheskikh processov v girokopii. Monographiya. - M: Radiotekhnika, 2005.
2. V.A. Matveev, Died V.I., Alekhin A.V. Proektirovanie volnovogo tverdotelnogo giroskopa. - M: Izd-vo MGTU im. AD Bauman, 1997.
3. V.F. Zhuravlev, D.M. Klimov Volnovoi tverdotelnii giroskop. - M: Nauka, 1985.
4. Lurie A.I. Teoriya uprugosti. - M: Nauka, chief editor physical Mat. lit., 1976.
5. Berezin I.S., Zhidkov E.G. Metodi vichislenii. So-2. M: GOS. ed. physical Mat. lit., 1952.
6. Bazhenov A. Kononenko, Dashenko A.F., Orobei V.F., Suryaninov N.G. Chislennye metody v mehanike. - Odessa: STANDARTY, 2005.
7. Khalutin S. P., Starostin I.E. Potencialno-potokovii metod modelirovaniya neravnovesnih processov// Izvestia of higher schools. Povolzhskiy region. Physico-mathematical Sciences. Penza: Publishing house of the University, 2012, So-2, C. 25 - 35.
8. Khalutin S. P., Tulaev M.L., Zhmurov B.V., Starostin I.E. Modelirovaniye slozhnykh elektroenergeticheskikh system letatelnykh apparatov. M: Izd-vo VUNTZ air force «VVA them. Professor N.E. Zhukovsky and Y.A. Gagarin, 2010, 188 S.

NUMERICAL SIMULATION OF THE ELECTRICAL TRANSPORT PROPERTIES OF SEMICONDUCTING ZIGZAG CARBON NANOTUBES

Sudorgin, S.A.

Volgograd, Volgograd State Technical University, VolSU

The transport characteristics of the semiconducting zigzag carbon nanotubes (electron conductivity and electron diffusion coefficient) were obtained analytically and analyzed numerically.

Keywords: carbon nanotubes, conductivity, diffusion coefficient, Anderson model

Currently, considerable interest is the generation of carbon nanostructures with specified characteristics. These structures may be applied in various fields of modern electronics, materials, chemistry and medicine [1, 2]. Transport properties of carbon nanotubes (CNTs) are one of the most important from the point of view for practical applications. Any solid surface coated with films of atoms or molecules adsorbed from the environment or left on the surface during the diffusion process under normal conditions [3]. Significant interest causes the study of the effect of atomic adsorption for different chemical elements and molecules on the electrical properties of carbon nanostructures.

The Anderson's Hamiltonian [4, 5] initially proposed for the description of the electronic states of impurity atoms in the metal alloys is often used in the theory of adsorption. This model has been successfully applied to study the adsorption of atoms on metal surfaces and semiconductors [6], the adsorption of hydrogen on the surface of graphene [7] and carbon nanotubes [8, 9]. We consider the hydrogen atomic adsorption influence for transport (conductive and diffusion) properties of “zigzag” single-walled carbon nanotubes in this paper. The interaction of hydrogen atoms, which adsorbed on the surface of carbon nanotubes is described within the framework of the periodic Anderson model. This model is well suited to describe the adsorption on the nanotubes surface, because the geometric configuration of the nanotubes determines their conductive properties. Transport coefficients (conductivity and electron diffusion coefficient) of CNT are calculated by solving the Boltzmann kinetic equation [10] in the relaxation time approximation. This technique has been successfully applied by authors for calculating the transport properties of ideal carbon nanotubes [11], graphene, bilayer graphene [12] and bilayer graphene nanoribbons [13].

State of the electrons in the crystal containing impurities in the π -electron approximation and in the nearest neighbor approximation is described in the periodic Anderson model by the effective Hamiltonian, having the following common form [5]:

$$H = \sum_{j,\Delta,\sigma} t_{\Delta} (c_{j\sigma}^+ c_{j+\Delta\sigma} + c_{j+\Delta\sigma}^+ c_{j\sigma}) + \sum_{l,\sigma} \varepsilon_{l\sigma} n_{l\sigma}^d + \sum_l U n_{l\uparrow}^d n_{l\downarrow}^d + \sum_{l,j,\sigma} (V_{lj} c_{j\sigma}^+ d_{l\sigma} + V_{lj}^* d_{l\sigma}^+ c_{j\sigma}) \quad (1)$$

where t_{Δ} is the electron hopping integral between the neighboring lattice sites of the crystal; U is the constant of the Coulomb repulsion of the impurity; $c_{j\sigma}$ and $c_{j\sigma}^+$ are the Fermi annihilation and creation operators of electrons in the crystal node j with spin σ ; $d_{j\sigma}$ and $d_{j\sigma}^+$ are the Fermi annihilation and creation operators of electrons on the impurities l with spin σ ; $n_{l\sigma}^d$ is the operator of the number of electrons on impurities l with spin σ ; $\varepsilon_{l\sigma}$ is the energy of

the electron by the impurity l with spin σ ; V_{lj} is the matrix element of hybridization of impurity electron l and atom j of the crystal.

The band structure of single-walled carbon nanotubes with adsorbed hydrogen atoms obtained using the Fourier transform of the creation and destruction operators of electrons in the crystal, and the Green function method takes the form [8, 9].

The external electric field is applied along the x axis directed along the axis of the nanotube. Method of calculation of the transport coefficients of electrons in carbon nanotubes is described in the papers [11 - 13]. Longitudinal component of the current density has the form.

$$j(x) = \sigma(\mathbf{E})\mathbf{E} + D(\mathbf{E}) \frac{\nabla_x n}{n} \quad (2)$$

The formulas for the transport coefficients of single-walled carbon nanotubes there are electrical conductivity and electron diffusion coefficient obtained for the case of a homogeneous temperature distribution and the linear approximation in the gradient magnitude of the electron concentration.

The conductivity tends to a constant value with increasing amplitude of the external electric field. The desire of the nonlinear conductivity of carbon nanotubes to a constant value is due to the limited number of charge carriers involved in the transport of electric current on the surface of the nanotubes. Fewer electrons are able to participate in the transfer of power with increasing amplitude of the electric field because other electrons already at lower values of the field by the conduction electrons become involved in the transfer of current. Adding one of the adsorbed hydrogen atom reduce the conductivity by a small amount (about $2 \cdot 10^{-3}$ S/m). Electrical conductivity decreases with the adsorption of hydrogen atom because that one of the electrons which localized in the crystallite forms a chemical bond with the impurity atom this atom is not involved in the process of charge transfer along the carbon nanotube. The electrical conductivity dependences of the external electric field magnitude for carbon nanotubes by (10,0) type, containing different concentrations of adsorbed hydrogen atoms were analyzed numerically. Increasing the number of adsorbed atoms decreases the electrical conductivity of «zigzag» carbon nanotube proportional to the amount of localized adsorption bonds. If you add one hydrogen adatom the conductivity of (10,0) carbon nanotube is reduced by 0.06%, if you add 100 adatoms the conductivity is reduced by 0.55%, the addition of 300 adatoms - 1.66%, if you add 500 adatoms the conductivity is reduced by 2.62%.

Dependence between the electron diffusion coefficient of the single-walled carbon nanotubes with adsorbed hydrogen atoms and the electric field amplitude has a pronounced non-linear. Electron diffusion coefficient initially increases and then decreases to a steady value with increasing electric field. This phenomenon is common to all systems with periodic and limited electron dispersion laws. Maximum value of the diffusion coefficient for semiconductor carbon nanotubes observed at the electric field strength of the order of $E \approx 4,8 \cdot 10^5$ V/m. If we add one adsorbed hydrogen atom, the electron diffusion coefficient reduced by 0.05%. This behavior of the electron diffusion coefficient in an external electric field is observed for different hydrogen adatom concentrations for semiconductor carbon nanotubes with different diameters when 100 adsorbed atoms added. At present one needs the study of transport and conduction properties of semiconductor carbon nanotubes with adsorbed hydrogen atoms for determining the operating parameters of nanoelectronic devices and for the miniaturization of the modern element base of microelectronics, such as transistors, and for creating new devices based on the unique properties of carbon nanotubes.

References

1. P. N., Diachkov, Electronic properties and applications of the nanotubes. BINOM, Laboratory of Knowledge, Moscow 2010, ISBN: 978-5-9963-0154-6.

2. M. K., Roko, R. S., Williams, P., Alivisatos, Nanotechnology in the near decade-Democracy. Forecast the direction of research. Mir, Moscow 2002, ISBN 5-03-003432-3.
3. L. A., Bol'shov, A. P., Napartovich, A. G., Naumovets, A. G., Fedorus, UFN, 122 (1977), 125-158.
4. P. W., Anderson, Phys. Rev., 124 (1961), 41-53.
5. A., Izyumov, I. I., Chashchin, D. S., Alekseev, The theory of strongly correlated systems. Generating functional method. Regular and Chaotic Dynamics, Moscow 2006, ISBN: 5-93972-502-3.
6. S. U., Davydov, S. V., Troshin, Solid State Physics, 49 (2007), 1508-1513.
7. S. U., Davydov, G. I., Sabirova, Letters ZHTF, 36 (2010), 77-84.
8. A. V., Pak, N. G., Lebedev, Chemical Physics, 31 (2012), 8287.
9. A. V., Pak, N. G., Lebedev, Journal of Physical Chemistry, 87 (2013) p. 994.
10. L. D., Landau, E. M., Lifshitz, Physical Kinetics. Fizmatlit, Moscow 2002, ISBN 5-9221-0125-0.
11. M. B., Belonenko, N. G., Lebedev, S. A., Sudorgin, Solid State Physics, 53 (2011), 1841-1844.
12. M. B., Belonenko, N. G., Lebedev, S. A., Sudorgin, Technical Physics, 82 (2012), 129-133.
13. S. A., Sudorgin, M. B., Belonenko, N. G., Lebedev, Physica Scripta, 87 (2013), 015602.
14. N. F., Stepanov, Quantum mechanics and quantum chemistry. Mir, Moscow 2001, ISBN 5-03-003414-5.
15. A. S., Buligin, G. M., Shmeliov, I. I., Maglevannaya, Solid State Physics, 41 (1999), 1314-1316.
16. S. A., Maksimenko, G. Ya., Slepian, Nanoelectromagnetics of low-dimensional structure. In Handbook of nanotechnology. Nanometer structure: theory, modeling, and simulation. Bellingham: SPIE press 2004 ISBN 1-86058-458-6.

ALGEBRAIC DESCRIPTION SENSOR FOR MEASUREMENTS OF LARGE MASSES

Sekashev V.A., Avdeuk O.A.

Volgograd, Volgograd State Technical University

Describes the output dependences of electric values of the measured at the example of a sensor for measuring large masses.

Keywords: automated software system, functional dependency, transition diagram.

The sensor is based on known physical transformation laws affecting physical quantity in value, directly convenient for perception by the end user or convenient for further transformations. With all the variety of sensors preferred are those that convert ultimately measured value in the electric signal [4, 5].

If to describe the work of sensors on the basis of: - measured value-output signal, and you will get:

$F(\Delta_i) = K\Delta_i$, where K – the coefficient of proportionality; Δ_i – the value of the measurand; $F(\Delta_i)$ – electric variable, dependent on the measured. If the design will be different, functional description will be different.

For construction of the automated software system to engage in the processing of a real functional converters of real physical quantities, it is necessary to build a knowledge base

about the most well-known components of the IMS with the ability to add new functional descriptions. Create soft automated system (SAS), using as a knowledge base database of all the elementary structures of IMS, presented in the form of a graph is impractical because it is necessary to take into account all the existing diversity of all measurement systems, even those that are slightly differ in structure [1-3].

Using the functional dependence of the electrical values of measured physical you can obtain the transfer function of the sensor. In the process of designing, specifying the parameter and mode of action of sensor enter the requested parameters of the existing sensor (or a component), and get a response, can the source component or not. For this assessment, you can use the scale with interest degrees of validity. For example, «Sensor <type> can ...%». Such a scale can be used for the selection of the ADC, normalizers, linearises, amplifiers, etc. Selection of components for the staging of signal processing necessary to produce taking into account the functional performance of existing component [1-3].

For example, the transformation of the mass of some real object into an electrical signal can be visualized in the following economies in the diagram:

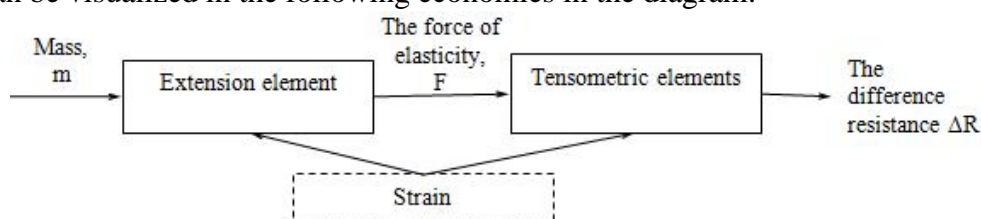


Fig. 1. Transition chart

To obtain the transfer function of the sensor weight is required extended set of physical quantities. Consider for a detailed example of the output of such dependence:

Let:

m – the measured value of the mass;

S – cross-sectional area of a torque element;

E – Young's modulus for the material element torque wrench;

ν – Poisson's ratio for the material element of dynamometric;

R_1, R_2, R_3, R_4 – resistance strain gauge cells connected by the bridge scheme Wheatstone bridge;

g – acceleration of gravity ($g \approx 9,81$);

K_{tm} – strain coefficient;

V_p – voltage sensor;

$U(m)$ – output signal.

Deformation of a cylinder or sleeve under the action of external forces can be used as a tool to measure these forces. This system, known as torque element is shown in Fig. 2. Typically, these devices are used for measurements of the masses in the range 48 ...600000 kg

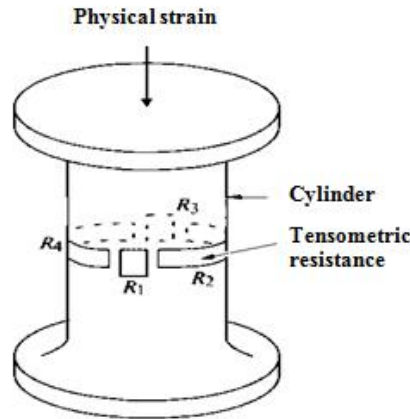
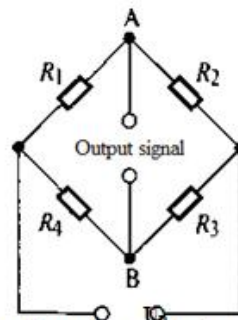


Fig. 2. Design of sensor weight


 Fig. 3. Connection scheme of strain gauge resistors
(on the basis of the bridge Uitsona DC)

Deformation of the sensor weight is often measured using a strain gauge sensor. As a rule, there are four identical тензотрa, each of which forms one of the shoulders Wheatstone bridge. If a torque wrench element is compressed, rebar strainmeters R1 and R3 are compressed. Value of deformation can be defined as $-(mg/SE)$, where m is measured mass, S - cross-sectional area of the element, and E is the Young's modulus of the material of element.

Rebar strainmeters R2 and R4 is also deformed. Their Poisson ratio for the material of this $+(vF/AE)$, where v deformation is element. Initially all rebar strainmeters have the same magnitude of resistance R . The loading of the sensor will change the resistance values, i.e.

$$R_1 = R_3 = R - \frac{RK_{tm}mg}{SE} \quad \text{and} \quad R_2 = R_4 = R - \frac{RK_{tm}vmg}{SE}.$$

There K_{tm} — strain coefficient. The difference in potential imbalances bridge can be defined as:

$$U(m) = V_p \left(\frac{R_1}{R_1 + R_4} - \frac{R_2}{R_2 + R_3} \right) = V_p \left[\frac{(1 - K_{tm}mg/SE) - (1 - K_{tm}vmg/SE)}{(1 - K_{tm}mg/SE) + (1 + K_{tm}vmg/SE)} \right]$$

$$\text{Besause } (K_{tm}mg/SE) \ll 1, \text{ the } U(m) = \frac{V_p K_{tm}mg}{2SE} (1 + v)$$

The use of four identical strain gauges eliminates the effects of temperature, since each shoulder of the bridge is exposed to peer exposed to temperature changes. If you look at this formula, we can see that $\frac{V_p K_{tm}g}{2SE} (1 + v)$ - the factor of proportionality depends on the properties of the sensor and the external environment - from the free-fall acceleration g (and it in different parts of the Earth varies on a small value, and the weightlessness, the sensor is not working), the value of the reference voltage, from the material (E and v), the square of a

deformable cross-section (S). In some cases, the value of the acceleration of gravity can be ignored when not important accuracy of the measured value. Size of a deformable cross-section of a construction parameter sensor.

References

1. Muha, Yu.P. Algebraicheskaya teoriya sinteza slozhnykh sistem: monografiya / Muha Yu.P., Avdeyuk O.A., Koroleva I.Yu.; VolgGTU. - Volgograd: RPK "Politehnik", 2003. - 320 s.
2. Muha, Yu.P. Informatsionno-izmeritelnyye sistemy s adaptivnyimi preobrazovaniyami. Upravlenie gibkostyu funktsionirovaniya: monografiya / Muha Yu.P., Avdeyuk O.A., Koroleva I.Yu.; VolgGTU. - Volgograd, 2010. - 303 s.
3. Muha, Yu.P. Teoriya i praktika sinteza upravlyayushchego i informatsionnogo obespecheniya izmeritelno - vychislitelnykh sistem: monografiya / Muha Yu.P., Avdeyuk O.A., Antonovich V.M.; VolgGTU. - Volgograd: RPK "Politehnik", 2004. - 220 s.
4. Aleynikov, A.F., Gridchin A., Tsapenko M. P. Sensors (Perspective directions of development) [Text] / Ed. by Professor M. P. Tsapenko. - Novosibirsk: Publishing house of the Novosibirsk state technical University, 2001. - 176 p.
5. Bolton, U., Pocket guide engineer-metrologist [Text] / W. Bolton. - Moscow: Publishing house «Dodeka-XXI», 2002. - 384 p.
6. Uvaysov S. U., Ivanov I. A method of ensuring controllability of electronics based on diagnostic modeling of heterogeneous physical processes // World Applied Sciences Journal. 2013. Vol. 24. P. 196-201.
7. Uvaysov S. U., Kofanov Ju. N., Sotnikova S. Ju. Programmnyy kompleks modelirovaniya fizicheskikh processov pri avtomatizirovannom proektirovanii istochnikov vtorichnogo jelektropitanija dlja slozhnykh bortovykh sistem // Dinamika slozhnykh sistem. 2012. № 3. S. 80-84.
8. Uvaysov S. U. Teksturovannye podlozhki iz splavov nikelja s tugoplavkimi metallami (W,Mo,Re) dlja sverhprovodjashhih kabelej vtorogo pokolenija // Izvestija vysshix uchebnykh zavedenij. Povolzhskij region. Tehnicheskie nauki. 2012. № 2(22). S. 126-137.
9. Uvaysov S. U., Aminev D. A. Algoritm raspredelenija propusknoj sposobnosti sistem registracii signalov ot mnogih datchikov // Datchiki i sistemy. 2012. № 5(156). S. 26-29.
10. Kofanov Ju. N., Sotnikova S. Ju., Uvaysov S. U. Dinamika optimizacionnogo processa pri identifikacii parametrov jelektronnykh sredstv // Dinamika slozhnykh sistem. 2012. № 3. S. 80-84.
11. Ivanov I. A., Uvaysov S. U., Koshelev N. A. Metodika obespechenija diagnostiruемости jelektronnykh sredstv kosmicheskikh apparatov po rangovomu kriteriju na rannih etapah proektirovaniya // Kachestvo. Innovacii. Obrazovanie. 2012. № 1. S. 60-62.

DEVELOPMENT OF AN ALGORITHM FOR AUTOMATIC LAYOUT AT THE LOCATION OF FRAGMENTS OF SCHEMATICS

Sekashev V.A., Avdeuk O.A.
Volgograd, Volgograd State Technical University

A summary of the process for the construction and study of the algorithm for layout fragments schematics on the structural-circuit design information-measuring systems.

Keywords: structural design, software system, graph.

After completion of structural engineering [1- 5], where the directed graph, you must go to the concept, replacing the graph nodes by circuit technology implementations of vertex functions, you can immediately get a schematic diagram of the developed IMS or other electronic device. A graph can be optimized according to the modified algorithm Бержа, or any of the known methods. The count must be final and vertex function should be specifically defined (amplifier a specific range of frequencies, low pass filter, AD, and so on) and circuit solution of each vertex function to have completed a description and certain physical parameters. Software system allows automated substitute graph vertex fragment of a concept, should issue a final version of the concept, having rectangular slices schemes in random order on the context of the display. This arrangement should be carried out in automatic mode.

How to build the algorithm? Obviously, for the realization of his need the following information:

1) The linear sizes of the fragments schematics (length W_n and width H_n each fragment of the principal scheme);

2) The number of fragments schemes n (coincides with the number of vertices of the graph);

3) Fill factor ($kz = \frac{\sum_{i=1}^n S_{\phi.c.}}{S_{\theta.c.}}$ the ratio of the sum of squares of fragments schemes to the total area of the display context scheme);

4) Indent step from the previous boundaries of the rectangular area s .

One of the implementations of this algorithm includes the following steps:

1) Calculation $\sum_{i=1}^n S_{\phi.c.}$ - the total area of all fragments created concept.

2) Calculate the area of a display context $S_{\theta.c.}$.

2.1) Allocated fragment with the highest linear dimensions (hence the largest area).

2.2) Calculation $\frac{S_{\theta.c.}}{S_{\phi.max}}$ - ratio of the total area of a display context of the entire

scheme of the square of the maximum fragment;

2.3) Knowing the linear dimensions of the maximum fragment scheme by dividing the minimum size to the proportion of the minimum size looked 1, we obtain the ratio of the species $1:W_{maxn}/H_n$ or $1:H_{maxn}/W_n$.

2.4) Each element of the proportions of the species species $1:W_{maxn}/H_n$ or $1:H_{maxn}/W_n$ is multiplied by the $\sqrt{\frac{S_{\theta.c.}}{S_{\phi.max}}}$.

2.5) The final result of the count $W_{\theta.c.}$ - the width и $H_{\theta.c.}$ - the width of the entire scheme.

3) Arbitrarily choose the rectangle diagrams of W_n and H_n and remember its number.

4) Select the first anchor point t_p (upper left coordinate the context of the display, pre-adding to the coordinates of the specified value s).

5) Adding to the coordinates of the t_p W_n and H_n (for X and Y respectively), we obtain the coordinates of the rectangle fragment concept.

6) Remember this rectangle.

7) Save the coordinates of the right - upper and left - bottom corner.

8) Randomly select the next rectangle and remember its number.

9) anchor taking into account s choose from a memorized in paragraph 7 of coordinates. The choice is made with a condition: if the selected coordinate of the right - upper value of s is added to the X coordinate, if the left - bottom - coordinate Y.

10) Check the condition of the rectangle within the boundaries of the display context. If not, make the sample to meet this condition, with a change not only the number, but the anchor point.

11) If the condition in paragraph 10, delete the coordinate memorized in paragraph 7, which was made binding, and add new ones, as in point 7.

12) Continue action item 8-11 until the length of the list of elements is equal to n .

13) If the condition of p. 12 fails, repeat p. 3-12 selecting items in a different order to get the result.

14) Save the resulting distribution in the form of an array or a file.

The weak side of this algorithm is a strong need for when fetching elements use a random number generator. This circumstance leads to more time working, and also to the non-determinism of the final results, which in our case is dependent on the successful choice of the sequence number of the element. It is obvious, that for the specified rectangular area and several rectangular areas, total area of which is always less than the size of the display context, multiple layout options.

Selection of the best layouts on the structural-circuit design depends connection fragments into a single scheme, when preference is given to conductors with minimal length.

How to join these fragments together? In addition to the well-known bus «GND» must be provided abstract однопроводные connectors that contain 2 output, which, when connected, are removed and replaced with a solid trunk line. Conditionally-graphical representation of these elements can be arbitrary designation.

The above algorithm was implemented in the machine language of a high level and tested on rectangular areas. It turned out that the choice of square display context random access of elements does not always lead to the final result. Therefore, for stable operation of the algorithm needs to be modified to exclude a random component in the choice of elements (instead, use a serial Robin), and also to exclude from the initial data, the fill factor.

1) The linear sizes of the fragments schematics (length W_n and width H_n each fragment of the principal scheme);

2) The number of fragments schemes n (coincides with the number of vertices of the graph);

3) Indent step at s .

One of the options implementations of this algorithm includes the following steps:

1) Take the first hosted rectangular element with a length of W_n and width H_n and remember its number.

2) Select the first anchor point t_p (upper left coordinate the context of the display, pre-adding to the coordinates of the specified the value s).

3) Adding to the coordinates of the t_p W_n and H_n (for X and Y respectively), we obtain the coordinates of the rectangle fragment concept.

4) Remember this rectangle.

5) Save the coordinates of the right - top, right, bottom, left - bottom corner.

6) Select next rectangle c serial number, different from the already positioned and remember its number.

7) Anchor point with regard to s choose from a memorized in paragraph 5 of coordinates. The choice is made with a condition: if the selected coordinate of the right - upper value of s is added to the X coordinate, if the left - the bottom - the Y co-ordinate, if the lower-right - and-coordinate X and y-coordinate.

8) Check the condition of not imposing posted a rectangular area on the already placed.

9) When the condition in point. 8 exclude coordinate from further consideration (replacing the value of X and Y -1), memorized in point. 5, which was made binding, and add new ones, as in point 5.

10) Continue actions p.6-9 to full view the list of all elements.

11) Remember the resulting location.

12) Perform steps 1-11 n times in order.

13) Of n derived locations, select location, occupying a minimum of space.

14) Save the resulting distribution in the form of an array or a file.

When this algorithm is not observed repeat. This algorithm is missing an opportunity to consider all permutations of elements in the list, which is $n!$, where n is the number of elements in the list. When the number $n \geq 10$ time of the algorithm operation will be very large. In our case, simulation of random sizes of rectangular regions in the range [1..350] in length and [1..250] the width of the algorithm when the number $n=10$ is 1 sec, the number of $n=30$ - 120 sec.

References

1. Muha, Yu.P. Algebraicheskaya teoriya sinteza slozhnyih sistem: monografiya / Muha Yu.P., Avdeyuk O.A., Koroleva I.Yu.; VolgGTU. - Volgograd: RPK "Politehnik", 2003. - 320 s.
2. Muha, Yu.P. Informatsionno-izmeritelnyie sistemyi s adaptivnyimi preobrazovaniyami. Upravlenie gibkostyu funktsionirovaniya: monografiya / Muha Yu.P., Avdeyuk O.A., Koroleva I.Yu.; VolgGTU. - Volgograd, 2010. - 303 s.
3. Muha, Yu.P. Teoriya i praktika sinteza upravlyayuschego i informatsionnogo obespecheniya izmeritelno - vychislitelnyih sistem: monografiya / Muha Yu.P., Avdeyuk O.A., Antonovich V.M.; VolgGTU. - Volgograd: RPK "Politehnik", 2004. - 220 s.
4. Novikov, F. A. Discrete mathematics for programmers [Text] / F. A. Novikov. - SPb.: Publishing house Piter, 2001. - 304 p.
5. Mathematical methods of Informatics problems and examples: Experience of use in the design of complex systems : textbook. manual [Text] / Avdeuk O.A., Gorbachev S.V., Mukha Y.P., Sekachev V.A., Siriamkin V.I., Titov V.S., Shirabakina T.A.; FSEI HPE «National research Tomsk state University».-Tomsk : Publishing house of Tomsk University 2012. - 483 p.
6. Uvaysov S. U., Ivanov I. A method of ensuring controllability of electronics based on diagnostic modeling of heterogeneous physical processes // World Applied Sciences Journal. 2013. Vol. 24. P. 196-201.
7. Uvajsov S. U., Kofanov Ju. N., Sotnikova S. Ju. Programmnyj kompleks modelirovaniya fizicheskikh processov pri avtomatizirovannom proektirovanii istochnikov vtorichnogo jelektropitanija dlja slozhnyh bortovyh sistem // Dinamika slozhnyh sistem. 2012. № 3. S. 80-84.
8. Uvajsov S. U. Teksturovannye podlozhki iz splavov nikelja s tugoplavkimi metallami (W,Mo,Re) dlja sverhprovodjashhih kabelej vtorogo pokolenija // Izvestija vysshih uchebnyh zavedenij. Povolzhskij region. Tehnicheskie nauki. 2012. № 2(22). S. 126-137.
9. Uvajsov S. U., Aminev D. A. Algoritm raspredelenija propusknoj sposobnosti sistem registracii signalov ot mnogih datchikov // Datchiki i sistemy. 2012. № 5(156). S. 26-29.

10. Kofanov Ju. N., Sotnikova S. Ju., Uvajsov S. U. Dinamika optimizacionnogo processa pri identifikacii parametrov jelektronnyh sredstv // Dinamika slozhnyh sistem. 2012. № 3. S. 80-84.
11. Ivanov I. A., Uvajsov S. U., Koshelev N. A. Metodika obespechenija diagnostiruемости jelektronnyh sredstv kosmicheskikh apparatov po rangovomu kriteriju na rannih jetapah proektirovanija // Kachestvo. Innovacii. Obrazovanie. 2012. № 1. S. 60-62.

THE MODELING OF SHEET SYMMETRIC ANTENNA WITH A LINEAR EXTENDING APERTURE FOR THE ARRAY

Parpula S. A., Girich V. S., Zayarniy V. P.
Volgograd, Volgograd State Technical University

The importance and relevance of the development of adequate mathematical models for the researched antenna, confirmed by experimental data is accounted for the necessity to obtain the agreed characteristics of the antenna systems based on them. For the calculation of directional pattern (DP) of sheet symmetric antenna whose change in the cross-section of the aperture is linear, perform the regularization for a finite number of sites so that each of them represented a slot of constant width, and calculate the DP entire antenna on their total contribution in the far zone of the field.

Keywords: antenna, directional pattern, aperture, regularization, microwave

Antenna and antenna devices in radio engineering systems are important functional link, characteristics which determine the characteristics of the remaining functional blocks of system. In this connection, development and research new antenna and antenna devices on their basis (include microwave band) are the increased interest and are relevant. The importance and relevance of the development of adequate mathematical models for the researched antenna, confirmed by experimental data is accounted for the necessity to obtain the agreed characteristics of the antenna systems based on them. For the calculation of directional pattern (DP) of sheet symmetric antenna whose change in the cross-section of the aperture is linear, perform the regularization for a finite number of sites so that each of them represented a slot of constant width, and calculate the DP entire antenna on their total contribution in the far zone of the field. For such stepwise approximation of continuous structure, the field in this zone is found as [1-3]:

$$E_{\theta}(\theta, \varphi) = \frac{j\omega\varepsilon w \cdot \sin \varphi \cdot e^{-jk_0 r}}{4\pi^2 r} \int_{-w/2}^{w/2} \frac{e^{jk_0 z' \cos \theta}}{\sqrt{\left(\frac{w}{2}\right)^2 - z'^2}} dz' \times$$

$$\times \int_0^L e^{jk_0 x' \sin \theta \cos \varphi} \cdot e^{k_x x'} \cdot \left[1 + e^{j\frac{\pi}{4}} F\left(v \cdot \sqrt{\frac{\pi}{2}}\right) + \frac{\sqrt{2}e^{-j\frac{\pi}{4}}}{\pi} \frac{e^{-j\frac{\pi}{2}v^2}}{v} \right] dx'.$$

Here $E(\theta, \varphi)$ – contribution in the field of the remote zone; θ, φ – angular coordinates in the E – and H – planes DP; w – width of n-th regular segment of waveleading structure; r – distance to the considered point of space; x, z – axes of coordinates.

$$F(v) = \int_0^v e^{-jt^2} dt \quad \text{– Fresnel integral,}$$

$$v = \sqrt{\frac{2k_0 x' \sin \theta (1 + \cos \phi)}{\pi}}.$$

ω – frequency of electromagnetic oscillations at the antenna input, k_0 – wave number, j – imaginary unit, t – time.

Calculations DP were produced for the antennas with the length L within $(1 \div 5\lambda)$ mm and width of aperture H within $(1 \div 3\lambda)$ mm at a frequency of 10 GHz, for E-plane electromagnetic oscillations [4, 5]. Figure 1 illustrates the directional pattern obtained in the result of modeling using the above formulas for the case $L = 150$ mm and $H = 60$ mm. Notice that width of the DP on the level of half of the capacity is about 30° , and the level of side lobes (LSL) is of the order of 0,05 from radiation power directly in front of the antenna (when $\theta=0$).

As a check on the adequacy of the obtained results was performed DP for one regular part (with $n=0$). These DP were compared with experimental results obtained for a regular antenna in [2, 4]. The comparative analysis of experimental data and modeling results showed that appeared divergence DP were insignificant. Best results are the same when the value of $\Delta w = \lambda_0/8$. This testifies of the validity of model concepts and possibilities of their use for simulation of DP of such antennas with any parameters, and DP a more complex antenna systems (e.g. arrays) on their basis.

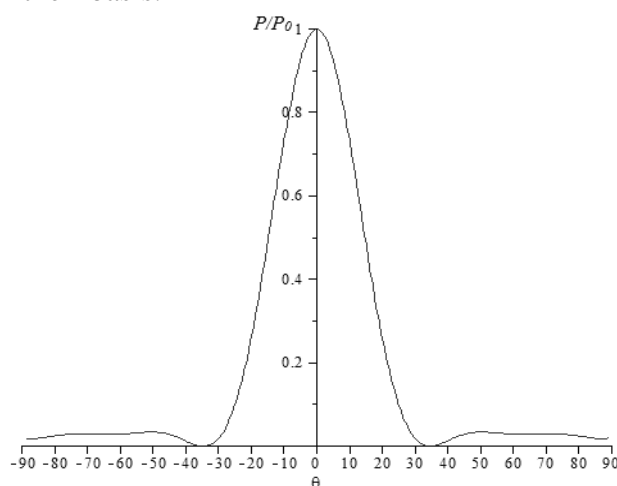


*Fig. 1 Directional pattern researched antenna for the case
 $L = 150$ mm, $H = 60$ mm.*

Calculation of the DP of the researched antenna when the width of the aperture was change (size H , at a constant length $L = 5\lambda = 150$ mm) in a large ($H = 3\lambda = 90$ mm) and small ($H = 1\lambda = 30$ mm) side showed the following. If increased the size of the antenna H , the main lobe DP significantly narrowed, and its width at the level of half of the capacity is about 20° . When reduced the size H , the main lobe DP significantly expanding and its width at the level of half of the capacity is about 46° . If increased the size of the antenna H , LSL increases, but does not exceed the level of 0.1 from the maximum power of radiation.

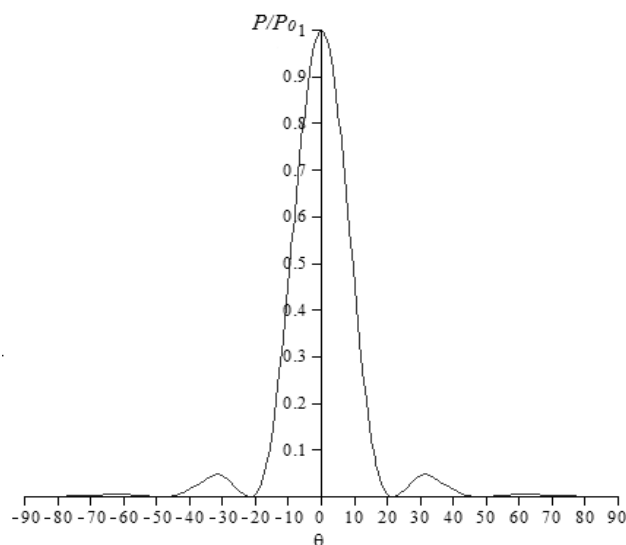


*Fig. 2 Directional pattern researched antenna for the case
 $L = 150 \text{ mm}$, $H = 90 \text{ mm}$*

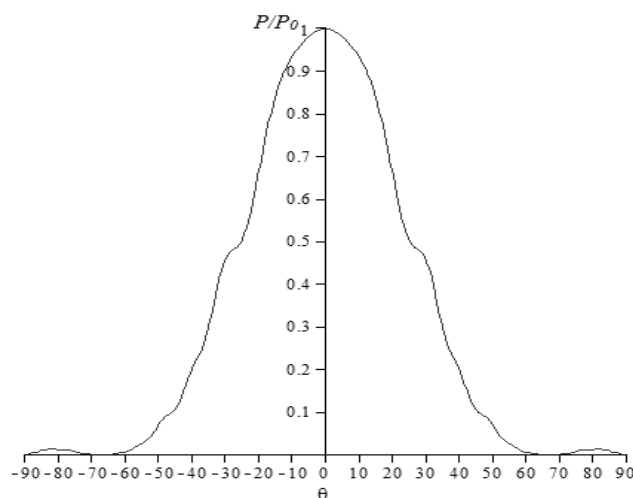


*Fig. 3 Directional pattern researched antenna for the case
 $L = 150 \text{ mm}$, $H = 30 \text{ mm}$*

From the received calculations, data shows that there is a clear dependence of the width of the main lobe of the DP studied sheet symmetric antenna with linearly changing aperture from the angle of aperture (size H). This allows the use of these types of antenna as the basic elements in more complex antenna systems, such as disk arrays [5], for the improvement and optimization of their electrodynamics characteristics. The model views allow you to predict and optimize the geometrical sizes of the basic elements for different antenna systems based on the investigated [6, 7]. The derived model views allow us to predict and optimize the geometrical sizes of the basic elements for different antenna systems based on the investigated [6, 7].

References

1. Janaswamy, R. Analysis of the transverse electromagnetic mode linearly tapered slot antenna / R. Janaswamy, D. H. Schaubert, D.M. Pozar // Radio Science. – v. 21. – P. 797–804.

2. Frolov, A. A. Izuchenie elelcrodimamicheskikh haracteristik antenn i antennih system SVH-diapozona / A. A. Frolov, Girich V. S., Zayarniy V. P.// Izvestij VUZOV «Radiofizika». – 2009. – T. 52. – №4. – C. 328 - 335.
3. Sharma, A. K. An Experimental investigations of Millimeter-Wave Fin Antennas / A. K. Sharma, R. M. Wilson, A. Rosen // IEEE Antennas & Propagation Society APS. – 1985. – Vol. 6. – P. 97-100
4. Bhat, B. Analysis, design and applications of fin lines / B. Bhat, S. Koul // Artech House. – 1987.
5. Frolov, A. A. Antenna krugovogo obzora sverhvisokochastotnogo diapozona / A. A. Frolov, Girich V. S., Zayarniy V. P.// Izvestij VUZOV «Radiofizika»– 2012. – T. 55. – № 10-11. – C. 697 - 703.
6. Frolov A. A. Diskovaj antenna krugovogo obzora na simmetrichnih chelevih izluchteley/ A. A. Frolov, Girich V. S., Girich S. A., Parpula S.A., Zayarniy V. P. // Fizika volnovih processov i radiotekhnicheskie: T. 15. № 4. 2012. C. 84-87.
7. Zayarniy V. P. Radiovizicheskie svoistva tverdotelnix sloistix structure s zarjdovoi svjziy: metodi informacionnoy vozmoznosti dlj ih opredelenij. – M.: Radio i svjaz, 2001. – 212 c.

EXPERIMENTAL STUDY OF SHEET SYMMETRIC ANTENNA WITH LINEAR EXPENDING APERTURE FOR ARRAYS

Parpula S. A., Girich V. S., Zayarniy V. P.
Volgograd, Volgograd State Technical University

Development and research new antenna and antenna devices include sheet antenna of the axial radiation of microwave band, and are of great interest and relevant. In this case, sheet antenna, made in the form of symmetric slots with linear expansion output (aperture), cut in metal plates with high conduction (copper, aluminium), with a thickness of 0.3 mm (Fig. 1), without the dielectric substrate, to be used in composition of disk arrays is addressed.

Keywords: antenna, directional pattern, level of side lobes, frequency, main lobe

Antenna and antenna devices in radio engineering systems are important functional link, characteristics which determine the characteristics of the remaining functional blocks of system. In this connection, development and research new antenna and antenna devices on their basis, include sheet antenna of the axial radiation of microwave band, and are of great interest and relevant. Such problems were studied in [1-3].

In this case, sheet antenna, made in the form of symmetric slots with linear expansion output (aperture), cut in metal plates with high conduction (copper, aluminium), with a thickness of 0.3 mm (Fig. 1), without the dielectric substrate, to be used in composition of disk arrays is addressed.

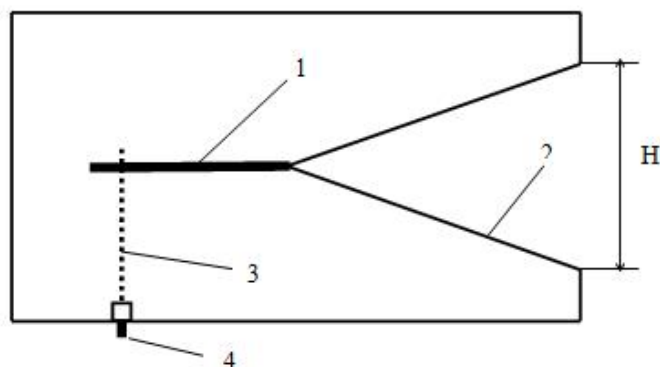


Fig. 1. The appearance of the researching antennas (1 – symmetrical slot line (SSL) ; 2 – dilative SSL; 3 – supply microstrip; 4 – coaxial connector)

Figures 2-4 gives the experimentally obtained directional patterns (DP) in the E – and H - planes for investigated antennas with a width of aperture $H=30$ mm (1λ), 60 mm (2λ) and 90 mm (3λ), respectively. The length of the antenna in all cases was the same ($L = 150$ mm). Measurement of the DP was made at a frequency of 10 GHz using the experimental plant and the techniques described in [4-6]. Their form remained almost unchanged in the frequency range of 5.9 - 12.5 GHz.

From the analysis of the DP it will be obvious that with increasing the aperture of the antenna, their main lobe, as in the case of design DP (for E - plane) is narrows. At the same time, the width of experimentally obtained DP half of the capacity was about 48° – for $H = 30$ mm (1λ), 32° - in the case $H = 60$ mm (2λ) and 20° - the case of $H = 90$ mm (3λ), which agrees well with the results of calculation. Level of side lobes (LSL) of the experimentally obtained DP slightly higher than the calculated and did not exceed 0.3 of maximum power.

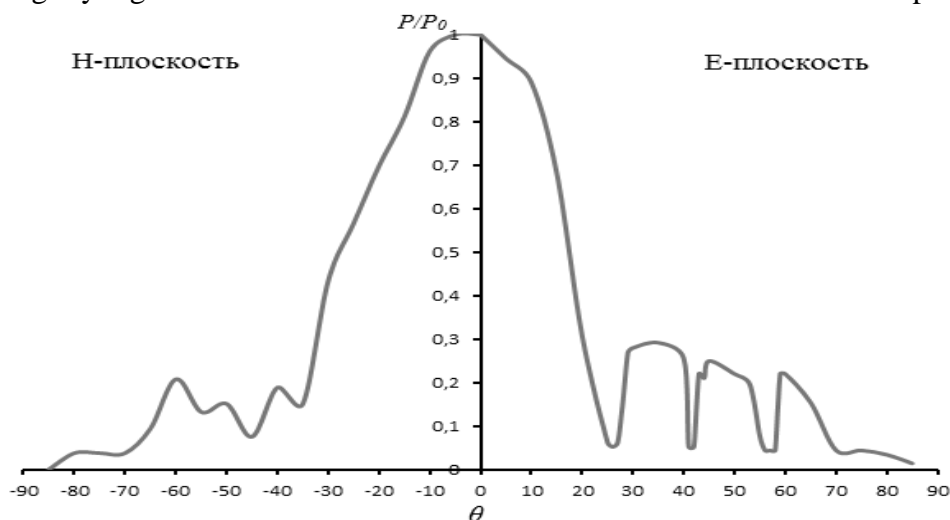


Fig. 2. Directional pattern researched antenna for the case $L = 150$ mm, $H = 30$ mm

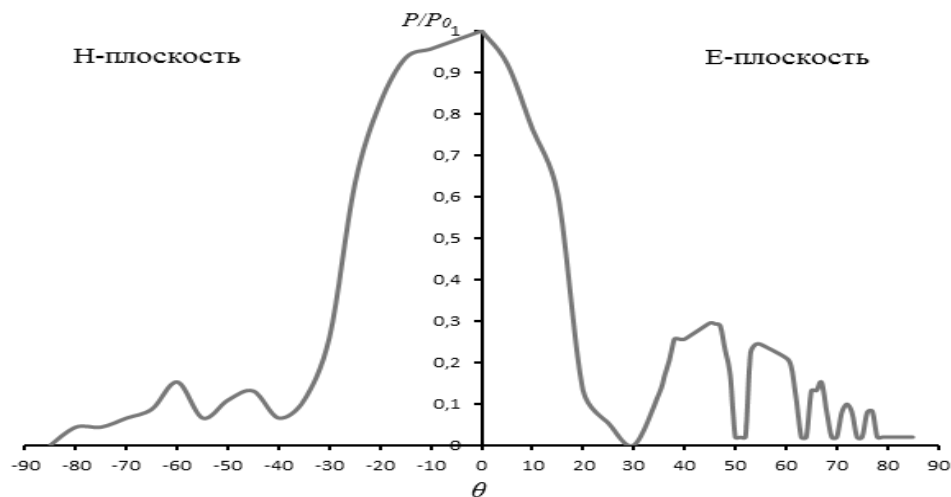


Fig. 3. Directional pattern researched antenna for the case $L = 150 \text{ mm}$, $H = 60 \text{ mm}$

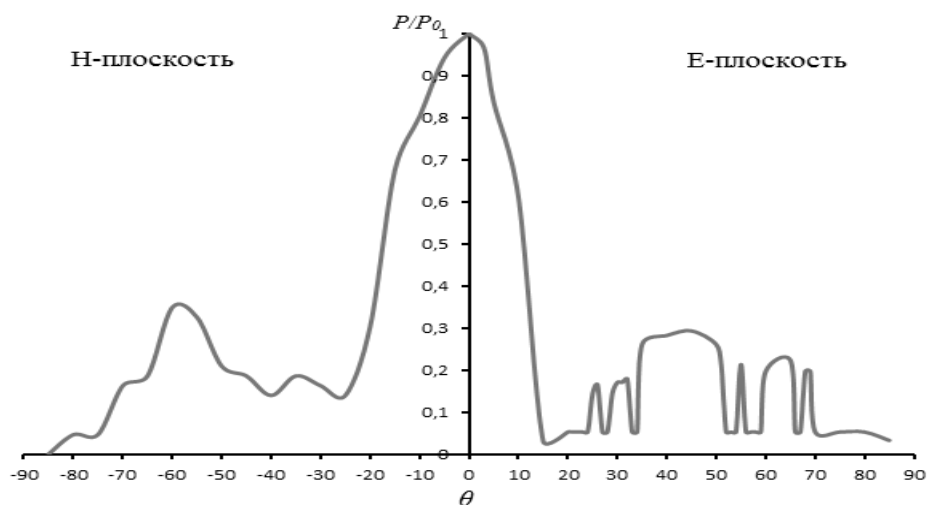


Fig. 4. Directional pattern researched antenna for the case $L = 150 \text{ mm}$, $H = 90 \text{ mm}$

From Fig. 2-4 that in the H – plane DP have the same pattern narrowing of the main lobes, as with E – plane. However, in H - plane main lobes of DP somewhat broader than in E - plane (for the same values of the aperture of the antenna), and had a value of about 58° – in case $H = 30 \text{ mm}$ (1λ), 54° - in case $H = 60 \text{ mm}$ (2λ) and 38° - in case $H = 90 \text{ mm}$ (3λ). There is a tendency to increase the LSL when increasing the aperture of the antenna, as well as in case of settlement of the DP.

From the received experimental result shows that there is a clear dependence of the width of the main lobe of the DP studied sheet symmetric antenna with linearly changing aperture from the angle of aperture (size H). This allows the use of these types of antenna as the basic elements in more complex antenna systems, such as disk arrays, for the improvement and optimization of their electrodynamics characteristics [7, 8].

References

1. Janaswamy, R. Analysis of the transverse electromagnetic mode linearly tapered slot antenna / R. Janaswamy, D. H. Schaubert, D.M. Pozar // Radio Science. – v. 21. – P. 797–804.
2. Sharma, A. K. An Experimental investigations of Millimeter-Wave Fin Antennas / A. K. Sharma, R. M. Wilson, A. Rosen // IEEE Antennas & Propagation Society APS. – 1985. – Vol. 6. – P. 97-100.

3. Bhat, B. Analysis, design and applications of fin lines / B. Bhat, S. Koul // Artech House. – 1987.

4. Frolov, A. A. Izuchenie elelrodinamicheskikh harakteristik antenn i antennih system SVH-diapozona / A. A. Frolov, Girich V. S., Zayarniy V. P. // Izvestij VUZOV «Radiofizika». – 2009. – T. 52. – №4. – С. 328 - 335.

5. Zayarniy V. P. Radiovizicheskie svoistva tverdotelnix sloistix structure s zarjdovoi svjzjy: metodi informacionnoy vozmoznosti dlj ih opredelenij. – M.: Radio i svjaz, 2001. – 212 c.

6. Frolov, A. A. Informacionno-upravljuzaj sistema dlj izmerenij xarakteristik antenn SVH-diapozona / A. A. Frolov, Girich V. S., Zayarniy V. P. // Izvestij VolgGTU. Ser. elektronika, izmeritelnaj tehnika, radiotekhnika i svyz. – 2008. – Вып. 2. – С. 77 - 80.

7. Frolov, A. A. Antenna krugovogo obzora sverhvisokochastotnogo diapozona / A. A. Frolov, Girich V. S., Zayarniy V. P. // Izvestij VUZOV «Radiofizika»– 2012. – T. 55. – № 10-11. – С. 697 - 703.

8. Frolov A. A. Diskovaj antenna krugovogo obzora na simmetrichnih chelevih izluchteley/ A. A. Frolov, Girich V. S., Girich S. A., Parpula S.A., Zayarniy V. P. // Fizika volnovih processov i radiotekhnicheskie: T. 15. № 4. 2012. С. 84-87.

DISK ALL-ROUND LOOKING ANTENNA BASED ON LINEAR EXPANDING SLOT LINES

Parpula S. A., Girich V. S., Zayarniy V. P.
Volgograd, Volgograd State Technical University

The directivity patterns of linear expanding symmetric slot lines arranged coaxially-symmetrically on disks was experimentally measured. The possibility of electrodynamic compatibility in the composition of coaxially located disk arrays was investigated.

Keywords: symmetric slot lines, disk arrays, directional pattern, electrodynamic compatibility, microwave

Development and research of electrodynamic characteristics of antenna systems, including microwave range, for the circular (or sector) review transceiver equipment is an important and topical, since such systems are needed in radio - videolocation, security systems, etc.

Solving the challenge of support for the sector (circular) review can be achieved, in particular, the design of disk structures, with the use of emitting elements in the form of linear expanding symmetric slot lines (SSL). The properties of such SSL have been studied and analyzed in [1, 2].

From the analysis of the characteristics of the directional patterns obtained for single linear expanding SSL follows that, if they are structurally are located on thre disk in the radial from the centre directions, so that the angle between them was equal to 45 that can accommodate up to 8 SSL. The full all-round visibility is virtually assured. However, the experiment showed that when placing an 8 SSL on one disk creates a significant overlap main lobes of the directional patterns of the neighboring SSL that does not provide acceptable electrodynamic isolation.

Measurements of the directional patterns (DP) of the antenna were carried out at the experimental device and using the techniques described in [3-5]. At first design was investigated, provided that single SSL added a second similar SSL, geometrically aimed in the opposite direction from the first and located on the same disk. Analysis of DP of such a

design, made in the form of thin aluminum disk without substrate, shows that in the frequency range from 6 GHz to 11.5 GHz their form remained practically unchanged. Outside of these boundary frequency appeared significant distortion of the DP as strip power SSL and used detect microwave diodes lacked broad wave-band. If necessary, extend the frequency range the possibility exists of change these elements at the more broadband.

The width of the main lobes DP for both SSL on the level of a half power in the specified frequency range varied from 22° to 50° , under changes of the angle of aperture slot each item, respectively, from $32,5^\circ$ to $10,5^\circ$.

The above characteristics for two opposite SSL allow to create a design in the form of an array has four SSL, located one after another at an angle of 90° on one disk (Fig. 1), and provide a good electrodynamic isolation. The resultant diagram pattern for the disk antenna with four SSL at a frequency of 10 GHz is shown in Fig. 2.

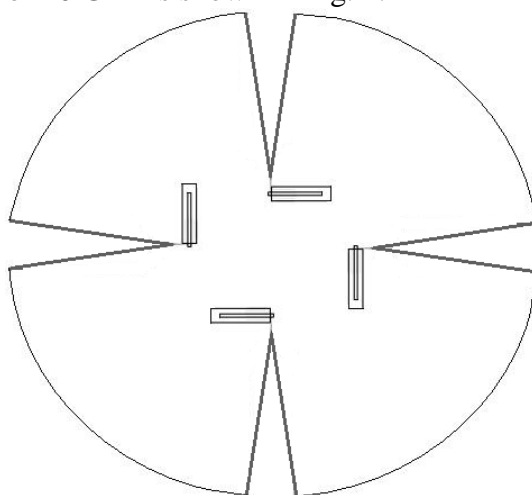


Fig. 1. The arrangement of the four SSL on the metal disk

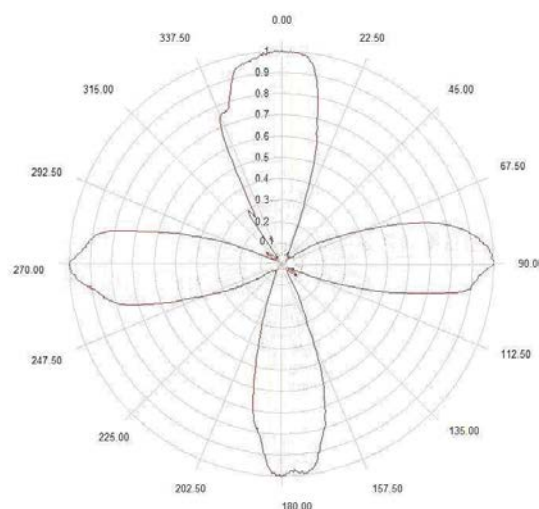


Fig. 2 Directional pattern of disk array with a four SSL

It is obvious that such a design is not yet provides overlap all the surrounding space (and even quite a broad sector). Therefore, the most optimal variant of a design of the disk array is a two similar, coaxially-located disks, azimuth shifted relative to each other at an angle of 45° (Fig. 3) and operating at different frequencies, which involves the spatial and frequency diversity directional patterns SSL. The possibility of changing the angle of aperture

SSL lets you modify the width of the main lobe of each SSL, that allows the best way to produce the electrodynamic isolation between DP corresponding SSL.

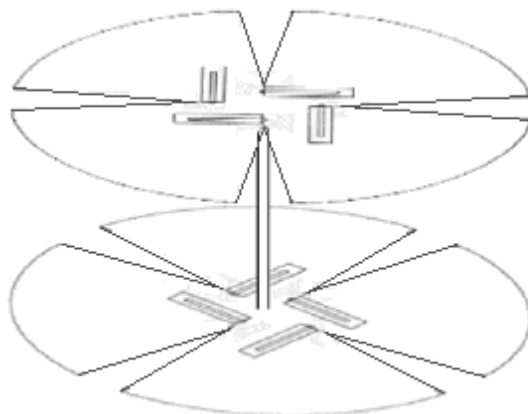


Fig. 3 Appearance of the all-round looking antenna

Such antenna design provides a circular (and any sector) review [4]. It has been found experimentally that the optimal distance between the disks, which ensures the required electrodynamic isolation between the SSL of the top and bottom disks, is about one wavelength (the average frequency of 10 GHz it is about 3 cm).

References

1. Janaswamy, R. Analysis of the transverse electromagnetic mode linearly tapered slot antenna / R. Janaswamy, D. H. Schaubert, D.M. Pozar // *Radio Science*. – v. 21. – P. 797–804.
2. Frolov, A. A. Izuchenie elektrodinamicheskikh harakteristik antenn i antennih system SVH-diapozona / A. A. Frolov, Girich V. S., Zayarniy V. P. // *Izvestij VUZOV «Radiofizika»*. – 2009. – T. 52. – №4. – C. 328 - 335.
3. Zayarniy V. P. Radiovizicheskie svoistva tverdotelnix sloistix structure s zarjdovoi svjzju: metodi informacionnoy vozmoznosti dlj ih opredelenij. – M.: Radio i svjaz, 2001. – 212 c.
4. Frolov, A. A. Antenna krugovogo obzora sverhvisokochastotnogo diapozona / A. A. Frolov, Girich V. S., Zayarniy V. P. // *Izvestij VUZOV «Radiofizika»*– 2012. – T. 55. – № 10-11. – C. 697 - 703.
5. Frolov A. A. Diskovaj antenna krugovogo obzora na simmetrichnih chelevih izluchteley/ A. A. Frolov, Girich V. S., Girich S. A., Parpula S.A., Zayarniy V. P. // *Fizika volnovih processov i radiotekhnicheskie*: T. 15. № 4. 2012. C. 84-87.

MOBILE ROBOT CONTROL BY VOICE COMMANDS

Egunov V.A., Abed O.A.

Volgograd, Volgograd State Technical University

Developing the interface of mobile robot using voice commands is discussed. Basic tasks required to create a similar interface, the basic requirements for it are formulated, described solution to this problem .

Keywords: mobile robot, voice commands, a robot control system.

Recognition of human speech is one of the complex scientific and technical problems. The problem of implementation of speech dialogue between man and hardware - an urgent task of modern cybernetics. Speech recognition task machine attracts the attention of specialists for a long time. Currently, users of computers and vehicles equipped with computers are people who are not specialists in the field of programming. Voice control problem arose, moreover, due to the fact that in some applications, it has become the only possible means of communication with the technique (in terms of congestion, dark or drastic changes in lighting, busy hands, highly focused attention on the object, which does not allow aside for a second, etc.) and also because of the impossibility of using other control options such as a wireless channel [1] .

To control mobile robot does not require a complete speech recognition problem, quite a few voice commands. Because this problem must be solved by means of robot control system, the aim of this work is to create additional interface robot control.

To achieve the goal of creating additional interface of mobile robot must perform the following tasks:

- analysis of digital audio signal processing and speech recognition systems;
- developing facial recognition software for mobile robot control commands.

To solve the problem of voice control of mobile robot have been developed functional requirements for the management system and put the following restrictions on the speech recognition task:

- voice commands management, is a separate short words;
- small set of commands (commands 10-20), which is sufficient to control for embedded systems and mobile robots.
- filtering the input signal from the intrinsic noise.

Work on the project began by reviewing the literature to find existing methods for analyzing speech. Also held a patent search devices performing feature extraction of speech signals, such as the start and end of words, the allocation of speech and noise removal

In general, this problem is computationally complex and places high demands on the performance of the central computing unit of the mobile robot [2]. The traditional model of automatic speech recognition suggests that by tracking the acoustic parameters and use one of the search tools on a set of standards can be set phonemic segments phonemic series. Then these series can be used for linguistic analysis on a higher tier highlight words, phrases and meaningless statements. Successful comprehension of spoken sentences (phrases) includes the use of a particular linguistic structure in combination with the most accurate sound information. In automatic speech recognition, great difficulties are processes detection and identification of certain groups of phonemes.

By creating the robot control interface for each word, which can be recognized by the system control points were obtained envelopes, their energy is calculated and determined measure of closeness between the signals. For the base of mobile robot compiled a dictionary of voice commands, which included four major commands set the direction of movement ("forward", "back", "left", "right"), and the command "stop".

This technology can be easily applied in various spheres of life, requiring automatic voice control mechanisms.

Later modeling of work of the device was completed. It was also developed a program for high level programming languages C # and C + + that implements the algorithm outlined speech recognition. The results showed the possibility of using the parameters allocated to the speech signals for speech recognition.

References

1. Egunov, V.A. Razrabotka mobil'nogo robota s navigatsionnoi sistemoi na baze odometrii / Egunov, V.A., Lebed', A.A. // Innovatsii na osnove informatsionnykh i kommunikatsionnykh tekhnologii (INFO-2013) : mater. X mezhdunar. nauch.-prakt. konf., g. Sochi, 1-10 okt. 2013 g. / MIEM NIU VShE [i dr.]. - M., 2013. - C. 417-418.

2. Egunov, V.A. Robotic Complex Central Processing Node Performance Requirements Assessment / Egunov, V.A., Kirnosenko, S.I., Andreev, A.E.. // World Applied Sciences Journal (WASJ). - 2013. - Vol. 24, Spec. Issue 24 : Information Technologies in Modern Industry, Education & Society. - pp. 37-42.

PARAMETER MEASURING OF CONSTELLATION DIAGRAMS IN PARTICULAR DVB-T SIGNALS

Ivo Lazar

European Polytechnic Institute, Kunovice, Czech Republic

Between analogue and digital television there is a significant qualitative difference in the sense of „purity“ of the TV picture without „snow.“ With the transition to digital television it is true that there has been reduced some demands on the received television signal – its level, but on the other hand, the capturing and processing of the DVB-T signal, in the edge zones of the reception range of the transmitter, is without these minimum levels quite difficult, and there then appears a so – called „kostečkovani“ (in Czech) – the phenomenon known as the Cliff effect.

Keywords: DVB-T, UHF ray, signal level, signal gain, multiplex, TV channel, YAGI antenna, signal amplification, signal attenuation, single-frequency network, bandwidth, impedance of the antenna, Cliff effect, CBER, MER, constellation diagram

INTRODUCTION

The actual signal DVB-T and its incidence according to coverage maps at the reception location does not guarantee that a particular multiplex will be detected and tuned by a DVB-T tuner. Not only the distance of the reception of the signal from the transmitter and its performance plays a key role, but also the terrain relief, whether a densely populated area with high-rise buildings, or various (hardly identifiable) interference sources, etc.

Another situation occurs when we receive signals from distant transmitters on the outskirts of potential reception, or if we receive a signal from a nearby transmitter distant only a few kilometers away from the reception site.

In the first case, we can hardly do without the large type of YAGI antenna with high gain in dBm (dBμV), and wideband amplifier and measuring the signal level in dBμV. In the second case near the transmitter it will be sufficient to have an omnidirectional antenna with a small profit, or simply a dipole.

Frequency spectrum of DVB-T

The multiplex channel consists of a frequency of 8MHz, the multiplex is radiated by a frequency spectrum of IV and V of the television band. One multiplex (MUX) with four to six TV programs by the analog television (ATV) took four to six discrete channels of 8 MHz. For this reason, all the MUXs are operated only in IV. and V. band on channels ranging from 21 to 69, with respective frequencies of 474–858 MHz. TV bands I. to III. are not used, thus eliminating the use of large antennas.

The Czech Radiocommunications calculated the using of the frequency spectrum in the 474–826 MHz (21 Ch to 65 Ch), with the 61 Ch to 65 Ch being used for experimental broadcasts.

Transmitters of public programs MUX 1 and transmitters of commercial programs MUX2, MUX3, MUX4, including MUX7 regional broadcast to 60 Ch.

Levels of analog and DVB-T signals

The minimum signal level required by the system to receive DVB-T is approximately 35 dB μ V at 75 Ω impedance of the antenna with a minimum signal / noise ratio 20 dB in the case of an ideal environment. In practical terms, this requirement corresponds to the equivalent of a minimum intensity of the electromagnetic field of 44 dB at a height of 10 m above the ground. In comparison with analog, wherein the counting of the 56 dB at the minimum signal / noise ratio 23 dB, the difference is about 12–20 dB higher in favor of the DVB-T.

Fewer demands on the level of DVB-T signals is achieved mainly due to the higher sensitivity and lower noise figure and high quality of TV receivers, set-top boxes.

Antenna gain of these reasons, and the only significant parameter in the covered DVB-T signal.

From the consumer's perspective there is an important difference between receiving analog and digital television, which will take effect when installing and adjusting the antenna reception quality picture and sound. For analog TV with poor reception, which was characterized by a speckling image improved by better routing and location of the antenna, increasing profit – in proportion to the noisy gradually disappeared. Each incremental, positive or negative step was reflected in the quality of picture and sound.

The expected success depended on the capture of one of the „starting signale“ close reach of the respective transmitter in the intended reception. This circumstance was to facilitate the analog TV to gradually improve reception is poor in income terms to the optimum, which unfortunately did not guarantee a perfectly clear picture, but the reception was satisfactory for viewing with a slight „snow.“

The principle of digital television does not switch from „no“ to a good income, and vice versa – is steep. Due to weather conditions or various signal interference from multiple sources at the receiving antennas or power, even a slight change in position of the antenna, the signal strength decreases and the stable TV reception suddenly „freezes“ or there begins the „Cliff effect“ and gradually disappears – and the screen goes black . These are the so-called Cliff effect accompanying DVB-T. [5]

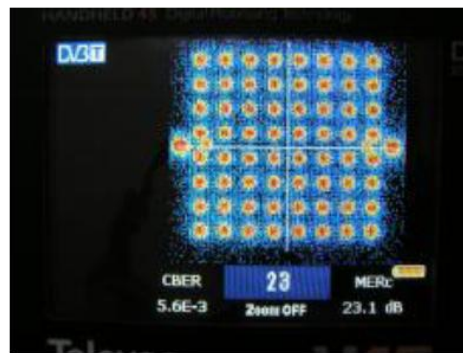
The various parameters of errant MER modulation measured signals

Slovak MUX:

The first one was a captured, amplified and measured signal on channel 23 from a transmitter propagated by the United Javorina–Nove Mesto nad Vahom. It is a Slovak MUX4 in which are disseminated the following TV programs that are paid (coded): [8]



Picture 1 The signal covering – V. Javorina, 23 Ch.



Picture 2 Constellation diagram, CBER a MERc 23 Ch.

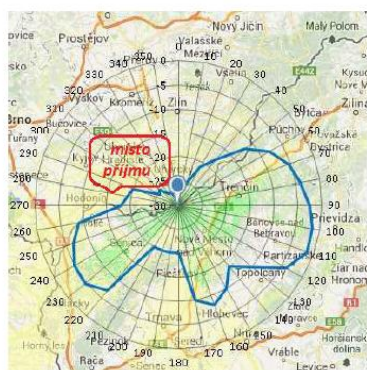
CBER error rate is 5.6×10^{-3} , ie six of error bits per thousand bits. Most set-top boxes and TV with DVB-T tuner should not have a problem to tune the channel. [8]

Slovak MUX3 contains nine public television and radio stations, is distributed from the transmitter United Javorina–Nove Mesto nad Vahom on channel 57. [2]

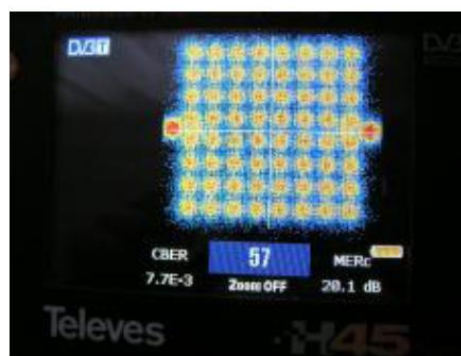




 :RÁDIO SLOVENSKO, :RÁDIO REGINA,
 :RÁDIO PATRIA, :RÁDIO FM, :RÁDIO DEVÍN, :RÁDIO KLASIKA,
 :RÁDIO LITERA, :RÁDIO JUNIOR, :RÁDIO SLOVAKIA INTERNATIONAL



Picture 3 The signal covering – V. Javorina, 57 Ch.



Picture 4 Constellation diagram, CBER a MERc 57 Ch.

CBER error rate is 7.7×10^{-3} , ie eight-bit error in a thousand bits. Approximately 80–90 % of set-top boxes and TVs with a DVB-T tuner should not have a problem to tune the channel. [2]

Slovak MUX2 is distributed from the transmitter United Javorina–Nove Mesto nad Vahom from a 56 channel contains a total of five TV channels: [8]

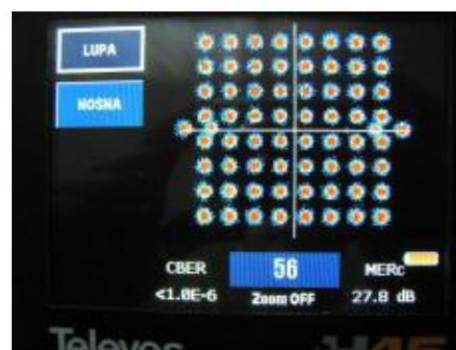








Picture 5 The signal covering – V. Javorina, 56 Ch.

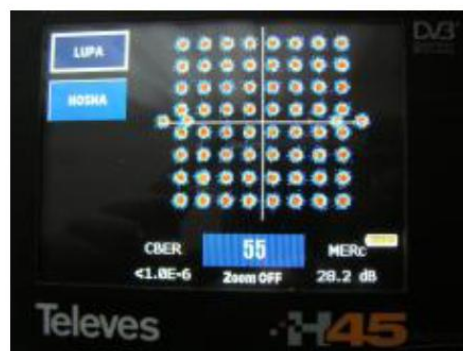


Picture 6 Constellation diagram, CBER a MERc 56 Ch.

Slovak MUX1 is distributed from the transmitter United Javorina–Nove Mesto nad Vahom from a 55 channel and contains a total of three television channels: [8]



Picture 7 The signal covering – V. Javorina, 55 Ch.



Picture 8 Constellation diagram, CBER a MERc 55 Ch.

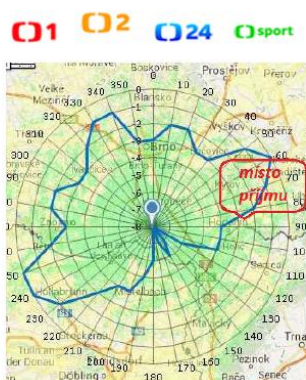
In both cases the measured error CBER $< 1.0E-6$, i.e. less than one bit error per million bits. The minimum error rate, including high gain in dB is due to line of sight to the transmitter from a distance of approximately 27 km at the receiving location. [2]

Czech MUX:

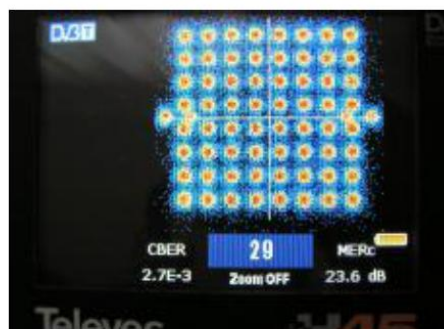
The reception location is within reach of several transmitters spread MUX 1–3 and MUX4, 7th

Brno–Kojal, Mikulov–Devin, Zlin–Tlusta Hora and MUX4 a 7 – Hungarian Fort Rovnina and Hodonin–Kaplansky. [8]

MUX1 Mikulov–Devin is distributed on channel 29 and includes a total of four public channels:



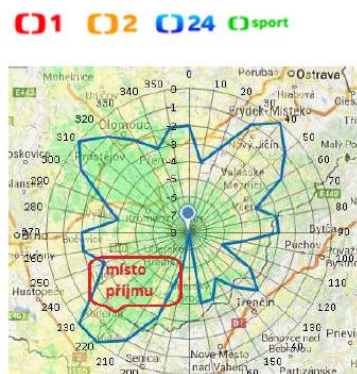
Picture 9 The signal covering – Mikulov–Devin, 29 Ch.



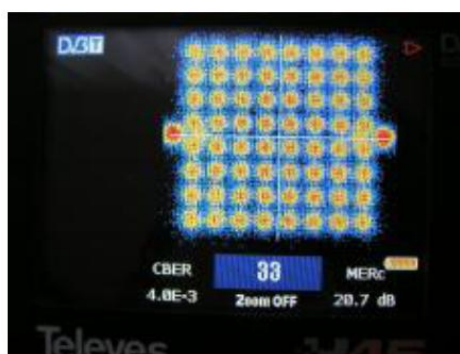
Picture 10 Constellation diagram, CBER a MERc 29 Ch.

CBER error rate is $2.7E-3$, ie, three error bits into a thousand bits. Almost all commercially available set-top boxes and boxes TV with DVB-T tuner should not have a problem to tune the channel. [2]

MUX1 Zlin–Tlusk Hora is distributed on channel 33 and includes a total of four public chan.



Picture 11 The signal covering – Zlin–Tl.Hora, 33 Ch.



Picture 12 Constellation diagram, CBER a MERc 33 Ch.

CBER error rate is $4.0\text{E-}3$, ie, three error bits into a thousand bits. Almost all commercially available set-top boxes and TV with DVB-T tuner should not have a problem to tune the channel. [2]

MUX2 Brno–Kojal is distributed on channel 40 with a total of five TV channels:



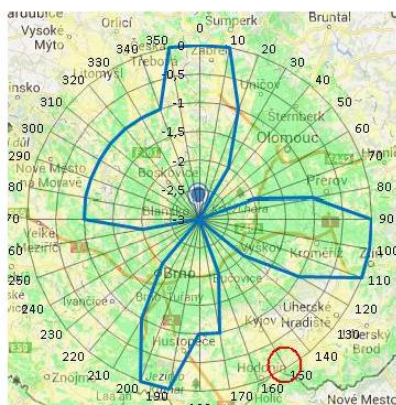
Picture 13 The signal covering – Brno–Kojal, 40 Ch.



Picture 14 Constellation diagram, CBER a MERc 40 Ch.

CBER error rate is $3.0\text{E-}5$, ie, three error bits per hundred thousand bits. Almost all commercially available set-top boxes and TV with DVB-T tuner should not have a problem to tune a channel. [2]

MUX3 Brno–Kojal is distributed on channel 59 and includes a total of six television channels.



Picture 15 The signal covering – Brno–Kojal, 59 Ch.



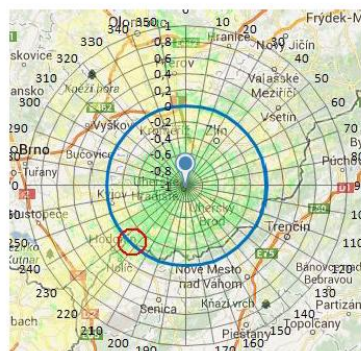
Picture 16 Constellation diagram, CBER a MERc 59 Ch.

CBER error rate is $3.9\text{E-}5$, four error bits per hundred thousand bits. All commercially available set-top boxes and TV with DVB-T tuner should not have a problem to tune the channel. The transmitter Brno–Kojal belong to their performance, the most powerful terrestrial transmitters DVB-T signal. [2]

Regional MUX 4 distributed in South Moravia and Zlin regions of the 46 and 42 channel contains a total of six television channels. [8]



42 K – Transmitter Rovnina, Uherské Hradiště



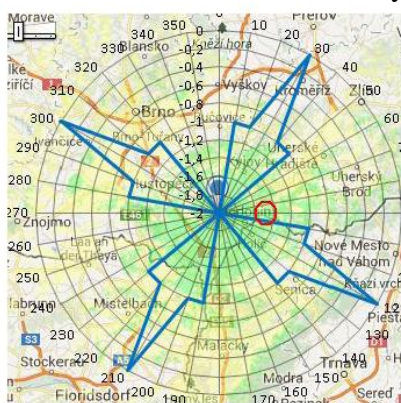
Picture 17 The signal covering – Uherské Hradiště, 42 Ch.



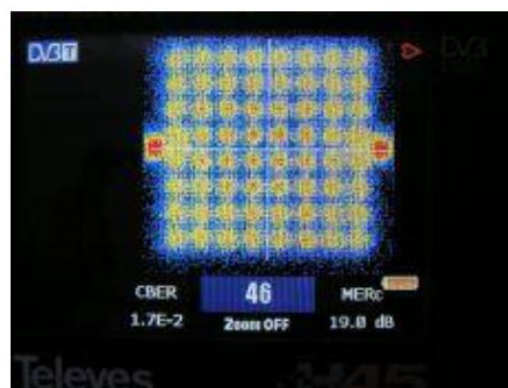
Picture 18 Constellation diagram, CBER a MERc 42 Ch.

CBER error rate is $1.2 \cdot 10^{-3}$, ie one bit error per thousand bits. All commercially available set-top boxes and TV with DVB-T tuner should not have a problem to tune channels. [2]

46 K – Transmitter Hodonin, Stary Podvorov [8]



Picture 19 The signal covering – Hodonín, 46 Ch.



Picture 20 Constellation diagram, CBER a MERc 46 Ch.

CBER error rate is $1.7 \cdot 10^{-2}$, i.e., two error bits per hundred bits. Some commercially available set-top boxes with lower sensitivity and TV with DVB-T need tuner to tune the channel problem. The graph indicates that there is a lot of noise present as a value CBER ($1.7 \cdot 10^{-2}$ before Viterbi corrector) and the value of the MERc (19.8 dB) is unsuitable for stable income. [2]

MUX4 falls in to regional DVB-T coverage through the local transmitters with lower performance.

Regional MUX4 and MUX7 is distributed from local transmitters with output up to 10 kW ERP

MUX 7 on-site broadcasts on channel 41 from the transmitter Uherske Hradiste Rovnina. The Czech television channel that launched in May 2013 was on the occasion of the sixtieth anniversary of the start of television broadcasting in Czechoslovakia.

Regional MUX7 offers the following programmes: [8]



Picture 21 The signal covering – Uherké Hradiště, 41 Ch.

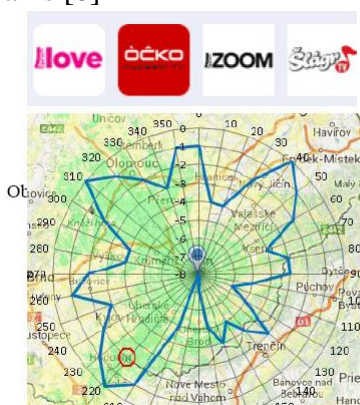


Picture 22 Constellation diagram, CBER a MERc 41 Ch.

CBER error rate is $2.7E-3$, ie, three error bits into a thousand bits. All commercially available set-top boxes and TV with DVB-T tuner should not have a problem to tune the channels. [2]

Obrazek 21: Pokryti signálu – Hodonin, 41 K

MUX3 propagated from the transmitter Zlin thick mountain on Channel 25 offers the following programs [8]



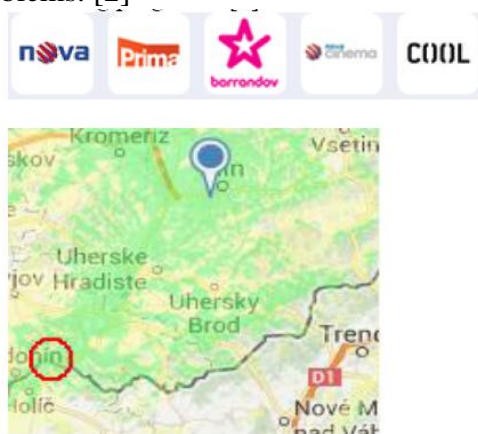
Picture 23 The signal covering – Zlín Tl. hora, 25 Ch.



Picture 24 Constellation diagram, CBER a MERc 25 Ch.

CBER error rate is $5.8E-6$ before Viterbi corrector, ie six bits of error per million bits. Noise at Mercy diagram is considerably less than in the case of 41,42 or 46 channel.

All commercially available set-top boxes and TV with DVB-T tuner tunes to a channel with no problems. [2]



Picture 25 The signal covering – Zlín Tl. hora, 49 Ch.



Picture 26 Constellation diagram, CBER a MERc 49 Ch.

MUX2 propagated from the transmitter Zlin thick mountain on Channel 49 offers the following programs: [8]

CBER error rate is $2.4\text{E-}6$ before Viterbi corrector, ie, three error bits per million bits. Noise at Mercy diagram is considerably less than in the case of 41,42 or 46 channel.

All commercially available set-top boxes and TV with DVB-T tuner tunes to a channel with no problems. [2]

Austria MUX:



Picture 27 The signal covering – Wien, 24 Ch.



Picture 28 Constellation diagram, CBER a MERc 24 Ch.

MUX1 propagated from the transmitter Kahlenberg Wien–distributed from 24 channels without any problems detected 120 km from the transmitter towards the Czech inland. QAM16 modulation is used, which has a „less demanding“ when MERC (measurement has been empirically determined that sufficient range of 18 dB). [2]



Picture 29 The signal covering – Wien, 34 Ch.



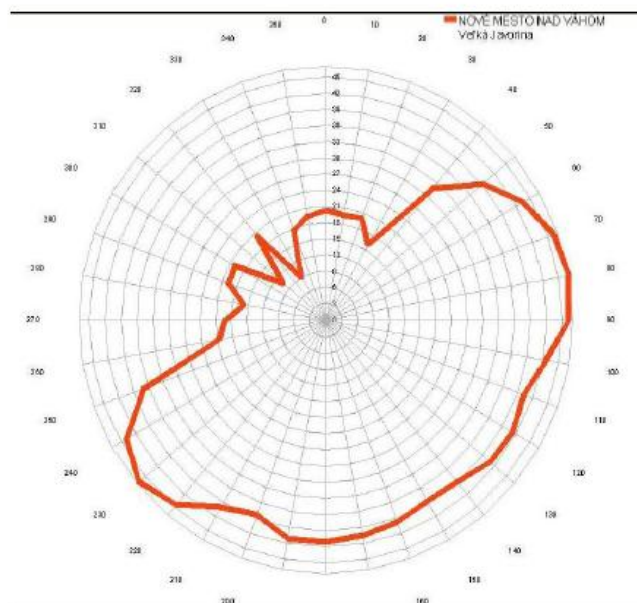
Picture 30 Constellation diagram, CBER a MERc 34 Ch.

MUX2 propagated from the transmitter Kahlenberg Wien – propagated from channel 34 is no problem detected 120 km from the transmitter towards the Czech inland. As in the first MUX QAM16 modulation is used. The signal has a „slightly“ worse parameters before Viterbi error corrector and Mercy, but it is good enough for remote reception at a distance of approximately 120 km from the transmitter. [6]

Bit error rate before correction CBER reaches values of $1.5\text{E-}6$, respectively. $5.4\text{E-}5$. These values guarantee a stable income from even a distance of over 100 km from the transmitter. [2]

CONCLUSION

From Velka Javorina Slovak transmitter antenna system transmitter does not transmits too much signal to Moravia and Silesia, is inhibited by approximately 25–35 dB. This limitation is clearly seen from the radiation patterns in the channels 55, 56 and 57 in a clear directionality toward western Slovakia.



Picture 31 The directivity of the signal from the transmitter Velká Javořina

Radiating power of individual transmitters due to the distance the signal reception falls on the very edge of the possible income (from 25 to 100 km) as the crow flies. Were therefore used large YAGI antenna with high gain (12–18 dBi).

Picture 31 The directivity of the signal from the transmitter Velka Javořina

For all Czech MUXs enough two antennas, looking toward the Brno–Kojal and Wien–Kahlenberg. On the other above antenna comes from the „other side“ of the MUX Uh. Fort–Rovný and Zlin–Thick mountains. The directors are angled toward the Hodonin–Kaplansky and vitriol for Slovak (Slovak regional channel MUX), then Kahlenberg Wien–horizontal directivity to 37°. [5]

Modulation error rate (MER)

It is one of the quality parameters of the DVB-T

For 64QAM modulation, which is used in case of Czech and Slovak MUX is the required minimum value of 22 to 24 dB, the optimal value is ≥ 25 dB.

16QAM modulation correspond to values lower MER 18–19 dB, optimally ≥ 19 dB.

Higher demands MER if 64 QAM is the number of bits required for transmission, wherein the transmission of one bit is needed to two states ($\log 0$, $\log 1$). The n bits are needed m modulation states according to the following formula:

$$nm^2$$

The main advantage lies in the multistate modulation bandwidth (the reserve), or vice versa, with the same bandwidth, it is possible to increase the baud rate.

Multistate modulation has the disadvantage that the signal becomes more sensitive to interference and more difficult to identify the symbol. Therefore, they are also subject to higher demands on the quality of the transmitted and received signal is required and a larger signal to noise ratio at the input of the demodulator in comparison with simpler modulation (FSK, PSK, etc.). [6]

Modulation	4QAM (QPSK)	16QAM	32QAM	128QM	256QM
Number of states	4	16	32	128	256
Number of bits per state	2	4	5	7	8

Max. transmission speed [Mbit/s]	56	112	140	196	224
Real transmission speed [Mbit/s] Bandwidth Occupancy 1,2 without FEC	47	93	117	163	187
Required distance of S/N v dB on demodulator without FEC for error rate 10e-6	13.6	20.4	23.5	26.4	28.4

Table 1 Parameters of particular modulations in required distance S/N

In addition, modulation error rate (MER) is an important measurement of other values DVB-T signal:

- The level of signal reaching the maximum level at 40–80 dB μ V antenna
- CBER – bit error rate before correction (2.0E-4) and a lower
- VBER – bit error correction ($\leq 9.0E-5$) is closely related to CBER.
- Envelope (spectral analysis) DVB-T signals
- Impulse response (echo) when the transmitter and signal reception occurs obstacle, such as a hill, etc.

In particular, the values of CBER and VBER depends stability of signal reception. From the measurements and the practical operation of DVB-T for three different STB from different manufacturers, it was found that all captured channels showed a steady income without downtime (kostečkovani) except K 46. [5]

List of transmitters and captured individual channels

23 – transmitter Javořina, Nove Mesto nad Vahom, Czech coded programs MUX4, vertical polarization, Pay

24 – transmitter Kahlenberg Vienna, Austria MUX1, horizontal polarization

25 – transmitter Zlin – thick mountain MUX3

29 – transmitter – Devin Mikulov, Czech MUX1, horizontal polarization

33 – transmitter Zlin – fat hora, Czech MUX1, horizontal polarization

34 – transmitter Kahlenberg Vienna, Austria MUX2, horizontal polarization

35 – Sklatica transmitter (local MUX), Slovakia

40 – transmitter Brno – Czech Kojal MUX2, horizontal polarization

41 – Fort transmitter Hungarian – Rovnina, Czech MUX7, horizontal polarization

42 – Fort transmitter Hungarian – Rovnina, Czech MUX4, horizontal polarization

46 – transmitter Hodonin – Kaplansky, Czech MUX4, horizontal polarization

49 – transmitter Zlin – fat hora, Czech MUX2, horizontal polarization

55 – Transmitter New Town n / weighting Javorina, Slovak MUX1, vertical polarization

- 56 – Transmitter New Town n / weighting Javorina, Slovak MUX2, vertical polarization
- 57 – Transmitter New Town n / weighting Javorina, Slovak MUX3, vertical polarization
- 59 – transmitter Brno – Czech Kojal MUX3, horizontal polarization

References

1. DIPOL Týdenní přehled – TV a SAT TV, CCTV, WLAN [online]. 1996-2013 [cit. 2010-06-14]. Dostupne z WWW: <http://newsletter.dipolnet.cz/dipol_tydenni_prehled_-_tv_a_sat_tv_cctv_wlan_inf_dipo_2010_24.htm>.
2. Měřicí přístroj Televes H45 [online]. 2000-2013 [cit. 2012-04-15]. Dostupne z WWW: <<http://www.parabola.cz/clanky/4621/merici-pristroj-televes-h45/>>.
3. Jak funguje kvadrurní amplitudová modulace [online]. 2002-2013 [cit. 2009-11-02]. Dostupne z WWW: <<http://www.internetprovsechny.cz/jak-funguje-kvadrurni-amplitudova-modulace/>>.
4. Měření digitálních signálů DVB-T [online]. 2010 [cit. 2010-04-22]. Dostupne z WWW: <<http://www.profidigital.cz/homepage/56-mereni-digitalniho-signalu-dvb-t.html>>.
5. Jak měřit DVB-T? [online]. 1998 [cit. 2009-12-01]. Dostupne z WWW: <<http://www.komsat.cz/aktualita/jak-merit-dvb-t>>.
6. Metody a způsoby měření parametrů digitálních signálů DVB-T [online]. 1999-2001 [cit. 2006-04-03]. Dostupne z WWW: <http://www.urel.feec.vutbr.cz/web_pages/projekty/clanky/mereni_dvb-t.htm>.
7. FAQ: Televizní přijímače [online]. 2013 [cit. 2013]. Dostupne z WWW: <http://www.videoprogress.cz/faq_tv.php>.
8. JIŘI PROCHAZKA: Interaktivní mapa vysílačů [online]. 2009 [cit. 2014]. Dostupne z WWW: <<http://www.mapavysilacu.cz>>.

“SMART HOUSE” CONTROL USING WIRELESS COMMUNICATION CHANNEL

Egunov V.A., Al-Saadi H.A.

Volgograd, Volgograd State Technical University

This work is devoted to organization of "smart houses" - automated houses controlled by computerized systems. One type of organization management system "smart house" using a wireless communication channel, based on ZigBee technology is investigated.

Keywords: smart house, wireless link, network ZigBee, module XBee.

Smart house - modern automated house, organized for the convenience of living people using high-tech devices. A "smart house" should be understood as a system that should be able to recognize specific situations occurring in the building, and appropriately respond to them: one system can control the behavior of others in advance elaborate algorithms. The main feature is the integration of intelligent building separate subsystems into a common managed complex. An important feature of the " smart house ", which distinguishes it from other methods of organization of living space, is that it is the most progressive concept of human interaction with the living space when a person with a single command sets the desired setting, and is automatic in accordance with the external and internal conditions sets and monitors the operating modes of all engineering systems and appliances.

During execution of the initial phase of the project specialized literature analysis was performed. As an initial project was designed sensor network management system, built on

technologies 1-wire. For these purposes was used sensor for measure the temperature, motion sensor and charge AT91SAM9 as coordinating center operates under a system of Linux. Software, such as 1 –wire driver, the server part of the program that controls the system in automatic mode, the Web serve were loaded to this embedded system. Web-site that reflects the state of the sensors and the current list of devices was created to facilitate the system management. Several options for managing the system were offered.

The main disadvantage of the developed system is the presence of a wired connection. Wired communication suggests laying a large number of cables, which certainly reduces the performance management system as a whole, including the reliability characteristics. Furthermore, all functions of the unit in this case are centralized, as shown in [1], during the growth of the complexity of the system leads to a significant increase in performance requirements of the central computer control unit.

It was decided to use the system management of the wireless link, so a comparative analysis of different wireless technologies was made. As a result, it was decided to focus on techniques ZigBee, which inter alia allows the decentralized control function.

The ZigBee specification regulates the stack of protocols for interaction of the network nodes, in which the upper layer protocols use the services provided by the lower level protocols. One of the main ideas of the ZigBee standard development was to provide the possibility of working in the same wireless network devices from different manufacturers. Obviously, to achieve interoperability at the application level ZigBee devices requires a standard language of communication. To achieve this task was developed library ZigBee-clusters ZCL (ZigBee Cluster Library).

ZigBee cluster is similar to a class in object-oriented programming and represents the aggregate of:

- ZigBee device (lighting device dimmer switch , counter) descriptions;
- device attributes (on / off, brightness, counter) descriptions;
- device commands (set the brightness level , take readings , turn on / off) descriptions

The market offers various options for hardware implementation of ZigBee. One of these modules is XBee. Modules are controlled via a standard UART- interface using AT-commands, and have developed enough additional features. XBee-PRO modules offer increased power output and thus a larger radius of action. Modules are available in three versions - with chip antenna with wire antenna and a connector for an external antenna.

As a result, the following control system structure was proposed. The control program (server side) is working on a standard PC, which XBee module is connected via a XBee-USB adapter. Through this module ZigBee-network can be managed. This network includes a certain number of nodes, each controls some segment of house equipment. Each node is a module XBee, coupled with the board Arduino Uno, through which actually occurs poll sensors and final control equipment. For convenience, each such XBee module installed in the Wireless Shield XBee.

References

1. Egunov, V.A. Robotic Complex Central Processing Node Performance Requirements Assessment / Egunov, V.A., Kimosenko, S.I., Andreev, A.E.. // World Applied Sciences Journal (WASJ). - 2013. - Vol. 24, Spec. Issue 24 : Information Technologies in Modern Industry, Education & Society. - pp. 37-42.

BLOCK IMPLEMENTATION OF ALGORITHMS FOR SOLVING SPARSE SYSTEMS OF LINEAR EQUATIONS WITH THE HIGH-PERFORMANCE COMPUTING TOOLS

Novokshchonov A.A., Nasonov A.A., Egunov V.A.
Volgograd, Volgograd State Technical University

The possibility of using vector instructions SSE and AVX CPUs in solving the systems of linear equations, and the possibility of using parallel computing with OpenMP are considered.

Keywords: SSE, AVX, SLAE, Vectorization, SIMD

Solving systems of linear algebraic equations - one of the major problems in computational linear algebra. A considerable part of numerical methods for solving linear and nonlinear problems involves solving systems of linear equations as an elementary step in the corresponding algorithm. Computing machinery development allowed to move from simple to more complex models, in the form of differential equations in partial derivatives and their discrete analogs on the grids. This transition led to the need of solving large sparse systems of linear algebraic equations with matrices of irregular structure. Systems appearing in practice are often sparse i.e. they contain a large number of zero elements, as well as have a large number of unknowns (for example, more than 1000 for the numerical solution of two-dimensional and three-dimensional problems of mathematical physics). Therefore, their solutions require significant technical resources, because the calculations take quite a long time. Using high-performance computing tools will reduce the cost of calculations. By these means solving SLAE algorithm can be optimized to obtain a more efficient algorithm (by the runtime).

In this paper LU-decomposition is used as a method of solving SLAE. Matrix of coefficients is partitioned into upper and lower triangular matrix. Since the matrix is sparse, it is more convenient to be stored in CSR (Compressed Sparse Rows) format. It is one of the most common and it represents a matrix in the form of three arrays: an array of values, an array of column numbers of these values and array of indexes of the beginning of the rows in the array of column numbers. Specifying storage matrices in this format, it is possible to reduce the amount of stored data. Sparse matrix elements can be not only numbers, but also small blocks (matrices). When solving SLAE, instead of multiplying number on number, a matrix-matrix multiplication can be obtained. Thus, in solving SLAE algorithm it is necessary to use algorithms for multiplication of small matrix-matrix or matrix-vector [3]. Those are functions AXPY and DOT of basic linear algebra subroutines (BLAS). For example, block AXPY is a direct generalization of point operation AXPY:

$$Y += X * A,$$

where A is a square matrix of size N x N, a rectangular matrix of X and Y have the dimension M x N, where M - the number of the rows in the matrix, N - the number of the columns. Block DOT is similar AXPY excepting a pre transpose of the matrix A.

The dimensions of these small matrices can vary depending on the type of the task. For solving SLAE of large dimension these "microalgorithms" of multiplication of small matrices can be invoked a huge number of times. By optimizing these microalgorithms, we increase the efficiency of the whole algorithm.

The first step of optimizing is using vector instructions of processor in microalgorithms. Now virtually all general-purpose microprocessors present sets of short vector instructions. This is an important architectural innovation of recent decades, which can significantly increase the processor performance in multimedia and computational problems

in which there is a data-level parallelism. Currently one of the most common methods of introduction of vector instructions in the program code is to use assembler code or the calls of special library functions (intrinsics). It is the most effective in terms of performance of the final code, however, it leads to increasing the complexity of development.

To perform vectorization, we can assume some degree of formalization that is necessary to fill the vector registers, perform with some vector operation, obtain the vector result and then disband this vector result and write in those memory cells in which this result should be. A typical vector instruction is an operation on two vectors in a memory or in the registers of a fixed length. These vector registers can be loaded from memory either in a single operation or in parts.

New technologies allowing to use vectorization add new registers and new instructions. For example, Pentium III added technology SSE (Streaming SIMD Extensions), which added to the MP 8 128-bit registers (XMM0-XMM7) and 70 new instructions including those for working with real numbers. However, although initially each register is treated as two values with a floating point of double precision ($2 * 64\text{-bit}$), operations can be applied to virtually all types, "fit" in 16 bytes. This means for example that there is an opportunity to add or multiply simultaneously two operands of four floating point single precision numbers with only one instruction, two – with double, two 64-bit integer, 16 8-bit integers, etc. Thus, to obtain the maximum benefit from the SSE, you should use such data structures that fit to the limit into these 128-bit registers.

Advanced Vector Extensions (AVX) – the extension for the x86 system instructions for Intel and AMD microprocessors, offered by Intel in March 2008. SIMD vector registers width increases from 128 (XMM) to 256 bits (registers YMM0-YYY15). Existing 128-bit SSE instructions will use the low half of new YMM registers without changing the high part. New 256-bit AVX instructions are added for working with the YMM registers. AVX instruction set contains analogues of 128 bit SSE instructions for real numbers. In this case, unlike the original, saving of the 128-bit result will null the upper half of the YMM register. 128-bit AVX instructions retain other advantages of AVX, such as new coding scheme, three operand syntax and unaligned memory access. It is recommended to abandon old SSE instructions in favor of the new 128-bit AVX instructions, even if two operands are enough. Due to the increasing size of the registers, two operands of eight numbers with single precision floating point can be multiplied with just one instruction, four – with double etc.

Therefore, it is advantageous to use different instructions for various sizes of blocks (small matrices). Optimal results are obtained when one row of the matrix is placed in one vector register. In other cases it is necessary to use additional functions of mixing, horizontal adding etc. When multiple block sizes are not multiple of 2, it is necessary to supplement the correct size with insignificant zeros.

For example, consider a microalgorithm of multiplication of small 4×4 matrices with double precision (double). In the initial implementation, it is the usual multiplication cycle:

```
for (int i=0; i<4; i++){
    for (int j=0; j<4; j++){
        double c = _cmatr[i*4+j];
        for (int k=0; k<4; k++)
            c += _amatr[k*4+i] * _bmatr[k*4+j];
        _cmatr[i*4+j] = c;
    }
}
```

Here _cmatr - resulting matrix, _amatr, _bmatr - multiplied matrices.

In this case, it is good to optimize the code using intrinsics AVX. The algorithm can be written in the following form:

```

__m256d a, b[4], c;
int i,j;
for (j=0,i=0; j<4; j++, i+=4)
    b[j] = _mm256_load_pd(_bmatr+i);
for (i=0; i<4; i++){
    c = _mm256_load_pd(_cmatr+i*4);
    for (j=0; j<4; j++){
        a = _mm256_broadcast_sd(_amatr+i+j*4);
        c = _mm256_add_pd(_mm256_mul_pd(a, b[j]), c);
    }
    _mm256_store_pd(_cmatr+i*4, c);
}

```

SSE algorithm is well suited for 4x4 matrix multiplication with single precision:

```

__m128 a, b[4], c;
int i,j;
for (j=0,i=0; j<4; j++, i+=4)
    b[j] = _mm_load_ps(_bmatr+i);
for (i=0; i<4; i++){
    c = _mm_load_ps(_cmatr+i*4);
    for (j=0; j<4; j++){
        a = _mm_set1_ps(_amatr[i+j*4]);
        c = _mm_add_ps(_mm_mul_ps(a, b[j]), c);
    }
    _mm_store_ps(_cmatr+i*4, c);
}

```

Comparing the results at different compilers almost triple acceleration was obtained (on average) compared with the initial implementation.

The second step of the algorithm optimization should be the introduction of OpenMP directives so as to conduct calculations on multiple cores. Since repeated calculations are independent, the result of parallelization is supposed to be the growth of acceleration in several times (depending on the number of cores).

These approaches to the optimization algorithm for solving systems of linear equations will reduce the computation time and make better use of available technical resources.

The work was commissioned by the engineering company "Tesis". Results of the study will be used in solving the system of linear equations in software package FlowVision [2].

References

1. Intel® Intrinsics Guide [Электронный ресурс]. URL: <http://software.intel.com/en-us/articles/intel-intrinsics-guide>.
2. Overcoming of Barrier between CAD and CFD by Modified Finite Volume Method [Text] / Aksenov A., Dyadkin A., Pokhilko V. // Proc. 1998 ASME Pressure Vessels and Piping Division Conference, San Diego, ASME PVP-Vol 377-1, 1998.
3. Kon'shin I.N., Sushko G.B., Kharchenko S.A. Trekhurovnevaya MPI+TBB+CUDA parallel'naya realizatsiya blochnogo iteratsionnogo algoritma resheniya SLAU dlya melkoblochnykh nestrukturirovannykh razrezhennykh matrits. Trudy Mezhdunarodnoi superkomp'yuternoi konferentsii "Nauchnyi servis v seti Internet: poisk novykh reshenii" (17-22 sentyabrya 2012 g., g. Novorossiisk), 2012, C. 522-528.

FPGA AS COPROCESSORS IN SOLVING PROBLEMS OF LINEAR ALGEBRA

Egunov V.A., Artyukh S.V.

Volgograd, Volgograd State Technical University

Using of FPGAs as coprocessors for solving linear algebra problems is discussed. The development of devices using HDL languages and high-level design tools FPGA is presented. It is described the process of developing software to communicate with the FPGA via PCI-E.

Keywords: design FPGA, coprocessor, Householder transformation, linear algebra.

Solving systems of linear algebraic equations, computing determinants, singular value decomposition, finding eigenvalues and eigenvectors of matrices, matrix inversion are important objectives in the field of scientific computing, and in solving huge count of applications.

As a basic matrix transformation for solving linear algebra and creation on its base of high-performance computing facilities, proposed QR-decomposition. Evaluation of the operating complexity and time for solving problems of this transformation with respect to other basic matrix transformations.

Problems of this type have a high complexity and their solutions require significant time costs [1]. To solve this problem, there are several approaches: the use of graphics cards as coprocessors, parallelizing calculations on multicore processors and multiprocessor systems, and the use of programmable logic integrated circuits as a coprocessor.

In this paper authors considers the latter approach. Currently, this approach is widely used by leading companies, particularly Intel, the implementation of embedded systems.

The first two approaches are difficult to find an application, for example, in the management of mobile robot [2], so it was decided to use the FPGA as a coprocessor. This method has some advantages and disadvantages.

FPGA contains several million gates, which allows getting results with a high speed. You can also improve performance by implementing a pipelined version of the algorithm.

However, implementation of algorithms on FPGA is consuming task. The implementation of the algorithm is divided into several stages. The first stage - a hardware implementation of the algorithm. It uses hardware description languages, the most popular is the Verilog HDL and VHDL. Also possible to use additional software. For example, the data processing algorithm can be implemented in the programming language C, and then using LegUp generates software code in Verilog. This conversion allow save time because to write the implementation of the algorithm in C, is much easier than on the hardware description language.

The second stage is selection of the driver for work with the board. In this work it was decided to use WinDriver. This software allows you to quickly get to work with the board, not thinking about writing drivers.

The final step is the implementation of the program, which will transmit and receive data from the FPGA.

To communicate with the FPGA used interface PCI-E. Implementing of data exchange at a high-speed interface, you can increase speed data transfers.

Thus, proposed several ways to improve the performance calculations of the basic linear transformations that have a positive impact on the work of the basic algorithm, for example, at a speed of decision-making mobile robot when moving in space.

Authors used algorithm of multidimensional reflection as matrix transformation.

On the first stage was designed language Verilog code for this conversion. Below is a portion of the file hausholder.v.


```

module hausholder(clk, start, iteration, a, b, c, d, tA, tB, tC, tStart, complete);
    parameter M = 32;
    parameter F = 15;
    input clk;
    input start;
    input[M-1:0] a;
    input[M-1:0] b;
    input[M-1:0] iteration;

    -----
    -----

    always @(posedge completeDiv)
        begin
            if(start == 1'b1 && regComplete == 1'b0)
                begin
                    regOutputA = -regA + (regSignB == 1'b0 ? tempBi1 : -tempBi1)
                        + (regSignC == 1'b0 ? tempCi1 : -tempCi1)
                        + (regSignD == 1'b0 ? tempDi1 : -tempDi1);
                    regOutputB = regB - (regSignB == 1'b0 ? tempAi1 : -tempAi1);
                    regOutputC = regC - (regSignC == 1'b0 ? tempAi1 : -tempAi1);
                    regOutputD = regD - (regSignD == 1'b0 ? tempAi1 : -tempAi1);
                end
            end
        end

    -----
    -----

endmodule

```

In the second phase was developed program in C language using FPGA firmware corresponding Verilog-code. Data exchange with the FPGA, as mentioned earlier, is carried out via PCI-E, as the driver used WinDriver. Below is a snippet of code that uses FPGA.

```

void Execute(UINT32 A, UINT32 B, UINT32 C, UINT32 D)
{
    unsigned int target_address = 0x0000;

    //Input values
    device->WriteValue32(A, target_address + 0 * sizeof(UINT32));
    device->WriteValue32(B, target_address + 1 * sizeof(UINT32));
    device->WriteValue32(C, target_address + 2 * sizeof(UINT32));
    device->WriteValue32(D, target_address + 3 * sizeof(UINT32));

    //Start signal
    device->WriteValue32(1, target_address + 4 * sizeof(UINT32));

    //Result
    UINT32 Res = device->ReadValue32(target_address + 0 * sizeof(UINT32));

    printf("a = %d\nb = %d\nc=%d\nd=%d\nModule = %d,%d", A, B, C, D,
        GetIntegerPart(Res), GetFractionalPart(Res));
}

```

```

bool Device::WriteValue32(UINT32 val, unsigned int address)
{
    DWORD dwStatus = WDC_WriteAddr32(hDev, 0, address, val);
    if (WD_STATUS_SUCCESS != dwStatus)
    {
        return false;
    }
    return true;
}

UINT32 Device::ReadValue32(unsigned int address)
{
    UINT32 Res;

    DWORD dwStatus = WDC_ReadAddr32(hDev, 0, address, (UINT32*)&Res);
    if (WD_STATUS_SUCCESS != dwStatus)
    {
        return 0;
    }
    return Res;
}

```

As FPGAs used Arria II GX EP2AGX125EF35C4. In the future, we plan to continue research, in particular the use of OpenCL to generate Verilog-code and the use of more powerful FPGA.

References

1. Egunov, V.A. Robotic Complex Central Processing Node Performance Requirements Assessment / Egunov V.A., Kirmosenko S.I., Andreev A.E.. // World Applied Sciences Journal (WASJ). - 2013. - Vol. 24, Spec. Issue 24 : Information Technologies in Modern Industry, Education & Society. - pp. 37-42.
2. Egunov, V.A. Ob ispol'zovanii lineinykh preobrazovaniy v upravlenii mobil'nym robotom / Egunov, V.A., Artyukh, S.V. // Izvestiya VolgGTU. Seriya "Aktual'nye problemy upravleniya, vychislitel'noi tekhniki i informatiki v tekhnicheskikh sistemakh". Vyp. 17 : mezhvuz. sb. nauch. tr. / VolgGTU. - Volgograd, 2013. - № 14 (117). - C. 82-84.

OPTIMIZATION OF BLOCK REALIZATION OF ALGORITHMS OF LINEAR ALGEBRA USING SIMD-INSTRUCTIONS OF THE PROCESSOR ON THE EXAMPLE OF INTEL® MIC SIMD.

Nasonov A.A., Novokshchonov A.A., Zavyalov D.V.
Volgograd, Volgograd State Technical University

The algorithms of linear algebra optimized using SIMD-instructions was developed and tested. It was developed in language C ++, with using XEON PHI SIMD. The compiler icpc (ICC) 14.0.1 was used, testing was held on the Intel Xeon Phi coprocessor and showed average acceleration approximately by 2-3 times.

Keywords: SIMD, linear algebra, Xeon Phi

For a long time microprocessors evolve toward the use of a large number of parallel operation. That is piping, a superscalar, vector operations - all this parallelism levels when we try to execute at the same time some arithmetical and logical actions. Vectorization also can be read as technology of simultaneous execution of instructions. Usually it call "parallelism of data" and imply changeover sequentially executed scalar operations by operations over a set of data.

Now practically all microprocessors of general purpose support sets of vector instructions. In the last decades this architectural innovation gave the significant increase in productivity on tasks of multimedia and computing character, which have a parallelism by data.

Usually vector instructions are introduced into the code by means of special library functions (intrinsics) or assembly code. This approach allows to increase productivity of a finite code, but, on the other hand, increases complexity of development.

In this work we will consider optimization block synthesis of the operation AXPY.

AXPY - - the operation of the 1st level of basic linear algebra Subprograms (BLAS). Represents a combination of a scalar multiplication and addition of vectors,

$$Y = \alpha * X + Y$$

where α is scalar, X and Y are vectors.

Usually for specifying of the data type, used in the operation, add the prefix. Thus, it is possible to select 4 main subtypes of the operation AXPY:

- 1) SAXPY – for real numbers of single precision
- 2) DAXPY – for real numbers of a double precision
- 3) CAXPY – for complex numbers of single precision
- 4) ZAXPY – for complex numbers of a double precision

It is possible to give the following code as the simplest implementation of the operation SAXPY:

```
void saxpy(float* x, float* y, int n, float a) {
    int i;
    for (i = 0; i < n; ++i)
        y[i] += a * x[i];
}
```

Block operation of AXPY represents direct synthesis of the point operation AXPY[4]:

$$Y += X * A,$$

where A instead of a scalar in the point version represents a square matrix of the N x N, and rectangular matrixes of X and Y have dimensionality of M x N, где M – number of rows in the matrix, N - number of columns.

Generally for execution vectorization we are required to fill in a vector register data from memory (in one or more operations), to execute on these data any vector operations and upload data from this register to a memory location where the result should be stored.

The new technologies, allowing to use vectorization, add new registers and instructions. So in Pentium III was added technology SSE (Streaming SIMD Extensions), which added to the microprocessor eight 128-bit registers (XMM0-XMM7) and 70 new instructions. SSE2, SSE3, SSE4, SSE4.1, SSE4.2, AVX, AVX-512 – further extension of this idea.

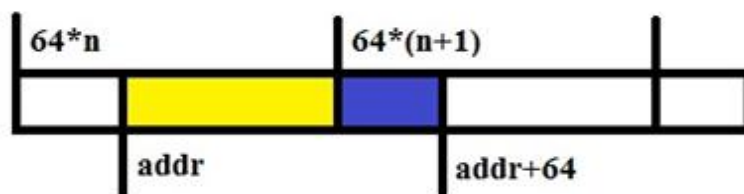
In the software packages intended for high-precision simulation modeling, operations over vectors, matrixes, and as their analogs for units of matrixes and vectors often are used. Algorithms of calculation are executed over a large number of data, and from them sufficient high-speed performance is required. In similar cases implementation straight solution is not the best option. It is possible to tear cycles manually is will give an acceleration, but only

insignificant.

One of options of vectorization with use intrinsics is AVX-512 (or Intel MIC SIMD). These vector instructions are available in the Intel® Xeon Phi™ coprocessor. As appears from the name in this case registers of long 512 bits are available to us. Use of these registers and instructions in case of small dimensionalities of units/matrixes unreasonably. But on the units which vector occupy a register half, the register and more, an acceleration can already be about 4-5 times. This result already significantly differs from last technologies, but too capacious registers superimpose the restrictions for use. This problem could be solved a call of the SSE and AVX commands, but, unfortunately, Intel® Xeon Phi™ doesn't support these technologies.

As it would be desirable to mark some features of operation of Intel MIC SIMD with not aligned memory. In the SSE and AVX technologies for loading / unloading of data the `_mm_load_ps/_mm_store_ps` functions and `_mm256_load_ps/_mm256_store_ps` respectively are used. Their options for operation with not aligned memory look as `_mm_loadu_ps/_mm_storeu_ps` and `_mm256_loadu_ps/_mm256_storeu_ps`. But in Intel MIC SIMD the situation is a little other. For operation with the aligned memory of function as are similar to the predecessors `_mm512_load_ps/_mm512_store_ps`. And here functions `_mm512_loadu_ps/_mm512_storeu_ps` for operation with not aligned memory in present family the coprocessor aren't implemented yet. But it is possible to work with it nevertheless, using a pair of functions for each of the operations (loading / unloading) - `_mm512_loadunpacklo_ps` + `_mm512_loadunpackhi_ps` / `_mm512_packstorelo_ps` + `_mm512_packstorehi_ps`.

Picture 1 shows the operation of these functions. `_mm512_loadunpacklo_ps (addr)` load register the yellow part (starting at `addr` to the first address aligned on 64-byte) and `_mm512_loadunpackhi_ps (addr + 64)` load register the blue part (starting with the first address aligned to 64 bytes after the address `addr`).



Pic. 1

Below is a verbal description of the algorithm that implements the operation for the dimension $N = 4$, $M = 4$.

1. Loading pointers to the original matrix with the required offset.
2. Load values of the first two rows of the matrix A in 1 ZMM register.
3. Distribute the data from these two lines of four other ZMM registers.
4. Load values of the first two rows of the resulting matrix C in 1 ZMM register.
5. Load values of the first row of the block vectors B in 1 ZMM register four times.
6. Multiply the resulting register of unit vector to first register with the data of the matrix A
7. Repeat steps 5 - 6 for the remaining three registers with the data from the matrix A and the three lines in the block vectors B.
8. Upload half of the values obtained from ZMM register addresses in the resulting matrix.
9. Repeat steps 2 - 8 for subsequent rows of the resulting matrix C and rows of the matrix A.

This implementation allowed to get acceleration in 3.5 times.

Concluding, it should be noted that the optimization of linear algebra algorithms using vectoring calculations yielded good results. Should take into account the time that the algorithms are not used such approaches to parallelization as OpenMP or MPI. Using these technologies should allow to improve the performance of optimized algorithms.

The work was commissioned by the engineering company "TESIS". Results of the research will be used in solving SOLE algorithms in software package FlowVision [3].

References

1. Intel® Intrinsics Guide [Электронный ресурс]. URL: <http://software.intel.com/en-us/articles/intel-intrinsics-guide>
2. Intel® Xeon Phi™ Coprocessor System Software Developers Guide [Электронный ресурс]. URL: <http://software.intel.com/en-us/articles/intel-xeon-phi-coprocessor-system-software-developers-guide>
3. Overcoming of Barrier between CAD and CFD by Modified Finite Volume Method [Text] / Aksenov A., Dyadkin A., Pokhilko V. // Proc. 1998 ASME Pressure Vessels and Piping Division Conference, San Diego, ASME PVP-Vol 377-1, 1998.
4. Kon'shin I.N., Sushko G.B., Kharchenko S.A. Trekhurovnevaya MPI+TBB+CUDA parallel'naya realizatsiya blochnogo iteratsionnogo algoritma resheniya SLAU dlya melkoblochnykh nestrukturirovannykh razrezhenykh matrits. Trudy Mezhdunarodnoi superkomp'yuternoi konferentsii "Nauchnyi servis v seti Internet: poisk novykh reshenii" (17-22 sentyabrya 2012 g., g. Novorossiisk), 2012, C. 522-528.

MATHEMATICAL MODEL AND pc PROGRAM FOR THE CALCULATION OF THE MACHINED FINISHED SURFACE ROUGHNESS IN TURNING THE STAINLESS STEELS WITH ADVANCE PLASTIC DEFORMATION

Bondarev A., Ingemansson A., Krainev D.
Volgograd, Volgograd State Technical University

A mathematical model which describes the regularities of formation a surface roughness in turning with advance plastic deformation (APD) on the workpiece surface has been created. The regression analysis has allowed revealing the dependence of the response function and the influence of each factor on the function. The formula for the calculation of an average arithmetic average roughness height Ra expanding possibilities of the cutting with APD application in machining practice has been offered.

Keywords: turning of stainless steels, advance plastic deformation, mathematical model for calculation surface roughness.

Improving the efficiency of material processing, particularly the hard-to-tread materials is the actual problem of modern engineering. This problem can be solved in different ways: by increasing the cutting tool integrity, the process efficiency and by the workpiece quality. The usage of modern information technologies should become one of the methods for the problem solving. The cutting with advance plastic deformation (APD), which combines the preliminary stages of the two-dimensional plastic deformation and of the subsequent stock removal with a cutting tool is a combined treatment method for gaining a comprehensive efficiency improvement on the directions listed above. The changes of the physical and mechanical properties of the processed material after the APD stage cause the formation of such conditions of physical processes in the cutting zone, which help to reduce

the chipmaker work, the load on the cutting edge and to improve the conditions for the contact interaction and for the formation of a new surface.

The APD turning the corrosion-resistant steels and the difficult-to-cut steels on the treated surface has been found to allow improving the microprofile of the obtained surface significantly and increasing the productivity of the cutting process [2], [3], [4]. The APD turning the corrosion-resistant steels of the ferrite grade, of the martensitic-ferritic grade and of the martensite grade is accompanied by the decrease of the arithmetic average roughness height Ra up to 2 times in comparison with the traditional treatment. The reserves of a significant productivity increase of the cutting process by obtaining similar values of the parameter Ra at higher values of the sliding feed of the deformed metal have been revealed.

It is necessary to create a mathematical model showing the effect of the basic processing parameters on the quality of the resulting surface for researching the patterns of the surface roughness forming of a corrosion-resistant steel workpiece in turning with APD, for the prediction results of the process and for the capability enhancement of the practical application of the cutting method in the light of its advantages. Our research task is to develop a PC program for calculation the parameters of the traditional cutting and cutting with APD based on this model.

The research has been carried out for precision turning (the cutting depth $t = 0,5$ mm) corrosion-resistant steel 20X13 (the delivery status, the rolled section, $\sigma_{0,2} = 440$ MegaPascal). Analogs of 20X13 are 420 and S42000 (USA) and X20Cr13 (Germany). The tool was presented as the replaceable multifaceted hard-alloy plates in form W ($\alpha = 0^\circ$ (ISO 1832-1991)); the nose radius is $r = 0,8$ mm. Processing was performed without cutting fluids. As the factors that determine the value of the response function (Ra) were selected: the cutting speed, the thermal conductivity of the tool material, the feed rate and the ratio APD.

$$R_{ADP} = \frac{h_{def}}{t}, \quad (1)$$

where h_{def} – the depth of the deformed surface layer, mm;
 t – the cutting depth, mm.

The natural and dimensionless values of the factors accepted in our research are presented in Table 1.

The effect of the APD machined surface on the turning process has been discovered to change. The increase in R_{ADP} to some value is accompanied by reduction of the cutting force, reaching the minimum at a certain relation of the depth of the deformed surface layer to the cutting depth (for the maximum efficiency in the machining of steel 20X13 this ratio equals 3.2). Further growth of the R_{ADP} reduces the efficiency of the process. The bottom level of the coefficient R_{ADP} is equal to zero (the cutting without advanced plastic deformation), but for the purpose of the model creation is accepted 0,001. It allows carrying out some additional calculations, including logarithming. At this assumption the depth of the deformed metal layer would be equal to 0,0005 mm and that is insignificant. Thus, this convention does not affect the result of the regression analysis.

For the research purposes the following most often applied mathematical models are accepted: the additive (linear) model and the multiplicative (sedate and indicative) models.

Table 1 - Natural values of the factors

Factors	Designation	Natural values		
Normalized value (level)	Z_i	-1	0	1
Cutting speed, m. per min	X_1	90	1 35	180

The thermal conductivity of the tool material, Wt/m*K	X_2	11 (TN20)	27 (T15K6)	50 (VK6)
Feed, mm/ rev	X_3	0,083	0,166	0,256
APD coefficient R_{ADP}	X_4	0,001	1.6	3.2

The problem of the usage the mathematical methods of the experiment planning consists in obtaining the mathematical description of the response function in form of a mathematical model, that connects this function with various factors. The data sufficiency depends on a type of the model and on the quantity of considered factors (four in this research) and is equal to:

$$\text{– for the additive model: } k_{\min} = 2^n = 2^4 = 16; \quad (2)$$

$$\text{– for the multiplicative models: } k_{\min} = 3^n = 3^4 = 81, \quad (3)$$

where k_{\min} – the number of independent trials with full factorial experiment;

n – the number of factors.

In modeling the formal assessment of the dependence existence of the response function from each of the considered factors has been received based on the pair correlation coefficient [5] which shows the existence probability of the linear relationship between two statistical selections of equal volume. The interrelation existence between the factors is also estimated approximately.

The carried-out calculations showed that the chosen factors are pairwise relatively independent and each of them has impact on the size of the response function (Table 2). The multifactor regression model has been constructed for an assessment of the efficiency of each factor.

In modeling the steps as described below are followed.

Table 2 - Calculated values of pair correlation coefficients

Compare values		Value coefficient steamy correlation	Existence linear Depending on	Character linear Depending on
$F_1 (v)$	$R (Ra)$	0.1051	Rare	Increasing
$F_2 (\lambda)$	$R (Ra)$	0.3651	Rare	Increasing
$F_3 (s)$	$R (Ra)$	0.6505	Most probably	Increasing
$F (R_{ADP})$	$R (Ra)$	-0.4810	Probably	Decreasing
$F (v)$	$F_2 (\lambda)$	0.0000	Not exist	-
$F (v)$	$F_3 (s)$	0.0000	Not exist	-
$F (v)$	$F (R_{ADP})$	0.0000	Not exist	-
$F_2 (\lambda)$	$F_3 (s)$	0.0000	Not exist	-
$F_2 (\lambda)$	$F (R_{ADP})$	0.0000	Not exist	-
$F_3 (s)$	$F (R_{ADP})$	0.0000	Not exist	-

The correct estimation of the influence factors on the character and the amount of the response function is possible provided by a comparability of the values of all factors and of the actual objective function. As the considered factors have various scales, rationing of the basic data has been carried out according to the rules [1, 5] corresponding the regression models of various specifications (Table 3).

Construction of the model after normalization involves the following, independent of its specification, sequential calculations [1, 5]: the calculation of the regression coefficients for the selected factors, the calculation of the regression coefficient, which determines the effect of random factors, the calculation of the normalized values of the response function, the calculation of Student's criterion, which determines the essential difference between the regression coefficients and zero, assessment of statistical significance and of the efficiency of the factors considered (for linear, power-mode and exponential models of all the analyzed factors are statistically significant), the calculation of the predicted normalized values of the response function based on the statistical significance of the factors, the calculation of the recovered (real) values of the response function for the normalized series, assessment of the adequacy of the constructed models in F-criterion size.

We tabulate the most essential results to analyze the received mathematical models (Table 4).

Table 3 - Normalization of the factor values and of the response function for constructing the power-law model

№	X_0	Normalized values					Natural values				
		Factors				Function	Factors				Function
		$X_1(v)$	$X_2(\lambda)$	$X_3(s)$	$X_4(R_{ADP})$	$Y(Ra)$	$X_1(v)$	$X_2(\lambda)$	$X_3(s)$	$X_4(R_{ADP})$	$R(Ra)$
1	1	-0.76	-0.87	-0.84	-0.974	-0.283	90.00	11.0 0	0.08 3	0,001	1.50
2	1	0.14 3	-0.87	-0.84	-0.974	-0.192	135.0 0	11.0 0	0.08 3	0,001	1.60
...											
80	1	0,14 3	0,88 9	0,85 6	0,977	0,594	135.0 0	50,0 0	0.25 6	3.2	2.80
81	1	0,78 7	0,88 9	0,85 6	0,977	0,434	180.0 0	50,0 0	0.25 6	3.2	2.50

Table 4 - Comparison of the regression models

Parameter	Model specification		
	Linear	Sedate	Exponential
Assessing the impact of factors			
Accidental factors	- 0.30	- 0.01	-0.01
Cutting speed	0.12	0.06	0.07
The thermal conductivity of the tool material	0.27	0.19	0.20
Feed	0.42	0.37	0.39
APD rate (R_{ADP})	- 0.20	- 0.22	-0.26
Validity of the adequate model, %	99.7	99.9	99.9
Error assessing			
Standard deviation	0,547	0,547	0,547
Table value of F – test	1,861	2,014	2,014
Estimated value of F -test	1,899	2,423	2,189
The average relative error, %	12.73	9.05	9.45

The data analysis allows definite conclusions (Table 4).

The average relative error (the divergence of the Ra values calculated on the model and received by practical consideration) of the linear model exceeds the similar parameters of the sedate and indicative models (12,73 % - the linear model, 9,05 % - the sedate model, 9,45 % - the exponential model). That is a limitation of a method. The random factors impact on the surface roughness is expressed by the corresponding regression coefficient and in the power-mode model and in the exponential model is 0.01 in absolute magnitude, that is negligible. In the linear model, the random factors efficiency is 0.3 in absolute magnitude, which is very important against the accepted factors in investigation. Thus, the sedate model and the exponential model facilitate the further prediction of the surface quality after turning with APD, as they allow definite conclusions that the cutting speed, the thermal conductivity of the tool material, the feed rate and the APD have more significant impact on the rate of a roughness. The comparison between the sedate model and the exponential one shows the accurate likeness of the simulation results. However, the preference should be given to the first model considering the smaller magnitude of error in calculating the objective function.

The regression coefficients of the sedate model and of the exponential model show that the surface roughness after turning with APD is affected by the following factors: the cutting speed, the thermal conductivity of the tool material, the APD, the feed rate in ascending order. With the increase of the cutting speed, there is some increase in the value of the arithmetic mean deviation of the profile (regression coefficient is to about 0.06 for the power-mode model). This objective law is explained by the growth of the instability of the cutting process (namely by the cycling chipmaking, which is specific for the processing stainless steels) with increasing the cutting speed. With increasing the thermal conductivity of the instrument material the surface roughness also deteriorates. This process is explained by the influence of the thermophysical properties of the contact pairs (tool-workpiece) on the character of the physical processes in the cutting zone. The influence of this factor (the regression coefficient 0.19 in the sedate model) is almost three times more than the cutting speed. The application of the APD can improve the quality of a workpiece (the regression coefficient -0.22 in the sedate model). The roughness of the received surfaces is known to get worse (the coefficient of regression +0,37 in the sedate model) with the increase in feed rate.

The values of the response function, received as a result of modeling, and the basic data are displayed in the charts (Fig. 1, 2, 3).



Figure 1 – Assessment of an error of linear model



Figure 2 – Assessment of an error of sedate model



Figure 3 – Assessment of an error of indicative model

On the ordinate axis the values of a roughness R_a indicator in *micron* are indicated and on the abscissa axis the serial numbers of the combinations of the processing modes are indicated. For descriptive reasons, the cut-offs corresponding to an interval of at the error of $\pm 5\%$ of the current value are plotted to the continuous line showing basic data. In the diagram (Fig. 1) the discrepancy between the linear model and the band of the allowed values of the response function is represented graphically. The comparison between the charts of the sedate model and the exponential model (Fig. 2, 3) allows some conclusion that they are sufficiently similar to the original data.

The regressive mathematical model of the impact of the major cutting parameters with APD to measure the arithmetic average roughness R_a of the finished surface can be realized in the form of the following relationship:

$$R_a = 1,33 \cdot V^{0,1} \cdot \lambda^{0,16} \cdot S^{0,4} \cdot K_{ADP}^{-0,04} \quad (4)$$

where V – the cutting speed, m/min ;

λ – the thermal conductivity of the tool material, $Watt/m \cdot K$;

S – the feed, mm/rev ;

R_{ADP} – the coefficient of the APD.

This formula allows calculating the value of roughness in the traditional turning and in the turning with APD, that is predicting the increase of the cutting effect completely at the technique being described and taking this fact into account in the technological machining route. The ranges of the factors variation (e.g., the speeds of $90-180 m/min$), and the processing conditions for the practical application are described above.

For the automatization the determining the arithmetic average roughness height based on the developed mathematical model a PC program for the calculation of the machined surface roughness values in the traditional turning and turning with APD has been created.

The program is designed for defining the value of R_a and the relative level of the efficiency increase of turning to reduce the arithmetic average roughness height when using APD compared with the traditional way for the subsequent adjustment of the base technological process. The program feature is the continued possibilities of determining the APD mode on the treated surface. It depends on the turning parameters and on the given technical conditions of the arithmetic average roughness height (average arithmetic deviation) of the obtained surface profile, on the supplement, on the updates, and on the development of the statistical and mathematical base necessary for the calculation. The screens where the program operation is displayed are presented in Fig. 4 and 5.

The program provides the following functions:

- calculation of the arithmetic average roughness of the finished surface while turning with APD and in the traditional turning;
- the calculation results output;
- the analysis of the consistency between the user-selected modes of treatment and the recommended values;
- enabling the user with the supplement, the data refinement and the development of the statistical and mathematical basis for the calculation of the arithmetic average roughness height of the treated surface while turning with APD and the traditional turning.

Figure 4 – Window of input of basic data

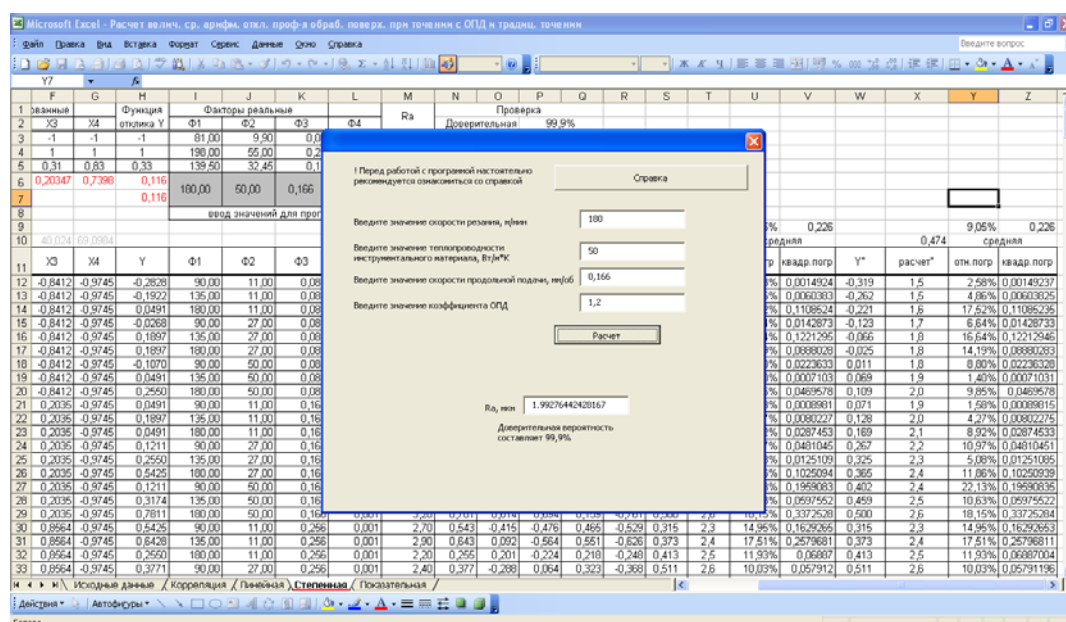


Figure 5 – Window with the calculation results of the size R_a of the processed surface when turning with APD

The proposed device can be used in the practice of mechanical metal processing, in scientific and educational study of the engineering technology and material processing. Thus, a mathematical model describing the regularities of roughness in turning with APD on the treated surface and in the traditional turning has been developed. It allows predicting the arithmetic average roughness height, determining the incremental amount of the cutting efficiency by reducing the value of the R_a parameter of the obtained surface with applying the APD and making the appropriate adjustments to the technological base, including the design phase. The regression analysis has revealed the dependence of the response function and the magnitude of the effect of each factor on it. Based on the regression coefficients the formation of the surface microgeometry after the turning, including the APD, is influenced by the following factors: the cutting speed (0.06), the thermal conductivity of the tool material (0.19), the APD (-0.22), the feed (0.37) in ascending order. All of the factors apart from the APD, increase the arithmetic average roughness height to a variable degree. The application of the APD provides the improved surface quality of the treated workpiece. The multiplicative regression models (the power-mode and the exponential models) reflect the laws of the workpiece surface formation when turning compared to the additive (linear) model more accurately. Based on the results of the regression analysis the multiplicative power-mode model is recognized as the most objective model. It is characterized by a minimum relative error and on the basis of the statistical analysis it is in agreement with the original data quite well. A formula for calculating the arithmetic average roughness R_a has been proposed. It expands possibilities for applying the cutting method with APD in machining practice. In order to automate the determining the value of the arithmetic average roughness height based on the developed theoretical model a PC program for the calculation the machined surface roughness values in the traditional turning and the turning with APD has been created.

Thus, a mathematical model allowing describing the regularities of roughness in turning the corrosion-resistant difficult-to-cut steels with APD on the treated surface has been developed. The regression analysis revealed the dependence of the response function and the magnitude of the effect of each factor on the response function. A formula for calculating the arithmetic average roughness R_a , expanding possibilities for applying in the cutting method

with APD in the practice of machining has been proposed and a program for the PC has been also developed.

References

1. Evdokimov, J. A. Planning and analysis of experiments in solving problems of friction and wear / Yu. A. Evdokimov, V. I. Kolesnikov, A. I. Teterin. - Moscow: Nauka, 1980. - 228 p.
2. Pat. Number 2399460 RF, IPC 23 in 1/00. Method of cutting machining with the advanced plastic deformation / Yu. N. Polyanchikov, P. A. Norchenko, D. V. Krainev, A. R. Ingemansson, L. A. Katchalov, L. S. Angelovskaya; GOU VPO VSTU. - 2010.
3. Improving the quality of the machined surface when turning with advanced plastic deformation / D. V. Krainev, A. R. Ingemansson, A. A. Bondarev, P. A. Azamatov, I. N. Kozachuhnenko / / Mechanical Engineering - the basis of technological development of Russia (TM-2013) Collection of scientific. Art. V int. scientific and engineering. conf., 22-24 May 2013 / South-Western state Uni [et al.] - Kursk 2013. - P. 354-357.
4. Development of a mathematical model of the roughness formation of the finished surface when turning with the advanced plastic deforming / A. R. Ingemansson, N. G. Zaitseva, D. V. Krainev, A. A. Bondarev / / Current trends in metalworking technologies and construction metalworking machines and components: Collection of scientific art. / VPO "Ufa State Aviation Techn. Uni." - Ufa, 2012. - P. 54-60. (Article or conference USATU)
5. Chigirinsky Yu. L. Stochastic modeling in mechanic engineering: Teaching guide / Y. L. Chigirinsky, N. V. Chigirinskaya, Yu. M. Bulls. - Volgograd: VSTU 2002. - 68 p.
6. Improving the efficiency of turning the grained structural carbon and alloy steels in using the advanced ray deformation plasticity / AA Bondarev, P. A. Azamatov, I. N. Kozachuhnenko, A. R. Ingemansson, DV Krainev / / Proceedings VSTU. Series "The progressive technology in mechanical engineering". Issue 9: Collection of scientific. Art. / VSTU. - Volgograd, 2013. - № 7 (110). - P. 11-14.

MODELING OF FORMATION AND GROWTH OF FLAME KERNEL IN SPARK IGNITION ENGINES (SIE)

Avdeuk O.A., Krokhaev A. V., Prihodkova I. V., Prihodkov K. V., Shumskij S.N.
Volgograd, Volgograd State Technical University

A principled approach to the modeling of the initial phase of combustion in SIE from the breakdown of the electrode gap spark plugs is considered. Based on these data explains the influence of some factors on the occurrence of cycle by cycle variability of combustion.

Keywords: spark ignition engines, modeling, flame kernel, cycle by cycle variability.

Interest in forming the initial flame kernel caused by its important role in the process of combustion in spark ignition engines (SIE). Duration of this stage takes a significant fraction of the total time of the combustion process in these types of Internal Combustion Engines (ICE).

By this duration we mean the period from breakdown on the spark plugs to the moment when the size of the flame kernel will become comparable with the integral scale of turbulence, for which the cylinder is determined by the size of the ICE combustion chamber, its shape and geometrical parameters of the intake valve [1, 2]. According to many authors

[3,4] it is the dynamics of flame kernel formation defines cycle-by-cycle combustion variability of the combustion process.

According to most researchers to improve the cyclic stability of the combustion process, which allows improving the lean operating limits, should seek an intensification of development of the combustion process in the initial stage

Experimental study does not allow identifying and analyzing the contribution of individual factors in the formation of cycle-by-cycle combustion variability, so urgent to get the theoretical study of the formation and evolution the initial flame kernel.

Based on original research [5,6] and the results obtained by other researchers [7], we divide the formation of flame kernel depending on the source of energy it receives into three periods.

The first period which we call “spark kernel formation” lasts from the moment of spark discharge prior to the intensive combustion of fuel-air mixtures in the forming flame. During this period using the energy stored in the electric capacity of the secondary circuit elements of the ignition system.

Beyond that the second period during which the formed spark kernel receives combustion energy both from released in the inductive discharge phase, and from combustion of fuel. This period is equal to the duration of the inductive phase of the discharge. After the cessation of the discharge comes the third period, during which the growth of flame kernel only ensured the energy released by the combustion of the fuel. The third period lasts as long as the size of flame kernel will not comparable with the integral scale of turbulence. It is assumed that the burning of the fuel in the second and third periods is subject to the laws of laminar burning [8]. After completion of the third period begins main combustion flowing through the turbulent mechanism.

Consider the first period of the formation of flame kernel - during the formation of the spark kernel which as mentioned above begins from the electrical breakdown of the spark plug. The breakdown of a few nanoseconds formed conductive channel with diameter d_s of about 40 microns [7, 9].

The energy released results in almost instantaneous rise in temperature to a value of about 104 K and pressures up to 102 bar.

At such temperatures, almost all molecules dissociate what consumes a significant portion of energy capacitive at breakdown phase. Thus to increase the thermal internal energy, ie temperature air-fuel mixtures in spark channel consumes only about 50% of the released energy in this phase. This energy can be calculated as:

$$E_{bd} = \frac{C_2 U_{bd}^2}{2}, \quad (1)$$

where C_2 – is a capacity of cells of the secondary ignition circuit and U_{bd} is a breakdown voltage.

In our opinion prior to the expansion of the plasma channel process of the heat supply at this moment can be considered isochoric with the assumption that the thermodynamic parameters of the cross section and length of the channel is constant.

The Law of energy for this process can be written as:

$$U_0 + \frac{C_2 U_{bd}^2}{2} \eta = U_1, \quad (2)$$

where η is a heat efficient of breakdown phase of electric discharge; U_0 - internal thermal energy of fuel-air mixture before spark discharge; U_1 - internal thermal energy of fuel-air mixture after the breakdown of the beginning of the expansion of the plasma channel.

If we accept the hypothesis that the spark channel walls are absolutely hard, we can assume that the mass of the fuel assembly in the channel breakdown persists until the end of the first period of ignition - spark kernel formation period.

Internal thermal energy of fuel-air mixture after the breakdown of the beginning of the expansion of the plasma channel can be written as:

$$U_1 = m_{ch} \cdot c_v(T_1) \cdot T_1, \quad (3)$$

where m_{ch} – mass of the air-fuel mixture on spark kernel and $c_v(T_1)$ – isochoric heat capacity mass presented as a function of temperature.

Statistical treatment of data [10] for the dissociated air given in the temperature range from 1500 to 6000 K allow to represent the $c_v(T_1)$ function as

$$c_v = 0,8855 \cdot \ln(T_1) - 5,6283 \left(\frac{kJ}{kg \cdot K} \right). \quad (4)$$

Due to the lack of reliable data about isochoric heat capacity on temperature over 6000 K obtained dependence has been extrapolated to $T > 6000$ K.

Pressure and temperature of the air-fuel mixture to the top of the plasma channel expansion can be determined based on the dependence of isochoric process and formulas (1) – (4).

Subsequently, the channel extends at a supersonic velocity, and the temperature and pressure of the air-fuel mixture therein are reduced. Due to the high rate of expansion by heat exchange with the environment can be neglected, i.e., to assume an adiabatic process.

It should be noted that, as an adiabatic respect to the external environment, the process is described with an internal heat supply due to recombination of ions and radicals occurred in the breakdown. Our calculations have shown that this leads to that the adiabatic index in this process is equal to about 1.2.

When the temperature reaches 3000 K, the conditions are created for forming of the final combustion products as result of the exothermic chemical reactions with the corresponding heat release. This completes the formation of the first period i.e. the spark kernel formation.

Its volume can be determined by known thermodynamic dependencies for adiabatic process. Assuming that the kernel has a spherical shape, it is easy to determine the radius r_2 .

The larger the radius r_2 , the more heat will be released during the subsequent combustion of air-fuel mixture in the formed initial flame kernel, the faster will be its development. When the radius r_2 called Zeldovich as critical radius of ignition [9], combustion subsequent development does not need to recharge the energy from the inductive phase of the discharge, and may be wholly due to the energy released in the flame kernel.

Mathematically, this condition has the form:

$$r_{cr} \geq 3\delta_l, \quad (5)$$

where δ_l is a thickness of the laminar flame front.

Value δ_l is inversely proportional to the normal velocity of the laminar flame u_l :

$$\delta_l = \frac{a}{u_l}, \quad (6)$$

where a is a thermal diffusivity of air-fuel mixture.

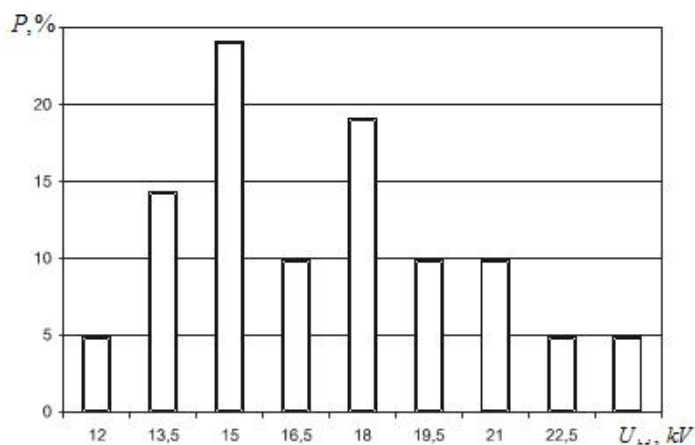
As can be seen, the lower the speed, the thickness of the flame front, and the critical radius of ignition is greater.

It is known that the normal velocity of the laminar flame depends on the composition of the mixture. When stoichiometric mixture of gasoline $\delta_l \approx 0.8$ mm and $r_{cr} \approx 2.4$ mm. They are increase both the depletion and enrichment of air-fuel mixture.

From the literature [7] and the proposed methodology for determining that the value of the flame kernel radius does not depend on the composition of the mixture and is entirely determined by the value of the breakdown voltage.

For typical range of engine operating values of the breakdown voltage from cycle to cycle are variable.

This is well illustrated by the histogram (Pic. 1) of cycle-by-cycle breakdown voltages obtained by testing of the commercial 4-cylinder gasoline engine.VAZ-21083. Variations of breakdown voltage entail changing the value of the flame kernel radius.



Picture 1. Histogram of cycle-by-cycle breakdown voltages
4-cylinder gasoline engine.VAZ-21083, $n = 2500 \text{ rpm}$, $M_e = 40 \text{ Nm}$

The table shows the values of the flame kernel radius for different values of breakdown voltage (electrode gap of 1 mm., the adiabatic index of 1.2.).

U_{bd}, kV	5	10	15	20	25
r_2, mm	0.1	0.4	1.0	2.1	3.7

Impossibility in each cycle to satisfy the condition (5) is then compensated in the second period of flame kernel formation by energy released in the inductive phase of the discharge.

Let to consider the second and third periods of the flame kernel formation. Modeling of processes in this period occurs when the following prerequisites and assumptions:

- Gases are ideal;
- Pressure is constant;
- Specific isobaric heat capacity are constant;
- Rate of convective currents are small compared to the speed of sound;
- negligibly small viscosity and body forces, and the impact of radiation;
- Flame kernel receives energy in the inductive phase during the discharge, and as a result of combustion in its volume;
- Heat is lost from the flame kernel in the spark plug electrodes, and the warm zone of the flame front.

Modeling of these periods is based on the basis of the equations of continuity, energy conservation and components written for the spherical coordinate system.

Simulation of the third period differs from the second in that after completion of the initial spark discharge flame kernel receives energy only from the burning of air-fuel mixture. Also assumed that the heat does not transmit into the spark plug electrodes due to the large thickness of the layer separated from the flame front. As a result, the energy equation in its application for the third period does not contain these terms.

The data generated by the model shows that with a decrease in the breakdown voltage rapidly decreases the radius of the initial nucleus of ignition. Since certain value, further reduction leads to the fact that the radius becomes smaller than a critical.

In this case, successful ignition becomes possible due to release energy in the inductive phase of the discharge, which occurs in the second period of the flame kernel formation.

To compensate for the instability of the breakdown voltage this energy is needed in almost all modes of engine with spark ignition

This especially actual issue when the engine modes close to idling. Ordinary for these regimes decrease density of air-fuel mixture causes a reduction in the breakdown voltage and leads to the fact that the radius becomes much less critical. That is why these regimes become noticeable role forcing parameters inductive discharge phase.

The model also explains the reason that the role of the inductive phase of the discharge increases for lean air-fuel mixture. With increasing excess air factor decreases normal laminar flame speed, and in accordance with (6) and increases its thickness accordingly increasing the critical radius. It requires allocating more energy in the inductive phase of the discharge

References

1. Bloss W., Herweg R., Ziegler G. Untersuchung der Flammer. – Kernbildung in Ottomotor // MTZ. – 1990. – V. – 51, № 5 – p. 202-209.
2. A.O. Zur Loye, F.V. Bracco Two-dimensional visualization of ignition kernels in an IC engine // Combustion and Flame, Volume 69, Issue 1, July 1987, Pages 59–69
3. Enzo Galloni. Analyses about parameters that affect cyclic variation in a spark ignition engine // Applied Thermal Engineering, Volume 29, Issues 5–6, April 2009, Pages 1131–1137
4. Yong M. Ciclic dispersion in the homogeneous – charge spark ignition engine – a liyerature survey // SAE Tech. Pap. Ser.– 1981 – № 810020. – 25 p.
5. Forsirovanie razvitiya nachalnogo ochaga goreniya v DVS s iskrovyim zazhiganiem // Zlotin G. N., Gibadullin V. V., Fedyanov E. A., Shumskiy S. N., Zaharov E. A., Svitachev A. Yu. Nauka proizvodstvu. – 2000. – № 1, s. 24-26.
6. Zlotin, G.N. Razvitie nachalnogo ochaga goreniya gomogennoy toplivovozdushnoy smesi v tsilindre DVS / G.N. Zlotin, K.V. Prihodkov, S.N. Shumskiy // Dvigatelistroenie. - 2007. - #3. - C. 7-10.
7. Heywood, J.B. (1988) Internal Combustion Engine Fundamentals. McGraw-Hill, New York
8. Ujiie Yasushige Spark ignition properties of combustion mixture under high – turbulence intensity conditions // JSME Inf. J. B. – 1994. – 37, № 3. –p.611 -617.
9. Zeldovich, Y. B., Barenblatt, G. I., Librovich, V. B., & Makhviladze, G. M. (1985). Mathematical theory of combustion and explosions.
10. Vargaftik N. B. Spravochnik po teplofizicheskim svoystvam gazov i zhidkostey. 1972 g.

φ - s – DIAGRAM MODELLING TECHNIQUES FOR TIRES

*Balakina E.V., **Borodin A.K., *Zotov N.M.

*Volgograd, Volgograd State Technical University, **Moscow, «PricewaterhouseCoopers Russia B.V.»

This article describes a new technique for computer modelling of $\varphi-s$ diagrams (dependencies of a braking coefficient of friction on a longitudinal sliding coefficient). The technique was developed by summarizing the outcomes of foreign experiments and the resulting analytical representation of the diagrams is suitable for computer modelling.

Keywords: computer modeling, $\varphi-s$ – diagrams, static friction coefficient and slip road surface.

1. Problem statement

Research questions of pavement loadings require development of certain mathematical models and their computer realization. These models describe the conditions related to the elastic wheel contact with the solid support surface. Such models are based on the brake $\varphi-s$ – diagrams, i.e. analytical dependencies of longitudinal tire-road braking coefficient of friction φ on longitudinal sliding coefficient of wheel s . Longitudinal sliding coefficient is the ratio of velocity of longitudinal contact sliding to the speed of the wheel axle. It varies between 0 and 1 or as a percentage (0 to 100%).

These analytical dependencies could be acquired by approximation of similar experimental dependencies. However, development of $\varphi-s$ – diagrams for each separate case is time-consuming and impractical. Therefore, a new technique of modelling $\varphi-s$ – diagrams is proposed. It is based on analytical representation of the diagrams suitable for computer modelling. The technique was developed by summarizing the outcomes of foreign experiments.

2. The description of modelling technique

Figure 1 shows experimental $\varphi-s$ – diagrams received by French and German researchers in 2001 and presented on the international colloquium in Italy [1].

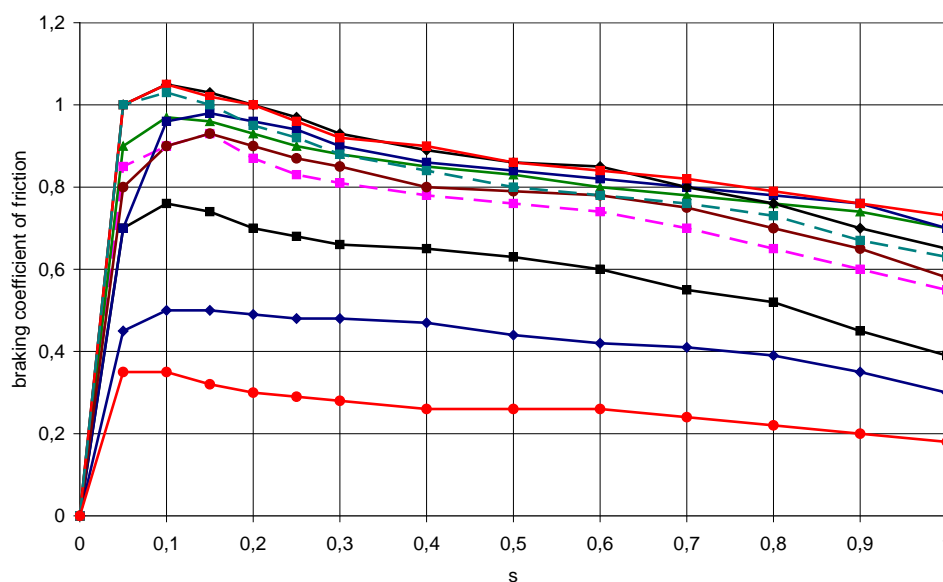


Fig. 1. Experimental $\varphi-s$ – diagrams for different types and conditions of pavements received by French and German researchers in 2001 and presented on the international colloquium in Italy

Figure 2 shows experimental $\varphi-s$ – diagram developed by Polish researchers in Warsaw, 2003.

Figure 3 shows experimental $\varphi-s$ – diagrams obtained by a Finnish researched from the University of Tampere, 2010 [3].

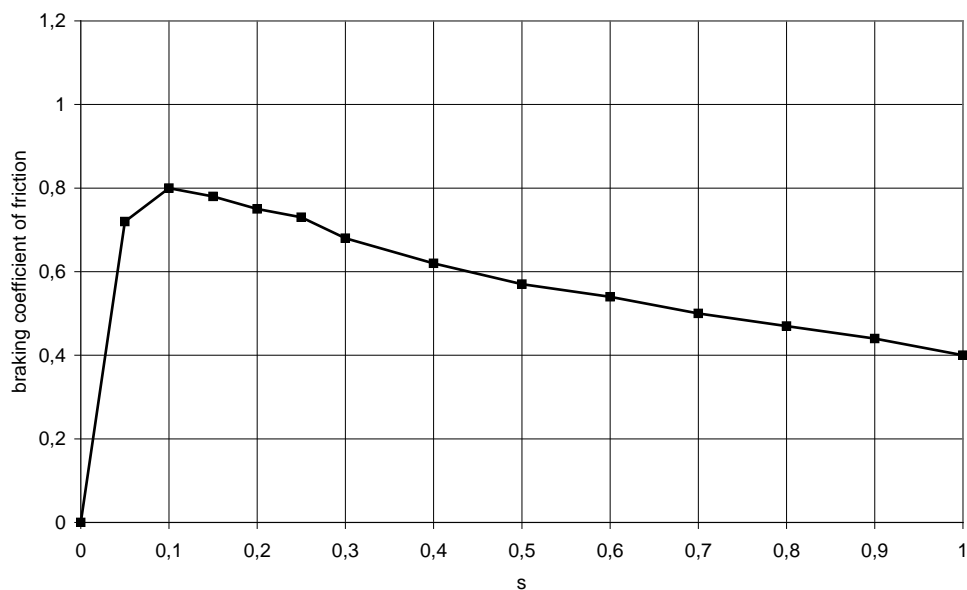


Fig. 2. Experimental $\varphi-s$ – diagram received by Polish researchers in Warsaw, 2003

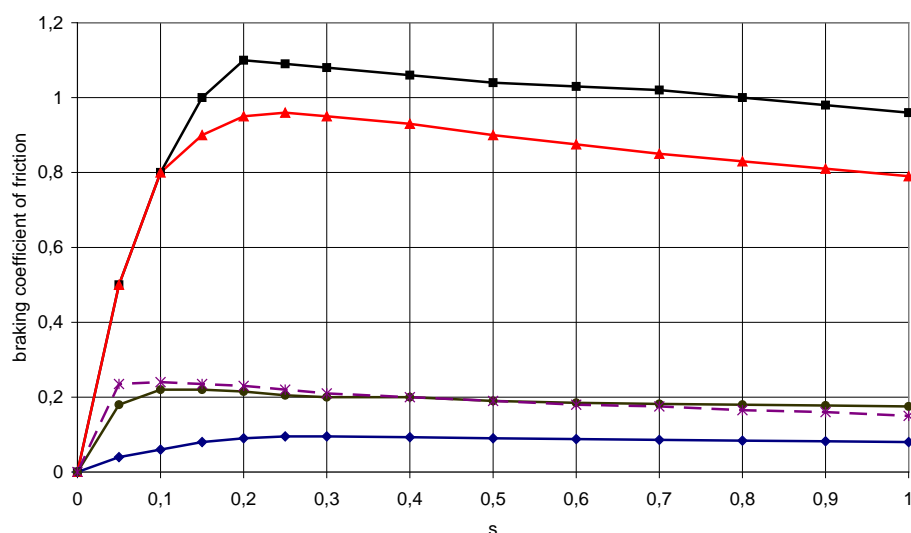


Fig. 3. Experimental $\varphi-s$ – diagrams for different types and conditions of pavements received by a Finnish researcher from University of Tampere, 2010

The obtained experimental data was processed and an average coefficient of static friction utilization in contact K was calculated. K is the ratio of the share of the static friction in contact used for realisation of surface longitudinal reaction to the total share of static friction in contact given the same s [4].

$$K = \frac{\varphi_{st}}{\varphi_{\Sigma st}} = \frac{\varphi(s) - f_{sl} \cdot s}{f_{st}(1-s)},$$

where s – coefficient of longitudinal sliding of a wheel;

φ_{st} – share of static friction in tire-road contact, used for realization of longitudinal reaction of a basic surface

$\varphi_{\Sigma st}$ – the general share of static friction in contact at set s ;

- $\varphi(s)$ – braking coefficient of friction at set s ;
 f_{sl} – coefficient of sliding friction (φ при $s=100\%$);
 f_{st} – coefficient of static friction (φ при $s=0\%$);
 $(f_{sl} \cdot s)$ – the general share of a sliding friction in contact at set s ;
 $f_{st}(1-s)$ – the general share of a static friction in contact at set s .

Figures 4, 5 and 6 represent the $K = f(s)$ dependencies, calculated using the values from Figures 1, 2 and 3 respectively.

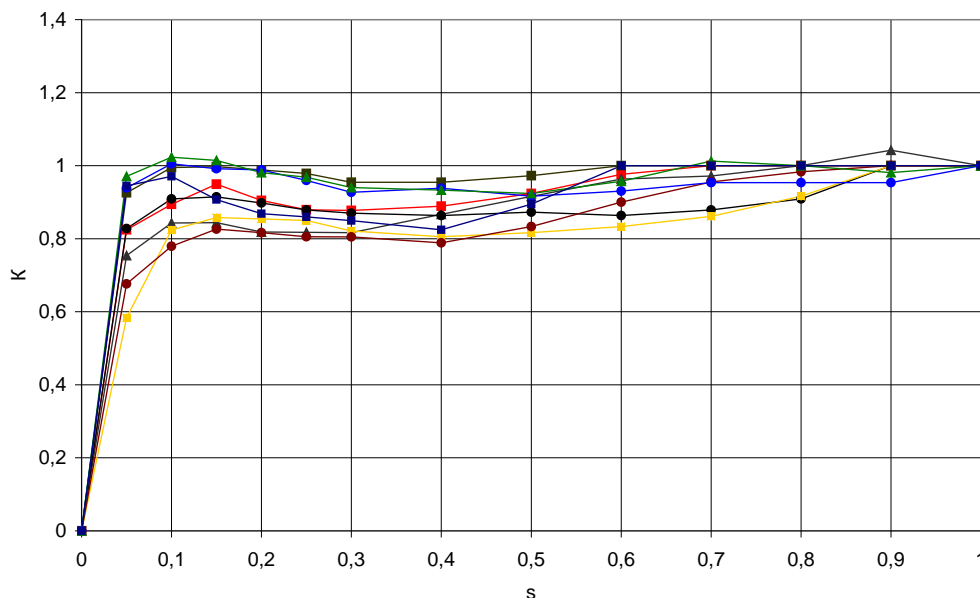


Fig. 4. The $K = f(s)$ dependences calculated using Figure 1 curve

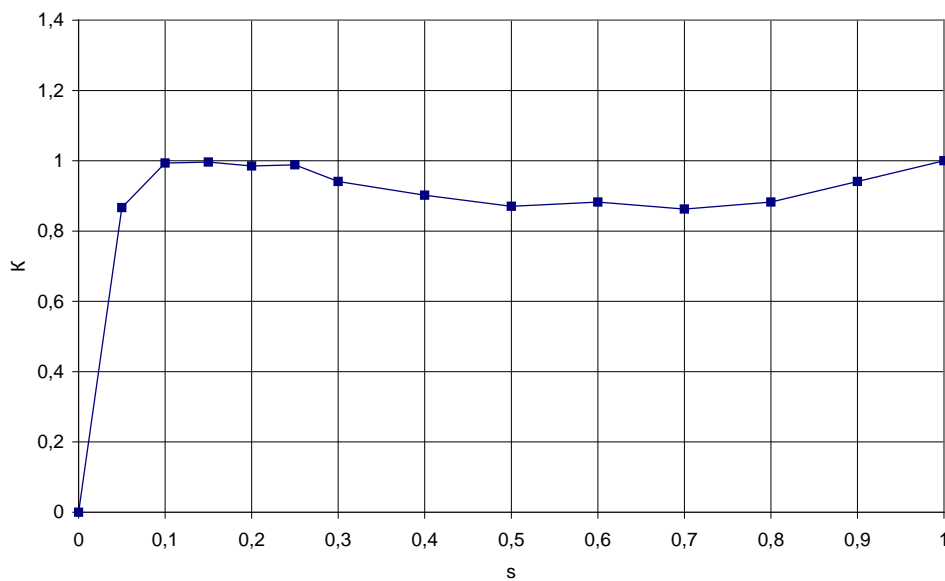


Fig. 5. The $K = f(s)$ dependences calculated using Figure 2 curve

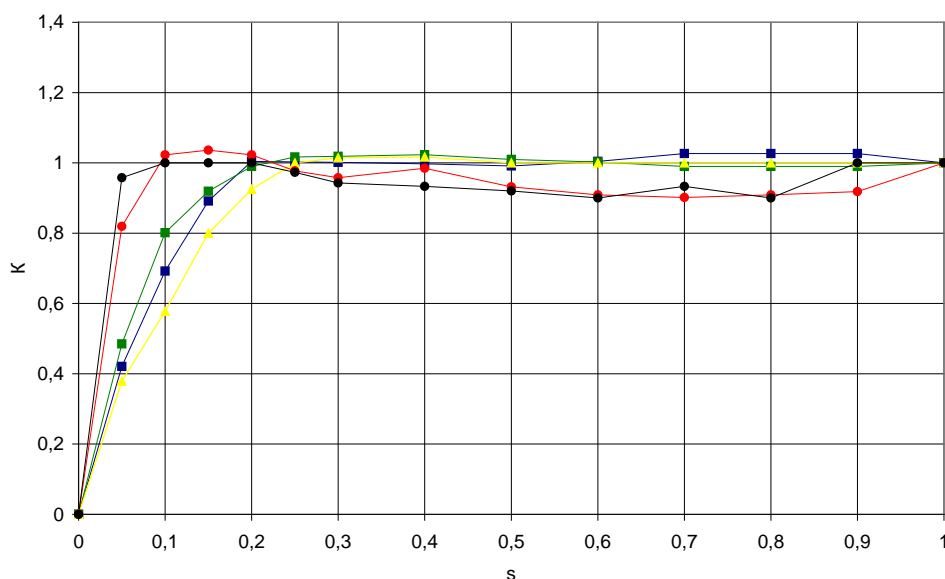


Fig. 6. The $K = f(s)$ dependences calculated using Figure 3 curve

Apparently, the $K = f(s)$ dependences have approximately the same shapes regardless the type or condition of the road surface. Based on this conclusion, all values from Figures 4, 5 and 6 are approximated by a general dependence shown in Figure 7.

It is a polynomial:

$$K = a + b \cdot s + c \cdot s^2 + d \cdot s^3 + e \cdot s^4 + f \cdot s^5 + g \cdot s^6 + h \cdot s^7 + i \cdot s^8 + j \cdot s^9$$

where s – coefficient of longitudinal sliding of a wheel ($s = 0 \dots 1$);

$a, b, c, d, e, f, g, h, i, j$ – constant factors.

Constants:

$a = 0,001814$; $b = 26,747630$; $c = -324,541748$;

$d = 2137,928850$; $e = -8375,670586$; $f = 20260,588666$;

$g = -30442,879724$; $h = 27611,479368$; $i = -13822,359721$; $j = 2929,705537$.

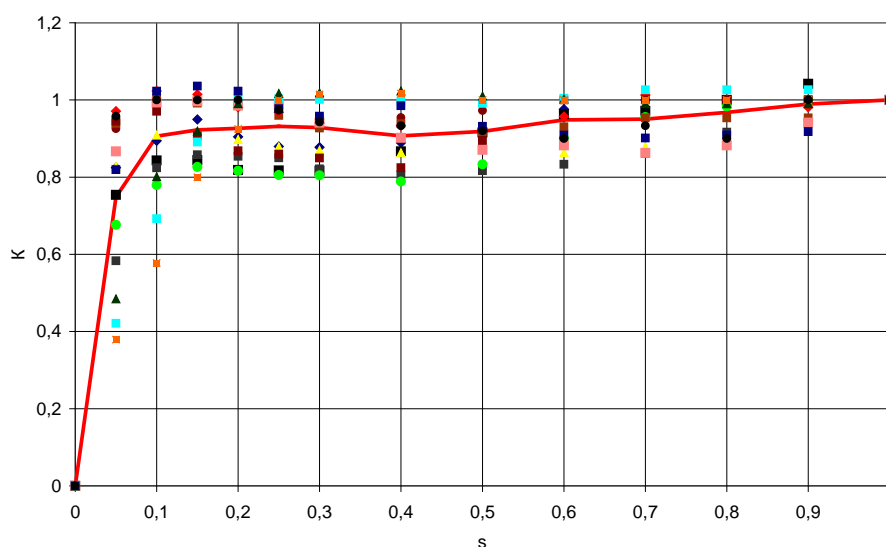


Fig. 7. The generalized approximated $K = f(s)$ dependence, fair for different tires and different types and conditions of road coverings

3. Discussion of results

The resulting $K = f(s)$ formula with an error not exceeding 10% (for $s > 0,1$) is valid for all types of non-studded tires and all types and conditions of pavements.

Solving the inverse problem, settlement $\varphi - s$ – diagrams are received:

$$\varphi(s) = f_{sl} \cdot s + K \cdot f_{st}(1 - s).$$

Coefficients of static friction and sliding should be set according to the type and condition of the road surface, based on the known data ranges. Calculation of $\varphi - s$ – diagrams using the proposed technique is expedient when there is no lateral force impacting on the car or bus, or when the impact is insignificant (no more than 15-20% of the weight of the vehicle).

More research is needed to assess the feasibility of the obtained formula for studded tires used in icy conditions because, as shown by result of experiments performed by a group of authors from MADI (The Moscow State Automobile & Road Technical University) [5], $\varphi - s$ – diagrams for studded tires on ice are fundamentally different from typical as their extremum is shifted towards $s \approx 0,5$. For all other types and conditions of pavements the proposed technique is valid for studded tires as well.

References

1. Y. Delanne, G. Schaefer, D. Lechner, V. Schmitt, G. Beurier. Vehicle Dynamics and tyre road friction performance models. – The report of the 2ND INTERNATIONAL COLLOQUIUM ON VEHICLE TYRE ROAD INTERACTION «FRICTION POTENTIAL AND SAFETY : PREDICTION OF HANDLING BEHAVIOR». – FLORENCE , FEBRUARY 23rd, 2001, 11p.
2. Wieslaw Grzesikiewicz, Janusz Pokorski, Bogumil Szwabik. Modelowanie i badania eksperymentalne przyczepnosci hamowanego kola. – Przegląd Mechaniczny. – 2003. – №10. – Warszawa. – P. 73-77.
3. Sami Koskinen. Sensor Data Fusion Based Estimation of Tyre-Road Friction to Enhance Collision Avoidance / A dissertation for the degree of Doctor of Science in Technology of the Faculty Automation, Mechanical and Materials Engineering, the Tampere University of Technology, 12 March 2010, 209 p.
4. E. Balakina. Improving the roadholding of a wheel car based on pre-project chassis parameter selection: monograph / E. Balakina. – Saarbrücken (Germany): LAP LAMBERT Academic Publishing GmbH & Co. KG, 2012. – 467 p.
5. Cristalniy S.R. Anti-lock braking system effectiveness problem for vehicles, equipped with studded tires / S.R. Cristalniy, N.V. Popov, V.A. Fomichev // Automotive Engineer Journal. - 2012. - № 2(73). - P.32-37.
6. NCHRP. Guide for Pavement Friction. National Cooperative Highway Research Program / J.W. Hall, K.L. Smith, L. Titus-Glover (Applied Research Associates, Inc. Champaign, IL), J.C. Wambold (CDRM, Inc. State College, PA), T.J. Yager (NASA Langley Research Center Hampton, VA), Z. Rado (Pennsylvania Transportation Institute University Park, PA). – Contractor's Final Report for NCHRP Project 01-43 Submitted February 2009.

The work was performed within the 14-08-00042A project of the Russian Foundation for Basis Research “New view on the development of research and modelling of interconnected contact phenomena of elastic wheel and solid surface”

COMPARISON OF CUMULATIVE DAMAGE FATIGUE LIFE MODELS UNDER AUTOMOBILE SERVICE LOADING BY THE EXAMPLE OF MEDIUM CARBON STEEL AISI 5140

Savkin A.N., Sedov A.A., Andronik A.V.
Volgograd, Volgograd State Technical University

Most successive models of cumulative fatigue evaluation are compared considering material strength degradation under variable amplitude loading. Analyzed models are adapted for spectrum loading evaluated via the multibody dynamics approach.

Keywords: degradation of material, cumulative damage, durability prediction.

Assessment of material strength degradation is one among many damage prediction methods in metal fatigue. Undoubtedly, phenomena of strength and plasticity properties variation is a well-known fatigue effect. [1, 2]

There is an abundant amount of nonlinear assessment models (more known as degradation models) in the papers that seem advantageous in contrast with linear one. The latter is based on physical description of strength degradation and failure as of the moment of match residual stress and actual maximal cyclic stress $\sigma_{a \max}$. Damage is commonly estimated in terms of physical strength and its value can be easily verified experimentally at the specific moment during test loading. Apparently, all existing models assume that residual strength is a cycle-depending decreasing function.

Equality of initial and static strength σ_B is a boundary condition any one of these models:

$$\sigma_r(0) = \sigma_B.$$

Failure event follows the formula (for particular case of constant amplitude loading, $n = N$):

$$\sigma_r(N) = \sigma_{a \max},$$

this implies that residual strength is equal to maximal cyclic stress, as previously mentioned. A number of degradation models with different authorship are listed in table 1. The authors of these models used in the research of composite materials, but we analyzed them and used for metals.

Let us briefly clarify an experimental work outlined in the paper. Tests were performed on a BISS 100kN servohydraulic test system in spectrum loading mode for specimens. Smooth cylindrical specimens made of medium carbon steel AISI 5140 used by way of example. The material choice is conditioned by widespread use in vehicle manufacturing owing to reasonably good fatigue, bearing and dynamic resistance and cheapness. Typical properties of the steel grade are given in table 2.

Noteworthy, amplitude stress random sample (fig. 1a) is generated via dynamic model of off-road vehicle built in multibody system “FRUND” [9]. Microprofile data of cobble road carpet with multiple bumps and holes were predetermined conditions. Vertical component of loading of off-road vehicle front suspension was selected for stress calculation because it is a leading cause of fatigue failures in suspension of off-road vehicle. Then stress sequence underwent “rainflow” processing and was transformed to symmetric load spectra.

Fatigue S-N curve can be approximated by the formulae (fig. 4, curve 0):

$$N_i = N_G \left(\frac{\sigma_{-1}}{\sigma_{ai}} \right)^m. \quad (1)$$

Degradation models

Table 1

Degradation models	Authors	№
$\sigma_r(n) = \sigma_u - \sum_{i=1}^n (\sigma_u - \sigma_{ai}) \frac{1}{N_i}$	[3]	(1)
$\sigma_r(n) = \sigma_u - \left[\sum_{i=1}^n (\sigma_u - \sigma_{ai})^{\frac{1}{C}} \frac{1}{N_i} \right]^C$	[4]	(2)
$\sigma_r(n) = \sigma_u - (\sigma_u - \sigma_{ai}) \left(\frac{n_i + n_{eqv(i-1)}}{N_i} \right)^{C_i},$ $C_i = C_1 \frac{\sigma_{ai}}{\sigma_u} + C_2, \text{ if } C_i < C_3, \text{ then } C_i = C_3,$ $n_{eqv(i-1)} = N_i \left(\frac{\sigma_u - \sigma_{r(i-1)}}{\sigma_u - \sigma_{ai}} \right)^{\frac{1}{C_i}} - \text{equivalent number of cycles}$	[5]	(3)
$\sigma_r(n) = \sigma_u - (\sigma_u - \sigma_{a \max}) \left[\frac{\sin \beta \frac{n}{N} \cos(\beta - \alpha)}{\sin \beta \cos \left(\beta \frac{n}{N} - \alpha \right)} \right], \alpha, \beta - \text{coefficients}$	[6]	(4)
$\sigma_r(n) = \left[\sigma_u^C - (\sigma_u^C - \sigma_{a \max}^C) \frac{n}{N} \right]^{\frac{1}{C}}$	[7]	(5)
$\sigma_r(n) = \sigma_u - (\sigma_u - \sigma_{a \max}) \frac{n^C}{N}$	[8]	(6)
where C – constant, C_i - variable		

Strength and fatigue properties of steel

Table 2

Steel grade	Static strength properties		Fatigue properties		
	σ_u , MPa	σ_y , MPa	σ_{-1} , MPa	N_G , cycles	m
Steel AISI 5140	957	640	390	$8 \cdot 10^5$	11,8

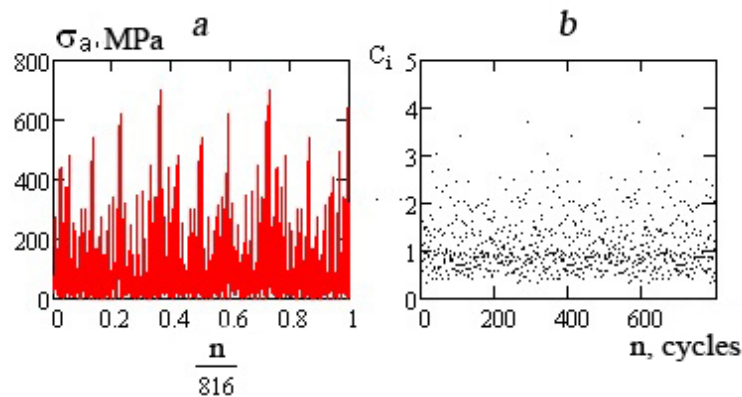


Fig.1. Plots of stress random sample caused by vertical loading of vehicle front suspension: *a* – stress amplitude versus number of cycles; *b* – amplitude interaction factor versus number of cycles by formulae (11).

In case of block loading (fig.1a) damage per loading block (8) is equal to:

$$D_b = \sum_{i=1}^{V_b} \left(\frac{\sigma_u - \sigma_{ri}}{\sigma_u - \sigma_{a \max}} \right), \quad (2)$$

where V_u - number of cycles in block. Consequently, number of cycles to failure:

$$N_p = \frac{V_b}{D_b}. \quad (3)$$

Linear model of degradation (1) is a simplest one among proposed in table 1. Parameters of fatigue curve S-N were used in the equation of linear model (7).

This model is true only for constant amplitude loading and tends to exhibit a crucial discordance between test and analytical data in case of variable amplitude loading (fig. 4, curve 1). Presence of correction factors, certainly empirical, in the models (2-6) reduces to more adequate results. The plot of generalized one-parametric scheme for metal strength degradation is given in fig. 2.

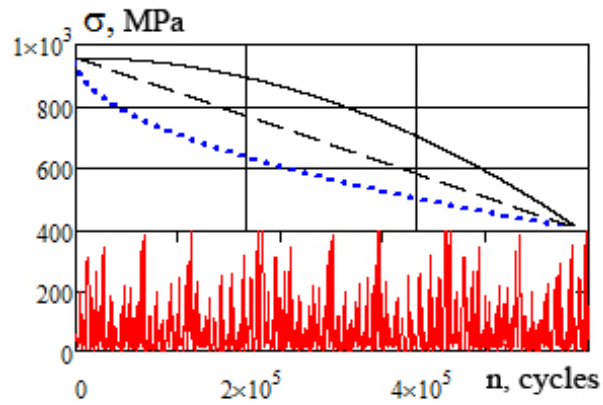


Fig.2. Metal strength degradation scheme under variable amplitude loading: 1 – linear model, 2 – decelerated model, 3 – accelerated model.

Let us assume that ultimate strength σ_u has a role of estimation parameter of metal strength degradation then degradation has various intensity of decreasing σ_u . Equality (2) describes linear approach ($C=1$). One may reveal decelerated degradation intensity of various metals and loading conditions ($C>1$) if strength varies gradually, and the greatest intensity of degradation falls in the last phase before failure. Accelerated degradation intensity ($C<1$) is also possible. Limit state occurs if metal ultimate strength descends to maximal working stress value. Models (2-6) meet this demand. Parameter C in these equalities (2-6), may be constant or feature a function. The latter is shown in following expression:

$$C_i = \left(\frac{1 - \log \frac{\sigma_{ai}}{\sigma_{-1}}}{1 - \log \frac{\sigma_{ai-1}}{\sigma_{-1}}} \right)^{C_i}, \quad (4)$$

moreover, C_i can be a sequence-sensitive parameter:

$$\sigma_r(n) = \sigma_u - \sum_{i=1}^n \left(\sigma_u^{C_i} - (\sigma_{ai})^{C_i} \right) \left(\frac{1}{N_i} \right)^{C_i}, \quad (5)$$

where σ_{ai} - current value of stress.

Plot of this parameter C_i versus number of cycles is given in fig. 1b.

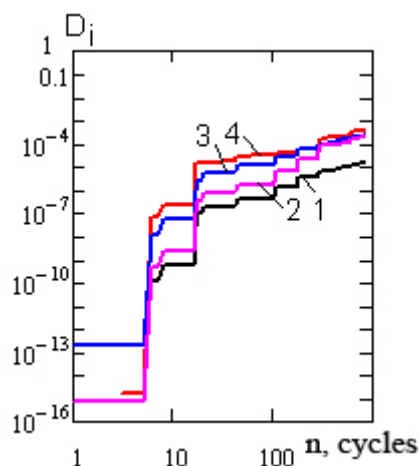
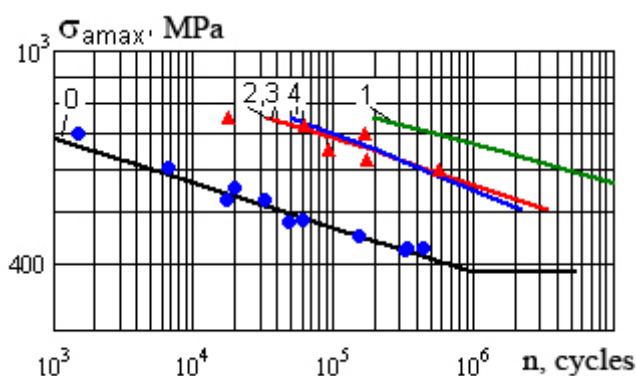


Fig.3. Fatigue damage D_i per block versus number of cycles for various degradation models: curve 1 – (1), curve 2 – (6), curve 3 – (2), curve 4 – (12).

Fatigue damage value cumulation D_i per loading block according to various models is graphically represented in fig. 3 assumed that $\sigma_{a \max} = 500$ MPa. Following models are compared: 1 – linear model (1), 2 – nonlinear model (2) with $C=0.8$, 3 – nonlinear model (6) with $C=0.95$, 4 – sequence-sensitive nonlinear model (12). As the result, cumulated damage D_i per loading block is the same for non-linear models (2), (6) and (12), however, linear model (1) demonstrates less conservative results.

Fatigue curves corresponding to the abovementioned models are shown in fig. 4. Following conventional numbers were used: 0 is for original fatigue curve, 1-4 is for analyzed models.



Pic.4. Fatigue curves for AISI 5140 steel under spectral loading according to degradation models.

There are results of experiments with constant amplitude (dots •) and variable amplitude (triangles ▲) in fig.4. Evidently, durability forecasts with using of degradation models (curves 2-4) are fit better to the test results of variable amplitude loading. Let us remark that a necessary condition of models adaptation is a presence of original fatigue curve and its parameters (in our case, asymmetric factor $R = -1$), and constant C also for model correcting. Calculation results with using of models 2 and 3 are similar: despite value of C is different, curves are almost matched. Fatigue curve for model 12 displayed results a few distinct from results of previous models, but close enough to them. Linear model 1 shows too

optimistic results likewise model of Palmgren-Miner. Sophistication of degradation models use attributed to the absence of physical sense of parameters and demand for special variable amplitude loading tests.

In the end, let us figure the conclusions:

1. Degradation models for damage cumulation and fatigue durability estimation have a widespread using in engineering and give physical sense of damage in metal.
2. Kinetics of degradation processes in various materials and loading conditions is a complex problem demanding further research of service loading.
3. Current paper highlighted that degradation models allow durability prediction under constant and variable loading both of materials and of structural elements.

References

1. Ivanova V.S. Priroda ustalosti metallov. /V.S.Ivanova, V.F.Terentev/ M., Metallurgiya, 1975, 456 p.
2. Savkin A.N. Prognozirovanie ustalostnoy vyiskonagruzhennyih konstruktsiy: monografiya/ A.N. Savkin, V.P. Bagmutov / VSTU,-Volgograd, 2013.-364 p.
3. Broutman L.J., Sahu S. A new theory to predict cumulative fatigue damage in fiberglass reinforced plastics. In composite Materials: Testing and Design (Second Conference) ASTM STP 497, p.170-188. American Society for Testing and Materials, 1972.
4. Post N.L., Lesko J.J., Case S.W. Modeling the variable 10 amplitude fatigue of composite materials: a review and evaluation of the art for spectrum loading. In review, Int. J.Fatigue, 2008.
5. Post N.L., Lesko J.J., Case S.W. Fatigue durability of E-gloss composites under variable amplitude loading the importance of load sequence. In Accepted for publication. Scientific Track proceedings of the European Wind Energy Conference, 2008.
6. Yao W.X., Himmel N. A new cumulative fatigue damage model for fiber-reinforced plastics. Composites science and technology no. 60, 2000, pp.59-64.
7. Post N.L., Lesko J.J., Case S.W. A new phenomenological model for the tension and compression residual strength of fiber dominated composite materials. In review, Composites Science and Technology, 2008.
8. Wahl N.K. Spectrum fatigue lifetime and residual strength for fiberglass laminates, Ph. D. Thesis, Montana State University, Bozeman, 2001.
9. Gorobtsov A.S. K raschetu dinamicheskogo napryazhennogo sostoyaniya elementov konstruktsiy mashin v sostave modeley mnogih tel /A.S. Gorobtsov, S.K. Karzov, A.N. Savkin// Prochnost materialov i elementov konstruktsiy: Trudy Mezhdunarodnoy nauchno-tehnicheskoy konferentsii (Kiev, 28-30 sep. 2010.) – Kiev: G.S. Pisarenko Institute for Problems of Strength of the National Academy of Sciences of Ukraine, 2011.
10. Uvajsov S. U., Kofanov Ju. N. Metodika vyjavleniya skrytyh defektov integral'nyh shem i apparatury // Nadezhnost' i kontrol' kachestva. Ezhemesjachnoe prilozhenie k zhurnalu "Standarty i kachestvo". 2013. № 11. S. 19-31.
11. Uvajsov S. U., Kofanov Ju. N., Sotnikova S. Ju. Programmnyj kompleks modelirovaniya fizicheskikh processov pri avtomatizirovannom proektirovanii istochnikov vtorichnogo jelektropitanija dlja slozhnyh bortovyh sistem // Dinamika slozhnyh sistem. 2012. № 3. S. 80-84.
12. Uvajsov S. U. Teksturovannye podlozhki iz splavov nikelja s tugoplavkimi metallami (W,Mo,Re) dlja sverhprovodjashhih kabelej vtorogo pokolenija // Izvestija vysshih uchebnyh zavedenij. Povolzhskij region. Tehnicheskie nauki. 2012. № 2(22). S. 126-137.

ON THE STEEL DAMAGE SIMULATION UNDER VARIABLE AMPLITUDE LOADING BY THE POWER, ENERGY AND STRAIN FAILURE CRITERIONS

Savkin A.N., Sedov A.A., Andronik A.V.
Volgograd, Volgograd State Technical University

Effort to describe effect of variable amplitude loading character on fatigue damage cumulation is made for a steel structural part. It is proposed to quantify the influence of loading character on durability through damage model incorporating the nonstationarity factor and the spectrum fullness factor. Experimental evidence and analytical results of the proposed model are correlated.

Keywords: spectrum loading, damage model, spectrum fullness factor.

Sufficient reliability of design and minimal essential safety reserve are two permanently desired aims of engineers. This is particularly significant for such high risk systems with crucial role of strength-weight ratio as transport systems. Design error in balancing between these two beacons fraught with both unrecoverable structural failure and hazard for people lives. Therefore, scientists and engineers already invented and incessantly continue their academic pursuits for fallouts prevention. Several effective damage models are analyzed below.

1. Evaluation of fatigue life under spectrum loading through power damage criterions. Certainly, quantification of chaotic state in spectrum loading gives a better understanding of influence of loading character on fatigue live of structures.

It is possible to estimate spectrum loading character through the spectrum fullness factor V by the formula [1]:

$$V = \left[\frac{1}{V_b} \left[\sum_{i=1}^{v_b} \left(\frac{\sigma_{ai}}{\sigma_{a\max}} \right)^m \right] \right]^{\frac{1}{m}}, \quad (1)$$

where V_b - duration (number of cycles) of loading block; σ_{ai} , $\sigma_{a\max}$ - values of i -th and maximal stress amplitude; m - slope of original fatigue curve in log-log coordinates.

Spectrum generation, especially intended for testing of various materials and structural components or simulation processes, is a hotly debated item in the scientific community. There are presented a lot of different approaches and concepts in the recent papers. For example, authors [2, 3] use the autocorrelation function of variable amplitude loading (hereafter referred to as VAL) for regions of stress sequence with intent to estimate spectrum irregularity. Autocorrelation is the cross-correlation function of external signal in different time points. The Rayleigh distribution is suited enough for the various real service loadings, and hence it was reasonably chosen for simulation. Loading simulation is based on the principle that components of two-dimensional vector are independent and distribute random variables according to the Rayleigh distribution.

Three loading spectrums with various autocorrelation and loading fullness factors were generated via autocorrelation approach on condition that duration of each block is 5000 cycles. All spectrums were processed by rainflow method and transformed to symmetric loading. Automobile service spectrums SAESUS, SAEBRACKET and SAETRANS were also subjected to this procedure for comparison generated sequences and well-known spectrums. The brief characteristics and appearance of these spectrums are given in table 1 and fig.1. Associated spectrum loading tests are completed on a servohydraulic machine BISS-100 for smooth specimens. Steel AISI 5140 has many applications in transport industry and thus this grade was selected for the tests.

Table 1
Properties of the normalized loading spectrums

Loading spectrum	Spectrum fullness factor V	Block loading durability V_b
CAL	1	N_i
Spectra A	0,676	5000
Spectra B	0,591	5000
Spectra C	0,52	5000
SAESUS	0,511	2484
SAEBRACKET	0,524	2496
SAETRANS	0,566	1494

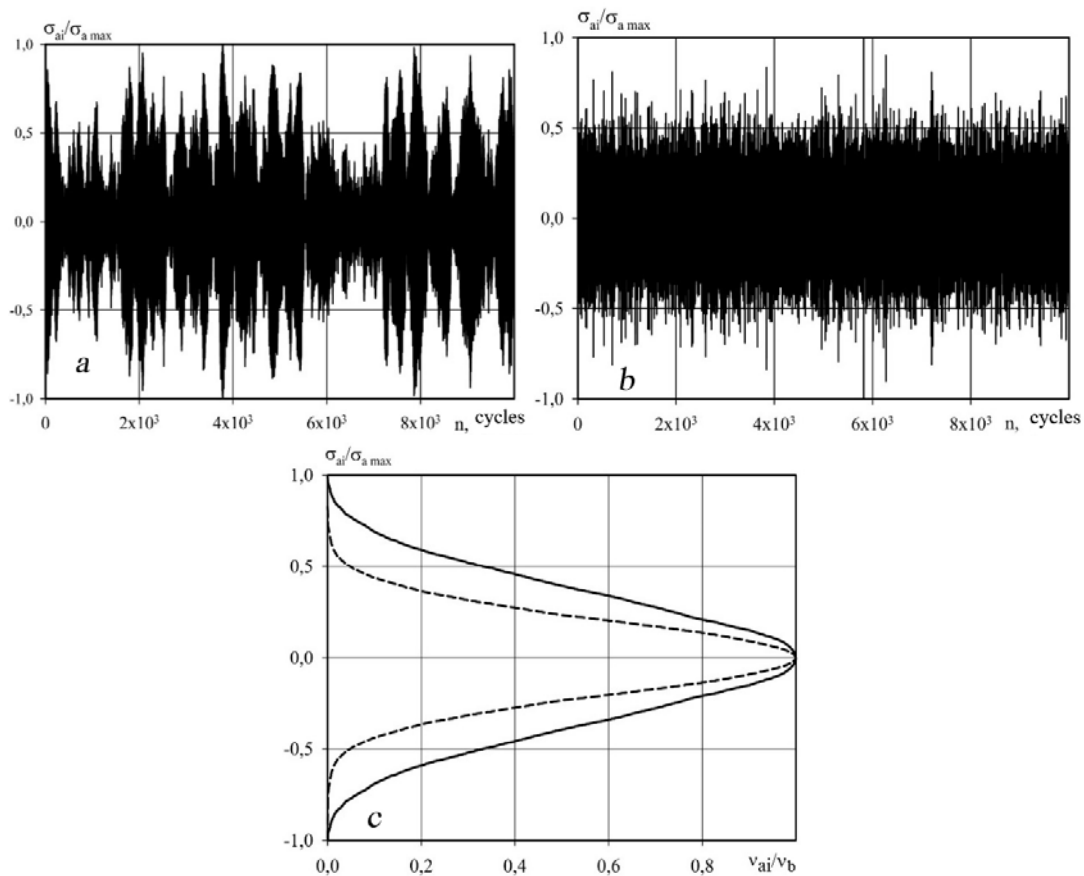


Fig. 1. Original and processed loading spectrums with various spectrum fullness factor V : a – block of the original spectrum A ($V=0,676$); b – block of the original spectrum C ($V=0,52$); c – processed spectrums (— spectra A, - - spectra C)

It is well known that fatigue curve (constant amplitude loading, hereafter referred to as CAL) follows the equality:

$$N = N_G \left(\frac{\sigma_{-1}}{\sigma_{a \max}} \right)^m, \quad (2)$$

where for AISI 5140 [4]: $\sigma_{-1} = 390 \text{ MPa}$; $m = 11,8$; $N_G = 8 \cdot 10^5 \text{ cycles}$.

Total fatigue life can be determined by expression:

$$N_{\Sigma} = N \cdot K, \quad (3)$$

where N – fatigue life under CAL, K - nonstationarity parameter of loading spectrum.

Resulting nonstationarity parameters of spectrums K for various models are given in table 2. K values were evaluated through transforming of fatigue damage equations according to the linear model [5], corrected linear model [6], and generalized model for random loading [7] (q is material constant and $q=3,83$ for steels):

$$N_{\Sigma} = \frac{N_G \cdot 10^{(1+q \lg m)(1-V)}}{\left(\frac{\sigma_{a \max}}{\sigma_{-1}} \right)^m} . \quad (4)$$

Table 2

Nonstationarity parameters of spectrum loading for fatigue life evaluation of steel

Damage model	Linear	Corrected linear	Based on spectrum character
Nonstationarity factor	$K_1 = \frac{1}{V^m}$	$K_2 = \frac{a_p}{V^m}$	$K_3 = 10^{(1+q \lg m)(1-V)}$

The test results under CAL (curve 1, fig. 2a) and VAL for the spectrum of A (points ●) and spectrum C (point ▲) are shown in fig. 2a. Curves 2 and 3 were obtained from equation (9), taking into account the coefficient K_3 unsteadiness as most closely describes the behavior of the material under different loading spectra. Distinctly, critical parameter of corrected linear model varies within the range $0 \leq D \leq a_p$, where $a_p < 1$. This model shows more adequate results than linear. Correlation of calculated life N_{an} by formula (4) and experimental result N_{exp} of steel AISI 5140 under different VAL spectrums is illustrated in fig. 2b. One can notice good correlation of these data in fig. 2b. Let us mark that correlation factor is $\mathcal{R}=0,817$, and root mean square is $S_{\sigma}=0,742$.

Table 3

AISI 5140 fatigue life prediction under spectrum loading by various damage models

Loading spectra	Spectrum fullness factor V	Nonstationarity factor by various models			Value of N_{Σ} of exp , cycles	Durability ratio $N_{\Sigma i} / N_{\Sigma exp}$ for models		
		K_1	K_2	K_3		1	2	3
CAL	1	1	1	1	2000	-	-	-
Spectra A	0,676	101,5	31,5	45	$1,3 \cdot 10^5$	1,56	0,49	0,69
Spectra C	0,52	936	137	282	$5,5 \cdot 10^5$	3,40	0,50	1,03

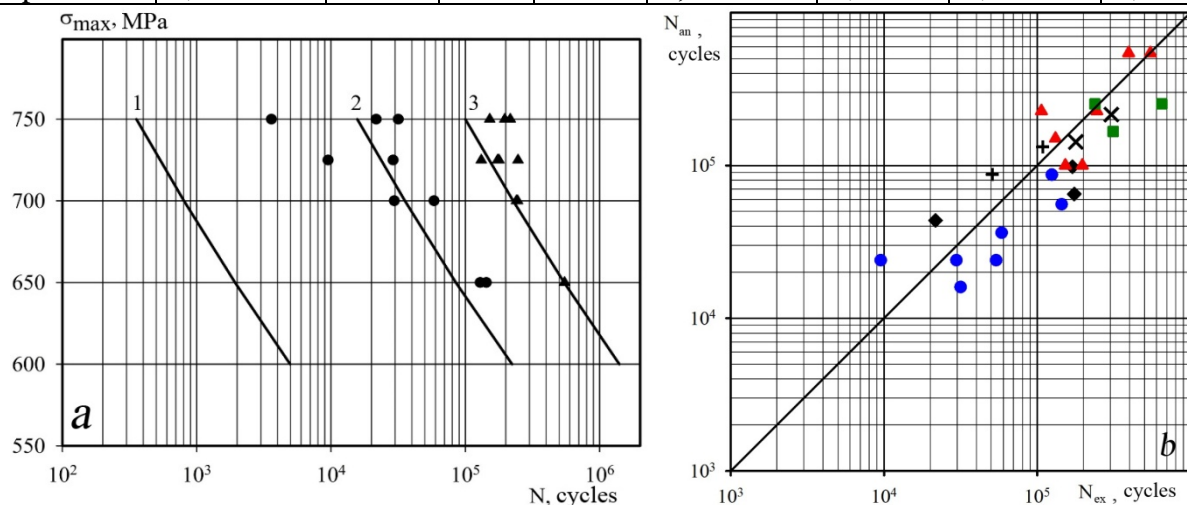


Fig. 2: 2a - Fatigue curves for AISI 5140 under CAL (curve 1) and generated spectrums (curve 2 is for the spectra A, curve 3 is for the spectra C); 2b - Correlation

evidence of analytical and experimental life under VAL spectrums (spectrums A - ●, C - ▲, B - ◆, SAESUS - ■, SAEBRACKET - ×, SAETRANS - +).

As a conclusion, fatigue life estimation of steel under VAL successfully covers the question of fracture behavior to some extent through power damage criterions. Moreover, loading character has an abundant effect on steel fatigue. The character is related to spectrum fullness factor V and cyclic strength parameters under CAL.

2. *Inelasticity and fatigue life relationship under VAL.* Evolution of inelastic processes in metals under cyclic loading is directly related to propagation of micro-plastic strains [8, 9]. These strains define kinetics of fatigue damage cumulation and lead to fracture.

Below is given analyzed development of hysteresis loop under VAL. Width loop evolution on applied of the narrowband normalized spectrums A (a) and C (b) with maximal stresses $\sigma_{a \max 1} = 700$ MPa and $\sigma_{a \max 2} = 650$ MPa is shown in fig. 3. Width loop is automatically evaluated in near-zero stress levels with accuracy of measurement in the order of 10^{-5} . Micro-plastic strain and stress amplitude are plotted against number of cycles for the spectrum A ($\sigma_{a \max} = 725$ MPa) in fig. 4a. One can observe typical leaps of strain caused by extreme stress values. Interestingly, fall of cyclic stress may invoke arrest of micro-plastic strain cumulation. Kinetics of the micro-plastic strain cumulation is shown in fig. 4b. It depends on hysteresis loop width $\Sigma \Delta \varepsilon_i$ related to spectrum fullness and maximal stress $\sigma_{a \max}$ in spectrum. Increasing of maximal stress is accompanied by decreasing of the micro-plasticity and life decreasing in the spectrum A (with spectrum fullness factor $V=0,696$).

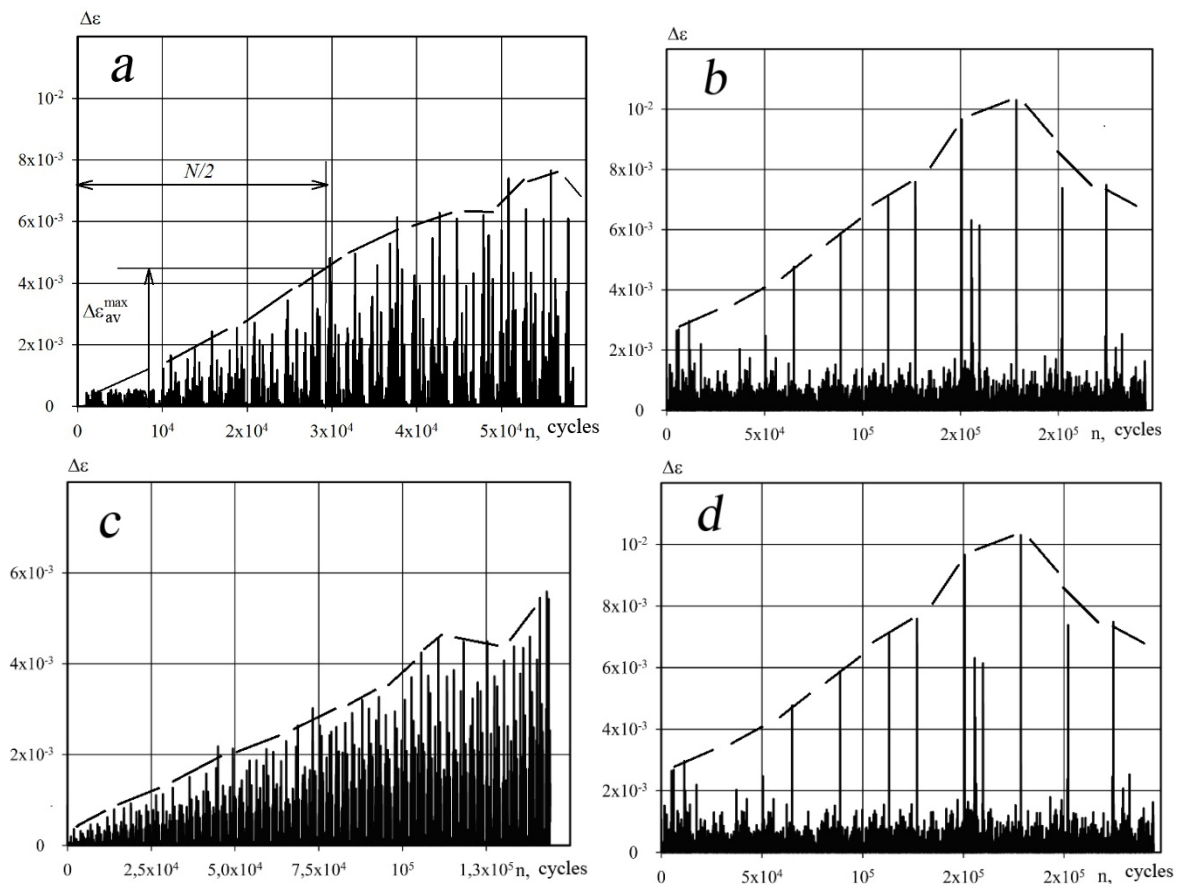


Fig. 3. The evolution of hysteresis loop under various spectrums with $\sigma_{a \max} = 700$ MPa (a – spectra A, b – spectra C) and $\sigma_{a \max} = 650$ MPa (c - spectra A, d - spectra C)

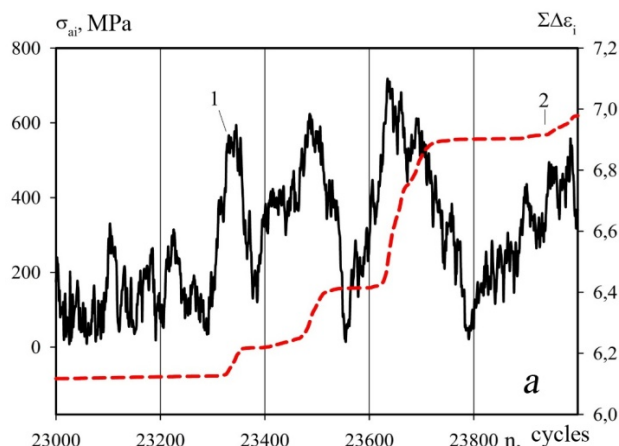


Fig. 4 - Fragment of maximal stress envelop curve (1) and micro-plasticity cumulation curve (2) in a distinct segment of VAL (spectrum A)

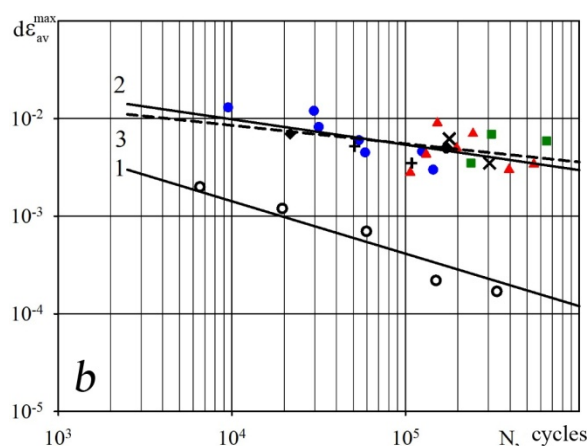


Fig. 5 – Plot of maximal loop width $\Delta\epsilon_{av}^{max}$ against fatigue life N for AISI 5140 (1 – curve for CAL, 2 – curve for VAL, 3 – curve for averaged VAL spectrum, ● - spectrums A, ▲ - C, ◆ - B, ■ - SAESUS, × - SAEBRACKET, + - SAETRANS)

Decreasing of maximal stress amplitude in combination with insignificant increasing of cumulated strain becomes a typical feature for the spectra C (with spectrum fullness factor $V=0,52$) when life exceeds 10000 cycles. However, cumulated micro-plastic deformation in the spectra C is greater than in the spectra A, essentially due to plenty of small stress amplitudes and bigger life.

Fatigue damage cumulation is primarily attributed to maximal hysteresis loop evolution in loading block, hence, it is possible to draw envelop curve of loop evolution based on maximal values (dashed line in fig. 3). The value $\Delta\epsilon_{av}^{max}$ corresponds to half-life under VAL and correlates with damage cumulation (fig. 3a). Curve of maximal loop width $\Delta\epsilon_{av}^{max}$ for CAL (curve 1) and for spectrum VAL (curve 2) are shown in fig. 5. Inelasticity in spectrums with various spectrum fullness factor V and parameters circumscribe one curve.

In the end, evolution of inelasticity properties under VAL within the fatigue life range $5 \cdot 10^3 - 10^6$ cycles is absolutely essential for durability estimation. All tests data under VAL with various spectrum fullness factors are situated along curve in coordinates $\lg \Delta\epsilon_{av}^{max} - \lg N$.

3. *Steel damage simulation under VAL by strain and energy criterions.* Fatigue fracture initiates in regions with local stress concentration (stress raisers). Variable micro-stresses lead to micro-plastic strain cumulation and finally crack appears when plasticity is

fully exhausted in overstrained volumes. Unfortunately, direct measurement of damage cumulation in local volumes is difficult. Therefore engineers use local stress-strain approach for fatigue life estimation of structural parts under cyclic loading. Cyclic stress-strain curve based on hysteresis loop evolution is used in this approach for fatigue resistance estimation. Expression for the cyclic curve is shown below:

$$\frac{\Delta \varepsilon}{2} = \frac{\Delta \varepsilon_e}{2} + \frac{\Delta \varepsilon_p}{2}, \quad (11)$$

where $\Delta \varepsilon$, $\Delta \varepsilon_e$, $\Delta \varepsilon_p$ - total, elastic and plastic strain components of hysteresis loop correspondingly.

Elastic strain component can be evaluated by expression:

$$\frac{\Delta \varepsilon_e}{2} = \frac{\Delta \sigma}{2E}. \quad (12)$$

Plastic strain component can be defined by formula:

$$\frac{\Delta \varepsilon_p}{2} = \left(\frac{\Delta \sigma}{2K'} \right)^{\frac{1}{n'}}, \quad (13)$$

where K' - constant; n' - coefficient of cyclic hardening (softening); E - elastic modulus.

Hence, cyclic strain curve corresponds to equation:

$$\frac{\Delta \varepsilon}{2} = \frac{\Delta \sigma}{2E} + \left(\frac{\Delta \sigma}{2K'} \right)^{\frac{1}{n'}}. \quad (14)$$

Fatigue curve equation is all-known:

$$\Delta \sigma = C \cdot N^B \quad (15)$$

In the end, Coffin-Manson equation is received [11]:

$$\frac{\Delta \varepsilon}{2} = \frac{\sigma_f'}{E} (2N_f)^b + \varepsilon_f' (2N_f)^c, \quad (16)$$

where σ_f' - true strength in tension mode; ε_f' - true plasticity; b, c - constants; $2N_f = N$ - number of cycles to fracture.

Various generated spectrums (table 1) were used for fatigue life calculations. Original material data for AISI 5140 are used for analysis in “Stoflo” program [10] (table 4).

Table 4

Original data for fatigue durability analysis of steel AISI 5140

S_u, MPa	σ_f', MPa	E, MPa	K', MPa	ε_f'	b	n'	c
976	1590	$2 \cdot 10^5$	1434	0.66	-0.075	0.14	-0.59

Fatigue curve (3) in fig. 5 is obtained by local strain-stress approach. It is evident that experimental values coincide to Coffin-Manson curve. Experimental results (dots in fig. 5) are independent of loading character, so one can see that experimental and analytical results correlate for various spectrums.

Damage estimation for steel AISI 5140 was estimated by energy criterions under VAL. Damage calculations are based on plasticity exhaustion d_{pl} and dissipation of elastic energy in material defined by hysteresis loop variation d_{el} .

$$d_{\Sigma} = d_{pl} + d_{el} \quad (17)$$

Plastic component of damage d_{pl} is evaluated by energy criterion:

$$d_{pl} = \sum_{i=1}^N \frac{D_i}{D_{cri}} \quad (18)$$

where D_i - dissipated energy per cycle of VAL per loop square:

$$D_i = k_F \Delta \varepsilon_i \sigma_{ai}, \quad (19)$$

where k_F , $\Delta \varepsilon_i$, σ_{ai} - parameters of hysteresis loop.

Critical energy value corresponding to fracture is defined by expression [12]:

$$D_{cri} = S_u \left(\frac{\sigma_p}{\sigma_{ai}} \right)^{\Theta}, \quad (20)$$

where $S_u=830$ MPa; $\sigma_p=1436$ MPa; $\Theta = 2.85$ - material constant.

Elastic part of damage can be estimated by formula:

$$d_{el} = \sum_{i=1}^N \frac{D_{eli}}{D_{el}^{cr}}, \quad (21)$$

where elastic component of dissipated energy per deformation cycle:

$$D_{eli} = \frac{\Delta \sigma_i \Delta \varepsilon_i}{2} = \frac{2 \sigma_{ai}^2}{E}, \quad (22)$$

where $\Delta \sigma, \Delta \varepsilon$ - stress and strain range per cycle; E - elastic modulus.

Critical elastic component of dissipated energy depends on fatigue endurance limit σ_{-1} and number of cycles for inflection point on fatigue curve N_0 :

$$D_{el}^{cr} = \frac{2 \sigma_{-1}^2 N_0}{E} \quad (23)$$

In the end, damage estimation by elastic component was received:

$$d_{el} = \frac{\sum_{i=1}^N \sigma_{ai}^2}{\sigma_{-1}^2 N_0} \quad (24)$$

It is well-known that damage variation depends on durability to fracture. Mixed mode of fracture considers both plastic and elastic damage cumulation components. Elastic component attributed with fatigue damage cumulation and, consequently, initiation and propagation of crack. By default, fracture occurs if $d_{\square} = 1$. Analytical fracture surfaces are shown for total damage d_{\square} based on proposed damage expressions in fig. 6: 1 – $d_{\Sigma} = d_{pl} + d_{el}$ is for linear model of damage; 2 – $d_{\Sigma} = d_{pl}^{\alpha} + d_{el}^{\beta}$ is for nonlinear model of damage and interaction of damage components. In this model nonlinear damage d_{\square} has decelerated character of plastic component d_{pl} ($\alpha \neq 0,05$) and accelerated character of elastic component d_{el} ($\beta = 2$) corresponding to kinetics of fatigue crack propagation.

Damage values d_{\square} by various models are plotted against number of cycles in fig. 7 for AISI 5140 under different spectrum VAL. Plasticity exhaustion model (fig. 7a) shows that total damage value $d_{\square} = 0,56$ (mean square deviation $s_d = 0,324$) is smaller than in proposed criterion. Linear damage model of mixed fracture mechanism (fig. 7b) approximates damage value to criterional one $d_{\square} = 0,7$ ($s_d = 0,332$). However, sufficient scatter of damage values for various spectrums and loading conditions is typical for this model. Nonlinear damage model demonstrates (fig. 7c) decelerated character of plastic component d_{pl} ($\alpha \neq 0,05$) and

accelerated character of elastic component d_{el} ($\beta \neq 2$) and fits experimental results to criterional parameter value $d_{\square}=0,991$ ($s_d = 0,039$).

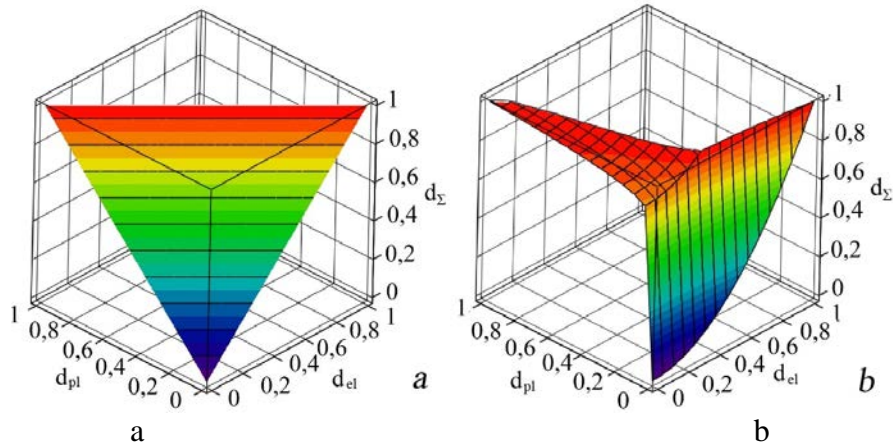


Fig. 6. Analytical fracture surfaces by linear (a) and nonlinear (b) models for cumulation of elastic and plastic components of damage d_{el} and d_{pl} .

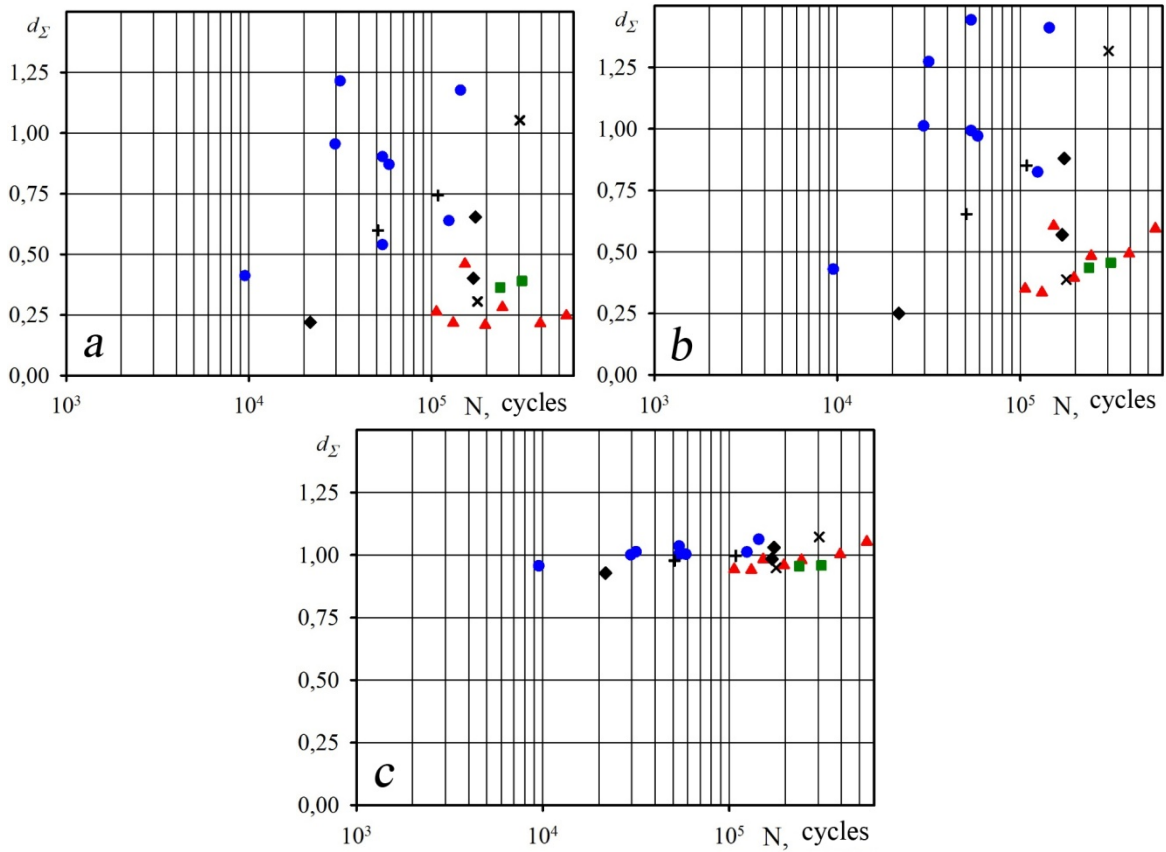


Fig. 7. Damage value d_{\square} according to various damage models and spectrum loading: a – $d_{\Sigma} = d_{pl}$ – by plasticity exhaustion model; b – $d_{\Sigma} = d_{pl} + d_{el}$ – by linear damage model in mixed fracture; c – $d_{\Sigma} = d_{pl}^{\alpha} + d_{el}^{\beta}$ – by nonlinear damage model in mixed fracture

Summary

1. Proposed equations and prediction methods highlighted surprising opportunity to create a new engineering practice for fatigue damage estimation using loading character term.

2. Phenomenological models for damage estimation under VAL demands a presence of fatigue curve parameters and spectrum loading character estimated by the spectrum fullness factor V .

3. Strain approach for fatigue life estimation under VAL based on Coffin-Manson equation and model for elastic and inelastic strains evolution demonstrates good correlation between experimental and analytical data. Proposed analysis is adequate in the range of strain amplitude $0,0002 < \Delta \varepsilon / 2 < 0,02$, as it is shown in [6], and cannot be extended, but may be applied to strain amplitudes as shown in this paper.

4. Fatigue estimation based on damage variation in mixed fracture mechanism in metals under VAL proves that damage cumulation components have nonlinear pattern of change.

References

1. GOST 25.507-85. Raschety i ispytaniya na prochnost v mashinostroenii. Metody ispytaniya na ustalost pri ekspluatatsionnykh rezhimakh nagruzheniya. Obschie trebovaniya, Izdatelstvo standartov, Moskva (2005), 19 p.

2. Sarkani Feasibility of Auto-Regressive Simulation Model for Fatigue studies, J. Structural Engineering, 116(1990), 2481-2495.

3. D.P. Kihl Stochastic fatigue concepts in welded surface ship structures. Departmental Report SSPD-90-173-25, US Navy: David Taylor Research Center, Bethesda, MD 200084-5000, 1990.

4. V.P. Bagmutov, A.N. Savkin O realizatsii razlichnykh podhodov k prognozirovaniyu dolgovechnosti konstruktsionnykh staley na osnove modelirovaniya povrezhdennosti pri neregulyarnom peremennom nagruzhenii, Trudy mezhdunar. nauch.-teh. konf. "Prochnost materialov i elementov konstruktsiy" (Kiev, 28–30 sentyabrya 2010 g.), G.S. Pisarenko Institute for Problems of Strength of the National Academy of Sciences of Ukraine, 2011, Kiev, 2011, pp. 594-602.

5. M.A. Miner, Cumulative damage in fatigue, Journal of Applied Mechanics. – 67 (1945), A159–A164.

6. V.P. Kogaev, N.A. Mahutov, A.P. Gusenko, Raschety detaley mashin i konstruktsiy na prochnost i dolgovechnost: Spravochnik, Mashinostroenie, Moskva, 1985.

7. A.N. Savkin, V.P. Bagmutov, Prognozirovanie ustalostnoy dolgovechnosti vyisokonagruzhenykh konstruktsiy, VolgGTU, Volgograd, 2013.

8. V.P. Bagmutov, A.N. Savkin Prognozirovanie dolgovechnosti konstruktsionnykh materialov pri regulyarnom i neregulyarnom nagruzhenii s uchetom razlichnykh mekhanizmov povrezhdeniya, VolgGTU, Volgograd, 2008.

9. A.V. Gurev, A.N. Savkin Rol mikroplasticheskikh deformatsiy v razvitii ustalostnykh povrezhdeniy v metallakh, in: Mekhanicheskaya ustalost metallov: Materialy VI Mezhdunarodnogo kollokviuma. Nauk. dumka, Kiev, 1983, pp. 122-129.

10. Rainflow Cycle Counting Excel Template with Macros. – 2011. – <http://www.storera.com/stoflo/>.

11. S.S. Manson Fatigue: a Complex Subject – Some Simple Approximations, Experimental Mechanics – Journal of the Society for Experimental Stress Analysis 5(1965), pp. 193-226.

12. V.T. Troschenko Deformirovanie i razrushenie metallov pri mnogotsiklovom nagruzhenii, Nauk. dumka, Kiev, 1981.

13. Uvajsov S. U., Kofanov Ju. N. Metodika vyjavleniya skrytykh defektov integral'nykh shem i apparatury // Nadezhnost' i kontrol' kachestva. Ezhemesjachnoe prilozhenie k zhurnalu "Standarty i kachestvo". 2013. № 11. S. 19-31.

14. Uvajsov S. U., Kofanov Ju. N., Sotnikova S. Ju. Programmnyj kompleks modelirovanija fizicheskikh processov pri avtomatizirovannom proektirovanii istochnikov vtorichnogo jelektropitanija dlja slozhnyh bortovyh sistem // *Dinamika slozhnyh sistem*. 2012. № 3. S. 80-84.

15. Uvajsov S. U. Teksturovannye podlozhki iz splavov nikelja s tugoplavkimi metallami (W,Mo,Re) dlja sverhprovodjashhikh kabelej vtorogo pokolenija // *Izvestija vysshih uchebnyh zavedenij. Povolzhskij region. Tehnicheskie nauki*. 2012. № 2(22). S. 126-137.

FATIGUE ANALYSIS OF THE AUTOMOBILE SUSPENSION ARM UNDER VARIABLE AMPLITUDE LOADING

Savkin A.N., Gorobcov A.S., Andronik A.V., Sukhanov M.A.
Volgograd State Technical University, Volgograd, Russia

Variable amplitude fatigue finite-element analysis is completed and reported for low arm and torsional bar of the offroad-vehicle suspension. Academic search of alternative materials is committed for providing the material replacement possibility of these structural parts. Calculation algorithms are given for applied engineering software, (multibody dynamics system FRUND and CAD SolidWorks). Critical fatigue regions and fatigue life values are defined.

Keywords: automobile fatigues, rainflow method, FRUND spectrum, stress correction.

Advances in automobile engineering allow relishing the performance, agility and comfort of modern passenger vehicles. Suspension is directly associated with all these characteristics and many others. One of the most popular is suspension with two lateral arms and torsional bar. It has amount of odds compared with rivals: reliability, small size, low metal intensity, negligible operation noise, tuning simplicity etc. Reasonable good set of technical parameters and exploitation convenience made this suspension type widespread among off-road and all-terrain vehicles. Though, cost of used materials and manufacturing processes is sufficiently high, especially for torsional bar [1]. Russian automobile manufacturers commonly use such expensive steels as AISI 6145, 9260, 9840. [2]

Automobile suspension is a basis of effective and safe transport exploitation and a foundation of driver and occupants comfort, particularly in off-road vehicle. This complex technical system undergoes tremendous value-, frequency- and direction-varying loading, minimizes it owing to elastic-dampening properties and transmits to sprung weight. Thus suspension may be subjected to crack appearance and fatigue fracture, so it explains the fatigue analysis necessity. Taking the above mentioned into consideration, question of cheap and effective material alternative certainly occurs for heavy-loaded low arm and torsional bar with concurrent retaining of fatigue and strength properties. It is proposed to use common and low cost steel grades used in automobile suspensions such as AISI 1045, 1074, 5140.

This issue can be resolved through finite-element analysis via medium-level CAD such as SolidWorks. Stress-life and strain-life methods are two well-known approaches to define implicit fatigue damage of structure. Detailed analysis of fatigue factors was demonstrated based on both stress-life and strain-life methods in the paper [3]. Interestingly, strain-life method showed itself more adequate for local plastic strain evaluation, but stress-life method is more popular in automobile design. However, there is only stress-life method in the code of SolidWorks. Note, that stress-life method brings several times longer fatigue life than strain-life method in presence of local near-yield stresses [4], and it is strongly recommended to admit maximal cumulated damage value $D=0,3$ rather than $D=1$ [5].

Historically, stress-life method is old and time-proved one for fatigue estimation. According to this approach fatigue primarily depends on loading, cyclic material properties, geometry, environment and associated Wohler's curve. Relationship between nominal stress amplitude and fatigue life represented by fatigue curve and expressed by formula [6]:

$$N_f = \left(\frac{\sigma_{-1}}{\sigma_a} \right)^m N_0, \quad (1)$$

where σ_a – stress amplitude; N_f – fatigue life; m – empirical exponent, defined by fatigue curve in the coordinates $\lg \sigma - \lg N$.

It is worth noting that multiple stress state is inherent for real structure parts. Nevertheless, most of experimental data for fatigue analysis were obtained for uniaxial symmetrical loading. Consequently, it is essential to follow one algorithm for correct description of relationship between external loading and stress tensors: 1) transform of a multiple stress state to equivalent uniaxial stress state; 2) schematize loading history from spectral variable amplitude loading to block variable amplitude loading; 3) consider mean stress effect via marginal amplitude curve. [7]

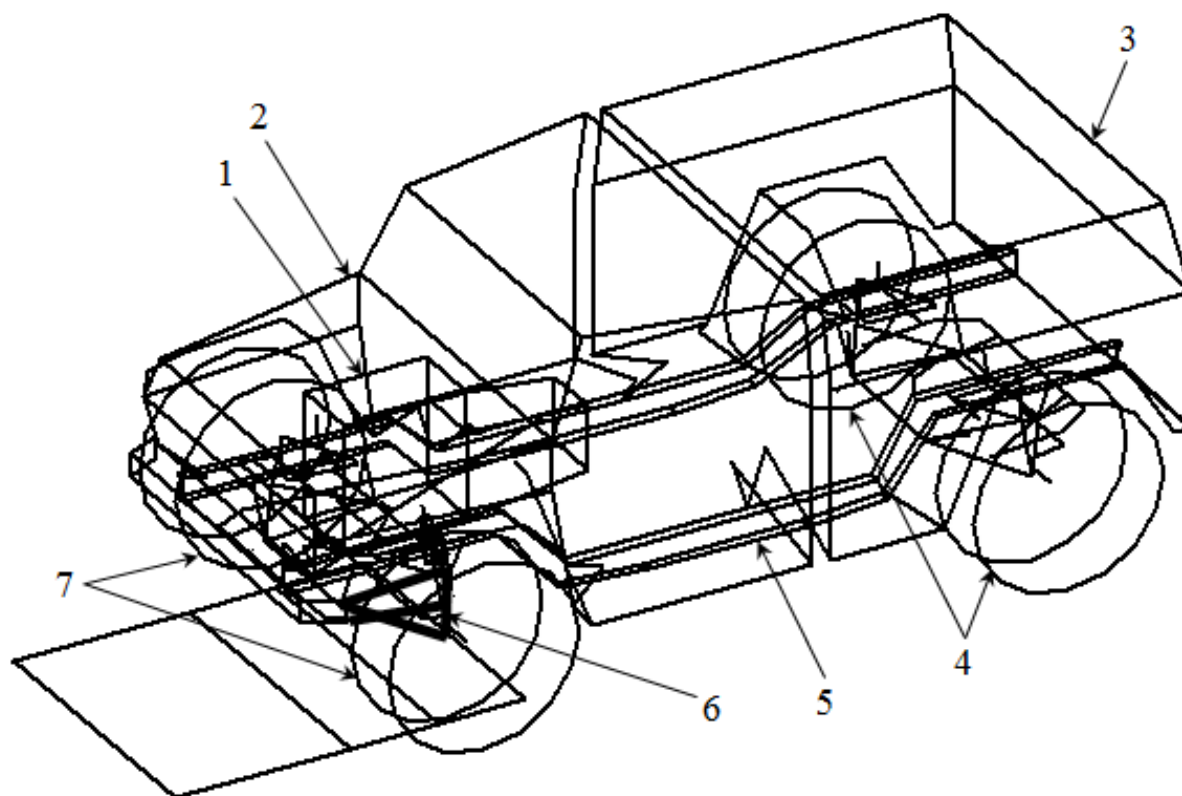


*Fig. 1 – Automobile dynamic model in multibody dynamics system FRUND:
1 – engine and gearbox, 2 – cabin, 3 – body, 4 – rear axle wheels, 5 – frame,
6 – low arm and torsional bar, 7 – front axle wheels.*

It was revealed that dominant contribution in fatigue damage attributed to high-frequency loading conditioned by road relief, so it is a rational decision to apply dynamic vehicle models with associated road profile [5]. Current research is restricted by straight linear motion on various road types with different, but constant speed in each simulation case. Automobile model assembled in multibody dynamics system FRUND (fig. 1) that is used for spectrum loading calculation [8]. There are major components, mechanisms and parts typical for off-road vehicle in the model. Loading signal contents 3 forces and 1 stability moment

(yaw moment) and comes from road to the automobile through tires. Spectrum loading sequences were generated in multibody dynamics system FRUND during vehicle exploitation on tarmac road, flat cobble road and cobble road with bumps and valleys corresponding to the experimental data of the Central Research Automobile and Motor Institute. Some of the above mentioned spectrums are shown on fig. 2. Vertical and horizontal loading spectrum caused by road and compressive loading spectrum caused by damper are used in each simulation case. 4 simulation cases were analyzed: generated spectrums for tarmac road used in 3 cases, flat cobble road and cobble road with bumps and valleys correspondingly, but spectrums of cobble road with bumps and valleys used in 4th case, however, generated vertical loading spectrum was replaced by standard automobile spectrum SAESUS for suspension loading [7].

Non-uniform mesh of second order solid tetrahedral finite elements (size 2 mm) was automatically created by means of Delaunay-Voronoi method for all the part volume during analysis. Kinematic (loads) and static (constraints) boundary conditions were defined based on assembly sequence and operating principle of the suspension [1]. Transformation of a multiple stress state to equivalent uniaxial stress state was committed via limit distortion strain energy hypothesis (von Mises model) [9]:

$$\sigma_{eq} = \sqrt{\frac{(\sigma_1 - \sigma_2)^2 + (\sigma_2 - \sigma_3)^2 + (\sigma_1 - \sigma_3)^2}{2}}, \quad (2)$$

where σ_{eq} – equivalent stress; $\sigma_1, \sigma_2, \sigma_3$ – principal stresses.

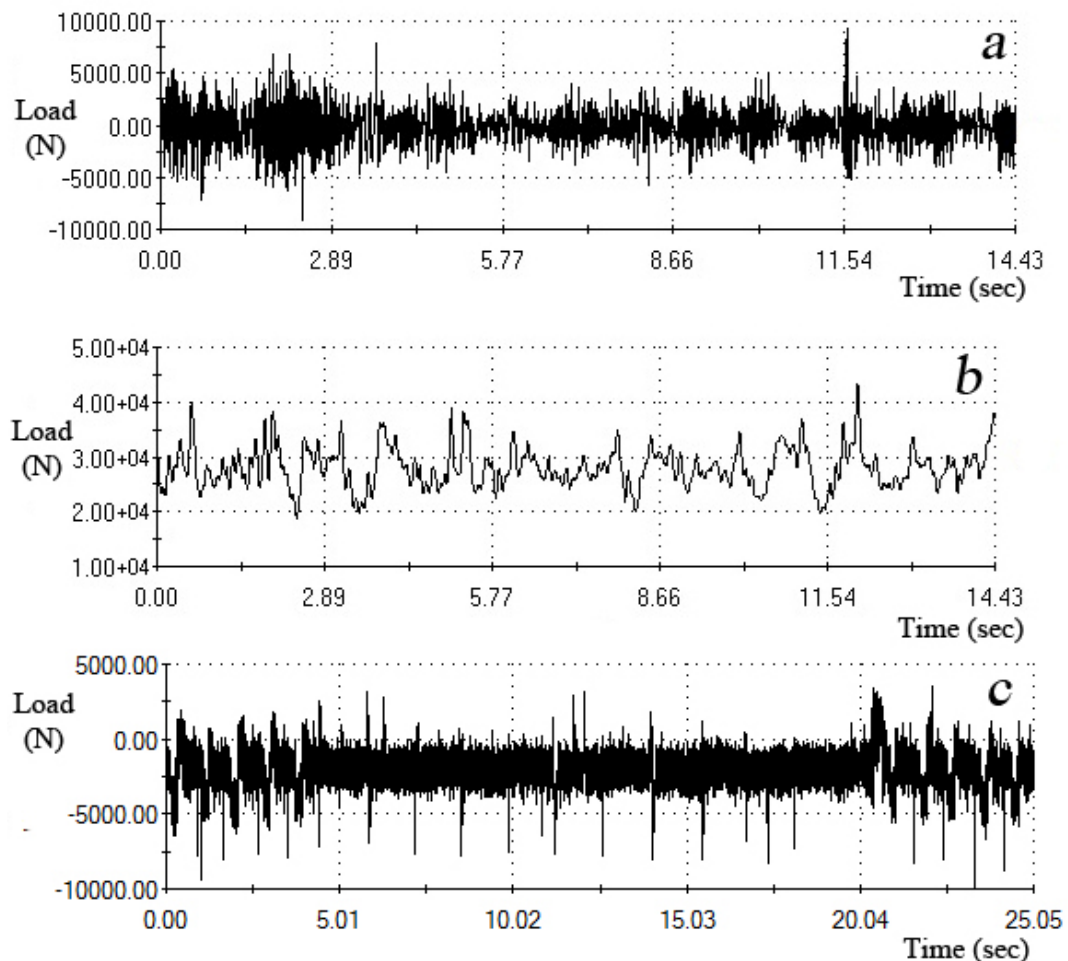


Fig. 2 – Loading spectrums for low arm: vertical spectrum caused by cobble road with bumps and valleys (a), compressive loading spectrum caused by damper (b), SAESUS spectrum (c).

Schematization of loading history was completed by rainflow method in SolidWorks. This makes possible to advance from loading history to the closed hysteresis loops sequence of stress (or strain) accounting loops as full cycles. There are rainflow I (for multiple loading as in the current research) and rainflow II modifications (in one scoop) of the method described in the paper [10].

Mean stress correction realized in SolidWorks by Gerber's formula for ductile materials [11]:

$$\sigma_{ca} = \frac{\sigma_a}{1 - \left(\frac{\sigma_m}{\sigma_u} \right)^2}, \quad (3)$$

where σ_{ca} – corrected alternating amplitude stress; σ_a – amplitude stress; σ_m – mean stress; σ_u – strength limit.

Palmgren-Miner's linear rule of damage cumulation forms the basis of fatigue life estimation in SolidWorks [12]:

$$\sum_{i=1}^{N_\Sigma} \frac{n_i}{N_i} = 1, \quad (4)$$

where n_i – number of cycles with current amplitude stress; N_i – number of cycles to fracture for constant amplitude loading; N_Σ – number of cycles to fracture for variable amplitude loading. Fracture is nothing but a strength loss of structure, expressly due to propagated macroscopic fatigue cracks according to Palmgren-Miner's model.

The fatigue analysis results showed that fatigue life diagram is almost the same at various combinations of spectrums and material assignments, apart from fatigue life values given in table 1. One of the fatigue analysis diagrams is given in fig. 3 for AISI 5140 steel under loading spectrums of the cobble road with bumps and valleys.

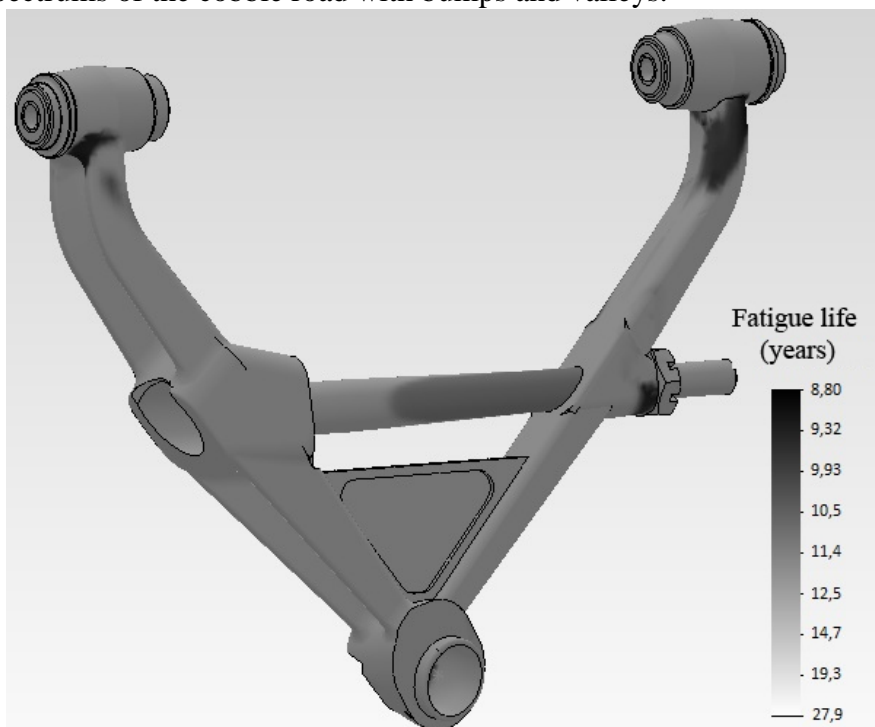


Fig. 3 – Fatigue life diagram of front suspension low arm (AISI 5140 steel)

Some conclusions proceeds from the table 1: 1) fatigue life attributed to exploitation of vehicle on the flat cobble road is 1,4 times longer than for the cobble road with bumps and

valleys; 2) fatigue life attributed to exploitation of vehicle on the tarmac road is 2,2 times longer than for the cobble road with bumps and valleys; 3) fatigue life calculated from combination of cobble road with bumps and valleys and SAESUS spectrum is 1,06 times longer than for the cobble road with bumps and valleys only.

Table 1

Fatigue life for various materials and loading spectrums

Steel grade (AISI)	Strength and fatigue properties, MPa				Fatigue life prediction (in years)			
	σ_u	σ_y	σ_{-1}	τ_{-1}	Tarmac road	Flat cobble road	Cobble road with bumps and valleys	Combination of spectrums (including SAESUS)
1045	570	315	280	170	4,48	2,85	2,05	2,16
1074	1130	980	392	350	6,27	3,98	2,87	3,02
5140	785	640	600	240	19,2	12,2	8,8	9,27
6145	1270	1080	676	519	20,6	12,7	8,9	10,4
9260	1470	1325	500	-	16,0	10,2	7,33	7,73
9840	1080	930	447	274	15,2	9,7	6,9	7,3

Using of generalized random sample of loading associated to typical exploitation cases of machine makes fatigue analysis more applicable. In the current research, it is enough to assign ratio between exploitation times on various type of road surface. We should notice that degradation of material properties was not accounted in the current work. So fatigue life for low arm made of the steel with the greatest fatigue resistance (AISI 6145) is equal to value:

$$L = \sum_{i=1}^3 a_i \cdot v_i \cdot t_i = 4,77 \cdot 10^6 \text{ km}, \quad (5)$$

where a_i - exploitation part for the current road type by mileage (0,684 - cobble road with bumps and valleys; 0,272 - flat cobble road; 0,044 - tarmac road) [13]; v_i - automobile speed for the current road type (45 km/h – cobble road with bumps and valleys, 60 km/h – flat cobble road, 90 km/h – tarmac road) [8]; t_i - fatigue life for every road type.

One can see that maximal fatigue damage appears close to lugs of the arm due to small radii of fillets (and associated reasonably high stress concentration), and in the torsional bar, especially near to fastening screw nut (see fig. 3). This fact is entirely conforms with real fatigue fracture of this suspension structure.

Conclusions

1. Fatigue calculations via multibody system FRUND and CAD SolidWorks are given for automobile suspension parts. This approach allows committing of nonlinear dynamics analysis and finite-elemental analysis for structures under external loading correspondingly.

2. Regions of stress raisers and possible fatigue fracture are defined for parts of automobile suspension.

3. According to fatigue analysis results, suggestion that low arm and torsional bar material may be replaced by AISI 5140 as an alternative of 6145 and 9260 steels. Associated fatigue life of structure was defined for various materials and road surface. Fatigue life of the low arm was defined ($4,77 \cdot 10^6 \text{ km}$ for AISI 6145) considering typical exploitation cases.

References

1. Raympel Y. Shassi avtomobilya - M.: Mashinostroenie, 1983. – 356 s.
2. Marochnik staley i splavov / A.S. Zubchenko, M.M. Koloskov, Yu.V. Kashirskiy and oth. – M.: Mashinostroenie, 2003. – 784 p.

3. Fatigue life prediction of lower suspension arm using strain-life approach / M. M. Rahman, K. Kadirgama, M. M. Noor, M. R. M. Rejab, S. A. Kesulai // *European journal of scientific research*. – 2009. - Vol.30. - #3. - pp. 437-450.
4. Svenson T., Johannesson P., Mare J. Fatigue life prediction based on variable amplitude tests-specific applications // *International journal of fatigue*. – 2005. - #27. – pp. 966-973.
5. Kim H.S., Yim H.J., Kim C.M. Computational durability of body structure in prototype vehicles // *International journal of automotive technology*. – 2002. - #3(4). - pp. 129-136.
6. Savkin A.N. Prognozirovanie ustalostnoy dolgovechnosti vyisokonagruzhennykh konstruktsiy: monografiya/ Savkin A.N. Bagmutov V.P.; VSTU, - Volgograd, 2013,- 364 p.
7. SolidWorks 2007/2008 Kompyuternoe modelirovanie v inzhenernoy praktike / A.A. Alyamovskiy, A.A. Sobachkin, E.V. Odintsov, A.I. Haritonovich, N.B. Ponomarev. – SPb.: BHV-Peterburg, 2008. – 1040 p.
8. Kompyuternye metodyi postroeniya i issledovaniya matematicheskikh modeley dinamiki konstruktsiy avtomobiley: monografiya / A.S. Gorobtsov, S.K. Kartsov, A.E. Pletnev, Yu.A. Polyakov. – M.: Mashinostroenie, 2011. – 463 p.
9. Mehanicheskoe povedenie materialov pri razlichnykh vidakh nagruzheniya / V.T. Troschenko, A.A. Lebedev, V.A. Strizhalo i dr. - K.: Logos, 2000. – 571 p.
10. Downing S.D., Socie D.F. Simple rainflow counting algorithms // *International journal of fatigue*. - 1982. - #1. – pp. 31-40.
11. Hanq D.A., Walters A.J., Beuth J.L. Development of an object-oriented fatigue tool // *Engineering with computers*. - 2000. – Vol. 16. – pp. 131-144.
12. Miner A. Cumulative damage in fatigue // *Journal of applied mechanics*. - 1945. - #12. – pp. 159-164.
13. Chernikov S.K., Ashihmin A.N. Matematicheskaya model dlya analiza NDS ramiy avtomobilya KamAZ i ee verifikatsiya // *Kazanskiy fiziko-tehnicheskii institut. Ezhegodnik*. – Kazan: FiztehPressyu - 2001. – pp. 187-193.
14. Uvajsov S. U., Kofanov Ju. N. Metodika vyjavleniya skrytykh defektov integral'nykh shem i apparatury // *Nadezhnost' i kontrol' kachestva. Ezhemesjachnoe prilozhenie k zhurnalu "Standarty i kachestvo"*. 2013. № 11. S. 19-31.
15. Uvajsov S. U., Kofanov Ju. N., Sotnikova S. Ju. Programmnyj kompleks modelirovaniya fizicheskikh processov pri avtomatizirovannom proektirovanii istochnikov vtorichnogo jelektropitanija dlja slozhnykh bortovykh sistem // *Dinamika slozhnykh sistem*. 2012. № 3. S. 80-84.
16. Uvajsov S. U. Teksturovannye podlozhki iz splavov nikelja s tugoplavkimi metallami (W,Mo,Re) dlja sverhprovodjashhih kabelej vtorogo pokolenija // *Izvestija vysshikh uchebnykh zavedenij. Povolzhskij region. Tehnicheskie nauki*. 2012. № 2(22). S. 126-137.

RESEARCH WORK SLIPCLUTCH IN A VIRTUAL ENVIRONMENT

Matlin M.M., Shandybina I.M., Lebskiy S.L., Polezhaev D.V.

Volgograd, Volgograd State Technical University

Methodology the study characteristics of the clutches in a virtual environment and run its software implementation.

Keywords: safety clutche, a study of the characteristics of clutches, clutch disc, clutch ball, jaw coupling clutch claw, modeling, 3D models, virtual lab, a virtual environment, software, software complex.

On chair «Elements of Machine and drawing-machine» for many years keep on creation and implementation of the virtual laboratory works. one of the most interesting is the exploration of the clutches [5]. Virtual environment significantly updated and expanded their study to carry out a study/

The study on computer specifications clutches have been built 3D models (Picturs 1,2) and clutches: circular, conical, spherical, claw, as well as the methodology for conducting experiments in a virtual environment. The methodology for the research of characteristics of safety clutches, the program is implemented as a virtual lab work and take out the patent for the program [5] The following are examples of on-screen forms, illustrate the module control of students knowledge on the topic of virtual laboratory work.



Picture.1. plant model

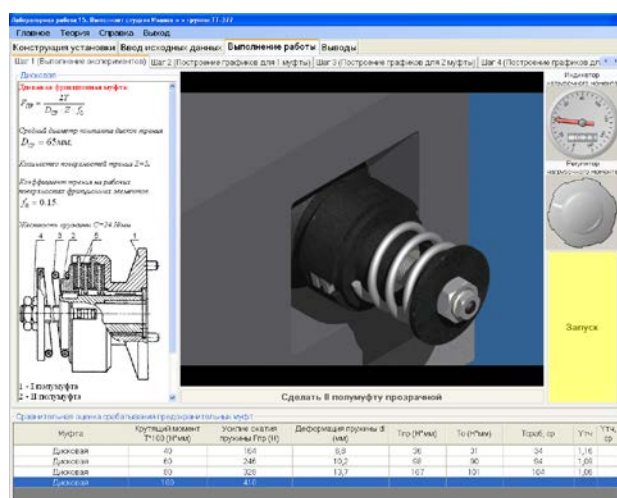
Picture 3 is presented on-screen form for choice of formulas and parameters in the calculation of the characteristics of the clutches are the same here all necessary comments and explanatory captions option choosing formulas for calculations are displayed in Picture 4

Pictures 4,5 shows examples of populating tables with experimental and calculated data and construct appropriate graphs.

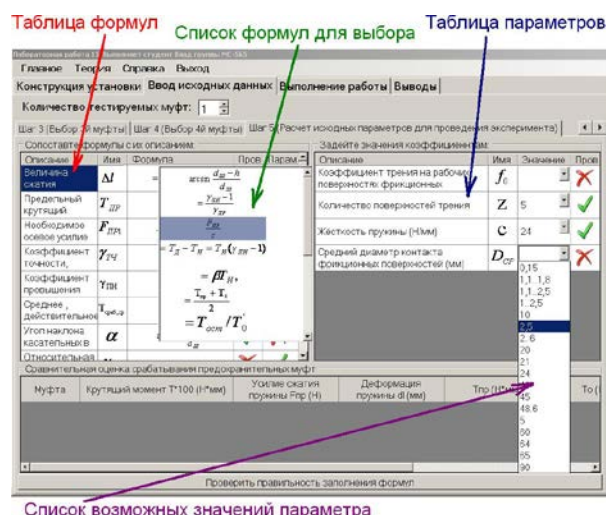
For documentation of work performed by computer support in the form of the generated report file in Microsoft Word format.

It contains basic formulas, experiments, numerical tables and graphs that illustrate the relationship between the different parameters in the end.

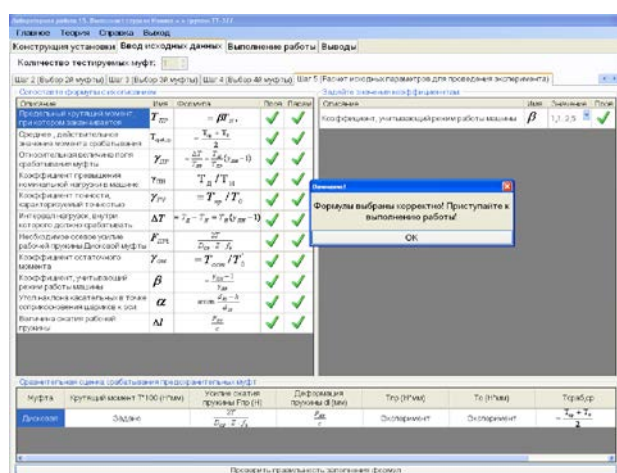
Using the proposed methodology and developed on the basis of the software enables the computer study of influence of various factors on the characteristics of the clutches for a large number of possible combinations of input data.



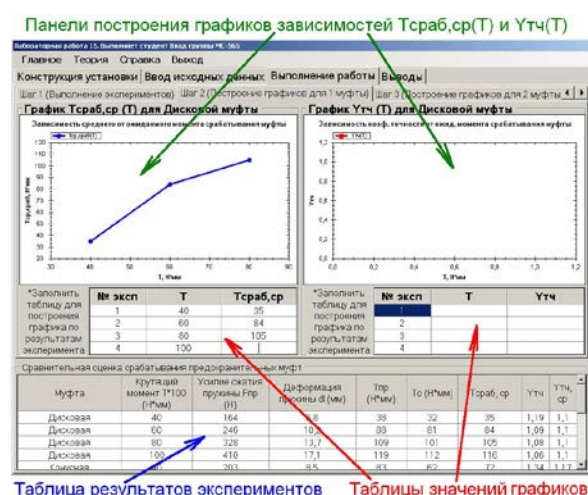
Picture 2: Experimental study of friction disk clutches



Picture 3 Control module knowledge



Picture. 4 Verifying the answer



Picture 5 Tables of experimental and calculated results

The practical value of the work lies in the originality of the software, its integrity and readiness as a virtual laboratory work in the educational process. It is planned to use the virtual laboratory work in distance education students full-time part-time and extra-mural form of teaching, as well as to the full-time students in order to enhance its effectiveness.

References

1. Matlin, M. M. Complex computer technology to study the courses of «Elements of Machine» and «TMM»/M.M. Matlin, S.Y. Kislov, I.M. Shandybina. Proceedings of the International Conference on the theory and mechanics of machines, mechanisms dedicated to the 100 anniversary of the birth of I.I. Artobolevskogo, Krasnodar, 2006, part 1.-p. 275-276
2. Laboratory workshop and control of students knowledge on computer/M. M. Matlin, I.M. Shandybina, S.Y. Kislov// «Theory of machines and machine elements» Tr. All. Rus. n-t. conf. with the participation of other countries. representatives, Moscow 10-12 Oct. 2008, devoted. 100-th anniversary of Prof. D.N. Reshetov/ MGTY. Be named N.E.Bauman.-2008.-249-251
3. Using virtual labs in the educational process of the course «Elements of Machine»/ M.M. Matlin, S.Y. Kislov, I.M. Shandybina, S.L. Lebskiy/ VolgGTU. series «New

educational systems and technology at the University», hunting rituals. *Wed. scientific calendar/VolgGTU, Volgograd, 2008.-vol. 5, no. 5, p. 145-147*

4. Certificate of state registration of the computer number 2009616726 «program to study the characteristics of the virtual safety clutches»/ Polezhaev D.V., Shandybina I.M, Matlin M.M., Lebskiy S.L., 2009.

5. Matlin M.M. Using virtual environments for laboratory practical course «Elements of Machine»/ M.M. Matlin, I.M. Shandybina, S.L. Lebskiy/ *Innovation Information Technologies: Mater. Intern. nauchn.-practical conference. Prague, Czech Republic, 22-26 April. 2013 4 volumes T.1.MIEMNIU HSE [etc.],-M., 2013. - p. 277-279.*

EVALUATION OF CYCLIC DAMAGE OF STRUCTURAL MATERIALS ON THE BASIS OF THE INTERACTIONS OF LOCAL DAMAGES

Stolyarchuk A. S., Korobov A. V., Vdovenko A. V., Gorunov A. I.
Volgograd, Volgograd State Technical University

The reported study was supported by RFBR, research projects № 14-08-00837 a and № 14-08-31712 мол_a

A procedure of evaluation of macrodamage at cyclic creep structural materials in the area of low-cycle fatigue is developed. This evaluation is carried out using entropy-probabilistic approach. The accounting of interactions between local damages at mesostructural level is entered. A comparison of calculated and experimental results is given.

Keywords: the mesostructural level, of entropy-probabilistic approach, of low-cycle fatigue.

At the present time many publications are devoted to research of low-cycle fatigue of metals and alloys with a polycrystalline structure. This interest to low-cycle fatigue is explained by constant increase in an energy saturation of modern designs. In this case materials of construction details are often operated out of Hook's law. There is a transition to the area of elasto-plastic strain. The result is a one-side strain accumulation which leads to the gradual depletion of the reserve plasticity (deformation damage). This phenomenon obtained a technical name – cyclic creep. Depletion of the reserve of plasticity at cyclic loadings occurs at accumulation of fatigue (cyclic) damage [1]. The mutual influence of these processes of damage (deformation damage and fatigue damage) in structural materials, in particular at mesostructural level, is insufficiently studied. The present study is devoted to studying this influence within the detected interactions between local damages at the mesostructural level.

The choice of the mesostructural level is caused by the following reasons. Firstly, at this scale level all mechanisms of damage of «previous» scale levels (atomic level, nanoscale level, microscale level) integrally show themselves. This defines the role of mesoscale level in the formation of the mechanical behavior of polycrystalline metal materials under loading [2]. Secondly, at this scale level the statistical character of local damages of previous levels is quantitatively displayed. It is known, that the statistical character disappears at the macroscale level. The above facts make rightful the application of entropy-probabilistic approach in the calculations which is based on a probabilistic evaluation of local damages at mesoscale level. At the present work the further arguments are carried out on the basis of this approach.

Earlier the entropy-probabilistic model for the evaluation of cyclic damage of polycrystalline structural materials was proposed [3] in the following form

$$\omega(\zeta) = q \int_0^{\zeta} S(\zeta) d\zeta. \quad (1)$$

Here ω and ζ are cyclic and deformation macrodamages of materials at the low-cycle fatigue; $S(\zeta)$ is a function of «unconditional entropy» [4] of damaged state which is defined as informational. In this case it is the uncertainty of the damaged macrostate by two types of mesodamages which have a probabilistic character. This uncertainty is set by Shannon's formula [5] (under mesodamages are understood local cracks or local deformations [3]); q is an empirical constant of material. As S is an unconditional entropy, formula (1) doesn't take into account possible interactions between local damages.

There is a systematic deviation of the calculated values from experimental values, despite essential working efficiency of entropy-probabilistic model (1). Qualitative regularities of this deviation are repeated even for materials with different lattice structure. For example, in the figure 1 the comparison of experimental (light points) values and calculated (curve 1) values ω for two structural materials is shown.

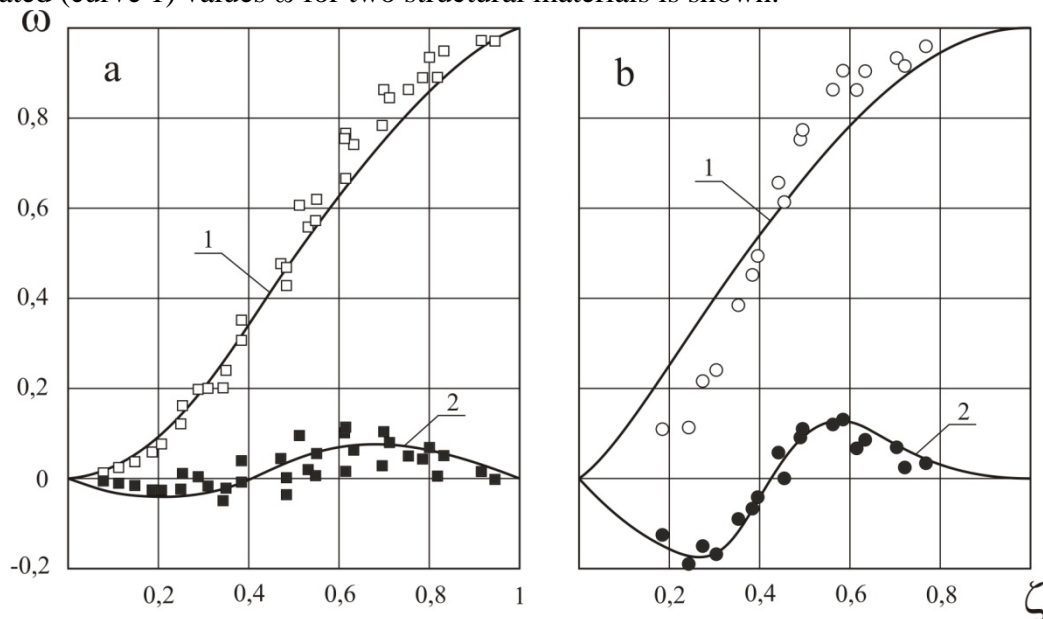


Figure 1 – Comparison of calculated values ω and experimental values for a titanium α -alloy (a) and steel 45 (b): 1 – evaluation on the basis of formula (1); 2 – disarrangement ω_* between calculated and experimental

We will call the value ω_* (curve 2) as a divergence between calculation values [on the formula (1)] and the values obtained in the experiment. We will take into account that the found divergence is associated only with the mutual influence of two processes damage (fatigue and creep) at the cyclic creep. This mutual influence can be estimated by means of the accounting of interactions between the corresponding two types of the local damages. This technique is based on a simple fact: local damages are concrete results of the two processes of damage. As it has been already mentioned, the formula (1) doesn't account such interactions.

We will set the task: to specify this formula by introducing into the calculations a correction factor ω_* . In the accepted statement it is logically to consider this correction factor as a function from interactions of the local damages at the mesostructural level that is described above. We will use the performances which are formulated in the general theory of communications for the solution of the problem.

In the general theory of communications for the accounting of the interaction between local sources of information (in our case – local damages) the concept of «conditional entropy» is used [4]. This entropy defines the exchange of information between local sources. As researches showed the interactions between local damages of elements of mesostructure (in particular at the cyclic creep) can be found on some indirect indicators. One of them is the periodic type of alternation of the correlated zones of mesodamages. In the figure 2 there are shown pictures of such correlations at the low-cycle fatigue of carbon steel. These pictures are built with the use of wavelet-analysis [6] at different surface conditions. Similar results are also obtained for other materials.

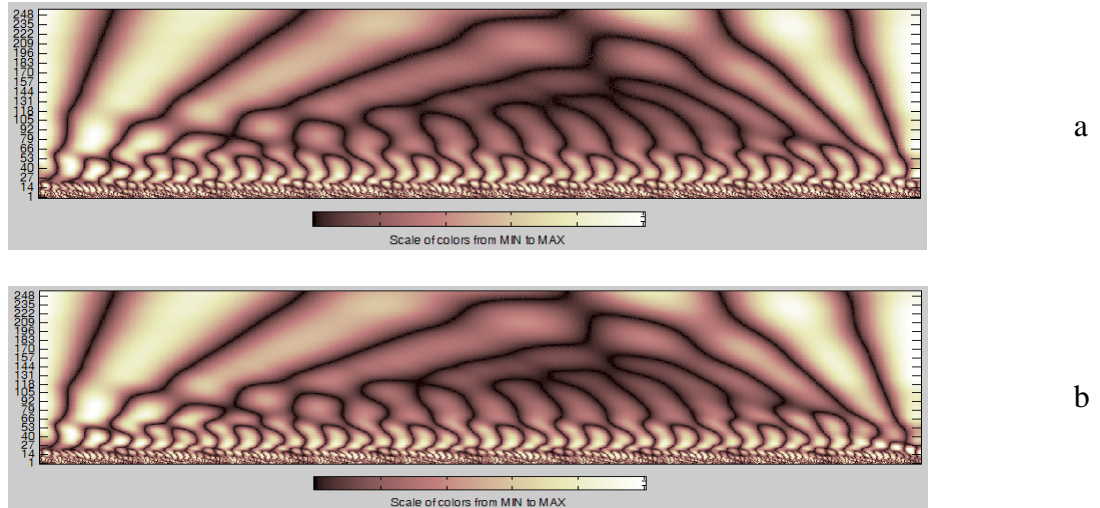


Figure 2 – A spectral recording of mesodamages for carbon steel in the initial state (a) and after surface plastic deformation (b)

These and other experimental facts [2, 7, 8] can be interpreted (in our opinion) as «exchange of information» about damages between structural components of structural materials (in other words about interactions between them). Moreover, these interactions are saved when the surface condition is changed (see figure 2).

We will introduce «function of interfaces» H of elements of mesostructure. Generally, this function should be considered as a complicated function from two arguments (from two types of damage at the macroscale level): $H = H(\omega, \zeta)$. Thus the complete differential of this function can be written as follows

$$dH = \frac{\partial H}{\partial \omega} d\omega + \frac{\partial H}{\partial \zeta} d\zeta. \quad (2)$$

In the work [3] the dependence of cyclic damage from deformation damage was accepted a priori. That is why, the formula (1) includes only one of the arguments (ζ). In order to make the developed decision coincide such a hypothesis, we should fix the following: $\omega = const \Rightarrow d\omega = 0$. Then, as for the studied special case we can see:

$$dH = \frac{\partial H}{\partial \zeta} d\zeta. \quad (3)$$

Using an entropy-probabilistic approach and taking into account the amendment ω_* , we obtain

$$\omega(\zeta) = q \int_0^\zeta S d\zeta + \omega_* = q \int_0^\zeta S d\zeta + q \int_0^\zeta \frac{\partial H}{\partial \zeta} d\zeta = q \int_0^\zeta \left(S + \frac{\partial H}{\partial \zeta} \right) d\zeta, \quad (4)$$

$$\text{where: } \omega_* = q \int_0^{\zeta} dH = q \int_0^{\zeta} \frac{\partial H}{\partial \zeta} d\zeta.$$

In expression (4) the partial derivative $\partial H / \partial \zeta$ makes sense of «conditional entropy». As it is known [4], the conditional entropy numerically reflects an exchange of information between local sources of information. In this case – between damaged elements of mesostructure. Thus in the proposed entropy-probabilistic approach the function $\partial H / \partial \zeta = F(\zeta)$ defines the interaction of two processes of damage of a material or, precisely speaking, the interaction of two fundamentally different information carriers about this phenomenon (two types of local damages).

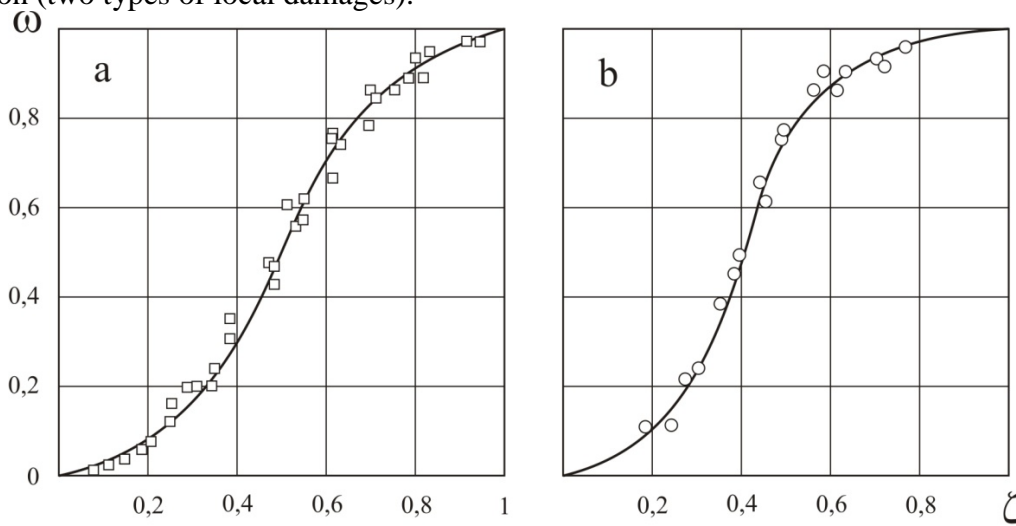


Figure 3 – Comparison of experimental and calculated [on a formula (4)] values ω for titanium α -alloy (a) and steel 45 (b)

In the figure 3 the test results of formula (4) are shown. This check showed good accordance to the experimental data. Besides, in the present work the modified entropy-probabilistic approach allows to estimate «conditional entropy» (in the adopted version) experimentally. This evaluation is necessary in the comparative analysis of various structural materials for the ability to interact between local damages at low-cycle fatigue at the mesostructural level.

References

1. Savkin, A. N. Prognozirovaniye ustalostnoy dolgovechnosti vyisokonagruzhennykh konstruktsiy: monografiya / A. N. Savkin, V. P. Bagmutov. – Volgograd, 2013. – 364 s.
2. Panin, V. E. Deformiruemoye tverdoe telo kak nelineynaya ierarhicheskaya organizovannaya sistema / V. E. Panin // Fizicheskaya mezomehanika. – 2011. – T. 14. – # 3. – S. 7-26.
3. Bagmutov, V. P. Description of Cyclic Creep on Basis of Entropic Approach / V. P. Bagmutov, A. S. Stolyarchuk // Mechanika. Kaunas. – 2000. – Nr. 1 (21). – P. 25-28.
4. Sovetov, B. Ya. Teoriya informatsii / B. Ya. Sovetov. – M.: Akademiya, 2010. – 432 s.
5. Shannon, C. A Mathematical Theory of Communication / C. Shannon // Bell System Tech. J. – 1948. – № 27. – P. 379-423, 623-656.
6. Astafeva, N. M. Veyvlet-analiz: osnovy teorii i primery primeneniya / N. M. Astafeva // Uspehi fizicheskikh nauk. – 1996. – T. 166. – # 11. – S. 1145-1170.
7. Bagmutov, V. P. Modelirovaniye deformatsionnoy struktury pri pulsiruyuschem rastyazhenii metallov / V. P. Bagmutov, A. S. Stolyarchuk, D. A. Griga // Kontseptualnoye

proektirovanie v obrazovanii, tehnike i tehnologii: Sb. nauchn. tr. / VolgGTU. – Volgograd, 2000. – C. 27-34.

8. Bagmutov, V. P. Vliyanie poverhnostnogo sloya na statisticheskiy harakter neobratimiyh mezodeformatsiy i povrezhdenie metallov pri tsiklicheskih nagruzheniyah / V. P. Bagmutov, A. S. Stolyarchuk, V. N. Arisova // Voprosyi materialovedeniya. – 2002. – #1 (29). – C. 364-372.

THE SIMULATION OF HCCI ENGINE PERFORMANCE BY THE SINGLE-ZONE NUMERICAL MODEL COMPLETED BY PHYSICALLY REASONABLE ADJUSTING FUNCTIONS

Itkis E.M., Kuzmin V.N., Fedyanov E.A.

Volgograd, Volgograd State Technical University

The single-zone model of methane-air mixture combustion in Homogeneous Charge Compression Ignition (HCCI) engine was developed. First modeling efforts resulted with the selection of the detailed kinetic reaction mechanism, most appropriate for the conditions of HCCI process. Then model was completed thus to simulate the performance of four-stroke engine and was coupled by physically reasonable adjusting functions. Validation of calculations against experimental data showed acceptable agreement.

Keywords: the single-zone numerical model, of four-stroke engine, by physically reasonable adjusting functions.

INTRODUCTION

Homogeneous Charge Compression Ignition (HCCI) is currently under widespread investigation. To limit the speed of combustion lean mixtures are used. If the mixture is too rich, the pressure rises too rapid and will generate knock-related problems. On the other side, lean equivalence ratios of fuel/air mixture inducted into the cylinder provide low NO- and particulate emissions, low fuel consumption. HCCI process seems promising when running engine on gas as fuel, especially on natural gas.

However, several problems with the HCCI combustion concept to reappear throughout the majority of investigations – two combustion control aspects. First, the ignition event and the ignition timing are not controlled. Second, the rate of heat release is not controlled too. It occurs due to insufficient understanding of HCCI technology. In conjunction with extensive experimental researches, computational models provide a good basis for exploring the HCCI combustion phenomena. Yet a direct numerical simulation of fluid mechanics combined with detailed chemical kinetic model is computationally complex. The typical method of the solution of the problem is simplification either in fluid mechanics or in chemistry part of the model. An example of the latter approach is the single-zone model, developed in Volgograd State Technical University. Its simulation of chemical kinetics is based on law of mass action and Arrhenius rate expression. This approach enables to explore numerically the implication of the inlet air-fuel ratio, initial mixture temperature and in-cylinder pressure on the ignition timing that is directly dependent on the pre-flame chemical reactions.

The paper is arranged as follows. In the first section the development of the model of the first stage of the ignition event – self ignition in the constant volume adiabatic reactor is presented. The results obtained made it possible to choose the most acceptable kinetic reaction mechanism of methane burning. The second section introduces one-zone numerical model of HCCI running process incorporating kinetic model mentioned. The results of the

study related to the validation of the model predictions against measurements enabled to define more accurately basic constants of the model.

SELECTION OF KINETIC REACTION MECHANISM

At the first step of the study the computational model of ignition and combustion in the constant volume adiabatic reactor is developed. Thus we excluded the influence of such factors as variable volume and wall heat transfer. The model mentioned represents the set of equations including the law of mass action and the Arrhenius rate expression to define the rates of three types of reactions:

$$\frac{dc_i}{d\tau} = \sum_j W_{ij}, \quad (1)$$

$$W_{ij} = \pm k_j c_\alpha, \quad (2)$$

$$W_{ij} = \pm k_j c_\alpha c_\beta, \quad (2a)$$

$$W_{ij} = \pm k_j c_\alpha c_\beta c_M, \quad (2b)$$

where W – denotes the reaction rate of a chemical specie i in reaction j ; α, β – standing for i values of species involved in mono-, bi- and three molecular reactions; τ – time; c_i – molar concentration of specie; c_M – molar concentration of active centers; k_j – the reaction rate constant of j -th reaction. The equation (2) is used for calculating the rates of monomolecular reactions, the equation (2a) – for bimolecular reactions and the equation (2b) – for three molecular reactions.

To our opinion the combustion process in HCCI engines can be presented as three sequential stages: the stage of pre-flame reactions, stage of active burning and the post-burning stage. For overcoming the combustion control problems mentioned above the main attention should be paid to studying of the first stage.

By means of the model the evolution of ignition and burning processes of air-methane homogeneous mixture in the constant volume adiabatic reactor was explored. The aim of the study was to determine the choice of kinetic reaction mechanism that shows best agreement of calculated pre-flame stage duration with corresponding experimental data. The necessity of such investigations is based on the fact that the majority of chemical kinetics models observed do not take into account the peculiarities of HCCI process.

The experimental data that serve as the baseline for comparison to the simulation results is generalized in reference [3]. The validation criterion of the model predictions against experiments is the pre-flame stage timing τ_i . Goldsborough [4] has shown that this stage is over when magnitude of current pressure exceeds the initial one more then 5 %.

In Fig.1 the effect of initial mixture temperature on duration of pre-flame reactions stage is shown obtained from experimental data [3] (lines 1–5) and from calculations with two versions of kinetic reaction mechanism: one by V. Y. Bacevich [5] (line 6) and the other developed in San Diego University [6] (line 7). The latter chemical kinetics model is often used to simulate the combustion processes in the flame front of air-methane mixture. Both experimental and computed data are taken for a stoichiometric mixture ($\alpha = 1.0$) at initial pressure $p_0 = 15$ bar. Initial mixture temperature T_0 varied from 800 to 2000K, corresponding to the conditions in the combustion chamber when the piston reaches TDC.

Obviously, values of pre-flame timing obtained with Basevich kinetics mechanism show good agreement with measurements for all initial temperature range, while those by San Diego University diverge dramatically at temperatures less then 1700K. Hence in further calculations the kinetics mechanism developed by Basevich was used.

SIMULATION OF HCCI PERFORMANCE

Next step was the study of heat release evolution in the variable volume reactor. The model was coupled by the set of equations: the energy conservation balance and the ideal gas equation:

$$\begin{cases} \frac{dQ}{d\varphi} + \frac{\alpha_{\Sigma}(T_W - T)}{\frac{\pi n}{30}} A = p \frac{dV}{d\varphi} + c_v m \frac{dT}{d\varphi}, \\ pV = mRT, \end{cases} \quad (3)$$

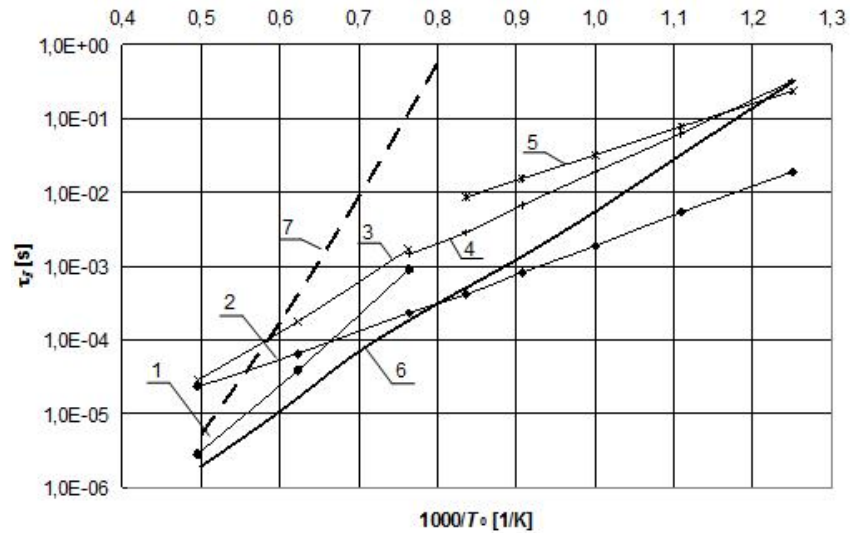


Fig.1. Comparison of the results from calculations with experimental data

where p , V , T – denote in-cylinder pressure, volume and temperature in the combustion chamber; φ – crank angle; m , R – are respectively the mass and individual gas constant of air-methane mixture; c_v – specific heat capacity of mixture at constant volume; Q – heat release during combustion process (calculated by the model depicted above); α_{Σ} – integral heat transfer coefficient; T_W – cylinder wall mean temperature; A – heat transfer area of the combustion chamber.

To date the calculation of convective component of heat transfer coefficient α_k is based on the Woschni's formula [7]. However taking into account results of investigations presented in (8) and (9) Woschni's formula was modified to enhance accuracy of heat loss prediction for HCCI engine operation:

$$\alpha_k = 819,5 \cdot \frac{p_r^{0,8} \cdot w^{0,8}}{T_r^{0,73} \cdot D^{0,2}}, \quad (4)$$

$$w = 2,28 \cdot c_m, \quad (5a)$$

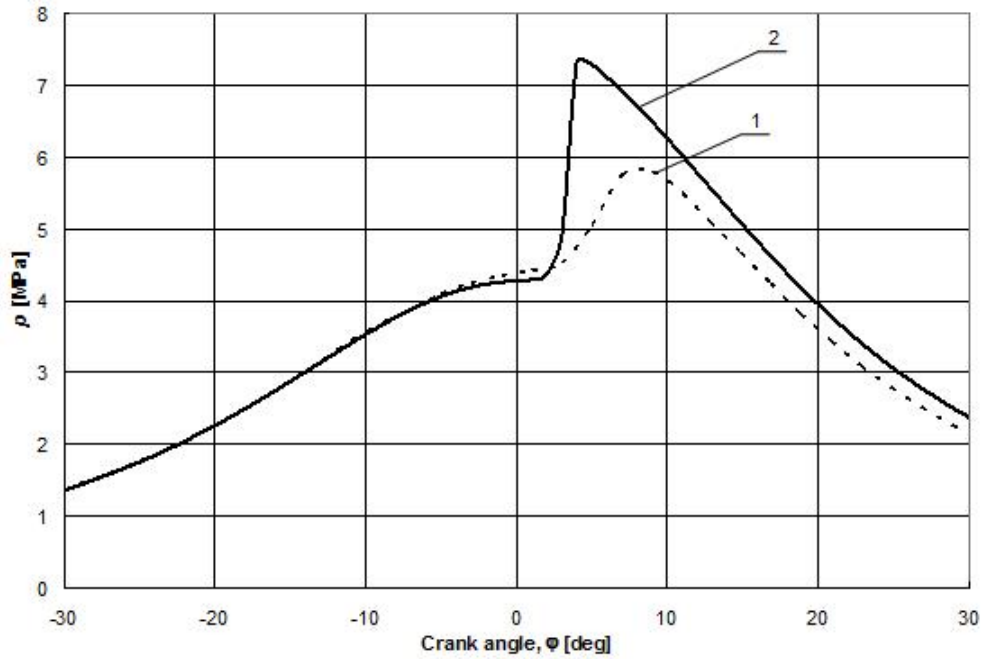


Fig. 2. Experimental (line 1) and calculated (line 2) pressure profiles

$$w = 2,28 \cdot c_m + 3,24 \cdot 10^3 \cdot \frac{V_s \cdot T_1}{6 \cdot p_1 \cdot V_1} \cdot (p_r - p_0), \quad (56)$$

where p – in-cylinder pressure; w – mean bulk speed; D_c – engine bore; T – mean in-cylinder gas temperature; c_m – mean piston speed; p_1 , T_1 , V_1 – respectively pressure, temperature and volume in the compression beginning; V_s – displaced volume; p_0 – in-cylinder pressure under motoring conditions. Two formulas are used for calculating: (5a) for compression process, (5b) for combustion and expansion.

Considering radiative heat transfer, the coefficient α_Σ is given by:

$$\alpha_\Sigma = \alpha_k + \varepsilon_{fl} \cdot C_0 \cdot \frac{\left(\frac{T}{100}\right)^4 - \left(\frac{T_W}{100}\right)^4}{T - T_W}, \quad (6)$$

where ε_{fl} – the emissivity of the flame; C_0 – ratio of absolutely black body radiation (Stefan-Boltzmann constant).

Numerical simulation of compression and combustion events of the HCCI-engine Volvo TD100 [10] was performed. The experimental data involved in the model was as follows. The engine was run at the speed $n = 1000$ rpm on air-methane mixture at fuel-air ratio $\alpha = 3,12$. Initial temperature and pressure at IVC were obtained by extrapolation of those from [10] at 60 CAD BTDC. The results of calculations and experimental data [10] are presented in the Fig. 2.

As seen from Fig.2 the model simulates the indicator process only qualitatively. Similar divergence of experimental data and calculations occur in some other researchers [2, 11]. Experimentally observed burning rates of lean air-fuel mixtures are significantly lower than calculated ones. Moreover, as shows the experimental data, this divergence follows the increase of burnt gas fraction in the reacting mixture.

To our opinion the reason of divergence mentioned is the specifics of HCCI performance that is burning of extra lean fuel/air mixtures. We can point out two main factors that have influence on burning rate. The first – comparison of calculated and experimentally

observed pre-flame reactions timing leads to the conclusion that this divergence follows the increase of α . The latter shows that the surplus air in the air-fuel mixture reduces the rate of burning reactions in the first and second burning stages. The second factor that decreases burning rates is the increase of the burnt gas fraction in the reacting mixture during active burning and post burning stages. Further, the modification of the model taking into account phenomena mentioned is presented.

It's known [13] that the duration τ_I of pre-flame reactions stage when the self ignition of air-fuel mixture occurs depends exponentially on the reciprocal value of temperature T and activation energy E_a of burning reaction:

$$\tau_I \sim \exp\left(-\frac{E_a}{R_\mu \cdot T}\right). \quad (7)$$

where R_μ – is the universal gas constant.

So the impact of air-fuel ratio on the pre-flame stage timing can be taken into account by varying of the activation energy magnitude by including the adjusting function k_α in the argument of exponential function. We suppose that the adjusting procedure of the activation energy should be implemented for all calculations of pre-flame and subsequent burning reactions that is to all elementary reactions of the kinetic scheme. As the magnitude of pre-flame reactions rate depends almost linear on air-fuel ratio and k_α is a multiplier to argument of exponential function thus its correlation with air-fuel ratio is assumed logarithmic:

$$k_\alpha = a_1 \cdot \ln(\alpha) + 1. \quad (8)$$

It provides, in particular, $k_\alpha=1$ for $\alpha=1$. Using the experimental data mentioned above, magnitude of $a_1=0.1341$ is calculated.

The slowing of fuel burning as a sequence of the increase of burnt gas concentration is also considered by the adjusting function. This function k_C simulating the burnt gas fraction impact is involved in the Arrhenius rate expression as an additional pre-exponential multiplier. The relationship between k_C and the instantaneous burning products fraction in the reacting mixture is represented as power function:

$$k_C = 1 - \left[\frac{C_b}{C_{b_{end}}} \right]^x, \quad (9)$$

where C_b , $C_{b_{end}}$ denote the instantaneous and final burning products fraction (burnt gas) both calculated for instantaneous state; x – an exponent. The analysis of experimental data determined the value of the exponent x as 0.16.

Thus, taking into account both adjusting functions, the rate constant for each chemical reaction incorporated in kinetics mechanism is computed by the modified Arrhenius equation:

$$K = k_C \cdot A \cdot T^n \cdot \exp\left(-\frac{k_\alpha \cdot E_a}{R_\mu \cdot T}\right). \quad (10)$$

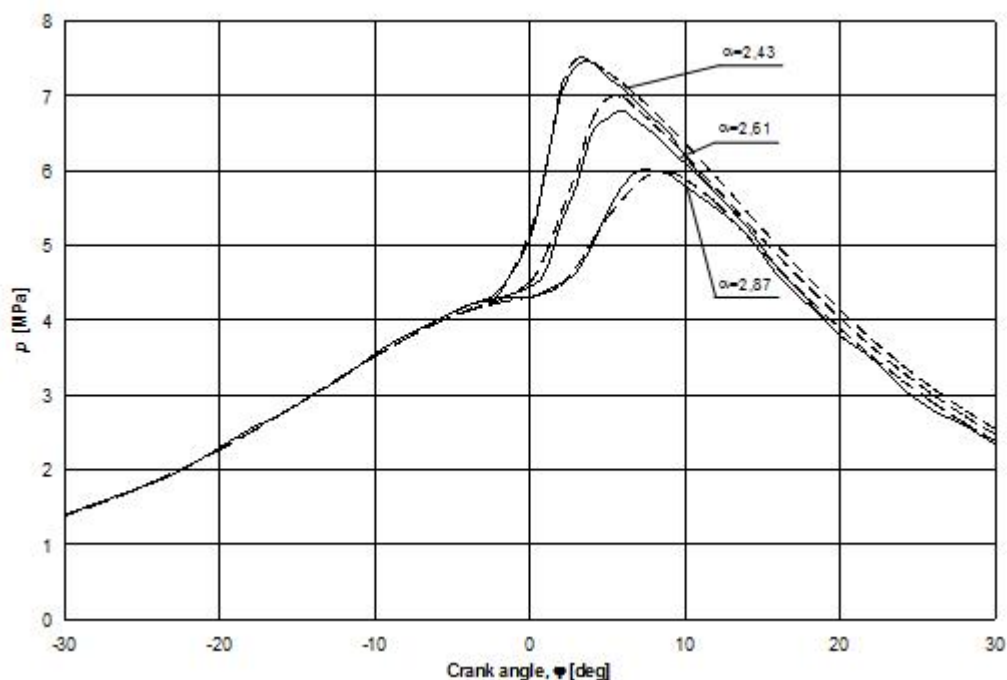


Fig.4. Comparison of experimental and computed (using the modified Arrhenius equation) pressure profiles obtained for the Volvo TD100 engine.

In Fig.4 as an example, the experimental pressure profiles obtained on the Volvo TD100 engine [2], and the results of calculations with modified Arrhenius equation are presented. Both experimental and computed profiles are obtained for 1400 rpm and three air-fuel ratios α (2.43; 2.61; 2.87). As shown in the figure the calculated profiles are in good agreement with experimental ones.

CONCLUSION

By means of the developed mathematical model numerical researches were performed, which enabled to choose the kinetic reaction mechanism of methane-air mixture burning, most appropriate for the conditions of HCCI process. Being completed to simulate the performance of four-stroke engine the model must be coupled with physically reasonable adjusting functions to obtain acceptable quantitative agreement of calculations with experimental data.

References

1. Daesu, J. Combustion analysis of natural gas/air mixture in an HCCI engine using experiment and chemical reactions calculation / J. Daesu, I. Kazuaki, I. Norimasa // Trans. Jap. Soc. Mech. Eng. B. – 2003. – № 681. – С. 1282 – 1289.
2. Homogeneous charge compression ignition engine: experiments and detailed kinetic calculations / P. Amneus [et al] // The Fourth Symposium on Diagnostics and Modeling of Combustion in Internal Combustion Engines. – 1998. – № 4. – С. 567 – 572.
3. Correlation of ignition delay with fuel composition and state for application to gas turbine combustion / S. Samuelsen [et al]; University of California. – Irvine, 2003. – Режим доступа: <http://www.clemson.edu/scies/UTSR/FinalSR084.pdf>, свободный.
4. Goldsborough S.S. Assessing the HCCI characteristics of n-heptane using a free piston rapid compression expansion machine / S.S. Goldsborough // The 4th Joint Meeting of the U.S. Section of the Combustion Institute; Combustion Institute. – Philadelphia, 2005. –

Rezhim dostupa: <http://www.eng.mu.edu/goldsborough/sgoldsb.CI.4th.Joint.Meeting.2005.pdf>.

5. Basevich V.Ya., Vedeneev V.I., Arutyunov V.S. Modelirovanie zaderzhek samovosplameneniya metanovozdushnykh smesey v dvigatele vnutrennego sgoraniya // FGV. – 1994. – № 2. – S. 7–14.

6. Hewson J.C. Skeletal Mechanisms for Methane-Air Flames including NO_x Chemistry / J.C. Hewson, M. Bollig; University of California. – San Diego, 1996. – Rezhim dostupa: http://maemail.ucsd.edu/combustion/Mechanisms/skeletal_table.html

7. Teoriya dvigateley vnutrennego sgoraniya / Pod red. N. H. Dyachenko. 2-e izd., pererab. i dop– L.: Mashinostroenie, 1974. – 552 s.

8. Fedyanov, E. A. Osobennosti teplootdachi v stenki tsilindra dvigatelya s samovosplameneniem gomogennoy toplivovozdushnoy smesi [Tekst] / E. A. Fedyanov, E. M. Itkis, V. N. Kuzmin // Vestn. VolgGTU. Ser. Protssy preobrazovaniya energii i energeticheskie ustanovki. Vyip. 2. – 2009. – № 7(55). – S. 72 – 74.

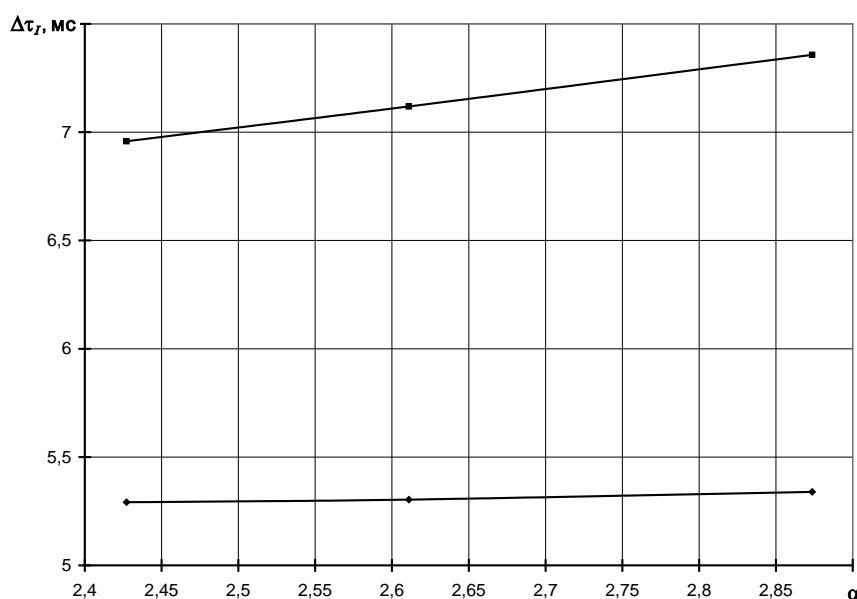
9. New heat transfer correlation for an HCCI engine derived from measurements of instantaneous surface heat flux / J. Chang [et al] // SAE transaction. – 2004. – № 113. – C. 1576–1593.

10. Analysis of a natural gas fuelled HCCI engine with exhaust gas recirculation using a stochastic reactor model / A. Bhave [et al]; University of Cambridge. – Cambridge, 1996. – Режим доступа: <http://journals.pepublishing.com/index/F13406581408046M.pdf>, свободный.

11. Soyhan, H. S. Evaluation of kinetic models for autoignition of automotive reference fuels in HCCI applications /H. S. Soyhan, J. Andrae // Turkish J. Eng. Env. Sci. – 2007. – № 31. – C. 383-390.

12. Golovitchev V.I., Atarashiya K., Tanaka K. Towards universal EDC-based combustion model for compression ignited engine simulations // SAE Paper. W.C. - 2003. - №2003-01-1849. – W.P.

13. Voinov, A. N. Protssy sgoraniya v byistrohodnykh porshnevnykh dvigatelyakh / A. N. Voinov.– M. : Mashinostroenie, 1965.– 212 s.



THE MODEL OF IONIC TRANSPORT IN A CELL WITH TWO MEMBRANES

Nikitin A. A., Gretsova N. V.

Volgograd, Volgograd State Technical University

The shape of ion concentration and potential was calculated in system with two membranes subject to external electrical field influence. The mathematical model was obtained by modifying the “reaction-diffusion” model.

Keywords: electrodiffusion, membrane, “reaction-diffusion” model, ionic transport.

The model of investigated system (figure 1) is one-dimensional cell with ion-exchange membranes on bounds. The cell is filled with binary electrolyte solution ($\text{Na}^+ - \text{Cl}^-$). The ions can flow inside and outside the cell only through the membranes. The solution is generally electrically neutral. There is potential drop on bounds with membranes caused by double electrical layer (figure 1, bottom) in Nernst’s diffuse delta-layer [1,2].

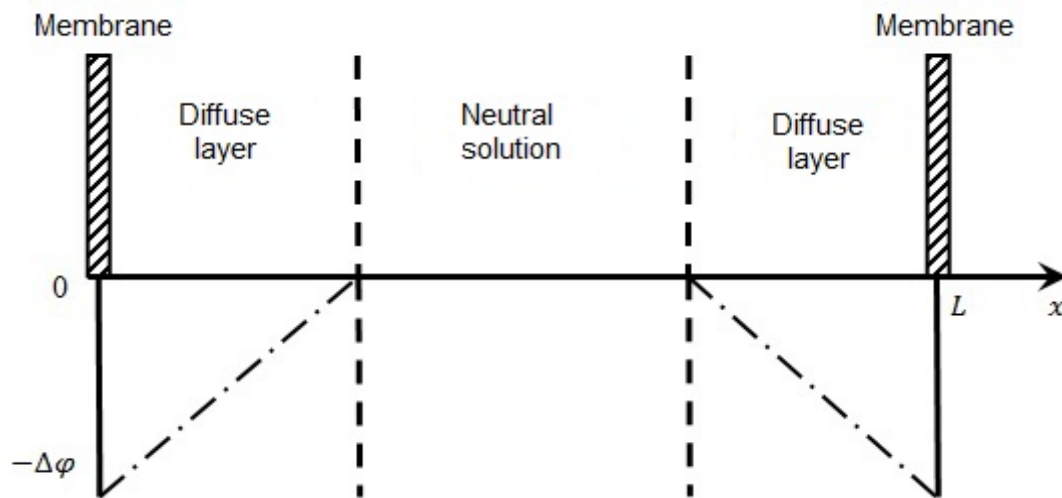


Figure 1 – The scheme of electrodiffusion of binary electrolyte in system with two membranes and potential distribution (– · –)

Ion transfer in diffusion layer is caused by two factors: electrical field and concentration gradient.

The system of differential equations (1) that describes ion transfer obtained with general physical considerations with use of Poisson’s equation, Nernst-Planck equation, mass conservation law. For calculation conveniences it is presented in dimensionless view:

$$\begin{aligned} \frac{\partial u_1}{\partial \tau} &= \frac{\partial}{\partial X} \left[K_{11} \frac{\partial u_1}{\partial X} + K_{12} u_1 \left(\frac{\partial u_3}{\partial X} + E^{\text{ext}} \right) \right], \\ \frac{\partial u_2}{\partial \tau} &= \frac{\partial}{\partial X} \left[K_{21} \frac{\partial u_2}{\partial X} + K_{22} u_2 \left(\frac{\partial u_3}{\partial X} + E^{\text{ext}} \right) \right], \\ \frac{\partial}{\partial X} \left(\frac{\partial u_3}{\partial X} \right) &= -\Phi(u_1 + \gamma u_2). \end{aligned} \quad (1)$$

There: $u_{1,2}$ – dimensionless concentration of ions, normalized on characteristic concentration of ions in intercellular space [3]; u_3 – dimensionless potential, normalized on value of potential drop in double electrical layer; $X = x/L$ – dimensionless length; $\tau = t/t_0$ – dimensionless time, t_0 – characteristic time of ion transmission through the cell that assignable from chemical reaction constants; $K_{i,j}$, Φ , γ – dimensionless coefficients.

The boundary conditions for the represented system are:

$$X = 0: u_3 = -1, \quad J_i^0 = 1 - A \cos(\omega' \tau) + B \sin(\omega' \tau);$$

$$X = 1: u_3 = -1, \quad J_i^L = 1 + A \cos(\omega' \tau) - B \sin(\omega' \tau);$$

where $A = (\sigma E_0) / J_i^{0,L}$, $B = \frac{(\varepsilon \varepsilon_0 E_0)}{J_i^{0,L}}$, $\omega' = \omega t_0$.

There is a concentration distribution of sodium ions calculated with influence of electrical field with 15 GHz frequency and power flux density 150 microwatt per square centimeter on figure 2. There are ion-exchange membranes on bounds of X coordinate. The distribution is smooth with one maximum when the electrical field is off. The dissipative structure with several maximums and minimums spreaded throughout all space appears when the electrical field is on.

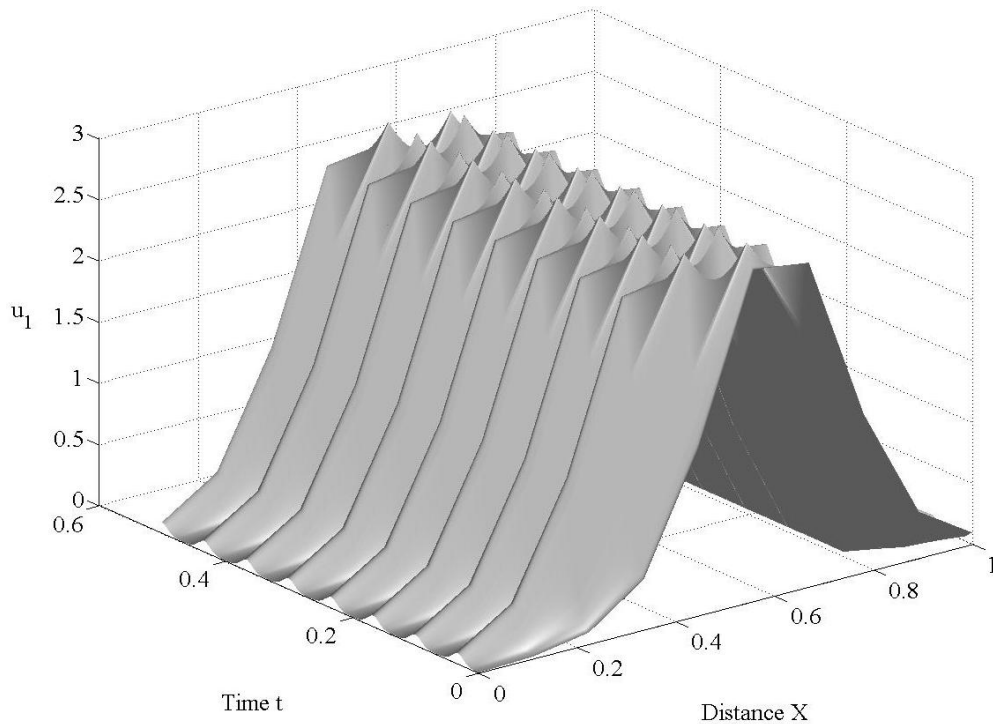


Figure 2 – Concentration distribution of sodium ions with EMF influence, frequency is 15 GHz

There are concentration time profiles of sodium ions on membranes on figure 3. Obviously, concentration oscillation frequency is equal to the frequency of external EMF. Oscillations on right and left membranes are in reversed phase, so it's like a pumping of ions from one membrane to another under EMF influence. The mean value of concentration on bounds with membranes is equal to the results of the other researchers [4,5].

Also, the concentration distribution of the second ion in system – potassium is identical in view to the sodium, but in reversed phase.

In compliance with obtained results the potential distribution was calculated for this system with a glance of potential drops on double electrical layers near membranes. There is also an oscillations of potential with external EMF frequency.

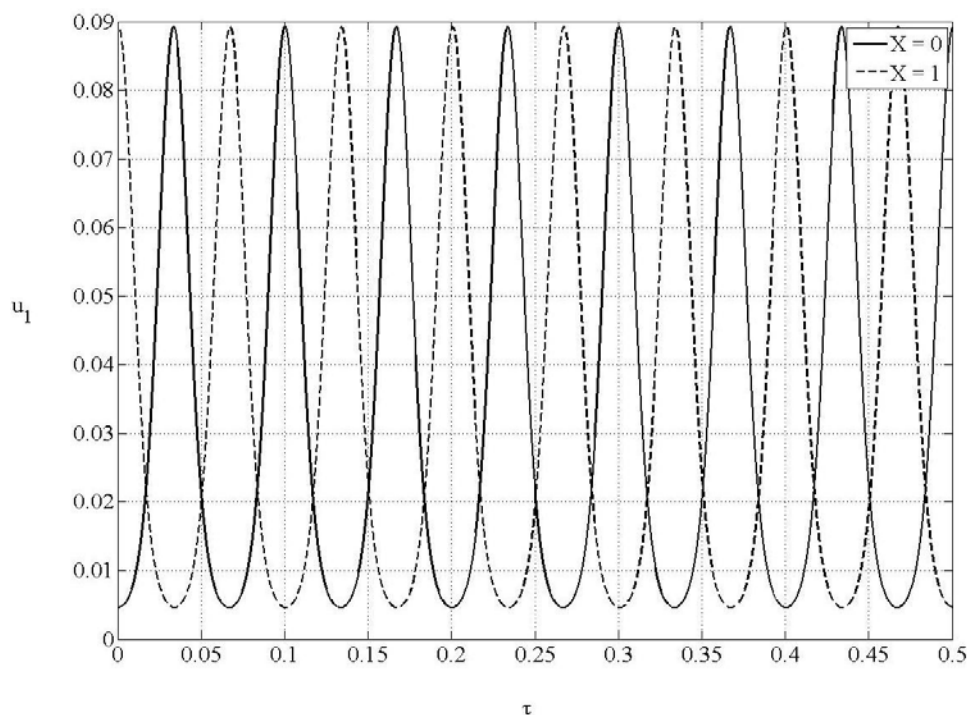


Figure 3 – Concentration time profiles of sodium ions on membranes

References

1. Markin V. S. Indutsirovannyi ionnyi transport. Moscow: Nauka, 1974. (in Russian)
2. Ivanitskii G. R. Matematicheskaya biofizika kletki. Moscow: Nauka, 1978. (in Russian)
3. Vol'kenshtein M. V. Obshchaya biofizika. Moscow: Nauka, 1988. (in Russian)
4. Plyusnina T. Yu. Vliyanie elektricheskogo polya na prostranstvenno-vremennye struktury v sisteme reaktsiya-diffuziya. Biofizika, 2000, 3(45), 495-501. (in Russian)
5. Chopchian A. S. In: Molodye uchenye – nauke i proizvodstvu: Proceedings of the conference, Staryi Oskol, 2007. Staryi Oskol: STI MISiS, 2007, 4(2), pp. 224-235. (in Russian)

NAVIGATION ALGORITHM FOR MOBILE ROBOT USING COMPUTER VISION SYSTEM WITH STRUCTURED-LIGHT CAMERA

Zhoga V.V., Kravchuk A.A., Skakunov V.N.
Volgograd, Volgograd State Technical University

This work was supported by RFBR (project number 12-08-00301-a).

Processing data from structured-light cameras, mapping and navigation methods for mobile robots were examined. Onboard system is built on single board computer Raspberry Pi Model B with software implementation of described algorithms.

Keywords: structured-light cameras, mobile robots, navigation and control algorithms.

Environment modeling and search for the path in an indeterminate environment are the tasks that autonomous mobile robots should be able to perform. In computer vision field, structured-light cameras such as Microsoft Kinect and ASUS Xtion PRO Live, which are able to obtain 3D picture of the environment, seem very promising. Main challenge in using the full

potential of these sensors on a mobile robot are limited computational resources available on-board [1,2].

In case of small mobile robots, physical size of sensors and onboard controllers are crucial [3]. For that reason, system capabilities of which are explored in this work is built on sensor ASUS Xtion PRO Live, which is rather small physically and microcomputer Raspberry Model B. Point clouds that Xtion PRO Live streams are very dense, but such amount of details is not necessary for environment modeling [4]. By lowering the detail of the point cloud, amount of processed points can be lowered drastically which allows algorithms for navigation and real-time control to be implemented on Raspberry Pi microcomputer.

In this work, problem of environment modeling and search for the path are solved using following methods:

- lowering cloud density;
- cutting off parts of scene;
- lowering cloud dimensions (plane projection);
- building the geometry model.

During the first stage of transformations, cloud density can be lowered without severe loss of precision in a following way: a voxel grid is built on the cloud, with cell size determining the amount of density reduction. After that all points inside each cell are approximated by the cell's centroid. This is a little slower than approximating them by just the cell's center but preserves underlying surface with less distortion.

Next step in preparing the cloud for environment modeling is cutting off excess points, which lowers amount of data to be processed. Points are being cut off in three areas:

- Points above certain height. These points do not represent an obstacle, but after projection on a plane, they'll appear as a potential obstacle.
- Points below certain height. As environment model is 2D, ground is represented by the plane and storing points, representing it, is excessive. Obstacles low enough that robot wouldn't need to go around them also fall in this area.
- Points further than certain distance. Accuracy of this type of sensors is very dependant on the distance, after a certain point measurement error can be comparable with received data. By introducing distance cutoff, amount of data to be processed can be reduced, and model distortion by the false obstacles can be avoided

Resulting cloud represents about the obstacles in robot's view, and it can be projected on a plane to lower data's dimensions.

After that, points are clustered using DBSCAN [5] algorithm. Defining trait of this algorithm is that cluster is defined not by distance from points to centroid of the cluster, but by whenever points are density-reachable from each other – points should be in certain zone from other point, and amount of points in that zone should be above certain threshold. This method has two advantages:

- works better with clusters of arbitrary form, as usual methods tend to form spherical clusters. Example – clusters that envelop others;
- can filter out the noisy data and avoid distortions thanks to density requirements..

Resulting clusters can be converted to geometric shapes by building around them the minimal convex hulls, that result in polygons. For hull building, Graham algorithm is used. This algorithm is based on traversing all points clock-wise. Points not belonging to the hull are filtered in process. Time of work for algorithm is only $O(n \lg n)$.

Like that, input point cloud is transformed into several geometric shapes, which can be used to build visibility graph or Voronoi diagram for navigation using A* method. This method is widely used for searching the optimal path on a graph. On every step every possible node that is reachable from current node is traversed. Next node is chosen by lower cost,

which consists of two components. First component of is the estimation of distance from this node x to the final one, usually denoted as $h(x)$. Unlike greedy algorithm, node x value also incorporates distance from the starting node, not just the previous one, denoted as $g(x)$. As every possible node is traversed, algorithm A^* is considered full, i.e. it will always find a solution if one exists.

Methods and algorithms used allow to tremendously lower the dimensions and amount of data to be processed during navigation of the mobile robot, thus lowering computational power requirements for the onboard system. For experimental testing of devised algorithm the prototype of wheeled mobile robot with computer vision system built with sensor ASUS Xtion PRO Live and microcomputer Raspberry Pi Model B installed onboard. Control system installed on robot includes DC motors drivers and sensor subsystem module with ultrasound and infrared range-finder sensors installed. Connection with operator's remote computer is established via WiFi channel. Experiments performed has shown that computational powers of microcomputer is enough for navigation using suggested algorithm in relatively simple scenes of working environment. Moreover, developed robot prototype allows development and testing of new navigation and control algorithms for autonomous mobile robots.

References

1. Bykov S.A., Leontiev V.G., Skakunov V.N. Application of 3D point clouds analysing methods in computer vision systems. // *Izvestiya VolgGTU. Seriya «Aktualnyie problemyi upravleniya, vychislitelnoy tekhniki i informatiki v tekhnicheskikh sistemah»*. Vyip. 13 : mezhvuz. sb. nauch. st. / VolgGTU. - Volgograd, 2012. - № 4 (91). - S. 37-41.
2. Bykov S.A., Skakunov V.N. Development of computer vision system for mobile robot using analysis of 3D point clouds. // *Innovatsionnyie informatsionnyie tekhnologii : mater. pervoy mezhdunar. nauch.-prakt. konf. , g. Praga, 23-27 apr. 2012 g. / Mosk. gos. in-t elektroniki i matematiki (MIEM) [i dr.]*. - M., 2012. - S. 253-255.
3. Zhoga V.V., Skakunov V.N., Eremenko A.V., Fedchenkov P.V., Gerasun M.B., Nesmiyanov I.A., Dyashnikov-Titov V.V., Pavlovsky V.E. Emergency rescue robot with high profile mobility. // *Ekstremalnaya robototekhnika : sb. dokl. mezhdunar. nauch.-tehn. konf. (Sankt-Peterburg, 23-25 noyab. 2011 g.) / Tsentr tekhnologii sudostroeniya i sudoremonta, TsNII robototekhniki i tehn. kibernetiki*. - SPb., 2011. - S. 165-168.
4. Zhoga V.V., Kravchuk A.A., Skakunov V.N. Application of sensor controllers in visual odometry systems of mobile robots. // *Innovatsii na osnove informatsionnyih i kommunikatsionnyih tekhnologiy (INFO-2013) : mater. H mezhdunar. nauch.-prakt. konf., g. Sochi, 1-10 okt. 2013 g. / MIEM NIU VSHe [i dr.]*. - M., 2013. - S. 318-320.
5. Martin T. Wells, et al. *Data Clustering: Theory, Algorithms, and Applications*, 2007, ISBN: 0898716233

STRUCTURE MULTIPROCESSOR DISTRIBUTED CONTROL SYSTEM OF THE MOBILE ROBOT

Zhoga V.V., Aniskov R.V., Merkulov A.A., Skakunov V.N.
Volgograd, Volgograd State Technical University

The work was performed with financial aid from RFBR (project № 12-08-00301-a).

The structure of a scalable multi-functional robot control system was developed, the functions and composition of unified modules - system components, integrated standard interfaces on-board multiprocessor distributed system remote control robot was determined.

Specificity of tasks in the implementation of an autonomous mobile robot mode allows you to select two levels of management. On the upper level, decisions on the formation of the main control the actuators depending on the desired mode of operation of the robot, and on the lower level functions are implemented assessment of the condition of the environment, and control thrusters. The requirements for computing resources, structure and distribution functions of the onboard control system is largely dependent on the type of remote control robot: remote or supervisory [1,2].

In this paper we define the functions and components of the system board on the lower level, for the remote control of robots with different types of propulsion and transport platforms: wheeled, tracked and walking. For small-sized robots designed a series of standard modules, considering features for control of electric DC motors and linear motors (in walking machines), as well as support for the sensor system consisting of subsystems global and local navigation, technical vision.

On the upper level as a leading processor, depending on the structural complexity of the mobile robot used microcomputer Raspberry Pi Model B or embedded processor module iMX53 OEM processor-based iMX536 architecture ARM Cortex-A8 and 800MHz. Both units have a wide range of integrated peripherals and high-speed global and local interfaces and allow you to create an arbitrary structure task-oriented multiprocessor control system with radial, bus or hybrid network architecture.

In the basic version control components of the device are designed as modular units consisting of two types: control modules thrusters (or electric actuator) with integrated sensors and state sensory subsystem modules. Control module and propulsion data preprocessing CPU board contains STM32F4Discovery, power amplifier IC VN3PS30P-E and controller

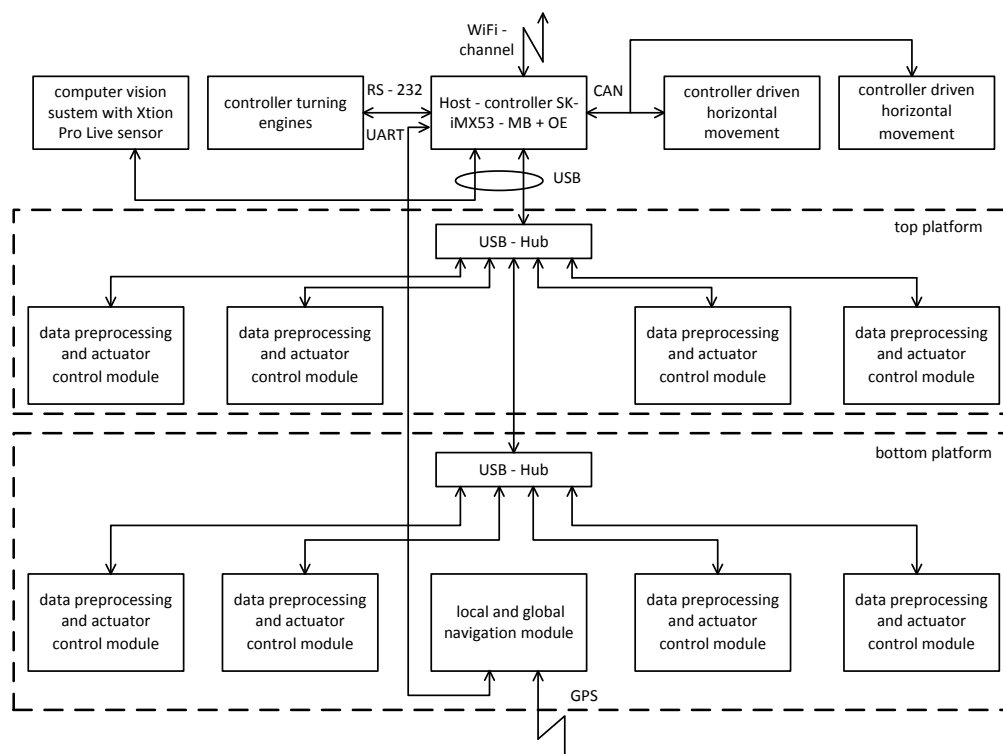


Fig.1 The structure of a multiprocessor system management walking robot

MPU 6050 with 3 -axis accelerometer and a gyroscope to measure the dynamic parameters of the suspension or platform support. Changing functions of the module depending on the type of propulsion provided by a software controlled settings peripheral

controller. The sensory subsystem based on the processor board STM32F3Discovery and contains a set of ultrasonic and infrared sensors. As rangefinders uses ultrasonic distance sensors MaxSonar-EZ (or HC-SR04), and to detect obstacles - infrared sensors Sharp GP2Y0A710K0F. In addition, the touch sensor module included global-positioning with GPS-receiver Tramble 67415. Both options modules are placed in the same type of body size 130x70x35mm, made of ABS- plastic with 3D printer Makerbot Replicator 2x.

Figure 1 shows a distributed multiprocessor system management structure of walking robots with orthogonal propulsors. The system includes modules designed to control thrusters preprocessing of data from sensors and position feedback signals, In addition, the system includes standard controllers actuators, control mechanisms, linear displacement and rotation platforms rescue robot high profile cross [3,4]. Propulsion control modules perform the functions of the signal generator job trajectory commands received from the host-controller, and also carry out a software implementation of digital filtering algorithms of data from inertial sensors separately for each vertical support and signal processing servo control feedback supports linear actuators.

The sensory system for the local and global robot navigation functions as measuring pitch and roll angles of the robot platforms, determine the current geographical coordinates. Noise filtering sensor readings performed programmatically by using Kalman-Bucy filter.

In computer vision system use camera ASUS Xtion PRO Line. Data exchange between system modules and host-controllers is made for USB-interface and communicate with a remote computer operator - for WiFi-channel.

Software developed for a multiprocessor control system includes three main components.

1. Robot control module that implements a graphical user interface, and allows you to set the parameters of the robot. The module operates as a Windows application on a personal computer (supervisor) operator, which communicates via a wireless connection with the module assignment software movement, and also allows you to view the camera image from the robot in real time.

2. The setting unit of the robot software that implements the control algorithm for the selected robot motion: rectilinear motion on a flat surface, the movement on uneven surfaces (with auto- leveling), crossing an obstacle, turn. The module operates as a server process on-board computer running Linux, provides the ability to connect a client application to perform basic supervisor algorithms displacement distribution produces peripheral controller commands and control the status of each of the propulsion.

3. Module interaction with peripheral controllers provides delegated management functions movers and get the working status of each controller produces the distribution of requests to peripheral controllers connected to the central controller via USB.

References

1. Aleynikov A.A., Skakunov V.N., Chumatchenko I.V. Remote control system for mobile robot. // Innovatsionnyie informatsionnyie tehnologii : mater. mezhdunar. nauch.-prakt. konf., g. Praga, Chehiya, 22-26 apr. 2013 g. V 4 t. T. 3 / MIEM NIU VShE [i dr.]. - M., 2013. - S. 106-109.
2. Pavlovsky V.E., Pavlovsky V.V. Scalable control robots Robocon-1. // Informatsionno-izmeritelnyie i upravlyayushchie sistemyi. 2013.T.11, № 4. S. 80-92.
3. Bykov S.A., Skakunov V.N. Development of a vision system of mobile robot based on the analysis of three-dimensional point cloud. // Innovatsionnyie informatsionnyie tehnologii : mater. pervoy mezhdunar. nauch.-prakt. konf. , g. Praga, 23-27 apr. 2012 g. / Mosk. gos. in-t elektroniki i matematiki (MIEM) [i dr.]. - M., 2012. - S. 253-255.
4. Zhoga V.V., Skakunov V.N., Eremenko A.V., Fedchenkov P.V., Gerasun V.M.,

Nesmiyanov I.M., Pavlovsky V.E., Rescue robot high profile cross. // Ekstremalnaya robototekhnika: sb. dokl. mezhdunar. nauch.-tehn. konf. (Sankt-Peterburg, 23-25 noyab. 2011 g.) / Tsentr tehnologii sudostroeniya i sudoremonta, TsNII robototekhniki i tehn. kibernetiki. - SPb., 2011. - S. 165-168.

USE THE VIRTUAL ENVIRONMENT FOR RESEARCH WELDED SEAMS WHEN STUDYING SUBJECT «ELEMENTS OF MACHINE »

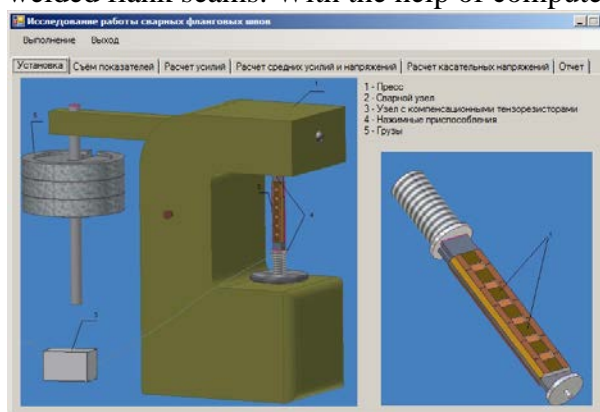
Matlin M. M., Shandybina I.M., Lebskiy S. L., Solovyev A.S.
Volgograd, Volgograd State Technical University

The technique of research of welded flank seams in the virtual environment is considered when subject «Elements of Machine»

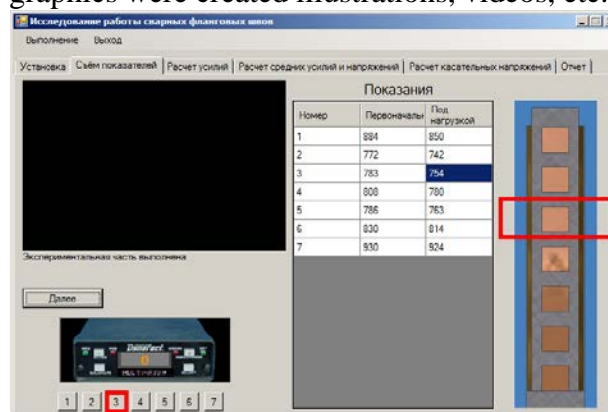
Keywords: research of work of welded seams, virtual environment, 3D modeling.

At the present stage of development of the higher school wide use of the virtual environment for studying of various subject matters is actual. Chair «Elements of Machine and drawing-machine» of VolG GTU worked out the complex of virtual laboratory works is developed for research of work of elements of machine and mechanisms studied subject «Elements of Machine» [1-5]. In particular, use of the virtual environment allowed to add and expand considerably opportunities studying and researches of welded flank seams [4, 5]

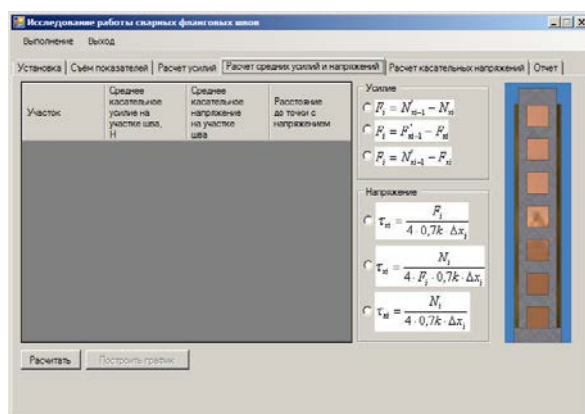
For researching on the COMPUTER were designed 3D models of plant (Picture. 1) and welded flank seams. With the help of computer graphics were created illustrations, videos, etc.



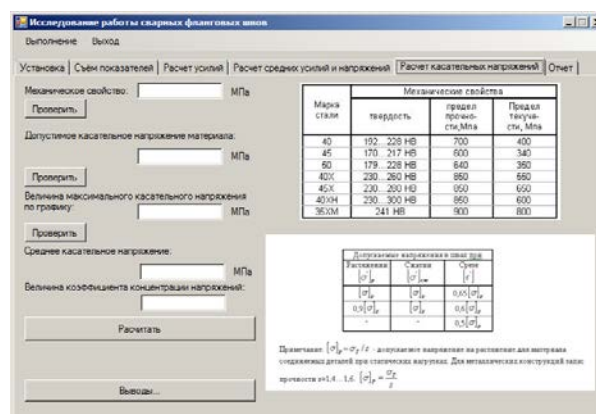
Picture 1 Description of installation



Picture 2. Experiment performance



Picture 3 Calculation of Averages of efforts



Picture. 4 Calculation of Tangent Tension

Based on the research methodology on real plant were identified and automated installation input of basic data, visualization of carrying out experiment with application 3D models (fig. 2), performance of calculations (rice 3-4 were allocated and automated.) graphic interpretation of results on the server or on the local computer.

The developed technique for studies of the welded seam has been soft flank is implemented as a virtual laboratory work (4). In Pictures 1-4 showing snippets of the virtual laboratory works on the research of welded joints of flank.

Document results performed on COMPUTERS in the form of the report file in Microsoft Word format. It contains formulas, experiments, numerical tables and graphs that illustrate the relationship between the different parameters in the end.

Introduction in educational process of virtual laboratory work on research of welded seams promoted increase of the general level of knowledge of students on discipline of «Elements of Machine».

References

1. Matlin, M. M. Complex computer technology to study the courses of «Elements of Machine» and «TMM»//M.M. Matlin, S.Y. Kislov, I.M. Shandybina. Proceedings of the International Conference on the theory and mechanics of machines, mechanisms dedicated to the 100 anniversary of the birth of I.I. Artobolevskogo, Krasnodar, 2006, part 1.-p. 275-276
2. Laboratory workshop and control of students knowledge on computer/M. M. Matlin, I.M. Shandybina, S.Y. Kislov// «Theory of machines and machine elements» Tr. All. Rus. n-t. conf. with the participation of other countries. representatives, Moscow 10-12 Oct. 2008, devoted. 100-th anniversary of Prof. D.N. Reshetov/ MGTY. Be named N.E.Bauman.-2008.-249-251
3. Using virtual labs in the educational process of the course «Elements of Machine»/ M.M. Matlin, S.Y. Kislov, I.M. Shandybina, S.L. Lebskiy/ VolgGTU. series «New educational systems and technology at the University», hunting rituals. Wed. scientific calendar/VolgGTU, Volgograd, 2008.-vol. 5, no. 5, p. 145-147
4. Certificate of state registration of the computer number 2009616726 «program to study the characteristics of the virtual safety clutches»/ Polezhaev D.V., Shandybina I.M, Matlin M.M., Lebskiy S.L., 2009.
5. Matlin M.M. Using virtual environments for laboratory practical course «Elements of Machine»/ M.M. Matlin, I.M. Shandybina, S.L. Lebskiy/ Innovation Information Technologies: Mater. Intern. nauchn.-practical conference. Prague, Czech Republic, 22-26 April. 2013 4 volumes T.1.MIEMNIU HSE [etc.],-M., 2013. - p. 277-279.

THE USE OF THE INFORMATION SYSTEM OF DISTANCE LEARNING FOR RATING STUDENT ACADEMIC PERFORMANCE IN THE COURSE “MACHINE ELEMENTS AND DESIGN PRINCIPLES”

Matlin M.M., Shandybina I.M., Popov A.V., Tetyushev A.A., Toporkova O.V.
Volgograd, Volgograd State Technical University

The article describes techniques of improving teaching process organization, student academic performance rating, and self-rating in the subject “Machine Elements and Design Principles” with the help of multimedia academic resources of “Moodle”.

The presented technique of student testing provides broad opportunities for students getting knowledge on their own as well as for teachers rating student academic performance.

Keywords: the system of distance learning “Moodle”, educational process in a higher education institution, testing, academic performance rating

At Volgograd State Technical University there has been constant work on development and implementation of computer technologies and distance learning resources into the educational process.

One of the directions in this work is the creation of a unified complex of methodological support in the course “Machine Elements and Design Principles”, which is designed for students of all modes of attendance.

Nowadays the availability of methodological materials plays the defining role in achieving educational aims. Availability is enhanced when multimedia academic resources are used, including groups of materials for the course study and academic performance testing on the subject.

One of the ways to implement a teaching materials complex for this subject is the dynamic learning environment “Moodle”

Its main advantages are:

1. The ability to use it for both distant and classroom education;
2. The simplicity and effectiveness of the web-interface;
3. Module design structure which can be easily modified;
4. The opportunity for students to edit their profiles (add photos and change different personal data and particulars);
5. Support of different course structures: “calendar”, “forum”, “topics”;
6. The opportunity to set messages via e-mail: news, forums, grades, teachers’ comments;
7. A rich set of modules - course components: “Chat”, “Feedback”, “Forum”, “Glossary”, “Assignment”, “Lesson”, “Quiz”, “Survey”, “Wiki”, “Workshop” etc.
8. The reflection of changes since last login always gives a quick overview of what has changed in the environment;
9. The ability to edit texts using the built-in editor (so one can edit resources, forum messages, notes etc.);
10. The ease of gradebook keeping;
11. The availability of a tracking report on the user’s being logged in and their work with graphics and different models (certain difficulties appeared when adding new questions into the system “Moodle” containing calculated dependences and calculated schemes).

Such a learning and teaching environment provides students with unique opportunities to acquire knowledge on their own as well as under a teacher’s guidance, and to prepare for individual testing according to the section of the course they are working on..

The Learning Management System “Moodle” has been designed to help educators create high quality online courses in different subjects and offers modular object-oriented dynamic learning environment. This environment enables students to master training materials via the Internet and provides access to numerous learning resources.

When implementing the “Moodle” environment there has emerged the necessity for development of a special technique and additional methodological support for testing in the course “Machine Elements and Design Principles”. Multimedia courses and a test bank have been developed for this purpose.

Using “Moodle” while teaching the course “Machine Elements and Design Principles”, educators get the opportunity to send messages to their students, give them tasks, collect and check the tasks, keep online gradebooks and students’ attendance on the roster, set up different resources of the course etc. With “Moodle”, students can study the subject by

sections online and get self-control of the sections studied, send the results of testing to their teacher and get their work assessment and advice in the form of messages and recommendations.

At the end of the term the teacher has the opportunity to check students' knowledge in the form of a test on the subject in general, and the settings of the "Moodle" system allow changing and giving grades for correct answers in accordance with the task difficulty and also editing the questions.

The whole process of teaching with the help of the "Moodle" system is carried out via the local University network or the Internet. In the latter case, students have to register and identify themselves to their teacher for further online advice.

The transition to the use of the "Moodle" system in the department "Machine Elements and Hoisting Machines" of Volgograd State Technical University has been preceded by much methodological work which can roughly be divided into the following stages:

1. The study of other higher institutions' cumulative experience of work in this system;
2. The training of the staff of the department "Machine elements and hoisting machines" to work in the "Moodle" system;
3. The development of a theoretical course of lectures in the subject "Machine Elements and Design Principles" in electronic form [1];
4. The development of questions for the test bank [2];
5. The importing of tasks into the test bank;
6. Test trials and question analysis according to their difficulty and students' understanding;
7. The correcting of the content of the test bank.

Initially, the tests were designed for one or several course sections, for the laboratory work report, and for the end-of-term test or exam [3].

The base of the test bank was laid by the materials designed at the department in electronic form and presented in the textbook "Machine Elements in Question and Answer Form" [2]. However the use of those materials in the "Moodle" environment required a totally new methodological approach not only to the formulation of questions but also answers and hints which is particularly vital when using Moodle's Adaptive mode [4].

At the present time, students have access to testing on the following course sections: "Spur Gears", "Bevel gears", "Worm gears", "Pulley Gears", "Spindles and Axes", "Sleeve-type and Frictionless Bearings", "Welded Connections". The tasks on the modules in the test bank include six question types: "true/false", "matching", "numerical", "short answers", "multiple choice multiple answers", "multiple choice single answer".

There are usually 10 questions for students' testing per section. Their choice is made with the help of random number generator.

At the present moment the total number of questions in different sections varies from 30 to 55. A numerical question type including calculation tasks enables us to increase their number dozens of times.

Pictures 1 and 2 show fragments of typical examples of test tasks.

The methodology for conducting testing includes several stages:

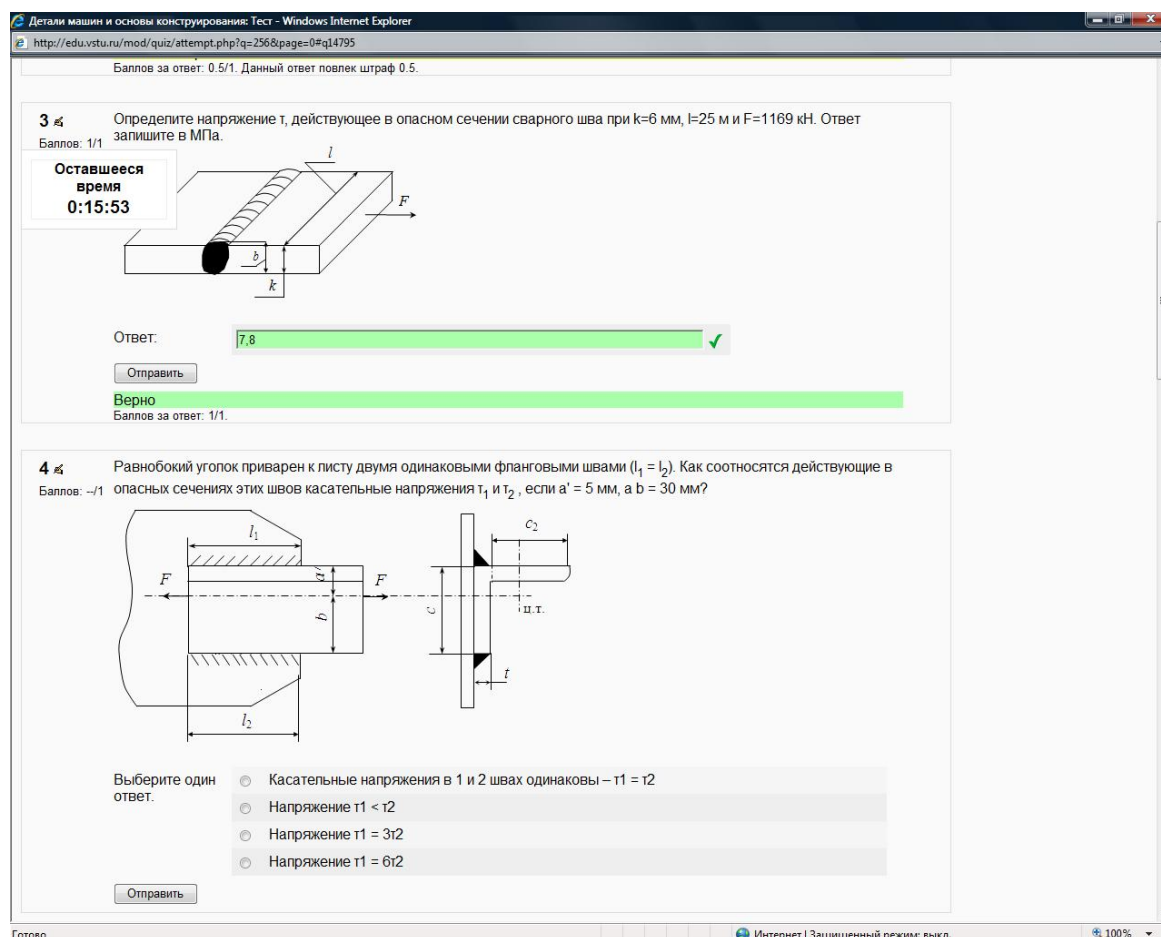
Stage 1. Preparing for testing

This stage involves configuring the system for a definite training program. It includes such actions as registration of test participants and giving them enrolment keys for authentication when logging in, setting boundaries for grades both for a group of questions depending on their difficulty and for the whole test, and defining the number of attempts allowed for a test trial and their time limit.

Stage 2. Authentication of a student and logging in.

It involves the following actions.

1. Getting from the teacher their personal ID in the form of enrolment key to be automatically enrolled in the course;
2. Opening the website <http://edu.vstu.ru> and following the link “Login”;
3. Entering Username, Password, Enrolment Key and logging in;
4. Opening the webpage of the course “Machine Elements and Design Principles”.



Picture 1.. An example of test tasks with a “numerical” answer and with a “multiple choice single answer”

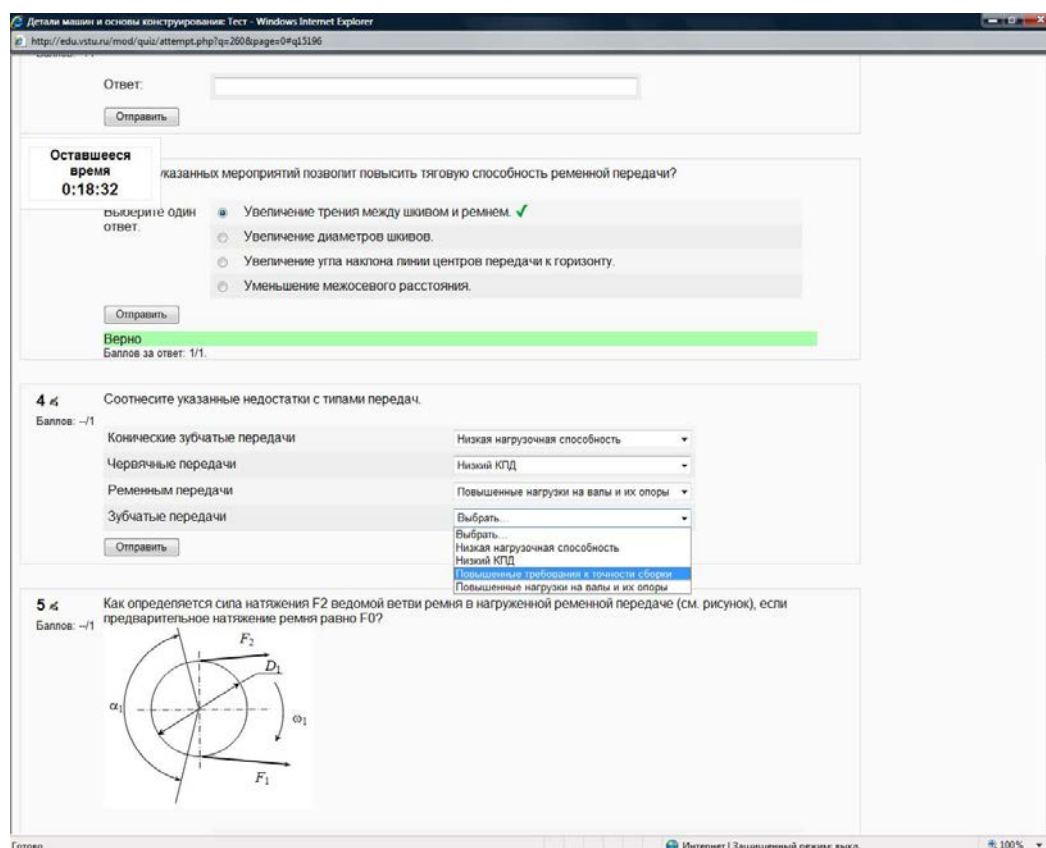
Stage 3. Conducting a quiz.

1. Choose a test from those offered and open to access sections by following the link “Quiz” in the chosen section.
2. Taking a quiz.

The quiz is considered to be finished either after the time specified by the time limit has run out or after clicking the button “Submit all and finish”.

3. After finishing the quiz students can review it.

There is an opportunity for students to retake a quiz by clicking the button “Re-attempt the quiz”. The number of attempts and the pause between them are specified by the teacher at the stage of preparing for testing.



Picture 2.. An example of test tasks with a “multiple choice single answer” and a “matching” answer

Stage 4. Teacher's analysis of the quiz results

The teacher should do the following:

1. Log in using their username and password;
2. Choose the group of test participants by filtering year, group, date, time etc.
3. Choose a certain student by using statistics of the quiz and go to the tab reporting their activity.
4. View the quiz responses of the chosen student.

The system allows the teacher to download in table format or charts any data concerning testing (including a detailed analysis of a particular question, student's responses, and the amount of time spent on it), message students' results and teacher's comments to their emails, analyze and keep statistics of students' academic performance, and make notes on student groups (picture 3 shows an example of quiz results statistics chart of a student group).

The developed technique and training system have passed testing in a real learning process of future Bachelors of Engineering. Testing was conducted for third year full-time students. 250 people took part in test trials.

Even the first testing experience has shown that the most difficult questions for students prove to be a numerical question type and multiple choice multiple answers questions. We have also found that it is easier for students to take topics of the course one after another and not all at one time.

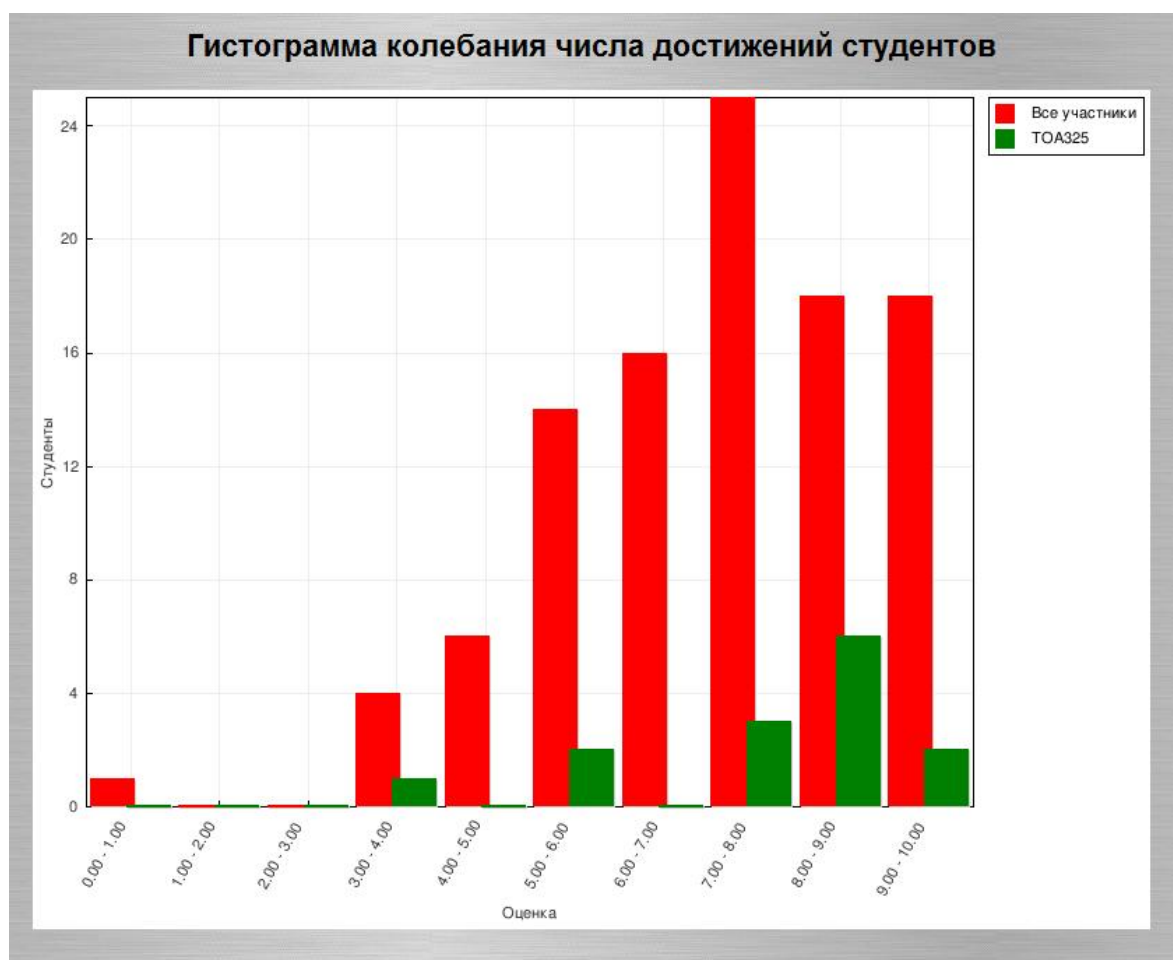
There is also an adaptive mode in the system. A system of hints has been developed for this purpose (picture 4) and access to the theoretical lecture course has been organized. Before the final test access to the section is open for several days for students to take tests at home using the adaptive mode. Expectedly, the best results were shown by the students who

had used an adaptive mode in the “Moodle” system which proves the efficiency of the developed technique.

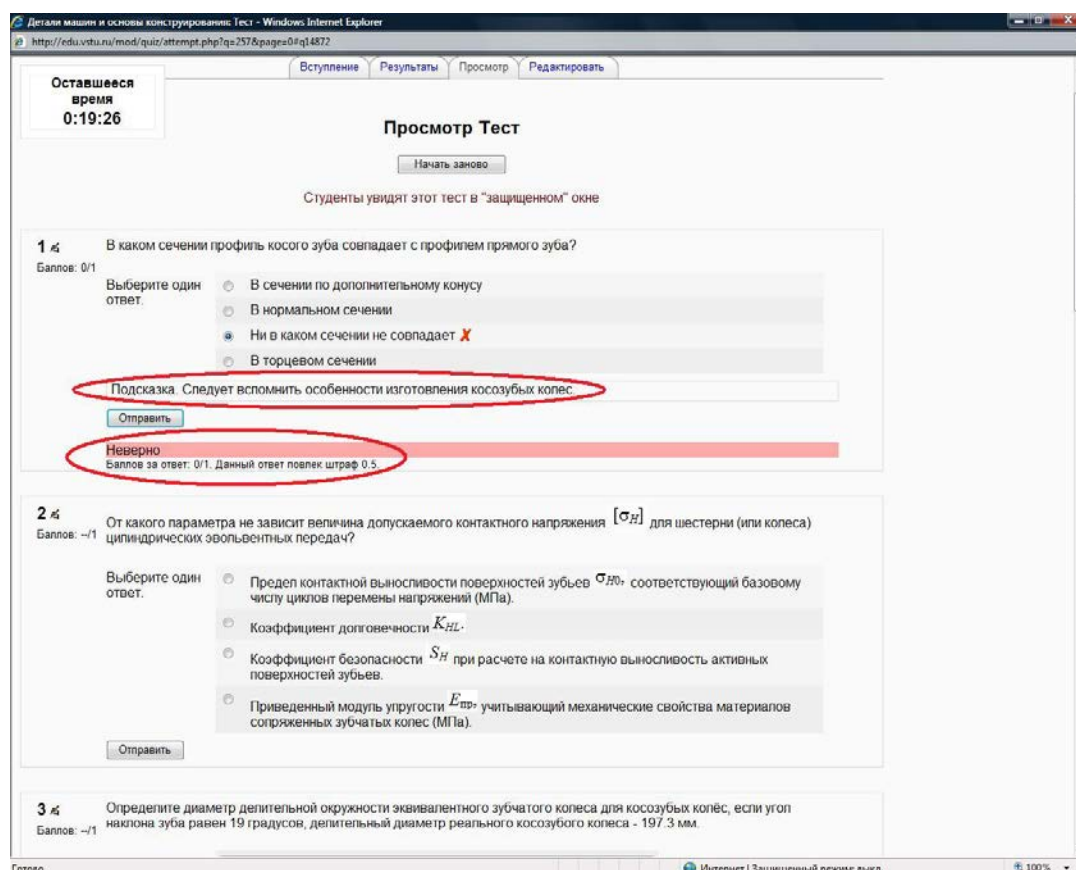
The analysis of the results of test trials allowed us to define more accurately the difficulty level of questions for students and consequently to differentiate points for the correct answer and penalties for wrong answers and re-attempting the quiz.

At present, there is no doubt that the use of “Moodle” system in the teaching process in the department “Machine Elements and Hoisting Machines” makes it possible to increase the attractiveness and quality of studying common technical subjects for students, ensures the objectiveness of knowledge evaluation, enhances students’ academic performance rating and reduces the necessary time for it.

At the present time, the level of the university’s equipment makes it possible to implement this educational activity with the use of distance technologies and provide students and teachers with access to the information resources via the Internet. Moreover, the majority of students studying at the University have the technical ability to access the Internet from home which makes the designed course also available at home at any time.



Picture 3. An example of quiz results chart of a student group



Picture 4. An example of a wrong answer with a hint and penalty for the second attempt.

References

1. Matlin, M. M. Osnovy raschjota detalej i uzlov transportnyh mashin (Basis for Calculations of Transport Machine Parts) : ucheb. posobie / M. M. Matlin, A. I. Mozgunova, S. L. Lebsky, I. M. Shandybina. – Volgograd: IUNL VolgGTU, 2010.– 279 s.
2. Matlin, M. M. Detali mashin v voprosah i otvetah Machine Elements: Questions and Answers) : ucheb. posobie / M. M. Matlin, A. A. Tetyushev, S. L. Lebsky, A. V. Popov, I. M. Shandybina [i dr.]; pod obshh. red. M. M. Matlina. – Volgograd: Izdatel'stvo VolgGTU, 2010. – 144 s.
3. Matlin, M. M. Sovershenstvovanie metodiki izuchenija kursa «Detali mashin i osnovy konstruirovaniya» studentami zaochnoj formy obuchenija (Improvement of Teaching Techniques in the Course “Machine Elements and Principles of Design) / M. M. Matlin, S. L. Lebsky, A. V. Popov, A. A. Tetyushev, I. M. Shandybina // Izv. VolgGTU. Serija «Novye obrazovatel'nye sistemy i tehnologii obuchenija v vuze». Vyp. 7: mezhvuz. sb. nauch. st. / VolgGTU. – Volgograd, 2011 – # 8. – S. 120-122.
4. Goremykin, I. V. Metodicheskie aspekty izuchenija discipliny «Detali mashin i osnovy konstruirovaniya» v srede «Moodle» (Methodological Aspects of Studying the Discipline “Machine Elements and Design Principles” in the “Moodle” Environment) / I. V. Goremykin, V. A. Kostyukov, A. V. Popov, A. A. Tetyushev, I. M. Shandybina // Izv. VolgGTU. Serija «Novye obrazovatel'nye sistemy i tehnologii obuchenija v vuze». Vyp. 8: mezhvuz. sb. nauch. st. / VolgGTU. – Volgograd, 2011 – # 10. – S. 31-33.

THE SELF-OSCILLATORY PROCESSES IN BIOLOGICAL SYSTEM OF THE BOUND TRIGGERS

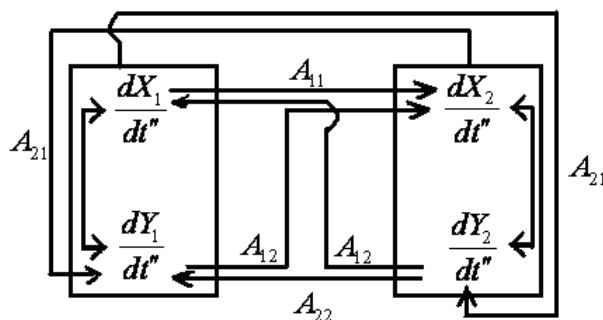
Gretsova H. V., Gretsov M. V.

Volgograd, Volgograd State Technical University

The mathematical model of communication between crates in zero approach as systems of the bound triggers are offer. Possibility of existence of the self-oscillatory modes are show at an equal initial reserve of a substratum.

Keywords: cell, biological trigger, auto-oscillations.

One of methods model operation of cellular systems are representation them as the bound triggers [1,2]. Crates and responses in them was bound among themselves by streams through a membrane. Because of similarity of parallel processes it are observ as influence of process of X_1 on process X_2 (according to Y_1 on Y_2), and cross cross influence. The first of them are process of "self-coordination" of modes in a crate. Second are the process of cross influence which is responsible for switching of system from a mode in a mode. In drawing 1 the plan of cross influence of processes of the first and second crate are g.



Drawing 1. The plan of interrelation of processes in two crates

Combined equations of the bound triggers in the dimensionless view:

$$\begin{aligned}
 \frac{dX_1}{dt''} &= \frac{L_1}{1 + \gamma Y_1^2} \cdot \alpha - X_1 + A_{11} X_2 + A_{12} \frac{L'_1}{1 + \gamma Y_2^2}, \\
 \frac{dY_1}{dt''} &= \frac{L_2}{1 + \gamma X_1^2} \cdot \alpha - Y_1 + A_{21} \frac{L'_1}{1 + \gamma X_2^2} + A_{22} Y_2, \\
 \frac{dX_2}{dt''} &= \frac{L_1}{1 + \gamma Y_2^2} \cdot \alpha - X_2 + A_{11} X_1 + A_{12} \frac{L'_1}{1 + \gamma Y_1^2}, \\
 \frac{dY_2}{dt''} &= \frac{L_2}{1 + \gamma X_2^2} \cdot \alpha - Y_2 + A_{22} Y_1 + A_{21} \frac{L'_1}{1 + \gamma X_1^2}.
 \end{aligned} \tag{1}$$

Coefficients of influence was spot by the matrix of coupling coefficients [3] similar to relations of Onzagera [4]:

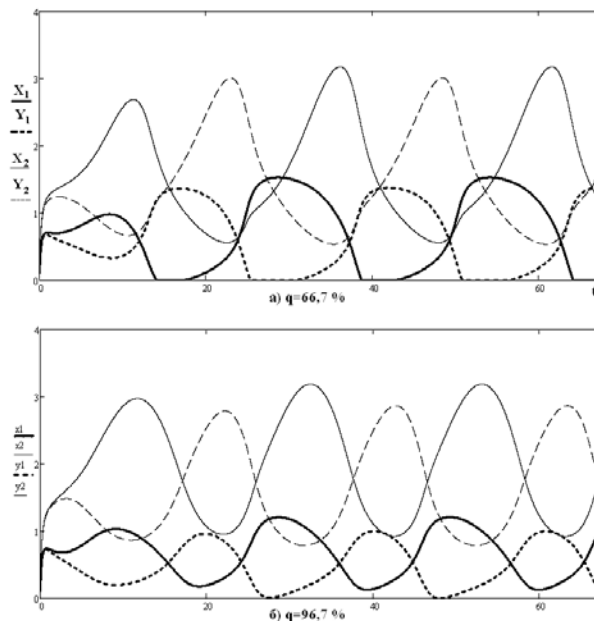
$$A_{ij} = \begin{bmatrix} A_{11} & A_{12} \\ A_{21} & A_{22} \end{bmatrix}. \tag{2}$$

The degree of conjugation of q (depth of communication of processes) are spot by a relation [4]:

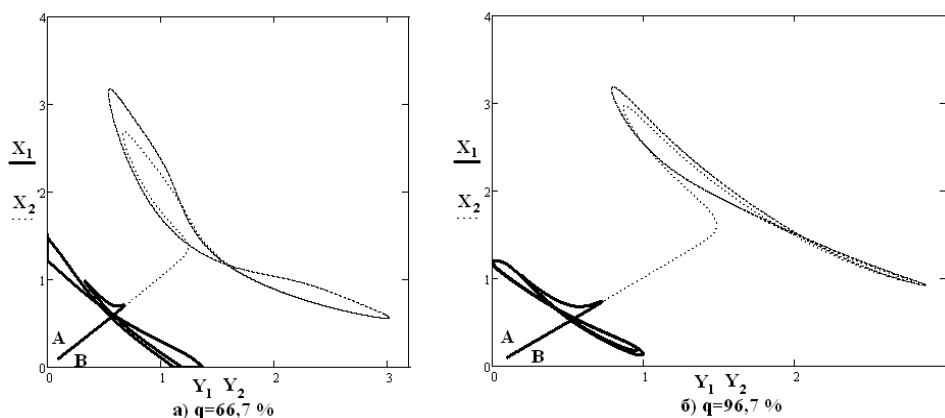
$$q = \frac{A_{12}}{\sqrt{A_{11}A_{22}}}. \quad (3)$$

The parametre α considered inhibition or activation of system of the bound triggers taking into account an external field.

In system (1) there was self-oscillatory processes at equality of an initial reserve of substrata. Then time scans was present in drawing 2, phase portraits at a various degree of conjugation – in drawing 3. On an abscissa axis in drawing 2 the normalised parametre who are translat during the dimensional time [3] are postpon.



Drawing 2. Time scan of system of the bound crates with an equal initial reserve of substrata



Drawing 3. Phase portraits of system of the bound crates with an equal initial reserve of a substratum at change of parametre of conjugation.

From drawing 2 and it are possible to see that in some time intervals of X (or Y) become zero, and process proceeded at the expense of pumping-over of a yield from the next crate. With pinch of a degree of conjugation the continuance of "idle time" of the first crate decreased. With pinch of a degree of conjugation time of stabilisation of a vibration amplitude of a second crate (drawing 3, table 1) are increment. Taking into account action of microwaves (inhibition or activation) time of stabilisation of a mode of system changed (tab. 1).

Table 1

degree of conjugation of q	Time between switchings, hour		
	the bound triggers without action	the bound triggers with activation by a field of 1 crate	the bound triggers with inhibition a field of 1 crate
66,7 %	37	65	25
96,7 %	33	44	19

Apparently from the table, the paradoxical effect are observ – inhibiting action one of responses led to diminution of time of switching, and activation – to magnification.

References

1. Romanovsky, Yu.M Mathematical model operation in biological physics / IO. M. Romanovsky, H. Century of Stepanova, D.S.Chernavsky. – M.: Science, 1975. – 344 with.
2. Gretsova, N.V.Model of action of an electromagnetic radiation of low intensity on the biological trigger taking into account passive transport of substances through a membrane of crate / N.V. Gretsova, A.G.Sheyin//Biomedical technologies and radiotronics. - 2006. - №4. - C. 4-14.
3. Model operation of the response of system of the bound crates on action of microwave radiation of low intensity by a method of triggers / Gretsova of N.V., Nikulin R. N., Gretsov of M. of Century, Nikulin M. P.//Biomedical radiotronics. - 2011. - № 6. - C. 4-11.
4. V.A.Biofizika's Timanyuk. Uch./. Century. And. Timanyuk, E.N.Zhivotova – Kharkov, Izd. NFAU Gold pages, 2003. – 705 with.

SYNTHESIS OF THE SYSTEM INTERFACE OF MULTICOHERENT MEASURING SYSTEMS ON THE BASIS OF NEURAL NETWORKS

Avdeuk O.A.

Volgograd, Volgograd State Technical University

In article we made statement of a new scientific problem – the theory of synthesis of the system interface of multicoherent measuring systems on the basis of neural networks.

Keywords: neural networks, measuring systems, system interface.

Modern technical systems and objects are difficult systems which are characterized not so much by a large number of the components (blocks), how many difficult structure of communications between them. They include in the structure of a network of information transfer of a functional and operating look, and the organization of interaction of all structural components of such systems is interfaced to performance of difficult managing directors of algorithms. The main part of the listed functions is assigned to the system interface as which understand set of methods and the means which have been functionally intended for the organization of an intrasystem information exchange. Therefore now topical issues of design of the system interface in difficult measuring systems. In [1,2] the device of the theory of categories for a task of the main measuring processes, the solution of problems of design of structure of SIIS, the system interblock interface was modified; the principle of construction on the basis of the developed measuring categories of full measuring category SIIS is offered;

algebraic operations of synthesis of the interface structures are developed; approach to design of the interblock system interface on the basis of the developed interface categories is offered; the concept of an error of the system interface is formulated. It was specified that in case of multichannel measuring systems there is a number of problems, for example, such as the accuracy of coordination of operation of channels, synthesis of optimum function of switching etc. One of versions of the decision are served by attraction of the device of the neural networks (NN) and the theory of multicoherent management. Really, as it is specified in [3], the NANOSECOND can be presented as supermultichannel measuring system with cross communications at which the number of output sizes is significantly less than number of entrance sizes, and any output size functionally depends on all set of entrance sizes or on any its part. This representation of measuring system on the basis of NANOSECOND completely answers concept of the multicoherent systems of automatic control (MSAC) which theory successfully develops to the present. It agrees [4], the block diagram of MSAR can be submitted in the form of several systems (channels) of regulation with cross communications between them. Thus each adjustable size can put in compliance the regulator and by that to define straight lines or separate channels of transfer of influence in object. Direct channels are allocated or on a technical sign, or on the basis of intensity and to speed of communication between regulator and adjustable size. The channel of transfer of the influences, originating in one separate system and enclosed in another, is called as cross communication. The most widespread multicoherent objects can be presented by two characteristic structures. The first kind of structure carries the structure name with direct cross connections. In such systems the entrance sizes x_i works through interference coefficients α_{ij} directly at this output size y_i , and α_{ii} – own coefficient of influence.

The second kind of structure carries the structure name with the return cross communications. In this type of structure not own output sizes y_i ($i \neq j$) affect through interference coefficients α_{ij} an entrance of i -go of a separate element of multicoherent system.

It is well known that structures with the return cross communications can be brought to structures with direct cross connections and vice versa.

In a type of complexity of multicoherent objects, there is some approaching to their synthesis. The first approach provides division of all system into some subsystems by number of separate channels. And cross communications aren't considered that can lead to model of the multicoherent system which isn't answering with the real. Therefore the greatest interest represents studying of multicoherent systems which on a functional sign can be dismembered on some parts – the functional blocks connected among themselves by branched structure of communications, on another, the interblock interface (fig. 1). Each block in this drawing represents a so-called multicoherent point, i.e. the object having some entrances and exits. Functions of transformation of information, the information transfer, operating functions etc. can be assigned to the multicoherent point (MP). In the MT set-theoretic form it can be presented in the following look:

$$MT_i = \{X_i, Y_i, F_i\},$$

where X_i – a set of entrance signals, Y_i – a set of output signals, F_i – a set of functional transformations, characteristic for this block.

Each MT, depending on a functional purpose, can be at different hierarchical levels of structure of transformation of information in multicoherent system. It is the starting moment at creation of a method of calculation of process of information transfer (both functional, and the managing director) in these systems.

Traditionally, multicoherent systems are usually described by the differential equations of very high order that causes not seldom difficulties at synthesis of these systems. Nevertheless, attraction of the theory of multicoherent systems at synthesis of the interblock interface of difficult measuring systems is an actual task. For this purpose it is necessary to

define terminology of multicoherent measuring systems on the basis of NS (MIS/NS), to attract adequate mathematical apparatus for the description of such systems (the theory of categories and functors), to create models of communication and a technique of synthesis of the MIS/NS system interface.

References

1. Mukha Ju. P., Avdeuk O. A., Antonovich V. M.. Teorija i praktika sinteza upravljajuwego i informacionnogo obespechenija izmeritel'no-vychislitel'nyh sistem: Monografija /VolgGTU. – Volgograd, 2004. – 220 s.2.
2. Mukha Ju. P., Avdeuk O. A., Koroleva I. Ju. Algebraicheskaja teorija sinteza slozhnyh sistem: Monografija/ VolgGTU.– Volgograd, 2003.– 320 s.
3. Mukha Ju.P., Skvorcov M.G. «IS/NS – klass IS dlja izmerenija integral'nyh parametrov»// «Biomedicinskie tehnologii i radiotekhnika», №4, 2003. – S.23–30.
4. Morozovskij V.T. Mnogosvjaznye sistemy avtomaticheskogo regulirovanija. – M: Jenergija, 1970. – 288 s.
5. Algebraicheskie operacii na interfejsnyh strukturah izmeritel'no-vychislitel'noj sistemy / Avdeuk O.A., Mukha Ju.P., Krohalev A.V., Prihod'kov K.V. // Innovacii na osnove informacionnyh i kommunikacionnyh tehnologij (INFO-2013) : mater. H mezhhdunar. nauch.-prakt. konf., g. Sochi, 1-10 okt. 2013 g. / MIJeM NIU VShJe [i dr.]. - M., 2013. - C. 161-163.
6. Avdeuk, O.A. Algoritm optimizacii vybora varianta mezhblochnykh svjazej izmeritel'no-vychislitel'noj sistemy / Avdeuk O.A., Mukha Ju.P. // Innovacii na osnove informacionnyh i kommunikacionnyh tehnologij (INFO-2013) : mater. H mezhhdunar. nauch.-prakt. konf., g. Sochi, 1-10 okt. 2013 g. / MIJeM NIU VShJe [i dr.]. - M., 2013. - C. 160-161.
7. Prihod'kova, I.V. Analiz apriornykh dannyh dlja izmeritel'nyh sistem s pomow'ju nejronnoj seti / Prihod'kova I.V., Koroleva I.Ju., Avdeuk O.A. // Innovacionnye informacionnye tehnologii : mater. mezhhdunar. nauch.-prakt. konf., g. Praga, Chehija, 22-26 apr. 2013 g. V 4 t. T. 2 / MIJeM NIU VShJe [i dr.]. - M., 2013. - C. 27-29.
8. Mukha, Ju.P. Analiz mnogosvjaznykh sistem na baze nejronnykh setej peredachi izmeritel'noj informacii v slozhnykh medicinskih kompleksah / Mukha Ju.P., Avdeuk O.A., Chuvaeva S.V. // Prilozhenie k zhurnalu "Fizika volnovykh processov i radiotekhnicheskie sistemy": po mater. VII mezhhdunar. nauch.-tehn. konf. - 2008. - [b/n]. - C. 347.
9. Mukha, Ju.P. Mnogosvjaznye sistemy na baze nejronnykh setej peredachi izmeritel'noj informacii v slozhnykh medicinskih kompleksah / Mukha Ju.P., Avdeuk O.A. // Informacionnye tehnologii v obrazovanii, tehnike i medicine : mater. mezhhdunar. konf., 21-24 sent. 2009 / VolgGTU [i dr.]. - Volgograd, 2009. - C. 123.
10. Uvaysov S. U., Ivanov I. A method of ensuring controllability of electronics based on diagnostic modeling of heterogeneous physical processes // World Applied Sciences Journal. 2013. Vol. 24. P. 196-201.
11. Uvajsov S. U., Kofanov Ju. N., Sotnikova S. Ju. Programmnyj kompleks modelirovanija fizicheskikh processov pri avtomatizirovannom proektirovanii istochnikov vtorichnogo jelektropitanija dlja slozhnykh bortovykh sistem // Dinamika slozhnykh sistem. 2012. № 3. S. 80-84.
12. 8. Uvajsov S. U. Teksturovannye podlozhki iz splavov nikelja s tugoplavkimi metallami (W,Mo,Re) dlja sverhprovodjashhih kabelej vtorogo pokolenija // Izvestija vysshih uchebnykh zavedenij. Povolzhskij region. Tehnicheskie nauki. 2012. № 2(22). S. 126-137.
13. Uvajsov S. U., Aminev D. A. Algoritm raspredelenija propusknoj sposobnosti sistem registracii signalov ot mnogih datchikov // Datchiki i sistemy. 2012. № 5(156). S. 26-29.

14. Kofanov Ju. N., Sotnikova S. Ju., Uvajsov S. U. Dinamika optimizacionnogo processa pri identifikacii parametrov jelektronnyh sredstv // Dinamika slozhnyh sistem. 2012. № 3. S. 80-84.

15. Ivanov I. A., Uvajsov S. U., Koshelev N. A. Metodika obespechenija diagnostiruемости jelektronnyh sredstv kosmicheskikh apparatov po rangovomu kriteriju na rannih etapah proektirovanija // Kachestvo. Innovacii. Obrazovanie. 2012. № 1. S. 60-62.

OBTAINING OF Cr_3C_2 -Ti HARD ALLOYS USING EXPLOSIVE PRESSING

Kharlamov V. O., Krokhaev A. V., Kuz'min S. V., Lysak V. I.

Volgograd, Volgograd state technical university

Attention focuses on the application of powder coatings and the shaping of hard alloys from powder mixtures (chromium carbide + metals) in explosive machining

Keywords: explosion, powder coating, hard alloy, chromium carbide, hardness

The experimental research of the materials received by explosive compacting of Cr_3C_2 with Ti powders mixes in a wide range stressing parameters¹ has shown that under certain conditions similar powder mixes are condensed to practically pore-free conditions and their hardness reaches 1100 HV (fig.1).

The researches held with FIB/SEM Quanta 3D FEG system have shown that phase composition of hard alloys doesn't change after explosive pressing, and redistribution of elements doesn't occur between phases in appreciable volumes (fig. 2).

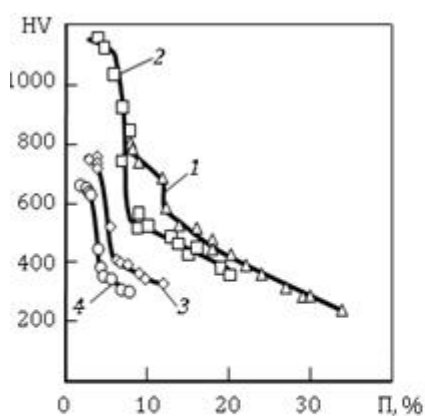


Fig. 1. Hardness versus porosity for hard alloys. Ti, vol. %:
(1) 20, (2) 30, (3) 40, and (4) 50.

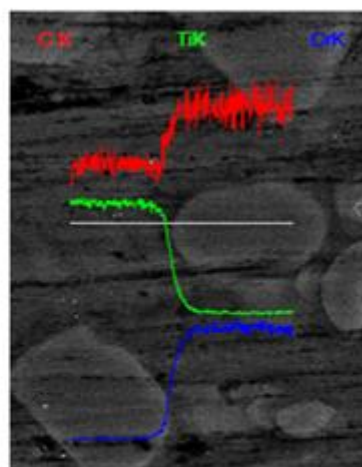


Fig. 2. Distribution of elements along the scanning line (SEM).

It is experimentally established that the bottom temperature's border of hard alloys's formation at the consolidation stage is 500-600 °C. Alloys's break character changes with intercrystallite on transcrystallite with excess of these temperatures that show about formation of strong interface (fig.3).

Transmission electron microscopy (Tecnai G2 20F) has shown that strong interphases look like layers with thickness about 50 nanometers different by structure both from carbide and from metal alloy's phases that allows to identify them as a «boundary phase» which formation provides consolidation of powder alloy's components (fig.4).

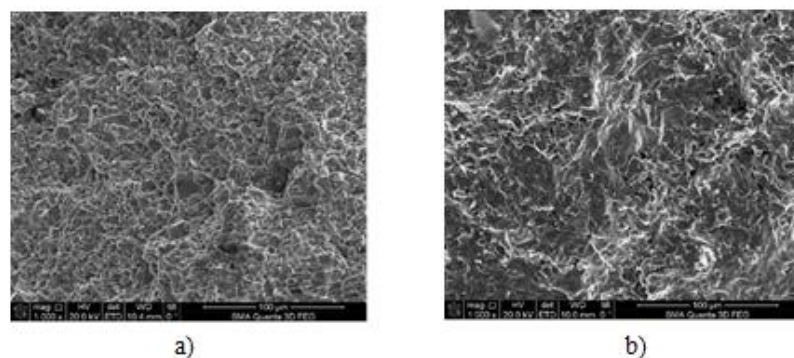


Fig. 3. Fracture Image for alloys of the Cr_3C_2 -Ti system (SEM): (a) intercrystallite and (b) transcrystallite.

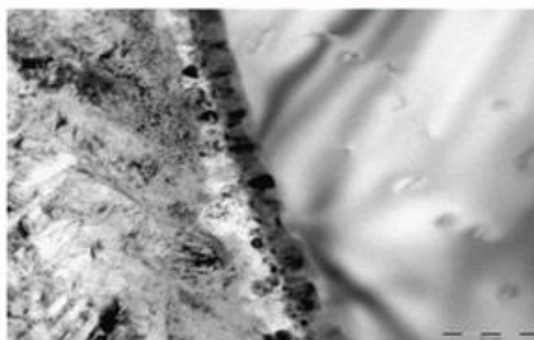


Fig. 4. Microstructure of the junction surface of the carbide and metallic phases in hard alloys of the Cr_3C_2 -Ti system (foil, TEM).

References

1. Russian Journal of Non Ferrous Metals, 2013, Vol. 54, No. 6, pp. 522–526. Allerton Press, Inc., 2013.

MANAGEMENT INFORMATION SYSTEMS - THROUGH IMPROVED FUNCTIONING OF URBAN PASSENGER TRANSPORT, AND QUALITY OF TRANSPORT SERVICES POPULATION

Dmitriev A.V., Rayushkina A.A., Shiryaev S.A., Shipilov E.S., Krashenninnikov A.V.
Volgograd, Volgograd State Technical University

Modern information systems for passenger traffic, improve the efficiency of urban transport and information support of all participants in the transport process, including passengers.

Keywords: passenger management system bus, information system management, passenger transportation, efficiency, quality, service.

Passenger management processes increasingly complex. This is due to the fact that with the growth of the urban population is expanding urban transport network increases the intensity of urban transport and traffic volumes grow.

Effective functioning of the passenger traffic is impossible without widespread deployment of intelligent transport systems (system priority traffic at traffic lights; positioning system of the vehicle automatic accounting of passengers, automatic fare

collection, etc.), based on modern technical means of monitoring and control movement of vehicles, including computers and advances in information technology.

Operating experience of automated control systems (ACS) transportation of passengers abroad has shown that these systems can improve the quality of public transport services and contribute to the improvement of transportation management technology [1, 2, 3].

Consider some of the above control systems:

1. Automatic payment system - a system of cashless travel on public urban transport through plastic cards, automating the process of collecting payment calculation that ensures the accuracy of settlement operations and effective control. Feature of the system of transport cards are in the system combi cards, namely, technical support various applications (algorithms), it is also convenient transport system card use in various fields, compliance with international standards, support for interregional payments.

Aspects of the expansion of the system of automatic payment:

- Transport aspect - the possibility of expanding not only in public transport, but also as payment collection terminals on toll motorways and paid parking;

- Aspect of electronic funds - the ability to use as a credit card and transactions on-line payment, banking and payment of utilities and taxes.

2. Management system bus - a high-tech system for public transport, which, firstly, provides passengers with information about the route of flight and estimated time of arrival, and secondly, the bus driver provides information about the movement and the situation on the road, a distance between buses, thirdly provides transportation company data for the effective control of vehicles and the distance between them.

3. Information system bus - a system that informs citizens with information about bus routes and estimated time of arrival in real time. This system provides extras users of public transport and enables the use of buses. The system lets you know the location of the passenger bus, its route and time of arrival on the mobile phone.

4. Speed control, monitoring compliance with parking regulations - installation of surveillance cameras in areas of high accident rate allows you to control the speed and adherence to the rules of parking drivers. Thus, improving safety on the roads and increase budget revenues by imposing fines on violators.

5. Automated parking (payment terminal) - Set the terminal payment in public areas and on roads near the office buildings will lead to relief urban traffic and increase revenues to the budget.

To optimize the management of passenger transportation needs such a management system that will maximize accurately estimate the parameters of the transport process and deadlines to respond flexibly to emerging bias. Using such a system will improve the technology of traffic control, increase the effectiveness of public transport services and improve the transport situation in the city.

References

1. Passazhirskie avtomobilnyie perevozki: Uchebnik dlya vuzov/ V.A. Gudkov, L.B. Mirotin, A.V. Velmozhin, S.A. Shiryayev; Pod red. V.A. Gudkova. – M.: Goryachaya liniya – Telekom, 2004. – 448s.
2. Ilin V. O sovershenstvovanii upravleniya passazhirskim gorodskim transportom // Avtomobilnyy transport. – 1999. – №7. – S. 42 – 44.
3. Shiryayev, S.A. Ispolzovanie IT-tehnologiy dlya avtomatizatsii sistem oplatyi proezda na obshchestvennom transporte / S.A. Shiryayev, O.V. Ustinova, A.A. Rayushkina // Innovatsionnyie informatsionnyie tehnologii : mater. pervoy mezhdunar. nauch.-prakt. konf. ,

g. Praga, 23-27 apr. 2012 g. / Mosk. gos. in-t elektroniki i matematiki (MIEM) [i dr.]. - M., 2012. - C. 497-499.

OPTIMIZATION OF $\text{Cr}_3\text{C}_2\text{-Ti}$ HARD ALLOYS USED IN SLIP BEARINGS

Krokhalev A. V., Kharlamov V. O., Avdeyuk O. A., Prikhod'kov K. V., Savkin A. N.,
Kuz'min S. V., Lysak V. I.

Volgograd, Volgograd State Technical University

A correlation is established between the antifrictional properties, structure, and hardness of hard chromium-carbide alloys. An explanation for this correlation is offered.

Keywords: explosion, powder coating, hard alloy, chromium carbide, hardness, antifrictional properties

Technical progress relies on the creation of new materials for frictional systems operating in extreme conditions, such as very high or very low temperatures, high slip velocities, high load, aggressive media, or exposure to radiation. Therefore, we need to develop new hard alloys and corresponding production methods.

Thus, slip bearings operating in contact with silicided graphite, in the presence of water, are currently manufactured from alloys of chromium carbide (Cr_3C_2) with nickel or Nichrome alloy obtained by pressing and sintering. Sintering may be eliminated if the nickel is replaced by titanium and explosive loading is employed [1,2]. By this means, also, the production of hard alloy may be combined with its application as a coating to the working surfaces of blanks for frictional systems.

In the present work, we study the frictional properties of such materials, identify the factors that determine the frictional characteristics at silicided graphite, and formulate recommendations regarding the optimal composition corresponding to minimal wear.

We study alloys containing 14, 22, 31, and 40% titanium binder, corresponding to $\text{C}_{0\text{Ti}}$ = 20, 30, 40, and 50 vol %, with the maximum hardness HV and density close to that of the monolithic material. Tests are conducted on a MI -1M frictional machine in a pin- ring configuration with incision, by the method in [3-6].

The influence of the titanium-binder content on these processes is shown in Fig. 1. These are complex curves, except for the minimum coefficient k_{\min} in liquid friction, which is practically constant with increase in the titanium-binder content. We now find the relation between the antifrictional properties, structure, and hardness of the alloys.

In boundary lubrication and seizure, the frictional coefficient is inversely proportional to the hardness HV, while the limiting load of boundary lubrication and seizure is proportional to the ratio V_{cp}/HV , where V_{cp} is the unit volume of carbide phase in the alloy structure (Fig. 2).

The dependence of k_{bo} and k_s on $(\text{HV})^{-1}$ is consistent with the theoretical notions in [7]: specifically, that the actual contact area at constant load is inversely proportional to the hardness of the softest frictional material (the chromium-carbide alloy, in the present case), at whose surface silicon-carbide projections enter the silicided graphite. Increase in the contact area boots the molecular component of the frictional force and the slipping-friction coefficient.

If we extrapolate the dependence of the frictional coefficients on $(\text{HV})^{-1}$ to zero, which corresponds to zero contact area, we may determine the mechanical component of the frictional coefficient: $b = 0.065$.

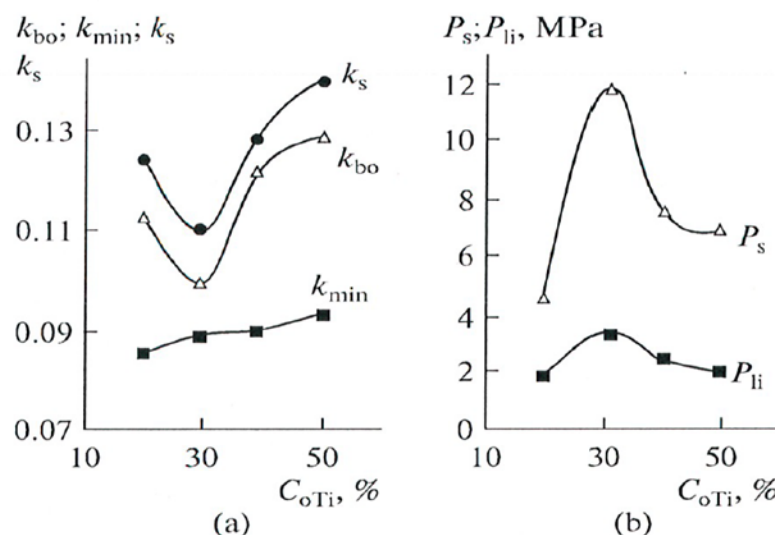


Fig. 1. Dependence of the antifrictional characteristics k_s , k_{bo} , k_{min} (a) and p_{li} , p_s (b) of hard chromium-carbide alloys with titanium binder on the titanium-binder

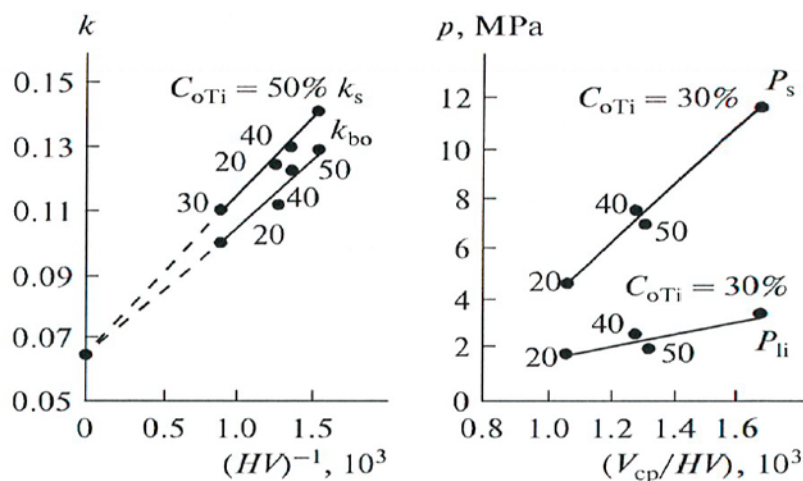


Fig. 2. Dependence of the antifrictional characteristics of the alloys on the hardness and unit volume V_{cp} of carbide phase.

The product of V_{cp} and $(HV)^{-1}$ is proportional to the actual contact area of the carbide phase with constant total contact load. It is obvious that the limiting load corresponding to liquid friction and the limiting load in seizure will depend on V_{cp}/HV , since the carbide phase is more resistant to deformation than the metallic matrix, while the thermal conductivity is lower. Therefore, increasing the contact area of the carbide phase will increase the local temperature and pressure at the actual contact area. In turn, for liquid friction, that should reduce the viscosity of the lubricant, reduce the carrying capacity of the liquid cushion, increase the likelihood of its collapse, and hence reduce p_{li} . In boundary friction, that leads to desorption of the monomolecular lubricant layers and increases the likelihood of their disintegration, with consequent decrease in p_s .

Thus, to improve the antifrictional properties of hard chromium-carbide alloys in contact with silicided graphite, in the presence of water, we must increase the alloy hardness as much as possible, with minimum unit volume of carbide phase in its structure.

For powder-based hard alloys produced from chromium carbide and titanium, these requirements are fully satisfied with 30% titanium binder. For these alloys, the antifrictional properties and wear resistance are greater than for tradition chromium- carbide alloys.

References

1. Russian Journal of Non-Ferrous Metals, 2013, Vol. 54, No. 6, pp. 522—526. © Allerton Press, Inc., 2013.
2. A.V. Krokhalev, V.O. Kharlamov, S.V. Kuz'min, V.I. Lysak, 2012, published in Izvestiya VUZ. Poroshkovaya Metallurgiya i Funktsional'nye Pokrytiya, 2012, No. 1, pp. 32-37.
3. Krokhalev, A.V., Avdeyuk, O.A., and Janta, A.I., Experimental study of frictional conditions in slip bindings, Izv. VolGTU, Ser. Progr. Tekhnol. Mashinostr., 2011, vol. 7, no. 13(86), pp. 20-23.
4. Russian Engineering Research, 2013, Vol. 33, No. 8, pp. 448—450. ©Allerton Press, Inc., 2013.
5. . V. Krokhalev, O.A. Avdeyuk, K. V. Prihod'kov, S. V. Kuz'min, V.I. Lysak, 2013, published in Vestnik Mashinostroeniya, 2013, No. 5, pp. 42—45
6. A.V. Krokhalev, V.O. Kharlamov, S.V. Kuz'min, V.I. Lysak, 2012, published in Izvestiya VUZ. Poroshkovaya Metallurgiya i Funktsional'nye Pokrytiya, 2012, No. 3, pp. 67-72.
7. Garkunov, D.N., *Tribotekhnika* (Frictional engineering), Moscow: Mashinostroenie, 1985.

FRICIONAL PROPERTIES OF HARD POWDER ALLOYS USING EXPLOSIVE PRESSING

Krokhalev A. V., Kharlamov V. O., Avdeyuk., O. A., Prihod'kov K. V., Savkin A. N.,
Kuz'min S. V., Lysak V. I.

Volgograd, Volgograd State Technical University

The frictional conditions in slip bearings are considered.

Keywords: explosion, powder coating, hard alloy, chromium carbide, hardness, antifrictional properties

Currently, hard alloys are produced by the compacting and sintering of source powder mixtures of high-melting carbides and metals, which limits the material composition first and foremost because of the chemical compatibility of alloy components and makes it impossible to radically improve their operating properties. These problems can be solved by the use of explosion energy during the compaction of powder carbides and metals mixtures. The explosive processing of powders makes it possible to simultaneously attain both pressures sufficient for compacting powders to a practically pore-free state and the temperatures required for the consolidation (welding) of structural components of powder materials in a single whole. The short-time action of high pressure and temperatures prevents the possibility of a secondary chemical interaction between components of alloys and the grain growth in their structure [1, 2].

We study alloys containing 14, 22, 31, and 40% titanium binder, corresponding to C_{0Ti} = 20, 30, 40, and 50 vol %, with the maximum hardness HV and density close to that of the monolithic material [1,2]. Tests are conducted on a MI -1M frictional machine in a pin- ring configuration with incision, by the method in [3].

In Fig. 1, we show the dependence of the frictional coefficient κ of the alloys in distillate on the unit load p_{un} . We see clear transitions from one set of frictional conditions to another, as is typical of Hersey—Stribeck diagrams [3, 4]. With increase in load, the frictional coefficient begins to decline (hydrodynamic and elas- tohydrodynamic lubrication). Then it increases to a certain value and remains constant for some time (mixed and boundary lubrication). With further increase in the load, the frictional coefficient again sharply increases to a new constant value (seizing).

From the plot of the frictional coefficient on the unit load, we may establish numerical values for the antifrictional properties of the alloys [5]: the limiting unit loads corresponding to stable predominantly liquid friction (p_{li}) and to boundary lubrication and seizing (p_s); the minimum coefficient k_{min} in predominantly liquid friction; and the frictional coefficients with boundary lubrication (k_{bo}) and seizure (k_s). The table presents the results of tests [6, 7].

To compare the properties of the proposed alloys and familiar antifrictional materials, we also conduct identical tests of SGP-0.5 silicided graphite and KKhN-20 chromium-carbide alloy with nickel binder, produced by traditional methods. Analysis of the results shows that, at silicided graphite, the frictional coefficients of chromium-carbide alloys with titanium binder are somewhat greater than those of silicided graphite itself, but lower than those of KKhN-20 chromium-carbide alloy with nickel binder.

The limiting load corresponding to predominantly liquid friction is somewhat greater for chromium-carbide alloys with 30% Ti than for the SGP-0.5-SGP-0.5 and KKhN-20—SGP-0.5 pairs. For chromium-carbide alloys with 50% Ti, the limiting load is somewhat less than for the alloy with 30% Ti and even less than for KKhN-20 alloy but still somewhat higher than for SGP-0.5 silicided graphite.

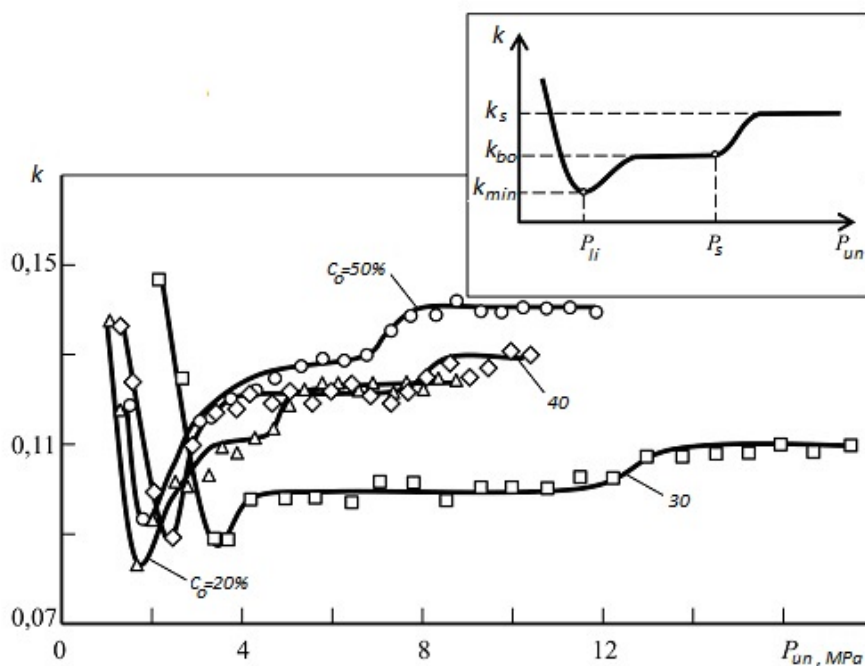


Fig. 1. Dependence of the frictional coefficient κ of hard chromium-carbide alloys with titanium binder on the unit load p_{un} .

The limiting load in seizure for explosively produced materials is significantly higher, while the wear is an order of magnitude less.

Characteristics of hard materials

Characteristic	Alloy based on Cr ₃ C ₂ with Ti content, %				SGP-0.5	KKhN-20
	20	30	40	50		
Minimum frictional coefficient (predominantly liquid friction)	0.085	0.089	0.090	0.093	0.054	0.123
Limiting load in stable predominantly liquid friction, MPa	1.8	3.3	2.4	1.9	1.4	2.6
Frictional coefficient with boundary lubrication	0.112	0.100	0.122	0.129	0.076	0.152
Limiting binding load, MPa	4.6	11.5	7.3	6.9	3.5	5.2
Frictional coefficient with binding	0.124	0.110	0.131	0.140	0.080	0.154
Pin wear per test cycle, mm ³	1.0	0.2	0.7	0.6	0.9	0.7
Wear of silicided-graphite counterbody, mg	29	1	8	10	34	18
Wear of counterbody (by volume), mm ³	12.1	0.4	3.3	0.2	14.2	7.5
Total wear of frictional pair, mm ³	13.1	0.6	4.0	0.8	15.1	8.2

References

1. Russian Journal of Non-Ferrous Metals, 2013, Vol. 54, No. 6, pp. 522—526. © Allerton Press, Inc., 2013.
2. A.V. Krokhaev, V.O. Kharlamov, S.V. Kuz'min, V.I. Lysak, 2012, published in Izvestiya VUZ. Poroshkovaya Metallurgiya i Funktsional'nye Pokrytiya, 2012, No. 1, pp. 32-37.
3. Krokhaev, A.V., Avdeyuk, O.A., and Janta, A.I., Experimental study of frictional conditions in slip bindings, Izv. VolgGTU, Ser. Progr. Tekhnol. Mashinostr., 2011, vol. 7, no. 13(86), pp. 20-23.
4. Moore D.F., Principles and applications of tribology, New York: Pergamon, 1975.
5. A.V. Krokhaev, V.O. Kharlamov, S.V. Kuz'min, V.I. Lysak, 2012, published in Izvestiya VUZ. Poroshkovaya Metallurgiya i Funktsional'nye Pokrytiya, 2012, No. 3, pp. 67-72.
6. Russian Engineering Research, 2014, Vol. 34, No. 2, pp. 85—88. © Allerton Press, Inc., 2014.
7. A.V. Krokhaev, O.A. Avdeyuk, K.V. Prihod'kov, A.N. Savkin, S.V. Kuz'min, V.I. Lysak, 2013, published in Vestnik Mashinostroeniya, 2013, No. 11, pp. 45-48.

SPATIAL MODEL OF ANKLE

Baydachenko V.A., Zemlyakov A.V., Tubol O.A.

**Volgograd, Volgograd State Technical University*

At creation of moving mechanical means it is necessary to consider smoothness of a course, in other words a movement antropomorfnost. One of the important factors influencing

smoothness of a course, the ankle joint which exact model allows to raise a movement antropomorfnost is.

Keywords: anthropomorphous movement, smoothness of a course, prosthetics, stability, spatial model, ankle, kinematic chain.

Creation of spatial model of foot an important task for modern science as data received at research of this model can be used for the solution of problems in a large number of problems of modern science: such as prosthetics in medicine, both the joint, and all ankle; for modeling of injuries of an ankle and their further prevention; in a robotics where active creation of anthropomorphous mechanisms, for calculation and creation of the mechanism of movement is conducted.

The ankle connects among themselves shin and foot bones thanks to what, the person makes movements to foot of feet and normally goes. Structure of an ankle joint rather difficult: in it some bones and system of cartilages connecting them among themselves and muscles are connected. Besides, round each joint the network of blood vessels and the nervous textures providing food of fabrics and coherence of movements in a joint is formed.

Anthropomorphous features of behavior of an ankle joint are defined by interaction of all structural components of a joint among themselves. Nature of interaction between structural elements of a joint is defined by system of the interrelations existing between these elements and muscular system of movement as a whole. Depending on spatial movement of the center of gravity of object as a whole smoothness and stability of movement is substantially regulated by muscular system and system of ligaments of a joint. All interactions thus have nonlinear character and establishment of nature of these not linearities defines efficiency of model of smooth movement.

The motive system of the person (anthropomorphous) as well as at other vertebrata shares on two components working in a tandem. The first is the rigid skeleton jointed by sheaves, it is passive part. The second is cross striped muscles in a set with sheaves. For ensuring stability of system aksialno the located passive motive device is constantly supported it by muscular system, I.e. active part of motive system. On it when modeling an ankle it is extremely important to consider this interaction.

One of important problems which will allow to solve creation of full-fledged spatial model of an ankle is prosthetics of the lost extremities.

There are many kinds of artificial limbs of an ankle from protozoa the plasti-napodobnykh of the shock-absorbers replacing dynamics of an ankle to single hi-tech copies, designed for today at universities of Germany and the USA imitating a set of parameters of a kinematic chain of the anthropomorphous motive device. The passive part of the anthropomorphous motive device is connected by the joints having various degrees of freedom. The elementary designs have one degree of freedom that characterizes the compelled type of movement of this kinematic chain thanks to what each of points of such system follows the trajectory. In the itself ankle has some degrees of freedom. The anthropomorphous motive device represents some links united in the kinematic chain having tens degrees of freedom that characterizes a qualitative measure of mobility, such as: corner of bending of an extremity, its angle of rotation along the axis and depreciation at the expense of sheaves and soft tissues of joints. These characteristics form a site of a surface on which the point with several degrees of freedom is capable to move in any way on an infinite set of trajectories. Such approach allows to create the mechanism, capable to provide the most approximate to the real anthropomorphous motive device, according to characteristics of smoothness of a course, stability, balance and as mobility.

References

1. Formalskiy, A.M. Peremeschenie antropomorfnyih mehanizmov. A.M. Formalskiy, - M.: Nauka, 1982. - 368 s.
2. Belokurov, V.I. Stend dlya ispytaniy proteza nizhney konechnosti cheloveka pri tsiklicheskom nagruzhenii // Problemyi prochnosti. – 2002. - #5. –s.128-132
3. Sapin, M.R. Karmannyiy atlas anatomii cheloveka. Sapin M.R., Nikityuk D.K., M., Elista: APP"Dzhangar", 1999., – 680 s.
4. Uvaysov S. U., Ivanov I. A method of ensuring controllability of electronics based on diagnostic modeling of heterogeneous physical processes // World Applied Sciences Journal. 2013. Vol. 24. P. 196-201.
5. Uvajsov S. U., Kofanov Ju. N., Sotnikova S. Ju. Programmnyj kompleks modelirovaniya fizicheskikh processov pri avtomatizirovannom proektirovanii istochnikov vtorichnogo jelektricitetnogo napitaniya dlya slozhnykh bortovykh sistem // Dinamika slozhnykh sistem. 2012. № 3. S. 80-84.
6. 8. Uvajsov S. U. Teksturovannye podlozhki iz splavov nikelja s tugoplavkimi metallami (W,Mo,Re) dlya sverhprovodjashchikh kabelej vtorogo pokoleniya // Izvestiya vysshikh uchebnykh zavedenij. Povolzhskij region. Tehnicheskie nauki. 2012. № 2(22). S. 126-137.
7. Uvajsov S. U., Aminev D. A. Algoritm raspredeleniya propusknoj sposobnosti sistem registracii signalov ot mnogih datchikov // Datchiki i sistemy. 2012. № 5(156). S. 26-29.
8. Kofanov Ju. N., Sotnikova S. Ju., Uvajsov S. U. Dinamika optimizacionnogo processa pri identifikacii parametrov jelektronnykh sredstv // Dinamika slozhnykh sistem. 2012. № 3. S. 80-84.
9. Ivanov I. A., Uvajsov S. U., Koshelev N. A. Metodika obespecheniya diagnostiruемости jelektronnykh sredstv kosmicheskikh apparatov po rangovomu kriteriju na rannih etapah proektirovaniya // Kachestvo. Innovacii. Obrazovanie. 2012. № 1. S. 60-62.

THE "REACTION - DIFFUSION" MODEL TAKING INTO CONSIDERATION THE ARBITRARY EXTERNAL MICROWAVE RADIATION

Vasich K.N., Gretsova N.V.

Volgograd, Volgograd state technical university

In work the model of transit of ions through a membrane like "reaction – diffusion" added taking into consideration of an external electromagnetic field is considered. The system is given to a dimensionless view that simplifies its application for calculation of biological systems.

Keywords: model "reaction – diffusion", concentration, potential, mobility, valence, microwaves.

Let's consider system "reaction – diffusion". [1, 2]

$$\begin{cases} \frac{\partial n_i}{\partial t} = -\frac{\partial J_i}{\partial x} + f(n_i), \\ J_i = -\frac{RTU_i}{F} \frac{\partial n_i}{\partial x} - n_i Z_i U_i \frac{\partial \varphi}{\partial x}, \end{cases} \quad (1)$$

where J_i – the streams of components described by the equations of Nernst-Planck, n_i – concentration of i of a type of ions, $f(n_i)$ – non-linear function which is responsible for ion concentration change due to chemical reactions occurring on a membrane, U_i – mobility of i of a type of ion, Z_i – the valence of i of a type of ion, T – absolute temperature, R – a gas

constant, F – a Faraday constant, $\frac{\partial \varphi}{\partial x}$ – strength of a self-consistent field which is formed by charges of ions.[1]

The Poisson equation will give the potential of a self-consistent field for the flat twodimensional case taken for simplicity

$$\frac{\partial^2 \varphi}{\partial x^2} = - \frac{4\pi F}{\varepsilon \varepsilon_0} \sum n_i Z_i = \Delta \varphi \quad (2)$$

We substituted the second equation of system in the first and we gained the equation for an ion concentration

$$\frac{\partial n_i}{\partial t} = \frac{RT U_i}{F} \frac{\partial^2 n_i}{\partial x^2} + Z_i U_i \frac{\partial n_i}{\partial x} \frac{\partial \varphi}{\partial x} + n_i Z_i U_i \frac{\partial^2 \varphi}{\partial x^2} + f(n_i) \quad (3)$$

Let's lead the gain equation to the dimensionless view by means of introduction of the following quantities: $c_i = \frac{n_i}{n_{0i}}$ – the dimensionless concentration, where n_{0i} – the reference concentrations of the positively and negatively ionized atoms on the different legs from a diaphragm, $\tau = \frac{t}{t_0}$ – the dimensionless time, where t_0 – the reference time of width of an ion through the canal, $\psi = \frac{\varphi}{\varphi_0}$ – the dimensionless potential, where $\varphi_0 = \frac{RT}{F Z_i}$, $r = \frac{x}{L}$ – the dimensionless distance, where L – depth of a membrane.

Transforming the equation, we gained

$$\frac{\partial c_i}{\partial \tau} = \frac{RT U_i t_0}{F L^2} n_{0i} \frac{\partial^2 c_i}{\partial r^2} + \frac{t_0 Z_i U_i \varphi_0 n_{0i}}{L^2} \frac{\partial c_i}{\partial r} \frac{\partial \psi}{\partial r} + \frac{n_i Z_i U_i \varphi_0^2}{L^2} \frac{\partial^2 \psi}{\partial r^2} + f(n_i), \quad (4)$$

where for simplicity of an entry we will introduce constants $D_i = \frac{RT U_i t_0}{F L^2}$ – dimensionless coefficients of diffusion of the positively and negatively ionized atoms, $B_i = \frac{U_i Z_i t_0 \varphi_0}{L^2}$ – ion mobility in an electric field.[1]

Let's view the system of equations, feature processes for a modification of concentration in a layer near to a membrane with concentrations c_1 and c_2 and the reference concentrations accordingly the positively and negatively ionized atoms n_{01} и n_{02} . [1]

$$\begin{cases} \frac{\partial c_1}{\partial \tau} = D_1 \frac{\partial^2 c_1}{\partial r^2} + B_1 \frac{\partial c_1}{\partial r} \frac{\partial \psi}{\partial r} + B_1 \frac{\partial^2 \psi}{\partial r^2} + f(c_1, c_2), \\ \frac{\partial c_2}{\partial \tau} = D_2 \frac{\partial^2 c_2}{\partial r^2} - B_2 \frac{\partial c_2}{\partial r} \frac{\partial \psi}{\partial r} - B_2 \frac{\partial^2 \psi}{\partial r^2} + g(c_1, c_2). \end{cases} \quad (5)$$

Let's take a Poisson equation to consider a self-consistent field

$$\frac{\partial^2 \varphi}{\partial x^2} = - \frac{4\pi F}{\varepsilon \varepsilon_0} \sum n_i Z_i = - \frac{4\pi F}{\varepsilon \varepsilon_0} n_{01} Z_1 (c_1 - c_2 \frac{Z_2 n_{02}}{Z_1 n_{01}}) = - \frac{4\pi F}{\varepsilon \varepsilon_0} n_{01} Z_1 (c_1 - c_2 Z \gamma), \quad (6)$$

where replacements $\gamma = \frac{n_{02}}{n_{01}}$ – the ratio of the reference ion concentrations, $Z = \frac{Z_2}{Z_1}$ – the ratio of valences of ions was injected.[1]

Then, resort to transition to the dimensionless potential, the Poisson equation became

$$\frac{\partial^2 \varphi}{\partial x^2} = \frac{\partial^2 \varphi}{\partial x^2} \frac{L^2}{L^2} \frac{\varphi_0^2}{\varphi_0^2} = \frac{\partial^2 \psi}{\partial r^2} \frac{\varphi_0^2}{L^2} = - \frac{4\pi F}{\varepsilon \varepsilon_0} n_{01} Z_1 (c_1 - c_2 Z \gamma) \quad (7)$$

$$\frac{\partial^2 \psi}{\partial r^2} = - \frac{4\pi F L^2}{\varepsilon \varepsilon_0 \varphi_0^2} n_{01} Z_1 (c_1 - c_2 Z \gamma) \quad (8)$$

Thus, the system of equations (5) and a Poisson equation (8) can be reduce to one general system who will state us an estimate of nonlinearity of a potential and concentration distribution in a membrane in the dimensionless view

$$\begin{cases} \frac{\partial c_1}{\partial \tau} = D_1 \frac{\partial^2 c_1}{\partial r^2} + B_1 \frac{\partial c_1}{\partial r} \frac{\partial \psi}{\partial r} + B_1 \frac{\partial^2 \psi}{\partial r^2} + f(c_1, c_2), \\ \frac{\partial c_2}{\partial \tau} = D_2 \frac{\partial^2 c_2}{\partial r^2} - B_2 \frac{\partial c_2}{\partial r} \frac{\partial \psi}{\partial r} - B_2 \frac{\partial^2 \psi}{\partial r^2} + g(c_1, c_2), \\ \frac{\partial^2 \psi}{\partial r^2} = -\chi(c_1 - c_2 Z), \end{cases} \quad (9)$$

where $\chi = -\frac{4\pi F L^2}{\varepsilon \varepsilon_0 \varphi_0^2} n_{01} Z_1$.

Let's take a concrete view of the electric field influencing a membrane, we will consider sizes of a membrane where L - breadth of a membrane, R - are more its radius. We will view a flat case for simplicity.

Configuration of a field we will take over as

$$\vec{E} = E_0 \cos(\omega t - \vec{k} \vec{r}),$$

where $\vec{r} = r_x \vec{i} + r_y \vec{j}$, \vec{i} and \vec{j} basis vectors of axes of x and y accordingly.

Then for a potential with sizes of a membrane of L on R it are possible to note by means of dissection on builders of an integral

$$\varphi = - \int_b^a \vec{E} \cdot d\vec{r} = - \int_0^R E_0 \cos(\omega t - kx) dx - \int_0^L E_0 \cos(\omega t - ky) dy \quad (11)$$

Wave amplitude E_0 we will express through intensity, us connection

$$I = v \varpi, \quad (12)$$

where v - rate of propagation of a wave, ϖ - an electromagnetic energy density.

Density of energy in turn we will write as

$$\varpi = \frac{\varepsilon_0 \varepsilon E_0^2}{2} \quad (13)$$

Then, consider formulas (12) and (13), we will gain for amplitude

$$E_0 = \sqrt{\frac{2kI}{\varepsilon_0 \varepsilon \omega}} \quad (14)$$

Return to a potential (11), we will gain at permutation of amplitude (14) expression

$$\varphi = - \sqrt{\frac{2kI}{\varepsilon_0 \varepsilon \omega}} \int_0^R \cos(\omega t - kx) dx - \sqrt{\frac{2kI}{\varepsilon_0 \varepsilon \omega}} \int_0^L \cos(\omega t - ky) dy \quad (15)$$

Let's take this integral by means of transition

$$dy = -\frac{1}{k} d(\omega t - ky)$$

It are possible to take an integral differently, ha us the trigonometry formula for decomposition of a cosine of a difference

$$\cos(\sigma - \gamma) = \cos \sigma \cos \gamma + \sin \sigma \sin \gamma$$

Then the potential will become

$$\varphi = \quad (18)$$

$$\begin{aligned} & \sqrt{\frac{2Ik}{\varepsilon_0 \varepsilon \omega}} \cos(\omega t) \int_0^L \cos(kx) dx + \sqrt{\frac{2Ik}{\varepsilon_0 \varepsilon \omega}} \sin(\omega t) \int_0^R \sin(kx) dx + \\ & \sqrt{\frac{2Ik}{\varepsilon_0 \varepsilon \omega}} \cos(\omega t) \int_0^R \cos(ky) dy + \sqrt{\frac{2Ik}{\varepsilon_0 \varepsilon \omega}} \sin(\omega t) \int_0^L \sin(ky) dy \end{aligned} \quad (19)$$

Exchange $\sqrt{\frac{2Ik}{\varepsilon_0 \varepsilon \omega}} = \Phi$, and then exchange $\mu = \Phi \frac{1}{k}$, and further leading to potential to the dimensionless view, we gained a potential in a general view

$$\psi = \frac{\mu}{\varphi_0} (\cos(\omega t t_0) \sin(kr) - \sin(\omega t t_0) \cos(kr))$$

For system (5) it are necessary to take derivatives (21)

$$\frac{\partial \psi}{\partial r} = \frac{\mu k}{\varphi_0} (\cos(\omega \tau t_0) \cos(kr) + \sin(\omega \tau t_0) \sin(kr)) \quad (22)$$

$$\frac{\partial^2 \psi}{\partial r^2} = \frac{\mu k^2}{\varphi_0} (-\cos(\omega \tau t_0) \sin(kr) + \sin(\omega \tau t_0) \cos(kr)) \quad (23)$$

Now it is possible to note a final view of the equations for system (9), consider (22) and (23)

$$\begin{cases} \frac{\partial c_1}{\partial \tau} = D_1 \frac{\partial^2 c_1}{\partial r^2} + B_1 \frac{\partial c_1}{\partial r} \frac{\mu k}{\varphi_0} (\cos(\omega \tau t_0) \cos(kr) + \sin(\omega \tau t_0) \sin(kr)) + \\ + B_1 \frac{\mu k^2}{\varphi_0} (\sin(\omega \tau t_0) \cos(kr) - \cos(\omega \tau t_0) \sin(kr)) + f(c_1, c_2), \\ \frac{\partial c_2}{\partial \tau} = D_2 \frac{\partial^2 c_2}{\partial r^2} - B_2 \frac{\partial c_2}{\partial r} \frac{\mu k}{\varphi_0} (\cos(\omega \tau t_0) \cos(kr) + \sin(\omega \tau t_0) \sin(kr)) - \\ - B_2 \frac{\mu k^2}{\varphi_0} (\sin(\omega \tau t_0) \cos(kr) - \cos(\omega \tau t_0) \sin(kr)) + g(c_1, c_2), \\ \frac{\mu k^2}{\varphi_0} (\sin(\omega \tau t_0) \cos(kr) - \cos(\omega \tau t_0) \sin(kr)) = -\chi(c_1 - c_2 Z \gamma). \end{cases} \quad (24)$$

As already it has been noted above, the yield model considered action of an external field on a membrane.

Model it are possible to term as doubtless pluses of this, at first, it the dimensionless view; secondly, the model considered a vacillation of potential gradients and concentration in a membrane.

References

1. Riznichenko, G.Yu. Lectures on mathematical models in biology [Text]. M.:RKHD, 2011. - 560 with. ISBN 978-5-93972-847-8
2. Wolkenstein, M. of Century. Blanket biological physics: Monography/m. V. Wolkenstein. - 2nd izd., Ispr. and top. - M.: Science, 1988. - 592 with.
3. Riznichenko, G. Yu. Lektsii po matematicheskim modelyam v biologii [Tekst]. M.:RHD, 2011. - 560 s.
4. Volkenshteyn, M. V. Obschaya biofizika: Monografiya / M. V. Volkenshteyn. – 2-e izd., ispr. i dop. - M.: Nauka, 1988. – 592 s.

SOME REGULARITIES OF SUMMATION OF FATIGUE DAMAGES UNDER CYCLIC CREEP OF MATERIALS

Stolyarchuk A.S., Vdovenko A.V., Korobov A.V., Tishenko P.O.
Volgograd, Volgograd State Technical University

The reported study was supported by RFBR, research projects № 14-08-00837 a and № 14-08-31712 мол_a, and within a basic part of state task of Ministry of Education and Science of the Russian Federation, research project № 2014/16

The problem of summation of fatigue damages under cyclic creep in the area of low-cycle fatigue of structural materials is studied. It was shown that the hypothesis of linear summation of fatigue damages under cyclic creep is a particular case of general approach, proposed by the authors. This general approach is based on the Volterra integral equation of the first kind, when applied to the study of this problem. The correctness of this application is determined by modern methods of building of ancestral theories of creep.

Keywords: fatigue damage, cyclic creep, low-cycle fatigue, mesostructural level.

The question of fatigue damages' summation remains one of the special problems in the calculation of the fatigue strength and life of highly loaded structures. This issue is being presently actively investigated in pure [1] and in low-cycle fatigue [2-4]. Despite numerous publications, this problem was not solved until recent time. For example, it was not solved in particular case of low-cycle fatigue. The cyclic creep is such a particular case of low-cycle fatigue. The quasi-static destructions of parts and elements of constructions made of advanced structural materials often arise under cyclic creep.

The entropy-probabilistic approach was applied in publications [2, 3] on the basis of information theory [5] for evaluation of the low-cycle fatigue damage in a quasi-static area's destruction *under stationary loading*. Herewith the structural material under load is considered as a global information system of *noninteracting* local sources of information – damaged "elements of structure". In this approach local damages of two types were accepted as a measure of the information. The damages are studied at mesostructural level of material. In the sequel this approach was extended to the case of *interacting* local sources of information [4].

The concept of *entropy of the damaged state* of the material, i.e. the uncertainty of this state, is introduced for calculation of fatigue damage in the mentioned approach. This uncertainty is put in correspondence with *the information entropy of Shannon* [6]. Depending on the adopted model of environment (with noninteracting or interacting mesostructural damages) the unconditional (or unconditional in conjunction with conditional) entropy of the damaged state of the material is introduced as a measure of uncertainty in the calculation formula.

The adopted entropy-probabilistic interpretation of uncertainty damaged state at meso-level allows to estimate the low-cycle damage of material (at macro-level) under cyclic creep in terms of the stationary cycle. Hereinafter the damage of material at the macro-level will simply be called "damage". This damage is described by the integral with variable upper limit – degree of ductility's exhaustion. Based on the obvious initial conditions the lower limit is assumed to be zero. In this case the integrand is a function of a certain "trajectory" of exhaustion of reserve of initial (static) material's plasticity. In this way damage depends on this trajectory – a very complicated even when is stationary loaded.

By described statement of the question we do not pose the problem to explore the regularities of low-cycle fatigue damage summation under *unsteady loading modes*. It is obvious, that under unsteady loading modes the specified trajectory becomes more complicated. As a result, the regularities of damages' summation can change. As mentioned above the problem of damages' summation is highly important for technical applications. Therefore the following application arises: it is necessary to estimate the low-cycle fatigue damages and their summation under unsteady loading and cyclic creep of materials. The present study is devoted to research of regularities of damages summation under unsteady loading in indicated fatigue's area. This problem is formulated here within the confines of information-entropy approach, posed in works [2-4].

To obtain the required solution in a generalized form we will follow the methodology of Boltzmann-Volterra. This methodology is used for example in continuum mechanics for building of ancestral theories of creep [7]. In our opinion, the mentioned circumstance allows us to apply this methodology for cyclic creep. We will enter the expression in the form of a Volterra's integral equation of the first kind [8] to find the low-cycle damage $\omega = n/N$ under cycle creep of material in case of unsteady ($\sigma = var$) loading. The cyclic creep will be considered as a relative value $\zeta = \varepsilon_n / \varepsilon_N$. This value ζ will be called "the degree of exhaustion" of ductility.

We use following designations: σ – maximum stress of cycle; n and N – current and destructive numbers of cycles; ε_n и ε_N – current and final deformations. A final deformation we define as deformation, which the material got at the moment of reaching the destructive number of cycle during cyclic loading. The measure of Hencky (logarithmic deformation) was chosen for estimation ε , because deformations of cyclic creep of materials, used in technics, may reach significant values – ten or more percent. Large deformations are caused by high power intensity and frequent forced mode of operation of modern machines and constructions. Listed and many other adverse operating conditions lead to the destruction of technical objects elements' under variable loads; in the particular case – from the low-cycle fatigue under "pulsating stress cycle" of these elements.

The above mentioned methodology was applied in work [9] to analyze the parameters of the model of cyclic creep damage's accumulation. Wherein the problem was considered under pulsating stress cycle (coefficient of skewness and minimum stress of cycle under pulsating stress cycle is equal to zero). As known [2, 4, 10] in this particular case the cycle creep of material is a maximum. Within methodology, adopted in this work, continuing previously formulated approach [3, 4], we form the expression to assess the low-cycle's damage under unsteady loading as an integral:

$$\omega(\zeta) = \int_0^{\zeta} U(\zeta, \eta) \sigma(\eta) d\eta. \quad (1)$$

In this expression "the history of loading" by stress σ till the "moment" ζ is defined by the function $\sigma(\eta)$, where η is dimensionless variable ($0 \leq \eta \leq \zeta$). The kernel $U(\zeta, \eta)$ of the linear integral equation (1) will be called "memory function" (or simple memory) of loading's history. As seen from the formula (1) the history of loadings will be considered not by time as it is customary in the ancestral theories of creep [7] but by degree of exhaustion ζ of static reserve of ductility $\ln(1+\delta)$ under cyclic creep in conditions of unsteady loads. The standard parameter of material's ductility – relative residual even elongation, determined by stretch's tests – is defined here by the letter δ . Herewith while mentioned in the preamble this problem is limited by the area of quasi-static damages under cyclic creep and it satisfies the condition: $\varepsilon_N = \ln(1+\delta)$.

As far as lower and upper limits of the recorded integral are finite, its kernel U and heterogeneous term ω are square-integrable [8]:

$$\|U\| \equiv \left\{ \int_0^1 \int_0^1 |U(\zeta, \eta)|^2 d\eta d\zeta \right\}^{1/2} < \infty, \quad (2)$$

$$\|\omega\| \equiv \left\{ \int_0^1 |\omega(\zeta)|^2 d\zeta \right\}^{1/2} < \infty. \quad (3)$$

The values $\|U\|$ and $\|\omega\|$ we accept as norm of kernel and inhomogeneous member accordingly. From adduced note it follows that these values are finite. Later on we need the expression (3) to solve the posed problem.

As stated above a lot of attention is paid now to the problem of the summation of fatigue damage during unsteady loading cycles. Wherein numerous hypotheses of damages' summation [1] for pure and for low-cycle fatigue are introduced and discussed. From this it follows that the problem of damages' summation remains open. While the question of the validity of the adopted model of damages' summation to the specific operating conditions comes out on top.

Let's consider this question with reference to our case – to accumulation of damages under cyclic creep of material. It is not difficult to show that in the particular case the

expression (3) is reduced to the hypothesis of Palmgren-Miner about summation of fatigue damages $\omega = \|\omega\|$ during unsteady loading (hypothesis of linear summation). Taking into account $0 \leq \zeta \leq 1$ and assumed that $\Delta\zeta_i = \Delta\zeta$ let's pass from the integral recording of this expression to its discrete form, typically used in applied tasks:

$$\omega = \sqrt{\sum_1^m \omega_i^2 \Delta\zeta_i} = (\Delta\zeta)^{1/2} \sqrt{\sum_1^m \omega_i^2} = Q \sqrt{\sum_1^m \omega_i^2}, \quad (4)$$

where m – is the number of stationary loading's intervals, which are under the influence of permanent, but various for different intervals, stresses. Suppose that m is a sufficiently large value. Therefore in formula (4) the sign of equality can be used instead of the approximate equality. In this expression minus sign is cast out, because it contradicts the physical sense of the problem (fatigue damages can not be negative by definition).

Let's introduce (4) in vector form:

$$\frac{1}{Q} \vec{\omega} = \vec{\omega}_1 + \vec{\omega}_2 + \dots + \vec{\omega}_m = \sum_1^m \vec{\omega}_i. \quad (5)$$

The recorded vector equation displays trajectory of storage by material fatigue damages under unsteady loading mode in conditionally adopted hypothetical space. To simplify the problem, we assume that this space is two-dimensional, although in the general setting that limit is not necessarily. Now project the left and right sides of equality (5) on vector $\vec{\omega}$:

$$\frac{1}{Q} \omega = \omega_1 \cos \varphi_1 + \omega_2 \cos \varphi_2 + \dots + \omega_m \cos \varphi_m = \sum_1^m \omega_i \cos \varphi_i,$$

where φ_i are angles between vectors $\vec{\omega}_i$ and vector $\vec{\omega}$. If $\varphi_i = 0$ (for all m), and taking into account the finite quantity of inhomogeneous member's norm (3), which for definiteness we denote by the letter «C», we get:

$$\frac{1}{Q} \omega = \sum_1^m \omega_i = \sum_1^m \left(\frac{n}{N} \right)_i = \frac{C}{Q}.$$

Setting $C/Q = 1$, for the considered particular case we obtain the hypothesis of linear summation of fatigue damages:

$$\sum_1^m \left(\frac{n}{N} \right)_i = \sum_1^m \frac{n_i}{N_i} = 1. \quad (6)$$

So the model of damages' summation in form (3) generalizes the expression (6). However, this model does not impose on the trajectory formed by the sum of the vectors $\vec{\omega}_1 + \vec{\omega}_2 + \dots + \vec{\omega}_m$, which represent particular fatigue damage, such strict restrictions as the hypotheses of Palmgren-Miner. Furthermore, it is known [1] that the hypothesis of Palmgren-Miner rarely matches up the experimental data. That is, using the condition (3) in applied task is preferable, if the integrand $\omega(\zeta)$ is known in advance (or it is defined by technical conditions of object's operating).

References

1. Savkin, A. N. Prognozirovaniye ustalostnoy dolgovechnosti vyisokonagruzhenyih konstruktsiy: monografiya / A. N. Savkin, V. P. Bagmutov. – Volgograd, 2013. – 364 s.
2. Stolyarchuk, A. S. Teoretiko-informatsionnaya model malotsiklovoy povrezhdaemosti materiala / A. S. Stolyarchuk // Progressivnyie metodyi i tehnologii polucheniya i obrabotki konstruktsionnyih materialov i pokryitiy: sb. tr. mezhdunarodn. nauchno-tehn. konf. / VolgGTU i dr. – Volgograd, 1997. – S. 59-60.

3. Bagmutov, V. P. Description of Cyclic Creep on Basis of Entropian Approach / V. P. Bagmutov, A. S. Stolyarchuk // *Mechanika*. Kaunas. – 2000. – Nr. 1 (21). – P. 25-28.
4. Bagmutov, V. P. Primenenie apparata prikladnoy teorii informatsii pri modelirovanii mekhanicheskogo povedeniya materialov / V. P. Bagmutov, A. S. Stolyarchuk // *Spravochnik. Inzhenernyi zhurnal*. – 2005. – № 6. – S. 21-25.
5. Sovetov, B. Ya. Teoriya informatsii / B. Ya. Sovetov. – M.: Akademiya, 2010. – 432 s.
6. Shannon, C. A Mathematical Theory of Communication / C. Shannon // *Bell System Tech. J.* – 1948. – № 27. – P. 379-423, 623-656.
7. Rabotnov, Yu. N. Elementyi nasledstvennoy mehaniki tverdykh tel / Yu. N. Rabotnov. – M.: Nauka, 1977. – 384 s.
8. Zon, B. A. Lektsii po integralnyim uravneniyam: Ucheb. posobie / B. A. Zon. – M.: Vyssh. shk., 2004. – 92 s.
9. Bagmutov, V. P. Issledovanie parametrov modeli nakopleniya povrezhdeniy pri tsiklicheskoy polzuchesti materialov / V. P. Bagmutov, A. S. Stolyarchuk, A. A. Tyiryimov // *Matematicheskoe modelirovanie i kraevye zadachi* (1-3 iyunya, 2005 god, g. Samara). *Trudy Vtoroy Vseros. nauchn. konf. Chast 1: Matematicheskie modeli mehaniki, prochnost i nadezhnost konstruktsiy*. – Samara: Samarskiy gos. tehn. un-t, 2005. – S. 48-52.
10. Strizhalo, V. A. Tsiklicheskaya prochnost i polzuchest metallov pri malotsiklovom nagruzenii v usloviyakh nizkikh i vysokikh temperatur / V. A. Strizhalo. – Kiev: Nauk. dumka, 1978. – 238 s.

SYSTEMS FOR DIAGNOSING AND PREDICTION OF EMERGENCY OPERATION MODES OF OVERHEAD POWER LINES

*Shilin A.N., *Shilin A.A., **Petrenko A.R.

*Volgograd, Volgograd State Technical University, **Volzhsky, National Research
University "Moscow Power Engineering Institute"

In the present article we propose a neurocomputing system for diagnosing and prediction of emergency operation modes of overhead power lines.

Keywords: overhead power lines, emergency operation, the electromagnetic field parameters of climatic factors, measurement converter, neurocomputer, data transmission, GSM / GPRS communication channel.

The neurocomputing system is based on registration of changes of the electromagnetic field around the power line and of the climatic factor parameters. Electromagnetic field changes are recorded by transducers that measure separately the electric and magnetic field components. The transducers register the electric field intensity E and the magnetic induction B created by all the wires of the line. The transducers are mounted on the support away from the wires, which greatly simplifies the installation and maintenance. Additionally, the system includes a weather station, which registers the basic climatic and environmental parameters respectively predicting wind and ice loads in the lines. The measured signals are processed using the neural computers trained to recognize and forecast emergency modes of overhead power lines. The information from neurocomputer of the network, and forecasts are transmitted via GSM / GPRS connection to the control panel.

The analysis of causality relations between the electromagnetic field characteristics and damages in the three-phase power system was realized for electrical mains with isolated neutral of 6 (10) 35 kV was performed. The analysis was realized for an ideal case, namely, where all the phase voltages are equal and the distances from the sensor to the wire are the

same. To develop identification criteria we considered separately the case of change in the total electric field intensity caused by the deviation of the phase voltages. On the basis of this analysis, the identification characteristics of emergency operation modes of overhead power lines are determined.

The developed device can improve the efficiency and immediacy in detecting the type of emergency mode for overhead lines. To solve the problem of forecasting of emergency modes network variables corresponding to climatic factor parameters and data are added to the basic neural.

References

1. Arcishevskii, Ya.L. *Opreделение mest povrezhdeniya linii elektroperedachi v setyah s izolirovannoi neutral'yu* / Ya.L. Arcishevskii. – M.: Vyssh.shk., 1989.
2. Neiman L.R., Demirchyan K.S. *Teoreticheskie osnovy elektrotehniki*. – M.: Energiya, 1981.
3. Ryudenberg R. *Perehodnye processy v elektroenergeticheskikh sistemah: Per. s angl.* – M.: Izdatel'stvo inostrannoi literatury, 1955.
4. P.m. 108149 Rossiiskaya Federaciya, MPK G 01 R 31/08. *Ustroistvo dlya opredeleniya mestopolozheniya i vida povrezhdeniya na vozdushnoi linii elektroperedachi* / A.A. Shilin, A.N. Shilin; VolgGTU. – 2011.
5. Shilin, A.N. *Informacionno-izmeritel'naya sistema opredeleniya povrezhdenii vozdushnoi linii elektroperedachi* / A.N. Shilin, A.A. Shilin // *Pribory*. – 2011. – 15. – S. 23–29.
6. Osovskii, S. *Neironnye seti dlya obrabotki informacii* / S. Osovskii. – M.: Finansy i statistika, 2004. – 344 s.
7. *Sistemy iskusstvennogo intellekta. Prakticheskii kurs: uchebnoe posobie* / pod red. I.F. Astahovoi. – M.: BINOM. Laboratoriya znaniy, 2008. – 292s.
8. Haikin, S. *Neironnye seti: polnyi kurs : per. s angl* / S. Haikin. – 2-e izd. – M.: Vil'yams, 2008. – 1104 s.

NEUROCOMPUTING SYSTEM FOR DIAGNOSING AND PREDICTION OF EMERGENCY OPERATION MODES OF OVERHEAD POWER LINES

*Shilin A.N., *Shilin A.A., **Petrenko A.R.

**Volgograd, Volgograd State Technical University, **Volzhsky, National Research University "Moscow Power Engineering Institute"*

The article presents a block diagram neurocomputer system for the diagnosing and prediction of the emergency operation modes in overhead power line. The system is based on the registration of the change of the electromagnetic field around the power line and of the climatic factor parameters. Measuring transducers monitor separately the electric and magnetic components of the electromagnetic field, as well as climatic parameters of the environment. The measured signals are analyzed using the neural computers trained to diagnose and to predict emergency operation. The information from the neurocomputer is transmitted via GSM / GPRS connection to the control center.

Keywords: overhead power lines, emergency operation, the electromagnetic field parameters of climatic factors, measurement converter, neurocomputer, data transmission, GSM / GPRS communication channel.

Actuality. At the present time one of the priority directions of scientific and technical progress in the world is the development of electric power engineering. This problem is particularly relevant for Russia, the energy system of which is characterized by high losses, high degree of wear and consequently by low level of reliability. One of the reasons for the low reliability of the energy system of Russia is a relatively high accident rate of overhead power lines. The overhead lines are the most unreliable elements in the energy system. This is due to the fact that the Russian overhead lines have a very large extent, and pass through territories of different character - steppes, forests, mountains, swamps and these areas significantly differ in climatic conditions. For example, the greatest negative impact on aircraft line crash comes from wind and ice loads. In order to reduce the recovery time after an accident of overhead lines it is necessary to determine quickly the location and the type of the crash. For long lines undergoing through difficult terrain, the recovery time is determined mainly by the time needed for searching the site of the accident. Therefore, for increasing the reliability of power supply it is necessary to introduce modern information-measuring systems (IMS) monitoring overhead power lines. IMS should be able to determine the location and the type of emergency mode and to predict such emergency regimes. It should be noted that IMS monitoring overhead power lines is a major part of smart grids. IMS allows one to identify the weakest and the most dangerous sections of the network and automatically to prevent accidents and to improve the reliability of electricity thereby.

In electrical energy industry there is a problem of an operational detection of the place and the type of the emergency mode of overhead power lines. There exist information-measuring systems for registering the type and the location of the damage which contain transducers mounted on supports to measure voltages and currents of each phase. The operation mode of the electrical line is determined by using the results of control currents and voltages with the help of logic schemes. If there is an emergency mode, the information about the place of the accident and the video is transmitted to the central dispatching board. The main disadvantage of such systems is the complexity of installation and maintenance. In addition, the information signals at emergency operation can take different values in a wide range, making it difficult to determine the type of accident.

The present article describes a neurocomputing system developed by the authors for diagnosing and prediction of emergency operation modes of overhead power lines. The system is based on registration of change of the electromagnetic field around the power line and of climatic factor parameters. The electromagnetic field changes are recorded by transducers that measure separately the electric and magnetic field components. The transducers register the electric field intensity \mathbf{E} and the magnetic induction \mathbf{B} created by all the wires of the line. The transducers are mounted on the support away from the wires, which greatly simplifies the installation and maintenance. Additionally, the system includes a weather station, which registers the basic climatic and environmental parameters respectively predicting wind and ice loads in the lines. The measured signals are processed using neural computers trained to recognize and forecast emergency modes of overhead power lines. The information from neurocomputer of the network, and forecasts are transmitted via GSM / GPRS connection to the control panel.

Identification criteria of regimes. For developing a neurocomputer system for diagnosing emergency conditions it is necessary to have the information about causality relations between the electromagnetic field characteristics and damages in the three-phase power system. With this purpose an analysis of these relations was realized for electrical mains with isolated neutral of 6 (10) 35 kV. The analysis was performed for an ideal case, namely, where all the phase voltages are equal and the distances from the sensor to the wire are the same. However, in real electric networks it is practically impossible to ensure the

equality of the phase voltages and the equality of all distances to the wire when installing the sensor. The variations of voltages in power supply systems is normalized by GOST and is equal to $\delta_U = \pm 5\%$. Therefore, to develop indication criteria we considered separately the case of change in the total electric field intensity caused by the deviation of the phase voltages.

The voltage proportional to the total electric field intensity for the case where the deviation is $\delta_U = \pm 5\%$ reads

$$U_{m\Sigma} = 0,085 \cdot U_m. \quad (1)$$

In the case where all phases work, the measured electric field intensity proportional to the voltage $U_{m\Sigma} = 0,085 \cdot U_m$, is slightly different from zero, and therefore to increase the reliability for mode diagnosis it is advisable to increase this deviation from zero using the asymmetry of the sensor location.

Similarly, changes in the magnetic field caused by the deviation of the phase currents at emergency operation modes have been identified. Thus, according to the recorded values of magnetic and electric fields one can determine the operation modes of energy network. The results of causality relations are presented in Table 1.

Table 1- Identification criteria for operating modes of the energy network.

Regimes	The electric field intensity is proportional to the total voltage		Induction of the magnetic field is proportional to the total current	
Normal regime	$0 < \sum U_m < 0,1U_m$ ($\sum U_m \approx 0,1U_m$)		$\sum I_m \approx 0,1I_m$	
Emergency regime	Before the place of accident	After the place of accident	Before the place of accident	After the place of accident
Loss of one phase	$\sum U_m \approx 0,1U_m$	$\sum U_m \approx U_m$	$\sum I_m \approx I_m$	$\sum I_m \approx I_m$
Loss of two phases	$\sum U_m \approx 0,1U_m$	$\sum U_m \approx U_m$	$\sum I_m \approx I_m$	$\sum I_m \approx I_m$
Loss of three phases	$\sum U_m \approx 0,1U_m$	$\sum U_m \approx 0$	$\sum I_m \approx 0$	$\sum I_m \approx 0$
Short circuit of one phase	$\sum U_m \approx \sqrt{3}U_m$	$\sum U_m \approx \sqrt{3}U_m$	$\sum I_m \gg I_m$	$\sum I_m \approx I_m$
Short circuit of two phases	$\sum U_m \approx \sqrt{3}U_m$	$\sum U_m \approx \sqrt{3}U_m$	$\sum I_m \gg I_m$	$\sum I_m \approx I_m$
Short circuit of three phases	$\sum U_m \approx 0$	$\sum U_m \approx 0$	$\sum I_m \gg I_m$	$\sum I_m \approx 0$

It should be noted that these relations are valid for the ideal case, namely, for a certain arrangement of transmitters and wires, and also in the absence of external fields. However, in real cases, the operation of the transmitter will be influenced by natural atmospheric fields that exist above the surface and are caused by different processes in the atmosphere. A great influence on the work of power lines are caused by climatic factors - rain, snow, humidity, ice, wind and lightning. In addition, the electromagnetic field of the air lines is greatly influenced by earth-wire transpositions [3]. Thus, for the development of information-measuring systems the presented above relations are only the fundamental basis and therefore the parameters and characteristics of the system should be adjusted to the influencing factors. An information-measuring system was developed on the basis of these relations [4,5].

Information-measuring system (Fig. 1) comprises a block of primary information processing, which consists of transducers measuring two quantities: the electric field **E** and

the magnetic field \mathbf{B} . The electric field transducers are represented by the capacitors C and the magnetic field transducers by coil inductors. Converters 1 and 2, record the total electric field intensity \mathbf{E} created by all the wires of the line. Converters 1 and 2 are set in a plane which is perpendicular to the wires of overhead lines with a relative angular offset φ round a circle.

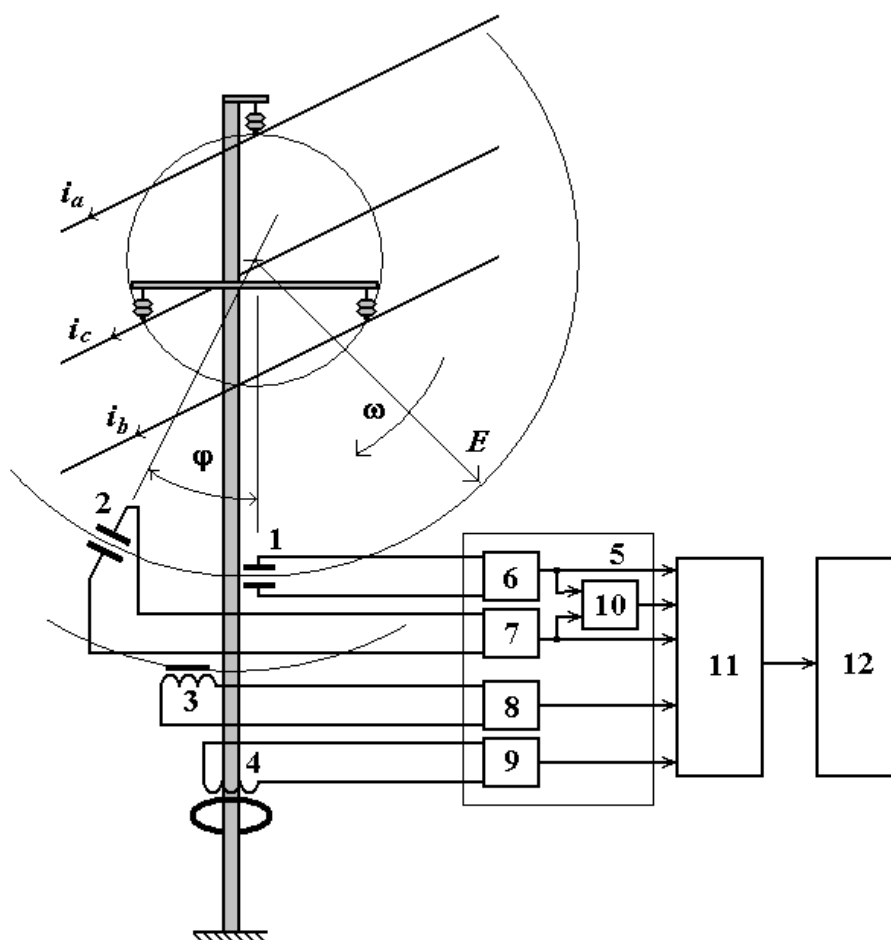


Figure 1 - Block diagram of the system neurocomputer

The measuring transducer of magnetic field 3 registers the magnetic field induction \mathbf{B} produced in wire lines. The measuring transmitter of short circuit current (CC) in support of the overhead lines 4 registers the magnetic field circuit current. The signals from the transducers 1, 2, 3, 4 come to the inputs of the signal processing block 5, which comprises a set of amplifiers 6, 7, 8, 9 and a phase shift detection unit 10, the input of which receives the signals from amplifiers 6 and 7. In a normal regime the electric field vector \mathbf{E} rotates with the angular velocity $\omega = 2\pi f$ relative to the center of a circle passing through the three wires of the overhead line. The signals from electric field measuring converters 1 and 2 have a difference in phase shift φ , which is determined by the angular displacement. It should be noted that the rotation of the electric field \mathbf{E} is caused by a timing offset of the phase voltages in a three phase system, and by the spatial arrangement of the wires [3]. Therefore, in the normal regime the unit signal is initiated by output 10. In the case of two phases the electric field vector pulsates, but does not rotate. Therefore, by analyzing the signals from the amplifiers 6 and 7 one can identify the phase where the breakage occurred. The signals from the amplifiers 6, 7, 8, 9, and from the unit of the phase shift determination 10 receives are sent to information processing unit 11 configured as a neurocomputer trained to be able to recognize the emergency modes.

The signals about emergency mode and its coordinate given by block 11 are transmitted via the transmission information unit 12 made as a GSM / GPRS modem to the control point.

Neurocomputing information processing unit. On the basis of this analysis, the identification characteristics of emergency operation modes of overhead power lines are determined and presented in Table 1. As the system's sensors measure the intensity and the induction of the electromagnetic field induced by the action of all the wires of overhead lines, the types of regimes can be recognized by the levels of sensor output signals. To translate analog data into binary code three-level threshold devices were used that convert the levels of the analog data signals into binary code. With the help of threshold voltage the levels of the voltage U_1-U_3 are converted into binary signals X_1-X_3 , and the levels of currents I_1-I_3 are converted into signals X_4-X_6 . The information in Table 1 may be represented in binary code. From Tables 1 we obtain Table 2 giving emergency operation modes of overhead lines in binary code, which is the basis for the design of a logic circuit diagnosis of emergency operation. From the analysis of the content of Table 2 it is seen that three pairs of emergency operation - loss of one and two phases, short circuit of one or two phases, open circuit or short-circuit of three phases after the accident site have the same identifying features, and therefore these same features can be concatenated. It should be noted that the threshold levels for each case may have different values. In addition there may be additional sensors and alarm levels, respectively.

Table 2 – Matching between mode types of the overhead line and sensor output signals

Regimes	Logic signals at the outputs of threshold devices, and phase sensor													
	Before the accident site							After the accident site						
	X_1	X_2	X_3	X_4	X_5	X_6	φ	X_1	X_2	X_3	X_4	X_5	X_6	φ
Normal regime	1	0	0	1	0	0	1	1	0	0	1	0	0	1
Loss of one phase	1	0	0	1	1	0	1	1	1	0	1	1	0	0
Loss of two phases	1	0	0	1	1	0	1	1	1	0	1	1	0	0
Loss of three phases	1	0	0	0	0	0	1	0	0	0	0	0	0	0
Short circuit of one phase	1	1	1	1	1	1	0	1	1	1	1	1	0	0
Short circuit of two phases	1	1	1	1	1	1	0	1	1	1	1	1	0	0
Short circuit of three phases	0	0	0	1	1	1	0	0	0	0	0	0	0	0

Table 2 of logic signals contains the output signal from the sensor phase designated by the variable φ . The signal, designated by variable I_{sup} , from the sensor of short circuit occurring in the support is inputted into the general logic scheme. Taking into account the combination of common identification criteria and the notations of outputs for the logic scheme that is under design, we obtain Table 3, which is an informational basis for the proposed scheme.

Table 3 - Logical combination modes line

Regimes	Output signal	Input signal						
		X_1	X_2	X_3	X_4	X_5	X_6	φ
Normal regime	Y_1	1	0	0	1	0	0	1

Loss of one or two phases before the accident site	Y_2	1	0	0	1	1	0	1
Loss of one or two phases after the accident site	Y_3	1	1	0	1	1	0	0
Loss of three phases before the accident site	Y_4	1	0	0	0	0	0	1
Loss or short circuit of three phases after the accident site	Y_5	0	0	0	0	0	0	0
Short circuit of one or two phases before the accident site	Y_6	1	1	1	1	1	1	0
Short circuit of one or two phases after the accident site	Y_7	1	1	1	1	1	0	0
Short circuit of three phases before the accident site	Y_8	0	0	0	1	1	1	0

From the analysis of the structural scheme of the diagnosing device and its work it is seen that this device works with fuzzy information, namely the comparator thresholds depend on the installation location, time of year and other external factors. Therefore, this device must adjust its parameters or should perform the instruction for operation, i.e the device must be an intellectual. To solve this problem it is advisable to use neural networks [6-8], which are able to perform a training at different non-formalized disturbing influences. The basics of the theory of neural networks is given [7] for having a reasonable choice of neural network.

The general view of an artificial neuron is shown in Figure 2.

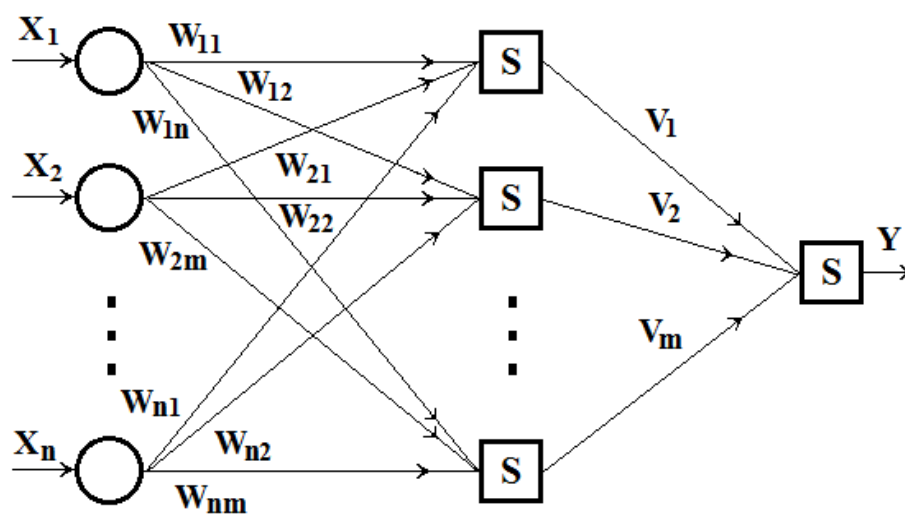


Figure 2 - General view of an artificial neuron

A set of input signals x_1, x_2, \dots, x_n is denoted by the vector X in the aggregate. Each synapse is characterized by the synapse connection and its weight w_i .

Each signal is multiplied by a corresponding weight w_1, w_2, \dots, w_n , and is sent to the summation unit. The set of weights in the aggregate is denoted by the vector W . The summation unit adds algebraically the weighted inputs, creating value S . Thus, the current state of a neuron is defined as a weighted sum of its inputs: $S = \sum_{i=1}^n x_i \cdot w_i$. The output of a neuron is a function of its state: $y = f(S)$, where f is the activation function [7].

Basing on the analysis of the neural network one can arrive at the following conclusion: the problem of detection of emergency operation modes can be solved by using

artificial neural networks because they allow one to perform the threshold functions, and with more functional features, and a three-level comparator is implemented by choosing the values of synapses connection.

In the detection device which is under design the logic device contains a single layer of logic elements, "AND". So, to implement the logic circuit using a neural network only one layer is sufficient, i.e. it is a relatively simple task. However, at further expansion of detection functions the number of layers may be increased.

Figure 3 shows the neural network to detect the emergency operation.

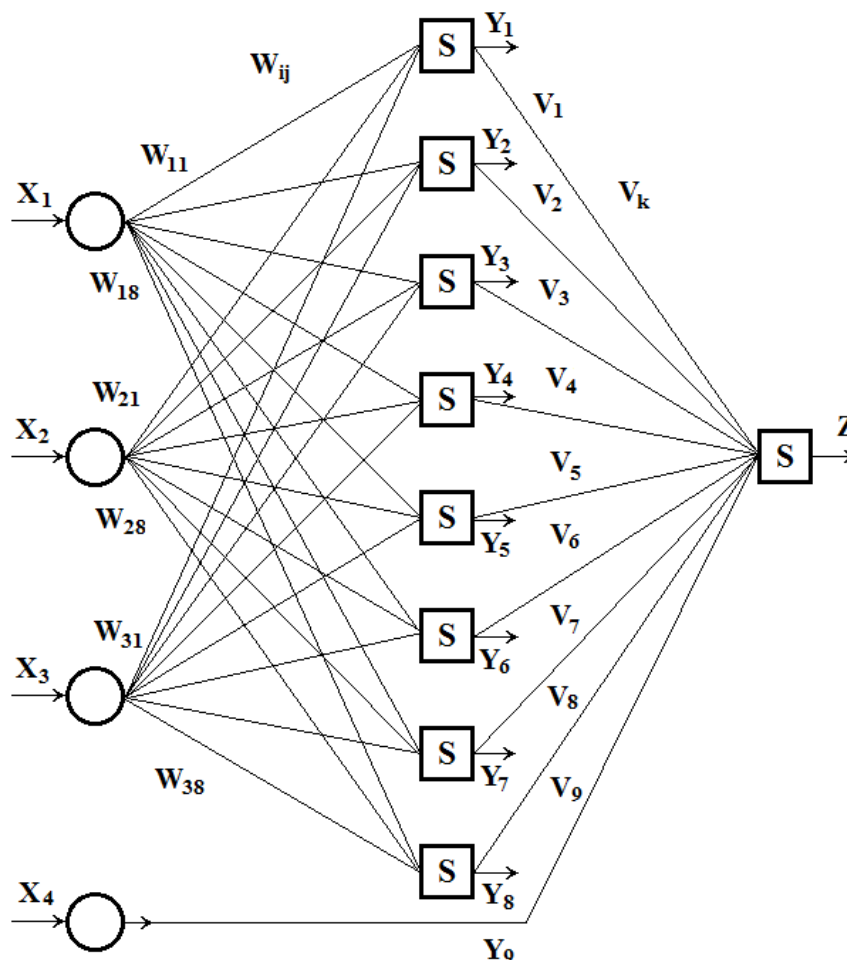


Figure 3 - A neural network to detect the emergency operation

From the analysis of existing training algorithms it follows that for neural network devices on emergency operation detection it is advisable to use a training algorithm with a teacher. Input vectors is convenient to specify values in simulated emergency conditions and for each set of weights and times of date.

Thus, the developed device can improve the efficiency and immediacy in detecting the type of emergency mode for overhead lines. To solve the problem of forecasting emergency modes of network the variables corresponding to climatic factor parameters and data are added to this basic neural.

References

1. Arcishevskii, Ya.L. Opredelenie mest povrezhdeniya linii elektroperedachi v setyah s izolirovannoi neitral'yu / Ya.L. Arcishevskii. – M.: Vyssh.shk., 1989.

2. Neiman L.R., Demirchyan K.S. Teoreticheskie osnovy elektrotehniki. – M.: Energiya, 1981.
3. Ryudenberg R. Perehodnye processy v elektroenergeticheskikh sistemah: Per. s angl. – M.: Izdatel'stvo inostrannoi literatury, 1955.
4. P.m. 108149 Rossiiskaya Federaciya, MPK G 01 R 31/08. Ustroistvo dlya opredeleniya mestopolozheniya i vida povrezhdeniya na vozduшной linii elektroperedachi / A.A. Shilin, A.N. Shilin; VolgGTU. – 2011.
5. Shilin, A.N. Informacionno-izmeritel'naya sistema opredeleniya povrezhdenii vozduшной linii elektroperedachi / A.N. Shilin, A.A. Shilin // Pribory. – 2011. – 15. – S. 23–29.
6. Osovskii, S. Neironnye seti dlya obrabotki informacii / S. Osovskii. – M. : Finansy i statistika, 2004. – 344 s.
7. Sistemy iskusstvennogo intellekta. Prakticheskii kurs: uchebnoe posobie / pod red.I.F. Astahovoi. – M.:BINOM. Laboratorii znanii, 2008. –292s.
8. Haikin, S. Neironnye seti: polnyi kurs : per. s angl / S. Haikin. – 2-e izd.– M.: Vil'yams, 2008. – 1104 s.

FEM SIMULATION OF PROCESSES OF ELASTIC-PLASTIC DEFORMATION OF MULTIPHASE POLYCRYSTALLINE MATERIALS

**Bagmutov V. P., **Bogdanov E. P.*

** Volgograd, Volgograd State Technical University, **Volgograd, Volgograd State Agricultural University*

The reported study was supported by RFBR, research projects № 14-08-00837 a and № 14-08-31712 мол_a, and within a basic part of state task of Ministry of Education and Science of the Russian Federation, research project № 2014/16

The procedure on a base of a finite element method, designed for modelling of processes of formations of plasticity deformations and microcracks in multiphase materials, for example, polycrystalline and composition materials is offered. The structures components can have an anisotropy of properties of elasticity, plasticity and strength with different directions of main axiss of mechanical properties. For polycrystalline materials with different types the cubic crystalline lattice the tangential stresses in systems of slipping, normal stresses on crystallographic planes of probable fracture are determined. The coefficients of concentration, statistical regularity distribution of local stresses and strains, both in a material as a whole, and on separate structural component are determined. For determination of formation of plastic deformations and fracture of composite materials consisting of isotropic parts are used the statistical criterions of failure, are designed by authors. The obtained results are a ground for optimization of structure of created materials, correction of criterions of a plastic flow and fracture for them, definition of a resource of a plasticity, and also of danger of a stress-strain state in a neighborhood of corner of a crack at different stressed states.

Keywords: Structure of a material; a modelling, finite element method, statistical approach, local deformation, micro fractures, yield criterion, failure criterion, fracture criterion.

Urgency of a problem. The development of technology, especially aerospace, predetermines more intensive usage of materials with composite structure. The components of

such structures sharply differ by the physico-mechanical properties. At development of such materials it is important to know about mutual influence of components of structure in their simultaneous deforming on concentrating of microstresses and local deformations. Heterogeneity of processes both the concentrating of microstresses and deformations defines of implicating of micro volumes in a plastic deformation and origin of fractures. This factor requires the reflection in general constitutive equations for elastic – plastic material. Necessity of technological treatments of such materials, which at standard tests have small plasticity, do actual problem of the registration of interaction of elements of structure on shaping of strength and plastic properties.

Ground of a design model. There is a great many of levels of detailing at modelling structure of a material. Thus the interactions separate atoms or dislocations or their bands, of separate parts of grains or average interaction of the whole grains are considered. In the given work some intermediate level, commensurable with a grit size in a polycrystalline material ("meso" a level) is considered. At this level by modern representations the installation of linkage between the characteristics micro and macro of properties of a material is possible.

For a solution of the explained problem concerning interaction of devices of structure of a material it is expedient to utilise a finite element method. It is bound that it algorithmically and ideologically is a method of the solution of such problems.

Reference sizes of a structural model. For usage of the algorithms of a mechanics of continua it is necessary, that the finite elements of structures had such sizes, at which concept about stress and deformation would have traditional sense. It is considered, that such mesh size is the magnitude about 10^3 interatomic distances ($2.. 3 \cdot 10^{-7}$). As the size of grains of materials used in technology, varies in breaking points ($1.. 300$) $\cdot 10^{-6}$ m, there is obvious an efficiency of detailed viewing of interactions of elements of structure on a base of a finite element method (FEM).

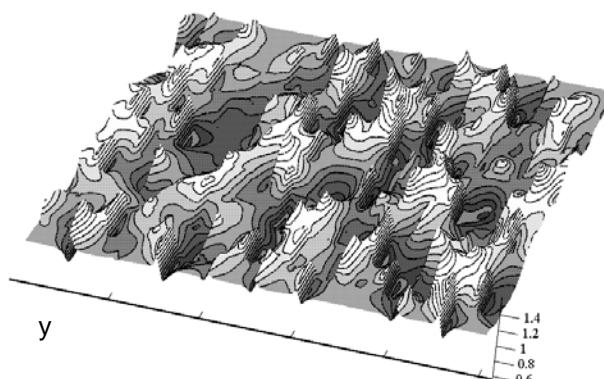


Fig.1 Microstress x_{yy} in model of iron from 100 grains at a tension $\sigma_{yy}=1$ n

By viewing polycrystalline materials it is necessary to take into account, that any restricted volume of finite number of grains, is some random sampling. It should be representative and reflect processes at a deforming proper in a material, instead of sample model. Therefore representative volume should consist of enough major number of grains. In a series of papers the linear magnitude of such volume was estimated on doubled of radius of a correlation of local deformations measured on base, is essentially a smaller grains size. The linear size of the underload crack was used also which it is necessary to consider as macroscopic. In all cases these estimates gave magnitude of the linear size of representative volume about 10 grains.

Form and arrangement of structure's elements. The known approaches to examination of a stress-strain state in polycrystalline materials do not take into account in all entirety the configuration, arrangement of grains, presence of interlayer on interface. It, as has

appeared, can essentially influence behavior of materials under loading. We designed specialized programs permitting it is easy to create a sample model of a polycrystal as a plate, consisting of square of grains of different magnitude, distinguished expedients of linking of corners of grains (three or four grains), and also from grains of the hexahedral form with interlayers of different thickness. Thus a level of digitization of a separate grain and any desirable number of grains in a sample model automatically can be set.

Assignment of elastic properties. For polycrystalline materials, in which the isolated areas of phases consisted of one crystal, the elastic properties of elements in laboratory axes depend on orientation of crystallographic axes of a grains. The orientation of axes sets by Euler's angles. In order that the model had effective properties of an isotropic polycrystal Euler's angles all three vary with an identical step. The assignment of alignments to adjacent grains in a model is yielded with the help of the generator of random numbers. There is an opportunity of reviewing of textures, when the change of one of corners does not happen at all or it varies with other step.

On Euler's angles are evaluated matrixes of direction cosines, and then for each grain the components of a tensor of elasticity C_{ijkl} and tensor of a compliance S_{ijkl} with the help of transformation of a tensor of the fourth rank are evaluated. A matrix of elastic properties $[D]$, linking components of vectors of microstresses $\{\xi\} = [\xi_{11}, \xi_{22}, \xi_{12}]^T$ and deformations $\{\varepsilon\} = [\varepsilon_{11}, \varepsilon_{22}, \varepsilon_{12}]^T$ for a plane strain (a) expresses through C_{ijkl} , and for a plane stress (b) through S_{ijkl}

$$[D] = \begin{bmatrix} C_{1111} & C_{1122} & C_{1112} \\ C_{2211} & C_{2222} & C_{2212} \\ C_{1211} & C_{1222} & C_{1212} \end{bmatrix} \quad (a), \quad [D] = \begin{bmatrix} S_{1111} & S_{1122} & 2S_{1112} \\ S_{2211} & S_{2222} & 2S_{2212} \\ 2S_{1211} & 2S_{1222} & 4S_{1212} \end{bmatrix}^{-1} \quad (b) \quad (1)$$

Here is taken into account, that zero components in the first case there is a strain tensor $\varepsilon_{33} = \varepsilon_{13} = \varepsilon_{23} = 0$, and in the second stress $\sigma_{33} = \sigma_{13} = \sigma_{23} = 0$.

The maximum coefficient of concentration of microstress for different stressed state. The solution of a problem for elastic deformation allows to receive the maximum coefficients of concentration anyone a component of microstresses. On coefficients of concentration and of known structural elements properties it is possible to estimate initial macroscopic stress, at which there are first local plastic detrusions or microfractures. The precision of such estimations, obviously, will depend on precision of evaluations of microstresses and of perfection of used criterions of a plastic flow and fracture.

For small elastic deformations the rule of a superposition is fulfilled, according to which microstresses or the local deformation in some point can be obtained for any stressed state, as the sum

$$\varsigma_{ij} = \sigma_1 (\bar{\varsigma}_{ij})_1 + \sigma_2 (\bar{\varsigma}_{ij})_2 + \sigma_3 (\bar{\varsigma}_{ij})_3. \quad (2)$$

Here $(\bar{\varsigma}_{ij})_k$ - microstress or local deformation is appearing from activity of $\sigma_k = 1$ (main unit macrostresses). Therefore for definition of stress and deformations in any element for an arbitrary view of a plane stress it is enough to yield calculation only for two different views of tensions. It is most convenient to make for uniaxial tensions by unity stress in two orthogonal directions. For an example in a fig. 1, 2 the fields of microstresses $\bar{\xi}_{yy}$ and microstrains $\bar{\varepsilon}_{yy}$ for a polycrystal of iron are shown at a monoaxial tension $\sigma_y = 1$. The gained components of tensors also will be $(\bar{\varsigma}_{ij})_k$, on which according to expression (2) is defined stress or deformations in any element at an different planar stressed state.

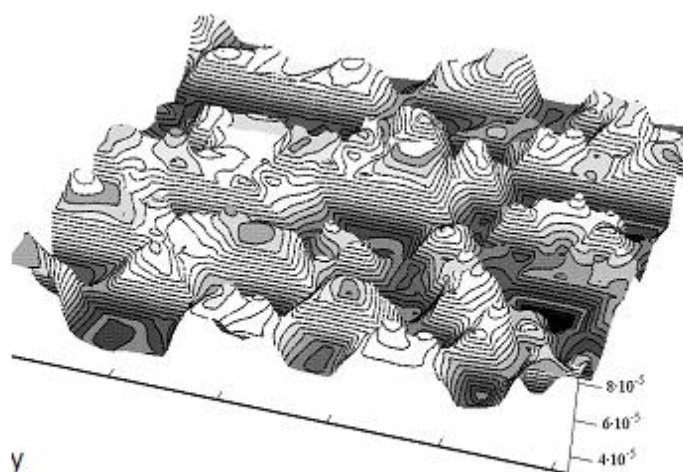


Fig.2 Microstrains ε_{yy} in model of iron from 100 grains at a tension $\sigma_w=1$

Criterion of plastic flow and strength for grains in a polycrystal. The definition of a macrostress, at which arise of the first plastic deformations in polycrystalline materials, was yielded according to the generalised law of the Schmid. As is known, at "restricted" slide in cubic crystals the plastic deformation can arise on 12 strictly restricted systems of slide $\{111\} \langle 110 \rangle$ for face-centred and $\{110\} \langle 111 \rangle$ for body-centred crystals. For both types of crystals 12 identical equations, defining magnitude of a tangential stress in system of slide on components of a tensor of microstresses expressed in crystal axes are gained. For "pencil" slide, which is most typical for body-centred crystals in requirements of room and heightened temperatures, the direction of slide $\langle 111 \rangle$ is defined only, and of slip planes can be is a lot of. And the generalised law of the Schmid is reduced to four equations, defining complete tangential stress on perpendicular planes to directions $\langle 111 \rangle$.

Definition of a macrostress, at which there are first microfractures was yielded according to an experimental rule, offered a Sonke, in which the strength of a crystal is defined by a critical rated stress on a plane cleavage. As is known, for many cubic crystals such family of planes is $\{001\}$. However, there are crystalline materials, which have a series crystallographic families of planes cleavage, and also such for which they are not present generally. Such materials have no a considerable anisotropy of strength. Therefore local criterion of fracture on a maximum normal microstress was applied to them.

Criterion of plastic flow and fracture for piecewise isotropic composition. For composition materials, the components consist of major number of variously oriented grains, and consequently can be considered as quasi isotropic. For definition of origin of plastic deformations and the fractures in such components were used statistical criterions designed in articles [1-6] on the basis of the modified approach Volkov S.D. [7]. In the monograph [7] is used by the phenomenological guess, about that that the variance of microstresses responsible for limiting state is proportional to work of deformation. As against it, in articles [1-6] the dependence of statistical distribution parameters of microstresses on a macrostress view obtained on three different models of a polycrystal are used. Thus the most reliable estimate of these dependencies was given by calculation on a finite element method. The results of calculations a FEM placed in area between lower estimates and upper gained with the help of the known analytical solutions.

The criterion of nonoriented plastic flow obtained on the basis of dependence of medial quadratic diversions of tangential stresses in various oriented systems of slide was applied to exposition of plastic deformations in materials consisting of crystals with a cubic lattice at "restricted" slide is

$$(1 + \chi) \sqrt{\sigma_1^2 + \sigma_2^2 + \sigma_3^2 + 2\rho_\tau(\sigma_1\sigma_2 + \sigma_1\sigma_3 + \sigma_2\sigma_3)} + 3(1 - \chi)\sigma_0/2 = \sigma_p^T. \quad (3)$$

Where $\rho_\tau = \mu_{kl}(\bar{\tau}_{nv})/D(\bar{\tau}_{nv})_k \geq -0,5$ - is correlation factor of random shearing stresses $(\bar{\tau}_{nv})_k$ and $(\bar{\tau}_{nv})_l$ in various oriented systems of slides, $\chi = \chi_s = \sigma_p^T/\sigma_c^T$ the ration the tensile yield point and of compression yield point. The magnitude $\rho_\tau = -0,5$ is underload of possible, otherwise ratio for hydrostatic compression or for all-round tension the variance of tangential microstresses should be subzero. On structure this expression will match to criterion Buginski-Jagn. But as against it, the statistical approach displays that the surface of plastic flow as a hyperboloid of one sheet can not be implemented. It follows from precise limitations on magnitude, incipient from the physical premise of obtained criterion, instead of is clean of formal or geometrical representations. For experimental definition of a correlation factor according to the formula (3) there are enough of results at three views of a stressed state.

As shown in article [4], the requirement of nonoriented plastic flow at low temperatures ensures for a series of alloys with a matrix having a body-centred cubic lattice, good correspondence to experimental dates, if magnitude of a correlation factor

As shown in article [4], the requirement of nonoriented plastic flow at low temperatures ensures for a series of alloys with a matrix having a body-centred cubic lattice, good correspondence to experimental dates, if magnitude of a correlation factor $\rho_\tau > (1 - 4\chi + \chi^2)/(1 + \chi)^2$. At these values and $\chi < 1$ in space of stress to criterion (3) will match the ellipsoid, displaced in area of all-round compression. Thus, according to the statistical approach of the offered models the surface of plastic flow can be closed, as in the field of multifold compression and multifold extension. That is at equality $\sigma_1 = \sigma_2 = \sigma_3$ as a result of interaction of anisotropic grains and presence of irregularities of crystalline structure the critical share of systems of slide can be activated. However it is obvious, that modification of the shape will not happen as a result of lack of preferred orientation of the activated systems of slide, and intensity of macroscopic deformation shall be $\varepsilon_e = 0$. Therefore points on a surface of flowability, when $\sigma_1 = \sigma_2 = \sigma_3$, are special, characterizing availability of a material for a plastic flow, which will happen only at presence of component of deviation tensor's of macrostresses.

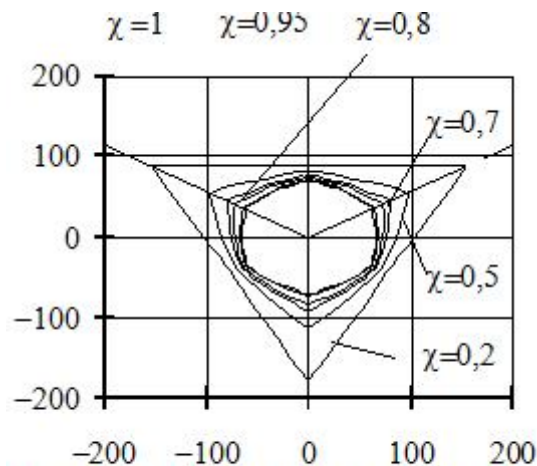


Fig.3 Yield envelopes based on formula (4) for different magnitude χ_s . View along the axis surfaces.

For polycrystals with the cubic type of a crystalline lattice, at origin of "pencil" slide, the stratum of flow from plastically deformed grains will be derivated. In them the local detrusion happens on slip planes, which orientation is close to a direction of a stratum of flowability, but direction of local detrusions are various.

For this case, the **statistical criterion of oriented (layered) plastic flow**, was designed. It is founded on association of statistical regularities of allocation of shear stresses of stressed

state. It was supposed, that the local yield strength linearly depends on a normal stress σ_v on a plane of stratum of plastic flow with

$$\tau_c = \tau_0(1 - \beta\sigma_v).$$

And the orientation of a stratum of plastic flow is defined by a maximum of work of a forming. According to Ostrovski A.A. is accepted, that the corner between a normal line to a stratum of plastic flow and σ_1 , depends on a stressed state $\cos^2\alpha = (2\sigma_1 - \sigma_2 - \sigma_3) / [3(\sigma_1 - \sigma_3)]$. An ensemble average of absolute values of tangential stresses on a layer of plastic flow $\langle |\tau_{nv}| \rangle = (\sigma_1 - \sigma_3) \sin 2\alpha / \pi$. Then the criterion of oriented plastic flow will accept a view [3, 4]

$$\begin{aligned} \tau_0[1 - \beta(\sigma_1 \cos 2\alpha + \sigma_3 \sin 2\alpha)] - ((\sigma_1 - \sigma_3) \sin 2\alpha) / \pi = \\ = Z_k \sqrt{D(|\bar{\tau}_{nv}|)_k (\sigma_1^2 + \sigma_2^2 + \sigma_3^2 + 2\rho_\tau(\sigma_1\sigma_2 + \sigma_1\sigma_3 + \sigma_2\sigma_3))}. \end{aligned} \quad (4)$$

Here $\rho_\tau = \mu_{km}(|\bar{\tau}_{nv}|)_k / D(|\bar{\tau}_{nv}|)_k \geq -0,5$, the correlation factor of random tangential stresses $(\tau_{nv})_k$ and $(\tau_{nv})_m$ on the variously oriented directions of slide located in a layer of flowability. The parameters $\tau_0, \beta, Z_k \sqrt{D(|\bar{\tau}_{nv}|)_k}, \rho_\tau$ can be expressed from four views of trials. At magnitude of a correlation factor $\rho_\tau \geq -0,5$ surfaces of plastic flow in space of stress are closed in the field of multifold compression and multifold extension, as well as for a criterion of nonoriented flowability. If for practical usage it is desirable to reduce number of necessary strength test, it is possible to assume that the alignment of a layer of flow does not depend on a view of a stressed state. And the layers of flow will be derivated on planes of the maximum macroscopic tangential stresses, when $\alpha = \pi/4$. Besides it is possible to put, that the magnitude of a correlation factor is underload and $\rho_\tau = -0,5$. Then a special case of a criterion of schistose plastic flow will accept a view [3, 4]

$$\sigma_1(\varphi - \chi + 1 - \sqrt{3}) + \sigma_3[1 - \varphi - \chi(1 - \sqrt{3})] + \sigma_e(1 + \chi - \varphi) = \sigma_p(2 - \sqrt{3}). \quad (5)$$

Here σ_e - intensity of stress. For the accepted simplifications at a multifold compression and multifold extension ($\sigma_e = 0$) there will not be of microstresses concentration and $D((\xi_{ij})) = 0$, that will match to an ideal single-phase polycrystal with boundaries of grains free of defects, not having in the composition of phases with other type of a crystalline lattice. The criterion (5) at different relations, also will match to a prism Tresca, to a cylinder of von Mises, to criterion Kovalchuk, to criterion Pisarenko-Lebedev.

For an estimate of strength of quasi isotropic materials having one family of planes cleavage, and consequently possessed of considerable local anisotropy of strength at a level of a grain - monocrystal, used a statistical criterion of nonoriented fracture. At its development the dependence of a variance of normal microstresses on all cleavage planes from stressed state was used. Thus it was supposed, what the fracture can arise on any of planes cleavage. The statistical criterion of nonoriented fracture will accept a view

$$\varphi \sqrt{\sigma_1^2 + \sigma_2^2 + \sigma_3^2 + 2\rho_\xi(\sigma_1\sigma_2 + \sigma_1\sigma_3 + \sigma_2\sigma_3)} + 3(\sqrt{2(1 - \rho_\xi)} - \varphi)\sigma_0 = \sigma_p \sqrt{2(1 - \rho_\xi)}, \quad (6)$$

Where $\varphi = \varphi^q = \sigma_p / \tau_{kp}$ - ratio of true stress at fracture for a extension and torsion; $\rho_\xi = \mu_{k\lambda}(\xi_{\{001\}}) / D(\xi_{\{001\}})_k - 0,5$ correlation factor of normal microstresses on variously oriented planes of one family. As the obtained criterion relates an opportunity of local fracture to stretching stress, and in the field of multifold compression at $\sigma_1 = \sigma_2 = \sigma_3$ in a continuous micrononuniform body the normal microstresses always are less than zero, the limiting

surface in space of stress in this band is unclosed. The magnitude can be retrieved from additional trial.

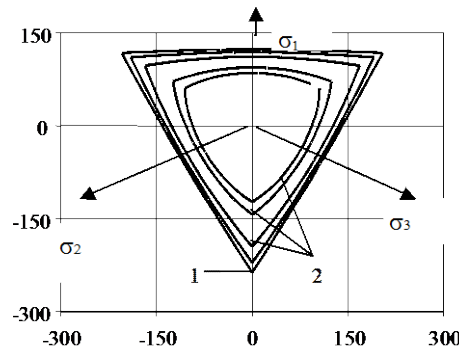


Fig.4 (1) - fracture envelopes based on maximum stress criterion and (2) - based on formula (7a) for different magnitude χ_q . View along the axis surfaces.

For materials with a small local anisotropy of strength the **criterion of oriented fracture** is used. At this mechanism of fracture it is supposed, that the microcracks arise on plane oriented perpendicularly to principal stress σ_1 , and fracture happens in those element of structure, where normal microstresses $\xi_{11} \geq \xi_c$, that is equivalent to neglect by a local anisotropy of strength. Such hypothesis is meaningful for polycrystals with a small local anisotropy of strength. To such materials, in particular, it is possible to refer refractory metals 5a and 6a of groups of Periodic system (vanadium, niobium, tantalum, chrome, molybdenum, tungsten). These metals have some sets of planes cleavage $\{100\}$, $\{112\}$, $\{113\}$, $\{110\}$. Taking into account a view the dependence of a medial quadratic diversion ξ_{11} from a stressed state and, that $\langle \xi_{11} \rangle = \sigma_1$ also is obtained [4]

$$\chi \sqrt{P\sigma_1^2 + \sigma_2^2 + \sigma_3^2 + 2Q(\sigma_1\sigma_2 + \sigma_1\sigma_3) + 2F\sigma_2\sigma_3} + (1 - \chi\sqrt{P})\sigma_1 = \sigma_p \quad (7),$$

Where $\chi_q \equiv S_k^p / S_k^{c*}$ - ratio of actual rupture limits at a tension and compression, $P = D(\bar{\xi}_{11})_1 / D(\bar{\xi}_{11})_3$, $Q = \mu_{12}(\bar{\xi}_{11}) / D(\bar{\xi}_{11})_3 < 0$, $F = \mu_{23}(\bar{\xi}_{11}) / D(\bar{\xi}_{11})_3 < 0$, and $P + 4Q + 2F + 2 \geq 0$. These parameters are defined on three different models of a polycrystal [4,5], besides they can be defined from additional aspects of trials [6]. This criterion generalisation of the theory of the maximum direct stresses at a microscopic level. The most simple aspect the requirement of oriented fracture accepts at usage of expressions for variances and covariances ξ_{11} , obtained on the basis of a hypothesis Voight about a homogeneity of deformations [5]

$$(1 - 4\chi_q/3)\sigma_1 + (\sigma_e\chi_q/3)\sqrt{(41 - 14\mu_\sigma + 9\mu_\sigma^2)/(3 + \mu_\sigma^2)} = \sigma_p \quad (7a)$$

Here $\chi_q < 3/4$, and μ_σ parameter Lode-Nadai.

The offered statistical criterions of strength give different results, as in the field of a biaxial extension, and biaxial compression. It is bound to usage of different local criterions of fracture and different regularities of change of statistical distribution parameters of microstresses calling fracture, from an aspect of a stressed state. The comparison of criterions of fracture with experimental data for a plane stress to perform, that the expression (6) enough well features experimental data at fragile fracture for materials possessing a considerable anisotropy of strength of grains. Such materials have one family of planes cleavage (typical representatives - alloys on a basis Fe). The expression (7) are given with good correspondence

for materials with a small anisotropy of strength, for example, alloys on the basis of a niobium, which have some sets of planes cleavage.

Solution at a elastic plastic deformation's for polycrystal. It is known that the activation 5 systems of slide suffice for deriving any strain state in a crystal grain. However, at "restricted" slide the cases are possible, when the stress at once in eight systems of slide reach identical magnitude. Besides in actual process of deformation in a polycrystal the amount of the activated systems depends on magnitude of a plastic deformation and at moderate deformations ≤ 3 . At input in a plastic deformation of one crystal grain, Stress-strain State in adjacent grains considerably varies. It can reduce that the stress in the earlier inactivated system of slide become more, than in active. The outcomes of experiments display, that change about the activated systems at moderate deformations happens extremely seldom. It testifies to origin of the latent hidden strengthening in passive systems. Now to develop the algorithm, which is taking into account the above-stated processes, being grounded on experimental results is obviously not possible. While it can be built only on a series of unfounded hypotheses, that reduces practical value of results. Thus considerably complicates computational process. Therefore alongside with the precise registration of an elastic anisotropy of crystal grains the plasticity anisotropy of grains was approximately considered. For this purpose the criterion of plastic flow such as von Mises for anisotropic materials was used which can be noted in a matrix aspect

$$F(\xi_{ij}, \kappa) = \{\xi\}^T [\Pi] \{\xi\} / \kappa^2$$

Here κ parameter of isotropic strengthening; $\{\xi\} = [\xi_{11}, \xi_{22}, \xi_{12}]^T$, - vector of stress; $[\Pi]$ - symmetrical matrix 3x3 from a component of a tensor of a plasticity of the fourth rank. Π_{ijkl} were defined by calculation with usage of the generalised law of the Schmid on yield strengths of a monocrystal testing in orthogonal directions with a tension and torsion. For the best approximation of a criterion of plastic flow with the help of a tensor of plasticity as principal axes of a plastic anisotropy the crystallographic directions [011], [01 1] and [001] are selected. Directions [011] and [001] are close to directions with extreme strength. For elements of a separate crystal grain the linear hardening $\tau_c = \tau_c^0 + h \sum |\gamma_p|$ is supposed. Here h the module of linear strengthening, and $\sum |\gamma_p|$ - total of relative magnitudes of plastic detrusions. The law of flow is used associate with a surface of flowability. The problem is solved in increments

$$\{\Delta\xi\} = [D] p \{\Delta\varepsilon\}.$$

Where the matrix of elastic plastic properties which are taking into account an elastic and plastic anisotropy and strengthening, on each step is evaluated [4]

$$[D]_p = [D] - [D][\Pi]\{\xi\}\{\xi\}^T[\Pi][D] \left[\frac{h}{\kappa^2 \tau_c^0} \left[\{\xi\}^T[\Pi]\{\xi\} \right]^2 + \{\xi\}^T[\Pi][D][\Pi]\{\xi\} \right]^{-1}. \quad (8)$$

$\kappa=1$ before origin of a plastic deformation . At formation of a plastic deformation in a element, its parameter of strengthening is augmented on

$$\Delta\kappa = h \{\xi\} \{\Delta\varepsilon\}_p / (\tau_c^0)^2$$

The solution is obtained with usage of a repetitive process, founded on a method of the elastic solutions.

Typical examples of application of designed procedures. The designed structure models of mechanical behaviour of inhomogeneous materials, have allowed to uncover features of their deformation and series of thin effects at different stressed state. The part from which with reference to polycrystal was surveyed above.

Elastic deformation for a two-phase alloy. Similarly expressions (2), microstresses or deformations in a random point in a flowing instant are possible to consider, as the sum, of

three dependent random variables. Then it is possible to note a general view of dependence of a variance of microstresses and deformations in a polycrystal from a stressed state

$$D(\xi_{ij}) = \sigma_1^2 D_1 + \sigma_2^2 D_2 + \sigma_3^2 D_3 + 2(\sigma_1 \sigma_2 \text{cov}_{12} + \sigma_1 \sigma_3 \text{cov}_{13} + \sigma_2 \sigma_3 \text{cov}_{23}) \quad (9)$$

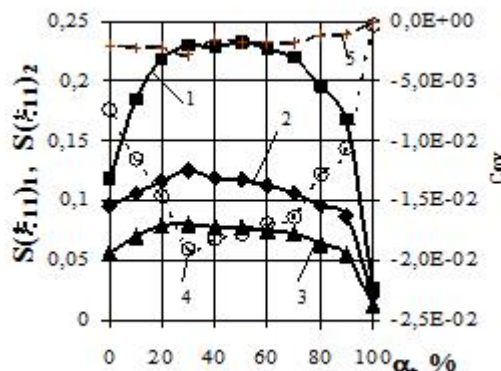


Fig. 5

Where D_k - variance $(\bar{\xi}_{ij})_k$, originating from a unit macrostress σ_k , and cov_{kl} - covariance of these magnitudes originating from unit macrostresses σ_k and σ_L .

The first phase of a two-phase material has at the crystal grains of body-centred, and second face-centred cubic crystalline lattices. And the level of an elastic anisotropy for component phases considerably differs. For cubic crystals the elastic anisotropy is convenient for characterising by relative parameter $\gamma = 2(S_{11} - S_{22})/S_{44}$. For isotropic crystal grains $\gamma=1$, and for materials $\gamma > 1$ this parameter is approximately equal to the ratio of maximum and minimum modulus of elasticity of crystal grain. In surveyed mixture for the first phase $\gamma=2.42$, and $\gamma=1.2$ for second. Besides, the medial modules of the first phase (rigid) in ≈ 2.8 times are more, than for second (soft). In a fig. 5 curves (1-5) display change of standard deviations $S(\bar{\xi}_{ij})_k = \sqrt{D(\bar{\xi}_{ij})_k}$ for microstresses $(\bar{\xi}_{ii})_1$, $(\bar{\xi}_{ii})_2$, $(\bar{\xi}_{12})_1$ and covariance $\text{cov}_{12}(\bar{\xi}_{11})$, $\text{cov}_{12}(\bar{\xi}_{12})$ from a share of a soft phase.

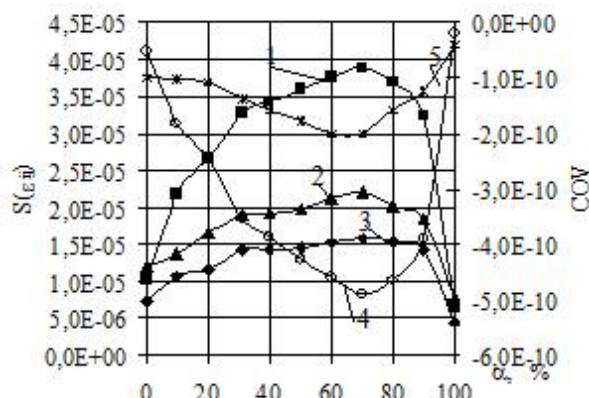


Fig. 6

In a fig. 6 the same parameters, but for local deformations are given. On variances and covariances of microstresses on the formula (9) it is possible to define variances of microstresses and deformations at any stressed state for a two-phase polycrystal with an arbitrary mixture. It is visible, that in mixture of phases in all surveyed variants the variance of microstresses is more, than in polycrystal consisting of one phase. And the maxima of concentration of microstresses is observed in region 30.. 40 % of the content of a soft phase.

The maxima of concentration for local deformations is observed at the content of the same amount, but rigid phase. On coefficients of concentration of tangential stresses in systems of slide the initial surfaces of plastic flow in first and in the second phases are obtained at different relations of phases. The initial surface of plastic flow of a polycrystal consisting completely of grains with a considerable elastic anisotropy ($\gamma=2,42$) is close to an ellipse of von Mises, and for a polycrystal from grains with a small anisotropy ($\gamma=1,2$) a little bit differs from a hexahedron of a Treska.

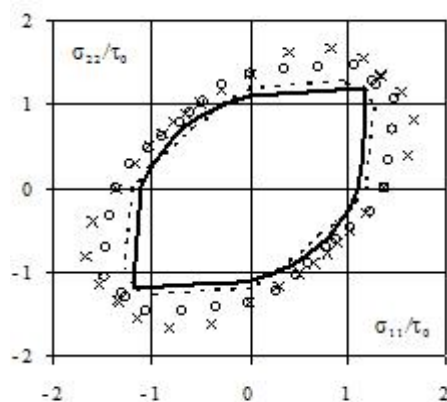


Fig. 7

Is obtained that as a result of interaction of anisotropic crystal grains of phases vary not only sizes of surfaces of flow, but also their form. In a fig. 7 in relative coordinates σ_{ii}/τ_0 , where τ_0 a critical tangential stress of a viewed phase, the initial surfaces of fluctuation for components of two mixtures are shown. The first mixture contains 90 % of a soft phase, second - 90 % of a rigid phase. The lines display a surface of plastic flow for a matrix. A solid line - for a soft matrix, dashed - for a rigid matrix. The crosses display an initial surface of plastic flow for inserts of a rigid phase (10 %), and circles for inserts from a soft phase. It is visible, that for both phases with change of their relation there is a transformation of an initial surface of flowability. For a soft phase with a small elastic anisotropy of grains, she it varies from a hexahedron of a Treska up to an ellipse. For mixture 50 % on 50 % (in a fig. 7 is not shown) displays calculations, that the plastic flow in soft and rigid phases for a biaxial tension occurs much earlier, than at a monoaxial tension (ratio $\approx 0,9$). Thus, the shape of an initial surface of plastic flow for mixture depends on a level of an elastic anisotropy of grains of different phases and phases relation. Besides, the relation of critical tangential stresses in systems of slide of viewed phases influenced, as an initial surface for mixture will be smaller on the sizes in co-ordinates ($\sigma_{11} - \sigma_{22}$) initial surface of plastic flow for a component. It is interesting to mark that the medial quadratic aberrations of tangential stresses in all 12 systems of slides calculated for all polycrystal differ from dependencies for single-phase polycrystal a little. It specifies that the basic influence on a variance of tangential stresses in all plurality of systems of slide give the orientation factor, instead of elastic anisotropy of grains.

Elastic plastic deformations for a single-phase material. At the solution of a problem for elastic - plastic deformations the interest represents to estimate, as depending on properties of structure there is a development of plastic deformations on element of structure of a material. The interest represents also change of macroscopic elastic propertys and definition of conditions of transition to common plastic flow of a material. These processes define strength and damping properties of a composition. Taking into account complexity of the solution of such problems and possible diversity the combination of components of an alloy becomes obvious, that in this direction there is a major field of activity.

Let's stop briefly only on results obtained for a single-phase material. In the solution of a problem according to a yield strength of a polycrystal by other methods many authors were engaged, therefore there is an opportunity to use their estimates for matching. For an example, we shall consider development of a plastic deformation in model of a polycrystal of α -iron. The magnitude macrostress, when the first elements of structure go into a plastic deformation, depends on the shape and modes of junction of grains. Thus $\langle \xi_{11} \rangle / \tau_c^0 \approx 1,6..1,8$. To the moment, when $\langle \xi_{11} \rangle / \tau_c^0 \approx 2,1..2,2$, that close to an estimate of a yield strength on Sachs, the share of plastically deformed element is makes 8.. 10 %, thus an imperfection of a coefficient of elasticity reaches the same magnitude. The input in a plastic deformation approximately 20 % of volume of element precede the moment of formation in some parts of a model of continuous bands from plastically deformed elements intersecting a model, which will be arising at small magnification of a loading. Thus the imperfection of a modulus of elasticity, defined for a model of a polycrystal on average values of microstresses and deformations is sharply augmented. Is established that at these stresses the small quantitative modifications of a portion of plastically deformed volumes reduce in a sharp qualitative modification of process of development of plastic deformations. There is a transition from a development of plastic deformations in zones of a material enclosed in elastic volumes, to formation of stratum of plastic macroscopic detrusion. That it is necessary to consider as transition to flowability. The relative yield strength of a polycrystal at this moment is equal approximately $\approx 2,5$, that will match to medial magnitude between estimates Sachs and Taylor-Bishop-Hill.

Though the curve of deformation obtained by calculation till a FEM, is a smoothly varying curve without presence on it of visual singular points, calculation of coefficients of a variation of microstresses $S(\xi_{11}/\langle \xi_{11} \rangle)$ and deformations $S(\varepsilon_{11}/\langle \varepsilon_{11} \rangle)$ presence displays of two stages of a development of inelastic deformations. At the first stage the level of concentration of deformations sharply increases, and the concentration of microstresses originating from interaction of elastic anisotropic grains, is reduced. After a small transient period, when the level of concentration of deformations is diminished, the during second stage occurs. At this stage relevant to developed plastic deformations, the level of concentration of stress and deformations is stabilised at some fixed level. This level also defines intensity of accumulation of damages of a further deformation.

Reference

1. Gurev, A. V. Vliyanie strukturnykh napryazheniy na prochnost polikristallicheskih materialov / A. V. Gurev, E. P. Bogdanov // Problemy prochnosti. – 1984. – №1. – S. 68-77.
2. Gurev, A. V. Zakonomernosti perehoda mikroplasticheskikh deformatsiy v makroplasticheskie dlya strukturno-neodnorodnykh materialov / A. V. Gurev, E. P. Bogdanov // Problemy prochnosti. – 1986. – № 6. – S. 35-41.
3. Bogdanov, E. P. Statisticheskie kriterii tekuchesti dlya razlichnykh mekhanizmov sdvigoobrazovaniya / E. P. Bogdanov, V. V. Kosarchuk, S. A. Kotrechko // Problemy prochnosti. – 1990. – № 3. – S. 35-40.
4. Bagmutov, V. P. Mikroneodnorodnoe deformirovanie i statisticheskiy kriteriy prochnosti i plastichnosti : monografiya / V.P.Bagmutov, E.P. Bogdanov; VolgGTU. – Volgograd, 2003. – 358 s.
5. Bagmutov, V. P. O vozmozhnosti ucheta tipa kristallicheskoy reshetki i anizotropii prochnosti zeren v kriteriyah razrusheniya / V. P. Bagmutov, E. P. Bogdanov // Problemy mashinostroeniya i nadezhnosti mashin. – 2004. – S. 24-30.
6. Bagmutov, V. P. Opredelenie parametrov statisticheskogo kriteriya razrusheniya dlya GPU materialov / V. P. Bagmutov, E. P. Bogdanov, I. A. Shkoda // Izvestiya VolgGTU. Seriya "Problemy materialovedeniya, svarki i prochnosti v mashinostroenii". Vyipusk 2: mezhvuzovskiy sbornik nauchnykh statey. – 2011. – № 5 (78). – S. 67-72.

7. Volkov, S. D. Statisticheskaya teoriya prochnosti / S. D. Volkov. – M.-Sverdlovsk: Mashgiz, 1960. – 176 s.

FORMATION OF A SINGLE MEDIUM, AS ASPECTS OF IMPROVING FOREIGN TRADE MARKET WORK FREIGHT TRANSPORTATION

Avilova E.D, Rayushkina A.A., Vaganova T.V, Shiryayev S.A., Fedotov V.N.
Volgograd, Volgograd State Technical University

The problems of creating a single information space in order to integrate the participants of foreign economic activity, improve performance and competitiveness of transport companies that will reduce overall costs and to achieve a new quality of transport services

Keywords: transportation, information, trade, logistics system, terminal network.

Economic globalization occurring at the moment, entails an increase in foreign trade relations and increase the volume of cargo in international traffic. Expansion of international relations requires new approaches to the development of the transport system using the new high-performance technologies for providing transportation services. One such approach today is to optimize the interaction of different types of transport, reduced downtime of vehicles, reducing transport and logistics costs, and improve the quality of logistics services.

Organization of information exchange in the process of foreign trade, a coordination interaction between the various structures involved in this kind of activity is not a simple task. Lack of timely, accurate and complete information from the participants of foreign economic activity may reduce the quality of transport and logistics services, duplication of functions performed, increase the volume of paper documentation and timing decisions. While the rapid assessment of information and acting upon competent managerial decisions allow for the required amount of foreign trade cargo transportation to the desired point on the optimal flowsheet, on time and with minimal costs [1].

Market transport and logistics and warehousing services is quite diverse and represented by numerous transportation companies. Each of them works in isolation, as has its specific advantages and disadvantages, both strengths and weaknesses in the organization of foreign trade transportation, perceiving his colleagues in the field as competitors. Therefore, to improve the efficiency of transport companies and, as a consequence, increase their competitiveness, it is necessary to create a single structure - a logistics center that will bring together businesses and organizations of different forms of ownership, will give them an opportunity to share the logistical infrastructure (transport, storage and information) due to the integration and coordination of logistics activities.

In order to achieve effective information security logistics processes to significantly reduce the overall costs and achieve a new quality of transport services, it is proposed the formation of a unified information space by integrating databases, technology and information systems participants transport and logistics processes. Such association has the potential to serve as a basis for the organization of a unified information environment of automated systems not only subjects of foreign economic activity of supply chains (FEA), but also by various federal agencies.

Today in this area there are already developments. For example, in the Russian customs service procedure is used to provide information via the Internet, enabling interaction with the customs service from anywhere in the world. As well as a perspective can be characterized on the basis of the establishment is currently being developed under the

auspices of the Russian Ministry of Transport of the automated control system of transport complex of the Russian Federation (ACS LC RF) environment, including "library" of national information standards, procedures and regulations of information exchange, the format of the documents and structures constituting their data. This information environment can serve as the basis of the automated system of foreign and mutual trade (ASVVT) of the Customs Union, as well as other automated systems ensure the logistics of foreign economic activity. Among them may be upgradable and unified automated information system (SAIS) of the FCS of Russia, developed and agencies engaged in control functions at the state border (FCS of Russia, Russian Federal Migration Service, the Federal Tax Service of Russia, Federal Service, Rostransnadzor, etc.), an interagency integrated automated information system (MIAIS).

Work on the creation of a common information space are also involved in the JSC «Russian Railways». At the heart of their development uses a unique digital backbone communications network that serves the company «Trans Telecom». Thanks to this modern network, today all operational information on traffic from all railways in real time falls into the MCC OJSC «Russian Railways», stored there and transferred to the Center for Transportation Management [2].

In general, the successful integration of foreign economic activity in the single information space will reach reduce processing time consignments terminal network, seaports, transshipment points, crossing the state border, as a consequence, increase transit cargo flows, the development of transport and customs technologies, information systems, transit infrastructure, formation and development of a balanced terminal and distribution network by creating terminals, multimodal terminal facilities that provide storage, customs and related services, the development of information security of the transport system to improve the quality of logistics customer service, quality of service approach to world standards [3].

Development of foreign relations by attracting foreign investment and partners formed logistics centers, ensuring a high level of logistics services of export-import operations in accordance with international standards. Logistic Centre should have a modern information system that allows online to solve all tasks assigned to it [4].

Information Management System for the logistics center should be a dynamic system of information processing and management of actual databases on the planning and execution of supply chains online. The foundation for such a system of information support logistics center can only be innovative enabling technologies in the field of Internet and telecommunications, uniting all participants of foreign economic activity.

References

1. Problems and prospects of the market for transport services in Russia after WTO accession / E.D. Avilova, T.V. Vaganova, S.A. Shiryaev, V.A. Gudkov, A.A. Rayushkina // Young scientist. – 2013. - № 5, Part 1. – C. 26-28.
2. Dubrovin, I.A New tools for the freight forwarder / I.A. Dubrovin // - Rail transport. – 2013. – № 12. – With. 52 - 54.
3. Prokofiev, D. Yu. Integrated management information system functioning multimodal transport and logistics center / D.Yu. Prokofiev, T.A. Prokofieva, V.I. Sergeev // In.: Siberia and the Far East in the long-term development of an integrated transport infrastructure Eurasia. – Irkutsk: Irkutsk State University of Railway Transport, 2011. – S. 464-503.
4. Panova, I.V. The concept of a cargo management at the interface between rail and water transport through the establishment of a logistics center – [electronic resource] / I.V. Panova, Sat proceedings of the international scientific-practical conference Internet «Scientific research and its practical application. Current status and the development of

'2012» – Mode of access: <http://www.sworld.com.ua/index.php/uk/transportation-312/transport-and-logistics-312/14138-312-706>

SIMULATION OF GEOMETRIC TRANSFORMATION IN OPTOELECTRONIC SYSTEMS WITH THE USE OF QUATERNION THEORY

Petrov S.A., Shilin A.N.

Volgograd, Volgograd State Technical University

Simulating method of geometric transformation in the optical marking system of large capacity shell-type products internal surface for set up tooling is considered in the article. The system contains rangefinder for cross-section profile of product body control. Proposed method is based on quaternion apparatus, allowing 3-D optical schemes simulating. All its operations are formalized that makes these substantially easy to realize on the computer.

Key words: assembly of large capacity shell-type products, shell of revolution, optic marking systems, pentaprism, quaternions.

Simulation problems. Reasonable selection of measuring optical schemes is one of the main stages of optoelectronic measuring apparatuses engineering because measuring optical schemes are exactly determine potential abilities of engineered systems. Measuring inaccuracies methodical components of optical and optoelectronic measuring apparatuses are determined by mathematical models of measuring optical schemes. Thus to make reasonable selection of measuring optical scheme with minimal methodical inaccuracy one needs mathematical modeling of geometric conversions in system using all scheme variants. It should be mentioned that measuring optical schemes can be rather complex and that is why the most formalized modeling methods convenient for computer technologies are required. Present modeling methods of geometric conversions are based on using theoretical trigonometry basis, analytic geometry and vector calculus. But formalization of all geometric conversions operations is needed for the computer modeling of optoelectronic apparatuses optical systems. For example, when calculating optical systems one needs to take into account the sign conventions: scheme vectors directions along optical axis, signs of points coordinates relative to the optical axis, sign of angle formed by ray and optical axis.

Analytic geometry apparatus utilization allows basic operations formalizing, but this method has a drawback when one models optical schemes: determination of sign before radical of formula for spacing between two points on coordinate plane calculation causes difficulties because a direction of a line is assigned instead of a ray direction. Thus, one requires equation generating for each coordinate, four equations in all, if the whole of coordinate plane is used for geometric conversions modeling. Besides, an analysis, being an operation that is more laborious and less formalized then equation generating, is carried out beforehand.

Vector calculus apparatus utilization hasn't allowed to gain substantial effect for geometric conversions in optical schemes because basic geometric operations aren't expressed by mathematical conversions of this apparatus directly. Thus, a selection of mathematical apparatus, which conversions makes all geometric operations quite easy to formalize, is the basic problem of geometric conversions modeling. By the same time, symbolic method of alternating current electric circuit calculation introduced by American scientist and engineer C. P. Steinmetz in 1897 year is used extensively in electrical engineering. This method allows to substitute vectors geometric operations by algebraic on the complex plane. Optical schemes modeling method has been designed on the base of

complex variable function theory (CVFT) analysis [1, 2]. But this mathematical apparatus is used for planar tasks solving, therefor the question about CVFT appliance for spatial tasks solving arises.

From science history it is known that one tried to solve spatial tasks with the use of CVFT. Thus hypercomplex numbers general theory embodied in a whole number of math and physics interface major appliances had been designed by the first quarter of the XX century.

Quaternion theory. Since quaternions are four-dimensional generalization of complex numbers apparatus, so these can be expressed this way: $\Lambda = \lambda_0 \cdot i_0 + \lambda_1 \cdot i_1 + \lambda_2 \cdot i_2 + \lambda_3 \cdot i_3$, where $\lambda_0, \lambda_1, \lambda_2, \lambda_3$ are unconditioned real numbers, which are called components of quaternion Λ , and i_0, i_1, i_2, i_3 are quaternion units. Applicable components λ_k and μ_k ($k = 0, 1, 2, 3$) of quaternions Λ and M are added when one adds these two quaternions. There is a quaternions interpretation that i_0 is identified with real unit and elements i_1, i_2, i_3 - with unit vectors $\vec{i}_1, \vec{i}_2, \vec{i}_3$ forming right-hand system in three-dimensional space. Then quaternion Λ can be represented by formal sum of scalar λ_0 and vector $\vec{\lambda}$ parts: $\Lambda = \lambda_0 + \lambda_1 \cdot \vec{i}_1 + \lambda_2 \cdot \vec{i}_2 + \lambda_3 \cdot \vec{i}_3 = \lambda_0 + \vec{\lambda}$, and rules of quaternion basis elements multiplication are represented by dot product and cross product in accordance with the formula: $\vec{i}_k \circ \vec{i}_j = -(\vec{i}_k, \vec{i}_j) + \vec{i}_k \times \vec{i}_j, k, j = 1, 2, 3$. Hence the product of two quaternions $\Lambda = \lambda_0 + \vec{\lambda}$ and $M = \mu_0 + \vec{\mu}$ with nonzero scalar part takes the form: $\Lambda \circ M = \lambda_0 \mu_0 - (\vec{\lambda}, \vec{\mu}) + \lambda_0 \vec{\mu} + \mu_0 \vec{\lambda} + \vec{\lambda} \times \vec{\mu}$. Rules that are mentioned above define quaternions algebra and properties resulting from it. We face with real numbers algebra utilizing quaternions with zero vector part and with complex numbers algebra utilizing quaternions with one dimension vector part.

The procedure being described in the source [3] has been utilized to elaborate the process of spatial geometric conversions relative to the baseline in pentaprism in this work.

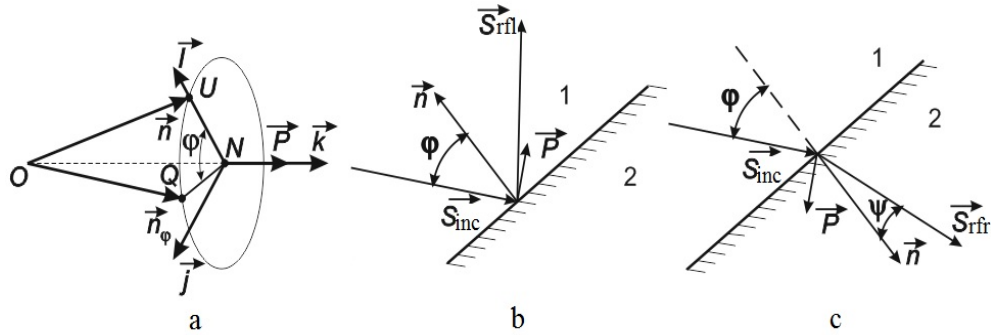


Fig. 1. The representation of a vector turn: a – pentaprism positioning; b – reflection, c – refraction of laser beam

A vector part of turn conversion can be obtained by direct geometric construction if the radius vector \vec{n} (fig. 1a) belongs to four-dimensional space. When a solid body rotates on a fixed axis, its points describe circumferences lying on a plane which is perpendicular to the rotation axis, and the radius vector \vec{n} with origin on the rotation axis describes conical surface and at the same time turns into the vector \vec{n}_φ . A turn around an axis which direction coincides with the direction of the unit vector \vec{k} at an angle φ is defined by scalar $\lambda_0 = \cos(\varphi/2)$ and vector $\vec{P} = \vec{k} \cdot \sin(\varphi/2)$. We need to use the expression to resolve the vector \vec{n}_φ into three mutually orthogonal directions $\vec{i}, \vec{j}, \vec{k}$: $\vec{n}_\varphi = \vec{n} \cos(\varphi) + \vec{k}(\vec{k}, \vec{n})(1 - \cos(\varphi)) + [\vec{k}, \vec{n}] \sin(\varphi)$. (1)

Authors utilize quaternions apparatus to make algebraic definitions of a beam reflection and refraction (fig.1b,c) in this work. A unit normal vector $\vec{n} = x_n \cdot \vec{i} + y_n \cdot \vec{j} + z_n \cdot \vec{k}$ and a vector describing an incident ray $\vec{S}_{inc} = x_{S_{inc}} \cdot \vec{i} + y_{S_{inc}} \cdot \vec{j} + z_{S_{inc}} \cdot \vec{k}$ are expressed in an orthonormal basis. A unit vector of the incident ray \vec{S}_{refl} can be found by a versor (unit quaternion) q of \vec{n} turn around the unit vector \vec{P} at an angle φ :

$$\vec{S}_O = q \cdot \vec{n} = (\cos \varphi + \vec{P} \cdot \sin \varphi) \cdot \vec{n} = \cos \varphi \cdot \vec{n} + [\vec{P}, \vec{n}] \cdot \sin \varphi, \quad (2)$$

where $\vec{P} = [-\vec{S}_{inc}, \vec{n}] / |[-\vec{S}_{inc}, \vec{n}]|$ and $\varphi = \arccos(|[-\vec{S}_{inc}, \vec{n}]| / (|-\vec{S}_{inc}| \cdot |\vec{n}|))$.

A unit vector of the refracted ray \vec{S}_{refr} can be found in a similar manner:

$$\vec{S}_{refr} = q \cdot \vec{n} = (\cos \psi + \vec{P} \cdot \sin \psi) \cdot \vec{n} = \cos \psi \cdot \vec{n} + [\vec{P}, \vec{n}] \cdot \sin \psi, \quad (3)$$

where $\psi = \arcsin(\sin \varphi / N_{12})$ is the refraction angle, N_{12} - relative refraction index, $\varphi = \arccos(|[\vec{S}_{inc}, \vec{n}]| / (|\vec{S}_{inc}| \cdot |\vec{n}|))$.

Modeling methodology. Controlled quantities analytical dependences of measuring circuit parameters are usually utilized for an analysis of optical measurements inaccuracies. One determines function increment through argument increment by applying analytical dependences of Taylor expansion. We can simplify the problem solving in practice by increments equations linearization, but this approach causes an inaccuracy of function increment calculation. Besides, it is quite difficult to estimate the linearization inaccuracy and most of all this inaccuracy value can be comparable with a value of an appropriate tolerance. That is why a simulation method would be appropriate for use to solve such tasks. The simulation method somewhat simplifies due to above assumptions, because maximum error can be found by extreme values from an inaccuracy zone.

One needs to set up equations of measuring optical scheme for modeling of inaccuracies formation processes. We have made some assumptions setting up equations of measuring optical scheme with the use of quaternions math apparatus:

- a) a cylinder is the form of an item inside surface, and a cross section of the cylinder is a circumference;
- b) a marking coordinate (point) on an item surface is defined by energy center of a laser beam;
- c) we used the laws of geometric optics when analyzing because a tolerance range size of the item geometrics considerably exceeds a wavelength of a laser beam;
- d) a divergence angle of the laser ray is an infinitesimal parameter and its radiation intensity is constant in the cross section;
- e) the distance between the laser emitter and the pentaprism is assessed without any inaccuracy;
- f) the laser beam enters the pentaprism through the center of its entrance facet;
- g) the law of random variables (angles) distribution is considered equiprobable.

The device (fig. 2a) consisting of the special clamps 1, the target 2, the laser rangefinder 3, the step motor with the control unit 4, the tripod 5, the laser cursor device 6 is applied to control cross sections deviations of towers bodies from circularity and to mark the plane in the “Volgogradneftemash” factory at present [4].

One determines the reference axis location with the use of the laser cursor device 6 and the target 2 before carrying out the plane marking and the circularity deviation of the cross section lying in this plane control. After that an operator sets the rotation angles of the laser rangefinder relative to the reference axis using the step motor control unit and performs the plane marking and the radius vectors measuring. The measuring results of current radius vectors and the relevant phase angles are transmitted to the computer calculating the

circularity deviation of the cross section. Pentaprism is utilized to provide the control plane perpendicularity to the reference axis in the device. And the reference axis beam can be used for the plane marking.

The rectangular coordinate system with the M_0 origin is determined by the right-hand triple $\vec{i}, \vec{j}, \vec{k}$ (fig. 2) before optical marking begins. The laser emitter is set in the working position M_1 being defined by \vec{h} using the positioner. The reference axis \vec{l} , which is usually specified parallel to the axis of the marking tower, is made visible by the laser beam. The pentaprism is utilized for the laser beam rotating in the marking plane of the item cross section determined by \vec{s} . So, the scanning of the item internal surface is implemented by the pentaprism being rotated around the reference axis. The laser beam path from M_2 inside the pentaprism is defined by $\vec{c}_1, \vec{c}_2, \vec{c}_3$ and the marking point M_9 is described by the ray \vec{r} at the item internal surface at the same time. Herewith the coordinates of the all points and vectors along the axis $\vec{i}, \vec{j}, \vec{k}$ is designated by x, y and z respectively.

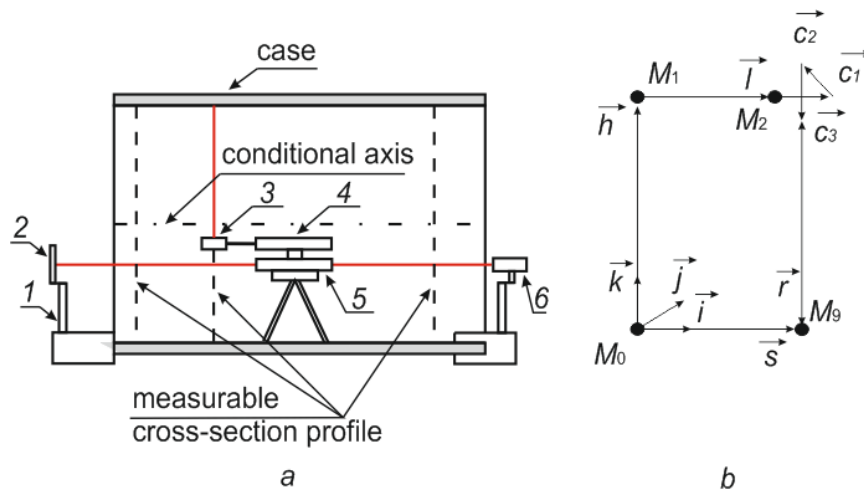


Fig.2. The device for the circularity deviation control and item body marking: a) the block representation b) the optical path scheme

The modeling main phases of the optical marking are shown in the fig. 3. The marking surface is defined in the discussed above coordinate system in the first phase:

$$(z - R)^2 + y^2 = R^2, \quad (4)$$

Where R is the radius of the item cross section. The coordinates of the M_1 and M_2 points are computed in terms of $\vec{h}, \vec{l} \in \vec{i}\vec{j}\vec{k}$ from the absolute values of these vectors according to fig. 2 in the second phase. The loop iterations of the five radius values of the marking item cross section represented by the numbers of the 200 random variables values are implemented with the equal step from 1000mm to 5000mm in the phases number 3 and 4. The internal angles of the pentaprism $\Theta_1, \Theta_2, \dots, \Theta_8$ (fig. 4) or its inclination angles to the coordinate planes are computed in the phases number 5 or 6 relative respectively depending on the parameter being analyzed. The coordinates of the pentaprism working planes normals $\vec{n}_1, \vec{n}_2, \vec{n}_3, \vec{n}_4$ and direction vectors $\vec{d}_2, \vec{d}_3, \vec{d}_4$ are specified originally in the 6th phase, moreover the \vec{n}_1 and \vec{d}_3, \vec{d}_4 are coincided with \vec{i} and \vec{k} relatively. After that the new coordinates of the mentioned above normal and directing vectors having been subjected to consecutive rotations around the basis vectors are calculated with the formula (1) for the mathematical description of the pentaprism positional errors. 720 iterations of the pentaprism elementary turns around the vector \vec{n}_1 are implemented within the uniform scan loop of the item marking cross section. Besides, the computing of the $\vec{n}_2, \vec{n}_3, \vec{n}_4$ and $\vec{d}_2, \vec{d}_3, \vec{d}_4$ new coordinates are also provided with

the formula (1) in the phase number 8. The coordinates of the $\vec{c}_{e1}, \vec{c}_{e2}, \vec{c}_{e3}, \vec{r}_{e1}$ unit vectors coinciding with $\vec{c}_1, \vec{c}_2, \vec{c}_3, \vec{r}_1$ (fig. 4) are calculated with formulas (2) and (3) in the 9th phase for mathematical formulating of the laser beam path inside the pentaprism. Then the coordinates of the M_3, M_4, M_5 points are to be found using $\vec{d}_2, \vec{d}_3, \vec{d}_4$ and after that the coordinates of the M_3, M_4, M_5 points – by the intersection of the pentaprism working surfaces with the M_2M_6, M_6M_7, M_7M_8 straight lines; to do this one needs to solve the equations set which is analogous to presented below:

$$\begin{cases} \frac{x_{M_6} - x_{M_2}}{x_{c_{e1}}} = \frac{y_{M_6} - y_{M_2}}{y_{c_{e1}}} = \frac{z_{M_6} - z_{M_2}}{z_{c_{e1}}}, \\ x_{n_2}x_{M_6} + y_{n_2}y_{M_6} + z_{n_2}z_{M_6} + (-x_{n_2}x_{M_5} - y_{n_2}y_{M_5} - z_{n_2}z_{M_5}) = 0. \end{cases} \quad (5)$$

The coordinates of the M_9 point are specified using the line M_8M_9 intersection with the item internal surface being determined by (4). The having been computed coordinates deviations from the nominal values are record and then the maximum is found according to the initial values thus the flatness error is calculated in the end.

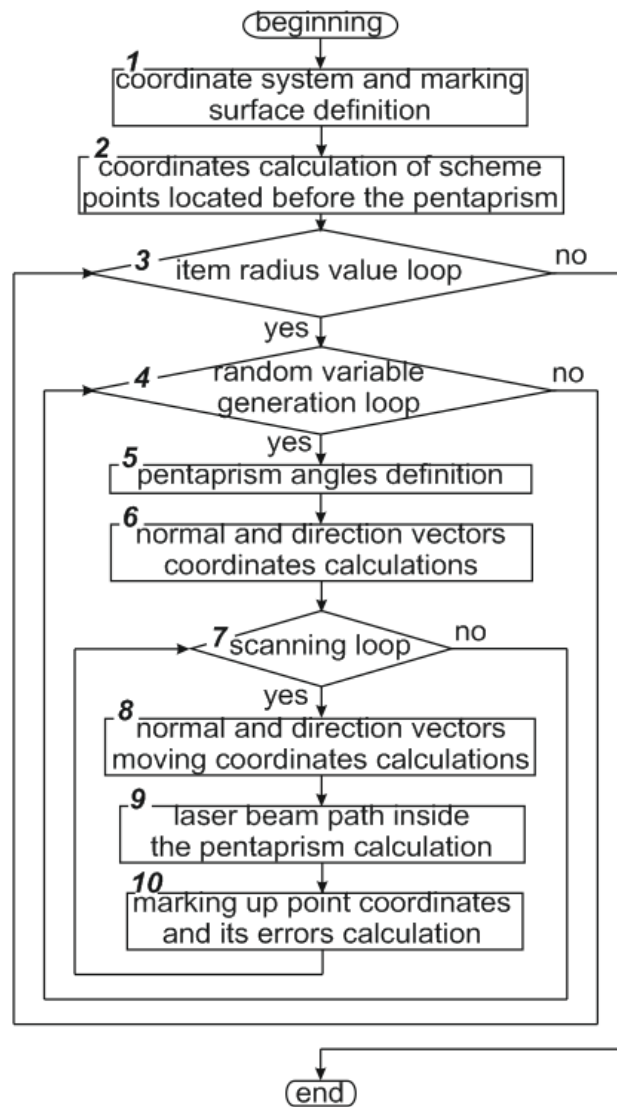


Fig. 3. The algorithm of the optical marking simulation

The diagrams of relationship between the maximum flatness error ΔX and the radius R of the marking cross section at constant 30 meters distance between this cross section and the coordinate origin have been obtained by means of the model having been developed by the authors (fig. 5). As the diagrams indicates the manufacturing errors of the pentaprism angles (fig. 5a: $1 - \pm 5''$, $2 - \pm 1'$) influence on the marking accuracy much stronger than the positional deviations from the reference axis (fig. 5b: $1 - \pm 3''$, $2 - \pm 1,5'$).

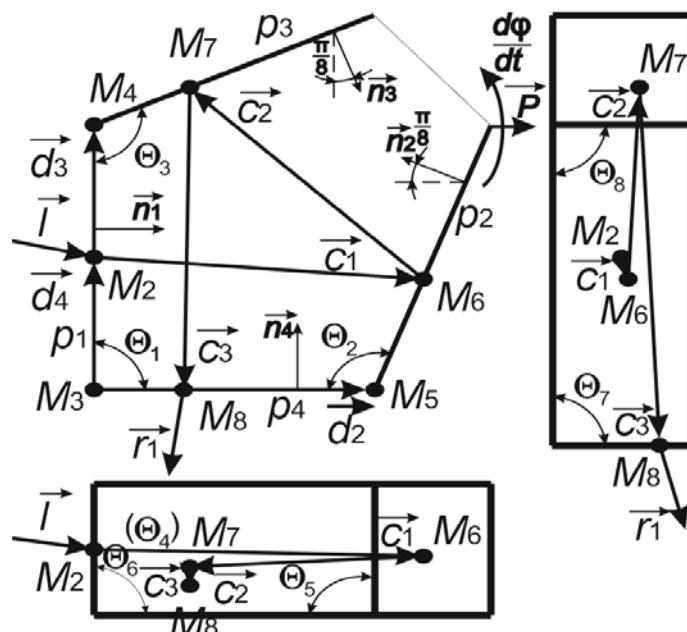


Fig. 4. The representation of the beam path inside the pentaprism

Thus, from the foregoing example it is seen that the pentaprism with at least $\pm 6''$ angle accuracy is to be utilized within the optical complex to provide $\pm 10^{-3}$ m tolerance of the flatness deviation. At the same time the positioner can be implemented on the base of standard coordinate stages utilizing rack-and-gear and worm-and-wormgear drives.

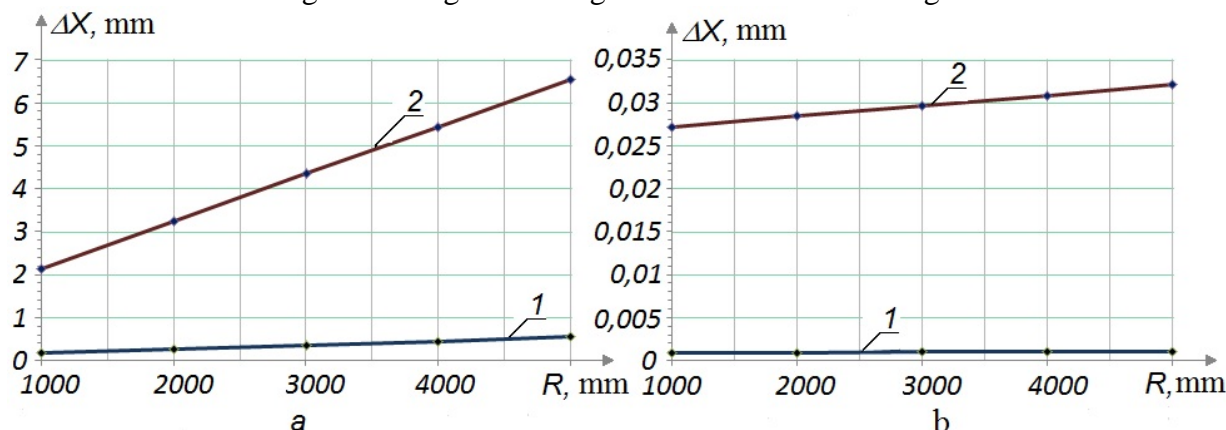


Fig. 5. The diagrams of relationship between the flatness deviation maximum and marking cross section radius: *a* – with the pentaprism manufacturing errors simulating; *b* – with the pentaprism positional deviations simulating

Conclusions. The based on quaternion theory and simulation computer-aided technique of the optical and optoelectronic devices inaccuracies analysis was considered. This technique appliance has been demonstrated with the example which confirmed its effectiveness. The optical schemes geometrics and component parts of the large-dimensioned

items optical marking systems can be reasonably chosen with the specified inaccuracies because of the carried out research results.

References

1. Shilin, A.N. (2004) Geometric transformation in optical systems modeling on the base of complex variable function theory. *Izvestiya vuzov. Priborostroeniye*, (1), 41-46.
2. Shilin, A.N. (1999) Geometric transformation modeling in optical measurements of items profile. *Izvestiya vuzov. Priborostroeniye*, (5), 44-47.
3. Khanukaev, U.I. (2013) About quaternions I. Finite movements of a rigid body and point, available at: http://02-07-90327.fizteh.ru/index/kvaternion1/f_otc1 (accessed 14 February 2014).
4. Petrov, S.A. (2011) Simulating of large capacity shell-type products optic marking system. *Izvestiya Volgogradskogo gosudarstvennogo tekhnicheskogo universiteta*, vol. 9, №11, 33-37.

PERSPECTIVES OF DEVELOPMENT OF INTERNET TECHNOLOGIES FOR AGRICULTURAL ENTERPRISES BASED ON TYPIFICATION IN UNIFIED WEB SPACE OF AGRARIAN KNOWLEDGE

Medennikov V.I., Salnikov S.G., Luppov V.V.

Moscow, Russian Institute of Agrarian Problems and Informatics named after A.A.Nikonov

In this paper we consider the possibilities of Web technologies for agricultural enterprises on the basis of typification within the framework of the Unified Web Space of Agrarian Knowledge (UWSAK).

Keywords: Agrarian knowledge, Web technologies, Information systems, Web site, Agroindustrial complex, Unified Web Space, Agricultural enterprise, Typical site.

According to world experience the most important problem for agrarian production development is improvement of integration processes based on information and telecommunication technologies. Their application permits farming producers to operate with significant volumes of information about goods, prices, services, firms and markets. This assists getting data fast, its accumulation, systematization and analysis for optimal managerial decisions.

According to estimations of the economists from the USA ([1]), qualitative and operational usage of information systems decreases production costs by 6% - 10% and distribution costs by 7% - 20%. Efficiency of information systems using for firms is estimated in reducing of stock materials in 3 – 4 times and reducing of current assets by 7% - 10%. Investments in products and services of information systems also increase labour productivity. Economists state that capital investments in information systems during past 10 years have had a significant influence on growth of gross domestic product (GDP) for many developed countries, that increased GDP per person by 0,3% - 0,8% in the OECD countries.

The above described effect can be feasible only with a complex and system approach to creation and implementation of information systems. Therefore only such an approach to the problem of informatization of agroindustrial complex (AIC) of the Russian Federation should be applied. There is also another significant aspect on this way. It implies that above described increase can be achieved only with a specific level of information systems development.

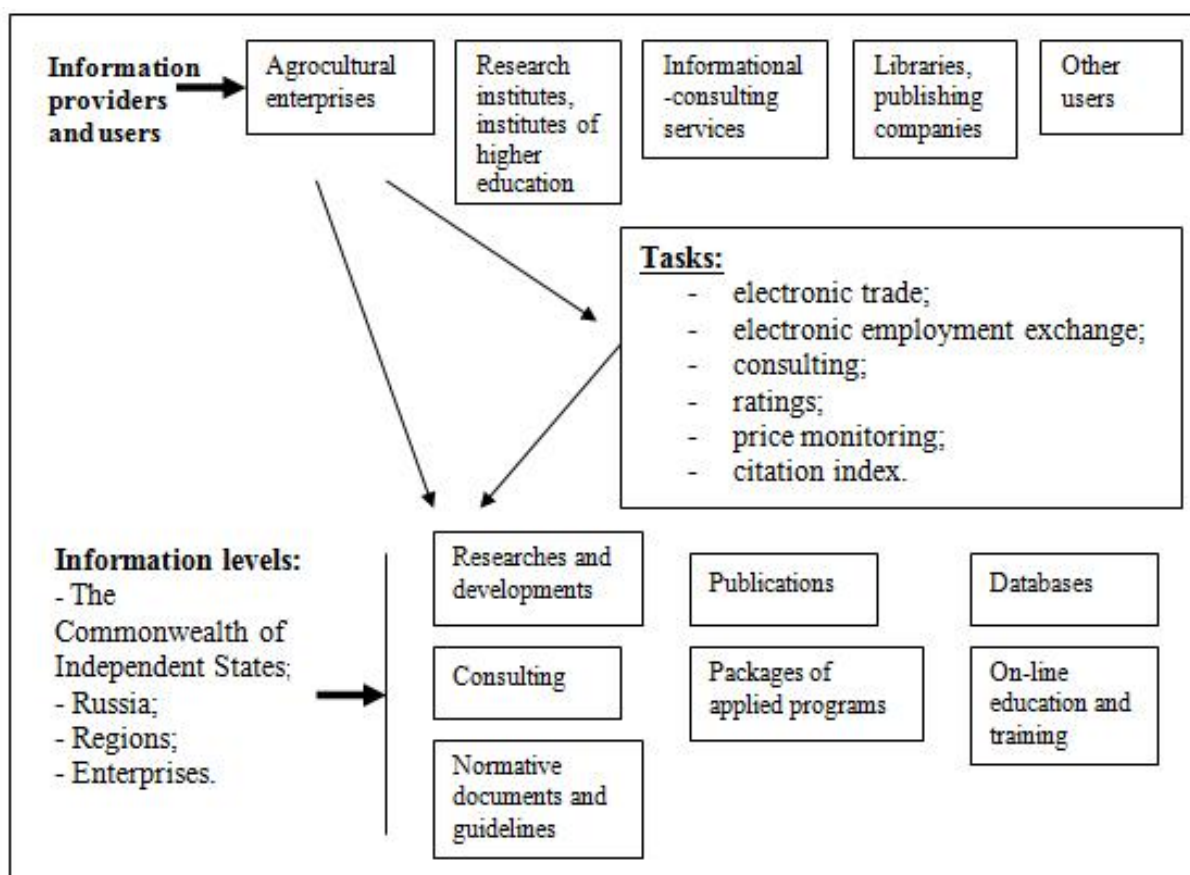
Ignoring this approach has resulted in the fact that information systems do not influence the development of productive forces of the Russian AIC, but are used mainly for purposes of advertisement and publicity. Internet for many leaders and managers is not more than «amusement» or additional, but not main, sales promotion tool.

Such state of affairs has some reasons. First of all, complex information systems are much more expensive than local program solutions for one single enterprise and may cost up to several million dollars. Therefore such work for AIC or for groups of enterprises must be developed by special engineering companies but they do not exist now in the Russian AIC. Secondly, there is a huge lack of IT specialists in the area of AIC information knowledge, because many professional engineers quit and are replaced by managers. Thirdly, within the Russian AIC there is not enough advanced production and sales promotion structures, which could require developed information systems.

Due to above reasons Russia at the present time remains behind other developed countries in all ways of informatization: software, amount of computers and information systems in using, communication systems, level of utilization of large-scale computing systems. And the significant aspect is that in Russia modern technologies of designing, creation and maintenance of information systems are being applied in industry very slowly. Informatization is currently more and more shifting by investments and innovation approaches to Internet space. But if the government structures pay little attention to these processes, it will bring only too large expenditures and scarce results, and even significant spent finances will not give expected effect.

The analysis of Web sites of research institutes of the Russian Agricultural Academy (RAA), the Russian Academy of Sciences, the Russian Academy of Medical Sciences, the Ministry of Education, the Agriculture Ministry, agricultural institutes of higher education and agricultural enterprises demonstrate that even Web sites with full and extensive content bring not so much utility because the users can extract only insignificant benefit from it. Information on those sites is not very clearly structured, concealed in different sections of sites, navigation is badly developed and does not permit making fast and complete information search. Besides, applying different approaches to design of Web sites, different data format and software - even on Web sites within one domain of knowledge – does not allow organize a unified system for regular replenishment from local sources of information and consequently does not allow effective unified search and analysis among all related sites. Only 25% of the most progressive agricultural enterprises included in Russian club AGRO-300 have own Web sites.

At the present time, as described in the researches of the past years, there are exist real capabilities and necessities to elaborate a typical Web site for agricultural enterprises. This conclusion may be made on the results of conducted studies on the problem of integration of all principal information elements in Internet: researches and developments, publications, advisory activity, technical standards, normative documents and guidelines that have been used in the above mentioned studied Web sites. There have been carried out modeling and estimation of feasibility to download large information volumes into an information carrier system of one provider. Queries response time have been also estimated during the modeling. Therefore, the results of the studies demonstrated that it is possible to merge all information of agricultural knowledge in the united database by the common provider. The operation of this database must be effected by a united database management system. The scheme of UWSAK is represented on picture 1.



Picture 1 Scheme of UWSAK

Creation of a typical site for agricultural enterprises must be done on a united database and must be located at one provider with modern database management system. Information must be organized according to classifiers used in Russia, such as state rubricator of scientific and technical information (SRSTI), Russian classifier of products (RCP) and others. This permits to analyze and process information for the purposes of sales promotion, for setting contacts of wholesalers and suppliers, for organization of manpower resources migration, for rating estimations, price monitoring and so on. But at the present time such approach to development of corporate agricultural Web sites in Russia is not realized. According to the above described approach and investigations ([3]) the following structure of a typical site for agricultural enterprises is suggested (Picture 2).

Structure of typical site of agricultural enterprise

About enterprise:

- history;
- areas of the business;
- guidance;
- organizational and production arrangement;
- contact information;
- cooperation with Russian and other organizations.

News:

- events;
- actions and procedures;
- business and jubilee meetings;
- seminars and workshops.

Economic and statistic information:

- income and profit;
- total enterprise area;
- area of agricultural land;
- production of agricultural crops and crop yield;
- production of animal breeding;
- farm equipment;
- other information.

Trade information (selling and purchasing):

- date of publication;
- name of product or service;
- type and sort of product or service;
- quantity, quality of product;
- lots and prices;
- package;
- delivery and purchase conditions.

Personnel:

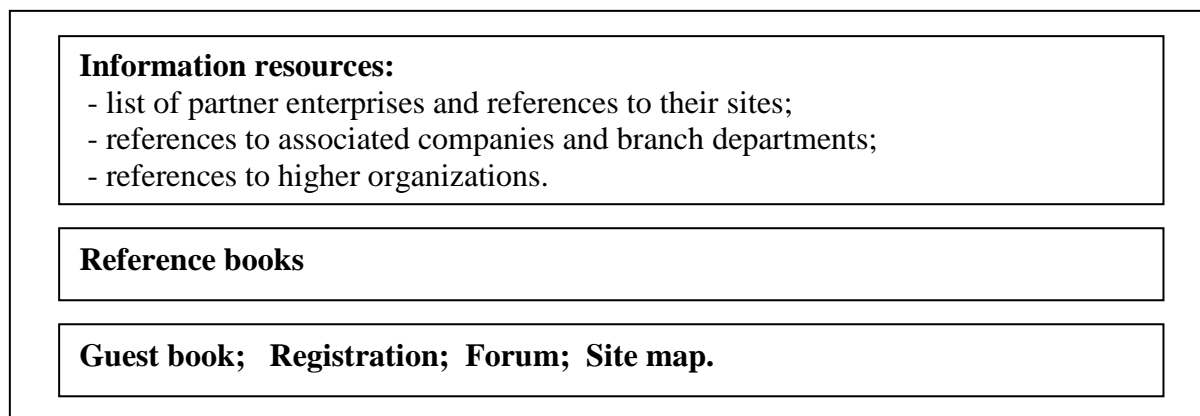
- quantity; - top staff; - managerial; -engineering; - operational staff.

Vacancies:

- position; - profession; - education; - salary; - requirements to applicants; - working and living conditions.

Scientific, applied and practical topics:

- publications; - researches and developments, - consulting;
- technical standards, - normative documents and guidelines;
- packages of applied programs; - on-line education;
- professional databases.



Picture 2 - Structure of typical site of agricultural enterprise

Full realization of this advanced project is a very hard task at the present time. Therefore initially it is proposed to create the integrated portal of the UWSAK based on unified database, catalogues, classifiers and convenient navigation system. Then it is necessary to create and reconcile normative documents and guidelines of software, to develop instructions and organize support service for enterprises while implementing their Web sites. Then it is necessary to organize digitization of all information materials (publications, researches and developments, technical standards, normative documents) and their download into the UWSAK. This centralized data preparation can minimize the expenditures.

At the next stage enterprises and institutes, which will join this project, may transform their sites for work with the unified database of the UWSAK. Typical sites may be provided to all enterprises that do not have yet proper own sites. At the next phases every enterprise will arrange information independently from its own site, and all information data will be available for all users on the portal of the UWSAK.

Realization of the UWSAK and typical sites of enterprises will allow to the Russian AIC to actualize a gross and essential step to the modern information community.

References

1. The Economist Intelligence Unit [Electronic resource]. 2011. URL: <http://www.eiu.com>.
2. SPARK – Systema professionalnogo analiza rynkov i kompanii [Electronic resource]. 2011. URL: <http://spark.interfax.ru/Front/index.aspx>.
3. Otchet o NIR, Analiz sostojanija i ob'emy informacionnykh resursov sel'skokhozjastvennykh predprijatij v Internet-prostranstve, VIAPI, 2011.
4. Otchet o NIR, Razrabotat' proekt otraslevoi programmy razvitija informatizatsii sel'skogo hozjaistva, VIAPI, 2004.
5. Otchet o NIR, Razrabotat' proekt programmy razvitija informatizatsii agrarnoi nauki, VIAPI, 2005.

MEDICAL MIXED-TYPE DATA CLUSTERING WITH MIXDC SOFTWARE

Alsova O.K., Uskova K.S.
Novosibirsk State Technical University

The paper describes the structure and functionality of a software system designed for mixed data cluster analysis (MixDC). In the system we have implemented a set of novel

clustering algorithms suitable for mixed data processing. This article contains description of a technique, used in MixDC to solve the problem of mixed medical data clustering and the results achieved with the help of this technic.

Keywords: cluster analysis, mixed data, software system, similarity matrix, clustering algorithm, ensemble approach.

1. Introduction

Clustering (the process of obtaining of «clusters» - groups of resembling objects) is one of the main problems of data mining today. Cluster analysis computational procedures are used in different areas of interest (medicine, sociology, economy and so on) and help to discover data regularities that were unknown before.

A lot of clustering algorithms and methods are now developed. Nevertheless, the vast majority can be used only if all variables which describe objects (e.g. all used in clustering process) are numeric. A few methods are suitable for nominal data analysis. Clustering of mixed-type data (when numeric, ordinal and numeric values are combined in one dataset) is the most difficult thing in this sphere. As a rule in reality object is often described by combination of mixed type variables and it is necessary to take all of them into account. This situation is specific for medical data processing for example.

Another clustering problem includes the choice and validation of variables (factors) set which is used in the grouping process, their statistical significance evaluation and ranging.

And finally, there is a problem of grouping solutions stability [1]. Clustering results can vary depending of the algorithm and its parameters, similarity measure and so on. Development and usage of ensemble algorithms is one of the ways to raise stability. In this case clustering results achieved either by usage of different algorithms or by one algorithm with different settings are used. After the ensemble is created the final solution can be found.

We have implemented the set of novel approaches and algorithms dedicated to solve the above problems [2, 3].

MixDC was used for analysis of real medical data about surgical treatment of patients of pathology of ascending aorta and aortic root (the dataset was furnished by Academician E.N. Meshalkin Novosibirsk Research Institute of Circulation Pathology). Database includes 20 factors (variables) estimated for 124 patients operated on ascending aorta and aortic arch with the help of different surgical techniques. Database contains 7 numeric, 2 ordinal and 11 nominal factors.

The process of mixed-type medical data clustering in MixDC software system as the results of this process are covered in this paper.

2. Structure and functionality of the system

MixDC software system is meant for cluster analysis of mixed-type datasets in any area of interest.

It consists of four main blocks: analysis block, clustering block, results evaluation block and visualization block. In analysis block the first-time analysis of data (for example cases and factors counting) is accomplished. Clustering block is used for separation the initial dataset in clusters. A user can choose one or more suggested algorithms and provide its (or their) parameters. Results evaluation block is focused on estimation of a solution accuracy degree. The system provides a user with some recommendations based on this estimation (for example the set of variables that should be used in future analysis). Visualization block involves graphical user interface and provides such things as parameters solicitation, visual presentation of analysis results.

Initial data can be input manually also MixDC supports automatic import from .xls files. Data must be represented as a table, its first line must contain factors' names. Values of variables apart from measurement scale must be represented in numerical form.

Before the start of cluster analysis process there is a possibility to choose a similarity measure and a clustering algorithm. A few algorithms (ensemble) can be used for getting more accurate results. The final result is formed by integration of solutions that were achieved with each of algorithms composing the ensemble.

After the end of clustering process a user can see the results in textual and graphical form and get a list of significant factors. The results can be saved on a local drive as .xls file.

3. Clustering algorithms. Ensemble approach

In the software we used our modifications of the Gower measure [4] and the measure of the matching of different scales [5]. These measures can be used for the calculation of the similarity between objects based on the mixed-type factors. Compared to the classic approach, we considered weights of the factors. The weight can be specified by a user if he has relevant information otherwise all weights are the same.

In our modification of the Gower measure the similarity between the i^{th} and j^{th} objects can be calculated as:

$$s_{ij} = \frac{\sum_{k=1}^p s_{ijk}}{\sum_{k=1}^p v_{ijk}}, \quad (1)$$

where s_{ijk} – the similarity by the k^{th} factor; v_{ijk} – the weight variable; p – the number of considered factors. The weight must satisfy the following equation $\sum_{k=1}^p v_{ijk} = 1$.

The similarity for the nominal and ordinal factors can be calculated as

$$s_{ijk} = 1, \text{ если } X_{ik} = X_{jk}, \text{ иначе } s_{ijk} = 0. \quad (2)$$

The similarity for the numeric factors can be calculated as

$$s_{ijk} = 1 - \frac{|x_{ik} - x_{jk}|}{R_k}, \quad (3)$$

where R_k – the range of variable values.

The modified measure which accords the different scales in a nutshell is a measure of distance and can be calculated for i^{th} and j^{th} objects.

For the numeric factors as

$$d_{\text{num}}(i, j) = \frac{|x_i - x_j|}{x_{\text{max}} - x_{\text{min}}} \quad (4)$$

For the nominal factors as

$$d_{\text{nom}}(i, j) = \frac{1}{m} \sum_{k=1}^m d(i, j)_s, \quad (5)$$

where m – the number of objects in a sample; $d(i, j)_s$ – the difference in the ratio of i^{th} and j^{th} objects to a s^{th} object.

For the ordinal factors as

$$d_{\text{ord}}(i, j) = \frac{1}{m-1} \sum_{k=1}^m d(i, j)_s. \quad (6)$$

The resulting distance between i^{th} и j^{th} objects is calculated as

$$d_{\text{res}}(i, j) = \sqrt{(v_1 d_{\text{num}}(i, j))^2 + (v_2 d_{\text{nom}}(i, j))^2 + (v_3 d_{\text{ord}}(i, j))^2}, \quad (7)$$

where v_1, v_2, v_3 – the weights of the factors.

The equation (7) is applied for the case then each object has one numeric, one ordinal and one nominal factor, but it can be expanded to the case of p factors of different types.

The MixDC provides the following clustering algorithms: the threshold algorithm [6] and the novel algorithm developed by authors based on the method of k-means. The measures described above can be applied for each of them.

In the threshold algorithm the only parameter is used (the threshold value, d_0). The objects are passed to the clustering consequently.

At the first step the first object O_1 is the kernel E_1 of the first cluster. Let at the m^{th} step k clusters with kernels E_1, \dots, E_k exist. For the object O_m : if $d(O_m, E_1) \leq d_0$ then O_m is in the first cluster; if $d(O_m, E_{i-1}) > d_0$ and $d(O_m, E_i) \leq d_0$, $2 \leq i \leq k$ then O_m is in the i^{th} cluster; if $d(O_m, E_i) > d_0$, $1 \leq i \leq k$ then O_m is the kernel E_{k+1} of the new $(k+1)^{\text{th}}$ cluster.

The novel algorithm is an iterative one. You have to specify a priori the number of centers of the clusters. The objects which have maximum distance between each other are chosen as centers.

Then the objects are distributed by the clusters. The distance to a cluster is calculated as the average distance from an included to the cluster object to each object in the cluster.

Let at the first step k objects O_1, \dots, O_k are chosen. These objects can be considered as centers of the clusters E_1, \dots, E_k .

At the second step we determine which cluster the object O_{k+1} belongs to. Then the distance between O_{k+1} and the centers of E_1, \dots, E_k is calculated separately by each factor using the equations (4-6). The object O_{k+1} belongs to the cluster the distance to which is minimum (7).

At the m^{th} step for each i^{th} cluster the average distance between the object O_{k+m} and other objects in the cluster is calculated separately by each factor.

For the numeric factors as

$$\bar{d}_{\text{num}}(i) = \frac{1}{n} \sum_{j=1}^n d_{\text{num}}(O_{k+m}, j), \quad (8)$$

where n – the number of objects in a cluster.

For the nominal factors as

$$\bar{d}_{\text{nom}}(i) = \frac{1}{n} \sum_{j=1}^n d_{\text{nom}}(O_{k+m}, j). \quad (9)$$

For the ordinal factors as

$$\bar{d}_{\text{ord}}(i) = \frac{1}{n} \sum_{j=1}^n d_{\text{ord}}(O_{k+m}, j). \quad (10)$$

The total average distance between the object O_{k+m} and the i^{th} cluster can be obtained as

$$\bar{d}_{\text{res}}(i) = \sqrt{\left(v_1 \bar{d}_{\text{num}}(i)\right)^2 + \left(v_2 \bar{d}_{\text{nom}}(i)\right)^2 + \left(v_3 \bar{d}_{\text{ord}}(i)\right)^2}, \quad (11)$$

The object O_{k+m} belongs to the cluster the total average distance to which is minimum (11).

The algorithm works until each object is clustered.

To improve the quality in the MixDC the ensemble approach is used. This approach is based on the usage of the algorithms combination. To obtain the final result the consistent similarity matrix is calculated.

In consideration of chosen factors L clustering methods are used. These methods form some groups. Then for each i^{th} group the $N \times N$ binary similarity matrix $S_i = \{S_i(j, m)\}$ is calculated, where $j, m = 1, 2, \dots, N$, $i = 1, 2, \dots, L$, N – the number of objects in original sample, L – the number of used clustering methods. At that $S_i(j, m) = 1$ if the objects O_j and O_m belong to one cluster, otherwise $S_i(j, m) = 0$.

Then the consistent similarity matrix $S = \{S(j, m)\}$ is formed as

$$S(j, m) = \frac{1}{L} \sum_{i=1}^L S_i(j, m) \quad (12)$$

The value of $S(j, m)$ is equal to the classification frequency for the objects to the same group in the set of groups G . The value closed to 1 means that the objects have high chance to be in the same group. The value closed to 0 means that the objects unlikely can be in the same group [1].

The obtained matrix can be used as input data for every hierarchical algorithm the result of which is the final solution.

4. Dialogue algorithm of data clustering in MixDC

Figure 1 illustrates the MixDC clustering process. The user selects factors and chooses methods that will go in the ensemble. As algorithms can be combined with different similarity measures the ensemble can include up to 4 methods.

On the first stage the system completes clustering with every selected method taking all chosen factors into account. Then significance of factors' influence the result is estimated. For numeric factors we use one way ANOVA to estimate the significance, for ordinal factors – nonparametric Kruskal-Wallis criteria is used, and χ^2 Pearson criteria is used for nominal factors significance estimation. The system forms a set of significant factors based on results of significance analysis.

To get more high quality solution the second stage of analysis should be made. Only significant variables chosen during the first stage are taken into account on the second one. Using the ensemble approach described above the system counts a consistent similarity matrix. This matrix is the initial information for any hierarchic algorithm; it is possible to use complete linkage method (by default), average linkage method or Ward's method.

All results (as final as intermediate ones) are represented to the user in textual description form and as a table and in the form of graphics and diagrams also.

5. Medical data clustering in MixDC

Neurological dysfunction (ND) is one of the most serious and socially important disease complications after surgical aggressions on ascending aorta and especially on aortic arch. Neurological dysfunction varies in severity: hypoxic encephalopathy, transient ischemic attack and stroke.

To identify the risk factors of ND contraction in early postoperative period and showing up the relation between ND severity and identified risk factors' values are important tasks of practical medicine.

Analysis of correlation between separated factors and ND couldn't discover statistically significant relations. As a part of the study there was made a hypothesis according to which ND is influenced by a combination of factors. Cluster analysis affords to separate sickness cases in groups, to identify significant (for this grouping) variables and to describe each group's patterns by ND severity and applied surgical techniques. So we can make a conclusion about relation between ND severity and a combination of risk factors.

First of all, we clustered described medical data taking all factors contained in database into account and then evaluated their significance.

The sets of significant factors differ when algorithm or similarity measure change. It's worth mentioning that the novel algorithm was more stable to similarity measure changes (significant factors sets were different in three positions) than threshold algorithm (significant factors sets were different in six positions). It can be explained with the fact that threshold algorithm compares distance between objects with some a priori specified value, but the novel algorithm adds objects to a cluster with the nearest center. That's why threshold algorithm results are more dependent on similarity measure distribution than clustering solutions achieved with the novel algorithm.

Aside from that, sets of significant factors achieved with the novel algorithm are bigger than ones achieved with the threshold algorithm.

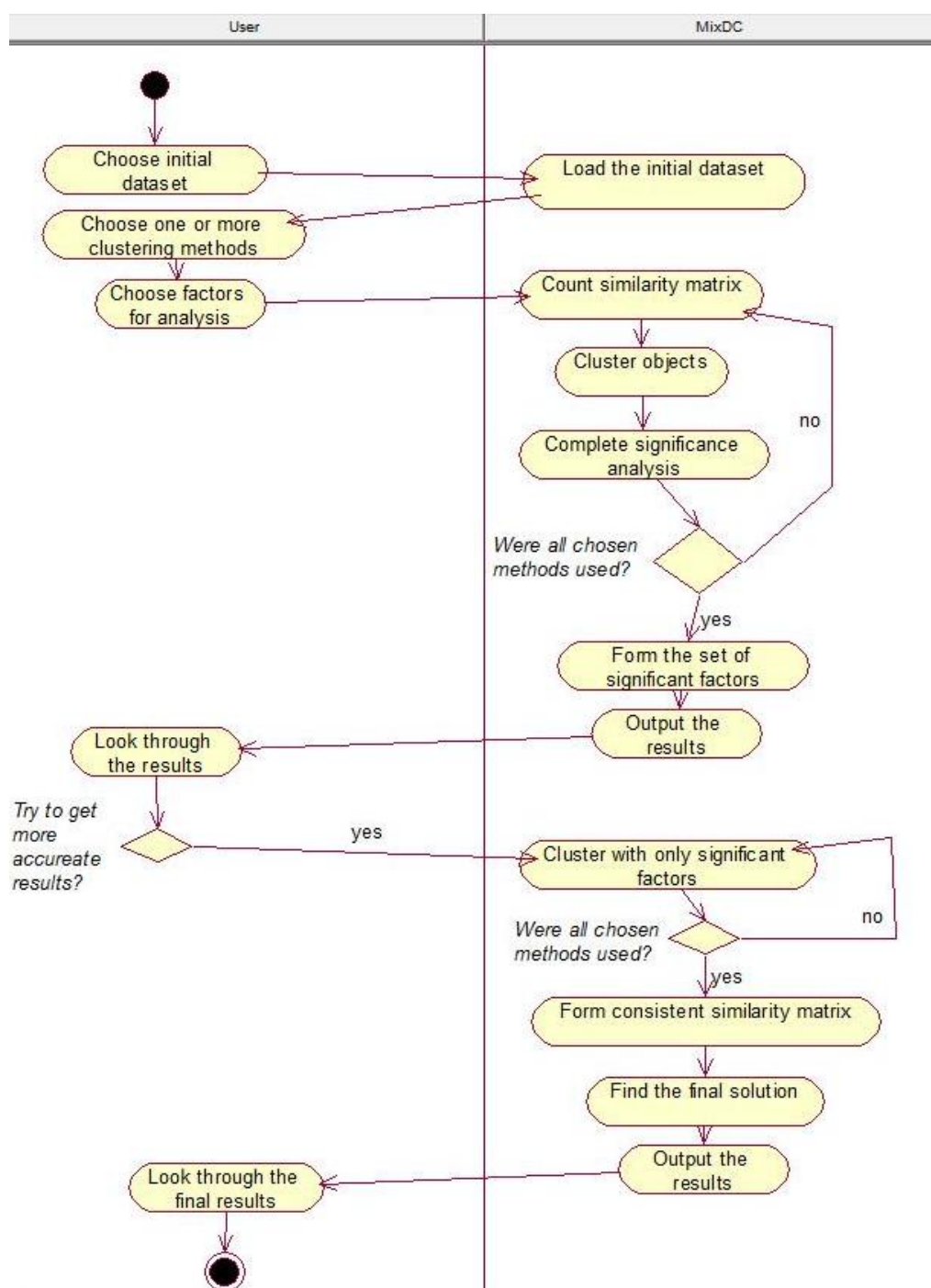


Figure 1. MixDC clustering process

At the same time some of the factors are included in a few of four sets, so it can be assumed that these very factors are the most important. To choose the final set of factors the system counts the frequency of including of each factor in significant set. This value changes from 0 to the number of algorithm in the ensemble and can be found in table 1.

Table 1. Factors significance

Factor type	Factor	Significance
	Gender	1
	Ethyology	2
	Previous cardiac surgery	2
	IHD – Ischemic Heart Disease	2

Nominal	AH – Arterial Hypertension	3
	CLD – Chronic lung disease	0
	Renal impairment	2
	Type of the arch reconstruction	4
	Borst procedure	3
	Brain perfusion	4
	Type of the aortic root reconstruction	3
Ordinal	ND - Neurological disfunction	3
Numeric	Age	2
	Hospital Stay time	2
	Height	0
	Weight	2
	CB – Cardiopulmonary bypass	1
	AO-Aortic occlusion (cross clamp time)	3
	CA-Circulatory arrest	4

The final set is formed with the user's participation; he can vary the frequency threshold in which the factor will be considered as significant one. In this particular case only factors with frequency more or equal to 3 ($\geq 75\%$) will be included in the result set. So we have a result set of 8 factors.

One the second stage the 4 methods ensemble was used again and only 8 chosen factors were taken into account. Hierarchic Ward's method was used to get the final decision. Figure 2 depicts the dendrogram of this process. The distribution of the significant factors' values by 4 clusters is illustrated in figures 3-8.

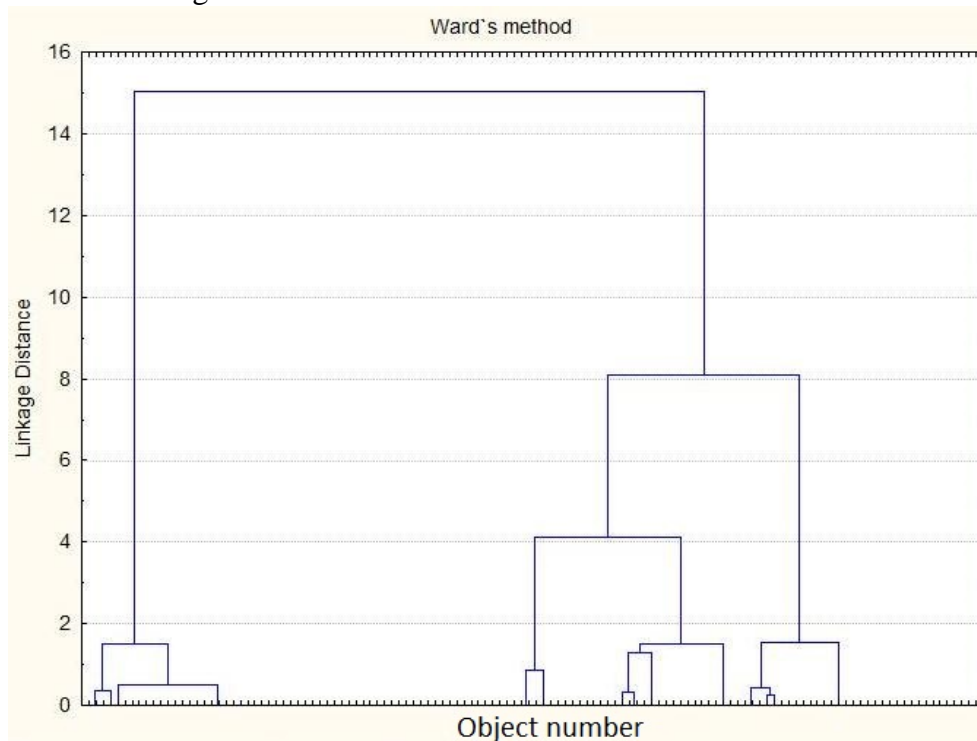


Figure 2. Dendrogram of Ward's method applied to consistent similarity matrix

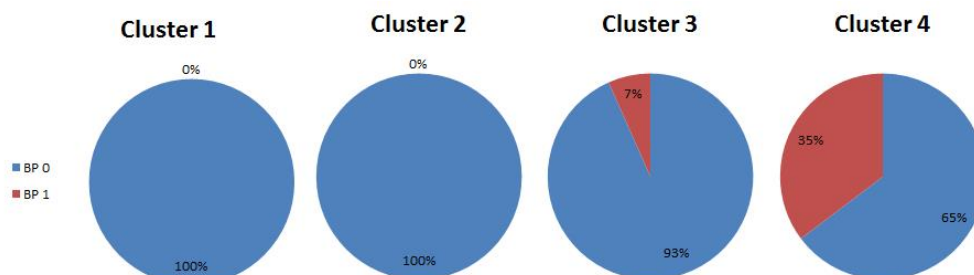


Figure 3. Borst procedure distribution by four clusters

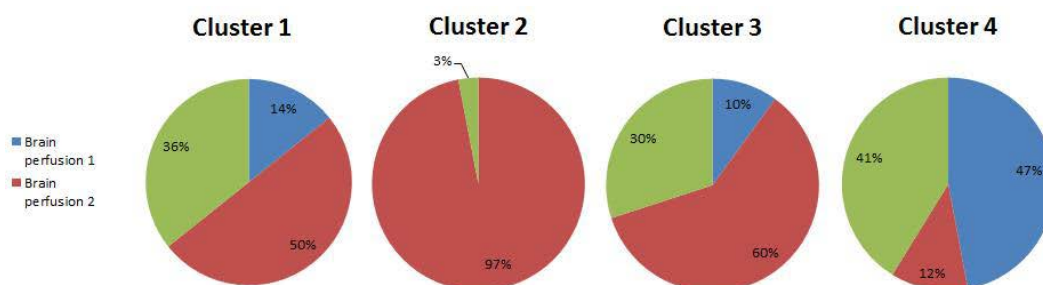


Figure 4. Brain perfusion distribution by four clusters

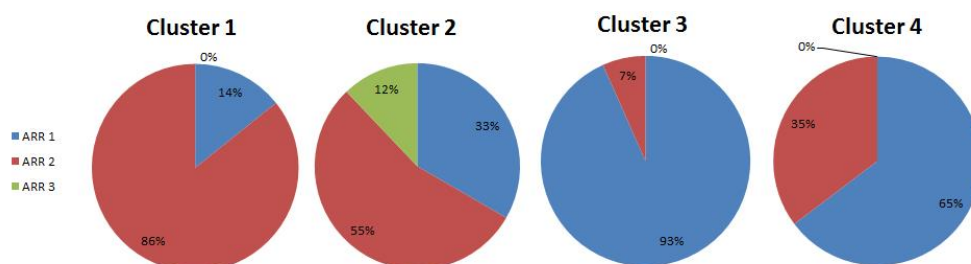


Figure 5. Type of the aortic root reconstruction's distribution by four clusters

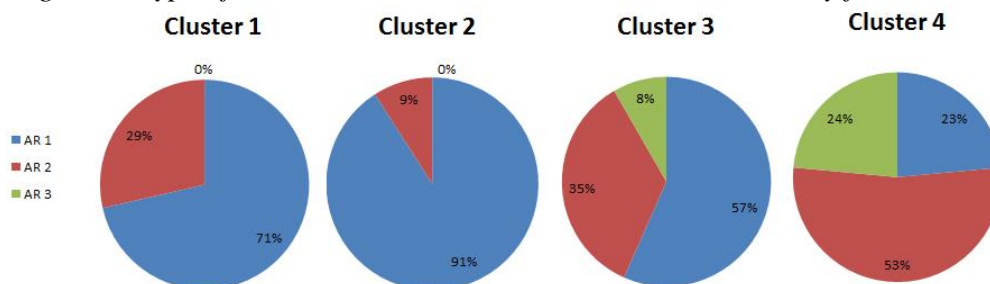


Figure 6. Type of the arch reconstruction's distribution by four clusters

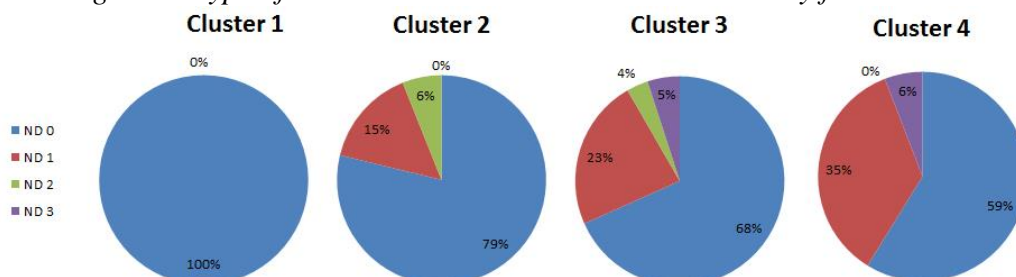


Figure 7. Neurological dysfunction's distribution by four clusters

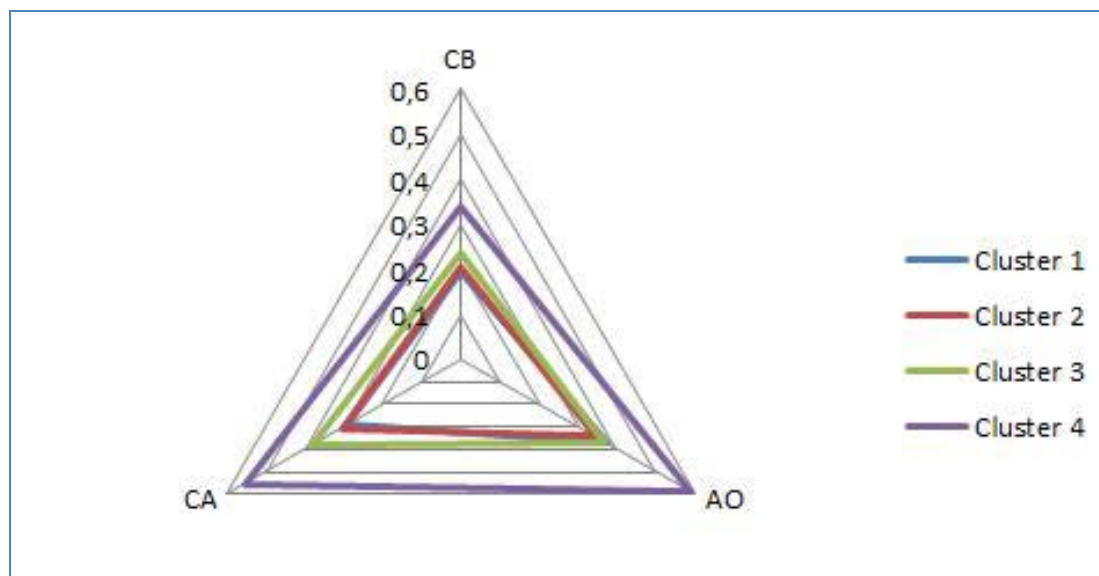


Figure 8. Numeric factors (Cardiopulmonary Bypass, Aortic Occlusion, Circulatory Arrest) normalized average values

Conclusion

MixDC software system provides a toolkit for mixed-type data cluster analysis. The process of finding of final result includes a few connected stages. The goal of first stage is to get a set of significant factors. Several clustering algorithms and the following significance analysis are used to reach this goal. Only significant factors are taken into account on the second stage. The final solution is formed with the help of ensemble approach and appears to be an integration of several clustering methods.

The system has been used to analyze data about surgical treatment of patients of pathology of aorta; four-cluster solution is the result of this analysis.

The achieved results can be explained logically. For example the disease severity, number of complications cases increase from first to fourth cluster. In the first cluster there were no ND cases. During the analysis it was found out that patients from the first cluster had endured the simplest types of the arch and aortic root reconstruction with the least time expenditures. In the fourth cluster we have the largest number of strokes (in comparison with other 3 clusters). And at the same time the most aggressive (in the context of complexity and operation duration) surgical technics were used in cases from this group.

References

1. Berikov V.B. Sovremennye tendencii v klasternom analize / V. B. Berikov // Federal'nyj portal po nauchnoj i innovacionnoj dejatel'nosti. Stat'i – pobediteli Vserossijskogo konkursnogo otbora obzorno-analiticheskikh statej po prioritetnomu napravleniju "Informacionno-telekommunikacionnye sistemy", 2008.
2. Alsova O.K. Programmnaja sistema klasternogo analiza dannyh smeshannogo tipa / O.K. Alsova, K.S. Uskova // Avtomatika i programmnaja inzhenerija, 2013. №1(3). – С. 75-81.
3. Uskova K.S. Struktura sistemy klasternogo analiza dannyh smeshannogo tipa / K. S. Uskova, O.K. Alsova // Sovremennye problemy tehniceskix nauk: sb. tez. dokl. Novosib. mezhhvuz. nauch. studen. konf. «Intel'lektual'nyj potencial Sibiri», Novosibirsk, 22-23 maja 2013. – Novosibirsk: NGASU. 2013. – С. 67.
4. Kim Dzh.-O. Faktornyj, diskriminantnyj i klasternyj analiz / Dzh.-O; per. s angl. A.M. Hotinskogo, S.B. Koroleva, nauch. red. I.S. Enjukova. – Moscow: Finansy i statistika, 1989. – 215 s.

5. Zagorujko N.G. Prikladnye metody analiza dannyh i znaniy / N.G. Zagorujko. – Novosibirsk: Izdatel'stvo instituta matematiki, 1999. – 270 s.

6. Ajvazjan S.A. Prikladnaja statistika i osnovy jekonometriki / S.A. Ajvazjan, V.S. Mhitarjan. – Moscow: JuNITI, 2001. – 1006 s.

USING THE UPGRADED PYROELECTRIC SENSOR IN ROBOTIC DEVICES.

Americanov A.A., Bogachev K.A., Korobova K.V., Lezhnyov E.V., Panasik D.S.
Moscow, National Research University "Higher School of Economics"

Currently interactive robotic devices are increasingly used to solve everyday problems. Now, their scope is not limited to high tech industries. They are increasingly used in daily life: in museums (interactive exhibits), large corporations (robots guides) in the entertainment field. In this paper we consider the possibility of using upgraded pyroelectric infrared sensor in robotics device, and the results of experimental studies.

Keywords: robotic devices, pyroelectric infrared sensor, experiments

Currently interactive robotic devices are increasingly used to solve everyday problems. Now, their scope is not limited to high tech industries. They are increasingly used in daily life: in museums (interactive exhibits), large corporations (robots guides) in the entertainment field.

The majority of such systems are combined a number of common tasks that they must perform. One of them is the mapping of the surrounding area and the discovery of man.

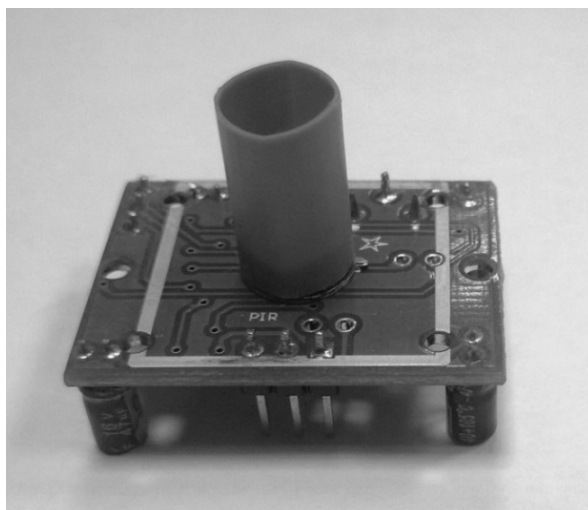
In most cases, these robotic devices available today are quite expensive, even in the case of self-assembly of functionally complete modules.

In this paper we consider the possibility of using an upgraded pyroelectric infrared sensor in devices of robotics and here are the results of experimental researches.

The pyroelectric infrared sensor detects infrared rays, based on its temperature dependence. This type of sensor detects the change in the infrared radiation range, namely, in its middle part - 5-15 microns (average healthy human body emits in the range of about 9 microns). From the perspective of the end user these sensors are simple to use and cheap, and therefore an integral part of the safety devices, security devices, automatic door systems, automatic lighting, as well as widespread in systems of "smart home", etc.

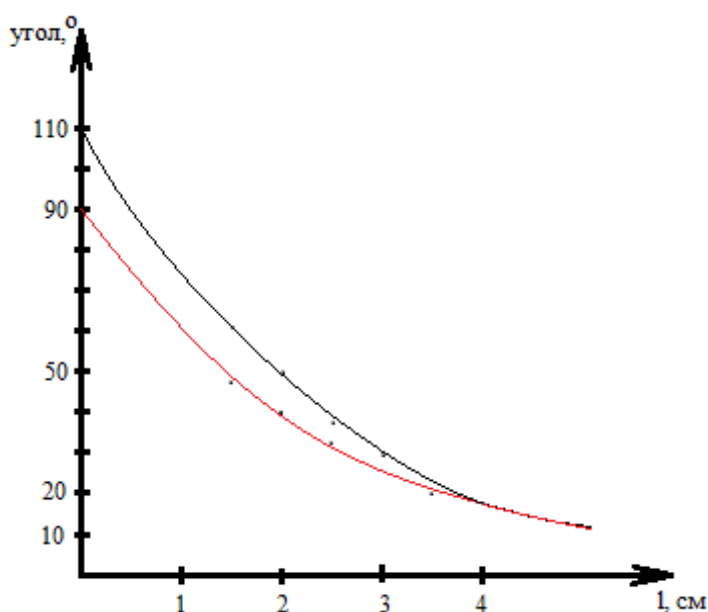
Fresnel lens is used in existing sensors to increase the viewing angle. This is an advantage in the detection units, but it is a disadvantage in relation to orientation or navigation devices because of the low accuracy of the angle determination of IR radiation signal arrival. To ensure the required pattern it is proposed to use the device limiting angles of the sensor.

The device is a removable aperture which sizes are defined by the laws of geometrical optics. The efficiency of an upgraded sensor was confirmed experimentally.



Picture 1 – Upgraded pyroelectric infrared sensor

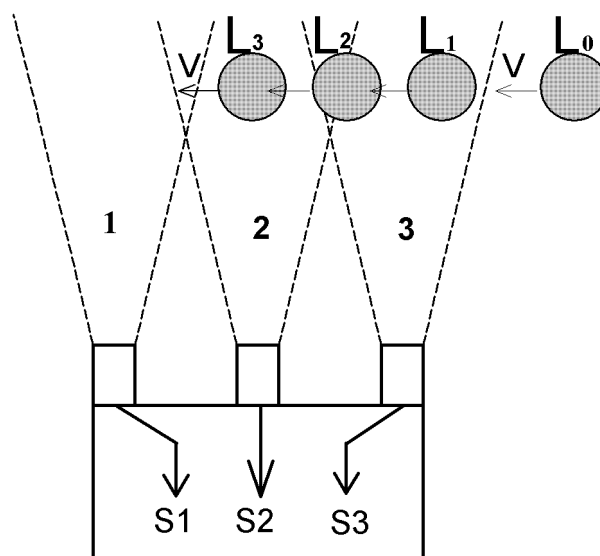
The experiment consisted of a practical definition of sensor's viewing angle. Picture 2 shows the experimentally obtained pattern LH sensor 778, that enables to set the required angle. The interference radiation is not taken into account in this experimental investigation.



Picture 2 – Schedule a viewing angle depending on the length of interchangeable sensor heads,

— : vertical position of the sensor,
 — : horizontal position sensor.

As a result of this upgrading, sensor can be used for device targeting, locating people or animals near the robot. Versatility and ease of this device allows its use in related areas: security systems and thermal control.

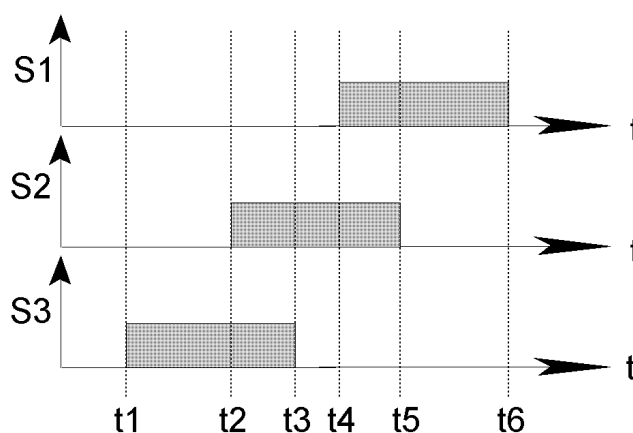


Picture 3

It is also possible to use such system of sensors in interactive robotics devices. An example of this application is shown in Picture 3.

1,2,3 designated zone detection sensors installed in front of the chassis. If the object which emits heat is detected, sensors form active signals S1, S2, S3.

Such system of sensors location helps to define clearly the direction of motion of the object relative to the chassis, as well as their relative positions.



Picture 4 - Timing diagram of the sensor system response when heat emitting object moves left

After contact with the heat emitting body (e.g., human) in the detection area of the sensor 3 (in a time interval $t_1 \dots t_2$), it generates an active signal S3. When an object moves from right to left, at time t_2 it reaches the detection zone of the sensor 2 remains in the detection zone of the sensor 3 (the signals S2 and the S3 are the active level). At time t_3 to come out of the detection area of the sensor 3 to the time t_4 is found only in the zone of the sensor 2 (only active output S2). At the time t_4 sensor 1 detects the object and form an active signal S1. From t_5 to t_6 active signal is generated only one sensor (signal S1). Analyzing this picture changes the sensor outputs, we can conclude the motion of the emitting body to the left with respect to the sensor system, and compute the relative speed of this movement.

By combining this system with other sensors positioning module for robotic devices and building terrain maps can be designed. The sensor system includes a pyroelectric infrared sensor, to determine the distance (sonar) and a video camera for image recognition allows you to explicitly specify the type of object in the zone. If an object is detected by the infrared sensor and its visual image is recognized image analysis system as a living object (person, animal), it will be assigned the status of the mobile - it should not be displayed on the map constructed as may at any time change its location. Maybe the system needs to determine only the distance to this object by using a distance sensor (ultrasonic or infrared sonar). In the case of detecting an object whose image is not defined as a living organism - it is stored in memory and displayed on the virtual map.

Described system will be implemented as an interactive robotic device on wheeled chassis. After validation of the proposed sensor system in an interactive device it is possible to develop and manufacture generic functional finished positioning module compatible with the popular microcontroller platforms (for example, Arduino) to fit different cybernetic mechanisms.

References

1. Korobova, K.V. Modernizatsiya piroelektricheskikh datchikov v ustroystvah robototekhniki / K.V. Korobova. // Nauchno-tehnicheskaya konferentsiya studentov, aspirantov i molodykh spetsialistov MIEM HSE. - M.: MIEM HSE, 2014.– s.
2. Lezhnev, E.V. Realizatsiya robota gida na baze apparatnoy vyichislitelnoy platformy Arduino / E.V. Lezhnev, A.A. Amerikanov, D.K. Kovalev // Nauchno-tehnicheskaya konferentsiya studentov, aspirantov i molodykh spetsialistov MIEM HSE. - M.: MIEM HSE, 2014. – s.

SPATIAL TECHNOLOGY ENVIRONMENT FOR THE IMPLEMENTATION OF INNOVATIVE SCIENTIFIC AND EDUCATIONAL PROJECTS

Linetskiy B.L., Sedova T.L., Tikhonov A.N., Trubochkina N.K.

Moscow, MIEM HSE

This article considers the project of the scientific and educational Center for integration of multimedia technologies in science, education and culture, as space-technological environment for the implementation of innovative scientific and educational projects of the 21st century, which should become the support for the master's programs, especially interdisciplinary, at the intersection of science, art and information technologies, and implementation of innovative scientific and commercial projects, which are to become a master's thesis.

Keywords: mathematics, fractals, information technology, multimedia equipment, high performance computing, education

The educational situation in the beginning of the 21st century demands significant changes in the system of training for highly qualified personnel. A person who has a higher education should be harmoniously developed and well-educated person, able to accumulate and apply achievements of domestic and foreign science and technology in their activities and to feel free and confident in the new environment. Amongst the most important conditions for determining the success of modern education reforms we can refer not only to the preparation of scientific and scientific-pedagogical personnel in the magistracy, including interdisciplinary, with the possibility of their subsequent training in postgraduate study, but

also to the creation of schools and centres on the basis of universities, where a new master's degree program will be implemented. Those will be equipped according to the latest scientific, technical and technological levels. The educational Center for integration of multimedia technologies in science, education and culture is one of such projects which is to become a support for innovative master programs, especially interdisciplinary, at the intersection of science, art and information technologies.

Currently there are global researches being carried out in the sphere of creating a new paradigm in education for the 21st century [1-8].

The increase in new computational capabilities of computers gives us an opportunity to look at some sections of mathematics. So, for example, fractal mathematics together with the enormous computational power of computers allows you to visualize the different models of dynamic systems of large dimension. For example: space, social systems, graphics.

In addition to increasing the computing power, another direction, which characterizes the 21st century education is an interdisciplinary paradigm at the stage of master programs and postgraduate programs. Mathematics, information and multimedia layers added on top of the basic education will allow to develop high quality modern 21st century experts - a new type of specialists, flexible and easily adaptable to the emergence of new concepts and technologies in the field of their activity.

The creation of such Centre will improve the quality of education, because in addition to the master's programs, it will create conditions for the innovative activities at the level of master's theses in the interdisciplinary fields. Thus having such a Centre will increase the University rating in the world of educational and scientific community.

The purposes for establishment of the Center are the following:

- improving the quality of University education through the integration and development of the foundations of the classical (mathematics and computer) and integration multimedia technologies creating the information products for innovative projects;
- raising the efficiency of scientific research in the field of creation of a systemic approach and implementation of projects in the field of multimedia technologies (MT) in science, art and culture;
- integration and consolidation of specialists of various directions of MT;
- development of methods to improve the effectiveness of the impact of information and assessment of the impact of MT on humans in various aspects for prompting to positive activities.

The main tasks of the Centre are the following:

- a review and analysis of the world experience in fundamental research in the field of integration of multimedia technologies (MT) in science, education and culture and the introduction of new knowledge in the educational process;
- development of new concepts, methodology and basic principles for the formation of information objects on the basis of a synthesis of information of different types (text, graphic static and dynamic, sound, touch) to enhance synergies impact on the human consciousness;
- development of methods of mathematical synthesis of various interactive information objects;
- development of methods for generating mathematical and computer information objects by areas: science, architecture, design, industrial design, computer painting, computer music, jewelry and film making, television, laser and light shows;
- computer modeling of information objects in these areas;
- development of recommendations on creation of the centers of integration of multimedia technologies (MT) in science, education and culture as experimental creative grounds in different educational forms (school community, University community, vocational and youth creative centers);

The meaning of the Centre model is that educational specialization tracks and interdisciplinary master's programs are formed based on innovative research in various fields of mathematics, information and multimedia technologies. Therefore the graduation works (term papers and diploma projects) become the basis for innovation or scientific projects and their subsequent development.

In this centre you can carry out the educational process in accordance with the new interdisciplinary master programmes. In such programmes basic higher education, e.g. in architecture (architects), design (designers), painting (artists), digital technologies (filmmakers), Directors and designers of TV shows, music (composers, sound engineers), etc. is supported by new knowledge in the field of mathematics, information and multimedia synthesis and simulation, and the course and graduation papers become the synergy of this new modern knowledge and the basic one.

In Pic.1,2 you can see mathematical and informational graphic art objects which can potentially become the examples of realization of the mathematical-multimedia knowledge of undergraduates after studying mathematics, information and multimedia technologies.

It should be noted that the fractal art objects have no size limitations, and the accuracy of visualization and image size depends only on the parameters in the mathematical models and computational capabilities of the computer. Therefore, designers will be able to synthesize relatively large size images without any loss of quality (Pic. 3).



Pic.1. Mathematical and informational graphic art objects (sketches for term papers and graduate works of architects)



Pic.2. Mathematical and informational graphic art objects (fractal painting [9])



Pic.3. Mathematical and informational graphic art objects fractal interior design panels [10])

These features can be used in other projects, for example in light shows (Pic. 4) and for creation of large stained-glass surfaces (Pic. 5).



Pic. 4. Sample of the innovative project «Light show» [11]



Pic. 5. Sample of the innovative project «Fractal stained glass» [12]

The practical value of the integration Center and master's degree programs

Fractal calculus mathematics is an effective technology of analysis and synthesis of 3D complex geometric forms and a generator of new innovative architectural and design solutions, which increases graphical diversity considerably faster than that of architects' and designers'.

Mathematics and information technologies in the above areas form an integral part of art-information technologies – the most important section of multimedia technologies.

The master's program can be recommended to the following students:

- bachelors, Architecture degrees:

- 270100 Architecture;
- 270300 Design of architectural environment;
- 270900 Urban development;

- bachelors, Design degrees:

- 070601.65: Designer (costume design; environmental design);
- 032401.65 Advertising Specialist;
- 070200.62 Theatre arts (decorations);

- designers, artists, musicians, goldsmiths, specialists in computer graphics, in the film and entertainment industry, TV, graduate students and professionals in these fields, etc.

The number of tracks of the master's programme in Computer Science (CS) “Mathematical, information and multimedia technologies in art and science, (Art Information technologies)” can be modified as required.

The innovation Center for integration of multimedia technologies in science, education and culture, created in line with the latest scientific and technical achievements, is to be used for the most complete implementation of interdisciplinary master's program in Computer Science (CS) «Mathematical, information and multimedia technologies in art and science, Art Informatics».

Creation of the Centre will improve the quality of education and provide conditions for the innovative scientific research in the interdisciplinary fields. It will improve the University rating in the global educational and scientific community and assist the achievement of its objectives.

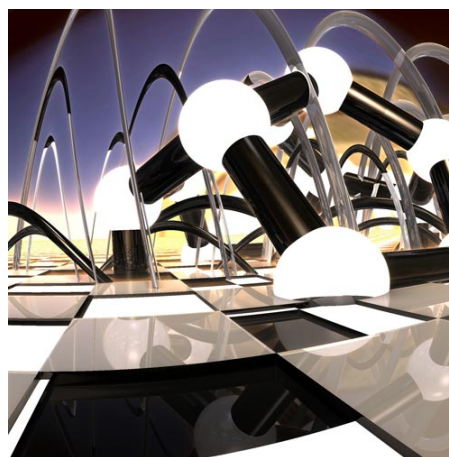
The synergetic effect from the synthesis of the capabilities of the Center and interdisciplinary master programmes will declare itself in the course papers and master dissertations.

The following art objects can become examples of innovative business projects:

- fabrics, paper, canvas prints etc. (Pic.6);
- files for art scenery and exhibitions (Pic.7);
- fractal video for TV and film industry (Pic.8).



Pic.6. Mathematical and informational graphic art objects - fabrics, paper, canvas prints, etc.



Pic.7. Mathematical and informational graphic art objects - files for art scenery



Pic.8. Mathematical and informational graphic art objects - fractal video [13]

Required equipment

Computing and multimedia equipment is required for creating and visualizing of fractals (Pic.9).



Pic.9. Light laboratory Center

Calculation of fractals is made on a multiprocessing computer complex with multi-core architecture. Calculation speed is directly proportional to the hardware performance rate.

The minimum recommended PC configuration to be used at home is Intel Core i5 processor or faster equivalent; RAM not less than 4 Gb; HDD volume of at least 500 Gb; video card GeForce GT 630 with the amount of graphics memory not less than 1 Gb or more productive equivalent.

Visualization of fractals (creation of interactive interiors, etc), is created through such multimedia objects as projection equipment and audio systems.

When creating interactive interiors projectors are installed along the perimeter of the room under the ceiling, so that the distance from the wall to the projector is in the range of minimum and maximum distance from the screen in accordance with the manufacturer's recommendations. Depending on the characteristics of projection equipment, a different number of projectors can be used to ensure 100% coverage of the walls. Calculations are made on the basis of the technical characteristics of equipment, as declared by the manufacturer.

Either a stationary bracket or a universal fastening can be used in order to fasten the projectors to the ceiling. Universal fastening allows you to move projectors parallel to the wall in the horizontal direction thus simplifying the process of adjustment.

Projectors with aperture of at least 4,500 lumens and physical sensor resolution not less than 1920x1080 pixels are recommended to ensure the highest quality of images.

Audio system should provide clarity of display and an even distribution of sound pressure in the premises. For small and medium-sized premises centralized sound systems located in one place can be used. For large areas use distributed system with devices placed on the perimeter or the ceiling. Thus the area of affect of each source and its pressure is lower.

Fractal art can be used to create interactive exhibitions in open spaces by projecting images on buildings and structures in good weather conditions, as well as by projecting images on the clouds. In this case, the selection of projection equipment and audio systems is carried out individually for each project.

Due to the universal nature of mathematics, information and multimedia technologies, it will be possible to carry out a vast range of scientific researches in the Centre. They can vary from modeling and visualization in art and society to modeling and visualization of the processes in space and the nanoworld.

Conclusion

This innovation Centre for integration of multimedia technologies in science, education and culture is to be developed in line with the latest scientific and technical achievements as a spatial technology environment for the implementation of innovative scientific and educational projects.

Establishment of the Center as the material and technological support for interdisciplinary master programmes will improve the quality of education and create conditions for the innovative scientific research in the interdisciplinary fields. It will improve the University rating in the global educational and scientific community and assist the achievement of its objectives.

References

1. Forbes, A. G., Savage, S., Höllerer, T. Visualizing and Verifying Directed Social Queries. IEEE Workshop on Interactive Visual Text Analytics for Decision Making. Seattle, Washington, October 2012.
2. Liu, Q., Han, Y., Kuchera-Morin, J., Wright, M. and Legrady, G. Cloud Bridge: a Data-driven Immersive Audio-Visual Software Interface. In Proceedings of the International Conference on New Interfaces for Musical Expression (NIME), Daejeon+Seoul, South Korea, 2013.
3. Fan Y.Y., Sciotto, F. M. BioSync: An Informed Participatory Interface for Audience Dynamics and Audiovisual Content Co-creation using Mobile PPG and EEG. In Proceedings of the International Conference on New Interfaces for Musical Expression (NIME), Daejeon+Seoul, South Korea, 2013.
4. Roberts, Charlie, and Wright M. The Web Browser As Synthesizer And Interface. In Proceedings of the International Conference on New Interfaces for Musical Expression. Daejeon + Seoul, Korea Republic, 2013.
5. Roberts, C., Forbes, A. and Höllerer, T. Enabling Multimodal Mobile Interfaces for Interactive Musical Performance. In Proceedings of the International Conference on New Interfaces for Musical Expression. Daejeon + Seoul, Korea Republic, 2013.
6. Savage, S., Forbes, A. G., and Höllerer, T. Utilizing Crowdsourced Databases for Social Media Question Asking. ACM CSCW 2013 Workshop on Social Media Question Asking. San Antonio, Texas, February 2013.
7. Han, Y., Han, B. Digi Sonus: An Interactive Fingerprint Sonification. In Proceedings of the ACM International Conference on Multimedia (MM). Nara, Japan, 2012.

8. Han, Y., Han, B. Virtual Pottery: An Interactive Audio-visual Installation". In Proceedings of New Interfaces for Musical Expression (NIME). Ann Arbor, Michigan, 2012.

9. Trubochkina N. K. Novyi promyshlennyy dizain i tekhnologii, kak rezul'tat matematicheskoy-komp'yuternykh fraktal'nykh issledovaniy // Kachestvo. Innovatsii. Obrazovanie. 2012. T. 84. № 5. S. 76-82.

10. <http://nadin.miem.edu.ru/>

11. http://nadin.miem.edu.ru/!!!_prez_Fract_Clouds/my_prez_F_Clouds.html

12. http://nadin.miem.edu.ru/new_works_v.html

13. http://nadin.miem.edu.ru/video_231212.html

TECHNIQUE OF APPLICATION OF BIOLOGICAL FEEDBACK ON THE BASIS OF STABILOGRAFIYA IN GYMNASTICS

Baulina O. V.
Penza, PENZGTU

In this article possibilities of application of a technique of a stabilografiya on the basis of biological feedback in gymnastics are considered. Proposed is methodology of rating of young athletes on the basis of stabile-graphic samples with feedback. Relevance of use of a technique of a stabilografiya for studying of biomechanical parameters of function of balance of a body of young gymnasts at a stage of selection is justified modernity diagnostic means, as for normal conditions so and for the rehabilitation of the various infringements and the body sustainability workout.

Keywords: stabilografiya technique, stabilo-measuring platform, gymnastics, selection of young gymnasts.

It is known that the person who is motionless, actually is in a condition of unstable balance, its center of gravity makes oscillatory micromovements. Sensitive indicators that display the status of various systems used in support of the balance of the body's vestibular system, are the characteristics of the hesitation as: amplitude, frequency, the direction, the average position of the projection on a plane of reliance. The measurement technique of above-mentioned parameters is based on use of a computer stabiloanalizator of "Stabilan-01" including the personal computer (stationary or the laptop), stabilo-measuring platform, a set of sensors for съема physiological signals (dynamometry, a miografiya, etc.), a complex of techniques and games exercise machines with feedback. The technique of a stabilografiya developed by V. S. Gurfinkel with coauthors still in 1952, with development of the computer equipment was repeatedly improved. Today a stabilografiya is a method of the quantitative, spatial and temporary analysis of biomechanical parameters of sustainability. From the production currently Stabile-graphic systems best meets the requirements for use in artistic gymnastics Stabile-Analyzer computer with biofeedback \"Stabilan-01\", available and at the chair of ITMMBS. This is computer stabilograf favourably differs from domestic and foreign analogs is that there are, five types of sensors for record and registration of physiological signals, namely:

- pulsometriya with the variation analysis;
- perimetric breath with the tensometric sensor;
- kistevaya silometriya with the tensometric sensor;
- stanovy silometriya with the tensometric sensor;
- by-passing miogrammy on the 4th the leads[1,2].

The technique of a stabilografiya got to relevance measurement and an assessment of statodinamichesky sustainability in different types of sports where ability to keep balance defines sports result. The greatest interest in use of a technique of a stabilografiya is represented by gymnastics. Control of a functional condition in the gymnastics on the basis of methods and means of a computer stabilografiya hasn't today alternatives because comfort and time of inspection, high sensitivity to deviations of a functional state, possibility of formation of individual and group standards, and also monitoring of current state of athletes. Besides, use in computer the stabilografakh of the biological feedback (BF) of various modalities allows to use them as the training devices directed on improvement of function of balance, coordination abilities, psychological stability, competent tactical thinking [3].

Control of a functional condition of gymnasts can be divided into the following types:

1) Selection both at an initial stage, and at certain stages of long-term training (from selection of kids in gymnastics section to a complete set of a national team of masters of sports).

2) Current inspection of a condition of various systems of an organism of the gymnast: cardiovascular, respiratory, various systems of TsNS, muscular, and also psychological state of the athlete.

3) Assessment of the general condition of the gymnast, his readiness for slozhnokoordinatsionny activity during training process, and also an assessment of influence of various load of adaptation processes of the athlete.

4) Stage survey allows to estimate a condition of athletes after performance of training loadings of a certain temporary period.

5) Complex medical examination of the athlete.

6) Rehabilitation actions for restoration of physical activity after various sports injuries [4-7].

Considering only the first type of control of a functional condition of athletes, I offered a choice technique from the general group of athletes of one age of the young gymnasts giving the Olympic hopes.

Technique of selection of children of 4-6 years at the initial stage of occupations by gymnastics

1 . Selection of beginners (children of a certain age (4-6 years)) according to the external physical data, wishing to go in for gymnastics.

2 . Research of function of balance and coordination of movements of each "izbranets" by means of a computer stabiloanalizator of "Stabilan-01".

To an assessment of a level of development of function of balance of young athletes it is planned to apply the test from 4 so-called "Romberg's poses", time (seconds) of deduction of each pose thus is registered. Romberg's test is carried out in four modes (figure 1) with a gradual decrease in square supports.



Figure 1

In the first position of a foot are shifted together, in the second – a foot are one for another on one line, the thumb of a hind leg touches a heel of front. In the third situation the examinee costs on one foot, the heel of the second is pressed to a knee of a basic foot. In the fourth pose "swallow" is shown. The exhaustion, overstrain, disease shorten time of preservation of a pose of Romberg.

Tests of stabilograficheskyy test of Romberg are usually carried out (feet to one line, a heel sock), for gymnasts I suggest to carry out this test in a pose "swallow" since exercise a swallow it is included in the list of Basic Elements young gymnasts (figure 2).



Figure 2

Romberg's test is the basic from the stabilograficheskikh of the tests, including tests with the opened and closed eyes, with use in the first case of visual stimulation in the form of alternating color circles on the screen, and in the second case – sound stimulation in the form of voice-frequency signals. Based on comparisons of indicators stabilogramm (Figure 4), you can determine the degree of Visual stability of standing, that is, the extent of feedback provided by the optical sensitivity-the so-called coefficient of Romberg.

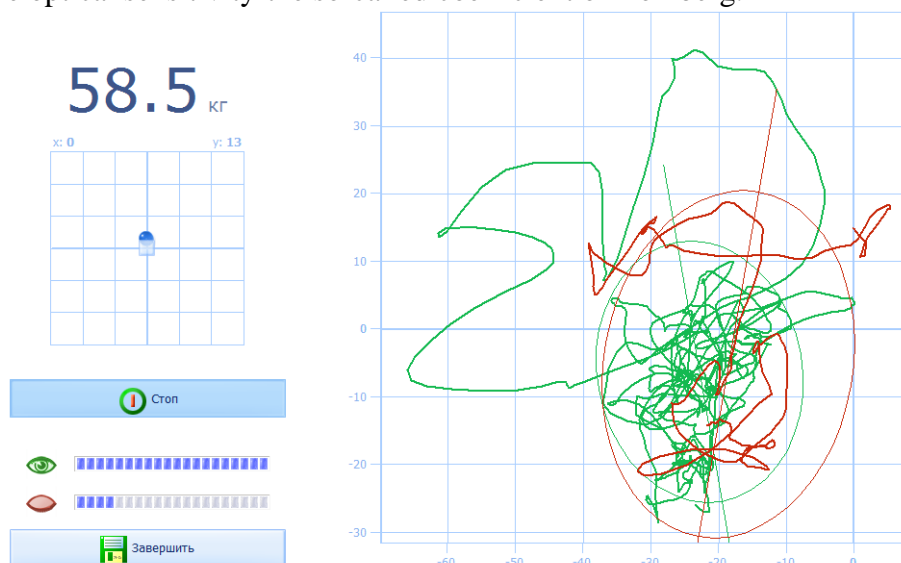


Figure 3

3 . Comparison of indicators with norms and transfer on one point for the indicator which isn't beyond norm, in an individual rating of the athlete.

4 . Conclusion of a summarizing rating assessment (in points) the gymnast by results of the carried-out tests.

5 . Distribution of young athletes on groups on results of the gained points in a rating (for example, "group of future Olympians" for perspective children with a high rating, and "group of health" for weaker).

6 . For a statistical assessment of adequacy of the forecast of success of selection of young athletes in a group of professional athletes and the analysis of dynamics of development of functionality of gymnasts preservation of results and their analysis in a database is provided.

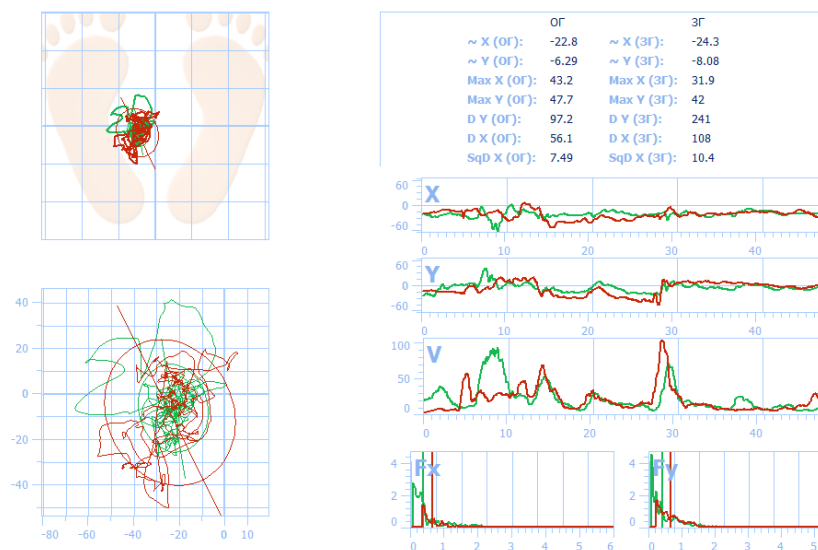


Figure 4

Thus, the technique has a place in the prospect of artistic gymnastics in order to enhance the effectiveness of trained and motivated athletes, and the use of computer Stabilographic method of biological feedback will improve not only the professionalism and efficiency of the gymnasts in all stages of sports training, but also the maximum involvement of the athletes in this sport.

References

1. Boloban B., Mistulova T. Stabilografiya: achievements, prospects: // Science in the Olympic sports: - 2000 . - Special release
2. S. S. Sliva Stabilografiya application in sports//the First All-Russian scientific and practical conference "Monitoring of physical development, physical readiness of various age groups of the population. Collection of reports. Nalchik, 2003.
3. Kazakova O. V., Shchipitsyn P. G. Stabilometricheskoye testing athletes of some specializations. - Southern Ural state university, Chelyabinsk.
4. Mistulova T.E. Metodika of a stabilografiya in scientific and methodical ensuring preparation of national teams of Ukraine//the Messenger of sports science. - 2008 . - № 4.
5. Istomin T.V. Akzhigitov R. F. Karamysheva T.V. Metodika of diagnostics and increases of resistance to stress of students: // Engineering Messenger of Don. - Rostov-on-Don, 2011 .
6. Mistulova T., Sliva S., Milenkaya S. Use of a technique of a stabilografiya in sports training and rehabilitation//Pedagogika, psykholohiya that mediko-biologichni to a problem

фізичного виховання і to sports: 3б. sciences. the ave. під an edition of Ermakov S. S. - Harkiv:khdadm (HHPI), 2004. -№24.

7. Istomina V. V., Istomin T. V., Karamysheva T.V. Stabilometriya application in post-urolological system of multidiagnostics and rehabilitation//the Biomedical Radio Electronics Magazine. - Moscow: 2011 .

BIOTECHNICAL LIFE SUPPORT SYSTEM

Istomina T.V., Kosenok N.Y.
Penza, PenzSTU

Human activities are related to the influence of various environmental factors. Human condition can deteriorate under the influence of various environmental factors, thus affecting the results of individual and collective (group) activities. Enhancing Human Security in the modern world requires creating a complex to control human physiological condition and location. Children and the elderly, as well as those whose professional activity is associated with extreme physical and psychological stress (military, emergency workers, athletes, and others), are potential users of such systems.

Keywords: the information model, biotechnical systems, wireless data transfer.

In terms of Russia, with its length of territory, long distances to centers of high-tech care, impossibility of rapid increase in their numbers to solve problems, for example the "therapeutic window " in acute coronary syndromes (2-3 hours), lack of social infrastructure for the development of universal quality health services, the biotechnical life support system can be a strategic solution to many social problems. Therefore a system is required for remote evaluation of the functional status of patients belonging to risk groups, and people working in extreme situations.

Creating a portable system for remote continuous personalized control of basic life functions of humans is associated with the solution a wide range of technical problems. The universal instruments for remote medical monitoring are absent, and automatic measurers of basic physiological parameters that have received recognition from clinicians are unusable "in the field."

Significant obstacle encountered when trying to use the standard gauges for monitoring the evolution of human functional state, is the need to accommodate on the body sufficiently massive metal detectors, multiple circular electrodes and compressing the artery cuff.

The aim of this work was to develop a portable "manpack" equipment and non-invasive (non-contributing mechanical perturbation) methods for recording the dynamics of physiological parameters.

The life support system draft was developed in the form of an instrumental complex, including biometric sensors and software equipment.

The manpack part provides reception of basic physiological parameters:

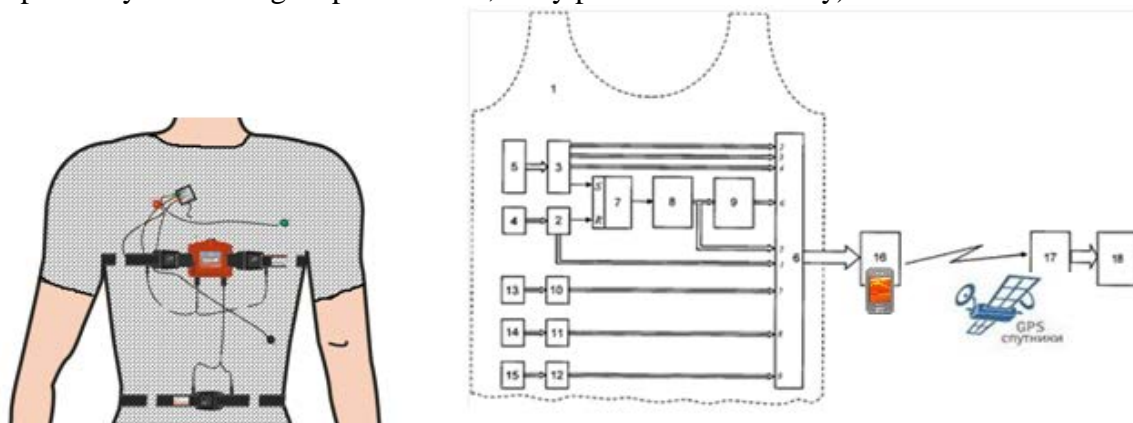
- pulse;
- respiratory rate;
- percent of blood oxygen saturation;
- mean blood pressure;
- skin temperature.

The instrumental complex evaluates the position and motion parameters:

- Position of the body;

- Motor activity; -
- Location (via GSM and GPS)

The system is an underwear (Fig. 1) with located in it temperature measurer, ECG recorder, pulse oximeter, the sensors of which are arranged to contact with sensitive areas of the controlled object body (which determine the skin temperature, heart rate, blood oxygen saturation percentage) as well as plethysmograph and accelerometer, inclinometer (respectively controlling respiration rate, body position and activity).



1 - breeches clothing; 2,3 - information outputs from the electrocardiograph and pulse oximeter (on photoplethysmogram, oxygen content of the red blood cells, and heart rate);

4 - ECG; 5 - pulse oximeter; 6 - primary data processing unit; 7 - RS-trigger; 8 - timer;

9 - blood pressure calculating block; 10,11,12- information outputs from thermometer induction plethysmograph, and accelerometer-inclinometer; 13 - thermometer; 14 - inductive plethysmograph; 15 - accelerometer – inclinometer; 16, 17 - TRD measured data via GPRS;

18 - data collection server. (Food: 1/2 AA Lithium Battery; check-in time: 24 hours; waiting time: 15 days; memory: 128 MB)

Figure 1. Composition of underwear clothing

The main principle of the system data acquisition and transmission is a minimum of user interaction. All communication settings are automatic. For data transmission the system uses GSM communication channel. The user must have a communicator (or a simple cellphone) with support for Bluetooth technology to collect data from a biometric system. The communicator connects to a data base located on a remote server via GPRS. Server provides access to user information through the facilities any Internet browser. The scheme of the system elements interaction is shown in Figure 2.



Figure 2. The principle of action of the life support system elements

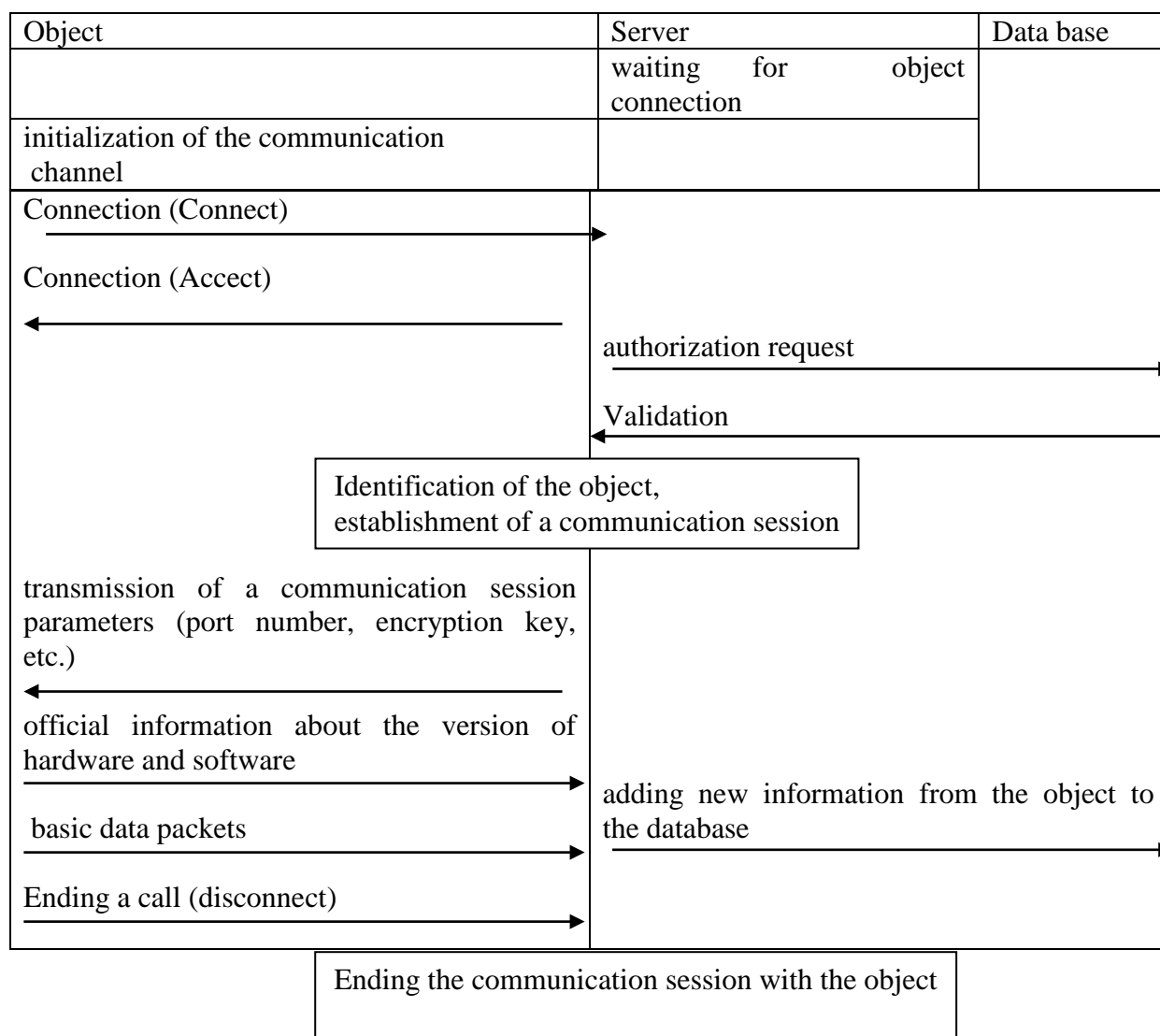


Figure 3. The scheme of interaction between the object, server and data base

The authorization of a person on the server happens through his phone number. If the phone with this number is registered in the database, the server will assign him a separate port for communication (Fig. 3).

The user access to the server is made via an Internet browser. To obtain the information, the user must go through the authorization process.

Upon successful login, the user passes to the main page that allows him to overlook the data on the movement and biometric information for each point in a given time interval.

To display the paths, the Google Map is used, the functions of the form selection (map, satellite, hybrid) and the zoom are supported.

The user can display the data about his movements for the whole or a designated period of time. For each waypoint, the following data is available:

- time to the nearest thousandth of a second;
- altitude above sea level;
- motion speed;
- respiratory rate;
- position of the body;
- physical activity (is going running , standing);
- temperature;
- blood pressure;
- pulse;
- the percentage of oxygen saturation of blood;
- battery level.

The novelty of the project:

1. Modification of the constructive solutions of special clothing, complexing the means of getting of data on biological specimen. Combining various types of modern sensors, both serially produced and certified, in a new system.

2. Integrating the advantages of a portable “manpacked” equipment and noninvasive methods of recording the dynamics of complex of basic physiological indicators - vital activity parameters.

3. Complex technique of tracking the physiological state of a person on a real-time basis, the algorithms of synchronous data processing and systematization, as well as data conversion for transmission via GPS- TV to the reception centers for analysis and rapid response.

The distinctive features of the system:

- Portable "manpacked" equipment;
- Noninvasive methods of recording the dynamics of physiological parameters;
- Transmission of information over wireless communication channels;
- Monitoring and evaluation of the physiological state of a person in extreme situations.

Technical significance (advantages over the existing analogues)

1. Life-support system includes devices for measuring physiological parameters of a human state, measured data transceiver via GPRS and data collection server. Thereby, the transceiver is designed with the provision of automatic transmission and reception of digital data files by the server upon the moment of supplying and removing power from the devices, data buffering in case of disconnection and automatic retransmission of data before confirmation of its integrity by the server.

3. The portable instrumental complex constitutes a temperature measurer, ECG, pulse oximeter with sensors providing possibility of contacting with sensitive parts of the body (determining skin temperature, heart rate, blood oxygen saturation percentage) as well as

plethysmograph and accelerometer - inclinometer (controlling respectively, respiratory rate, body position and activity) .

2. The instrumental complex is equipped with the RS- 232port or analog output, while the transceiver consists of a hardware module of accumulation and transmission of data via the Ethernet network or GSM to the server of data collection and wireless modules for data transmission from devices to a hardware module, thereby the wireless data transmission modules are adapted for network of Bluetooth standard and are provided with the interface for device connection.

Scope of application of life support systems:

Agencies: welfare services, emergency services, defense industry, sports associations.

Individuals: pensioners, emergency workers, soldiers, athletes, public transport drivers, bank, office, supermarket, etc. security guards.

For example, the authors analyzed the advanced technologies of development of defensive means and combat equipment in the world's leading powers. It was found that the armies of the United States, France and Germany have conceptual designs, which mean the fighter's employment of night vision systems, positioning and navigation systems, improved aiming systems, new dynamic protection means.

In the complexes FELIN (France), Land Warrior (USA), IdZ-ES (Germany) three main elements are used - protection, communication and weapons system, situational awareness. Modular communications equipment allows video and voice data transmission. Digital display, combined with a system of GPS, allows displaying the ground situation on a real-time basis along with its transferring to the combat command and control centers. But in the above mentioned sets of equipment there is no system capable of monitoring the soldiers' physical condition.

In this way, the article discusses the draft of a biotech life support system in the form of a portable complex for continuous remote monitoring of physiological status and location of a person.

References

1. Kosenok NY. Modern aspects of safety in the use of personal body armor. Magazine. Global Security, № 3. - M.: WASCs 2010. – 116p. (Pp. 67-78).
2. Istomina TV, Kosenok NY Biotechnical autonomous life support system. The utility model application of 28.10.2013.
3. Biosensoruy: osnovy i primeneniya 2007.
Grin N., Staut Y., Teylor D.
4. Prikladnaya anatomiya i biologiya 2005.
Himchenko V.I., Shtrak M.B.

BOURBAKI'S STRUCTURE THEORY IN THE PROBLEM OF MULTI-COMPONENT SIMULATION MODELS SYNTHESIS

Brodsky Yu. I.
Moscow, CC RAS

The work is devoted to the application of Bourbaki's structure theory to substantiate the synthesis of simulation models of complex multicomponent systems, where every component may be a complex system itself. An application of the Bourbaki's structure theory offers a new approach to the design and computer implementation of simulation models of complex multicomponent systems – model synthesis and model-oriented programming.

Keywords: simulation, complex multi-component systems, model synthesis, model-oriented programming, parallel and distributed computing.

To get an informal comprehension of what a complex multicomponent system is, let us quote a prominent specialist in the field of complex systems and their simulation, correspondent member of the USSR Academy of Sciences, N.P. Buslenko:

“A complex system is a complex object whose parts can be regarded as systems, logically combined into a single entity, in accordance with certain principles or defined set of relations” [1, 2].

Fully agreeing on an intuitive level that the complex system itself may consist of complex systems, we do not undertake to give a rigorous definition of this concept. However, the concept of a model of the complex system will be defined quite formally, as a species of structure in the sense of N. Bourbaki [3]. From this point of view, a complex system – is what a model of complex system can represent adequately enough.

A species of structure is a development of the concept of a set. A base set is supplied with a structure of some species - a certain type of relations between its elements, and depending on this relationship, the set can become, for example, a group, or a lattice, or a vector space, or in our case – a simulation model of a complex system. The mathematical object, for example a specific linear space, is an instance of the structure of the respective species.

The structuralism method [4], which ideologically goes back to F. Klein's Erlangen program [5], and turned out to be quite popular and productive in the twentieth century, offers to consider further various mappings of base sets and look for the invariants of these mappings. The school of correspondent member of RAS Yu.N. Pavlovsky at CC RAS, in recent decades developed the geometric theory of decomposition [6-9], where with the help of Bourbaki's Structure Theory they are trying to find simple representations of various mathematical objects - their reductions and decompositions.

In this work, devoted to the synthesis of a complex system model from models of its component, we are mostly interested in the extension of the species of structure on consolidate base sets of mathematical objects, endowed with the species of structure from the “model-component” family. An invariant under the integration of base sets of simulation models is the method of simulation calculations organization, proposed below.

Model synthesis as an alternative to the object-oriented analysis, a method of describing and synthesis of simulation models of complex multi-component systems, has been developing in the CC RAS Department of Simulation Systems since the late 80's. Its main ideas were described in the works [10-14]. However, the term “model synthesis” was firstly proposed only in [10]. In the base of the model synthesis method lays the concept of the model-component.

From the position of the software systems development, the model-component is similar to the object of object-oriented analysis. But in addition to the characteristics it is equipped with not only the methods that can do something useful, but with some equivalent of an operating system which is always ready to give standard answers to the standard requests from the internal and external environment of the model.

From a formal point of view, the model-component is a mathematical object, which has as the base set an aggregate of sets of internal and external characteristics of the model, methods (what the model is able to do) and events (what the model should be able to respond.) At the mentioned base set a species of structure “model-component” is defined. It has two remarkable features:

1. The species of structure “model-component” provides a standard and unambiguous way to organize the computational process of simulation for all objects

provided with this species of structure. This means that you can create a universal program that can run on any implementation of a simulation model, if that is a mathematical object with the species of structure “model-component”.

2. A family of species of structure “model-component” turns out to be closed under the operations of integration of the models-components into the model-complex. That is that the model-complex constructed from the set of models-components, proves to be a model-component itself and so may be included in new models-complexes.

The second property allows us form from the models-components fractal constructions of any complexity. The first property encourages us not to despair because of the complexity of computational process, which is obtained as a result of such an overcomplicated fractal construction.

A model-oriented programming paradigm is proposed for the software implementation of complex multi-component models, where the unit of software design is a model-component – a more aggregated construction than the object in the object-oriented analysis.

It will be shown that the model-oriented programming allows to eliminate the imperative programming [14] – the most difficult for both the development and the debugging. Furthermore, the resulting executable code has a high degree of parallelism and the degree of the code parallelism increases with the model complexity increasing. This fact may offer a scope for applications of model-oriented programming in high-performance computing systems, including not only tasks related to the simulation, but either complex program systems with multi-component organization.

The Species of Structure “Model-Component”

Let us try to define formally a mathematical object that represents an elementary simulation model of a complex system.

We introduce a one-parameter family of species of structure Σ_N . A member of that family is called a “model-component”. Parameter N of the family is the number of processes in the model-component. Meaningful processes are similar to system services of computer operating system. Formally processes of the model-component will be defined below by typical characterizations (10) and axioms R_9 .

$$\begin{aligned} \Sigma_N = & \langle X, M, E, \{M_j\}_{j=1}^N, \{E_j\}_{j=1}^N; \\ & x \subset X, \quad a \subset X, \quad s \subset M, \quad f \subset M, \\ & \{m_{j,real} \subset M_j \times M\}_{j=1}^N, \\ & \{e_{j,real} \subset E_j \times E\}_{j=1}^N, \\ & \{m_{j,in} \subset M_j \times \beta(X)\}_{j=1}^N, \\ & \{m_{j,out} \subset M_j \times \beta(X)\}_{j=1}^N, \\ & \{e_{j,in} \subset E_j \times \beta(X)\}_{j=1}^N, \\ & \{m_j^0 \subset M_j\}_{j=1}^N, \\ & \{sw_j \subset E_j \times M_j \times M_j\}_{j=1}^N, \\ & \{p_j \subset \beta(M_j) \times \beta(E_j) \times M_j \times \beta(E_j \times M_j \times M)\}_{j=1}^N; \\ & R_1: (x \cup a = X) \& (x \cap a = \emptyset), \\ & R_2: (s \cup f = M) \& (s \cap f = \emptyset), \\ & R_3: \left\{ \left(\forall m \in M_j \right) \left(\exists ! \tilde{m} \in M \right) \left(\{m, \tilde{m}\} \in m_{j,real} \right) \right\}_{j=1}^N, \\ & R_4: \left\{ \left(\forall e \in E_j \right) \left(\exists ! \tilde{e} \in E \right) \left(\{e, \tilde{e}\} \in e_{j,real} \right) \right\}_{j=1}^N, \end{aligned}$$

$$R_5: \left\{ \left(\forall m \in M_j \right) \left(\exists ! r \in \beta(X) \right) \left(\{m, r\} \in m_{j,in} \right) \right\}_{j=1}^N,$$

$$R_6: \left\{ \left(\forall m \in M_j \right) \left(\exists ! r \in \beta(x) \right) \left(\{m, r\} \in m_{j,out} \right) \right\}_{j=1}^N,$$

$$R_7: \left\{ \left(\forall e \in E_j \right) \left(\exists ! r \in \beta(X) \right) \left(\{e, r\} \in e_{j,in} \right) \right\}_{j=1}^N,$$

$$R_8: \left\{ \left(\left(\forall e \in E_j \right) \left(\exists ! r \in M_j \times M_j \right) \left(\{e, r\} \in sw_j \right) \right) \& \right.$$

$$\left. \& \left(\left(\{e, r\} \in sw_j, \{\tilde{e}, \tilde{r}\} \in sw_j, r = \tilde{r} \right) \Rightarrow (e = \tilde{e}) \right) \right\}_{j=1}^N$$

$$R_9: \left\{ p_j = \left\{ M_j, E_j, m_j^0, sw_j \right\} \right\}_{j=1}^N,$$

$$R_{10}: \text{there are no identical elements in the sets } X, M, E,$$

$$R_{11}: \text{organization of simulation calculations axiom}.$$

Here N – is the number of processes in the model. Everywhere $\left\{ \dots \right\}_{j=1}^N$ means that the contents of the braces is repeated through a comma N times, while the index j is replaced by $1, \dots, N$.

Principal base sets of the species of structure are $X, M, E, \left\{ M_j \right\}_{j=1}^N, \left\{ E_j \right\}_{j=1}^N$. There are no auxiliary base sets. The set X is the set of characteristics of the model, occasionally, we will divide it into two subsets: $X = \{x, a\}$, where x – are the internal characteristics of a model that, in accordance with the closeness hypothesis completely determine its status, and a – its external characteristics, that by the same closeness hypothesis completely defines its interaction with all the rest world.

$$x \subset X, a \subset X, \quad (1)$$

This is the first typical characterization of our species of structure, and the first axiom of the species of structure $R_1: (x \cup a = X) \& (x \cap a = \emptyset)$ completes the definition of the internal and external characteristics of the model.

The set of different implementations of methods-elements $M = \{s, f\}$, – elementary skills of our model, among which we will sometimes distinguish two subsets: s – slow, realizing a smooth dependence of the internal characteristics of the model from its internal and external characteristics, if for example, $\dot{x} = F(x, a)$, then, $x(t + \Delta t) \approx x(t) + F(x(t), a(t))\Delta t$, and fast f – which implement the internal model characteristics jumps: $\Delta x = G(x(t), a(t))$.

$$s \subset M, f \subset M, \quad (2)$$

$R_2: (s \cup f = M) \& (s \cap f = \emptyset)$. The second typical characterization and the second axiom – the situation is just the same as in the case of characteristics.

The set of different implementations of methods-events E , associated with the model. Events – are something that our model must respond to. The method-event – is a method that gets as an input a subset of model characteristics, and gives as an output a non-negative number, indicating that the event occurred if the output is zero, or the forecast time-to-event, if the output is positive.

Note that in the sets X, M, E there are no identical elements. For X , this follows from the fact that we are talking about the model, and the principle of not increasing the number of entities beyond the necessity (Occam's Razor) encourages us to avoid unnecessary duplication of the same characteristics as of the phenomenon simulated, either of its links with the outside world. As for M and E , the words "a set of different implementations," emphasizes the uniqueness of the methods in these sets.

We will talk about the processes of the model-component. The processes are what can occur in the model simultaneously. It was said above that N is the number of processes. The

formal definition of the process will be done later. Each process p_j has the set of its methods-elements M_j and its many methods-events E_j . This concludes the description of the base sets.

We now continue the introduction of the typical characterizations on the base set $X, M, E, \{M_j\}_{j=1}^N, \{E_j\}_{j=1}^N$ and impose on these characterizations certain requirements – axioms of species of structure.

$$m_{j,real} \subset M_j \times M, R_3: (\forall m \in M_j) (\exists ! \tilde{m} \in M) (\{m, \tilde{m}\} \in m_{j,real}). \quad (3)$$

For each process p_j a mapping is defined of its methods-elements M_j into the set of implementations M . Thus, for each $m \in M_j$ there is uniquely determined its implementation $\tilde{m} \in M$.

$$e_{j,real} \subset E_j \times E, R_4: (\forall e \in E_j) (\exists ! \tilde{e} \in E) (\{e, \tilde{e}\} \in e_{j,real}). \quad (4)$$

For each process p_j a mapping is defined of its methods-events E_j into the set of implementations E . Thus, for each $e \in E_j$ there is uniquely determined its implementation $\tilde{e} \in E$.

$$\{m_{j,in} \subset M_j \times \beta(X)\}_{j=1}^N, R_5: \left\{ (\forall m \in M_j) (\exists ! r \in \beta(X)) (\{m, r\} \in m_{j,in}) \right\}_{j=1}^N. \quad (5)$$

Internal and external characteristics of the model are connected with the input parameters of methods-elements of the j -th process. Inclusion determines what subset of the model characteristics is passed to each of the methods-elements.

$$\{m_{j,out} \subset M_j \times \beta(X)\}_{j=1}^N, R_6: (\forall m \in M_j) (\exists ! r \in \beta(X)) (\{m, r\} \in m_{j,out}). \quad (6)$$

Output parameters of methods-elements are connected to the internal characteristics of the model.

$$\{e_{j,in} \subset E_j \times \beta(X)\}_{j=1}^N, R_7: \left\{ (\forall e \in E_j) (\exists ! r \in \beta(X)) (\{e, r\} \in e_{j,in}) \right\}_{j=1}^N. \quad (7)$$

Internal and external characteristics of the model are connected to the input parameters of methods-events of the j -th process. Inclusion determines what subset of the model characteristics is passed to each of the methods-events.

The typical characterizations

$$\{m_j^0 \subset M_j\}_{j=1}^N \quad (8)$$

defines the initial methods-elements of the processes.

The next portion of typical characterizations and axioms follows:

$$sw_j \subset E_j \times M_j \times M_j, R_8: \left\{ (\forall e \in E_j) (\exists ! r \in M_j \times M_j) (\{e, r\} \in sw_j) \right\} \& \left\{ (\{e, r\} \in sw_j, \{\tilde{e}, \tilde{r}\} \in sw_j, r = \tilde{r}) \Rightarrow (e = \tilde{e}) \right\}_{j=1}^N. \quad (9)$$

Switching of methods-elements is defined for each process. If it is possible under certain conditions to switch j -th process from the execution of the method $A \in M_j$ to the execution of the method $B \in M_j$, the unique method-event $e_{AB}(x, a) \in E_j$ is to be created, to calculate and predict the moment of that switching. According to the closeness hypothesis, such a condition may be only a certain combination of internal and external characteristics of the model $\{x, a\} \in X$, – there are nothing at all but model's characteristics in the virtual world of the model. The event of the type $e_{AA}(x, a)$ is also possible. It does not switch the method-element $A \in M_j$ to any other, but only interrupts its execution (for example, to synchronize the results of its calculations with the other processes of the model). Thus, the time and the order of the elements switching of each process are determined by what happens inside and outside of the model. The mappings from events to switches are bijections for all processes.

$$\{p_j \subset \beta(M_j) \times \beta(E_j) \times M_j \times \beta(E_j \times M_j \times M)\}_{j=1}^N, R_9: \{p_j = \{M_j, E_j, m_j^0, sw_j\}\}_{j=1}^N \quad (10)$$

By relation (10) the processes of the model are determined, j – index of the process, which changes from 1 to N . The sets M_j, E_j – are sets of elements and events of the j -th process; m_j^0 – its initial element; sw_j – elements switching rules. Processes – are what may run in parallel in the model, something like when the operating system of the computer at the same time has several system services running. Each process consists of sequential alternation of a finite number of methods-elements. The alternation of elements in the process is event-driven. Distinguished within the process methods-elements and methods-events, generally speaking, may have the same realizations in M , and, accordingly in E . The difference between the methods having the same realizations, from the point of view of the process, maybe for example, in the way of commutation of their parameters with characteristics of the model. Not prohibited (although not recommended) just “synonyms”.

Finally, we supplement the axioms of the species of structure “model-component” R_1 – R_9 with two more:

The axiom R_{10} requires that the sets X, M, E have no identical elements. Note that the verification of compliance with this axiom is not formalized and is left to the discretion of the model developer. What should be considered the same and what differs in the model, – depends of its semantics.

The axiom R_{11} sets the following rules to run any kind of the object of species of structure “model-component”. First, it is believed that at the beginning of the simulation step current methods-elements of all processes and all of the internal characteristics of the model are known (at the first step - there are the initial values of the internal characteristics and the initial methods-elements of processes). Secondly, observability of the external characteristics at any moment is assumed. Further,

1. The events associated with the current elements of the processes are computed. The correlation of events with the current elements of the processes is determined by the rules of switching (7). The events can be computed in parallel, but to promote the computing process further, you should wait for completion of the computation of all the events. If there are events occurred, it is checked whether there are transitions to the fast elements. If there are any - the fast elements run (they become current). They can also be computed in parallel, but to advance the computing process further, you should wait for completion of all the calculations of the fast elements, and then return to the beginning of the item 1. If there are no transitions to fast elements - the transitions to the new slow elements are made, and then return to the beginning of the item 1.

2. If there is no occurrence of the events, from all the forecasts of the events is selected the nearest $\Delta\tau$.

3. If the standard step of modeling Δt does not exceed the predicted time to the nearest event $\Delta t \leq \Delta\tau$, – we compute the current slow elements with the standard step Δt . Otherwise, we compute them with the step to the nearest predicted event $\Delta\tau$. Slow elements can also be computed in parallel, with expectation of completion of the latter.

4. Return to the beginning of the item 1.

Thus, the family of species of structure “model-component” is fully defined, and even in some measure explained.

The Synthesis of the Model-Complex from Models-Components

Now suppose that there are two mathematical objects with species of structure “model-component” Σ_N and $\Sigma_{N'}$, with the base sets $X, M, E, \{M_j\}_{j=1}^N, \{E_j\}_{j=1}^N$

and $X', M', E', \{M'_j\}_{j=1}^{N'}, \{E'_j\}_{j=1}^{N'}$ correspondingly. Let us define a model-complex, composed from these models-components. As the base set of the complex, we take the following set:

$$X \cup X', M \cup M', E \cup E', \{M_j\}_{j=1}^{N+N'}, \{E_j\}_{j=1}^{N+N'};$$

where $\{M_j\}_{j=1}^{N+N'}$ and $\{E_j\}_{j=1}^{N+N'}$ mean $M_1, \dots, M_N, M'_1, \dots, M'_{N'}$ and $E_1, \dots, E_N, E'_1, \dots, E'_{N'}$

correspondingly. The unions of the sets $M \cup M'$ and $E \cup E'$ we treat in the usual sense:

$$M \cup M' = \{m : (m \in M) \vee (m \in M')\},$$

$$E \cup E' = \{e : (e \in E) \vee (e \in E')\}.$$

As for the sets X and X' , let us take that they do not have intersections, i.e., even if $X \cap X' \neq \emptyset$, we assume that we are able to distinguish the characteristics from X and from X' by their origin. So elements from $X \cap X' \neq \emptyset$ are included in the union $X \cup X'$ twice, as $X \cap X' \subset X$ and as $X \cap X' \subset X'$, and are treated as different elements. The meaning of this assumption - we put together two models-components, but they do not still interact with each other - each lives its own life, as if it was alone.

We show that on the basic sets of the model-complex the species of structure $\Sigma_{N+N'}$ from the family "model-component" can be set. Now we will check the following typical characterizations:

$$x \cup x' \subset X \cup X', \quad a \cup a' \subset X \cup X', \quad (11)$$

$$s \cup s' \subset M \cup M', \quad f \cup f' \subset M \cup M', \quad (12)$$

$$\{m_{j,real} \subset M_j \times (M \cup M')\}_{j=1}^{N+N'}, \quad (13)$$

$$\{e_{j,real} \subset E_j \times (E \cup E')\}_{j=1}^{N+N'}, \quad (14)$$

$$\{m_{j,in} \subset M_j \times \beta(X \cup X')\}_{j=1}^{N+N'}, \quad (15)$$

$$\{m_{j,out} \subset M_j \times \beta(X \cup X')\}_{j=1}^{N+N'}, \quad (16)$$

$$\{e_{j,in} \subset E_j \times \beta(X \cup X')\}_{j=1}^{N+N'}, \quad (17)$$

$$\{m_j^0 \subset M_j\}_{j=1}^{N+N'}, \quad (18)$$

$$\{sw_j \subset E_j \times M_j \times M_j\}_{j=1}^{N+N'}, \quad (19)$$

$$\{p_j \subset \beta(M_j) \times \beta(E_j) \times M_j \times \beta(E_j \times M_j \times (M \cup M'))\}_{j=1}^{N+N'}; \quad (20)$$

and axioms:

$$R_1: (x \cup x' \cup a \cup a' = X \cup X') \& ((x \cup x') \cap (a \cup a') = \emptyset),$$

$$R_2: (s \cup s' \cup f \cup f' = M \cup M') \& ((s \cup s') \cap (f \cup f') = \emptyset),$$

$$R_3: \left\{ \left(\forall m \in M_j \right) \left(\exists ! \tilde{m} \in M \cup M' \right) \left(\{m, \tilde{m}\} \in m_{j,real} \right) \right\}_{j=1}^{N+N'},$$

$$R_4: \left\{ \left(\forall e \in E_j \right) \left(\exists ! \tilde{e} \in E \cup E' \right) \left(\{e, \tilde{e}\} \in e_{j,real} \right) \right\}_{j=1}^{N+N'},$$

$$R_5: \left\{ \left(\forall m \in M_j \right) \left(\exists ! r \in \beta(X \cup X') \right) \left(\{m, r\} \in m_{j,in} \right) \right\}_{j=1}^{N+N'},$$

$$R_6: \left\{ \left(\forall m \in M_j \right) \left(\exists ! r \in \beta(x \cup x') \right) \left(\{m, r\} \in m_{j,out} \right) \right\}_{j=1}^{N+N'},$$

$$R_7: \left\{ \left(\forall e \in E_j \right) \left(\exists ! r \in \beta(X \cup X') \right) \left(\{e, r\} \in e_{j,in} \right) \right\}_{j=1}^{N+N'},$$

$$R_8: \left\{ \left(\forall e \in E_j \right) \left(\exists ! r \in M_j \times M_j \right) \left(\{e, r\} \in sw_j \right) \right\} \& \\ \& \left\{ \left(\{e, r\} \in sw_j, \{ \tilde{e}, \tilde{r} \} \in sw_j, r = \tilde{r} \right) \Rightarrow (e = \tilde{e}) \right\}_{j=1}^{N+N'}$$

$$R_9: \{p_j = \{M_j, E_j, m_j^0, sw_j\}\}_{j=1}^{N+N'},$$

$$R_{10}: \text{axiom of uniqueness of the model-component characteristics calculation,}$$

R_{11} : organization of simulation calculations axiom.

We see that the typical characterizations (11) – (20) and axioms $R_1 - R_9$ are valid, because as for the component Σ_N , either for $\Sigma_{N'}$, the typical characterizations and corresponding axioms $R_1 - R_9$ (1) – (10) are valid.

For example, consider the most bulky typical characterizations (20). Suppose first $1 \leq j \leq N$, then by (10) holds:

$$\begin{aligned} p_j &\subset \beta(M_j) \times \beta(E_j) \times M_j \times \beta(E_j \times M_j \times M) \subset \\ &\subset \beta(M_j) \times \beta(E_j) \times M_j \times \beta(E_j \times M_j \times (M \cup M')). \end{aligned}$$

Let now $N < j \leq N + N'$. Then by (10) again holds:

$$\begin{aligned} p'_j &\subset \beta(M'_j) \times \beta(E'_j) \times M'_j \times \beta(E'_j \times M'_j \times M') \subset \\ &\subset \beta(M'_j) \times \beta(E'_j) \times M'_j \times \beta(E'_j \times M'_j \times (M \cup M')). \end{aligned}$$

From the above we can conclude that our complex is a mathematical object from the family of species of structure “model-component” $\Sigma_{N+N'}$.

Similarly we can check the rest of the typical characterizations and axioms up to (20) and R_9 .

Axiom of behavior R_{11} by definition is such that applies to any object from the family “model-component”.

Now let us discuss the axiom R_{10} of unambiguity of the model-component characteristics calculation.

As we „forced“ the decision that

$$X \cap X' = \emptyset, \quad (21)$$

then the unambiguity follows from that which take place for each of the components. However, our components still do not interact with each other - they are simply combined together formally.

Pay attention to the fact that there cannot be a formal criterion of the condition (21). Only the developer can check their validity, basing on his understanding of the model subject area. However, if the developer has indicated that the condition (21) is violated, and has concretized what this violation is, we can point to a formal sequence of actions to correct the situation.

Note that if we understood the system characteristics association in the most common way:

$$X \cup X' = \{y : (y \in X) \vee (y \in X')\},$$

then, it is not difficult to see that the typical characterizations (11) - (20) and axioms $R_1 - R_9$ would also be fulfilled. In the case $X \cap X' \neq \emptyset$, interaction would occur between the components due to the intersection of their characteristics. However, it would be impossible to guarantee the uniqueness of the united characteristics calculation (axiom R_{10}). The closure hypothesis does not prohibit to two methods-elements of different processes (originally belonging to different components), simultaneously modify the same characteristic, if this characteristic belongs to $X \cap X'$.

Let us try to find out the reconciliation of the two above extremes. First we assume, that still all the characteristics combined formally are distinguishable, i.e. $X \cap X' = \emptyset$. Second, assume that from the substantive point of view, on the contrary, some of the characteristics of the components are the same (for example, two models-components are trying to give the weather forecast for tomorrow), that is, from the point of view of the model semantics $X \cap X' \neq \emptyset$.

Let us start with the easiest. Let intersect external characteristics of our component, for example, at the characteristic \tilde{a} . This means that the external characteristic $a_i = \tilde{a}$ of the first model and the external characteristic $a'_j = \tilde{a}$ of the second, reflect the same (otherwise they would differ) factor of the external to our model world. From the general concepts about unity and objectivity of the external world, should follow that the values of these characteristics (of course, correctly identified) should coincide, and therefore, to the model-complex is quite enough one of them. Exclude for definiteness a' from $X \cup X'$. Then in all commutation relationships (15) and (17), where a' presents, it should be replaced by a , that will allow these ratios keeping the message in the model-complex. If to someone the considerations about "unity and objectivity of the world" doesn't seem too convincing, further, to resolve the intersection of the internal characteristics of the components will be offered another method which can be applied in this case as well.

Suppose now that there intersects a set of internal characteristics of one model-component with a set of external characteristics of the other. For example, suppose $x \cap a' = \tilde{y} = x_i = a'_j$. This means that if in the second model-component the characteristic a'_j was not simulated, but was a factor of the outer world, in the model-complex this characteristic is explicitly simulated as the first model-component internal characteristic x_i . Therefore, the model-complex external characteristic of the second component $\tilde{y} = a'_j$ becomes an internal characteristic of the first model-component $\tilde{y} = x_i$. Therefore, the external characteristic a'_j should be deleted from the model-complex external characteristics, and all of the commutation (15) and (17), which include $\tilde{y} = a'_j$, are to include $\tilde{y} = x_i$ instead.

Thus, in full compliance with the humorous programmer's proverb: "Documented bug becomes a feature", we can not only integrate the components into the complex, but also use in the simulation of the complex that some of the components, perhaps simulate something that without them did not simulate any others. So we get some benefits from the complexity of the model while building complexes.

Finally, suppose that there is an intersection of the internal characteristics of the model-component. Unfortunately, the concerns about unity and objectivity of the world are not convincing as in the case of the external characteristics. On the contrary, it is well known that there may be dozens of different weather forecasts or exchange rates. Let the internal characteristics of two models-components intersect in a characteristic $\tilde{x} = x_1 = x_2$. It is proposed to supplement the set $X \cup X'$ by a new characteristic \tilde{x} . The task to calculate the value of this characteristic is left for a special model-component, which has external characteristics x_1 and x_2 , and the internal characteristic \tilde{x} . An algorithm to calculate it – is left at the discretion of the developer. In the commutation relations (15) – (17), in those correspondences, where present x_1 and x_2 ; they must be replaced by \tilde{x} .

Thus, the models-components allow association into a model-complex with possible (but not obligatory) commutation of some of internal characteristics of some components with certain external characteristics of others, possible addition to the initial set of components some extra to eliminate ambiguities, and correction in part of relations (15) – (17) for some components. As was shown, the resulting model-complex has a species of structure "model-component" and thus, may be a component of some new models-complexes.

This way you can build models of an arbitrarily complicated fractal design, computational processes of which, however, is completely determined by the axiom R_{11} of the family of species of structure "model-component".

Organization of simulation calculations, as an invariant under the integration of models-components into complexes, allows completely solve the task of complex

multicomponent systems simulation models describing and synthesis. The class of models was highlighted [10] (namely, satisfying in every point the closeness hypothesis and with piecewise-smooth, continuous on the left trajectory), for which the proposed organization of simulation calculations leads to the successful synthesis of the model.

Thus, the construction of a large software system that implements simulation modeling, is divided into foreseeable stages of declarative describing of components and complexes of the model, as well as writing on universal programming languages, but in the functional paradigm, of methods-elements, and methods-events of components. Debugging declarative descriptions of the models-components and models-complexes, as well as functional programs that implement the methods, is based on the principle – debugged and forgotten. Imperative programming [14] thus is completely excluded from the project, making it easier to design and debug.

The proposed concept of complex systems simulation has been realized in series of simulation models implemented under the influence of the model-oriented programming paradigm. For example, some episodes of Reagan's SDI functioning were simulated, the model of interaction of several countries was created. Also the tools for complex systems simulation were created: the system MISS [13], and the software for the workstation of peer-to-peer system of distributed simulation [11].

This work was supported by the Russian Foundation for the Basic Research, project 13-01-00499-a.

References

1. Buslenko N.P. Simulation of Complex Systems Moscow: “Nauka”, 1978, 400 p. (in Russian)
2. Buslenko N.P. Complex System //An article in the Great Soviet Encyclopedia, 3-ed., Moscow: “Soviet Encyclopedia”, 1969-1978. (in Russian)
3. Bourbaki N. Elements of Mathematics, Theory of Set. Springer, 2004, 414 p.
4. Gretskey M.N. Structuralism (philosopher) //An article in the Great Soviet Encyclopedia, 3-ed., Moscow: “Soviet Encyclopedia”, 1969-1978. (in Russian)
5. Klein F. A comparative review of recent researches in geometry //Complete English Translation is here -<http://arxiv.org/abs/0807.3161>
6. Pavlovsky Yu.N. A Geometrical Theory of Decomposition and Some its Implementations Moscow: CC RAS, 2011, 93 p. (in Russian)
7. Pavlovsky Yu.N., Smirnova T.G. Introduction into Geometrical Theory of Decomposition. Moscow: FAZIS, CC RAS, 2006, 169 p. (in Russian)
8. Pavlovsky Yu.N., Smirnova T.G. A Problem of Decomposition in Mathematical Modeling. Moscow: FAZIS, 1998, 272 p. (in Russian)
9. Elkin V.I. Reduction of Nonlinear Controlled Systems. Decomposition and Invariance under Disturbance. Moscow: FAZIS, 2003. 207 p. (in Russian)
10. Brodsky Yu.I. Model Synthesis and Model-Oriented Programming Moscow: CC RAS, 2013. 142 p. (in Russian)
11. Brodsky Yu.I. Distributed Simulation of Complex Systems Moscow: CC RAS, 2010, 156 p. (in Russian)
12. Brodsky Yu.I., Pavlovsky Yu.N. Developing an Instrumental System for Distributed Simulation. //Information Technologies and Computing Systems, N4, 2009, P. 9-21. (in Russian)
13. Brodsky Yu.I., Lebedev V.Yu. Instrumental Simulation System MISS. Moscow: CC AS of the USSR, 1991, 180 p. (in Russian)

14. Brodsky Yu.I., Mjagkov A.N. Declarative and Imperative Programming in Simulation of Complex Multicomponent Systems //Vestnik MSTU Ser. Natural sciences. Spec. Issue, N4, "Mathematical modeling" - 2012. - P. 178-187. (in Russian)
15. Ponomarev I.N. Introduction into Mathematical Logic and Species of Structures: Textbook. Moscow: MIPT, 2007, 244 p. (in Russian)
16. Laplace P.S. The System of the World. Dublin, University Press 1830, 524 p.
17. Booch G., Rumbaugh J., Jacobson I. UML. User Guide, 2-ed., – Addison-Wesley, 2005, 475 p.
18. Fowler M. UML Distilled, 3-ed., – Addison-Wesley, 2004, 192 p.

PERFORMANCE TOOL FOR FAST DETECTION OF JAVA STRUCTURES

Bublík T.

Prague, College of information Management, Business Administration and Law

This paper presents general results on the Java source code snippet detection problem. We propose the tool which uses graph and subgraph isomorphism detection. A number of solutions for all of these tasks have been proposed in the literature. However, although that all these solutions are really fast, they compare just the constant static trees. Our solution offers to enter an input sample dynamically with the Scriphon language while preserving an acceptable speed. We used several optimizations to achieve very low number of comparisons during the matching algorithm.

Keywords: AST, Java, tree matching, Scriphon, source code recognition

It is usual that programs, consisting of a large source code, are becoming chaotic, and many times described illnesses start to appear (code duplicity, weak reusability, etc.). Maintaining a source code is a serious issue. There are a lot of tools and guides on how to approach this issue. The tool, described in this work, serves to programmable Java source code scanning. This tool is based on the Scriphon language which was developed for these purposes in the scope of this work. A script, which describes a source code structure and its properties, can be written in this language. This allows defining dynamic properties of searching requirements. Next, an abstract syntax tree (hereinafter AST) is created dynamically from this script. Meanwhile, a similar tree is created from given Java source, and these two trees are matched by a graph matching algorithm. However, not only graph shapes are compared, also trees properties are considered. To obtain results faster, several graph optimizations are used during this process. And it is possible to scan higher amount of source code classes during a relatively short time.

Typical usage of this approach is as follows: A user wants to find something, not easily describable, in a large program. But he or she knows that it could be there. He or she can use our tool and try to find at least the similar snippet of indented code. Therefore, a user performs a searching procedure, and specifies the input script based on the received results. By repeating this procedure, he or she filters the unintended results, and finally gets the desired code snippet.

Our tool is useful not just for the fast Java sources scanning, but for example, for a better definability of search conditions.

Another usage area of our tool can be a clone's detection problem. By using other clones detection tools, a material for further research can be gathered. For example, the non-ideal clones are difficult to detect and the output of such programs isn't unequivocal in many

cases. However, it can be classified by Sripthorn, and a common searching script based on such output can be.

A graph is an ordered pair $G = (V, E)$ where V is a finite, non-empty set of objects called vertices, and E is a (possibly empty) set of unordered pairs of distinct vertices i.e., 2-subsets of V called edges. The set V is called the vertex set of G , and E is called the edge set of G . If $e = \{u, v\} \in E(G)$, we say that vertices u and v are adjacent in G , and that e joins u and v . We'll also say that u and v are the *ends* of e . The edge e is said to be *incident* with u (and v), and vice versa. We write uv (or vu) to denote the edge $\{u, v\}$, on the understanding that no order is implied. Two graphs are *equal* if they have the same vertex set and the same edge set. But there are other ways in which two graphs could be regarded the same. For example, one could regard two graph as being “the same” if it is possible to rename the vertices of one and obtain the other. Such graphs are identical in every respect except for the names of the vertices. In this case, we call the graphs *isomorphic*. Formally, graphs G and H are isomorphic if there is a $1-1$ correspondence $f: V(G) \rightarrow V(H)$ such that $xy \in E(G) \leftrightarrow f(x)f(y) \in E(H)$. This function f is called an isomorphism.

A tree is a connected graph that has no cycles (i.e., a connected acyclic graph).

The graph matching problem is actually the same as the problem of finding the isomorphism between the graphs. Moreover, matching the parts of a graph with a pattern is the same challenge as the finding the isomorphic subgraph. There are many approaches to this topic [2].

Subgraph isomorphism is useful to find out if a given object is part of another object or even of a collection of several objects. The maximum common subgraph of two graphs g_1 and g_2 is the largest graph that is isomorphic to a subgraph of both g_1 and g_2 . Maximum common subgraph is useful to measure the similarity of two objects. Algorithms for graph isomorphism, subgraph isomorphism and maximum common subgraph detection have been reported in [3, 4, 5, 6].

A more general method to measure the similarity of two graphs is graph edit distance. It is a generalization of string edit distance, also known as Levenshtein distance [7].

Another approach measuring the similarity of two graphs is a distance measure based on the maximum common subgraph between g_1 and g_2 . With increasing work being done in the field of maximum common subgraph detection, these measures are growing in popularity. In [8], a graph distance measure based on the maximum common subgraph of two graphs is introduced.

It is shown that the well-known concept of maximum common subgraph distance is a special case of graph edit distance under particular edit costs. Consequently, algorithms originally developed for maximum common subgraph detection can be used for edit distance computation and vice versa for the considered edit costs. Furthermore, in [9] the concepts of maximum common subgraph and minimum common supergraph are combined to derive a graph distance measure and in [10], graph distances based on the minimum common supergraph denoted as the *graph union* are discussed.

A number of graph matching algorithms are known from the literature [11, 12, 13, 14]. All of these methods are guaranteed to find the optimal solution, but require exponential time and space. Suboptimal or approximate methods, on the other hand, are polynomially bound in the number of computation steps, but may fail to find the optimal solution.

In [15], inexact graph matching is performed by calculating the Levenshtein distance on the eigenvectors of the graphs. Another approach illustrated in [16] converts the adjacency matrix into a string, then uses the leading eigenvector to impose a serial ordering on the string.

Graphs are then matched by applying string matching techniques to their string representation. A different idea is pursued in [17, 18] where eigen(sub)space projections and vertex clustering methods are explored.

Whereas in [18] the objective of the method is to work in the eigenspace of the graphs, in [17] similar subgraphs are matched based on their vertex connectivities defined in the common subspace.

There exists a lot of searching types which can be used to detect a clone [19]. The textual approaches belong to basic ones. These approaches are easy to implement, on the other hand, because of a large excess of non-program material contained in source code, they suffer from a whole range of ailments. For example, checking a variable scope could be very challenging issue by using textual comparisons.

The token-based comparisons are the next group of approaches needs to be considered. This kind of approaches divides a source code into the tokens sequences which are compared to each other. This is little more robust than the textual ones, because it doesn't work with unnecessary text material like spaces, comments etc. However, this approach still does not handle a variable or a method scope.

More effective algorithms are the tree-based. There exist two approaches to them: metric-based and tree-based. The metric-based ones use the Java source generated metrics. These metrics are then compared with the metric generated from original sources. The tree-based methods are base on abstract syntax subtrees comparison. These methods are used in our work. They are little more difficult to implement, but they are very effective and they offers more searching options. On contrary, the algorithms based on these methods are more time consuming comparing to other types.

Ira D. Baxter was a pioneer in this area [20]. He proposed a solution using the subtrees hashing into the buckets. And only the same bucket trees are being compared.

Another solution proposed Wahler [24]. He converted AST into XML and applied data mining techniques on it. The remaining question is the speed of XML processing procedures. Further, an interesting option proposed [21]. They serialized generated AST and compared just the suffix tree tokens of it. The proposed algorithm is very fast. It is able to detect a clone in a linear time.

The lack of these algorithms is the inability to detect snippets dynamically. They suppose a constant and unchanging original pattern. On the opposite, our solution offers the usage of the dynamic input based on a scripting language. This means that the input could be conditioned or iterated, and the searching tree changes according to the searched tree properties. Even the variables can be used. For example, a user can declare the "clazz" variable of type Class, and use it later for the name comparison:

```
Class clazz
  Block StmtNum=2)
  if (clazz.Name=="HelloWorld")
  ...
  else
  ...
```

This example means that we search the class with two statements inside, and if the name of this class is "HelloWorld", then we search something, else we search something else.

Within this work, a new programming language named Scripthon, capable of these functionalities, was developed. Using this language, it is possible to describe a code structure with properties, and it is even possible to change the properties of a searching sample in dependence of searched segment properties.

Scripthon is a dynamically typed, interpreted, and non-procedural language. Its translation into a tree-expressing form and its usage is very similar to the usage of any other

modern script languages. The complete definition of the Scripthon language semantics is beyond the scope of this paper, can be found in [1].

Because the language is designed to be just a scripting language, there are no special constructions starting a script. This language is neither a pure object-oriented language. The input for a compiler is a text with a sequence of commands. This sequence describes consecutive statements in Java source code. Commands with a variable detail degree correspond to a variable length code segment. A detail level is not fixed, and can vary in every command. One command can correspond to a line of source code; other one can describe a whole class in Java. A Scripthon structure is very similar to the structures of the others contemporary dynamic programming languages. Individual commands are separated by lines. There is no command separator in Scripthon. Inner parts of blocks are tab nested. A block is not delimited by any signs; just a hierarchy of tabulators is used.

Looking for a method with a specific name? Suppose we have the most common Java code:

```
public class HelloWorld {
    public static void main(String[] args) {
        System.out.println(args);
    }
}
```

Let's suppose we are looking for the method named "main". It's easy. A user just starts a text search dialog (usually by CTLF + F shortcut) and performs a searching procedure. Unfortunately, this will find a lot of miscellaneous results. With Scripthon, we can search just methods:

```
Meth(Name="main")
```

Moreover, we want just the public and static ones:

```
Meth(Name="main"; Rest=[public, static])
```

Even more, the most specific searching criteria for the main method are:

```
Meth(Name="main"; Rest=[public, static]; Ret=void; ParNum=1;
ParTypes=[String[]]; ParNames=["args"])
```

With Scripthon, we can define a method call inside the main method:

```
Meth(Name="main"; Rest=[public, static])
    MethCall(Name="System.out.println"; Params=["args"])
```

Scripthon supports also a block of code description. We can define properties of block by this way:

```
Class(Name="HelloWorld")
    Meth(Name="main")
        Block(StmtNum=1; Order=false)
```

Again, this example corresponds to a given "hello world" example. There is one statement inside the main method and the order of statements doesn't matter. Another interesting Scripthon's keyword is the word "Any". It is useful for an indefinite searching. It means the searched statements can be anything, or empty. To describe the code above, we can write:

```
Meth(Name="main")
    Any()
```

But the desired code can look like this:

```
public static void main(String[] args) {
    int i = 1;
    i++;
    System.out.println(args);
}
```

And we can find this by the following script:

```
Meth(Name="main")
Any()
MethCall(Name="System.out.println")
```

There are several more keywords supported by Scripthon. For example, Init() for a variable initialization, Loop() for a common loop, etc. Finally, with the presented examples, it is easy to find a singleton in code:

```
Class() class
Block(Order=false;Consecutive=false)
Meth(Name=class.Name;Rest=private)
MethCall(Ret=class.Name;Rest=[public, static])
```

The only unmentioned parameter here is the “consecutive” parameter. It means that the statements inside block must not be consecutive. These statements just need to be contained somewhere in the given block.

The Java Compiler API is used to get AST from the given Java sources in the first iteration. This API is free and is contained in Java SDK. It provides access to control the Java compiler, and one of the compilation outputs is an abstract syntax tree of the given sources. Just one condition needs to be met. The Java sources must be compilable.

While browsing the Java source code, the tree, with the nodes enhanced by four numbers, is created. These numbers are the natural numbers named left, right, level and level under. The first and the second number (left, right) denote the order index of a node in the tree preorder traversal. Therefore, an ancestor’s left index is always smaller than its children left index, while the right index is always bigger than any children’s right index. The level number denotes the level in a tree hierarchy of vertices, and the level under number denotes a number of levels under the current node (compare with the method described in [22]).

Suppose that x and y are two nodes from a tree; the following rules are valid for these values.

- The y node is an ancestor of x and x is a descendant of y if $y.\text{left} < x.\text{left} < y.\text{right}$
- The y node is a parent of x and x is a child of y if 1) $y.\text{left} < x.\text{left} < y.\text{right}$ and 2) $y.\text{level} = x.\text{level} - 1$
- The node x has $((x.\text{left} - x.\text{right}) - 1)$ sub-nodes.

All these data are acquired during a single pass through the tree. Obtaining this information is not a time consuming operation, because it is made during the tree production process. On the other hand, the number of comparisons can be significantly reduced with these numbers.

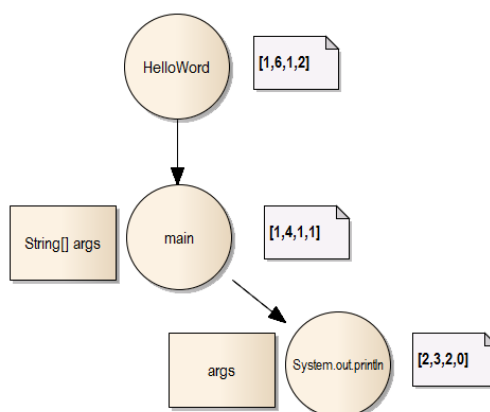


Figure 1. Example of AST with indexes

With this information (Fig. 1), we know how many children are contained in the currently processing node, or whether a node is a leaf. Thanks to it, a lot comparisons need not to be performed. For example, comparing this script:

```
Meth(Name="main")
```

```
Block(StmtNum=4)
```

with this Java code:

```
public static void main(String[] args) {
    System.out.println(args);
}
```

means that these two nodes are compared (Fig. 2.)

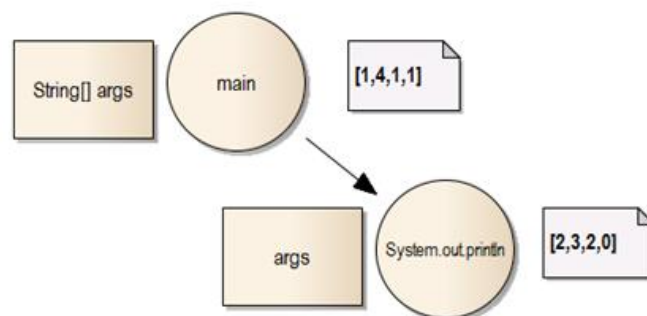


Figure 2. Node “main” with one child

But the left and right indexes signalizes that the “main” node does have just one child, however, we search for a method with 4 statements. So that, this code does not corresponds to the script, and any other comparisons are not needed.

The complete process is little bit complex, but the top overview is easy. Before the main matching procedure, two processes take place. The first one starts immediately after a user enters a Java sources path. It compiles and optimizes AST obtained from the sources. This process is done just once, because the sources are always the same in scope of this process. It runs on the background. The second process starts immediately after a user enters a searching script. It compiles the script and, if it is not done, waits for the first process.

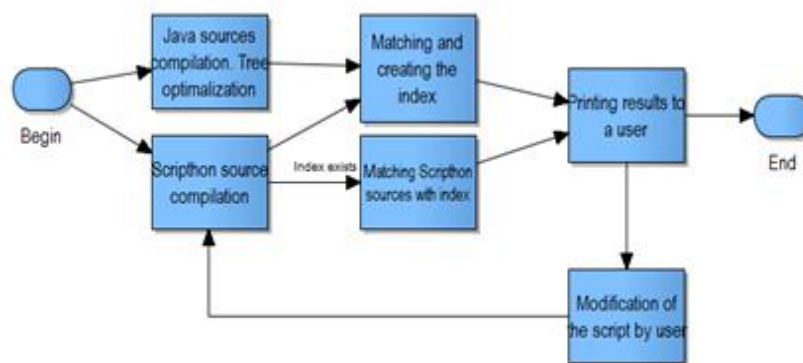


Figure 3. Complete process

Next, the first iteration is performed. Matching is performed together with index building during this iteration. After that, results are presented to a user. It is supposed that a user improves the entered script according to the results. And then the algorithm runs again with only difference. Only the nodes corresponding to the index of changed Scripthon part are considered.

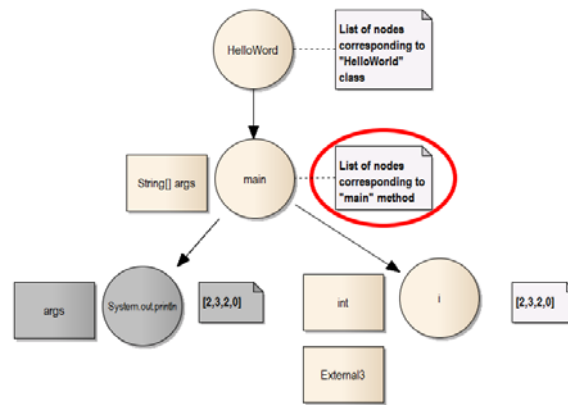


Figure 4. Indexing of nodes

Figure 4 shows how the indexing works. Let's suppose the same "HelloWorld" example from the beginning of this paper. The index into the group of corresponding Java sources is assigned to all non-leaf nodes. When a user changes the input script, the new and the old corresponding trees are compared. In our example (Fig. 4), the "System.out.println" method call was changed to the initiation the variable "i" of type int. This is indicated by gray colour. The node which contains this change is then detected by the tree matching algorithm. It is clear that the set of corresponding Java sources to this node remains the same. Therefore, only this set needs to be considered in the next search iteration.

These top level listings show how the matching algorithm works:

```

1 for(Class c from classes)
2   for (Statement s from statements)
3     match = compare(c.node, s)
4     if (!match)
5       break
6   if (match)
7     addToResults(c)
8
9 compare(Node n, Statement s)
10  match = optiMatch(n, s)
11  if (match)
12    if (n.allProperties matches
13      s.allProperties)
14      addResultsForThisStatement(n, s);
15    for (n.children, s.children)
16      match = compare(...)
17      if (!match)
18        return false
19  else return false
20  return match
21
22 optiMatch(Node n, Statement s)
23  checkTreeSizes(n, s)
24  checkLevels(n, s)
25  checkChildrensNumber(n, s)
26  return resultOfChecks

```

All the source classes are iterated in a loop (line 1). Next, all the Scripthon statements are then iterated inside this loop (line 2). The “compare” method is called inside the second loop. This method compares all the sub-statements with the node from the outside loop. If there is a match, the founded result is added to the group of results (line 7), otherwise the inner loop is beaked (line 5). According to the line 15, the “compare” method calls itself recursively. First, it checks the match with prepared optimizations (line 10). The “optiMatch” method (line 21) checks the structure of trees and tries to exclude the node by tree sizes mismatch, by levels number mismatch or children number mismatch. If the “optiMatch” method return false, then the node is excluded from further considerations (line 18). On contrary, when the optimizations do not exclude the node, all the children of the statement and node are compared in the “compare” recursive call (line 15). But before that, we know about the correspondence between the current statement and the current node, therefore it is saved into memory on the line 13. If the entire children set matches, the current node is considered equal, and true is returned from the “compare” method (line 19). Otherwise, false is returned (line 17). Finally, if is the node equals to all the Sripthon statements, it is saved into the results set (line 7).

Because the non-constant trees are compared, the complexity determination of our algorithm is not an easy task. Syntax trees are always little bit different and since we compare the characteristics of the nodes according to a user input, the comparison is always different. To begin, it is possible to emerge from the complexity of the subtrees comparing algorithm. The subtree comparison problem is NP-hard. And according to [23], the complexity is $O((n_1 + n_2)^2)$, where n_1 is number of the first tree nodes whereas n_2 is number of the second tree nodes. There exist also several improvements [25].

Our algorithm, however, is based on the use of information on the required sample tree. Thanks to this information, a lot of comparisons can be saved. Moreover, the whole tree is traversed just once during the first run. During next runs, just the data, corresponding to the node containing the change, are considered. Unfortunately, also the commands increasing the comparisons number can be written in Scripthon. For example:

```
Any()
MethCall(Name="someName")
```

This script must run over all statements in the source code up to the “someMethod” method. If the code before this method is large, several more comparisons must be done. And moreover, it must be done even in the case if there is no such method. This means n more comparisons in the worst case. Another example:

```
Block(Order=false)
```

```
...
```

This command identifies the statements in a block. But if the statements order doesn't matter, the algorithm must compare all the children of the “Block” node. If the first statement corresponds to the last child, there will be n more comparisons. And if the second statement corresponds to the penultimate child, there will be $n - 1$ more comparisons. In conclusion, there could be $\sim n^2$ more comparisons in the worst case.

To assess whether the implemented optimization makes sense, the algorithm is equipped with the ability to switch off the optimization globally. If we note how many comparisons actually occur in the case of enabled optimizations, we obtain the basis to assess whether our optimization are meaningful. We chose a project with 800 Java classes as a test sample. Then several search iteration were run over this project.

When testing with disabled optimizations, nodes 142 275 comparisons were performed. On the other hand, with enabled optimization, there was a big difference between the first run, with index gathering function, and the following rounds, with using this index. In

the first case, there were 28 268 comparisons, whilst in the second case, there were 6 800. As can be seen, the second comparisons numbers are much lower.

A quite common computer with Windows 7, 2,4 GHz CPU and 8 GB memory was used to test the time complexity of our algorithm. Used Java version was 1.7.0_51. To show real benefits of our solution, we performed several search procedures with disabled and also with enabled optimizations. We tried to identify several important parts which could, by their time, reflect the actual contribution of the whole work. Without optimizations, the algorithm runs over all input classes by the “brute force” method. In this case, no results caching and no indexing was used. We compared the obtained times with times of optimized algorithm version in Fig. 5.

First round	Without optimizations	Optimized
Time of Java compilation	38 469 ms	39 542 ms
Time of Scripthon compilation	35 ms	33 ms
Time of search	962 ms	170 ms
Total time	39 441 ms	39 924 ms

Second round	Without optimizations	Optimized
Time of Java compilation	0 ms	0 ms
Time of Scripthon compilation	48 ms	44 ms
Time of search	888 ms	151 ms
Time of search with change detection	68 ms	15 ms
Total time	1 062 ms	208 ms
Total time with change detection	118 ms	62 ms

Figure 5. Times table

As can be seen from the tables, measurements were carried out in two phases. The first table shows the times received always in the first run of the algorithm. Both tables have two columns to indicate whether the time was with or without the optimizations. The first significant difference is the time of compilation which is not used in the second run. It is zero, because it does not occur in further runs.

Next row represents the times of Scripthon code compilation process. Because there weren't significant differences between the searching scripts, these times are almost the same. Another row shows the times of the own matching process. There is a big difference between these times. Optimized version is about 5 times faster, however, according to the first table, this time is completely lost in the compilation time. To make matters worse, the total time is even bigger than the time without any optimization!

The second table contains one more row. This row shows the time of matching process with help of the index created in previous runs. In this case we used this script:

```
Class()
Any()
Meth(Name="add")
Init(Name="errors")
```


For the further runs, the only change was a name in the “Init” statement. The algorithm used just the nodes corresponding to “Meth(Name=“add”)” in this case. In other words, the algorithm considered just the classes with methods named “add”. As can be seen, if there is no need to compile the entire sources again, and if the algorithm has an index created from the previous runs, the matching time acceleration is enormous. Then the complete process runs for a tiny fraction of the time needed to run the same task without any improvement.

Our project showed that the source recognition can be speeded up highly. The significant contribution for the speed is the caching the nodes corresponding to statements. Although this approach speeded up the process, however, it is necessary to say that this applies just for further runs. In the case of the first runs, compilation of sources takes a lot of time. But there exist a lot of improvements. For example, the compilation can start already during script writing.

This project shows the usability of programmable and dynamic code recognition in an acceptable time. Currently, the project is used just for science purposes, but we want to add all the workaround to make it other users. We consider also the use of the tree indexing methods to achieve even a higher speed of the matching process in the future.

References

1. Tomáš Bublík., Miroslav Virius.: “New language for searching Java code snippets,” in: ITAT 2012. Proc. of the 12th national conference ITAT. diar, Sep 17 – 21 2012. Pavol Jozef Safrik University in Kosice. p. 35 – 40.
2. Christophe-André M. Irniger, “Graph Matching - Filtering Databases of Graphs Using Machine Learning Techniques,” 2005, ISBN 1-58603-557-6.
3. B.D. McKay, “ractical graph isomorphism,” In Congressus Numerantium, volume 30, 1981, pages 45–87.
4. J.R. Ullmann, “An algorithm for subgraph isomorphism,” Journal of the Association for Computing Machinery, 1976, pages 31-42.
5. G. Levi, “A note on the derivation of maximal common subgraphs of two directed or undirected graphs,” Calcolo, 1972, pages 341-354.
6. J. McGregor, “Backtrack search algorithms and the maximal common subgraph problem,” Software-Practice and Experience, 1982, pages 23-34.
7. G.A. Stephen, “String Searching Algorithms,” World Scientific, 1994.
8. H. Bunke and K. Shearer, “A graph distance metric based on the maximal common subgraph,” Pattern Recognition Letters, 1998, pages 255-259.
9. M.-L. Fernandez and G. Valiente, “A graph distance metric combining maximum common subgraph and minimum common supergraph,” Pattern Recognition Letters, 2001, pages 753-758.
10. W.D. Wallis, P. Shoubridge, M. Kraetz, and D. Ray, “Graph distances using graph union,” Pattern Recognition Letters, May 2001, pages 701-704.
11. A. Sanfeliu and K.S. Fu, “A distance measure between attributed relational graphs for pattern recognition,” IEEE Transactions on Systems, Man, and Cybernetics, 1983, 353-363.
12. W.H. Tsai and K.S. Fu, “Error-correcting isomorphisms of attributed relational graphs for pattern recognition,” IEEE Transactions on Systems, Man, and Cybernetics, 1979, pages 757-768.
13. M.A. Eshera and K.S. Fu, “A graph distance measure for image analysis,” IEEE Transactions on Systems, Man, and Cybernetics, 1984, pages 398-408.

14. E.K. Wong, "Three-dimensional object recognition by attributed graphs," In H. Bunke and A. Sanfeliu, editors, *Syntactic and Structural Pattern Recognition- Theory and Applications*, World Scientific, 1990, pages 381-414.
15. R. Wilson and E.R. Hancock, "Levenshtein distance for graph spectral features," In J. Kittler, M. Petrou, and M. Nixon, editors, *Proc. 17th Int. Conference on Pattern Recognition*, volume 2, 2004, pages 489-492.
16. A. Robles-Kelly and E.R. Hancock, "Graph edit distance from spectral seriation," *IEEE Transactions on Pattern Analysis and Machine Intelligence*, 2005, pages 365-378.
17. T. Caelli and S. Kosinov, "Inexact graph matching using eigensubspace projection clustering," *Int. Journal of Pattern Recognition and Artificial Intelligence*, 2004, pages 329-355.
18. T. Caelli and S. Kosinov, "An eigenspace projection clustering method for inexact graph matching," *IEEE Transactions on Pattern Analysis and Machine Intelligence*, 2004, pages 515-519.
19. Ch. K. Roy, J. R. Cordy, and R. Koschke. 2009. "Comparison and evaluation of code clone detection techniques and tools: A qualitative approach," *Sci. Comput. Program.* 74, 7 (May 2009), pp. 470-495.
20. I. D. Baxter, A. Yahin, L. Moura, M. Sant'Anna, and L. Bier. 1998. "Clone Detection Using Abstract Syntax Trees," in *Proceedings of the International Conference on Software Maintenance (ICSM '98)*. IEEE Computer Society, Washington, DC, USA, pp. 368-377.
21. R. Koschke, R. Falke, P. Frenzel, "Clone Detection Using Abstract Syntax Suffix Trees, Reverse Engineering," 2006. WCRE '06. 13th Working Conference on, ISBN 0-7695-2719-1, 2006, pages 253-262.
22. J. T. Yao and M. Zhang. 2004. "A Fast Tree Pattern Matching Algorithm for XML Query," in *Proceedings of the 2004 IEEE/WIC/ACM International Conference on Web Intelligence (WI '04)*. IEEE Computer Society, Washington, DC, USA, pp. 235-241.
23. G. Valiente, "Algorithms on Trees and Graphs," Springer, ISBN 3540435506, 2002, page 170.
24. V. Wahler, D. Seipel, J. W. von Gudenberg, and G. Fischer, "Clone detection in source code by frequent itemset techniques," In *SCAM*, 2004.
25. R. Shamir, D. Tsur, "Faster Subtree Isomorphism," In *Journal of Algorithms*, Volume 33 Issue 2, 1999, pages 267-280, doi:10.1006/jagm.1999.1044

SYNTHESIS OF ADAPTIVE CONTROL FOR NONLINEAR SYSTEMS

Kharkov, V.P.

Moscow, "NaukaSoft" Experimental Laboratory

Synthesis algorithm of adaptive control by nonlinear systems is considered. This algorithm allows finding such control which provides change coordinates of a condition of object on the set (desirable) trajectory at the expense control of the law of control. The developed law of control allows reducing a mean-square error of control to the values close to zero. The object of control represents observable dynamic system.

Keywords: optimal control, adaptation control, Lyapunov equation, inverse problems of dynamics.

Let the operated and observable dynamic system which mathematical model is represented the differential operator is given

$$\frac{dx(t)}{dt} = f(a, x, u, t, \varphi), \quad (1)$$

where $x(t) = (x_1, x_2, \dots, x_n)^T$ is the n -dimensional state vector; a - r -dimensional parameter vector; $u(t) = (u_1, u_2, \dots, u_m)^T$ - m -dimensional vector control functions; $\varphi(t) = (\varphi_1(t), \varphi_2(t), \dots, \varphi_n(t))^T$ - the controllable external revolting influences being set function of time. Let's believe that all elements of a vector belong to space L_2 ; the vector function is supposed variables continuous and continuously differentiated on set x, u, φ .

It is required to find such control $u(t)$ which provides change of coordinates of a condition of object (1) on the set trajectory $y_K(t)$. Thus it is necessary that ratios between components of state vector which should be carried out along a trajectory of movement of system (1) are representable in a look

$$F(x, y_K) = 0, \quad (2)$$

where $F(\bullet)$ - m -dimensional vector-valued function, differentiated n times.

It is necessary to define control u in the form of function of the coordinates states of the system (1) and coordinates of a desirable trajectory.

The solution of this task we will define from a condition that $F(x, y_K)$ aspires to zero under the set law. And this law of change $F(\bullet)$ can be set by any for example differential operator.

For definiteness we believe that function $F(\bullet)$ looks like

$$F(x, y_K) = x_1(t) - y_{K1}(t). \quad (3)$$

Then taking into account the requirement of analytical communication of control and operated coordinates of a condition the law of change $F(x, y_K)$ can be chosen in the form of the linear homogeneous differential equation of the n -order

$$F^{(n)}(x_1, y_K) + \lambda_{n-1}F^{(n-1)}(x_1, y_K) + \dots + \lambda_0 F(x_1, y_K) = 0, \quad (4)$$

where $\lambda_j, j = 0, 1, \dots, n-1$ - any positive numbers providing stability of system (4).

Taking into account model (1) equation (4) will register in a look

$$B_l + \lambda_{l-1}B_{l-1} + \dots + \lambda_1 B_1 + \lambda_0 F(x, y_K) = \sum_{j=1}^l \gamma_j, \quad (5)$$

Thus the management law satisfying to a condition (3) is defined by the solution of the equation (5) rather required functions $u(t)$. For finding of control the way which is not demanding obvious permission of the equation (5) relatively can be in certain cases offered $u(t)$. Let's designate:

$$Q(x, u, \dots, u^{(l-1)}) = \sum_{j=1}^l (\lambda_j B_j - \gamma_j) + \lambda_0 F(x, y_K),$$

then

$$Q'(x, u, \dots, u^{(l-1)}) = \frac{\partial Q}{\partial x} f(x, u) + \sum_{j=0}^{l-1} \frac{\partial Q}{\partial u^{(j)}} u^{(j+1)}. \quad (6)$$

If exists $\frac{\partial Q}{\partial u^{l-1}}^{-1}$ then the equation (5) will correspond in a look

$$u^{(l-1)} + \alpha_{l-2} u^{(l-2)} + \dots + \alpha_1 u = - \left(\frac{\partial Q}{\partial u^{l-1}} \right)^{-1} \left(\frac{\partial Q}{\partial x} \right) f(x, u).$$

Let's present the vector equation l - order in the form of dimension Cauchy system $(m \times l)$

$$\dot{\hat{u}}(t) = \hat{b}\hat{u}(t) + \hat{G}\hat{z}(t), \quad (7)$$

where \hat{b} - the numerical matrix which has been written down in the form of a matrix of Frobenius and nonzero elements of the last m - are made lines of matrixes $\alpha_j, j=1, 2, \dots, l-1$; \hat{G} - a matrix; $\hat{z}(t)$ - the right part of the initial equation, $\hat{u}(t)$ - the dimension vector $(m \times l)$ the first m -th which component define required control.

Thus if initial control $u(t_0)$ is chosen so that $Q(x(t_0), u(t_0), \dots, u^{(l-1)}(t_0)) = 0$, that solution $\hat{u}(t)$ of the equation (7) satisfies during every moment of time to the equation (3). It is natural that the described ways of calculation of control $u(t)$ provide performance of a condition (3) that is each operated coordinate satisfies

$$\lim_{t \rightarrow \infty} (x_j - y_{\text{sci}}) = 0, j = n_1, n_2, \dots, n_m; i = 1, 2, \dots, m.$$

Practically all variety of methods of synthesis of the control return problems of dynamics based on the concept allows building algorithms of control on the basis of full mathematical models of the operated processes reflecting fundamental properties of real objects. The deviation of the actual properties of object from their aprioristic representation causes expediency of development of systems of the control using identification of object of control in real time. Such systems usually belong to the class of adaptive systems.

The idea of a combination of control with simultaneous parametrical identification is known long ago and has gained rather wide circulation. Recently other approach to the current identification has started to be developed. Here it is recommended to carry out estimation of parameters in interests directly controls and quality of identification to characterize an average square of a difference of operated and wished processes

$$J = \int_{t_0}^{t_k} (x(t) - y_{\text{sc}}(t))^2 dt. \quad (8)$$

As real operated process contains, both dynamic, and static mistakes in tracking of the set trajectory of flight there is a problem of synthesis of the adaptive management which main objective consists in control of the law of control so that the mean-square error (8) would aspire to zero. It is necessary that desirable process steady. Then for creation of adaptive management we will use property of the closed system which is that the behavior of linear or nonlinear object in space of conditions is defined by the linear differential equation.

Let's present the equation of desirable operated process provided that the model of process is known precisely in the form of Cauchy

$$\dot{x}_\lambda(t) = A_\lambda x_\lambda(t) + b_\lambda y_{\text{sc}}, \quad (9)$$

where $x_\lambda^T = (x_{1\lambda}, x_{2\lambda}, \dots, x_{n\lambda})^T$ - n -dimensional state vector; A_λ, b_λ - matrix of dimension $(n \times n)$ and look vector column

$$A = \begin{bmatrix} 0 & 1 & 0 & \dots & 0 \\ 0 & 0 & 1 & \dots & 0 \\ \vdots & \vdots & \vdots & \ddots & \vdots \\ 0 & 0 & 0 & \dots & 1 \\ -\lambda_0 & -\lambda_1 & -\lambda_2 & \dots & -\lambda_n \end{bmatrix}, B_\lambda = \begin{bmatrix} b_{n-1} \\ b_{n-2} \\ \vdots \\ b_0 \end{bmatrix}.$$

Entry conditions of system (9) can be defined for example proceeding from a vector of a condition of real movement at the moment of time $t = t_0$ that is at the moment of system inclusion. The vector B_λ in (9) is written down in a general view and $b_0 \equiv \lambda_0$. In a similar form "real" operated process is representable. "Real" process here is understood as the process received provided that $u(t)$ is determined by aprioristic data on structure and parameters of mathematical model of object of control. Taking into account it is possible to present the equation of operated process in a look

$$\dot{x}(t) = (A\lambda + \Delta A)x(t) + (B_\lambda + \Delta B)y_{sc}.$$

For linear objects (1) matrix ΔA as appears from (9) has the first $(n-1)$ the lines consisting of zero. The last line of this matrix consists of elements $\Delta\alpha_j, j = 0, 1, \dots, n-1$ and their estimates that is

$$\Delta A_{nj} = \Delta\alpha_j + \Delta\hat{\alpha}_j.$$

Let's enter a vector $e(t)$ characterizing an error of a mismatch

$$e(t) = x(t) - x_\lambda(t). \quad (10)$$

As the vector $x_\lambda(t)$ can be calculated according to the equation (9) and $x(t)$ on a condition is measured that $e(t)$ is completely known.

The differential equation to which satisfies a vector $e(t)$ looks like

$$\dot{e}(t) = A_\lambda e(t) + \Delta A x(t) + \Delta B y_{sc}.$$

It is obvious that matrixes ΔA and ΔB contain parameters which can be changed in time according to some law so that the error of a mismatch aspired to zero. Let's notice that in order that $x(t)$ aspired to $x_\lambda(t)$ that is $x_1(t) \rightarrow y_{sc}(t)$, it is necessary elements of matrixes ΔA and ΔB also to direct to zero at $t \rightarrow \infty$.

Let's assume that change of parameters $\{\Delta A\}_{nj}$ and $\{\Delta B\}_{nj}, j = 1, 2, \dots, n$ is subordinated to some system of the differential equations in expanded state space $\Omega = \{e, A_1, \Delta B\}$.

Here A_1 - the vector of dimension n made of the last line of a matrix ΔA . It is known that asymptotic stability of expanded system in space Ω defines exact tracking of desirable process $x_\lambda(t)$. And it is fair even at unequal initial conditions $x_1(t_0)$ and $x_\lambda(t_0)$.

Asymptotic stability of expanded system we will investigate by means of Lyapunov function. Let's enter Lyapunov function in the form of a square-law form

$$V(e, A_1, \Delta B) = e^T p e + A_1^T A_1 + \Delta B^T \Delta B,$$

where $p = p^T$ - numerical positively certain matrix.

The full derivative of function $V(e, A_1, \Delta B)$ taking into account models of operated process is defined by the scalar equation

$$\begin{aligned} \dot{V}(e, A_1, \Delta B) = & e^T(t) [A_\lambda^T p + p A_\lambda] e(t) + A_1^T C^T p e(t) + e^T(t) p C A_1 + \\ & + y_{\mathcal{M}} \Delta B^T p e(t) + e^T p \Delta B y_{\mathcal{M}} + \dot{A}_1^T A_1 + A_\lambda^T \dot{A}_1 + \Delta B^T \dot{\Delta B} + \dot{\Delta B}^T \Delta B. \end{aligned}$$

Here C - a matrix at which all lines are equal to zero and the last line is equal to values a vector component $x^T(t)$. If to choose the law of change A_1 and B in a look

$$\begin{aligned} \dot{A}_1(t) &= -C^T p e(t), \quad A_1(0) = 0, \\ \Delta \dot{B}(t) &= -p e(t) y_{\mathcal{M}}, \quad \Delta B(0) = 0. \end{aligned} \quad (11)$$

that the derivative of function of Lyapunov will be defined by the following equation

$$\dot{V}(e, A_1, \Delta B) = e^T(t) [A_\lambda^T p + p A_\lambda] e(t).$$

As the matrix A_λ on Hurwitz condition always will be the numerical matrix $p = p^T > 0$ satisfying to Lyapunov equation

$$p A_\lambda + A_\lambda^T p = -Q, \quad (12)$$

where Q - any numerical positively certain matrix.

If the matrix p satisfies (11) when the matrix A_λ under condition of a Hurwitz condition it guarantees that the derivative $\dot{V}(e, A_1, \Delta B)$ everywhere is negative, except of some variety M . The variety M is characterized by that at $e(t) = 0$ a derivative $\dot{V}(e, A_1, \Delta B) = 0$.

For asymptotic stability of expanded system performance of conditions is necessary

$$V > 0, \quad \dot{V}(t) < 0 \quad (13)$$

in any point of space of conditions except for the beginning of coordinates.

If algorithm of adaptation (10) to choose in a look

$$\begin{aligned} \dot{A}_1(t) &= -C^T p e(t) - \mathcal{G} A_1(t), \\ \Delta \dot{B}(t) &= -p e(t) y_{\mathcal{M}} - \omega \Delta B(t), \end{aligned} \quad (14)$$

where \mathcal{G}, ω - it is positive certain weight matrixes a condition (12) it is carried out everywhere except for the beginning of coordinates. Therefore for algorithm (13) asymptotic stability in expanded space is reached. It means that identification of parameters of the closed control system is possible only on the indignant trajectories of movement of the incorporated system. Further as the reasons of indignation of a trajectory will be understood or change $y_{\mathcal{M}}(t)$ or a deviation of entry conditions from balancing values. This statement will rather fully be coordinated with a basic provision of a problem of identification in interests of management.

From (10) and (14) follows that for successful identification of parameters of model of the closed system it is required to know all vector of a condition. Besides, if to consider that

$x(t)$. Therefore for adaptation it is represented to more reasonable to construct such algorithm which would use only target coordinate.

For this purpose we will use not a minimum-phase form of representation of initial system upon transition from model of a look (5) to Cauchy system. Though the offered approach is suitable and for the equation (4) general views but at an algorithm statement for definiteness we believe that $n = 2$. Let's enter the variables which values are defined by formulas

$$\begin{aligned} Z(S) &= W_1(S) x_\lambda(S), \\ \gamma(S) &= W_1(S) y_{\text{жс}}(S), \end{aligned} \quad (15)$$

where S - Laplace operator; $W_j(S)$ - the transfer function which concrete look is defined by

initial transfer function. For the accepted assumptions $W_1(S)$ looks like $W_1(S) = \frac{1}{S + \tau}$,

where τ - known positive number. Generally the denominator of transfer function $W_1(S)$ should be a steady $(n - 1)$ - order polynomial.

The equation of operated process, taking into account the accepted designations and assumptions, we will write down in the form of the equation of the first order

$$Sx_\lambda(S) = d_\lambda x_\lambda(S) + \eta_\lambda Z_\lambda(S) + b_0 \gamma_\lambda(S), \quad (16)$$

where d_λ, η_λ - the constant factors defined from expression

$$W(S) = \frac{\frac{b_0}{S + \tau}}{S^2 + \lambda_1 S + \lambda_0}.$$

For $W(S)$ the second order we have

$$d_\lambda = -(\lambda_1 - \tau); \quad \eta_\lambda = -(\lambda_0 - d_\lambda \tau).$$

Expressions (15) and (16) presented in a frequency form we will write down in a time domain in the form of system of the differential equations of the first order

$$\begin{vmatrix} \dot{x}_\lambda \\ \dot{z}_\lambda \\ \dot{\gamma}_\lambda \end{vmatrix} = \begin{vmatrix} d_\lambda & \eta_\lambda & b_0 \\ 1 & -\tau & 0 \\ 0 & 0 & -\tau \end{vmatrix} \bullet \begin{vmatrix} x_\lambda \\ z_\lambda \\ \gamma_\lambda \end{vmatrix} + \begin{vmatrix} 0 \\ 0 \\ 1 \end{vmatrix} y_{\text{жс}}. \quad (17)$$

Let's notice that the system (17) represents object (5) at $n = 2$ in not to the minimum initial form.

Similarly considered above we will enter error vector

$$e(t) = g(t) - g_\lambda(t), \quad (18)$$

where $g_\lambda^T(t) = (x, z, \gamma)$ - a state vector (17); $g(t)$ - a vector having structure $g_\lambda(t)$ for real operated process.

The differential equation to which satisfies a vector $e(t)$ looks like

$$\dot{e}(t) = \tilde{A}_\lambda e(t) + \Delta \tilde{A} g(t), \quad (19)$$

where $\tilde{A}_\lambda, \Delta \tilde{A}$ - matrixes of known structure

$$\tilde{A}_\lambda = \begin{vmatrix} \alpha_\lambda & \eta_\lambda & \lambda_0 \\ 1 & -\tau & 0 \\ 0 & 0 & -\tau \end{vmatrix}, \Delta\tilde{A} = \begin{vmatrix} \alpha - \alpha_\lambda & \eta - \eta_\lambda & b_0 - \lambda_0 \\ 0 & 0 & 0 \\ 0 & 0 & 0 \end{vmatrix}.$$

Lyapunov function in this case we choose in the form of square-law function

$$V(e, \tilde{A}_1) = e^T R e + A_1^T A_1.$$

Here $R = R^T$ - a numerical positive and certain matrix; A_1 - the vector which elements are equal to the corresponding elements of the first line of a matrix $\Delta\tilde{A}$.

The derivative $\dot{V}(e, \tilde{A}_1)$ taking into account formulas (18) and (19) is defined by the equation

$$\dot{V}(e, \tilde{A}_1) = e^T (\tilde{A}_\lambda R + R\tilde{A}_\lambda^T) e + \tilde{A}_1^T \tilde{c}^T R e + e^T R c \tilde{A}_1 + \tilde{A}_1^T \dot{\tilde{A}}_1 + \tilde{A}_1^T A_1, \quad (20)$$

where \tilde{c} - a matrix at which the first line is equal $g(t)$ and other lines are equal to zero.

From (20) follows that if algorithm of estimation of parameters of mathematical model of real operated process to choose in a look

$$\frac{d}{dt} \tilde{A}_1(t) = -\tilde{c}^T R e(t), \quad (21)$$

that we have

$$\dot{V}(e, \tilde{A}_1) = e^T (\tilde{A}_\lambda R + R\tilde{A}_\lambda^T) e.$$

We believe that the matrix \tilde{A}_λ satisfies to a condition

$$\tilde{A}_\lambda R + R\tilde{A}_\lambda^T = -T,$$

where T - any numerical positive and certain matrix. Then the considered system which state vector it is equal (e^T, A_1^T) it is steady according to Lyapunov.

The algorithm of formation of control is supplemented with two differential equations

$$\dot{g}_\lambda(t) = \tilde{A}_\lambda g_\lambda(t) + \tilde{b}_\lambda y_{\text{жс}},$$

$$\dot{\tilde{A}}_1 = -\tilde{c}^T R e(t).$$

So, the algorithm of adaptation which is not demanding measurement of a full state vector but only operated coordinate and fictitious variables is received.

References

1. Sage E.P., White Ch.S. Optimum control of systems. - M: Radio and communication, 1982.
2. Krutko P.D. Return problems of dynamics of operated systems. Linear models. - M: Science, 1987.
3. Petrov V.M., Vorobyov A.V., Kulikov V.E., Kharkov V.P. Way of plane flight control. Patent for the invention. RUS 2249540 2/6/2003.
4. Verba V.S., Kapustyan S.G., Merkulov V.I., Kharkov V.P. Optimization of radio-electronic control systems. Methods and synthesis algorithms of optimum control. Part 1. Classification of methods of the solution of a problem of optimum control. Method of dynamic programming. Principle of a maximum of Pontryagin. // Information and measuring and managing directors of system. 2012. Vol.10. No. 12. Page 3-16.

5. Halyutin S.P. Problems of creation of steering drives for control systems of flight. //Sensors and systems. 2003. No. 7. Page 22-26.

MONITORING AND DIAGNOSIS OF OBSERVABLE DYNAMICAL SYSTEMS BY THE USE OF COMBINED GOODNESS-OF-FIT TESTS

Chernodarov, A.

Moscow, “NaukaSoft” Experimental Laboratory

This paper is devoted to the problem of increasing the diagnosis confidence, diagnosis operativeness, and diagnosis depth in observable dynamical systems (DSs). The proposed solution of the above problem relies on the decomposition of DS diagnostic models, on the application of combined goodness-of-fit tests, and on the processing of observations in “forward” and “backward” time. The results of experimental studies are given.

Keywords: dynamical system, diagnosis, goodness-of-fit tests

1. An Observable Dynamical System as the Object of Monitoring and Diagnosis

At present, the problem of increasing the reliability of dynamical systems (DSs), which are part of complex engineering objects and which significantly affect their safety still remains topical. Analytical approaches to the solution of the problem mentioned above are based on the detection, counteraction, and prevention of faults. To accomplish this, in observable DSs, use is made of diagnostic models and external information. A technology for the formation of such models relies on a mathematical description of the functioning of both the reference (unperturbed) DS and an actual (perturbed) DS. The ideal vector $Y(t)$ and the actual vector $Y_p(t)$ of state parameters are made to correspond to such DSs; these vectors are described by the following differential equations:

$$\text{for the ideal DS:} \quad \dot{Y}(t) = F[Y(t)]; \quad (1)$$

$$\text{for an actual DS:} \quad \dot{Y}_p(t) = F[Y_p(t)] + G(t)\xi(t), \quad (2)$$

where $\xi(t) = [\xi_1(t) \dots \xi_r(t)]^T$ is the vector of disturbances that affect the DS, which is characterized by the covariance matrix $M[\xi(t)\xi^T(t-\tau)] = Q(t)\delta(t-\tau)$; $\delta(t-\tau)$ is the delta-function; $M[\dots]$ is the operator of mathematical expectation; $G(t)$ is the matrix of disturbance intensities.

Parameters of the ideal DS and the actual DS are related by the following error equation:

$$\frac{dx(t)}{dt} = \dot{x}(t) = A(t)x(t) + G(t)\xi(t), \quad (3)$$

where $x(t) = \Delta Y(t) = Y_p(t) - Y(t)$ is the vector of DS errors; $A(t) = \frac{\partial F[Y_p(t)]}{\partial Y}$ is the matrix of coefficients that characterize the dynamics of variation of DS errors.

The estimates $\hat{x}(t)$ of DS errors are obtainable through the use of an optimum Kalman filter (OKF) [1] by processing the following observations:

$$z(t) = h[Y_p(t)] - h[Y(t)]_{SEI}, \quad (4)$$

where $h[Y(t)]_{SEI}$ is an observed value formed by the sensor of information that is external (SEI) with respect to the DS, and the above observed value has the model $h[Y(t)]_{SEI} = h[Y(t)] + \mathcal{G}(t)$; $\mathcal{G}(t)$ is the vector of perturbations in a measuring channel, which has the covariance matrix $M[\mathcal{G}(t)\mathcal{G}^T(t-\tau)] = R(t)\delta(t-\tau)$.

In the OKF, the interrelation of observations (4) and DS errors is taken into account via the following mathematical model:

$$z(t) = H(t)x(t) + \mathcal{G}(t), \quad (5)$$

where $H(t) = \frac{\partial h[Y(t)]}{\partial Y}$ is the matrix for the relation of observed parameters and the vector of DS errors.

An observable dynamical system with the OKF in an error estimation loop can be represented by a diagram shown in Figure 1, where U is the vector of control actions; CAMS is a computer-aided monitoring system; CC is a coordinate converter. It should be noted that as a SEI, use can be made of the mathematical model of the reference DS.

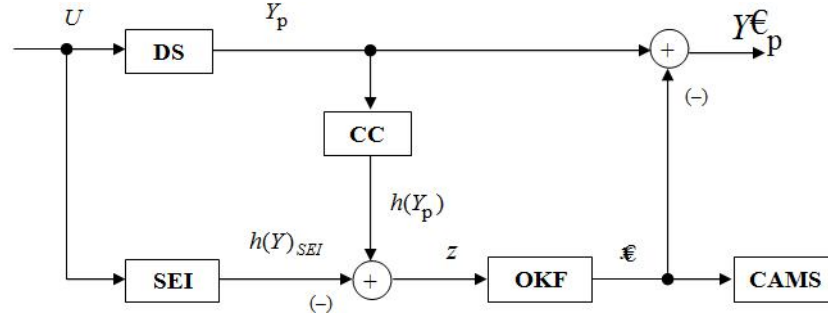


Figure 1. Block diagram of an observable DS with the OKF in an error estimation loop

The CAMS can depend for its functioning on the estimation of DS errors. In that case, however, it will be necessary to put each set of DS technical states in correspondence with its own equations of the form (3). Moreover, the problem of making DS current status consistent with the appropriate model from the bank of estimation filters arises [2, 3], but this is difficult to attain in practice. That is why, it is expedient to elaborate monitoring algorithms on the basis of equations of the form (3), which are tuned to the DS serviceable condition. In view of this, diagnostic parameters can be formed which have to reflect a deviation of the DS actual condition from its serviceable condition. The above-mentioned parameters are selected so that formalized tolerances can be justified for them.

The purpose of this paper is to increase diagnosis confidence in observable dynamical systems on the basis of combined goodness-of fit tests.

2. Monitoring by a Generalized Parameter on the Basis of the χ^2 Test

Statistical properties of the optimum Kalman filter permit one to form diagnostic parameters on the basis of the following vector of residuals:

$$v_i = z_i - H_i \Phi_i \hat{x}_{i-1} = [v_{1(i)} v_{2(i)} \dots v_{j(i)} \dots v_{l(i)}]^T, \quad (6)$$

where $z_i = z(t_i)$ is the vector of observations at the i -th instant of time; Φ_i is the transition matrix for the vector of errors, which is determined from the solution of the following differential equations:

$$\frac{d\Phi(t, t_{i-1})}{dt} = \dot{\Phi}_i = A(t)\Phi(t, t_{i-1}) \quad \text{for} \quad \Phi(t_{i-1}, t_{i-1}) = E,$$

where E is an identity matrix of the appropriate dimension.

It is known [3, 4] that for a DS the model of errors of which is tuned to the serviceable condition the vector of residuals has the Gaussian (normal) distribution with zero expectation and the covariance matrix α_i , i.e., $v_i \in N(0, \alpha_i)$ (7).

Taking into consideration the principle of orthogonality of optimal estimations $M[e_i g_i^T] = 0$, we can show that

$$\alpha_i = M[v_i v_i^T] = H_i \Phi_i P_{i-1} \Phi_i^T H_i^T + R_i, \quad \text{where } P_i = M[e_i e_i^T]; \quad e_i = x_i - \hat{x}_i. \quad (8)$$

The application of the traditional OKF presupposes simultaneous processing of all components of the vector z_i of observations, having regard to predicted values of the estimates $\hat{x}_{i/i-1}$. Therefore, to monitor the DS status, it was necessary to check whether the vector v_i is an l -dimensional Gaussian sequence. In practice, however, the solution of this problem is a matter of some difficulty. In this connection, computationally more compact diagnostic parameters are formed on a basis of the vector of residuals. Such parameters rely on the following convolution of the vector v_i of residuals with the use of the covariance matrix α_i :

$$J_i = v_i^T \alpha_i^{-1} v_i. \quad (9)$$

In quadratic form (9), elements of the matrix α_i are considered as normalizing factors that take into account information about the required DS statistical characteristics.

It can be shown [4] that if the vector v_i of residuals has the Gaussian (normal) distribution, quadratic form (9) is distributed as χ^2 with l degrees of freedom, namely:

$$J_i \in \chi^2(l, 2l), \quad (10)$$

i.e., the dimension l of the vector of residuals is equal to the mathematical expectation of the parameter J_i and to one-half of its variance.

Thus, relation (10) determines a necessary condition for DS correct operation. Inasmuch as the quadratic form J_i combines all of the l components of the vector v_i of residuals, it may be considered as a DS generalized parameter.

DS correct operation can be put in correspondence with the range of permissible values of the parameter J_i . When a tolerance on the above-mentioned parameter is justified, it is essential to take into account both numerical characteristics for the χ^2 distribution and a given significance level for the monitoring criterion. In the implementation of these requirements, use can be made of the properties of the quantile $a(l)$ for the χ^2 distribution, namely:

$$P\{J_i > J_{T, a(l)}\}, \quad (11)$$

where $J_{T, a(l)}$ is a tabular value of the parameter J for the given quantile $a(l)$ and for the number l of degrees of freedom; $a(l)$ is the quantile of order a , $a \in (0, 1)$.

An analysis of tabular data shows that quantile (11) reflects the “three-sigma rule” with a sufficiently high accuracy. Such a rule finds use in the processing of normal random scalars and it reduces to the following.

The normal random variable ξ takes on different values that are close to its mathematical expectation with a high probability, namely:

$$P\{|\xi - M[\xi]| \geq k\sigma\} = \begin{cases} 0.3173..., & k = 1; \\ 0.0455..., & k = 2; \\ 0.0027..., & k = 3. \end{cases} \quad (12)$$

For $k=3$, relation (12) reflects the rule of 3σ for the normal distribution law. Hence, we can state with fiducial probability 0.9973 that a necessary condition for the random variable ξ to belong to the normal law is the following:

$$|\xi| \leq |M[\xi]| + 3\sqrt{D[\xi]}, \quad (13)$$

where $D[\dots]$ is an operator for variance.

By analogy with rule (13) and with consideration for the quantile 0.02 (l) we can state with fiducial probability 0.98 that a necessary condition for the parameter J_i to belong to the χ^2 distribution is the following:

$$J_i \leq \gamma_l^2 = M[J_i] + 3\sqrt{D[J_i]} = l + 3\sqrt{2l}. \quad (14)$$

Thus, the quantity γ_l^2 determines the range of permissible values of the parameter J_i in the DS correct operation. In view of the tolerance γ_l^2 , DS monitoring by a generalized parameter on the basis of the χ^2 test reduces to testing the following conditions:

$$\left. \begin{array}{l} \text{if } J_i \leq \gamma_l^2, \text{ there are no faults in the DS;} \\ \text{if } J_i > \gamma_l^2, \text{ there are faults in the DS.} \end{array} \right\} \quad (15)$$

Monitoring by the generalized parameter J_i permits one to estimate the DS status as a whole, without analyzing the question of due to which of the parameters of the vector of observations a fault has most probably taken place. In actual practice, the need arises for estimation of the DS status for each of the components of the vector z_i , i.e., for execution of DS diagnosis with a depth of an observed parameter.

3. Diagnosis by a Generalized Parameter on the Basis of the χ^2 Test

The diagnosis problem can be solved if observation errors are statistically independent (uncorrelated), i.e., if the matrix R_i in relation (8) is a diagonal matrix. If observations are cross-correlated, their preliminary decomposition is performed [4]. Taking this into account, it is apparently possible to carry out channel-wise (element-by-element) processing of the vector of observations (6) and to analyze the status of each of the l measuring channels. For example, in order to monitor the j -th measuring channel, use can be made of the normalized residual $\beta_j = \nu_j / \alpha_j$, where α_j is a scaling parameter; $j = \overline{1, l}$. When observations are processed in “forward” time, the residual ν_j is the difference $\nu_j = z_j - \hat{z}_j$ in value between the actual observation z_j and the predicted observation $\hat{z}_j = H_j \hat{m}_j$, where

$\hat{m}_j, \hat{x}_{i/i}$ are estimates of the DS error vector x_i at the i -th step after the j -th component and the whole of the vector z_i of observations are processed, respectively. H_j is the row vector of

coupling coefficients. Statistical properties of the parameter β_j^2 can be used for the construction of decision rules. For the above parameter, by analogy with generalized parameter (9), for $l=1$, a necessary condition for DS correct operation can be formed for each of the observation channels, namely:

$$\beta_j^2 \in \chi^2(1, 2) \quad (16)$$

or by the rule of 3σ , for the quantile $\alpha(1) = 0.02$,

$$\beta_j^2 \leq \gamma_1^2 = M[\beta_j^2] + 3\sqrt{D[\beta_j^2]} = 1 + 3\sqrt{2} \cong 5.2. \quad (17)$$

When the tolerance γ_1^2 is taken into account, DS channel-wise monitoring by the χ^2 test reduces to testing the following conditions:

$$\left. \begin{array}{l} \text{if } \beta_j^2 \leq \gamma_1^2, \text{ there are no faults in the DS for the } j\text{-th channel of observations;} \\ \text{if } \beta_j^2 > \gamma_1^2, \text{ there are faults in the DS for the } j\text{-th channel of observations.} \end{array} \right\} \quad (18)$$

4. Diagnosis by a Generalized Parameter on the basis of the \mathcal{G}^2 Test

The application of the χ^2 test allows us to detect current faults in a DS. In actual practice, the need also arises for the accumulation and analysis of information about DS operation over a certain period of time. Using the retrospective data as the base, the appropriate diagnostic parameters may be determined. A technology for the sequential processing of components of the vector of observations permits one to form such parameters from the sample of residuals on a moving time interval. For this purpose, use can be made of the ergodic properties of output parameters of the OKF that is “a priori” tuned to the DS correct operation. Such parameters are variances of the residuals in each of the l channels of DS status observation. The predicted value α_j of variance in the j -th channel of observations

at the i -th instant of time is determined by relation (8), and its estimate $\hat{\alpha}_j(i)$ is determined using the actual sample of residuals, i.e.,

$$\hat{\alpha}_j(i) = \frac{1}{N-1} \sum_{k=i-N+1}^i [v_{j(k)} - \bar{v}_{j(i)}]^2; \quad j = \overline{1, l}, \quad \text{where } \bar{v}_{j(i)} = \frac{1}{N} \sum_{k=i-N+1}^i v_{j(k)} \text{ is an}$$

estimator of the mathematical expectation of the residual in the j -th channel of observations at the i -th instant of time; N is the number of samples of the residual on the moving time interval $T = [t_{i-N+1}, t_i]$.

As a parameter that characterizes the DS status on the time interval T , the quotient of the actual variance $\hat{\alpha}_j$ and the predicted variance α_j can be accepted, i.e.,

$$F_j = \hat{\alpha}_j / \alpha_j. \quad (19)$$

By analogy with expression (7), a necessary condition for DS correct operation for the j -th channel of observations is the following normal distribution of the residual v_j :

$$v_j \in N(0, \alpha_j). \quad (20)$$

It is known [5] that when condition (20) is satisfied, parameter (19) has the \mathcal{G}^2 distribution (Fisher distribution), namely:

$$F_j \in \mathcal{G}^2(a, b), \quad (21)$$

where $a = \frac{N}{N-2}$; $b = \frac{4N(N-1)}{(N-2)^2(N-4)}$ are tabulated values of the mathematical expectation and variance for the parameter F_j .

If we use the rule of 3σ (13), for the quantile $a = 0.02$ and $N = 20$, condition (21) can be represented as

$$F_j \leq \eta_1^2 = M[F_j] + 3\sqrt{D[F_j]} = a + 3\sqrt{b}. \quad (22)$$

When the tolerance η_1^2 is taken into account, DS channel-wise monitoring by the \mathcal{G}^2 test reduces to testing the following conditions:

$$\left. \begin{array}{l} \text{if } F_j \leq \eta_1^2, \text{ there were no faults in the DS for the } j\text{-th channel of observations} \\ \quad \text{on the time interval } T = [t_{i-N+1}, t_i]; \\ \text{if } F_j > \eta_1^2, \text{ there were faults in the DS for the } j\text{-th channel of observations} \\ \quad \text{on the time interval } T = [t_{i-N+1}, t_i]. \end{array} \right\} \quad (23)$$

Procedure (23) supplements test (18) in the interests of improving the diagnosis confidence.

5. Diagnosis by the χ^2 / \mathcal{G}^2 Combined Goodness-of-Fit Test

In the implementation of DS diagnosis procedures, the problem of detecting outliers against the background of sudden and gradual failures arises. When recognizing such faults, it is apparently possible to counteract outliers without switching the DS off. The solution of the problem mentioned may be based on combining the χ^2 and \mathcal{G}^2 tests. Indeed, the inclusion of the procedure of diagnosis by the χ^2 test in the structure of an estimation filter permits one to detect current faults in a DS (both outliers and failures). The diagnostic parameter F_j , which is formed for estimation of the DS status by the \mathcal{G}^2 test is determined from a set of the ν_j residuals on a moving time interval. Outlying signals used to compute such a parameter are averaged, and they have an insignificant influence on the results of diagnosis by the \mathcal{G}^2 test. At the same time, gradual failures and sudden ones which are characterized by constant biases of the residuals with respect to their nominal values cause the diagnostic parameter F_j to be out of tolerance. Therefore, if faults are detected by both of the tests, a failure has more probably occurred in the j -th channel of observations, and if faults are detected only by the χ^2 test, an outlier has most probably taken place.

A technology intended to counteract faults reduces to the following. When there is no discordance, the residual ν_j is processed by the OKF, a failure is counteracted by connecting a redundant channel, and an outlier is counteracted by the adaptive robust processing of the residual with the use of the influence function $\psi(\beta)$ [4]. This function determines the level of confidence in incoming observed values.

The procedures presented here make it possible to carry out DS diagnosis with a depth of the component of the vector of the residuals v_i . At the same time, in practice, the necessity for detection of faults for each component of the vector of DS status arises.

1. Diagnosis of Dynamical Systems on the Basis of Complex Processing of Experimental Data in “Forward” and “Backward” Time

DS diagnosis with a depth of components of the state vector (SV) can be performed on a basis of the coprocessing of observation signals in “forward” (filtering) and “backward” (smoothing) time. In this case, at the stage of smoothing, the set of SV components can be extended with respect to the base SV that is formed in filtering. The parameters that characterize the design features of a DS can be included in the state vector, too.

Generalized parameters that respond to a discrepancy between the SV components enter structurally in the following quadratic form:

$$J_i = v_{i/N}^T \Delta P_i^{-1} v_{i/N}, \quad (24)$$

where $v_{i/N} = \delta_{f(i)} - \delta_{s(i)} = T\Phi_{i+1}^{-1}\hat{x}_{i+1/N} - \hat{x}_{i/i}$; $\delta_{f(i)} = x_i - \hat{x}_{i/i}$;

$$\delta_{s(i)} = \Phi_{i+1/N}^{-1}(x_{i+1} - \hat{x}_{i+1/N}); \quad \Delta P_i = P_{i/i} + T\Phi_{i/N}^{-1}P_{i+1/N}\Phi_{i/N}^{-T}T^T;$$

$\hat{x}_{i/i}, \hat{x}_{i/N}$ are estimates of the SV x_i at the i -th instant of time, and these estimates are obtained from observations at the stage of filtering and smoothing, respectively; $P_{i/i}, P_{i/N}$ are the covariance matrices of the above estimates; $\Phi_{i/N}$ is the transition matrix for an extended SV; T is the matrix of coupling between the extended SV $\hat{x}_{i+1/N}$ and the base SV $\hat{x}_{i/i}$; $\Phi^{-T} = (\Phi^{-1})^T$.

Stable smoothing ($|\delta| < 3\sigma$), which reflects the good DS state is characterized by the following distribution of the residual $v_{i/N}$ and the quadratic form J_i :

$$v_{i/N} \in N(0; \Delta P_i); \quad J_i \in \chi^2(n; 2n), \text{ where } n \text{ is the SV dimension.}$$

In view of the statistical properties of the χ^2 distribution and in view of the rule of 3σ , necessary conditions can be formed for the good state (“no” outliers and “no” failures) of the DS as a whole, i. e., $J_i \leq n + 3\sqrt{2n}$ and for the j -th component of the SV in particular, i. e.,

$$J_{i(j)} = J_{i(j-1)} + \frac{\tilde{v}_{i/N(j)}^2}{\Delta D_{i(j)}} \leq \gamma_j^2 = j + 3\sqrt{2j}, \quad \text{where } \tilde{v}_{i/N} = \Delta U_i^{-1} v_{i/N};$$

$\Delta U_i^{-1}; \Delta D_i^{-1}$ are an upper triangular matrix with identity diagonal and a diagonal matrix, respectively; these matrices are obtained by the following orthogonal transformation:

$$\Delta P_i^{-1} = \Delta U_i^{-T} \Delta D_i^{-1} \Delta U_i^{-1}; \quad (25)$$

$\Delta D_{i(j)}^{-1}$ is the j -th element of the diagonal matrix ΔD_i^{-1} .

Taking into account decomposition (25) and the properties of the Fisher statistic [4]

$$F_j = \frac{\hat{\alpha}_{(i/j)}}{\Delta D_{(i/j)}} \in \mathcal{G}^2(a, b),$$

one can form a necessary condition for the operable DS condition (“no” failures) for the j -th component of the SV, i.e., $F_j \leq \eta_j^2 = a + 3\sqrt{b}$,

where $\hat{\sigma}_{(i/j)}$ is an estimate of the variance of the residual $v_{i/N(j)}$ on a moving time interval. For DSs, a diagnosis diagram that is based on the postprocessing of experimental data is shown in Figure 2, where $Q_i; \Gamma_i$ are the covariance and transition matrices for the vector of DS perturbations.

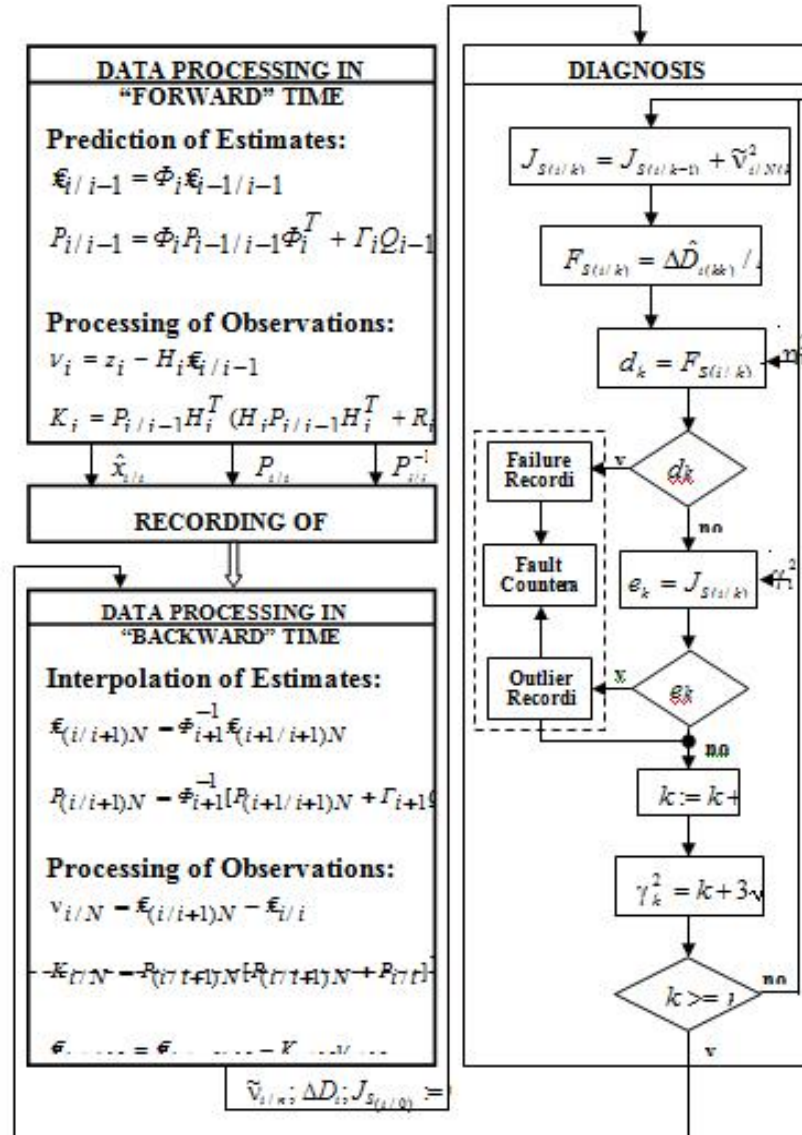


Figure 2. Block diagram of the diagnosis of dynamical systems on the basis of joint procedures of optimal filtering and smoothing

7. Analysis of the Results of Studies

In Figures 4 and 5, characteristic results of the studies of an algorithm for the diagnosis by the recorded data are presented using a one-channel inertial navigation system (INS) as an example. An accelerometer failure at the 500-th second has been simulated. Such a failure indirectly makes itself evident during filtering for the velocity observation channel when the generalized parameter β_V^2 is above upper tolerance. In postprocessing the recorded estimates and during the diagnosis by the algorithm shown in Figure 2, it is possible to determine which of the INS sensors – an accelerometer or a gyro – has most probably caused a fault. Figures 3 and 4 show the dynamics of variation of the estimates of both the bias of the

a_x accelerometer output signal and the ω_x gyro drift when velocity observations are processed in “forward time” and when the estimates mentioned are refined in “backward time”. During the post-flight diagnosis, a failed accelerometer is isolated if the generalized parameters J_{Saj} (the χ^2 test) and F_{Saj} (the g^2 test) are above upper tolerances (see Figure 3). It can also be seen (see Figure 4) that the accelerometer failure has had an insignificant influence on the variation of the generalized parameters $J_{S\omega j}$ and $F_{S\omega j}$, which characterize the status of the ω_x gyro. Thus, combined processing of observations in “forward” and “backward” time enables us to solve diagnosis problems with a depth of the component of the state vector of a dynamical system.

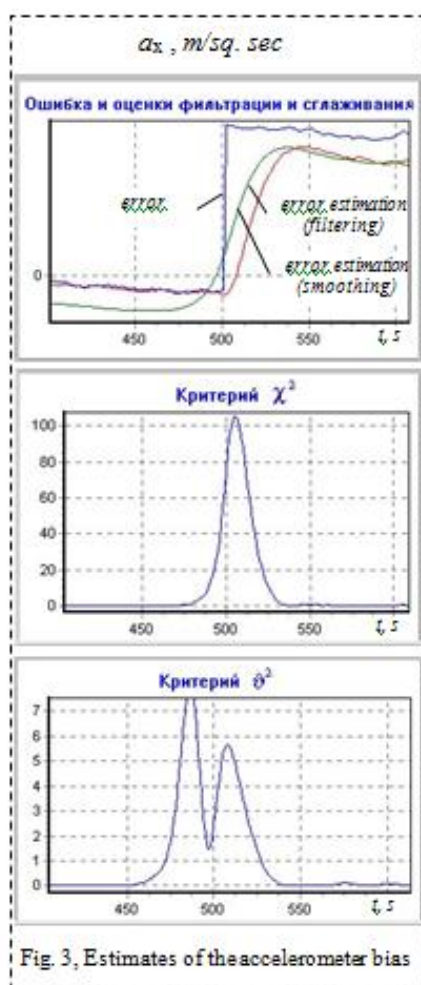


Fig. 3. Estimates of the accelerometer bias

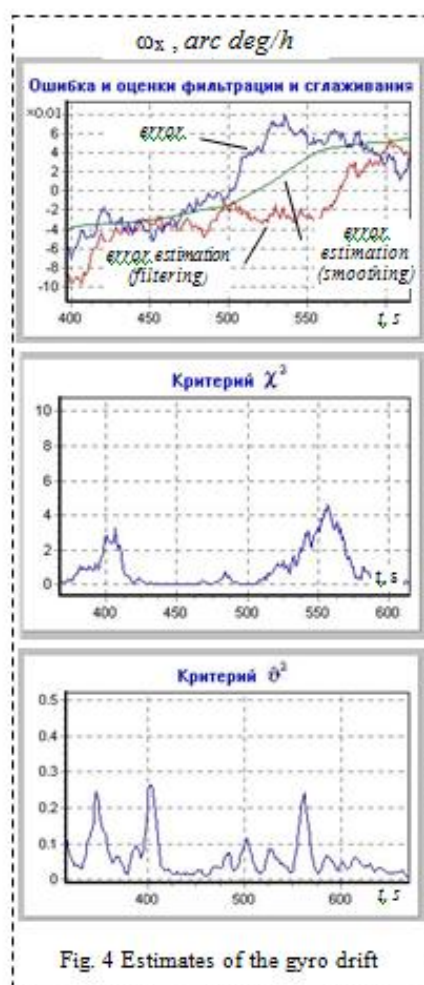


Fig. 4 Estimates of the gyro drift

Conclusions

The diagnosis technology presented here permits one to detect DS faults with a depth of the component of the state vector on a basis of the joint procedures of optimal filtering and smoothing of experimental data, to increase the confidence and operativeness in the detection of and counteraction to faults through the analysis of generalized state parameters by the use of combined goodness-of-fit tests, to select outliers against the background of failures.

References

1. I.N. Sinitsin. Kalman and Pugachev Filters [in Russian]. – M.: Logos, 2007. – 776 p.

2. S.P. Dmitriev, N.V. Kolesov, A.V. Osipov. Information Reliability, Monitoring and Diagnosis of Navigation Systems [in Russian]. – SPb: CSRI «Electropribor», 2003. – 207 p.
3. J.J. Gertler. Fault Detection and Diagnosis in Engineering Systems. – N.Y.: Marcel Dekker, 1998. – 484 p.
4. L.P. Kolodezny, A.V. Chernodarov. Reliability and Engineering Diagnostics [in Russian]. – M.: Zhukovsky and Gagarin Air Force Academy, 2010. – 452 p.
5. V.S. Korolyuk, N.I. Portenko, A.V. Skorokhod, and A.F. Turbin. A Handbook of Probability Theory and Mathematical Statistics [In Russian]. – M.: Nauka, GRFML, 1985. – 640 p.

COMPUTER USAGE IN THE ANALYSIS OF VALIDITY OF DECISION MAKING CRITERIA.

Klochkov, U.S., Mikshina, V.S.
Surgut, SurGU; Surgut, SurGU;

This article aims to basic requirements for checking the validity of decision making support system indicators using a computer. The analysis algorithm of the validity of decision-making indicator will be considered in the article and the requirements to the algorithms on computers, determining the validity of the indicator, will be defined. As an example the indicator of stock market behavior RSI will be used.

Keywords: indicator, criterion, validity, the decision support system, RSI.

The introduction of computer technology leads to the widespread use of making decision support systems. Part of these systems provides a recommendation as a signal (to commit acts) in the case of fulfillment of conditions of specified indicator. The indicator is understood as a complex index of system parameters, allowing to analyze the condition of the system. An important issue is determining the validity of the indicator. The validity of indicator consists in the universality over various data and efficiency of the recommendations based on the signals generated by the indicator. As an example, let us consider the application of the *RSI* indicator with automatic deciding to purchase stocks of JSC "Gazprom" with the frequency of data every 5 minutes. In reviewing the model of decision-making system some generalizing assumptions will be taken:

1. purchase and sale of stocks in the experimental data does not affect the movement of the market;

2. you can always buy or sell stocks at a typical price (1) of the current period:

$$TP = (HIGH + LOW + CLOSE) / 3, \quad (1)$$

where TP – typical price, $HIGH$ – the highest price in the period, LOW – the lowest price in the period, $CLOSE$ – the closing price of the period.

Period (timeframe) – time interval used for grouping quotation in the construction of elements of price chart.

Quotation – the price (the rate, the interest rate) of a product, which is set by a buyer or seller, according to this price they are ready to buy or sell.

Note that the work of almost any indicator depends on the external and internal parameters. The following parameters can be identified for *RSI*:

1. The level of smoothing. The smoothed indicator *RSI* (2) is the most frequently used. The notation RSI_K will be used in the article, where K – the period of *RSI* smoothing.

$$RSI(K) = 100 \frac{U(K)}{U(K) + D(K)}, \quad (2)$$

where $U(K)$ – sum of positive changes in closing prices of recent K periods, $D(K)$ – sum of negative price changes for those periods in which the trade session was closed with a decrease in relation to the closing price of the previous period.

2. Criteria for buying in:

a. Desired income percentage P . A desired income is the income at which the transaction will be closed.

b. The maximum period of validity of the transaction T_{max} . The period at which the transaction is closed, regardless of whether it brings a profit at the moment or not.

c. Threshold value of the indicator. There are rules which form RSI signals both for buying and selling (usually it is crossing values in 30 and 70, the type of signal depends on the direction of the function). For already formed signals there is a threshold repealing the last signal – the intersection value of 50 in the direction opposite to the direction of a formed signal. That is a signal to close the transaction, even if it did not bring income.

The usage of computers allows to determine the optimal parameter values directly. But exhaustive search stumbles upon a requirement of limiting parameters. The value of parameter for transaction closing is not limited, that is why exhaustive search is forbidden. Thus, even using the possibilities of computers it is necessary to set empirical restrictions for the criteria. For example, such restrictions for RSI may be the following:

1. The desired profit value can not exceed 50 ($P \leq 50$) (theoretically a leap by 50% during the maximum period is possible, but the probability of such events is very low).

2. The step h between the values of desired profit we will take equal 0.5%.

3. The short term periods are assumed those for which $T_{max} \leq 15$.

These limits may be changed if it is necessary to make more accurate or more advanced analysis. For example, within a period, you can use a step profit h of 0.1 %, resulting in a more accurate value, but will not affect the overall conclusions regarding the use of the indicator. The 15 days limit is selected empirically as limiting concepts of short term investments. In addition, the profit earned through a long term can be obtained not as a result of the correct response indicator, but as a stochastic variable.

Analysis of simultaneous changes of all parameters leads to a large amount of data that are difficult to analyze. To start the analysis we fix the values of variables $P = 5\%$ and $T_{max} = 5$ and analyze the effect of smoothing N on the resulting profits. We assume that every time the indicator signals we form a rate on the maximum number of stocks with a limited amount of 5000 rubles. Rates can be of 2 types: a long position (purchase stocks available for sale) and a short position (sale of stocks, which are not available at the moment, with a engagement of subsequent repayment).

As a control sample we use the data of quotations of stocks OAO Gazprom in 2011 – 2013 years (Table 1).

Table 1

Stocks quotation data. Stocks of JSC “Gazprom” in 2011–2013

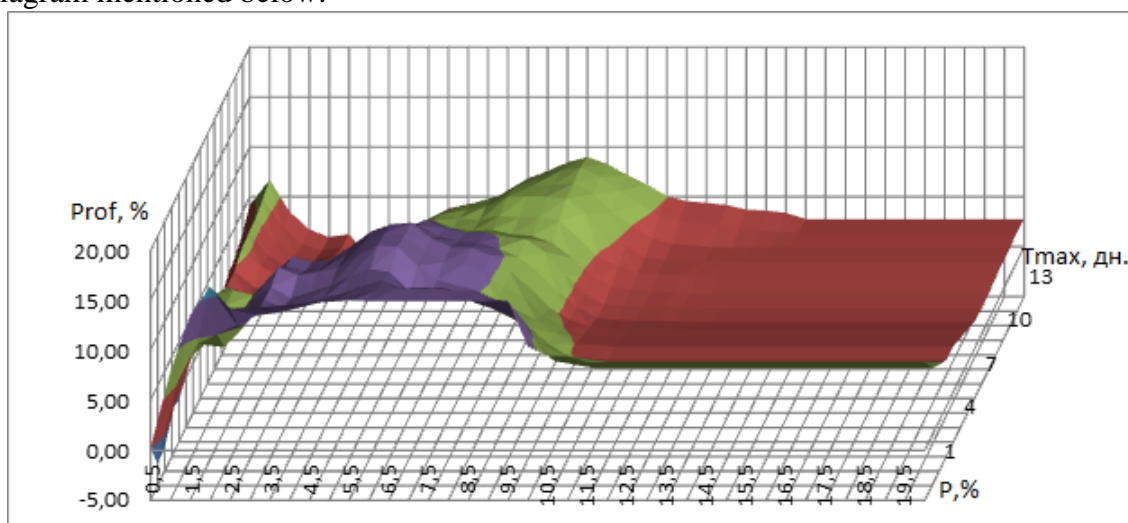
2013 year									
	RSI_1	RSI_2	RSI_3	RSI_5	RSI_10	RSI_20	RSI_40	RSI_60	RSI_80
N	13701	9565	7481	5196	2787	1223	409	155	59
N ₊	4084	3379	3070	2545	1644	726	232	76	24
N _{Tmax}	5883	4077	3173	2223	1141	518	162	63	22
N _P	908	607	486	339	187	65	35	14	6
Sum	95997	55537	46155	27061	10663	–6832	–2405	–4152	–2025
Max	700103	528627	419675	335934	232061	148213	79199	49651	24660
Prof	13,71	10,50	11,00	8,05	4,59	–4,61	–3,04	–8,36	–8,21
2012 year									

	RSI_1	RSI_2	RSI_3	RSI_5	RSI_10	RSI_20	RSI_40	RSI_60	RSI_80
N	14116	9924	7735	5355	2818	1232	385	127	61
N ₊	3448	2990	2809	2429	1569	718	211	68	30
N _{Tmax}	6240	4355	3379	2332	1259	509	143	52	25
N _P	755	532	431	280	137	64	21	5	3
Sum	93296	66785	56442	39950	20057	11778	3172	1205	310
Max	723169	513538	414552	331371	206949	142698	59144,3	49036,9	39222,4
Prof	12,90	13,00	13,62	12,06	9,69	8,25	5,36	2,45	0,79
2011 year									
	RSI_1	RSI_2	RSI_3	RSI_5	RSI_10	RSI_20	RSI_40	RSI_60	RSI_80
N	13017	9061	7178	5033	2683	1170	377	152	67
N ₊	3434	2945	2696	2311	1526	692	199	69	26
N _{Tmax}	4505	3147	2523	1805	960	437	146	51	21
N _P	1938	1350	1050	735	389	154	42	18	6
Sum	57892	42516	25248	8647	1379	-9482	-7613	-4984	-2654
Max	737046	503378	433339	319630	230444	146008	77972,8	44281,3	34217,6
Prof	7,85	8,45	5,83	2,70	0,60	-6,49	-9,76	-11,26	-7,76

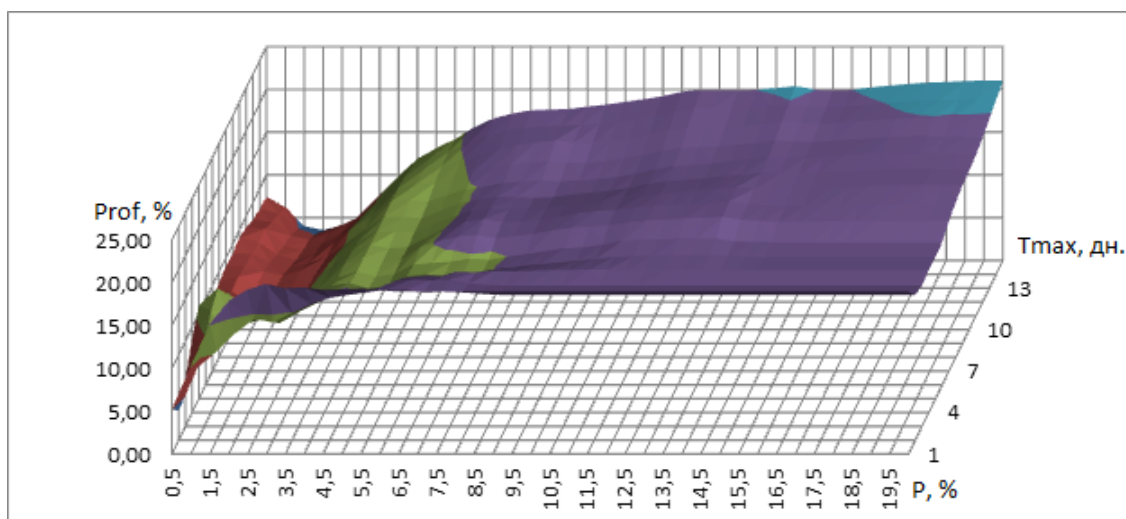
In the table 1 N – the number of indicator activation cases (made rates), N_+ – number of transactions, which brought profit, N_{Tmax} – number of transactions closed because of time limit T_{max} , N_P – number of transactions closed because of attainment the desired income, Sum – total income during the period, Max – the highest amount of all transactions, which are active at the same moment (this number is needed for using all indicator's signals), $Prof$ – profit on invested funds as a percentage, it is calculated as Sum/Max (if we change the amount of invested funds, Sum will change too, but the ratio will not change).

As we can see from analysed data, the increase of K leads to a decrease of $Prof$ and if K become rather big, $Prof$ will become less than zero. The value of parameter K influences on making decision using RSI and we can also note that the optimal value of K is not permanent. Thus, in 2013 the optimal value of K was 1, in 2012 – 3, in 2013 – 2. The most efficient value was 1.

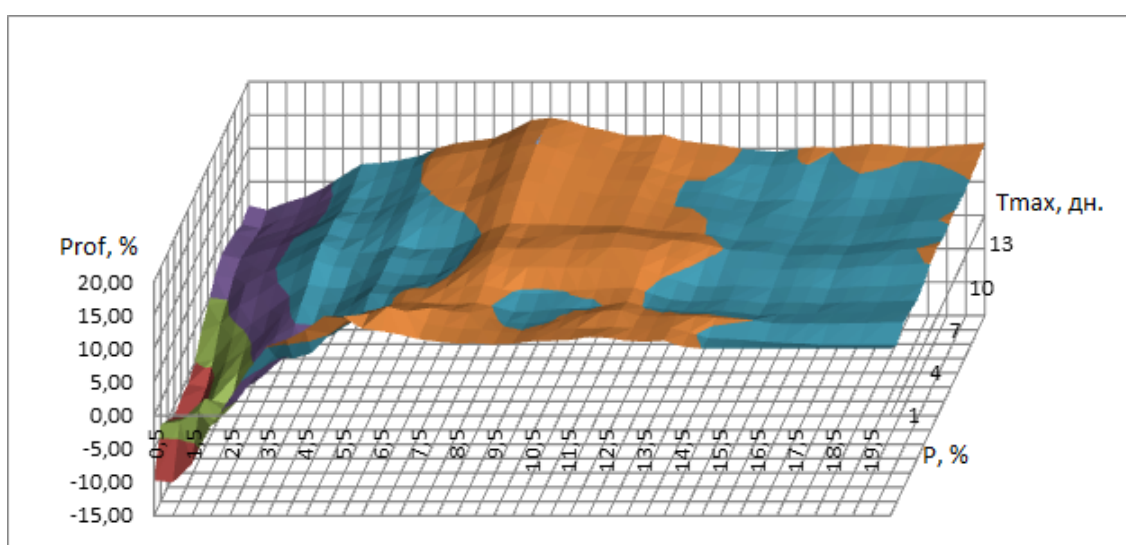
Let us now analyze the influence of P and $Tmax$ on $Prof$. On the basis of presented data the dependence $Prof = f(P, T_{max})$ was figured out and the result was presented within three diagram mentioned below.



Pic. 1. The dependence $Prof = f(P, T_{max})$. Year 2013, RSI_1.



Pic. 2. The dependence $Prof = f(P, T_{max})$. Year 2012, RSI_1 .



Pic. 3. The dependence $Prof = f(P, T_{max})$. Year 2011, RSI_1 .

The analysis of these diagrams is resulted by a conclusion that the values of RSI_1 are not permanent in time and this indicator is not universal and cannot be used in long term case in automatic mode.

To sum up, in this article basic requirements for analysis algorithm of the validity of decision-making support system indicators using a computer are considered:

- carrying out the heuristic analysis of the data to avoid infinite intervals of values;
- use different time intervals to confirm or disprove quality and constance of indicator work
- analysis of the behavior of optimal indicator values within different time intervals.

References

1. Klochkov, U.S., Mikshina, V.S. Analysis of indicators for shades of automatic control dynamic investment portfolio. Materials of X International Scientific and Practical Conference Innovation based on information and communication technologies, Sochi, 2013, ISSN 2226-6690.

2. R. Pardo, Design, Testing and Optimisation of Trading System, Moscow, 2002, ISBN 5-902270-01-4.

DEVELOPMENT OF NEW DESIGN OF FIBER-OPTIC DIFFERENTIAL PRESSURE SENSOR

Savochkina M.M.
Penza, Penza State University

The purpose of this scientific research is to develop new design of fiber-optic differential sensor based on existing fiber-optic pressure sensor. I used basic terms of engineering and rational mechanics, fiber optics, analytical geometry, sensitivity theory and math modeling to reach my goal.

Introduction

The demand for sensors is growing fast due to the rapid development of automated control systems, the introduction of new technological processes, the transition to flexible automated manufacturing.

Modern engineering level demands sensors not only to have high metrological characteristics, but also to have high reliability, durability, stability, small size, weight and power consumption, compatibility with microelectronic information processing devices at a low cost and low complexity of manufacturing. Fiber-optic pressure sensors (FOPS) satisfy these requirements to the maximum extent.

Currently available sensors and pressure measuring systems based on physical principles such as capacitive, resistive strain gage, inductive etc. In these systems electricity is used as a physical medium, therefore requires additional protection circuits against accidental spark overshoot.

In this research I tried to use an engineering solution from patent RU 2290605. This patent describes an attenuator type of fiber-optic excessive pressure sensor. My goal is to develop the fiber-optic differential pressure sensor (FODPS).

1 Basic concept of fiber-optic differential pressure sensor (based on patent RU 2290605[1])

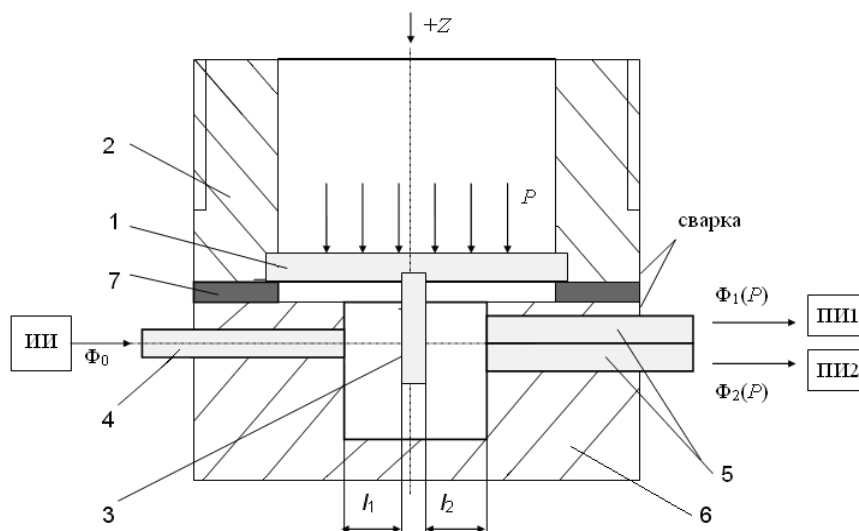


Figure 1 - Simplified structural layout of fiber-optic excessive pressure sensor with cutoff attenuator

Membrane 1 rigidly connected to the fitting 2 (welded, for example) or it is part of fitting 2. Differential cutoff attenuator (shutter) 3 rigidly attached (welded) to the center of membrane. Shutter 3 has round bore, which is opposite to end of feeding optical fiber (FOF) 4 and ends of receiving optical fibers (ROF) 5 of first and second measuring channels accordingly. FOF 4 and ROF 5 rigidly fixed in case 6. Spacer plate 7 used for adjustment of optical fibers against round bore in cutoff attenuator 3. Adjustment is made by changing the thickness of spacer plate 7.

Pressure perceived by membrane 1, wherein attenuator 3 travels vertically between FOF 4 and ROF 5. Shutter 3 movement changes the intensity of light flux coming into ROF. Measuring information transducer in this scheme is differential fiber-optic transducer of microdisplacement (FOTMD).

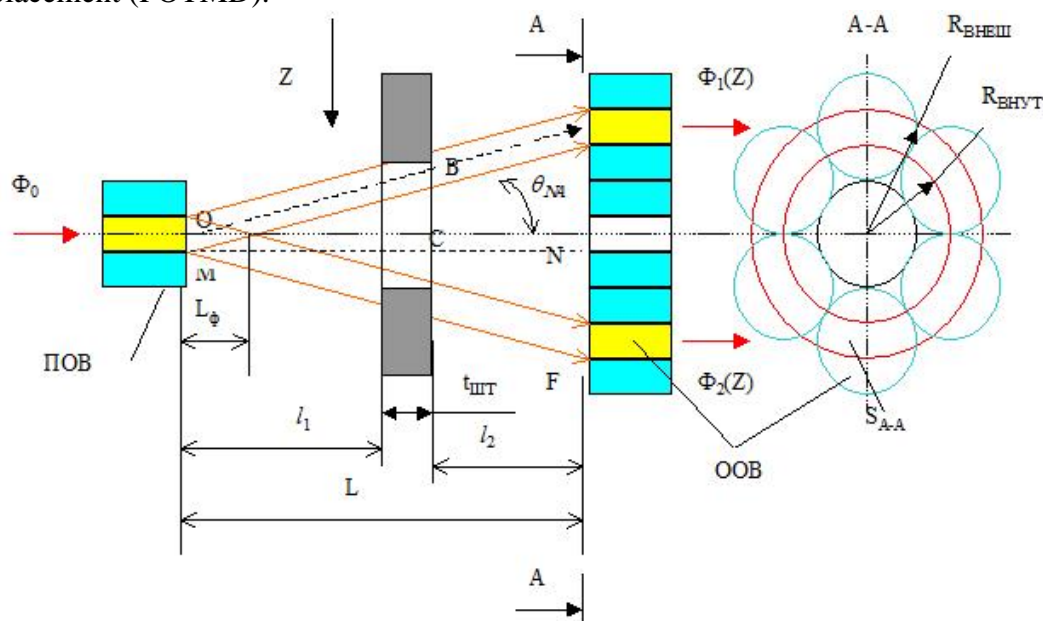


Figure 2 – Simplified structural layout of differential FOTMD with cutoff attenuator and round bore

Operation concept of FOTMD (ref. fig. 1 and 2).

From source III through feeding optic fiber 4 light flux Φ_0 going to attenuator 3. Under the influence of the measured physical quantity (pressure) attenuator moves by an amount Z toward ends of receiving optic fiber. That movement changes intensity of light fluxes $\Phi_1(Z)$ and $\Phi_2(Z)$. Light fluxes going through optic fiber to the radiation receivers (photosensitive semiconductor diodes) ПИ1 and ПИ2 of first and second measuring channels. Radiation receivers convert optical signals into electrical signals I_1 and I_2 . That signals going to input of information processing device.

2 Transfer function of differential fiber-optic transducer of microdisplacement with cutoff attenuator

Transfer function of FOTMD depends from modulation system of optical signal in measurement zone. Modulation of optical signal in FOTMD operating due to the overlap of the light flux by moving opaque screen.

Transfer function $\Phi(Z)$ of FOTMD with cutoff attenuator and round bore be of the form [1]:

$$\Phi(Z) = K_0 K_{шт}(Z) \Phi_0, \quad (1.1)$$

K_0 - coefficient, characterizing the distribution of light in the area of measurement;
 K_{opt} - transmittance of «feeding optical fiber-attenuator-receiving optical fiber» route;
 Φ_0 - light flux from source on FOF end.

It is necessary that the coefficient K_0 is equal to 1. Obviously, when $K_0 = 1$, behavior of the conversion will be evaluated by the behavior of the optical path transfer function, i.e., coefficient $K_{\text{opt}}(Z)$.

Analytical model of measuring transducer when light flux is controlled by attenuator with round bore moving along Z-axis depicted on figure 3.

$$K_{\text{opt}}(Z) = K_{\text{opt}_1}(Z) K_{\text{opt}_2}. \quad (1.2)$$

When FOF and ROF placed coaxially:

$$K_{\text{opt}_1}(Z) = \sum_{i=1}^{n/2} \frac{S_{Z_i}}{S_C} = \frac{\sum_{i=1}^{n/2} S_{Z_i}}{n S_C}, \quad (1.3)$$

$$K_{\text{opt}_2} = \frac{n S_C}{2 S_{A-A}}, \quad (1.4)$$

n —quantity of ROF;

S_{Z_i} —lighted part of ROF core cross-section;

S_C —ROF core cross-section area;

S_{A-A} —light flux cross-section area in image plane A-A (placement of receiving optical fibers ends).

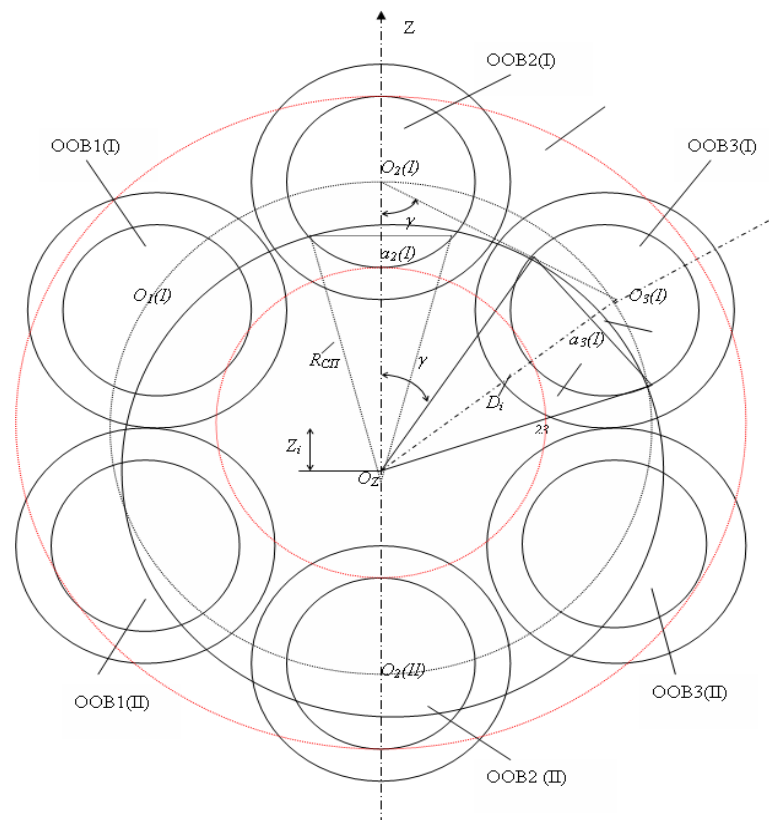


Figure 3 – Analytical model of fiber-optic transducer of microdisplacement with cutoff attenuator and round bore

Accordingly to figure 3:

$$S_{A-A} = \pi R_{BHEII}^2 - \pi R_{BHNT}^2, \quad (1.5)$$

R_{BHEII}, R_{BHNT} – outer and inner diameter of light flux cross-section in image plane A-A (placement of receiving optical fibers ends).

$$R_{BHEII} = d_{OB} + r_C, R_{BHNT} = d_{OB},$$

d_{OB} – OF diameter, r_C – radius of OF core.

Then

$$S_{A-A} = \pi r_C^2 (2d_{OB} + r_C), \quad (1.6)$$

determined by selected optical fiber parameters.

Insert (1.3) - (1.6) into (1.2), we obtain

$$K_{III}(Z) = \frac{\sum_{i=1}^{n/2} S_{Zi}}{2S_{A-A}} = \frac{\sum_{i=1}^{n/2} S_{Zi}}{2\pi r_C^2 (2d_{OB} + r_C)}. \quad (1.7)$$

Cross-section area S_Z determined by attenuator travel along Z-axis.

As an example let's find out S_Z for OOB3:

$$S_{Z3} = S_{13} + S_{23}. \quad (1.8)$$

Area S_{Z3} contains sum of 2 circular sectors S_{13} and S_{23} , formed by the intersection between the two circles: r_C radius, which is equal to OF core radius, and R_{CII} radius, which is equal to light flux cross-section area going through round bore in attenuator in A-A plane.

$$R_{CII} = L \tan \Theta_{NA}, \quad (1.9)$$

L – distance between FOF end and plane which contain ROF ends;

Θ_{NA} – OF aperture angle.

L distance is selected so light flux in A-

A plane completely overlaps ROF ends in neutral shutter position (when $Z=0$)

From MNF triangle:

$$L = \frac{d_{OB}}{\tan \Theta_{NA}}.$$

Then $R_{CII} = d_{OB}$.

According to figure 3

$$S_{Z3} = \frac{r_C^2}{2} \left(\frac{\pi \alpha_3}{180} - \sin \alpha_3 \right) + \frac{R_{CII}^2}{2} \left(\frac{\pi \beta_3}{180} - \sin \beta_3 \right). \quad (1.10)$$

But

$$\sin \frac{\alpha_3}{2} = \frac{a_3}{2r_C}; \sin \frac{\beta_3}{2} = \frac{a_3}{2R_{CII}}. \quad (1.11)$$

Accordingly

$$\alpha_3 = 2 \arcsin \frac{a_3}{2r_C}, \quad \beta_3 = 2 \arcsin \frac{a_3}{2R_{CII}}. \quad (1.12)$$

Then, using expressions (1.7) - (1.12) for S_{Z3} we get:

$$S_{Z3} = \frac{r_C^2}{2} \left[\left(\frac{\pi}{90} - \arcsin \frac{a_3}{2r_C} - \sin \left(2 \arcsin \frac{a_3}{2r_C} \right) \right) + \right. \\ \left. + \frac{R_{CII}^2}{2} \left[\left(\frac{\pi}{90} - \arcsin \frac{a_3}{2R_{CII}} - \sin \left(2 \arcsin \frac{a_3}{2R_{CII}} \right) \right) \right] \right]. \quad (1.13)$$

By analogy with the definition of S_{Z3} solve for S_{Zi} , we get

$$S_{zi} = \frac{r_c^2}{2} \left[\left(\frac{\pi}{90} - \arcsin \frac{a_i}{2r_c} - \sin \left(2 \arcsin \frac{a_i}{2r_c} \right) \right) + \right. \\ \left. + \frac{R_{\text{CH}}^2}{2} \left[\left(\frac{\pi}{90} - \arcsin \frac{a_i}{2R_{\text{CH}}} - \sin \left(2 \arcsin \frac{a_i}{2R_{\text{CH}}} \right) \right) \right] \right], \quad (1.14)$$

$i = 1, \dots, n$; where n – quantity of receiving optical fibers.

Analysis of formulas (1.13), (1.14) shows that they be distinguished by a_i parameters. Let's find out a_i parameters.

As an example let's find out $a_3(I)$ of third ROF of first measuring channel OOB3(I) (fibers is placed above Y-axis).

From $A_3O_3(I)O_Z$ triangle

$$a_3 = A_3B_3 = 2 \sqrt{r_c^2 - \left(\frac{D_3}{2} + \frac{r_c^2 - R_{\text{CH}}^2}{2D_3} \right)^2}. \quad (1.15)$$

By analogy with a_3 and D_3 find a_i and D_i , where $i = 1, \dots, n$; where n – quantity of receiving optical fibers.

$$a_i = 2 \sqrt{r_c^2 - \left(\frac{D_i}{2} + \frac{r_c^2 - R_{\text{CH}}^2}{2D_i} \right)^2}. \quad (1.16)$$

Generally, if there is n ROF, placed on the equal distances from optical axis, distance $D_i(I)$ of first measuring channel for fibers placed above Y-axis, counts by formula (1.17), and for second measuring channel fibers placed below Y-axis counts by formula (1.18).

$$D_i(I) = \sqrt{(R_{\text{CH}} + z_i)^2 + R_{\text{CH}}^2 - 2R_{\text{CH}}(R_{\text{CH}} + z_i) \cos \frac{360^\circ}{n}}, \quad (1.17)$$

$$D_i(II) = \sqrt{(R_{\text{CH}} - Z_i)^2 + R_{\text{CH}}^2 - 2R_{\text{CH}}(R_{\text{CH}} - Z_i) \cos \frac{360^\circ}{n}}. \quad (1.18)$$

For the special case, if there is 6 ROF placed on the equal distances from optical axis (seventh fiber runs through the center, providing symmetrical cable design), formulas (1.17) и (1.18) be as follows:

$$D_i(I) = \sqrt{(R_{\text{CH}} + z_i)^2 + R_{\text{CH}}^2 - 2R_{\text{CH}}(R_{\text{CH}} + z_i) \cos 60^\circ}, \quad (1.19)$$

$$D_i(II) = \sqrt{(R_{\text{CH}} - Z_i)^2 + R_{\text{CH}}^2 - 2R_{\text{CH}}(R_{\text{CH}} - Z_i) \cos 60^\circ}. \quad (1.20)$$

With regard of (1.7) - (1.12), (1.18) formula (1.1) for 1 measuring channel (first, for example) be as follows:

$$\Phi_1(Z) = \frac{\Phi_0}{2\pi r_c (2d_{\text{OB}} + r_c)} \times \\ \times \sum_{i=1}^{n/2} \left\{ \frac{r_c^2}{2} \left[\left(\frac{\pi}{90} - \arcsin \frac{a_i}{2r_c} \right) - \sin \left(2 \arcsin \frac{a_i}{2r_c} \right) \right] + \right. \\ \left. + \frac{R_{\text{CH}}^2}{2} \left[\left(\frac{\pi}{90} - \arcsin \frac{a_i}{2R_{\text{CH}}} \right) - \sin \left(2 \arcsin \frac{a_i}{2R_{\text{CH}}} \right) \right] \right\}, \quad (1.21)$$

a_i , D_i defined by (1.16) – (1.18); R_{CH} – (1.19).

Analysis of formula (1.21) depicts that transfer function of differential fiber-optic transducer of microdisplacement with cutoff attenuator is determined by the following parameters:

- r_c core radius, d_{OB} outer diameter, Θ_{NA} aperture angle of OF (i.e. type of used OF);
- quantity of ROF n ;
- distance L between feeding and receiving fibers.

2 Development of the fiber-optic differential pressure sensor (FODPS)

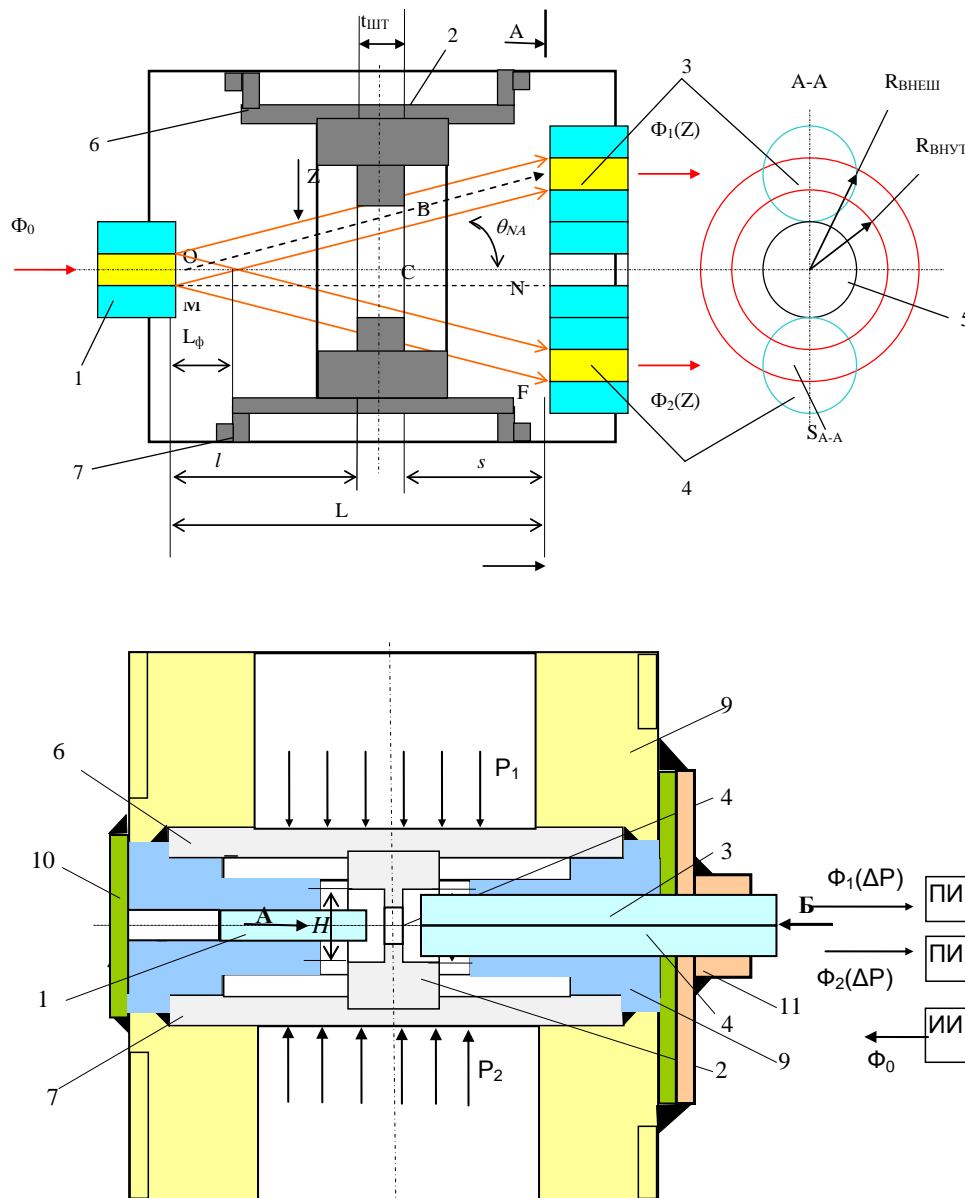


Figure 4 – New fiber-optic differential pressure sensor:

a– Analytical model,

b– Simplified structural layout

FODPS contain: feeding optical fiber (FOF) 1; rod (attenuator) 2 with bore; receiving optical fiber 3 of first measuring channel; ROF 4 of second measuring channel; technologic piece of optical fiber 5; membranes 6 and 7 with solid center (for positive and negative pressure). (ref. figure 4,b).

The left boundary of the bore in rod 2 placed on l distance from end of ROF 1, determined by formula (2.1).

$$l > d_c / 2 \tan \theta_{NA}, \quad (2.1)$$

d_c – OF core diameter

d_{ob} – OF outer diameter

θ_{NA} – OF aperture angle

The right boundary of the bore in rod 2 placed on distance from end of ROF 3 and 4 of first and second measuring channels. Ends of ROF 3 and 4 of first and second measuring channels placed on L distance from FOF 1.

Technologic optical fiber 5 is necessary for symmetrization of ROF 3 and 4. Around technologic optical fiber 5 placed receiving ends of ROF 3 and 4, divided into two equal-size groups of fibers symmetrically arranged one above the other in the direction of rod 2 travel Z (corresponds to the displacement of the center of the membranes under the influence of pressure). Quantity of ROF in the first and second measuring channels are equal to each other (for example, one for each channel).

Optical fibers is rigidly fixed in case, which made of two parts 2 and 6 (ref. figure 4,b). FOF 4 link up with light flux source ИИ and FOF 5 of first and second measuring channels are links up with radiation receivers ПИ1 and ПИ2.

Operation concept of FODPS (ref. figure 4).

Part of light flux from radiation source through FOF 1 going to measuring zone. Light flux Φ_0 from FOF 1 with aperture angle Θ_{NA} falling on shutter in rod 2, coming through it (ref. figure 4,a). Part of light flux $\Phi_1(Z) = \Phi_1(\Delta P)$ coming through bore in shutter and falling on receiving ends of ROF 3 of first measuring channel; other part of light flux $\Phi_2(Z) = \Phi_2(\Delta P)$ falling on receiving ends of FOF 4 second measuring channel. Excess of “positive” pressure over “negative” causes deformation of the membranes 6 and 7; whereby rod 2 moves, which causes bore (in rod 2) movement for Z distance in relation to ROF 3 and 4. Bore movement changes the intensity of light fluxes $\Phi_1(Z)$ and $\Phi_2(Z)$ coming through ROF 3 and 4 to the radiation receivers (photosensitive semiconductor diodes) ПИ13 and ПИ14. Radiation receivers convert optical signals into electrical signals I_1 and I_2 . That signals going to input of information processing device (IPD).

IPD is placed in 100...2000 meters away from the fire hazardous zone in accessible area.

IPD divides signals I_1 and I_2 which compensate for variations in the LED radiation intensity and the light flux uninformative loss of the optical fiber bends, since their attitude does not depend on these factors. To increase the sensitivity of the conversion ratio of the can generated difference of signals I_1 and I_2 to their sum.

Summary

- Specified design parameters of membranes and attenuator of fiber-optic differential pressure sensor (FODPS)
- Given recommendations about design of fiber-optic differential pressure sensor (FODPS)

References

1. Pivkin A.G., Murashkina T.I., Badeeva E.A. *Patent RU 2290605, MPK6 G01 L 19/04* 27.12.2006.
2. Kolomiets L.N., Badeeva E.A., Murashkina T.I., Pivkin A.G. *Funktsiyapreobrazovaniyadifferentsial'nogo VOD davleniyaotrazhatel'nogotipa // Aviakosmicheskoe priborostroenie.-2007.-№8*
3. Kolomiets L.N., Badeeva E.A., Murashkina T.I. *Opredelenieusloviirealizatsiidifferentsial'nogopreobrazovaniyasignalov v volokonno-opticheskikhpreobrazovatelyakh davleniyaotrazhatel'nogotipa // Aviakosmicheskoe priborostroenie.-2011.- №11*

DISTRIBUTED COMPUTER CONTROL SYSTEM FOR ELECTRON SPECTROMETER, GATHERING AND MATHEMATICAL PROCESSING OF ELECTRON SPECTRA

Valyukhov, D.P., Djudjun, D.E.; Zubrilov, V.G.

Dept. of Physics, Electrical engineering & Electronics., North-Caucasus Federal University, Stavropol, Russia

Hardware-software PC-based complex for control of X-ray photoelectron spectrometer (XPES) has created. Its use could fully automate the receipt of the XPS spectra of the samples surface and save obtained spectra in accessible formats (xls, jpg, bmp) for subsequent processing of measurement results. The work has reduced complexity, increased accuracy, speed and convenience of measurement.

Keywords: X-ray photoelectron spectroscopy, distributed computer control system, hardware-software complex

Modern methods of samples surface analysis by photoelectron spectroscopy, Auger electron spectroscopy and mass spectrometry of secondary neutral particles ejected from the surface during etching of the samples, are resource-intensive. Computer control system of collection and mathematical processing allows to automate these processes, and modern computer facilities make it easy to handle large volumes of data.

For a long time, such systems were implemented as monolithic architectures with predetermined functionality provided by hard-related hardware and software components. Functional properties of such systems were almost impossible to expand, as they were able to perform only those functions that were laid at the design stage. However, the current requirements for these systems, are largely associated with the ability to constantly expand and increase their functional properties.

Figure illustrates a block diagram of the hardware system which controls X-ray photoelectron spectrometer, realized on the basis of the National Instruments Data Acquisition Board (DAQ). Such boards can include a number of DACs, ADCs, counters, digital inputs/outputs.

Versatility of data acquisition boards allows to assemble complex hardware and software systems based on DAQs. The flexibility of such architectures can easily implement the necessary functionality. You can select the mode of each acquisition board node with the help of software (eg, package Lab VIEW).

Consider the example of the complex system operation. The electron cannon ejects photoelectrons from the sample surface during the analysis. These electrons are accelerated and focused by energy analyzer “cylindrical mirror”. Braking voltage applied from the high-voltage amplifier (OPS - Operational Power Supply) is used for separation of the electron energy; magnitude of this voltage is set at channel 1 of digital-to-analog converter (DAC). Electrons with appropriate energy reach the channel electron multiplier (CEM). CEM signal is fed to the 2 channel board of amplitude selection (AS). Upper and lower levels of selection are specified by the 2nd and 3rd channel of DAC, that allows to remove noise and bursts of energy. Digital pulses are generated at the outputs of amplitude selection board when the input signal level exceeds the level of selection. The outputs of the AS board are connected to the inputs of counters (counter 1 and counter 2). The difference in the values obtained by counting pulses during a certain period of time corresponds to the number of pulses in the range located between the lower and upper levels of selection. A smooth increase of the OPS input voltage allows to scan in the required energy range.

Almost all of the blocks are realized on one board. This reduces interference from external fields, increases performance and reduces the workload of the personal computer system bus, freeing the CPU from the interrupt processing on several boards. Thus saved CPU time enables advanced signal processing during scanning in a multitask software.

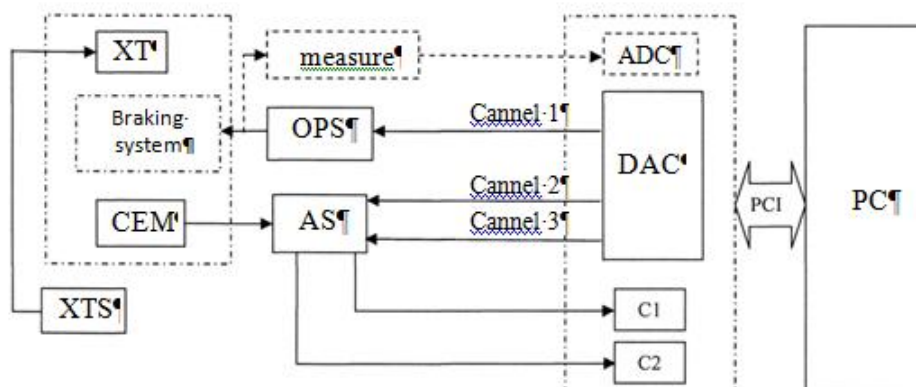


Figure - Block diagram of XPES control and registration of XPS spectra and electron spectra: XTS - X-ray tube supply; XT - X-ray tube; CEM-channel electron multiplier; OPS - Operational Power Supply, AS - amplitude selection block.

DIVISION OF A POPULATION OF ELEMENTS INTO A GIVEN NUMBER OF DISCERNIBLE PARTS

Enatskaya N.Yu., Khakimullin E.R.
Moscow: MIEM, HSE.

Two statements of the problem for the division of a population of elements into a given number of discernible parts with and without limitations applied to their dimensions or compositions are distinguished. Under conditions of these statements, the problem under consideration with varying quality of elements by their discernibility is resolved in the following aspects (sub-problems): explicit enumeration of the results of element division schemes, determination of their total quantities, the problem of result indexing in the basic permutation schemes with repetitions, calculation of probabilistic distributions of all possible results and their modelling in the division schemes under study.

Introduction

In the problem aspects given in the abstract, let us differentiate analytical solving of individual sub-problems that would give results in the form of accurate formulae and construction of numerical methods for their precise and approximate solving. First and foremost, the question is in finding the total number of results, which may be presented in the form of a function of their parameters (the count of population and the number of its parts) or an algorithm of procedure development for result enumeration of the studied scheme as an extension of their enumeration, and approximate calculation of the number of scheme results using probabilistic modelling.

Let us particularly emphasize the constructibility of full visual enumeration of all scheme's results for practical application, which means a possibility to find their number in the absence of explicit formula. In the considered problem of calculating the number of results of dividing a set of elements into parts with their explicit enumeration under any limitations of division part dimensions, in particular, this will be defined by extension of the

rejection result provided by limitations from full enumeration of the results obtained from schemes for dividing a population of elements into a given number of parts without limitations. Basing on enumeration of results of schemes their probabilistic distributions are also calculated. Moreover, this gives way for simple modelling of results for the scheme of population division into parts without limitations by their enumeration lists and with limitations.

In case of establishing mutual correspondences between kinds of results and their numbers in the sequence of results obtaining during their full enumeration, hereinafter called the indexing problem, we obtain additional opportunities in finding the last obvious content result as an explicit formula for the number of scheme results (with regard to established indexing discipline for all enumerated states) and "rapid" modelling of the scheme results by a single random number via the result number selection.

The results will be treated in order of solving of listed sub-problems according to schemes of discernible and indiscernible elements division in the population into parts without limitations of their dimensions and compositions and with such limitations.

Obviously, in more familiar terms of particle permutations by cells, the division scheme without limitations of the parts is equivalent to the permutation scheme of discernible or indiscernible particles by discernible cells (in the amount of division parts) having no free cells at all combinations. In population division schemes with limitations of dimensions and compositions of the parts, they are transferred to corresponding levels and compositions of cell filling at particle permutations. In these terms hereafter we'll sequentially study schemes in the above listed directions. Further on, by default, we will mean the division scheme with no limitations. To put it differently, this will be indicated by the short name: the division scheme with limitations.

Let us define the scheme of permutations with repetitions, i.e. the permutation scheme for discernible particles by discernible cells, as the basic permutation scheme, because it has the highest number of results as compared with the schemes under consideration, the list of results for which may be obtained via certain rejections of results in the basic scheme. Let us study all results of the basic permutation scheme individually, in as much detail as possible.

§1. Listing of results and indexing problems in the basic scheme

As defined above, by the basic scheme a permutation scheme with repetitions, i.e. permutations of r discernible particles taken n discernible cells with no limitations at a time and with total number of results $N_1^* = n^r$, is meant.

1. Explicit enumeration of results in the permutation scheme with repetition

For explicit enumeration of all n^r results in this scheme, let us compose a random process of sequential, unit-wise independent permutation of particles in increasing order of their numbers (1 through r) with the results indexing in increasing order of the permutation cell numbers for the last particle. Designation $E_j^{(i)}$ means the j -th state at the i -th step (after permutations of i particles in the cells) and is described by an n -dimensional vector, each component of which contains the numbers of particles in each cell, and their components are listed in the order of cells indexing. When writing down a component containing more than one number of particles, we will parenthesize them. Let us explain the above mentioned using an example.

Example 1. Let $n = 3$, $r = 2$. The number of results in the scheme is $3^2 = 9$.

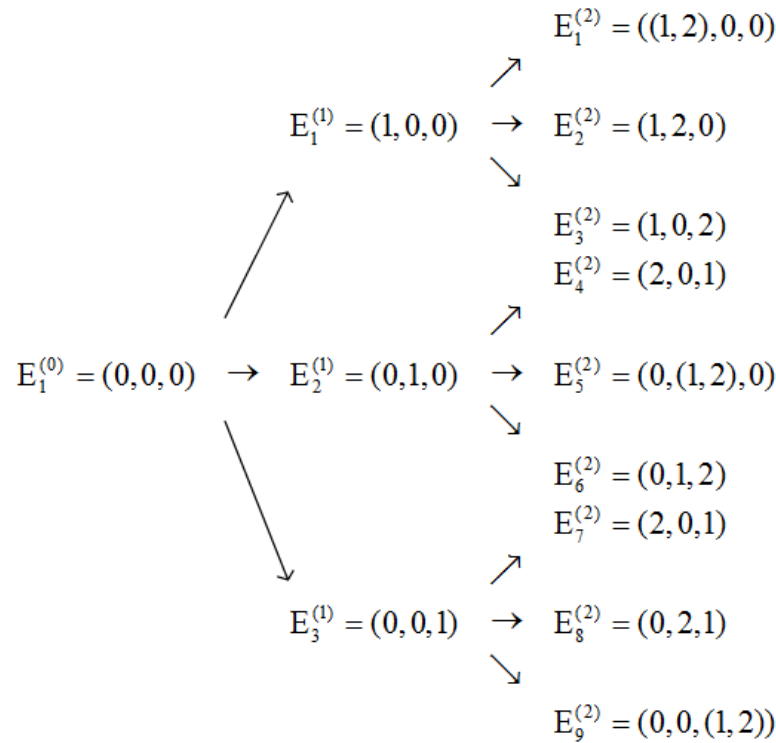


Fig. 1

I.e. by the graph, at the second step 9 equiprobable results are obtained again.

Calling the above suggested notation of the scheme result the first, for further consideration let us suggest the second notation of the scheme results at the r -th step, so that the j -th result (state) will be written down in the form of $R^{(j)} = (R_1, \dots, R_i)$ enumeration of parenthesized, comma separated cell numbers, sequentially containing particles with numbers from unit to r . (Each vector R consists of r components.) For instance, the fifth result on the second step in the first notation $E_5^{(2)} = (0, (1,2), 0)$, in the second notation (see Fig. 1) will be written down as

$R = R^{(5)} = (2,2)$. (Let us omit the result number, when it is defined in the text unambiguously.)

2. Indexing of scheme results

Definition of enumeration fullness for all results of schemes in §1 and convenience of its further application requires solution of direct and inverse indexing problems, i.e. finding the result R for each scheme under consideration by its number N and vice versa: finding number N of the given result R of the scheme.

For solving the indexing problems, let us agree to use the second notation of the scheme results, i.e. the form $R = (R_1, \dots, R_r)$, where R_i is the number of a cell containing the particle with number i , $i = \overline{1, r}$. The result number N of the scheme will be given in the form of $N = N_r = (N_1, \dots, N_{r-1})$, where N_r is the result number on the i -th step and procedure of results listing (item 1), i.e. after permutation of i particles taken at n cells at a time, $i = \overline{1, r}$.

Direct indexing problem

The form of result R with the given number N should be found.

The problem is solved by determination of R_i in the order from $i = r$ to $i = 1$ by formulae that follow from the enumeration procedure for the scheme results (see item 1). Let us denote $N = N_r : N_{i-1}^* = \left\lceil \frac{N_i + n - 1}{n} \right\rceil$, $i = \overline{2, r}$. Then target values R_i are calculated by the formulae

$$R_r = N(\bmod n); R_i = \left[\frac{N_{i+1} + n - 1}{n} \right] \bmod n. \quad (1)$$

Let us show a numerical example.

Example 2. Let $r = 3$, $n = 3$, $N = 10$. For calculations check, let us plot a graph of states, extending it by one more step, to $r = 3$, in the example 1

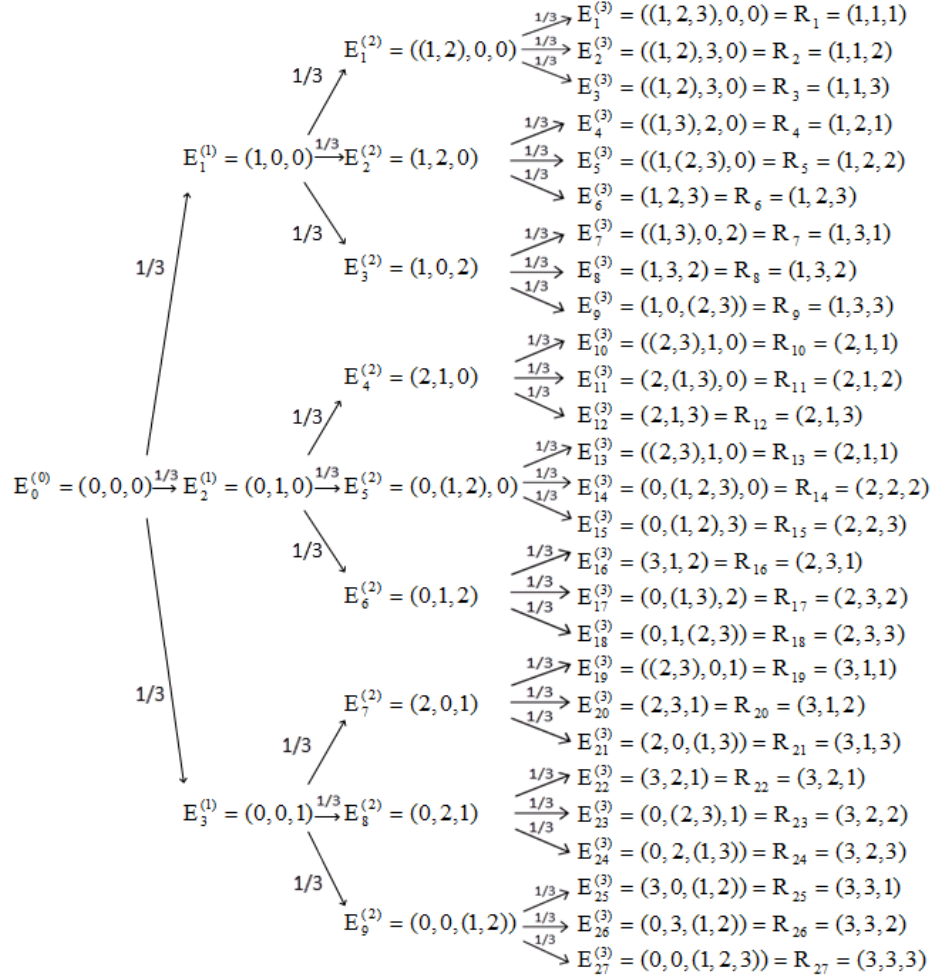


Fig. 2

Then according to Fig. 2 in the second notation we must obtain the state $R=(R_1, R_2, R_3)=(2, 1, 1)$. Let us now determine vector R components by formulae (1):

$R_3=10(\bmod 3)=1$, $N_2^*=[(10+3-1)/3]=4$; $R_2=4(\bmod 3)=1$, $N_1^*=[(4+3-1)/3]=2$; $R_1=2(\bmod 3)=2$, i.e the state $R=(2, 1, 1)$ as by Fig. 2 is obtained.

Inverse indexing problem

Number N of the scheme result given in the second notation of $R=(R_1, \dots, R_r)$ form should be found.

The problem is solved by determination of N by the formula deduced from the enumeration procedure for the scheme results (see item 1):

Let us denote $N = N_r : N_{i-1}^* = \left[\frac{N_i + n - 1}{n} \right]$, i.e. Then target values R_i are calculated by the following formulae:

$$N = \sum_{i=1}^{r-1} (R_i - 1)n^{r-i} + R_r \quad (2)$$

Let us show a numerical example.

Example 3. Let $r = 3$, $n = 3$, the second notation state used in the formula (2) is $R = (2, 1, 1)$.

For calculations check, let us use the state graph from the Example 2, wherefrom it follows that its number $N = 10$, where in Fig. 2 the state R is presented in the corresponding first notation $R = ((2,3), 1,0)$. Let us now calculate the value N by the formula (2): $N = (2 - 1)3^2 + (1 - 1)3^1 + 1 = 10$ that coincides with the result in Fig. 2.

§2. The problem of division of r discernible elements into n discernible parts

Total number M_1 of results of this scheme is known as Stirling number of the second kind:

$$M_1 = \frac{1}{n!} \sum (-1)^j C_n^j (n-r)^r \quad (3)$$

For solving other sub-problems defined in the abstract in this scheme, let us interpret the population division under consideration in permutation terms: a scheme of r discernible particles permutation taken at n discernible cells at a time having no empty ones is studied. For this purpose, some combinatorial schemes will be used.

For the first auxiliary scheme, let us consider more general analogous scheme of permutations with no limitations for the number of particles in cells with the given total number of particles r , the above-called basic one, considered in §1. The number of results in such a scheme is $N_1^* = n^r$. This scheme is called the permutation scheme with repetitions.

For the second auxiliary scheme, the interchange scheme of r discernible elements with the known number of results $N_1^* = r!$ with consecutive division of each interchange into n non-empty parts.

For the third auxiliary scheme, the permutation scheme is used, i.e. the scheme of selecting n elements from r at $n \leq r$ with the known number of results $N_3^* = A_r^n$. This scheme may be studied via the interchange and combination schemes in view of the known formula. $A_r^n = n! C_r^n$.

1. Auxiliary results

Let us pay attention to enumeration procedures of combinatorial schemes used, except for the basic permutation scheme with repetition studied in §1

A. Interchange scheme

This scheme occurs in case of ordering of n discernible elements against each other or is a case of permutations of n discernible particles by n discernible cells so that each cell contains precisely one particle. Total number of the scheme results is $n!$.

Explicit enumeration of the results in the interchange scheme with the solution of direct and inverse indexing problems is considered in [2].

B. Combination scheme

As is known, the combination scheme occurs in case of permutation of r indiscernible particles by n discernible cells with the limitation: a single particle is located in each cell.

Total number of scheme results is C_n^r - the number of combinations of n taken r at a time, where n is the number of cells; r is the number of particles.

Explicit enumeration of the results in the interchange scheme with the solution of direct and inverse indexing problems is considered in [3].

C. Interpreting of results of C_{n-1}^{r-1} division scheme for ordered set into parts

Obviously, the interpretation of interest coincides with that for permutation of r indiscernible particles n discernible cells taken at a time without empty cells, and is formulated as the rule from [1]: sizes of parts of element division located in the fixed order

are obtained as differences between locations of neighbouring elements selected by the combination scheme C_{n-1}^{r-1} , with the unit added for end parts of division.

D. Permutation scheme

As it is known, the combination scheme occurs in case of permutation of r discernible particles by n discernible cells with the limitation: a single particle is located in each cell.

Due to the equality $A_n^r = n!C_n^r$, the explicit enumeration procedure for results in the permutation scheme follows from the procedures in items B and A described in [2] and [3], and conducted in the following sequence: the results of the combination scheme (item B) are enumerated, and to each result the enumeration procedure for all interchanges of the interchange scheme result elements (item A) is applied.

2. Enumeration of division results and numerical determination of their number

Let us suggest different approaches for solving the set problem as algorithms.

Numerical methods for solving this problem may be obtained from the basic and the first auxiliary scheme (A) by the analysis with rejection of particular results and using the third auxiliary scheme by direct enumeration of results of interest for the set division into given number of parts. (These approaches to enumeration of results also relate to the set division scheme with limitations with the only difference that direct enumeration of results in the division scheme without limitations will require rejection of results by these limitations.)

Algorithm 1

We will use the first auxiliary scheme as follows: if we visually list all its results, i.e. the results of permutation scheme with repetitions, then the rejection of alternatives with empty cells will give an explicit enumeration of all divisions, the total number, M_1 of which will be found from the initial scheme. Thus the problem is reduced to enumeration of all results of this auxiliary permutation scheme with repetitions.

Algorithm 2

The first auxiliary scheme (A) for interchanges of r discernible elements will be the first phase of the required division algorithm in the initial scheme. At the second phase, each interchange will be divided by all C_{n-1}^{r-1} methods into n non-empty parts. The elements in each part will be arranged in the ascending numbers order, and repetitive results at different initial interchanges of all r elements will be rejected. As a result, we'll get a listing of all division alternatives in the initial scheme. Total number of these divisions is M_1 . Here the initial problem is reduced to the listing of $r!$ interchanges and enumeration of C_{n-1}^{r-1} divisions of each interchange for non-empty parts.

Algorithm 3

Results of the set division into the given number of parts will be directly enumerated by selecting at the first stage of n from r particles with the minimal numbers at their permutations in n cells by nA_{n-1}^{r-1} methods (since the particle with number 1 is the mandatory inclusion of this selection, and we just have to choose one of n cells for it, the rest $n - 1$ particles are chosen from $r - 1$ according to the permutation scheme) with further permutation (at the second phase) of the rest $r - n$ particles by n cells so that they do not change minimal numbers of particles in cells, previously defined. This means that cells permissible for equiprobable permutation of each of $r - n$ particles will contain particles with minimal numbers which are smaller than the particle number permuted at the second phase.

Here the number of scheme results will be calculated by all selections of minimal particle numbers with different composition in cells (i.e. regardless of their location in discernible n cells) and, therefore, compositions of the rest $r - n$ particles, by calculating minimal numbers in cells for each number n fixed among them, which minimal numbers are smaller than this fixed one. Let us assume that resulting from the i -selection of minimal

numbers of particles in n cells for these $r-n$ particles the numbers of particles selected with the smallest numbers are $n_{i_1}, \dots, n_{i_{r-n}}$. Then the target

number M_1 of the set division results is obtained from the formula:

$$M_1 = n! \sum_{i=1}^{C_{r-1}^{n-1}} \prod_{j=1}^{r-n} n_{i_j}$$

Thus, calculation of the number M_1 requires the list of all C_{r-1}^{n-1} selections of minimal particle number compositions (except for the particle numbered 1) in cells. How to derive this list, see item 1. Let us numerically explain calculation of the number of a part of scheme results at their i -th fixed selection, which is defined by the number of permissible permutations of the rest $r-n$ particles by n cells.

Example 4. Let $n = 5$, $r = 8$, and the i fixed composition of minimal particle numbers be 3,4,1,8,6. Then particles with numbers 2,5,7 remain unselected. For them, respectively, we get: $n_{i_1} = 1$, $n_{i_2} = 3$, $n_{i_3} = 4$, whence we get the number of permissible permutations of the rest 3 particles by 5 cells as follows: $1 \cdot 3 \cdot 4 = 12$.

Note 1. In case of simpler first two algorithms of enumeration and M_1 number calculation, the third algorithm is obviously more economic in terms of the memory volume used and time spent.

Note 2. When the number M_1 is calculated by enumeration of the division results, coincidence with the result of formula (1) serves as verification for its fullness.

3. Probabilistic distribution of the results of set division into the given number of parts

To find probabilistic distribution of r elements set division into n parts in this scheme (the set elements and division parts are discernible), let us indicate on the graph edges easily calculated probabilities (in the permutation interpretation) of state-to-state transitions in the basic scheme described in item 1, §1. This is done for consecutive unit-wise adding of particles basing on equiprobable occurrence of a particle in any cell and indiscernibility of cells during new state formation. Then regarding independence of particles permutation at each step, probability of each result in the basic scheme will be obtained by multiplying probabilities on the graph edges in the path leading to the state under consideration.

To find probabilistic distribution of all required set divisions meeting all permutations of r particles by n cells without empty ones, let us sum the probabilities of such permutations up by the graph and divide by this sum the probability of each result, obtained above for all permutations of particles by cells in the basic scheme. (As above, in the division scheme with limitations, the probability of any result meeting the limitations is with replacement of particle permutations by cells with no empty cells by permutations meeting the required limitations for the cell filling level.) Due to equal probability of particle permutations by cells in the basic scheme, for the results of interest we also get equiprobable distribution (in all cases, both without limitations of with them).

Example 5. Let $n = 3$, $r = 4$. Find probability distribution for the division results a) without limitations; b) with the limitation: precisely two particles permuted in the first cell; c) with the limitation: in the first cell, particles with prime numbers are permuted (i.e. in this example, these are particles with numbers 1, 2, 3).

Let us perform these calculations using the graph of transitions (Fig. 2) described for enumeration of states in the basic scheme (§1), with corresponding probabilities for $n = 3$, $r = 3$ indicated on edges of state-to-state transitions, and mentally extending it by one more step, to the given value $r = 4$. This can be easily done using results indexing in the basic scheme, assumed in §1, according to the listing algorithm for its results at the 4th step in the given cases of division a)-c).

To solve the problem, let us put in line quantities of results at the 4th step from each state at the 3rd step (Fig. 2) in the given cases.

- a) 0,1,1,1,1,3,1,3,1,1,1,3,1,0,1,3,1,1,1,3,1,3,1,1,1,1,0;
- b) 0,1,1,1,0,1,1,1,0,1,0,1,0,0,0,1,0,0,1,1,0,1,0,0,0,0,0;
- c) 0,1,1,1,1,2,1,2,1,1,1,2,1,0,0,2,0,0,1,2,1,2,0,0,1,0,0.

According to the given cases, we get the following quantities of results: 36, 12, 24, respectively; whence (considering the number of results in the basic permutation scheme with repetitions equal to $3^4 = 81$) we get:

in the case a) that division of the given set into 3 parts without empty parts among all divisions into 3 parts has a probability of $36/81=4/9$, each such division among all divisions of the set into 3 part exactly having the probability of $1/36$;

in cases b) and c) that for the set division into 3 parts exactly, meeting the limitations of cases b) and c) has probabilities $12/36=1/3$ and $24/36=2/3$, respectively, each result in the cases mentioned having the probability of $1/36$.

4. Modelling of the results of set division into the given number of parts

The first method

Using solved right-hand indexing problem in the basic scheme, a "quick" modelling by selecting one of n^r numbers of the results is performed, and from this modelling the type of result is found, which is thus modelled. Among modelled results we preserve those without empty cells or in the scheme with limitations - the results related to them.

The second method

By this algorithm and the algorithm from [1], results of the basic scheme are modelled with rejection of results incorporating empty cells, or in the scheme with limitations - the results related to them.

5. Approximate calculation of the number of set divisions into the given number of parts.

The target number M_1 of divisions of a set from r elements into n parts can be found by the method of proportions in case of probabilistic modelling of results for a scheme similar to the basic one with the number of results n^r as follows: a sufficiently great number D_1 of results in the basic scheme is modelled, and number D_2 of the results without empty cells among them is determined. Then the target number M_1 is approximately calculated from the proportion $M_1/n^r=D_2/D_1$. In the scheme of division with limitations, number D_2 represents the number of results with particle permutations by cells meeting these limitations.

Note 3. In the set division scheme into the given number of parts considered the latter calculation is only sensible in the scheme with limitations, because in the scheme without limitations, a precise formula for calculation of M_1 number is given in (3). This reasoning is given to illustrate the general approach of approximate calculations of the number of set divisions using probabilistic modelling in other schemes in the absence of simple explicit formulae for it.

§3. The problem of division of r indiscernible elements into n discernible parts

The total number of results M_2 of this scheme called in the classical combinatorics the permutation scheme with repetitions without empty cells at $r \geq n$, is known and gives

$$M_2 = C_{r-1}^{n-1} \quad (4)$$

The number of results in the division scheme with limitations is obtained in [5] and provides rather complicated explicit calculation of by a recurrence relationship. Therefore, another idea about its calculation may be practical.

1. Enumeration of division results of the scheme and numerical determination of their number

All results of this set division scheme into the given number of parts are enumerated according to the results enumeration algorithm in the combination scheme with interpretation

of indiscernible particle permutations by discernible cells without empty cells (§2, items B, C). (As mentioned above, the number of such divisions is known from (4).) For the scheme with limitations, results not related to them should be rejected. Their number will give the target number of given set divisions.

2. Probabilistic distribution of the results of set division into the given number of parts

This problem is solved by analogy to item 3, §2, with the graph of the random process of consecutive unit-wise permutation of particles by three cells for enumerating results of the scheme from §2 substituted by the corresponding graph for enumerating results of the set division scheme considered in §4 by n cells.

In case of the division scheme with limitations, probabilities of corresponding results are calculated the same.

3. Modelling of the results of set division into the given number of parts

According to the algorithm given in [4] for the combination scheme with repetitions, let us model its results. In case of modelling results of the scheme with limitations, we reject results of the combination scheme with repetitions according to these limitations,

4. Approximate calculation of the number of set divisions in the scheme with limitations

The target number M_3 of divisions of the set of r elements into n parts may be found by the method of proportions in case of probabilistic modelling of results of the combination scheme with repetitions described in item 3, with the known number of results C_{n-1}^{r-1} as follows: a rather large number D_1 of its results is modelled and the number D_2 is determined from them, which meets these limitations. Then the target number M_3 is approximately calculated from the proportion $M_3/n^r = D_2/D_1$.

References

1. Enatskaya, N.Yu., Khakimullin, E.R. The method of graphs for solving problems of enumeration combinatorics. Information-control systems (in press)
2. Enatskaya, N.Yu., Kolchin, A.V. Combinatorial analysis of the interchange scheme. Proceedings of Korelsky Scientific Center RAS (in press).
3. Enatskaya, N.Yu., Kolchin, A.V. Combinatorial analysis of the combination scheme. Proceedings of Korelsky Scientific Center RAS (in press).
4. Enatskaya, N.Yu., Khakimullin, E.R. On division of a number into fixed number of addendums of limited size. Part 2 Innovative information technologies in science. Prague-2013, April 22-26.

AUTOMATIC DIGITAL ELEVATION MODELS CREATION FROM RASTER TOPOGRAPHIC MAPS

Dobroserdov O.G., Miroshnichenko S.Yu.
Kursk, Southwest State University

Digital elevation models (DEM) along with the thematic layers set including buildings and structures, hydrography, greenery, road net are the main components of geographic information systems' (GIS) digital maps (DM) [1, 2]. DEMs are required to solve a wide range of problems in logistics, mobile communications, as well as for surveillance and monitoring performed by air drones for the sake of emergency services, ecological and security organizations.

Raster topographic maps of different scales that were scanned from paper originals contain relief elements which provide information to create DEMs. The key relief elements are isometric lines (isolines) and height marks. Topographic maps provide the most financially efficient way to create DEMs, however it requires significant time investments to transform isolines into vectors (vectorize) in case this operation is performed by operator manually (up to one week for a skilled operator to process one map sheet).

Software complexes for computer-aided vectorization reduce time costs in 2-5 times by significant simplification of raster-to-vector isolines transformation process [3], but still have few functional limitations that are blocking the further performance growth (up to several hours per one map sheet):

1. The closely situated isolines can't be automatically separated if the source map region has a saturated relief.
2. Height marks automatic recognition or automatic height assignment for isolines are not provided.
3. Microtopography overlapping with isolines can't be automatically localized or eliminated.
4. Software operator has to be quite highly skilled to provide enough DEM precision.

Consequently, there is an actual problem of further time costs reduction for DEMs creation from topographic maps. This problem can be solved by developing the methods of topographic maps digital processing and recognition that provide close isolines separation, height marks recognition, isolines height assignment and microtopography elimination. Moreover the advanced topographic maps processing software based on the developing methods will have less requirements for operator skills.

The following topographic elements are used to create DEM from a map [4]:

1. Relief isometric line is a closed line on a map, which any point has the same height from the sea level. The difference between neighbor lines is called the isoline step and is determined by the map scale and the shown terrain relief (height transition values). Isolines are displayed by the following colors:

- 1.1. Brown (close to red) color corresponding to the isolines located on a dry land (fig. 1a).

- 1.2. Blue color used to mark isolines in the regions of glaciers and mountains snowpacks (fig. 1b), coastlines of constant and varying hydrography (fig. 1c), sea-bed relief (fig. 1d).

2. Height value is numeric sequence corresponding to elevation of certain point or isoline on a map. There are the following height mark types:

- 2.1. Height mark displays the elevation from the sea level of some neighbor point (generally on a high ground top or a reference point) marked by a special symbol (dot, triangle, rectangle etc). It is drawn by the black color (fig. 1e).

- 2.2. Shore line height used for varying hydrography and drawn by the blue color (fig. 1f).

- 2.3. Isometric line height shows the elevation value of a line in which discontinuity it is situated. It is drawn by the brown color (fig. 1g,h).

Microtopography elements (washouts, sand bumps etc) show insignificant relief details with height transitions less than one isoline step and are used only to specify some relief form features.

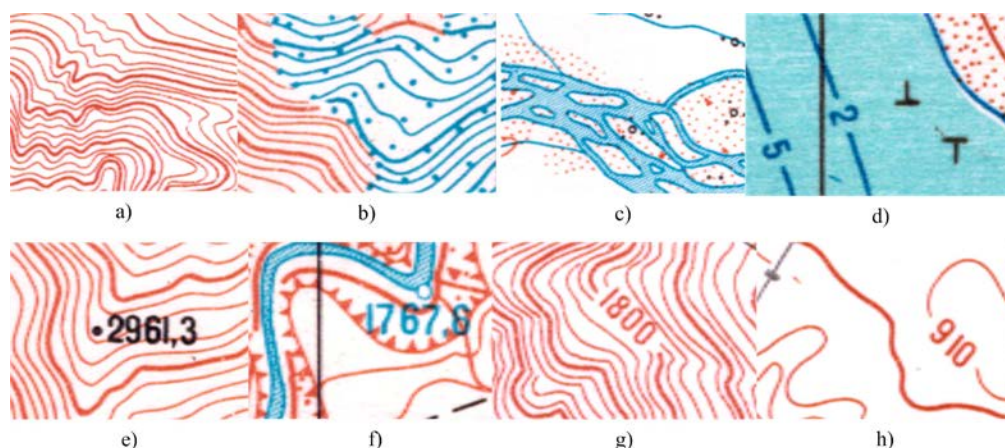


Fig. 1. Main topographic map relief elements

The described relief element set on a topographic map is used to create DEM automatically by the method containing the following steps:

1. Isolines raster-to-vector transformation.
2. Height values localization, recognition and type identification.
3. Regular DEM creation.

The key to isolines raster-to-vector transformation is the detection of their centers producing singly connected line representation that is the most suitable for vector encoding [5].

The central line part on a topographic map is a brightness function local minimum in orthogonal to line direction in the current point, that in most cases coincide with brightness gradient direction (except regions of line intersections or source media defects).

Using this feature we created the nonlinear dimensional FIR-filter [5], represented by a sliding window of 3 by 3 points size, that provides brightness function local minimums detection in gradient vector direction with step of $\pi/4$ radians. Gradient direction is calculated by Elder and Zucker local scale estimating edge detection method using local brightness function features of source topographic map [6]. The result of the filter application is shown on fig. 2.

Detected isolines' central parts of brown and blue colors are directly encoded into vector representations.

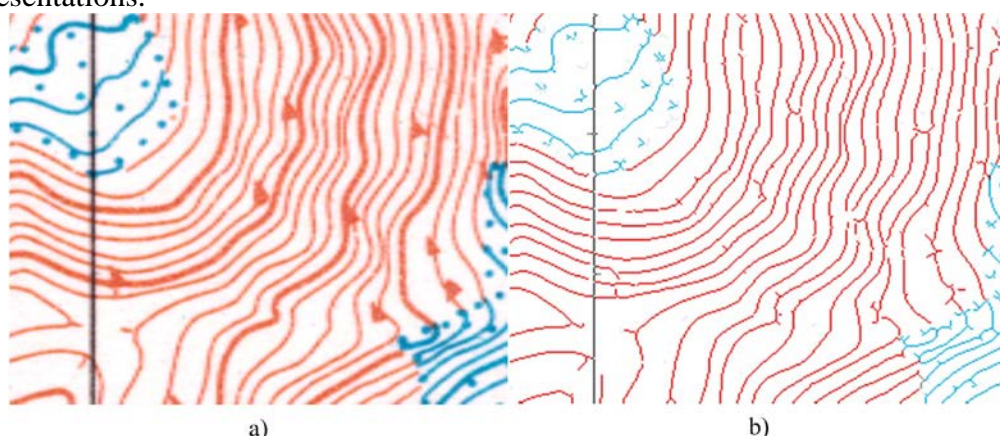


Fig. 2. Isolines center parts detection

Height values detection and recognition are performed using source topographic map color segmentation [5] with further numeric sequences search by contour analysis methods [7].

Raster topographic map color segmentation matches each pixel to one of a priori defined color classes set including brown, blue, green, black and white (fig. 3b). Segments of brown, blue and black colors are transformed into vectors by encoding their borders with other segments and matched to one of digit etalons by a shape comparing with contour analysis methods.

Contour analysis mathematical apparatus provides a calculation of segment similarity degree to digit etalon independently from their mutual scale and rotation angle along with ability to define these parameters. Topographic map segments with similarity degree to one of digit etalons above 80% (fig. 3c) are grouped into numeric sequences representing height values. The following parameters are considered in grouping: digit color, rotation angle and scale related to etalon. Created sequences are semantically verified to avoid possible false recognitions of isolines parts as ones or sevens. The recognized value is checked to comply with permitted height range, isoline step multiplicity (for isoline heights), permitted rotation angles (fig. 3d).

Recognized height values are bound to special markers (dots, circles, rectangles, triangles for height marks or contour dots for shore line heights) and to isolines.

Every isoline height on the map has to be calculated to create a regular elevation model. Isoline height is defined using three most close recognized height values by counting an intersections number of other isolines with vector aimed to each of heights. The obtained non regular model is converted to a regular one (fig. 4) using triangulation.

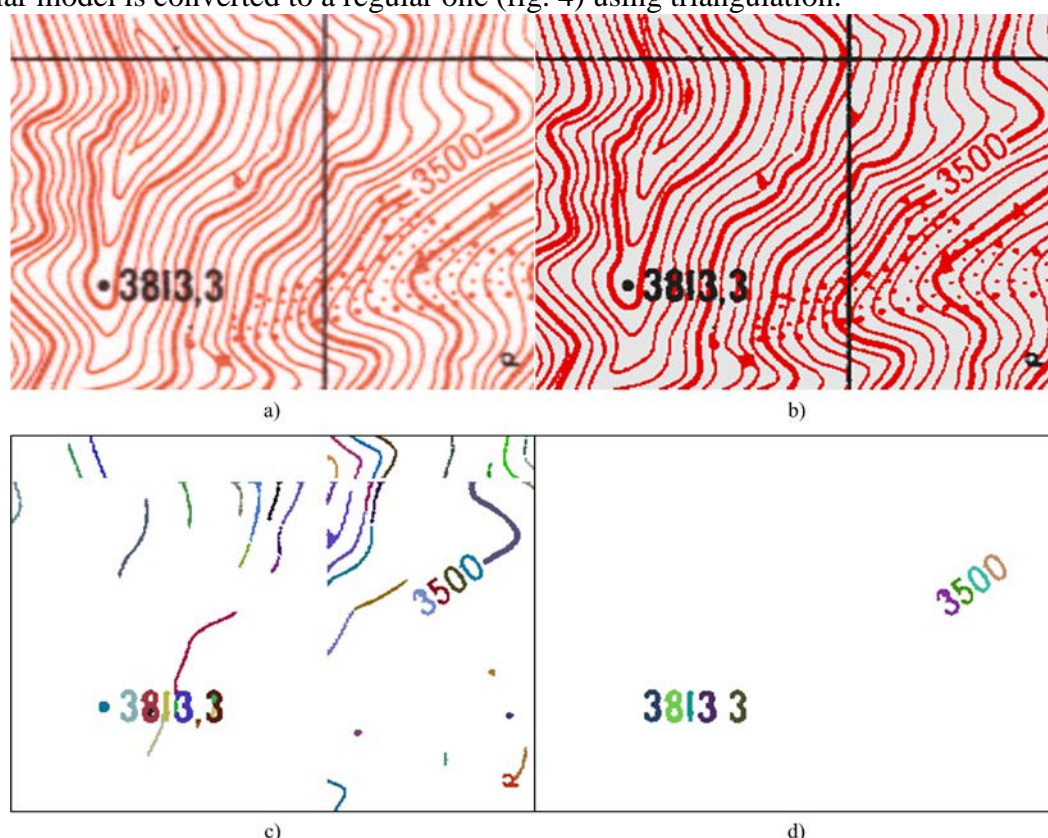


Fig. 3. Source topographic map (a) color segmentation (b), values recognition (c) and numeric sequences creation (d)

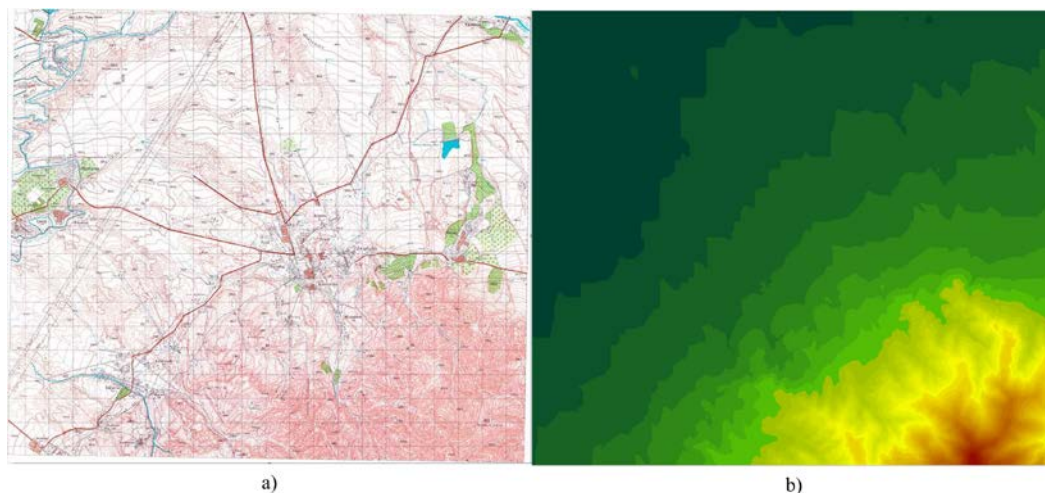


Fig. 4. Regular DEM (b) based on the topographic map (a)

The described methods is taken as basis for software complex for automatic DEM creating from topographic maps that allows to reduce time costs up to several hours per map sheet by automatic close isolines separation, height values recognition and isolines heights calculation.

References

1. D.E. Andrianov, Geoinformatsionnye sistemy: issledovanie, analiz i razrabotka – M.: Gosudarstvennyi nauchnyi tsentr Rossiiskoi Federatsii – VNIIGeosistem, 2004. 184s.
2. A.I.Martynenko, Informatika i elektronnaya Zemlya: fundamentalnye nauchnye problemy / Sistemy i sredstva informatiki. Vyp. 11. – M.: IPI RAN, 2001. PP. 94-112.
3. Easy Trace. Intellekтуalnoe programmnoe obespechenie dlya vektorizatsii kart: <http://www.easytrace.com/site/russian/news/news.html>.
4. Osnovye polozheniya po sozdaniyu i obnovleniyu topograficheskikh kart mashtabom 1:10 000, 1:25 000, 1:50 000, 1:100 000, 1:200 000, 1:500 000, 1:1 000 000. M.: RIO VTS, 1984.
5. R. Gonzalez, R. Woods, Digital Image Processing, Addison-Wesley Publishing Company, 1992.
6. J.H. Elder, S. Zucker, Local Scale Control for Edge Detection and Blur Estimation // IEEE Transactions on Pattern Analysis and Machine Intelligence. Vol. 20, No 7. 1998. PP. 699-716.
7. Ya. A. Furman, Vvedenie v konturnyi analiz i ego prilozhenie k obrabotke izobrazhenii i signalov // M.:FIZMATLIT, 2002. 592s.

DESIGNING AND DEVELOPING INTELLIGENT INFORMATION SYSTEMS TO SUPPORT MEDICAL FACILITIES

Dunin V. O., Egorov V. A.
Russia, Penza, Penza State University

Separate questions of designing cloud services and application delivery to the end user. The conceptual model of the organization of ancillary services for the medical facility.

Keywords: cloud technology, medical treatment, virtualization, intelligent systems.

Given the current trends in the development of information technology, we propose the implementation of an information system to support medical institutions capable of

aggregating and analyzing data, providing users with information on possible trends of current medical situation, analyze the market and provide operational support to users on the basis of integrated catalogs patients.

The subject is to create a specialized single information system, aggregating the results of recent developments in the field of medicine, with connectivity and clustering around a single core information differently – designed information systems not only support but also optimize the provision of medical services, and as a result, increasing quality research and techniques for treating various diseases, as well as facilitating their widespread use in medical practice. Information system, to solve such problems circle can be equated to an expert system.

The tasks solved should be assigned tasks to be undertaken by people experts in a particular subject area. To solve any problem in the ES – used some knowledge base describing the regularities of the domain. ES – an information system that uses mathematical algorithms to solve the problem domain, and having a knowledge base. Tasks imposed on the ES can be solved by different approaches, some of them are discussed below. Feature of the solution of such problems is the large number of unknown variables, then use linear methods for solving impossible. Support system of medical institutions – some system that facilitates the interaction of health workers, patients in a medical institution. Likewise, the system allows you to collect and to predict, on the basis of aggregate data derived from the monitoring of patients, the general trends in the development of mass diseases, illnesses, etc.

The solution of these problems can be done by linear methods. Using these methods, to solve the problem using an algorithm tough action. Example of application of the linear method – a situation in which you need to determine the temperature of the patient. Thermometer readings should be within a certain range, this range is the normal state, an unstable condition and dangerous condition. When you receive the temperature data can be unambiguously judge the patient's condition.

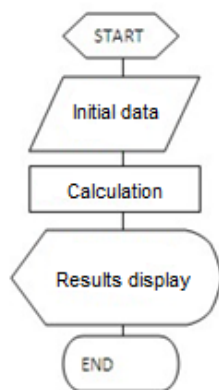


Figure - 1 circuit linear algorithm

Currently 99 % of systems work on linear algorithms (as for the tasks it is enough). Example - site content filtering system, or a system of filtering junk e- mail (spam). Filtering is used to implement a set of rules, based on which a determination is made - in the query searched keywords, or use a specific list of domain names (and similarly with the system spam filtering). A typical system is shown in Figure 1.

These problems can be classified as follows:

- interpretation of the data;
- diagnostics;
- monitoring;
- design;

- forecasting;
- master scheduling;
- optimization;
- training;
- management;
- Debugging.

These kinds of tasks require decision making under conditions of insufficient data, a large number of "raw" information, operating conditions, large amounts of data. The general scheme of such systems is presented in Figure 2.

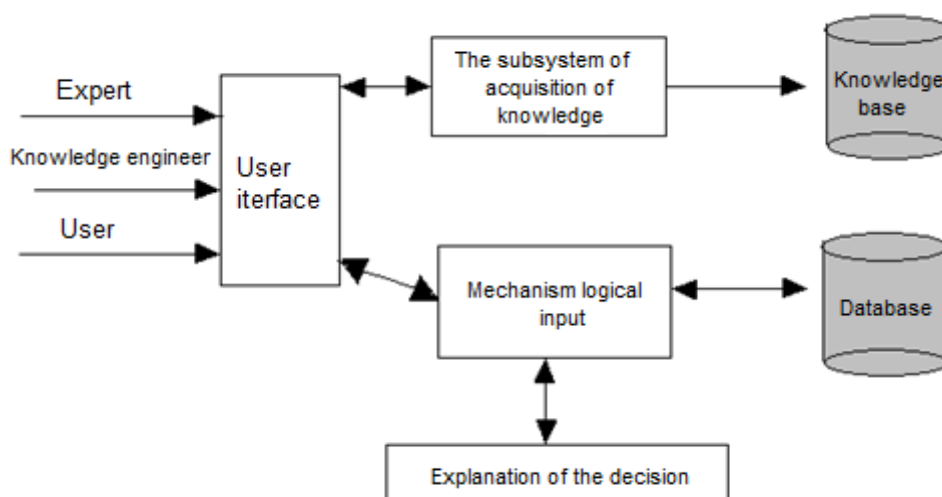


Figure 2 - The general scheme of the expert system

The inference engine is designed to produce new facts on the basis of comparison of the original data from the main memory and knowledge from the knowledge base. This mechanism allows to generate conclusions, perceiving facts introduced as elements of rules, finding rules, which include input facts and actualizing those parts which correspond to the facts entered. In the usual case, the output mechanism may perform one or both of the following operations:

- verification of the truth of a fact: the true fact is considered, if the inferred according to the laws of formal logic from the available facts and rules;
- finding a set of parameter values of a rule under which the rule is transformed into a true fact.

The main rule of inference in traditional logic is the rule that we judge the truthfulness of statements B on the truth of the statements A and $A \rightarrow B$. A fuzzy set in a non-empty space

X is the set of pairs $\langle x, \mu_A(x) \rangle$, where $\mu_A(x)$ – membership function of the fuzzy set A. This function assigns to each element x its degree of fuzzy sets A.

Explanations subsystem - the software part, allowing us to obtain a response to the questions: "How was obtained or that decision?" And "How the decision was made?" Tracing the process output decision containing fragments used the knowledge base. Knowledge Base - a body of knowledge related to a certain subject area and formally presented so that on the basis of their reasoning could be carried out. Model of knowledge representation can be divided into 3 types:

- Production models that allow us to represent knowledge in the form of sentences like: "IF condition THEN action."
- Such models have a significant drawback: the accumulation of a sufficiently large number of rules, they begin to contradict each other.

In ES uses a number of elements that are implemented within the software application that describes the subject area. Among the entities include:

- network models or semantic networks - usually represented by graphs that display the meaning of a complete image . nodes of the graph correspond to the concepts and objects , and the arcs - relationships between objects ;
- frame-based models , which are based use so-called frames - data structure to represent a conceptual object. information relating to the frame , contained in its constituent slots that can be terminal or be framed themselves , forming an entire hierarchical network ;
- User Interface - subsystem which allows to organize the user interaction with the system;
- interface developer is a software environment that allows you to make corrections in the working code ;
- debugging and testing the adequacy of the system operate programmer engineer and expert cognitive science ;
- Cognitive engineer - specialist in artificial intelligence , designed and built an expert system . usually the knowledge engineer acts as an intermediary between the expert and the knowledge base ;
- expert - a person who knowingly deemed competent in a particular subject area.

In Figure 3 is a diagram using the system, describing the interaction between the various users of the system.

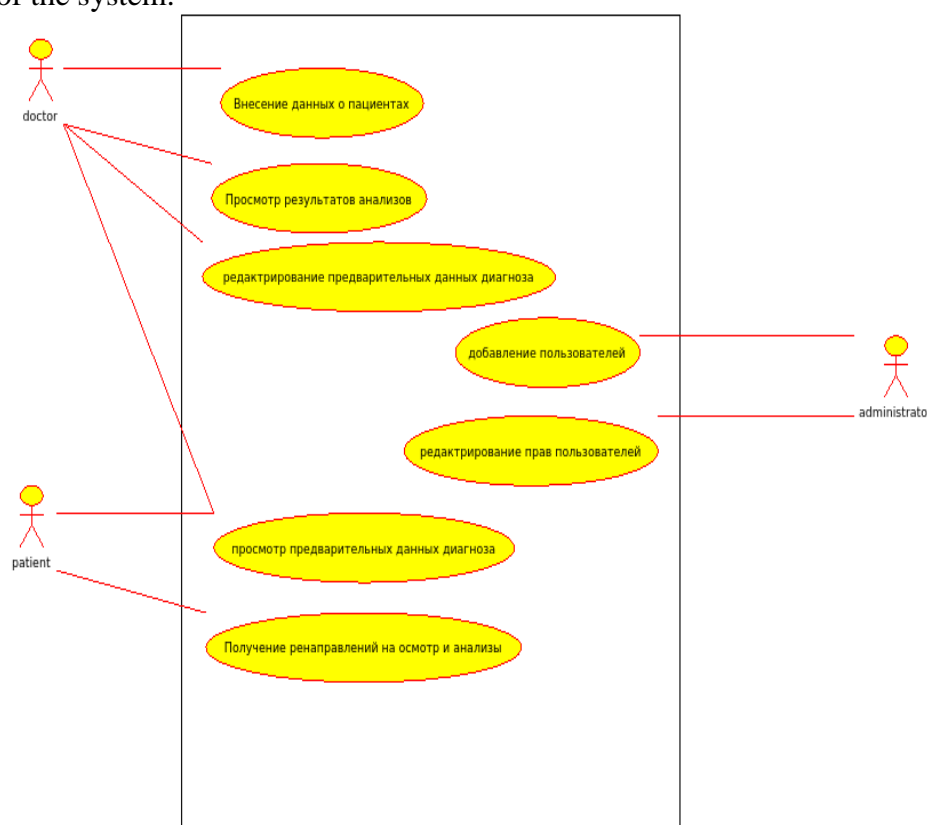


Figure 3 - UML diagram use

Standard scheme ES generally represents the system as a reference , which gives access to a shared specialist knowledge base, formed by experts thematic area that definitely helps in making difficult decisions , but sometimes this is not enough because sometimes can make a difference and the human factor [4] .

In health care, the correct decision depends on many factors and data obtained during various medical procedures and tests, in reading which may arise misinterpretations and errors, which may exclude the addition of user feedback with the system and the introduction of a DBMS to store patient records. Detail of schema changes is shown in Figure 4.

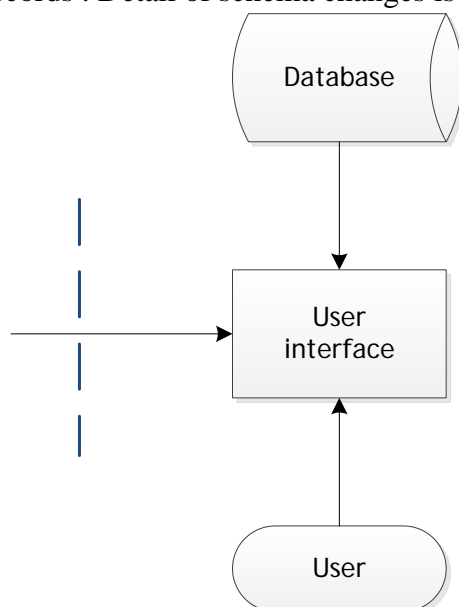


Figure 4 - fragment of an interactive expert system with user feedback

On the one hand, the introduction of the possibility of storing medical records is only a means to document and additional means of data storage. On the other - keeping and analyzing previous test results, it is possible to observe the dynamics of indicators displaying the indicators on the chart (Figure 5).

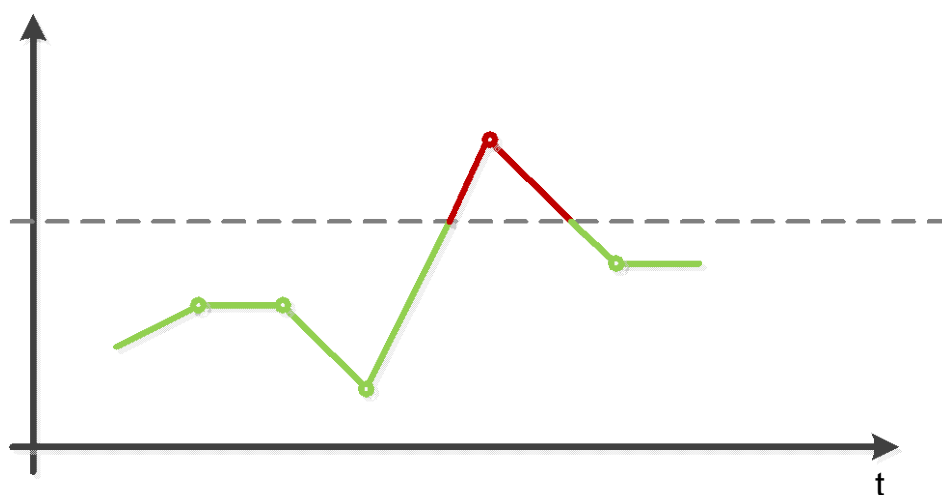


Figure 5 - dates dynamics of evaluable patients

Given the specifics of the application, you should cancel the need to use the system with maximum portability, which is solved by use of tablet and laptop computers and client-server technology. Diagram of the system is shown in Figure 6.

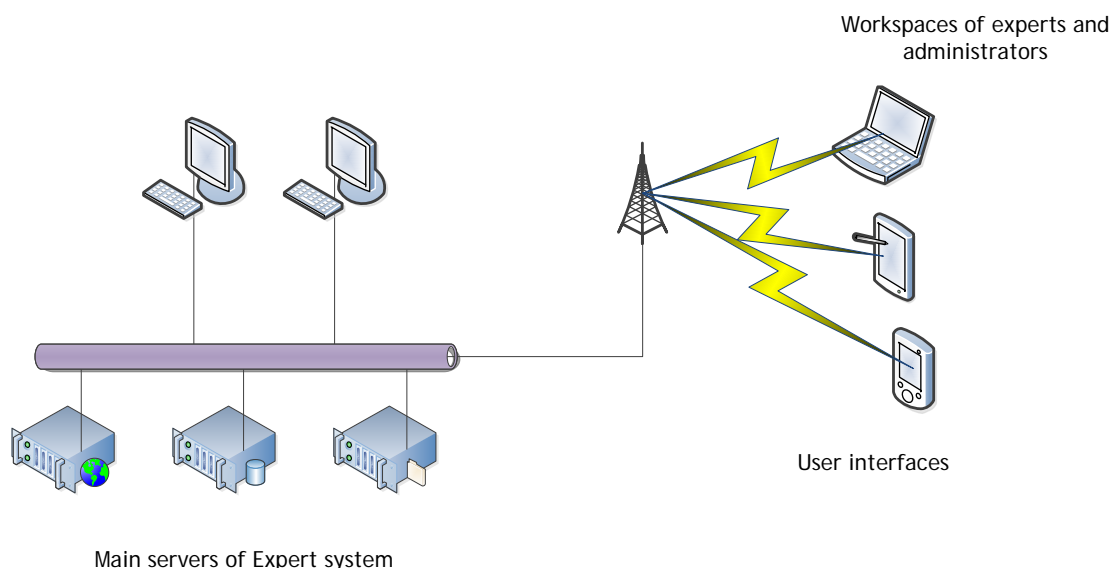


Figure 6 - ES interactive diagram

Central servers interactive expert systems store information and reference data, recharged and edited by experts, as well as data analysis and case histories of patients clinics and hospitals. Users of the system with the help of working with laptop client software installed on secure communications and wireless networks have access to the servers getting the opportunity to work with the required information. In order to improve the overall effectiveness of the system is proposed to use a cluster virtualization, which will reduce the overhead of system operation to a minimum.

As a result, the information system will create a specialized single database and perform various forecast trends in the field of medicine, as well as enable connectivity and clustering around a single information hub different directional IP not only support but also optimize the provision of health services, and as a result, improve the quality of treatment of various diseases.

Commissioning such interactive expert system will enhance the health care system, providing an opportunity as doctors clinics and ambulance paramedics to ensure timely and correct care for the sick and injured, as well as to analyze in advance and be prepared to solve complex medical problems.

References

1. Ponjatie, osobennosti i primery jekspertnyh sistem – YourLib.net. URL: <http://yourlib.net/content/view/12924/153/> (data obrashhenija 13.01.2014)
2. Dzhekson P. Vvedenie v jekspertnye sistemy. M.: Vil'jams, 2001. 624 s.
3. Dzharatano D., Rajli G. Jekspertnye sistemy: principy razrabotki i programmirovaniya. M.: Vil'jams, 2006. 1152 s.
4. Taunsend K., Foht D. Proektirovanie i programmaja realizacija jekspertnyh sistem na personal'nyh JeVM. M.: Finansy i statistika, 1990. 320 s.
5. Uotermen D. Rukovodstvo po jekspertnym sistemam. M.: Mir, 1989. 388 s.
6. Onlajn diagnostika zabolevanij po simptomam. – URL: <http://simptomus.ru/> (data obrashhenija 09.01.2014)
7. Obzor rynka kompleksnyh medicinskih informacionnyh sistem. – URL: http://www.kmis.ru/site.nsf/pages/2009_obzor_kmis.htm (data obrashhenija 16.12.2013)
8. T.V. Istomina, V.A. Egorov «Perspektivnye napravlenija razvitiya IT-industrii dlja analiza bol'shih ob#jomov dannyh v sistemah issledovaniya bioorganizmov» – Innovacionnye

tehnologii v jekonomike, informatike i medicine. VII Mezhregional'naja nauchno-prakticheskaja konferencija studentov i aspirantov. Sbornik statej. Penza: Izd-vo Penz. gos. tehnol. akad., 2011. – 266 s. – s. 20-21.

9. T.V. Istomina, V.A. Egorov, V.O. Dunin. Perspektivy razvitija jekspertnyh informacionnyh sistem dlja povyshenija urovnja kachestva zdravooohranenija // «XXI vek: itogi proshlogo i problemy nastojashhego pljus»: Nauchnoe periodicheskoe izdanie. – Penza: Izd-vo Penz. gos. tehnolog. Akad., 2012 – 220 s. – s. 92-96.

10. V.O. Dunin, V.A. Egorov. Perspektivy sozdaniya i razvitija informacionnoj sistemy s jelementami intellektual'nogo poiska, analiza i obrabotki biomedicinskoj informacii // Prikaspijskij zhurnal: upravlenie i vysokie tehnologii. – 2013. – № 3 (23). – S. 162-168

EXPERIENCE IN THE USE OF THE WCF SERVICE IN A GAME APPLICATION FOR WINDOWS PHONE.

Mikitchuk, A.
Saratov, SSEI

Games for Windows Phone are very popular in the Marketplace, and many of them use the services located in the Internet. Technology Windows Communication Foundation (WCF) allows for networking between the game and services.

Keywords: game development, Windows Phone, Windows Communication Foundation.

Operating system Windows Phone provides several scenarios for using remote services: classes for working with the protocol HTTP, sockets, or WCF. WCF technology allows you to use the C # language to write code, configuration files for tune the security and data transport layer for transmission data types are used .NET Framework. To host the service on the Internet is enough to have hosting that supports ASP.NET.

IDE Microsoft Visual Studio for Windows Phone allows you to create client applications for WCF- services. In Visual Studio in the current solution you must add URL link to the service. If the service is running, the IDE displays a list of methods exposed by the service, create a namespace to work with them and a configuration file describing the network interaction with the service.

To use the methods of service in a client application must create an object of class work with the service and call the appropriate method of induction provided by this class. An asynchronous method allows continuing gameplay while the remote service is engaged in calculations. After calculation service on the client corresponding event occurs. To handle the response from the service should use this event handler. Sometimes when working with a remote service can raise exceptions, so it is advisable to handle them to avoid hovering gaming application. That is to inform the user of error, suggest an error report developers and continue gameplay. When debugging work with the service recommended enabling tracing and debugging in the web.config configuration file on the server side.

This algorithm of working with WCF- services was used to create the game application augmented virtuality for Windows Phone. Augmented Virtuality - an innovative technology that lets create the game worlds based on real objects. Scenario of using this technology: a player makes a photo and along the contours on this photo are arranged game objects that make up the game world. Recognition algorithms are hard for mobile devices, so all the calculations runs remotely. Remote service is based on WCF. To create game map client must call service method GetMap, which passed an argument array byte, derived from

photos. The method returns a variable of type string, which is stored the game map in the agreed format. Upon completion of this method is invoked on the client event GetMapComplete. This event handler stops the game loop and stored game map in memory. If there is an error, the player is informed about this. After that gameplay continues.

Thus, WCF technology is relevant tool to create the server-side game applications for Windows Phone.

References

1. Ch. Petzold, Programming Windows Phone 7 Series, Microsoft Press 2011, ISBN: 978-0-7356-4335-2.
2. S. Pugachev, S. Pavlov, D. Soshnikov, Razrabotka prilozhenii dlya Windows Phone 7.5. SPb.: BHV-Peterburg 2012, ISBN 978-5-9775-0873-5.

GRAPHENE AS A MATERIAL FOR A NEW GENERATION OF HEAT SINKS

Merkulev A.Yu., Trusov V.A., Yurkov N.K.
Penza State University

The article is devoted to the unique material graphene, which in the future it may become the basis of heat sinks of the new generation. Describes its characteristics and properties, advantages and disadvantages .

Keywords: graphene, nanotubes, heat sink, specifications, features, advantages, disadvantages

One of the most difficult, tasks being solved by the development of electronics, - heat dissipating electronic equipment (EE). The current stable tendency to reduce the size of the EE acuteness of this problem is not reduced, and constantly grows stronger with increasing the power of the device and the less physical volume [1, 2].

For the manufacture of cooling systems EE use materials with high thermal conductivity and low thermal resistance [3]. However, under forecasts of experts, cooling systems classic made from aluminium and copper soon not be able to provide a normal thermal regime of the EE. Trying to solve the growing problem, scientists are conducting research aimed at the creation of various composite materials with higher thermal characteristics.

In 2004, two Russian scientists - Konstantin Novoselov and Andre Geim have made great strides, they managed to obtain a material with unique properties, graphene. On the properties of graphene scientists knew long ago, but the problem was how to get one. Novoselov and Game have solved this problem by adhesive tape. By means of multiple overlays tape on a layer of graphite and subsequent avulsion was obtained by a layer of graphene one atom thick. According to experts, graphene can radically transform not only modern electronics, but with major changes in the process of thermal design EE.

Graphene is a two-dimensional material with a hexagonal crystal structure, it is unusual mechanical and electrical properties. According to the tensile strength he surpasses steel up to 200 times the speed of conductivity is comparable with the speed of light, and the weight of the film graphene thickness in one atomic layer size of a football field is less than 1, the electrical resistivity of the material at room temperature is about 1 $\mu\text{ohm}\cdot\text{cm}$, which is 35% less than that of copper. The unique electronic properties of graphene are manifested, and in optics. Its thermal conductivity is 10 times more than that of copper [4]. On Fig. 1 shows the crystal structure of graphene carbon atoms arranged in a lattice «honeycomb»[5].

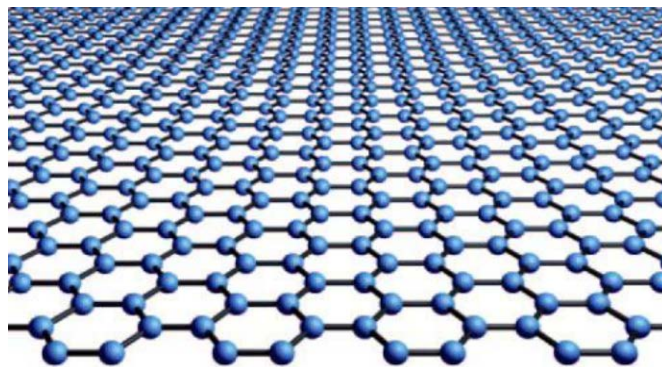


Fig. 1. Crystal structure of graphene.

Possibility of use of a decanter for heat removal from elements of electronics is discussed for a long time. In the experiments made in 2008, the coefficient of heat conductivity of the suspended single-layer decanter at the room temperature reached 3000–5000 W • m⁻¹ • K⁻¹. This value surpasses indicators of the diamond, one of the best conductors of heat. Measurement of heat conductivity of a decanter carry out by means of a contactless method of confocal microraman spectroscopy [1].

It was recently opened the amazing property of graphene, which makes possible to manufacture a nearly ideal heat sink: a layer of carbon one atom thick can serve as a «mediator», allowing grow vertical nanotubes on nearly any surface, including on the surface of the diamond. One can predict that the nanotubes easy to get and on the surface of the heat sinks of aluminum and copper. Thus, turning them into the heat sink with the advanced surface.

Results of the research conducted by Rice university together with the Honda company, will allow to grow up nanotubes on substrates which were considered for this purpose as the absolutely unsuitable earlier. Scientists showed it, having grown up nanotubes on a diamond surface. Diamond very well, is five times better than copper, carries out heat. But the area of its surface radiating this heat, is very small. Grafen, on the contrary, actually consists only of a surface. The same can be told and about carbon nanotubes which represent the decanter twisted in tubes. The wood of the vertical nanotubes which have been grown up on a surface of diamond, will disseminate heat as the radiator having million edges. Such ultrathin heat sink will give the chance to save significantly space in compact microprocessor devices. Scientists from research institute of the Honda company grew up a decanter on a copper foil a standard method of sedimentation from a steam phase.

Then they transferred decanter sheets from a foil to surfaces of samples from diamond, quartz and various metals. For further researches samples were transferred to Rice's university where on them grew up nanotubes. Good results were received only with a single-layer decanter, and defective – wavy and morshchinistny – sheets worked best of all. Defects of a decanter took the sprayed particles of the catalyst on the basis of iron on which nanotubes started growing. As researchers consider, the decanter promoted growth of nanotubes, interfering with a congestion of particles of the catalyst in groups. The hybrid structure from a decanter and the nanotubes which have been grown up on a metal substratum (for example, copper), has high general electric conductivity. Such structures can be used in designs of powerful electrochemical elements where will provide low contact resistance between current collectors and active materials [6].

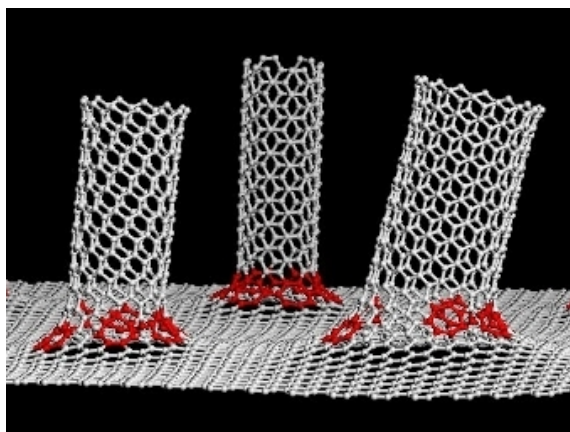


Fig.2 Connection graphene and nanotubes in a single covalent sheet of carbon.

Modern materials, intended for the removal of heat from electronic components have to have a number of mandatory properties [1]:

- have good thermal conductivity;
- have a high electric strength;
- be flexible;
- easy to handle woods;
- issued with a glutinous layer on one or both sides on customer's request;
- be environmentally friendly, does not release hazardous emissions when heated;
- have an affordable price.

Thus, graphene has all the required properties for the effective removal of heat, but today, it is very expensive, because there is no effective method of its production for the introduction into industrial production. Meanwhile, the work of many scientists in the field of production of graphene on an industrial scale is possible to expect the appearance in the near future of a new class of heat sinks and cooling systems, EE. These heatsinks will have record low thermal resistance, thereby reducing the load on the crystal heatloaded item [7,8].

Thus, the decanter possesses all necessary properties for effective heat removal, but today it very expensive as is absent an effective way of its receiving for introduction in industrial production. Meanwhile work of a large number of scientists in the field of receiving a decanter commercially, allows to count on emergence shortly a new class of heat sinks and EE cooling systems. Such heat sinks will possess record-breaking low value of thermal resistance that will lead to decrease in load of a crystal of the heatloaded element [7,8].

References

1. Vladimir Kosnyrjov. Teploprovodnye materialy kompanii Bergquist [Jelektronnyj resurs]. Rezhim dostupa: http://www.power-e.ru/2008_2_118.php
2. Goryachev N.V. Konceptija sozdaniya avtomatizirovannoj sistemy vybora teplootvoda jelektroradiojelementa / N.V. Goryachev, N.K. Yurkov // Sovremennye informacionnye tehnologii. 2010. № 11. S. 171-176.
3. Merkul'ev A.Ju. Sistemy ohlazhdenija poluprovodnikovyh jelektroradioizdelij / A.Ju. Merkul'ev, N.V. Goryachev, N.K. Yurkov // Molodoj uchenyj. — 2013. — №11. — S. 143-145.
4. V.Judincev «Nanojelektronika stremitel'no nabiraet sily»// Jelektronika: Nauka, Tehnologija, Biznes, 2009.S.82
5. Novoselov K.S. Grafen: materialy Flatlandii / Novoselov K.S. // Uspehi fizicheskikh nauk. 2011. T. 181. № 12. S. 1299-1311.

6. Majk Uil'jams, Rut Djevid. Brillianty, nanotrubki najti obshhij jazyk v grafene. Bergquist [Elektronnyj resurs]. Rezhim dostupa: <http://news.rice.edu/2013/05/28/diamonds-nanotubes-find-common-ground-in-graphene/>
7. Yurkov N.K. Systems of Coriolis flowmeters in the field / N.K. Yurkov, K. V. Gudkov, M. Yu. Mikheev, V. A.Yurmanov // Measurement Techniques. N.Y., Springer, November 2012, Volume 55, Issue 6, pp 132-139.
8. Goryachev N.V. Programma inzhenerenogo raschjota temperatury peregreva kristalla jelektroradiokomponenta i ego teplootvoda / N.V. Goryachev, A.V. Lysenko, I.D. Grab, N.K. Yurkov // Trudy mezhdunarodnogo simpoziuma Nadezhnost' i kachestvo. 2012. T. 2. S. 242-243.
9. Andreev P.G. / Modelirovanie pereotrazhatelej radioluchevykh sistem obnaruzhenija. / Avtoreferat dissertacii na soisk. uch. step. kand. tehn. nauk: — Penza: PGU, 2005 g. — 22 s.
10. Goryachev N.V. Teplovaja model' smennogo bloka issleduemogo ob#ekta / N.V. Goryachev // Trudy mezhdunarodnogo simpoziuma Nadezhnost' i kachestvo. 2012. T. 1. S. 263-263.
11. Yurkov N.K. Measurement of the parameters of three-element nonresonance two-terminal networks at a fixed frequency / N.K. Yurkov, M. V. Klyuev, E. V. Isaev // Measurement Techniques. N.Y., Springer, Issue 11, February 2013, Volume 55, Issue 6, pp. 1267-1274.
12. Goryachev N.V. Programmnye sredstva teplofizicheskogo proektirovanija pechatnykh plat jelektronnoj apparatury / N.V. Goryachev, N.K. Yurkov // Molodoj uchenyj. 2013. № 10. S. 128-130.
13. Yurkov N.K. A finite-element model of the thermal influences on a microstrip antenna / N.K. Yurkov, E.Yu. Maksimov, A.N. Yakimov // Measurement Techniques. N.Y., Springer, Vol. 54, No. 2, May, 2011. P. 207-212.
14. Goryachev N.V. Algoritm funkcionirovanija komp'juternoj programmy stenda issledovanija teplootvodov/ Grab I.D., Goryachev N.V., Lysenko A.V., Yurkov N.K.//Trudy mezhdunarodnogo simpoziuma Nadezhnost' i kachestvo. 2011. T. 1. S. 244-246.
15. Yurkov N.K. Electromagnetic screening of the elements of a high-voltage vacuum divider / N.K. Yurkov, Buts V.P., Smirnov E.N., Ryshov A.A. // Measurement Techniques. N.Y., Springer, Vol. 54, No. 2, May, 2011. P. 200-206.
16. Goryachev N.V. Struktura avtomatizirovannoj laboratorii issledovanija teplootvodov / N.V. Goryachev, I.D. Grab, A.V. Lysenko, N.K. Yurkov // Trudy mezhdunarodnogo simpoziuma Nadezhnost' i kachestvo. 2011. T. 2. S. 119-120.
17. Andreev P.G. Primenenie CAD sistem v proektirovanii radiojelektronnykh sredstv / P.G. Andreev, N.A. Talibov, P.M. Osipov // Trudy mezhdunarodnogo simpoziuma Nadezhnost' i kachestvo. 2007. T. 1. S. 146-148.
18. Brostilova T.Ju. Metodika rascheta konstruktivnykh parametrov opticheskoy sistemy razrabatyvaemogo volokonno-opticheskogo preobrazovatelja davlenija / T. Ju. Brostilova, S. A. Brostikov // Nadezhnost' i kachestvo : tr. Mezhdunar. simp. — Penza : Izd-vo PGU, 2012. — T. 2. — S. 43–44.
19. Goryachev N.V. Struktura i programmno-informacionnoe obespechenie informacionno-izmeritel'nogo laboratornogo kompleksa / N.V. Goryachev, A.V. Lysenko, N.K. Yurkov // Izvestija Juzhnogo federal'nogo universiteta. Tehnicheskie nauki. 2012. T. 130. № 5. S. 169-173.
20. Goryachev N.V. Konceptual'noe izlozhenie metodiki teplofizicheskogo proektirovanija radiojelektronnykh sredstv / N.V. Goryachev, N.K. Yurkov // Sovremennye informacionnye tehnologii. 2013. № 17. S. 214-215.

21. Brostilov S.A. Matematicheskoe modelirovanie processov otrazhenija i rasprostraneniya jelektromagnitnyh voln v tonkoj gradientnoj dijelektricheskoj plastine / S. A. Brostilov, E. V. Kuchumov // Nadezhnost' i kachestvo : tr. Mezhdunar. simp. – Penza : Izd-vo PGU, 2011. – T. 1. – S. 281–283.
22. Andreev P.G. Mikroprocessornye sistemy v uchebnom processe / P.G. Andreev, I.Ju. Naumova, N.K. Yurkov, N.V. Goryachev, I.D. Grab, A.V. Lysenko // Trudy mezhdunarodnogo simpoziuma Nadezhnost' i kachestvo. 2009. T. 1. S. 161-164.
23. Goryachev N.V. Podsystema rascheta sredstv ohlazhdenija radiojelementov v integrirovannoj srede proektirovanija jelektroniki / N.V. Goryachev, I.D. Grab, A.A. Ryzhov // Izvestija vysshih uchebnyh zavedenij. Povolzhskij region. Tehnicheskie nauki. 2010. № 4. S. 25-30.
24. Brostilov S.A. Volokonno-opticheskij datchik davlenija na osnove tunnel'nogo jeffekta / S. A. Brostilov, T. I. Murashkina, T. Ju. Brostilova // Izvestija vysshih uchebnyh zavedenij. Povolzhskij region. Tehnicheskie nauki. – 2010. – № 4. – S. 106–117.25.
- Goryachev N.V. K voprosu vybora vychislitel'nogo jadra laboratornogo stenda avtomatizirovannogo laboratornogo praktikuma / N.V. Goryachev, N.K. Yurkov // Sovremennye informacionnye tehnologii. 2009. № 10. S. 128-130.
26. Trifonenko I.M. Obzor sistem skvoznogo proektirovanija pechatnyh plat radiojelektronnyh sredstv / I.M. Trifonenko, N.V. Goryachev, I.I. Kochegarov, N.K. Yurkov // Trudy mezhdunarodnogo simpoziuma Nadezhnost' i kachestvo. 2012. T. 1. S. 396-399.
27. Goryachev N. V., Grab I. D. , Petelin K. S. , Trusov V. A. , Kochegarov I. I. , Yurkov N. K. Avtomatizirovannyj vybor sistemy okhlazhdeniya teplonagruzhennykh elementov radioelektronnykh sredstv [Automated selection of cooling system of thermally loaded elements of radioelectronic facilities]. Priaspiskiy zhurnal: upravlenie i vysokie tekhnologii [Caspian Journal: Management and High Technologies], 2013, no. 4, pp. 136-143
28. Sivagina Ju.A. Obzor sovremennyh simpleksnyh retransljatorov radiosignalov/ Ju.A. Sivagina, I.D. Grab, N.V. Goryachev, N.K. Yurkov // Trudy mezhdunarodnogo simpoziuma Nadezhnost' i kachestvo. 2012. T. 1. S. 74-76.
29. Goryachev N.V. Informacionno-izmeritel'nyj laboratornyj kompleks issledovanija teplootvodov jelektroradiojelementov / N.V. Goryachev, A.V. Lysenko, I.D. Grab, N.K. Yurkov // Trudy mezhdunarodnogo simpoziuma Nadezhnost' i kachestvo. 2012. T. 2. S. 239-240.
30. Goryachev N.V. Proektirovanie topologii odnostoronnih pechatnyh plat, sodержashhih provolochnye ili integral'nye peremychki / N.V. Goryachev, N.K. Yurkov // Trudy mezhdunarodnogo simpoziuma Nadezhnost' i kachestvo. 2011. T. 2. S. 122-124.
31. Goryachev N.V. Indikator obryva predohranitelja kak jelement pervichnoj diagnostiki otkazov RJeA / N.V. Goryachev, N.K. Yurkov // Trudy mezhdunarodnogo simpoziuma Nadezhnost' i kachestvo. 2010. T. 2. S. 78-79.
32. Goryachev N.V. Programmnye sredstva teplofizicheskogo proektirovanija pechatnyh plat jelektronnoj apparatury / N.V. Goryachev, N.K. Yurkov // Molodoj uchenyj. 2013. № 10. S. 128-130.
33. Andreev P. G. Osnovy proektirovanija jelektronnyh sredstv: ucheb. posobie/ P. G. Andreev, I. Ju. Naumova//Penza: Izd-vo PGU, 2010.-124 s.
34. Padolko E. P. Osnovnye ponjatija imitacionnogo modelirovanija i postroenie imitacionnoj modeli sistemy massovogo obsluzhivaniya/ E. P. Padolko//Sovremennye informacionnye tehnologii. 2012. № 15. S. 43-45.

HISTORY OF DEVELOPMENT OF ELECTRO-MUSICAL INSTRUMENTS IN RUSSIA

Joao A.J. Gromkov N.V.
Penza, Penza State University

This article it is talking about some features of historical developments and scientific achievements in the field of development and production of electro-musical instruments in the time of the USSR.

Electro-musical instruments in Russia started to develop at the end of XIX - the beginning of the XX century and passed an interesting and peculiar way in a century. Electro-music is a result of cooperation of radio technicians and musicians.

Electronic musical instruments (EMI) call tools in which at musical electric energy it will be transformed to the sound. In the majority of EMI to this purpose by applying various electronic devices - generators, amplifiers and modulators [1].

Source of a sound is the acoustic radiator (loudspeaker) raised by electric fluctuations of sound frequency from 20 Hz to 20 kHz [10].

Electric fluctuations are generated with the subsequent strengthening in electronic amplifiers. Influencing generators and amplifiers, the performer changes frequency and amplitude of electric fluctuations and thus achieves the necessary frequency and loudness of sounding of EMI.

There are two types of EMI with free intonation, like a human voice and strings. To bow instruments they allow taking sounds of any height within their range. In them generators with frequency reconstructed in the course of execution are applied. The second look keyboard electro-musical instruments with the fixed intonation, such as, in a piano and body; they have a set of in advance adjusted generators [4].

The first data on use of electro-mechanical generators for receiving sound fluctuations belong to the middle of the XIX century. In 1885 German scientist E.Lorentz used a principle of the electric breaker for excitement of strings and tuning forks [3].

Depending on the circuit decision distinguishes melodic (single voice) and polyphonic tools. Single voice tools allow reproducing only one melody without accompaniment that is at present time to receive only one sound. They apply as the soloist for imitation of a peculiar "electronic" sounding at execution of modern rhythms.

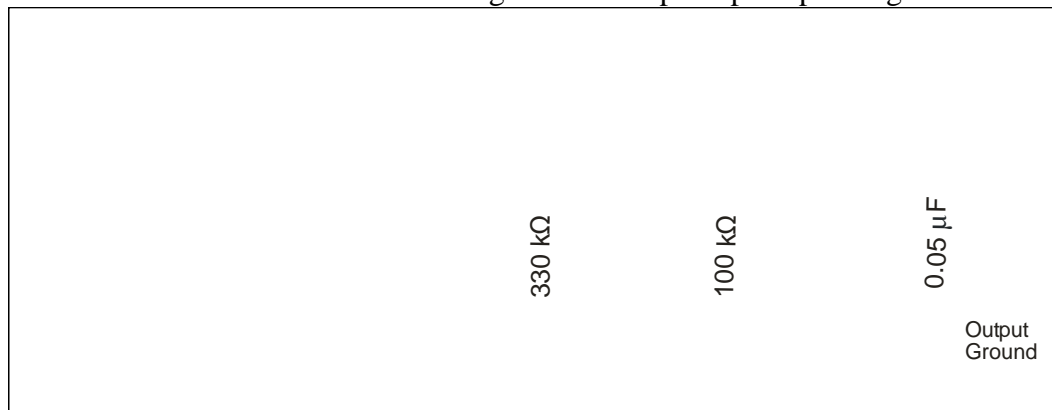
The tool some tones (it is possible to press at the same time some keys) allow to reproduce Polyphonic tools at the same time and to execute both a melody, and accompaniment [2].

On a way of education electro-musical instruments are subdivided on adapterize and electronic.

In adapterize electro-musical instruments mechanical fluctuations of a sounding body (strings, decks) will be transformed to electric fluctuations of sound frequencies by means of a sound pickup - the adapter. These fluctuations amplify in the amplifier of low frequency and move in a loudspeaker [5].

The widest application as sound pickups for shchipkovy musical instruments was received by electro-magnetic adapters. They have a number of advantages in comparison with the sound pickups, based on other principles of action (piezoelectric, electrodynamic, etc.): high mechanical durability, safety in operation, absence of reproduction of extraneous noise, rather wide range of reproduced frequencies.

The electric circuit of an electromagnetic sound pickup adapter is given in drawing 1.



Drawing 1 - The Electric circuit of an electromagnetic sound pickup: 1-constant magnets; 2-steel string; 3-core; 4 coils; 5, 6-resistors; 7-condenser; 8-plug nests

Basic element of a sound pickup is not closed constant magnet (1) (they can be a little). On a way of passing of magnetic power lines in this case on the steel core (3) coils (4) are established. Constant magnets with coils are placed in the adapter in such a manner that at its installation on a guitar its steel strings (2) get to an action field of power lines of magnets. The principle of action of a sound pickup is based on change of size of a magnetic stream of the constant magnets passing through the core and a steel string. Two coils (4) placed on the core have the identical and coordinated windings. The fluctuating string changes a magnetic stream with the frequency, equal frequency of fluctuation of a string. In this regard in coils the electromotive power with the frequency, equal frequency of change of a magnetic stream is directed. The electric signals received in coils move on an adapter entrance of the amplifier of low frequency. For volume control of sounding the resistor resistance (5) included in the scheme as a potentiometer serves. The resistor (6) which has been switched on consistently on the rheostatic scheme, changes a timbre [8].

In principle adapterize it is possible for any acoustic tool - string, wind. Thanks to an adapterize and the subsequent strengthening of a sound in the amplifier of low frequency the tool becomes on force of sounding in one row with other orchestral tools and can be used for solo, ensemble and orchestral execution of pieces of music, accompaniment, and also for the educational purposes.

The first single-voice electronic musical instrument on the lamps, received practical application was constructed in 1921 in our country. In honor of his founder, the Soviet physicist of I. S. Theremin, this tool with spatial management in height of a sound it was called «Theremin». The tone height in it changed by means of approach to the aerial and removals of a hand of the performer from it. The aerial of theremin - the metal core connected to an oscillatory contour of the generator. Management of loudness was made in the similar way, in some subsequent updating - by means of a pedal. Theremin it was shown in 1921 at the 8th All-Russia electro-technical congress. V.I.Lenin approved the invention and even tried to play this instrument. Having highly appreciated advantages of the new tool, it pointed to need of continuation of works in the field of electronic musical instruments [1].

In Theremin fluctuations of sound frequency arise as palpation of fluctuations of two high-frequency generators frequency of one which copes the performer. In the late twenties Theremins were widely adopted abroad. In 1927 Theremin acted with concerts on theremin at the Frankfurt musical exhibition, then in other cities of other countries in Western Europe and North America [3].

The beginning of distribution of EMI in our country was marked by this invention.

After the creation of Theremin enthusiasts of electromusic - engineers and radio fans in commonwealth with musicians found out that there is a lot of and fruitfully work in this area. There are new tools, their designs and circuit decisions are improved, performing possibilities got extended. In the 20-30th they got popular after the invention of some new things such new tools as sonar, violena, emirithone, ekvodin [7]. From spatial management of a sound pass to more convenient - fretboard, and then to the most available - keyboard. The first Soviet keyboard single-voice EMI - "companola" was designed by I.D.Simonov in 1937 and was repeatedly used in broadcasts. After that keyboard management in height of tone it was entered in emirithone and ekvodin.

In the 30th models of various adapterizovanny electro-musical instruments - guitars, balalaikas, violins, violoncellos, and also keyboard tools [9] were developed.

During 1925-1930 at the State institute of history of arts (GIII) the musical and acoustic laboratory under the direction of at first Kovalenkov, then L.G.Nemirovsky and E.A.Sholpo worked, it works on studying of acoustics of musical instruments, mikrotemperatsiya, an electric sound recording were carried out, etc.

In the 50th of this year Korsunsky and I.D.Simonov designed lamp electronic harmonic in which loudness of a sound was regulated by depth of pressing a key, then transistor [9].

In 1930 in Leningrad the Central musical and acoustic laboratory transformed two years later at the initiative of the academician N.N. Andreeva in Research institute of the musical industry in which many outstanding scientists-physicists worked: H.H. Andreev, A.V. Rimsky-Korsakov, I.I.Kuznetsov, A.A. Harkevich, G.A. Ostroumov, N.A. Deaconov, N.I. Ugolnikov, Ya.M. Gurevich, L.S. Vagin, etc. At the institute the big complex of works was on studying materials for musical instruments, mechanisms of interaction of strings and a deck in a piano and shchipkovy tools, to research of mechanical properties of keyboard mechanisms, sound education systems in wind instruments, on equipment creation for record and the analysis of properties of sounds of musical instruments etc. was carried out. The institute closely cooperated with the branch research laboratory created in 1932 at the factory «Red October» under the direction of N.A. Dyakonova, and also with the factory of A.V. Lunacharsky on studying and developing new models of grand pianos, guitars, balalaikas and other string instruments. Results of these works found late reflection in A.V.Rimskogo-Korsakova's book and H.A. Dyakonova «Musical instruments. Research and calculation methods» and three volumes of the collection «Works Research institute of the musical industry». Before the Second World War the institute in Leningrad was closed [11].

In Moscow under the direction of Professor N. A.Garbuzova in 1921 the state institute of a musical science (SIMS) which existed till 1931 was created. After that H.A. Garbuzov created at the Moscow conservatory Research musical institute (RMI), having allocated in it acoustic laboratory. From the middle of the 1930th was in it A.A.Volodin, one of leading experts in area of electro-musical instruments, the author of the book «Electro-musical tools» worked. The laboratory was engaged in studying of acoustics of musical instruments, a singing voice, psychology of perception of musical sounds etc. In it there are acoustics, psychologists, musicologists, such as of this year Korsunsky, S.S. Skrebkov, with L.S. Thermen, Yu.N. Rage, E.V. Nazaykinsky, P.N. Zimin, I.D. Simonov at different times worked, etc. The laboratory of musical acoustics ceased to function in 1991. On its base in the 1992nd the Studio of electronic music and the Thermen-center under the direction of A. Smirnov was created [4].

In 1967 on the basis of factory of musical instruments "Dawn" the Research design institute of technology of the musical industry (RDITMI) which should provide requirements of production was created near Moscow. Some results of the research works executed in it on

musical acoustics found reflection in Kuznetsov's directory «Acoustics of musical instruments» [9].

In 1957 under control of Vyacheslav Meshcherin the first Soviet collective of electro-musical instruments was created. The ensemble was created as experimental at musical edition of All-Union Radio. As it was formulated in the official document, the ensemble was created «with a view of use of electro-musical instruments in radio - and telecasts, and also tape recordings». The idea is supported by such outstanding musicians, as Dmitry Dmitriyevich Shostakovich and Dmitry Borisovich Kabalevsky [12].

Vyacheslav Meshcherin collected a circle of adherents - engineers, designers, musicians, and they together started to work over creation of new tools. Thus, in the single copy of the Kamertonny piano, electronic Germanium, Ekvodin were born. Also musical "arsenal" of ensemble of Meshcherin included electrobodies, theremins, an electro harp; on bayans, violins, the Hawaiian guitars established adapters (sound pickups). Participants of ensemble which developed a reverberator. Ten musicians cooperated with collective [12].

Tools appeared very little, less, than in a symphonic orchestra of usual structure. They stood in a hall mixed up with lecterns and chairs, from them cables to tables on which devices in identical gray casings were piled up lasted.

The ensemble helped hundreds of TV programs, animated films and radio of performances.

In the 90th Meshcherin's ensemble entered in new "incarnation" - supplied already modern, mainly digital import synthesizers. The structure of an orchestra became purely electronic, there were new possibilities of tembral processings of a sound. However Meshcherin kept the main thing - individual style, unique musical handwriting. And - surprising business - "serious" Japanese synthesizers sounded as it was warm and lyrical, as well as our "Youth" and theremins in far the 60th [12].

But, unfortunately, electro-musical instruments did not enjoy such support of the state, as other directions of acoustics (hydroacoustics, ultrasonic acoustics and so forth) therefore many prominent scientists-physicists, started to be engaged in musical acoustics, were reoriented on these areas of a science (S.N. Rzhavkin, A.V. Rimsky-Korsakov, A.N. Rivin). For the same reason it was not created as a large research in institutes on musical acoustics, works proceeded only in separate laboratories at the Leningrad conservatory, at the Moscow conservatory and at a number of productions [1].

List of electro-musical instruments of production USSR [6]:

- Polyphonic body "Faemi-1M";
- Portable electro-body "Quintet";
- Portable electro-body "EM-14 Electronics";
- Small-sized four-part keyboard electro-musical instrument of "Formanta-mini";
- Body with sintezator sounding "Solaris" (Estradin-314);
- A keyboard electro-musical instrument - a polyphonic prefix to a piano "Manual";
- A keyboard electro-musical prefix to "Klaviol's" piano;
- Portable electro-body "Lel";
- Electro-body "Prelude";
- Portable keyboard polyphonic electronic tool "Youth-1122", "Youth-1132";
- The combined two-channel electronic tool «Formanta EMS-01»;
- Electronic piano "EM-15 Electronics".

Outstanding results in the field of studying of acoustics of vocal speech were received at this time under the direction of the professor of V.P. Morozov. Have begun the researches on acoustics of a voice at physiology Institute of Setchenov in Leningrad, it organized a laboratory for the studies of a singing voice in the Leningrad conservatory. There in 1960-1968 the big complex of researches on acoustics of vocal speech which were executed, and

then were continued in Moscow at the Institute of psychology of the Russian Academy of Sciences (The center «Art and a science») and in the Moscow conservatory. Problems of nonverbal communication, perception of speech and singing, acoustic parameters and their communication with the emotional content of vocal speech, etc. were investigated [5].

V.P. Morozov published fifteen monographs, among them «Secrets of vocal speech» (1967), «Biophysical bases of vocal speech» (1977), «Art and a communication science: nonverbal communication» (1998), «Art of resonant singing» (2002), etc.

It should be noted that acoustics of speech was given a lot of state attention in connection with studying of problems of its recognition and synthesis, large research institutes were engaged in these questions in the 1960-90th years. From acoustic works of this period it is possible to note works of such known scientists as L.A. Chistovich, L.Ya. Myasnikov, V.I. Galunov, Yu.A. Dubrovsky, A.V. Ventsov, V.G. Mikhaylov, M.A. Sapozhkov, V.N. Sorokin, etc.

We got used to the piano sounds only as a piano, a clarinet only as a clarinet and not differently. Electric ways of a timbre-creation already now allow to create EMI with any various timbres, especially attractive in this sense it is necessary to consider possibility of electric synthesis of new timbres of high musical quality. Besides, the sphere of art creativity of the performer can join management of spatial characteristics of a sound - reverberation, dimensions and the sound generation direction.

It is necessary to state the advantages of electro-musical instruments and also their almost unlimited possibilities in sense of use of sound ranges on height and loudness [1].

Shortcomings of modern EMI are so considerable that in some cases interfere with their wide introduction in musical practice. Small reliability, low stability of a system, "electric" coloring of sounding first of all concern them. However now there are all conditions for the creation of EMI of the highest class. Only such electro-musical instrument which besides high operational qualities in everything will be subordinated to the will of the performer for it is possible to consider sounding highly artistic only under condition of flexible management of the performer in all parameters of a sound can become: in height, dynamics, timbre.

Abroad electro-musical instruments gained very big distribution. A number of specialized firms are engaged only in production and sale of EMI, mainly polyphonic - electrobodies. In the second half of the last century in the Soviet Union a number of electrotools serially was issued as the Retakkord models, the series "Estradion", "Romantika", "Meridian", "Gamma", "Ekvodin", "Unost". As a base for creation of these tools long-term works of the Soviet inventors served this case. To a great regret, with disorder of the USSR in Russia scientific development in this direction was sharply reduced and the Russian musicians - professional performers and composers are compelled to be content with foreign development and tools.

Now the huge range of the electro-musical instruments which producers are such firms as «Roland», «CASIO», «YAMAHA» is abroad presented.

Further research of this direction in music, can impulse to scientific development of new original electro-musical instruments on the basis of modern achievements of electronics, promoting and increasing the level of music education, involving young and talented musicians, to adjust the production of EMI, thereby having increased the growth of the industry of Russia.

It is possible to hope that improvement of existing designs, studying of foreign experience, commonwealth of designers and musicians will allow to create in the near future of the domestic EMI meeting the highest operational and art requirements.

References

1. Voloshin V. I., Fedorchuk L.I. Electromusical instruments, M, "Energy", 1971;
2. Korsunsky C., Simonov I., Electro-musical instruments, M. - L., 1957;
3. Thermen L., Physics and musical art, M., 1966;
4. Volodin A., Electronic musical instruments, M., 1970;
5. Voloshin V., Fedorchuk L., Electromusical instruments, M., 1971;
6. Kuznetsov L., Prospects of development of electromusical instruments, вып. 2, M., 1973;
7. Mol A., Fuchs V., Kessler M., Art and COMPUTER, M., 1975;
8. Medvedovsky D., Guzevich O., Electromusical shchipkovy instruments, L., 1979;
9. Musical acoustics in Russia: <http://www.zvintsov.ru/zvintsov/muzykalnaya-akustika-v-rossii>;
10. Electromusical instruments. Musical encyclopedia, 1973-1982): <http://www.musenc.ru/html/6/6lektromuz3kal5n3e-instrument3.html>;
11. Development history. Musical acoustics: <http://www.paintpit.ru/muzykalnaya-akustika-v-rossii.html>;
12. Inventors and pioneers of electronic music. Ensemble of electromusical instruments under the direction of Vyacheslav Meshcherin: <http://www.fingus.ru/publ/34-1-0-214>.

INVESTIGATION LISSAJOUS ORBITS AROUND THE L2 LIBRATION POINT OF THE EARTH-MOON SYSTEM

Fedorenko, J.V.
Moscow, NRU HSE

This paper covers space mission design with a use of a massive object flyby to move a spacecraft to asteroids, comets and other objects of the Solar system. Libration points (which are also known as Lagrange points) are often used to implement these tasks in similar projects.

If the Earth-Moon system is considered stationary and consisting of two massive bodies, a spacecraft, which is assumed to be a small body, can be left stationary in the libration points, also called Lagrange points, because the gravitational forces from the two bodies are balanced there. Consider the massive bodies rotating around their common center of mass with a constant angular speed. Such systems will possess 5 points, where the gravitational forces are balanced by the centrifugal one, which leads to a small body at any one of such points to remain stationary in the rotating reference frame.

Missions to the Earth-Moon L2 libration point can be of interest both as a starting stage for remote objects of the Solar System, and for exploration of the back side of the Moon. The possibility of missions to L2 point utilizing Lunar flybys is studied in [1-3]. Libration point L2 is the only one of the five Earth-Moon Lagrange points, which lies directly behind the Moon relative to the Earth.

Placement of a spacecraft on an orbit around L2 point will allow communicating with other equipment, for example, on the surface of the far side of the Moon, which would be impossible to realize directly from the Earth. In this case, the spacecraft position allows its operation as a relay station between a control center on the Earth and a mobile unit collecting scientific data on the far side of the Moon [4].

Two types of periodic orbits are known around libration points, which were described by Hechler in [5]. These trajectories have been well studied and implemented in practical missions.

This paper discusses families of Lissajous orbits, which are optimal for exploration of the far side of the Moon possessing relatively small trajectory amplitudes, which makes them beneficial for missions of certain types. On the other hand, a spacecraft on a Lissajous orbit around L2 can pass behind the Moon and lose communications with the Earth for a certain duration of time. Such problem was discussed by Farquhar in [6], where it was shown that stretches of trajectory can be found such that significant spacecraft visibility time is provided. At the same time, due to Lissajous orbits being aperiodic, the shape of the orbit and characteristics of spacecraft visibility are dependent on the spacecraft position at the time of orbital insertion.

The research conducted in this work provided estimates of spacecraft visibility parameters as a function of Lissajous orbital insertion position and amplitudes of this orbit. Three parameters were determined: maximum time of continuous spacecraft visibility t_v , maximum time of continuous spacecraft occultation behind the Moon t_h , and the ratio of the total occultation time to the total time on the orbit k . The dependence of these parameters on the orbital amplitudes A_y , A_z and phases φ_y , φ_z , defining the spacecraft position at the starting moment of time, was considered [7,8]. Calculated values of parameters t_h , t_v and k have shown that increasing amplitude leads to increased periods of visibility from the Earth, while the periods of continuous occultation and the ratio of the total occultation time to the total time on the orbit decrease.

Linearized system of differential equations was used to describe the spacecraft motion around Earth-Moon L2 point:

$$\begin{cases} \ddot{x} - \dot{y} - (2B_{L2} + 1)x = 0, \\ \ddot{y} + 2\dot{x} + (B_{L2} - 1)y = 0, \\ \ddot{z} + B_{L2}z = 0, \end{cases} \quad (1)$$

where x , y , z are axes of a Cartesian coordinate system (x -axis is parallel to the L2-Moon line, z -axis points up from the orbital plane), $B_{L2} \approx \left[\frac{(1-\mu)}{(1+\gamma_{L2})^3} + \frac{\mu}{\gamma_{L2}^3} \right]$, where $\mu = 1/(1+M_R)$ is the normalized reduced mass (M_R is the ratio of Lunar to Earth mass) and γ_{L2} is the Earth-Moon distance. Numerical value of parameter $B_{L2} = 3.19042$ [5].

Solutions for this system can be represented as:

$$\begin{cases} x_n = kA_y \sin(\omega_y t + \varphi_y), \\ y_n = A_y \cos(\omega_y t + \varphi_y), \\ z_n = A_z \sin(\omega_z t + \varphi_z), \end{cases} \quad (2)$$

where A_y , A_z , φ_y , φ_z are amplitudes and phases in y and z axes, correspondingly, t is time, $\omega = \frac{2\pi}{T}$, $T_y = 14.65$ days, $T_z = 15.23$ days.

All three parameters under study are π -periodic, therefore, their behavior was studied only within the square $(0,0)(\pi,\pi)$. To prove this, if the spacecraft is occulted for a given set of values $(\varphi_y, \varphi_z, t)$, it will also be occulted for values $(\varphi_y + \pi, \varphi_z, t)$, $(\varphi_y, \varphi_z + \pi, t)$ и $(\varphi_y + \pi, \varphi_z + \pi, t)$.

Therefore:

$$V(t, \varphi_y, \varphi_z) = V(t, \varphi_y + \pi, \varphi_z) = V(t, \varphi_y, \varphi_z + \pi) = V(\varphi_y + \pi, \varphi_z + \pi, t), \quad (3)$$

where V is determined by the formula:

$$V(t, \varphi_y, \varphi_z) = \begin{cases} 1, & (y^2(t) + z^2(t)) < R^2 \\ -1, & (y^2(t) + z^2(t)) \geq R^2 \end{cases} \quad (4)$$

According to expression (2):

$$y(t, \varphi_y + \pi) = A_y \sin(\omega_y t + \omega_y + \pi) = -A_y \sin(\omega_y t + \omega_y) = -y(t, \varphi_y), \quad (5)$$

$$z(t, \varphi_z + \pi) = A_z \sin(\omega_z t + \omega_z + \pi) = -A_z \sin(\omega_z t + \omega_z) = -z(t, \varphi_z), \quad (6)$$

Therefore:

$$y^2(t, \varphi_y + \pi) = y^2(t, \varphi_y), \quad (7)$$

$$z^2(t, \varphi_z + \pi) = z^2(t, \varphi_z), \quad (8)$$

The equality (3) follows simply from equations (4), (7) and (8).

Apart from π -periodic dependence of the studied parameters on phases φ_y and φ_z , it was explored numerically and qualitatively. It was shown that increase of orbital amplitude leads to improved communication conditions for the spacecraft according to all parameters under study: maximum time of continuous spacecraft visibility is increased, and the maximum time of continuous spacecraft occultation behind the Moon and the ratio of the total occultation time to the total time on the orbit are decreased. The obtained results allow us to determine the range of values of φ_y и φ_z providing the maximum value of continuous spacecraft visibility time. It is shown that continuous spacecraft visibility time can reach 92.27 days for amplitude combination $A_y = 5000$ km and $A_z = 5000$ km, 114.10 days for $A_y = 5000$ km and $A_z = 10000$, 152.36 days for $A_y = A_z = 10000$ km, 159.71 days for $A_y = 10000$ km and $A_z = 15000$ km, as well as 167.52 days for amplitude combination $A_y = A_z = 15000$ km.

The results obtained in this work, will be used for trajectory design of a spacecraft with transfer to a Lissajous orbit around Earth-Moon L2 point for exploration of the far side of the Moon.

References

1. Nikolaeva Yu. A. Raschet okon zapuska kosmicheskogo apparata dlya traektorii Zemlya – tochka L2 sistemy Zemlya-Luna / Nikolaeva Yu. A., Aksenov S.A., Dunham D / International Scientific – Practical Conference INNOVATIVE INFORMATION TECHNOLOGIES, 2013, Prague, pp.567-573.
2. Aksenov S.A. Komputernoe modelirovanie missii k tochke libracii L2 sistemy Zemlya-Luna / Aksenov S.A., Efremova E.V., Dunham D. / International Scientific – Practical Conference INNOVATIVE INFORMATION TECHNOLOGIES, 2013, Prague pp. 545-548.
3. D. Dunham, R. Farquhar, N. Eismont, E. Chumachenko, New Approaches For Human Deep-Space Exploration / ISSFD / 2012, California.
4. Fedorenko Yu. V. Ocenka vremeni vidimosti kosmicheskogo apparata pri dvizhenii vokrug tochki libracii L2 sistemy Zemlya-Luna / Fedorenko Yu. V., Aksenov S. A., Dunham D. / International Scientific – Practical Conference INNOVATIVE INFORMATION TECHNOLOGIES, 2013, Prague, pp. 573-578.
5. Herschel, Planck and Gaia Orbit Design / M.Hechler , J.Cobos // Libration PointOrbits and Applications / Gomez G, Lo M.W. and Masdemont J.J., Eds. Singapore: World Scientific Publishing, 2003.
6. Farquhar, R.W. The Control and Use of Libration-Point Satellites / Robert W. Farquhar / Goddard Space Flight Center Greenbelt, Maryland 20771, 1970.
7. Fedorenko Yu. V. Analiz I optimizaciya orbit Lissazhu vokrug tochki libracii L2 Zemlya-Luna / Fedorenko Yu. V., Aksenov S. A. / Nauchno-tekhnicheskaya konferenciya studentov, aspirantov I molodykh uchenykh MIEM NIU VSHE. Tezisy dokladov / NIU VSHE, 2013, Moskva c. 17-18.
8. Fedorenko Yu. V. Ocenka vozmozhnosti nabludeniya kosmicheskogo apparata nakhodyaschegosya na orbite Lissaju vokrug tochki libracii L2 sistemy Zemlya-Luna / X

Konferenciya molodykh uchenykh Fundamentalnie I prikladnie kosmicheskie issledovaniya / 2013, IKI RAN c.129-130.

NEW IT-SOLUTIONS FOR BREAKTHROUGH RESEARCH IN NANO- AND BIOELECTRONICS

O.E. Gluhova, A.S. Kolesnikova, M.M. Slepchenkov, G.V. Savostyanov
Saratov State University, Saratov, Russia

The aim of this work is a developing of software and information complex, capable to perform high-precision simulations of technologies of new materials creation and testing of devices based on them. The main structural elements of the complex are modules that implement high-performance numerical experiments and multifunction graphical user interface. Using the developed complex is expected to solve the problem of developing the concept of the organization and synthesis of new materials with advantages of living objects and components of the electronic devices.

Keywords: software and information complex, computational modeling, IT- solutions, nano- and bioelectronics.

Introduction

Conducted by experts of NRE HSE (2011), Massachusetts Institute of Technology, McKinsey Global Institute (2013) analysis of the global economy current state and forecasting of its development prospects found twelve promising High-Tech technologies and directions that would lead to economic growth and to improving of life quality in ten-fifteen years. Among them there are information technologies, which should support development of robotic technologies, design of new nanomaterials and nanodevices that in sum will provide remote monitoring of the human health; will allow producing mechanized prostheses and «exoskeletons» that help people to have no problems with movement.

New IT-solutions will virtually allow to create new technologies, new materials, to test future work of nanodevices in order to find the optimal parameters to forecast work of constructed devices. One of the key points is creating perfect fundamentally-new multi-purpose nanomaterials and bringing them to the functional state. The principal novelty means the development of new generation materials bearing functions of living objects (that are capable of self-organization, self-assembly, rebuilding of tertiary and even secondary structure to achieve the greatest effect of the energy and stability) and herewith serving as structural elements of electronic devices able to conduct current, to work as switches, to store and to transfer energy, to respond on external electric fields, to serve as mechanical micro- and nanodetails, to withstand mechanical stresses and etc. Such materials would highly increase progress in development of nanobioelectronics, nanomedicine, sensing and in the area of integrated circuits superelements design.

Development of such universal modern nanomaterials is very cost because it requires high-tech solutions, erudite staff, information and intellectual resources that fit the modern demands of international standards. All these factors in common cause the gap between the scientific and technological potential and the effect of implementation. One of the ways to overcome it is reliable preliminary comprehensive virtual study of material and devices testing based on it.

The purpose of this work is to provide software and information complex (SIC) that can simulate the technology of new nanomaterials for various purposes creation, the design of nanodevices and bioelectronics, testing of its work. SIC is supposed to solve the problem of

conception development of organization and synthesis of new materials with the advantages of living objects and components of electronic devices: self-assembly of the basic elementary fragments, self-organization, which lies in such arrangement of own atomic-molecular structure that provides the most favorable configuration from energy point of view, adjustable electronic conductivity; controlled thermal conductivity, high strength and elasticity, other requirements of bionanoelectronic devices and live machines. It is also planned to do the following developments: new ways of proteins as an ion pump, as carriers of electronic charge in order to create integrated bioelectronic systems, solar panels of new generation, etc.; fundamentally new breakthrough application of micelles phospholipid layers, lipoproteins and similar biological macromolecules self-organization for self-assembly of transistors and other elements of the integrated circuits on graphene, for fabrication of nanowires, nanocomposite multilayer films; a new mechanism for controlling the physical properties of bilayer / few-layer graphene by phospholipid layers; the way of manipulating by biomacromolecules at various substrates including graphene by external electric field, a new method of motion control by encapsulated in nanotubes objects by biomolecular systems.

Solution of formulated tasks will promote progress in the field of nano- and microelectronics, will bring it to a new level of development associated with application of biological systems and will give a new impulse to the development of nanomedicine and sensory. A new generation of materials will play a great role in the field of "robotic technology" for the design of prostheses and mechanized "exoskeletons" that realize needs of people who have problems with movement.

New IT- solutions

Software and information complex (SIC) based on a combination of dynamic programming language Python and programming language C++. Using a high level language Python provides the universality of the implemented modules and the ability to quickly and easily expand their functions. For convenience, the SIC is automatically documented using the intrinsics of language Python (PyDoc). The complex consists of two main elements: 1) a module that provides high-performance numerical experiments; 2) the module that implements the multifunctional GUI.

Libraries for scientific calculations Numpy, Scipy are used for effective implementation of the calculation module. The most demanding to performance modules are implemented in the programming language C++ using Boost-Python. Thus, the SIC uses both the advantages of dynamic programming languages (Python), and the high speed of compiled programming languages (C++).

The compute module of SIC is adapted for work on massively parallel cluster computing systems (using library mpi4py, implementing MPI standard (Message Passing Interface)), and for work on hybrid architectures (using the technology of parallel computing on GPU InVidia CUDA) that makes SIC of universal complex, allowing to solve the problems of high dimension.

Graphical interface is implemented on the basis of libraries PyOpenGL, PyQt4 and matplotlib. It enables the construction of molecular models, the task of computer simulation modes, and processing of the obtained calculation results.

Solution of problems of nanoelectronics

Currently, intensive researches were carried in the field of nanoscale electronic devices. Material, which is based on carbon nanostructures, is one of the most popular materials for the creation of such devices. Uniqueness and breadth of properties these materials led to the development prospects of new direction electronics. New direction electronics is carbon nanoelectronics, which is based on the use of carbon nanostructured materials (carbon nanotubes, fullerenes, graphene and its modifications and other carbon nanostructures). At the same time for the successful development of carbon nanoelectronics

solve the problem of controlling the properties of carbon nanoobjects constituting the element base of a new generation of electronics is necessary.

Carbon nanotubes (CNTs) are widely used in emission vacuum devices, microwave devices [1] and x-ray sources [2]. However, the question of the parameters optimization of the cathode based on the carbon nanotubes remains actual question still. It is found that material on based on baboo-like carbon nanotubes will be the most promising material for nanoemitter. In favor of the choice of this material is the fact that bamboo-like nanotubes have better strength and emission properties compared with hollow nanotubes. In particular, it was shown in papers [3] and [4] that bamboo-like nanotubes with diameter ~ 2 nm are stable nanotubes smallest diameter (Fig. 1). Earlier it was shown that extended bamboo-like nanotube with diameter ~ 2 nm and the distance between the bridges of 2.8 nm are superior in emission ability infinite hollow nanotubes by 0.1 eV [4]. Consequently, greater emission current can be produced with the cathode point based on bamboo-like nanotubes.

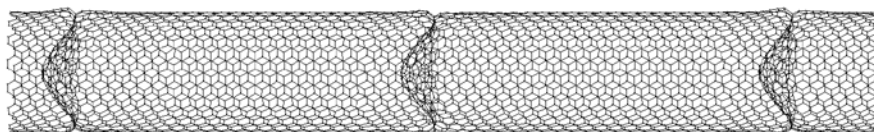


Fig. 1. Bamboo-like nanotubes with diameter ~ 2 nm with thee bridges

In recent years, researches directed on the solve of the problem of creation and application of compact sources of electromagnetic radiation in the terahertz range of frequencies were intensively conducted. Creating such high sensitivity devices ~ 1 micron in size can be achieved by using carbon nanotubes as a base material for construction.

The authors have proposed a model of nano emitter device capable of generating radiation tera and gigahertz ranges (Fig. 2). Open carbon nanotube armchair (10, 10) the length of 10.3 nm and the diameter of 1.39 nm formed the basis of the proposed model nanoemitter [5]. Chains of few C_{60} were encapsulated with one end of the nanotube. These fullerenes connected by a chemical bond with each other and with the wall nanotube. Free charged fullerene was placed in a space of tube next to a chain of fullerenes. In the initial state of the studied system this fullerene is located in the potential well formed by van der Waals interactions between the charged fullerene molecule and a chain of several fullerenes. When an external electric field of free charged fullerene oscillates in the potential well, accompanied by radiation of frequency in the terahertz range.

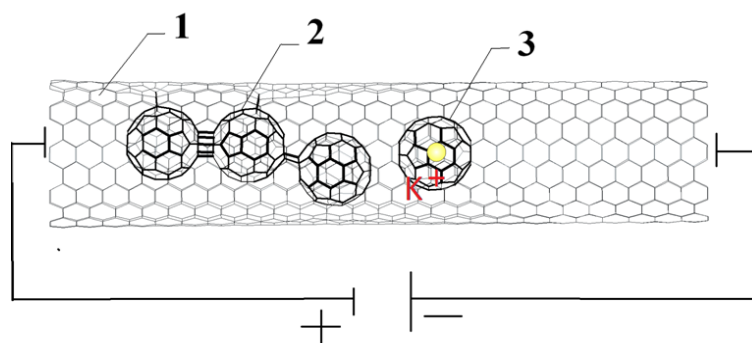


Fig. 2. Model nanoemitter: 1 – carbon nanotube; 2 – chain of C_{60} , chemically related to each other and with the wall nanotubes; 3 – free positively charged C_{60} fullerene.

New vector of development of carbon nanoelectronics associated with the use of nanotechnology to construct graphene nanodevices. Use of graphene nanostructures to create emission electronics devices is particularly a promising (nanoemitters in cathodes) [6,7]. For

efficient use of graphene as a material of nano-emitters problem reducing the amount of work function necessary to solve. Axial compression deformation is one of the most effective ways to control emission characteristics of graphene. The results of numerical experiment on axial compression of graphene nanoribbons armchair 71 Å length and width 22 Å showed that increasing the amount of deformation of 10% ionization potential of the investigated structures decreased by 0.1 eV [8]. It should be noted that 10% compressed graphene sheet having the lowest value of the ionization potential for ongoing research in the compression process has acquired the same arc.

Solution of problems nanobioelectronics

Preparation of nanoobjects without impurities in the final product is one of the problems in nanobioelectronics. The proposed solution of this problem is to provide a method of polymerization of nanobioobjects using the original model nanoautoclave developed OE Glukhova [Invention patent number 2360864 - "Method of low molecular weight polymers - C₂₀ fullerene dimers"]. Nanoautoclave is the device for generating of high pressures, ensuring the implementation of certain types of reactions [9]. The proposed model nanoautoclave (nanoreactor) is based on a hybrid of carbon compounds, which is closed at both ends of the nanotube, in which one of the edges of the potential wells is located a shuttle molecule (Fig. 3). Pressure on the substance in the opposite potential hole in the edge of the CNT can provide the controlling motion of the molecule shuttle. Ionized C₆₀ fullerene acts as such a molecule. The ionization of fullerene is achieved by its doping with ions of alkali metals (potassium, lithium) [10]. The fullerene begins to move from one potential well to another under an external electric field.

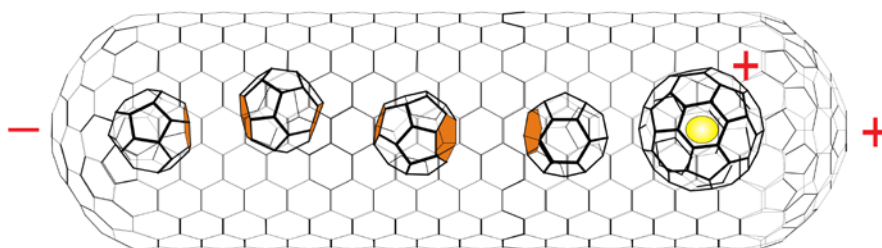


Fig. 3. Location fullerene C₂₈ in a capsule in the initial equilibrium state of the system.

Number of fundamentally new physical laws is already established using the proposed model of nanoautoclave. It was found that the formation of oligomer of the four C₂₈ fullerenes inside nanotube is possible [11]. This process is observed at a pressure of 37.73 GPa created by charged fullerene C₆₀, which moves under the influence of an external electric field. The feasibility of the synthesis process of the dimer consisting of two molecules of fullerene C₂₈ was demonstrated by model nanoautoclave [9].

Another actual problem of nanobioelectronics is the identification of the patterns behavior of nanobioobjects in the nanospace. Nanospace is some nanoscale cavity. The object in this cavity remains isolated and unaffected at external influence. Structure of the nanobioobject, its rotational and vibrational states, interaction with other objects can be studied in a similar nanospace. In particular, the results for the theoretical study of molecules of retinol in vitro in the nanospace of carbon nanotube with a radius of 6.25 nm are presented in [12] (Fig. 4). It is found during the study that the free rotation of retinol observed experimentally possible only if its connection with fullerene. Individual molecule retinol likely will not rotate because it held a strong van der Waals attraction of the tube walls. Branched configuration of retinol prevents rotation of molecule in a deep potential well.

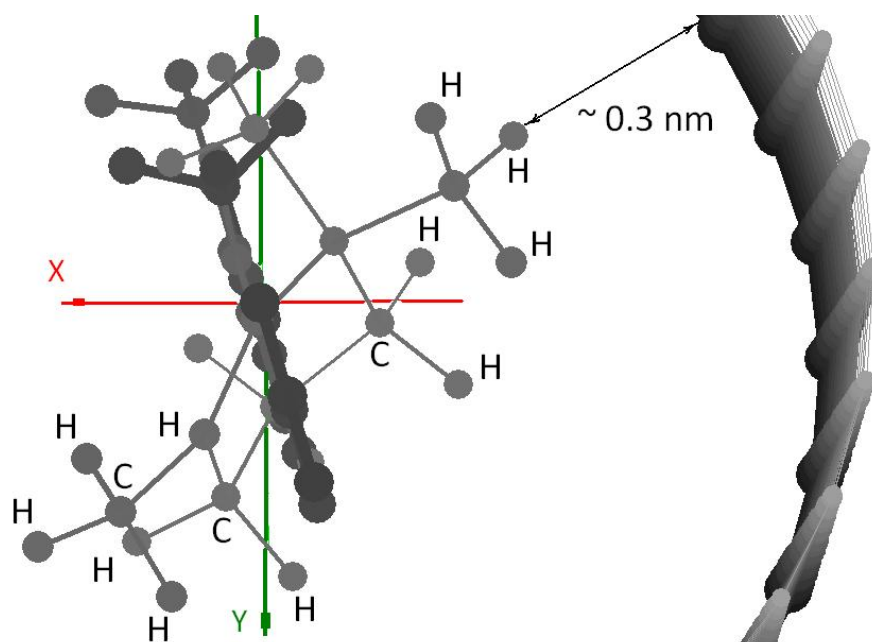


Fig.4. Fragment of complex retinol-nanotube

Conclusions

Ways to solve problems of nanoelectronics and nanobioelectronics were found. New IT-solutions provide a breakthrough research in biosensors, nanotechnology and functional medicine.

References

1. K. B. K. Teo, E. Minoux, L. Hudanski, F. Peauger, J. P. Schnell, L. Gangloff, P. Legagneux, D. Dieumegard, G. A. J. Amaratunga, W. I. Milne, *Nature*, 437 (2005), 968
2. S. H. Heo, H. J. Kim, J. M. Ha, S. O. Cho, *Nanoscale Research Letters*, 7: 258 (2012), 1-5.
3. O.E. Glukhova, A.S. Kolesnikova, M.M. Slepchenkov, *Journal of Molecular Modeling*, 19 (2013), 4369-4375.
4. O.E. Glukhova, A.S. Kolesnikova, *Journal of Physics: Conference Series*, 393 (2012), 012027-1-012027-4.
5. O.E. Glukhova, I.S. Nefedov, A.S. Kolesnikova, M.M. Slepchenkov, O.A. Terentev, V.V. Shunaev, *Proceedings of SPIE*, 859611(2013), 1-6.
6. L. Chen, M. Zhang, W. Wei, *Journal of Nanomaterials*, 2013 (2013), 1-8.
7. H. Park, S. Chang, J. Jean, J. J. Cheng, P. T. Araujo, M. Wang, M. G. Bawendi, M.S. Dresselhaus, V. Bulović, J. Kong, S. Gradečak, *Nano Lett.*, 13 (2013), 233–239.
8. O.E. Glukhova, M.M. Slepchenkov, *Nanoscale*, 11 (2012), 3335-3344.
9. O.E. Glukhova, *Journal of Molecular Modeling*, 17 (2011), 573-576.
10. N. Krawez, A. Gromov, R. Tellmann, E. E. B. Campbell, *Electronic properties of novel materials. - Progress in molecular nanostructures*, XII International Winterschool, Kirchberg, Tyrol, Austria, 1998, p.368
11. O.E. Glukhova, A.S. Kolesnikova, M.M. Slepchenkov, *Journal of Molecular Modeling*, 19 (2013), 985-990.
12. O.E. Glukhova, I.V. Kirillova, I.N. Saliy, M.M. Slepchenkov, *Proceedings of SPIE*, 7911(2011), 1-11.

PHYSICAL GROUNDS OF THE INFORMATION STORAGE AND REORDERING IN MAGNETIC NANOCCLUSERS

Kagan M.Yu.^{a,b}, Abrameshin A.E.^a

^a*Moscow Institute of Electronics and Mathematics, National Research University Higher School of Economics*, ^b*Moscow, P.L. Kapitza Institute, Russian Academy of Sciences*

This paper proposes a method of identifying some blocks in the scientific text to use this information for calculating the weights of semantic network nodes and arcs. This method is based on the application of fuzzy controllers.

Keywords: semantic network, scientific text, formal text sing of, fuzzy controllers

Essential feature of many systems with the colossal magnetoresistance (CMR-systems) [1, 2] is an instability in the wide range of the parameters with respect to the nanoscale electronic phase-separation, which leads to the formation of small ferromagnetic (FM) droplets or ferrons in the insulating antiferromagnetic (AFM) or charge-ordered (CO) matrices [3, 4, 5]. The ferromagnetic droplets randomly located in the insulated matrix (as blueberries in the pie), have the spherical or ellipsoidal shape [6] and represent the real nanoobjects with a radius in the range of $R \sim 10\div 15 \text{ \AA}$ (3-4 interatomic distances). Inside the ferrons we typically have $30\div 100$ FM ordered local spins and one conductivity electron (or hole) located in the center of the droplet. Thus a droplet has a large magnetic moment of the order of $50\div 100$ Bohr magnetons. There is a magneto-dipole interaction between the droplets and hence phase-separated state of CMR-systems (of manganites, ruthenates, cobaltates and other complex magnetic oxides) represents a super-paramagnet.

In the same time the effect of colossal negative magnetoresistance (the drastic reduction of the resistivity in field) can be naturally explained via the droplet growth in an external magnetic field which increases a degree of metallicity in the system and thus substantially reduces the resistivity. Note that CMR-effect can reach the values of $10^2\div 10^3$ in manganites. The electron transport in phase-separated state is defined by the spin-dependent tunneling of the conductivity electron from one metallic FM-droplet to a neighboring one via the insulating barrier. If the droplet concentration increases and we are close to the percolation threshold, then the mean distance between neighboring droplets becomes small enough and the network of the tunneling bridges (or tunneling contacts) is formed. In this case we deal with a phenomenon of the tunneling magnetoresistance [7]. Moreover applying already weak magnetic field we can measure the contact resistance and thus control the electric current across the contact. In this way we can read the information in accordance with the main principles of the spintronics.

With respect to the possible magnetic realization of the quantum computer, we can say that the quantum bit (qubit) in the FM-droplet itself with a large magnetic moment oriented parallel or antiparallel to the easy axis of the magnetization. To write the information we have to apply high magnetic field to polarize FM-droplets.

In the same time an entangled two qubit state in this scheme is just a system of two neighboring droplets connected by a tunneling bridge and interacting via magnetic dipole potential. The network of FM-droplets or ordered nanocomposite Fe/Cr; Co/Cu and tunneling bridges between them could be used as a memory device.

The similar scheme for magnetic realization of the quantum computer can be connected with large magnetic molecules and resonance tunneling of the spin states in them.

The most serious obstacle on the way of the creation of the magnetic qubits is connected with a large amplitude of $1/f$ -noise in a phase-separated state [4].

There are other interesting application of the nanoscale phase-separated CMR-systems for optoelectronics and fabrication of the metamaterials. One of them is based on the strong variation of the optical and infrared transmission coefficient in a magnetic field. The new physical device which is constructed by a group of prof. Sukhorukov in Ekaterinburg [8] is called a modulator of infrared radiation. Another application proposed by prof. Kaul on the Chemical Faculty of Moscow State University [9] is connected with the fabrication of magnetic lens based on manganite high- T_C heterostructures.

Another problem interesting for nanophotonics and nanoplasmonics was first addressed by the group of profs. Kugel and Rakhmanov in Moscow Institute for Theoretical and Applied Electrodynamics. Together with prof. Sarychev [10] they proposed to create on the surface of a bulk metal an artificial layer with a periodic superstructure of small metallic droplets in the CO or AFM insulating matrix. In this geometry we can study the angular and frequency dependence of the transmission (T) and reflection (R) coefficients for the electromagnetic wave which incident on the surface from the vacuum side. Then form the resonance peaks (or drops) in these coefficients at some critical angles, corresponding to the resonance excitation of the surface plasmon modes, we can define their collective spectrum which is promising for the amplified sensitivity in the Raman spectroscopy. Note that even more promising for practical applications is a so-called GMR-effect (giant magnetoresistance) [11] which is closely connected with CMR-effect and is based on the geometry of magnetic superlattices consisting of alternating layers of FM and non FM-metals. These multilayer structures represent high resistance and low resistance current paths in a weak applied magnetic field and can be used for the fabrication of the GMR memory cells and GMR magnetic field sensors.

References

1. Jonker G.H., van Santen J.H. // *Physica* – vol. 16 – 1950 – p. 337.
2. Jin S., Tiefel T.H., et al. // *Science* – vol. 264 – 1994 – p. 413.
3. Nagaev E.L. // *Sov. Phys. Uspekhi* – vol. 39 – 1996 – p. 781.
4. Rakhmanov A.L., Kugel K.I., Blanter Ya.M., Kagan M.Yu. // *Phys. Rev. B* – vol. 63 – 2001 – p. 174424 / Kagan M.Yu., Kugel K.I. // *Sov. Phys. Uspekhi* – vol. 44 – 2001 – p. 553 / Kagan M.Yu., Khomskii D.I., Mostovoy M.V. // *Eur. Phys. Jour. B* – vol. 12 – 1999 – p. 217.
5. Mott N.F., Davis E.A. *Electronic processes in non-crystalline materials*/ Clarendon Press – Oxford – 1971 / Mott N.F. *Metal-Insulator Transitions*/ Taylor & Francis – London, 1984.
6. Kagan M.Yu. *Modern Trends in Superconductivity and Superfluidity. Lecture Notes in Phys.* – vol. 874 / Springer-Verlag – Dodrecht, Heidelberg, New York, London, 2013 – Chaps. 15, 16.
7. Julliere M. // *Physics Letters A* – vol. 54 – 1975 – p. 225.
8. Sukhorukov Yu.P., Loshkareva N.N., Telegin A.V. // *Techn. Phys. Lett.* – vol. 29 – 2003 – p. 904.
10. Sarychev A.K., Boyarintsev S.O., Rakhmanov A.L., Kugel K.I., and Sukhorukov Yu.P. // *Phys. Rev. Lett.* – vol. 107 – 2011 – p. 267401 / Shalaev V.M., Sarychev A.K. *Electrodynamics of Metamaterials* / World Scientific Publishing Company – Singapore, 2007
11. Fert A. // *Sov. Phys. Uspekhi* – vol. 178 – 2008 – p. 178 / Grunberg P., Schreiber R., Pang Y., Brodsky M.B., and Sowers H. // *Phys. Rev. Lett.* – vol. 57 – 1986 – p. 2442
12. Zverdin A.K. // *Sov. Nature (Priroda)* – № 12 – 2000 – p. 11.

THE PATIENT-PHYSICIAN RELATIONSHIP IN REMOTE HEALTHCARE MONITORING

Korsakov I.N. , Atabaeva V.D., Vorobyeva E.E.

Institute of Information Technologies, National Research University Higher School of Economics, Russia

Market growth of personal medical device comes from a number of factors:

- Aging population requiring more attention;
- Patients with chronic diseases may measure blood pressure and blood glucose at home;
- Reducing the cost of these devices;
- Ease of use and availability of medical devices;
- Risen cost of a series of medical tests.

This article discusses the new challenges that arise in the relationship doctor - patient in the remote Monitoring human healthcare. With the advent of a greater variety of low-cost medical devices, as well as low-cost high-quality mobile communication system will allow the system to tell the Remote Healthcare Monitoring System has also become possible. This system should be as ready to doctors and patients themselves. there is a new quality in the interaction between doctor and patient. Considers a new model of doctor-patient relationship in the light of the transfer of active interaction to the virtual world.

Keywords: physician-patient relationship, Internet, empowerment, health information, health care consumer.

Introduction

The Institute of Medicine identifies patient centeredness as a core component of quality health care.[1] Patient centeredness is defined as: **Healthcare** that establishes a **partnership among practitioners, patients, and their families** (when appropriate) to ensure that decisions respect patients' wants, needs, and preferences and that patients have the education and support they need to make decisions and participate in their own care. [2]

Patient-centered care is supported by good provider-patient communication so that patients' needs and wants are understood and addressed and patients understand and participate in their own care. Physicians practicing patient-centered care improve their patients' clinical outcomes and satisfaction rates by **improving the quality of the doctor-patient relationship**, while at the same time **decreasing the utilization of diagnostic testing, prescriptions, hospitalizations**, and referrals. Patient-centered practitioners focus on improving different aspects of the patient-physician interaction by employing measurable skills and behaviors. This type of care can be employed by physicians in any specialty, and it is effective across different disease types. Given the sensitive nature of healthcare information, and the high degree of dependence of health professionals on reliable electronic medical records, the issues of integrity, security, privacy, and confidentiality are of particular significance and must be clearly and effectively addressed by health and health-related organizations and professionals. Two factors make the matter a subject of great significance: the intrinsically sensitive nature of patient data; and the growing use of network computing, particularly the Internet, for healthcare information processing. We will get using remote healthcare monitoring a number of benefits for both patients and physicians.

Business process level of potential functionalities for a Patient-Centered Health Information System

The health information technology focuses on the use of Electronic Medical Records (EMR) by clinicians, but patients need access to EMR either. Outside of health care, the public routinely uses computers and smart phones to access information and perform tasks with a click of a button, patients seek similar ease in accessing health information.

A technology that **should respond** to this need is Remote Healthcare Monitoring System with personal health record (PHR). Initially, Personal Health Records (PHR) were merely an electronic substitute for the home medical file. The simplest function of the Personal Health Record is to store similar information, often entered by the patient. The user may be asked prompting questions about health behaviors and diagnoses, but the answers come mainly from the user's memory or home records. Although patients are the ultimate authority on some details, such as eating habits and symptoms, **they may not be as precise** about diagnoses, medications, and laboratory values. More advanced PHRs address this problem by linking electronically to clinical information in EMRs or claims data. These systems provide a portal to clinical information, but too many deliver unmodified content to the patient, who may have difficulty understanding the terminology or putting the information in context. For example, a patient may not know whether to be concerned about specific medical term. A higher function of PHRs is to interpret content—to explain technical information in language that patients easily understand or to render clinical advice, as when personal health records call attention to overdue screening tests or the need to reduce blood pressure or serum lipid levels. The highest level of functionality is to help patients take action. Information is plentiful on the Internet, but some PHRs give patients vetted information, such as a health encyclopedia or hyperlinks to useful resources. Some Personal Health Records personalize information for the individual patient and some can incorporate motivational messages to help patients take action to confront challenges, such as weight loss or smoking. The Personal Health Record offers a platform for applications or decision aids that help patients weigh difficult tradeoffs. By assisting with self-management, offering logistical support for appointments, and providing follow-up, personal health records can extend care beyond the clinical encounter. This must be done in coordination with the patient's physician, a level of functionality that many standalone systems lack. Trust comes when the Personal Health Record has the endorsement of the physician and is designed to interface seamlessly with care delivery, as when output is shared and the personal health record refers patients back to their physician for assistance or helps them prepare for upcoming office visits.[5] Thus, the usual procedure visit a specialist through the system of remote monitoring of health allows the doctor to prepare for the arrival of the patient, to get acquainted with Electronic Medical Record, as well as the patient did not need long to tell that it led to a doctor. That, ultimately, will significantly reduce the time for a doctor that will lower the cost of treatment.

Discussion

A model for shifting personal health records to become patient centered, which stratifies these interactions by arbitrarily defined levels, is Remote Healthcare Monitoring System.

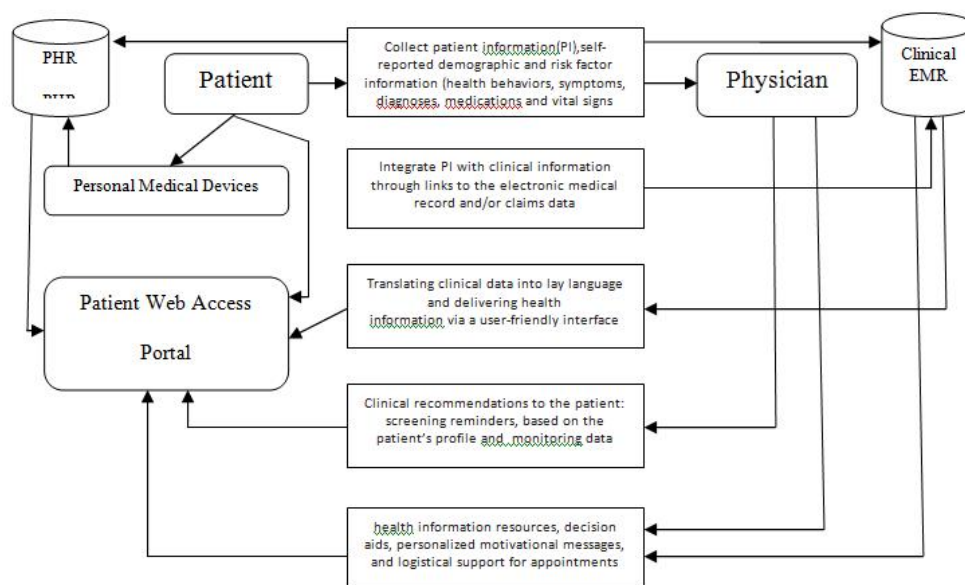


Figure 1. Business Model for Patient-Physician Relationship

Conclusion

Patients, armed with their smart phones and home computers, want real access to their electronic medical records and that many individuals would be willing to switch doctors to have it. Physicians shows the majority believe patients should only have limited access to their electronic records.

When patients are part of the record-keeping process, such as self-tracking their personal health information, it can increase their understanding of their condition and the required treatment.

Not only are patients demanding that their physicians communicate with them electronically, but physicians are already discovering that this media can be an important tool in managing the mounting demands and time pressures facing their practices. Thus it makes sense for physician practices to begin getting experience in expanding their use of electronic communications. Doing so will help their practices evolve with this new technology and start the process of exploring the unique mix of telephone, email, internet, and web site uses that will best meet their practice needs. The process of engaging the patient in the treatment process believes the key to success for many chronic diseases. The patient must understand the main points of his disease. The doctor has an effective way to influence and monitor the patient out of the hospital.

In particular, implementation of glycemic control in patients with diabetes type 2 with each year becomes more expensive, primarily due to the steady increase in the number of patients with the disease, and the lack of glycemic control entails the risk of cardiovascular disease in patients with diabetes type 2. Implementation of systems, such as patient health monitoring subsystem with diabetes type 2, will improve glycemic control this population of patients, without increasing the cost of its implementation, as well as to relieve the doctors and give more time for patients by remote glycemic control.

Acknowledgment

The work was carried out with the financial support of the Ministry of education and science of the Russian Federation (the contract № 02. G 25.31.0033)

References

1. Institute of Medicine. Crossing the quality chasm: a new health system for the 21st century. Washington, DC: National Academies Press; 2001.
2. Institute of Medicine. Envisioning the National Health Care Quality Report. Washington, DC: National Academies Press; 2001.
3. Korsakov I. N., Kuptsov S. M., Raznometov D. A. Personal Medical Wearable Device for Distance Healthcare Monitoring X73-PHD // International Journal of Scientific & Engineering Research. 2013. Vol. 4. No. 12. P. 2321-2328
4. Tang PC, Ash JS, Bates DW, Overhage JM, Sands DZ. Personal health records: definitions, benefits, and strategies for overcoming barriers to adoption. *J AmMed Inform Assoc.* 2006;13(2):121-126
5. Alex H. Krist, MD, MPH; Steven H. Woolf, MD, MPH A Vision for Patient-Centered Health Information Systems *JAMA.* 2011;305(3):300-301

MULTI-CHANNEL ALGORITHM COMPENSATION ECHO SIGNALS IN TELECOMMUNICATION HANDSFREE SYSTEMS

Kropotov Y.A.

*Murom Institute (branch) of Vladimir State University named after Alexander and Nikolay
Stoletovs*

Described the characteristics of adaptive compensation algorithm echoes in the range of values significant delays in telecommunication handsfree systems. It is shown that the considered algorithm provides fast convergence and a high degree of echo cancellation when the adaptive filter is configured around a localized neighborhood delays.

Keywords: compensation algorithm, echo, telecommunication system, adaptive filtering

The need for echo cancellation arises when building telecommunications systems audio exchange, handsfree systems [1]. The difficulty of solving this problem is largely caused long delays in the channels propagation echo that for these systems can reach values of the order of five hundred milliseconds or more [2, 3, 4]. Under these conditions, a filter with finite impulse response, which is part of the compensator must have order equal to several thousand, which significantly reduces the rate [2, 3]. Can solve this problem by introducing a block adaptive filters, each of which provides compensation only in the range of delays, localized in the vicinity of some important values. In this case, the order of the filter is markedly reduced, and if the number of channels of the echo is within from three to five, and the total number of adjustable coefficients holds substantial gain.

The aim of this work is the consideration of the characteristics echo compensation algorithm, based on time selection and the method of least squares. The parameters of the channel echoes their significant delay values and damping are taken from the results of its known correlation analysis. Accepted and known reference signal - echo source signal.

Scheme compensating adaptive filter in one of the channels of the echo is shown in fig.1.

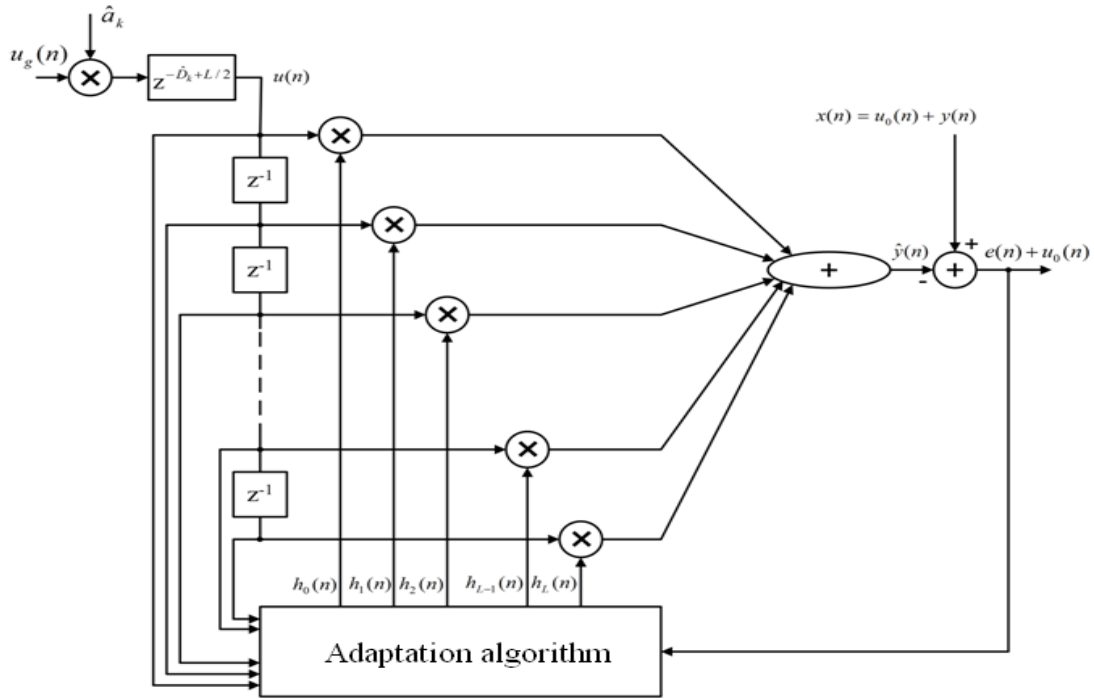


Fig. 1. Adaptive compensation scheme in a single channel echo

In this figure, the variable \hat{D}_k refers to estimate in k -channel delay echo, \hat{a}_k – normalizing factor (estimated attenuation in a channel) and L - the order of the filter. The signal at the input of the interference canceller $u(n)$ is delayed by the amount $(\hat{D}_k - L/2)$ of the reference signal $u_g(n)$, $u(n) = \hat{a}_k u_g(n - \hat{D}_k + L/2)$.

Echo the microphone input has in this view

$$x(n) = u_0(n) + y(n)$$

Where in order to simplify, to the useful information signal $u_0(n)$ allocated to the components of the echo channels of the other delay values and $y(n)$ represents only be offset component which can be represented as [1]

$$y(n) = a_k u_g(n - D_k).$$

Here D_k and a_k – thus delay and attenuation of the k -echo channel. Evaluation of this component is formed by the adjustment device shown in fig. 1 symbol $\hat{y}(n)$, where $\hat{y}(n) = a_k u_g(n - D_k) * h_k(n)$, $h_k(n)$ – the impulse function of the channel. Estimation error $e(n) = y(n) - \hat{y}(n)$.

The output signal of the comparison circuit $x(n) - \hat{y}(n)$, the averaged over a plurality of implementation equals

$$E(x(n) - \hat{y}(n))^2 = E(u_0(n) + y(n) - \hat{y}(n))^2 \quad (1)$$

where, E – the symbol of mathematical expectation. If we consider that $u_0(n)$ and $y(n) - \hat{y}(n)$ are uncorrelated, then the expression (1) can be written as

$$E(u_0(n) + y(n) - \hat{y}(n))^2 = E(u_0^2) + E(y(n) - \hat{y}(n))^2,$$

which implies that the minimum value of the error $e(n)$ is achieved when $y(n) \approx \hat{y}(n)$.

The output signal of the adaptive filter can be represented as

$$\hat{y}(n) = \sum_{l=0}^L u(n+l)h_l(n) = \mathbf{u}^T(n)\mathbf{h}(n),$$

$$\text{where } \mathbf{h}(n) = \begin{pmatrix} h_0(n) \\ h_1(n) \\ \vdots \\ h_L(n) \end{pmatrix} \text{ and } \mathbf{u}(n) = \begin{pmatrix} u(n) \\ u(n-1) \\ \vdots \\ u(n-L) \end{pmatrix} \text{ — the vectors of coefficients of the adaptive}$$

filter and the reference signal samples $u(n)$, respectively.

Error learning can be written as

$$e(n) = x(n) - \mathbf{h}^T(n)\mathbf{u}(n).$$

It should be noted that the gradient of the error is equal to the vector of the coefficients $\nabla_h e(n) = -\mathbf{u}(n)$.

In the method of least squares adjustment coefficients of the adaptive filter implementation is found from the condition of minimum loss function

$$\begin{aligned} Q(n) &= \frac{1}{M+1} \sum_{l=0}^M \lambda^{2l} e^2(n-l) = \frac{1}{M+1} \sum_{l=0}^M \left(\lambda^l x(n-l) - \lambda^l \mathbf{h}^T(n)\mathbf{u}(n-l) \right)^2 = \\ &= \frac{1}{M+1} \left(\mathbf{x}(n) - \mathbf{U}^T(n)\mathbf{h}(n) \right)^T \left(\mathbf{x}(n) - \mathbf{U}^T(n)\mathbf{h}(n) \right), \end{aligned}$$

where parameter λ is taken from the from the interval $0 < \lambda \leq 1$, vector

$$\mathbf{x}(n) = \begin{pmatrix} \lambda^0 x(n) \\ \lambda^1 x(n-1) \\ \vdots \\ \lambda^M x(n-M) \end{pmatrix},$$

and the matrix $\mathbf{U}(n) = \begin{pmatrix} \lambda^0 \mathbf{u}(n) & \lambda^1 \mathbf{u}(n-1) & \dots & \lambda^M \mathbf{u}(n-M) \end{pmatrix}$.

In this notation, the minimization of the loss function (2) leads to solutions having the form

$$\hat{\mathbf{h}}(n) = \left(\mathbf{U}(n)\mathbf{U}^T(n) \right)^{-1} \mathbf{U}(n)\mathbf{x}(n). \quad (3)$$

Equation (3) for values $M = L$ and $\lambda = 1$ - this equation Wiener filter that determines the stationary solution, which is used to estimate the effectiveness of adaptive filters [1]. Adaptation algorithm based on loss function (2) can be obtained by using Newton's method [3].

Given that the gradient of the function (2) is

$$\nabla_h Q(n) = \frac{-2}{M+1} \mathbf{U}(n) \left(\mathbf{x}(n) - \mathbf{U}^T(n)\mathbf{h}(n) \right),$$

and the Hessian matrix –

$$\nabla_h^2 Q(n) = \frac{-2}{M+1} \mathbf{U}(n) \left(\mathbf{x}(n) - \mathbf{U}^T(n)\mathbf{h}(n) \right),$$

desired equation can be written as

$$\mathbf{h}(n+1) = \mathbf{h}(n) + \alpha \left(\mathbf{U}(n)\mathbf{U}^T(n) \right)^{-1} \mathbf{U}(n)\mathbf{e}(n). \quad (4)$$

Here, the coefficient α of the selected interval $(0, 1]$ and the error vector given by the expression

$$\mathbf{e}(n) = \mathbf{x}(n) - \mathbf{U}^T(n)\mathbf{h}(n).$$

Note that the matrix multiplication $\mathbf{U}(n)\mathbf{U}^T(n)$ is the dimension $(L+1) \times (L+1)$ is the Gram matrix. Its components are the inner multiplication of rows $\mathbf{U}(n)$ of the matrix

dimension $M + 1$. This means that a value $M < L$ of the matrix $\mathbf{U}(n)\mathbf{U}^T(n)$ is a degenerate, which precludes the application of equation (4). In what follows it is assumed that $M \geq L$.

When modeling the echo signal was represented by the sum of three delayed copies of the reference speech signal propagation delays in the channels 120, 240 and 360 ms, and the damping coefficient of 0.7, 0.5 and 0.3, respectively.

The following results were obtained in three changes of adaptive filters 128 order. At the same time as an error at their training was used, the total error given by the expression

$$e(n) = x(n) - \sum_{k=1}^r \mathbf{h}_k^T(n) \mathbf{u}_k(n),$$

where the summation is over all the coefficients r of adaptive filters (in this case $r = 3$).

Modeling was carried out both by the formula (4), and in its modifications, the resulting loss function

$$Q(n) = \frac{1}{M+1} \sum_{l=0}^M \lambda^{2l} e^2(n-l).$$

The adjustment results of the filter coefficients are presented learning curve shown in fig. 2 for the size of the error vector $M = 200$. Fig. 2 shows the ratio of the error echo canceller to its maximum value in the interval training iteration number (sample number). Fig. 3 and 4 show the original speech signal to the reconstructed echo and background speech signal.

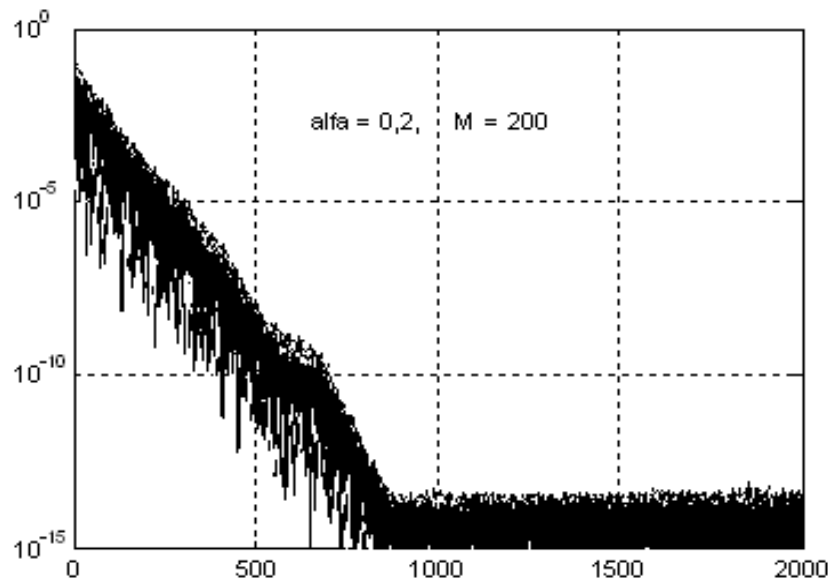


Fig. 2. Curve adjustment of filter coefficients

Modeling algorithm echo compensation based on significant delay channels showed its high rate of convergence. Also, the modeling showed that the level of compensation and speed settings, this algorithm has better performance than, for example, the steepest descent gradient algorithm [3].

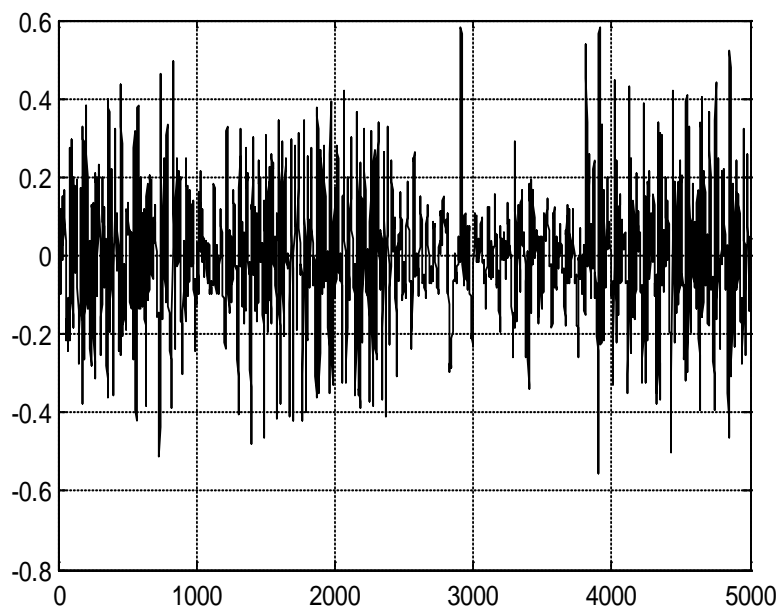


Fig. 3. Fragment of the original signal against echo

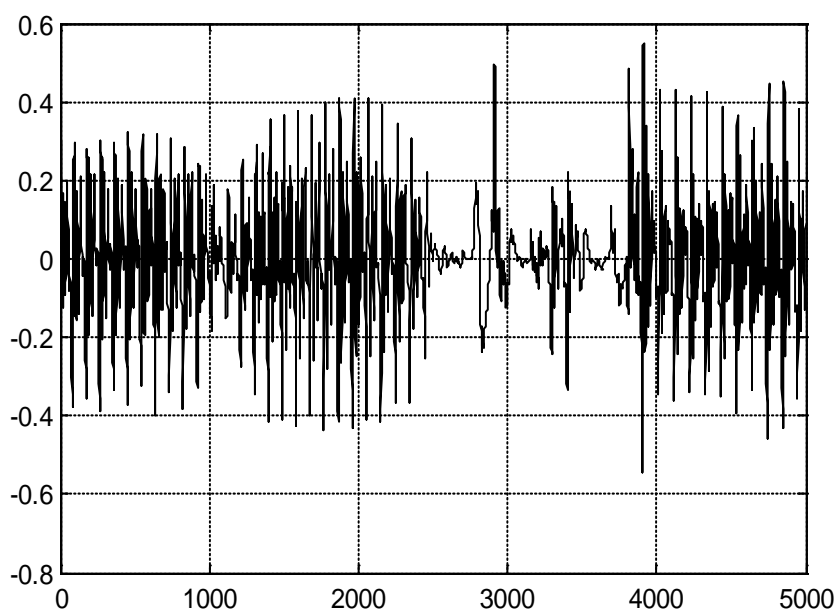


Fig.4. Fragment recovered signal after the echo cancellation

References

1. Kropotov Y.A. O korrelyacionnom ocenivanii parametrov modelej akusticheskikh eho-signalov. / Y.A. Kropotov, V.A. Ermolaev /Voprosy radioelektroniki, seriya OT, 2010. - Vol. 1. - C. 46 - 50.
2. Widrow B. and Stearns S. D. Adaptive Signal Processing. New Jersey: Prentice-Hall, Inc., 1985. 440 p.
3. Breining, C. and et al. Acoustic echo control: An application of very-high-order adaptive filters. IEEE Signal Processing Magazine, 1999, No. 7, pp. 42 – 69.

4. Cohen I., Benesty J., Cansot S. Speech processing in modern communication. Berlin Heidelberg: Springer, 2010. 342 p.

ACTIVE PROTECTION SYSTEM OF RADIO-ELECTRONIC FACILITIES

Lysenko A.V., Zatylnik A.V., Yurkov N.K.
Penza State University, Russia

The basic methods of vibroprotection, allowing to lower influence of external vibrating influences are examined in this article. The new method to reduce vibration amplitude of radio-electronic facilities (REF) bearing construction is offered. The new construction of active anti-vibration clamber is shown.

Keywords: vibration, amplitude, mechanical fluctuation, anti-vibration clamber, construction.

Introduction

Now mechanical loadings, and also a frequencies range of their influence on REF is growing [1-3]. There are various means of vibroprotection of REF: dampers, springs, liners, anti-vibration clammers (passive, adjustable, active), etc., which allow to reduce influences of vibration strains on all range of frequencies [2, 3].

The most effective are active amortisation systems [4-7], because they include elements with the additional energy source, allowing to change brackets rigidity of anti-vibration clammers in addition to damping elements. This makes it possible to reduce influence of vibration strains on REF [8].

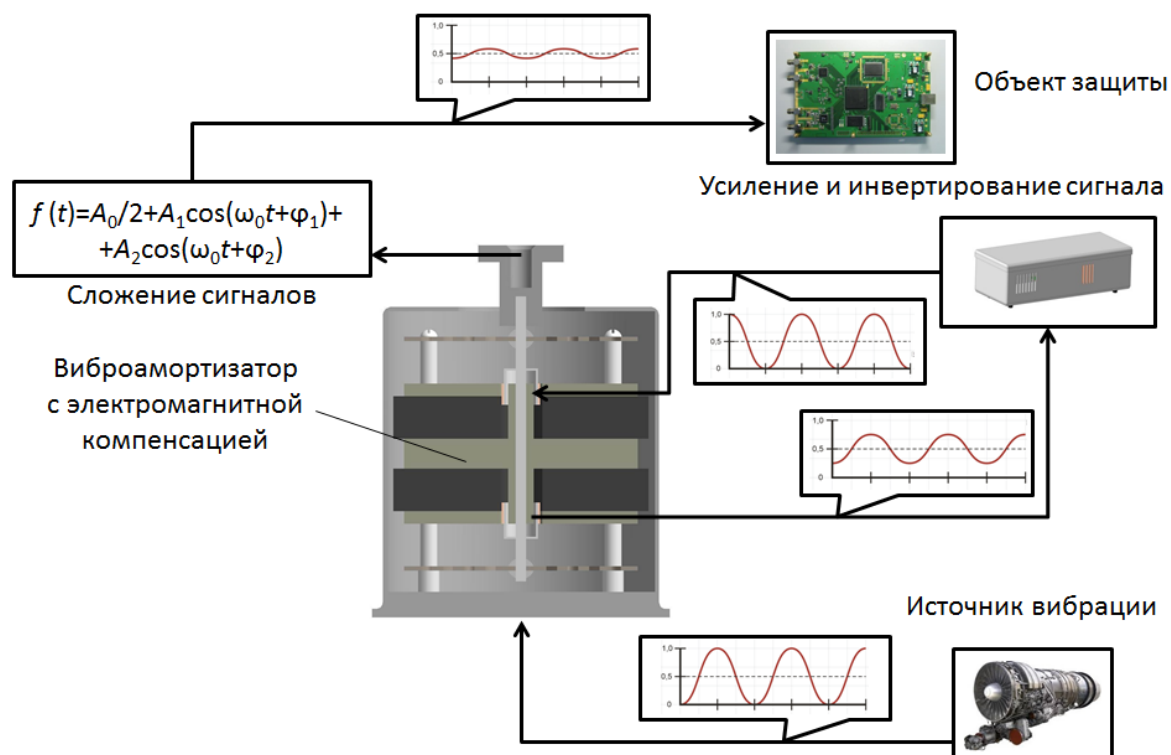
Active amortisation systems are intended for vibration amplitude reduction not only on resonant frequencies, but also on all demanded range of frequencies due to compensating signals introduction and the way of change of rigidity adjustable brackets of amortization systems realization [9, 10]. But it evokes construction of active anti-vibration clamber complication because of additional means of vibrations measurement introduction and also increase of their cost, therefore application of such protection means is proved only in unusual cases of important REF. Besides in many cases vibroprotection is sufficient on resonant frequencies because influence on REF other range is not so strong [11-13].

Thus, there is a sharp necessity of creation of structurally simple means of REF active vibroprotection, realizing a high-performance method of vibration strains reduction on resonant frequencies.

The method of electromagnetic compensation

Modern tendencies of development in the radio-electronic industry allow us to offer a new construction of the active anti-vibration clamber, differing simplicity and corresponding with the above-stated requirements [14, 15]. For creation of this anti-vibration clamber the method of electromagnetic compensation of fluctuations amplitude of bearing REF constructions is offered (pic. 1). The method contains the feedback entered by means of an additional constructive element.

The introduced method of electromagnetic compensation is realized on the basis of interaction between the anti-vibration clamber and the processing block which displaces signal acting on it in a phase.



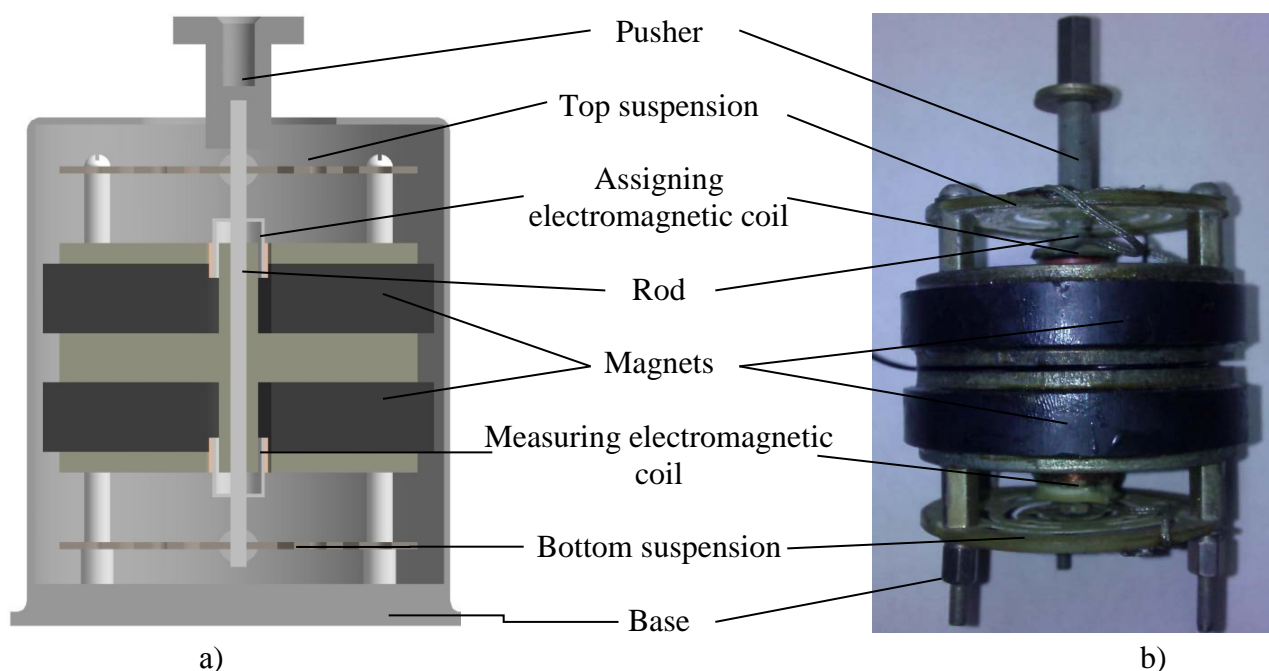
Picture 1 – The method of electromagnetic compensation of fluctuations amplitude of bearing REF constructions

The introduced method of compensation of amplitude of fluctuations of bearing REF constructions allows to get rid of necessity of measurement of external influence amplitude. Thereby it allow to lower cost of active system of REF amortization.

The construction of the active anti-vibration clamber

It is necessary to develop a new anti-vibration clamber construction for realization of the offered method. It will allow to compensate fluctuation amplitudes of bearing REF constructions due to introduction of new elements which provides antiphase fluctuations [16, 17].

The experimental model of the construction of the active anti-vibration clamber has been developed by the department «Construction and manufacture of radio equipment» of Penza state university. It contains the exploring electromagnetic coil placed on a rod of the anti-vibration clamber that allows to form a reference signal without use of the additional measuring equipment and devices (pic. 2).



Picture 2 – Anti-vibration clamber construction:

a) – Physical anti-vibration clamber construction, b) – Photo of experimental model of anti-vibration clamber

The anti-vibration clamber with electromagnetic compensation consists of the electromagnetic coil fixed on a rod in a constant magnetic field, which allows to measure amplitude value of the external vibrating influence, acting on the anti-vibration clamber. The rod is fixed on top and bottom suspensions which serve as membranes. The signal from the electromagnetic coil enters in the processing block where amplification of signal in amplitude is realized, the phase mismatch is inputted, and also there are digital-to-analog and return transformations. From the output of the processing block signal goes on the assigning coil, located on the same rod as the measuring coil, but in a magnetic field of the second constant magnet. As a result there is the vibrating influence shifted in phase concerning entrance influence. Superposition of two vibrating signals on one rod provides the compensating effect extinguishing external vibrating influence and reducing amplitude of REF vibrations as a whole.

The distinctive feature of the this anti-vibration clamber construction is the arrangement of measuring (serving as a sensor) and assigning coils on one rod that allows to compensate external vibration.

Conclusion

The method of electromagnetic amplitude of external vibrating influence in the active anti-vibration clamber has been offered. This method allows to get rid of additional means of amplitude of external influences measurement. It promotes to decrease the cost of active system of REF amortization. Also the anti-vibration clamber construction with the electromagnetic compensation is developed. It allows to lower loads due to introduction of a phase mismatch considerably.

References

1. Yurkov, N.K. Avtomatizaciya proizvodstvennyh processov izgotovleniya radioelektronnyh sredstv : ucheb. posobie / N. K. Yurkov, A. V. Zatylnkin, V. G. Nedorezov. – Penza : Izd-vo PGU, 2012. – 120 s.

2. Zatylnkin, A.V. Algoritm provedeniyja proektnyh issledovaniy radiotekhnicheskikh ustroystv opytno-teoreticheskim metodom / A.V. Zatylnkin, I.I. Kochegarov, N.K. Yurkov // Nadezhnost' i kachestvo: tr. Mezhdunar. simp. Tom 1 / pod red. N. K. Yurkova. – Penza : Izd-vo Penz. gos. un-ta, 2012. – S. 365-366.
3. Goryachev N.V. Struktura avtomatizirovannoy laboratorii issledovaniya teplootvodov / N.V. Goryachev, I.D. Grab, A.V. Lysenko, N.K. Yurkov // Trudy mezhdunarodnogo simpoziuma Nadezhnost' i kachestvo. 2011. T. 2. S. 119-120.
4. Goryachev N.V. Programma inzhenernogo raschyota temperatury peregreva kristalla elektroradiokomponenta i ego teplootvoda / N.V. Goryachev, A.V. Lysenko, I.D. Grab, N.K. Yurkov // Trudy mezhdunarodnogo simpoziuma Nadezhnost' i kachestvo. 2012. T. 2. S. 242-243.
5. Zatylnkin, A.V. Sistema adaptivnogo testirovaniya na osnove nechetkogo logicheskogo vyvoda / A.V. Zatylnkin // Nadezhnost' i kachestvo: tr. Mezhdunar. simp. Tom 1 / pod red. N. K. Yurkova. – Penza : Izd-vo Penz. gos. un-ta, 2013. – S. 237-239.
6. Lysenko, A.V. Analiz osobennostey primeneniya sovremennykh aktivnykh sistem vibrozashchity dlya nestacionarnykh RES / A.V. Lysenko, G.V. Tankov, D.A. Ryndin // Trudy mezhdunarodnogo simpoziuma Nadezhnost' i kachestvo. 2013. T. 2. S. 155-158.
7. Zatylnkin, A.V. Algoritm i programma rascheta staticheskikh neopredelimykh sistem amortizatsii bortovykh RES s kinematischeskim vozbuzhdeniem / A.V. Zatylnkin, A.V. Lysenko, G.V. Tankov // Innovatsii na osnove informatsionnykh i kommunikatsionnykh tekhnologiy. 2013. T. 1. S. 223-225.
8. Lysenko, A.V. Metodika modelirovaniya vneshnykh mekhanicheskikh vozdeystviy na bortovuyu RES / A.V. Lysenko, E.A. Danilova, G.V. Tankov // Innovatsii na osnove informatsionnykh i kommunikatsionnykh tekhnologiy. 2013. T. 1. S. 226-228.
9. Bannov, V.Ya. Avtomatizirovannyi stend issledovaniya procedury formirovaniya testovogo vozdeystviya pri provedenii diagnostiki logicheskikh shem elektronnykh ustroystv / V.Ya. Bannov, E.V. Saprova, A.V. Zatylnkin // Nadezhnost' i kachestvo: tr. Mezhdunar. simp. Tom 1 / pod red. N. K. Yurkova. – Penza : Izd-vo Penz. gos. un-ta, 2011. – S. 32-34.
10. Zatylnkin, A.V. Innovatsii v obrazovatel'nykh uchrezhdeniyakh i interaktivnye programmy obucheniya / A.V. Zatylnkin // Nadezhnost' i kachestvo: tr. Mezhdunar. simp. Tom 1 / pod red. N. K. Yurkova. – Penza : Izd-vo Penz. gos. un-ta, 2011. – S. 340-344.
11. Goryachev N.V. Informatsionno-izmeritel'nyy laboratornyy kompleks issledovaniya teplootvodov yelektoradiyeyelementov / N.V. Goryachev, A.V. Lysenko, I.D. Grab, N.K. Yurkov // Trudy mezhdunarodnogo simpoziuma Nadezhnost' i kachestvo. 2012. T. 2. S. 239-240.
12. Goryachev N.V. Opyt primeneniya sistem skvoznogo proektirovaniya pri podgotovke vypusknoy kvalifikatsionnoy raboty / N.V. Goryachev, N.K. Yurkov // Izvestiya Penzenskogo gosudarstvennogo pedagogicheskogo universiteta im. V.G. Belinskogo. 2011. № 26. S. 534-540.
13. Zatylnkin, A.V. Metod svyazannykh sistem v modelirovanii processa obucheniya / A.V. Zatylnkin, V.B. Almametov, I.I. Kochegarov // Izvestiya vysshikh uchebnykh zavedeniy. Povolzhskiy region. Tekhnicheskie nauki. – 2010. № 4 (6). – S. 86-89.
14. Gorjachev N.V. Sovershenstvovanie struktury sovremennogo informatsionno-izmeritel'nogo kompleksa / N.V. Goryachev, N.K. Yurkov // Innovatsionnye informatsionnye tekhnologii. 2013. T. 3. № 2. S. 433-436.
15. Lysenko, A.V. Osobennosti razrabotki tipologii ustroystv amortizatsii radioelektronnykh sredstv na osnove fasetnoy struktury / A.V. Lysenko // Trudy mezhdunarodnogo simpoziuma Nadezhnost' i kachestvo. 2013. T. 2. S. 151-155.

16. Zatylnik, A.V. Modelirovanie izgibnyh kolebaniy v sterzhnevyykh konstrukciyah RES / A.V. Zatylnik, G.V. Tankov, // Nadezhnost' i kachestvo: Trudy mezhdunarodnogo simpoziuma / Pod red. N.K. Yurkova – Penza: IIC PGU, 2006, s. 320-323.

17. Lysenko, A.V. Konstrukciya aktivnogo vibroamortizatora s jelektromagnitnoy kompensaciey / A.V. Lysenko, D.V. Olhov, A.V. Zatylnik // Innovacii na osnove informacionnyh i kommunikacionnyh tehnologiy. 2013. T. 1. S. 454-456.

GSM MODULES IN ENERGY EFFICIENT M2M-SYSTEMS

Kolganov A., Sviridov A.

Moscow, MIEM, NRU «Higher School of Economics»

This article briefly presents several architectures for M2M-devices. One of them is based on an external microcontroller with additional gsm modem unit and another one – on the base of multifunctional gsm-module. A comparative analysis of these schemes is given. Proposed analysis of energy consumption of modern GSM modules.

Keywords: m2m-systems, power consumption of gsm-modules

Machine to machine (M2M) refers to technologies that allow both wireless and wired systems to communicate with other devices of the same type. M2M is a broad term as it does not pinpoint specific wireless or wired networking, information and communications technology.

Most of devices in M2M application developed in wearable or vehicle-transportable modification so for information exchange uses existing widespread GSM networks. For organization of communication between systems functionally complete modules are applied. Initially modem in such interactions perceived as terminal equipment, performing the role of data transmission only and the formation of the data and their processing perform other functional units of the device. In this approach, modem is a device used in communication systems for physical linking of information signal with the medium of distribution where it can not exist without adaptation. Thus the modem is one of peripheral devices connected to the equipment.

The market of M2M devices and systems is very dynamic in its development and in this dynamic well traced the tendency to minimization of devices. In this situation the first priority goal to extend the functionality of modems, their ability to independently process the data and work on their own without external processor. However it should be understood that when you increase the functionality of a separate node - increases and its energy consumption, therefore the replacement of several individual elements of the system as a single module may not always be beneficial in terms of energy efficiency and flexibility of control this nodes. For example, consider two possible schemes of building the device that may be used for communication in the M2M-systems. Usually in such systems various environmental parameters are controlled (e.g., humidity, temperature, pressure and other) or internal control system parameters such as voltage, current consumption. But for the analysis of the circuits of the device and evaluation of its energy efficiency this is not essential.

Figure 1 shows diagram of the device, consisting several sensors, LCD display and microcontroller with external GSM modem.

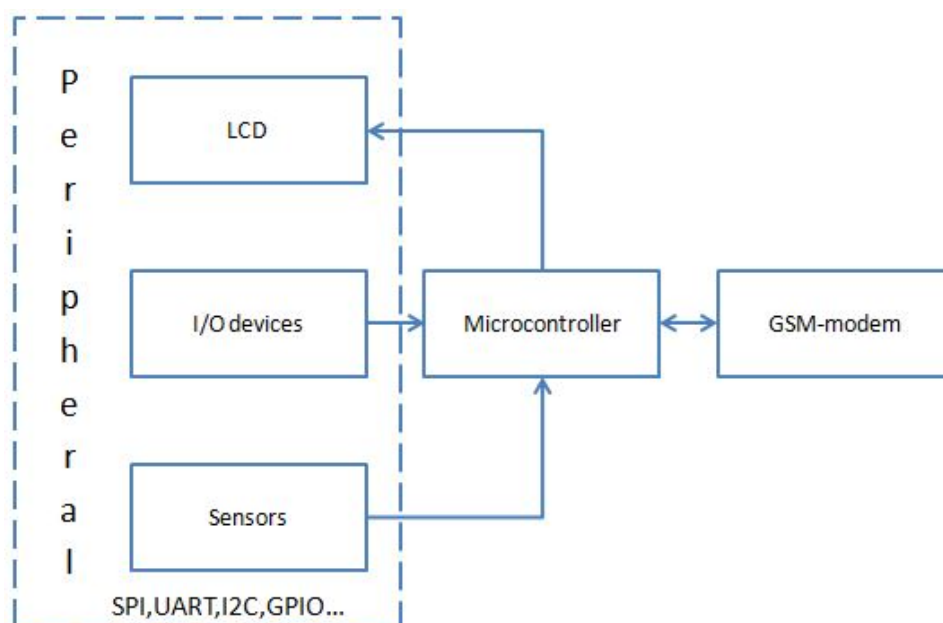


Figure 1. Diagram of the device with a separate microcontroller and GSM-modem

With this structure all of communications between peripheral occur through a central microcontroller unit. This scheme has a number of advantages, including the ability to choose the microcontroller for specific task. Developer is not limited in this context and he able to select any model from wide line of microcontrollers with different working frequencies, flash and ram memory size, etc. An important advantage is the possibility of choice from special lines of microcontrollers with low power consumption that are currently represented by different companies on the market. These microcontrollers with a corresponding firmware allow to obtain very low current consumption in various working modes. When implementing a «sleep» mode such chips allow to achieve consumption currents in dozens of microamps, which is very important when using batteries to power the device.

Power consumption of modern gsm-modems in different modes can reach an average of 500-600 milliamps. Comparison of modules on the average current consumption and physical size is presented in Table 1.

Table 1. Comparison of energy consumption and physical size for modern GSM-modules

Model	Size, mm	Energy consumption (avg.), mA Voltage supply, V
Quectel		
GSM/GPRS M10	29.0 × 29.0 × 3.6	230-520 mA
GSM/GPRS M80	23.0 × 25.0 × 2.6	230-520 mA
GSM/GPRS M85	24.5 × 25.3 × 2.6	230-520 mA
GSM/GPRS M95	19.9 × 23.6 × 2.65	230-520 mA
UMTS/HSDPA UC15	29.0 × 29.0 × 2.5	240-540 mA 3.3-4.3 V
UMTS/HSPA+ UC20	32.0 × 29.0 × 2.5	280-520 mA 3.3-4.3 V
Telit		

UMTS/HSDPA UE910-EU V2 AUTO	$28.2 \times 28.2 \times 2.2$	270-700 mA 3.4-4.2 V
LTE LE920 AUTO	$34 \times 40 \times 2.8$	260-700 mA 3.4-4.2 V
GSM/GPRS GE864-QUAD AUTO V2	$30 \times 30 \times 2.8$	160-420 mA 3.4-4.2 V
Sagemcom		
GSM/GPRS HiLo V2	$27 \times 27 \times 3.6$	190-360 mA 3.2-4.5 V
UMTS/HSDPA HiLo 3G	$27 \times 27 \times 4.8$	260-610 mA 3.2-4.5 V
SIMCOM		
GSM/GPRS/EDGE/UMTS/HSDPA SIM5216	$36 \times 26 \times 4.5$	< 470 mA 3.3-4.2 V
GSM/GPRS/EDGE/UMTS/HSDPA SIM5320	$30 \times 30 \times 2.9$	<550 mA 3.3-4.2 V
GSM/GPRS SIM900	$24 \times 24 \times 3$	< 440 mA 3.3-4.2 V
GSM/GPRS SIM800H	$15.8 \times 17.8 \times 2.4$	< 450 mA 3.4-4.4 V
SierraWireless		
GSM/GPRS SL6087	$25 \times 30 \times 2.65$	100-420 mA 3.2-4.8 V
GSM/GPRS/EDGE/HSPA+/ EVDO SL9090	$25 \times 30 \times 2.35$	730 mA 3.2-4.8 V
Gemalto		
Cinterion AHS2	$33 \times 29 \times 2.4$	180-400 mA 3.3-4.2 V
FIBOCOM		
G510	$20.2 \times 22.2 \times 2.5$	230-350 mA 3.3-4.5 V
uBlox		
LEON-G1 series	$18.9 \times 29.5 \times 3.0$	<400 mA 3-4.5 V
SARA-G3 series	$16.0 \times 26.0 \times 3.0$	<300 mA 3-4.5 V
LISA-U2 series	$22.4 \times 33.2 \times 2.6$	<500-800 mA 3.3-4.4 V

When designing a device it is important to remember that all gsm-modules have a peak current during data transmission through GSM network which can be up to 2.5 A. In accordance with this requirement, it is necessary to choose a power supply that can provide this impulse current without voltage drop. This is a critical moment in the calculation system of power supply of the device, as most modems operate at voltages from 3V. In this case if not to consider the possible voltage drop during an impulse and supply voltage drops below 3V than data transfer through the modem may be failed or there will be a complete shutdown of gsm-module. And it means the loss of communication with the system where it is installed.

The following Fig.2 shows typical pulse cycle during working gsm-module Quectel M95 and shows a voltage drop in the supply battery cell.

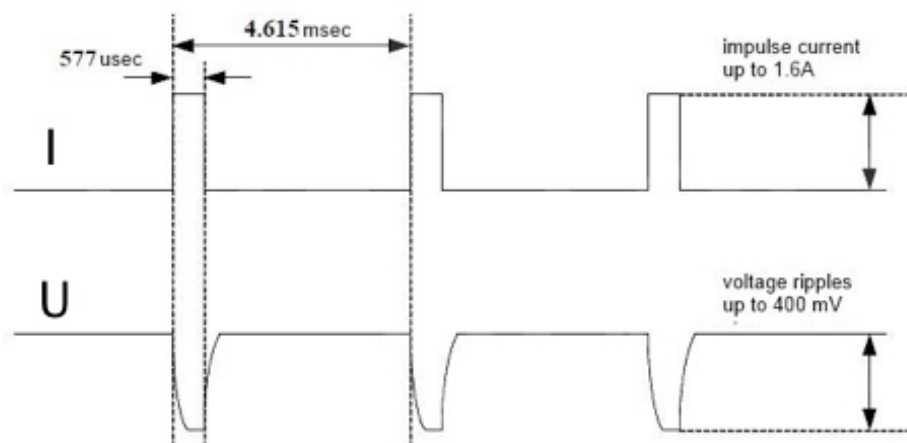


Figure 2. Typical pulse cycle during working GSM-module Quectel

Another possible scheme for constructing the device may be a structure where the main functions of the microcontroller performs a modem. This gsm-module realizes functions of central controller for peripheral and communication options for M2M communication. This scheme is shown in Fig.3.

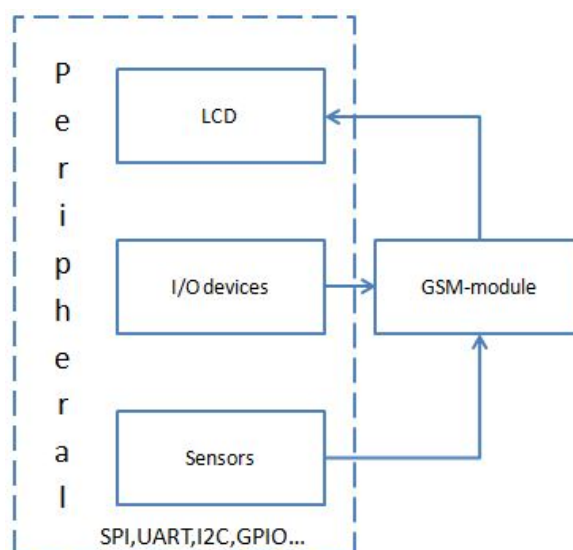


Figure 3. Scheme of device based on multifunctional GSM-module

Using modern gsm-modules can significantly extend the functionality of a modem and thereby simplify the overall architecture of the developed system up to the complete replacement of external microcontroller functions. Manufacturers of these modules offer a range of technologies to expand the functionality. For example, the Sierra Wireless in their solutions proposes to use developed by them real-time operating system OpenAT which manages a gsm module and implements all of functionality on its basis: GPIO, I2C, SPI and other interfaces for communication with peripherals. The Telit company in their modules embeds the Python language interpreter and all further work with the module and external interfaces are based on its functionality. Scheme of device based on multifunctional gsm-module in combination with these technologies significantly simplify the development of the system and reduce the time to get a working prototype of device as most of the functionality implemented by manufacturer of module. The majority of firms provides ready to use software library to work with TCP/IP, SMS and other protocols.

Modern gsm-modules are not only able to transmit and receive data through gsm networks but also to interact with various types of peripherals, process data, perform functions that had previously been assigned only with an external microcontroller. These modules simplify development and reduce its time but the device becomes bound to a particular vendor as internal software is closely linked with the firmware and infrastructure, which was designed by the manufacturer.

References

1. Uvaysov S.U., Ivanov I.A. Informatsionnaya model' protsessa proektirovaniya kontroleprigodnykh radioelektronnykh sredstv // Informatsionnye tekhnologii. 2011. № 12. S. 41-45.
2. Uvaysov S.U., Bushmeleva K. I., Bushmelev P. E., Plyusnin I. Modelirovanie optimal'nykh parametrov ustroystv distantsionnogo zondirovaniya // Izmeritel'naya tekhnika. 2011. № 3. S. 39-42.
3. Uvaysov S.U., Ivanov I.A. Obespechenie kontroleprigodnosti radioelektronnykh sredstv v ramkakh CALS-tekhnologii // Kachestvo. Innovatsii. Obrazovanie. 2011. № 1. S. 43-46.
4. Ivanov I.A., Uvaysov S.U., Koshelev N. A. Formirovanie naborov testovykh signalov dlya kontrolya kachestva elektronnykh sredstv kosmicheskikh apparatov // Kachestvo. Innovatsii. Obrazovanie. 2011. № 11. S. 84-88.
5. Ivanov I.A., Uvaysov S.U., Koshelev N. A. Metodika obespecheniya diagnostiruемости elektronnykh sredstv kosmicheskikh apparatov po rangovomu kriteriyu na rannikh etapakh proektirovaniya // Kachestvo. Innovatsii. Obrazovanie. 2012. № 1. S. 60-62.
6. Uvaysov S.U., Aminev D.A., Optimizatsiya RAID massiva dlya dostizheniya maksimal'noi proizvoditel'nosti sistem registratsii dannykh // Kachestvo. Innovatsii. Obrazovanie. 2012. № 12. S. 93-96.
7. Uvaysov S.U., Ivanov I.A. method of ensuring controllability of electronics based on diagnostic modeling of heterogeneous physical processes // World Applied Sciences Journal. 2013. Vol. 24. P. 196-201.
8. Uvaysov S.U., Aminev D. A., Lisitsyn I. Yu. Zashchita bortovoi sputnikovoi navigatsionnoi sistemy ot kratkovremennogo propadaniya elektropitaniya i elektromagnitnykh pomekh // Tekhnologii elektromagnitnoi sovmestimosti. 2013. № 3(46). S. 45-49.
9. Uvaysov S.U., Ivanov I.A., Gol'dberg O. D., Ivanov O.A. Obespechenie kachestva kharakteristik istochnikov bespereboynogo pitaniya v usloviyakh pomekh, vyzvannykh nelineinoi nagruzkoi // Tekhnologii elektromagnitnoi sovmestimosti. 2013. № 3. S. 55-64.

ILLUSTRATIVE MODELING OF COALITION FORMATION

Mashkov, V., Barilla, J., Simr, P.
Usti nad Labem, University J.E. Purkyne

The paper tackles the challenging task of coalition formation from the agents of alliance. Under alliance it is understood a set of agents that agree to share some of their private information and cooperate eventually. Coalition is formed every time when a request is received from an in-need entity. Coalition formation is a non-trivial task. It requires correct description and preliminary modeling in order to be solved effectively. There are several tools that allow providing and carrying out coalition formation modeling. In this paper, we show and illustrate how the Petri Nets can be used for such modeling.

Keywords: agent, alliance, coalition formation, Petri nets

1. Introduction

We consider an agent in broad sense as either technical or social entity. Agents can group and, thus, form alliances and coalitions. In this paper, we adhere to the concept of alliance suggested by M. Pechoucek et. al [1]. The alliance is defined as a set of agents that agree to share some of their private information and cooperate eventually.

During alliance formation, each agent receives public information from the agents that have already agreed to participate in the alliance. After performing analysis of this information, some of the agents can take a decision about their refusal or inability to cooperate with particular agents, although giving their agreement to participate in executing certain tasks of the alliance. Thus, the alliance can be formed with the account of the revealed refusals [2], [3]. Information about agents' refusal has to be further considered by each agent to determine the coalitions in which it is prepared to participate.

As distinct from alliance, in coalition all agents agree to cooperate with each other. In the paper, we restrict our consideration to the group-rational agents (i.e., agents that are more interested in achieving the common goal than in their own benefits).

For describing interactions among the agents and for modeling alliance and coalition formations the following formal description techniques and tools are used: finite state machines [4], Petri Nets [5], languages such as LOTOS [6] and SDL [7], language Z [8], modeling languages based on UML such as Agent UML [9], Erlang/OTP platform [10]. Among the above mentioned techniques and tools we suggest to opt for Petri Nets, since:

- they offer a simple way of how to graphically represent the coalition formation procedure elements (such as agents' capabilities, agents' ability and willingness to communicate, and restrictions imposed on task execution);
- they allow us to easily make changes in modeling procedure;
- there exist many high-quality modeling tools for solution of Petri Net.

The rest of the paper is organized as follows. Section 2 gives a short description of agents' communication during formation of coalitions. Section 3 reminds the basics of Petri Nets. Section 4 describes how Petri Nets can be used for modeling coalition formation procedure. Section 5 contains analysis of the results of the performed modeling and recommendations made on their basis. Conclusions are finally made in Section 6.

2. Communications among the agents during coalition formation

During coalition formation each agent has to decide when and with which other agents to communicate. This decision is made on the basis of available to him information about other agents' capabilities and on the strategies which they adhere. We consider the agents that are more interested in maximum efficiency of tasks execution in shortest possible time rather than in gaining any direct benefits from their participation in the coalition. From this preference it follows that agents should be honest to each other in pursuing a coalition goal. It is implied that an agent doesn't change its previous decision to cooperate with particular agent when it gets the offer from another agent (i.e., the decision once made cannot be reversed). It is also expected that each agent provides correct information about its capabilities which will be held fixed in process of coalition formation. When an agent receives an offer from another agent, the delay with a reply should not be caused by waiting for a more attractive offer.

In general, an agent can be either active or passive. If the agent is passive, it only waits for offers from other agents and replies to the received offers. If the agent is active, it also offers the other agents to collaborate in the coalition. In this paper, we assume that all agents will be active since each of the agents is keen on shortening the period of coalition formation.

Generally, two approaches to coalition formation are possible. Namely,

- coalition formation with preliminary exchange of information about agents' capabilities;
- coalition formation without preliminary exchange of information about agents' capabilities.

In the paper, we consider the latter approach, and also assume that each agent believes that the capabilities of all the agents are equal.

At the beginning of coalition formation, agents form interim coalitions (i.e., coalitions that can be further extended by adding new agents and, thus, increasing their capability). When capability of interim coalition has become greater or equal to the value required to perform the coalition tasks, the coalition formation ends and the formed coalition is considered as final.

3. Basics of Petri Nets

Petri Nets were designed by Carl Adam Petri in 1962 in his PhD Thesis “Kommunikation mit Automaten” [11]. The basic idea is to describe state changes of system via transitions. The main elements of Petri Net are places and transitions that may be connected by directed arcs. Thus, the graphical structure of a Petri Net is a bipartite directed graph. Nodes of this graph are divided into two groups called places and transitions. Arcs connect only nodes of different groups. Transitions symbolize actions or events, whereas places symbolize states or conditions. When conditions are met, an action can be performed (in terms of Petri Nets, transition “fires”). Transition has a certain number of input and output places representing the pre-conditions and post-conditions of the event, respectively. Places can contain a certain number (nonnegative integer) of tokens. The presence of a token in a place is interpreted as holding the truth of the condition associated with the place. Tokens can be also interpreted as available resources needed for carrying out of an action. Since each place is marked with a certain number of tokens, it is possible to write an m -vector, where m is the total number of places. This m -vector is called as marking and is denoted as $M = \{m_1, m_2, \dots, m_n\}$, where $m_i, i=1..n$, is the number of tokens in place p_i in marking M .

Graphically, places, transitions, arcs and tokens are represented by circles, bars, arrows and dots, respectively (see Fig. 1).

In Fig. 1, places p_1 , p_2 and p_3 are drawn as circles, transition t_1 as bar and tokens as black dots, respectively. Arcs are labeled by weights. In an ordinary Petri Net (i.e., when all of its arc weights are 1's) labels are omitted. A label indicates the number of tokens which is needed in order that transition can fire. After transition firing, this number of tokens will be withdrawn from the corresponding place.

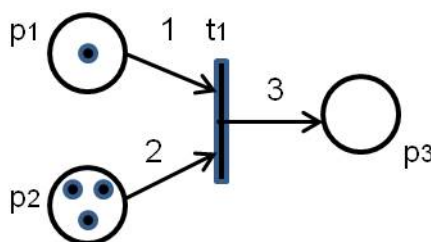


Figure 1. Graphical representation of simple Petri Net.

The behavior of many systems can be described in terms of system states and their changes. In order to simulate the dynamic behavior of a system, a state or marking in a Petri Nets is changed by moving the tokens into the places after transition firing. A transition t is enabled (i.e., can fire) if each input place p_i is marked with at least $w(p_i, t)$ tokens, where $w(p_i, t)$ is the weight of the arc from place p_j to transition t . A firing of an enabled transition t

removes $w(p_j, t)$ tokens from each input place p_j , $j=1, \dots, k$, and adds $w(t, p_r)$ tokens to each output place p_r , $r=1, \dots, s$, where $w(t, p_r)$ is the weight of the arc from t to p_r .

For Petri Net depicted in Fig.1, the firing of transition t_1 removes one token from place p_1 , two tokens from place p_2 and adds three tokens to output place p_3 . The firing of an enabled transition will change the token distribution (marking) in Petri Net. For the example under consideration, initial marking is $M_0=(1,3,0)$. After transition firing the marking has changed to $M_1=(0,1,3)$. Generally, a sequence of firings will result in a sequence of markings. A marking M_α is said to be reachable from a marking M_β if there exists a sequence of firings that transforms M_α to M_β . The set of all possible markings reachable from M_0 is denoted by $R(M_0)$. The reachability problem for Petri Nets is the problem of checking if $M_n \in R(M_0)$ for a given marking M_n .

Petri Nets are a powerful tool for modeling real systems since they allow take into consideration such features of system activities as concurrency (or parallelism), synchronization, limited resources, sequence, mutual exclusion (conflict) etc. (see Fig. 2).

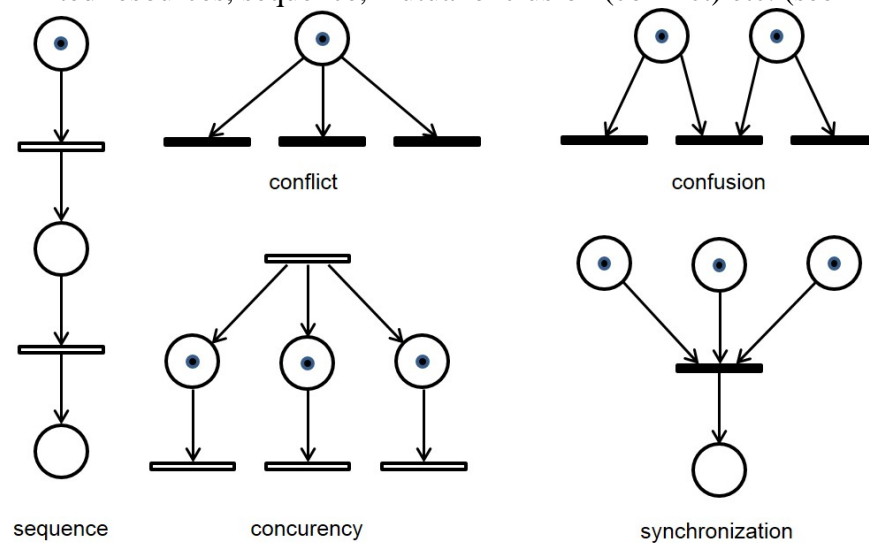


Figure 2. Primitive structures of Petri Net

It is worth noting that the conflict may be resolved in a purely probabilistic way, by assigning appropriate probabilities to the conflicting transitions. Carl Adam Petri originally proposed Petri Nets without any notion of time. However, for performance evaluation and scheduling problems of dynamic systems, it is desirable and useful to account time delays of the events associated with transitions. Such Petri Nets are called as timed Petri Nets if the delays are deterministically given, or as stochastic Petri Nets if the delays are probabilistically specified. Application of timed Petri Nets is available in such areas as communication protocols, performance evaluation, manufacturing etc. In the stochastic Petri Nets, time was naturally associated with activities that induce state changes, hence with the delays incurred before firing transitions.

For modeling specific features of activities or events of the systems, some special constructs in Petri Nets are usually exploited. As an example, for modeling priorities of transitions, the inhibitor arcs are often used. An inhibitor arc (see Fig. 3) from place p_1 to transition t_1 modifies the enabling rule so that the transition t_1 can fire only if place p_1 has no tokens. The inhibition function is displayed by a circle-headed arc.

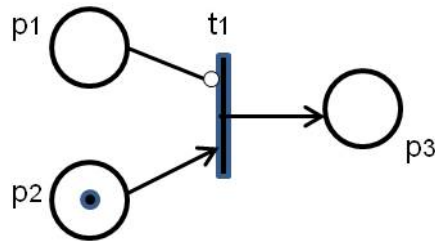


Figure 3. Petri Net with inhibitor arc.

4. Using Petri Nets for modeling of coalition formation

Petri Nets are a graphical tool for the formal description of the flow of activities in complex systems. In our case, the activities which should be modeled are the communications among the agents of an alliance aimed at forming interim and final coalitions.

In order to show how Petri Net can be used to describe agents' communications, we start with simple example when alliance consists of only three agents, particularly, agent A, agent B and agent C. Agent's capability can be measured and expressed via number of tokens. For the example under consideration, we assume that for carrying out the task facing the coalition the capabilities need to be equaling to four tokens. We also assume that the distribution of tokens among the agents is as follows: agent A has one token, agent B has two tokens and agent C has three tokens.

In Fig. 4, places P_1 , P_2 and P_3 represent the states of agents A, B and C, in which the corresponding agent cannot negotiate other agents for some reasons. For instance, at the start of coalition formation, an agent may continue in performing its own main tasks. As another reason why an agent cannot immediately start negotiation consists in that an agent may require some time to prepare for the negotiations. Timed transitions t_A , t_B and t_C allow simulating the lapse of time while the agent cannot negotiate. Timed transitions t_1 , t_2 and t_3 simulate the time when the corresponding agent either waits for an offer or tries to contact other agents to form the interim coalition. Places P_4 , P_5 and P_6 represent the states of agents A, B and C, in which the corresponding agent can contact or be contacted by other agents. Arcs from places P_4 , P_5 and P_6 to timed transitions t_{k1} , t_{k2} and t_{k3} allow simulating the preferences of the agents regarding their intention to communicate with particular agent. These preferences can be expressed with probabilities. Timed transitions t_{k1} , t_{k2} and t_{k3} allow simulating the amount of time required for negotiation between two agents. Places P_4 , P_5 and P_6 represent the events of interim coalition formation. For example, if place P_{10} has three tokens, it means that interim coalition AB is formed (i.e., agents A and B have agreed and prepared to cooperate). How many times interim coalition can be formed is set by the number of tokens in special place. For interim coalitions AB, AC and BC these places are P_7 , P_8 and P_9 , respectively. In Fig. 4, places P_7 , P_8 and P_9 contain one token each. It means that each interim coalition can be formed only once. Immediate transitions t_5 and t_6 simulate the logical operation "OR", i.e., $AC \vee BC$. Both interim coalition AC and BC can be considered as final coalition since four and five tokens that the associated places P_{11} and P_{12} have are enough for performing coalition tasks. In contrast, interim coalition AB cannot perform coalition tasks, and thus agents A and B should continue in search of further agents to form the final coalition.

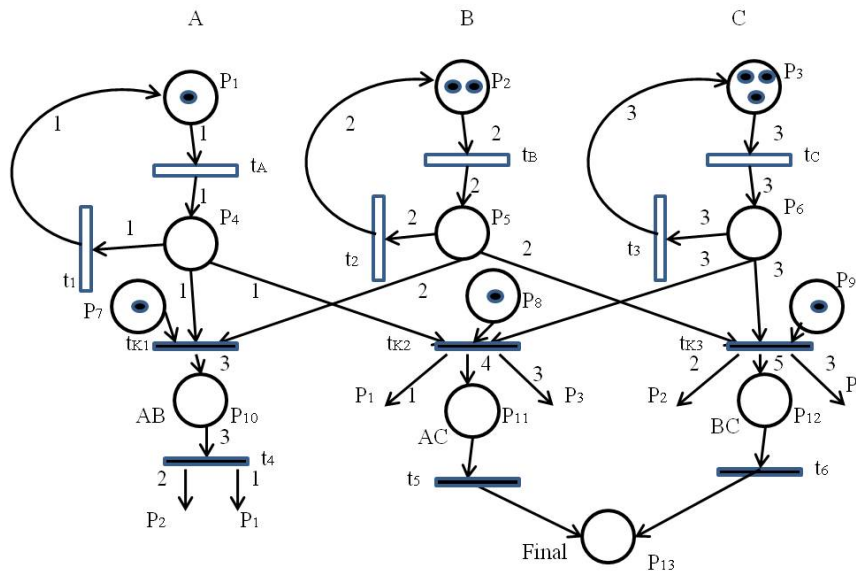


Figure 4. Petri Net modeling coalition formation.

In the example under consideration, we simulate such agent's features as:

- agent's engaged and free periods (i.e., availability for negotiations);
- agent's preferences in the choice of agents for communications;
- agent's capabilities.

We also simulate the coalition capabilities by summarizing the capabilities of the agents that form the coalition. By using agent's preferences it is possible to model coalition formation when some agents refuse to communicate and negotiate with each other, i.e., deal with the agents of restricted alliance. It is especially important when restricted alliance includes great number of agents. In this case, Petri Net modeling coalition formation will allow to find out the possible deadlocks and to estimate the probability of their occurrences. A deadlock occurs when current interim coalitions are unable to perform coalition tasks and cannot be expanded for the reason of agents' refusals to negotiate with each other.

5. Modeling and its results

We provide modeling for the simple example when only three agents are available. Nevertheless, this modeling includes most of the features that pertain to more complex cases. Since Petri Net that we have designed for modeling coalition formation (see Fig. 4) includes probabilistically defined timed transitions, it relates to Stochastic Petri Nets.

There exist many modeling tools for solution of Stochastic Petri Nets. For our research we have chosen Sharpe [12] for the following reasons:

- Sharpe enables both developing graphical Petri Nets and reading input and output matrices that represent Petri Nets. This is very important for our purposes since graphical representation of Stochastic Petri Nets is very difficult or even impossible when the number of places is great. This problem can be solved by designing the Petri Net generator whose output can be read and used by Sharpe. Similar generator was designed by us for Petri Nets simulating mutual checks in multicore processors [13];

- Sharpe has the tools for providing analysis of the model;
- Sharpe has a friendly interface.

Petri Nets simulating coalition formation when only three agents can be engaged in this process can be plotted directly in the proper window of Sharpe.

While performing the modeling we varied such parameters as period of time when an agent is available for negotiations. In Petri Net, this parameter is set by value of rate t_1 (associated with free period of agent A), by value of rate t_2 (for agent B) and by value of rate

t_3 (for agent C). We also varied the preferences of separate agents. In Petri Net, these preferences are set by the corresponding probabilities assigned to arcs connected to places P_1 , P_2 and P_3 , respectively.

Fig. 5 shows how the probability of final coalition formation depends on the time devoted to coalition formation.

In Fig. 5, time is measured in arbitrary unit. For example, value 10 of t can be interpreted as either 10 ms or 10s or 10h or 10 days etc. Probability of final coalition formation was determined for several different values of rate of transition t_1 . Rates of transitions t_2 and t_3 were set equal to rate of transition t_1 . For instance, for the case when rate of transition t_1 equals to 0.1 the sought probability P_k reaches the value near to 1 after approximately 3 arb. units from the start of coalition formation process. From Fig. 5 we can infer that the dependence of probability P_k on time t is of exponential type.

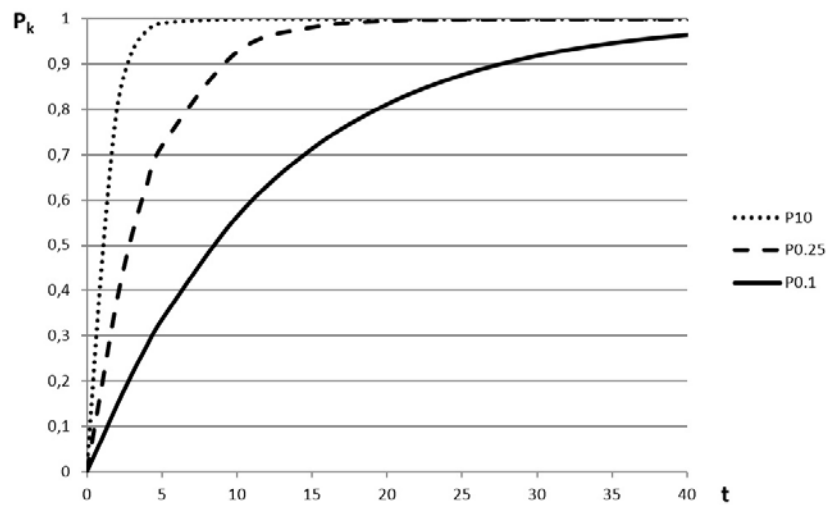


Figure 5. Probability of final coalition formation, P_k .

Fig. 6 shows the time required to form the final coalition for the case when coalition BC has low preferences (case of T_{k2}) and for the case when coalition BC has high preferences (case of T_{k1}).

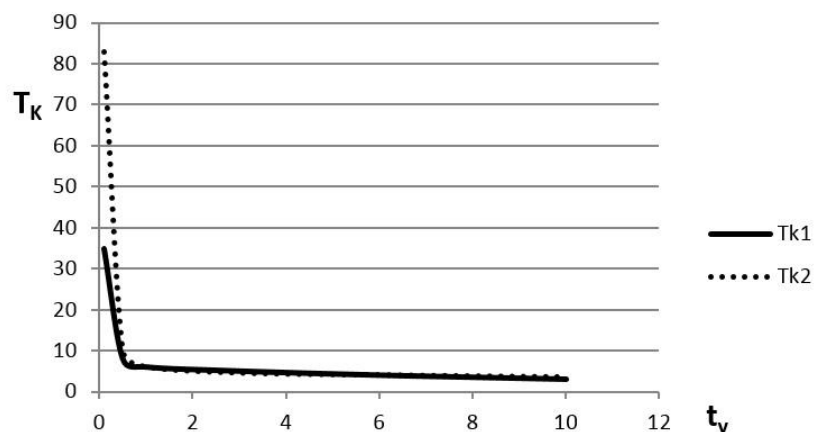


Figure 6. Time required to form the final coalition, T_k .

We varied the rates of transitions t_1 , t_2 and t_3 . Time t_v in Fig. 6 is determined as

$$t_v = \frac{1}{\text{Rat}t_1} = \frac{1}{\text{Rat}t_2} = \frac{1}{\text{Rat}t_3}$$

Fig. 6 shows that preferences of the most powerful coalition, BC, (i.e., coalition that has the greatest capabilities) essentially impact the time T_k . Fig. 6 also shows that increasing t_v above the value of 1 do not allow to considerably decrease time T_k . Thus, the value of 1 for t_v can be considered as “optimal” in certain sense.

Fig. 6 allows us to make prediction (with probability equal to 0.95) about the time of final coalition formation. For the considered example, this time is approximately equal to 4 arb. units for $t_v > 2$.

6. Conclusions

Our research deals mainly with the issues concerning interaction and collaboration of distributed multiple agents. Cooperation among agents makes it possible to create the effective groups, since agents acting in a team fashion could essentially increase their capabilities, and thus, be able to offer more services and/or to perform tasks more effectively than acting individually. Examples of groups of agents are alliance and coalition. Initially, agents form an alliance, i.e., preliminary agreement to cooperate. When tasks arise, the agents of the alliance form coalition to carry out particular tasks. Generally, there can be formed several coalitions, although only one coalition will perform the emerged tasks. Thus, all possible coalitions should be estimated, and the “best” coalition should be chosen.

Coalition formation process has many parameters that are probabilistically defined. Therefore, it is very difficult to determine all possible coalitions that can be formed with the agents of alliance, especially when the total number of agents is large. Even more difficult task is the task of estimating the probability of formation for different coalitions. These tasks can be solved only on the basis of corresponding modeling. There are several ways of how to perform this modeling. We preferred to exploit Petri Nets for providing modeling of coalition formation for the reasons mentioned above.

We did not aim to provide complete modeling, but only wanted to show that Petri Nets is a very effective tool for determining and estimation of possible coalitions. With the help of Petri Net we can predict the time needed for coalition formation. We can also determine the probability of formation of all possible coalitions, including the formation of the “best” coalition. We can evaluate how separate parameters influence the main characteristics of coalition formation process.

For providing analysis of a designed Petri Net, we used special tool called Sharpe. With the help of Sharpe we can obtain all the characteristics of coalition formation that are of interest. For the case when the number of agents is small, Sharpe allows graphical representation of coalition formation. With graphical representation of coalition formation it is easy to make changes of different model parameters and to estimate how these changes could influence the process of coalition formation.

We expect that Petri Net will be very efficient for predicting the coalition formation with the agents of restricted alliance (i.e., alliance in which not all agents agree to cooperate with each other). When agents’ refusal to cooperate with each other take place, there is a possibility of a situation called as deadlock. Petri Net allows to find out such situations before coalition formation process begins, and allows to estimate the probabilities of such situations. Agents of the alliance will be informed about possible deadlocks, and thus, they will be prepared and will know what to do to proceed with coalition formation.

When number of agents of alliance is very large, graphical representation of coalition formation is very difficult or even impossible. Nevertheless, it is possible to design Petri Net generator whose output can be used by Sharpe. Hence, Petri Nets can be used to model coalition formation also for the case with large number of agents.

References

1. M. Pechoucek, V. Marik, J. Barta, A knowledge-based approach to coalition formation. *IEEE Intelligent Systems*, 7(3), 2002, 17-25.
2. V. Mashkov, Restricted alliance and coalition formation. *Proc. of IEEE/WIC/ACM International Conf. on Intelligent Agent Technology*, Beijing, 2004, 329-332.
3. V. Mashkov, Coalition formation with unreliable agents. *Proc. of IASTED International Conference on Knowledge Sharing and Collaborative Engineering*, St.Thomas, US Virgin Islands, 2006, 138-143.
4. M. Barbuceanu, M. Fox, COOL: A language for describing coordination in multiagent system. In *First International Conference on Multi-agent Systems (ICMAS-95)*, San Francisco, USA, 1995, 17-24.
5. R. Cost, et al., Modeling agent conversation with colored Petri nets. In J. Bradshaw, ed., *Autonomous Agents'99 Special Workshop on Conversation Policies*, 1999.
6. J. Koning, Algorithms for translating interaction protocols into a formal description. In K. Ito, ed., *IEEE International Conference on Systems (SMC-99)*, Tokyo, 1999.
7. C. Iglesias, M. Garrijo, J. Gonzales, J. Velasco, Design of multi-agent system using mas-commonkads. *Proceedings of ATAL 98, Workshop on Agent Theories, Architectures and Languages*, LNAI 1555, Springer-Verlag, Paris, 1998, 163-176.
8. M. d'Inverno, M. Luck, Formalising the contract net as a goal-directed system. In W. de Velde and J. Perram, ed., *Agent Breaking Away, MAAMAW 96*, LNAI 1038, Springer-Verlag, 1996.
9. B. Bauer, J. Muller, J. Odell, An extension of UML by protocols for multi-agent interaction. In *International Conference on Multiagent Systems (ICMAS'00)*, Boston, USA, 2000, 207-214.
10. J. Fiser, V. Mashkov, Alliance and coalition formation. *Journal of Applied Computer Science*, Vol. 18, No. 1, 2010, 19-38, ISSN 1507-0360.
11. C.A. Petri, *Kommunikation mit Automaten*. Bonn: Institut für Instrumentelle Mathematik, Schriften des IIM Nr.3, 1962. Also, English translation "Communication with Automata", New York: Griffiss Air Force Base, Tech., Rep., RADC-TR-65-377, Vol.1, Suppl. 1, 1966.
12. R.A. Sahner, K.S. Trivedi, Reliability modeling using SHARPE. *IEEE Transactions on Reliability*, R-36(2), 1987, 186-193.
13. V. Mashkov, J. Barilla, P. Simr, Applying Petri Nets to modeling of many-core processor self-testing when tests are performed randomly. *Journal of Electronic Testing (JETTA)*, Vol.29, No.1, 2013, 25-34.

MEASURING DEVICE FOR CALIBRATION OF MECHANICAL CONVERTING SYSTEM OF FIBER-OPTIC DIFFERENTIAL PRESSURE SENSOR

Golev D.M.

Penza, Penzenskii Gosudarstvennyi Universitet

I developed the measuring unit, which can be used for experimental appraisal of math modeling, engineering specifications of fiber-optic pressure sensor. Appliance of this unit in design phase can greatly reduce material and time expenses for testing and alignment of fiber-optic sensor in comparison with known methods of finalization engineering specifications of FOPS

Introduction

Wide implementation of fiber-optic sensors (FOS) in aerospace and aeronautical equipment calls for contemporary technologies, which lower the prime cost and improve machinability. Most complicated development stages are alignment and adjustment of FOS's optical system. It is essential for minimize expenses at that stages. In this context we must develop measuring unit for experimental evaluating of engineering specifications of mechanical converting system.

On the first stage of research fiber-optic route was excluded from sensor and calculation of mechanical converting system take place. For experimental evaluating of math modeling was developed the measuring device. It can be used to check engineering specifications of fiber-optic differential pressure sensor.

Appliance of sensor prototype, which utilizes only mechanical converter system, can greatly reduce the cost of design phase. Lack of fiber-optic route and electronic information processing device spare developers from numerous fiber-optic differential pressure sensor tests during design phase.

1 Mathematical modeling for characterization of mechanical converting system

Differential fiber-optic transducer of microdisplacement provides high sensitivity of optical signals transduction and high modulation percentage (up to 30%) of optical signal and linearity of transfer function if shutter travels along Z-axis up or down between ends of optical fibers and equals approximately $0,25...0,5d_c$ [1].

Parameters used for calculation of sensors' optical system:

Optical fiber TKhO .735.123 TU

Optical fiber diameter $d_{OB}=500$ micron

Core diameter $d_c=200$ micron

Aperture angle $\Theta_{NA}=12^\circ$

Optical system construction establishes the following requirements:

bend of central part of membrane must fall within the limits of $50...100$ mym

round bore in the shutter of transducer must travel between ends of optical fibers within the limits of $50...100$ micron.

Initial data for calculation:

- pressure $P = 0...100 \text{ kgf/cm}^2 = 0...1 \text{ kgf/mm}^2$,

- membrane thickness $h = 0,25...0,50 \text{ mm}$,

- bend of central part of membrane $W = 50...100 \text{ micron}$

- elasticity modulus of membrane material (36NKhTYu alloy),

$E=195000 \text{ N/mm}^2$.

Main results of calculation must be:

- thickness of membrane h , mm,

- membrane radius R , mm.

Pressure applied to membrane cause bending of center of membrane W_{max} and tension σ_{max} . Maximal values of this parameters calculated by formula (3.1):

$$W_{max} = \frac{3(1 - \mu^2)R_m^2 P}{16Eh^3}, \quad (3.1)$$

$$\sigma_{max} = \frac{3r^4 P}{4h^2} \leq [\sigma],$$

W_{max} – maximal bend of membrane under pressure, micron;

R_m, h – radius and thickness of membrane, mm;

E - elasticity modulus of membrane material, N/mm^2 , for 36NKhTYu alloy:

$E = 195000$; $\text{H/mm}^2=1988,4 \text{ kgf/mm}^2$;

μ - Poisson's ratio of membrane material; for 36NKhTYu alloy: $\mu=0,3$;

σ – maximal allowed tension, N/mm²;

$[\sigma]$ – maximal nominal allowed tension, N/mm², for 36NKhTYu alloy:

$[\sigma] = 1200 \text{ N/mm}^2 = 122,3 \text{ kgf/mm}^2$.

Results of mathematical modeling depicted in tables 1,2,3 and figures 5 and 6.

Table 1

Pressure $P, \text{ kgf/mm}^2$	Thickness of membrane $h, \text{ mm}$	Membrane radius $R, \text{ mm}$	Bend of membrane $W, \text{ micron}$
0,1	0,25	5	13,7
0,1	0,25	6	19,8
0,1	0,25	7	27
0,1	0,25	8	35,15
0,1	0,25	9	44,48
0,1	0,25	10	54,92
0,1	0,25	11	66,45
0,1	0,25	12	78,08
0,1	0,25	13	92,81
0,1	0,25	14	107,64

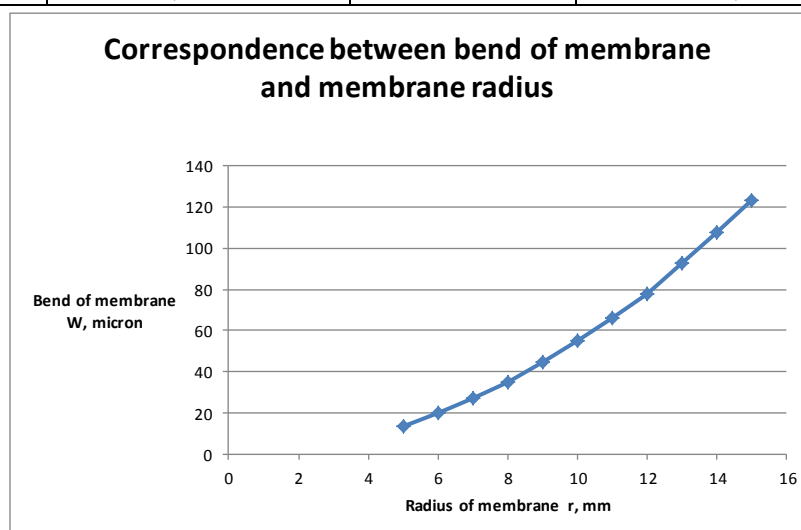


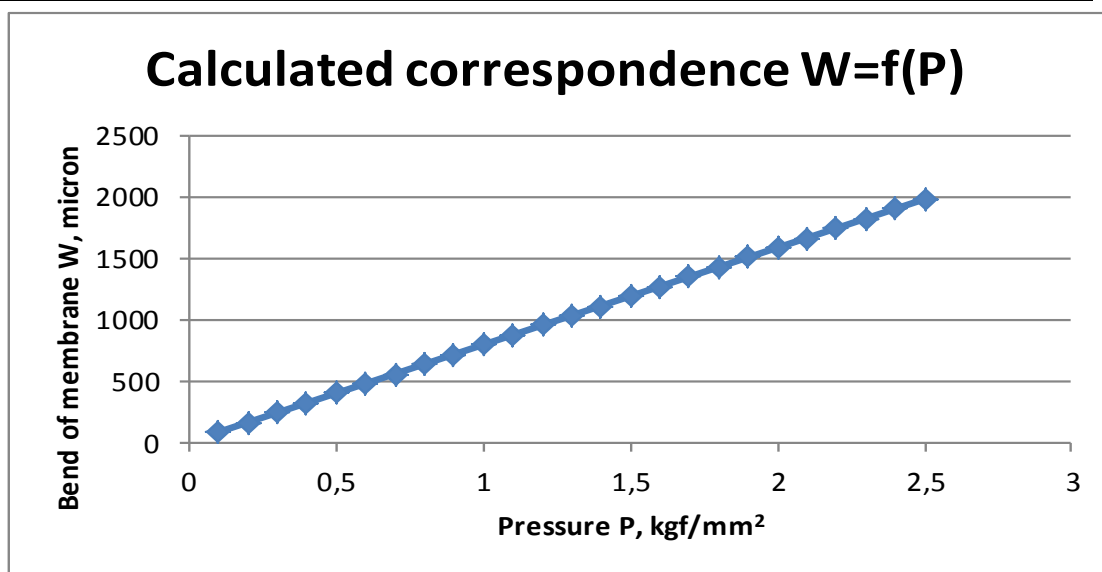
Figure 1 – Calculated correspondence $W_{max}=f(r)$

Table 2

Pressure $P, \text{ kgf/mm}^2$	Thickness of membrane $h, \text{ mm}$	Membrane radius $R, \text{ mm}$	Bend of membrane $W, \text{ micron}$
0,1	0,25	11	66,5
0,25	0,25	7	67,3
0,25	0,25	8	87,9
0,25	0,3	9	64,4
0,5	0,25	5	68,6
0,5	0,3	6	57,2
0,5	0,3	7	77,9
1	0,25	4	87,9
1	0,3	4	50,8
1	0,3	5	79,4
1	0,4	7	65,69

Table 3

Radius of membrane R , mm	Thickness of membrane h , mm	Pressure P , kgf/mm ²	Bend of membrane W , micron
12	0,25	0,1	79,08109
12	0,25	0,2	158,1622
12	0,25	0,3	237,2433
12	0,25	0,4	316,3244
12	0,25	0,5	395,4054
12	0,25	0,6	474,4865
12	0,25	0,7	553,5676
12	0,25	0,8	632,6487
12	0,25	0,9	711,7298
12	0,25	1	790,8109
12	0,25	1,1	869,892
12	0,25	1,2	948,9731
12	0,25	1,3	1028,054
12	0,25	1,4	1107,135
12	0,25	1,5	1186,216
12	0,25	1,6	1265,297
12	0,25	1,7	1344,379
12	0,25	1,8	1423,46
12	0,25	1,9	1502,541
12	0,25	2	1581,622
12	0,25	2,1	1660,703
12	0,25	2,2	1739,784
12	0,25	2,3	1818,865
12	0,25	2,4	1897,946
12	0,25	2,5	1977,027

Figure 2 - Calculated correspondence $W=f(P)$

2 Development of measuring device for calibration of mechanical converting system of fiber-optic differential pressure sensor

To approve mathematical calculation I developed measuring device for calibration of mechanical converting system of fiber-optic differential pressure sensor (figure 3).

Measuring device consist of pressure calibrator, stand (which connected to massive base), meter clock gauge and measured fiber-optic differential pressure sensor. Meter clock gauge bracing and coupling device fixed on stand.

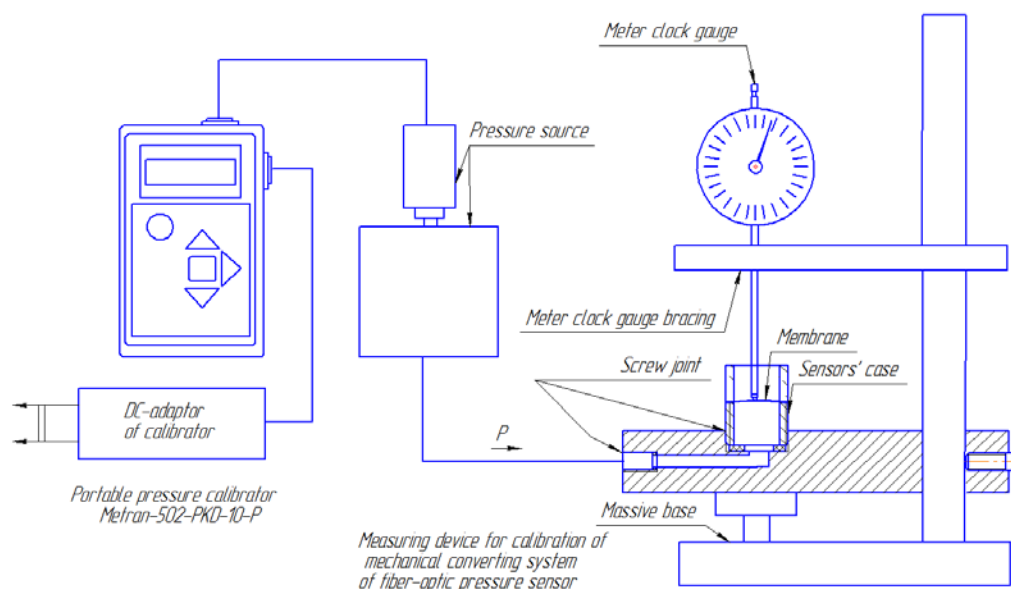


Figure 3 - Measuring device for calibration of mechanical converting system of fiber-optic differential pressure sensor

Portable pressure calibrator such as Metran-PKD-10 TU 4212-002-36897690-98 can be used in measuring device. Metran-PKD-10 consist of electronic indication block, pressure control block, pressure source (pneumatic hand pump), electrical cable and pneumatic cable (figure 4).



Figure 4 - Portable pressure calibrator Metran-502-PKD-10P

Portable pressure calibrator Metran-502-PKD-10P used for precise measuring and reproduction of excessive pressure and exhaustion within the limits of 0...25000 kPa with precision up to 0,1%.

It contains pneumatic hand pump N2,5M as a source of excessive pressure (within the limits of 0...2,5 MPa) in measured sensor.

In measuring device used meter clock gauge with precision within 0,5 micron. Measuring rod of meter clock gauge in neutral position (0 on the scale) contacts with center of top membrane. Pressure applied to the bottom membrane. Calibrator connected with sensor with pneumatic cable by screw joint in the base of sensor.

During experimentation stage can be used prototype of sensor without fiber-optic route (without optical fibers). Prototype contains mechanical converting system with calculated parameters. That engineering solution can reduce cost of development stage.

3 Method of experimental approval of calculated correspondence $W=f(P)$

Portable pressure calibrator must be tested by reference pressure gauge accordingly to instruction manual for Metran-PKD-10 TU 4212-002-36897690-98.

Calibrator connects to measured sensor. Pressure applied to bottom membrane with pneumatic hand pump. Centers of membranes connected by rod and can transfer force from bottom membrane to the top. Bend of the top membrane W measured by meter clock gauge. Results of experiment can be used to create experimental correspondence $W_{exp}=f(P)$, which can be compared with calculated correspondence $W_{calc}=f(P)$.

If experimental correspondence and calculated correspondence coincide by 90%, then parameters of mechanical converting system can be applied to construction of fiber-optic differential sensor. Otherwise necessary to recalculate parameters and retry experiment/

Summary

- developed measuring unit for mechanical converting system calibration of fiber-optic differential pressure sensor

Applying of sensor prototype unit, which utilizes only mechanical converter system, can greatly reduce the cost of design phase. Lack of fiber-optic route and electronic information processing unit release from numerous fiber-optic differential pressure sensor tests during design phase.

References

1 Badeeva E.A., Pivkin A.G., Murashkina T.I., Tekhnologicheskie osnovy proektirovaniya VOD davleniya dlya iskro-, vzryvo-, požaroopasnykh i Kolomiets L.N., Badeeva E.A., Murashkina T.I., Pivkin A.G. nzhenerno-tekhnicheskikh ob'ektov // Nadezhnost' i kachestvo: Tr. Mezhdunar. simp.– Penza: Izd-vo Penz. gos. un-ta, 2011. – T. 2.

2 . E.P. Osadchii Proektirovanie datchikov dlya izmereniya mekhanicheskikh velichin - Moscow: Mashinostroenie, 1979.

3 Kolomiets L.N., Badeeva E.A., Murashkina T.I., Pivkin A.G. Funktsiya preobrazovaniya differentsial'nogo VODD otrazhatel'nogo tipa. // Aviakosmicheskoe priborostroenie. – 2007. – № 8. – S. 17–22

UDC [681.2/.51:621.3]:57.042/.047::004

METHODS OF PROTECTION FROM ADVERSE FACTORS THAT MAY AFFECT AUTOMATED INFORMATION AND MEASUREMENT SYSTEMS

Botvinkin P., Kamaev V.
Volgograd State Technical University

This work was partially funded by the Ministry of Education and Science of Russian Federation within the basic part (task 2586 of project № 2014/16).

In this paper are analyzed the most possible adverse factors, which may affect automated information and measurement systems. The main methods of protection from them are described.

Keywords: AIMS, automated information-measuring systems, equipment protection, information security.

Wide-spreading and accelerating implementation of automation in almost all spheres of activity has led to a radical restructuring of the measuring equipment: now in its task, along with the measurements also includes information servicing of a researched (controlled) object, which includes automatic collection, presentation, delivery, storage, registration, formation, processing and analysis of information obtained from separate measurements. [5]

Automated information-measuring system (AIMS) is a set of devices, which providing automatic collection, storage, processing, analysis and delivery to a human operator the necessary information about the properties, status and settings (including historical) of the set of objects. [3, 15]

Use of AIMS formed by complex of various measuring instruments, now receives extensive development, and its study in the disciplines of measurement and metrology is becoming increasingly important. [11, 16]

The most important aspects of the functioning of electronic measurement system are the continuity of its work and the accuracy of the information obtained through it. [10, 11]

Malfunctions of the automated systems, including violations of the data protection regime can lead to serious consequences. [6, 7]

After analyzing the possible adverse factors, the following directions of protection of electronic measuring systems can be denoted:

- protection from natural factors: climate, sunlight, extreme temperatures, rain, high relative humidity, high atmosphere pressure, dust, sand, lightning;
- protection from biological agents: animals (insects, rodents), fungi, mold;
- protection from technogenic effects: power surges, corrosive environments, radiation;
- protection from malicious human intervention: mechanical effects of electric and magnetic fields, information protection.

Let's review the listed directions.

Natural influences are determined by a combination of factors (physical, chemical, thermobaric, etc.) capable of exerting direct or indirect, immediate or mediate impact on both the performance of the nodes and the accuracy of the AIMS as a whole.

In Russia the current related standard is GOST 14254-96 (Russian National Standard, harmonized with IEC 529-89) "Degrees of protection provided by enclosures", which defines the requirements in terms of resistance of enclosures and electrical equipment in general to external impact factors, as well as the methods and modes of controlling and testing to check for compliance with enclosures' electrical protection level sets.

The standard [4] indicates the degree of protection provided by enclosures. Electrical protection index (IP) consists of two digits. The first shows the protection against ingress of

solid particles inside the structure: from zero to six. The second shows protection against moisture: from zero to eight.

Along with the indicators of protection against external influences there are concepts of climatic performance and allocation category. Climatic performance shows in which temperature range the device is operated. Allocation category defines a number of external factors (such as humidity) in place of the product's exploitation.

If the automated water meters are used, it is possible to increase their durability by special magnetic filters [1], which allows to sift metal fractions contained in the water passing through the water meter.

In the case of a wired connection of the nodes of AIMS, rodents can damage cables connecting them and cause serious consequences, including the entire system failure. Damage can be dealt to the sensor cables, electric power cables and LAN cables.

One of the oldest methods of protection is the installation of mechanical traps and poison baits. Also the popular and rather effective method is the use of ultrasonic and high-voltage rodent repellent devices. [2]

In addition to damage to the cables and wires, rodents, along with insects can harm penetration of electrical devices, causing a short circuit and resulting in a failure of the electrical system components.

Avoiding exposure to biological factors on the operation of any system (including AIMS) should be carried out at the level of organization by implementing the necessary measures and compliance with applicable sanitary and epidemiological rules. When measuring units are installed outdoors, their shells should be protected against the ingress of foreign objects.

Devices protection from power surges can be performed by special equipment which is designed to turn off automatically when the voltage changes and automatic switching-on after a specified period of time after the normalization of voltage. Voltage relays are used to protect electrical devices connected to the network from dangerous power surges. With all the harmful voltage changes (increase or decrease, abrupt or gradual) the relay will disconnect connected devices from the power source as long as the supply voltage returns to acceptable limits. [12]

Such surge protection can be used to protect individual nodes of AIMS against power surges caused by both technogenic and natural (lightning) reasons.

The easiest way to protect against malicious mechanical human intervention is physical limitation of access to the locations of nodes, node installation in hard-to-reach places. If AIMS' nodes are installed in the room, the best way of protection of these facilities is using door locks, installation of the components in a lockable mounting cabinets, etc.

However, these measures are not always able to prevent the physical access of intruders to AIMS' nodes. For example, the design features of water meters lead to their susceptibility to the effects of the magnetic field. An attacker is able to use a common magnet to affect the readings of the meter.

To protect nodes of AIMS from malicious magnetic effects, special shielding shells are usually applied, and sensors of the device are located at a maximum distance inside beneath the casing.

Well-proved counter sealing may achieved by usage of special capsule with magnetic fluid. In case of exposure to the magnetic field installed on the device, the liquid in the capsule shifted irrevocably, and readings from the damaged seal thus deemed invalid.

Another way to intervene into the integrity of AIMS is unauthorized connection to the communication channels between system components, which may cause serious system failure or data fraud. Usually this channel is a wired or wireless local area network. When

connected to a local network, which connects the nodes of AIMS, the attacker is able to gain access to the data transmitted between the nodes. [9]

In the case of a wireless network to improve safety should be used resistant-to-hacking encryption protocols and cryptography keys. In the case of a wired network the best way is to ensure the reliability of the data transmitted between the receiver and a data source, e.g., using encryption and digital signatures.

Also possible that an attacker gains access to data from outside. This unfavorable scenario is the most common for systems with client-server organization, as well as for systems that provide access to information through web interfaces.

Vulnerability of the system increases if it allows the remote access via the Internet, or the part of the data transfers between the individual components of AIMS via the Internet or cellular networks (very common in municipal telematics and navigational systems of ground transportation). In this case seems necessary to use the cryptographic protocols, which provide secure communication (e.g. SSL), and digital signatures. Effective method of protection is also restricting access to server-side system by filtering client IP-addresses, for example, by firewalls.

Malicious attempts to change the meters and counters, as well as attempts to gain unauthorized access, or in any way affect the information inside the AIMS, punishable under Article 159 of the Criminal Code of the Russian Federation — "Fraud".

How do the data transmitted and stored in the AIMS is of great importance. Let's take for example the case in which AIMS is an automated navigation system for supervisory control of ground transportation. An attacker, who gains access to the data transmitted within the system, can bring serious loss or damage to data, change the amount of over mileage cars, intercepting signals from alarm buttons installed in the interior of the car, etc.

If such a system provides the ability to control via a web interface and does not have an adequate level of information security, an attacker, who gains unauthorized access, may even physically harm the nodes of the system and the property of involved organizations.

Data transmitted and stored in AIMS may also reflect the financial condition of the organizations and commercial secrets. [8, 13, 14]

Getting unauthorized access to such information is punishable under Article 158 of the Criminal Code of the Russian Federation — "Theft".

AIMS protection from vulnerabilities and malicious human impact is relevant and challenging. To ensure an adequate level of protection, required a multifaceted approach in each case depending on the type of AIMS and the most likely and potentially dangerous adverse factors. In general, the task of protecting of these systems involves the use of special technical, technological, software and hardware solutions, and should be developed and implement as a set of measures to comply with the constitutive and legislative standards, rules and regulations.

References

1. Astashonok G.N. Fil'try s magnitnoj obrabotkoj vody [Filters with magnetic water treatment]. *Ehnergoehffektivnost' [Energy efficiency]*, 2003, no. 4, p. 10.
2. Bakhtyeva N.G. Rezul'taty issledovaniya vliyaniya na gryzunov ehlektrofizicheskix metodov [Results of the study of electrophysical methods impact on rodents], *Vestnik ChGAA [News of Chelyabinsk State Academy of Agroengineering]*, 2012. vol. 60, pp. 21-23.
3. Botvinkin P.V., Luk'yanov V.S. Avtomaticheskoe upravlenie parametrami potrebleniya ehnergeticheskix resursov na osnove poluchennoj statisticheskoy modeli [Automated management of energy resources' consumption based on statistical model]. *Izvestiya Samarskogo nauchnogo centra Rossijskoj akademii nauk [Proceedings of the*

Samara Scientific Center, Russian Academy of Sciences]. 2011, vol. 13, no. 4-4, pp. 1069-1071.

4. GOST 14254-96 (IEC 529-89). Stepeni zashhity, obespechivaemye obolochkami [Degrees of protection provided by enclosures].

5. Gusinskij A.V., Kostrikin A.M., Voroshen' V.A. and others. Informacionno-izmeritel'nye sistemy: Ucheb. posobie po prakt. zanyatiyam dlya stud. metrolog. i radiotexn. spec. vsex form obucheniya [Information-measuring systems Tutorial on practical training for students of metrological and radio engineering specialties of all forms of learning]. In 2 parts, Part 1. Minsk, Publisher: BGUIR, 2003, 40 p.

6. Kamaev V.A., Lezhebokov V.V. Razrabotka i primeneniye modeli avtomatizirovannykh sistem upravleniya informacionnymi processami k zadache monitoringa sostoyaniya oborudovaniya [The automation system of information processes model design and its application to the equipment state monitoring issue]. Vestnik komp'yuternyx i informacionnyx tekhnologij [Bulletin of computer and information technology], 2009, no. 9, pp. 18-22.

7. Kamaev, V.A., Natrov V.V. Analiz metodov ocenki kachestva funkcionirovaniya i ehffektivnosti sistem zashhity informacii na predpriyatiyax ehlektroehnergetiki [Analysis of methods of assessment of functioning quality and efficiency of information security for electricity companies]. Izvestiya Volgogradskogo gosudarstvennogo tekhnicheskogo universiteta [News of Volgograd State Technical University], 2007, no. 1, pp. 74-76.

8. Kamaev V.A., Natrov V.V. Metodologiya obnaruzheniya vtorzhenij [Intrusion Detection Methodology]. Izvestiya Volgogradskogo gosudarstvennogo tekhnicheskogo universiteta [News of Volgograd State Technical University], 2006, no. 4, pp. 148-153.

9. Kamaev V.A., Natrov V.V. Modelirovanie i analiz informacionnoj bezopasnosti organizacii [Modelling and the analysis of the condition of information security of the organization], Zashhita informacii. Insajd. [Information Security. Inside.], 2009, no. 4, p. 16.

10. Kamaev V.A., Shcherbakov M.V., Brebels A. Intellekturnye sistemy avtomatizacii upravleniya ehnergobezbezheniem [Intelligent automation systems for energy consumption control]. Otkrytoe obrazovanie [Open Education], 2011, no. 2-2. — pp. 227-231.

11. Kamaev V.A., Shcherbakov M.V., Brebels A. Sistemy avtomatizacii upravleniya ehnergobezbezheniem [Automation systems for energy consumption control]. Otkrytoe obrazovanie [Open Education]. 2010, no. 2, p. 227.

12. Ltd. «UKRRELE». Ustrojstva zashhity ehlektropriborov ot perepadov napryazheniya [Devices for protection against electrical surges]. Available at: <http://www.ukrrele.com/devices-protection.htm>

13. Nguen D.X., Kizim A.V., Kamaev V.A., Bykov D.V. Povyshenie nadezhnosti ehkspluatatsii programmno-informacionnykh sistem ehlektronnogo dokumentooborota putem primeneniya specializirovannykh algoritmov zashhity [Increasing reliability of software and information systems electronic document management by applying specialized security algorithms]. Izvestiya Volgogradskogo gosudarstvennogo tekhnicheskogo universiteta [News of Volgograd State Technical University], 2011, vol. 11, no. 12, pp. 144-147.

14. Shcherbakov M.V., Kamaev V.A., Shcherbakova N.L. Metodika resheniya zadachi identifikacii dinamiki sistem na korotkix intervalax nablyudeniya s primeneniem konnektivistskix modelej [Connectionists systems framework for dynamics identification on the short observed period]. Izvestiya Yuzhnogo federal'nogo universiteta. Tekhnicheskie nauki. [News of Volgograd State Technical University. Technical Science.], 2012, vol. 126, no. 1, pp. 72-77.

15. Tyukov, A., Brebels, A., Shcherbakov, M., Kamaev, V.: A concept of web-based energy data quality assurance and control system. ACM International Conference Proceeding Series. 2012. pp. 267-271.

16. Tyukov, A., Ushakov, A., Shcherbakov M., Brebels A., Kamaev V.: Digital signage based building energy management system: solution concept. World Applied Sciences Journal. Issue 24 (Information Technologies in Modern Industry, Education & Society). pp. 183-190.

MEDICAL ASPECTS OF RESEARCH GUNNER'S HEALTH

Mironova A.S.

Penza, Penza State Technological University

Work is devoted to the identification of health parameters affecting the result of his firing and methods for their study.

Keywords: stabilometry, center of pressure, the common center of mass, multidagnostic system biofeedback, athletes, methodology, sample.

Professional gunners must have specific psychological and physical training to be effective in workout. Many factors affect to the health of athlete. This article discusses the medical records specific to this sport like gunning. Let's consider the medical aspects of training gunners more amply.

Certainly an important factor affecting the stability and, consequently, on the effectiveness of training and shooting of sportsman, is a psychological condition of the athlete. Stress levels, or rather, the degree of control over their psychological state, just determines exercise performance and accuracy of the athlete.

Pulse dynamics and the degree of humidity of the palm (sweating) of athlete can be considered as an indicator of the level of stress.

The most important aspect needed to succeed in this sport as gunning is stability while maintaining a certain body positions.

During the centuries of human evolution one of the most efficient and resistant to the destructive factors of dynamical systems has formed - functional system antigravity (FSA), in which the activities of vestibular mechanisms play a leading role. People in the first hours of its prenatal development exists in terms of the gravitational field of the Earth. [1]

There is science, which study mechanisms for maintaining vertical posture in health and development of several pathological conditions, and also compensatory mechanisms involved in the regulation. Name of this particular area of human knowledge is posturology (latin postura - pose). Highlight the relevance of the medical and biological areas into a science proves the existence of several associations in the posturology particularly authoritative Association française de posturologie [2].

Holding vertical pose of the person is accompanied by its micro oscillating (in comparison with the size of a man) process, which is very rarely noticeable by visual observation of the natural act of a comfortable state. There are fairly complex harmonic oscillations as a common center of mass (CCM) and the center of pressure (CP) feet to the bearing surface, which due to objective circumstances are not the same amplitude and phase character.

CP - is an integral point on the supporting plane, which surround a geometric body - man, having first a different density of body tissues and, secondly, not installed as unbending direct beam, but is constantly changing in the joints of the body mutual configuration its

segments, like "averaged" in real time during maintaining its vertical rack. Thus, we emphasize that the CP is not a mapping human CCM projections to the bearing surface and oscillatory processes CCMs and CP are not identical (their identification - a common mistake made by many doctors). Common property of the CP and CCM projections stable standing (not falling) is the only person that they are located within the boundaries of the support of human origin (eg, iambic triangle).

Statokinezimetriya (stabilometry) - a method for qualitative and quantitative analysis of the oscillatory process in the plane CD supports a vertically mounted or that is used less often, a sitting person. The method is used to assess the function of balance and mechanisms for maintaining human upright posture - both in normal and in various pathological conditions. Preferred is recognized in the world scientific literature, the term statokinezimetriya (literal transcript - measurement of human movement, i.e. oscillatory process CSD inevitably arise during their static security man, arbitrary maintain upright posture). [3]

To investigate the athletes used multidagnostic system with biofeedback (figure 1).



Figure 1. Multidagnostic system with biofeedback (photo department ITMMBS PSTU)

The system supports to work in the programming mode, with the help of which was made up of individualized assessment methodology functioning of the postural system.

In this technique includes a phased over 10 samples: samples with open and closed eyes, the sample turns from the right and left eyes at 30°, the sample with head rotation to the right and to the left by 60°, the sample with the torso turns to the right and to the left by 30°, sample on a soft mat on a rigid surface and with the rise angle of the foot with a different angle of inclination, etc.

Express information after the examination for a doctor is a protocol containing graphics dynamics area of an ellipse, as a function of equilibrium in %, severity of fluctuations in the frontal and sagittal planes, as well as 9 coefficients postural system:

- Romberg coefficient to estimate the role of vision;
- plantar coefficient evaluating the role of the feet;
- temporomandibular coefficient evaluating the role of the temporomandibular joint;
- two coefficients of rotation of the eye;

- two coefficients turn heads;
- two coefficients turn of the trunk .

Last three pairs of coefficients reflect respectively function proprioceptors eyes, neck and lumbar spine [4].

Thus, the use of stabilograph heart rate monitor sensor and sweat as well as a comprehensive methodology primeneneiem operate the equipment and interpret the results of consultations with a psychologist and general practitioners to help professional athletes and their coaches to watch the body as an arrow behaves before during and after the shot, draw conclusions and adjust the training process , achieving the desired results.

References

1. Napalkov D.A., Ratmanova P.O., Kolikov M.B. Apparatnie metody diagnostiki i korrektsii funktsional'nogo sostoyaniya strelka. –M.: MAKSS Press, 2009. – 212 s.
2. Shestakov M.P., Shelud'ko E.A., Abalyan A.V., Fomichenko T.G. Issledovanie koordinatsionnoi struktury sportsmenov v vidakh sporta s assimichnym vypolneniem dvizheniya, Izvestiya YuFU. Tehnicheskie nauki. Tematicheskii vypusk "Meditsinskie informatsionnye sistemy". – 2010. – № 9. – С. 174-178.
3. Dotsenko V.I., GU Nauchnii tsentr zdorov'ya detei RAMN, Nauchno-meditsinskaya firma "Statokin", Moskva
4. Sliva S.S., Voinov I.D., Sliva A.S. Stabiloanalizatory v adaptivnoi fizicheskoi kul'ture i sporte, ZAO "OKB "Ritm", g. Taganrog, Russia

CREATE A CLOUD DATABASE IN A PRIVATE DATA CENTER USING WINDOWS AZURE PACK

Miroshkin V.M.

*Saratov socio economic unstitute branch Russian economic university G.B. Plekhanov,
Saratov*

Cloud platforms are gaining immense popularity among developers of applications, technical specialists and companies seeking to reduce their costs. Windows Azure Pack an open and flexible cloud platform that enables you to quickly create, deploy, and manage applications in a private data center (PDC).

Keywords: Windows Azure Pack, cloud database, MySQL in the cloud

Operating system Windows Server 2012 R2, based on the concept of the Microsoft Cloud OS allows you to create and provide global services in the cloud containing new features for virtualization, management, data storage. Despite the basis Cloud OS Windows Server 2012 R2 provides the ability to manage cloud services in Windows Azure. For these purposes the company Microsoft developed the Windows Azure Pack.

Windows Azure Pack unfolds in Windows Server 2012 and allows you to get a set of technologies in Windows Azure without additional investments. Windows Azure Pack imposes no restrictions on use and connection to the database is physically located on different servers as Windows and Linux servers. Using a cloud-based database gives the opportunity not only flexible scaling, but also the transfer of data with both desktop and mobile applications.

The purpose of the work - unwrapping own cloud-based storage that is running Windows Server 2012 using Windows Azure Pack. This technology is a new product from Microsoft which allows to produce a functional fully similar to Windows Azure.

Based on the technical specifications cloud storage must be distributed MySQL database to store user data, ratings and pictures downloaded from the app running a Windows operating system Windows Phone.

Before you deploy Windows Azure Pack, you need to prepare the working environment Windows Server 2012 R2. To do this, install the components for Windows Server: Microsoft .NET Framework 3.5 Service Pack (SP) 1, .NET Framework 4.5 Extended with ASP .NET Windows 8, Microsoft Web Platform Installer 4.6. The next step is to configure IIS 8.0 and SQL Server 2012 for user portals, portals management for administrators clouds and usage portal. Then install and configure MySQL Server for Windows that after installing the Windows Azure Pack connect MySQL database as a cloud.

After you install and configure all the above components, you can proceed to install Windows Azure Pack. This requires the browser to jump at localhost:30091 and in the immediate window, the configuration of the Windows Azure Pack enter data SQL server: the address of the server name, database name, database administrator password, required to keep accounts of administrators and users of Windows Azure Pack.

After installing Windows Azure Pack in addition to the portals of the administrator and users become available: provider connection MySQL, SQL, website setup and configuration.

The portal administrator can manage the users of the cloud, and cloud services. Database services are used cloud storage that can connect to the MySQL database, SQL located on different servers running both Windows Server and Linux. Services of cloud storage services allow you to manage connections, monitoring and scaling databases like MySQL and SQL.

Above described algorithm installation and configuration was used for the deployment of private data processing and storage center SSEU REU them. G.B. Plekhanov. Uses a database to store user data, ratings and pictures. The database currently contains over 6000 unique records.

We developed and integrated into a private cloud MySQL database. The database will provide a high data access rate and flexible scaling as necessary. Cloud MySQL database provides high reliability, thanks to the automatic backup to the other server. The stability of the database is provided by technology, Cloud OS is Windows Server 2012 R2, and Windows Azure Pack expanded the possibilities of cloud services. So, Windows Azure Pack has allowed not only to solve the problem, but also to get practical experience deploy to the cloud resources in a private data center.

INCREASING THE PRECISION OF METROLOGICAL CHARACTERISTICS OF SMART SENSORS IN LARGE SCALE MONITORING SYSTEMS

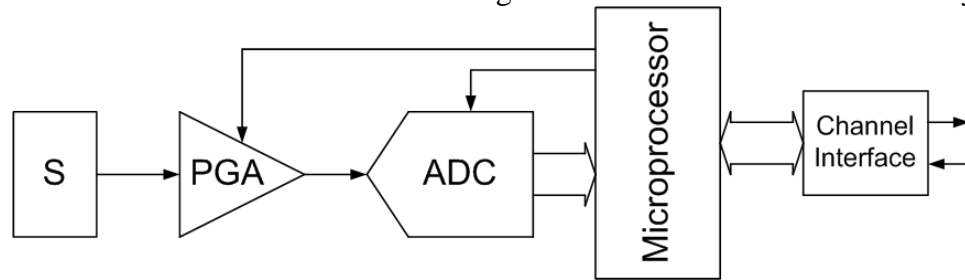
Mixeev M.Yu., Yurmanov V.A., Kuts A.V., Piskaev K.Yu., Volodin K.I.
Penza State Technological University, Russia

The article considers the questions of increasing accuracy of smart sensors. There was carried out a comparative analysis of schemes of normalization of signals with auto-correction of the bias voltage and methods of weight integration.

Keywords. Smart sensor, weight functions, offset voltage of amplifiers, auto-zeroed amplifiers, analog-to-digital converters.

Modern monitoring systems are based on smart sensors (SS). Simplified structure of smart sensor is shown in Figure 1. Smart sensor usually consists of the sensor (S),

programmable gain amplifier (PGA), analog-to-digital converter (ADC), control device (often microprocessor based) and the channel interface. Smart sensors generate the required amount of measurement data that is used in decision-making about the state of the controlled object.



S – sensor; PGA – programmable gain amplifier; ADC – analog-to-digital converter

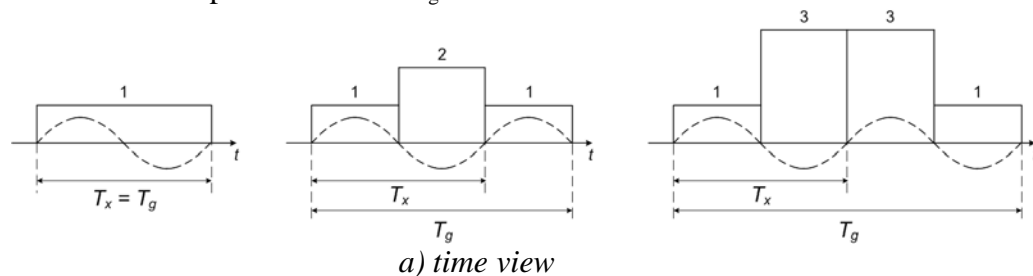
Figure 1 – Smart sensor simple structure

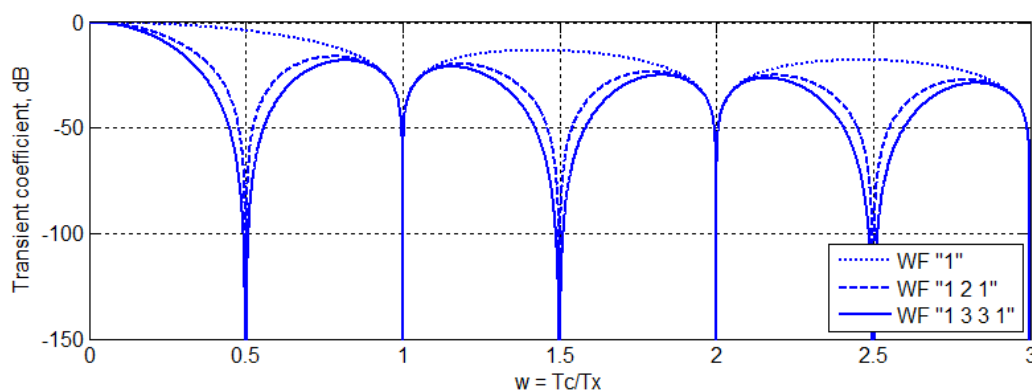
The particular realization of process of analog-to-digital conversion allows to receive higher metrological characteristics by removing extended lines of communication between the sensor and ADC. That is performing by means of microprocessor operations, such as calibration and considering the influence of environmental parameters on the characteristics of the smart sensor, also reducing the load on the communication channels.

Next, consider the solution to this problem on the example of the use of an ADC integrating type (IADC). Currently, these ADCs achieved the highest conversion accuracy: sigma-delta ADC ($\Sigma\Delta$ -ADC) have more than 20 bits [2].

Smart sensors adaptation to different requirements of "precision–performance ratio" is implemented by simply changing the time of conversion. Increased accuracy in 2 times, usually leads to a decrease in performance during the same time. Obvious is the desire to control this criterion more efficiently. The accuracy in the future, we will understand the closeness of the measured numerical values obtained to the true values of the measured value [1]. In addition, we will not consider the metrological characteristics of primary sensors (Fig.1) and communication interfaces characteristics. Additional limiting factor in the analysis, we assume an additional amount of computational resources of smart sensor.

The analysis showed that the area of solving the problem is limited to the theory and practice frequency response function (FRF) form transformation of PGA and IADC. Implementation of the known methods IADC with the necessary frequency properties best meets the constraints posed weighting method of integration. For example, the use of weight functions (WF) of the form «1», «1 2 1», «1 3 3 1» (Fig 2a) and etc. improves the inhibition of the variable components of the input signal to the 38, 56 and 90 dB, respectively [3]. Figure 2b shows the frequency response of the weighting functions of the form «1», «1 2 1» and «1 3 3 1», which the relative frequency corresponds the ratio of period of WF T_g to the period of the variable component T_x : $w = T_g/T_x$





b) frequency response
Figure 2 – Weight functions

However, the PGA circuit needed to align the sensor outputs with IADC impose a limit on the accuracy of smart sensor. Requirements for this circuit defined field of application, but there are several major - high input impedance, low current, high CMRR, low temperature drift (current and voltage). Effect of temperature component parameters need not be considered, as it is slowly varying size and is easily corrected. There remain only the parameters which depend on the input signal - this is the noise level, and its main component - the offset voltage variation of the input signal.

One of the main ways to reduce the offset voltage of amplifiers are circuits with automatic correction. An example is the series AD8553, AD8555, AD8556, AD8557 Analog Devices [4]. Consider the features of automatic correction schemes use the example of the instrumentation amplifier AD8555. Model AD8555, designed for measuring systems based on a bridge circuit, such as a pressure measuring system [4]. This IA is built on a three operation amplifiers and has a scheme for automatic bias correction.

“Auto-zeroed” technology minimize input offset errors. According datasheet offset voltage value does not exceed the 10mV at temperatures ranging from -40°C to $+125^{\circ}\text{C}$. Input offset voltage drift - 65 nV/ $^{\circ}\text{C}$. Detailed description of the amplifier with automatic zero correction can be found at the Analog Devices official website [4].

As a disadvantage manufacturer specifies that by operating the electronic switches in the circuit takes charge of the capacitors and a number of other effects which result in the occurrence of impulse noise on the internal clock frequency and its harmonics. These noises are large compared with its own wideband noise amplifier and may be a source of error, if they fall in the information signal bandwidth. These disturbances may cause intermodulation distortion signal, whereby the output signal components appear at frequencies equal to the sum and difference frequencies of the signal and the compensation circuit. In practice, a slight difference in the gain of the amplifier in different phases offset compensation leads to the fact that the gain in a closed feedback circuit is changed by a small amount with the clock frequency. The magnitude of intermodulation distortion depends on this small difference in gain, and has no direct relationship to the noise generated by an clock. Intermodulation and harmonic distortion products typically from -100 dB to -130 dB relative to the signal in a closed feedback loop, significantly less than the values corresponding to the accuracy of 20 bits. Therefore, to suppress the specified distortion necessary to form frequency response of the integrating ADC in consideration of the distortion of this implementation PGA.

Further instrumental errors as described, there are errors arising during use of the chip in the schemes. In real circuits noise that creates elements at work is broadband, in order to understand its impact on the operation of this scheme we use the following reasoning.

Assume that used ideal op amp offset voltage which is equal to zero. Therefore, it is necessary to consider only the signals caused by the above reasons. From the theory of

spectral analysis of known, that power spectral density can be represented as a Fourier integral of the correlation function of the random process (as an expansion of a random function on an infinite sum of elementary harmonic oscillations with a continuous spectrum).

Figure 3 (top) shows the harmonic component and its discrete values taken at a frequency correction FK equal to the frequency of the harmonic. It is seen that as a result of the correction process of the spectrum component is transferred to the zero frequency value.

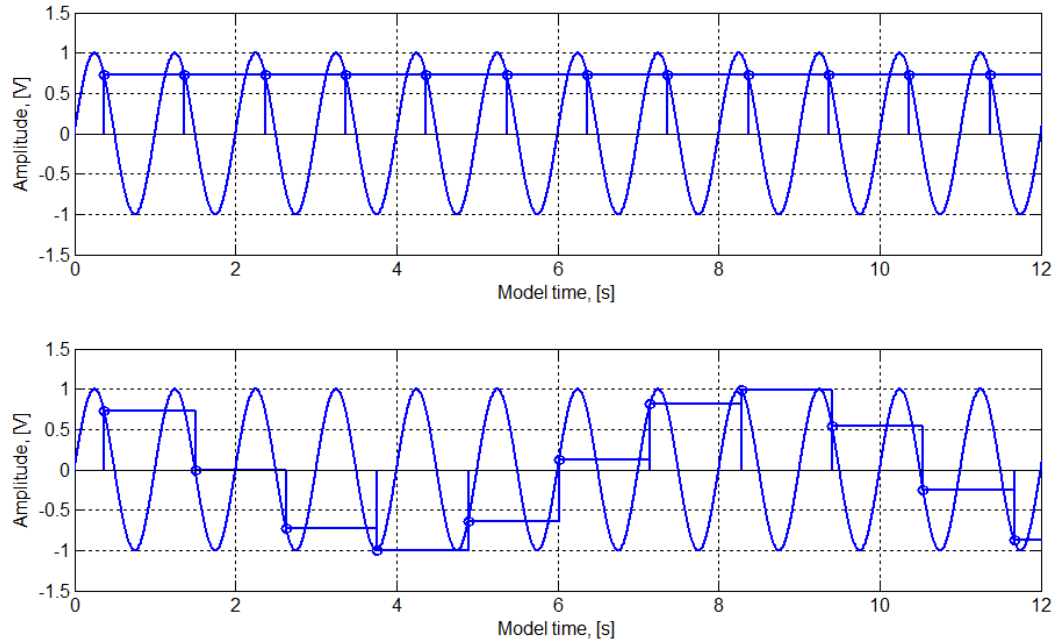
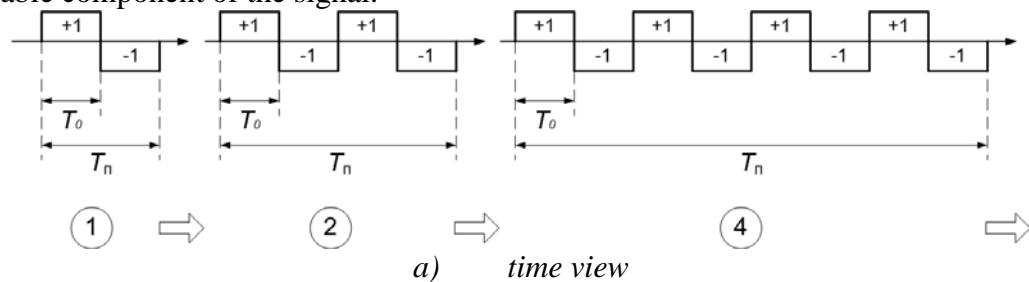


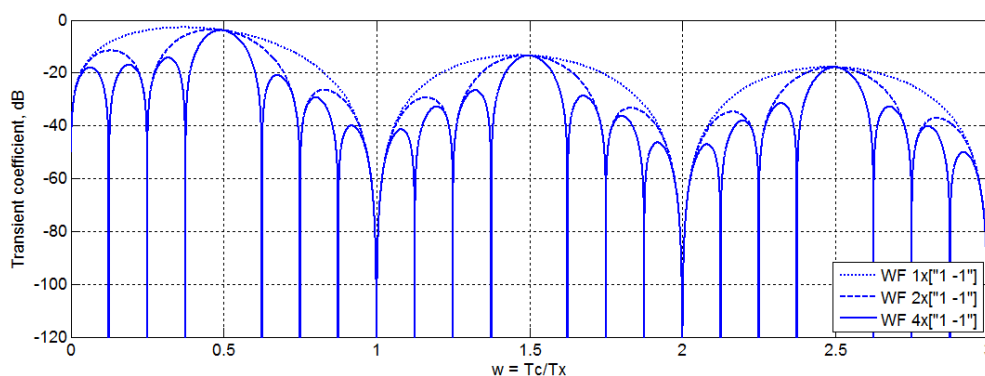
Figure 3 – Sampling process of the signal harmonic components

This phenomenon is known as the aliasing effect, some sources it is known for mimicry frequencies. Thus, the spectral components of a random process, multiples of the frequency correction will be moved to the zero frequency, then there will be a constant offset. Figure 3 (bottom) shows the process of a harmonic component whose frequency is slightly lower than the frequency correction. It can be seen that in this case, a correction process generates in the output signal spectrum of the harmonic component.

Consequently, there are additional sources of error in the PGA, the occupied bandwidth of the desired signal, which significantly increases the amount of computational resources required for further processing conversion. This is the major drawback of the method of correction for instantaneous values. Thus, the automatic correction amplifiers do not satisfy the requirements for accuracy.

Another well-known [3], and the authors believe more promising by increasing the precision not only the PGA and SS in general, is the use of WF type shown in Figure 4a. This class WF theoretically allows the complete suppression of permanent and partial suppression of the variable component of the signal.





b) frequency response

Figure 4 – Internal noise suppress weighting functions

To this type of frequency response applied to its own noise conversion tract, and for the useful signal frequency response would have the form corresponding to Figure 2, it is necessary to implement specified in Figure 4a WF in PGA. Theoretically it is possible to implement only two ways.

In the first way should be implemented WF "+1-1" consistently in the PGA and IADC. In this case, a useful input signal modulated in accordance with the coefficients WF will be restored in by IADC demodulating same coefficients, which is equivalent to the implementation of the WF type "1". The internal noise of the elements in this case should not be subject of the first modulation.

In the second way, the implementation of WF "+1-1" PGA carried internal noise elements modulation base and WF for IADC should be as shown in Figure 2.

In the first variant, the accuracy of reference weighting coefficients directly determines the efficiency of the process. To ensure the accuracy of the converter is not worse than 20-bit accuracy at the coefficients must be at least 6 significant digits. In the latter case, the requirement for precision tasks weighting coefficient decreases by a factor equal to the ratio of maximum values of the input signal and the inherent noise.

The task of implementing PGA transmission coefficients "+1-1" with great accuracy is very difficult. All existing schematics, starting from [7] and discussed above to IA AD8555 require switching elements in the input circuit and ensure the independence of the values of the intrinsic noise of the input values. As an example, Figure 5 shows the dependence of the offset voltage of the operational amplifier. Is seen that variations in the bias voltage over a range of changes comes to 17uV.

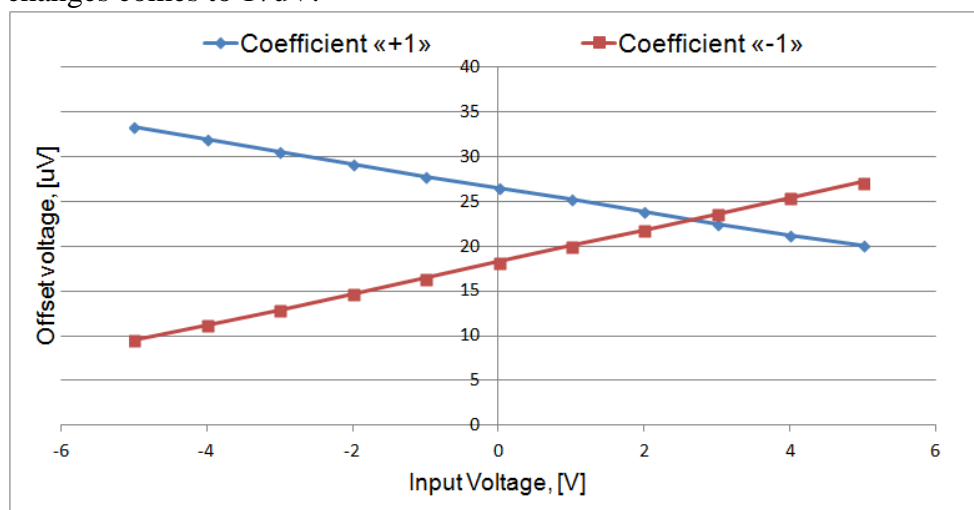


Figure 5 – Offset (bias) voltage vs input voltage for OP37 opamp PSpice-model

Thus, the construction of precision smart sensors with accuracy more than 20 bits is limited metrological characteristics known schemes PGA based on the Op Amps. The analysis showed that the construction of the PGA based on current amplifiers with automatic correction does not provide these characteristics. Known WF coefficients "+1-1" theoretically allows for perfect interference suppression internal noise elements. Of technology to achieve the required accuracy at the coefficients, but all existing schematics have a size according to the values of the internal noise of the input signal is much larger than the quantum of 20 bit ADC.

Consequently, the formation of a more effective exchange of accuracy performance smart sensors associated with a particular solution of the problem of creating a corresponding analog structures PGA.

References

1. Ornatskiy P.P. (1983). *Tekhnicheskie osnovy informacionno-izmeritel'noy tekhniki*. Kiev: Vischa shkola. Golovnoe iz-vo. (in Russian)
2. Kester U. (2007). *Analog to digital conversion*. Moscow: «Tehnosfera». (in Russian)
3. Shahov E.K., Mihotin V.D. (1986). *Integriruyushchie razvertyvayushchie preobrazovateli napryazheniya*. Moscow: Energoatomizdat. (in Russian)
4. Analog Devices: official website datasheets and appnotes. <http://www.analog.com>
5. Gromkov N.V. (2009). *Integriruyushchie razvertyvayushchie preobrazovateli parametrov datchikov sistem izmereniya, kontrolya i upravleniya: monografiya*. Penza: Penza state university press. (in Russian)
6. Shahov E.K. (2006). $\Sigma\Delta$ -ACP: Processy perediskretizatsii, sheypinga shuma kvantovaniya i decimatsii. *Datchiki i sistemy*, vol 11., p. 50 - 57.
7. Horovic P., Hill U. (1981) *Iskusstvo shemotekhniki*. (in Russian)

MODERN STATE OF THE PROBLEM OF THE DEFINITION OF THE DISEASE AS A RESULT OF THE VIOLATIONS OF ADAPTATION

Kulikova, O. A.

Penza State technological University (Penza, Russia)

In this work the problem of determining the current status of the disease resulting from the violation of adaptation to endogenous and exogenous factors. Analysis of influence of external and internal factors on the live system, in particular, assessment and monitoring of physiological, immunological and biochemical parameters identify a possible methods of diagnostics and prognosis of the disease.

Keywords: methods of diagnostics, immunological and biochemical parameters.

Of particular interest for biology and medicine, is the study of living systems under the influence of exogenous factors, the study of which is one of the important clinical problems. Numerous clinical observations and experimental data analysis of violations of the functional systems of the body to treat hypertension and its complications have developed and offer methodological approaches to assessment of adaptational possibilities of the organism.

Objective: to study the problems of a disease as a result of the adaptation of violations to research adaptive and homeostatic mechanisms of functional systems of the organism.

The criterion of optimization of adaptation is considered persistence or minimal changes vitally important parameters in a limited number. Consideration of the specific physiological, immunological and biochemical systems of the body suggest ways to assess the severity of the condition and prognosis of the pathological process.

Allocation of external and internal factors leading a living system in a state of illness, allows to describe and analyze functional (reversible) and organic (irreversible) changes.

The disease is always the result of disruption of the normal regulation of functions by the regulatory mechanisms at the cellular, molecular, organ - system or organismal levels.

At the present stage of studying the mechanisms of adaptation at pathological conditions deal with methods of evaluation of adaptational possibilities of the organism from the point of view of the impact of external or internal factors.

In this regard, the main requirement for the conduct of biomedical research studies are:

- proper organization (study design) and mathematically grounded way to randomization;
- clearly marked and travellers comply with criteria of inclusion and exclusion of studies;
- the correct use of statistical methods of data processing.

Etiological factors of development of the severity of the condition are hypoxia, intoxication disorders and immune conflict. This creates prerequisites for the development of violations of systems of regulation of immune-biochemical metabolism. It is known that the adjustment processes require changes in the level of metabolic reactions. In particular, it is known that, with the development of hypertension of II-III degree is the activation of neutrophilic leukocytes, macrophages and other cells that can produce antibodies and their synthesis of the neurotransmitters. Development of autoantibodies to regulatory peptides is a complex multicomponent system, which is a universal adaptive system of the body: it prevents damaging action of neurotransmitters and their metabolites, providing them with linking and modification, preventing their devastating impact on the body's cells and their membranes. It is known that the formation of autoantibodies to the neurotransmitters and the degree of regulation largely determines the transition irreversible change in irreversible and adaptive changes in pathological. Each phase synthesis of antibodies corresponds to the mechanism of regulation. Thus, the interlinking of the changes in the processes of synthesis of antibodies to the neurotransmitters can determine the degree of adaptation to internal and external factors.

Therefore, the methodological approaches to the assessment of adaptational possibilities of the organism in terms of environmental damage (environmental damage is the damage to the environment, expressed in physical units of measurement. For example, the amount of pollutants entering the environment; the number of permanently the natural resources used and so on must be based on perceptions of the General mechanisms of adaptation (adaptation) of living systems to extreme conditions.

Study of autoantibodies to the neurotransmitters in the blood serum of patients with essential hypertension important for the objective evaluation of the adaptive forces of the organism.

Standardization estimation of the patient severity condition is required in forecasting the course of pathology, for which reveal the adaptive capacity of the body based on the analysis of clinical and laboratory control from the point of view of system approach. When laboratory control use the required set of laboratory tests for monitoring the systems of organism functioning, based on the results of laboratory analysis.

However, General principles for the evaluation of adaptive opportunities of an organism based on the requirements for the conduct of biomedical research, denoting practice properly organized by clinical trial, based on the approaches of system analysis. Assessment

of the level of functioning of system of blood circulation can be done according to performance criteria that divide the indirect and direct. To direct the performance criteria include recovery, reducing mortality, morbidity, quality of life improvement. Indirect criteria reflect the positive change in any of the examined parameters such as the normalization of blood pressure, reduction in blood levels of urea, creatinine, enzymes, etc.

Standard assessment of the degree of severity of patients is needed in forecasting the course of disease in patients with cardiac pathology using the required set of laboratory tests and, accordingly, the results of research. For the diagnosis and prediction of the severity of the condition in hypertensive patients it is important to study systems of the natural detoxification of the organism, in particular serum components, capable to neutralize products increased synthesis of regulatory peptides - natural antibodies to them. It is assumed that autoantibodies contribute to capture and removal from the body products of cellular metabolism and are capable to transport functions.

A solution of the urgent medical-social problems related to evaluate the immune status of the formation of risk groups, diagnostics, treatment and prevention of hypertension, associated with the development of new methods of the analysis of immune-biochemical adaptations of functioning of systems of blood circulation.

Fundamental research on the border of immunology and medicine revealed that under pathology of any genesis is a disturbance of the functioning of the immune system. found new diagnostic markers, reflecting the initial stages of the development of hypertension and the formation of its complications. The possibility of using new methods of enzyme immunoassay for the determination of natural antibodies to the neurotransmitters in practical medicine in this category of patients. this method can serve as a method of definition of natural antibodies in biological fluids.

For the evaluation of the immune status of the results obtained using this method, you can:

- conduct diagnostics of pathological changes in the human body;
- conduct early diagnostics of existing or only beginning diseases;

Supplement the received analytical data of clinical and biochemical parameters and the level of cells of the immune system, that will allow to receive more complete information about the immune status of an organism of the patient; evaluate and adjust clinico-laboratory diagnostics of the patient; to offer the individual program of patient examination.

To identify the most informative qualitative and quantitative characteristics of the used methods of research evidence. In biology and medicine one of the main methods of research evidence is mathematical modeling. under the mathematical model is the relation between multiple variables, expressed in the language of the different equations and their systems. At a pathology of cardiovascular system mathematical modeling is used to predict the severity of the state of development of possible complications functional systems of the body. Theoretical model to results of clinical and laboratory monitoring of.

Technology mathematical modelling in medicine allows to objectify the choice of indicators to assess the severity of the condition and treatment outcome of the patients. it includes the following stages :

- development of a specialized database, necessary for formation and accumulation of information about patients to solve a particular task;
- selection and ranking of informative parameters; obtaining of a number of mathematical equations that describe the relationship between parametric criterion status (outcome) and a set of the most informationally significant indicators;
- selection of the optimal equation and checking it out on an independent sample; the decision of actual research problem by comparing the calculated (projected) source of disease (condition) with the real. evaluation of the efficiency of the diagnostic and treatment methods.

Of particular interest for biology and medicine is modeling of living systems in extreme conditions, that allows to more adequately assess the dynamics of the severity of the patient and to predict the outcome of the disease in the process of clinical and laboratory monitoring.

In ecology and medicine under extreme conditions understand the impact of external factors that translate a living system in a critical state, the study of which is one of the relevant clinical problems.

For survival in the critical conditions of living system, to adapt, to organize, mobilize, that requires changes in the level of metabolic reactions of the organism. Therefore the mathematical model should be based on perceptions of the general mechanisms of adaptation (adaptation) of living systems to extreme conditions.

The criterion of optimization of the body is considered persistence (homeostasis) or minimal change a limited number of vital parameters.

Conclusion: consideration of specific physiological, immunological and biochemical systems of the body, as well as calculation of external and internal factors leading a living system in extreme condition to describe and analyze functional (reversible) and organic (purchased, the change of the living system and possible ways of its diagnostics and prediction.

References

1. N.N. Belyaeva, Cyto - histological criteria of risk of development of ecologically caused diseases. Hygiene and sanitation, 5 (2006), 17 - 19.
2. V.L. Gaponov, Review of adequacy of model of dispersion of harmful substances in exhaust gases of automobiles. Ecology and industry of Russia, 11 (2007), 30 - 31.
3. A.A. Gromov, M.V. Kruchinina, Innovative technologies in the prevention of cardiovascular disease. Proceedings of the III National Congress of physicians, M, Ed. «Bionics», 2008, 59 - 60.
4. N.Y.Kelina, V.V. Pikulin, T.Y. Mamelina, O.A. Kulikova, The methodology of the evaluation of patients with cardiac pathology on the basis of immune-biochemical analysis with regard to ecological background of the region. The Technology of living systems, (7) 2012, 65-69.
5. V.N. Titov, Fundamental medicine. Unity of physical chemistry, methods of General biology and medicine in determining the etiology and pathogenesis of diseases of the person. Clinical laboratory diagnostics. 1 (2005), 3 - 8.

PROCEDURE FOR CREATING DATABASE PARTITIONON THE CHARACTERISTICS OF RELIABILITY OF MECHANICAL ELEMENTS

Monakhov M.A.

Moscow, NationalResearchUniversity“Higher School of Economics”

The issues of the development of data bank on the base of characteristics of reliability of mechanical elements for the system ASONIKA-K-SCH are studied in the research. The procedure of working up of data bank section by DBCS Oracle is described in the study.

Keywords: radio electronic equipment, reliability, mechanical elements, data bank, ASONIKA-K.

This study (research grant № 14-05-0038) supported by The National Research University - Higher School of Economics' Academic Fund Program in 2014. The effect of

mechanical elements (ME) is not taken into account in assessing reliability in radio electronic equipment (REE) in the currently accepted techniques[1]. American Standard NSWC-11[2] contains mathematical models of failure rates of ME, which form the basis of the development of the database section of the system ASONIKA-K-SCH on the base of characteristics of reliability of mechanical elements.

Oracle is used as a database control system (DBCS) in the system ASONIKA-K, so the same DBCS is used when the section of characteristics of ME reliability is developed. Detailed description of the database of the system ASONIKA-K is given in [3,4].

Section structures of database are universal and allow you to add various guides and standards. Database tables contain parameters, symbols and keys to have a link with the main table. The data sets are often repeated, so each set of data in the table has a unique identification number that allows you to save data volume of tables.

Database section is developed to assess the reliability of ME, with the help of which failure rates of mechanical elements will be set. Detailed description of the section structure is given in [5,6].

Database section with ME also has a number of tables, which are common to all classes. This is due to the fact that a number of application parameters and empirical coefficients are repeated for different classes of ME. The table of conversion rates is common to all classes of ME that are based on the standard NSWC-2011[1], as the standard is written in the American system of measures, and the system ASONIKA-K-SCH focused on the user working in the SI system.

Another feature of the database is the independence of the tables of different classes of ME from each other. That means when the data or the table structure of one class are changed, tables of other classes remain unchanged. Obviously, in this case the number of ME classes stored in the DB is almost unlimited and DB can be expanded to any number with the appearance of new classes of ME[3,4]. Example of the database structure of class ME “Filters” is given in [7].

The structure of each class is constructed depending on the mathematical model of failure rate. For example, the failure rate model of the class “Filters” has the form:

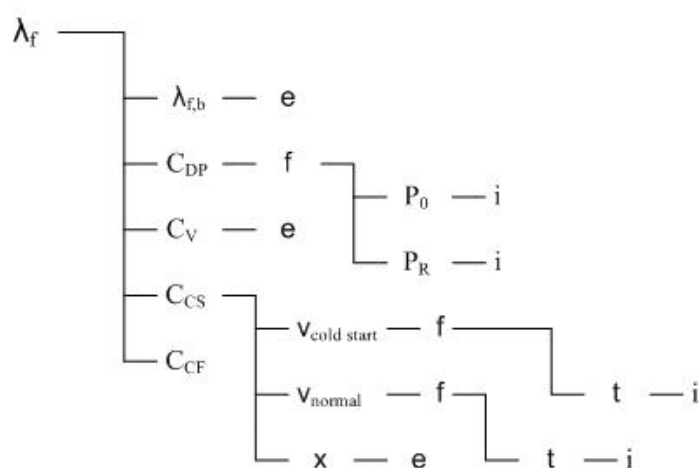
$$\lambda_f = \lambda_{f,b} \cdot C_{DP} \cdot C_V \cdot C_{CS} \cdot C_{CF}, \quad (1)$$

where: CDP is correction factor of pressure; CV is correction factor of the instrument cluster; CCS is correction factor of the effect of the liquid viscosity; CCF is correction factor of the pore size of the filter element and the cyclic rate of flow.

Each correction factor is either contained in the database, or is based on a formula, factors of which are either contained in database or are entered by the user, and in some rare cases have their own formula. Therefore, all data necessary for calculation, are divided into three groups:

- The group of e - factors which are contained in the database
- The group of f - factors which are calculated by the formula
- The group of i - factors that the user enters.

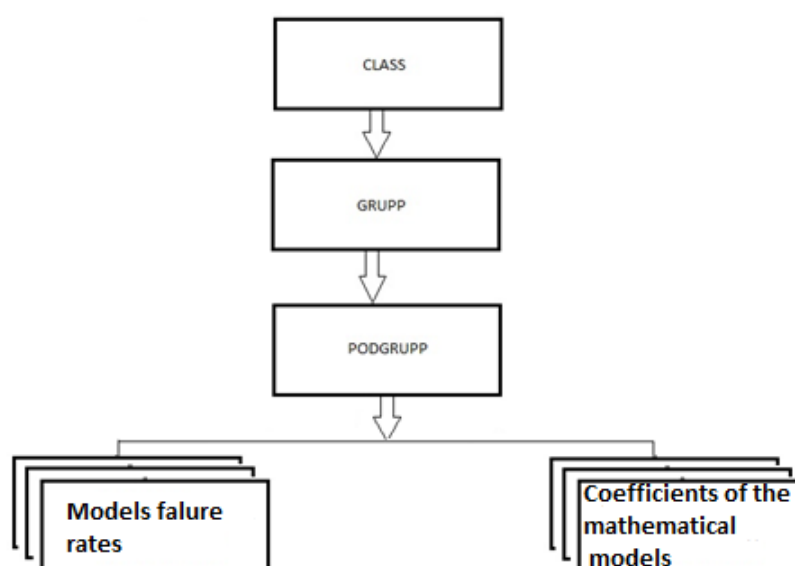
The tree of all factors of this class is created, which is based on the classification above (picture 1).



Picture 1 – the tree of factors of the class “Filters”

The tables of the class included in database system are created on the base of “The tree of factors” (picture 1).

The DB tables have a clear hierarchy (picture 2).



Picture 2 – Hierarchy of DB tables

A list of all classes of the components used in the REE compiled in the main table «CLASS». This table shows strict conformity of component class name with its serial number, which is the main part of the class hierarchy in REE or ME, and SQL- queries, under which the entire set of reference data needed to calculate the failure rate returns from the database. All components are divided into " classes " divided into " Constructive-technological groups " and " Subgroups ", in which there are references to tables with coefficients necessary for the calculation.

Each ME has its own parameter values. Each ME is tied to any group and (or) the subgroup, it is achieved by matching numbers in columns «NomGrupp» and «NomPodgrupp» of main class table and numbers in the tables «Grupp» and «Podgrupp» respectively. All information on the group or subgroup, connected with a particular ME by the method described above. They include basic failure rate λ_b , basic failure rate in storage mode λ_{sg} , etc.

In Picture 3, the main table of class "filters" is given as an example.

Name	Type	Nullable	Default	Comments
TYPE	VARCHAR2(100)	<input checked="" type="checkbox"/>		
CONSTRTU	NUMBER	<input checked="" type="checkbox"/>		
CONSTRDOC	NUMBER	<input checked="" type="checkbox"/>		
NOMGRUPP	NUMBER	<input checked="" type="checkbox"/>		
NOMPODGRUPP	NUMBER	<input checked="" type="checkbox"/>		
PRIMER	VARCHAR2(100)	<input checked="" type="checkbox"/>		
PR	NUMBER	<input checked="" type="checkbox"/>		
PORI	NUMBER	<input checked="" type="checkbox"/>		
LAMDA_B	NUMBER	<input checked="" type="checkbox"/>		
SW	NUMBER	<input checked="" type="checkbox"/>		
*		<input checked="" type="checkbox"/>		

Picture 3 - DBCS Oracle: The main table of class "Filters"

As you can see from Picture 3, the name of shortened element type («TYPE»), is stored in the main class table, ME of any class also has a unique number, which is stored in the field «CONSTRTU», which allows you to store several parameters in the database for one ME. Base failure rate for each item is stored in the field «LAMDA_B» and identifiers of groups and subgroups are stored in the fields «NOMGRUPP» and «NOMPODGRUPP». The other fields in this table are subject to change in accordance with the classification of the coefficients of the selected class[8-10].

Thus, the procedure for developing a new section of database for the system ASONIKA-K - SCH involves the following steps:

- Classification of parameters and coefficients in the mathematical model of the failure rate;
- Construction of the "Tree of coefficients";
- Construction of the "Hierarchy of tables";
- Design of a logical model of the database section.

The above procedure can be used as a base for developing database on the characteristics of reliability of ME of other classes, listed in the standard NSWC-2011.

References

1. OST 4G 0.012.242-84. Apparatura radioelektronnaya. Metodika rascheta pokazateley nadegnosti.
2. NSWC-11 Handbook of reliability prediction procedures for mechanical equipment.
3. Avtomatizaciya proektnih issledovaniy nadegnosti radioelektronnoq apparaturi: Nauchnoe izdanie / V.V. Zhadnov, U.N. Kofanov, N.V. Malyutin i dr. - M.: Radio i svyaz', 2003. - s.
4. Zhadnov V.V. Upravlenie kachestvom pri proectirovanii teplonagruzhennih radioelektronnih sredstv: Uchebnoe posobie. / V.V. Zhadnov, A.V. Sarafanov. - M.: SOLON-PRESS, 2012. - 464 s.
5. Monakhov, M.A. Razrabotka modeli informacionno-spravochnoy bazi danih dlia ocenki bezotkaznosti elektronnih sredstv s uchetom mehanicheskikh elementov. / M.A.

Monakhov. // Nauchno-tehnicheskaya konferenciya studentov, aspirantov i molodih specialistov. - M.: MIEM HSE, 2014. - s.

6. Monakhov, M.A. Razrabotka bazi dannih programmnoy kompleksa ASONIKA-K dlya rascheta nadegnosti radioelektronnoy apparatury s uchetom mehanicheskikh elementov. / M.A. Monakhov. // Nauchno-tehnicheskaya konferenciya studentov, aspirantov i molodih specialistov. - M.: MIEM HSE, 2013. - s.

7. Monakhov, M.A. Razrabotka bazi dannih dlya sistemi ASONIKA-K-SCH po harakteristikam nadegnosti mehanicheskikh elementov klassa «Filtri». / M.A. Monakhov, V.V. Zhadnov. // Sovremennye problemi radioelektroniki: sb. nauch. tr. / nauch. red. G.Y. Shaydurov; otv. za vip. A.A. Levickiy. - Krasniyarsk: Sib. feder. un-t, 2013. - s. 366-369.

8. Monakhov, M.A. Issledovanie modeli intensivnosti otkazov mehanicheskikh elementov klassa «Pruzhini» / M.A. Minakhov, V.M. Fokin, I.L. Lushpa. // Innovacionnye informacionnye tehnologii: Materiali mizhdunarodnoy nauchno-prakticheskoy konferencii. Tom 3. - M.:MIEM HSE, 2013. - s. 443-446.

9. Monakhov, M.A. Issledovanie modeli intensivnosti otkazov prugin skrudivaniya. / M.A. Minakhov, V.M. Fokin, I.L. Lushpa. // Novye informacionnye tehnologii v avtomatizirovannih sistemah. Materiali shestnadcatogo nauchno-prakticheskogo seminar - M.: MIEM HSE, 2013. - s. 128-131.

10. Monakhov, M.A. Issledovanie modeli intensivnosti otkazov volnoobraznih kol'cevih prugin. / M.A. Minakhov, V.M. Fokin, I.L. Lushpa. // Новые Новые informacionnye tehnologii. Tezisi XXI Mezhdunarodnoy studencheskoy shkoli-seminara. - M.: MIEM HSE, 2013. - s. 122-123.

PHYSICAL EFFECTS AND PROBLEMS IN GAMMA-ELECTRONICS

Mozgovoi Yu.D, Khritkin S.A.

Moscow Institute of Electronics and Mathematics, National Research University Higher School of Economics (MIEM NRU HSE)

The physical effects and problems within the scientific direction "Gamma- electronics (γ - electronics)", which studies the interaction of the electron and positron fluxes with the electromagnetic field in the γ - range of wavelengths, as well as problems of production and the prolonged existence of the electron-positron substance (EPS) with extremely high stored energy released in the process of collective slow annihilation have been considered. We discuss the possible quantum analogues of classical high-power microwave devices in the interaction of charged particles multipath different sign. The basic stages of work, corresponding to the possible experiment in gamma- electronics with streams of electrons and positrons have been indicated.

Keywords: gamma-electronics, electron-positron substance, electron and positron beams, the method of large particles, the macroscopic quantum theory, Schrodinger and Poisson equations, macroscopic wave function, super-liquidity, super-plasmoid, collective interaction.

1. Introduction

Considered a new scientific direction - GAMMA ELECTRONICS (γ electronics), which explores the interaction of the electron and positron beams with electromagnetic fields in the γ - wavelengths. In scientific monograph [1] formulated a hypothesis about the possibility of prolonged existence of metastable electron-positron substance (EPS) with unique properties: extremely high stored energy released in the process of collective slow

annihilation; properties of macroscopic quantum electron-positron super-liquidity implemented in large volumes, the possibility of resonance EPS self-organization to obtain macroscopic quantum super-plasmoids [1-5].

The uniqueness of the EPS consists in that it is a combination of three types of fundamental particles (electrons, positrons and virtual γ - quanta), self-assembled in a single macroscopic quantum state. Electron and its antiparticle - the positron is an elementary particle, the structures of which are not observed at distances greater than 10^{-16} cm. They are not subject to strong (nuclear) interaction. Their spin $\frac{1}{2}$ and they obey Fermi-Dirac statistics, entering the number of fermions. Electron refers to the number of leptons, the positron is antilepton. Neutral particle is a γ -quantum. Gamma photon has zero charge, zero rest mass and a single spin. He obeys Bose-Einstein statistics, as boson. Particles and antiparticles annihilate, turning into γ - quanta only in pairs. Electron-positron pair (e^-e^+) are stored energy $1.02 \text{ MeV} = 1.6 \cdot 10^{-13} \text{ J}$ released during annihilation [6-9].

In EPS theory are important properties of particles ensembles. In particular, separately taken electron as an elementary particle is not identical to the positron, at the same time neutral in charge of electrons and positrons group could be identical [4]. Certain groups of electron-positron pairs can acquire the properties of neutral systems. This is due to the symmetry with respect to the transformation, called "charge conjugation". EPS is formed by the Bose-Einstein condensation of electrons and positrons at high particle density and forms macroscopic electron-positron field with nonzero rest mass (matter field) in contrast to the electromagnetic field radiation (γ -quanta field - particles with zero rest mass). Known example of EPS are hydrogen-like atoms-positronium and molecules of positrons [6-9].

Positronium atom which is in S-state (singlet), undergoes 2-photon annihilation, which is characterized by the lifetime $\tau(2\gamma)=1.25 \times 10^{-10} \text{ n}^3 \text{ sec}$. Lifetime at 3-photon annihilation in the triplet state $\tau(3\gamma)=4 \times 10^{-7} \text{ n}^3 \text{ sec}$. Positron lifetime before annihilation is usually small, but can be significantly increased by making the superfluid or superconducting EPS macroscopic quantum state. Many problems are removed at transition to the system of delocalized electrons and positrons at particle densities corresponding of metal super-state. EPS's electrons and positrons that are in S-state near their Fermi surfaces can form Cooper pairs of electrons and positrons. Pairs are bosons and in the area of macroscopic parameters form superfluid electron and positron pairs condensate. In groups of particles with an equal number of electrons and positrons $N_e=N_p > 2$, the principle of identity and charge conjugation, consider allowing macroscopic resonant mechanism of the exchange interaction between groups of electrons and positrons. Condensation occurs in the form of a superfluid neutralized liquid based on double electron-positron pairs [1, 6-9].

It is known that as a result of short-term exposure to pulsed high-current relativistic flow on a specially prepared to experiment with the system under the action of γ -quanta arise clouds of electrons and positrons with high bulk density of particles, sufficient for the emergence of collective interaction, which leads to compensation of the Coulomb field with forming of macro-plasmoids and their union into electron-positron condensate. Construction of theory and experiment organization from the outset admits the existence of an effective mechanism for multiple productions of positrons in pairs with electrons under the influence of a powerful gamma burst [1].

At high density of surrounding particles newly born particles are screened and they represent quasiparticles. In this case, the collective process of identical particles self-organization has to go faster than annihilation process of electron-positron pairs. Self-organization of interaction processes leads to unite groups of electrons and positrons into macroplasmoid with compensated the Coulomb field and the same wave fields of electrons and positrons, which corresponds to the macroscopic appearance of an electron - positron.

Macroplasmoid must be boson capable to condensation based on Bose-Einstein statistics [1, 6-9].

Formed spatially developed active region (electron-positron plasma) and produced multipath direct and counter flows in drift tubes (moving charged plasma). The streams may converge into a focus scope of electron optical system. Sources of radiation in the frequency range close to the frequency of the annihilation of electrons and positrons are considered to be promising. To describe such devices is possible to use synchronism of electron beam with field and flow fluctuations [10-13]. Microwave electronics experience shows that highly nonlinear processes must be described using discrete models of the electron beam. Let the number of electrons per unit volume is large enough to have valid average system description. At the same time the smallness conditions of the particles collision are performed. Therefore, the transition can be accomplished to the macroscopic quantum description of the charged particles active medium [1-5].

Computational modeling of electron-positron medium carried by the methods of classical nonlinear theory [10-13] and the macroscopic quantum theory in the interactions of the electron and positron beams with electromagnetic field [1-5].

Light carriers plasma is considered as collisionless with collective interaction [14, 15]. Within the theory of plasma, arise problems on the interaction of several groups of opposite sign charges, related to the experiment possibilities [16-17].

Hydrodynamic approximation equations of the classical theory for quantum electron-positron plasma are valid, if the spatial variation of the particle density is sufficiently small. Here the wave functions of the electrons Ψ_e and positrons Ψ_p have the form of macroscopic wave functions of the superfluidity theory [18]. Connection establishment of a quantum theory wave model and models of large particles is useful for understanding the role of the characteristic distances between the particles. We carried out a Schrödinger and Poisson equations joint decision for the macroscopic wave functions of electrons and positrons [1-5].

The possibility of prolonged existence of metastable EPS with extremely high stored energy released during slow annihilation has been discussed. Dynamic EPS self-organization based on the collective effect of the identity of the groups of particles consisting of an equal number of electrons and positrons, and it accompanied by phase self-focusing. Within the limits of an extended active volume phase becomes slowly changing, and the substance in the volume is a unified whole. Processes occurring in the material are described by macroscopic particle wave functions of the electrons and positrons, as well as the two-particle wave function of the electron-positron pairs - Dirac field. Squared modules of functions equal to the density of the corresponding particles. Phases of functions allow simultaneous measurement along with amplitudes. Macroscopic electron-positron field is obtained after averaging of the microscopic field.

EPS with a long lifetime is the result of condensation of many particles or pairs groups of electrons and positrons at high density. In some cases EPS is the analog electron-positron-ionic substance, where a part of positrons can be replaced by positive ions, and in superconductors the ions can be replaced by positrons. The average distance between the microparticles of various EPS embodiments is in the range of $1 \div 100 \text{ \AA}$. This distance is much larger than the area of annihilation of electron-positron pairs $dA \sim 10^{-11} \text{ cm}$ and, thus, provides a slow (or delayed) annihilation.

To investigate of macro-processes is applicable the EPS representation as a collisionless plasma with electric interaction. Electrons and positrons are satisfy Fermi-Dirac statistics, however, the electron and positron Cooper pairs, as well as electron-positron dual-pairs are bosons, and may be in the macroscopic quantum states, representing a single entity - or superconducting or superfluidity condensate. These objects are objects of high mass (heavy bodies), the interaction with which significantly reduces the probability of annihilation.

Periodic alternation of positive and negative charges of the particles at the initial stage of interaction also significantly reduces annihilation probability.

2. Methods for calculating the interaction of electron and positron fluxes in the classical and quantum treatment

To study the electron-positron substances used classical model of large particles and quantum macroscopic models of single-particle wave functions. In contrast to the point kinematic approach of quantum electrodynamics, the particles are treated as deformable clots charge. Allowance for the influence of space charge forces on the small volumes movement allows to find conditions for the Coulomb field compensation and to explore the establishment of a lower dynamic mode (electron-positron plasmoid) as superliquidity. Electron-positron matter reveals itself in the forms of substance, field and energy. Collisionless processes in the material studied in the plasma approach framework of the macroscopic classical and quantum theories. In the classical area have been introduced phase ensembles of large particles and investigated resonance processes at the spontaneous and stimulated emission, defining characteristics of the self-consistent interaction.

In quantum theory, ensembles correspond to single-particle wave functions of the electrons and positrons, which are squares of the modules equal to the particle density. At large number of particles can be determined and measured simultaneously field's amplitudes and phases. Solution of the Schrödinger and Poisson equations allows exploring the classical and quantum analogues of radio physics and electronics devices, including relativistic high-power pulse generators with a field of dynamic mode.

Within the validity of the "cold" collisionless two-component plasma model, transition to simplified equations for degenerate (quantum) and non-degenerate (classical) charge carriers is valid. Let considered plasma components are in motion. In the case of slow variation of amplitudes and phases should be implemented transition to the hydrodynamic equations. The reveal relation between wave model and large particles model is helpful, for example, to understand the role of characteristic distances (Coulomb forces action radius R_0 in the classical model and the de Broglie wavelength λ in the quantum problem).

Modes with high efficiency in high-power electron devices are achieved by the resonant interaction of electron bunches and electromagnetic field. Experience powerful microwave electronics shows that highly nonlinear processes must be described using discrete models of electron beam. Let the number of electrons per unit volume is large enough to have rightly average system description. In this case are carried conditions of the smallness particles collision. Therefore, can be accomplished the transition to the macroscopic quantum description of the active medium.

In modeling the processes of interaction plays an important role dualism and flow field. Electrons are described by a macroscopic wave function and used quantum principle of identity of particles. When creating models system of interacting particles, electrons (or positrons) are presented in the form of a stream of charged liquid. In fact, in the analysis of the interaction is taken into account spreading bunches of electrons and positrons, considered at different times. Considered displacement and deformation of individual fragments of bunches of electrons and positrons in the system, the space-charge forces are taken into account at each step of the integration of non-stationary equations.

Dirac equation in the nonrelativistic approximation transforms into the Schrödinger equation for two macroscopic particle wave functions of the electrons and positrons related Coulomb interaction. Within the field approach we assume that in the Dirac equation, as in the Schrödinger equation, we can introduce interconnected single-particle wave functions of the electrons and positrons, the sum of which on condition of compensation charge coincides with the two-particle wave function of the Dirac theory. Particle density is also summarized. Such assumption follows from the saturation effect at the exchange interaction of identical

particles. We also point to the fact that the Dirac equation can be regarded as the equation of electron-positron field with the two-particle wave function ψ [1, 19].

To describe the collective processes in electron-positron-ion collisionless plasma, according to the general procedure [1] we are introduced macroscopic single-particle wave functions of electrons, positrons and ions with selected amplitudes and phases

$$\Psi_e(x, y, z, t), \Psi_p(x, y, z, t), \Psi_i(x, y, z, t).$$

Components of the electron-positron plasma are described as condensate, using macroscopic wave functions $\Psi_{e,p}$ with a coherent phase $S_{e,p}$ [1]

$$\Psi_{e,p}(R, t) = \Psi_{e,p}(R, t) \exp[iS_{e,p}(R, t)].$$

Unlike conventional problems of quantum theory, the product $\Psi\Psi^* = |\Psi|^2$ is not related to the probability density of a single particle but is a particle density $n = |\Psi|^2$. At large number of particles is allowed simultaneous measurement the phase S and the density n . Squares wave functions of charged particles in the framework of macroscopic quantum theory are associated with the charge density of the particles and their concentrations following expressions [1-5].

$$|\Psi_e|^2 = n_e, \quad |\Psi_p|^2 = n_p, \quad |\Psi_i|^2 = n_i.$$

Introduction to the theory of macroscopic single-particle wave functions of the electrons Ψ_e and positrons Ψ_p allows consideration of electron and positron fluid drops with charge density $\rho_e = -|e| |\Psi_e|^2$, $\rho_p = |e| |\Psi_p|^2$ and signifies that a physically small volume V_p all the same type of particles (electrons, positrons, or ions) behave as ordered and the same identical particles without relatives (twin, triple, and other discrete) interactions.

In all cases is important close relationship of the charge density and the potential $\Phi(x, y, z, t)$ in the Poisson equation [1-5]

$$\Delta\Phi = \frac{|e|}{\varepsilon} \left(|\Psi_e|^2 - |\Psi_p|^2 - Z|\Psi_i|^2 \right).$$

Schrödinger equation for the wave functions have the form [1-5]

$$\begin{aligned} i\hbar \frac{\partial \Psi_e}{\partial t} &= H_e \Psi_e, & H_e &= -\frac{\hbar^2}{2m} \Delta + U_e, \\ i\hbar \frac{\partial \Psi_p}{\partial t} &= H_p \Psi_p, & H_p &= -\frac{\hbar^2}{2m} \Delta + U_p, \\ i\hbar \frac{\partial \Psi_i}{\partial t} &= H_i \Psi_i, & H_i &= -\frac{\hbar^2}{2M} \Delta + U_i, \end{aligned}$$

where U_e, U_p, U_i - potential energy of electrons, positrons and ions (charge $Z|e|$) in the Coulomb field with potential Φ

$$U_e = -|e| \Phi, \quad U_p = |e| \Phi, \quad U_i = Z|e| \Phi.$$

A grid method for calculation of nonstationary processes in two-dimensional and three-dimensional approximation is described in detail in [1].

Formation of electrons and positrons condensations in the classical theory is considered by the method of large particles. At the initial time, electrons and positrons are staggered. If the distance between particles is less than the size of large particles, then we are observed separately disposed accumulation of electrons and positrons. Thickenings with the passage of time under the influence of Coulomb forces are blurring. If the rate of spreading is small and large particles of model are enough for discrete description of the spatial distribution of the charges, the classical solution becomes similar solution of the wave problem.

Important role of the vector potential \mathbf{A} in the consideration of macroscopic quantum processes and with allowance magnetic field. Possible quantum effects at $\mathbf{E}=\mathbf{B}=0$ and if the vector \mathbf{A} is nonzero, then he is responsible for the phase shift of the wave functions. Raises a number of physical effects, including the Aharonov-Bohm effect [9, 19, 20].

Let us write the basic equations describing the interaction of electrons, positrons and ions taking the field vector potential. Vector potential \mathbf{A} , the magnetic induction \mathbf{B} and the vector of current density \mathbf{j} are related by $\Delta\mathbf{A}=\mu_0\mathbf{j}$, $\mathbf{B}=\mu_0\text{rot}\mathbf{A}$.

Schrödinger equation for the considered macroscopic wave functions is written considering the vector potential [1, 6, 9, 20]

$$\begin{aligned} i\hbar \partial\Psi_e/\partial t &= H_e\Psi_e, & H_e &= 1/2m(\mathbf{p} - e/c\mathbf{A})^2 + U_e, \\ i\hbar \partial\Psi_p/\partial t &= H_p\Psi_p, & H_p &= 1/2m(\mathbf{p} - e/c\mathbf{A})^2 + U_p, \\ i\hbar \partial\Psi_i/\partial t &= H_i\Psi_i, & H_i &= 1/2M(\mathbf{p} - e/c\mathbf{A})^2 + U_i, \end{aligned}$$

where the vector $\mathbf{p} = (-i\hbar\nabla)$ - momentum operator.

We are interested in the special role of the vector potential \mathbf{A} in the quantum domain when considering macroscopic processes. Fundamentally that formula includes interaction vector \mathbf{A} , and not the vectors \mathbf{E} and \mathbf{B} . To clarify the model assume that at the initial time thickening of electrons and positrons have the form of spherical clouds, radii of which are not greater than the Compton wavelength ($\sim 4 \cdot 10^{-11}$ cm) and can be close to the classical electron radius $r_0 = 10^{-13}$ cm. Nested inside each other, which are identical in everything except the charge sign, spherical clouds (clumps) of electrons e^- and positrons e^+ together form an electron-positron pair (microdroplet condensation). The wave equation can be considered as the equation for the potential field Ψ , produced by electron-positron pairs, responsible for the force interaction. Function Ψ should be considered as a two-particle operator in the space of occupation numbers of the second quantization theory. He has nonzero matrix elements corresponding to the absorption of the electron and positron.

3. Possible quantum analogues of power microwave devices and basic stages of experimental works

Multibeam electron-positron flux with alternating signs charges rays is considered. Streams of charged particles are introduced into the interaction region by drift tubes. The main effects of the interaction are developing in separately taken drift tube. Relativistic high-current electron accelerators with single pulses are often used as generators of powerful γ - radiation [1, 10] caused by radiative losses during bremsstrahlung. Gamma-radiation at electron energy more than 10 MeV is absorbed by the target material and is spent on a large number of electron-positron pair's creation.

Permissible level electron energy high-current beam 12-15 MeV implemented on accelerator "Aurora" in the U.S. terawatt pulse power and pulse energy of 10 MJ. To obtain pulses of positrons with energies of $1 \div 10$ MJ and to development corresponding works in the pulse energy need a specialized high-current electron multibeam accelerator of terawatt power level with energies of electrons greater than 50 MeV. The use of radial or volume location of beams and controls particle fluxes is natural. Devices for producing positrons contain special target where the electrons are decelerated, creating directed γ -quanta flows, which are distributed over a specified volume of the positrons source. Then unless measures are taken for the positrons conservation occurs electron-positron annihilation with the release of energy 1.02 MeV per pair [1].

Usually at longitudinal interaction flow and field are considering Cherenkov radiation and bremsstrahlung. In weakly relativistic and relativistic areas the individual radiation spectrum is smeared in frequency and has a maximum at low frequencies. In the case of sufficiently large voltage synchronism processes are accompanied by the establishment of a single phase of the oscillations, which is typical for the nonlinear theory. This feature of the process allows using the methods of nonlinear theory. Analogy with the theory of non-relativistic wave systems is possible. Radiated field is localized within the Cherenkov cone, which is important in the study of energy processes.

As follows from the foregoing discussion [1-5, 10] there are several milestones appropriate of the experiment possibilities in the gamma-electronics with relativistic electrons and positrons fluxes:

- obtaining pulsed relativistic electron flux in the accelerator laboratory;
- bremsstrahlung of relativistic electrons when passing the target with the generation of directed streams of gamma rays;
- short pulse action of powerful convergent gamma-ray flux on the medium in the region of the focal spot, with the implementation of multiple electron-positron pairs production;
- obtaining and ensure long existence of electron-positron pairs by gamma rays action;
- pairwise exchange interaction of different sign particles clumps;
- deceleration of newly emerged particles with transition from binary collisions to the collective process of merging groups of identical particles into the same or different signs charges condensations;
- nonlinear exchange process with synchronization oscillation in the entire region rapidly flowing compensation of the Coulomb field and increase of the wave field around a common center, which leads to self-organize the system into condensate spherical shape.

The calculations have shown that under optimal space charge forces the particles at first collected into separated in space groups of the same sign charge. We select paired groups of electrons and positrons, similar in size and magnitude of the charge. Serves as a convenient model system of pairs of large particles of different sign, for example, charged balls in three-dimensional approximation. Using special vacuumed devices γ - rays fluxes can effectively manage and transform into electron-positron pairs and then to multibeam secondary flows with alternating beams of slow electrons and positrons.

In the next layer behind it, electrons and positrons lose energy during collisions with the matter layer and turn into flows of slow electrons and positrons. Important layer is formed separated in space control electrodes with the alternating voltage sign. On the output of this layer are obtained multibeam streams with changing of the particle charge sign. Only under special deceleration of charged particles and the use of converging optics can be raised the particle density up to values of the order $n = 10^{19} \div 10^{21} \text{ cm}^{-3}$. At high electron energies decreases substantially energy spread of interacting particles. Main role is played effect of electron-positron pairs (photo effects and the Compton Effect are not significant). The greatest clarity in the use of devices achieved in the case of spatially developed systems of Cherenkov and klystron types.

Currently, many of the options of resonance processes described with macroscopic wave functions of electrons and positrons using a simplified distribution charges function of large electron and large positron types are investigated. Nonlinear effects in the exchange interaction have much in common with classical processes in nonlinear media. In classical area nonlinear processes lead to the optimization of the grouping in microwave generators [6,7]. In quantum area is important inverse problem - minimizing radiation with increasing lifetime of the plasmoid by moving to slow or delayed annihilation. In a free state superplasmoid is spherical in shape. Inhomogeneities near the it exhibits properties of superpenetration primarily into a dielectric. Exchange processes in a ball modeled using macroscopic wave functions of electrons and positrons of quantum theory. In particular, it is shown that the equality of the wave functions of electrons and positrons, as well as passing the plasmoid through the insulator is possible without changing the properties in the case of dynamic compensation of the Coulomb field.

Resonance effects in the quantum exchange interaction leads to self-organization of the active volume of the charged medium and continue until the dynamic compensation of the

Coulomb field and the establishment of a dynamic electron-positron mode. It should be noted the close relationship of identity effect under charge conjugation and dynamic compensation effect of the Coulomb field in the entire volume. In the macroscopic ground state are important slowly varying centrally symmetric field (S-wave), the radial structure is determined by collective effects. Macroscopic quantum state is a special electron-positron medium formed by particles of matter (electrons and positrons) and the field of virtual photons. In quantum theory, a large number of plasma particles de Broglie waves are transformed into charge-density waves.

Conclusion

The physical effects and problems in gamma-electronics, studying the interaction of electron and positron fluxes with the electromagnetic field in γ -range of wavelengths, as well as problems of production and the prolonged existence of the electron-positron substance (EPS) with extremely high stored energy released in the process of collective slow annihilation are presented. The possible quantum analogues of classical high-power microwave devices with longitudinal interaction (klystrons, relativistic TWT and BWO) at the interaction of multipath beams of different sign charged particles are considered. The basic stages of work, corresponding to the possible experiment in gamma-electronics with relativistic electrons and positrons streams are marked.

References

1. Kanavets V.I. Electron–Positron Substance: From Positron to Superliquid and Ball Lightning (Pedagogicheskoe Obshchestvo Rossii, Moscow, 2009) [in Russian].
2. Kanavets V.I., Mozgovoi Yu.D., Khritkin S.A. Exchange Interaction of Electron and Positron Bunches // Journal of Communication Technology and Electronics. 2010. V. 55. No 4. P. 469-474.
3. Kanavets V.I., Mozgovoi Yu.D., Khritkin S.A. Feasibility of Quantum Analogues of Classical Microwave Devices on Longitudinal Interaction // 14th IEEE International Vacuum Electronics Conference (IVEC-2013). Paris, France. 2013. P. 215-216.
4. Kanavets V.I., Mozgovoi Yu.D., Khritkin S.A. Resonance Effects in the Quantum Exchange Interaction of Electron and Positron Beams // 14th IEEE International Vacuum Electronics Conference (IVEC-2013). Paris, France. 2013. P. 282-283.
5. Kanavets V.I., Mozgovoi Yu.D., Khritkin S.A. Self-Organization of the Electron-Positron Medium // 14th IEEE International Vacuum Electronics Conference (IVEC-2013). Paris, France. 2013. P. 288-289
6. Sokolov A.A. Introduction to quantum electrodynamics. (Nauka, Moscow, 1958) [in Russian]
7. Goldansky V.I. Physical chemistry of the positron and positronium. (Nauka, Moscow, 1968) [in Russian].
8. Arifov U.A., Arifov P.U. Physics of slow positrons. 1971. [in Russian]
9. Berestetsky V.B., Livshits E.M., Pitaevsky L.P. Quantum electrodynamics. (Nauka, Moscow, 1980) [in Russian].
10. Bugaev S.P., Kanavets V.I., Koshelev V.I., and Cherepenin V.A. Relativistic Multiwave Microwave Generators (Nauka, Novosibirsk, 1991) [in Russian].
11. Kanavets V.I., Mozgovoi Yu.D., and Slepko A.I. Radiation of High-Power Electron Currents in Resonant Slow-Wave Structures (Mosk. Gos. Univ., Moscow, 1993) [in Russian].
12. Kanavets V.I., Mozgovoi Yu.D., Khritkin S.A. Synchronization of electron generators based on small volumes of an active resonance medium obtained upon electrostatic focusing // Journal of Communication Technology and Electronics. 2003. V. 48. No 6. P. 687-690.

13. Kanavets V.I., Mozgovoi Y.D., Khritkin S.A. Self-Excitation and Synchronization in a Multibeam Microwave Generator with Electron-Oscillator Flows // Journal of Communications Technology and Electronics. 2006. Vol. 51. No. 3. P. 339-344.
14. Aleksandrov A.F. and Rukhadze A.A. Lectures on the Electrodynamics of Plasmalike Media (Mosk. Gos. Univ., Moscow, 1999) [in Russian].
15. Aleksandrov A.F. and Rukhadze A.A. Lectures on the Electrodynamics of Plasmalike Media: Nonequilibrium Media (Mosk. Gos. Univ., Moscow, 2002) [in Russian].
16. Cassidy D.B., Mills A.P. The production of molecular positronium. Nature, September, 2007. Vol. 449, P. 195-197.
17. Fortov V.E. Extreme States of Substance on the Earth and in Space (Nauka, Moscow, 2008) [in Russian].
18. Tilli D.R., Tilli J. Superfluidity and Superconductivity. New York: Reinhold (1974)
19. V.G. Levich, Yu.A. Vdovin, and V.A. Myamlin, Theoretical Physics; an Advanced Text (Fizmatgiz, Moscow, 1962; North-Holland, Amsterdam, 1970), Vol. 1, 2.
20. Bohm D. Quantum Theory (Prentice-Hall, New York, 1951; Nauka, Moscow, 1965).

DEVELOPMENT SEQUENCE DIAGRAM OF NEURAL NETWORK IDENTIFICATION OF A COMPLEX SIGNAL USING THE UNIFIED MODELING LANGUAGE UML 2.0

Murashkina E.N.

Penza State Technological University, Russia

We develop a sequence diagram of a neural network identification of a complex signal using Unified Modeling Language UML 2.0. Neural network acts as a structural-parametric models. The structure of an artificial neural network expert changes. Parameters are automatically determined in the learning process. Constructed diagram need for further study of complex signals and construction of the system identification using artificial neural networks.

Keywords. Neural network, complex signal, identification, sequence diagram, UML 2.0.

Identification of complex signal is one of the fastest growing technologies in the moment. This is due to the wide use of complex signals and for transmitting encoding information. Examples of systems of identification complex signals can serve as an access control system, vehicle identification and biometric systems.

Develop a sequence diagram of neural network identification of a complex signal using the Unified Modeling Language UML 2.0. is the aim of this study.

The UML is a graphical modeling language for general purposes. It is intended for the specification, visualization, design and documentation of all artifacts created for developing software systems [1].

The main purpose UML is to provide a formal, a convenient and a universal means. It helps reduce the risk of differences in interpretation of specifications, beg the development process models, as well reduce the economic and temporal modeling.

Interaction diagrams are used to model the interaction of objects in UML. Interaction of objects can be seen in time. The sequence diagram is used to represent temporal characteristics of transmitting and receiving information between objects [2].

Objects involved in the interaction and showing possible association with other static objects are shown on the sequence diagram. Dynamics of the interaction of objects in time for sequence diagrams is the key.

The sequence diagram is two dimensions. One is left to right in the form of vertical lines. Each line represents the line of life of an individual object involved in the interaction.

The vertical axis is the second time measurement sequence diagrams. The upper part of the diagram corresponds to the initial time. Interaction of objects implemented via messages. They sent some other objects. Messages are shown as horizontal arrows with the message name. They form the order in time of their occurrence.

Posts located at the sequence diagram above initiated before those that are below. The scale on the time axis is not specified as a sequence diagram models the ordering of interactions temporal "earlier-later."

The sequence diagram of the neural network identification of a complex signal illustrated in figure 1.

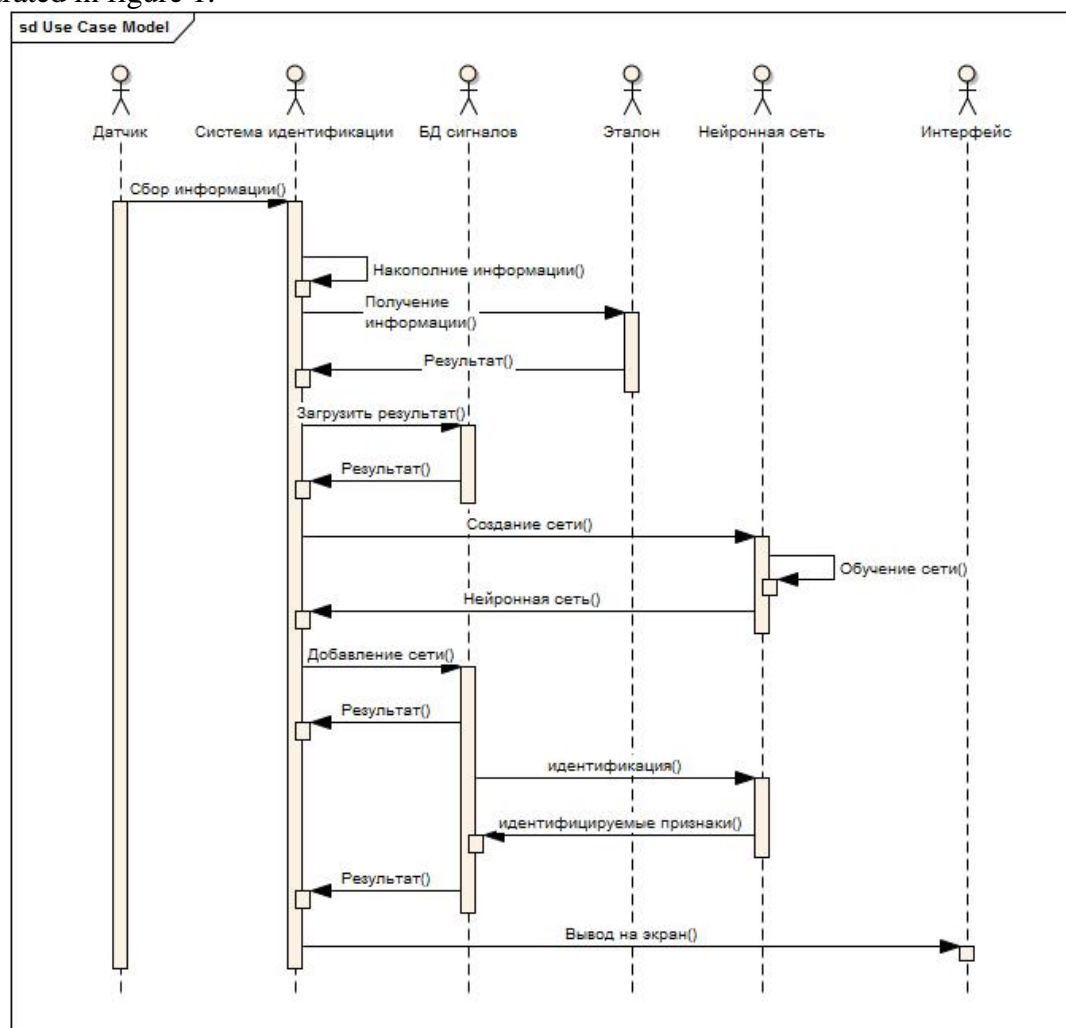


Figure 1 - The Sequence diagram of the neural network identification of a complex signal

We receive information from the source of the reference signal for the neural network identification signals of complex shape. Training the neural network will be using this information. The signal coming from the sensors located around the perimeter of the test portion in a system of identification. Identification system stores information for more accurate data analysis. The resultant signal is compared with the stored database signals.

We create a neural network based on the obtained results. The neural network is trained. The process of identification of parameters of a complex signal is done by the trained neural network. Neural network is an adaptive a model structural-parametric. The structure of an artificial neural network expert changes. Parameters are automatically determined in the learning process.

So, we have constructed a sequence diagram of neural network identification signals of complex shape in the study. Constructed diagram need for further study of complex signals and construction of the system identification using artificial neural networks.

References

1. Grady Booch, James Rumbaugh, Ivar Jacobson, Introduction to UML from the creators of the language. Per: Mukhin - M: DMK Press, 2011 - 496s.
2. D. Yu. Ivanov, FA Novikov Basics modeling UML: Textbook. allowance. - St. Petersburg. Univ Polytechnic. University Press, 2010. - 249C
3. A.I. Galushkin Neural Networks - M: Hot Line - Telecom, 2012. - 496.
4. V.V. Perkov System digital data transmission signals of complex shape (RU Patent 2024198).
5. A.B. Scherban, V.V. Soloviev, M.V. Tyurin, E.N. Murashkina. Structural approach to the analysis of the complex systems. Modern information technology: Collected papers of international scientific and technical conference. Issue. 14. - Penza: PSTA, 2011. - S. 72-76

MICROWAVE MEDICAL ELECTROD BASED ON SLOW-WAVE SYSTEM

Shaymardanov R.V., Elizarov A.A.
Russia, Moscow, MIEM HSE

The hereby article considers microwave methods of based on slow-wave systems for internal organs treatment. Application of various methods are revealed, the electrodynamic analysis of an electrode based on slow-wave system like the “ribbed coaxial line” is carried out. Application prospects of such structure are defined in creation various microwave devices for treatment internal organs diseases, such as prostate gland disease.

Keywords: microwave slow-wave system, medical electrode, ribbed coaxial line.

Some time ago the only ways of prostate gland disease (PGD) treatment were: lifelong application of medicines or surgical intervention. Though both of these treatment methods can be effective, they have a number of serious side effects: headache, dizziness, slackness, chemical intoxication for medicamentous treatment, and a syndrome of water intoxication of an organism, structurization urethra tissues, urine incontience, impotence in case of surgical intervention.

The surgical method today is recognized to be the most effective method of PGD treatment, however it is contraindicated to some groups of patients especially at early stage of disease or possible complications when carrying out operation, including in case of aged patients. As this disease is spread generally in elderly people, existence of accompanying serious diseases limits application of this method.

Conductivity of biofabrics has ionic character. Important property of biofabrics is dependence of their conductivity and relative dielectric permeability on current frequency. In this sense it is accepted to say that the specified electric properties of biofabrics possess dispersion.

Transurethral microwave thermotherapy (TUMT) is distinguished among many new and innovative low-invasive methods of physical intracavitary organs therapy. When carrying out TUMT the desirable result is receiving a cavity and release an urethra from compression, illustrated on Fig.1, i.e. receiving effect closest to the operational surgical intervention result.



Figure 1. Appearance of a prostate gland whis compressed urethra.

Heat induced by microwave radiation is used for the specified purposes. Control of the reached levels of temperature in biotissues is exercised during a medical session. If the temperature exceeds 55°C the biotissues gland necrosis process begins. Microwave radiation was not chosen incidentally for biotissues diseases treatment – it possesses two important properties, firstly, it delivers warm deeply in tissues, and, secondly, its power is possible to regulate.

It is clinically proved that the last generation of TUMT has efficiency comparable to surgical influence at early stages of DGP, at the same time thermotherapy is the simpler, ambulatory, profitable method which allows to carry out DGP treatment practically without restrictions for patients to whom surgical intervention is refused due to a state of health. Thus use of the general anesthesia is not required, and the session lasting originally of about one hour, is reduced till 30 minutes. The scheme of procedure of application of therapy is given in Fig.2.

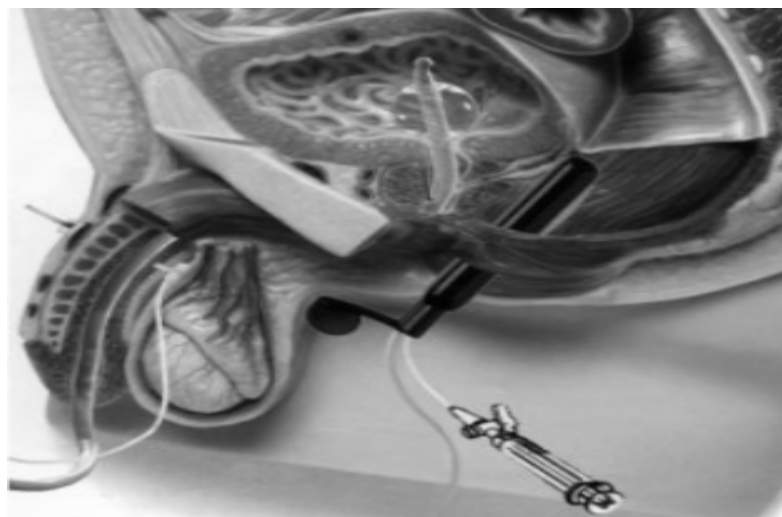


Figure 2. Transurethral microwave thermotherapy procedure application.

Applied now spiral electrodes for the urology consisting of the microwave generator, the control unit, system of circulation, temperature sensors and the radiating antenna which has been built in a special catheteris presented on Fig.3.

The device has the generator using the working frequency of 915 MHz and radiation power, changing from 0 to 80 W. According to safety requirements for the modern equipment for thermotherapy the top limit of radiation power can't exceed the specified value. Radiation power of 20 W is sufficient for achieving temperature close to 44°C in biotissues of a prostate gland. Radiation power of 80 W allows to warm gland biotissues up to the temperatures of exceeding 55°C that allows to cause a coagulative necrosis of biotissues. With the frequencies used for microwave thermotherapy (between 900 MHz and 1300 MHz), penetration depth of an electromagnetic field in a prostate gland is about 15 mm. With a frequency of 100 MHz, that is at a radiofrequency, depth of penetration makes 100 mm, and at 2450 MHz – the frequency used in household microwave ovens – depth of penetration makes 10 mm.



Figure 3. Spiral urological electorde.

This electrode has a number of shortcomings:

- The electrode with a wide pass-band is not always required.
- Heat removal from a spiral can be complicated.
- High output power can not be received and burns of fine epitaxial biotissues of an internal organs directly adjacent to the device are possible.

For treatment of a prostate gland disease at early stages, a narrow-band emitter with dielectric filling on the basis of the coaxial ribbed line is suggested to be used.

This electrode is created on the basis of new approaches to usage of slow-down structures. Similar emitters have a number of peculiarities:

- Ensuring of exact localization of electromagnetic energy in an irradiated body part.
- Change of a local heating zone of an intracavitary radiator, both on length, and on azimuth.
- Change of radiation zone square.

Such electrodes are hi-tech, have small overall dimensions, small weight which increases comfort of treatment in comparison with a traditional surgical method of treatment. Also the narrow-band electrode is necessary for effective treatment. But even in this case its slowing down coefficient remains rather high thanks to existence of dielectric filling by a layered material with the set properties for local heating of biotissues. The offered electrode demands practical realization in the small geometrical parameters related to physiological specifics of its use.

As known, wave impedance of the coaxial line is defined by the relation of diameters of conductors and can be changed over a wide range [2]. Besides, the geometrical length of

such lines can be reduced if surface of one or both conductors of the coaxial line make ribbed Fig.4 [3, 4].

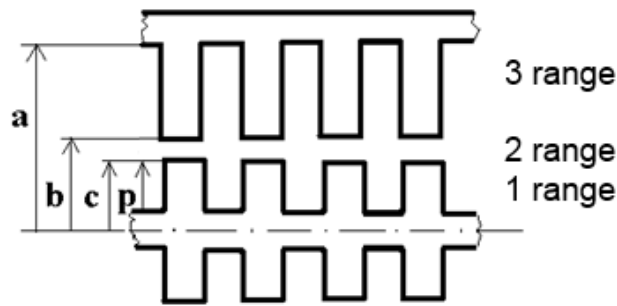


Figure 4. Model of the ribbed coaxial line.

General view of the coaxial line with ribbed conductors dispersive equation was for the first time received in paper [5]:

$$\frac{I_1(\tau) + \frac{\tau}{k\sqrt{\varepsilon}} I_0(\tau) bct(kc, kp)}{K_1(\tau) - \frac{\tau}{k\sqrt{\varepsilon}} K_0(\tau) bct(kc, kp)} = \frac{I_1(\tau a) + \frac{\tau}{k\sqrt{\varepsilon}} I_0(\tau a) bct(ka, kb)}{K_1(\tau a) - \frac{\tau}{k\sqrt{\varepsilon}} K_0(\tau a) bct(ka, kb)}, \quad (1)$$

where

$$bct(x, y) = \frac{J_1(x)N_0(y) - N_1(x)J_0(y)}{J_0(x)N_0(y) - N_0(x)J_0(y)}. \quad (2)$$

is Bessel cotangent, J_0, J_1, N_0, N_1 - Bessel functions, I_0, I_1, K_0, K_1 are the modified Bessel functions; β – the phase constant connected with a transverse constant τ and wave number k as:

$$\beta^2 = \tau^2 + k^2, \quad k = \omega\sqrt{\varepsilon_0\mu_0}. \quad (3)$$

ω is the angular frequency, ε_0 and μ_0 are the permittivity and permeability of vacuum.

Dispersion equation takes a form:

$$\left[1 - \tau \frac{K_0}{K_1}(c\tau)y_1\right] \left[1 - \tau \frac{I_0}{I_1}(a\tau)y_3\right] = \varphi_{11}(a\tau, c\tau) \left[1 + \tau \frac{I_0}{I_1}(c\tau)y_1\right] \left[1 + \tau \frac{K_0}{K_1}(a\tau)y_3\right]. \quad (4)$$

Received equation analysis shows that it breaks up in two independent equations, the solution of each allows to find phase constants of the slow-waves extending near a ribbed surface:

$$1 - \tau \frac{K_0}{K_1}(c\tau)y_1 = 0, \quad (5)$$

in “diaphragm wave guide”:

$$1 - \tau \frac{I_0}{I_1}(a\tau)y_3 = 0. \quad (6)$$

Generally, the received dispersion equation has two decisions - for inphase and antiphase waves excitement. Taking into account coefficients the dispersion equation will be transformed to a quadratic equation and takes a form:

$$\frac{\tau^2}{k_2^2} - \frac{\tau}{k_2} \frac{R_1(1 + \varphi_{10}) + R_3(1 + \varphi_{01})}{1 - \varphi_{00}} + R_1 R_3 \frac{1 - \varphi_{11}}{1 + \varphi_{00}} = 0. \quad (7)$$

In this case in strong interaction between electrodes and antiphase excitement we will receive:

$$\frac{\tau}{k_2} \approx \frac{R_1(1+\varphi_{10})+R_3(1+\varphi_{01})}{1-\varphi_{00}} - \frac{R_1R_3(1-\varphi_{11})}{R_1(1+\varphi_{10})+R_3(1+\varphi_{01})}, \quad (8)$$

for inphase excitement:

$$\frac{\tau}{k_2} \approx \frac{R_1R_3(1-\varphi_{11})}{R_1(1+\varphi_{10})+R_3(1+\varphi_{01})}. \quad (9)$$

Received equation follows us in idea that in antiphase excitement case phase constant has bigger value in comparison with inphase excitement.

Wave slowing down in this system depends on the relation of the geometrical sizes of an electrode and ε , as analysis showed:

$$N = \beta / k \approx \sqrt{\varepsilon \ln(b/p) / \ln(a/c)}. \quad (10)$$

Dependence of wave slowing down (N) with relation of geometrical parameters of an electrode (c, b, p, a) is given in Fig.5 at $\varepsilon = 1$. The received theoretical ratios qualitatively confirmed according to results of physical experiment.

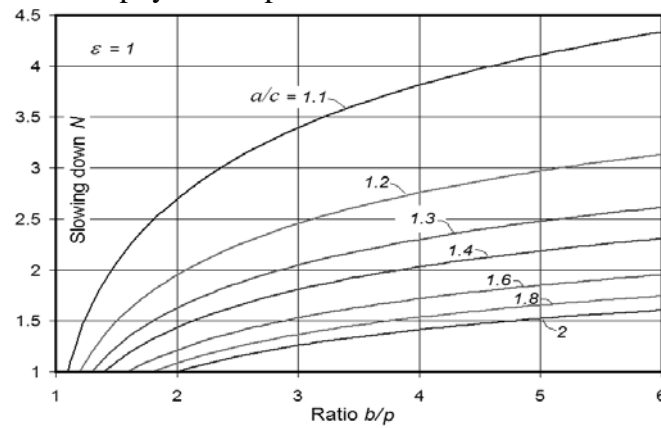


Figure 5. Wave slowing down from electrode geometry.

The coaxial ribbed line offered to development was simulated in the user program of the Ansoft HFSS v.12 company is giving in Fig.6. For the working frequency of 2450 MHz, the total length of an electrode was chosen equal 80 mm, diameter of an electrode – 24 mm.

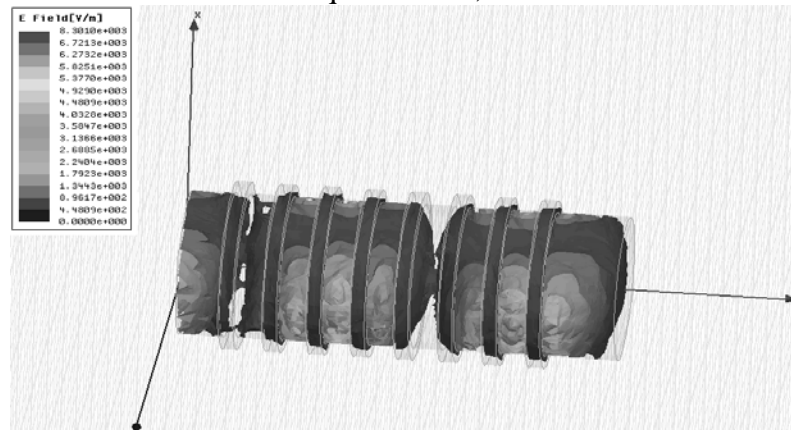


Figure 6. Modelling of the coaxial ribbed line.

Operating an electromagnetic field and dielectric permeability between a ridge surface and the screen, it is possible to achieve the demanded slowing down coefficient with a set

working frequency [7]. Electric field distribution near the surface has periodic structure. The wave extends from microwave input port to output port without attenuation.

It was shown that possibility of use of an electrode based on the coaxial ribbed line for transurethral microwave thermotherapy. The theoretical ratios received as a result of the electrodynamic analysis allow to calculate electromagnetic slow-wave phase speed change in the coaxial line with ribbed conductors and they are in good compliance with results of physical experiment. Application of such structure represents practical interest at creation electrodes for physical therapy.

Acknowledgements

The authors wish to acknowledge the funding, received within the research grant (No.13-05-0017) under The National Research University Higher School of Economics.

References

1. V.V. Ocavitov, "Practice of TUMT operations", M: "Mirmed", 2005.
2. T.I. Izyumova, V.T. Sviridov, "Waveguide, Coaxial and Strip Lines", M: Energiya, 1975, 112 p.
3. A.A. Yelizarov, Yu.N. Pchelnikov, "Radio-Wave Elements of Technological Devices with the Use of Electro-Dynamic Slow-Wave Structures", M: Radio and Communications, 2002, 200 p.
4. Yu. N. Pchelnikov, V. A. Pisarevskiy, R.M. Dymshits, and N. I. Dannikov, Patent SU 1117740, B. I. # 37, 1984.
5. Yu.N. Pchelnikov, "Coaxial Line with Ribbed Electrodes", M: Izd.- MIEM, 1985, 19 p.
6. Pchelnikov Yu. N. and Yelizarov A. A., "Calculation of Wave Impedance of Slow-Wave Systems at Relatively Low Frequencies", Journal of Communications Technology and Electronics, 1995, Vol. 40, # 8, p. 4-7.
7. A.A. Yelizarov, R.V. Shaymardanov, "Electrode research based on the coaxial ribbed line for treatment of a good-quality prostate gland giperplaziya" in material of V Troitsk conference: Medical physics and innovations in medicine, TKMF-5, Troitsk, 2012, Vol.2, p. 294-296.

AN APPROACH TO COMPLEX SYSTEMS SENSITIVITY ESTIMATION ON THE BASIS OF REGIONS OF ACCEPTABILITY

Nazarov D.

Vladivostok, Institute of Automation and Control Processes

The task of analysis of analog systems sensitivity to their parameter variations is considered. An approach to sensitivity estimation based on application of information on the system regions of acceptability is offered.

Keywords: computer-aided design, reliability, system sensitivity, region of acceptability.

Introduction

Analog system design usually includes a task of its components parameter sizing with account of reliability requirements. Manufacturing, storing and especially exploiting of engineering systems are unavoidable associated with parameter variations under both environmental and internal factors which may lead to system performances variation. Variations of system performances can be qualified as system fault and bring to adverse

consequences. Reliable engineering system design should include research of parameter variations and their influence on system performances. One of the approaches to parameter variations research is based on exploiting of information on regions of acceptability. Region of acceptability (RA) is a set of points inside system parameter space which yield proper system performance. Exploration of RA allows to research parameter variations without expensive computations of system performances.

Region of Acceptability Definition

From a consumer point of view, a system has its performance characteristics (gain, temperature, voltage, etc.). The performances are given as m -vector (1):

$$\mathbf{y} = (y_1, y_2, \dots, y_m) \cdot \quad (1)$$

From a design point of view, any system consists of elements/components that perform their functions. These elements are considered to be atomic. Thus, system parameters are considered as the n -vector:

$$\mathbf{x} = (x_1, x_2, \dots, x_n) \cdot \quad (2)$$

System parameters (2) are usually bounded with tolerances (3):

$$\mathbf{x}_{\min} \leq \mathbf{x} \leq \mathbf{x}_{\max} \cdot \quad (3)$$

System performances (1) depend on parameters (2) of system elements (system parameters). System topology is defined by the model (4) which relates system parameters (2) to the system performances (1):

$$\mathbf{y} = \mathbf{y}(\mathbf{x}) \cdot \quad (4)$$

System components are influenced by different factors like ambient temperature, supply voltage, radiation, etc. These factors are usually taken into account in the model (4) as operational parameters and cannot be controlled by the designer. Operational parameters and aging factor cause deviations of system parameters which, consequently, cause system performances deviations. Usually, system performances (1) are constrained by performance specifications (5):

$$\mathbf{y}_{\min} \leq \mathbf{y}(\mathbf{x}) \leq \mathbf{y}_{\max} \quad (5)$$

The deviations of system parameters may cause violation of performance specifications (5) that means system failure. The task of parametric synthesis [1] as one of design stages consists in nominal parameters choosing to meet the performance specifications (4) with the account of system parameter deviations during operating cycle. The solution of this task is often associated with determination of a region of acceptability as defined in (6):

$$D_x = \{\mathbf{x} \in \mathbf{R}^n \mid \mathbf{y}_{\min} \leq \mathbf{y}(\mathbf{x}) \leq \mathbf{y}_{\max}\} \cdot \quad (6)$$

The region of acceptability and schematic illustration of system parameter deviation from nominal values \mathbf{x}^0 at the moment t_0 to gradual parametric failure at the moment t_2 are presented in Figure 1.

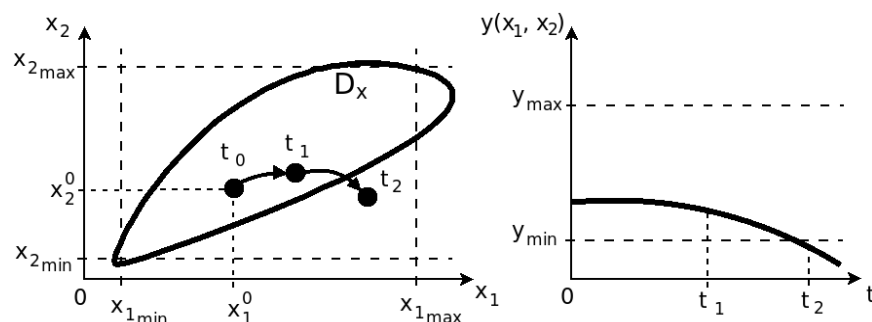


Figure 1. The region of acceptability and gradual parametric failure.

Grid Representation of a Region of Acceptability

As it was said before, the approximation of a n -dimensional region with a discrete set of elementary hyper-parallelepipeds (boxes) is used in this work. The basis of such representation of a region is a n -dimensional regular grid inside a bounding box (circumscribed box [1] or parameter tolerances box (2))

Grid nodes (7) define corners of the elementary boxes:

$$x_{ij} = x_{i0} + j \cdot h_i, \quad (7)$$

where $i=1,2,\dots,n$ is an index of a parameter, $j=0,1,\dots,q_i$ is the node index for i -th parameter (the first node $x_{i0} = x_{i \min}$), $h_i = (x_{i \max} - x_{i \min}) / q_i$ is the grid spacing for i -th parameter, q_i – is the amount of “quanta” – the atomic intervals into which the range $[x_{i \min}, x_{i \max}]$ is divided. For each x_i inside a “quantum” $\partial y / \partial x_i = 0$ is supposed. Every “quantum” is indexed with $k_i = 1, 2, \dots, q_i$, thus the set of indices (k_1, k_2, \dots, k_n) identifies an elementary box. It is supposed that every point \mathbf{x} inside an elementary box yields the same performances as its central point $\mathbf{x}_c(k_1, k_2, \dots, k_n)$ with the coordinates defined in (8):

$$x_{i_c}^{k_i} = x_{i0} + k_i \cdot \frac{h_i}{2}, \quad \forall i = 1, 2, \dots, n. \quad (8)$$

Every point $\mathbf{x}_c(k_1, k_2, \dots, k_n)$ acts as a sampling point for elementary box identified by the indices (k_1, k_2, \dots, k_n) . System performances (1) are calculated for every elementary box's sampling point using the model (3). Then these performances are compared with performance specifications (4). Thus, for every elementary box, the binary function (9) is calculated:

$$F_{D_x}(k_1, k_2, \dots, k_n) = \begin{cases} 1, & \mathbf{y}_{\min} \leq \mathbf{y}(\mathbf{x}_c(k_1, \dots, k_n)) \leq \mathbf{y}_{\max} \\ 0, & \text{otherwise} \end{cases}. \quad (9)$$

The function (9) determines the membership of a sampling point in the region D_x . Let us denote the set of elementary boxes B_g , then the function (9) defines a partitioning (10) of this set:

$$B_g = B_g^0 \cup B_g^1, \quad B_g^0 \cap B_g^1 = \emptyset. \quad (10)$$

The subset B_g^1 is the approximation of the region of acceptability D_x , constructed with a discrete set of elementary boxes, defined with a regular grid.

The region of acceptability approximation with a grid is defined with the model (11):

$$G_R = (n, B, Q, S), \quad (11)$$

where n is the amount of designable system parameters (2), $B = \{(x_{i \min}, x_{i \max}), \forall i=1, 2, \dots, n\}$ is a bounding box, defined by the constraints (3) in system parameter space, $S = (s_1, s_2, \dots, s_n)$ is a set of membership indicators that store results of membership function (9). Every indicator $s_p \in \{0, 1\}$ displays the membership of the corresponding elementary box in subset B_g^1 or B_g^0 , $R = q_1 \cdot q_2 \cdot \dots \cdot q_n$ is the amount of elementary boxes and, consequently, the amount of membership indicators. The one-to-one correspondence between indices (k_1, k_2, \dots, k_n) and the index p of an indicator in the set S is defined in (12). It is evident, that zero-based indices are preferable.

$$p = k_1 + q_1 \cdot (k_2 - 1) + q_1 \cdot q_2 \cdot (k_3 - 1) \cdot \dots \cdot q_1 \cdot q_2 \cdot \dots \cdot q_{n-1} \cdot (k_n - 1). \quad (12)$$

The process of the region of acceptability construction on the basis of the model (11) was described in the work [2]. Briefly, this process consists in complete enumeration of the values of index p with calculation of corresponding indices (k_1, k_2, \dots, k_n) , calculation its sampling point (8), calculation of membership function (9) and assigning its result to the indicator s_p . The illustration of the result of this process and indicators assignment is presented in Figure 2.

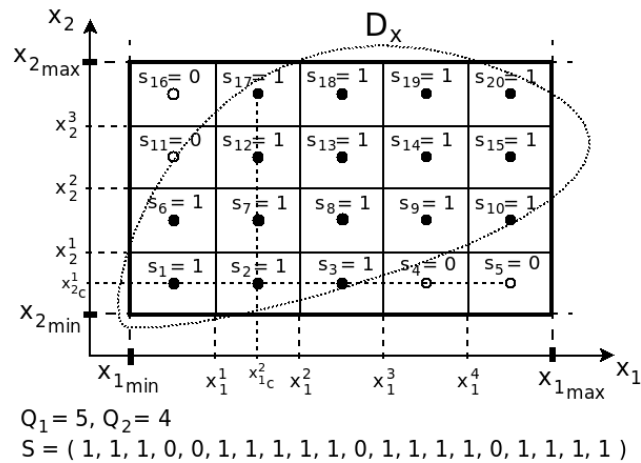


Figure 2. A region of acceptability approximation with a regular grid.

System Sensitivity Estimation based on Region of Acceptability

Sensitivity estimation is based on calculation of distances from every elementary box to the border of RA. In the terms of grid representation of RA, the border of RA is a set of elementary boxes with indices (k_1, k_2, \dots, k_n) and corresponding membership indicator $s_p = 1$ that have at least one neighbor with $s_p = 0$ or at least one index $\exists j: k_j = 1 \vee k_j = q_j$. Neighbor box differs only one coordinate: $\exists! j \in \{1, 2, \dots, n\}: k_j^* = k_j \pm 1, k_i^* = k_i, i \neq j$ (Figure 3).

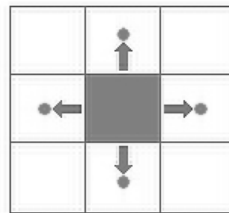


Figure 3. Neighbor boxes for 2-dimensional space

Every elementary box is given a weight of minimum distance to RA border measured for a specified parameter k_i (Figure 4).

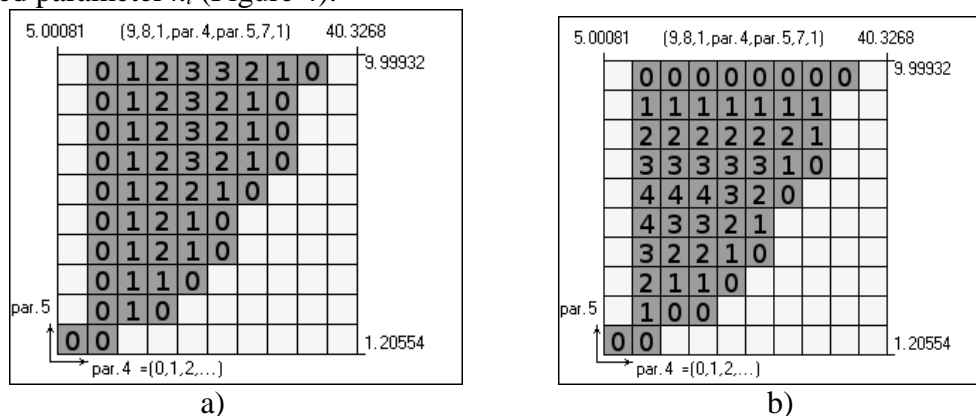


Figure 4. System sensitivity analysis for specified 2D section of RA.

- a) *minimal distance calculation for parameter 4;*
- b) *minimal distance calculation for parameter 5;*

Figure 4 illustrates that considered system is more sensitive to variations of 4-th parameter than 5-th.

Conclusion

Regions of acceptability can be applied to estimation of sensitivity of analog systems. Grid representation of RA allows calculating distances to RA border to estimate relative sensitivity of the system to parameter variations. The algorithm requires complete enumeration of elementary boxes inside RA which has exponential complexity. Nevertheless, this complexity often can have less computational cost than system performances calculation.

This work is supported by Russian Foundation of Basic Research No. 14-08-31291

References

1. O.V. Abramov, Y.V., Katueva, and D.A. Nazarov, “Reliability-Directed Distributed Computer-Aided Design System,” Proc. Of the IEEE International Conference on Industrial Engineering and Engineering Management. Singapore, 2007, pp. 1171 – 1175.
2. O.V. Abramov, D.A. Nazarov, “Regions of Acceptability for Reliability Calculation and Creation,” Proceedings of the 7th International Conference on “Mathematical Methods in Reliability: Theory. Methods. Applications. (MMR2011)” / edited by Lirong Cui & Zian Zhao. - Beijing: Beijing Institute of Technology Press, 2011, pp. 600 - 606.

NONLINEAR TRANSPORT AND OPTICAL PROPERTIES OF QUANTUM DOTS FOR NANOMEDICINE

V. D. Krevchik¹, M. B. Semenov¹, R. V. Zaitsev¹, P. V. Krevchik¹, A. K. Aringazin², K. Yamamoto³

¹*Penza State University of Russia, Russia,* ²*Eurasian National University, Kazakhstan,*

³*International Medical Center, Japan*

The aim of this work is theoretical and experimental study of the effect of doping for semiconductor quantum dots on their photoluminescence (PL), which has important applications both for nanomedicine and nanoelectronics devices to create the controlled properties. An experimental study of the surface treatment effect for quantum dots (QDs) of CdSe on their photoluminescence (PL) has been fulfilled. It is shown that the highest intensity of photoluminescence yield QD with surface treated by the donor electron impurity. The role of the QD doping by impurities has been theoretically studied. It is shown that the PL intensity in this case can be increased considerably. The development of the 1D - dissipative tunneling theory for structures with quantum dots in the system of combined AFM / STM in an external electric field at a finite temperature has been proposed. The probability of the 1d - dissipative tunneling in a double-well model oscillator potential in the external electric field with accuracy of the pre-exponential factor has been calculated. Theoretical investigation of features for the field dependence of the tunnel probability is allowed to offer the controlled growth method of colloidal gold QD, based on the transformation of the oscillator double-well potential in the external electric field. The applicability of nanoscale dots (QD) from colloidal gold for nanomedicine has been discussed. For example, QD from colloidal gold are used as carriers of drugs, as well as for the diagnosis and treatment of cancer. Optical response for QD from colloidal gold (surface enhanced Raman spectroscopy) is 200 times brighter than for semiconductor quantum dots. Optical and transport properties of the doped semiconductor QDs with bio-conjugated shells can be used as fluorescent labels for imaging of biological objects and in nanomedicine for the diagnosis and treatment of a number of serious diseases, including cancer.

The problem of controllability for 2D - tunnel bifurcations in systems with quantum molecules in a dielectric matrix of a metamaterial in the external electric field at finite

temperature has been investigated. Usage of the quantum tunneling with dissipation theory to study the interaction of quantum molecules with contact environment is productive, because, despite of the instanton approach usage, it is possible to obtain the main results in the analytical form with account of the environment influence on the process of tunneling, whereas other commonly used approaches give not such possibility. A theoretical study of the electric field influence on the 2D-quantum tunneling for quantum molecules in the matrix of a metamaterial (with negative effective permittivity) at finite temperature has been fulfilled in the instanton approximation. It is shown that a stable regime of 2D - bifurcations in such matrix can take place in a more narrower range of parameters than in case of usual dielectric matrix. An important problem in this case is to identify the range of experimentally realizable values of the relative dielectric permittivity (including negative values) for the matrix environment, which allow to realize the 2D – bifurcations regime. A range of the control parameters (electric field, temperature, and the relative permittivity of the metamaterial matrix), in which the regime of stable 2D - bifurcations in the system of quantum molecules, as well as in the system "AFM / STM cantilever – quantum dot or quantum molecule" can take place, has been theoretically investigated.

1. Introduction

The last few years the number of experimental and theoretical research in the field of optics for nanostructures with impurity centers has dramatically increased. Success in the development of methods for the synthesis of fluorescent nanocrystals (quantum dots (QDs)) with desired properties and methods for functionalizing of the QD-surface has opened ways of the new class of fluorophores creation for many biological and medical applications. Fluorescent nanocrystals are detected as individual objects with usage of conventional fluorescence microscopes that can help to visualize the processes at the single molecule. The advantage of nanocrystals in comparison with organic fluorophores is their high brightness due to the large value of the absorption coefficient, a unique high photostability and the narrow, symmetrical peak of emission. The wavelength of photoluminescence (PL) for nanocrystals is strictly dependent on their size, and for all colors of nanocrystals the excitation of only one radiation source is necessary. Such unique properties of nanocrystals make its as ideal fluorophores for ultrasensitive, multicolor detection in biological and medical diagnosis that requires registration of many parameters simultaneously.

Currently, a new class of materials, known as metamaterials [1], with unique properties in a certain frequency range, is of great interest. Metamaterials are the artificial composite materials consisting of a dielectric or conductive elements that form a regular structure, which are characterized by a negative effective permittivity and permeability (ϵ and μ) and, accordingly, a negative refractive index. On the basis of such materials it is possible to develop a number of unique devices [1], such as flat electromagnetic lenses that do not have the diffraction limit (superlens), masking the shell, and so such properties cause the increased interest in their practical implementation. In addition, the problem of control for nanostructures, which are in the matrices of metamaterials, is of great interest. In this paper we investigate the problem of controllability for 2D - tunnel bifurcations in systems with quantum molecules in a dielectric matrix of the metamaterial in the external electric field at finite temperature. Usage of the quantum tunneling with dissipation theory to study the interaction of QM with contact medium is productive, because, despite of usage of the instanton approach it is possible to get the main results in an analytical form with account of the environment effects on the tunneling process, which it is not possible in other often used approaches [2]. It is experimentally possible to observe earlier theoretically predicted 2D - bifurcations for QD from colloidal gold in the matrix of a conventional insulator on the tunneling current-voltage characteristics in the system of combined AFM / STM [2]. An

important problem is to reveal the experimentally realizable range of values of the relative dielectric constant for the matrix environment, allowing 2D – bifurcations regime, including negative values, which corresponds to the matrix of metamaterials. The aim of this work is to theoretically study the range of control parameters (electric field strength, temperature, and the relative dielectric constant of matrix of the metamaterial), in which the regime of stable 2D - bifurcations in the QM system can be realized, as well as in system with " the cantilever needle of combined AFM / STM - QD or QM". Special attention is paid to the problem of control in a two-dimensional dissipative tunneling for system of interacting QM, simulated by 2D - oscillator potential in the medium with negative dielectric permittivity in an external electric field.

2. The fluorescence intensity of the quantum dots in the water depends on the surface processing

Various materials, such as semiconductor, metals and lattices are used for synthesize the quantum dots with recent nano-technology. Many kinds of characters on the quantum dots have been reported on quantum dot films of semiconductor and electron packed metals. One of the important characters, we focus on the surface treatment of the quantum dot. The cytotoxicity is reported to depend on the surface processing. That is the interaction of the surface of the molecules of the cell and the surface of the quantum dot plays a key roll for the safety for human being and the environment. The size of the aggregation also depends on the surface treatment. The intensity of the fluorescent light and the surface treatment of the quantum dot will be studied in this report.

2.1. Material and methods

Red colored quantum dot and yellow colored quantum dot was made as from Cadmium and selenium by the hot soap method with trioctylphosphine oxide (TOPO). Then, the shells of both of the quantum dots were covered with mercapto-zinc. Here, we obtain the quantum dots that are not solvable to the water. Then, the surface of the quantum dots, TOPO were exchanged by the water solvable molecules such as 11-mercapto-undecanoic acids and mercapto-glycerol. Vero cell, the kidney cell of the African green monkey, was cultured with the standard methods. Fluorescent microscope system (OLYMPUS) was used for the observation. Measurement of the photo-luminescent spectra with the time course was done by JASCO fluorescence spectrophotometer. Measurement of the zeta potential and the particle size was done by zeta potential and particle size measurement system (SYSMEX).

2.2. Results and discussion

The more the emission light is dosed, the larger the fluorescent intensity of the quantum dot becomes, which is known as the light memory effect [1]. This effect was found not in the water but in the dry film at first. We have found this memory effect also occurs in the water with the appropriate surface processing of the quantum dot. This effect does not continue infinitely. That is after a while, the intensity of the fluorescent come to the maximum and, after that, comes down. The wavelength of the fluorescent light becomes short in the meantime. One of the ideas for the movement of the wavelength of the fluorescent to the short wave length is the light etching. It is reported the quantum dot of the mercapto-cadmium can be produced with the laser light etching from the bulk material. In our case of cadmium seren quantum dot, it might also true. But we have not any data for the evidence of the difference of particle size yet. Another idea for the effect would be the oxidization of the quantum dot by laser light dose. The electron might skip away from the surface might lead to the oxidization from the outside of the quantum dot. So far now, we use the Cd/Se quantum dot with the ZnS processed as the surface of the particle. As this nano-particle is not water soluble, we use mercapto undecanoic acids, mercapto glycerol, and mercapto amine for the surface processing to get the hydrophilicity. We measured the zeta potential of the surface of these three different treated quantum dot. The quantum dot treated with the mercapto undecanoic acids is

negatively charged, that with the mercapto amine is positively charged and that with the mercapto glycerol is the neutral. The quantum dot treated with mercapto-organic acid showed the highest intensity of the fluorescent light, the quantum dot treated with mercapto glycerol the middle, and the quantum dot treated with mercapto-organic amine, the lowest intensity. Zeta potential from the minimum to the maximum is just the reverse order with the intensity of the fluorescent light, (from strong to weak). It seems the surface electric potential has the key role for the fluorescent intensity. Different surface treatment will result in the different zeta potential of the quantum dot. In the previous study, we have reported the cytotoxicity is also depend on the surface treatment rather than the inside, the quantum dot itself. The conjugation of the quantum dot with the bio-molecule such as protein, sugar and nucleic acids will change the zeta potential which lead to speculate that the measurement of the zeta potential of the bio-molecule predict roughly the fluorescent intensity of the conjugated bio-molecule quantum dot complex.

2.3 The electron donor agent and the intensity of the fluorescent light

We added the electron donor agent in order to see if the intensity of the fluorescent light of the quantum dot will become strong. We used sodium azide for the electron donor agent. We used the quantum dot, the surface of which was treated with mercapto-undecanoic acids for this experiment. In this study, we have some evidence of the importance of the surface electric potential of the quantum dot to get the strong fluorescent light. We have studied to add the electron scavenger agents into the water solution of containing the water soluble quantum dots. The fluorescent light became very weak. Under this condition, we added the electron donor agents and found the recover of the strong fluorescent. One of the application for this effect is the way to recover the fluorescent light and to find the quantum dot tagged cell in the organ with the microscope.

3. The influence of two-dimensional dissipative tunneling on probability for two-photon ionization of d - center in a system of two interacting quantum molecules

Currently, two-photon (TF) spectroscopy is widely used for studying of the band structure in low-dimensional systems [1,2] as a non-destructive method for the information readout in three-dimensional optical memory devices [3], to study the coherence properties of radiation [4], and also in many other applications. Development of technology for creation of quantum molecules (QM) (tunnel-coupled QDs) requires broadening of the TF – spectroscopy possibilities, in particular, in relation to investigation of the dissipative tunneling features. Usage of the science of quantum tunneling with dissipation to study the interaction of QM with contact medium is productive, because, despite the use of the instanton approach it is possible to get the main results in an analytical form for the effects of environment on the tunneling process, which it is not possible in other often used approaches. One of the aims of this work is the theoretical study of TF impurity absorption in QM, under 2D-dissipative tunneling in the presence of an external electric field.

3.1 The two-photon impurity absorption spectra features for quantum molecules

Probability of two-photon ionization for D(-) – center in quantum dot $W(2\omega)$ with the parabolic confinement potential under influence of external electric field with account of the Lorentz broadening for energy levels of virtual and final states in QD, can be written as

$$W(2\omega) = B_0 \sum_{n_1, n_2, n_3} \frac{\left[(\beta^{-1}(n_1 + n_2 + n_3 + \frac{1}{2}) - W_0^* + \eta^2)^2 + \hbar^2 \Gamma_0^2 / E_d^2 \right] X^{-2}}{\left[(\beta^{-1}(n_1 + n_2 + n_3 + \frac{1}{2}) - W_0^* + \eta^2 - X)^2 + \hbar^2 \Gamma_0^2 / E_d^2 \right] ((n_2/2)!(n_3/2)!)^2} \times$$

$$\times \left\{ \frac{\exp(x_0^{*2} / a_0^{*2}) \Gamma(\beta(\eta^2 - W_0^*) / 2 + 7/4)}{\pi(\beta(\eta^2 - W_0^*) / 2 + 3/4) \Gamma(\beta(\eta^2 - W_0^*) / 2 + 1)} \left[(\beta(\eta^2 - W_0^*) / 2 + 3/4) \times \right. \right.$$

$$\left. \left. (\psi(\beta(\eta^2 - W_0^*) / 2 + 7/4) - \psi(\beta(\eta^2 - W_0^*) / 2 + 1)) - 1 \right] \right\}^{-1} \times$$

$$\times 2^{-5(n_1+n_2+n_3)-3} \cdot n_1!n_2!n_3! \int_0^\infty dt (1-e^{-2t})^{-1/2} \exp[-(\beta(\eta^2 - W_0^*) + n_2 + n_3 + 3/2)t] \times$$

$$\times \sum_{m=0}^{[n_1/2]} (-1)^m f(x_0^*, t) \frac{\exp(f(x_0^*, t)/4)}{m!(n_1 - 2m - 1)!} \left[x_0^*(n_1 - 2m - 1) \sum_{k=0}^{[(n_1 - 2m - 1)/2]} \frac{f(x_0^*, t)^{-k}}{(n_1 - 2m - 2k - 1)!k!} - \right.$$

$$\left. - a_0^*(n_1 - 2m) \sum_{k=0}^{[(n_1 - 2m)/2]} \frac{f(x_0^*, t)^{1-k}}{2(n_1 - 2m - 2k)!k!} \right]^2 \times \frac{\Gamma_0}{(3\beta^{-1}/2 - W_0^* + \eta^2 - X)^2 + \hbar^2 \Gamma_0^2/E_d^2},$$

where $B_0 = 2(a_0^* \beta \lambda_0)^4 (a_d \alpha^*)^2 \hbar I_0 / E_d$; λ_0 - the local field coefficient; α^* - the fine structure constant with account of dielectric permittivity; I_0 , ω - intensity and the light frequency, correspondingly; $X = \hbar \omega / E_d$ - the photon energy in units of effective Bohr energy; $f(x_0^*, t) = x_0^{*2} (2e^{-t} + e^{-2t}) / a_0^{*2}$; $\psi(x)$ - logarithmic derivative for Γ - function. The calculation process has identified the following selection rules: the optical transitions from the impurity level are possible only to the size-quantized states of QD with even quantum numbers n_2, n_3 and with the value of the quantum number $n_1 = n'_1 + 1$ ($n'_1 = 0, 1, 2, \dots$). The tunnel probability $\Gamma_0 = B \exp(-S)$ for quantum molecule has been calculated in frames of the tunneling with dissipation theory.

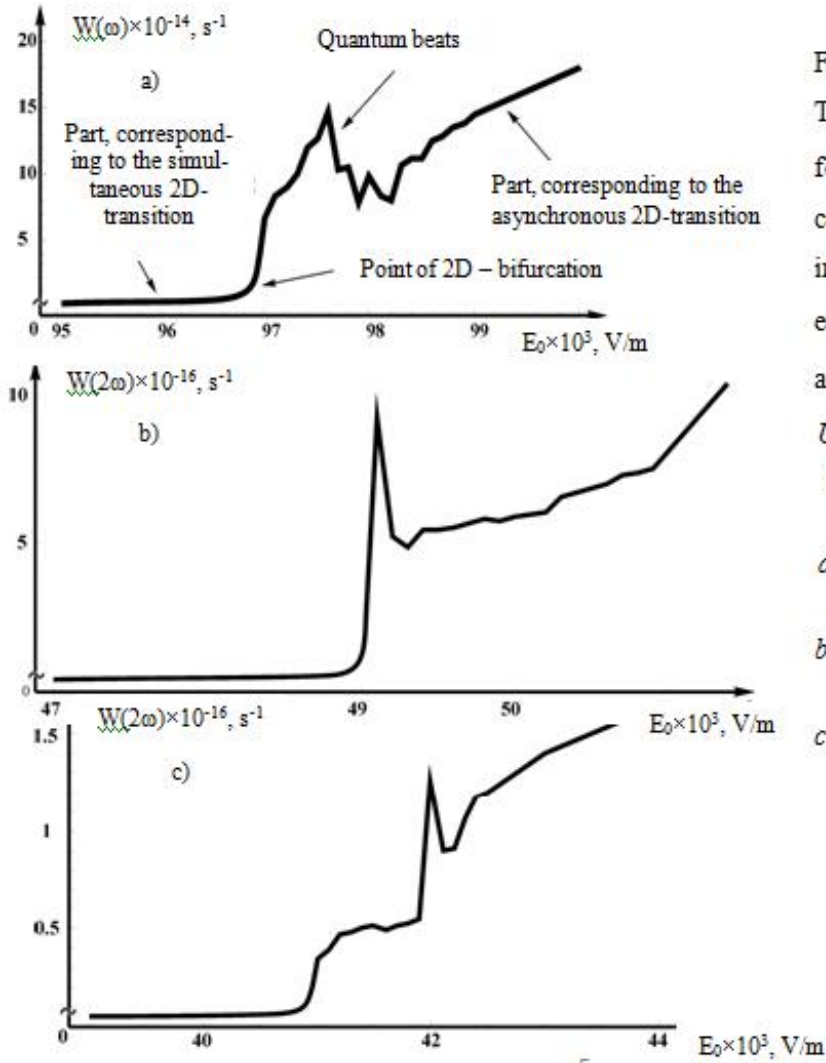


Fig. 1 The dependence of TF- ionization probability for $D^{(-)}$ - center in system, consisting of two interacting QM from intensity of external electric field E_0

at

$$U_0^* = 250, \alpha_0 = 1, b_0 = 1.5, \eta_i$$

$$\varepsilon_L = 1, \varepsilon_C = 1:$$

$$a - \alpha = 0.38, \varepsilon_T = 1;$$

$$b - \alpha = 0.37, \varepsilon_T = 1;$$

$$c - \alpha = 0.37, \varepsilon_T = 1.5.$$

3.2. Features of the tf – impurity absorption under 2d – dissipative tunneling

Fig. 1 shows the calculated dependence of the TF- ionization probability of the $D^{(-)}$ - center in system consisting of two interacting QM from the magnitude of the external electric field under 2D- dissipative tunneling. It can be seen from Fig. 1 that for the field dependence

of the TF – impurity absorption probability corresponds the characteristic kink point - bifurcation - as a result of change in the dissipative tunneling regime from synchronous to asynchronous. It is evident, too, that in a small neighborhood of the bifurcation point, the regime of quantum beats, associated with the existence of competing solutions under search of 2D - instanton, can be realized. It can be seen, that with increase of coupling constant α the bifurcation point is shifted to the region of more strong fields (cf. Fig. 1a and Fig. 1b), due to the symmetry change of 2D - potential by increasing of the Coulomb repulsion for the tunnel particles. A similar situation occurs with decreasing temperature (parameter ε_T) (cf. Fig. 1c and 1b). With reduction of the parameter ε_T the 2D – tunnel probability is reduced and hence, the more high value of the external electric field is required to the increase of the potential asymmetry. Thus, the effects of bifurcations and quantum beats are strongly depended on such parameters of 2D- tunneling, as temperature and the interaction constant of tunnel particles. The role of the external electric field is reduced to the restoration of 2D – potential asymmetry, which is necessary for the appearance of 2D- bifurcations.

4. Probability of 2d - tunneling under external electric field in matrix of the metamaterial

We consider the simultaneous tunneling transfer of two particles which weakly interact with each other. If there is no interaction, each of the particles moves independently in its own double-well potential. We will study the effect of the particle interaction on the tunneling regime change from synchronous to asynchronous (the effect of 2D - bifurcation ([2-10])) as a function of interaction with the heat - bath in an external electric field. With the introduction of the interaction between particles in the dipole - dipole approximation, we choose V_{int} in the form of a harmonic "attraction" potential

$$V_{\text{int}} = - \frac{\alpha(q_1 - q_2)^2}{2}. \quad (1)$$

The function of the potential energy for interaction can be represented as a series in powers of parameter $\frac{(q_{1t} - q_{2t})^2}{R_0^2}$, where q_{1t} and q_{2t} - are tunnel coordinates, R_0 - the distance between the tunneling "channels". For the Coulomb repulsion of the particles in the medium (ε_0 - dielectric constant, ε - relative dielectric constant) we get

$$V_{\text{rep}} = \frac{e^2}{\varepsilon\varepsilon_0|R|} = \frac{e^2}{\varepsilon\varepsilon_0 \sqrt{R_0^2 + (q_{1t} - q_{2t})^2}} \gg \frac{e^2}{\varepsilon\varepsilon_0 R_0} - \frac{1}{2} \frac{e^2}{\varepsilon\varepsilon_0 R_0} \frac{(q_{1t} - q_{2t})^2}{R_0^2}. \quad (2)$$

Hence, $\alpha = \frac{e^2}{\varepsilon\varepsilon_0 R_0^3}$. (where $\varepsilon < 0$ for the metamaterial matrix). Negative harmonic

potential energy (the second term in the expansion) appears, therefore, as an effective attractive interaction, although the potential is always repulsive. This negative contribution reduces repulsive potential of its maximum value in R_0 . The constant component

$U(R_0) = \frac{e^2}{\varepsilon\varepsilon_0 R_0}$ may be included in the definition of the potential energy for the individual

particles $U(q_1)$ and $U(q_2)$. The influence of an electric field can be accounted for by the

renormalization parameter $a = \tilde{a} = a_0 + \frac{|e|E}{\omega_0^2}$, $b = \tilde{b} = b_0 - \frac{|e|E}{\omega_0^2}$. For 2D - parallel transfer with

account of the particles interaction and with the renormalization of the potential parameters in an external electric field, we obtain the renormalized potential in the next form

$$U_p(q_1, q_2) = \frac{2\tilde{U}_p(q_1, q_2)}{\omega^2} = (q_1 + a)^2 \theta(-q_1) + \left[-(b^2 - a^2) + (q_1 - b)^2 \right] \theta(q_1) + (q_2 + a^2) \theta(-q_2) + \left[-(b^2 - a^2) + (q_2 - b)^2 \right] \theta(q_2) - \frac{\alpha^*}{2} (q_1 - q_2)^2. \quad (3)$$

We assume that two particles interact independently with the harmonic thermostat (a heat – bath). This interaction is considered in the bilinear approximation. Oscillatory dynamics of the medium is described by the Hamiltonian (we have used the system of units, in which $\hbar = 1$, $k_B = 1$, and the mass of the oscillators are 1).

$$H_{ph} = \frac{1}{2} \sum_i (P_i^2 + \omega_i^2 Q_i^2). \quad (4)$$

Each of the tunneling particles (electrons or effective charges) interacts with the oscillator thermostat as follows:

$$V_{p-ph}^{(1)}(q_1, Q_i) = q_1 \sum_i C_i Q_i, \quad V_{p-ph}^{(2)}(q_2, Q_i) = q_2 \sum_i C_i Q_i, \quad (5)$$

As in [3], we are interested in the probability of transfer per unit time or, strictly speaking, only in the exponential part of it, which can be written in the Langer form

$$\Gamma = 2T \frac{\text{Im} Z}{\text{Re} Z}. \quad (6)$$

To calculate Γ , it is convenient to represent the partition function in the form of the path integral [1-10]

$$Z = \prod_i \int Dq_1 Dq_2 DQ_i \exp[-S\{q_1, q_2, Q_i\}]. \quad (7)$$

Here S is the sub-barrier action for the entire system. The imaginary part $\text{Im} Z$ appears due to the decay of the energy levels in the initial well of the potential energy. The validity of this approach requires that the dissipation would be enough strong, so, the only incoherent decay is realized [3].

The integral (7) can be taken over the phonon coordinates [3], in result we obtain

$$S\{q_1, q_2\} = \int_{-\beta/2}^{\beta/2} d\tau \left[\frac{1}{2} q_1^2 + \frac{1}{2} q_2^2 + V(q_1, q_2) + \int_{-\beta/2}^{\beta/2} d\tau' D(\tau - \tau') [q_1(\tau) + q_2(\tau)] \times [q_1(\tau') + q_2(\tau')] \right], \quad (8)$$

$$\text{where } D(\tau) = \frac{1}{\beta} \sum_{n=-\infty}^{\infty} D(v_n) \exp(i v_n \tau), \quad (9)$$

$\beta = \hbar / (k_B T)$ - inverse temperature (we assume that $\hbar = 1$ and $k_B = 1$), $v_n = 2\pi n / \beta$ is the Matsubara frequency, and

$$D(v_n) = - \sum_i \frac{C_i^2}{\omega_i^2 + v_n^2} - \sum_i \frac{C_i^2}{\omega_i^2} + \xi_n. \quad (10)$$

The trajectory that minimizes the Euclidean action S , can be found from the equations of motion. The moments of time, τ_1 and τ_2 , in which particles transfer the top of the barrier, are determined by the following equations:

$$q_1(\tau_1) = 0, \quad q_2(\tau_2) = 0. \quad (11)$$

Once a path is found, the equation (11) can be represented in the following form:

$$\sinh \varepsilon \left[\cosh \tau \coth \beta^* - \sinh \tau - \coth \beta^* \right] + \frac{1}{1 - \alpha^*} \sinh \left(\varepsilon \sqrt{1 - \alpha^*} \right) \left[\cosh \left(\tau \sqrt{1 - \alpha^*} \right) \times \right.$$

$$\begin{aligned}
& \times \coth\left(\beta^* \sqrt{1-\alpha^*}\right) - \sinh\left(\tau \sqrt{1-\alpha^*}\right) + \coth\left(\beta^* \sqrt{1-\alpha^*}\right) \Big] = 0, \\
& 3 - \frac{4}{1+b^*} - \frac{1}{1-\alpha^*} + \cosh \varepsilon \left[\sinh \tau \coth \beta^* - \cosh \tau - 1 \right] + \sinh \tau \coth \beta^* - \cosh \tau + \\
& + \frac{1}{1-\alpha^*} \cosh\left(\varepsilon \sqrt{1-\alpha^*}\right) \left[\sinh\left(\tau \sqrt{1-\alpha^*}\right) \coth\left(\beta^* \sqrt{1-\alpha^*}\right) - \cosh\left(\tau \sqrt{1-\alpha^*}\right) + 1 \right] - \\
& - \frac{1}{1-\alpha^*} \left[\sinh\left(\tau \sqrt{1-\alpha^*}\right) \coth\left(\beta^* \sqrt{1-\alpha^*}\right) - \cosh\left(\tau \sqrt{1-\alpha^*}\right) \right] = 0. \quad (12)
\end{aligned}$$

As we have shown in [2], the solution of this system reveals the bifurcation of the 2D - tunneling trajectories, i.e. at a certain temperature β^* or the potential asymmetry parameter associated with the applied electric field $b^* = b/a$, or the interaction factor $\alpha^* = 2\alpha/\omega^2$ (where $\alpha = \frac{e^2}{\varepsilon \varepsilon_0 R_0^3}$ depends on the relative permittivity of the medium (a heat – bath) for metamaterials $\varepsilon < 0$). Numerical analysis of the system (12) can also allow to identify the fine structure for tunnel transition in the vicinity of the bifurcation point, namely the regime of quantum beats for the parallel transport of tunneling particles. As a result, the probability of 2D - tunneling with exponential accuracy is defined as $\Gamma = \exp(-S)$. The system of equations (12) decision reveals the bifurcation for 2D- tunnel paths for certain values of temperature or for the potential asymmetry parameter (which is connected with the value of an external electric field), or for the interaction factor α , which depends on the relative negative dielectric constant for metamaterials. Numerical analysis of the system (12) can also identify the fine structure for transition in the vicinity of the bifurcation point, i.e. regime of quantum beats for the parallel transport of tunneling particles (in this case apart from the trivial solutions of (12), additional solutions are appeared). The dependence of the tunneling probability on the electric field is shown in Fig. 2. In this figure, the area of the stable 2D – bifurcations is realized. In the vicinity of this point (as in the neighborhood of interruption point for 2D - bifurcation) the quantum beats mechanism is realized, where mechanisms for synchronous and asynchronous transfer for tunneling particles are competing. Region for realization of the 2D – bifurcations stable effect is revealed, as also corresponding limits of the 2D – bifurcation existence are analyzed under change of the control parameters (the inverse temperature β , the relative dielectric constant of the heat–bath - ε for the metamaterial matrix, and the asymmetry parameter for 2D – potential of interacting QM b, which is weakly nonlinear depended on the magnitude of the external electric field).

5. Conclusion

Thus, optical and transport properties of the doped semiconductor QD with bio - conjugated shells can be used as fluorescent labels for visualization of biological objects and in nanomedicine for diagnosis and treatment of a number of serious diseases, including cancer. The experimental check of the predicted effects, such as 2D - bifurcations and quantum beats in the field dependence of the TF - ionization probability for $D^{(-)}$ - center in system, consisting of two interacting QM, is also planned. The predicted effect can be used in high-precision devices of opto-and nano-electronics with controllable characteristics. Thus, the dependence of the electric field strength, at which the stable 2D-bifurcations are realized, on the value of the inverse temperature, has been investigated in this work. In contrast to conventional dielectric matrix in the case of the metamaterial matrix, region of the stable 2D-bifurcations is narrowed considerably, probably due to the sign inversion of the tunneling particles interaction. It should be noted, that the theoretical results, obtained in this article, do not have any quantitative comparison with the experiment, and are only qualitative meaning.

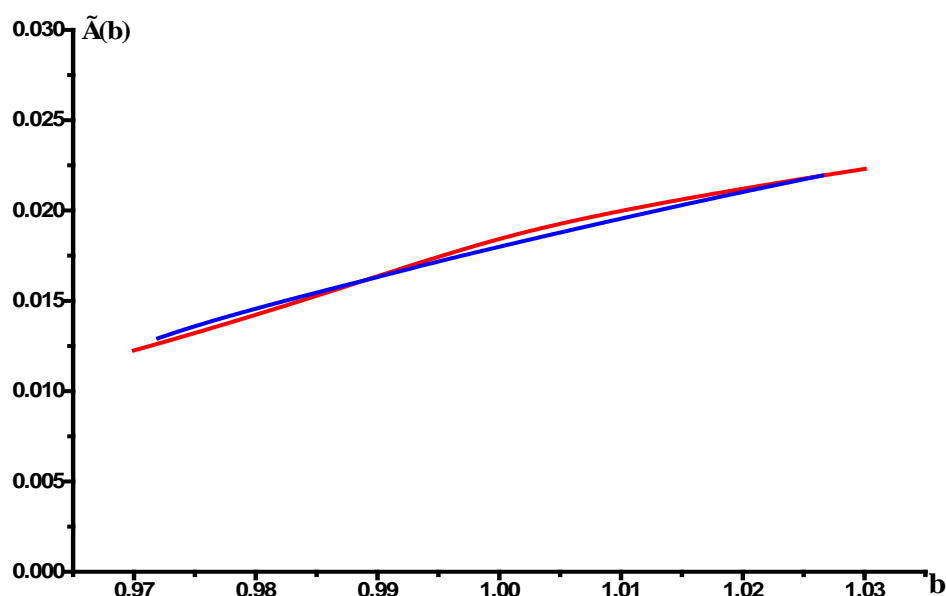


Fig. 2. The dependence of the tunneling probability on the electric field.

References

1. Atusi Kurita, Yasuo Kanematsu, Takashi Kushida Observation of optical memory effect due to interference of multiply scattered light by using a focused beam.// Journal of Luminescence - vol. 98, no. 1, pp. 325-329, 2002 DOI: 10.1016/S0022-2313(02)00287-9
2. Caldeira A.O., Leggett A.J. Influence of dissipation on quantum tunneling in macroscopic systems // Phys. Rev. Lett. – 1981. – V. 46. – № 4. – P. 211–214.
3. Larkin A.I., Ovchinnikov Yu.N. Quantum tunneling with dissipation// JETP Letters – 1983. – V. 37. – № 7. – P. 322–325.
4. Ivlev B.I., Ovchinnikov Yu.N. The decay of metastable states in the presence of close-barrier trajectories// JETP – 1987. – V. 93. – № 2(8). – P. 668–679.
5. Competing tunneling trajectories in a 2D potential with variable topology as a model for quantum bifurcations / V.A. Benderskii, E.V. Vetoshkin, E.I. Kats, H.P. Trommsdorff // Phys. Rev. E. – 2003. – V. 67. – P. 026102.
6. Transfer processes in low - dimensional systems/Edited by: Yu.I. Dahnovsky, V.D. Krevchik, V. Ya. Krivnov, M.B. Semenov, K. Yamamoto. UT Research Institute Press, Tokyo, Japan, (2005), 690 p.
7. Controllable dissipative tunneling. Tunnel transfer in low-dimensional systems (editors: A.J. Leggett, A.K. Aringazin, M.B. Semenov, V.D. Krevchik, Yu.N. Ovchinnikov, K. Yamamoto), M., Fizmatlit 2011-2012, 495 P.
8. Aringazin A.K., Dahnovsky Yu.I., Krevchik V.D., Semenov M.B., Ovchinnikov A.A., Yamamoto K. Two-dimensional tunnel correlations with dissipation // Physical Review B, vol. 68, 2003, P. 155426.
9. I.B. Vendik, O.G. Vendik, M.A. Odit Isotropic metamaterial based on ferro - ceramic spherical inclusions // FSS, 2009, v.51 (num.8), p. 1499-1503.
10. Transfer processes in low - dimensional systems, UT Research Institute Press, Tokyo, Japan, (2005), 690 p., (editors A.J. Leggett, V.D. Krevchik, V.Ya. Krivnov, M.B. Semenov, K. Yamamoto).

NUMERICAL SIMULATION OF THE NATURAL GAS FLOW IN THE SECTION OF THE GAS PIPELINE

Eremin D.V., Ivanov F.F.

Surgut State University, Khanty-Mansiysk Autonomous Region - Ugra

The article considers the numerical simulation of the natural gas flow in the curved section of the gas pipeline in three-dimensional formulation to determine the hydrodynamic parameters of the flow and the level of mechanical effects on the inner wall of the pipe.

Keywords: main gas pipeline, linear part, pipes, natural gas, numerical simulation, gas dynamics

In the general case in hydrodynamics both gas and fluid flows are described by Navier-Stokes differential equations of the motion of viscous compressible fluid (1) which express the law of momentum conservation and by the continuity equation (2) which expresses the law of mass conservation [5]. Here are these equations written in vector-tensor form:

$$\frac{\partial(\rho \vec{u})}{\partial t} + \nabla \cdot (\rho \vec{u} \otimes \vec{u}) = -\nabla p + \nabla \cdot \tau + \vec{F} \quad (1)$$

$$\frac{\partial \rho}{\partial t} + \nabla \cdot (\rho \vec{u}) = 0 \quad (2)$$

where t is time, \vec{u} is the flow velocity vector field at a given time, p is fluid pressure at a given point, ρ is fluid density, \vec{F} is the vector of body forces and τ is the viscous stress tensor:

$$\tau = \mu \left((\nabla \otimes \vec{u}) + (\nabla \otimes \vec{u})^T - \frac{2}{3} \delta (\nabla \cdot \vec{u}) \right)$$

where μ denotes the coefficient of dynamic viscosity. In mathematical expressions of the article the following notation is used: \otimes – tensor product, ∇ – Hamiltonian operator, δ – Kronecker delta and T – matrix transpose operation.

In the general case the liquid density ρ and dynamic viscosity μ are depend from the pressure p of the fluid and the absolute temperature T , that is $f(p, T)$. On the other hand, if the absolute temperature and the pressure of a liquid are a function of spatial coordinates x, y, z and of time t , we get that ρ and μ are the functions of the species $f(\vec{r}, t)$, where $\vec{r} = (x, y, z)$ is the radius vector of the point of the three-dimensional Euclidean space.

Considering isothermal $T = \text{const}$ and incompressible $\rho = \text{const}$ flow and taking viscosity constant $\mu = \text{const}$ we can conclusion that the equation is describing the motion of the fluid and the continuity equation is simplified. So, in the equation of motion (1) the density can be taken out from a sign of the time derivative, respectively, in the equation of continuity (2) the derivative of the density of time equals zero $\partial \rho / \partial t = 0$. As a result of transformation of the initial equations we obtain respectively that the equation of motion (3) and the continuity equation (4) for incompressible fluid are:

$$\frac{\partial \vec{u}}{\partial t} + (\vec{u} \cdot \nabla) \vec{u} = -\frac{1}{\rho} \nabla p + \nu \cdot \Delta \vec{u} + \vec{F} \quad (3)$$

$$\nabla \cdot \vec{u} = 0 \quad (4)$$

where $\nu = \mu / \rho$ is kinematic coefficient of viscosity and Δ is the Laplace operator. For modeling of the turbulence is used k - ε model of turbulence in which the differential equation of the kinetic energy (5) and the equation of the dissipation rate of the turbulent energy (6) are:

$$\frac{\partial(\rho k)}{\partial t} + \nabla \cdot (\rho k \vec{u}) = \nabla \cdot \left(\left(\mu + \frac{\mu_t}{\sigma_k} \right) \nabla k \right) + G_k - \rho \varepsilon \quad (5)$$

$$\frac{\partial(\rho \varepsilon)}{\partial t} + \nabla \cdot (\rho \varepsilon \vec{u}) = \nabla \cdot \left(\left(\mu + \frac{\mu_t}{\sigma_\varepsilon} \right) \nabla \varepsilon \right) + \frac{\varepsilon}{k} (C_{\varepsilon 1} G_k - C_{\varepsilon 2} \rho \varepsilon) \quad (6)$$

where k is the kinetic energy of turbulence, ε is the dissipation rate of kinetic energy, μ_t is turbulence viscosity, σ_k and σ_ε are turbulent Prandtl number, G_k is the generation of turbulence kinetic energy due to the mean velocity gradients and $C_{\varepsilon 1}$, $C_{\varepsilon 2}$ are an empirical constants.

In the modeling of the turbulence the hydrodynamic parameters that describe the flow are sum of average value of that parameter and fluctuating component of that parameter, for example for local velocity we have: $\vec{u} = \bar{\vec{u}} + \vec{u}'$, where $\bar{\vec{u}}$ is the mean value of the velocity at certainly point in the space, \vec{u}' is fluctuating value of the local velocity.

The kinetic energy of the turbulence is expressed through the fluctuating components of the vector of local velocity:

$$k = \frac{1}{2} (\overline{u_x'^2} + \overline{u_y'^2} + \overline{u_z'^2})$$

Dissipation rate of kinetic energy of turbulence is expressed through the components of the tensor of turbulent stresses (Reynolds stress tensor):

$$\varepsilon = 2\nu_t \overline{e'_{ij} e'_{ij}}$$

The Reynolds stress tensor appears as:

$$e'_{ij} = \frac{\partial u'_i}{\partial x_j} + \frac{\partial u'_j}{\partial x_i}$$

Turbulence viscosity is expressed:

$$\mu_t = \rho C_\mu \frac{k^2}{\varepsilon}$$

The physical parameters of the flow of natural gas presented below (tab.1).

Table 1

The physical parameters of the flow of natural gas

Parameter	Symbol	Value
<i>Mean pressure</i>	p	4,4 MPa
<i>Mean velocity</i>	v	14,29 m/s
<i>Gas density</i>	ρ	35,35 kg/m ³
<i>Viscosity dynamically coefficient</i>	μ	$1,277 \cdot 10^{-5}$ kg/m · s

Reynolds number is calculated by the following formula [5]:

$$Re = \frac{\rho v d}{\mu}$$

where v is the average velocity and d is inside diameter of the pipe. For the given physical parameters the Reynolds number equals to $3,61 \cdot 10^7$, that value indicates on the turbulent fluid flow regime.

Basic geometrical model of the pipeline section presented on the illustration below (fig.1).

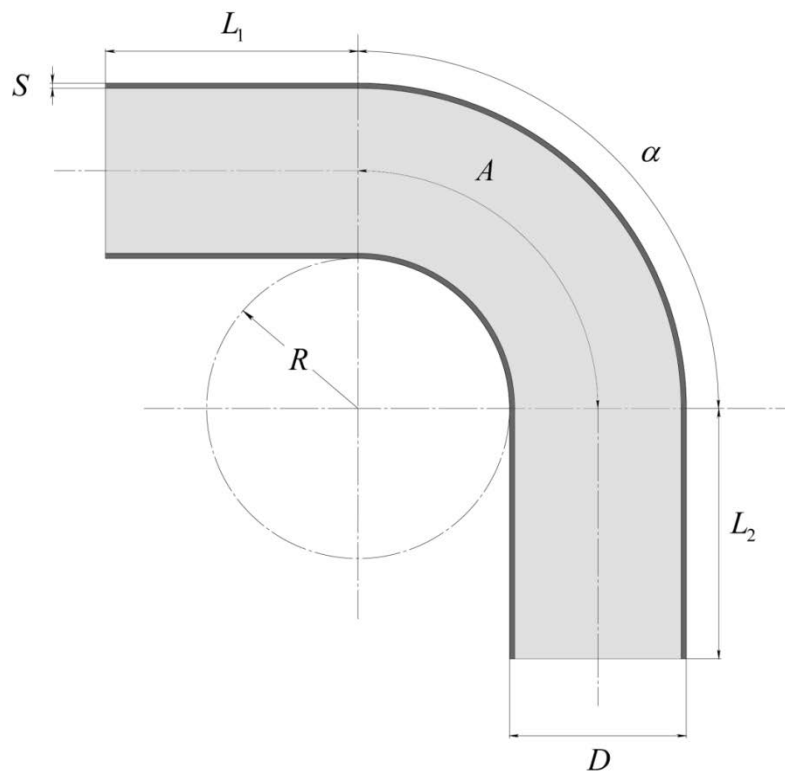


Fig.1. Sketch of bend.

The basic geometrical parameters of the model of the pipeline presented below (tab.2).

Table 2

Geometrical parameters of pipe

Parameter	Symbol	Value
Outer diameter	D	920 mm
Thickness of pipe's wall	S	7 mm
Curvature angle	α	90°
Curvature radius	R	3,4 m
Initial section length	L_1	9 m
Terminal section length	L_2	7 m
Inner diameter	d	913 mm
Length of the curved	A	6,063 m

Numerical simulation was made at various values of the angle of the pipeline on the curve α , which takes values from the range $(10^\circ - 90^\circ)$ increments 10° . Radius of the bend of a gas pipeline that accepts values from the range $(1,0 \text{ m} - 8,2 \text{ m})$ increments $1,2 \text{ m}$.

The length of the curved of the centerline at the bend is calculated by the following formula (7) which expresses the basic mathematical ratio of geometrical parameters of the pipe bend.

$$A = \alpha \frac{\pi}{180} \left(R + \frac{D}{2} \right) \quad (7)$$

The results of calculations by the formula (7) for the length of the arc plot centerline for all the corners and radii of curvature are presented below (tab.3). The maximum length value A is achieved when the maximum values of the angle α and radius R .

Table 3

The length of a bend with various geometrical parameters

		The radius of curvature, m						
		1,0	2,2	3,4	4,6	5,8	7,0	8,2
The bend angle, °	10	0,255	0,464	0,674	0,883	1,093	1,302	1,511
	20	0,510	0,929	1,347	1,766	2,185	2,604	3,023
	30	0,764	1,393	2,021	2,649	3,278	3,906	4,534
	40	1,019	1,857	2,695	3,533	4,370	5,208	6,046
	50	1,274	2,321	3,368	4,416	5,463	6,510	7,557
	60	1,529	2,786	4,042	5,299	6,555	7,812	9,069
	70	1,784	3,250	4,716	6,182	7,648	9,114	10,580
	80	2,039	3,714	5,390	7,065	8,741	10,416	12,092
	90	2,293	4,178	6,063	7,948	9,833	11,718	13,603

The illustration below (fig.2) presents slices of cross-sections of pipes on a bend pipe at an angle 90° with profile of modulus of the velocity. The maximum value of the velocity is $20,0718 \text{ m/s}$ and consequently minimum value is $2,60631 \text{ m/s}$.

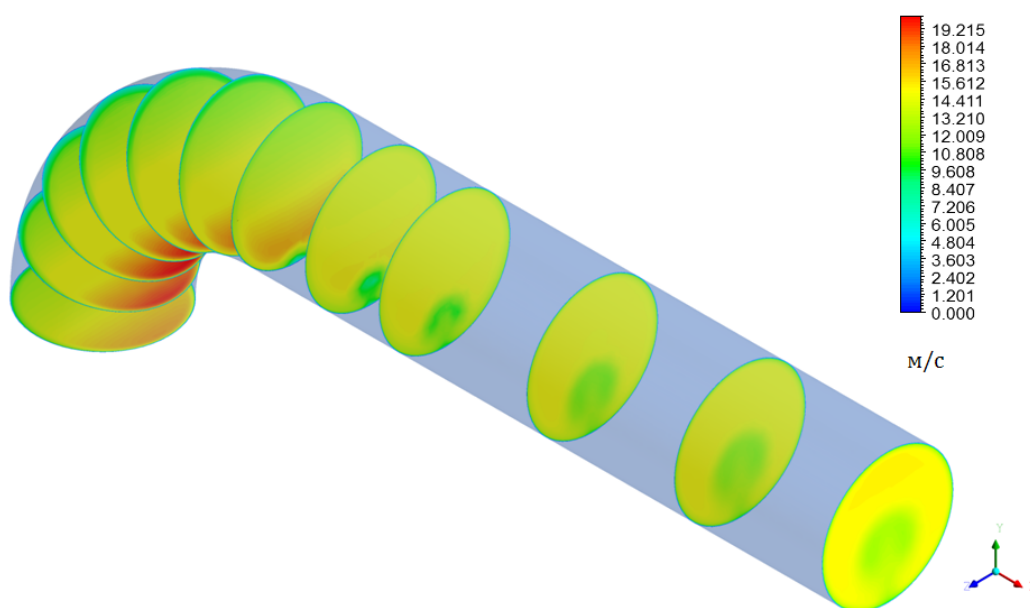


Fig.2. Profiles modules speed on the cross-sections of the tube.

Below the following illustration (fig.3) are represented sections with the projections of the velocity of gas flow in the relevant sections.

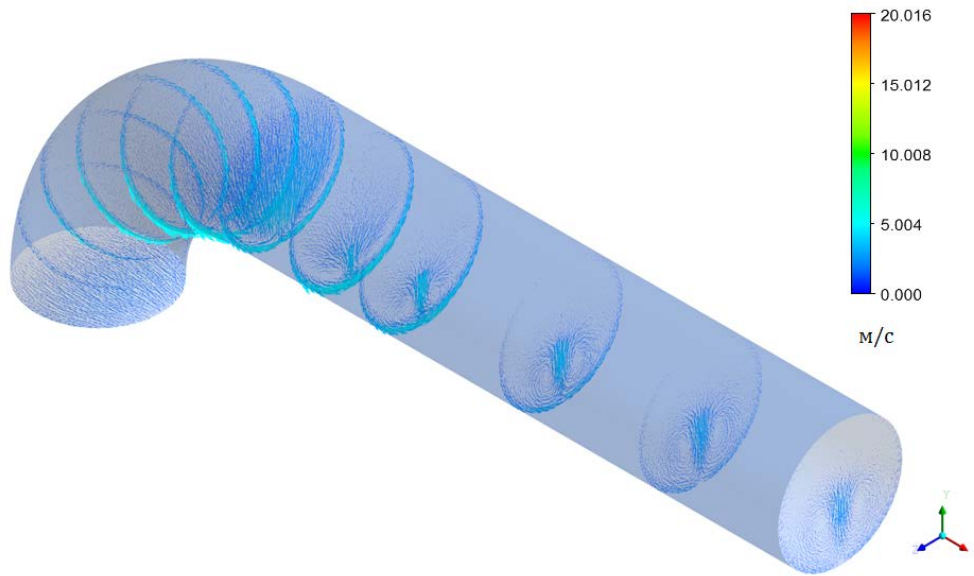


Fig.3. The projection of the velocity vectors of the cross sections of pipe.

Below is the vortex core region (fig.4), which is received by the computation of the values of the absolute helicity, equals to the absolute value of the dot product of velocity vector and vorticity vector.

$$H = |\vec{u} \cdot \vec{\Omega}|$$

where $\vec{\Omega} = \text{rot } \vec{u}$ is the rotor of velocity.



Fig.4. The vortex core region.

Below are the (fig.5) of the trajectory of motion of the liquid particles, which colored by corresponds to the absolute value of the velocity of motion in the corresponding point of the space.

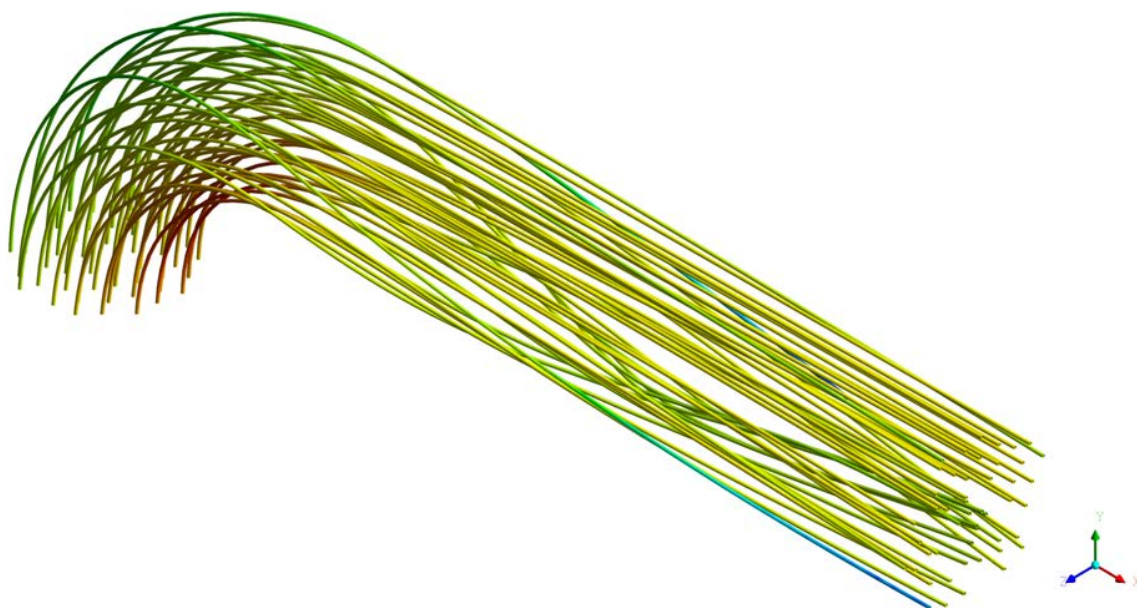


Fig.5. The trajectory of motion of the liquid particles.

On the outer side of the bend arise increased tension as a result of increased load from the gas flow on the bend. The illustration below (fig.6) shows an area ($2,13844 \text{ m}^2$) of the inner wall of the tube with pressure more than 1400 Pa .

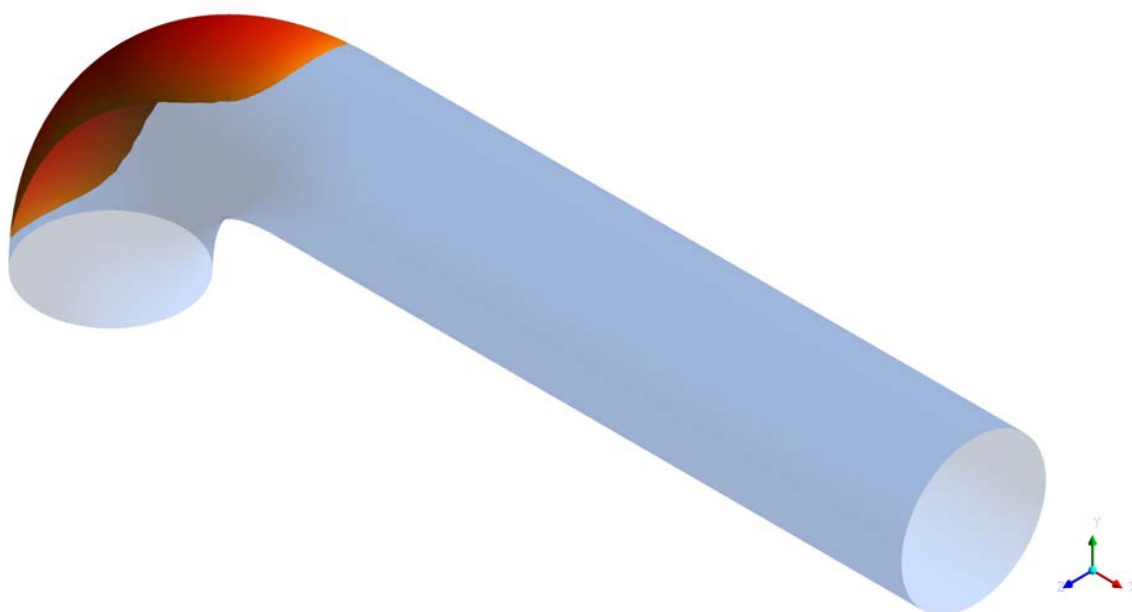


Fig.6. The area of the pipe's wall with a certainly pressure.

So, after series of numerical experiments for different values of geometrical parameters such as the angle of bend and bend radius were obtained values of the maximum pressure created on the inner wall of the pipe in a curved section of the pipeline (tab.4).

Table 4

The maximum values of pressure

	The radius of curvature, m
--	-----------------------------------

		1,0	2,2	3,4	4,6	5,8	7,0	8,2
The bend angle, °	10	1080,19	1072,34	994,394	923,031	870,924	825,126	776,658
	20	1658,23	1376,28	1136,09	1013,59	915,052	846,233	810,952
	30	1864,87	1446,99	1221,48	1064,78	955,376	889,381	841,414
	40	2074,25	1597,52	1266,23	1098,06	972,882	916,800	832,142
	50	2332,14	1593,62	1318,39	1134,29	1045,71	962,569	905,016
	60	2484,82	1726,32	1445,38	1209,79	1045,75	963,100	924,977
	70	2494,48	1832,83	1393,06	1200,05	1102,00	985,598	941,918
	80	2621,22	1781,54	1496,57	1355,50	1104,25	1020,44	961,362
	90	2737,25	1849,89	1498,67	1312,37	1217,30	986,694	962,028

The illustration below shows (fig.7) the profile of the pressure on the inner wall of the pipe in three projections for the angle 50° and radius of curvature 4,6 m .

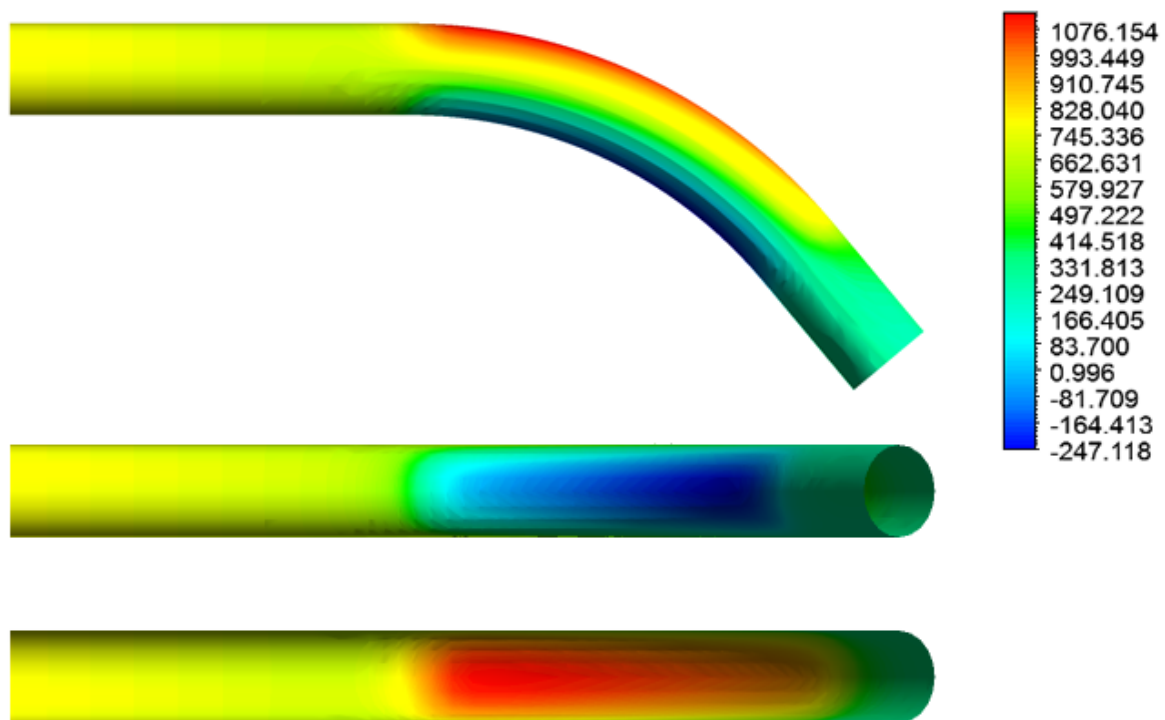


Fig.7. Profiles of the pressure on the inner wall of the pipe.

It shows the increase of the pressure outside of the bend and the decrease of this one inside of the bend. The illustration (fig.8) shows a surface that approximates the values of maximum gas pressure which obtained in the calculations on the curved section of the pipe.

The finish results of modeling and surface approximation show that the functional relationship of the maximum value of the pressure on the inner wall of the pipeline of curvature and rotation axis of the pipe in the area of bending radius is non-linear.

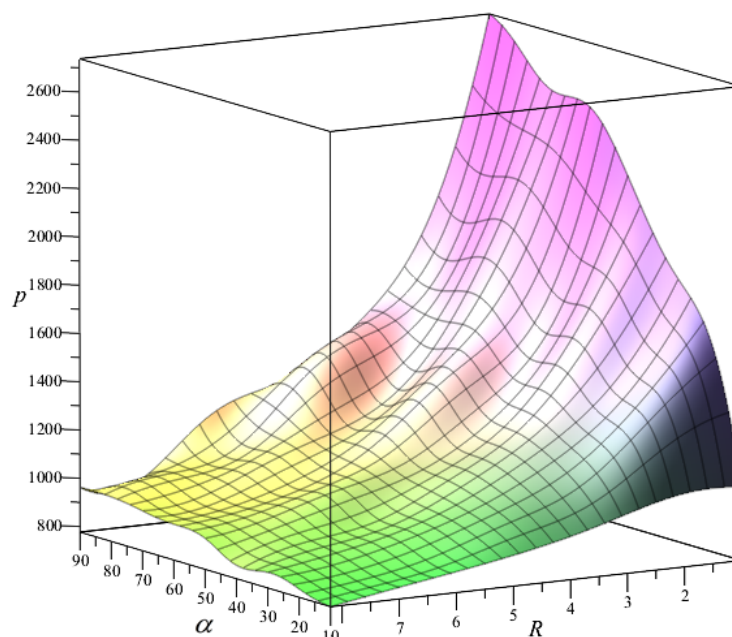


Fig.8. The dependence of the maximal pressure from the corner and bend radius.

References

1. Avramenko M. I. O k-ε modeli turbulentnosti / M.I. Avramenko. - 2e izd., pererab. i dopoln. - Snezhinsk: Izd-vo RFJAC — VNIITF, 2010. - 102 s.
2. Aliev R. A., Belousov V. D., Nemudrov A. G. Truboprovodnyj transport nefti i gaza: Ucheb. dlja vuzov/ R. A. Aliev, V. D. Belousov, A. G. Nemudrov i dr.— 2-e izd., pererab. i dop.— M.: Nedra, 1988. - 368 s.
3. Brehdshou P. Vvedenie v turbulentnostq i ejo izmerenie / P. Brehdshou. - M.: Mir, 1974. – 279 s.
4. Idelqchik I.I.Spravochnik po gidravlicheskim soprotivlenijam / Pod red. M.O. Shtejnberga // Mashinostroenie. – 1992. – 672 s.
5. Kudinov A.A. Gidrogazodinamika: Uchebnoe posobie / A.A. Kudinov. – M.: INFRA-M, 2013. – 336 s. - (Vysshee obrazovanie).
6. Kuzminov A.V., Lapin V.N., Chernyj S.G. Metod rascheta turbulentnyx techenij neshzimaemoj zhidkosti na osnove dvuxslojnoj (k-e)-modeli / A.V. Kuzqminov, V.N. Lapin, S.G. Chernyj // Vychislitelqnye texnologii. - 2001. - T.6, #5. - S.73-86.
7. Kurnosov M.M. K vyboru modelej turbulentnosti dlja raschetov teplogidravlicheskix parametrov v soedinenijax truboprovodov RU tipa VVEHR / M.M. Kurnosov. - FGUP OKB «Gidropress», Podolsk.
8. Cade M. A., W. Lima C. P. B., Farias Neto S. R. and Lima A. G. B. Natural Gas Laminar Flow in Elliptic Cylindrical Pipes: A Numerical Study // Brazilian Journal of Petroleum and Gas. 2010 Vol. 4(1)
9. O. Saheed Ismail, George T. Adewoye. Analyses and Modeling of Laminar Flow in Pipes Using Numerical Approach // Journal of Software Engineering and Applications. 2012. Vol. 5
10. Olumuyiwa A. Lasode, Tajudeen O. Popoola, and B. V. S. S. S. Prasad. Numerical Study of Liquefied Petroleum Gas Laminar Flow in Cylindrical Elliptic Pipes. // World Academy of Science, Engineering and Technology International Journal of Mechanical, Industrial Science and Engineering. 2013. Vol. 7(6).

11. Charnyj I.A. Neustanovivsheesja dvizhenie realnoj zhidkosti v trubax / I.A. Charnyj.– M., Nedra, - 1975. – 296 s.

METHODICAL ERRORS OF DIELECTRIC PARAMETERS OF FERROELECTRICS MEASUREMENT

Pecherskaya, E. A., Pecherskaya R.M., Shepeleva, .Yu.V., Kuznetsova O.N., Ryabov D.V.
Penza State University

Electrophysical model of the ferroelectric capacitor which takes into account electrical capacities and resistance characterizing the physical effects in ferroelectrics is analyzed. Causes of methodical errors appearing are determined, formulas for calculating them are made. The results of modeling of electrodes capacity influence on the result of dielectric loss tangent measurement are presented.

Keywords: ferroelectric, methodical error, model, measurement.

Ferroelectric heterostructures have a number of unique properties including high values of specific inductive permittivity and specific capacity with minimal topological sized. That is why the ferroelectric materials are used in the creating of storage device capacitor elements with an arbitrary sampling, in transistor elements of integrated circuits as gate dielectrics. The requirement of miniaturization of nano- and microsystem technology products indicates the actuality of the use of thin ferroelectric films. The most common methods of their forming are methods of chemical deposition from solutions (the extraction method from a solution, the method of moving meniscus, the method of spraying particulate), the method of physical sputtering, the method of chemical vapor deposition, the method of deposition of atomic layers [1]. And the structure (thickness, uniformity, defects) and the dielectric material parameters (capacitance, specific permittivity, dielectric loss tangent) and their dependences of on control actions, methodological, errors, in particular due to electrodes impedances influence depend on the method of films forming. Automated measurements of dielectric parameters of ferroelectrics have instrumental and methodological errors. The analysis of instrumental errors using automated measuring system developed at the department “Nano- and microelectronics” of Penza State University is set out in [2, 3]. At was used functional and metrological analysis methodology, it was described in [4, 5].

Electrophysical model of ferroelectric capacitor (figure 1) takes into account:

- capacity C – equivalent parallel connection of capacities characterizing the own field of electrodes, if there is not ferroelectric between them (vacuum), capacitance caused by linear kinds of polarization-electron and ion, spontaneous polarization capacity;
- resistance R – equivalent parallel connection of resistance causing energy loss by spontaneous polarization and ferroelectric resistance to electrical conductivity current;
- R_k, C_k – resistance and capacitance of electrodes. Their values depend on the method of forming of ferroelectric structure: metal – insulator – metal.

The metrological analysis of the equivalent electric model is carried out for two particular cases:

- 1) If $R_k = 0$ the equivalent capacitance $C_{eq} = C + C_k$, the equivalent tangent of dielectric loss D_{eq} is defined by the formula $D_{eq} = \frac{tg\delta}{1 + \frac{C_k}{C}}$, where $tg\delta = 1/\omega RC$ - nominal

tangent of dielectric loss of a ferroelectric. As $\lim_{C_K \rightarrow 0} \left(\frac{tg\delta}{1 + \frac{C_K}{C}} \right) = tg\delta$ the result of measurement D_{eq} is decrising to true meaning $tg\delta$, so $D_{eq} \leq tg\delta$ and depends on C_{eq} . The methodical error of dielectric loss tangent measuring in the absolute form $\Delta D(C_K)$ is always negative: $\Delta D(C_K) = -\frac{tg\delta}{1 + \frac{C_K}{C}}$. In particular, if $C_K \ll C$ the methodical error $\Delta D(C_K)$ is minimized and its influence can be neglected.

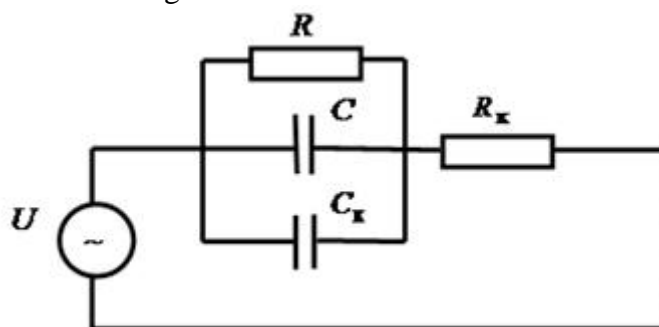


Figure 1 – The equivalent electrical model of a ferroelectric based on electrode impedances: U – voltage

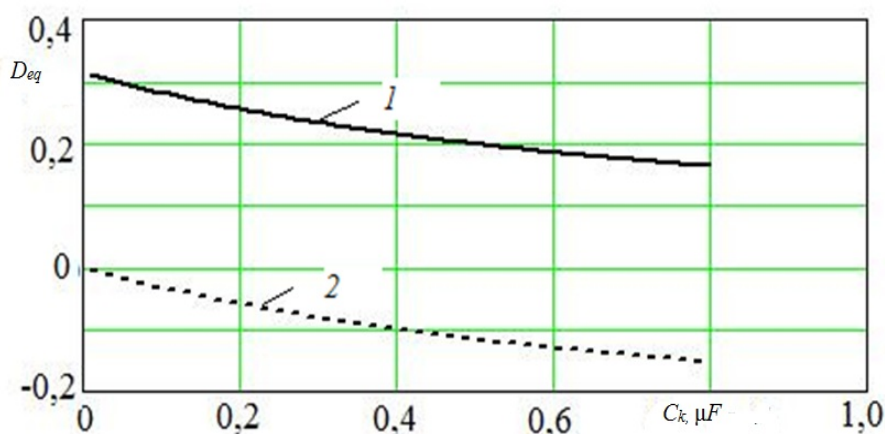


Figure 2 – The effect of the parasitic capacitance C_K : 1 – dependence of the dielectric loss tangent; 2 – dependence of the absolute methodical error of dielectric loss tangent measurement $\Delta D(C_K)$

For the examined sample of ferroelectric ceramics at the temperature $T = 25^\circ C$ the next values are determined experimentally: $C = 0,8611 \mu F$, $tg\delta = 0,3147$, $C_K \leq 1 pF$. In this case, the specific methodical error of dielectric loss tangent measurement is not more than 0,0001 %.

2) If $C_K = 0$ for a sample with small losses and $R \rightarrow \infty$ the equivalent capacitance is estimated by the formula $C_{eq} = \frac{C}{1 + \omega^2 C^2 R_K^2}$ measuring the capacitance we

have a decreased value of C_{eq} , because $\lim_{R_k \rightarrow 0} \left(\frac{C}{1 + \omega^2 C^2 R_k^2} \right) = C$. The methodical error in the absolute form is: $\Delta C = -\frac{C}{1 + \frac{1}{(\omega C R_k)^2}}$. So, for the tested ferroelectric ceramic capacitor at

the temperature $T = 25^\circ C$ it is set that $R_k \leq 6,25 \text{ M}\Omega$ that leads to a depreciatingly small value of ΔC . The represented method of methodical errors estimating caused by the influence of capacitance and electrodes resistance can be used to improve the reliability of dielectric parameters measurements of ferroelectrics.

References

- 1 Vorotilov K.A. Perspective technologies of ferroelectric heterostructures forming for integrated circuits C3Y / K.A. Vorotilov, A.S. Sigov // Fundamental problems of radioelectronics instrument – making: a collection of articles of VI International scientific and Technical Conference (Moscow, 23–27 October 2007 г.). – M.: MIREA, 2007. – P. 1. – P. 7–23.
- 2 Pecherskaya E.A. The use of the Sawyer -tower method and its modifications to measure the electrical parameters of ferroelectric materials//Measurement Techniques. 2007. - T. 50. - № 10. - P. 1101-1107.
- 3 Metrological analysis of a plant for measuring electro physics properties of ferroelectric samples with linear dimensions of micrometer range. Pecherskaya E.A. Journal of nano- an microsystem technique. - 2007. № 12. P. 43 – 47.
- 4 Methodology application of functional and methrological analysis to quality of materials examination of micro- and nanoelectronics/ Pecherskaya E.A. Fundamental problems of radioelectronics instrument making. 2007. T. 7. № 2. P. 94-98.
- 5 Methods and tools for study of active dielectrics for nanoindustry: systematic approach: Pecherskaya E.A. Monograph / E.A. Pecherskaya: Penza State University, Penza, 2008. – 129 c.

PARAMETERS INTERDEPENDENCY ANALYSIS OF UNIVERSITIES INTERNATIONAL RATINGS BASED ON QUALITY CONTROL TOOLS

Pecherskaya, E. A., Pecherskaya R.M., Shepeleva, Yu. V., Mihailov, A. A., Rybakova, N. O.
Penza State University

An analysis of the main indicators of the world leading Universities ratings based on quality systems methodology is presented Ishikawa cause – effect diagram designed. It allows to systematize ratings indices and group them depending on key activities according to developed the University business model. It contributes to the (development method) of University efficiency improving to enter the world leading ratings.

Keywords: ranking, University, business model, cause – effect diagram

At present, the entry the world leading University ratings such as the Academic Ranking of World Universities (ARWU); Quacquarelli Symonds (QS World University Rankings); the Times of Higher Education – World University Rankigs (THE - QS); Webometrics; Perfomance Ranking of Scientific Papers for World Universities is an actual strategic task for the Russian Universities. It is motivated by a number of advantages both for

the Universities and for their stakeholders (table 1). As stakeholders are examined the main partners of higher education institutions: applicants, students, potential employers, other Universities – partners, scientists and the world community teachers.

Table 1 – The main advantages of University entry into international ratings

Object	Advantages
1 University	Status raising to ensure competitiveness in the educational market, research and innovation activity.
2 Applicants, potential students, postgraduate program students	Chance of University which meets their demands in terms of an educational services consumer.
3 Researchers, the world community teachers	Choosing a workplace the rating gives an opportunity to compare potential employers by educational, innovative and other indicators.
4 Universities - partners	Choosing a partner with high rates on the required area of expertise and science researches.
5 Other stakeholders	An information about the University status as a business partner.

Key partners	Key activities	Valuable proposals	Relationships with clients	Customer segments
1. Providers of (equipment, logistics, communication and connection services)	1. Education (full, external, extra mural, remote and postgraduate additional, raising the level, retraining of region staff)	1. Theoretical and practical knowledge's (high quality specialists)	1. Reception commission, different forms of vocational guidance work	1. Enterprises, organization by economics spheres (production, medicine)
2. Enterprises – clients of graduates (on purpose directions)	2. Scientific and innovation activity	2. Patents and other scientific workings	2. Additional education based on a budget and a contract basis	2. Ministries and departments
3. International cooperation (exchange)	3. Production activity (in service sphere also)	3. Diploma status	3. Public lectures, seminars	3. International associations
4. Banking and investment spheres	Key resources	4. Level raising	Distribution channels	
5. Scientific cooperation	1. Intellectual resources (patents, author rights, data bases)		1. Information resources, University data bases (on graduates, patents, workings)	
	2. Staff (professor – teacher staff, educational staff, additional)		2. Advertisement (vocational guidance, conferences)	
	3. Material security (buildings, constructions, equipment)		3. Purpose directions of graduates	
Cost structure		Revenue flow		
1. Resources (rent, payment of connection and communication means, purchase of equipment by key activities)		1. Budget		
2. Advertisement, information activity		2. Clients		
3. System of staff financial incentives		3. Sponsors (charity)		
4. Taxes		4. Contract activity, grants		
		5. Licenses (incomes from intellectual activities also)		

Figure 1 – University business model

So, University ratings can have an indirect influence on the formation of relationship between Universities and their stakeholders. These relationships are generally taken into account in the University business model, shown in figure 1. It was built by common

recommendations stated on [1, 2]. Thus, the proposed business model includes the following basic elements: key partners, key activities, key resources, valuable proposals, client relationships, distribution channels, customer segments, cost structure, revenue flow. The content of these elements is determined by University specific policy. In this paper the so - called model of entrepreneurial University, which is characterized by its orientation to the commercialization of production and dissemination is described. The features and functions of the entrepreneurial University are shown very exhaustively and detailed in [3].

It should be noted that the represented business model can be spread in future by strategic planning of University development. It is expedient to take into account changes of corrections between factors in each structural elements frames. For example, the model «key partners» (stakeholders) contains the following components: suppliers (equipment, logistics, connection and communication services), enterprises – clients of graduates (on purpose directions), international cooperation (exchange), banking and investment spheres, scientific cooperation. Aim of partners is to ensure a competitive functioning of the University, to reduce casts, etc towards the creation of an entrepreneurial University. Accounting the developed model of the University of future as well as University strategic stresses of 2020, we can predict an increasing role of international and scientific cooperation including innovative sphere. By analogy you can identify redistribution between components of the model describing relationships with customers, key resources, etc taking into account identified strategic stresses and challenges. Thus, under strategic stresses are referred the following factors: globalization of education, knowledge economy, education technologization, internationalization of education, the content of educational programs, financing of education. These stresses lead to system challenges and problems, which must be solved by Universities to remain the competitiveness under conditions of changing external factors. One of the factors of the competitiveness is a set of indicators of educational University scientific research activity, which are obviously retraced in various ratings of Universities indifferent degrees. To raise the efficiency of decisions on improving of University indices on the basis of quality control tools such factors as causes influencing the main place in world leading international ratings are analyzed in this paper. Ones of the effective tools are cause – effect diagrams of Ishikawa which are widely used in the analyses of complex technical problems, for example give a possibility to identify key process parameters that effect the product characteristics [4, 5] and in the solution of social problems to systematize causes effecting the final indices of activity.

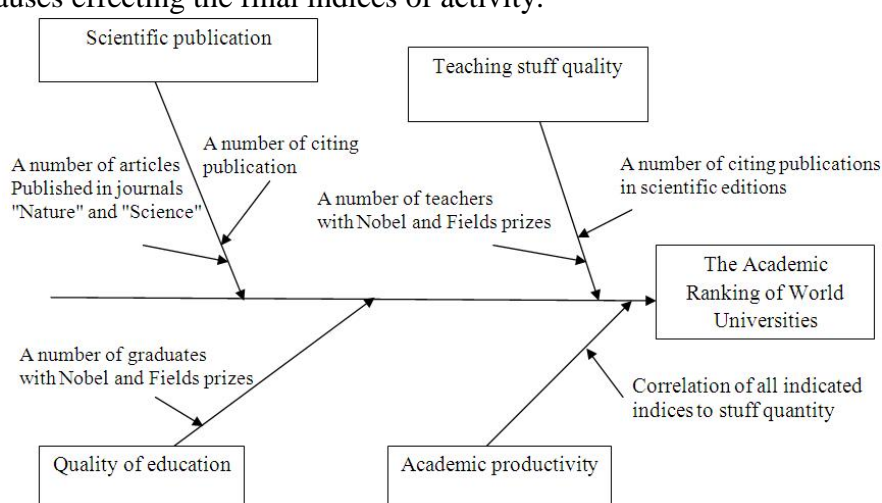


Figure 2 – The cause – effect diagrams Ishikawa, containing the reasons influencing indexes of estimation of activities of university according to a rating the Academic Ranking of World Universities (ARWU)

Developed in accordance with methodology of evaluation of Universities world leading ratings activity diagrams of Ishikawa show what indicators effect a specific rating. In particular, figure 2 is a diagram of Ishikawa corresponding to the methodology of the Academic Ranking of World Universities (ARWU).

The cause – effect diagrams for Quacquarelli Symonds (QS World University Rankings); the Times of Higher Education – World University Rankings (THE - QS); Webometrics; Performance Ranking of Scientific Papers for World Universities are composed by analogy. The analysis of cause – effect diagrams allow to systematize the interdependence of indicators and group them in accordance to key activities displayed on the business model. The application of the optimization theory and other methods of system analysis gives an opportunity to develop guidelines improving the efficiency of the University activity and its structural subdivisions, to improving enter into the status world leading ratings.

References

- 1 Building of business models: strategist and innovator handbook. Alexander Osterwalder, Yves Pine, M.: Alpina Publisher, 2013. – 290 p.
- 2 Konstantinov G.N. Strategic management: concepts. M. : Business Aliment, 2009. – 239 p.
- 3 Konstantinov G.N., Filonovich S. R. What is an entrepreneurial university? // Problems of education. 2007. №1. - P.49-62.
- 4 Pecherskaya E.A. Methods of optimal technological process determining for thin-film strain gauges construction / Pecherskaya E.A., Pecherskaya R.M., Popchenkov D.V. // Innovative information technology. - 2013. T. 2. № 2. - P. 339-345.
- 5 Pecherskaya E.A. Systematization of quality indicators of high-temperature thin-film strain gauges / Pecherskaya E.A., Popchenkov D.V., Soloviev V.A. Innovative information technology. 2012. - № 1. P. 302-305.

THIRD ORDER INTERMODULATION DISTORTION REQUIREMENTS FEAUTERES FORMULTI-CHANNEL RADIO RECIEVER

Pilkov A. V. Radomsky A. N.

«Academician A. L. Mints Radiotechnical Institute», Moscow

In this article third order intermodulation distortion requirements for analog part of multi-channel receiver are observed. The test method is offered, which provides to interpret the one-channel analog part measurement results to receiver as a whole.

Keywords: third order intermodulation distortion susceptibility level, multi-channel receiver with digital processing, requirements interpretation.

Introduction

At the design and testing stage of multi-channel receivers with digital signal processing the need to interpret the integral requirements for radio receiver to components: antenna system, analog and digital parts. In this article features of third order intermodulation distortion susceptibility level requirements for analog part of multi-channel receiver with digital processing are observed. The test method is offered.

1. Third order intermodulation distortion susceptibility level requirements for analog part of multi-channel receiver

Scheme of the concerned multi-channel receiver, which consists of m analog channels, analog-to-digital converters (ADC), combiner (Σ) and digital signal processing block (DSPB) is shown on fig.1.

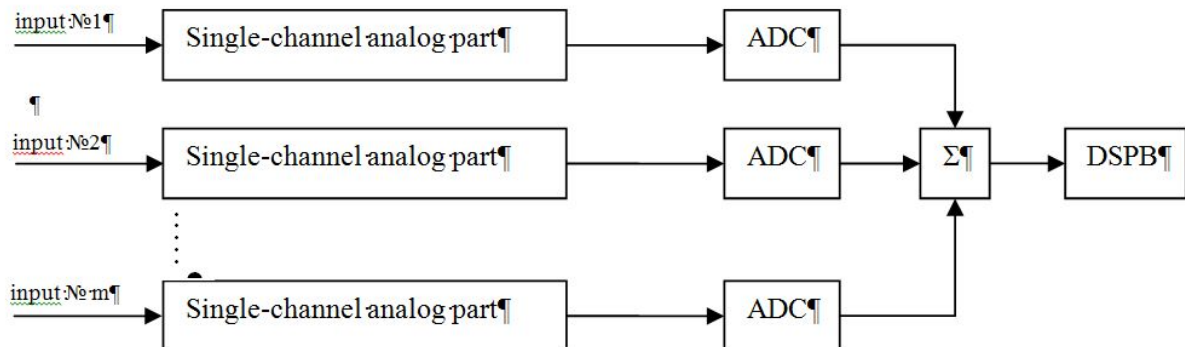


Fig.1. Scheme of the concerned multi-channel receiver

In case of realizing third order intermodulation distortion susceptibility level measurements according to standardized technique the following complexity is occurs:

- need to output ADC data conversion for analyzing intermodulation distortion;
- need to simultaneous control signal injection on every analog input.

According to standards [2], third order intermodulation distortion susceptibility level requirement (N_3 , dBm) is set for receivers. Taking into account that intermodulation distortion occurs mainly in to analog part of receivers, it's necessary to provide the fulfillment of the requirements at the analog part design stage. Consequently interpret requirements for analog part problem arises.

Dependence of output intermodulation distortion level is shown on fig.2. $IM3_{\text{channel}}$ and $IM3_{\Sigma}$ are third order intermodulation distortion levels at output of each analog channel and at analog signals combiner output, correspondingly [3]. For construction of this dependence, integral $IP3$ of analog receiving part should be determined [4].

Third order intermodulation distortion susceptibility level requirement for each analog channel is suggested to be N_3 , but at the same time output intermodulation response into operation frequency range of receiver must be at δ_{IM3} , dB below output noise level of analog channel $P_{n_out_ch}$. δ_{IM3} value defines intermodulation response increasing due to m channels combining and derive from the following equation:

$$\delta_{IM3} = 10\lg(m) - \Delta_{IM3_ \Sigma} - 10\lg(m^{1/2}), \quad (1)$$

m – number of channel in multi-channel receiver.

$\Delta_{IM3_ \Sigma}$ – output intermodulation distortion level response after combiner relative to output noise level, dB;

$10\lg(m^{1/2})$ – value of output noise level increasing ($P_{n_out_ \Sigma}$) relative to analog channel output noise level ($P_{n_out_ch}$).

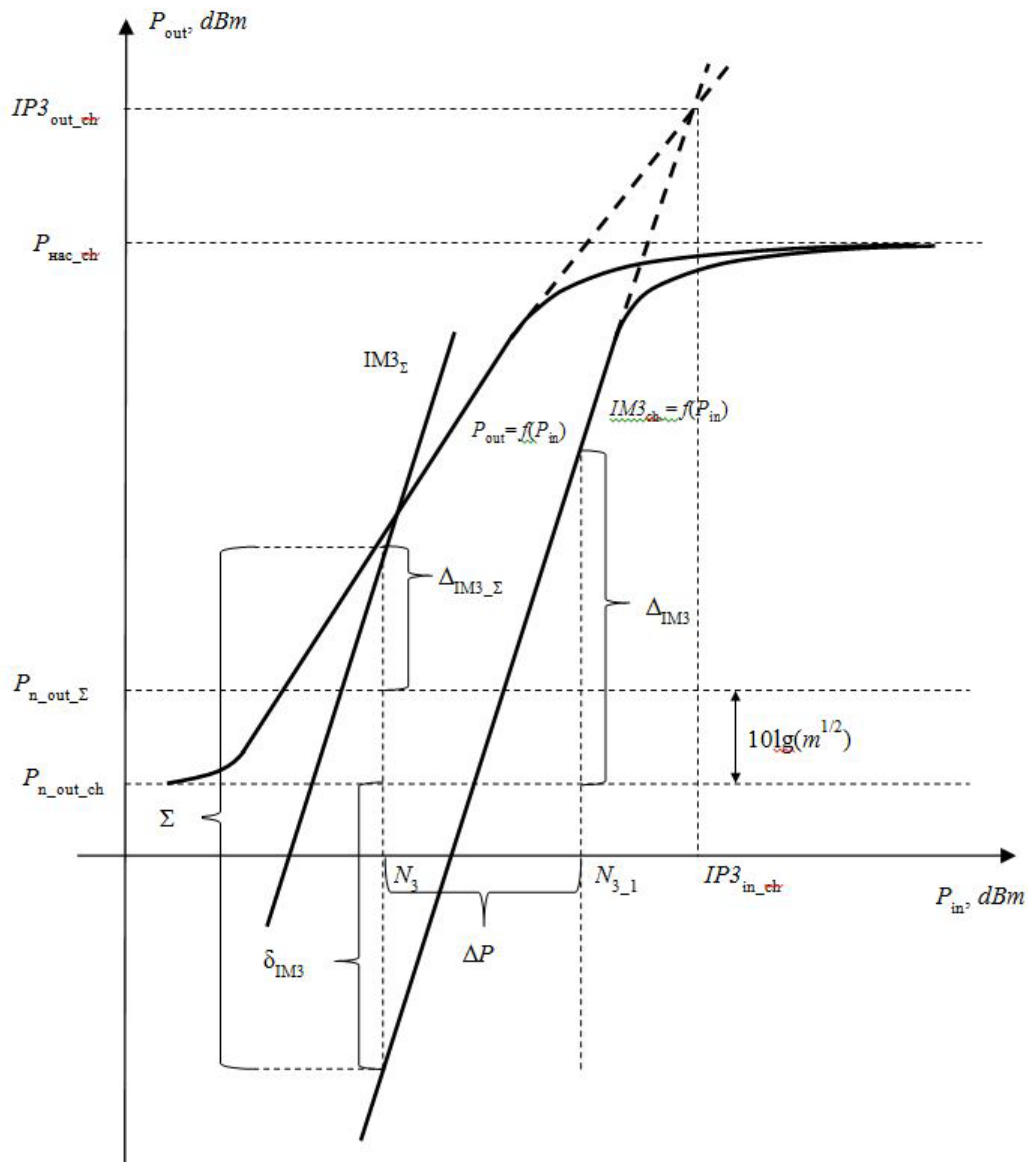


Fig.2. Third order intermodulation distortion levels at output of each analog channel ($IM3_{ch}$) and at analog signals combiner output ($IM3_{\Sigma}$)

After conversion, equation (1) becomes:

$$\delta_{IM3} = 10\lg(m^{1/2}) - \Delta_{IM3_ \Sigma}$$

The test procedure is suggested in the next section of the article.

2. Test technique requirements for levels of susceptibility to intermodulation

According to the above requirements, the third order intermodulation response level should be no less than δ_{IM3} dB below the analog channel output noise level. Taking into account that the intermodulation response is proportional to third power relative to produced input signal, for realization of the measurement is proposed to increase input signal levels to a value N_{3_1} which provides occurrence of the intermodulation response acceptable level Δ_{IM3} at analog channel output. Δ_{IM3} value chosen from the condition the possibility of measuring the intermodulation response by standard methods.

Compliance with requirements criterion evaluates into equation:

$$\Delta P = (N_{3_1} - N_3) \leq (\Delta_{IM3} - \delta_{IM3})/3,$$

$$N_{3_1} \leq N_3 + (\Delta_{IM3} - \delta_{IM3})/3$$

Technique confirmed by experiment. Proposed form of requirements and test procedure were used in the development and testing of phased array antenna receiver.

Conclusion

Suggest form of third order intermodulation susceptibility level requirements makes it possible to interpret general requirements for receiver to one analog channel. Test results of one analog channel, which derived according suggest test procedure allows to make preliminary conclusion about compliance with receiver intermodulation susceptibility level requirements.

It is recommend to design separately analog and digital of radio receiver for realization proposition realization he proposed test procedure. It is inadmissible to integrate in the same package analog channel output and ADC input in an effort to provide test equipment connection directly to analog channel output.

References

1. Izmerenie parametrov EMS RES / Mikhaylov. A.S. M.: Svyaz, 1980, 200 s, il.
2. GOST 23611-79 Sovmestimost tekhnicheskikh sredstv elektromagnitnaya. Terminy i opredeleniya. Izdanie s izmeneniyami № 1, 2, utverzhdannymi v iyune 1987, iyune 1988 g. – Izdatelstvo standartov, 1979. – 16 s.
3. Finkelshtein M.I. Osnovy radiolokatsii: Uchebnik dlya vuzov. – 2-e izd., pererab. i dop. – M.: Radio i svyaz, 1983. – 536 s., il.
4. Teoriya i tekhnika priema diskretnykh signalov TSSPI: Uchebnoe posobie. – M. «Radiotekhnika», 2005. – 144 s.: il.

ON THE THEORY PARAMETRIZATION OF THE THREE-DIMENSIONAL ROTATIONS GROUP ABSOLUTE RIGID BODY. METHODS AND APPENDICES

Perelyayev S. E., Perelyaev D.S.

Moscow Institute of Electromechanics and Automatics

In the report the basic rules of the theory of a parameterization of group of three-dimensional rotations of an absolutely firm body in finite-dimensional vector space are stated. The issues raised are of grate interest to the experts in dynamics of a rigid body and have been rather intensively discussed in re-cent decades in works on the theoretical mechanics. It is connected, first, to increase of interest to dynam-ics of rotary movements of a firm body caused, in particular, by direct communication of this problem with questions of movement and management of mobile objects (space vehicles, planes, helicopters etc.) and secondly, with powerful penetration into applied tasks of the theoretical mechanics of new mathemat-ical methods of geometrical-topological character, for which dynamics of a rigid body represents rather in-teresting and beneficial capabilities.

The problem of a parameterization of mathematical operation of rotation in three-dimensional Euc-lidean space for the first time mathematically was strictly formulated in 1776 by the L.Euler and since then constantly attracts in itself attention. The basic application the given task has received in the theory rigidly connected with a mobile object of strapdown inertial navigating systems (SINS) at integration of kinematics differential equations of rotation for definition of orientation of a rigid body in three-dimensional space, environmental us.

The consecutive application of modern topological methods in a kinematics of a rigid body has ap-peared rather fruitful and has allowed besides uniformity of a statement,

mathematical clearness, clearness and severity of the proofs to receive new original results. In particular, the connection between all kinematics parameters is established and the orderly account of the unified theory of a parametrization rotation of real three-dimensional space. The set of turns of a firm body in three-dimensional space forms group of three-dimensional rotations.

This group represents three-dimensional configuration variety of all situations of a firm body with one motionless (fixed) point. Any point of such variety (conditional designation $SO(3)$) corresponds to a point of the closed sphere B in radius equal p is glad. Between set of rules of a firm body and points of a sphere B the mutual - unequivocal conformity is not present, as the turn concerning a positive direction of an axis of rotation on a corner p is glad. Represents same, as turn concerning a negative direction of same axis on the same corner p .

Thus, on a surface of a sphere B (bivariate of sphere $2S$) pairs opposite of points represent the same rotation from group $SO(3)$.

Having identified opposite points of a surface of a sphere B , we shall receive space $\square B$, representing turns by a continuous image and taking place with all turns of a firm body in mutually - unequivocal (1-1) conformity.

The space of configurations of a firm body is entered as set of his rules special image allocated structure of analytical variety. The kind of spaces of configurations of a firm body, as generally, and in special cases of his movement is established. Space of configurations of a firm body with one motionless point - three-dimensional material projective space $3RP$. Here dimension of configuration space (named by number of degrees of freedom) is equal to three.

At an identification of rules of a firm body with the operators of turns around of this point the space of configurations gets structure of group $SO(3)$ and Whether turns to group. In three-dimensional Euclidean space the rotation of a firm body concerning a motionless point is usually described analytically with the help of orthogonal matrixes of the third order. The set of all orthogonal matrixes with a positive de-determinant forms group - $SO(3)$. The set of all orthogonal matrixes of the third order is nine-dimensional space R^9 . Therefore $SO(3)$ there is a subset R^9 and can be considered as a subspace in topological space R^9 of all matrixes 3×3 .

This group $SO(3)$ homeomorphisms $3RP$, having the structure of three-dimensional projective space. The task of orientation of a firm body is considered in two aspects: local and global. Thus are considered not only global and unequivocal, but also the global one-to-one methods of a parameterization, and also basic parameters of orientation, with which help are entered those or other methods parameterization and probably definition of an angular rule of a firm body.

The problem global and mutual - unequivocal parameterization of group of three-dimensional rotations of a firm body is one of the most interesting tasks of applied mathematics and analytical mechanics.

In these cases the task of orientation of a firm body contacts to an investment of space of configurations or his covering space in appropriate Euclidean spaces. The generalizing concept of a matrix of parameters of orientation is entered. The comparative analysis various kinematics parameters is resulted which are applied to definition of orientation of the connected basis of maneuverable object. The analysis of parameters will be carried out by criterion of mutual unambiguity of definition of orientation of object and them not singular points.

In the report the researches, carried out by the author, of the basic methods of introduction a global one-to-one parameterization of space of rotations of a three-dimensional rigid body (from the mathematical point of view methods of an investment $SO(3)$ in R^n) are submitted. Except for researches of widely known methods by nine-dimensional (with the

help of a matrix directing cosines) and six-dimensional (with the help two columns of this matrix) parameterizations, is resulted and is analyzed modified six-dimensional parameterization of Stupelnagel, which is necessary for the description little-known six-dimensional parameterization of H.Hopf.

Is resulted belonging to Hopf result about impossibility of an investment) $SO(3)$ in four-dimensional space R^4 , that is about impossibility global one-to-one four-dimensional parameterization is reduced. Thus is shown, that any set four-dimensional of parameters (quaternion, biquaternions, complex variable of Kayley-Kleins and quadriplex numbers of Ljush etc.) is displayed on space of parameters smoothly and unequivocally, but is not mutual - is unequivocal.

That is two different four-dimensional of parameter, for example quaternion (qq,-), represent one and too rule of a body at his rotation. Therefore four-dimensional parameterization global (has no singular points) and two-place.

For group) $SO(3)$ in space R^3 the minimal number of parameters three, and the maximal number of really used parameters is equal to nine. Besides there is a certain number most known three and four-dimensional of parameters of an arrangement. Taking into account the large number of all known parameters and their updating (all only known more to than eighteen, not speaking about an even lot, which it is really possible to set), for the analysis of methods global mutual - unequivocal parameterization of group) $SO(3)$ the elements of the mathematical device of topology of varieties are used.

Except for widely known methods global and unequivocal parameterization with use four-dimensional of parameters - quaternion (individual and any length), biquaternions of Clifford's, complex variable of Kayley-Kleins and quadriplex numbers of Lush's, in the report is considered to six, seven and eight-dimensional parameters of orientation.

Use six-dimensional of variable orientation of any length, allows to carry out an investment of group) $SO(3)$ in space of parameters. Kinematics differential equations, which are received for modified six-dimensional, symmetric, linear and have no singular points. The number of the equations of communication is equal to three. Application of hypercomplex Kayley numbers (octantions), as elements eight-dimensional of algebra above a field of real numbers, also allows to enter global and mutual - unequivocal eight-dimensional parameterization.

The differential equations of rotation of a firm body received on the basis eight-dimensional numbers of Kayley, also symmetric, linear also have no the special points. However thus it is required to decide five equations of connection. All elementary operations of addition and multiplication octantions are based on alternative eight-dimensional to algebra Kayley-Dicsons, turning out from algebra generalized quaternion by application of procedure Dicsons. The algebra of Kayleys is algebra with unequivocal division and with unit alternative, but not associative and noncommutative.

The application of modern superhigh-speed vector-matrix processors allows directly to use to five, six, seven, eight and nine-dimensional methods parameterization depending on object of application and cost of the specialized calculator.

At absence of the rigid requirements on mutual unambiguity of the decision of a task of definition of any orientation of a firm body in space of three measurements most effective four-dimensional in parameters are the quaternion and quadriplex numbers of Ljush. The differential equations of movement of a bodies expressed in four-dimensional variable, linear, have no singular points and all one equations of communication require.

In conclusion of the report five basic methods local (three-dimensional) parameterizations are considered: with application of corners of orientation, vector of final turn of Rodriguez, vector of Gibbs, vector of orientation and material linear-fractional parametrizations of Kayley.

The given researches show, what methods parameterizations allow to decide a problem of global mutual - unequivocal definition of any orientation of the connected basis in three-dimensional space, and what methods decide this task in the local areas. It has allowed to develop the theory parameterizations of three-dimensional group of rotations of an absolutely firm body and to close a question of search any new exotic kinematics of parameters for the decision of the put problem.

In the applied plan the theory parameterization allows the researchers and developers SINS of various assignment on early design stages to make an intelligent choice for the benefit of those or other parameters of orientation. The given decision is accepted depending on the put tasks and presence of the onboard processor with those or other functionalities (real speed, length of a digit grid, circuit realization of a "floating" point, volume of operative memory).

The basic application the methods global and local parameterizations find at an integration of kinematics equations of any movement of a rigid body concerning a motionless point in tasks of orientation of space vehicles and difficult controlled mechanical systems.

References

1. Chelnokov Yu. N (2006), Quaternion and Biquaternion model and methods of a rigid body mechanics and their application. Geometry and kinematics of motion. M: Fizmatlit, 2006. 512 p.
2. Perelyaev S. E. (2009), On the correspondence between the Three – and Four-Dimensional Parameters of the Three-Dimensional rotation Group. ISSN 0025-6544 Mechanics of Solids, 2009. Vol 44, No. 2, pp. 204-213. Allerton Press, Inc., 2009

POLYIMIDES FOR THE PROTECTION OF SPACECRAFT EQUIPMENT

Afanasyeva M. A.

National Research University - Higher School of Economics, Moscow Institute of Electronics and Mathematics

The aim of this paper is to observe modern problems of spacecraft equipment reliability caused by electric charging and discharging phenomena, effects of high-energy irradiation and to review properties of such a material like polyimide as an example for the optimal use for the protection of the spacecraft equipment.

Space radiation appears to have caused noise pulses and temporary satellite failure on a number of satellites, especially at high orbits where significant fluxes of particles with energies above 1 keV are found. To date, high energy electrons ($1 \text{ keV} < E < 1 \text{ MeV}$) appear to present a problem but other particles have not been adequately investigated. Some satellites are equipped with spectrometers measuring particle spectra.

The creation of discharge pulses is complex. It begins with the tracing of radiation-induced electrical charge in insulated components and the associated development of electric fields. Spontaneous electric breakdown pulses may then form in the regions of high static electric field. The collapsing electric fields induce pulses in electric wiring or circuits and thereby upset or damage the circuits if the pulse is of sufficient magnitude.

When evaluating the electric charging threat to spacecraft, reliability analysts will calculate the rate of charge introduced into the insulators from space, and attempt to balance this against the rate of charge leakage from the insulators. The charge leakage current density

is assumed to be equal to the electric field in the insulator (V/cm) divided by the bulk resistivity (Ωcm) of the insulator. The bulk resistivity of the insulator is typically found in the material handbooks and is based on International Electro-Technical Commission (IEC) or American Society for Testing and Materials (ASTM) test methods. As the insulator in space accumulates charges, the electric field rises until the leakage current equals the accumulation current, or until the insulator "breaks-down" and generates a pulse. Insulators in space often have only one metallized side so they are different from typical electronic materials.

It is known that polyimides can be made conductive by pyrolysis. Irradiation by high-energy particles such as electrons and protons produces the same effects in solids as does pyrolysis. If one sufficiently pyrolyzes polyimide it will not store dangerous amount of charge in spacecraft applications. Therefore, it may be possible to simply irradiate polyimide to reduce its resistivity in order to prevent pulsing in space, yet maintain other desirable properties.

As more spacecraft flight hours were accumulated at higher orbits, researchers found instances of unusually high charging, sometimes as high as -10 kV as evidenced by the shift of the charged particle spectra. It could be assumed that the charged particle spectra have changed but the straightforward explanation of this effect is still not available. Concomitant with the appearance of large spectral shifts there seems to occur a significantly enhanced probability of anomalous responses in the satellite electrical systems. In addition, the large spectral shifts occur with highest probability during times of geomagnetic activity, i.e. when solar activity associated with solar transients actually causes a perturbation of the earth's magnetic field at sea level. It is known that satellite polymeric films, when subjected to laboratory simulations of space radiations, do produce discharge pulses of approximately 10 A with a width of the order of 10 ns. General analysis of satellite electrical systems has shown that they may well be susceptible to such pulses.

Most spacecraft have a thermal control blanket which surrounds the spacecraft. A slightly conductive film is coated on or imbedded within the blanket and connected to the conductive spacecraft frame to allow charge from the blanket material to "bleed" to the frame. The charging/ESD properties of thermal blankets have greatly improved and this problem is much less significant than it was before. However, almost no improvement has been made to other parts of spacecraft.

Behind the outer thermal blanket are many insulated components that can be charged by the high energy particles that pass through the blanket. The blanket prevents the cold space plasma from limiting the charging of insulated surfaces behind the blanket. Typical insulated surfaces are: cable jackets, thermal blankets, standoff insulators, thermal paint, open connectors, component encapsulations, fiber optic cables, cable bundle wrap, cable ties, optical windows, etc. Sufficient particle fluxes penetrate deeper into electronics boxes to charge insulators such as: circuit boards, wire insulation, connectors, integrated circuit encapsulations, capacitor cases, etc. Inside the satellite the plasma potential is not relevant unless it can penetrate the spacecraft.

To qualify a material for space application, its properties appropriate for that environment must be taken into account. Contrary to this advice, resistivity measurements for insulators are usually performed in the earth atmosphere according to ASTM method D 257-99, with some humidity present and with electrodes attached to the sample. In [6] and [8] were repeated such atmospheric tests to find resistivity in "Kapton" polyimide of the order of $1.4 \times 10^{16} \Omega\text{cm}$, in agreement with the handbook values. Such a resistivity predicts a charge decay time constant of $\tau = (1.4 \times 10^{16} \Omega\text{cm}) (8.85 \times 10^{-14} \text{F/cm}) (3.12) = 64 \text{min}$. Thus, charging by space radiation may be incorrectly assumed by an analyst or spacecraft designer to quickly (1 h) relax. But under the space environment, the resistivity of "Kapton" polyimide has been found to be $>5 \times 10^{19} \Omega\text{cm}$, and of the LaRC-SI polyimide to be $>5 \times 10^{20} \Omega\text{cm}$, much

greater than the resistivity determined by ASTM methods. Inappropriate resistivity values have been frequently assumed for space applications.

Resistivity and electric charge storage properties of LaRC-SI and Kapton polyimide samples were studied in vacuum, both before and after 50 kGy Co60 gamma irradiation. In different tests, slow (4 keV) electrons were used to charge open surfaces of 50 μm polyimide to about 500 V while the opposite surfaces were copper metalized and grounded. The subsequent decay of surface voltage can be interpreted as a current through the resistivity of the dielectric. The same samples tested by classical ASTM and IEC methods provided resistivities of the order of $10^{16} \Omega \text{ cm}$, but when tested using the vacuum charge decay the resistivity was 5×10^{19} - $5 \times 10^{20} \Omega \text{ cm}$ or more.

Charging with low energy electrons produced resistivity data reasonably similar to that produced by charging with 4 keV electron beams. The gamma irradiation, followed by one month of rest under no bias, reduced the resistivity by a factor of 2 in both materials. Raising temperature from the normal 20-50 °C, reduced the resistivity in Kapton, but the reduction was not observable in the LaRC-SI material. Even after 20 days of "constant-bias" the rate of fractional charge loss continued to decline indicating that polarization current rather than an ideal resistivity may be the cause of most voltage decay, and that the true resistivity is higher than the values determined here, and much higher by several orders of magnitude than the values determined by classical ASTM and IEC test procedures.

The electric field plays a dominant role as a causative agent in irradiated insulators. However, if we had applied the same electric field using batteries, would the statistics of pulsing remain the same? Or does the radiation influence the processes of pulse formation so that the same field in irradiated insulators makes more frequent pulses or a different ratio of number of large pulses to number of small pulses? Until these questions are answered, one cannot use high voltage alone to test irradiated dielectrics for pulsing capability; one must use radiation with an adequate simulation of the in-service radiation.

For example, it is suspected that the fiberglass-filled materials pulse more frequently because the fields at the fiber tips increase and initiate more frequent pulses.

Radiation alters the conductivity of materials. If the fiber material becomes more conductive while the binder conductivity remains constant, the pulse rate will increase. But if the fiber conductivity remains constant while the conductivity of the binder increases, then both the field enhancement and the pulse rate will decrease.

High-energy irradiations often lead to high space-charge voltages in thick samples. The problem of blocking contacts is substantially mitigated because large electric fields appearing in this case enforce conduction across the contact. This happens because radiation-generated carriers cross the contact before being thermalized, and because the voltage generated at the blocking contact is small relative to the voltage generated across the thick insulator. Yet the issues persist, and the work begun by B. Gross and others for thick insulators should be continued.

We owe much of the progress to Professor B. Gross. At present, the wide availability of computers allows one to simulate the full transport process in order to avoid the limitations of the box model used by him. The effects of the electric field inside the insulator on the range of high-energy electrons can now be accounted for. Laboratory simulations provide a method to experimentally determine the dependence of secondary electron emission on electric field strength at the surface of insulators. The occurrence of partial discharges has been correlated with the evolution of the internal space charge fields. The rate of spontaneous partial discharge pulses in spacecraft insulation has been correlated with the flux of fast electrons of the space plasma. Spacecraft surface voltage also correlates with the fast electron flux.

Partial discharges at the surface of irradiated insulators in vacuum are associated with a burst of gas, which modifies or controls the surface discharge process. Perhaps the gas results from the Lichtenberg figures noted by Gross. The conditions for the loss of the integrity of glass bulbs by electron bombardment of high-voltage electron tubes have been investigated as well. Improved Compton Diodes have resulted from detailed studies of the currents in irradiated material structures.

The works of Gross have helped us to formulate our future investigations. The normal-incidence one-dimensional approach has been successful and this encourages us to attempt a three dimensional analysis. The conditions that allow radiation to produce an insulator breakdown are being increasingly clarified. The nature of spontaneous discharge pulses is being established. Knowledge of radiation effects in semiconductors is beginning to assist in the understanding of the insulator effects. The detailed delineation of fast electron transport and penetration allows one to experimentally address the issue of conduction currents with increased accuracy.

References

1. A. Tyutnev, A. Vannikov, G. Mingaleev, Radiation electrophysics of organic dielectrics. Moscow, 1989 (in Russian);
2. A. Tyutnev, V. Saenko, E. Pozhidaev, N. Kostyukov, The dielectric properties of the polymers in the fields of ionizing radiation. Moscow, 2005 (in Russian);
3. N. Adrova, M. Bessonov, Polyimides – a new class of heat-resistant polymers. Moscow, 1968 (in Russian);
4. V. Milnichuk, E. Klinshpont, V. Tupikov, Fundamentals of radiation resistance of organic materials. Moscow, Energoatomizdat, 1994 (in Russian);
5. B. Gross, Charge Storage in Dielectrics, a Bibliographical Review on the Electret and Related Effects, Elsevier, Amsterdam, 1964;
6. B. Gross, J. Polymer Science 27, 1958;
7. A. R. Frederickson, Progress in high-energy electron and x-irradiation of insulating dielectrics, Braz. J. Phys. vol.29 n.2 Sao Paulo, 1999 ;
8. A.R. Frederickson, C.E. Benson, J.F. Bockman, Measurement of charge storage and leakage in polyimides, Nuclear Instruments and Methods in Physics Research B 208, 2003;
9. A. R. Frederickson, Electric discharge pulses in irradiated solid dielectrics in space, IEEE Transaction on Electrical Insulation Vol. EI-18 No.3, 1983;
10. A.R. Frederickson, Upsets Related to Spacecraft Charging, IEEE Transaction on Electrical Insulation Vol. 43. No. 2, 1996

SENTIMENT ANALYSIS AS THE METHOD OF INFORMATION EXTRACTION

Posevkin R.

St. Petersburg National Research University of Information Technologies, Mechanics and Optics

The paper examines sentiment analysis methods. Also take up stages of sentiment analysis process based on dictionaries.

The problem of management of the text represents a great interest for different spheres and the institutes of society operating with text documents. Especially it belongs to education, journalism, culture, the publishing which efficiency are caused by quality of the text, and work skills with it are a part of professional requirements [1]. However, information is

represented in a natural language in an unstructured look [2]. Structured information can be received by polls that attracts with itself increase in financial investments and quantity of labor costs. Thus, development of the automated system of natural language processing is an actual task.

Sentiment analysis — this developing direction of the computational linguistics which main objective is identification in the document of emotionally stained lexicon and an emotional assessment of objects the author. The emotional assessment expressed in the text, also is called as a tonality, or a text sentimentality. The emotional component expressed at the level of a lexeme or a communicative fragment, is called as a lexical tonality (or to a lexical sentimentality).

The similar analysis type can be used for collection of statistical data about the relation of a certain class of people to this or that subject or an event. Thus, having collected responses and correspondence of people at forums, it is possible to define public opinion of rather recently accepted legislative initiatives.

The text tonality as a whole is defined by a lexical tonality of units making it and rules of their combination [3].

The tonality of the text is defined by three factors:

1. Subject of a tonality;
2. Tone assessment;
3. Object of a tonality.

The subject of a tonality is the author of the text, object of a tonality — about what or whom about goes speech in the text. Tone an assessment can it is provided in one of the following types:

- Binary (positive / negative);
- Ternary (positive / neutral / negative);
- Ranged.

There are three main methods of determination of a tonality of the text:

1. Vector analysis methods of text analysis. Represents comparing with earlier labeled reference casing in process of closeness and text classification to this or that assessment based on comparing.

2. Search of a lexical tonality in the text using advance made tone dictionaries (lists of patterns) using the linguistic analysis

3. The hybrid method.

The first method requires existence beforehand the labeled reference casing on the basis of which there is a training of algorithm of comparing. This method doesn't allow to carry out the deep analysis of the text, that is to reveal and show an emotiveness at the sentence level. In a developed software the method based on dictionaries of a tonality is used. This method is more flexible: he allows not only to show chains of tone lexicon, but also to receive syntactically correct emotional expressions. In case of good filling of tone dictionary lists this method allows to reach a good completeness.[3].

The sentiment analysis, that is developed, consists of several stages. First, the linguistic parcer making the morphological analysis, a lemmatization and defining parts of speech of each word works. Then all words are labeled according to dictionary lists of tone lexicon. If the word isn't found in the list, it is considered neutral. After that primary parse is launched: words and phrases integrate in tone chains. At the last stage in a sentence the object of a tonality is selected and its sentiment is defined.

References

1. Bessmertny I., Dzhaliashvili Z., Maksimov V., Markin D. Lingua marking control of the text. Materials of the X International conference «Application of New Technologies in Education» Troitsk: Fund of new technologies in education "Baytik", 1999.
2. Ermakov S., Ermakova L. Valuation methods of an emotional painting of the text. Vestnik of the Perm university, №1(9) 2012. P. 85 – 89.
3. Pozelskaya A., Solovyov A. Method of determination of emotions in texts in Russian. Materials of annual International conference on computational linguistics and intellectual technologies «Dialog 2011». RGGU publishing, 2011. C. 510 – 523.

PRESELECTOR OF WIRELESS SIGNALS OF SATELLITE NAVIGATION SYSTEMS

Sviridov A., Kolganov A.

Moscow, MIEM, NRU «Higher School of Economics»

This article discusses the preselectors for global navigation satellite system (GNSS) implementations ways under conditions of small scale navigation equipment production for special customers. The comparative analysis of technical characteristics of perspective low-noise amplifier (LNA) of leading vendors is carried out. The optimum variant of preselector has been chosen and implemented.

Keywords: low-noise amplifier (LNA), GPS/GNSS, high-gain, navigation

The preselector, is necessary for a receiving device quality of operation improvement and in most cases represents the functional structure consisting of the LNA and the band-pass filter (BPF), as shown in Fig. 1. The preselector is used for amplification of weak signals of satellite navigation systems GPS and GLONASS in operating frequency ranges of 1575.42 MHz and 1598 – 1606 MHz respectively, coming from navigation satellites; provides minimum noise figure of the receiver, weakening out-of-band signals and noises [1].

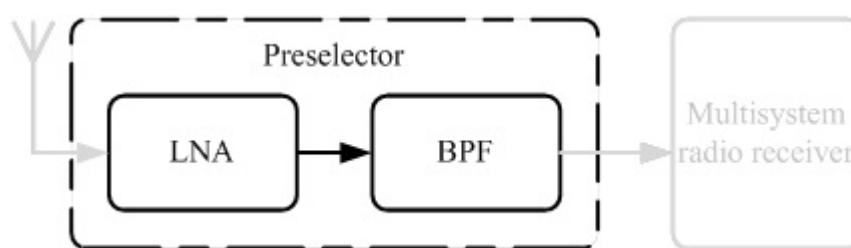


Figure 1. The functional diagram LNA

The preselector must have noise figure $NF \leq 4$ dB, work in 50Ω system, have input and output value of standing wave ratio on voltage $VSWR \leq 2$ and provide gain in operating frequency range of $Total\ Gain \approx 26...30$ dB. In case of implementation of these requirements, the subsequent stages noise of an analog path of a navigation radio receiver practically doesn't affect aggregate value of noise figure of whole receiver. [2].

LNA can be implemented on the microwave transistor or on an integrated microcircuit (IC). In comparison with IC, the microwave transistor without the discrete elements of external circuits possesses smaller noise figure. However testing of circuit and matching it are time consuming and in most cases results to a deterioration of the noise factor. IC has inside matching to the line with an impedance 50Ω and the noise figure is a little more than at the microwave transistor. Therefore application of chips for design of LNA is more important in

small-scale production for equipment of a household and special purpose and it is expedient to use microwave transistors in single precision equipment.

BPF is a passive element intended for suppression of hindering signals out of operating range of frequencies. The main parameters of BPF are band-pass range and signal strength loss coefficients: in band-pass range and beyond its limits. Nowadays the ceramic BPF and BPF which operation is based on the principle of surface acoustic waves (SAW BPF) are the most popular. This filters have an average loss of 3 dB in bandwidth.

For an amplifier which functional diagram of a preselector are shown in Fig. 1 we will select one of perspective chips of LNA. The main parameters of IC LNA are shown in Table 1.

Table 1. Electrical Specifications

Parameter	BGA715L	BGU8007	MAX2658	MAX2659
Noise Figure, dB	0.7	0.75	0.8	0.8
Gain, dB	20.0	19.0	17.7	20.5
Input 1dB Compression point, dBm	-15.5	-11.0	-10.0	-12.0
Maximum RF Input Power, dBm	10.0	0	5.0	10.0
Integrated 50Ω Output Matching Circuit	+	+	+	+
Supply Voltage, V	1.5 – 3.3	1.5 – 2.5	1.6 – 3.3	1.6 – 3.3
Supply Current, mA	3.3	4.6	7.7	4.1

As an example we will take MAX2659. This IC has 20.5 dB gain, 0.8 dB noise figure. The MAX2659 is applied in means of avionics, means of telematics and sea navigation.

The general transmission ratio of the preselector of Fig. 1, *Total Gain (dB)* is calculated as:

$$Total\ Gain\ (dB) = G_{LNA} + G_{BPF} \quad (1)$$

where G_{LNA} – gain LNA [dB],

G_{BPF} – Inserted loss BPF [dB]

$$Total\ Gain = 20.5\ dB + (-3.0\ dB) = 17.5\ dB$$

One stage of LNA doesn't provide sufficient level of transmission ratio, therefore preselector implementation according to the functional diagram of Fig. 1, for realization of requirements [2] of IC is impossible. To meet the requirements for transmission ratio and noise figure it is expedient to do the preselector according to the multistage diagram as shown in Fig. 2. In this form of preselector is represented by the amplifier with two identical stages and one ceramic band pass filter.

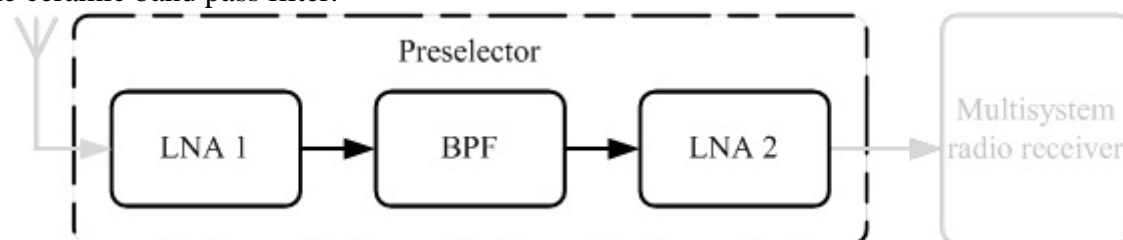


Figure 2. The functional diagram of the multistage preselector

Using IC LNA MAX2659 and one SAW BPF in such diagram, the general transmission ratio of the preselector, is calculated as:

$$Total\ Gain = G_{LNA1} + G_{BPF} + G_{LNA2} \quad (2)$$

where G_{LNA1} , G_{LNA2} – LNA gain of the first and second stages, respectively, [dB],

G_{BPF} – Inserted loss BPF [dB].

$$Total\ Gain = 20.5\ dB + (-3.0\ dB) + 20.5\ dB = 38.0\ dB$$

The calculated value of transmission ratio of the functional diagram (Fig. 2) with a reserve meets the requirement imposed to the preselector for gain amount.

One more important parameter of radio receivers of GNSS is a general noise figure of all device. The general noise figure of the device can be counted by Harold Friis [3] formula, via the noise factor F_{sys} :

$$F_{sys} = F_1 + \frac{F_2 - 1}{G_1} + \frac{F_3 - 1}{G_1 \times G_2} + \dots \quad (3)$$

where $F_1, F_2, F_3 \dots$ – noise factor of the first, second and subsequent stages, respectively [unit]; $G_1, G_2 \dots$ – gain of the first, the second and subsequent stages, respectively, [unit].

F and G in (3) are dimensionless quantities.

Value of the noise factor was historically measured as dimensionless quantities, the modern term – noise figure of NF is a logarithmic representation of the noise factor F , equal:

$$NF = 10 \log_{10} F \quad (4)$$

Equation of noise figure for multistage NF_{sys} systems from (3) and (4):

$$NF_{sys} = 10 \log \left(10^{\frac{NF_{LNA1}}{10}} + \frac{10^{\frac{NF_{BPF}}{10}} - 1}{\frac{G_{LNA1}}{10}} + \frac{10^{\frac{NF_{LNA2}}{10}} - 1}{\frac{G_{LNA1}}{10} \times \frac{G_{BPF}}{10}} \right) \quad (5)$$

where NF_{LNA1}, NF_{LNA2} – noise figure of the first and second stages of the LNA preselector, [dB];

NF_{BPF} – BPF noise figure is equal to transmission ratio in bandpass range on the module, [dB];

$G_{LNA1}, G_{LNA2}, G_{BPF}$ – transmission ratio of the first and second stages of LNA and also BPF, respectively, [dB].

Using a equation (5) we will receive:

$$NF_{sys} = 10 \log \left(10^{\frac{0.8\ dB}{10}} + \frac{10^{\frac{3.0\ dB}{10}} - 1}{10^{\frac{20.5\ dB}{10}}} + \frac{10^{\frac{0.8\ dB}{10}} - 1}{10^{\frac{20.5\ dB}{10}} \times 10^{\frac{-3.0\ dB}{10}}} \right) = 0.84\ dB$$

Thus the functional diagram of the preselector of Fig. 2 has: $Total\ Gain = 38.0\ dB$ и $NF_{sys} = 0.84\ dB$, that completely meets requirements. Such functional diagram in case of need allows to use as input LNA, IC with small gain, for example BGU8007 or MAX2658 as the second stage that increases the general transmission ratio of the preselector and compensates losses in BPF.

Based on the technical documentation of LNA the electric circuit of one stage, Fig. 3 was developed; printed circuit board (PCB), Fig. 4 are also designed.

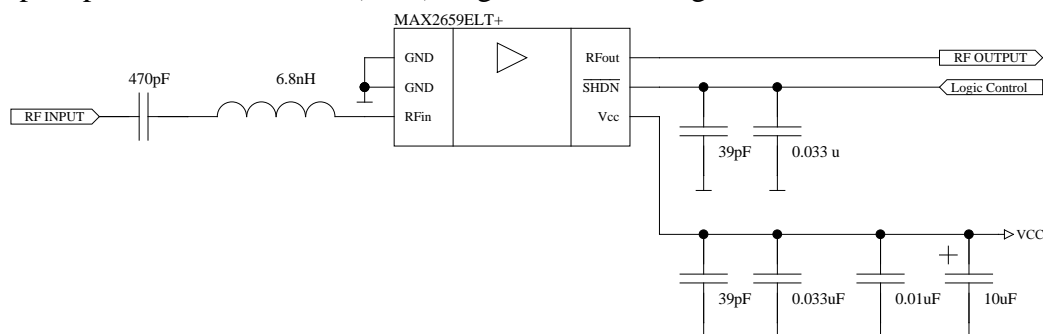


Figure 3. Electric circuit of one stage

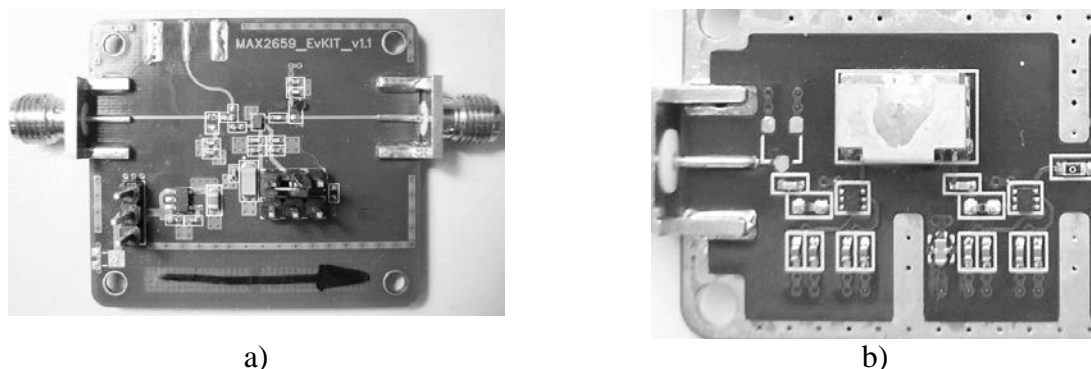


Figure 4. a - Evaluation board of one stage of LNA, b - PCB functional diagram, Fig. 2.

Measured in the range of frequencies 1575 – 1606 MHz by network analyzer, the main technical characteristics of printed circuit boards, fig. 4, are shown in Table 2.

Table 2. Electrical Specifications

Parameter	Total Gain, dB	NF_{sys} , dB	VSWR
Evaluation board LNA MAX2659	19.5	1.25	1.11
PCB functional diagram, Fig. 2	32.5	1.37	1.23

After analyzing the values in the table, we can conclude that the practical implementation is difficult to achieve the values of technical parameters specified in the technical documentation for IC. The difference with the calculated values occurs because of unmanageable various destabilizing factors: distortion of copper lines, the range of the dielectric constant of core and prepreg.

Deviations of the measured technical characteristics of preselector from the requirements is small and can be ignored because the conditions [2], specified above are met.

References

1. Aminev D.A., Sviridov A.S., Suchkov D.V., Uvaysov S.U. Embodiment of the input path receiver of satellite navigation system // V kn.: Innovatsii na osnove informatsionnykh i kommunikatsionnykh tekhnologii: Materialy mezhdunarodnoi nauchno-prakticheskoi konferentsii. / Gl. red., Uvaysov S.U.; Otv. red. Ivanov I.A. –MOSCOW: MIEM NIU VShE, 2013, C. 329-331.
2. GLONASS. Printsipy postroeniya i funktsionirovaniya / Pod red. A.I. Perova, V.N. Harisova. Izd. 4-e pererab. i dop. – MOSCOW: Radiotekhnika, 2010. 800s.
3. Agilent. Fundamentals of RF and Microwave Noise Figure Measurements. Application note 57-1. URL: <http://cp.literature.agilent.com/litweb/pdf/5952-8255E.pdf> (дата обращения: 29.01.2014).
4. Uvaysov S.U., Ivanov I.A. Informatsionnaya model' protsessa proektirovaniya kontroleprigodnykh radioelektronnykh sredstv // Informatsionnye tekhnologii. 2011. № 12. S. 41-45.
5. Uvaysov S.U., Bushmeleva K. I., Bushmelev P. E., Plyusnin I. Modelirovanie optimal'nykh parametrov ustroystv distantsionnogo zondirovaniya // Izmeritel'naya tekhnika. 2011. № 3. S. 39-42.
6. Uvaysov S.U., Ivanov I.A. Obespechenie kontroleprigodnosti radioelektronnykh sredstv v ramkakh CALS-tekhnologii // Kachestvo. Innovatsii. Obrazovanie. 2011. № 1. S. 43-46.

7. Ivanov I.A., Uvaysov S.U., Koshelev N. A. Formirovanie naborov testovykh signalov dlya kontrolya kachestva elektronnykh sredstv kosmicheskikh apparatov // Kachestvo. Innovatsii. Obrazovanie. 2011. № 11. S. 84-88.
8. Ivanov I.A., Uvaysov S.U., Koshelev N. A. Metodika obespecheniya diagnostiruемости elektronnykh sredstv kosmicheskikh apparatov po rangovomu kriteriyu na rannikh etapakh proektirovaniya // Kachestvo. Innovatsii. Obrazovanie. 2012. № 1. S. 60-62.
9. Uvaysov S.U., Aminev D.A., Optimizatsiya RAID massiva dlya dostizheniya maksimal'noi proizvoditel'nosti sistem registratsii dannykh // Kachestvo. Innovatsii. Obrazovanie. 2012. № 12. S. 93-96.
10. Uvaysov S.U., Ivanov I.A. method of ensuring controllability of electronics based on diagnostic modeling of heterogeneous physical processes // World Applied Sciences Journal. 2013. Vol. 24. P. 196-201.
11. Uvaysov S.U., Aminev D. A., Lisitsyn I. Yu. Zashchita bortovoi sputnikovoi navigatsionnoi sistemy ot kratkovremennogo propadaniya elektropitaniya i elektromagnitnykh pomekh // Tekhnologii elektromagnitnoi sovместимости. 2013. № 3(46). S. 45-49.
12. Uvaysov S.U., Ivanov I.A., Gol'dberg O. D., Ivanov O.A. Obespechenie kachestva kharakteristik istochnikov bespereboynogo pitaniya v usloviyakh pomekh, vyzvannykh nelineinoi nagruzkoi // Tekhnologii elektromagnitnoi sovместимости. 2013. № 3. S. 55-64.

USING COMMON ONTOLOGY OF SOFTWARE REQUIREMENTS FOR AUTOMATED REQUIREMENTS FORMALISATION TOOL'S DEVELOPMENT.

Pustovalova N.

Russia, Novosibirsk State Technical University

The paper discusses a common ontology of software requirements based on different classifications and approaches. The ontology was designed for automated system formalization of software requirements. Some templates used for natural language requirements formalization in the automated system are presented.

Keywords: software requirements, formalization, templates, domain area ontology.

The contemporary practices of requirements engineering allow for several different classifications of requirements. The choice depends on the life cycle of the model, process maturity and approaches used in an organization, developers' skills, customers' needs for standardization of the product and its development process. As a result, extra resources are needed to reconcile the artifacts that are created not only based on different classifications, but also in the form of documents following different standards.

As the author's research of software requirements formalization and potential for its automation clearly demonstrates, different requirements classifications exist and are used across the field to generate artifacts. It is not uncommon that even within a single practice, there is no consensus as to how to create artifacts of specific types. To a certain degree, it can be explained by the fact that creation procedures are rather of advisory (non-mandatory) nature and are specific to domain objects for which the artifacts in question are created.

As an example, let us consider a *Technicheskoe zadanie* (Requirements Specification) UML class diagram created according to the GOST 19.201-78 standard (Soviet and later Russian national standards.), *Vision*, *SRS* etc. These documents define the structure and format of the description, but leave significant discretion to developers in terms of content.

The research of Internet communities/forums for requirements engineers shows that practical recommendations proposed by individual groups or experts can differ significantly, despite the existence of well-established works that are (or at least should be) familiar to every professional in the field, such as [1, 2, 3, 4]. Therefore, there remains the need to discuss and define a number of issues concerning terminology and methodology. It is particularly true for Russian specialists. Historically, since the Soviet era, the paradigms and procedures of software development and documenting this process have been governed by the GOST standards. By the time the Russian developer community became exposed to Western approaches and methods, it had already established its own methodology for handling requirements in the software development process, which ensured a systematic approach and comprised such important concepts as enterprise architecture and quality management.

Nevertheless, the Russian and Western approaches to requirements engineering do share a number of common features, such as distinguishing between functional and non-functional requirements within the specification structure. Such shared features can serve as key points, or points of reference for developing a common ontology of requirements specifications. The ontology can further be enhanced with additional elements/components/ with respect to specific artifacts.

The author has studied document forms and artifacts created to handle/process requirements within different frameworks and developed a number of templates for a software program that automates requirement formalization, quality control, and management, which allow writing requirements in a natural language with respect to the their type and in accordance with general guidelines.

Figure 1 shows a common ontology that summarizes requirements classifications from [1, 2, 3, 4, 5], RUP guidelines [6] (particularly UML), and GOST standards (protocols 19 to 34) [7,8]. Imposing this limitation helps take into consideration all the approaches to requirements specifications in a comprehensive manner, while at the same time presenting the most common and widely used requirements documenting and modeling tools that need to be reconciled during the development process. The below requirements formalization templates have been developed for this ontology.

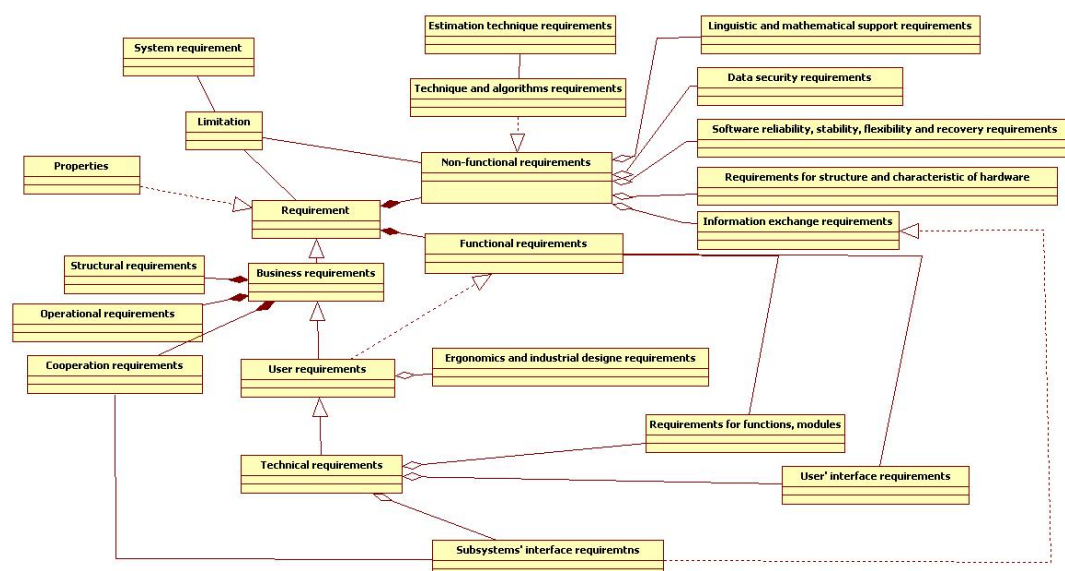


Figure 1. Common requirement's ontology

In templates the mandatory/obligatory structure elements are denoted as 1, and the non-mandatory/non-obligatory elements are denoted as 2.



Figure 2. Schematic presentation of mandatory and non-mandatory template elements.

1. Business requirements (fig. 3) describe requirements sources and are generally defined by business indicators

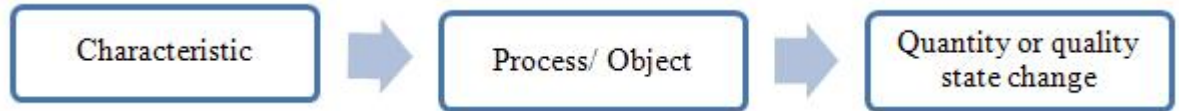


Figure 3. Business requirement's template

Example: increase sales by 3.5% due to additional analysis capabilities in the context of different categories.

2. User requirements (fig. 4)



Figure 4. User requirement's template

Example: ordering sales manager based on items ordered by customer sees elements complete their required amount of interchangeable brand, based on the availability of goods in stock.

3. Limitations (fig. 5)

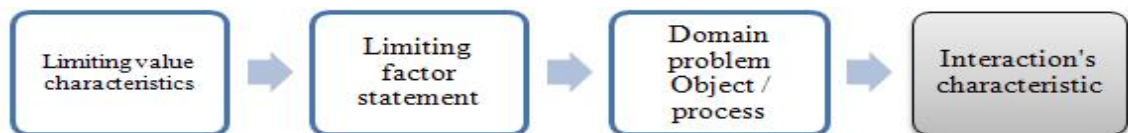


Figure 5. Limitation's template

Example: developed subsystem should use the data from an existing enterprise information systems database, based on Oracle.

4. Functional requirements (fig. 6)



Figure 6. Functional requirement's template

Example: The main screen form of subsystem "Analyse sales". When the sales manager push the button "Show alternatives", software answer must be the screen form "Alternatives". As a respond to query from enterprise information system database software presents screen form "Alternatives" read-only. This screen form contains information about products that are purchased to fully complete in order, and which are analogous to different manufacturers, according to their completeness.

5. Non-functional requirements (fig. 7)

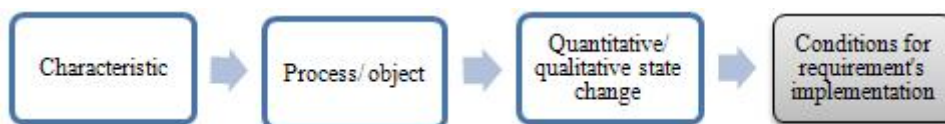


Figure 7. Non - functional requirement's template

Example: Enterprise information system database access must be in real-time mode. If sales manager push the button "Show alternatives", while the form "New Order" is created, the answer about additional products must be received over 10 seconds.

6. Technical requirements (fig. 8)

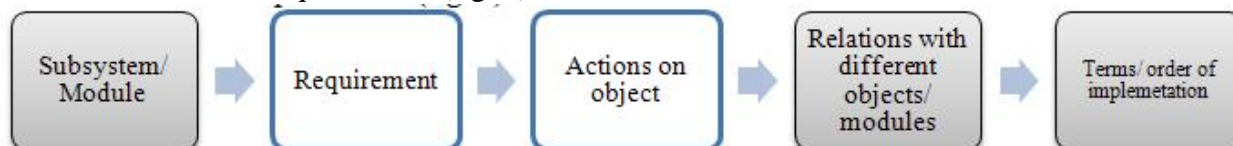


Figure 8. Technical requirement's template

Example: Subsystem "Analyse sales" allows you create, edit and delete the object "Product description", which contains the same fields as in the subsystem "Logistics", but with an indication of the complete data and interchangeable products from different manufacturers. The data on this product are recorded in the source database table "Product", and data completeness and interchangeability are recorded in a separate new database table "Configuration."

7. Specific/additional requirements divided into categories – instances of other templates (e. g. for implementing specific procedures and documents, such as GOST standards) or embedded/nested templates:

— System (special-case limitation) (fig. 9):

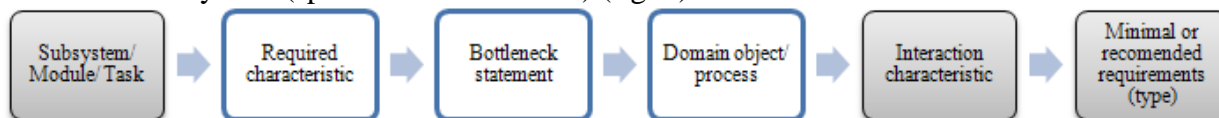


Figure 9. System requirement's template

— Hardware structure and features (special-case non-functional requirements) (fig.10):

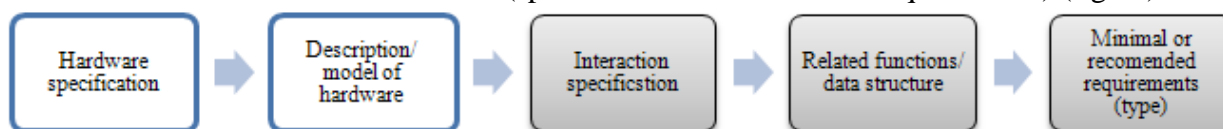


Figure 10. Hardware structure and feature's template

— Ergonomical and industrial design requirements (special-case non-functional requirements) (fig.11, 12):



Figure 11. Ergonomical and industrial design requirements' template (type 1)



Figure 12. Ergonomical and industrial design requirements' template (type 2)

— Linguistic and mathematical support requirements (special-case non-functional requirements) (fig.13):

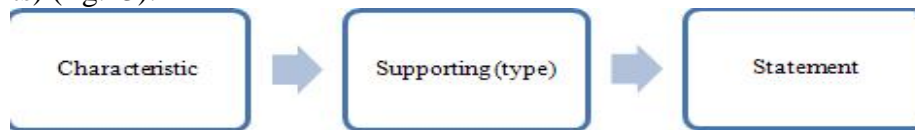


Figure 13. Linguistic and mathematical support requirements hardware's template

— Software reliability (special-case non-functional requirements) (fig.14):

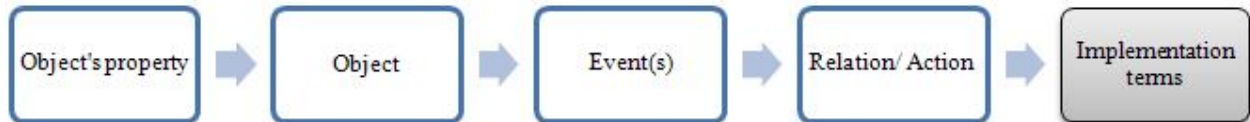


Figure 14. Software reliability requirement's template

— Technical security and data security (special-case non-functional requirements) (fig.15):

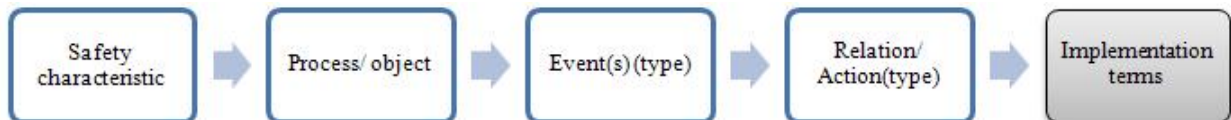


Figure 15. Technical security and data security requirement's template

— Access control (special-case data security requirements) (fig.16):

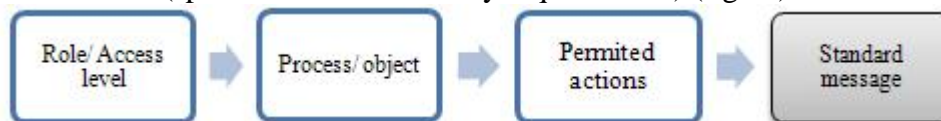


Figure 16. Access control requirement's template

— Estimation technique (related with non-functional requirements) (fig.17):



Figure 17. Estimation technique requirement's template

— Information/data environment (special-case technical requirements) (fig.18):

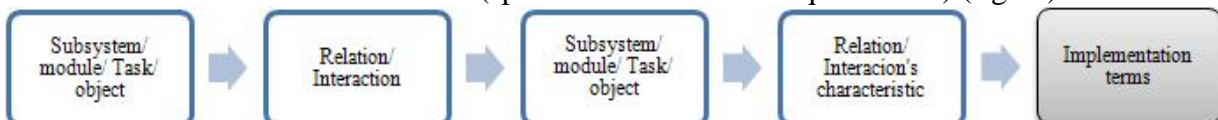


Figure 18. Information/data environment requirement's template

— Data structure and design/organization (special-case information/data environment requirements) (fig.19):



Figure 19. Data structure and design/organization requirement's template

— Feature implementation (special-case technical requirements) (fig.20):

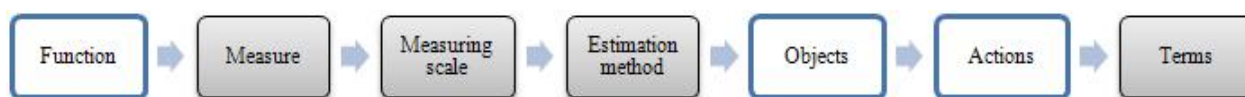


Figure 20. Feature implementation requirement's template

— Data exchange methods (additional technical requirements) (fig.21):



Figure 21. Data exchange methods requirement's template

After the requirements are formalized based on templates, their processing can be automated. Among the most important characteristics of requirements are unambiguity and self-consistency. Every natural language allows (grammatical/syntactical/lexical/verbal) constructions that can be understood differently by different recipients. Each analyst who works on a number of projects is accustomed to using certain expressions and verbal constructions. Moreover, if a database of finalized documents is kept in an organization, one can use it as a reference or partially reuse individual documents e.g. when developing a new software program version or template solutions.

The presented ontology can be used for developing automated requirements processing systems as well as for educational purposes. In reality, an entry-level requirements analyst has to deal with large/overwhelming amounts of information concerning practical terminology used in the field and needs to shape his or her own idea of how certain objects are related to each other.

Figure 22 presents a class "Requirement" structure. This figure shows a variety of attributes that are used by the program for data entry and processing requirements. It is worth noting that the class represented in the same view like it is implemented in the developing software tool structure. Not to be mixed up with the base ontology, presented at Figure 1. It is a conceptual framework for developing software tool, and must be complemented with additional slave classes of technical nature.

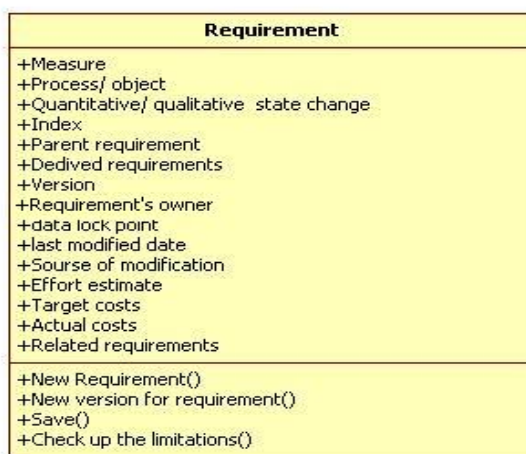


Figure 22. Class «Requirement».

Characterize the class attributes. The first three of these "Measure", "Process/ object" and "Quantitative/ qualitative state change" are used for natural language requirement's states saving. Next, attributes required for the organization of the trace. "Index" (requirement address in the hierarchy), "Parent requirement" and "Devided requirements" - store data about the links in the vertical hierarchy of requirements specifications. "Version", "Requirement's owner", "date lock point", "last modified date", "Source of modification", these slots are

contains values for control the requirements trace by time. Attribute "Related requirements" is associated with the class allows us to characterize the semantic relations between requirements, such as duplication, contradiction. The other attributes are designed for storing information used to manage the project. For example, lets show those requirements that have a short implementation period, and, for example, a high priority. These data can be obtained and processed on the basis of the specification data set stored in the class of "Requirements" and "Requirement's attribute".

Let us consider the author's personal teaching experience. In Software development and standardization course, students are assigned the tasks of modeling UML diagrams (specifically, use case diagrams) and drawing up software documentation as per the GOST 19 protocol (specifically, Requirements Specifications). Among the most common mistakes students make are substituting one type of requirements for another and insufficient level of detail in description. Students, therefore, have difficulty understanding what specific types of requirements are designed for, how they are applied and what their role is in a particular document structure. The templates are not only useful for the ontology, but also help determine which format it is advisable to use with which types of requirements.

References:

1. Karl E. Wiegers. Software Requirements. Microsoft Press, 2003.
2. Dean Leffingwell, Don Widrig. Managing Software Requirements: A Unified Approach First Edition. Addison-Wesley, 2002.
3. Alistair Cockburn. Writing Effective Use Cases. Addison-Wesley, 2001.
4. Leszek A. Maciaszek. Requirements Analysis and System Design: Developing Information Systems with UML. Addison-Wesley, 2002.
5. Orlic S. Основы Программной Инженерии (по SWEBOK). (Osnovi programnoi ingenerii (po SWEBOK) "Software engineering principals (by SWEBOK)". Retrieved from <http://swebok.sorlik.ru/>.
6. Jacobson I., Booch G. and Rumbaugh J. The Unified Software Development Process. Reading, MA: Addison-Wesley Longman, 1999.
7. GOST 19.201-78. Technicheskoe zadanie, trebovania k sodержaniu I oformleniu. Retrieved from http://www.rugost.com/index.php?option=com_content&view=article&id=54:19201-78&catid=19&Itemid=50
8. GOST 34.602-89. Technicheskoe zadanie na sozdanie avtomatizirovannoy sistemy. Retrieved from http://www.rugost.com/index.php?option=com_content&view=article&id=96:gost-34602-89&catid=22&Itemid=53
9. Maglinec U.A. (2007). Analiz trebovaniy k informacionnym sistemam: conspect lekcyi. Krasnoyarsk, Russia. Retrieved from <http://ivan-shamaev.ru/wp-content/uploads/2013/06/Information-systems-analysis-and-requirements-analysis.pdf>
10. Karl E. Wiegers. More About Software Requirements: Thorny Issues and Practical. Advice Microsoft Press, 2006.

SIMULATION OF A CYLINDRICAL ROD STRETCHING PROCESS DURING HOT DEFORMATION

Puzino Y.A.

Moscow, MIEM NRU HSE

This aim of this paper is the interpretation of the results of mechanical testing of materials to determine their properties under hot deformation. As an example, a simulation of rod stretching in superplasticity mode was considered. Comparing obtained data with the analytical solution was conducted.

Keywords: deformation, superplasticity, mathematical simulation, aluminum

Optimization of technological modes of products manufacturing using gas forming in superplastic conditions requires simulation of metal forming during deformation. To obtain correct results one must correctly set the initial and boundary conditions, including mechanical properties of materials, which are stress-strain and strain rate at a given temperature. For these dependencies special mechanical testing of materials is done [1]. In this case, the type of test usually depends on the process technology which will be simulated with the help of the obtained information. The most convenient tests for hot-forming processes are tests of uniaxial and biaxial stretching. In some cases uniaxial stretching is rather than others, because they allow control strain rate.

Phenomenology of tensile tests was studied in detail in the work [2], where special attention is paid to the effects of strain rate sensitivity of tensile metals. The stability problem of deformation in a tensile test was also investigated and common sustainability criteria were formulated. Also there were investigated the problems of stability of deformation in a tensile test and were derived basic stability criteria. In addition, the assessment of the propagation velocity heterogeneity was made, when the deformation is unstable. But these works rest on analytical methods that do not allow detailed study of the heterogeneity of the metal flow under deformation.

To take into account these phenomena, it is necessary to carry out the simulation of the tests. The results of such an analysis, conducted for compression tests are presented in the papers [3,4].

This work deals with simulation and analysis of tensile tests of superplasticity state using the finite element method (FEM). Simulation was performed using the developed CAD \ CAE system.

The plan of this work is as follows: in section «Program» the program structure is introduced, in section «Simulation » conditions of the uniaxial stretching test and simulation of tensile test in superplasticity state is discussed. Section «Results» consists of review and analysis of the results.

Program

Developed system consists of two parts: a preprocessor and a core. The user works with the preprocessor in the following sequence:

- 1) Selecting a task (stretching).
- 2) Working with sketch. User must create or download metamodel (sketch) of the object under study. User can export its sketch using common format *.dwg or draw it by itself.
- 3) Construction of the finite element mesh. This component allows you to select the length of the segments of the partition (it determines the size and number of triangles filling a region), as well as the concentration point and the radius (Figure 1). This makes it possible to increase the accuracy of calculations in the necessary area, while not greatly increasing the number of triangles, which affects the performance of the program.

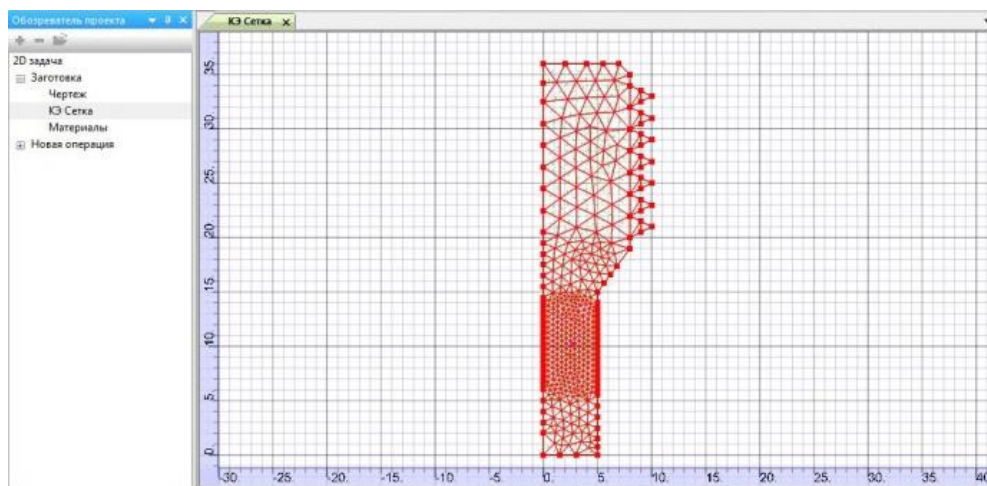


Fig.1. Finite element mesh with the concentration area.

4) Setting the operations. Operations in this system are used to set the tools which act on the workpiece, and set trajectories of those tools.

5) Instruments component. Similarly to paragraph 2, instruments is created or downloaded in sketch form that will interact with the workpiece. User can set the reference point, which indicates how the tool will move in space (Figure 2): in what direction with which the linear and angular velocity. Movement as possible in a straight line, and on the arc trajectory.

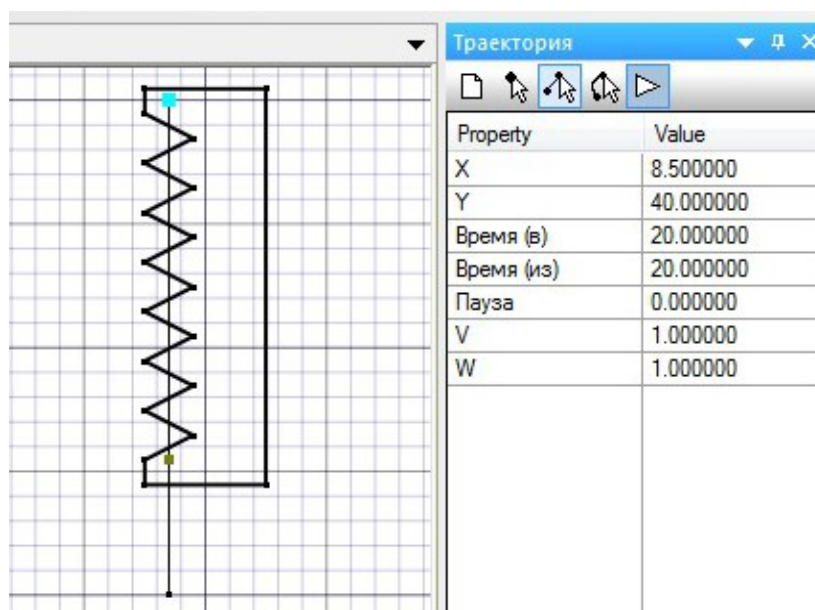


Fig.2. Instrument and its trajectory.

6) Trajectories module. For each instrument is given its own trajectory displacement. The trajectory is predetermined by reference points, which indicate the linear and angular velocity of the tool. Reference points connected by segments or arcs (portions of circles).

7) Assembly component. It is an amalgamation of the results of all previous components and the creation of a single task file for further calculations in the core program. At any time, you can edit any previous stage and re-create the file assignment.

8) Last step: preview and analyze the result in the preprocessor. Optionally, the user can display the line gradient and level parameters such as strain, its intensity, the rate of deformation, stress, etc.

We should also consider the calculation of task file in the kernel. This includes reading task file, the correctness of the data analysis, exercising of boundary conditions, materials, temperature, parameter calculation and graphical display of results of calculations. For each calculation of a folder is created with the log files (the file name assignment), which logs the desired physical quantities.

Simulation

Tensile experiments are one of the main methods of testing material for the study of mechanical properties at high temperature superplasticity. These experiments prominently in many industrial processes, like hot sheet forming: they allow you to define intervals of superplasticity, parameters of materials at specified temperatures and intensities, depending on the intensity of the stress and deformation strain rate intensity [5].

Superplastic materials exhibit the ability to severe plastic deformation without discontinuity, if forming occurs in a narrow range of strain rates specific to each alloy and temperature-dependent. In the study of superplastic materials, it is necessary to maintain a constant strain rate in the workpiece. This is achieved by conducting an experiment according to a special pattern in which traverse rate is changed during the uniaxial experiment by the following formula (2)

$$\varepsilon = \ln \frac{l}{l_0} \quad (1)$$

$$\dot{\varepsilon} = \frac{1}{l} \cdot \frac{dl}{dt} \quad (2)$$

As a test task was chosen axisymmetric problem: tensile test using a special loading program [6]. The planned extension of the working portion of the cylindrical rod was 300%. Parameters required for this test were calculated – the condition of constant strain rate, traverse speed and trajectory. Initial temperature: 415 °C. As a material the aluminum alloy was selected (AMg6 in Russia). Its properties are described by Smirnovs formula:

$$\sigma = \sigma_s \frac{\sigma_0 + K \dot{\varepsilon}^{m_v}}{\sigma_s + K \dot{\varepsilon}^{m_v}} + h \varepsilon, \quad (3)$$

where σ – stress, σ_s – yield strength, σ_0 – threshold stress, K and m_v – viscosity parameters, h – hardening parameter, ε and $\dot{\varepsilon}$ – strain and strain rate respectively.

The following parameters were set to workpiece and the tool. Dimensions of the working part (narrow): length – 5 mm, height – 15 mm. Given that the task is axisymmetric, it is enough to simulate the behavior of quarter of workpiece (right upper part). Boundary conditions are as follows: the lower left corner is embedded on the bottom and left sides of the symmetry condition is given. The movement is given with predetermined speed by traverse which is attached to the right upper side of the workpiece (the region with the edges). The tool moves along the predetermined path (upward) at a rate controlled during the experiment [7].

Results

As a result of the experiment (Figure 3) were obtained values of the forces and loads at the medial section of the cylindrical rod (where $y = 0$). The simulation was performed taking into account the size control of cross-sectional area and without it. Size control section area implies that we consider the ideal of cylinder rod and therefore its cross-sectional area at the base changes also ideal.

Figures 4, 5 show a comparison of analytical calculations and simulation results.

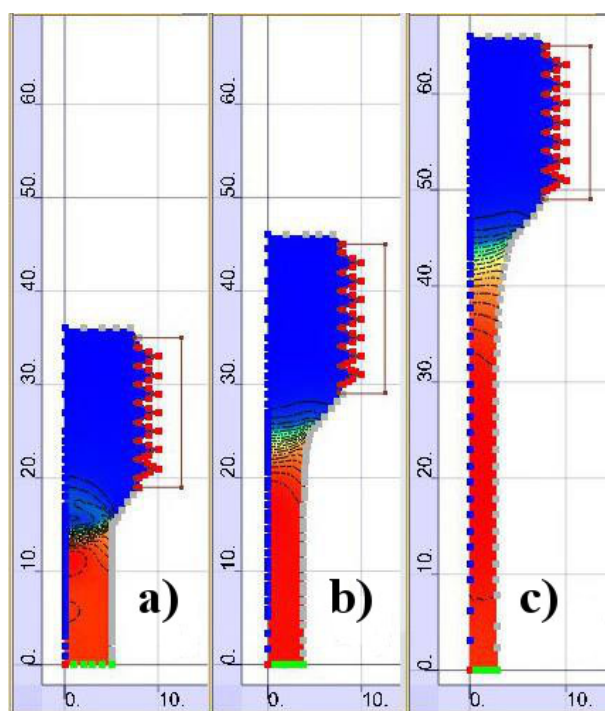


Fig.3. Line intensity and deformation levels of the rod in the calculations
(a – 1, b – 2000, c – 6000 sec)

As we can see, during the first minutes of the stretching process deviation from the analytical solution is in the range of 10% to 25%, but further reduced to 0.5 – 1% (using the area control) and to 1 – 5% (without).

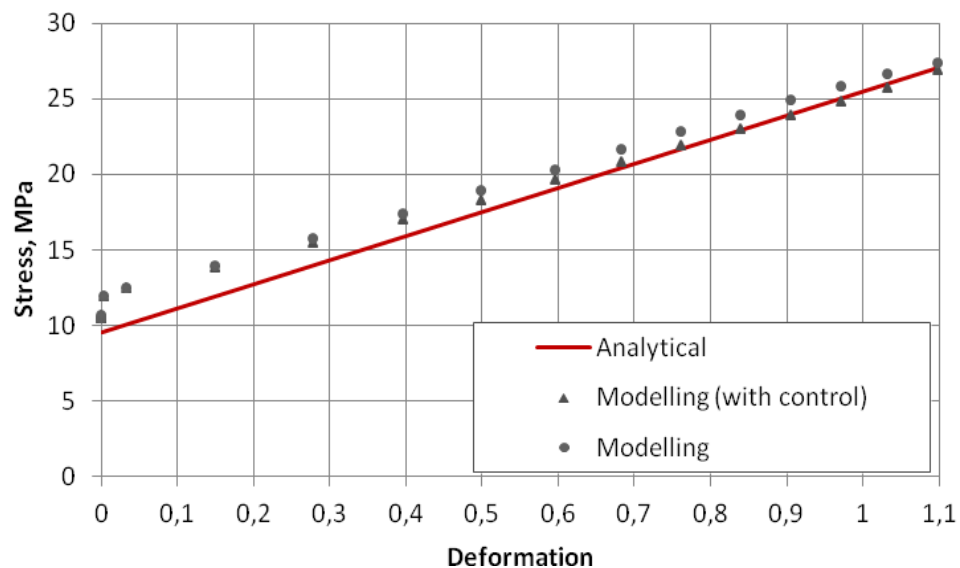


Fig.4. Stress-strain dependence

The average deviation was less than 7% (with the control) and 9% (without) for the time calculation. Large deviation values provide justification for further system improvement.

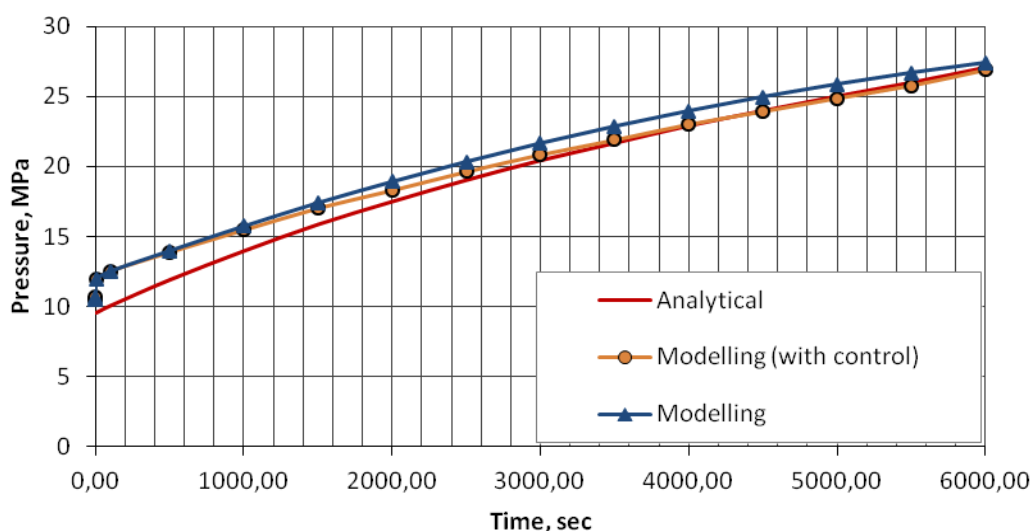


Fig.5. Pressure-time dependence

In this paper simulation of axisymmetric stretching rod was produced with a special loading program using the developed system. There were calculated such values as forces, loads and stress-strain relation. The simulation results showed that the simplified interpretation of the test results may give a huge error in the initial stage of the experiment, which lead us to further investigations.

References

1. O.M. Smirnov, M.A. Tsepin, E.N. Chumachenko, *Sverhplastichnost': materialy, teoriya, tehnologiya*. Moscow: Publishing house «Librokom», 2009. – 320 p.
2. E.W. Hart, Theory of tensile test. *Acta Metallurgica*, vol. 15, 1967. pp 351-355.
3. J. Kliber, S. A. Aksenov, R. Fabik, Numerical study of deformation characteristics in PSCT volume certified following microstructure, *Metalurgija*, Vol. 4(2009), pp 257-262.
4. S. A. Aksenov, E. N. Chumachenko, J. Kliber, R. Fabik, Inverse analysis of a plane strain compression test results for the purpose of material mechanical and microstructural properties study, *HUTNIK*.- №8.- 2009, pp 555-557.
5. I.Yu. Zakhariev, Determination of parameters of superplastic aluminum alloy AMg6 based on gas forming // In book: 12-th International Conference «Aviation and Cosmonautics – 2013». Abstracts. St. Petersburg. : Masterskaya pečati, 2013, pp. 192-194.
6. Puzino Y.A., Aksenov S.A., "Imitacionnoe modelirovanie mehanicheskikh ispytaniy v rezhime sverhplastichnosti s ispolzovaniem specialnoi programmy nagruzheniya zagotovki", *Trudy XIV Vserossiiskoi nauchno-tehnicheskoi konferencii i shkoly molodyh uchenyhaspirantov i studentov AKT-2013*, Voronezh, OOO Firma «Elist»; 2013, pp. 138-143.
7. Puzino Y.A., Aksenov S.A., "Modelirovanie mehanicheskikh ispytaniy v rezhime sverhplastichnosti s ispolzovaniem specialnoi programmy nagruzheniya", *Materialy X Mezhdunarodnoi nauchno-tehnicheskoi konferencii "Innovacii na osnove informatsionnykh i kommunikatsionnykh tehnologiy"*; 2013, Sochi, MIEM NRU HSE, pp. 463-465.
8. V.N. Chuvildeev, M.Y. Gryaznov, V.I. Kopylov, A.N. Sysoev, B.V. Ovsyannikov, A.A. Flyagin, *Mechanicheskie svoystva mikrokristallicheskogo alyuminievogo splava AMg6*, *Vestnik Nizhegorodskogo universiteta im. N.I. Lobachevskogo*, 2008, № 4, pp. 35–42.

ALGORITHMS FOR GATHERING WIRELESS WEARABLE SENSORS INFORMATION IN REMOTE HEALTHCARE MONITORING

Raznometov D. A., Korsakov I.N.

*Institute of Information Technologies, National Research University Higher School of
Economics, Russia*

The aim of this paper is to summarize recent developments in the field of wearable sensors and systems that are relevant to the field of remote healthcare monitoring. The major articles focused on the application of wearable technology to monitor elder people and patients with chronic diseases at home. Currently clinical applications of wearable technology are undergoing assessment. The home remote monitoring system derives from clinical monitoring system. The Patient Monitors are expensive and need special knowledge to use it. Patients need external help just to connect and disconnect from Patient's Monitor. As a result, wearable and easy to use sensors start to use not only in remote home monitoring, but in hospitals as well, such as floor sensor pad, chair sensor pad, bed sensor pad with heart rate detection.

Applications, such as heart rate detection, described in this review papers include those that focus on health and wellness, safety, home rehabilitation, assessment of treatment efficacy, and early detection of disorders. The integration of wearable and ambient sensors is discussed in the context of receiving vitals sign and activities of elder people and patients with chronic diseases. The main problem of home sensor like ECG still have to have knowledge how and where to put electrode as well as not very clearly the purpose of 1 Lead ECG sensor, it still complicated, but mostly used for Heart Rate detection. We believe that we may find easy way, like special algorithms, to get Heart Rate. Additional work is required to advance medical devices including wearable, portable and ambient sensors in a clinic.

Keywords: Wearable sensors, Home monitoring, Telemedicine, eHealth, mHealth

Introduction

As the manuscripts in this field is vast, we have limited the scope of this paper to include wearable sensors, portable and ambient sensors that measure health parameters such as vital signs for disease management and prevention health monitoring systems. In our project we concentrated the review on the following vital sign parameters: electrocardiogram (ECG), oxygen saturation (SpO₂), heart rate (HR), Photo Plethysmo Graphy (PPG), blood glucose (BG), respiratory rate (RR), and blood pressure (BP) [1,2]. Physiological monitoring could help in both diagnosis and ongoing treatment.

Wireless communication is relied upon to transmit patient's data to a mobile phone or an access point and relay the information to the Center of Remote Healthcare Monitoring and Emergency Intervention (CRHREI) via the Internet or 3G Network. Emergency situations are detected via data processing implemented throughout the system and an alarm message is sent to an emergency service center (ESC) to provide immediate assistance to patients. Even cheap fall detector sensor or heart rate detector very helpful in most cases. Family members are alerted in case of an emergency but could also be notified in other situations when the patient requires assistance with, for instance, taking his/her medications. Attending doctor may monitor the patient's health remotely and receive reports of deviations from the normal state of the patient's physician for making decisions on the patient's treatment. Despite the potential advantages of a remote monitoring system relying on wearable, portable and ambient sensors as the one described above, **there are significant challenges ahead** before such a system can be utilized on a large scale. These challenges include technological barriers such as

limitations of currently available battery technology (low consumption) as well racial prejudices to use of medical devices for household-based clinical monitoring system.

Wearable systems for patients' remote monitoring contains of three main tasks:

- the sensing and data collection hardware and algorithms to collect physiological(vital signs) and movement data(accelerometer);
- the communication hardware and software to send data to a CRHREI;
- the **data analysis algorithms** to extract information from physiological and movement data.

Electronic chip manufactures, such as Analog Devices, Texas Instruments, Microchip technology inc have development and deployment of wearable, portable and ambient sensors systems for patients' remote monitoring.[5]

Chip manufacturers have been producing chips even smaller and more complete functionality, such as specialized ECG-chip, have allowed researchers to develop miniature circuits entailing sensing capability, front-end amplification, microcontroller functions, and radio transmission. The ADS1293 from Texas Instruments is a highly integrated low-power analog front end (AFE) which features three high-resolution ECG channels.

We have own development of wearable 3-channels ECG [6]. The Wireless Heart Rate Monitor with Bluetooth low-energy (BLE) is intended as a reference design that researchers can use to develop end-products for battery-powered, 3-channel health and fitness electrocardiogram (ECG) applications. As a part of monitoring system we used a MicroElectroMechanical Systems (MEMS) accelerometer to monitor patients' activities. The accelerometers are usually used in Medical devices as:

- Implantable medical devices (AXL)
- Pacemakers, defibrillators, neuro-stimulators
- Concussion detection in sports (high g AXL)
- Helmets, patches, mouth guards
- Motion detection and body motion reconstruction (AXL, GYRO, MAG, PS)
- Man down, rehabilitation and training, personal emergency response systems (PERS), improved straight line motion, tilt detection for safety
- Instrument guidance in surgery (AXL, GYRO)
- Health care and wheel chairs/scooters (AXL, GYRO, PS)

The example shown in Figure 1 demonstrates how sensors can be embedded in a garment to collect, for instance, electro cardio graphic and electro myo graphic data by weaving electrodes into the fabric and to gather movement data by printing conductive elastomer-based components on the fabric and then sensing changes in their resistance associated with stretching of the garment due to subject's movements.

Most wearable, portable and ambient sensors is not invasive sensors, but for individuals with type 1 diabetes for real-time continuous blood glucose data we have to use invasive sensor for now, there are some non invasive glucose meters in clinical trials. Glucose levels were determined every 30-60 s and Bluetooth transmission signal with glucose data occurred every 5 minutes. This sensor was to be combined with an implantable insulin pump, which will be control of blood glucose levels via the delivery of variable amounts of insulin.

An example of this technology is the MITHril system [4]. Such systems by design were not suitable for long-term health monitoring. One is the promises technologies is Bluetooth Low Energy (BLE), the low consumption and easy established paring communication - the key why BLE became more popular now. Mobile operating systems including Windows Phone, iOS, BlackBerry, Android, and as well as OS X and Windows 8, natively support Bluetooth low energy. The Bluetooth SIG predicts more than 90 percent of Bluetooth-enabled smartphones will support the low energy standard by 2018.

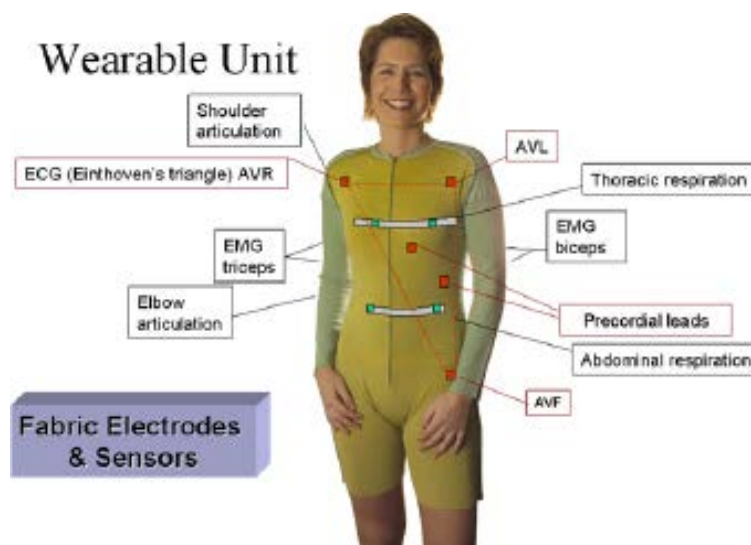


Figure 1. Example of e-textile system for remote, continuous monitoring of physiological and movement data. Embedded sensors provide one with the capability of recording electrocardiographic data (ECG) using different electrode configurations as well as electromyographic (EMG) data. Additional sensors allow one to record thoracic and abdominal signals associated with respiration and movement data related to stretching of the garment with shoulder movements. (Courtesy of Smartex, Italy).

Sensors and Algorithms

Electrocardiography has been used for many years as a key, non-invasive method in the diagnosis and early detection of coronary heart disease. For interoperability standard in healthcare systems usually used ISO/IEC 11073(73X) Medical / Health Device Communication Standards is a family of ISO, IEEE, and CEN joint standards addressing the interoperability of medical devices.

The ISO/IEEE 11073 standard family defines parts of a system, with which it is possible, to exchange and evaluate vital signs data between different medical devices, as well as remote control these devices. This modular approach makes it relatively easy to add support for a new type of device. More device specialization standards are on the road, including:

- IEEE P11073-10406 - Device specialization - Basic ECG (1 to 3-lead)
- IEEE P11073-10413 - Device specialization - Respiration rate monitor
- IEEE P11073-10418 - Device specialization - INR (blood coagulation)
- IEEE P11073-10419 - Device specialization - Insulin pump
- Modification of existing standards:
- IEEE Std 11073-10404 - Device specialization - Pulse Oximeter (revision)
- IEEE Std 11073-10417 - Device specialization - Glucose Meter (revision)
- IEEE Std 11073-10441 - Device specialization - Cardiovascular fitness and activity monitor (revision to add 3D accelerometer / physical activity monitor data)

One-lead ECG recorders may be used for monitoring the heart rate in association with regular exercise, workouts, and sports activities. The actual recordings need to be done while the body is **not moving, to avoid artifacts from the muscles**. However, "resting" measurements can nonetheless be done during exercise and while the heart is responding to the exercise by briefly interrupting the activity long enough to obtain a recording or immediately after finishing the activity. In most cases, we need not ECG signal for aggregation, we just need signal from sensor good enough to get Heart Rate for monitoring purpose.

The basic functions that we deal with the sensors:

- *Monitors physiological data;*
- *Capture raw data;*
- *Process raw data;*
- *Communicate data;*
- *Display data.*

The most important step is Process raw data, because it very noisy and have some artifacts. The actual sensors send information to the micro-controller. The software is designed to handle the following activities:

- *Data acquisition*
- *ADC Lead off detection*
- *DC signal removal*
- *Multi band pass filtering*
- *ECG lead formation*
- *QRS (HR) detection*
- *RR Detection*
- *Bluetooth communication*

Thus, QRS (HR) detection is an important part of many ECG signal processing systems.

QRS detection algorithms

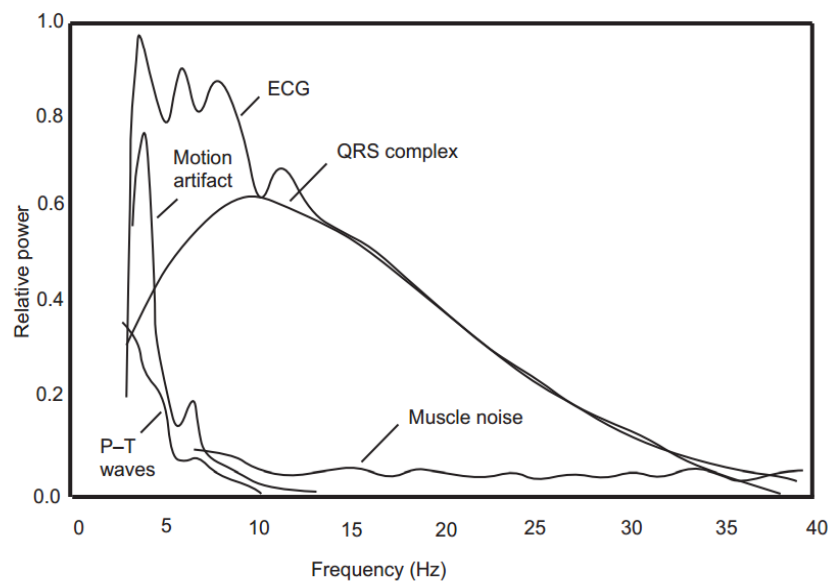


Figure 2. Spectrum of signal from sensor

Differentiation forms the basis of many QRS detection algorithms. Since it is basically a high-pass filter, the derivative amplifies the higher frequencies characteristic of the QRS complex while attenuating the lower frequencies of the P and T waves. An algorithm based on first and second derivatives originally developed by Balda et al. (1977) was modified for use in high-speed analysis of recorded ECGs by Ahlstrom and Tompkins (1983). Friesen et al. (1990) subsequently implemented the algorithm as part of a study to compare noise sensitivity among certain types of QRS detection algorithms. Figure 4. shows the signal processing steps of this algorithm.[7]

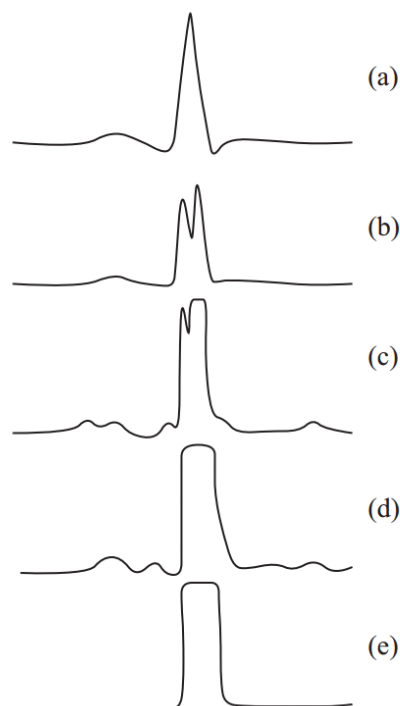


Figure 3. Various signal stages in the QRS detection algorithm based on differentiation.

(a) Original ECG. (b) Smoothed and rectified first derivative. (c) Smoothed and rectified second derivative. (d) Smoothed sum of (b) and (c). (e) Square pulse output for each QRS complex.

Conclusion

Low noise 1-Lead ECG with 24 bit analog to digital conversion and robust algorithm against noisy environment, artifacts etc. and relatively easy computation are one of the benefits proposed solution for HR detection problem. There are a lot of various algorithms based on ECG signal averaging used for High-Resolution ECG (HRECG) e.g. [9, 10].

Proposed 1 Lead ECG, method and algorithm are effective for relatively quick ECG Heart Rate detection as well as preprocessing stage for searching R pointers. The described HR detection algorithm is also robust against artifacts and non-stationary degradation factors.

Acknowledgement

The work was carried out with the financial support of the Ministry of education and science of the Russian Federation (the contract № 02. G 25.31.0033)

References

1. Teng X-F, Zhang Y-T, Poon CCY, Bonato P: Wearable medical systems for p-Health. *IEEE Reviews in Biomedical Engineering* 2008, 1:62-74.
2. Bonato P: Wearable sensors and systems. From enabling technology to clinical applications. *IEEE Eng Med Biol Mag* 2010, 29:25-36.
3. Brand O: Microsensor integration into systems-on-chip. *Proceedings of the IEEE* 2006, 94:1160-1176.
4. DeVaul R, Sung M, Gips J, Pentland A: MITHril 2003: applications and architecture. *Seventh IEEE International Symposium on Wearable Computers* 2003, 4-11.
5. Shyamal Patel, Hyung Park, Paolo Bonato, Leighton Chan and Mary Rodgers: A review of wearable sensors and systems with application in rehabilitation. *Journal of NeuroEngineering and Rehabilitation* 2012, 9:21

6. Korsakov I. N., Kuptsov S. M., Raznometov D. A. Personal Medical Wearable Device for Distance Healthcare Monitoring X73-PHD // International Journal of Scientific & Engineering Research. 2013. Vol. 4. No. 12. P. 2321-2328.
7. X. Alfonso and T. Q. Nguyen, —ECG beat detection using filter banks, IEEE Trans. Biomed. Eng., vol. 46, no. 2, pp. 192–202, Feb.1999
8. Z. Piotrowski and K. Rózanowski Telecommunications Institute, Military University of Technology Kaliskiego 2, 00-908 Warsaw, Poland
9. R.E. Herrera, J.T. Cain, E.G. Cape, G.J. Boyle, *A High Resolution ECG Tool for Detection of Atrial and Ventricular Late Potentials*, Computers in Cardiology, p. 629.
10. E. Laciár, R. Jane, *An Improved Weighted Signal Averaging Method for High-Resolution ECG Signals*, Computers in Cardiology, 2001, p. 69, Digital Object Identifier 10.1109/CIC.2001.977593.

RESEARCH METHODS OF COOLING SYSTEMS

Grab I.D., Sivagina U.A., Goryachev N.V., Yurkov N.K.
Penza State University

Reliability and stability of parameters of electronic devices is largely determined by the correct observance of a temperature mode. Thus, the challenge for designers is to provide the desired thermal regime of all the elements, units and devices of radio-electronic equipment.

Keywords: reliability, cooling systems, heat sinks, mathematical models.

Reliability of semiconductor devices is largely determined by the correct observance of their temperature mode. Failures of semiconductor devices often occur as a result of thermal breakdown under bad conditions of the dissipation of heat generated in the electronic components. [1-9] However, the surface of a semiconductor device does not always provide the necessary heat transfer to the environment, therefore, the temperature of heat transfer can exceed the allowable maximum. Therefore, the challenge for designers is to provide the required thermal regime of all the elements, units and devices of radio-electronic equipment. [10]

Different kinds of heat sinks are used to create the balance conditions between heat generation and heat dissipation. The most simple and effective heat sinks are radiators, representing metal structures that artificially increase the cooling surface of semiconductor devices, thereby improving heat dissipation [11].

Individual tasks of investigation of thermal modes of radio-electronic elements are effectively accomplished by such famous systems of computer-aided design as ANSYS, Analog Workbench, Qfin, T-Flex, APM FEM, Betasoft, COSMOS, COLDPLATE, Mentor Graphics, Microwave Office, MSC Nastran, PRAC, etc.

The test natural investigations are necessary to monitor the adequacy of the model, however, as the analysis shows, such systems do not allow to analyze the data of a natural experiment.

So, the integrated investigation of cooling systems on models or on a physical object is necessary for the broad-scale research of cooling system [2].

Figure 1 shows the algorithm of natural model investigation of cooling systems.

This algorithm allows carrying out the investigation of cooling systems in the following ways:

1. If a real object or a model exists, the data of the experimental investigations are used to calibrate the mathematical models and to control the accuracy of approximate solutions. It can be used when evaluating the adequacy of the model. The application of demonstrational possibilities of mathematical models during the investigation of a real cooling system allows to visualize the processes that take place inside the object [3].

2. If the capabilities of the experimental installation are not sufficient for the broad-scale research, the application of mathematical models provides an opportunity to expand the boundaries of a natural experiment and to get new information about processes outside the laboratory installation.

3. When designing a new cooling system, an experimental prototype is developed with its following investigation on the experimental installation according to the results of mathematical modeling. The problem of optimization to reduce costs and to unweight the structure is solved.

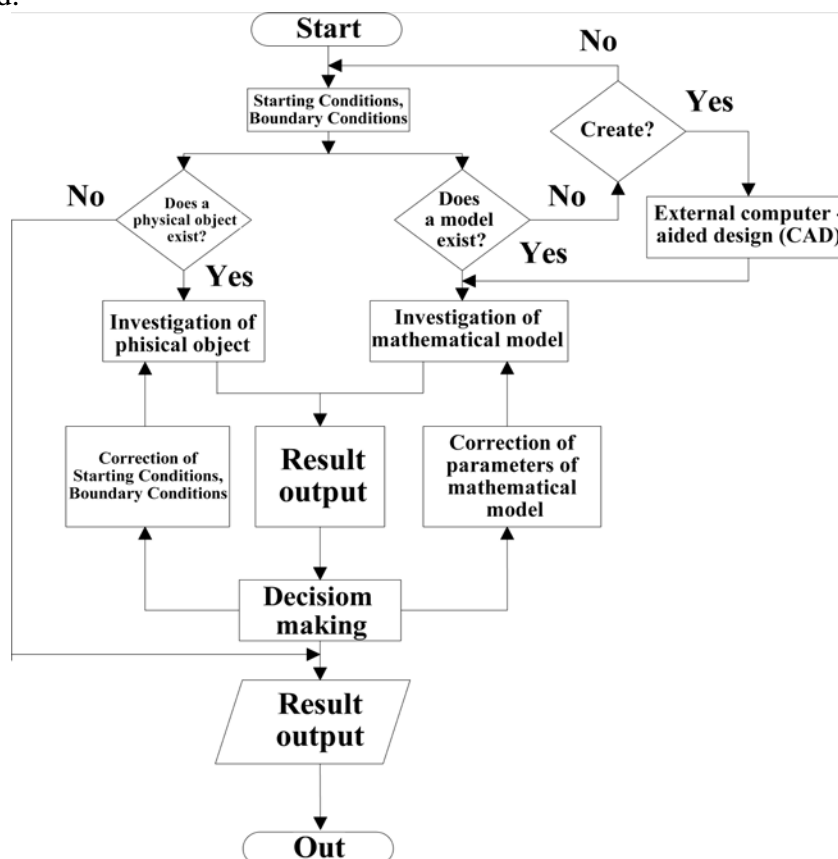


Fig. 1. The algorithm of natural model investigation.

Thus, the joint application of the demonstrational possibilities of mathematical models during the investigation of cooling systems on the laboratory test makes the transition to a new level in the development of the research systems.

In this case, the data captured by the sensors are the input data for the model that makes it possible to search simulation of the investigated physical process in different parameters and limitations and to define or to clarify the structure and parameters of the mathematical model with experimental data.

References

1. Makvecov E.N. Modeli iz kubikov. M.: Sov. Radio, 1978. – 192 s.
2. Samarskij A.A., Vabishhev P.N. Vychislitel'naja teploperedacha. - Moskva: Editorial URSS, 2003.

3. Yurkov N.K. Systems of Coriolis flowmeters in the field / N.K. Yurkov, K. V. Gudkov, M. Yu. Mikheev, V. A.Yurmanov // Measurement Techniques. N.Y., Springer, November 2012, Volume 55, Issue 6, pp 132-139.
4. Yurkov N.K. A finite-element model of the thermal influences on a microstrip antenna / N.K. Yurkov, E.Yu. Maksimov, A.N. Yakimov // Measurement Techniques. N.Y., Springer, Vol. 54, No. 2, May, 2011. P. 207-212.
5. Yurkov N.K. Electromagnetic screening of the elements of a high-voltage vacuum divider / N.K. Yurkov, Buts V.P., Smirnov E.N., Ryshov A.A. // Measurement Techniques. N.Y., Springer, Vol. 54, No. 2, May, 2011. P. 200-206.
6. Yurkov N.K. A method of automatic verification of Coriolis flowmeters in the field / N.K. Yurkov, K. V. Gudkov, M. Yu. Mikheev, V. A.Yurmanov// Measurement Techniques. N.Y., Springer, May 2012, Volume 55, Issue 2, pp 151-155.
7. Yurkov N.K. Measurement of the parameters of three-element nonresonance two-terminal networks at a fixed frequency / N.K. Yurkov, M. V. Klyuev, E. V. Isaev // Measurement Techniques. N.Y., Springer, Issue 11, February 2013, Volume 55, Issue 6, pp. 1267-1274.
8. Yurkov N.K. Programma inzhenerenogo raschjota temperatury peregreva kristalla jelektoradiokomponenta i ego teplootvoda / N.K. Yurkov, N.V. Goryachev, A.V. Lysenko, I.D. Grab // Trudy mezhdunarodnogo simpoziuma Nadezhnost' i kachestvo. 2012. T. 2. S. 242-243.
9. Goryachev N.V. Teplovaja model' smennogo bloka issleduemogo objekta / N.V. Gorjachev // Trudy mezhdunarodnogo simpoziuma Nadezhnost' i kachestvo. 2012. T. 1. S. 263-263.
10. Goryachev N.V. Utochnenie teplovoj modeli smennogo bloka issleduemogo objekta / N.V. Goryachev, I.D. Grab, N.K. Yurkov // Trudy mezhdunarodnogo simpoziuma Nadezhnost' i kachestvo. 2013. T. 1. № 1-1. S. 169-171.
11. Goryachev N.V. Modelirovanie teplovych rezhimov pri proektirovanii radiojelektronnoj apparatury / Goryachev N.V. // Trudy mezhdunarodnogo simpoziuma Nadezhnost' i kachestvo. 2009. T. 1. S. 330-332.
12. Goryachev N.V. Algoritm funkcionirovanija sistemy podderzhki prinjatija reshenij v oblasti vybora teplootvoda jelektorradiojelementa / N.V. Gorjachev // Trudy mezhdunarodnogo simpoziuma Nadezhnost' i kachestvo. 2012. T. 2. S. 238-238.
13. Lysenko A.V. Informacionno-izmeritel'nyj laboratornyj kompleks issledovanija teplootvodov jelektorradiojelementov / A.V. Lysenko, N.V. Goryachev, I.D. Grab, N.K. Yurkov // Trudy mezhdunarodnogo simpoziuma Nadezhnost' i kachestvo. 2012. T. 2. S. 239-240.
14. Goryachev N.V. Konceptual'noe izlozhenie metodiki teplofizicheskogo proektirovanija radiojelektronnyh sredstv / N.V. Gorjachev, N.K. Jurkov // Sovremennye informacionnye tehnologii. 2013. № 17. S. 214-215.
15. Andreev P. G. Zashhita radiojelektronnyh sredstv ot vneshnih vozdeystvij:ucheb. posobie / P. G. Andreev, I. Ju. Naumova // Penza : Izd-vo PGU, 2012. – 130 s.
16. Yurkov N.K. Sistemy ohlazhdenija poluprovodnikovych jelektorradioizdelij / N.K. Yurkov, A.Ju., Merkulev, N.V. Goryachev // Molodoj uchenyj. — 2013. — №11. — S. 143-145.
17. Goryachev N.V. Programmnye sredstva teplofizicheskogo proektirovanija pechatnyh plat jelektronnoj apparatury / N.V. Goryachev, N.K. Jurkov // Molodoj uchenyj. 2013. № 10. S. 128-130.

18. Trusov V.A. Stend issledovaniya teplovyh polej jelementov konstrukcij RJeS/ V.A. Trusov, N.V. Goryachev, I.D. Grab, A.V. Lysenko, P.G. Andreev //Trudy mezhdunarodnogo simpoziuma Nadezhnost' i kachestvo. 2008. T. 2. S. 162-166.

19. Yurkov N.K. Struktura i programmno-informacionnoe obespechenie informacionno-izmeritel'nogo laboratornogo kompleksa / N.K. Yurkov, N.V. Goryachev, A.V. Lysenko // Izvestija Juzhnogo federal'nogo universiteta. Tehnicheskie nauki. 2012. T. 130. № 5. S. 169-173.

20. Goryachev N. V., Grab I. D. , Petelin K. S. , Trusov V. A. , Kochegarov I. I. , Yurkov N. K. Avtomatizirovannyi vybor sistemy okhlazhdeniya teplonagruzhenykh elementov radioelektronnykh sredstv [Automated selection of cooling system of thermally loaded elements of radioelectronic facilities]. Priaspiskiy zhurnal: upravlenie i vysokie tekhnologii [Caspian Journal: Management and High Technologies], 2013, no. 4, pp. 136-143

APPLYING THE AUTOMATED SYSTEM FOR THE DETERMINATION OF EMOTIONS IN THE EDUCATION'S TASKS FOR PEOPLE WITH DISABILITIES

Rozaliev V.L., Orlova Yu.A.

Russia, Volgograd, Volgograd State Technical University

The article shows how to apply the system for training children with hearing disabilities. This paper presents the main idea of a new approach to automated identification of human emotions based on analysis of body movements, a recognition of gestures and poses. Methodology, models and automated system for emotion identification are considered. To characterize the person emotions in the model, body movements are described with linguistic variables and a fuzzy hypergraph for temporal events, which are transformed into the expression in a limited natural language.

Keywords: human emotions, gestures and movements, fuzzy temporal event, Kinect, the language of the deaf

There are a lot of modern information technologies incorporated into the human life such as Internet, robotics, games, video monitoring, and so on. The main purpose of these information technologies is to improve a human-computer interaction. But, for instance, a replacement of real persons by automated systems is impossible without overcoming the barrier of man-machine relationship [1]. The inability of machines to recognize and show emotions is one of the impeding factors. The development of telecommunication technologies changes the interpersonal communication. Very soon people will use virtual communications, which will be more effective and easy to learn but could not express emotions. At the same time emotions play a vital role in the human life. Emotions influence on cognitive processes [2] and decision making [3]. So, it is important to recognize and identify the human emotions and use them.

We developed a new approach to the identification of human emotions that is based on description and analysis of body movements, recognition of gestures and postures specific for the emotional states. In this paper, we present the methodology, models and the automated system, which are realized the suggested approach.

The process of identifying human emotional response is based on the idea of how the human manifests his/her emotions [4], [5].

Now various companies are actively developing automated systems for recognition, identification and transmission of emotional reactions. Many of these systems use web solutions based on a model SaaS (Software as a Service). There are also different ways for

determining emotional states such as by voice, facial expression, body movements, physiological parameters, and so on. [2], [6], [7], [8]

The proposed approach to emotion identification are based on recognition and analysis of human gestures and poses. [9] First of all, we recognize a person on video images using a technology for markerless motion capture with the digital video camera Microsoft Kinect. Video pictures are presented in the special animation format - the BVH-file, which describes poses of body skeleton and contains motion data. Such technology allows visualizing and analyzing different movements of person, determining areas of static or dynamic postures of micro and macro movements.

To detect the borders of movements, the motor activity of person is analyzed. For the separation of postures, we suggest a special notion of activity, which depends on what part of body performs the movement. We describe the typical body movements with linguistic variables and fuzzy hypergraphs for temporal events, and transform these descriptions into the expressions in a limited natural language, which characterize the person emotions. The identification of human emotional reactions such as joy, sadness, anger, etc is provided by the detailed analysis of postures, gestures and motions.

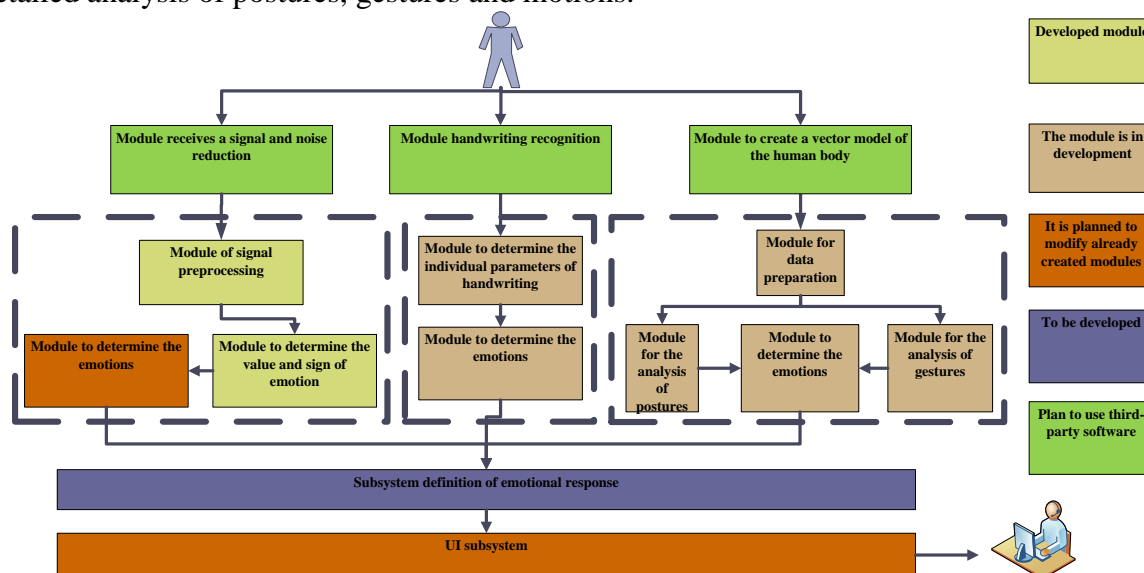


Figure 1. The architecture of system for identification of human emotional reactions

The architecture of computer system developed for identification of human emotional reactions is shown on Fig. 1 [10]. The input of the system are moving images, sound samples and handwriting texts. The output of the system is information about the emotional state of the real person, which is expressed in a limited natural language.

In order to define human emotional reactions by body movements, we use the vector model of skeleton [11], which is obtained from video information captured with the digital video camera Microsoft Kinect.

Kinect camera allows obtaining three-dimensional image in all lighting conditions and without any requirement to the actor, who is in the frame. Data from Kinect represented as a hierarchy of nodes of the human skeleton. Rotation of one joint with the other, is presented in the form of quaternions (the role of the rotating vectors perform the bones of the skeleton) and the offset is represented as a 3 dimensional vectors in local to each node coordinate system.

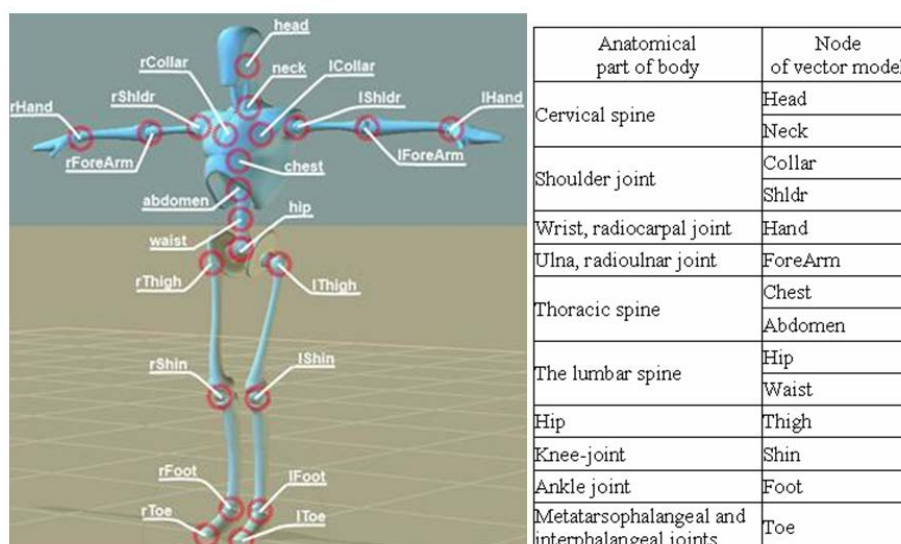


Figure 2. The vector model of body skeleton and correspondence between anatomical parts of body and nodes of the vector model

To obtain BVH-file, we have developed a new method consists of the following steps:

1. Getting data from the camera Kinect.
2. Determine the displacement of nodes relative to the parent node.
3. Record the hierarchy of key units in accordance with the specifics of the BVH-format.
4. Conversion of quaternions to the Euler angles.

With the vector model of body movements, presented as a BVH-file may work most of the currently existing animation packages.

Vector model of the human body is the formalized representation of the movement of the person, where as vectors are presented bones of the human skeleton, and the angles between them correspond to the rotation angles of the main nodes of the human body in relation to each other. The vector model of skeleton consists of 22 nodes, which correspond to different anatomical joints with one, two or three axes of rotation (Fig.2).

Using information on structure of body skeleton presented in the vector model and motion data contained in BVH-files, which describe poses of skeleton, we formalize the concept of motor activity of person expressed in gestures as follows [12]:

$$A(\Delta t) = \sum_{n=1}^m (T_n(\Delta t) \cdot k_n) \quad (1)$$

Here m is a number of time series describing movement of the body parts, $T_n(\Delta t)$ is a variation of the n -th time series for the time Δt , k_n is a coefficient that characterizes influence of the body parts on the body motion for the n -th time series.

The influence coefficient can be calculated as the following sum

$$k_n = \sum_{i=1}^{j_n} p_i \cdot q_{ni} \quad (2)$$

where i is a index of the body part, j is a number of the moving body parts, q_{ni} is a ratio of the body part in the total body mass, p_i is a gender coefficient of proportionality. According to biomechanical studies the averaged values of ratio q_{ni} for adults are equal to 6,9% for head, 15,9% for the upper section of trunk, 2,1% for shoulder, 16,3% for the middle section of trunk, 1,6% fore forearm, 11,2% for the lower section of trunk, 0,6% for brush, 14,2% for thigh, 4,3% for lower leg, 1,4% for foot. The gender coefficient p_i is equal approximately to 1 for all parts of man body, and differs for various parts of woman body.

Another important characteristic of body movement is a mobility of the joint, which is measured in morphology by values of the angles of flexion-extension, abduction-reduction, internal-external rotation as follows:

$$M_{joint} = \text{angle} (\text{Fold} + \text{Straightening}, \text{Bringing} + \text{Abduction}, \text{In} + \text{Out}) \quad (3)$$

The maximum spine mobility is a sum of the angles of the left and right rotation around the longitudinal axis of the body.

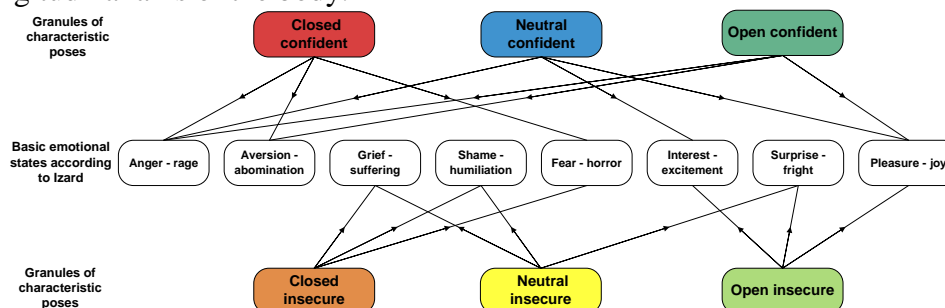


Figure 3. Compliance granules poses and basic emotional states

For automatic separation video districts of the individual poses and gestures, we introduce additional parameters, defined by the user: the minimum duration of the movement, the level of activity for poses, the level of activity for the movements. Next, we construct a graph of activity and find areas of the postures and movements [12, 13].

Poses discussed in detail in the works B. Birkenbil, G. Wilson, D. Morrison, A. Pease, were merged into granules, based on a similar interpretation. As it is impossible to unequivocally define the current posture emotional state of a person, we define the granules, which belong to the posture. This allowed us to increase the reliability of a particular emotional state. Compliance granules poses and basic emotional states by K. Izard is shown on Fig. 3.

We use information about emotional reactions to control the education of children with hearing disabilities. Briefly describe another developed by us system. The system is aimed for recognition and translation in real time gestures of the Russian language of the deaf in the text and the text in gestures. The system is intended for training of children with hearing disabilities and adults who need to learn sign language. It will be used in a test mode in school for children with limited hearing. But already now receives positive reviews.

Problem use Kinect to recognize the small gestures of hands is still unresolved, despite the successful application of Kinect to recognizing faces and tracking of the human body. The main reason for this low resolution depth map sensor.

In sign languages in communication, information is transmitted via several channels: directly through hand gestures, facial expressions, lip shape, position of the body and head. Hand gestures described via hand position, direction of movement, shape and direction of hands. The first stage of recognition is a segmentation of the image received from Kinect to find the hand or both hands. Development of a method for finding the hand in the picture is one of the most complicated problems in the process of creating a system of recognition of gestures.

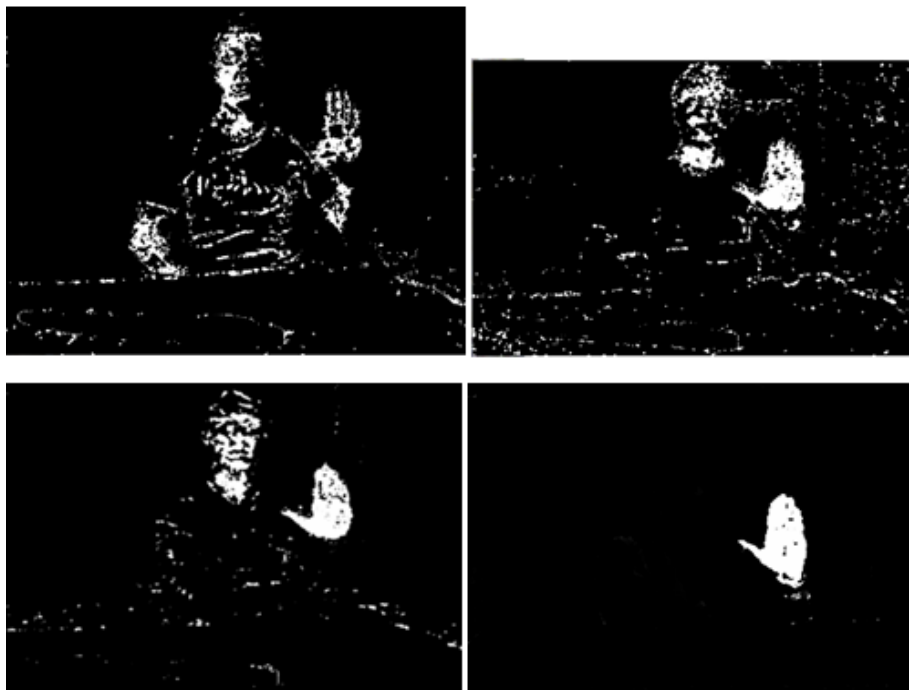


Figure 4. Finding hands on the image

There are several signs that can be used to detect the object on the image: the appearance, shape, color, distance to the subject and context. When detecting faces in the image, a good sign is the appearance, as the eyes, nose and mouth are always about the same proportions.

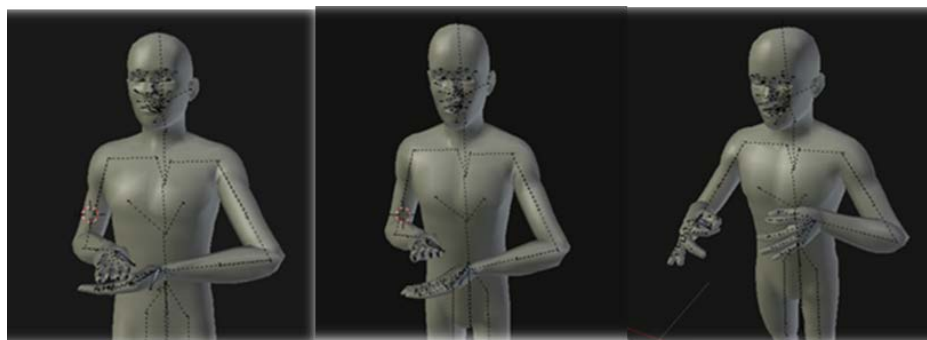


Figure 5. Animated demonstration gestures

Therefore, to find hands, we first find the face of a man, define its color and highlight the closest object. Accept his hands. Next we apply the developed method for finding the hands and define user gesture. An example of the recognition the user's hand is shown in Fig.4.

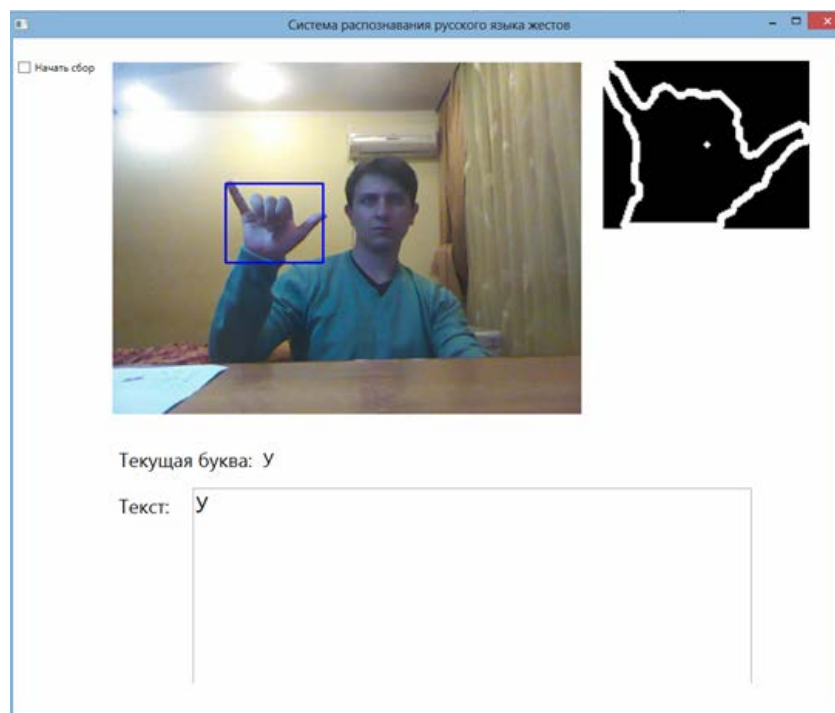


Figure 6. Show gesture language of the deaf

The system works as follows. The user enters text. The system displays an animated image of the gesture. A sample output of the animated gesture is shown in Fig. 5. User-child repeats movement. Example showing the user gesture is shown in Fig. 6. The movement is recognized and checked for correctness. If not correct, the movement is shown again. If correct, then enter the new text. If the user starts to receive a closed posture characteristic of anger, resentment, it is informing the administrator and learning process can be stopped.

The identification of the human emotional states is closed to the problem of understanding what is the normal behavior. The variety of "normal" behavior is great. So it is difficult to draw the line between acceptable and unacceptable behavior. The automation of the human emotion recognition can help to solve many problems of relationships between people and avoid possible misunderstanding.

Automated systems for the human emotion identification by gestures and movements can be useful and necessary in various areas such as communication of deaf people; education/learning; emergency services; monitoring unstable emotional state of pilots, drivers, operators of complex technical system, etc; monitoring public places to prevent illegal and extremist actions, and so on. [14]

In the future, we intend to use the developed approach to determine the emotional response by the handwritten text, and to animate human gestures and motions described in a limited natural language.

Acknowledgements. This work is supported by the grants of Russian Foundation for Basic Research 12-07-00266-a, 12-07-00270-a, 13-07-00351-a, 13-07-00459-a, 13-07-00461-a.

References

1. Orlova, Ju.A. Analiz i ocenka jemocional'nyh reakcij pol'zovatelja pri rechevom vzaimodejstvii s avtomatizirovannoj sistemoj / Orlova Ju.A., Rozaliev V.L. // Otkrytoe obrazovanie. - 2011. - № 2. - С. 83-85.
2. D. Bernhardt Emotion inference from human body motion. University of Cambridge Computer Laboratory, Cambridge, pp: 227, 2010

3. Petrovskij A.B. Teorija prinjatija reshenij. – M.: Izdatel'skij centr «Akademija», 2009.
4. Il'in, E.P. Jemocii i chuvstva / E.P. Il'in. - SPb: Piter. 2001. - 752 s.
5. Rozaliev V.L., Zaboлева-Zotova A.V. Modelirovanie jemocional'nogo sostojanija cheloveka na osnove gibridnyh metodov // Programmnye produkty i sistemy: mezhdunarodnyj nauch.-prakt. zhurnal. – Tver', 2010 – Vyp.2 (90). – S.141-146.
6. Coulson M. Attributing emotion to static body postures: Recognition accuracy, confusions, and viewpoint dependence. *Nonverbal Behavior*, 28, pp. 117-139, 2004.
7. N. Hadjikhani and B. Gelder. Seeing fearful body expressions activates the fusiform cortex and amygdale. *Current Biology*, 13, pp. 2201-2205, 2003.
8. R. Laban and L. Ullmann, The mastery of movement. Princeton Book Company, London, pp: 210, 1988
9. A. Zaboлева-Zotova, V. Rozaliev and A. Bobkov, Automated identification of emotional states. In the Proceedings of the 24th International Conference of Systems Research, Informatics and Cybernetics, pp: 21-25, 2012
10. A. Zaboлева-Zotova, Y. Orlova, V. Rozaliev and A. Bobkov, Emotional state recognition based on the motion and posture. In the Proceedings of the Workshop Operations Research and Data Mining, pp: 161-169, 2012.
11. Avtomatizacija postroenija vektornoj modeli tela cheloveka / Rozaliev V.L., Orlova Ju.A., Shpirko A.A., Dorofeev N.S. // Jeletrotehicheskie i informacionnye komplekсы i sistemy. - 2013. - № 2, t. 9. - C. 102-106.
12. L. Bernshtein, Models of representation of fuzzy temporal knowledge in databases of temporal series. *Journal of Computer and Systems Sciences International*, 48 (4), pp: 625-636, 2009.
13. Orlova, Ju.A. Obzor sovremennyh avtomatizirovannyh sistem raspoznavanija jemocional'nyh reakcij cheloveka / Orlova Ju.A., Rozaliev V.L. // Izv. VolgGTU. Serija "Aktual'nye problemy upravlenija, vychislitel'noj tehniki i informatiki v tehnikeskikh sistemah". Vyp. 10 : mezhvuz. sb. nauch. st. / VolgGTU. - Volgograd, 2011. - № 3. - C. 68-72.
14. Razvitie sistemy avtomatizirovannogo opredelenija jemocij i vozmozhnye sfery primenenija / Zaboлева-Zotova A.V., Orlova Ju.A., Rozaliev V.L., Bobkov A.S. // Otkrytoe obrazovanie. - 2011. - № 2. - C. 59-62.

CONVERGENCE OF MULTIPLE ITERATIVE SOLUTION OF LINEAR ALGEBRAIC SYSTEMS WITH A FULLY VARYING MATRIX USING A SINGLE CALCULATED INITIAL PRECONDITIONER

Salov V.K., Gazizov T.R., Nikitina O.A.

Television and Control Department, Tomsk State University of Control Systems and Radioelectronics, Tomsk, Russian Federation

Convergence of multiple iterative solution of linear systems is investigated. Several parameters of structure under consideration are changed leading to change of entries in arbitrary parts of a matrix or to full change of the matrix. LU-factorized matrix S , obtained for initial parameters of structure, is used as a preconditioner. To investigate the convergence of the solution, iterations are continued until the relative norm of the residual vector was larger than 10^{-16} . The proposed approach may decrease considerably the time of multiple iterative solution of linear systems. Estimates of the speed up will be presented in final paper.

I. Introduction

Numerical solution of electrostatic problems often reduces to the solution of linear algebraic system $\mathbf{S}\boldsymbol{\sigma}=\mathbf{v}$, where \mathbf{S} – $N \times N$ sized dense matrix describing a structure, $\boldsymbol{\sigma}$ – unknown vector of charge density on conductors and dielectric boundaries, while \mathbf{v} – prescribed voltage. For this purpose, boundaries of structure are divided into N segments. The increase of N increases the computational accuracy. As is known, when direct methods are used the time required for linear system solution is proportional to N^3 and can be considerable. The use of iterative methods allows tenfold speed up of the linear system solution [1], but convergence of solution depends on many parameters including the type of the problem solved, therefore the usage of them is still limited. Preconditioner usage in iterative methods allows to speed up the convergence of the solution of linear system with dense matrix but, in such a case, the time for preconditioner matrix factorization is also spent.

However, problems in which there is a need to solve a linear system with similar matrix many times exist, for example, multiple computation of per unite length capacitance of structure with its geometrical and electrophysical parameters changing [2]. Similar problem arises during structure optimization by gradient methods. In such a case, single factorized matrix \mathbf{S} can be kept and used as a preconditioner matrix in order to compute capacitance of other structures. Such approach has been proposed and tested on example of calculation of coupled microstrip line capacitance with relative permittivity changing [2]. The matrix obtained by zeroing the matrix \mathbf{S} entries, which are lower than defined drop tolerance, and by ILU(0) factorization has been used as a preconditioner [3]. Simple formulas for analytical estimation of the obtained speed up have been derived. Its important corollaries have been formulated which determine the choice of iterative solution parameters and possibilities to obtain additional speed up. Particularly, it was shown, that the use of LU-factorization instead of ILU(0) may be more effective for large number of solved linear systems. However, the partial and very week changing of linear system matrix, requiring just 1–3 iterations for obtaining the solution has been considered. The iterative process has been continued until the relative norm of the residual vector was larger than 10^{-6} . However, convergence of the solution with increasing the number of iterations has not been considered.

In this paper, convergence of multiple iterative solution of linear systems is investigated. Several parameters of structure under consideration are changed leading to change of entries in arbitrary parts of a matrix or to full change of the matrix. LU-factorized matrix \mathbf{S} , obtained for initial parameters of structure, is used as a preconditioner. To investigate the convergence of the solution, iterations are continued until the relative norm of the residual vector was larger than 10^{-16} .

II. The description of the numerical experiment

Geometrical parameters of the structure have the following values: the width of the conductor $w=400\text{ }\mu\text{m}$, the thickness of the conductor $t=10\text{ }\mu\text{m}$, the thickness of the substrate $h=200\text{ }\mu\text{m}$, the relative permittivity of the substrate $\epsilon_r=1.3$, the distance from the edge of conductor to the edge of structure is $2000\text{ }\mu\text{m}$. Every boundary of the structure is divided into 300 subintervals. Fig. 1 shows the cross section of structure.

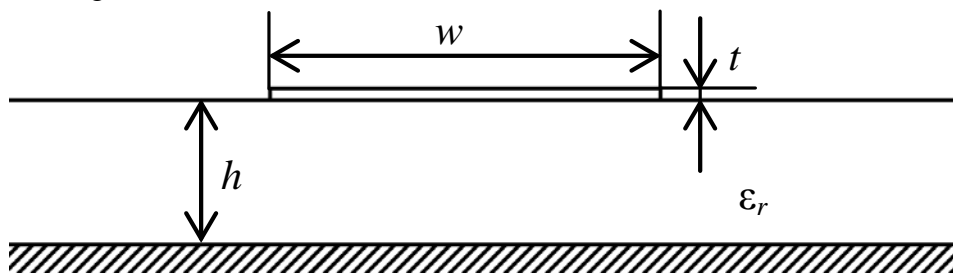


Fig 1. Cross section of structure under consideration

The algorithm of multiple computation of the per unit length capacitance of the structure:

1. Creation of the structure with geometrical and electrophysical parameters from the initial data ($w_0, h_0, t_0, \varepsilon_{r0}$).
2. Computation of \mathbf{S}_0 matrix entries by the method of moments [4] and factorization of the matrix.
3. Calculation of the per unit length capacitance of the structure.
4. For $i=1, 2, \dots, 10$
 - Value change of one of the initial parameters ($w_i=w_{i-1}+\Delta w, h_i=h_{i-1}+\Delta h, t_i=t_{i-1}+\Delta t$, or $\varepsilon_{ri}=\varepsilon_{ri-1}+\Delta\varepsilon_r$).
 - Creation of the structure using new parameters ($w_i, h_i, t_i, \varepsilon_{ri}$).
 - Matrix \mathbf{S}_i computation.
 - Solving linear system $\mathbf{S}_i\boldsymbol{\sigma}_i=\mathbf{v}$ by BiCGStab method with preconditioner taken as a factorized matrix \mathbf{S}_0 .
 - Calculation of the per unit length capacitance of the structure.

During the solving of linear system by the iterative method, after the every (j -th) iteration the residual norm is obtained as $r_j=\|\mathbf{v}-\mathbf{S}_j\mathbf{x}_j\|_2/r_0$, where \mathbf{x}_j – vector of the solution obtained after the j -th iteration, $r_0=\|\mathbf{v}-\mathbf{S}_0\mathbf{x}_0\|_2$, \mathbf{x}_0 – vector of the initial guess (unit vector). Iteration method parameters: maximum number of iterations – 50, condition of iterations break out – $r_j<10^{-16}$.

III. Convergence of the iterative solution

A. Change of ε_r

Fig. 2 shows residual norm after the j -th iteration for $\varepsilon_r=1.5, 1.7, \dots, 3.3$. It is clear, that for the ε_r increasing to 2.7 the number of iterations required for the same residual norm is increasing. Residual norm r_j reaches the value of 10^{-2} for $\varepsilon_r>2.7$ and does not reduce if the iterations are continued and, in such a way, the solution does not converge.

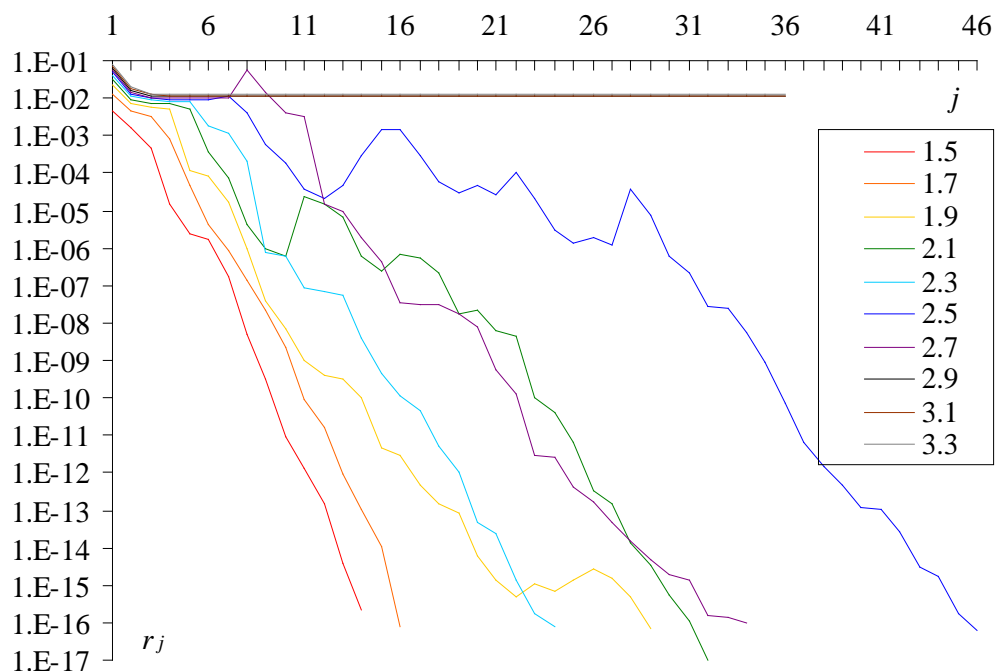


Fig 2. Dependence of residual norm on the j -th iteration for $\varepsilon_r=1.5; 1.7; \dots, 3.3$

B. Change of w

Fig. 3 shows residual norm after the j -th iteration for $w=475, 550, \dots, 1150 \mu\text{m}$. It is clear from the plot that for increasing the w the number of iterations is increasing. The solution is obtained for the value of w changed to 850. For greater values the method did not converge but when $w=1075 \mu\text{m}$ r_j reached the value of $2.5 \cdot 10^{-16}$ during the last iteration.

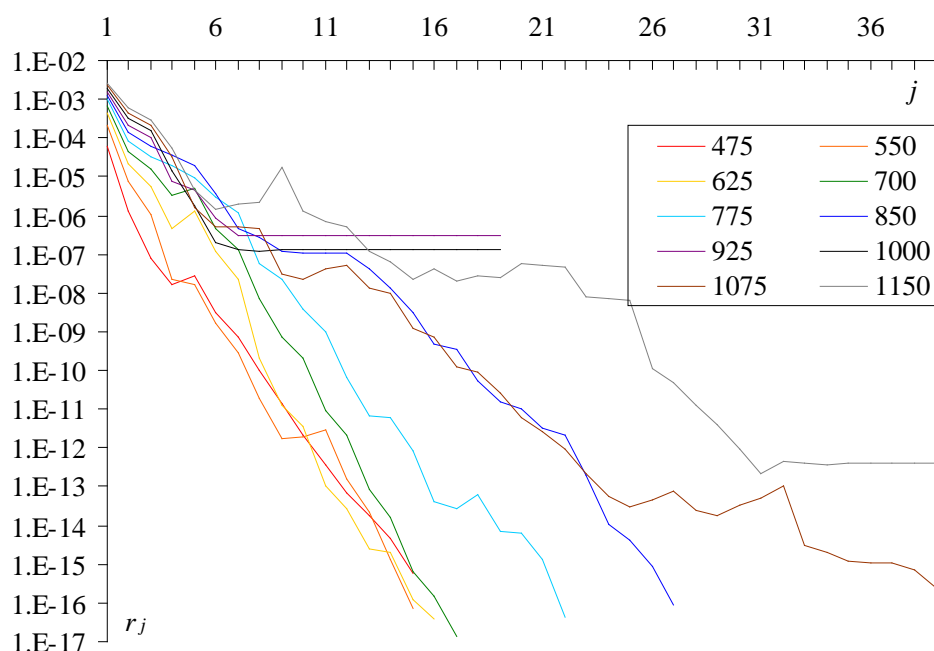


Fig. 3 Dependence of residual norm on the j -th iteration for $w=475, 550, \dots, 1150 \mu\text{m}$

C. Change of t

Fig. 4 shows residual norm after the j -th iteration for $t=15, 20, \dots, 60 \mu\text{m}$. As in the previous experiments, it is clear that the increase of the parameter increases the number of iterations. The solution is obtained for the value of t changed to 25 μm . For $t=30 \mu\text{m}$ r_j reached the value of $1,77 \cdot 10^{-16}$ during the last iteration. For greater values the solution did not converge.

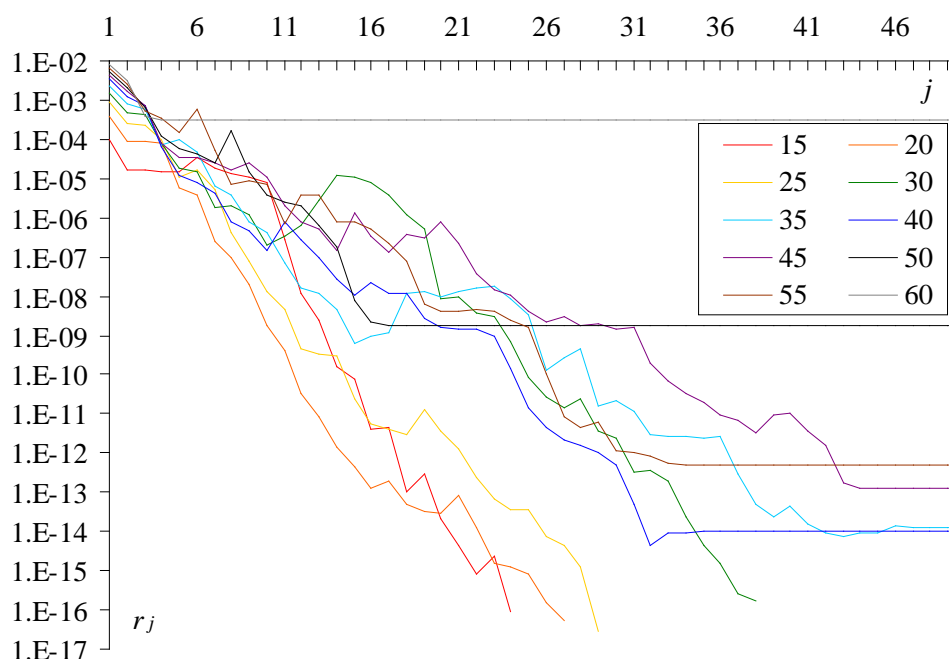


Fig. 4. Dependence of residual norm on the j -th iteration for $t=15, 20, \dots, 60 \mu\text{m}$

D. Change of h

Fig. 5 shows residual norm after the j -th iteration for $h=250, 300, \dots, 700 \mu\text{m}$. The number of iterations required for the convergence increases as the h increases. For $h=250$ r_j achieved the value of $1.21 \cdot 10^{-16}$. For $h>450$ the method did not converge, residual norm reach achieved the value 10^{-3} .

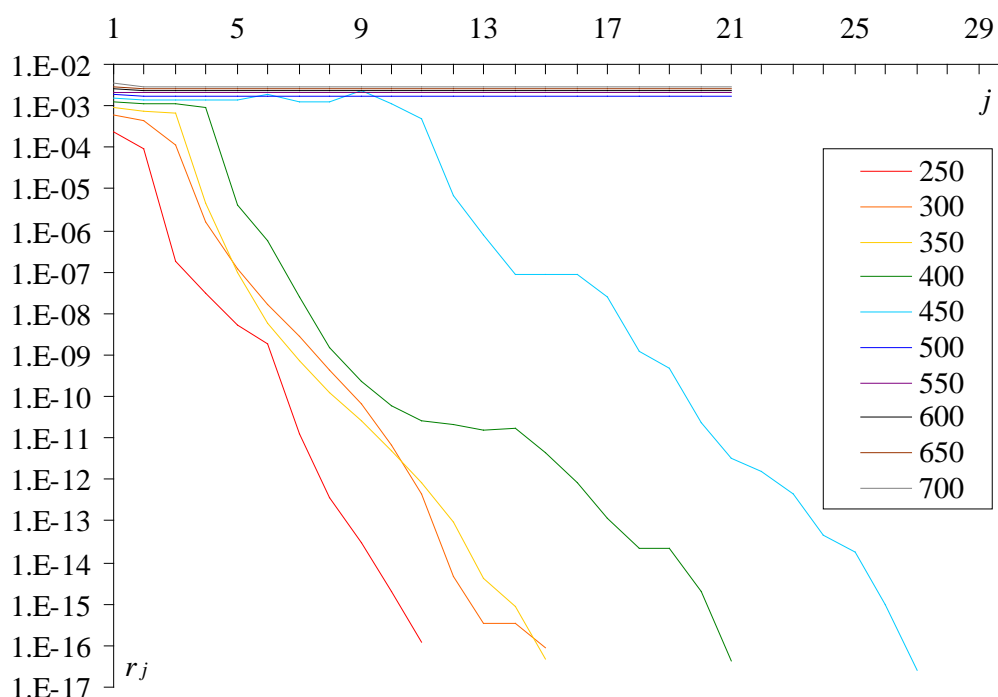


Fig. 5. Dependence of residual norm on the j -th iteration for $h=250, 300, \dots, 700 \mu\text{m}$

IV. Conclusion

Thus, it is possible to use as a preconditioner the factorized matrix computed from initial parameters to solve by the iterative method the linear system for other parameters. But as the difference between the values of these parameters increases (by factor 2–3) the number of iterations also increases. Therefore, it is important to know the maximum number of iterations when the time required for solving by the iterative method is less than by the direct method. If the solution does not converged, then it is possible to recalculate preconditioner by means of calculation of matrix \mathbf{S} for current parameters of structure and by following factorization of the matrix, thereby, guarantying the solution convergence for total range of changing the parameters.

In any case, the proposed approach may decrease considerably the time of multiple iterative solution of linear systems. Estimates of the speed up may be easily performed.

References

1. Kuksenkov S.P., Gazizov T.R. Dense Linear System Solution by Preconditioned Iterative Methods in Computational Electromagnetics. Proc. of the 19-th Int. Zurich Symp. on EMC. Singapore, May 19–22, 2008, pp. 918–921.
2. Akhunov R.R., Kuksenkov S.P., Salov V.K., Gazizov T.R. Multiple iterative solution of linear algebraic systems with a partially varying matrix. Journal of Mathematical Sciences, 2013. To be published. Transl. from Zapiski Nauchnykh Seminarov POMI, Vol. 419, 2013, pp. 16–25.

3. Y. Saad. Iterative methods for sparse linear system. Second edition with corrections. January 3rd, 2000.

4. Gazizov T.R. Analytic expressions for Mom calculation of capacitance matrix of two dimensional system of conductors and dielectrics having arbitrary oriented boundaries. Proc. of the 2001 IEEE EMC Symposium, Montreal, Canada, August 13–17, 2001. Vol. 1. P. 151–155.

SAMPLING DATA PROCESSING – APPROACH TO SPEEDING UP ITERATIVE ALGORITHMS ON MAPREDUCE MODEL

Mityakov A. V, Tatarinov U. S.

Saint Petersburg Electrotechnical University "LETI"

In this paper we propose a method of sampling data to increase the performance of iterative algorithms on MapReduce model. A method proposed for selective data update based on priorities.

Keywords: MapReduce, iterative algorithms, sampling data

Iterative algorithms. Iterative algorithms are an important class of algorithms that underlie many others: machine learning, graph algorithms, reference analysis and others. The main idea of iterative algorithms is that data are processed in a cycle and the output of one iteration is the input of the next one until a certain condition is true. As the amount of data in various fields of human activities are growing distributed data processing systems become necessary. The most popular and well-known systems of this kind are various implementation of MapReduce models, for example, Apache Hadoop.

The performance of iterative algorithms on MapReduce model is possible but it is noticeably less efficient in comparison with various more specialized systems. Disadvantages of MapReduce model for the execution of iterative algorithms are associated with one of the main advantages of this model – namely, fault-tolerance. An iterative algorithm in the MapReduce model is a sequence of MapReduce-tasks (pairs of Map and Reduce phases), running in a loop until a certain condition fulfills. In order to provide fault tolerance, the results of each MapReduce task are stored in a distributed file system. The next iteration is forced to load data again as an input from a distributed file system. The cost of network IO is the main factor that adversely affects the performance of iterative algorithms on MapReduce model.

There are various system of iterative algorithms execution that devoid of this shortcoming [1]. All these solutions are essentially different variants of balance between fault-tolerance and performance. At the same time in terms of performance they mainly focus on reducing network input/output.

In this paper, we consider the possibility of reducing both network and disk input/output by selective data processing on each iteration.

Figure 1 shows a generalized scheme of existing systems for iterative algorithms execution (the main differences appear on the lower level of specific implementations).

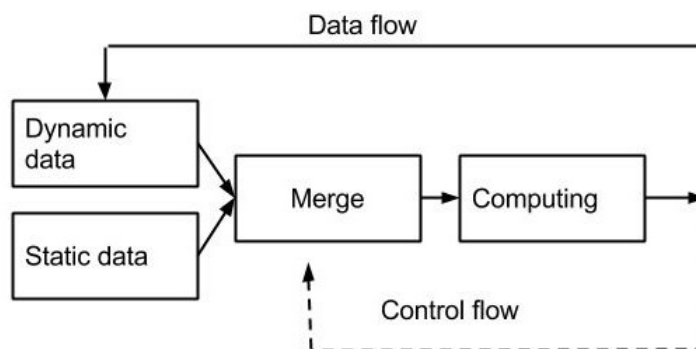


Figure 1.

Data streams in the system may be divided into two types: static and dynamic. The static part of the data (e.g. the structure of the graph) does not change between iterations and is cached in the cluster nodes. The static part is usually the biggest and significant economy of network traffic is achieved in nodes due to its caching. The dynamic part is the result of the algorithm work on a particular iteration. Before starting a new iteration the static and dynamic parts are merged to produce the actual terms of the algorithm data set for the current iteration.

As an extension of this architecture we propose to introduce a control flow in addition to the data flow, which would set a multitude of data (keys) for processing in the next iteration.

Sampling data processing. In the MapReduce model all available to node data are processed on the Map phase. So even if it is known what kind of data in the current iteration can be omitted we still have to process them. This is due to the fact that at the moment of the Map phase execution we have no information about what data is processing in parallel Map-nodes. Therefore, we can decide whether to process specific data only post facto on the Reduce step. The basic idea of the selective processing method is to reduce the intervals between which we can make a decision and to execute a correction of a selection.

We propose to modify the model to provide an algorithm developer a way to set what data should be processed in the next iteration.

As an example, let us consider a shortest path search algorithm in the graph. In our previous work [2] the results of this algorithm on two real public graphs (Amazon Ads and YouTube Ads) are represented. The experiment is conducted in order to compare the amount of data to be processed in an unmodified version of MapReduce and in case of feedback to adjust a selection. The results of the experiment are shown in Figure 2.

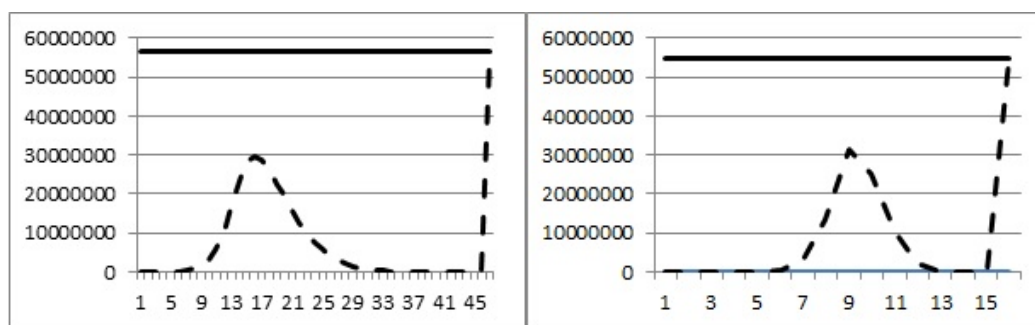


Figure 2.

As seen from the figure, the possibility of forming the selection for processing in the next iteration allows to reduce the amount of processing data from 50% to 90%. In this paper we extend this approach by introducing the concept of priority.

Sampling data processing with priorities. The basic idea underlying the proposed approach is the following assumption: “The order in which data is processed affects the speed of the whole algorithm”.

Priority execution means the following. At each iteration only K data items with highest priority according to some criterion are processed. At the same time K is much less than the total amount of available data. Thus, the total number of iterations increases but because of small amounts of data they are processed much faster. Next, on a specific example we will demonstrate that data processing in priority order may significantly reduce the execution time by using different heuristic approach.

Let us refer to the shortest path search algorithm in the graph. An example of heuristics for this algorithm is an analogy with the sequential implementation of this algorithm - Dijkstra algorithm. Dijkstra is an example of "greedy" algorithm - every time a path with the least weight is chosen in a graph. In a typical implementation of MapReduce model usage of this heuristic is not possible, but it is quite possible to describe it on the level of a prioritized selection.

We conducted an experiment to find out whether this heuristics allows to reduce the total amount of data transmitted over the network in a parallel version of the algorithm. We modify the algorithm in a way that each iteration processes K vertices with the smallest current distance. The results of this experiment are shown in Figure 3.

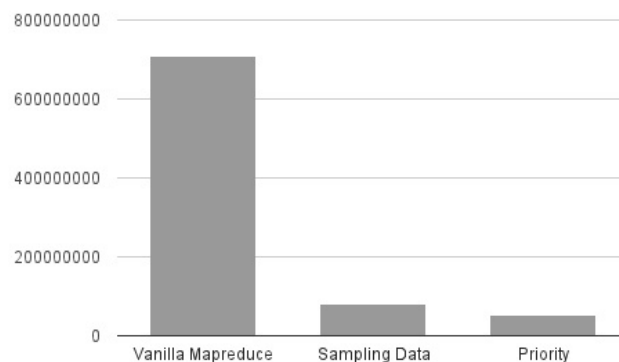


Figure 3.

As the diagram shows the use of processing priorities reduces the amount of network traffic up to 38% in comparison with the manual selection of data and up to 700% in comparison with the classical MapReduce model implementation. This is achieved at the expense of two additional iterations.

The overall system architecture. In order to get a more accurate time estimates of the effectiveness of the proposed method and its applicability to other algorithms it is necessary to implement a specialized framework. The general scheme of the framework supporting the selective data processing is presented at Figure 4.

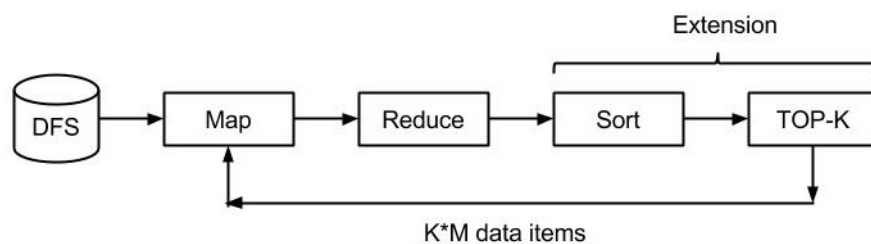


Figure 4.

Compared with the base implementation of MapReduce model we propose three additional components:

1. Indexation
2. Sorting
3. Selection of Top-K elements

Let us consider each of the elements in more detail.

Indexation. The base implementation of MapReduce model assumes that the Map nodes sequentially process all data available to them. We would like to decrease the available data to some subset and update only it. To avoid sequential read we need to know where exactly on the disk the needed data are located. To construct the index, we need to make one complete pass through the data. Since on the first iteration of any iterative algorithm a selection is not formed yet we use the first iteration to build index of data. As an algorithm for indexing different algorithms may be used depending on available memory. We consider the situation (in our opinion the most relevant one) when the memory is cheap and a large amount of it may be used, but in this case the data fetch time based on index is really important. In this regard, we use an indexing algorithm based on B-TREE.

Sorting. One of the key, in our opinion, factors of the MapReduce model popularity nowadays is a low entry threshold for writing distributed algorithms. A developer should implement only two functions: Map and Reduce. All other tasks of routing data, fault tolerance and monitoring the progress are implemented by MapReduce framework. In developing the architecture of our system we tried to be guided by the same principle.

Sampling can be performed in two modes: manual and automatic. In the manual mode, the developer of the algorithm indicates what data should be processed in the next iteration in the implementation of the Reduce function by himself. In automatic mode, the developer is required along with the implementation of the Map and Reduce functions also specify the implementation of the SORT function:

```
int function SORT( ReduceValue1, ReduceValue2 )
```

The function takes two values derived from the function Reduce as parameters. And the result values are: -1 ($rv1 < rv2$), 0 ($rv1 == rv2$) or 1 ($rv1 > rv2$).

In the case of the automatic selection formation Reduce-nodes work results are sorted according to the SORT function and the first K elements fall into the selection for the next iteration.

Sorting algorithm is essentially a modified version of the "merge sort" algorithm. Modifications of the algorithm is connected with the fact that since the second iteration in the Reduce-nodes have already presented sorted data from the last iteration. Therefore, only values that have changed are sorted. Then they are merged with the data from the last iteration.

Selection of Top-K elements. The main parameter on which we can influence is the maximum number of elements in the sample. The queue can be of two types : local (for each Map node), and global - is shared to all nodes. Shared queue leads to the problem of fragmentation of the workload between the compute nodes . So theoretically one node can get 99% of all processed data. Presence of a barrier [3] in MapReduce model forces Reduce nodes to wait while all Map nodes are finished. In this regard, the fragmentation of the selection by the nodes can be a serious performance problem. The solution to this problem is the introduction of local queues for each node. At the same time we should ensure that the size of the queue is about the same to increase the probability that all Map nodes finish at the same time. It is also worth noting that the same queue size is not always guarantee equal time spent on data processing.

Value of the parameter K is an important factor affecting the performance of the algorithm. In particular, when K is close to the maximum number of existing vertices at the

nodes there is no sense in selective update. On the other hand, when K is close to 0 - the cost of starting a new iteration and transfer data is much more than benefits from this approach. In this regard, the optimum value of K is an important parameter in the presented method, and requires further investigation.

Results. Controlling the data to be processed in the next iteration by itself may reduce the execution time by reducing the amount of disk and network IO operations. The method of prioritized selective update for a number of algorithms allows to apply heuristics to improve their time efficiency. The presented experiment with the graph search algorithm with applying heuristic assertions that we should first go over shorter paths can increase the efficiency of the algorithm in comparison with its implementation on the base selective update up to 38% and by 700% in comparison with classical MapReduce model.

To study the applicability of this approach to other algorithms, we are implementing a software framework to support a prioritized selective data processing.

References

1. Mityakov A. V., Tatarinov U. S. Podhody k effektivnomu ispolneniyu iterativnyh algoritmov na modeli MapReduce. // *Isvetiya LETI*, Vyp. 2, 2014 C. 30-41.
2. Mityakov A. V., Tatarinov U. S. MapReduce: Problema polnogo perebora v iterativnyh algoritmah i podhod k resheniyu. // *21 century: fundamental science and technology III Vol. 2*, Moscow, 2014.
3. A. Verma, N. Zea, B. Cho, I. Gupta, and R. Campbell, "Breaking the MapReduce stage barrier," in *CLUSTER 2010*, Heraklion, Crete, Greece, 2010, pp. 235 –244.

MULTIAGENT APPROACH FOR DEVELOPING HYBRID INTELLECTUAL SYSTEM

Semenov, A.

Orenburg, Orenburg State University

In this work we consider the aspects of developing software system with hybrid architecture. The multiagent system methodology presenting modern tendency in the sphere of new technologies is in its basis.

Keywords: multiagent system, hybrid intellectual system, soft computing, contextual diagram.

Nowadays one of the main tendencies in developing hybrid systems is distributed artificial intelligence (DAI). The technology of multiagent systems is oriented towards joint use of scientific and technical achievements and advantages of models and artificial intelligence methods. Multiagent systems can be built by the principle of distributed intelligence as an integration of separate intellectual systems having their own knowledge base and means of reasoning. The author of this publication understands by agent the program essence able to act for goal achievement determined by a user.

Agent is a program module which can perform assigned functions or the ones of another agent (a man whose functions it reproduces) [1]. For hybrid intellectual system modules development with multiagent system theory application we chose 3 basic types of architectures [2]:

- architectures which are based on principles and methods of work with knowledge
- architectures based on behavioral model stimulus- response type;
- hybrid architectures.

Hybrid architectures allow to combine possibilities of all approaches, including soft computing.

To solve given problem the contextual diagram which presents the general description of hybrid intellectual system and its interaction with external data are shown in figure 1.

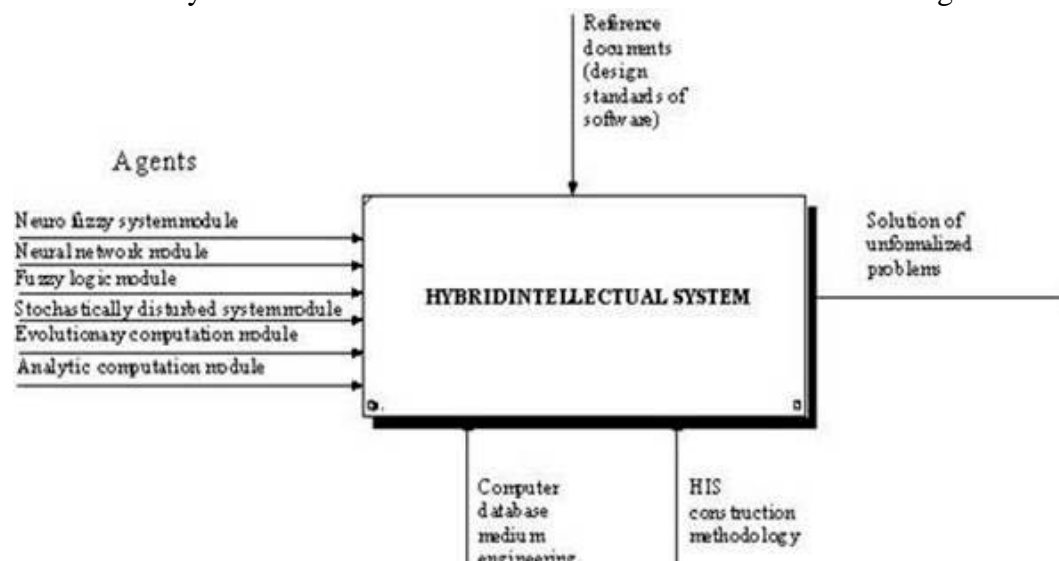


Figure 1 – Functional model of GIS. Context diagram of IDEFO.

To create HIS and develop modules C-# was taken as programming language, supporting standard SQL, having components for making reports and diagrams, transaction supporters, utility programs for database work, is simple and fast for program creation.

The following algorithms were developed and realized in programs in the course of researches: fuzzy modeling for expert or control system; adaptive system for neuro fuzzy output (ANFIS); neural network emulator, expert system basing on Bayesian approach to inference. frame-based expert system, genetic algorithms for learning neural networks and optimization problem solution, machine-learning algorithm, expert system for multicriteria evaluation for power supply systems.

The test was held with the use of well-known applications. The developed modules are approved by unformalized problems solution in different subject fields in the course of lab(oratory) work and practical training in computer software and automation systems department of Orenburg State University [3-5].

The further research is determined by organization and loosely coupled agent algorithms jointly functioning for general problem solution, development data base for learnt neural networks, inference algorithms, knowledge base and intellectual interface for HIS.

References

1. Pospelov D. A. Multiagent systems- present and future // Information technologies and computer system; -1998, -No1. 14-21.
2. Kolesnikov A. V., Kirikov I. A. Methodology and technology of complex problem solutions via hybrid intellectual systems. RAS, 2007.-387.
3. Certificate No 2009616955 Russian Federation. Fuzzy interference system. Certificate about state computer program registration/ Semenov A.M, Soloviev N.A, Tsygankov A.S.; application 15.12.2009.
4. Certificate No 2009616955 Russian Federation. bundled software ESMOS; Certificate about state computer program registration Semenov A.M, Semenova L.A. application 15.12.2009.

5. Semenov A.M., Semenova N.G., Krylov I. B. Knowledge base of intellectual technical discipline learning system // Reporter of Orenburg State University. 2013. No19 (115). 232-239.

DOUBLE-LEVEL EXPERT SUPPORT SYSTEM OF MAKING DECISION IN THE CHOICE OF ELECTRIC SYSTEMS DEVELOPMENT MODEL

Semenova, L.
Orenburg, Orenburg State University

The problem of choosing a model of development of electric power systems were examined in the light hierarchical approach, multicriteriality evaluation and suspense of the original information. The structure and algorithm of the software system, designed to support decision-making for the development of electric power systems, were presented.

Keywords: electric power system, multicriteria analysis, decision support system, the theory of fuzzy sets.

Modern electrical power systems are complex, multilinked, spaced hierarchical objects functioning in conditions of their structure, parameters and operating regime variability. It defines the problem of their control including the choice of electric system development.

Making decision in the choice of electric systems development should be referred to such problems which solutions by existing methods is difficult due to complexity of formalization process.

First of all, one should use an hierarchical principle when choosing electric system development model. According to it the problem of model development choice is divided into several simple and technologically and data interrelated tasks which could be solved in all steps of territorial hierarchy control referred to different time levels (figure 1).

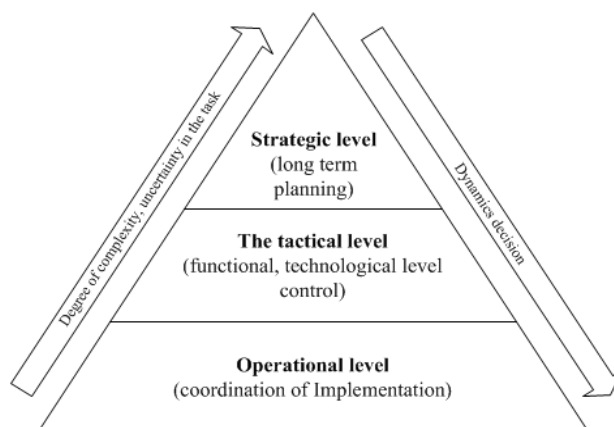


Figure 1 – levels of making decision.

Decomposition in the time aspect consists in dividing general decision-making task of electric systems development into the ones referred to 3 temporal hierarchy control levels: long-range strategical planning, tactical planning and operational control (figure 1).

By such general task decomposition for each level new alternative development systems are specified and established by means of their detailed consideration in technological and territorial aspects. Each of these levels is directed towards one relevant task and the first task is in data collection and system analysis.

Thus, considering hierarchical (decompositional) approach to the choice of electric systems development model, firstly, it will consist in the choice of more preferable strategy by the sum total of criteria from multitude of all possible alternatives and, secondly, in defining best values (more rational) of system parameters for the chosen strategy (coordination level for taking decision is not considered in this work).

Secondly, the complexity of process formalization in choosing an electric system development model is conditioned by the presence of uncertainty related to the number of factors such as: impossibility to take into account all peculiarities of the problem; data insufficiency of the system etc. Moreover multipurpose situation of making solution, when in most of cases they need consideration of several conflicting estimation criteria of electric system development models should also be taken into account.

The optimal variant electric system development choice in terms of uncertainty could be performed mathematically in the following way:

$$a^* = \underset{a_i}{opt} \{f_k(a_i, s_n), a_i \in A\} \quad (1)$$

$$\forall a_j, a_m \in A, \text{ if } a_j \succ_{c_k} a_m : f_k(a_j, s_n) \{<, >\} f_k(a_m, s_n),$$

where a^* – is an optimal development variant from set of alternatives, $A = \{a_1, a_2, \dots, a_i\}$;

c_k – k criterion of solution from set $C = \{c_1, c_2, \dots, c_k\}$;

$f_k(a_i, s_n)$ – criterion value of k -criterion for i -alternative subject to possible situations (of uncertainty) $s_n \in S = \{s_1, s_2, \dots, s_n\}$;

the sign «<» or «>» is defined by the character of criterion: minimization or maximization.

To make detailed analysis of taken solutions in electrical power engineering, to estimate their validity and to give appropriate recommendations is impossible without intellectual data-computing means specially developed for these purposes. That's why a big progress in solution of such problems, evidently, may be achieved by combining widely used traditional mathematical models and methods with new information technologies possibilities supported by means of artificial intelligence in a way the advantages of ones would compensate the disadvantages of others [2].

One of the fastest developing and promising directions is the one connected with the use of artificial intelligence technologies which involve neural networks, expert systems, indistinct logic, genetic algorithms etc. [3]. Their principal ideas differ considerably from standard computing methods copying either “human” ways of problem solution or “natural, genetic” process development. For example, neural networks have ability to learn, indistinct logic systems use such terms as uncertainty or partial/approximate truth. All these systems can supplement each other increasing the possibilities of optimal solution in the choice of electric system development model.

Making decision support systems can be called the first developments in the sphere of artificial intelligence. They combine strict formal methods and solution search models with heuristic ones based on expert knowledge and intelligent interacting modules.

The process of taking managerial decision in the sphere of electrical power engineering are similar to data processing in any intellectual system. A standard system structure of making solution can shown by the following blocks (figure 2): knowledge base with reasoners; intellectual solver; intellectual planner; system explanation system; intelligent interface with user. Such problem-solving systems can differ significantly by their architecture and functions, but they always use to a degree the above mentioned blocks. At the same time the most difficult problem-solving functions basing on reasoners with the use of knowledge base data are realized in “intellectual resolvent” block.

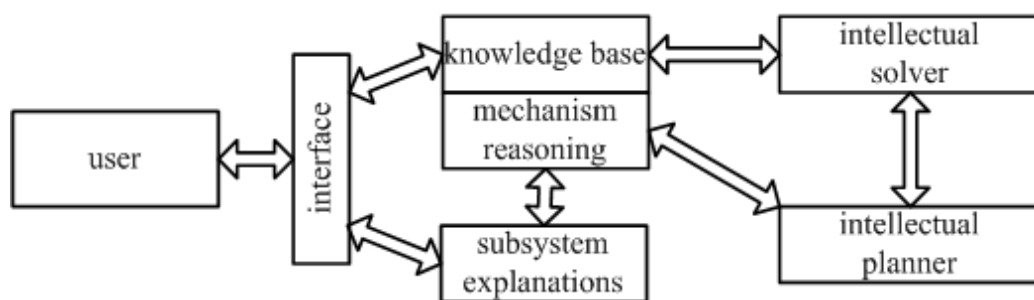


Figure 2 – standard expert system structure.

The author, taking in account decompositional approach, developed a software package “ESMOS” which represents double-level decision-making support system for the choice of electric systems development model using a single infobase [3].

The first level involving experts consists in qualitative evaluation of possible electric system development model strategies and the choice of the most preferable one by the sum total of criteria. To this effect the following expert evaluation methods are realized in software “ESMOS”: pair comparison, generic regulation, evaluation itself and algorithms of getting coefficient expert competence and expert group forming.

The second level performs computing experiments for an optimal parameter value determination of the system for the chosen strategy. At the given level the systems parameter choice is carried with the use of fuzzy-set theory which makes it possible to build multiple criteria model for variants evaluation with due regard for uncertainty of the part of initial information.

In general case, when there is k of purposes and m of limitations, the optimal final solution is determined by all purposes and limitations crossing:

$$\mu_D(x) = \mu_{c_1}(x) \wedge \mu_{c_2}(x) \wedge \dots \wedge \mu_{c_k}(x) \wedge \mu_{g_1}(x) \wedge \mu_{g_2}(x) \wedge \dots \wedge \mu_{g_m}(x), x \in X. \quad (2)$$

where $\mu_{c_k}(x)$ is a membership function of fuzzy objectives (make decision criterion);

$\mu_{g_m}(x)$ – membership function of fuzzy constrain.

The software includes all attributes of make decision support systems: database (information about experts; information about equipment installed in substations; retrospective and predictable power consumption level etc.); knowledge base (model development estimation by economical, technical and technocentric criteria); solvers (programs for choice of an optimal electric systems development model); simple interface.

The software consists of the following modules shown in the figure 3. The module Main is the principal one, made for other modules interaction, database connection and for main menu providing. Matrix module, which consists of two initial and one result-matrixes makes main matrix operations. DBase module makes operations with database. Kompetent module realizes algorithm to get competence coefficient of experts and form expert group. ParnyhSr, Rang, NepOcenka make pair comparison, generic regulation, evaluation algorithms for electric systems strategy determination. Discontir, Energy, NeOtpusk, DILiniy, Structur modules performs calculation algorithms of the chosen evaluation variant criteria (discounted costs, energy consumption, low-power level, cable length, optimal electric systems structure). SelStrateg module implements user interface for detecting optimal strategy parameters.

Figure 4 shows the functional diagram of “ESMOS” software package.

Figure 5 presents window “ESMOS” form with the results of nomenclatorial parameters choice of “substation modernization” strategy.

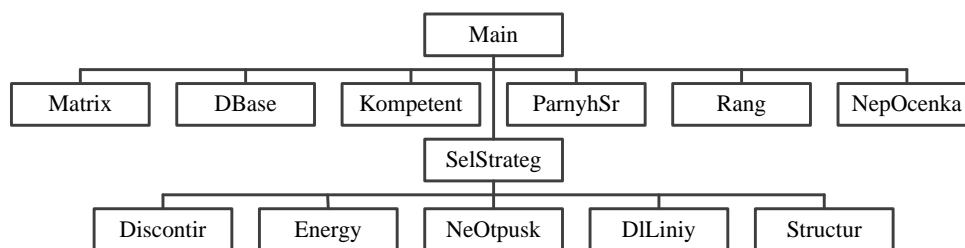
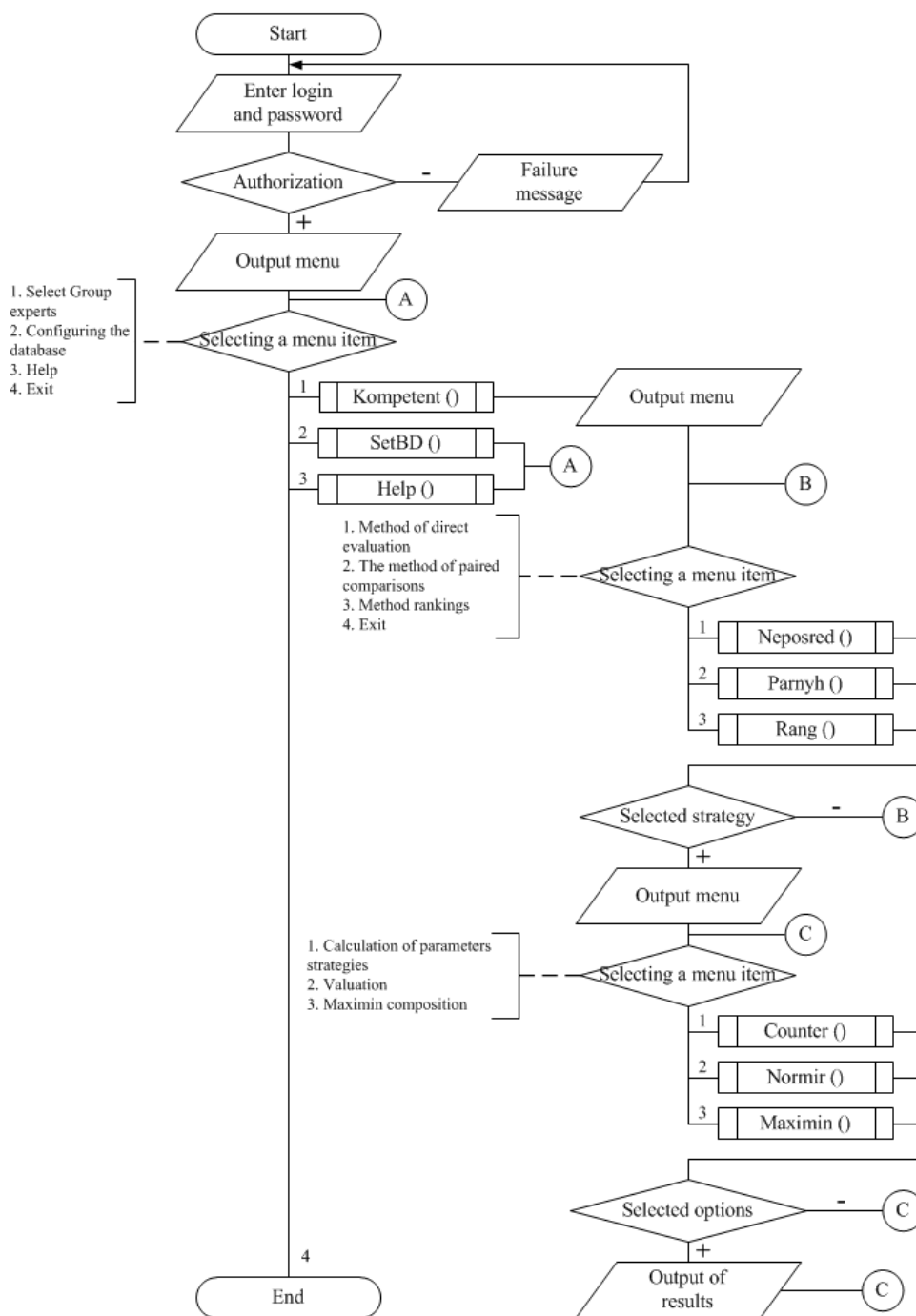


Figure 3 – modular software package construction.



Figures 4 – shows the algorithm of “ESMOS” software package.

Расчет параметров стратегии развития

РасчетБаза ДанныхЗакрыть

Расчет численных значений параметров частных критериев

Дисконтированные затраты					Потери электроэнергии					Недоотпуск электроэнергии					Протяженность трасс КЛ						
	2*25	16:25	3*16	2*1		2*25	16:25	3*16	2*1		2*25	16:25	3*16	2*1		2*25	16:25	3*16	2*16:25	2*25:16	2*25:6
1.05	0,19923	1,0	0,917410,7		1.05	0,81042	1,0	0,618510,3		1.05	0,0	0,488411,0	0,67		1.05	0,62806	1,0	0,80883	0,35002	0,0	
1.1	0,19936	1,0	0,917350,7		1.1	0,81293	1,0	0,621440,3		1.1	0,0	0,488411,0	0,67		1.1	0,62806	1,0	0,80883	0,35002	0,0	
1.15	0,19950	1,0	0,917370,7		1.15	0,81543	1,0	0,624360,3		1.15	0,0	0,488411,0	0,67		1.15	0,62806	1,0	0,80883	0,35002	0,0	
1.2	0,19964	1,0	0,917350,7		1.2	0,81793	1,0	0,627280,3		1.2	0,0	0,488411,0	0,67		1.2	0,62806	1,0	0,80883	0,35002	0,0	
1.25	0,19977	1,0	0,917370,7		1.25	0,82035	1,0	0,630160,3		1.25	0,0	0,488411,0	0,67		1.25	0,62806	1,0	0,80883	0,35002	0,0	
1.3	0,19991	1,0	0,917370,7		1.3	0,82283	1,0	0,630070,3		1.3	0,0	0,488411,0	0,67		1.3	0,62806	1,0	0,80883	0,35002	0,0	
1.35	0,20006	1,0	0,917250,7		1.35	0,8253	1,0	0,635940,3		1.35	0,0	0,488411,0	0,67		1.35	0,62806	1,0	0,80883	0,35002	0,0	
1.4	0,2002	1,0	0,917270,7		1.4	0,82772	1,0	0,638750,3		1.4	0,0	0,488411,0	0,67		1.4	0,62806	1,0	0,80883	0,35002	0,0	

Критерий оптимальной структуры

Значения функций принадлежности					Значение функции принадлежности = 0,52, Стратегия 3 Параметры стратегии: Число трансформаторов 3 Мощность трансформаторов 16, 16 и 16 МВА				
	2*25	16:25	3*16	2*16:25		2*25:16			
Дисконт.Затраты	0,58832	1,0	0,793650,40		0,200	0,52	0,52	0	
Потери Эл.Эн.	0,58832	1,0	0,793650,40		0,52	0,52	0,52	0,396	0
Недоотпуск Эл.Эн.	0,58832	1,0	0,793650,40		0	0,488	0,52	0,52	0,357
Протяженность трасс КЛ	0,58832	1,0	0,793650,40		0,52	0,52	0,52	0,35	0
Построение Оптим.Структуры	0,58832	1,0	0,793650,40		0,52	0,52	0,52	0,403	0

Figure 5 – presents window “ESMOS” form with the results of nomenclatorial parameters choice of “substation modernization” strategy.

The developed software enables to analyze electric system structure, energy consumption of some objects, to form expert group, to choose an electric system development model specifying its parameters.

Software package “ESMOS” is a universal one since, depending on the assigned task (purpose of research), such modules can be used independently or in combination with each other. “ESMOS” is an open perspective system able to be modernized (changes can be inserted in its content, the number of modules can be increased etc.) as the problem of electric systems development model choice remains actual.

References

1. Novye informatsionnye tekhnologii v zadachakh operativnogo upravleniya elektroenergeticheskimi sistemami / N. A. Manov [i dr]. – Ekaterinburg : UrORAN, 2002 – 202 s.
2. Semenova L. A. K razrabotke metodik prinyatiya reshenii po razvitiyu elektroenergeticheskikh sistem / L. A. Semenova // Energetika: sostoyanie, problemy, perspektivy :- Vserossiiskaya nauchno-tekhn. konf. – Orenburg: OGU, 2010. – С. 17-21.
3. Kamnev V. I. Preimushchestva i vozmozhnosti primeneniya tekhnologii iskusstvennogo intellekta dlya optimizatsii raboty elektroenergeticheskikh system I oborudovaniya / V. I. Kamnev, I. M. Ibraghimov // Izvestiya Akademii promyshlennoi ekologii. – 2003. No 1. – С. 10-21.
4. Svidetel'stvo o registratsii programmy dlya EVM “ESMOS”/ Semenov A. M., Semenova L. A; Rospatent. No 2009616955; zayavl. 15.10.09; opubl. 15.12.09.

INFORMATION MODEL OF REMOTE HEALTHCARE MONITORING SYSTEM

Shalkovsky A.G., Kuptsov S.M.

Institute of Information Technologies, National Research University Higher School of Economics, Russia

The article discusses the status of work in the field of remote monitoring of human health. Without Legal framework, the telemonitoring and mHealth will not meet its full potential. One complicated factor is that even thru terms such as Telemonitoring,

Telemedicine, Telehealth, eHealth, mHealth, personal health still have very similar meaning. Despite all the advantages of telemonitoring in Russia on the need for fundamental studies of telemonitoring as a branch of medicine. Absence of such studies may lead to negative consequences, including the threat of a patient's life.

Introduction

The relations among the Russians to their health has improved dramatically , including this due to the implementation of the National Programme "Health". The part of this Programme is Russian Healthcare Information Infrastructure (RHII). At the patient level, progress toward an RHII would greatly empower individual patients to assume a much more active, controlling role in decision making and in implementing their own health care (i.e., applications that could help bring about a shift from hospital/clinic-based, clinician-directed care to **home-based, clinician-guided self-care**). In time, the RHII would also provide a platform for the implementation of new information/communications systems, such as wireless integrated medical microsystems (medical sensors and algorithms combined with microelectronics and wireless interfaces), which would enable the remote capture and continuous communication of a patient's physiological data to care professionals, thereby increasing the likelihood of the timely diagnosis and treatment of illnesses. In 2007, implemented within the framework of the research project " Theory and practice of the use of mobile devices and telecommunications in medicine and the educational process " became the winner of interdisciplinary research projects Moscow State University. In September 2013 in Moscow held a scientific -practical conference " High-tech services and solutions for remote monitoring of the health status and health care". The conference was attended by leading representatives of the regional ministries and departments of health in most regions of the Russian Federation, heads of medical institutions , social services and operational support . Was marked by great practical interest to the creation of the medical model of care focused on the patient , which would solve two major objectives : **to reduce the cost of medical services and on the other hand increase the availability of health care**, which ultimately lead to better quality of life for patients with chronic diseases. The second component of the need to seek to reduce the cost of services is to **increase life expectancy**.

Almost all participants indicated the major problems that hinder the development of services for remote monitoring. Lacks the necessary legal framework and must provide targeted government funding for the development of remote healthcare monitoring is and its integration with existing Russian Healthcare Programs and Standards.

As they age, many people are no longer able to live alone and unaided, for reasons ranging from simple frailty to specific conditions such as dementia. Accordingly, the need for integrated care comes through particularly strongly in the issue of long-term or social care, most of which is geared towards older people. Although theoretically differentiated from medical care, both are closely intertwined: long-term care is largely only necessary because of health deterioration and its standard is directly relevant to maintaining, or sometimes even restoring, health. Most countries addressing this issue are understandably focusing on ways to improve the provision of home care, rather than invest in more institutional care. From the standpoint of cash-strapped government, home care is economically **much more attractive**.

Some of these innovations are truly novel. In Japan, for instance, “nurse robots” are being built to help care for elderly patients, along with service robots that assist them at home. With the oldest population in the world, the Japanese government is openly encouraging such innovations. Video demonstrations show robots performing functions such as lifting patients out of wheelchairs and placing them on beds. Toshiba’s latest model can open doors and handle trays, and is equipped with a camera for remote monitoring. The university’s Institute of Digital Healthcare to develop teams of robots for use in health settings. Rather than

replacing nurses, as the Japanese are trying to do in some settings, the project is developing robots that are meant to perform a few clearly defined functions—such as cleaning or monitoring hospital hallways—so that human nurses have more time to care for patients. The concept of robot nurses may be exciting to some and controversial to others, but is only one aspect of the technology-based research aimed at enabling older people to live better lives. A wide range of innovations is being developed, often grouped under the umbrella of telemedicine, to allow healthcare professionals to monitor and assess the health of individuals from information transmitted by phone or the Internet or some other means. Products include Massachusetts Institute of Technology's "smart personal advisers", which use radio-frequency identification and wireless technology to make an individual's personal diet information available on a screen-based device that offers them in-store guidance while shopping for food, and intelligent cardiopulmonary decision systems, which apply telemedicine to provide early detection of and warning about patients at risk of congestive heart failure. Parameters showing patients during their illness to help them better understand the disease that leads to better outcomes. Doctors also benefit associated with relief patient monitoring. Insurance companies increase the attractiveness of the market for new medical technologies and profit from lower costs for medical services .

This simplicity and accessibility to market has led to the emergence of services avalanche huge number of companies from the health centers to developers of medical devices and software. Whilst remote healthcare monitoring applications have considerable potential to aid professionals in delivering healthcare, it is not widely appreciated that use of these new technologies may also introduce significant new risks to patients. Also of concern is that even when high quality interventions are developed, they frequently fail to live up to their potential when deployed in the "real world"; a major factor contributing to this paradox is professional resistance to their introduction and use due in part to relative lack of sophistication and an a risk adverse culture of practice. A lack of regulatory framework and systematic approach to the new field of medicine may lead **to threats to the life of the patient**. It is the lack of remote monitoring system of health research as a branch of medicine has led to such results .

Informational Model: Classification

General provisions and requirements for information systems (IS) organizations and health care institutions are defined in the standard Russian organizations [2].

These requirements determine the composition of the recommended IS and application functions are aimed primarily at the interface between IS and different organizations of health facilities, which include :

- Ministry of Health ;
- Government Territorial (institutional) health management ;
- Medical management of ministries and departments ;
- State health surveillance ;
- Federal Fund MLA;
- Territorial funds (TFOMS);
- TFOMS Affiliates and their representation;
- Insurance medical organizations ;
- Health facilities ;
- Spa facilities ;
- Medical schools.

he standard used by the functional classification of IS , according to which there are five classes of IS functionality :

1. Medical technology IS's intended for information support of diagnosis, treatment, rehabilitation and prevention of patients in health care settings .
2. Reference information systems containing medical information banks for information services of medical institutions and health management services .
3. Statistical IS health authorities .
4. Research IS, designed to inform medical research in clinical research institutes .
5. IS training designed to inform learning processes in medical schools .

The lack of an actual accepted classification and terminology of different information systems for health care. This is due to the long period of informatization autonomous medical institutions and the active development of complex systems, providing broad functionality and fall under several categories, the highest classification. According to the Association for the development of health information technology , as of 2012 has more than 600 software solutions for health care, of which 23 - limited edition IIA . Between separate and often incompatible software hampered mutual exchange of information at the health facility and summary information needed to manage health at the regional level and the industry as a whole.

According to [6] RHII is defined as "a set of technologies, standards, applications, systems, values and laws that support all aspects of individual health, health care and public health. It includes an information model for Internet protocols, common standards, safety standards, knowledge transfer processes with the possibility for the flow of information based on three fronts:

1. personal health,
2. health care providers,
3. public health.

The Russian Healthcare Information Infrastructure would provide a platform for the application of a wide range of proven and emerging information, communications technologies that could have a dramatic impact on health care processes and outcomes. The following discussion explores the promise of an RHII for each level of the health care delivery system. At the level of the organization, steps toward RHII would greatly facilitate the integration and analysis of clinical, administrative and financial data to measure and improve quality, patient-centeredness, and efficiency of health care.

The components of a RHII can be divided into three interrelated categories:

1. health care data standards and technical infrastructure;
2. core clinical applications, including EHRs, systems, digital sources of medical knowledge, and decision-support tools;
3. information/communications systems.

Technical Infrastructure and Data Standards

If health care data are standardized, they become understandable to all users. The, Patient Safety, considered three key groups of standards [7]:

- Data interchange formats. The standard formats for electronically encoding data elements and can also include document architectures for structuring data elements as they are exchanged and information models that define relationships among data elements in a datagram (HL7 messages).
- Terminologies. The medical terms and concepts used to describe, classify, and code the data elements and data expression languages and syntax that describe relationships among the term sand concepts. It may used Ontology Methods, like SNOMED.
- Knowledge. Standard methods of electronically representing clinical guidelines, medical literature, and other information required for computerized decision support. As a Terminologies it may also used Ontology Methods.

For each group of standards identified key priorities and describes the current efforts that have led and funded by the federal government. In this area of data-interchange formats, in which engineering has played an important role, a number of major standards, address some of the required domains:

- medical images ([DICOM])
- administrative data
- clinical data (HL 7)
- prescription data
- medical device data (ISO 1073-X)

Electronic Health Records (EHR)

The ability to share electronic health information both internally and externally with healthcare organizations has been accepted as a method to improve the quality and delivery of care. When health care providers have access to complete and accurate information, patients receive better medical care. EHRs can improve the ability to diagnose diseases and reduce—even prevent—medical errors, improving patient outcomes. However, the rate of progress toward realizing this vision has been glacial.

The EHR is a compilation of clinical and clinically related information and is used as the primary communication tool for planning and delivering patient care. Ensuring that health information is associated with the patient to whom it pertains is key to ensuring patient safety. EHR systems should have alerts and prompts that notify the user when the potential for an incorrect association exists.

Russian Ministry of Health in November 2013 approved the composition of EHR. Sections in the structure of the card :

- **Card holder** : contains information about a medical organization , which is responsible for the creation and storage of patient cards .

- **Patient:** personal data of the patient - his full name, gender, age, date of birth, identification number of its electronic medical record SNILS , policy number CHI information about insurance companies, etc. It also indicates the presence of harmful and (or) hazardous working environments , occupation and level of education.

- **A representative of the patient** : information concerning the official representatives of the patient (relatives , guardians , attorneys , chief physician at home kids). Information is necessary to harmonize treatment decisions - for example, if the child is unconscious or in a state of drug and alcohol intoxication .

- **Maintenance of the Register** : the inclusion of the patient in a particular case. The information on whether a patient has the right to provide free and discounted drugs through the budget of the Russian Federation .

- **Metrics** patient's height, weight, body proportions, blood pressure, pulse , etc.

- **Map patient** : blood group, group health , health and development bias , having a disability , bad habits , drug intolerance , allergic and family (with the list of diseases), medical history, list of dropped childhood diseases , the availability of vaccines. Obstetrical history - pregnancy outcomes , gynecological diseases transferred IVF.

- **The results of research** : information about all of diagnostic , laboratory and ultrasound . Map stored registration number laboratory responsible for the analysis , the date of the study , etc.

- **Clinical examinations:** the result of each medical examination will be kept on the map as introduced electronic medical records . Recorded name will be indicated doctor , symptoms, diagnosis , designated research PURPORT doctor, etc. Also in this section there is a subsection "Observation of the newborn "

- **The patient's condition** : the reduction of the time of admission to the clinic , information about his condition at the time of admission and at discharge . In section we

prove the time was called "first aid" when it came to the patient, the time of arrival to the emergency department, in what condition the patient was taken to the police (eg, intoxicated), etc.

- **Pregnancy and childbirth** : section consists of 41 sub detailing procedures for delivery of the patient.

- **Diseases and complications** : This section contains information about recent patient diseases. Accumulated information is also needed to make a decision on the appointment or award of disability benefits. Filled with information about whether to recommend to the patient and whether to VMP medico- pedagogical correction.

- **Hospitalization and treatment**: information about all areas of treatment and hospitalization. Include designated drugs during treatment. Guidance on the course of chemotherapy, radiation therapy, gormonoimmunoterapii, antiparkinsonian treatment, thrombolytic therapy, treatment of an episode of acute coronary syndrome, special treatment and spa.

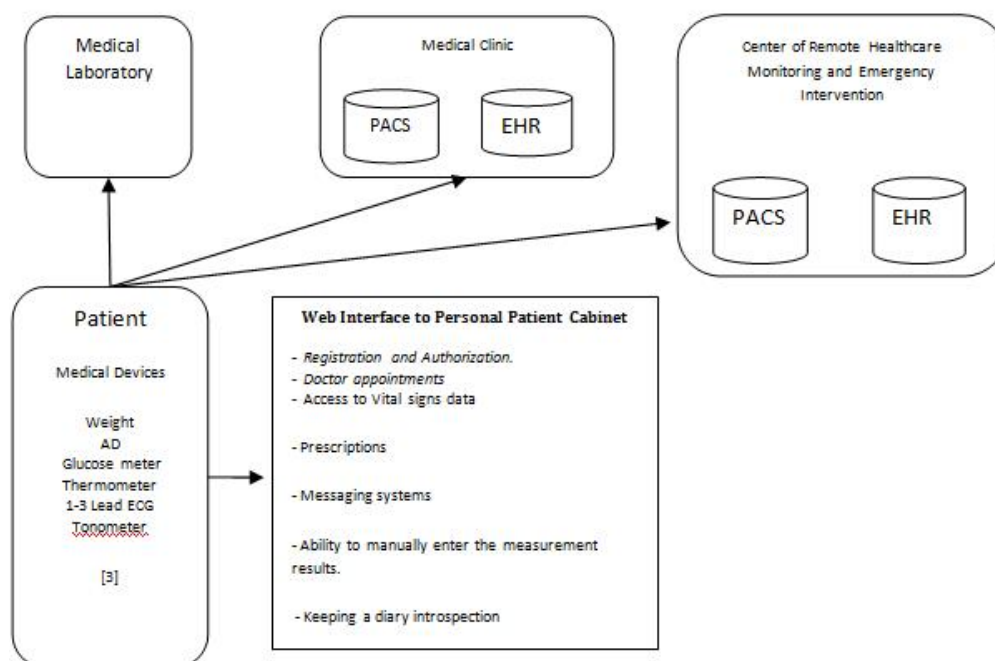
- **Interventions and procedures**: information about all medical interventions and procedures performed. Can also serve as a basis for a decision on awarding disability and providing subsidized medicines.

- **Support SMEs** : information about what specialized (high-tech) medical care was provided to the patient. Including indicate why it was denied a NSR.

- **Prescriptions for medicines**: Section allows you to monitor the patient and health care provider number of prescriptions, the amount of doses and duration of drug treatment.

- **Temporary incapacity** : Information on all outstanding patient disability sheets - details of the document, the reason for the issuance of a duration sheet who was issued.

Functional model



Conclusions

Provision of quality health care, such as a new remote monitoring of human health, requires that doctors and patients have access to complete patient information and decision-support tools, and access to Electronic Medical Records and personal account of the patient, as well as the relationship between the doctor and the medics and doctors at a medical facility.

Internet have provided patients with unprecedented access to health information and has made possible a more continuous, asynchronous communication between patients and their health care institution (with any form of ownership).

These technologies for asynchronous communication allowed the development of self-care educational tools and modules which facilitates informed decision-making, health, and giving patients access to information of specific diseases.

In the case of remote health monitoring system (ASDMZ) many of the challenges and opportunities associated with the establishment of permanent information and communication networks, increased communication and exchange of information between patients and doctors.

The patients have a real opportunity to receive quality medical care but also to participate actively in the process of treatment, to receive more information about new medicines and technologies.

The system of remote health monitoring practically change entire information model of ambulatory treatment patients.

Acknowledgement

The work was carried out with the financial support of the Ministry of education and science of the Russian Federation (the contract № 02. G 25.31.0033)

References

1. Metodicheskie rekomendaczii po sostavu, sozdavaemy'x v 2011 – 2012 godax v ramkax realizaczii regional'ny'x programm modernizaczii zdavooxraneniya, prikladny'x komponentov regional'nogo urovnya edinoj gosudarstvennoj informaczionnoj sistemy' v sfere zdavooxraneniya, a takzhe funkczional'ny'e trebovaniya k nim (ot 14 noyabrya 2011 g. [Http://www.minzdravsoc.ru/docs/mzsr/informatics/40](http://www.minzdravsoc.ru/docs/mzsr/informatics/40).
2. Standart organizaczii «Informaczionny'e sistemy' v zdavooxranenii». Obshhie trebovaniya STO MOSZ 91500.16.0002-2004. Moskva 2004
3. Korsakov I. N., Kuptsov S. M., Raznometov D. A. Personal Medical Wearable Device for Distance Healthcare Monitoring X73-PHD // International Journal of Scientific & Engineering Research. 2013. Vol. 4. No. 12. P. 2321-2328
4. Tang PC, Ash JS, Bates DW, Overhage JM, Sands DZ. Personal health records: definitions, benefits, and strategies for overcoming barriers to adoption. *J AmMed Inform Assoc.* 2006;13(2):121-126
5. Alex H. Krist, MD, MPH; Steven H. Woolf, MD, MPH A Vision for Patient-Centered Health Information Systems *JAMA.* 2011;305(3):300-301
6. Prikaz Ministerstva zdavooxraneniya i soczial'nogo razvitiya Rossijskoj Federaczii ot 28 aprelya 2011 № 364 «Ob utverzhenii Konczepczii sozdaniya informaczionnoj sistemy' v zdavooxranenii». 7. National Academy of Engineering (US) and Institute of Medicine (US) Committee on Engineering and the Health Care System; Reid PP, Compton WD, Grossman JH, et al., editors. Building a Better Delivery System: A New Engineering/Health Care Partnership. Washington (DC): National Academies Press (US); 2005. Available from: <http://www.ncbi.nlm.nih.gov/books/NBK22832/>

TO THE QUESTION OF EVALUATING THE RELIABILITY OF FUNCTIONING OF THE ELEMENTS OF THE TELECOMMUNICATION ENTERPRISE-WIDE NETWORKS

Safonova, I. E., Zhelenkov, B. V., Goldovskii, Y. M., Tsyganova N. A.
Moscow, MGUPS(MIIT)

Examines the problem of calculation of reliability of functioning of the elements of the corporate telecommunications network that are critical to the delay of the results of calculations. In particular, describes the method for assessing the reliability of the network for devices located in partial operable state.

Keywords: telecommunication enterprise-wide networks, reliability, devices.

The essential characteristic of a telecommunication enterprise-wide network is reliability. Reliability is not enough to define the level of quality, it is necessary to assess the reliability quantify and compare a variety of objects by their reliability. With this purpose, parameters and criteria of reliability [1]. The reliability of telecommunication enterprise-wide network, as in any system, is determined by the reliability of its constituent elements, so you should assess the reliability of your network - as a complex hierarchical system [2, 3].

Element of the network can be considered a server, a workstation, a communication channel, and so on. The degree of aggregation of elements in each case is determined by the purpose of the research and the nature of the selected index of reliability. To assess the reliability of the networks use the following features: availability, security, fault tolerance [3].

To date, remain insufficiently studied methods of estimation of reliability of devices of telecommunication networks, critical to delay the results of a calculation. This is manifested in the inadmissibility of queries wait in the queue and it is impossible to reopen the computational process after the occurrence of failures.

Let the device (element) telecommunication enterprise-wide network, for example, the server may fail or when servicing applications, or in the free state, or of that, and in another state. In many cases, coordination with the real situation gives the assumption that the network element fails randomly in time t . This can cause extremely negative consequences for the functioning of the network and the work of the whole Corporation.

In [4] considered the problem: 1 - server failure in the free state when, after a moment t_0 received the application, and the server have not yet fails and the server fails before received the application; 2 - a server failure during servicing user requests. This article considers the problem of partially working status of the device (element) telecommunication enterprise-wide network critical to delay calculations. Here is a short description of the developed method.

Service user requests can be interpreted as the execution of the device some amount of work that corresponds to the different requests of independent and, with common distribution $\varpi_1, \varpi_2, \dots, \varpi_n, \dots$ identically distributed random values function $R(t)$. Almost every time the device has a capacity of $E(t)$. If we assume that its capacity is constant $E(t)=E$, then a statement of the problem will be reduced to a problem of maintenance with anticipation, and the distribution function of the service time will be equal to $R(F(t))$. At the moments of time when the device is in a failed state, can be considered a power equal to zero, a functioning state corresponds to a non-zero power.

Device network can be in each moment of time in one of n States 1, 2, ..., n , the i -th state corresponds to the value of power, equal E_i . The transition from one state to another occurs randomly: if at the moment t the device is in the i -th, then at the moment Δt it can go

in the j -th state. Such a condition is to form a Δi -m state, during homogeneous Markov process $s(t)$ [5].

In this set up the main characteristics of the service user requests are: the distribution of the value of the work that must run a device from t to the service of those applications that to the moment t is already available; the distribution of waiting time applications.

The process $s(t)$ does not depend on the service. From any condition it is possible to switch to any other state i for awhile. According to the ergodic theorem [4] there is ergodic distribution process $s(t)$ assigned probabilities $p_i = \lim_{t \rightarrow \infty} p\{s(t) = i\}$ for $1 \leq i \leq n$. The average output power of the device network can be defined as

$$\bar{E} = \sum_{i=1}^n E_i p_i. \quad (1)$$

Of ergodic theorem:

$$\frac{1-p_i}{\rho} P_0(t) \mid \frac{1}{T} \int_0^T E(t) dt - \bar{E} > \varepsilon. \quad (2)$$

where T - is the duration of the employment period.

Loading device ρ :

$$\rho = MO \frac{(1-T)\varpi_i}{\bar{E}}. \quad (3)$$

Because the distribution of the process $s(t)$ at any point in time is given by functions:

$$F_i(x, t) = \sum_{i=0}^n f(s_i(t)), \quad F_i(x) = \lim_{t \rightarrow \infty} F_i(x, t), \quad (4)$$

so, consequently, we obtain theorem. Theorem 1. A necessary and sufficient condition for the existence of the ergodic distribution of the process $s(t)$ is the inequality (2). When this condition limits (4) satisfy the system of integro-differential equations:

$$E_i F_i(x) - \sum_{i \neq j} F_i(x) F_j(x) + \int_0^{\Delta t} F(x, t) dF(x) + E_j F_j(x) = 0, \quad 1 \leq i \leq n. \quad (5)$$

The proof of the theorem is given in [4].

If mark $\Phi_i(s) = \int_0^\infty e^{-\Delta t} dF_i(t) dt$ by $1 \leq i \leq n$, $a_{ij} = F_{ij}(0)$ for $1 \leq i \leq n$, $h(s) = \int_0^\infty e^{-\Delta t} dF_0(t)$, and

apply to the system (5) the Laplace transform, then:

$$\Phi_i(s) \{E_i(t) - [1 - h(s)] - \sum_{i=1}^n F_i(t)\} + \sum_{j=1}^k F_j(x, t) = h(s) a_{ij} E(t), \quad 1 \leq i \leq n, 1 \leq j \leq k. \quad (6)$$

The system of equations (6) has a unique analytic solution $\Phi_i(s)$, $1 \leq i \leq n$ for $Re\{s\} > 0$, if the constants a_i , appearing in the right parts of these equations correspond to their probabilistic sense - equal probabilities $F_{ij}(0)$.

Must establish that in some neighborhood of the point $x=0$ determinant

$$\Delta(x) = \begin{vmatrix} \Phi_1(s)E_1(t) - [1 - h(s)] - \sum_{i=1}^n F_i(t) & \dots & a_{n1} \\ a_{12} & \dots & a_{n2} \\ \dots & \dots & \dots \\ a_{1n} & \dots & \Phi_n(s)E_n - [1 - h(s)] - \sum_{j=1}^k F_j(x, t) \end{vmatrix} \quad (7)$$

does not vanish. When $x=0$ this determinant is zero (sum of items in each column of this determinant is equal to zero). According to the rule of differentiation determinants:

$$\Delta'(x) = [\Phi_i(s)E_i(t) + h'(s)] \begin{vmatrix} \Phi_2(s)E_2(t) - [1 - h(s)] - \sum_{i \neq 2} F_2(t) & \dots & a_{n2} \\ \dots & \dots & \dots \\ a_{n2} & \dots & \Phi_n(s)E_n(t) - [1 - h(s)] - \sum_{j \neq n} F_{nj}(x, t) \end{vmatrix} + \dots \quad (8)$$

substituting $x=0$, one can obtain:

$$\Delta'(0) = [\Phi_i(0)E_i(t) + h'(s)] \begin{vmatrix} -\sum_{j \neq 2} F_2(t) & \dots & a_{n2} \\ \dots & \dots & \dots \\ a_{n2} & \dots & -\sum_{j \neq n} F_{nj}(0, t) \end{vmatrix} + \dots \quad (9)$$

or, if you mark this decomposition, the coefficient on the $[\Phi_i(0)E_i(t) + h'(s)]$ which are Δ_i . The system of equations defined by the probabilities p_i :

$$p_i \sum_{j \neq i} a_{ij} = \sum_{j \neq i} p_i a_{ij}, \quad 1 \leq i \leq n. \quad (10)$$

Because the process $s(t)$ is ergodic, then this system has the unique solution [4], then of the first n paragraph of equations of this system can discard the equation so that the rest of the system will have the same the only solution. Therefore, according to the Cramer's rule:

$$p_1 : p_2 : \dots : p_n = \Delta_1^* : (-\Delta_2^*) : \dots : (-1)^{n+1} \Delta_n^*, \quad (11)$$

where Δ_i^* - determinant of the matrix resulting from crossing the i -th column and the last row in the matrix of the system n equations.

For all i , concluded between 1 and n , $\Delta_i = (-1)^n \Delta_i^*$, or for all i - $\Delta_i = (-1)^{n+1} \Delta_i^*$. Then $\Delta_i = \varpi_i p_i$. It is necessary to notice, that $\sum_{i=1}^n E_i p_i = \bar{E}$, a $\sum_{i=1}^n p_i = 1$ and:

$$\Delta'(0) = \varpi \bar{E} (1 - \rho) \neq 0. \quad (12)$$

For the distribution function of time-out: if the application was submitted to the moment of time t , the wait time before commencement of the service will depend on the status of the device at a given time and the work that it has to run to the end of the maintenance of existing applications. If $t^*(t)$ - standby time prior to the service

$$\Phi(s) = \lim_{t \rightarrow \infty} P_0(t^*(t)), \text{ that}$$

$$\Phi(s) = \sum_{i=1}^n \int_0^\infty F_i(x, t^*) dF_i(t^*). \quad (13)$$

The functions $F_i(x, t^*)$ satisfy the system of differential equations:

$$\frac{\partial F_i(x, t^*)}{\partial x} + E_i \frac{\partial F_i(x, t^*)}{\partial t^*} + \sum_{i \neq j} a_{ij} F_i(x, t^*) = \sum_{i \neq j} a_{ij} F_i(x, t^*). \quad (14)$$

If during the period from t to $t+t^*$ device not changed state, then $t^*(t+\Delta t) \leq t+t^*$, otherwise $t^*(t) \leq t+\Delta t$.

To determine functions $F_i(x, t^*)$ and $F_i(t^*)$, there are two equations:

$$\left. \begin{aligned} \frac{\partial F_i(x, t^*)}{\partial x} + E_i \frac{\partial F_i(x, t^*)}{\partial t^*} + a_i[F_i(x, t^*)] &= 0 \\ \frac{\partial F_i(t^*)}{\partial t^*} + E_i \frac{\partial G_i(t^*)}{\partial t^*} + a_i[F_i(t^*)] &= 0 \end{aligned} \right\}. \quad (15)$$

Boundary conditions are the following relations:

$$F_i(t^*, E_i t) = e^{-(\Delta t + t^*)}. \quad (16)$$

If $t^*(t)$ close to $E_i t$, over time t^* transition process $s(t)$ in the following state - of $s'_i(t)$ in $\bar{s}_i(t)$. Therefore

$$P_0(t) = \int_0^{\infty} e^{-(\Delta t + t^*)} dt \int_0^{E_i} e^{-t} F_i(t^*) F_i(x, t^*) dt^* \quad i = 1, 2, \quad (17)$$

from (17) is obtained:

$$a_i(F_i(x, t^*) - a_i F_i(x, t^*)) + E_i \int_0^{\infty} e^{-(\Delta t + t^*)} F_i(t^*, E_i t) dt = 0$$

$$a_i(F_i(t^*) - a_i F_i(t^*)) + E_i \int_0^{\infty} e^{-(\Delta t + t^*)} F_i(t^*, E_i t) dt = 0 \quad (18)$$

By theorem 1 and using (16) - (17):

$$\Phi_i(s') = (E_i + a_i)[F_i(x, t^*) - a_i F_i(x, t^*)] + (E_i) \frac{(1-T)}{h(s) + E_i}$$

$$\Phi_i(\bar{s}) = E_i + a_i[F_i(t^*) - a_i F_i(t^*)h(s)] \quad (19)$$

The developed method of calculation of reliability of devices of corporate telecommunication networks, critical to the delay of the results of calculations allows to determine and predict the probability of failure of any element of the network. The performed experimental verification method has shown, that the accuracy of the results is sufficient to assess the reliability of networks and their elements, and reliability indicators correspond to the international standards [2, 6].

References

1. K.A.Polyakov, I.E.Safonova, V.V.Ivanov, Grafovaya model' rascheta apparaturnoi nadezhnosti korporativnoi telekommunikatsionnoi seti // Telekommunikatsii. 2012. № 12., 7 – 9.
2. I.E.Safonova, On one Approach to Modeling Enterprise-Wide Function-Oriented Computer Networks. Telecommunications and Radio Engineering. Begell House. Inc. Publishers - Vol. 71, № 12, 2012, 1087 - 1101.
4. Safonova I.E. Metody i modeli otsenki osnovnykh kharakteristik korporativnykh funktsional'no-orientirovannykh setei v SAPR [Tekst]/ I.E.Safonova - M.: MIEM, 2007. - 344 s.
5. Ushakov I.A. Veroyatnostnye modeli nadezhnosti informatsionno-vychislitel'nykh sistem [Tekst]/ I.A.Ushakov - M.: Radio i svyaz', 1991. - 132 s.
6. Polyakov K.A., Safonova I.E., Goldovskii Y.M. Optimizatsiya apparaturnoi nadezhnosti korporativnykh telekommunikatsionnykh setei // Telekommunikatsii. - 2013. - № 3., 6 – 9.
7. Safonova I.E. Formalizatsiya postanovki problemy adaptatsii i sinteza korporativnykh funktsional'no-orientirovannykh setei // Komp'yutery v uchebnom protsesse. - 2009. - № 6., 7 - 14.

NUMERICAL MODELING OF THE PROCESSES OF COAGULATION AND DISPERSION OF DROPS IN ELECTRIC FIELD

Tarantsev K. V.

Penza State University, Penza, Russia

Results of the physical and mathematical modeling of the processes of producing and disintegrating water—oil emulsions using the COMSOL Multiphysics software, as well as of electric fields, velocity fields, and pressure fields, under boundary conditions that correspond

to the apparatuses under development are presented. Based on the analysis of the data obtained, different versions of the design of electric dispersers and electric dehydrators are proposed.

Keywords: electric dispersers, design, modernization, physicochemical characteristics, emulsion, model fluids, drop diameter, field strength

Analytical calculation of processes of destruction and the interaction of water droplets in oil in an electric field is only possible for a limited number of cases. That is why numerical modeling of the processes of creation and destruction of emulsions in electric fields is a promising area of research.

Taylor [1] did theoretical analysis of droplet deformation under the influence of an external electric field. Relationship between the droplet D and the deformation strength of the electric field he represented as:

$$D = \frac{9f_d(R, Q, \lambda)}{8(2 + R)^2} Ca_E$$

where $f_d(R, Q, \lambda)$ is a function of

$$f_d(R, Q, \lambda) = R^2 + 1 - 2Q + \frac{3}{5}(R - Q) \frac{(2 + 3\lambda)}{(1 + \lambda)}$$

Accuracy of the theory for small deformations Taylor drops proved by several authors [2]. Sherwood [3] based on the method proposed settlement boundary integrals of Laplace's equation and the Stokes equation, i.e. divided the problem into two parts: the calculation of the electric field, the calculation of the velocity field in liquids. Initially, he has calculated electric field distribution on the surface of the drop, and after the jump of the electric field at the interface was calculated, he has determined fluid velocity field.

In [4, 5] analyzed the mechanisms of deformation and fracture drops. The influence of the relative viscosity on the stability of drops and defined the limits of applicability of the proposed method of boundary integrals was studied. Authors [6, 7] have considered the final deformation of water droplets, but have neglected by the effects of viscosity, which play an important role for emulsions.

Model of weakly conducting fluid with the two drops was used in [8]. Viscous interactions between two drops were investigated in [9]. But the effect of the relative motion of the droplets not taken into account.

The motion of two drops in a uniform electric field using a weakly conducting fluid was studied in [10]. Mutual influence of turbulence and electric field on the behavior of emulsions was studied in [11-14]. Shown, that turbulence promotes rapprochement drops, while the electric field destroys the adsorption film and increases the likelihood of a successful merger of droplets in contact.

Previously we have reported the results of studies of processes of destruction and merging of droplets in weakly conducting liquids received by numerical methods [15-17].

In this paper, we present the model of fracture and merge droplets in weakly conducting liquids, which in the Navier-Stokes equations take into account additional Coulomb and polarization forces.

The results are compared with the results of other authors using dimensionless parameters.

The processes of the dispersion and coagulation of water in low-conducting fluids were modeled using COMSOL Multiphysics software. The electrocoagulation unit proposed in COMSOL was taken as the basis. This unit employs two modules, i.e., the *AC/DC Module* and the *Microfluidics Module*. The *AC/DC Module* makes it possible to model dc and ac

electric fields in a working zone with various shapes and dimensions, as well as to determine the spatial and time distributions of the parameters such as the electric conductivity and dielectric constant. The *Microfluidics Module* includes applications that describe the flow dynamics in both a homogeneous and multiphase fluid in the working zone under the effect of various volume forces.

These processes were modeled based on the equations that describe the flow of an incompressible fluid between two electrodes for the schemes shown in Fig.1. A low-conductive fluid with one or two water drops moves between the electrodes. The top and bottom boundaries are the entry and exit of the low-conductive fluid; the charged and grounded electrodes are arranged on the right and left.

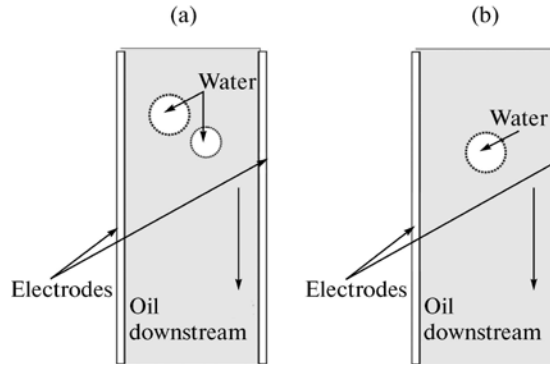


Fig. 1. Schematics of the model of (a) the coalescence and (b) the disintegration of water drops.

The system of equations that is solved during the modeling includes the generalized version of the Navier—Stokes equations with an additional electric field force and the flow continuity equation:

$$\begin{cases} \rho \frac{\partial u}{\partial t} + \rho(u \cdot \nabla)u = \nabla \cdot [-pI + \eta(\nabla u + (\nabla u)^T)] + \\ + F_{st} + \rho g + F, \\ \nabla \cdot u = 0, \end{cases},$$

where ρ is the density (kg/m^3), u is the flow velocity (m/s), η is the dynamic viscosity ($\text{Pa}\cdot\text{s}$), p is the pressure (Pa), I is the identity tensor, $\eta(\nabla u + (\nabla u)^T)$ is the viscous stress tensor, g is the acceleration of gravity (m/s^2), F_{st} are the forces at the interface (N/m^3), and F is the additional electric field volume force (N/m^3).

To trace the movement of the phases at the interface of the fluids, the following system of equations is used:

$$\begin{cases} \frac{\partial \phi}{\partial t} + u \cdot \nabla \phi = \nabla \cdot \frac{3\chi\sigma\varepsilon}{2\sqrt{2}} \nabla \psi, \\ \psi = -\nabla \cdot \varepsilon^2 \nabla \phi + (\phi^2 - 1)\phi, \end{cases},$$

where σ is the surface tension coefficient (N/m); ε is the numerical parameter (m) that determines the thickness of the interface of the fluids, i.e., the zone where the phase variable ϕ changes from -1 for water to $+1$ for oil; and χ is the numerical parameter that characterizes the mobility of the interface.

The electric potential was calculated as follows:

$$-\nabla \cdot (\varepsilon_0 \varepsilon_r \nabla V) = 0,$$

where ε_0 is the dielectric constant in vacuum and ε_r is the relative dielectric constant of the fluid.

The relative dielectric constant was determined as a function of the internal volume fractions of both fluids as follows:

$$\varepsilon_r = \varepsilon_{r1} Vf1 + \varepsilon_{r2} Vf2,$$

where ε_{r1} and ε_{r2} are the relative dielectric constants of oil and water, respectively; $Vf1$ is the volume fraction of the first fluid, i.e., water; and $Vf2$ is the volume fraction of the second fluid, i.e., oil.

The electric field's strength was calculated using the following formula:

$$E = -\nabla \cdot V.$$

The electric force in the Navier—Stokes equation was found as follows:

$$F = -\frac{\varepsilon_0 \varepsilon_r E^2}{\sigma_e} \nabla \sigma_e.$$

The electric conductivity was determined as a function of the internal volume fractions of both fluids as follows:

$$\sigma_e = \sigma_{e1} Vf1 + \sigma_{e2} Vf2,$$

where σ_{e1} and σ_{e2} are the electric conductivities of castor oil and water, respectively.

Figure 2 shows the results of the numerical modeling of the process of the disintegration of water drops with different electric conductivity (saltiness) in an oil product under the effect of an electric field. The modeling was carried out for 4 mm in diameter water drops with an electric conductivity of $3 \times 10^{-4} \text{ (ohm cm)}^{-1}$ placed into the 70 x 40 mm interelectrode space. Figure 2a illustrates the results of calculating the distribution of the electric field potential in the vicinity of the drop interface. The results of calculating the velocity field (Fig. 2b) allow us to draw the conclusion that the two vortices that appear in the continuum are responsible for the pattern of the disintegration of the drop. The application and amplification of the electric field lead to the retardation of the drop. The interaction of the incoming flow with the drop results in the formation of a Carman track. Behind a stationary or slowly moving object, vortices appear that interact with the mobile interface. The drop deforms and then disintegrates along the electric force lines. The study's results have shown that the mechanism of the disintegration of the drop is governed by not only its dimensions but also, to a substantial extent, by the hydrodynamic and electrophysical properties of the fluids that form the emulsion, as well as by the electric parameters of the system.

The conductivity of the oil and water strongly depends on the concentration of various substances in them; as a result, the electric conductivity of the oil emulsions is governed not only by the amount of water contained and its dispersity but also by the amount of salts and acids dissolved. The experiments and modeling were carried out using model fluids with properties whose range overlaps to the best extent possible the properties of the available water-oil emulsions.

A full-scale experiment was previously performed to study the behavior of a water drop in castor oil. The properties of castor oil are within the range of the possible hydrodynamic and electrophysical properties of oil. In addition, castor oil is transparent, which makes it possible to easily observe and record the occurring processes.

Time = 0.545 Surface: Volume fraction of fluid 1 (1)

Contour: Electric potential (V) Contour: Volume fraction of fluid 1 (1)

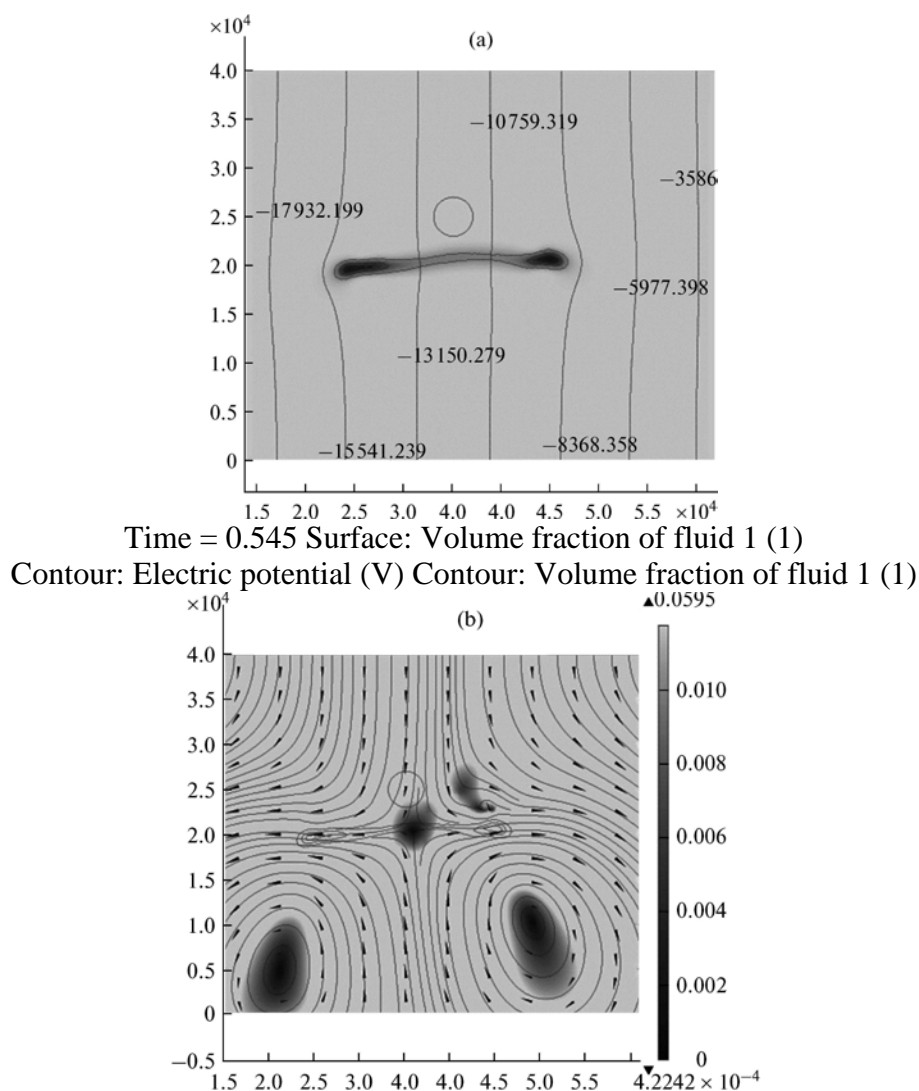


Fig. 2. Results of the numerical modeling of the disintegration of water drops with electric conductivity of $3 \times 10^{-4} \text{ (Ohm cm)}^{-1}$ in oil products obtained at potential difference between the electrodes of 4 kV/cm and the initial drop diameter of 4 mm: (a) electric field; (b) velocity field.

Numerical simulation results are presented as the degree of deformation

$$D = \frac{d_{\max} - d_{\min}}{d_{\max} + d_{\min}} \quad (d_{\max} \text{ and } d_{\min} - \text{the maximum and minimum diameters of deformed drop})$$

from the electric capillary number and Weber number $We = \frac{\varepsilon_0 \varepsilon R_0 E_\infty^2}{\sigma}$. If $D > 0$, the drop is pulled across the field (prolate spheroid), and if $D < 0$, the drop is compressed by the field (oblate spheroid)

The results of physical experiments deformation of water droplets in castor oil presented in Figure 3. It is clear that up to the strain $D = 0,07$, the experimental results agree with those obtained analytically based on the theory of small deformations of weakly conducting liquids proposed by Taylor. For large deformations observed significant deviation from analytical calculation.

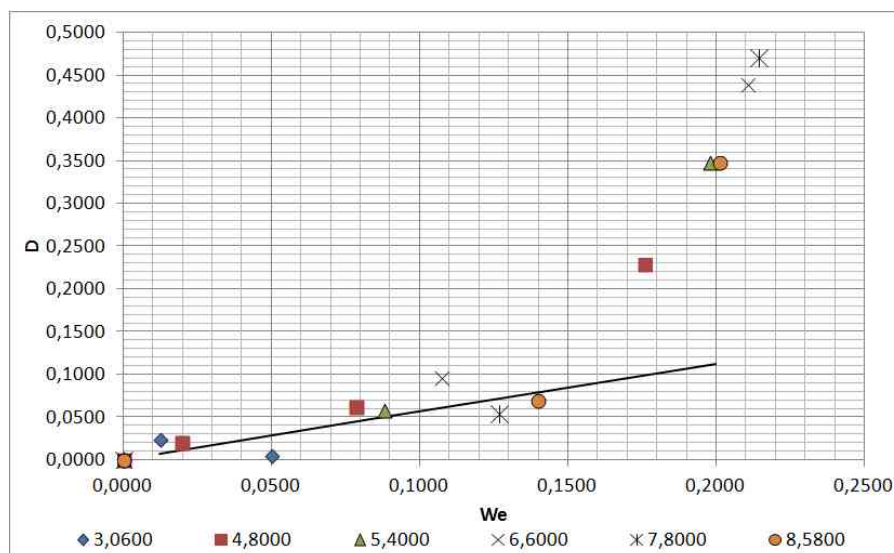


Fig. 3. Effect of Weber number We on the degree of deformation D drops of water in castor oil: solid line - results of analytical calculation of the theory of small deformations of weakly conducting liquids proposed Taylor; markers - results of physical experiments for droplet with different diameter, mm.

This indicates the adequacy of the proposed numerical model and the possibility of using this model to predict the behavior of weakly conducting liquids for small deformations.

References

1. G. Taylor, Proc. R. Soc. London, 291 (1966), 159.
2. J. Q. Feng and T. C. Scott, J. Fluid Mech., 311 (1996), 289.
3. J. D. Sherwood, J. Fluid Mech., 188 (1988), 133-146.
4. Etienne Lac and G. M. Homsy, J. Fluid Mech., 590 (2007), 239-264.
5. O. O. Ajayi, Proc. R. Soc. Lond., 364 (1978), 499-507.
6. P. R. Brazier-Smith, Phys. Fluids, 14 (1971), 1-6.
7. P. R. Brazier-Smith, S. G. Jennings, J. Latham, Proc. R. Soc. Lond., 325 (1971), 363-376.
8. C. Sozou, J. Fluid Mech., 91 (1975), 541-546.
9. X. Zhang, O. A. Basaran, R. M. Wham, AIChE J., 41 (1995), 1629-1639.
10. J.C. Baygents, N. J. Rivette, H.A. Stone, J. Fluid Mech., 368 (1998), 359-375.
11. P. Atten, J. Electrostat., 30 (1993), 259-270.
12. O. Urdahl, N. J. Wayth, H. Fordedal, T. J. Williams, A. G. Bailey, In: Encyclpedic Handbook of Emulsion Technology, Marcel Dekker, New York 2001, 679-694.
13. I. G. Harpur, N. J. Wayth, A. G. Bailey, T. J. Williams, O. Urdahl, J. Electrostat. 40 & 41 (1997), 135-140.
14. J. D. Friedemann, P. J. Nilsen, O. Sother, J. Sjoblom, In: 4th International Symposium on the Chemistry and Physics of Petroleum-Water Emulsions II (2001).
15. K. V. Tarantsev, A.V. Korosteleva, Chemical and Petroleum Engineering, 49 (2013), 1-2, 92-98.
16. K.V. Tarantsev, E.G. Krasnaya, V.A. Chirkov, I.A. Ashikhmin, Chemical and Petroleum Engineering, 49 (2013), 7-8, 435-439.
17. K. V. Tarantsev, Surface Engineering and Applied Electrochemistry, 49 (2013), 5, 414-422.

THE CALCULATION OF THE VIBROINSULATORS' FAILURE RATE

Lushpa I.L.

Moscow, National Research University "Higher School of Economics"

The questions of an assessment of reliability of the vibroinsulators which are applied to protection of radio-electronic means from vibration influences were considered. The calculations of intensity of refusals of springs for various techniques were given. It is shown that application of the technique, which considers influence of features of constructive and technological execution, allows to solve not only calculation problems, but also providing demanded level of characteristics of reliability of vibroinsulators.

Keywords: reliability, radio-electronic means, reliability, vibroinsulators, springs, failure rate

This study (research grant № 14-05-0038) supported by The National Research University - Higher School of Economics' Academic Fund Program in 2014. In the process of exploration of the majority of types of radio-electronic means (REM) are subjected to the vibration. The frequency and acceleration of vibration influences can be quite various depending on the sources of influence and their arrangement concerning REM constructions, so the design of REM, that operating in the conditions of vibration influences, have to meet the requirements of durability and stability.

One of the more effective measures to struggle against vibration is the vibroprotection of REM by various vibroinsulation systems, the essence of which is that between the REM and the object of installation are placed devices – vibroinsulators which weaken vibration impacts on the design.

The shock-absorber (vibroinsulator) is a structure uniting an elastic and damping element. The elastic forces in the shock-absorber are created by steel springs, the elastic component hardness of rubber or polymer components, elasticity of metalrubber or a cable. Forces of resistance (damping) in the design of the shock-absorber is formed as a result of dry friction in the material of elastic and damping elements and viscous friction.

Depending on the type of the elastic element and the way of damping vibroinsulators are divided into the following groups: the rubber-metal; spring-loaded with air damping; spring-loaded with frictional damping; all-metal with structural damping [1].

Figure 1 shows the form of insulator type DO.



Figure 1 – Vibroinsulator

Figure 2 shows the sketch of the design of vibroinsulator type DO.

The material of the spring is the steel 65 [2]. Main technical characteristics of vibroinsulators type DO are given in tables 1 and 2.

Table 1 - Characteristics of vibroinsulators type DO

Brand	Load P,	Vertical	Height in	Sediment of the	The	Weight,
-------	---------	----------	-----------	-----------------	-----	---------

	N		rigidity , N/cm	the free state	spring under load, mm		number of working coils	kg
	Work.	Prev			Work.	Prev.		
DO-38	122	152	45	72	27	33,7	5,6	0,3
DO-39	219	273	61	92,5	36	45	5,6	0,4
DO-40	339	424	81	113	41,7	52	5,6	1
DO-41	540	674	124	129	43,4	54	5,6	1
DO-42	942	1177	165	170	57,2	72	5,6	1,8
DO-43	1648	2060	294,3	192	56	70	5,6	2,4
DO-44	2384	2979	357	226	66,5	83	5,6	3,65
DO-45	3728	4660	441,5	281	84,5	106	5,6	6,45

Table 2 - Characteristics of vibroinsulators type DO

Brand	Sizes, mm						
	A	A ₁	B	D _{cp}	d	d ₁	d ₂
DO-38	100	70	60	30	3	12	8,5
DO-39	110	80	70	40	4	12	8,5
DO-40	130	100	90	50	5	12	8,9
DO-41	130	100	90	54	6	14	10,5
DO-42	150	120	110	72	8	14	10,5
DO-43	160	130	120	80	10	14	10,5
DO-44	180	150	140	96	12	14	10,5
DO-45	220	180	170	120	15	16	12,5

Note:

1. The Deformation (sludge spring) under the load, which is different from that indicated in the table, changes in proportion to load.

2. For vibroinsulators of all types the total number of rounds of a spring is 6,5.

3. For the vibroinsulators DO-38, DO-39 $S = 2$ mm, for other vibroinsulators $S = 3$ mm, S_1 is respectively 5 and 10 mm. In the rubber gaskets in all cases $d_1 = d_2 + 3,5$ mm.

Apparently from figure 1 the main element of vibroinsulator of the type DO is the spring, so its characteristics of reliability are defined by the reliability exactly this element. According to the classification of GOST 27.003 [3] springs relate to the products of general purpose type I (highly reliable accessory intersectoral application), continuous and long application, nonrestorable, unattended, transition which transition to the limit state does not lead to catastrophic consequences, worn out, growing during storage. For such products the following indicators of reliability are normalized:

- failure rate - λ
- average resource - $T_{p.Cp}$
- medium term persistence - $T_{c.Cp}$

Let required value λ of the vibroinsulator DO-38 is $5 \cdot 10^{-7}$ 1/h⁻¹

Consider the calculation of the failure rate of the vibroinsulator's DO-38 spring under the following conditions:

- Amplitude of acceleration of vibration: $40 \text{ m} / c_2$;
- Range of frequencies: from 1 to 300 Hz;
- Working temperature: 50°C ;
- Limit temperature: 70°C ,

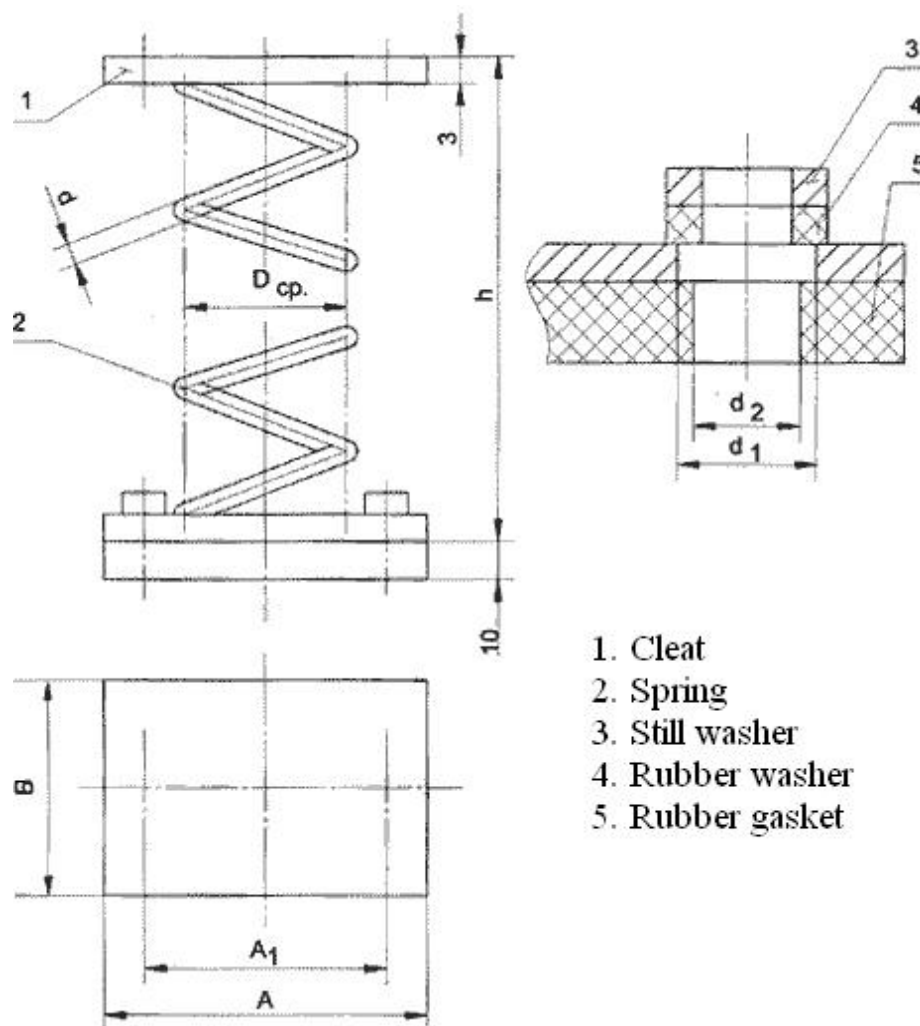


Figure 2 – The design of vibroinsulator

Which corresponds to class 1, group 1.9 «Equipment based on railway platforms,» on the classification of GOST RV 20.39.304 [4].

The choice of methods of calculation of indicators of reliability of the mechanical and electromechanical elements applied in practice is rather limited [5-7].

For the calculation we will use the technique given in [8] according to which the mathematical model of the failure rate of the spring is the following:

$$\lambda_e = \lambda_0 \cdot a_1 \quad (1)$$

where: λ_0 - failure rate of a spring in the nominal mode and normal conditions (ambient temperature 20 ± 10 °C, relative humidity of air is 30-70%; atmospheric pressure $0,825 \dots 1,06 \cdot 10^5$ PA; lack of vibration and blows); a_1 – the coefficient taking into account the design features of the spring, the conditions of production and spring operation.

The value of the coefficient a_i is calculated by the formula:

$$a_1 = K_{11} \cdot K_{12} \cdot K_{13} \cdot K_{14} \cdot K_{15} \quad (2)$$

where: K_{11} - the coefficient taking into account the of vibration; K_{12} - the coefficient taking into account the influence of blows; K_{13} - the coefficient taking into account the influence of climate; K_{14} - the coefficient taking into account the influence of quality of service; K_{15} - the coefficient taking into account the influence of quality of production.

The values of coefficients $K_{11} - K_{14}$, received according to the tables provided in [8], are presented in table 3.

Table 3 – The values of correction coefficients of a formula (2)

The coefficient	The classification characteristic	The value
K_{11}	Enterprises of metallurgical heavy machinery. Railway transport. (unamortized equipment)	8.0
K_{12}		4.0
K_{13}	Climate is temperate, midland (not heated, unpackaged room)	1.3
K_{14}	The transport	1.5
K_{15}		0.5

The value given in [8] for the class of «Spring» is $0.05 \cdot 10^{-6}$ 1/h.

Then, operational failure rate of the spring of the vibroinsulator DO-38 is:

$$\lambda_e = 1.56 \cdot 10^{-6} \text{ 1/h.}$$

As follows from the received result, the calculated value exceeds demanded that requires the adoption of measures to increase reliability.

The analysis of the table 3 shows that coefficients K_{11} and K_{11} (see table 3) have the greatest impact on value λ .

However, to reduce their values by the use of vibroinsulator DO other denomination is not possible, since when using this technique, the values of the coefficients K_{11} and K_{11} will not change, as they depend on the characteristic «Railway transport» (see table 3).

Therefore we will use the technique given in the standard [9]. Mathematical model for the class «Spring» has the following form:

$$\lambda_s = \lambda_{sp,b} \cdot C_G \cdot C_{DW} \cdot C_{DC} \cdot C_N \cdot C_Y \cdot C_L \cdot C_K \cdot C_{CS} \cdot C_R \cdot C_M \quad (3)$$

where: $\lambda_{sp,b}$ - basic failure rate of the spring; C_G , C_{DW} , C_N , C_Y , C_L , C_K , C_{CS} , C_R , C_M - correction coefficients.

The value of the coefficient C_G , taking into account the size of the module of rigidity of a material, calculated by the formula:

$$C_G = \left(\frac{G_M}{11.5 \cdot 10^6} \right)^3, \quad (4)$$

where: G_M is the module of rigidity of a material of a spring.

The value of the coefficient C_{DW} taking into account the value of the thread diameter is calculated by the formula:

$$C_{DW} = \left(\frac{D_w}{0.085} \right)^3, \quad (5)$$

where: D_w - diameter of the thread.

The value of the coefficient C_{DC} taking into account the value of the diameter of the coil is calculated by the formula:

$$C_{DC} = \left(\frac{0.58}{D_C} \right)^6, \quad (6)$$

where: D_C - the average diameter of a spring.

The value of the coefficient C_N taking into account the number of active coils calculated by the formula:

$$C_N = \left(\frac{14}{N_A} \right)^3, \quad (7)$$

where: N_A - number of active coils.

The value of the coefficient C_Y taking into account the resistance to stretching the material of spring is calculated by the formula:

$$C_Y = \left(\frac{190}{T_s} \right)^3, \quad (8)$$

where: T_s - strength of a material at the gap.

The value of the coefficient C_L taking into account the impact of precipitation coil springs is calculated by the formula:

$$C_L = \left(\frac{L_1 - L_2}{1.07} \right)^3, \quad (9)$$

where: L_1 - L_2 - draught spring.

The value of the coefficient C_K taking into account the impact of compression is calculated by the formula:

$$C_K = \left(\frac{K_w}{1.219} \right)^3, \quad (10)$$

where: $K_w = \frac{4 \cdot r - 1}{4 \cdot r - 4} + \frac{0.616}{r}, \quad r = \frac{D_C}{D_w}.$

The value of the coefficient C_{CS} , taking into account the impact of the frequency of loading coil, calculated by the formula:

$$C_{CS} = \frac{CR}{300}, \quad (11)$$

where: CR - the frequency of loading of a spring.

The numerical values of the parameters necessary for calculation of the coefficients of C_G , C_{DW} , C_N , C_Y , C_L , C_K , C_{CS} , C_R and C_M , are given in table 4.

Table 4 – The values of the parameters used in formulas (4)-(11)

Sign	Name	Value	Unit	Note
G_m	Module of rigidity	$8.0 \cdot 10^3$	kgf/mm ²	GOST 14959
D_w	Diameter of a thread	3	mm	See table 2
D_c	Diameter of a spring	30	mm	See table 2
N_a	The number of active coils	5.6	PCs	See table 2
T_s	Tensile of strength	80	kgf/mm ²	GOST 14959
L_1 - L_2	Deposit of spring	27	mm	See table 1
K_w	Compression of spring	1.145	-	-
CR	Frequency of the load	300	Hz	GOST RB

				20.39.304
C_R	Corrosion influence	1	-	-
C_M	Quality of the production process	1	-	-

The numerical values of coefficients of model (3) received as a result of calculation are summarized in table 5.

Table 5 – The values of the model's coefficients (3)

Sign	Value
C_G	0.949
C_{DW}	2.658
C_{DC}	0.014
C_N	15.625
C_Y	4.657
C_L	0.99
C_K	0.829
C_{CS}	1

The basic failure rate for this group that given in the standard [9] is $23.8 \cdot 10^{-6}$ 1/h.

Then, operational failure rate of a spring of the vibroinsulator DO-38, is:

$$\lambda_{sp} = 5.128 \cdot 10^{-5} \text{ 1/h.}$$

As follows from the received result, the calculated value λ also exceeds the demanded that requires the adoption of measures to increase reliability. So for providing demanded level it is necessary to choose vibroinsulator DO other denomination.

The analysis of table 5 shows that the greatest impact on magnitude λ has C_{DW} , C_N and C_Y coefficients.

Find in how many time you need to reduce λ_{sp} for providing demanded level of failure rate:

$$\frac{\lambda_{sp}}{\lambda} = 98.94.$$

However it is impossible to reduce value of coefficients of C_N and C_Y because for production of springs of all face values of vibroinsulators DO the same brand of steel is used and they have an identical quantity of working rounds (see table 1). Besides, with increasing $d(D_w)$ (see table 2) the value of coefficient of C_{DW} according to (5) also increases.

The analysis of mathematical models of failure rate of the class "Springs" of the standard [9] that was given in works [10-12] has shown that the greatest impact on λ_{sp} has a parameter $D_C(D_{cp})$. Changing this value (see table 2) leads to change the value D_w that, according to (5), (6) and (10) leads to a change in the coefficients C_{DW} and C_{DC} and C_K .

For the vibroinsulators DO-42 the values of these coefficients are:

$$C_{DW} = 50.412;$$

$$C_{DC} = 7.474 \cdot 10^{-5};$$

$$C_K = 0.867.$$

Besides, since value of load of a vibroinsulator remains invariable, so $L_1-L_2 = 7.435$ mm, and the value C_L will be 0.021.

In this case operational failure rate of a spring of the vibroinsulator DO-42 is:

$$\lambda_{sp} = 1.111 \cdot 10^{-7} \text{ 1/h,}$$

that meets the set requirements.

Thus, it can be concluded that the technique given in [8], is more simple than technique standard [9]. However, if the results received with its help are not satisfactory, it is necessary to apply a technique standard [9] in which at calculation of failure rate are considered both constructive and technological features of springs, and mechanical characteristics of materials.

References

1. Il'inskiy, V.S. Zashita REA i pretsizionnogo oborudovaniya ot dinamicheskikh vozdeystviy. / V.S. Il'inskiy - M.: Radio i svyaz', 1982. - 296 s.
2. GOST 14959-79. Prokat iz ressonno-pruzhinnoy uglerodistoy i legirovannoy stali.
3. GOST 27.003-90. Nadezhnost' v tehnikе. Sostav i obshchie pravila zadaniya trebovaniy po nadezhnosti.
4. GOST RV 20.39.304-98. KSOTT. Apparatura, pribory, ustroystva i oborudovanie voennogo naznacheniya. Trebovaniya stoykosti k vneshnim vozdeystvuyuschim faktoram.
5. Zhadnov, V.V. Metody i sredstva ocenki pokazatelej nadezhnosti mehanicheskikh i e'lektromechanicheskikh e'lementov priborov i sistem. / V.V. Zhadnov. // Datchiki i sistemy. - 2013. - № 4. - s. 15-20.
6. Zhadnov, V. Methods and means of the estimation of indicators of reliability of mechanical and electromechanical elements of devices and systems. / V. Zhadnov. // Reliability: Theory & Applications: e-journal. - 2011. - Vol. 2, No 4. - p. 94-102.
7. Markin, A.V. Metody ocenki nadyozhnosti elementov mexaniki i elektromexaniki elektronnyx sredstv na rannix etapax proektirovaniya. / A.V. Markin, S.N. Polesskij, V.V. Zhadnov. // Nadyozhnost'. - 2010. - № 2. - s. 63-70.
8. Shavykin, N.A. Otsenka pokazateley bezotkaznosti mehanicheskikh elementov produktsii priborostroeniya. / N.A. Shavykin, B.P. Petruhin. // Datchiki i sistemy, № 6, 2006. - s. 28-35.
9. NSWC-11 Handbook of reliability prediction procedures for mechanical equipment.
10. Lushpa, I.L. Issledovanie modeli intensivnosti otkazov mehanicheskikh elementov klassa «Pruzhiny». / I.L. Lushpa, M.A. Monahov, V.M. Fokin. // Innovatsionnye informatsionnye tehnologii: Materialy mezhdunarodnoy nauchno-prakticheskoy konferentsii. Tom 3. - M.: MIEM NIU VShE, 2013. - s. 443-446.
11. Lushpa, I.L. Issledovanie modeli intensivnosti otkazov volnoobraznykh kol'tsevykh pruzhin. / I.L. Lushpa, M.A. Monahov, V.M. Fokin. // XXI Mezhdunarodnaya studencheskaya konferentsiya-shkola-seminar «Novye informatsionnye tehnologii»: tez. dokl. - M.: MIEM NIU VShE, 2013. - s. 122-123.
12. Lushpa, I.L. Issledovanie modeli intensivnosti otkazov izognutykh kol'tsevykh pruzhin / I.L. Lushpa, M.A. Monahov, V.M. Fokin. // X Vserossiyskaya nauchno-tehnicheskaya konferentsiya «Nauchnye chteniya po aviatsii posvyaschennye pamyati N.E. Zhukovskogo»: sb. tez. dokl. - M.: Izdatel'skiy dom Akademii im. N.E. Zhukovskogo, 2013. - s. 415-419.

THE FORMATION PROCESS OF NANOCLUSTERS IN THE METAL SURFACE LAYER, INITIATED BY NONLINEAR TUNNELING DYNAMICS IN THE ELECTROSTATIC FIELD

Artemov I. I., Krevchik V. D., Simonov N.P.
Penza State University of Russia, Russia

One of the possible mechanisms for the nanoclusters formation in the metal surface layer under the cavitation regime for sound capillary effect, has been considered. Physical basis of this mechanism is electron exchange between nanoparticles by dissipative tunneling with subsequent formation of dipoles. As a result, the mechanism of the dipole-dipole interaction can turn on between the nanoparticles themselves, and with the interior of the broken bonds in microcracks due to the electrostatic image forces, which leads to the formation of nanoclusters. It is shown, that the effective Young's modulus of the nanostructured surface layer is defined by the relation between the rate of tunneling transfer in an electric field and the frequency of the ultrasonic wave. It is found that in the case of the dense regular chain of microcracks the effective Young's modulus of the surface layer is mainly determined by Young's modulus of the nanoparticles material. The obtained theoretical results can form the basis of technology to improve the efficiency of grinding, including and for rather brittle materials. For example, the results of the experiment on the processing of ferrite materials using the process fluid, modified by the copper nanoparticles are showed a reduction of roughness by 12%. By electron microscopy data, the surface of the treated material becomes more homogeneous due to overgrowth of microcracks net by the copper nanoparticles.

1. INTRODUCTION

One of the possible mechanisms for the nanoclusters formation in the microcracks (MC) – volume of the metal surface layer in the cavitation regime of sonocapillary effect, has been theoretically investigated. The physical nature of the mechanism under consideration is the following. At the first stage, the cavitation cloud arises in the volume of coolant with nanoadditives with the following slamming of cavitation bubbles at the MC- base and with formation of cumulative jets. This jets, which carry nanoparticles (NP) fall into the canal of MC. This situation is repeated with the period of the ultrasonic wave, during this period the cluster is formed from NP in a volume of MC. At this stage, due to thermal activation, a process of the electron exchange between NP arises because of dissipative tunneling. The result is the formation of dipoles, and the mechanism of dipole - dipole interaction between NP and with dangling bonds of the MC- inner cavity is turned on because of the electrostatic image forces through, that gives in result formation of nanoclusters. The effective Young's modulus of the nanostructured surface layer E^* is a function of the frequency ω_s of the ultrasonic wave and of the probability of dissipative tunneling Γ_0 :

$$E^* = E_0 \frac{N_H^{(MT)}}{N_H} \cdot \frac{2\pi}{\omega_s} \cdot \Gamma_0, \quad (1)$$

where E_0 – Young's modulus of the NP material; $N_H^{(MT)}$ - the number of NP in the MC - volume; N_H - the NP number in the coolant volume. It follows from (1) that the value of E^* essentially depends on the ratio between the rate of tunneling and the frequency of ultrasonic waves. Formalism of the dissipative tunneling theory in an adiabatic, quasi-classical instanton approximation [1] is used to tunnel chemical dynamics for calculation of Γ_0 .

2. CALCULATION OF THE DISSIPATIVE TUNNELING PROBABILITY

We consider the adiabatic tunneling reactions in which the parameter Landau-Zener is great: $\frac{\Delta^2}{\hbar u |F_2 - F_1|} \gg 1$, (where Δ - electronic matrix element of the interaction between the initial and final states, u - speed of the transferred particle, $F_{1,2}$ - forces at the intersection point of the terms). State of the reaction system in an environment characterized by a multi-dimensional potential surface (similar to the statement of the problem in the tunnel chemical kinetics [9-11])

$$U_i = \sum_{i=1}^N \frac{1}{2} \omega_{0i}^2 (x_i + x_{0i})^2, \quad U_f = \sum_{i=1}^N \frac{1}{2} \omega_{0i}^2 (x_i - x_{0i})^2 - \Delta I \quad (2)$$

The Hamiltonian of the system (along the tunneling coordinate)

$$\hat{H} = \frac{p_1^2}{2} + v_1(y_1) + y_1 \sum_{\alpha=2}^N C_\alpha y_\alpha + \frac{1}{2} \sum_{\alpha=2}^N (p_\alpha^2 + \omega_\alpha^2 y_\alpha^2), \quad (3)$$

where C_α - interaction coefficients with oscillator modes of the medium. Tunneling probability per unit time is defined as [2, 3]

$$\Gamma = 2T \frac{\text{Im } Z}{\text{Re } Z} \quad (4)$$

where $Z = \prod_\alpha \int D y_1 \int D y_\alpha \exp[-S\{y_1; y_\alpha\}]$ - partition function of the system that

can be represented as a path integral. $y_\alpha(-\beta/2) = y_\alpha(\beta/2)$, (here $\beta \equiv T^{-1}$ or $\beta \equiv \frac{\hbar}{kT}$, where \hbar and k are set equal to unity). Semi-classical (instanton) action is defined as [2, 3, 9]

$$S\{y_1\} = \int_{-\beta/2}^{\beta/2} d\tau \left[\frac{1}{2} \dot{y}_1^2 + v(y_1) + \frac{1}{2} \int_{-\beta/2}^{\beta/2} d\tau' K(\tau - \tau') y_1(\tau) y_1(\tau') \right], \quad (5)$$

$$v(y_1) = v_1(y_1) - \frac{1}{2} \sum_{\alpha=2}^N \frac{C_\alpha^2}{\omega_\alpha^2} y_1^2, \quad (6)$$

$$\zeta_n = v_n^2 \sum_{\alpha=2}^N \frac{C_\alpha^2}{\omega_\alpha^2 (\omega_\alpha^2 + v_n^2)}, \quad (7)$$

where $v_n \equiv 2\pi nT$ - is the Matsubara frequency.

The renormalized potential energy of the particle along the coordinates of tunneling in the case of a two-well model, Fig. 1 takes the form

$$v(q) = \frac{1}{2} \omega_0^2 (q + q_0)^2 \theta(-q) + \left[\frac{1}{2} \omega_0^2 (q - q_1)^2 - \Delta I \right] \theta(q), \quad (8)$$

$$q = y_1 + \frac{\Delta I}{2\lambda}, \quad \omega_0^2 = \omega_1^2 - \sum_{\alpha=2}^N \frac{C_\alpha^2}{\omega_\alpha^2}, \quad q_0 = \frac{\lambda}{\omega_0^2} - \frac{\Delta I}{2\lambda}, \quad q_1 = \frac{\lambda}{\omega_0^2} + \frac{\Delta I}{2\lambda},$$

$$\lambda^2 = \sum_{i=1}^N \omega_{0i}^4 x_{0i}^2$$

It is assumed that the main contribution to the action $S(q)$ gives the trajectory (instanton) that minimizes the functional (5) and subordinate to the Euler – Lagrange equation

$$-\ddot{q}_B(\tau) + \frac{\partial v(q_B)}{\partial q_B} + \int_{-\beta/2}^{\beta/2} d\tau' K(\tau - \tau') q_B(\tau') = 0, \quad q_B(\tau) = q_B(\tau + \beta) \quad (9)$$

The solution (9) we seek in the form:

$$q_B(\tau) = \beta^{-1} \sum_{n=-\infty}^{\infty} q_n \exp(iv_n \tau) \quad (10)$$

$$q_B(\tau) = -q_0 + \frac{2(q_0 + q_1)\tau_0}{\beta} + \frac{2\omega_0^2(q_1 + q_0)}{\beta} \sum_{n=1}^{\infty} \frac{\sin v_n \tau_0 \cdot \cos v_n \tau}{v_n(v_n^2 + \omega_0^2 + \zeta_n)} \quad (11)$$

Then

$$S_B = 2\omega_0^2(q_0 + q_1)q_0\tau_0 - \frac{2\omega_0^2(q_0 + q_1)^2\tau_0^2}{\beta} - \frac{4\omega_0^4(q_0 + q_1)^2}{\beta} \sum_{n=1}^{\infty} \frac{\sin^2 v_n \tau_0}{v_n^2(v_n^2 + \omega_0^2 + \zeta_n)}. \quad (12)$$

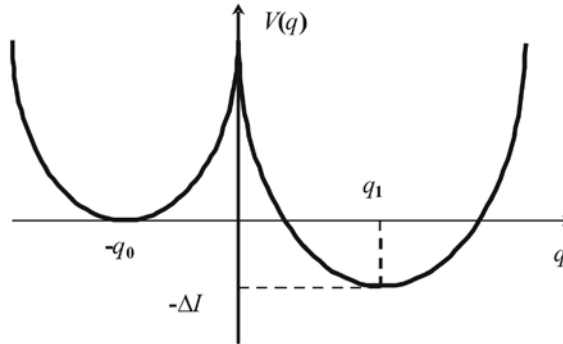


Fig. 1. The potential energy of the particle along the tunneling coordinate (two-well model).

In the case of interaction with a selected local mode action (12) takes the form

$$2S = (q_1 + q_0)(3q_0 - q_1)\omega^2\tau_0 - \frac{4\omega^2(q_0 + q_1)^2(\tau_0)^2}{\beta} - \frac{\omega^2(q_0 + q_1)^2}{2\tilde{\gamma}} \left\{ \frac{(\omega^2 - \tilde{x}_2)}{\sqrt{\tilde{x}_1}} \left(\operatorname{cth}\left(\frac{\beta}{2}\sqrt{\tilde{x}_1}\right) - \frac{1}{\operatorname{sh}\left(\frac{\beta}{2}\sqrt{\tilde{x}_1}\right)} \left(\operatorname{ch}\left[\left(\frac{\beta}{2} - 2\tau_0\right)\sqrt{\tilde{x}_1}\right] - \operatorname{ch}\left[\left(\frac{\beta}{2}\right)\sqrt{\tilde{x}_1}\right] + \operatorname{ch}\left[\left(\frac{\beta}{2} - 2\tau_0\right)\sqrt{\tilde{x}_1}\right] \right) \right\} -$$

$$-\frac{(\omega^2 - \tilde{x}_1)}{\sqrt{\tilde{x}_2}} \left\{ \operatorname{cth} \left(\frac{\beta}{2} \sqrt{\tilde{x}_2} \right) - \frac{1}{\operatorname{sh} \left(\frac{\beta}{2} \sqrt{\tilde{x}_2} \right)} \left(\operatorname{ch} \left[\left(\frac{\beta}{2} - 2\tau_0 \right) \sqrt{\tilde{x}_2} \right] - \operatorname{ch} \left[\left(\frac{\beta}{2} \right) \sqrt{\tilde{x}_2} \right] + \right. \right. \\ \left. \left. + \operatorname{ch} \left[\left(\frac{\beta}{2} - 2\tau_0 \right) \sqrt{\tilde{x}_2} \right] \right) \right\}, \quad (13)$$

$$\text{where } \tilde{x}_{1,2} = \frac{1}{2} \left(\omega^2 + \omega_L^2 + \frac{C^2}{\omega_L^2} \right) \mp \frac{1}{2} \sqrt{\left(\omega^2 + \omega_L^2 + \frac{C^2}{\omega_L^2} \right)^2 - 4\omega^2 \omega_L^2} \\ \tilde{\gamma} = \sqrt{\left(\omega^2 + \omega_L^2 + \frac{C^2}{\omega_L^2} \right)^2 - 4\omega^2 \omega_L^2}.$$

The same formula (13) in the Bohr units takes the form:

$$S = \frac{1}{2} \frac{E_d}{\hbar} a_d^2 \varepsilon_0^{*2} l_1^2 \left(\frac{l_2}{2l_1} \tau_0^* - \tau_0^{*2} \varepsilon_T^* - \right. \\ \left. - \frac{1}{2\gamma^*} \left\{ \frac{(\varepsilon_0^{*2} - x_2^*)}{\sqrt{x_1^*}} \left(\operatorname{cth} \left(\frac{\sqrt{x_1^*}}{2\varepsilon_T^*} \right) - \frac{1}{\operatorname{sh} \left(\frac{\sqrt{x_1^*}}{2\varepsilon_T^*} \right)} \left(2\operatorname{ch} \left[\left(\frac{1}{\varepsilon_T^*} - 2\tau_0^* \right) \frac{\sqrt{x_1^*}}{2} \right] - \operatorname{ch} \left[\frac{\sqrt{x_1^*}}{2\varepsilon_T^*} \right] \right) \right) - \right. \right. \\ \left. \left. - \frac{(\varepsilon_0^{*2} - x_1^*)}{\sqrt{x_2^*}} \left(\operatorname{cth} \left(\frac{\sqrt{\tilde{x}_2}}{2\varepsilon_T^*} \right) - \frac{1}{\operatorname{sh} \left(\frac{\sqrt{\tilde{x}_2}}{2\varepsilon_T^*} \right)} \left(2\operatorname{ch} \left[\left(\frac{1}{\varepsilon_T^*} - 2\tau_0^* \right) \frac{\sqrt{\tilde{x}_2}}{2} \right] - \operatorname{ch} \left[\frac{\sqrt{\tilde{x}_2}}{2\varepsilon_T^*} \right] \right) \right) \right) \right\}, \quad (14)$$

$$\text{где } x_{1,2}^* = \frac{1}{2} \left(\varepsilon_0^{*2} + \varepsilon_L^{*2} + \frac{\gamma_0^*}{\varepsilon_L^{*2}} \right) \mp \frac{1}{2} \sqrt{\left(\varepsilon_0^{*2} + \varepsilon_L^{*2} + \frac{\gamma_0^*}{\varepsilon_L^{*2}} \right)^2 - 4\varepsilon_0^{*2} \varepsilon_L^{*2}} \\ \tilde{\gamma} = \sqrt{\left(\varepsilon_0^{*2} + \varepsilon_L^{*2} + \frac{\gamma_0^*}{\varepsilon_L^{*2}} \right)^2 - 4\varepsilon_0^{*2} \varepsilon_L^{*2}}.$$

$$\tau_0^* = \frac{1}{\varepsilon_0^*} \operatorname{Arcsh} \left[\frac{a^* - b^*}{a^* + b^*} \operatorname{sh} \frac{\varepsilon_0^*}{2\varepsilon_T^*} \right] + \frac{1}{2\varepsilon_T^*} \\ \varepsilon_T^* = \frac{\hbar}{\beta E_d}, \quad \varepsilon_L^* = \frac{\hbar \omega_L}{E_d}, \quad \beta = \frac{\hbar}{\varepsilon_T^* E_d}, \quad \varepsilon_T^{*2} = \frac{4U_0^*}{q_0^{*2}}, \quad U_0^* = \frac{U_0}{E_d}, \\ l_1 = a^* + b^*, \quad l_2 = 3a^* - b^*, \quad a^* = \frac{q_0}{a_d}, \quad b^* = \frac{q_1}{a_d}, \quad \gamma_0^* = \frac{\hbar^4 C^2}{E_d^4}, \quad \frac{q_1}{q_0} = \frac{b^*}{a^*} = \frac{b}{a}. \quad (15)$$

With the exponential accuracy, the tunneling probability Γ is estimated as $\Gamma_0 \propto \exp(-S)$.

3. DEPENDENCE OF THE PROBABILITY OF DISSIPATIVE TUNNELING ON TEMPERATURE, THE PHONON MODE FREQUENCY AND THE INTERACTION CONSTANT WITH THE CONTACT MEDIUM

The temperature dependence of the tunneling probability Γ_0 for NP in the MC - volume is shown in Fig. 2. Tunneling probability is sensitive to the frequency of the phonon modes and to the constant of interaction with the contact medium (Fig. 3).

From the point of view of the physics of this process the obtained results are expected: the efficiency of electron - phonon interaction increases with increasing of the phonon mode, that is accompanied by a corresponding increase in the tunneling electron energy and leads to an increase in the probability of tunneling transition (the transition from the curve "1" to a curve "2", Fig. 3); increase of the coupling constant increases the medium viscosity contact, i.e. to the growth of its "degree of dissipation" and to the corresponding decrease in the probability of tunneling (transition from curve "1" to the curve "3" in Fig. 3). Fig. 3 shows a number of interesting features of tunneling in the considering system. First, under coincidence of the radii of the NP the effect of lockout for electron wave function takes place (a characteristic minimum in Fig. 3). The interest to this effect has increased significantly in recent years in connection with the study of the dynamic control of the electronic states in a double quantum dot in a weak dissipation [12].

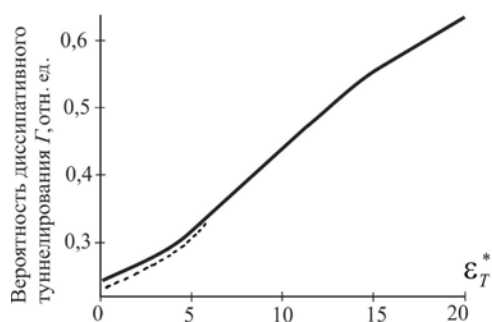


Fig. 2. Dependence the dissipative tunneling probability of Γ (in relative units) on ε_T^* - quantities for NP in the MC - volume.

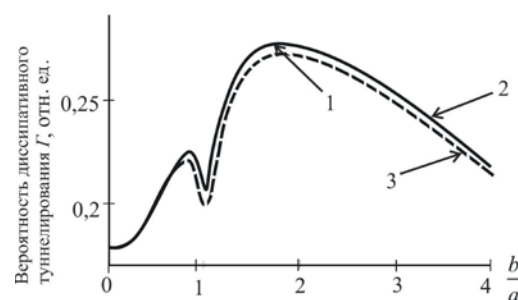


Fig. 3. Dependence the dissipative tunneling probability of Γ (in relative units) from the value of the asymmetry parameter $\frac{b}{a}$

- 1 - $U_0^* = 200, \varepsilon_T^* = 3, \varepsilon_L^* = 1, \gamma_0^* = 10$; 2 - $U_0^* = 200, \varepsilon_T^* = 3, \varepsilon_L^* = 10, \gamma_0^* = 10$;
3 - $U_0^* = 200, \varepsilon_T^* = 3, \varepsilon_L^* = 1, \gamma_0^* = 50$.

4. CONCLUSION

Thus, the ability to use the science of quantum tunneling with dissipation to the study of thermo – control for tunneling process in MC with NP, has been demonstrated; that opens new possibilities to obtain a surface layer of details with the pre-given properties.

References

1. Landau L.D., Liphshits E.M. Quantum mechanics (non-relativistic theory). V.3.– M.: Nauka, 1989.
2. Caldeira A.O., Leggett A.J. Influence of dissipation on quantum tunneling in macroscopic systems // Phys. Rev. Lett. - 1981. - Vol. 46, N 4. - P. 211 - 214.
3. Larkin A.I., Ovchinnikov Yu.N. Quantum tunneling with dissipation// JETP Letters - 1983. - V. 37, N 7. - P. 322 - 325.

4. Gorokhov D.A., da Silveira Rava A. Ultrasharp crossover from quantum to classical decay in a quantum dot flanked by a double – barrier tunneling structure // <http://arXiv.org/abs/cond-mat/0308023> .
5. Foa Torres L.E.F., Lewenkopf C.H., Pastawski H.M. Coherent versus sequential electron tunneling in quantum dots // <http://arXiv.org/abs/cond-mat/0306148> .
6. Thielmann A, Hettler M.H., Konig J, Schon G. Shot noise in tunneling transport through molecules and quantum dots // *Phys. Rev. B.* – 2003. – Vol. 68. – P. 115105 ;
7. Khanin YU.N., Vdovin E.E., Dubrovsky Yu.V. Resonant tunneling in single-barrier heterostructures GaAs/AlAs/GaAs // *FTP.* – 2004. – V. 38, num. 4. – P. 436-447.
8. Ternov I.M., Zhukovsky V. Ch., Borisov A.V. Quantum mechanics and the macroscopic effects. – M.: MSU, 1993. – 198 P.
9. Dahnovsky Yu.I., Ovchinnikov A.A., Semenov M.B. Low-temperature chemical reactions as tunnel systems with dissipation // *JETP.* 1987. V. 92. num. 3. P. 955-967.
10. Aringazin A.K., Dahnovsky Yu.I., Krevchik V.D., Semenov M.B., Ovchinnikov A.A., Yamamoto K. Two-dimensional tunnel correlations with dissipation // *Physical Review B.* 2003. V. 68. P. 155426-1 – 155426-12.
11. Ovchinnikov A.A., Dahnovsky Yu.I., Krevchik V.D., Semenov M.B., Aringazin A.K. The principles of controlled modulation of low-dimensional structures. Moscow, UNC DO. 2003. 510 P.
12. Burdov V.A., Solenov D.S. Dynamic control of the electronic states in a double quantum dot in a low dissipation // *JETP.* 2004. V. 125. num. 3. P. 684-692.

INFORMATION PROCESSING METHODS IN VISUAL SENSOR NETWORKS

Karpov A.V.

Moscow, National Research University Higher School of Economics

In this paper we discuss information processing methods in visual sensor networks, analyze methods of increasing energy efficiency of visual sensor networks, associated with image processing on the end devices, propose new method, and review problems which should be research.

Keywords: visual sensor networks, image processing, energy efficiency

INTRODUCTION

Camera sensor network (wireless image sensor network, visual sensor network, smart cameras network) – is a wireless sensor network, where small low-power cameras are used as the main sensor in a system. There are a lot of limitations in such networks, these are computational power, bandwidth, energy resources. The main goal of deployment camera network is remote acquiring of information about surveillance objects and its transmission to the central node of a system for a long time.

Since images size is much more than scalar data size, acquired from temperature or humidity sensors in usual sensor networks and it has limited resources, then the key problem in camera sensor networks is the energy efficiency.

The aim of our work is to increase energy efficiency of wireless camera sensor networks with autonomous power sources. For this purpose is necessary to research information processing methods in such networks.

In this paper we discuss applications of camera sensor networks, information processing methods, analyze methods of energy efficiency increasing of camera sensor networks associated with image processing on the end devices, and propose new method.

This study (research grant No 14-05-0064) was supported by The National Research University–Higher School of Economics’ Academic Fund Program in 2014- 2015.

IMAGE PROCESSING IN VISUAL SENSOR NETWORKS

The main task of visual sensor network is remote distributed monitoring, using small low-power cameras [1,2,3,4,5]. We can determine three types of applications with respect to the desired end-user information in visual sensor networks:

- applications that require to transmit images;
- applications that images transfer are not required and necessary information contained in the images;
- mixed type of applications, when the information contained in the images, and transfer images themselves are necessary.

The main part of the applications refers to the second type as the receipt and transmission of images is not the aim of a system deployment. Image is only an intermediate form of information representation, needed for its collection by the end-device, equipped with a camera. Examples of such applications are: monitoring of intruder detection, monitoring of plant diseases, tracking objects, monitoring of rare species of birds and animals.

In the monitoring system can determine two principles of information processing:

- 1) centralized, when all information, obtained by end-nodes of the system, is transmitted to the central user-node which spends its further processing.
- 2) distributed, when information is processed by end-nodes.

Today photo and video surveillance systems built on centralized information processing method, when the cameras, distributed in the district surveillance, are obtain images and sent them to the user in the control center, where the images are processed, reproduced and stored. Because the amount of transmitted data is large, such networks have high bandwidth requirements.

In [6] the authors identify levels of intelligent video monitoring. Under the intelligent video monitoring, authors mean any surveillance solution, in which video processing performs directly on the camera-node and thus, reduces bandwidth requirements.

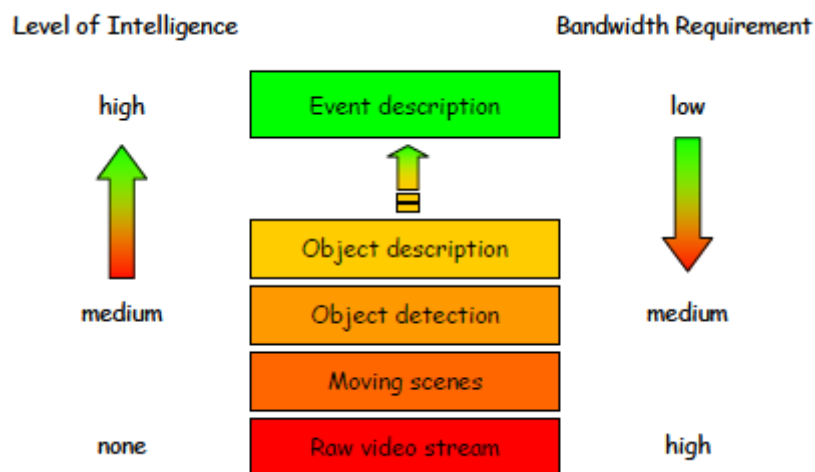


Figure 1. Intelligence surveillance levels

There is no intelligence of a network in existing video monitoring systems (Figure 1). In the video monitoring systems, where image processing is performed on the end devices, we can highlight four levels of intelligence:

- 1) At the first level, the camera nodes use a motion detection scheme such that only moving scenes are streamed to the surveillance center.

2) At a second level, the camera nodes can perform object detection and classification such that only moving scenes containing persons or more general objects of interest are forwarded.

3) At the third level, the smart camera nodes can collaborate to identify objects and only transmit their textual description along with a snapshot.

4) At the fourth level, a network of smart cameras can possibly just notify the surveillance center in case of events of interest by providing a hybrid textual/visual or fully textual description of the event.

Thus, with increasing levels of intelligence, when image processing performs on end-devices, decrease bandwidth requirements, since transmits less data, however, increase demands to the computing resources of the end-nodes, producing data processing. Since end-devices are autonomous, then energy resources are extremely limited and its effective using is the main topic of research many authors.

Consider the factors affecting energy networks: nodes hardware characteristics of the network, the frequency of data collection and transmission, which depends on the application, protocols of physical and link layers, network architecture, which determines the number of device levels, network topology, the routing protocol, as well as the total amount of transmission data. The efficiency of the network mainly determined by the amount received/transmitted information with respect to energy costs. To increase energy efficiency of a network is necessary to maximize the amount of useful information, transmitted over the network, and minimize the total energy consumption of network nodes.

Next, we analyze some methods, associated with data processing in visual sensor networks.

Image processing methods for the end devices are:

a) using of intraframe compression algorithms.

All compression algorithms can be divided into two categories: lossless (RLE, LZW, etc.) and lossy (JPEG, JPEG 2000, fractal compression algorithm, etc.). Lossy compression algorithms widespread as they provide a greater degree of compression than lossless algorithms, despite the fact that image quality is reduced.

In [7] authors studied the question of balance between the computational costs on the side of the camera-node and low-power transmission costs of images over the network. Authors review the application where camera takes metering from a counter. Before transmitting images, the authors conduct its preprocessing, performing downsampling.

b) image preprocessing at the node (background subtraction [8], motion detection [9], for example, based on pixel differences among frames, binarization, edge detection, etc.). Thus, the total amount of information is decreasing.

c) object recognition on the images on the end-nodes.

Proposed method can refer to distributed method of information analysis. It assumes the implementation of the object recognition process on the side of the end-nodes. Analysis results are transmitted to the other devices of a network. This should allow to significantly reduce the amount of transmission data over the network, their volume is becoming comparable to the volume of data using temperature, pressure, light sensors.

There is a range of problems which should be investigated in the development of the method.

First, to determine what kind of image processing algorithms and pattern recognition can be used for low-power devices with limited resources.

Second, to identify groups of objects that can be effectively recognized locally on the end-devices. If an object is more complex, then more time is required for its recognition, and respectively more energy resources are consumed. But is not the fact also that if the frequency

of the processor is lower, then the less energy will be spent in the computation. It's not the fact that the less energy will be spent in the computation if the frequency of the processor is lower.

Third, identify what kind of characteristics (resolution, color depth, etc.) should be taken images, which the distance to the surveillance object should be to be able to recognize it.

Fourth, to determine how the network devices should interact with each other (network algorithm).

These and other questions should be investigated in the development of method that will increase energy efficiency of the visual sensor networks.

CONCLUSION

Object recognition on the side of low-power end-devices can be used as a method of increasing the energy efficiency of the visual sensor networks with independent power sources. In the article we discuss some methods of image processing on the camera-nodes, define the tasks for further study, it is shown that to increase the efficiency of the network should improve its intelligence, that is, to conduct the information processing on end-devices. The proposed method can be implemented in applications, which are not required images transmission from the end-nodes to the central node.

References

1. J. Lloret, I. Bosch, S. Sendra, A. Serrano «A Wireless Sensor Network for Vineyard Monitoring That Uses Image Processing». // *Sensors*. 2011. Vol.11. Pages 6165-6196.
2. Kays, R., B. Kranstauber, et al. «Camera traps as sensor networks for monitoring animal communities». // *The 34th IEEE Conference on Local Computer Networks*. 2009. Pages 811-818.
3. Bir Bhanu, Chinya V. Ravishankar, Amit K. Roy-Chowdhury, Hamid Aghajan, Demetri Terzopoulos «Distributed Video Sensor Networks». // Springer-Verlag London Limited. 2011.
4. Teresa A. Dahlberg, Asis Nasipuri, Craig Taylor «Explorebots: A Mobile Network Experimentation Testbed». // *SIGCOMM'05 Workshops*. August 22–26, 2005.
5. Primož Skraba, Leonidas Guibas «Energy Efficient Intrusion Detection in Camera Sensor Networks». // *DCOSS'07*. Springer-Verlag Berlin Heidelberg 2007. Pages 309-323.
6. S. Hengstler, D. Prashanth, S. Fong, H. Aghajan «MeshEye: A Hybrid-Resolution Smart Camera Mote for Applications in Distributed Intelligent Surveillance». // *IPSN'07*, April 25–27, 2007, Cambridge, Massachusetts, 2007.
7. L. Ferrigno, S. Marano, V. Paciolo, A. Pietrosanto, «Balancing computational and transmission power consumption in wireless image sensor networks», *IEEE International Conference on VECIMS*, 2005
8. H.H.Kenchannavar, S.S.Kudtarkar,U.P.Kulkarni, «Energy Efficient Data Processing In Visual Sensor Network», *International Journal of CS & IT*, 2010
9. R.Zilan, J.M.Barcelo-Ordinas, B.Tavli, «Image Recognition Traffic Patterns for Wireless Multimedia Sensor Networks», *Wireless Systems and Mobility in Next Generation Internet*, 2008

ISSUES OF LONG-HOP AND SHORT-HOP ROUTING IN WIRELESS AUDIO SENSOR NETWORKS

Karpov I.V.

Moscow, National Research University Higher School of Economics

This paper considers the problem of communication range selection of nodes for transmitting audio data with a predetermined Quality of Services (QoS) in Wireless Audio Sensor Networks (WASN). The various strategy of routing selection is viewed from the perspective of network lifetime and energy efficiency. We consider routing strategies with minimum and maximum communication ranges and propose a hybrid routing for audio data transmission.

Keywords: wireless audio sensor networks, long-hop, short-hop, energy-efficiency, lifetime

1. INTRODUCTION

Wireless Audio Sensor Network belongs to the class of Wireless Sensor Networks (WSN) consisting of distributed autonomous nodes with different sensors. A microphone uses as the collection data sensor in WASN. Usually obtained information is stored in nodes and sent upon request or using stream to a main point of network – base station. Because all nodes in the network are autonomous and powered by batteries the problem of network lifetime is relevant [1]. The main purpose of this work is to increase the lifetime of WASN.

To increase the network lifetime is necessary to reduce the power consumption of sensors included in the system, through using hardware with small power consumption, energy-efficiency medium access and routing protocols. Furthermore, to decrease the energy consumption of WSN is used data preprocessing on the nodes that reduce the amount of information for transmitting. However, using compression for WASN is unacceptable, because it takes additional preprocessing delay that affects on QoS [2].

2. SHORT-HOP ROUTING

Basic standard in WSN is IEEE 802.15.4, which defines physical and data link layers according to the OSI model and does not provide a dynamic channel switching within a single network. Since nodes share the same area, competing for it, there is a risk of collisions during data packet transmission, which increases the time delivery, packets lost and quality of service.

In [3] proposed a spatial reuse of channel, which keeps the transmission range as short as possible, avoiding the contention of the channel with other nodes (Fig. 1).

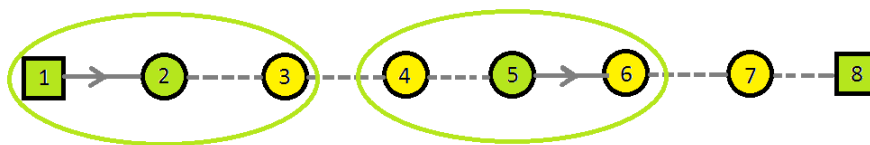


Fig. 1. The network with spatial reuse of channel

In other words, the delivery of information from source to destination nodes is going many hops over a short distance (short-hop routing). For example, nodes 2 and 5 only see neighboring nodes and do not interfere with each other during data transmission. As a result the channel capacity increases. Thereby, while decreasing power transmission, the energy resources are stored. Moreover, the spatial transmission media can be released, but increase the number of retransmissions, time delivery of packets and probability of disconnect between nodes.

According to research [4], with increase the number of nodes in the network, the overhead transmission costs will also increase. Approximately 70% of energy resources spend on the transferring of useful data in the network with 100 nodes and 30% are overhead. But the network with 300 nodes spend 40% of energy for useful data and 60% of all energy are overhead. Furthermore, when the number of nodes increases in the network, the overall energy costs in the system also increase, because it takes more packet transmission. However, the minimum energy costs account for the network with a minimum communication range (Fig. 2).

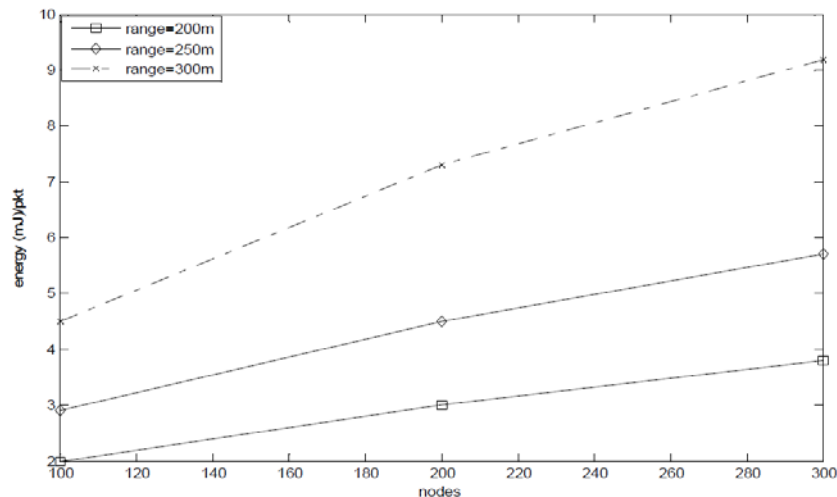


Fig. 2 E energy consumption per packet for different transmission ranges [4]

In [5] describes the reasons for the data transfer over long distances is most appropriate than the data transfer over short distances, because:

- short routing requires information coding\decoding at each nodes, which leads to additional delays and energy waste;
- in many WSNs, where sensors are randomly distributed, the high power level required for good network connectivity;
- the data transfer can be proceed with deviations from the straight route to the point of gathering information, which can also leads to additional energy waste;
- increase the number of retransmitting nodes increase the probability of failure on a route and complicate coordination process such network;
- the nodes with short-hop routing and located near the base station, denied faster, that leads to decrease of network lifetime;
- the extra data retransmission also leads to energy waste in broadcast (multicast).

Thus, the long-hop routing is better than short-hop routing for data transmission.

3. LONG-HOP ROUTING

When the audio data is transmitting over the long distances from source to destination node with overlapping in the coverage area we assume the long-hop routing (Fig. 3).

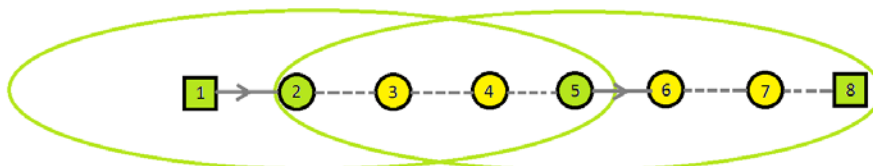


Fig. 3 Network with shared channel

For example, the TOR (Tree-based Opportunistic Routing) supposes data retranslation only those nodes that closest to the destination node [6]. The nodes 2 and 5 in Fig. 3 cover several neighbor nodes that allow to data transmission from node 1 to node 8, using node 5

and ignoring node 3 and 4. The packet delay is reduced due to the long-hop routing in the network with many nodes. In other words, the QoS for long-hop routing is higher, because the number of attempts to shared channel for data transmission are minimal, but under certain conditions, specifically, depending on network density and traffic network.

The short-hop routing provides the worse QoS, due to small probability of packet delivery, the number of nodes, involved to the data transmission, are more and consequently, the packets delay has more time delivery. As a result, the energy costs for additional data are increased and the network lifetime is decreased. To diminish the disadvantages of two routing strategy we propose to use a hybrid routing.

4. HYBRID ROUTING

By hybrid routing we mean the union of two types of routing strategy, discussed above. It is assumed that the nodes with a dynamic regulation of the communication range (from long to short distances) will have a longer lifetime with the defined characteristics of QoS (Fig. 4).



Fig. 4 Network with hybrid routing

In Fig. 4 node 1 has a small communication range and node 5 has maximum. The audio data transmission from the node 1 to the node 8 is carried out through the nodes 2 and 5. Since the long-hop routing consumes more energy resources than short-hop routing, then eventually the energy resources of node 5 will be the smallest over time, so when a certain threshold achieved, it is necessary to switch transmitter of the node 5 to the short communication range and node 2, for example, to the long communication range. The network lifetime can be increased by using the short-hop and long-hop strategies.

The authors use different wireless network models that lead to incorrect results in favor of one or the other routing strategies. For example, a successful reception of data can be incorrect determined, when the disk model is used, as well as the physical model [7]. In [8] authors propose to use the Nakagami-m model (Nakagami-m fading model) for evaluation of the data channel instead of Rayleigh channel model (Rayleigh fading model), which does not take into account the number of characteristics of the channel. Thus, the used tools have a large influence on the evaluation of the system performance (energy consumption, transmission delays, packets loss). In this case, it is necessary to choose the right model of WSN, which would take into account the most important parameters for evaluation of network performance in different routing strategies. Since we consider the class of Wireless Audio Sensor Networks that QoS and power consumption are defining characteristics of the network.

5. CONCLUSION

In this paper we discuss the problem of audio data delivery with QoS in Wireless Audio Sensor Networks. The main purpose of this study is to increase the lifetime of the network using the hybrid routing, which combines long-hop and short-hop routing strategies. Each method has advantages and disadvantages. Since the use of certain models and routing algorithms produce different results, it is necessary to choose the most accurate network and channel models of Wireless Audio Sensor Networks for further research.

This study (research grant No 14-05-0064) was supported by The National Research University–Higher School of Economics’ Academic Fund Program in 2014 – 2015.

References

1. Voskov L.S., Efremov S.G. The problem of increasing lifetime of the autonomous wireless sensor networks in the systems of data collection and the way of to solve it // *Sensors and systems*. №4 (167), 2013 – p. 2-9.
2. Karpov I.V. Wireless Audio Sensor Networks. Quality of Services and energy efficiency, Quality. Innovation. Education. №10 (101), 2013. – p. 47-52.
3. Brunelli D., Maggiorotti M. [et al.], Analysis of audio streaming capability of ZigBee networks // *Wireless Sensor Networks, Lecture Notes in Computer Science*, 2008, vol. 4913, 2008. – P.189-204.
4. M. Tarique, A. Hossain, R. Islam and C. Akram Hossain Issues of Long-Hop and Short-Hop Routing in Mobile Ad Hoc Networks: A Comprehensive Study // *International Journal of Network Protocols and Algorithm*, vol.2 №2, 2010. – P. 107-131.
5. M. Haenggi, Twelve reasons not to route over many short hops // *Vehicular Technology Conference*, 2004, VTC2004-Fall, vol. 5, 2004. – P.3130-3134.
6. Li L., Xing G. [et al.], Adaptive Voice Stream Multicast over Low-power Wireless Networks, Technical Report MSU-CSE-10-16, Computer Science and Engineering, Michigan State University, East Lansing, Michigan, 2010.
7. P. Gupta and P. R. Kumar, The Capacity of Wireless Networks // *IEEE Transactions on Information Theory*, vol. 46, pp. 388–404, 2000.
8. Caleb K. Lo, Sriram Vishwanath, Robert W. Heath Jr, An Energy-Based Comparison of Long-Hop and Short-Hop Routing in MIMO Networks // *Vehicular Technology*, IEEE Transactions on vol. 59, 2010. – P. 394-405.
9. J-H. Chang and L. Tassiulus, Energy conserving routing in Wireless Ad Hoc Networks, In the Proceedings of IEEE INFOCOM, March, 2000, – P. 22-31.

IDENTIFYING SEMANTIC CONTENT-BLOCK OF TERMS AND RELATIONS IN SCIENTIFIC TEXTS

Ayusheeva N.N., Kusheeva T.N.

Ulan-Ude, East Siberia State University of Technology and Management

This paper proposes a method of identifying some blocks in the scientific text to use this information for calculating the weights of semantic network nodes and arcs. This method is based on the application of fuzzy controllers.

Keywords: semantic network, scientific text, formal text sing of, fuzzy controllers

Introduction. Scientific texts in accordance with the typology of private nonfiction texts are on a par with the texts of mass communication and the official business texts. Scientific text has its own peculiarities of language and style. Consider the main features of the narration of scientific text. Scientific text is characterized by *logic*, which correlates with the main stages of scientific work: setting and understanding the problem, study the experience of predecessors, offer solutions of the problem, its proof and argumentation, generalization of data, summarizing. Stylistic feature of the scientific text is its *accuracy*. Accuracy is achieved by using a single-valued expressions, terms, words with clear lexical and semantic combinability. *Abstraction and generalization* are also main characteristics of the scientific text. Scientific text cannot be submitted without the *cliché* – steady turn of speech, ready turn of speech, standard, easily used in certain conditions. In scientific text clichés which are expressed by formal text signs of (markers, connectors, indicators), widely

used as a means which provides an unambiguous and objective narration of information, as well as facilitating its perception.

Traditionally established forms of communication between scientists predetermines a clear structure of scientific texts. Typically, there are three semantic unit: introduction, main part, conclusion. In turn, the main part may be deeper detailed. Scientific texts are not only characterized by a clear structure, but also the fact that each semantic element has its own, only inherent therein, formal text signs of. They can be used to distinguish the individual aspects of the content in the text, track the development of the author's thoughts, reflect compositional logical connection between the keywords of the text, to characterize the degree of objectivity of information and indicate the author's attitude to the statement [3]. The presence of formal signs of and their analysis can facilitate automatic definition of semantic blocks in scientific text, which is important for solving the problem of building a semantic network of scientific texts in part of weights computation of network nodes and arcs [1, 2].

Major aspects of building a semantic network. In a text document semantic network nodes are terms of the text, and the arcs represent the relationship between the terms. The weighting coefficients are typically used to quantify significance of terms and relations.

Existing methods for calculating the weighting coefficients of text semantic network nodes and arcs based on the use of text statistics, such as the word or term frequency in the document, in a collection of documents, the inverse word or term frequency, the total number of words or terms, the number of terms links with each other and etc. Besides these indicators, in our opinion, should be in the calculation of the weighting coefficients to use information about the compositional structure of a text document. Then, the terms and relationships found in the block A will have a different weight than the terms and relations which are used in the block B.

Some linguists relate the compositional structure of a text document with the notion of semantic content-block. Scientific text consists of a logically selected content-block: setting and understanding the problem (The problem), the block of study experience predecessors (The experience), the block of presentation ways to resolve the problem, its proof and argumentation (The decision), the block of the data generalization and summarization (The total). A method of allocation of formal text signs of used to identify each block. These formal signs of are used with high probability in a specific block. Besides above blocks can be distinguished in the texts the so-called additional units, which play an important role to reflect the communicative, aspect, semantic, informative, functional and semantic structure of scientific text:

- to describe a well-known and proven fact (The fact);
- for expression of the author (The Conviction);
- to ensure the inter-phrase connection (connector);
- to provide the information, the opposite pretext (opposite);
- to reflect information about the often / rarely recurrent events (Repeat);
- to reflect the development of the information (Development);
- to clarify the information (Clarification).

For sufficiently small texts which are scientific articles, the presence of additional blocks is not characteristic: some blocks may be missing, some blocks can be very small.

Description of the identifying method. As noted above, the significance of terms and relations are quantified as the weight coefficients. The main criteria for the significance of the terms may include [1]:

- the frequency of occurrence of the term in a document: if the document term is more common, it forms a relationship with other terms;
- the text category, which includes the term: terms of thematic text string will be more important than the terms of textual modality;

– semantic content-block in which the term occurs: term that occurs in the main unit, be more useful to reflect meaning than the term, which met in the additional unit.

In turn, the significance of the relationship in semantic network depends on two criteria [2]:

- frequency of co-occurrence of terms in this relationship;
- relationship utensils to the semantic content-block: relations that bind the two terms, for example, in block «The total» more informative to determine the meaning of the text than the relationship found in other blocks.

A method of allocation of formal text signs of is used to define utensils the term or relationship to a particular block. This method is well suited for clichéd scientific texts. At the same time in the presence of distinct markers and indicators specific semantic units, which are given in earlier works, there are a large number of formal text sings of that can occur in any content-block.

For example, the indicator *"In conclusion ..."* clearly indicates the presence of the block "The total" and it is rare to find in the block "The problem". On the other hand, the indicator *"that way"*, pointing to the block "The total", most likely can be found in other blocks of the test text. Therefore, for the definition of the term or relationship to a particular semantic content-block can use fuzzy logic, constructing fuzzy controller.

The input to fuzzy controller receives fuzzy linguistic variables "PLACE IN THE TEXT" and "CHARACTERISTIC SIGNS OF BLOCK". At the output of the fuzzy controller get variable "SEMANTIC CONTENT-BLOCK". Linguistic variable "PLACE IN THE TEXT" let on a universal set of values from 0 to 100 that represent meaningful place in the text: 0 – beginning of text, 50 – mid text, 100 – end of text. Term-set of linguistic variable «PLACE IN THE TEXT» can form a fuzzy variables *"at the beginning of the text"*, *"not at the beginning of the text, but not in the middle"*, *"in the middle of the text"*, *"not at the end of the text, but not in the middle"*, *"at the end of the text"*, etc. The linguistic variable «CHARACTERISTIC SIGNS OF BLOCK» let set on a partially ordered set of formal text sings of. Partial order was given by ranking of frequency of formal text sings of in a given block. For example, select 25 indicators, which are located on the number axis points from 1 to 25. The first should stand indicator that most often occur in the block "The problem", and the last to stand indicator that most often occur in the block "The total". It should be recalled that we are considering only the basic building blocks of scientific texts, which include setting and understanding the problem (The problem), the block of study experience predecessors (The experience), the block of presentation ways to resolve the problem, its proof and argumentation (The decision), the block of the data generalization and summarization (The total) [2]. The sequence corresponds to the transfer of their compositional arrangement of these sequence blocks in the scientific text. Term-set of the linguistic variable "CHARACTERISTIC SIGNS OF BLOCK" can be represented by the following fuzzy variables *"indicates a block of 'The problem'"*, *"indicates a block of 'The experience'"*, *"indicates a block of 'The decision'"*, *"indicates a block of 'The total'"*.

To define the fuzzy sets method for determining membership functions with a standard set of graphs used. It is obvious that for a definition of fuzzy sets *"at the beginning of the text"* and *"indicates a block of 'The problem'"* it is necessary to use Z–figurative function of accessory. For a definition of fuzzy sets *"at the end of the text"* and *"indicates a block of 'The total'"* S–figurative function of accessory is necessary. For a definition of fuzzy sets *"not at the beginning of the text, but not in the middle"*, *"in the middle of the text"*, *"not at the end of the text, but not in the middle"*, *"indicates a block of 'The experience'"* and *"indicates a block of 'The decision'"* it is possible to use bell-shaped function of accessory. We will set all parameters of accessory functions on the basis of an expert assessment and then experimentally to check.

For realization of fuzzy inference it is necessary to make rule set. We will accept that degree of confidence of the validity of the received subconclusion of each rule will be identical and equal by default 1. The rule set includes such rules as:

- 1) If term is "at the beginning of the text" AND the marker is "indicates a block of "The problem" THEN the semantic context-block is "The problem";
- 2) If term is "not at the beginning of the text, but not in the middle" AND marker is "indicates a block of "The experience" THEN the semantic context-block is "The experience";
- 3) If term is "in the middle of the text" OR "not at the end of the text, but not in the middle" AND marker "indicates a block of "The decision" THEN the semantic context-block is "The decision";
- 4) If term is "at the end of the text" AND marker is "indicates a block of "The total" THEN semantic context-block is "The total".

Consequents of rules are set by obviously accurate values. Therefore we will be based on application of the simplified algorithm of fuzzy inference. Thus, using the fuzzy controller is described, it will be possible to determine which block belongs analyzed the term or the relation.

Discussion and conclusions. For carrying out computing experiments the fuzzy controller was realized. Schemes of system architecture of building of a semantic network of the scientific text and the developed fuzzy controller are given in figure 1. In the system of building of a semantic network the following modules are obviously designated: module of management of database of formal text signs of, module of terms/relations extraction, module of calculation of weight coefficients. Except them in system there are still other modules which in this context aren't considered. In figure 1 it is possible to judge existence of such modules on dots and the module with number n .

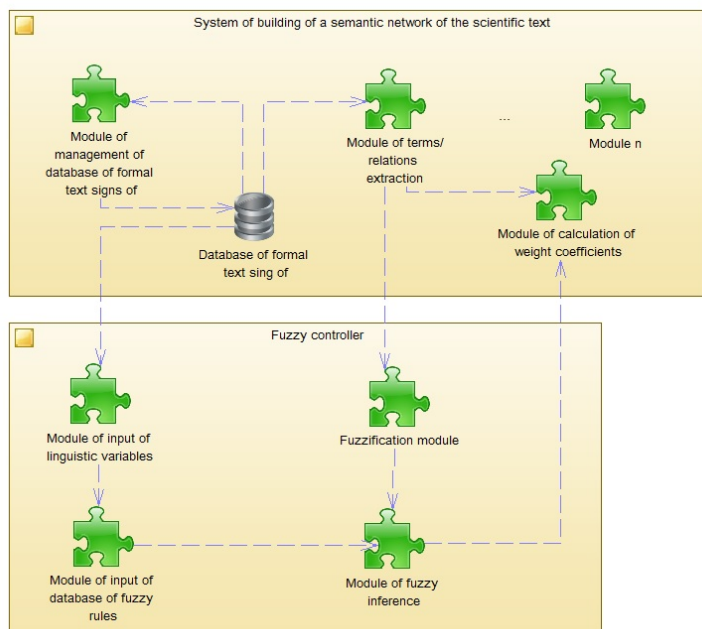


Figure 1 – Interaction of system of building of a semantic network of the scientific text and fuzzy controller

The module of terms/relations extraction is one of the main components of system of building of a semantic network. It finds terms and the relations, and also defines formal text signs of which meet in the text. From this module information about the term or the relation in

the text, namely a place and a formal sign of which met in one offer or the paragraph with the term or the relation arrives on the fuzzification module. The database of formal text signs of which can be supplemented, specified, reduced is conducted in system. The module of input of linguistic variables addresses to this database when the terms of the linguistic variable "CHARACTERISTIC SIGNS OF BLOCK" creates.

The module of input of database of fuzzy rules allows to create new rules, to edit the entered rules, addressing to the module of input of linguistic variables. The module of fuzzy inference, having obtained entrance data from the fuzzification module, calculates value of the output variable "SEMANTIC CONTEXT-BLOCK" which arrives in the module of calculation of weight coefficients of terms and the relations of the scientific text. Results of experiments on definition of the semantic context-block of the terms allocated in the investigated text are given in the table.

Table – The results of the fuzzy controller

№	Term	Place in the text	Formal text sing of	Semantic context-block
1	2	3	4	5
1	"razlichnyi sposob predstavleniya" (different ways of presenting)	1,665345	"v stat'e" (in article)	The problem
2	"soderzhanie vyskazyvaniy" (propositional content)	1,823949	"v stat'e" (in article)	The problem
3	"estestvennyi yazyk" (natural language)	1,982553	"v stat'e" (in article)	The problem
4	"pomoshch' semanticheskikh setei" (help of semantic networks)	2,141158	"v stat'e" (in article)	The problem

Continued Table

1	2	3	4	5
5	"arkhitektura sistemy sneps" (system architecture sneps)	43,61618	"v rezul'tate" (as a result)	The total
6	"postroenie semanticheskoi seti" (building a semantic network)	43,85408	"v rezul'tate" (as a result)	The total
7	"znanie" (knowledge)	44,09199	"v rezul'tate" (as a result)	The total
8	"razlichnyi istochnik" (various sources)	44,2506	"v rezul'tate" (as a result)	The total
9	"vopros" (question)	45,83664	"v rabote" (in this paper)	The experience
10	"mekhanizm" (mechanism)	47,10547	"v rabote" (in this paper)	The experience
11	"kontseptual'nyi graf" (conceptual graph)	47,18477	"v rabote" (in this paper)	The experience
12	"sovremennoe opisanie sostoyaniya" (modern description of the state)	47,58128	"v rabote" (in this paper)	The experience
13	"formalizm kontseptual'nykh grafov" (formalism of conceptual graphs)	47,81919	"v rabote" (in this paper)	The experience
	...			

From the table we see that the first four terms are located in the beginning the text. To it point small values of the Place in the Text parameter. These terms are a part of one sentence. In the same sentence the indicator "*v stat'e*" (*in article*) which is indicated the block by the Problem met. The value of the output variable "SEMANTIC CONTEXT-BLOCK", meaning that these terms meet in the Problem block, is true. For terms 5-8 the semantic context-block is defined not absolutely truly. We see that the terms met in the first half of the text and therefore can not be placed in block "*The total*", which should compositionally complete scientific text. As a whole the received results are accepted, but rather big percent of mistakenly identified blocks (about 40%) demands completion of fuzzy rules and algorithms of definition of the next formal text signs of.

Thus, the method of identifying of semantic context-block offered in this work can be applied to calculation of weight coefficients at building of a semantic network of the scientific text. For improvement of results of a method in the long term it is necessary to expand database of fuzzy rules and to analyze the formal text signs of which have met not only in one offer the term or the relation, but also in the environment next to them.

References

1. Ayusheeva N.N. Razvitie sposoba vychisleniya vesovykh koeffitsientov vershin semanticheskoi seti nauchnogo teksta / N.N. Ayusheeva, T.N. Kusheeva // Teoreticheskie i prikladnye voprosy sovremennykh informatsionnykh tekhnologii: Materialy XI Vseros. nauch.-prak. konf. – Ulan-Ude: Izd-vo VSGUTU, 2012.
2. Ayusheeva N.N. Sposob rascheta vesovykh koeffitsientov dug semanticheskoi seti nauchnogo teksta / N.N. Ayusheeva, T.N. Kusheeva // Global'nyi nauchnyi potentsial. – №7(28). – 2013. – С. 51-55.
3. Blyumenau D.I. Informatsionnyi analiz/sintez dlya formirovaniya vtorichnogo potoka dokumentov / D.I. Blyumenau. – SPb.: Professiya, 2002. – S. 110-166.

THE DETERMINATION OF AMg6 ALLOY SUPERPLASTIC CHARACTERISTICS BASED ON THE FREE BULGING TEST

Zakhariev I. Yu.

Moscow, MIEM NRU HSE

The main aim of the present work is to get the first approximation of AMg6 alloy superplastic characteristics. In this study, constant pressure free bulging for superplastic material is analyzed by some simple analytical methods to determine the constants of the superplastic AMg6 alloy.

Keywords: mathematical modeling, free bulging, superplasticity, aluminum

This work is devoted to the mechanical properties determination of the aluminum alloy AMg6 using its superplastic properties. These properties based on the data of hot superplastic forming process.

Gas Superplastic forming allows producing the complex shape goods with a single operation. The development of pressure regimes of superplastic forming is a complex challenge, which requires mathematical and computer modeling to meet the requirements for mechanical properties of the forming material products obtain [1].

AMg6 alloy is used in the aerospace industry especially for fuel tanks fabrication; it is also used in the manufacture of frames and bodies of railway wagons, ships bulkheads, in the automotive and chemical industries. The mechanical properties of superplastic materials may

be characterize by using high-speed sensitivity of the equivalent stress to the strain rate, which manifests itself when forming in narrow speed ranges depending on the temperature of forming. For determination of the material mechanical properties and identification of superplasticity ranges, it is necessary to conduct a series of mechanical experiments of hot forming [2].

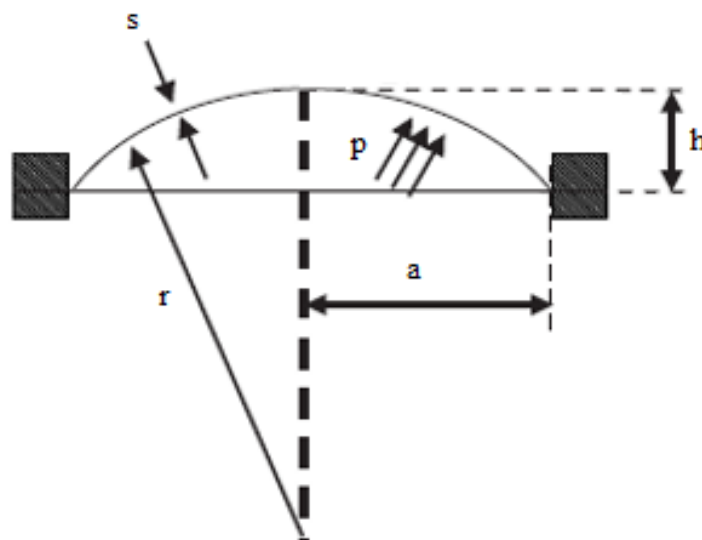


Fig. 1. The forming process scheme

All necessary parameters of superplastic material can be define by biaxial stretching. However, further computer modeling the implementation of these data requires further clarification. Figure 1. illustrates a diagram of a biaxial stretching test, which is a free dome forming at a given pressure regime. Interpretation of the results of such tests is a challenging task that should be done step by step, using the simulation of the forming process to improve the model of the mechanical properties. The first approximation of the mechanical properties can be obtained by using methods described in the literature.

The first approximation of the mechanical properties of the AMg6 alloy based on the gas forming test results with constant pressure was received. The carried out Tests for different values of pressure and time in Irkutsk Technical University [3].

As the initial data were obtained: the pressure acting on the workpiece, the initial thickness of the workpiece, the radius of working area, the temperature on the upper and lower tooling and height depending on the thickness on the dome apex shown in Figure 2.

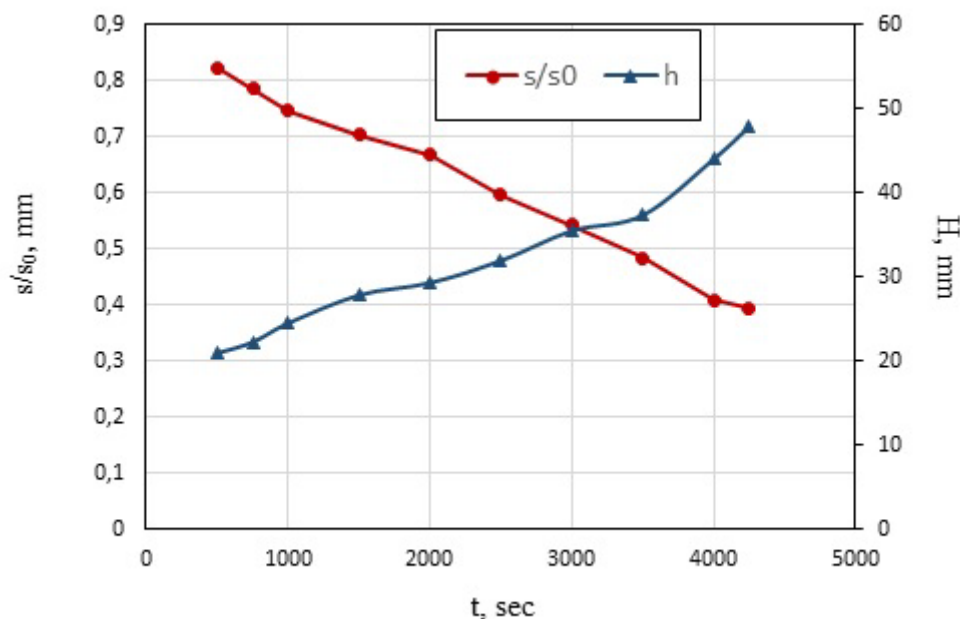


Fig. 2. The dependence of the thickness and height of the dome on the time

For determining the experimental dependence of the equivalent stress of equivalent strain rate and equivalent strain, the following formulas were used [4]:

$$r = \frac{a^2 + h^2}{2h} \quad 1.$$

$$\sigma = \frac{pr}{2s} \quad 2.$$

$$\varepsilon = \ln \left(\frac{s_0}{s} \right) \quad 3.$$

$$\dot{\varepsilon}(t) = \frac{\varepsilon(t + \Delta t) - \varepsilon(t - \Delta t)}{2\Delta t} \quad 4.$$

where p is the internal pressure, s_0 and s are the initial and current thickness at the dome apex, a is the radius of working area, r is the radius of the dome and h is the height of the dome.

Further analysis was carried out using a reverse method of Nelder – Mead. The most common equation describing the rheological behavior of polycrystalline superplastic materials is the Bekofen equation [5, 6]:

$$\sigma = K \dot{\varepsilon}^m \quad 5.$$

where K is the strength coefficient, n is the hardening index and m is the strain rate sensitivity index. However, due to lack of data on the microstructure of the alloy as the equation of state was chosen the Smirnov equation adding hardening function [7, 8, 9].

$$\sigma_0 = \bar{\sigma}_s \frac{\bar{\sigma}_0 + k \dot{\varepsilon}^{m_v}}{\bar{\sigma}_s + k \dot{\varepsilon}^{m_v}} \quad 6.$$

$$\sigma = \sigma_0 + H \varepsilon \quad 7.$$

Where $\bar{\sigma}_0$ is the threshold voltage below which the metal does not flow, $\bar{\sigma}_s$ is the yield strength, k , m_v are the parameters characterizing the material viscosity and remaining constant over a wide range of strain rates, H is the hardening function.

Thus, a preliminary model for the mechanical properties of AMg6 alloy for a temperature range 400 - 430 °C was constructed, and process conditions identified for further experimental studies. Figure 3 shows a comparison of experimental and simulated equivalent stress dependency on the strain rate for various values of the strain.

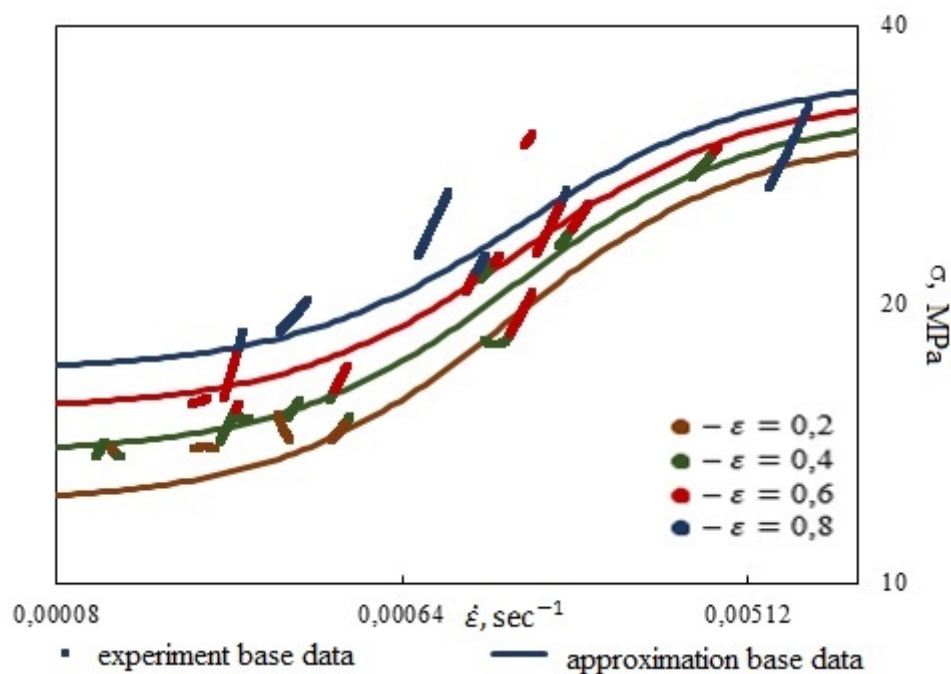


Fig. 3. Depending of the equivalent stress on the strain rate

The interval of the superplasticity can be received by using rate sensitivity coefficient. Rate sensitivity coefficient can be find by applying equation.

$$m(\dot{\varepsilon}) = \frac{d \ln(\sigma)}{d \ln(\dot{\varepsilon})} = \frac{m_v k_v \dot{\varepsilon}^{m_v} (\sigma_s - \sigma_0)}{(\sigma_0 + k_v \dot{\varepsilon}^{m_v})(\sigma_s + k_v \dot{\varepsilon}^{m_v})(\sigma_s + H)} \quad 8.$$

Rate sensitivity coefficient is shown on Figure 4, thus alloys closest interval to the superplasticity is obtained when $\dot{\varepsilon} = 0,7 \cdot 10^{-3} \div 0,2 \cdot 10^{-2} \text{ s}^{-1}$.

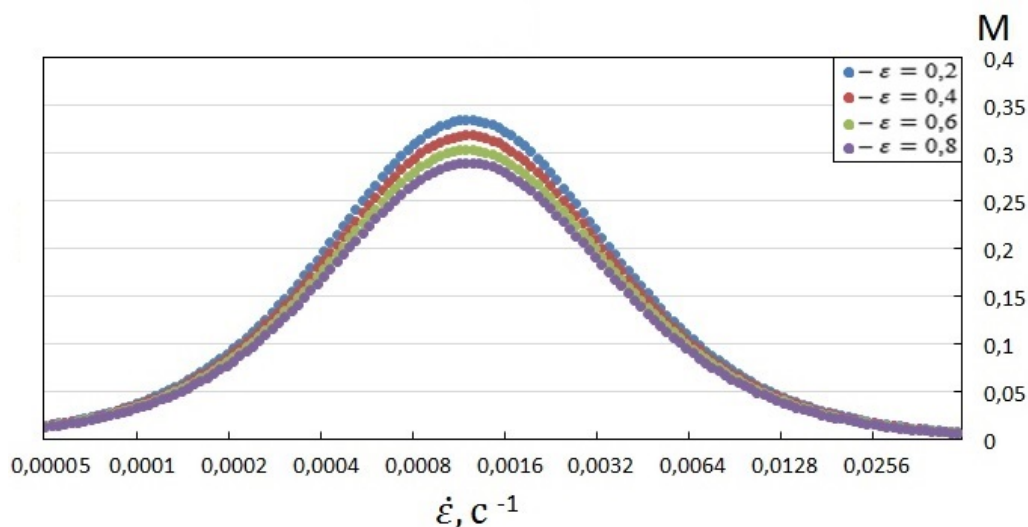


Fig. 4. Rate sensitivity coefficient

Figure 5 shows the correlation coefficient between the experimental and the obtained values of the equivalent stress:

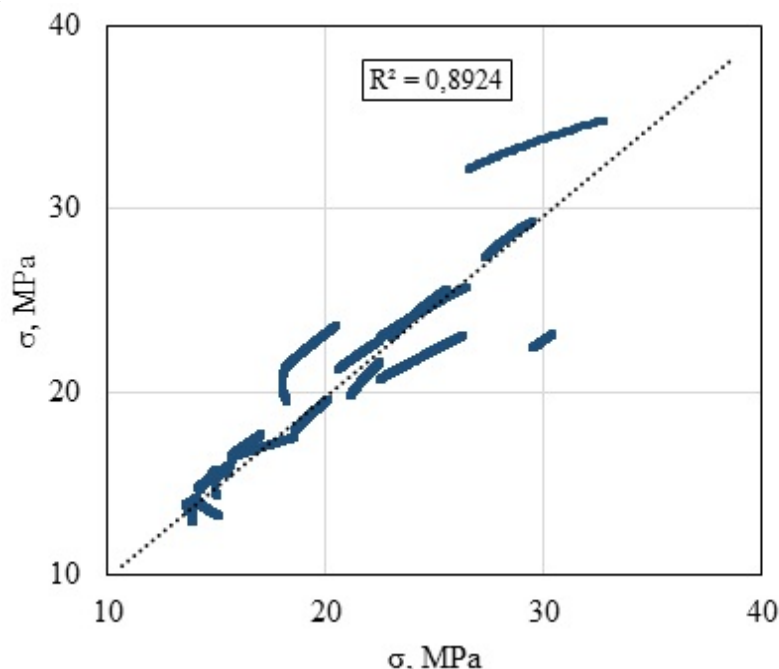


Fig. 5. Correlation between the experimental and the obtained values of the equivalent stress

The results will be used in future work, the purpose of which is to refine the estimate obtained using simulations and the construction of an adequate model of the mechanical properties of the alloy under superplastic conditions. This will allow further develop and test a methodology interpreting the results of mechanical tests on the biaxial tensile strain in hot conditions.

References

1. Sverchplastichnost': materialy, teoriya, technologii E.N. Chumachenko, O.M. Smirnov, M.A. Tsepin, Moscow "Librokom" publishing house, 2009. – 320.
2. J. Kliber, S. A. Aksenov, R. Fabik, Numerical study of deformation characteristics in PSCT volume certified following microstructure, Metalurgija, Vol. 4(2009), pp. 257-262.
3. A.K. Shmakov, V. Mironenko, K.K. Kirishina, A.S. Stanislavchik, V.V. Kotov, Effect of the average velocity of the free part of the semifinished product on the process of pneumothermal forming in the superplastic regime, Metallurgist 57 (1-2), 2013, pp. 8-12.
4. G. Giuliano, S. Franchitti, On the evaluation of superplastic characteristics using the finite element method, International Journal of Machine Tools & Manufacture 47 (2007) 471-476.
5. G. Giuliano, Constitutive equation for superplastic Ti-6Al-4V alloy, Materials & Design, 2008, Vol. 29, 7, 1330-1333.
6. Bakofen W., Turner I., Avery D., Superplasticity in an Al-Zn alloy, Trans ASM, 1964, v.57, p.980-990.
7. O.M. Smirnov, Obrabotka metalov davlenijem v sostoyanii sverchplastichnosti, Moscow, Mashinostrojenie, 1979. 184.

8. A.K. Ghosh and C.H. Hamilton, Influences of material parameters and microstructure on superplastic forming, Metallurgical and Materials Transactions A Vol 13 Number 5, May 1982 733-743.

9. S.A. Aksenov, E.N. Chumachenko, I.V. Logashina, Tensile testing of TI-AL-V alloy superplasticity, Materials Science forum, T. 762. C. 392-397.

MODELING THE INTRODUCTION OF MECHANICAL INFLUENCES IN THE DESIGN OF RADIO-ELECTRONIC FACILITIES

Zatylnik A.V., Tankov G.V., Golushko D.A.
Penza State University, Russia

The mathematical model of occurrence and development of mechanical tension in rod designs of radio-electronic facilities (REF) is offered in this article. The idea is finished to program realization.

Keywords: vibration, amplitude, mechanical oscillations, bar.

Products of the modern radio-electronic industry concern to complex high technology products of which are made great demands [1-4].

Application of methods of mathematical modelling enables to carry out researches of physical processes progressing in designs of REF, to determine their dynamic characteristics. It is a basis for prognostication behavior of a product in the set conditions of operation.

Therefore, development of the software capable to spend the analysis of peak-frequency characteristics of a researched design is an actual problem.

Bar designs can make various fluctuations. For definition of amplitudes, mechanical tension in elements of rod designs we shall consider the equation of their movement at the forced fluctuations [5, 6.]. Bend fluctuations in a bar are described by next equation:

$$EJ \frac{\partial^4 \varpi}{\partial x^4} + \rho S \frac{\partial^2 \varpi}{\partial t^2} = 0, \quad (1)$$

where $\varpi(x, t)$ – displacement of bar points perpendicularly elastic axis; E – module of Jung; J – the moment of inertia of section relative to the axis of a perpendicular plane of a bend; ρ – density of a material: S – the area of a bar cross-section.

Having marked rigidity of a bar bend as $C_s = EJ$ we shall consider losses of energy at fluctuations in the form of the force proportional to speed of deformation [2]. In the right part of the equation we shall add external force $F(x, t)$, exciting fluctuations and applied in fastening points. Then the equation of the forced fluctuations of a bar bend will look as follows:

$$C_s \frac{\partial^4 \varpi}{\partial x^4} + \eta \frac{\partial}{\partial t} C_s \frac{\partial^4 \varpi}{\partial x^4} + \rho S \frac{\partial^2 \varpi}{\partial t^2} = F(x, t), \quad (2)$$

where η – coefficient of material viscosity.

According to a method of finite differences we shall replace a continuous bar with set of discrete elements with step of splitting on an axis x , equal h_x . Weight of each discrete element we shall concentrate in its center - the unit laying on an axis x . Forces of interaction between discrete elements it is replaced by elastic connections between units. We shall receive the geometrical discrete model of a bar consisting from n of units, connected by elastic connections.

Having replaced the first derivative on time in the left part of the equation (2) its difference analogue, and believing, that $L(\omega) = \frac{\partial^4 \varpi}{\partial x^4}$ we shall write down it in the form of:

$$C_s L(\varpi)_t + \frac{\eta}{\tau} [C_s L(\varpi)_t - C_s L(\varpi)_{t-\tau}] = -\rho S \frac{\partial^2 \varpi}{\partial t^2}, \quad (3)$$

Where τ - the step of time sampling, and force $F(x, t)$ is considered in entry conditions.

Having removed the brackets and having grouped similar members (3), we shall receive:

$$-\left[\frac{(1 + \frac{\eta}{\tau}) C_s}{\rho S} L(\varpi)_t - \frac{\eta C_s}{\rho S} L(\varpi)_{t-\tau} \right] = \frac{\partial^2 \varpi}{\partial t^2}, \quad (4)$$

Considering, that the second derivative of moving on time is acceleration a of unit, we shall write down the equation (4) in the form of $a = \frac{\partial^2 \varpi}{\partial t^2}$. Then having replaced the second derivative on time a difference analogue, we shall receive:

$$-\tau^2 a = \varpi_x(t + \tau) - 2\varpi_x(t) + \varpi_x(t - \tau).$$

Let's transform the equation (4) to a kind of the obvious difference equation:

$$-\tau^2 a + 2\varpi_x(t) - \varpi_x(t - \tau) = \varpi_x(t + \tau),$$

Which, being is added boundary and entry conditions, forms an obvious difference the scheme. It in a combination to geometrical model gives the settlement model of a core simply enough sold on the computer. The interface of the developed program is shown in figure 1.

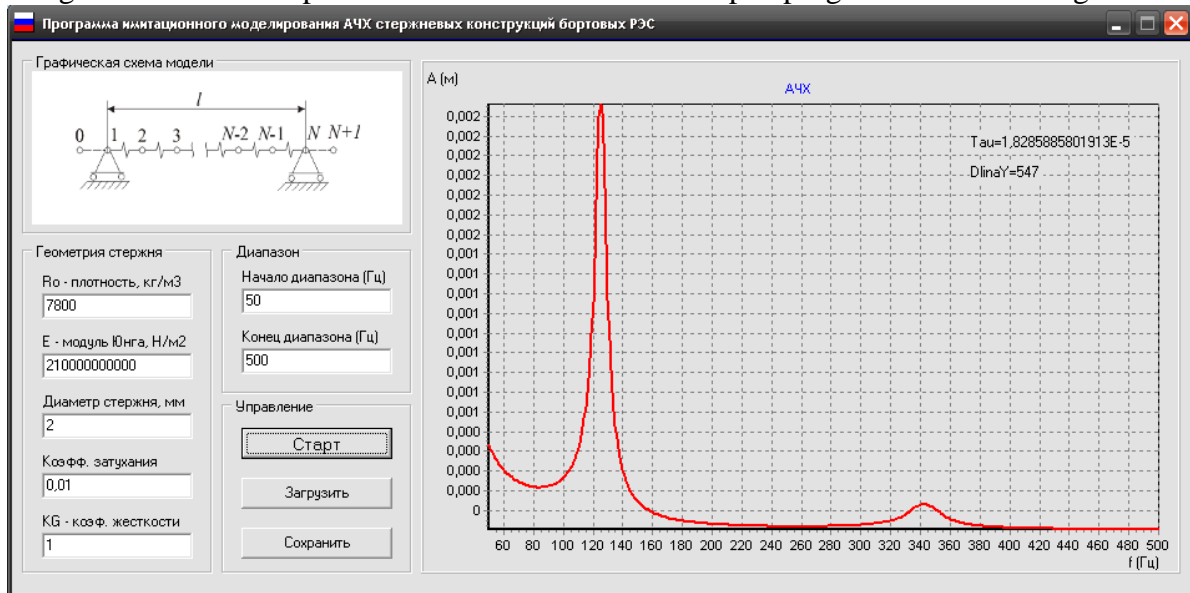


Figure 1 – Interface of the program of imitating modeling peak-frequency characteristics designs onboard REF

The structure of the program allows the user to enter data necessary for carrying out of calculations, to see results and to keep them in a file.

The basic program contains the list of all used modules and some the executed operators providing creation of the necessary windows and connection of the program with

Windows. The code of procedures and functions settles down in an executed part of the module which can be hidden from the user.

Thus, the developed program of imitating modelling of bar peak-frequency characteristics designs onboard REF will be useful for REF engineers-designers and as can be recommended to application in educational process [7-9] in technical colleges.

References

- 1 Zatylnkin, A.V. Algoritm provedeniya proektnykh issledovaniy radiotekhnicheskikh ustroystv opytno-teoreticheskim metodom / A.V. Zatylnkin, I.I. Kochegarov, N.K. Yurkov // *Nadezhnost' i kachestvo: tr. Mezhdunar. simp. Tom 1 / pod red. N. K. Yurkova.* – Penza : Izd-vo Penz. gos. un-ta, 2012. – S. 365-366.
- 2 Bannov, V.Ya. Avtomatizirovannyi stend issledovaniya procedury formirovaniya testovogo vozdeystviya pri provedenii diagnostiki logicheskikh shem elektronnykh ustroystv / V.Ya. Bannov, E.V. Saprova // *Nadezhnost' i kachestvo: tr. Mezhdunar. simp. Tom 1 / pod red. N. K. Yurkova.* – Penza : Izd-vo Penz. gos. un-ta, 2011. – S. 32-34.
- 3 Nedorezov, V.B. Avtomatizatsiya proizvodstvennykh processov izgotovleniya radioelektronnykh sredstv: ucheb. posobie / V.G. Nedorezov. – Penza : Izd-vo PGU, 2012. – 120 s.
- 4 Olhov, D.V. Sistema obrabotki yeksperimental'noy informatsii v proektnykh issledovaniyakh radiotekhnicheskikh ustroystv / D.V. Olhov, // *Izvestiya YUFU. Tekhnicheskie nauki.* – 2012. № 5. – S. 94-99.
- 5 Tankov, G.V. Modelirovaniye izgibnykh kolebaniy v sterzhnevyykh konstruktsiyakh RES / G.V. Tankov, // *Nadezhnost' i kachestvo: Trudy mezhdunarodnogo simpoziuma / Pod red. N.K. Yurkova* – Penza: IIC PGU, 2006, s. 320-323.
- 6 Leonov, A.G. Upravleniye issledovaniyami modeley radiotekhnicheskikh ustroystv na etape proektirovaniya / A.G. Leonov, N.K. Yurkov // *Prikaspiyskiy zhurnal: upravleniye i vysokie tekhnologii: nauchno-tekhnicheskiy zhurnal - Astrahan': Izdatel'skiy dom «Astrahanskiy universitet», 2012. – № 1(17). – S. 138-142.*
- 7 Almametov, V.B. Innovatsii v obrazovatel'nykh uchrezhdeniyakh i interaktivnyye programmy obucheniya / V.B. Almametov // *Nadezhnost' i kachestvo: tr. Mezhdunar. simp. Tom 1 / pod red. N. K. Yurkova.* – Penza : Izd-vo Penz. gos. un-ta, 2011. – S. 340-344.
- 8 Laboratornyy kompleks v arkhitekture IKOS kak osnova formirovaniya umeniy / I.D. Grab, N.V. Goryachev, V.B. Almametov, V.Ya. Bannov // *Nadezhnost' i kachestvo: Trudy mezhdunarodnogo simpoziuma. Tom 1: / Pod red. N.K. Yurkova* – Penza: Izd-vo Penz. gos. un-ta, 2008, s. 213-215.
- 9 Zatylnkin, A.V. Metod svyazannykh sistem v modelirovanii processa obucheniya / A.V. Zatylnkin, I.I. Kochegarov // *Izvestiya vysshikh uchebnykh zavedeniy. Povolzhskiy region. Tekhnicheskie nauki.* – 2010. № 4 (9). – S. 56-61.

INTELLIGENT SYSTEM “OBJECT-MODEL-APPLICATION RESULT”

Gubarev V.V., Abalov N.V., Bulgakova N.V., Gorodov E.Y., Kuragin A.V., Melnikov G.A.,
Terehov R.V., Fedorov E.I.
Novosibirsk, NSTU

The main idea outlined in this paper is to describe intelligent consulting system structure and principles, which is oriented to provide aid for researchers in data and knowledge collecting and processing about investigated object, which are applied in

conditions of different kind of vagueness met on each stage of research from task definition stage to result application stage.

Keywords: data, knowledge, models, methods, algorithms, measurement, processing, analysis.

Not only in study, but also in practice, there is a situation, when the expert in one of subject area has to solve the tasks from other subject area, where he hasn't enough competence. In this case, he has to ask an expert from other subject area, who usually isn't competent in subject area of first expert. So there is a need for a cooperative work of both experts from different subject areas, which isn't always applicable because of weak connection of expert competences in solved task. The situation can become even worse, if first experts (from now and on – “Customer”) isn't able to provide a task description in terms and form of second expert (from now and on “Implementer”) from other subject area. Those cases can't be resolved without iterative procedure of cooperative task definition by the “Customer” and way of solving definition by “Implementer”. Those cases are common for situations, when “Customer” task assumes knowledge mining, data regularity search and other subtasks solution for “Customer” object investigation (such as researching, designing, describing, controlling, ...) by mixed Data relative to object. By Data we mean conjunction of signals, data or knowledge in case of information carriers. So, the “Implementer” is an different nature object modeler expert in different aspects of its functionality and Data collection and manipulations, required to achieve aims, provided by “Customer”.

Those situations are met more and more often last years. It promotes from following facts:

1. Measurement and computing techniques enhancement;
2. Techniques application in fields, where there were no formal accurate methods, or its application were limited;
3. “Customers” dissatisfaction about current results of their task solutions;
4. Big Data problem appearance.

The main aim of that paper is to expose the ideas and provide the description of interactive intelligent system, which can assist the “Customer” and the “Implementer” in solving the application task, provided by “Customer” through all stages of technological process in dialog mode, with aid of object Data collection, detection, interpretation and application of empirical knowledge, in particular regularity contained in that Data. Specifically, it allows to cooperatively move through the chain of operations in process of “Customer” task solution – from its formal verbal definition, clarification to results acquirement and interpretation of concrete results of initially poorly defined task description. It also must be mentioned, that we have to take into account concrete manifestation of both investigated object and conditions, that are applied in reality while task solution, in task definition.

This paper contains functions, applied by each system block, implemental editions of each block, the main examples for models storage, methods storage and algorithms storage constructions and “Customer” – “Implementer” interaction procedures in dialog mode.

2. System Structure

In order to achieve the mentioned aim, the system approach is used by authors. In particular the development and functionality of “Object-Model-Application result” (OMAR) is considered from three aspects: OMAR, as one unit; by each consistent part; and as an part of supersystem, that includes environment with investigated object and conditions for its operating, field of application, user qualification, technological process of object investigation and collected data and knowledge and so one. Integrated scheme is provided on Fig. 1.

OMAR includes blocks, which can be optional for some cases. For example, if the “Customer” provides initial formalized task description, there is no need for block 1. If the empirical data is already acquired, the block 4 will not be used. If all data is represented in one scale, there is no need for calling block 11 and so one.

Blocks from 1st to 9th are oriented to corresponding stages tasks solution. Let's consider main features of technological process for application task solution blocs, including all operations for task definition and step-by-step result acquirement, expected by “Customer”. We'll describe it complexly by example of statistical methods application and Data analysis in condition of need for providing the required level of results qualities in out gate of 8th stage of technological process.

Purpose of first block is obvious. “Implementer” and “Customer” clarifies the verbal task definition for investigated object, using that block.

Later, with help of blocks 2, 9-16, “Implementer” provides task definition formalization, including following operations:

1. Class definition, which investigated object refers to (by its mathematical representation);
2. A priory data acquirement;
3. Measurement scales definition, data models and knowledge, which were used by investigated object Data acquirement, or which will be used by Data mining;
4. Data acquirement possibilities research in passive (observation) or active experiment;
5. Model class definition;
6. Measurement plan composition, underling object features, which are to be measured and measurement algorithms and its transformation into counting signals and also its features and parameters;
7. Experiment planning (block 3), organization and its execution (block 4);
8. Provisional processing and initial (experimental, selected) data transformation, including exploration analysis and execution operations, which allows to convert initial data to the form for further result acquirement by selected algorithms with the best or required quality.
9. Required features and/or its parameters measurement operation execution over corrected data (block 6), including provided selection sectioning operations, provided by algorithms, evaluation shifts or shifts compensations, robust evaluation, randomization, dynamical functions arguments changes, and so one (for example, see [1]);
10. After evaluation transform operation and evaluation processing as operands for indirect measurements for quality enhancement, its control, including filtration, evaluation smoothing, its combinations and so one [1]. If the initial data is provided by “Customer”, corresponding operations are not executed. Those operations executions are carried by using blocks 13-16.

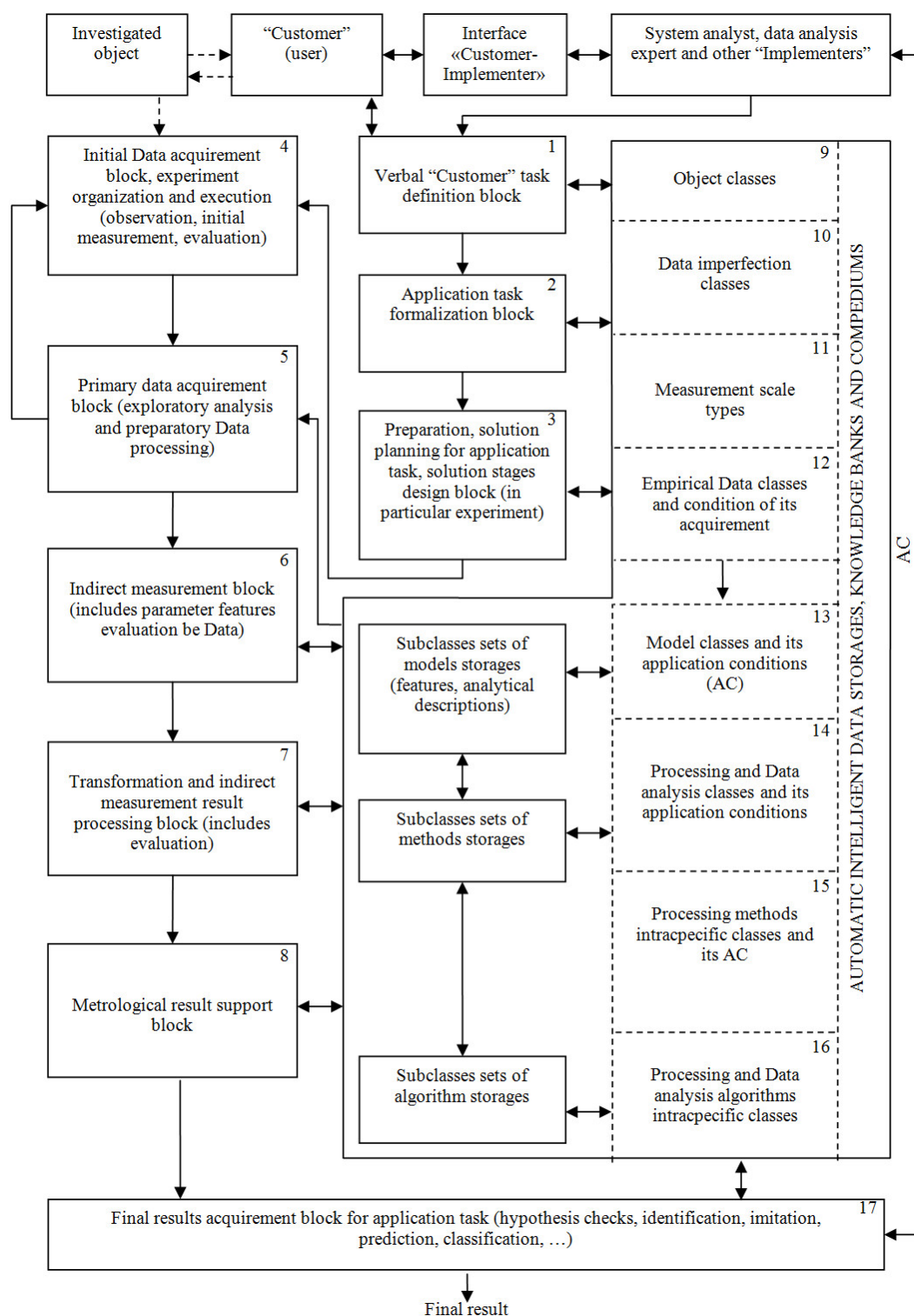


Figure 1. Integrated block-scheme of OMAR system

3. System Blocks Implementation Aspects

Developed OMAR system, by its nature, provides functions of intelligent consulting system for every user, including "Implementer" and "Customer", and with aid from "Implementer", it can be said, that it is dialog system of preparation and decision making. Because of that, main blocks are based on methods and resources of artificial intelligence. In particular, blocks 9-16 are performed in form of expert subsystems, which integrated scheme

is provided on Fig. 2. The purpose and principles of elements composition on scheme Fig. 2, basically, corresponds to the one, described in theory of expert systems (for example, see [2]).

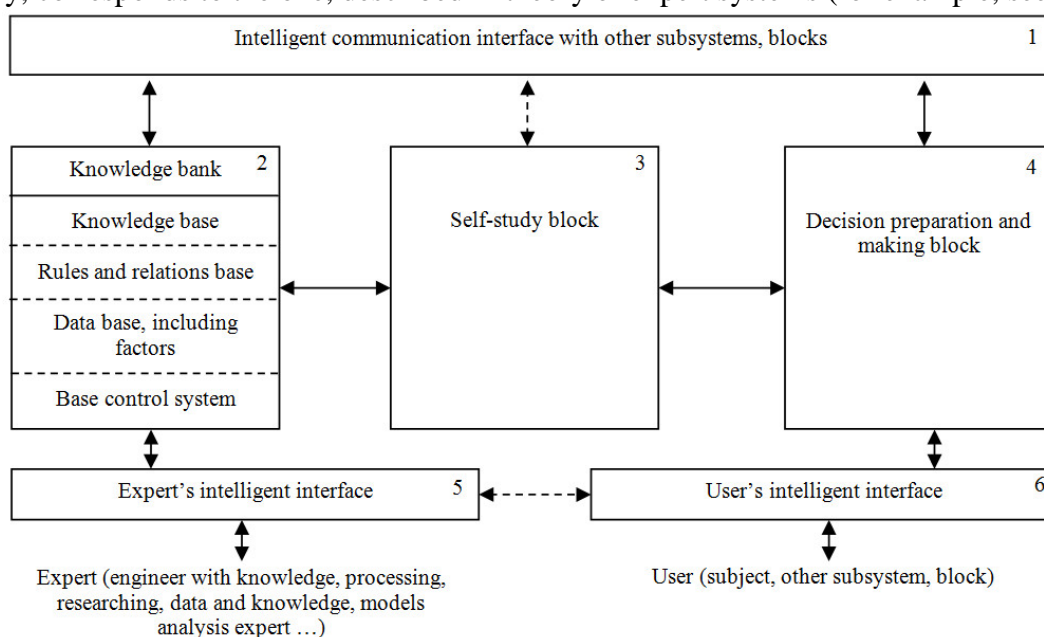


Figure 2. Integrated scheme of expert subsystem as a part of OMAR

For object classes, measurement scales, models, methods and algorithms selection automation, its subset are formed into storages, in particular models storage, methods storage and algorithms storage. Let's recall, that under the term models storage we understand the ordered set of models, satisfying requirements of simplicity, fullness, minimal redundancy, description and investigation levels in application for concrete subject area [1,3]. Points on construction, features description and models storage applicability are fully described in [1, 3, 4]. The terms methods storage and algorithms storage [for example, see [5, 6)] are introduced by analogy with models storage. We should highlight the following two features of models, methods and algorithm storages in that paper – on one hand, description and investigation level and, possibility of set existence from storage on the other.

The first feature is connected with the fact that description and investigation level of storable elements (models, methods, algorithms, ...) into storages must be enough, but with minimum redundancy for solution of most task, provided by users interactions. In particular, elements of storage must be followed by examples of different task solutions, which uses those elements, and also with its advantages and disadvantages in application to those tasks and with respect to relation with other similar elements. The storages, by itself, must include examples of the best models, methods, algorithms for different task solutions in different conditions, and examples of its metrological support, and also examples of data imitation algorithms, similar to initial and or corresponding to concrete models.

The second feature refers to the need of solution for the following situation: according to requirements of elements simplicity, fullness and minimal redundancy into the storage on the one hand, there must be enough elements to solve the required user task in specified subject area, using only elements from storage. And on the other hand, number of those elements hasn't to be redundant, which allows to lower the time cost, exclude unexplainable element duplicates from the same storage and so one. This situation solution is end up into following options. At first, multiple storages creation, consist of equal by difficulty nonrecurring elements, different in aspects of construction "mechanisms" and investigated objects functionality and its existence and/or research conditions. Such storages can accept different options of modeling results interpretation for investigation and results of objects

cognition. Second, we can use two step modeling procedure for object investigation. This means, that on the first stage, we select one storage from the predefined set of storages, and on the second stage, the search of appropriate element (model, method, algorithm) takes place. This situation, for example, takes place when empirical distributions are divided by typical model of probability distribution [1, 3, 4]. The main theoretical aspects of distribution models storage with different options of model ordering and its filling are described in [1, 3, 4]. Some aspects of data analysis methods selection automation are considered in [6]. The authors are developing software and informational provision of that system.

Conclusion

As a conclusion, there is a list of two primary tasks, which need to be solved for OMAR system creation:

1. Application tasks systematization and comparative study from the point of identification of object models and Data, methods, Data analysis and processing algorithm, measurement scales, typical conditions of object functioning and experimenting, used in those tasks. This point is critical for blocs 9-16, taking into account operations, executed in blocks 1-8.
2. Classes, subclasses types and models families, methods and its implementing algorithms for Data analysis and processing classification, model, method and algorithms storages composition and its set for different application tasks (block 13-16).

References

1. Gubarev V.V. Algoritmy spektral'nogo analiza sluchainykh signalov / V.V. Gubarev – Novosibirsk, izd-vo NGTU, 2005. – 660 s.
2. Smolin D.V. Vvedenie v iskusstvennyi intellekt: konspekt lektsii / D.V. Smolin – M.: FIZMATLIT, 2007. – 264 s.
3. Gubarev V.V. Veroyatnostnye modeli: spravochnik v 2-kh chastyakh / V.V. Gubarev – Novosibirsk: NETI, 1992. – Ch.1. – 196 s.; Ch.2. – S.197-421.
4. Gubarev V.V. Avtomatizatsiya analiticheskogo opisaniya empiricheskikh raspredelenii / V.V. Gubarev // N.: Izmeritel'naya tekhnika, 2012. - №5. – S.13-18.
5. Gubarev V.V. Automation of analytic descriptions of empirical distributions / V.V. Gubarev // Measurement Techniques, 2012. - V.55. - №5–P.506-513.
6. Gubarev V.V. Osnovnye opredeleniya termina «Bol'shie dannye» / V.V. Gubarev, E.I. Fedorov // Estestvennye i tekhnicheskie nauki, 2013. - №2. – S. 235-242.
7. Gubarev V.V. Avtomatizatsiya vybora metodov analiza empiricheskikh dannykh / V.V. Gubarev, E.I. Fedorov, N.V. Bulgakova // Informatsionnye i telekommunikatsionnye tekhnologii, 2013. - №19. - S. 29-34.

PARKING SYSTEM OF HIGH RELIABILITY

Dianov V.N., Gevondian T.A.
Moscow State Industrial University. Moscow

The questions of the safety of vehicles in the parking lot. To improve the reliability of equipment proposed to use differential and integral sensors failures. The system can be used in navigation, in particular when driving to prevent its collision with other vehicles or fixed obstacles when maneuvering and setting the parking lot.

Recently, due to a sharp increase in road transport , primarily cars, parking problem escalated [1]. In this regard , is an urgent task of increasing the life of the parking system and,

as a consequence, components and units of the car, as well as reducing failures and failures in its work .

The effect of increasing the reliability of the parking system is proposed to achieve by introducing into it various kinds of contact and non-contact sensors , including differential and integral that detect and eliminate sources of failures with respect to time of their lives. At the same time as informative parameters used changes of amplitude- frequency characteristics , increased electromagnetic radiation , the appearance of the effect of differentiation and integration of signals. [2] .

Existing technical solutions, in particular contained in Parktronic <http://www.tpmaster.ru> [1] , have a significant drawback device - low reliability of detecting sources of failures in the system. Therefore, expansion capability to detect hidden defects in the form of elements and nodes failures due to the introduction of additional contact and contactless sensor failures with the addition of intellectual properties by differentiation and integration of bad signals , as well as internal and external electromagnetic interference in the corresponding processing information is very timely.

This problem is solved by the fact that the parking system comprising an electronic control unit connected to the ultrasonic sensors and blind spot sensors front and rear circuits , and outputs associated with the right and left warning LEDs and indicator , power supply, connected to an electronic control unit , further comprising a contact or contactless sensors malfunctions mounted respectively on lines of communication and interface tire or in the vicinity of 1-2 cm from the communication interface or bus for detecting internal and external noise sources in the form of disruptions connector / connectors , interface tires, control, ground and power supply, the system is capable of algorithmic (differential, integral, and if necessary, and integro- differential) signal processing with said sensors failures [3].

The problem is solved by the fact that as informative parameters when detecting failures sources selected change of amplitude-frequency characteristics , increased electromagnetic radiation , the appearance of the effect of differentiation and integration of signals. Note that the system is adapted to reception of the amplitude -frequency characteristics of power failure in the frequency range from zero or DC up to several gigahertz.

It is important that the system is capable of non-contact detection of electromagnetic radiation from the source of malfunctions in the frequency range from a few hertz to a few gigahertz. The system is adapted to determine the source of failure of the contact into the micro-annulus , and formation of microcracks in communication lines and connectors, and a small fraction of the capacitive component and units of picofarads therein , followed by a large impedance to 107 ohms , and the receiver signals to the above CMOS - structure and formation effect differentiation signals.

The proposed system is adapted to determine the source of failure proximity upon formation microresonant circuits and electromagnetic radiation in them by passing an electrical signal. When this contact and contactless sensors failures arranged to operate in the frequency range from a fraction of hertz to several gigahertz. Contact sensors failures can be implemented in CMOS inverters .

The problem is solved in that the proximity sensors failures implemented on passive (LC- elements) microresonant oscillation circuits . It is particularly important that the system is configured to determine at operation two or more contact sensors to the source of the failure element or failure node earlier by the sensor response time .

The problem is solved in that the system is configured to determine , while triggering two or more proximity sensors as the source of failure of failures or external electromagnetic interference effects .

The problem is solved in that the system is adapted to majorization signals with an odd number of proximity sensors failure.

The problem is solved in that the system is configured to determine when triggered contact and proximity sensors as sources of failures of internal electromagnetic interference.

The problem is solved in that the system is adapted to determine the source of contact failure on the effect of signal integration, solving thus the problem of finding an integral failure.

Problem of determining error conditions and sources of failures in the form of lines and connectors to change the frequency response, high electromagnetic radiation, differentiation electrical signals based on the representation of hidden defects mentioned elements of the apparatus in the form of micro-annulus, microasperities microcracks of microscopic particle and thereby forming microresonant contours and mikroemkostey.

The task of integrating the informative parameters of electrical signals when the failure is based on the integral representation of latent defects in the form of increased device (tens and hundreds of times) ohmic resistance constituting integrating unit followed mikroemkostyu included (eg, hundredths of a pF).

Fig. 1 is a block diagram of the parking system of high reliability. The system comprises an electronic control unit 1, unit of ultrasonic sensors and blind spot sensors front circuit 2, a block of ultrasonic sensors and sensors rear blind zone circuit 3, 4 LED warning right, left 5 LED warning indicator 6, block pitaniya 7 and contact sensors failures (CBC) 8-19, proximity sensors failures (OBD) 20-25. When a unidirectional force signals PDR set at the beginning (at step signal) lines - CBC 12, 14, 16, 18 and the end - 13 DPT, 15, 17, 19. In the general case the number of sensors can be large, depending on the particular link and resolution sampling desired for it, where necessary fixation failure.

The diagram (Fig. 1) are shown and proximity sensors malfunctions 20 - 25 set in the vicinity of diagnosable elements or nodes. No. BSS chosen based on their sensitivity, the link length, and in the general case can be large. As CDS and BDS may have as an autonomous and centralized display (in Figure 1 is not shown).

Park Assist is activated automatically when reverse gear. If the distance to the obstacle is more than 2 meters, the display is missing. When the distance becomes less than 2 meters, the display shows the digital display. By reducing the distance to 1.5 meters and less than an audible alarm, the frequency beeps increases as you get closer to an obstacle. LED segments of the left and right side of the display indicate the direction in which the obstacles. If both sides of the display lights up an equal number of segments, the obstruction is in the middle.

Front sensors are activated after two second on the brake pedal and stop working automatically after 10 seconds. When an obstacle in a meter zone from the front bumper distance to it will be displayed on the device. By reducing the distance of less than 60cm in addition to displaying on the display device will supply intermittent beeps, while reducing the distance of less than 30cm beeps become continuous.

In parallel with the work units and blocks 1 - 7 in "on-line" work and sensors CDS (8 - 19, 1) and the BSS (20 - 25, Figure 1) installed on the communication lines between the nodes and blocks one - 7 and monitor data communication lines for the presence of latent defects manifest as failures, or the presence of internal (external) electromagnetic interference. Usually hidden defects appear as micro-annulus, microcracks microasperities of microscopic particle and thereby forming microresonant contours that can lead to system failure.

Operation algorithm CBC 8 - 19 next. For example, the simultaneous actuation of two contact sensors 16 and 17 malfunction indicating failure output terminal pair "plug - socket" the electronic control unit 1, which transmits signals via said terminal pair, and also

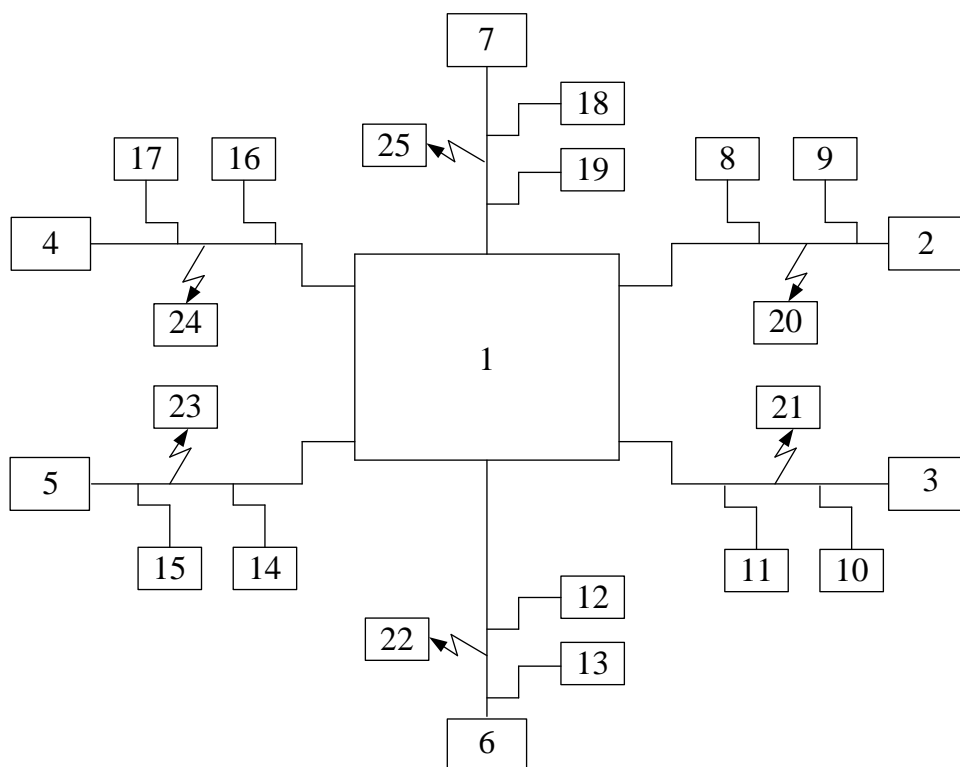
through the communication line to the right warning LED 4 . Fire only one sensor DPT 17 says about the source of failures in the communication between blocks 1 and 4. Additional activation of the proximity sensor failures (OBD) 24 will indicate a breach (eg , poor contact) in the insulating (" earth") bus and appearance of internal exposure to electromagnetic interference (noise) . Similarly functioning CDS and BDS in other lines of communication interface or tires.

CBC implementation is quite simple and is , for example, to connect to the corresponding points of small capacitors (tenths and hundredths of PF) and parallel with comparators with independent display or output connected to a microcontroller (electronic control unit) that are configured on the target voltage level failure (eg , 5 volts) . Then, when the failed link in violation of or in pairs in a defective contact point is formed (for example, before giving up - cliff) a large series resistor (in the tens or hundreds of times greater than the resistance in normal functioning of the link or contact pair) . This resistance in series with the capacitance forms included integrating network with the accumulation of electric charge on the vessel , which can be recorded as a failure of self-contained means of indication or a microcontroller (electronic control unit) .

The principle of operation is based on BSS registration of additional (beyond permissible) electromagnetic radiation source failures due to the formation microresonant contours. Implementation of these sensors are also quite simple and , in a particular case , can be built on passive LC - elements established at a distance of 1 - 2 cm from the proposed source of failures. Ideology incorporating BSS and the algorithm of their functioning in the device is similar to CBC . The main difference (besides informative parameter) - in the value fixed by the signal depending on the distance to the source of failures. Signals from the BDS can be used for further processing or MC, or (if necessary) to have autonomous registration system (Display) .

Crash sensors mounted , for example by clips . Simultaneous operation of BSS on the various lines of communication and does not trigger CDS evidence about the source of failures in the form of an external electromagnetic interference. Simultaneous operation of CDS and BDS says internal electromagnetic interference .

Simultaneous operation of CDS and BDS (except one) on a single communications line captures the failed state of the line and broken (refusal) condition is not triggered proximity sensor failure. Centralized system of signals with BDS this link (for example, using a microprocessor system) defines a faulty OBD, in particular using a majority signal processing (in Figure 1 is not shown).



Фиг. 1. Блок-схема парковочной системы

Should pay attention to the performance of microminiature CBC and BDS and small dimensions and weight of said sensors, which together with the prospect of nanotechnology applications in transport is not difficult at their introduction .

Conclusions

1. Ask parking scheme and considered high reliability .
2. Dopolnenie scheme differential and integral sensor failures can increase the information content of the system, in particular , in determining the survivability of stock or residual resource .

References

1. Parktronic , <http://www.tpmaster.ru>
2. Dianov VN Integro-differential diagnosis of failures in combinational circuits (see this volume) .
3. Dianov VN Ghevondian TA, IM Belousov , Lyuminarsky ES, Doucet SG Parking system . The utility model application number 2013144952 /11 (069499) . Priority FIPS certificate from October 22, 2013 .

INTEGRO-DIFFERENTIAL DIAGNOSIS OF FAILURES COMBINATIONAL CIRCUITS

Dianov V.N.

Moscow, Moscow State Industrial University

In theory failures prompted to enter a new concept: a differential failure, malfunction integral, integro-differential failure. On an example of active elements (transistors, integrated

circuits) combinational circuits shows a practical sense of the concepts introduced, particularly in the detection and recording of these types of failures.

To control the reliability of modern electronics (CEA) is necessary to diagnose the state of its elements, obtained in a variety of signals. In combination (or digital) circuits built on logic elements (such as "AND", "OR"), one of the informative parameters characterizing the quality of the operation is the transition from one state to another (eg, from "0" to "1"). In cases where the signal propagation time within the cell is sufficiently small, switching delay can not be ignored. But with increasing frequency of change of input signals in real circuits begins to affect the influence of the propagation time of the signal inside the cells. Such delays may cause erratic operation of devices, leading to failures. Especially the problem of failures relevant in today's processors due to the delays of signals at frequencies of the order of units of gigahertz. In particular, a conventional wire with a plurality of bends near the board in such a high frequency operation becomes inductance.

Delay in the element depends on a number of factors (technological, supply voltage, load, communication lines). Not only the delay chain speed limit, but generate false signals in the circuit, which could be dangerous if connecting circuit elements on the memory. In this case, the error does not disappear with time. Such false alarms called risk failure. [1]

Distinguish between static and dynamic risk failure. Static failure risks arise if the input signals when changing the output state should not change. Dynamic risk of failure occurs if the change of state circuit provided for the output signal. By virtue of the time difference may shift multiple switching signals output from "0" to "1" and vice versa.

The most versatile and widely used methods therefore address the risks of failure are timing and gating. When clocking around digital device divorced single system timing (clock) signals provide a record of information in the data registers in a time that exceeds the longest process of uncertainty, ie the largest delay for all paths of the circuit. If you need a clear signal from the risks of failure, and not remember it, the method of sampling, implemented by the relevant building combinational circuit.

All methods developed to eliminate the risks of failure in combinational circuits, into three groups: structural, functional, and design and technology. Structural methods aim at obtaining the desired properties of the device at a constant algorithm for its operation. Functional methods associated with changes in the algorithm works, in particular the change in the coding of the input states. Design and technological methods focused on generating desired restrictions on the level of use of mathematical models. Structural methods can be directed at changing the internal structure, i.e. reconfiguration scheme, in case of failure of a circuit element. Functional methods of failure must be capable of reprogramming scheme.

However, all the methods described, involving the elimination of the risks of failure in combinational circuits are, in our view, a number of disadvantages, the main ones are as follows.

First. Failures occurring suggests their probabilistic rather than deterministic. As a result - passive methods fault diagnosis and control.

Second. Consider only failures in the active elements (transistors, integrated circuits) and entirely the left to the detection and registration of failures in passive elements (contact track PCBs, contact LSI and VLSI devices, power bus shielding conductors, connectors).

Third. Also in the left side of the impact and influence of external electromagnetic interference and power circuits.

Therefore, the existing degree of reliability and resiliency to ensure equipment is proposed to add-fail and demand issues sboustoychivostyu Especially build-fail equipment in outer instrument given the increase in the life cycle of spacecraft from 2 to 15 years [2].

Lifecycle Management when it should be based on information about the precursors of failure.

Another important area of application non-fail equipment is military equipment. To this end, developed GOST devoted to different methods of estimating the frequency of single failures of integrated circuits [3]. Questions build -fail based on recording equipment failures on various sources of informative signs and documented in the literature [4].

Novelty detection solutions and fault logging for technical means using methods patented active diagnostics and has considerable domestic priority, particularly in comparison with the United States about 10 years: cm. RF [5] - [9], USA - [10] - [13]. Patenting decisions on failures in the United States noted in such firms as "General Electric" [10] "Katerpiler" [12], as well as one of the world leaders in the field of supercomputers - "IBM" [13].

Recently, the concept of "failure" as before the concept of "failure" is increasingly being used, in addition to military equipment in general industrial equipment and specialized. This fact is confirmed, for example, a series of GOST standards on this subject [14] - [17].

All these domestic guests as well as foreign sources for the failed category (patents) are characterized by random or statistical estimates, despite the variety of definitions of "failure". However, in some cases, is important not only the fact of failure detection and reporting, but also required to know and characteristics of this failure, for example, the lifetime of failure, his borderline (properly, failure) or an intermediate state, external or internal manifestation of it (for example, a manifestation of failure as external, internal, or low-frequency electromagnetic interference) time or frequency nature of its manifestations, etc.

In connection with the foregoing, it is proposed the theory of failure especially in the theory of reliability and security, enter the following concepts: "differential failure", "integral failure", "integrodifferential failure".

Earlier in the existing methods of detecting and recording sources of failures was first proposed by the differential method [18]. The method allows to fix the source of failure in the passive elements of CEA - communication lines, interface tires, tire power and grounding connectors, tire management. All of the above elements with the existing latent defects and acquired during the operation in the form of micro-cracks, micro-annulus, partial breaks, low-quality contacts in connectors, supplemented in the electrical equivalent circuits mikroemkostyami [19].

Subsequent high input resistance ohmic load (eg, tens of megohms in CMOS circuits) together with an educated mikroemkostyu defect created the preconditions for the differentiation of passing through this chain of useful signals, and hence registering a latent defect in the form of failure. This, in turn, allows you to record the initial stage (beginning) of the offending state (failure) of the element.

On the other hand, in the further destruction of the element in fixed source of failure of its electrical resistance increased in tens and hundreds of times. Example. Connector RPPM 27-90 used in domestic supercomputer, in particular, a series of "Elbrus", in good condition and has enabled the ohmic resistance of the order of 20 - 30 milliohms. In the failed state (e.g., before rupture) this resistance is increased to hundreds of ohms. Including additional parallel mikroemkost same CMOS load, as a result, we have been integrating circuit. This circuit can be used as a harbinger of failure element [4] in the intermediate state of the offending element, that is, after the failure of the differential lock and until after the integral failure to diagnose the state of a latent defect can, for example, using kodoimpulsnyu modulation signals [20].

Thus, introducing the concept of "differential failure" and "integral failure", have the opportunity to a more detailed description (early failure, late failure) of the same failure. Combining these concepts into one, in integrodifferential failure, we can talk about the stock

already survivability item in the failed state, or the lifetime of failure [21]. In turn, knowledge of the parameter "lifetime of failure" can uniquely identify such an important parameter of the system as a "residual life" [22].

With respect to the logic element combinational circuit should be noted that the change of state of a serviceable condition to the state precursor failure occurs exponentially with a particular index or constant exponent [23]. Naturally, the transition to the element of "0" to "1" will be not immediately, but within a finite time, ie front time is finite ($\tau_{fr} \neq 0$). Using the well-known formula, the parameter can be "front time" to reconcile with the upper cut-off frequency of failure f_{gr} ($\tau_{fr} \approx 0,35 / f_{gr}$) [24]. Received by the upper limit frequency of this failure can be fixed differential contactless using informative parameter "electromagnetic radiation" [25]. There also described a principle of proximity sensor failure, and its original implementation proposed in [26].

Integral state failure occurring after the state differential failure will fit over a low frequency, given the increase in the pulse rise time. Range duration of fronts to integral differential failure can be determined either experimentally (to use), or by simulating error conditions, taking into account effect of different data delay time of the test element. Ideology of the integro-differential sensor fault condition is configured, for example, at two frequencies (top and bottom) corresponding to the differential and integral element of error conditions, set out in [8] and has been implemented, in particular, in [27].

It should be noted that the detection and registration of failures on differential and integral characteristics, as well as fixing the intermediate between the symptoms associated with intellectual processing of bad signals detected due to intellectual property in the passive elements [28]

In particular, in the failed state of elements was recorded a number of informative features, different from other states of the elements ("regularly", "failure"). Unable to identify these conditions and due to the original processing kodoimpulsnyh signals, particularly when they are processed simultaneously in the time and frequency domains [29] and [30]. Experimental tests have confirmed this assumption expressed a priori, which allowed all of the results registered as opening with the issuance of the relevant documents of the Russian Academy of Natural Sciences [31].

Detection and registration of differential failure, showed appearance or presence of a latent defect, were first proposed for implementation in the automotive sensors [32].

Detection and registration failure integral fixing forthcoming transition element of the failed states in refusal, were first obtained by sensors - flowmeters [33].

Detection and registration of integro-differential failure determining the duration (lifetime) of failure, have been proposed for the diagnosis of single and multilayer printed circuit boards [34], [35]. To the detection and registration differentsalnyh and integral failure resolved in parking systems of high reliability [36].

Findings

1. In theory failures introduced new concepts: a differential failure, malfunction integral, integro-differential failure.

2. On an example of active elements (transistors, integrated circuits) combinational circuits shows a practical sense of the concepts introduced, particularly in the detection and recording of these types of failures.

References

1. Vorobyev N.V. Methods of analysis of combinational circuits to the risks of failure .. // Chip News/- 1997. Number 12.

- 2 . Danilin N.S., Kolesnikov N.P. Lifecycle Management spacecraft based on information about the precursors of failure . Network electronic journal " Systems Engineering », № 8, 2010
- 3 . GOST RV 20.57.415 . Methods of estimating the frequency of single failures of integrated circuits.
- 4 Dianov V.N.. Conceptual features of build -fail equipment / / Automation and Remote Control . 2012 . Number 7. P.119 - 138.
- 5 . Dianov V.N. A method for controlling electrical connectors . RF patent number 2001413 , 1993 . BI Number 37. 6 C.
6. Dianov V.N. A method for detecting latent defects connectors. RF patent number 2003126 , 1993 . BI Number 42.9 C.
7. Dianov V.N. Method contactless control of electrical connectors . RF patent number 2003993 , 1993 . BI Number 43. 5 C.
8. Dianov V.N. A method for controlling electrical connectors . RF patent number 2050555 , 1995 . BI Number 35. 10. C.
9. Dianov V.N. Martynuk D.V. Dianov S.V. A method for controlling electrical connectors . RF Patent number 2001412 , 1993 , Bull . № 37-38, 4 C
- 10 . U.S. patent number 6336065 , IPC G 06F 11/25 of 2003
11. U.S. patent number 6324655 , IPC G 06F 11 /00 of 2003 .
12. U.S. patent number 6363332 , IPC G 06F 15 /00 of 2002 .
13. U.S. patent number 6341360 , IPC G 06 F 11/00 , G 01R 31/28 from 2003 .
14. GOST RV 20.39.302 - 98. Integrated system of common technical requirements.
15. GOST RV 20.57.305 - 98. Comprehensive quality assurance system .
16. GOST R UCO / IEC 15408 2 - 2008.Kriptografiya .
17. GOST R 50 922-96 . Information Security. Basic terms .
18. Dianov V.N. Fault diagnosis in electronic equipment / / Vestnik MSTU. N.E. Bauman. Series "Instrument " . 2007 .
Number 2 (67) , pp. 16 - 47.
19. Dianov V.N. Failures in technical systems . Monografiya.M . : Mechanical Engineering , 1999 . Pp. 97 .
20. Dianov V.N. Integro- differential pulse code- modulation in the diagnostics of complex objects hidden defects . International Scientific - Practical Conference "Innovative Information Technologies" (I2 T). Prague - 2012 , April 23 - 27. C.403 - 405.
21. Belousov I.M. , Dianov V.N. Method for determining the survivability of stock item in the failed state. Internftional Scientific - Practical Conference "Innovative Information Technologies (I2T). Part 2 Innovative Information Technologies in Science. Prague - 2013 , April 22 - 26. C.473 - 478.
22. Dianov V.N. The concept of improving the reliability of non-destructive testing equipment / / 10th Europ. Conf. on Non-Destructive Testing (ECNDT). Moscow, 2010 . Abstracts. Part 2 . P. 248 - 250 .
23. Dubnitskiy L.G Harbingers of failures in electronic products . AM Radio and Communications . 1989 .
24. Dianov V.N Contactless testing and diagnostics connector HPC / / Questions electronics . Ser. EVT . 1992 . MY . 6. Pp. 93 -101 .
25. Dianov V.N. Automatic and electronic systems of vehicles increased reliability . Monograph. ID " League " , Kolomna. 2009 . 320 P. .
- 26 .. Dianov V.N. Tsarev B.D., Dianov S.V. Poliker B.E. Sensor electrical signals / / RF Patent number 2,064,189 . 1996 . Bull. Number 20 , p.7 .
27. Nekrasov V.N , Savostin Y.M Hydroacoustic antenna . RF Patent № 2201041 from 21.07 . 2000 . IPC 7 H04R 1/44 A; 7 H04R 29/00 , 7 G01S 15 /00 B.

28. Dianov V.N. Intellectual properties of passive elements of electronic equipment . Proceedings of the eighth international . symposium. " Intelligent Systems ". INTELS'2008, Russia , Nizhny Novgorod, June 30 - July 4, 2008 , pp. 56 - 61
29. Vyushkov Y.A., Dianov V.N. Asynchronous electric with PWM control . Copyrights . testimony. USSR number 365789 . BI 1973 . Number 6.C.2
30. Plyushkin K.V., Sarkisov A.A., Vlasov D.V, Dianov V.N. Intelligent Fault Diagnosis actuators and sensors using code - Vyushkova Dianova / / Control, Diagnostics . 2006 . Number 4 (94). 5 C .
31. Dianov V.N. Severtsev N.A., Yevtushenko YG Property passive elements to increase the amount of electronic equipment readable information about the system under the influence of electrical oscillations . Scientific discovery in the field of reliability theory , the theory of security (diploma 47 -S). Scientific discoveries in 2012 . Collection of summaries of scientific discoveries , scientific ideas. P.44 -46 . RANS edition .
32. Dianov V.N. , A.A. Sarkisov A.A., Vlasov D.V. Method and apparatus for intelligent fault diagnosis of automotive sensors. RF patent number 2292578 , 2007 . Bull. Number 3 .
33. Dianov V.N., Cherepova E.A., Egorova A.O. , Kulikova O.N. , Stasenok K.O., Babayan B.Yu. Flowmeter sensor with detection of sources of failures. Patent for utility model number 86732 , 2009 . Bull. Number 25.
34. Dianov V. N. 2006 IEEE Active Diagnostics of the Failures in Printed - Circuit - Boards. Moscow State Industrial University, Russia. EMC - Zurich in Singapore 2006 17 th International Zurich Symposium on Electromagnetic Compatibility, 27 February- 3 March 2006 , Singapore, Suntec International Convention & Exhibition Centre. P. 194 - 197.
35. Dianov V.N. Puzanov A.V., Mironov M.N Baryshnikov D.A., AI Medvedev A.I. Apparatus for testing printed circuit boards with the detection of latent defects . Patent for utility model number 91767 , 2010 . Bull. Number 6.
36. Dianov VN, TA Ghevondian Parking system of high reliability . (See this collection) .

COMPUTER SIMULATIONS OF ELASTIC COPONENTS OF NANO- AND MICROELECTROMECHANICAL SYSTEMS

Vasil`ev V.A., Kalmykova M.A., Chernov P.S.
Penza State University, Russia

The modeling of elastic components of nano- and microelectromechanical systems during design is discussed. Numerical simulations of deformations in membranes with rigid center are considered. The solution of a problem of optimization is shown.

Keywords: computer modeling, numerical simulation, finite element methods, nano- and microelectromechanical systems

In tasks of measurement monitoring, and control within the first proposal there are problems of improving accuracy, stability, information content, reliability, etc. [1–12].

In creating thin-film nano- and micro-electromechanical pressure transducer systems, there arises the problem of obtaining an elastic component with given characteristics [6, 11]. An elastic component is one of the basic elements of these systems which transforms the measured quantity into a deformation or displacement. The creation of improved nano- and micro-electromechanical systems sensors (N&MEMS) based on them requires a systematic approach to their design employing modern computer technologies.

A membrane is used most widely as the elastic element. The construction with a rigid center is shown in Fig. 1 of thin-film N&MEMS tensoresistor pressure sensor. Thin-film tensoresistor pressure sensors (TTPS) exhibit the optimum combination of metrological, structural, and engineering characteristics with the highest resistance to the action of the factors listed above compared with sensors with a similar designation of different conversation principles. Therefore TTPS provide measurement of the absolute majority of pressure parameters for liquid rocket engines. Thin-film N&MEMS, intended for TTPS (Fig. 1) consist of heterogenic structure 1, sealed lead-outs 2, delivery wiring 3, peripheral base 4, membrane boundary 5, membrane 6 and a rigid center 7.

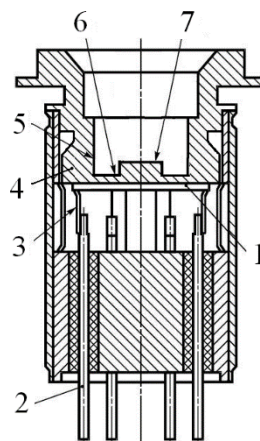


Fig. 1. Thin-film N&MEMS with a membrane: 1) heterogenic structure; 2) sealed lead-outs; 3) delivery wiring; 4) peripheral base; 5) membrane boundary; 6) membrane; 7) rigid center.

A typical heterogeneous structure of a thin-film N&MEMS consists of several nano- and microsize layers formed on a metal membrane with a microroughness height not more than 50–100 nm. Analyses of well-known designs of pressure transducers with thin-film resistance strain gauge systems have demonstrated that the most common elements consist of layers, such as a dielectric layer 1, resistance strain gauge (chromium–nickel) layer 2, adhesive layer 3, and contact (conducting) layer 4 (Fig. 2). For these later studies, the resistive layer may be 40–60 nm thick. The layers are successively grown on an elastic element (most often in the form of a metallic membrane) by a method of heat-induced evaporation) in a vacuum or by magnetron sputtering.

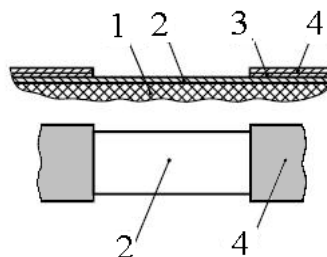


Fig. 2. Elements of a thin-film resistance strain gauge system comprising several layers: 1) dielectric layer; 2) resistance strain gauge layer; 3) adhesive layer; 4) contact (conducting) layer.

Use of heterogeneous structures in thin-film N&MEMS for TTPS is promising. The advantage of heterogeneous structures appears under certain conditions, ratios of parameters and characteristics of the components. The amount and quality of information obtained using heterogeneous structures is mainly determined by the physical properties of their materials.

In spite of the considerable amount of research performed by scientists of different countries, the possibilities of constructing and analyzing thin-film N&MEMS for TTPS are far from exhausted. In developing and creating new more improved systems and sensors based on them, simulation should play an important role.

Simulation of information conversion in N&MEMS with heterogeneous structures as a rule is constructed on the basis of physical models taking account of the internal properties of the structure and an external effect. The physical model of simple elements such as a simple membrane, substrate, thin film, and others, within the composition of thin-film N&MEMS pressure sensors, has been studied quite sufficiently. Moreover, some promising systems with heterogeneous structures and areas for modeling them connected with information conversion in structures, has not been studied sufficiently.

For membranes with a rigid center, the analytic expressions are applicable only for a limited range of membrane radii, far from the rigid center, and cannot give the deformation near this center [6]. Computer simulation can be used to calculate the deformations of elastic components with complicated shapes in nano- and microelectromechanical systems. The finite element method has come into widespread use for solving problems involving mechanical deformations because of its many advantages and relative simplicity of implementation on a computer.

Simulations of the deformations of a membrane with a rigid center have been used to find the zones with positive and negative radial deformations and to determine the deformations for different ratios of the radii of the rigid center and the membrane.

Fig. 3 shows the dependences of extrema positive $\varepsilon_{r\max}$ (curve 1) and negative $\varepsilon_{r\min}$ (curve 2) relative radial deformations on the flat surface of a membrane with a rigid center. The curve 3 represents the inverted curve 2 (that is $|\varepsilon_{r\min}|$). It is established that the minimum difference between $|\varepsilon_{r\min}|$ and $\varepsilon_{r\max}$ corresponds $\frac{r_c}{r_m} = 0,42$. Here r_c is the radius of the rigid center; r_m is the radius of the membrane. Thus sizes of relative deformations accept close and greatest values.

Deformations of a membrane with a rigid center (cf. Fig. 1) were calculated with condition $\frac{r_c}{r_m} = 0,42$. The dependence of the relative radial deformations of a membrane on the relative radius of a membrane with rigid center ($\frac{r_c}{r_m} = 0,42$) is shown in Fig. 4. Here x is the current radius x ; r_b is the basis radius.

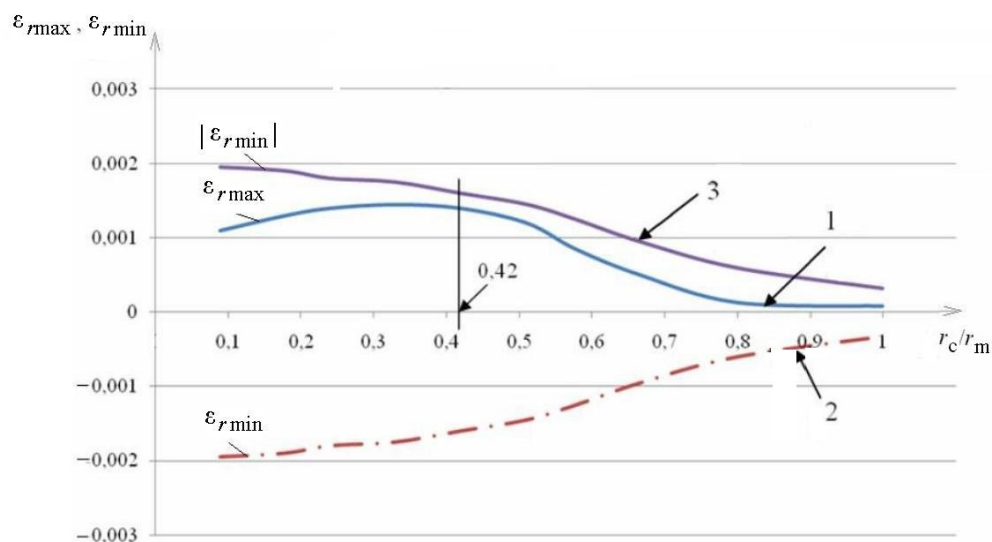


Fig. 3. The dependences of extrema positive ε_{rmax} and negative ε_{rmin} relative radial deformations on the flat surface of a membrane with a rigid center.

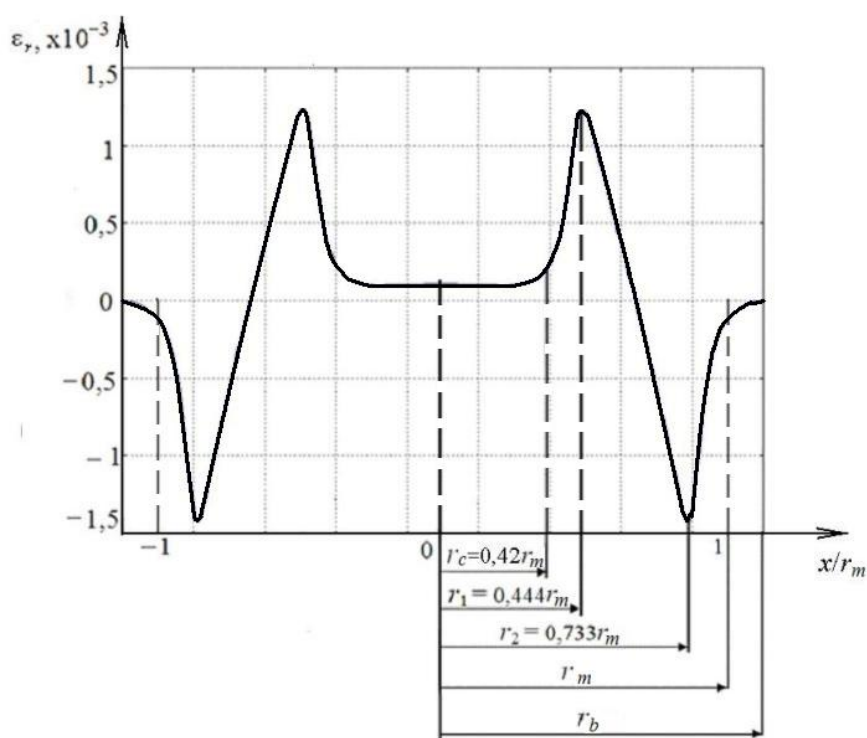


Fig. 4. Relative radial deformations on the flat surface of a membrane with rigid center.

Knowledge of the zones with positive and negative deformations of the membranes with a rigid center and of the values of the deformations in these zones is needed for optimum placement of strain gauges on a membrane when designing nano- and micro-electromechanical systems for strain resistance pressure sensors. So, an optimum place for strain gauges (thin film tensoresistor) on a membrane (with a rigid center $r_c = 0,42r_m$) is $r_1 = 0,444r_m$ and $r_2 = 0,733r_m$.

In membranes with a rigid center the radial deformations assume both positive and negative values. The diameter choice of the rigid center $r_c = 0,42r_m$, the greater is the relative variation in the radial deformations and, consequently, the higher the sensitivity of the transducer.

References

1. V. A. Vasiliev, P. S. Chernov Modeling and estimation of the parameters of the morphology of the surfaces of thin films of nano- and micro-electromechanical systems // Measurement Techniques. – USA, New York: Springer, 2013. Volume 55, Issue 12, Page 1350–1355.
2. V. A. Vasil'ev, P. S. Chernov Study of the Influence of the Substrate Temperature and the Deposition Rate and Time on Surface Morphology// Journal of Surface Investigation. X-ray, Synchrotron and Neutron Techniques. – USA, Dover: Pleiades Publishing, Inc., 2013, Vol. 7, No. 3, pp. 565–571.
3. V. A. Vasiliev, P. S. Chernov Smart sensors, sensor networks, and digital interfaces general problems of metrology and measurement technique // Measurement Techniques. – USA, New York: Springer, 2013. Volume 55, Issue 10, Page 1115 – 1119.
4. V. A. Vasil'ev, P. S. Chernov Modeling the Growth of Thin Film Surfaces// Modeling the Growth of Thin Film Surfaces // Mathematical Models and Computer Simulations, 2012, Vol. 5, No. 6, pp. 622–628.
5. V. A. Vasiliev, N.V. Gromkov Combining integrating scanning frequency converters with pressure sensors // Measurement Techniques. – USA, New York: Springer, 2012. – V. 55. – N 8 – P. 932–935.
6. E. M. Belozubov, V. A. Vasiliev A. I., Zapevalin and P. S. Chernov Design of elastic components of nano- and microelectromechanical systems // Measurement Techniques. – USA, New York: Springer, 2011. – V. 54. – N 1 – P. 21–24.
7. E.M. Belozubov, V.A. Vasil'ev, and N.V. Gromkov Problems and Basic Research Directions in the Field of Thin-film Nano- and Microelectromechanical Systems of Pressure Sensors // Automation and Remote Control – USA, Pleiades Publishing, Ltd., 2011, Vol. 72, No. 11, p. 345 – 352.
8. E. M. Belozubov, V.A. Vasil'ev, N.V. Gromkov Thin-film nano- and micro-electromechanical systems – the basis of contemporary and future pressure sensors for rocket and aviation engineering // Measurement Techniques. – USA, New York: Springer, 2009. – V. 52. – N 7 – P. 739–744.
9. E. M. Belozubov, V. A. Vasil'ev, D. A. Izmailov Effect of thermal shock on a membrane-type transducer // Measurement Techniques. – USA, New York: Springer, 2009. – V. 52. – N 2. – P. 155 – 160.
10. E. M. Belozubov, V.A. Vasil'ev, N.V. Gromkov Minimization of the effect of temperature on thin-film nano- and microelectromechanical systems and pressure sensors based on them // Measurement Techniques. – USA, New York: Springer, 2009. – V. 52. – N 8 – P. 853–858.
11. E.M. Belozubov, V.A. Vasil'ev, P.S. Chernov Simulation of Deformations in the membranes of pressure transducers // Measurement Techniques. – USA, New York: Springer, 2009. – V. 52. – N 3. – P. 271 – 276.
12. S.U. Uvaysov, I.A. Ivanov A method of ensuring controllability of electronics based on diagnostic modeling of heterogeneous physical processes // World Applied Sciences Journal. 2013. Vol. 24. P. 196 – 201.

THE TASK OF DETERMINING THE NUMBER OF TEST PULSES TO EVALUATE THE RESISTANCE OF ENGINE CONTROL SYSTEM OF A VEHICLE TO ELECTROMAGNETIC RADIATION OF LIGHTNING

Nikolaev P.A., Nikolaev A.D.
Togliatti

The problems of testing the engine control system of a vehicle for resistance to the lightning are considered in this paper. An approach of calculating the amount of affecting pulses required to assess the resistance of control system.

Keywords: test, lightning, control system, vehicle.

Currently, the number of vehicles, as well as number of onboard electrical equipment is growing. Therefore the likelihood of operation breakdowns of onboard systems under electromagnetic influence increases. In this regard the problem of electromagnetic compatibility of vehicles is becoming more urgent. This field is constantly under study. There are tests that the vehicle must necessarily pass. However, not enough attention is paid to a number of effects in the automotive field, which can affect the performance of the onboard systems and, respectively, safety. One of those effects is lightning. Physics of this phenomenon has been well studied and there are many books, one of which is [1].

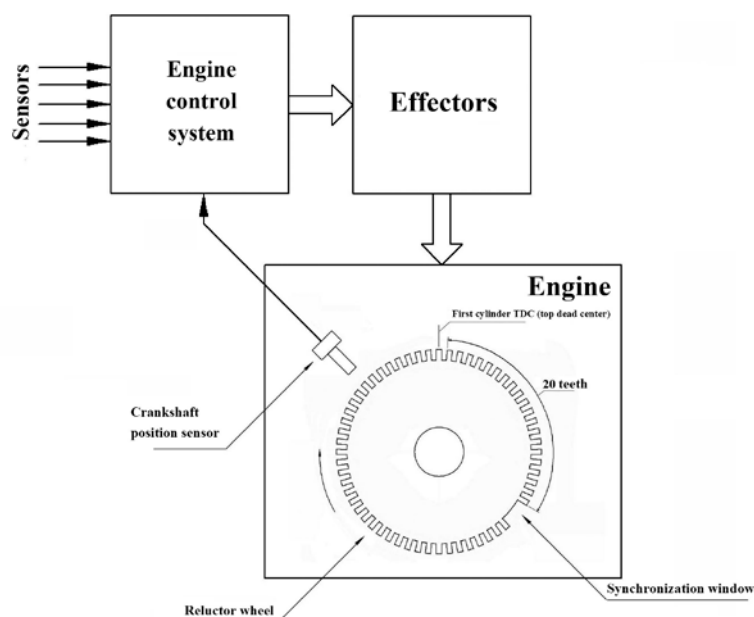
Resistance of onboard electric equipment to lightning radiation must be assessed based on the large coverage areas and thus massive and powerful electromagnetic effects on the vehicles. Back in 1983 SAE recommended to test vehicles for resistance to lightning radiation with amplitude 5 kV/m

Currently modern car is equipped with sophisticated electronic systems. The cornerstone of everything is electronic engine control system. Malfunction or failure of this system could affect the safety. Therefore it is important to solve the problem of determining the amount of impacts to objectively assess EMC of control system.

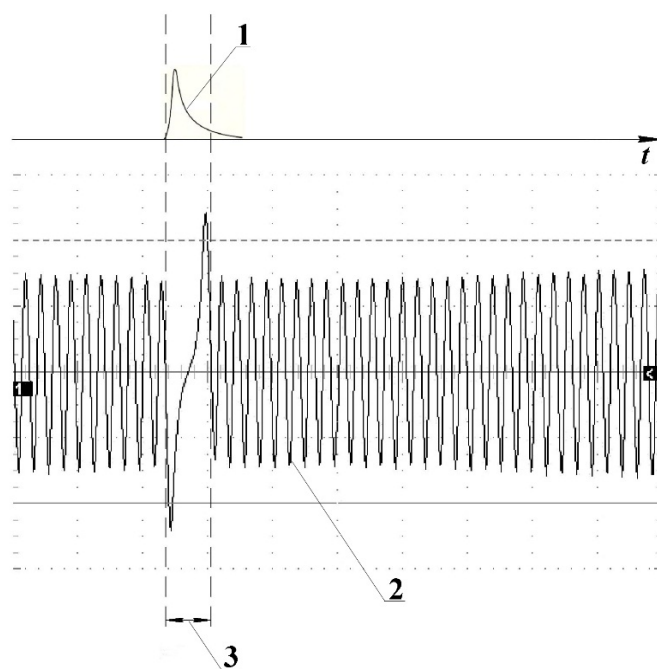
It is well known car engine control is carried out by feedback circuits from various sensors. The most important channel is the control channel for the crankshaft position sensor. In practice, the following scheme is used in almost all cases. The reluctor wheel from a magnetic material with teeth Scheme 60-2 (i.e. two teeth are cut to ensure synchronization) is attached to the crankshaft of the engine. Each tooth as well as the corresponding slot reflects 30 turn of the crankshaft. Information about the position of the pistons and crankshaft speed enters the engine control unit. Primary converter here is the crankshaft position sensor of induction type. This control channel is schematically shown in Pic.1.

As shown in [2] the most critical for engine control is the failure at the moment of synchronization. Therefore the EMC of engine control system can be most fully evaluated when the pulse radiation generated by the lightning hits engine control system in a time slot of synchronization (Pic. 2).

As can be seen from the analysis of literature temporal pulse parameters of the lightning vary widely, but for the test we can take as the basis pulse with $T_{rp} = 50$ ms.



Pic. 1. Channel engine control channel based on crankshaft position sensor



Pic. 2. Evaluation of EMC of engine control system

1 - pulsed radiation generated by a lightning (schematically) 2-signal generated by the driving disk, 3 - time slot of synchronization

It is necessary to learn how to relate to each other the duration of electromagnetic exposure of lightning and synchronization at different operating modes of the engine.

Obviously, the larger is the rpm, the less is the time slot of synchronization. Typical maximum rpm is 6000 min^{-1} . Rpm of certain types of motorcycle engines can reach 20000 min^{-1} . Time slot of synchronization is calculated as follows

$$T_{\text{synch}} = \frac{2}{n} \text{sec}, \quad (1)$$

where n - rpm (min^{-1}).

For $n = 6000 \text{ min}^{-1}$ - $T_{\text{synch}} = 333 \text{ ms}$, and for $n = 20000 \text{ min}^{-1}$ - $T_{\text{synch}} = 100 \text{ ms}$. It follows that the lightning impulse will never completely overlap a temporary synchronization window. Therefore the probability of hitting a single impulse of lightning into the temporary synchronization window (event A) for the teeth scheme 60-2 is equal to

$$P(A) = 1/30 \quad (2)$$

Ultimately the problem is reduced to find required number of not synchronized test impulses of lightning where at least one impulse with a specified probability would hit into the temporary synchronization window.

When impact is not synchronized each subsequent impulse of lightning does not depend on the other. Now we turn to the opposite case: \bar{B} – no hitting of impulses to the temporary synchronization window. We use the rule of multiplication of independent events. Then the hit probability $P(B)$ is at least one impulse from N series is equal to

$$P(B) = 1 - P(\bar{B}) = 1 - [1 - P_1(A)] \times [1 - P_1(A)] \times [1 - P_N(A)] \quad (3)$$

As $P_1(A) = P_i(A) = P_N(A)$, and also taking into account (2), we obtain

$$\left(\frac{29}{30}\right)^N = 1 - P(B) \quad (4)$$

Taking the logarithm of (4), we obtain

$$N = \log_{\frac{29}{30}} [1 - P(B)] \quad (5)$$

Expression (5) is the starting point for finding the required number N of test impulses of lightning. To calculate it is necessary to set the probability $P(B)$. For the most accurate assessment of the resistance of engine control system of a vehicle it is necessary to choose $P(B)$ within limits of 0,95 till 0,99.

References

1. Baluk N.V High-power electromagnetic pulse: effects on electronic means and methods of protection. [Text] / N.V. Baluk, L.N. Kechiev, P.V.Stepanov. – M.: "Group ITD", 2007. - 478 p.
2. Nikolaev P.A. Effect of impulse interference on the control system of combustion engines. [Text] / P.A.Nikolaev, A.D.Nikolaev / / EMC Technology. 2010. - №4 (35). - C.12-17.

THE METHODS OF STATISTICAL ANALYSIS AND DATA MINING IN INFORMATION SYSTEM FOR IMMUNE-BIOCHEMICAL TESTS

V.N. Elizarov; N.Y. Kelina;
Penza State Technological University

This article is devoted review of the data analysis methods using for building information system for immune-biochemical tests. The paper describes the statistical and data mining methods which can be used in laboratory information systems.

Keywords: immune-biochemical tests, laboratory information systems, data mining.

The issue of enlarging possibilities of using information systems in medicine is very serious now. The increasing of performance and improving data processing algorithms contributes increasingly high degree of computerization in hospitals. One of the most important benefits of using computers is the laboratory analysis, for example, the blood test or

hemanalysis. In addition it should provide information support processes of special investigations, in particular, the new scientific field of biochemistry associates with the functioning of the humoral immune system. This field is developing intensively in the last decade. Modern approach to the choice of laboratory tests of homeostasis disorders determines the relevance of immunological and biochemical monitoring of patients with hypertension and coronary heart disease [2].

In the [1] proposed the structure of building Laboratory Information System (LIS). The blocks for processing of measurement results will be considered especially. It should perform the following functions:

1. The statistical processing of the experimental results by any kinds of methods including the assessment tendencies in the values of estimated parameters and factors;

2. Methods of Data Mining и Knowledge Discovery in Data.

For example, we need to use a set of values of all patients hospitals for classify patients. But if we want to determine the impact indicators for a disease specific patient we need to know the changes of indicators over time.

For all methods of data processing is important the quality of source data. It is often the cause of failure [3]. Because data are rarely purposefully accumulating for analysis, it often contains errors, gaps, anomalies.

Some steps to prepare for the analysis of patient data will be considered [3].

1. The description of the factors that could potentially affect the process.

2. The expert evaluation of the significance of factors.

3. The formalization of the data. Quantitative data can be easily represented as a number. But if we need to represent the qualitative data its will be the problem. For example, the character of the disease is difficult to describe numerically, but we can describe it by the categories - chronic/acute, etc.

4. The "cleaning" the data. We must correctly evaluate the data. For example, the address of the form "g. Penza, ul. Clara Zetkin 1 m. 1" can be represented in the form "Penza, Clara Zetkin 1-1" or "g. Penza, street Cl. Zetkin 1, 1", etc. To minimize this type of error we should enter the data from the list of existing values.

5. The reduction of the dimension of data. The large dimensionality of the data does not necessarily imply to more detailed analysis. The set of values may include the data which does not affect the process. These data increases the model and the computational cost, it reduces the accuracy of the analysis. Also some features can be combined, for example, height and weight of the patient that can be represented by the ratio height/weight.

The task of statistical processing based on multivariate statistical analysis. Multivariate statistical analysis is the section of mathematical statistics. It examines the methods of collection and processing of multivariate statistical data. These data are systematized and processed to determine the nature and structure of the relationships between the components of the multivariate attribute and obtain practical conclusions [4].

For example, there is a collection of patient data which contains some of the indicators: X_1 - sex, X_2 - age, X_3 - place of residence, $X_4 \dots X_k$ - information about the results any of laboratory tests. Thus, we obtain a set of N observations on the k -dimensional vector of values for each patient $P = (X_1, X_2, \dots, X_k)N$.

The typical problems that can be solved by methods of multivariate statistical analysis, such as:

- examine the relationship between the components of the random vector $P = (X_1, X_2, \dots, X_k)N$, based on the observed values.
- determination which of the observed parameters X_1, X_2, \dots, X_k have the greatest impact on the disease;
- classification of patients according to some criterion.

The task of intelligent processing methods based on Data Mining. It extractions of non-trivial, "hidden" knowledge (facts, structures, relationships) from a wide array of unrelated at first glance, information. Data Mining uses models based on learning: decision trees, decision rules, neural networks, etc.

Data Mining helps to solve the following types of tasks:

- 1) Clustering. It's grouping objects on the basis of the object's properties;
- 2) Classification. It sets the dependencies between the discrete output variable (label of class) and the input variables;
- 3) Regression. It sets the relations between continuous output variable and input variables;
- 4) Association. It reveals regularities between related objects.

Clustering can be used for segmentation of patients. Segmentation is merges objects on any grounds. After this it is convenient to work with a group of patients (cluster). Problem of clustering refers to a broad class of problems of unsupervised learning.

The using of Clustering is subdivided to the following stages:

- selection the set of objects for clustering;
- definition of a set of variables, by which will be assessed a set of objects (if you need you can normalize this variables);
- calculation of measure of similarity between objects.
- using the cluster analysis to create groups of similar objects (clusters).
- presentation of analysis results.

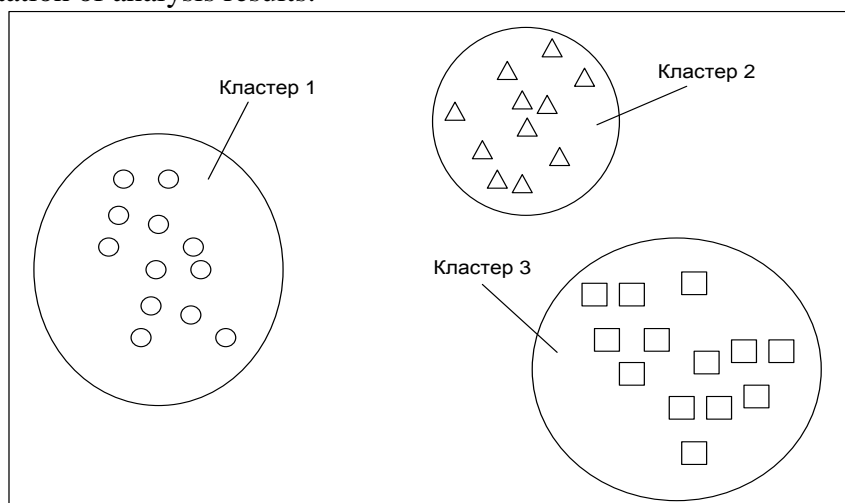


Figure 1 – Example of clustering

Clustering is a partition of a set of objects X into m (m - integer) clusters (subsets) Q_1, Q_2, \dots, Q_m . Each object must belong to only one cluster.

A formal statement of the problem of classification is as follows: let X is the set of object's characteristics, Y is the finite set of class label attributes. Function of the distance between objects was defined as $\rho(x, x')$. There is a set of training examples $X^m = \{x_1, \dots, x_m\} \subset X$. We need to split the set into disjoint subsets, called clusters, so that each cluster consists of objects that are close by the metric ρ , and objects of different clusters differed substantially. Each object $x_i \in X^m$ was attributed by class label attribute y_i .

The clustering algorithm is a function $\alpha: X \rightarrow Y$ which assigns the class label attribute $y \in Y$ to any object $x \in X$. The set Y in some cases known in advance, but often we seek to determine the optimal number of clusters in terms of a quality criterion clustering.

The clustering (unsupervised learning) differs from the classification (supervised learning). In clustering the labels of initial objects does not specified, and the set Y may be unknown itself.

When procedures for measuring the proximity of objects are developing we should eliminate the following difficulties: the ambiguity of the choice of normalization method and determining the distance between objects.

The main methods of determining the proximity between objects are shown in Table 1.

Table 1 – The basic distance function

Distance function	Description	Formula
Euclidean distance	Euclidean distance is the most popular in the cluster analysis. Geometrically, it is best to combine objects in globular clusters.	$\rho(x, y) = \sqrt{\sum_i^n (x_i - y_i)^2}$
Hamming (city block) distance	In most cases, Manhattan distance leads to results similar to the Euclidean metric, however, this measure reduces the impact of individual emissions (compared using Euclidean distance), because here the coordinates are not squared.	$\rho(x, y) = \sum_i^n x_i - y_i $
Tchebyshev distance	Tchebyshev distance is recommended to use when you need to define two objects as "different" if they differ in any one dimension.	$\rho(x, y) = \max(x_i - y_i)$

Clustering problem can be represented as a discrete optimization problem. So we need to attribute the clusters object x_i by the label y_i , so that the value of the selected functional quality took the best value. There are many varieties of quality features. Each clustering method can be regarded as an exact or approximate algorithm for finding the optimum of some function[6].

The average intracluster distance should be as small as possible [5]:

$$F_0 = \frac{\sum_{i < j} [y_i = y_j] \rho(x_i, x_j)}{\sum_{i < j} [y_i = y_j]} \rightarrow \min$$

The average intercluster distance should be as much as possible:

$$F_0 = \frac{\sum_{i < j} [y_i \neq y_j] \rho(x_i, x_j)}{\sum_{i < j} [y_i \neq y_j]} \rightarrow \max$$

If clustering algorithm calculates the centers of clusters μ_y , $y \in Y$, then we can define functionals which computationally more efficient. Sum of the average intracluster distances should be as small as possible:

$$\Phi_0 = \sum_{y \in Y} \frac{1}{K_y} \sum_{x_i \in y} \rho^2(x_i, \mu_y) \rightarrow \min,$$

where y_i – class label attributes, x_i – objects, ρ – measure of distance, μ – the center of mass of the cluster, $K_y = \{x_i \in X^l \mid y_i = y\}$ – cluster with the label y .

Sum of intercluster distances should be as much as possible:

$$\Phi_1 = \sum_{y \in Y} \rho^2(\mu_y, \mu) \rightarrow \max,$$

In practice, the ratio of the pair of functional is calculated to account for both inter-cluster and intra-cluster distance:

$$F0/F1 \rightarrow \min \text{ or } \Phi0/\Phi1 \rightarrow \min.$$

The k-means algorithm and its variants, the Kohonen network (a special type of neural networks) are used for clustering.

Cluster analysis can be used as a stand-alone tool to gain insight into the distribution of data, to observe the characteristics of each cluster, and to focus on a particular set of clusters for further analysis. Alternatively, it may serve as a preprocessing step for other algorithms, such as characterization, attribute subset selection, and classification, which would then operate on the detected clusters and the selected attributes or features.

Classification is used when you know the set of classes to which the object should be classified according their characteristics. For example, the patient should be referred to one or another group or the disease should be diagnosed based on the observable symptoms. In fact, the classification is the assigning an object the certain class label attribute.

A formal statement of the problem of classification is as follows: let X is the set of object's characteristics, Y is the finite set of class label attribute. There is an unknown target dependency. This is mapping $y^* : X \rightarrow Y$, whose values are known only at the facilities of the set of training examples $X^m = \{(x_1, y_1), \dots, (x_m, y_m)\}$, generated according to the probability measure P . We need to construct an algorithm $\alpha : X \rightarrow Y$, which capable to classify an arbitrary object $x \in X$ [8].

Data classification is a two-step process [7]. In the first step, a classifier is built describing a predetermined set of data classes or concepts. This is the learning step (or training phase), where a classification algorithm builds the classifier by analyzing or "learning from" a training set made up of database tuples and their associated class labels. A tuple, X , is represented by an n -dimensional attribute vector, $X = (x_1, x_2, \dots, x_n)$, depicting n measurements made on the tuple from n database attributes, respectively, A_1, A_2, \dots, A_n . Each tuple, X , is assumed to belong to a predefined class as determined by another database attribute called the class label attribute. The class label attribute is discrete-valued and unordered. It is categorical in that each value serves as a category or class. The individual tuples making up the training set are referred to as training tuples and are selected from the database under analysis. In the context of classification, data tuples can be referred to as samples, examples, instances, data points, or objects.

Classification is widely used in medical diagnosis. The patients are represented in the role of objects. Values is describing the results of tests, symptoms of diseases and treatment methods. Examples of binary attributes: gender, presence of headache, presence of weakness. The ordinal value is the severity of the condition (normal, moderate, severe, very severe). The quantitative characteristics is age, pulse, blood pressure, hemoglobin, the dose of the medicament. Attributive description of the patient is, in fact, the formal history of the disease. The worth of such systems is that they are able to instantly analyze and summarize a huge amount of precedents. This option is not available for doctor.

The classification algorithms are the following: decision trees (classification rules), Bayesian classifier, metric classifiers. Bayesian classifier is a wide class of classification algorithms based on the principle of maximum a posteriori probability. The likelihood function of each class is calculated for the classified object. Then the posterior probabilities of classes is calculated [6]. Object belongs to the class for which the posterior probability is maximized. Metric classifier (similarity-based classifier) - a classification algorithm based on the calculation of estimates similarity between objects. The k-nearest neighbor algorithm is

the simplest classifier. It classifies that the object belongs to the class which contains the most similar object.

The function of the distance between objects is introduced to formalize the notion of similarity. As a rule, the strict requirement that this function was the metric is not presented.

The regression is used to establish relationships between the factors. Between the tasks of classification and regression much in common. In particular, they help to find the relationship between the input and output characteristics.

The association rules helps identify patterns, for example, the dynamics of the disease flow of the patient or group of patients, depending on the place of residence.

A simple algorithm is usually more rough, but it's easier to explain the results. The most powerful algorithms can find complex nonlinear effects, but their interpretation is a challenge. In practice, it is necessary to find a compromise between accuracy and simplicity.

For estimating the amount of stored laboratory data of patients (blood test results, immuno research), we assume that:

- Π - the set patients (individuals participating in research), cardinality of the set $N=|\Pi|$;
- $G = \{G_1, G_2, \dots, G_n\}$ - the set groups of parameters characterizing the state of the human organism;
- G_i - i-th group of indicators;
- n – number of groups of indicators (cardinality of the set G);
- $P_i = \{p_{i1}, p_{i2}, \dots, p_{iq}\}$ - the set of indicators of i-th group which characterizing the state of person;
- $\Phi = \{\Phi_1, \Phi_2, \dots, \Phi_m\}$ - set of factor groups which are taken into account during research;
- m – number of factor groups (cardinality of the set Φ);
- $\Phi_i = \{\phi_{i1}, \phi_{i2}, \dots, \phi_{i\mu}\}$ - many factors of i-th group, which are accounted during research.

Then, the stored data can be estimated as the number of "single" records (excluding accumulation over a period) in the database

$$V = |\Pi| \sum_{i=1}^n |G_i| \sum_{j=1}^m |\Phi_j|,$$

at $|\Pi| \sim 100$; $n = 1$, $m = 1$; $q \approx 10$; $\mu \approx 10$ we obtain $V \sim 10^4$ records,

at $|\Pi| \sim 100$; $n = 10$, $m = 10$; $q \approx 10$; $\mu \approx 10$ we obtain $V \sim 10^6$ records.

The value of ~ 100 taken on the basis of the required volume of statistical data to provide reliable statistical estimates of the results of biochemical studies. When forming the time series data volume during the year may increase by an order.

There are many factors that significantly affect the correctness of the immuno-biochemical testing. we should accommodate these factors to create a modern LIS for immuno-biochemical studies, which provides storage and rapid processing results of laboratory tests. Also, we need to implement a number of methods of information processing capabilities for a comprehensive research.

References

1. Otkrytye innovacii – vklad molodezhi v razvitie regiona: sbornik materialov regional'nogo molodezhnogo foruma : v 2 t. – Penza: Izd-vo PGU, 2013. – T.1. s.93-96.
2. Kelina N.Yu., Pikulin V.V., S.N. Chichkin, P.V. Nekrasov. Razrabotka specializirovannoj informacionnoj sistemy dlja immuno-biohimicheskikh issledovanij /

Informacionnye resursy i sistemy v jekonomike, nauke i obrazovanii: sbornik statej II mezhdunarodnoj nauchno-prakticheskoj konferencii.- Penza: Privolzhskij Dom znaniy, 2012. - s. 47-50.

3. Paklin N.B., Oreshkov V.I. Biznes-analitika: ot dannyh k znanijam: uchebnoe posobie. 2-e izd., ispr. – SPb.: Piter, 2013. – 704 s.: il.

4. Bureeva N.N. Mnogomernyj statisticheskij analiz s ispol'zovaniem PPP «STATISTICA»: Uchebno-metodicheskij material po programme povyshenija kvalifikacii «Primenenie programmnyh sredstv v nauchnyh issledovanijah i prepodavanii matematiki i mehaniki». - Nizhnij Novgorod: 2007. - 112 s.

5. Voroncov K.V. Algoritmy klasterizacii i mnogomernogo shkalirovanija. Kurs lekcij. MGU, 2007.

6. Informational and analytical resource dedicated to machine learning, pattern recognition and data mining - www.machinelearning.ru/

7. Jiawei H., Micheline Kamber. Data Mining: Concepts and Techniques. San Francisco, 2006. 743 p.

AN ATTRACTOR OF THE DIFFERENTIAL INCLUSION FOR THE MULTILAYER OCEANIC GENERAL CIRCULATION MODEL

Ipatova, V. M.

Dolgoprudny, Moscow Institute of Physics and Technology

We consider the autonomous differential inclusion for the quasi-geostrophic multilayer model of oceanic general circulation. It is proved that the differential inclusions have a compact invariant global attractor.

Keywords: attractor, differential inclusion, multivalued mapping, model of oceanic general circulation, partial differential equation

Many of natural objects (including the atmosphere and oceans of the Earth) are the chaotic systems. Investigation of their predictability needs the in-depth study of the dynamics of the system by describing a minimal uniformly attracting set, which is called an attractor [1-5]. Geophysical fluid dynamics models can describe the natural processes approximately only, so they are obviously having an error and containing the uncertainty [6-8]. Differential inclusion is a direct extension of a concept of differential equation to the case of inexactly given dynamics of the system and incomplete information about it. Differential inclusions are widely used now in optimal control, physics, economics, demography, and other areas [9-13]. A relatively new field is the theory of attractors of multivalued dynamical systems.

A multivalued mapping G for each non-negative moment of time t and each element of the metric space X assigns a nonempty set of the same metric space. G is called a multivalued semiflow (m-semiflow) in X if:

- 1) G is the identity map on X when $t = 0$;
- 2) for all non-negative t, s and all $x \in X$ we have the inclusion $G(t + s, x) \subset G(t, G(s, x))$. M-semiflow is strict if the latter inclusion is replaced by the equality, ie $G(t + s, x) = G(t, G(s, x))$.

A set $P \subset X$ is called an attracting set of m-semiflow G if for each set B bounded in X and for every neighborhood of P there is a time $T > 0$ such that the image of B is contained in the selected neighborhood at all $t \geq T$.

A set $A \subset X$ is called a global attractor of m-semiflow G if:

- 1) A is an attracting set of G ;
- 2) A is negatively semi-invariant, ie $A \subset G(t, A)$ at all $t \geq 0$;
- 3) A is contained in the closure of any attracting set of G (minimality property).

The following theorem gives the sufficient conditions for the existence of a global attractor.

Theorem 1 [14, 15]. *If the m -semiflow G has a compact attractive set and for any $t \geq 0$ the graph of mapping $G(t, \cdot)$ is closed, then G has a compact global attractor. In the case of a strict m -semiflow the attractor is invariant, ie $A = G(t, A)$.*

Suppose a multivalued mapping F for each value $t \geq 0$ assigns a nonempty set of the space E . An integrable branch of the mapping F on the interval $[t_0, t_1]$ is called a single-valued function f belonging to the space of Lebesgue-Bochner $L_1(t_0, t_1; E)$, such that $f(t) \in F(t)$ at almost all $t \in [t_0, t_1]$. The set of all integrable branches of F on the interval $[t_0, t_1]$ will be denoted $L_F(t_0, t_1)$.

Let Ω be a bounded domain in \mathbb{R}^2 with a piecewise smooth boundary $\partial\Omega$. We consider the water cylinder whose projection onto the horizontal plane is Ω . This cylinder is divided across its depth into N layers of mean height H and constant density p_k . Within each layer we introduce a geostrophic stream function ψ_k . Consider the following multilayer quasi-geostrophic ocean general circulation model [1, 5, 16, 17].

$$\begin{cases} \frac{\partial \Delta \psi_1}{\partial t} + J(\psi_1, \Delta \psi_1) + \beta \frac{\partial \psi_1}{\partial x} + \frac{f_0}{H} w_1 - \mu \Delta^2 \psi_1 = f_1, \\ \frac{\partial \Delta \psi_k}{\partial t} + J(\psi_k, \Delta \psi_k) + \beta \frac{\partial \psi_k}{\partial x} + \frac{f_0}{H} (w_k - w_{k-1}) - \mu \Delta^2 \psi_k = 0, \quad k = \overline{2, N-1}, \\ \frac{\partial \Delta \psi_N}{\partial t} + J(\psi_N, \Delta \psi_N) + \beta \frac{\partial \psi_N}{\partial x} + \frac{f_0}{H} (J(\psi_N, h_b) - w_{N-1}) + \nu \Delta \psi_N - \mu \Delta^2 \psi_N = 0, \end{cases} \quad (1)$$

where $w_k = \frac{f_0}{g_k} \left(\frac{\partial}{\partial t} (\psi_{k+1} - \psi_k) + J(\psi_k, \psi_{k+1}) \right)$ is a vertical velocity on the interface between

the layers numbered k and $k+1$; $g_k = g \frac{(p_{k+1} - p_k)}{p_{k+1}} > 0$ is a reduced coefficient of gravity; g

is the acceleration of gravity; f_0, β, μ, ν are positive constants (f_0 is an average value of the Coriolis parameter, β is the gradient of the Coriolis parameter, μ is a viscosity factor, ν is the bottom friction coefficient), $h_b = h_b(x, y)$ is the bottom relief function; $f_1 = f_1(x, y, t)$ is

the wind stress vorticity strength function; $\Delta = \frac{\partial}{\partial x^2} + \frac{\partial}{\partial y^2}$ is the Laplace operator,

$J(a, b) = a_x b_y - a_y b_x$ is the Jacobian.

The system (1) is supplied with the conditions on the boundary of the domain Ω

$$\psi_k|_{\partial\Omega} = C_k(t), \quad \Delta \psi_k|_{\partial\Omega} = 0, \quad k = 1, \dots, N \quad (2)$$

and the water mass conservation law

$$\int_{\Omega} w_k d\Omega = 0, \quad k = 1, \dots, N-1. \quad (3)$$

After that, solutions to (1)–(3) can be determined up to a constant, depending of time. We choose one additional condition $\int_{\Omega} \psi_1 d\Omega = 0$. Then, using (2) and (3) we find

$$\int_{\Omega} \psi_k d\Omega = 0, \quad k = 1, \dots, N. \quad (4)$$

System (1), (2) and (4) now supplied with the initial conditions at $t = h \geq 0$

$$\psi_k|_{t=h} = \psi_k^0(x, y), \quad k = 1, \dots, N. \quad (5)$$

By $\|\cdot\|$ we denote the norm in the real space $L_2(\Omega)$; $|\Omega|$ is the area of Ω ; $W_2^n(\Omega)$, $n = 1, 2$ are the Sobolev spaces of functions that are square integrable in Ω with its derivatives up to order n ; $W_2^1(\Omega) = \{\varphi \in W_2^1(\Omega) | \varphi|_{\partial\Omega} = 0\}$; $W_{2,0}^2(\Omega) = W_2^2(\Omega) \cap W_2^1(\Omega)$.

For vector-valued functions $u = (u_1, \dots, u_N)$ define the spaces $E = (L_2(\Omega))^N$, $E_1 = \left(W_2^1(\Omega)\right)^N$, $E_2 = \left(W_{2,0}^2(\Omega)\right)^N$.

We denote $\varphi_k = \psi_k - C_k$, ie $\nabla \varphi_k = \nabla \psi_k$, $\varphi_k|_{\partial\Omega} = 0$, and rewrite the problem (1)-(2), (4)-(5) in the form

$$\Phi(\varphi) \equiv (F(\varphi); T_h \varphi) = (f; \varphi^0), \quad (6)$$

where

$$\varphi = (\varphi_1, \dots, \varphi_N), \quad f = (f_1, \dots, f_N), \quad \varphi^0 = (\varphi_1^0, \dots, \varphi_N^0); \quad F(\varphi) = (F_1(\varphi), \dots, F_N(\varphi));$$

$$T_h \varphi = \varphi|_{t=h};$$

$$F_k(\varphi) = \frac{\partial \Delta \varphi_k}{\partial t} + J(\varphi_k, \Delta \varphi_k) + \beta \frac{\partial \varphi_k}{\partial x} + \frac{f_0}{H}(w_k - w_{k-1}) - \mu \Delta^2 \varphi_k +$$

$$+ \delta_{k,N} \left[\frac{f_0}{H} J(\varphi_N, h_b) + \nu \Delta \varphi_N \right], \quad \delta_{k,N} \text{ is the Kronecker symbol,}$$

$$w_k = \frac{f_0}{g_k} \left(\frac{\partial}{\partial t} (\varphi_{k+1} + C_{k+1} - \varphi_k - C_k) + J(\varphi_k, \varphi_{k+1}) \right), \quad k = \overline{1, N-1},$$

$$w_0 = w_N = 0, \quad C_k = -\frac{1}{|\Omega|} \int_{\Omega} \varphi_k d\Omega.$$

Hereafter we assume $h_b(x, y) \in W_2^2(\Omega)$. Solvability of the problem (6) was studied in [1, 16]. Shall assume that $f \in L_2(h, T; E)$ for any $T > h$ and denote $\varphi(x, y, t) = V_f(t, h)\varphi^0$ the solution to (6) at the time $t \geq h$. Thus defined the continuous operators $V_f(t, h): E_1 \rightarrow E_1$ and $V_f(s, t)V_f(t, h) = V_f(s, h)$ for all $s \geq t \geq h \geq 0$.

Suppose we are given a function $f_1^0 \in L_2(\Omega)$ and positive constants r_k , $k = \overline{1, N}$. Define on $\square_+ = [0, +\infty)$ the multivalued mappings

$$F_1(t) = \left\{ \zeta \in L_2(\Omega) \mid \|\zeta - f_1^0\| \leq r_1 \right\}, \quad F_k(t) = \left\{ \zeta \in L_2(\Omega) \mid \|\zeta\| \leq r_k \right\}, \quad k = \overline{2, N},$$

$$F = (F_1, F_2, \dots, F_N).$$

Consider the differential inclusion

$$\Phi(\varphi) \equiv (F(\varphi); T_h \varphi) \in (F; \varphi^0). \quad (7)$$

The solution of the differential inclusion (7) on the interval $[h, T]$ will be called the solution of the equation (6) when a right-hand side of the equation is an integrable branch $ff \in L_F(h, T)$ of the multivalued mapping F . We denote $Z(t, \varphi^0)$ the set of solutions to (6)

for $h = 0$, $t \geq 0$ and $\varphi^0 \in E_1$. Obviously, $Z(t, \varphi^0)$ is not empty and the mapping $Z: \mathbb{R}_+ \times E_1 \rightarrow P(E_1)$ is a strict m-semiflow. By using a priori estimates [5] and weak convergence of solutions [16, 17] we verify that the m-semiflow Z satisfies all the conditions of Theorem 1. Namely, we have the following result [15].

Theorem 2. *M-semiflow $Z: \mathbb{R}_+ \times E_1 \rightarrow P(E_1)$, generated by the differential inclusion (7), has a compact invariant global attractor $A \subset E_2$.*

References

1. Bernier Ch. Existence of attractor for the quasi-geostrophic approximation of the Navier-Stokes equations and estimate of its dimension. *Advances in Mathematical Sciences and Applications*, 4:2 (1994), 465-489.
2. Dymnikov V.P., Gritsoun A.S. Climate model attractors: chaos, quasi-regularity and sensitivity to small perturbations of external forcing. *Nonlinear Processes in Geophysics*, 8:4 (2001), 201-209.
3. Filatov A.N., Ipatova V.M. On globally stable difference schemes for the barotropic vorticity equation on a sphere. *Russ. J. Numer. Anal. Math. Modelling*, 11:1 (1996), 1-26.
4. Ipatova V.M. On uniform attractors of explicit approximations. *Differential Equations*, 47:4 (2011), 571-580.
5. Ipatova <http://www.reference-global.com/doi/abs/10.1515/RJNAMM.2011.008-aff1#aff1> V.M. Uniform attractors of finite-difference schemes for the multilayer quasigeostrophic model of ocean dynamics. *Russ. J. Numer. Anal. Math. Modelling*, 26:2 (2011), 143-159.
6. Ipatova V.M. Convergence of the numerical solution of the variational data mastery problem for altimetry data in the quasigeostrophic model of ocean circulation. *Differential Equations*, 34:3 (1998), 410-418.
7. Agoshkov V.I., Ipatova V.M. Study of variational data assimilation problem for a model of tide dynamic in adjacent seas. *Russ. J. Numer. Anal. Math. Modelling*, 21:2 (2006), 111-138.
8. Agoshkov V.I., Ipatova V.M., Zalesnyi V.B., Parmuzin E.I., Shutyaev V.P. Problems of variational assimilation of observational data into ocean general circulation models and methods for their solution. *Izvestiya, Atmospheric and Oceanic Physics*, 46:6 (2010), 677-712.
9. Polovinkin E.S., Smirnov G.V. On one approach to the differentiation of multivalued mappings and necessary conditions for optimality of solutions to differential inclusions. *Differents. Uravneniya*, 22:2 (1986), 944-954.
10. Balashov M.V., Polovinkin E.S. M-strongly convex subsets and their generating sets. *Sbornik: Mathematics*, 191:1 (2000), 25-60.
11. Polovinkin E.S., Ivanov G.E., Balashov M.V., Konstantiov R.V., Khorev A.V. An algorithm for the numerical solution of linear differential games. *Sbornik: Mathematics*, 192:10 (2001), 1515-1542.
12. Zakharov V.K., Polovinkin E.S., Yashin A.D. Mathematical model of a state. *Doklady Mathematics*, 75:2 (2007), 208-212.
13. Polovinkin E.S. On the calculation of the polar cone of the solution set of a differential inclusion. *Proceedings of the Steklov Institute of Mathematics*, 278:1 (2012), 169-178.

14. Kapustyan O.V., Mel'nik V.S., Valero J., Yasinsky V.V. Global attractors of multi-valued dynamical systems and evolution equations without uniqueness, Kyiv: Naukova Dumka, 2008.
15. Ipatova V.M. Attractors of differential inclusions for models of the atmospheric and oceanic dynamics, containing multivalued functions. *Nelinejny'j mir*, 11:8 (2013), 545-553.
16. Agoshkov V.I., Ipatova V.M. Solvability of the altimeter data assimilation problem in the quasi-geostrophic multilayer model of ocean circulation. *Computational Mathematics and Mathematical Physics*, **37**:3 (1997), 348-358.
17. Agoshkov V.I., Ipatova V.M. Convergence of solutions to the problem of data assimilation for a multilayer quasigeostrophic model of ocean dynamics. *Russ. J. Numer. Anal. Math. Modelling*, **25**:2 (2010), 105-115.

CHARGED BOARD EVENT ANALYSIS USING CIRCUIT SIMULATOR FOR PCB MOUNTED MOSFET

Kusnetsov V.V., Kechiev L.N.
Russia, Moscow, MIEM HSE

The model of CDM ESD impact on MOS transistors mounted on printed circuit boards is considered. The results of modeling is compared to results of ESD testing for test boards. The MOS transistor failure level decreasing is researched.

Keywords: ESD, CBE, CDM, circuit simulator, MOSFET

ESDs devices can accumulate static charge. If it then contacts massive metal parts (for example insertion head), rapidly discharge occurs from ESDs device to metal object. This event is known as Charged Device Model (CDM) [1].

CDM rating of ESDs devices depends on many factors. Mainly component package design determines CDM rating. Equivalent package capacitance determines charge amount, that can be accumulated by ESDs component. CDM ESD event modelling was considered in [2, 3]. In [4] is reported, that CDM ratings for ESDs devices, mounted on PCBs, decrease dramatically. So, if 3500 V CDM rating falls to 900 V, when component mounted on 12x12 inch PCB. ESDA White Paper [5] even introduces new ESD model — Charged board event model. The researches of this subject was started only in 2007-2008. There is no exact data for CDM ratings for specific ESDs devices and PCBs.

The purpose of this paper is to independently check results, declared in [4]. CDM impact model was developed and experimental measurements were taken for this purpose. The object of our research was International Rectifier power MOSFETs. Circuit model for CDM and CBE ESD events is proposed. Physical parameters of object is replaced by equivalent circuit components parameters in our model.

CDM ESD event equivalent circuit for component with multiple pins is shown on figure 1. This circuit can be reduced for components with three or two pins, such as diodes and transistors.

This equivalent circuit can be simulated using general purpose circuit simulators, such as PSpice. Transient analysis need to be performed for this equivalent circuit. Open-source circuit simulator Qucs was selected for performing simulation in this research. The advantage of Qucs is that it is free and open-source and allows to perform transient analysis with

picoseconds step, because not all commercial circuit simulators support picosecond transient analysis.

International Rectifier power MOSFET IRF510 was chosen as object of this research. MOSFET is basic unit of all modern semiconductor components, and results obtained for MOSFET can be extended to more complex semiconductor devices. This MOSFET has class C4 (1000 V) CDM rating.

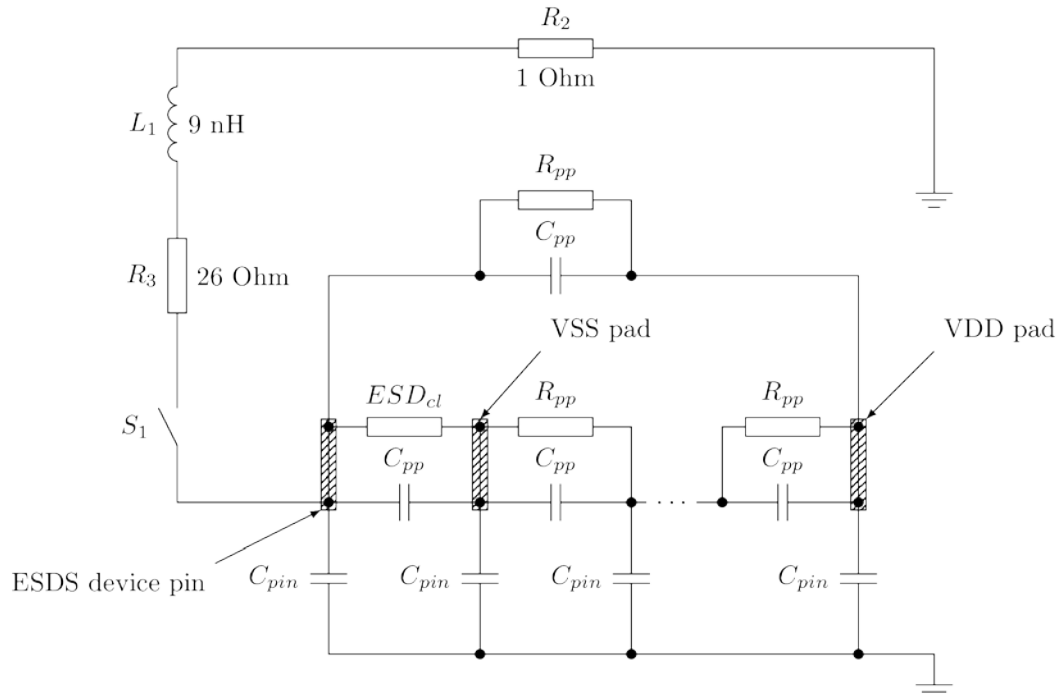


Figure 1. The CDM ESD event equivalent circuit. R_2 — current sensor resistor; R_3 — arc resistance; $C_{pin}=1-5\text{pF}$ — ESDS device pin to ground capacitance; $C_{pp}=1-5\text{pF}$ — pin to pin capacitance; $R_{pp}\gg 1\text{M}\Omega$ — leakage resistance; ESD_{cl} — ESD clamp circuit.

Now having CDM event equivalent circuit, we can simulate CDM impact for IRF510 MOSFET using Qucs. IRF510 under CDM impact in Qucs shown on figure 2. Standard library model for IRF510 was used without any special adaptations. C2 on this figure is capacitance of PCB ground plane, connected to source. If there is no PCB, it can be set to few picofarads.

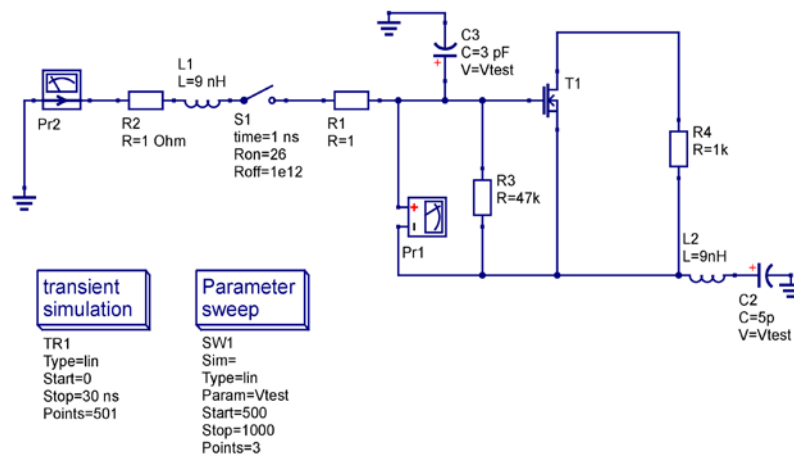


Figure 2. IRF510 under CDM impact in Qucs.

We can perform transient analysis for this circuit and research gate-source voltage (V_{gs}) waveform. If V_{gs} voltage exceeds gate dielectric breakdown level (75 - 80 V for IRF510), MOSFET fails. Having V_{gs} waveform, we can determine CDM voltage level at which transistor fails. To simulate CBE event it is need to increase C2 to PCB capacitance (for example $C_{pcb}=190$ pF for test board).

Resulting transient MOSFET gate voltage waveform is shown on figure 3. Test voltage is 250V. You can see, that peak gate voltage exceeds breakdown level (75 V for IRF510). It means, than MOSFET must fail after CDM event. If test board accumulates static voltage at level 250V, and MOSFET gate then contacts to ground, CDM event occurs and MOSFET fails.

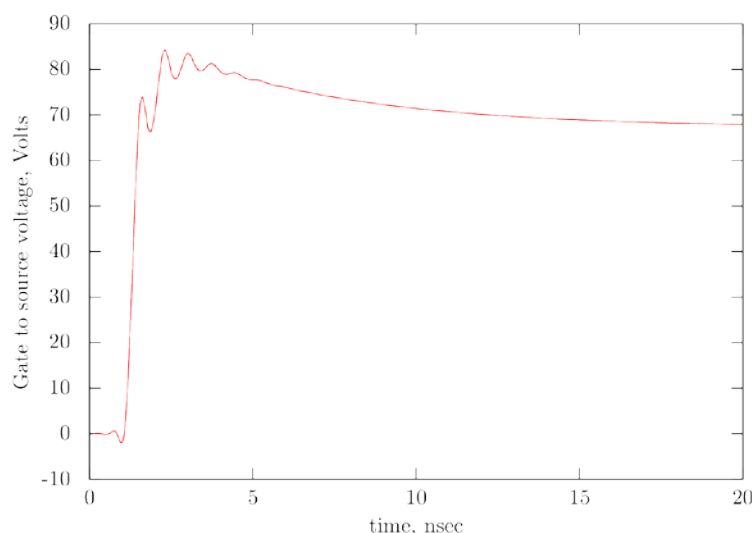


Figure 3 . CDM discharge voltage waveforms into gate of IRF510. MOSFET mounted on PCB. Test voltage 250V.

To determine CBE rating for other MOSFETs and other PCBs, it is need to do following. MOSFET spice model can be found in MOSFET datasheet and needs no adaptation. Gate dielectric breakdown voltage also can be found in datasheet. At first it is need to measure capacitance of copper polygon on PCB, connected to MOSFET source, to ground. It can be measured using general RCL-meter. Than C2 capacitance value on figure 2 need to be replaced by measured value. Transient gate voltage waveform may be obtained using transient simulation of circuit shown on figure 2. If peak gate voltage exceeds breakdown voltage at current test voltage V_{test} , MOSFET fails after CDM ESD impact. You can manually increase test voltage V_{test} , or use parameter sweep to determine test voltage at which peak gate voltage exceeds breakdown level.

Analysis of this model shows, that massive copper polygons on PCBs, connected to MOSFET source, store additional charge. When discharging, this charge travels to ground through MOSFET and makes additional voltage overshoots at MOSFET gate. Using this simulation method we can find CDM rating for PCB mounted MOSFET. So, CDM rating for IRF510 with test board was founded. It is 250 V. CDM rating for this transistor decreased in 4 times.

Now we can fabricate test PCB, mount IRF510 on it and perform CDM tests, using CDM ESD testing setup. Schematic of this setup is shown on figure 4. After perform test, we can compare CDM ratings, founded by modeling and by experimental testing. We should obtain same results.

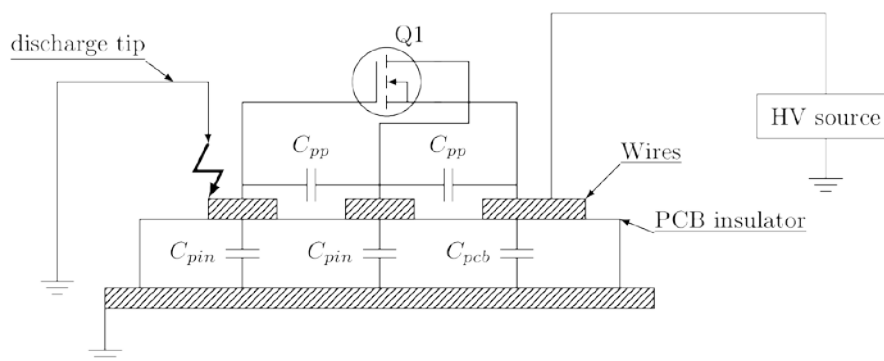


Figure 4. MOSFET mounted on PCB under CDM impact in test setup. C_{pcb} — equivalent capacitance of ground plane connected to MOSFET source.

Failure level for IRF510 founded by experimental way was also 250 V, as for our circuit model. Difference is less than 5 % between CDM rating, founded from circuit model and CDM rating obtained experimentally. Data obtained in [4] was experimentally checked. Indeed, CDM rating for MOSFET decreases in few times. Reduction factor is more than 50 %. CDM ESD event is dangerous even for power MOSFETs, mounted on PCBs.

Having PCB capacitance value, which can be measured with general purpose equipment, and using our CDM and CBE circuit simulation method, CDM ratings for PCB mounted MOSFETs can be found.

References

1. L. N. Kechiev and E. D. Pozhidaev. Zashita elektronnykh sredstv ot vozdeystviya staticheskogo elektichestva. Moscow: ID «Technologii», 2005.
2. M. D. Ker, C. Y. Lin, and T. L. Chang. Layout styles to improve CDM ESD robustness of integrated circuits in 65-nm CMOS process. In International Symposium on VLSI Design, Automation and Test (VLSI-DAT), pages 374–377, Hsinchu, Taiwan, April 2011.
3. M. S. B. Sowariraj, C. Salm, T. Smedes, A. J. Tom Mounthan, and F. G. Kuper. Full chip model of CMOS integrated circuits under charged device model stress. In 7th annual workshop on semiconductor advanced for future electronics, Veldhoven, Netherlands, November 2004.
4. J. Colnar, J. Trotman, and R. Petrice. Decreased CDM ratings for ESD-sensitive devices in printed circuit boards. In Compliance, pages 38 – 41, September 2010.
5. Industry Council on ESD Target Levels. White Paper 2: A Case for Lowering Component Level CDM ESD Specifications and Requirements, April, 2010.

ELECTROSTATIC POTENTIAL METER WITH HIGH INPUT OVERSHOOTS ROBUSTNESS

Kusnetsov V.V.
Russia, Moscow, MIEM HSE

Contact electrostatic potential meter is presented. This device has high input overvoltage robustness. It can withstand 10 kV peak ESD impulse or 250 V DC voltage directly applied to its input. Measurement range can be from 5V to few kilovolts. Inverse mode vacuum tubes used in this device.

Keywords: electrostatic discharge, electrostatic potential, electric field meter, induction probe, capacitive potential divider

There are two main methods for measuring electrostatic voltages and field strength: induction probe method and field mill method [1, 2]. All of those methods are non-contact methods. Distance from object to field meter sensor need to be carefully set. This is fallback of those methods. It is not always possible. For contact methods it is not need to do that. But measurement object can carry electrostatic voltage up to few kilovolts. ESD occurs after contact with field meter probe and field meter input can be damaged by ESD pulse.

The purpose of this research is to develop contact electrostatic voltage meter with extra high input overshoots robustness.

We developed electrostatic potential meter, which has lower measurement range from 5 V and can withstand ESD pulses up to 10 kV. This features were obtained using in this device inverse mode vacuum tube circuitry [3]. Inverse mode tube is driven by negative plate voltage. Control grid is connected to positive voltage source. Plate voltage drives control grid current. This mode of tube operation has very high input impedance up to 100 TOhm.

Contact electrostatic voltage meter circuit is shown on figure 1.

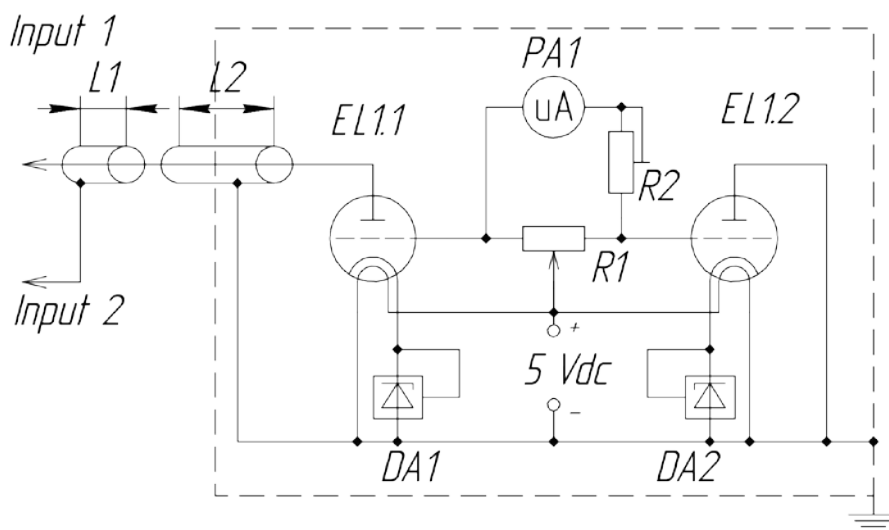


Figure 1 . Contact electrostatic potential meter

This is differential bridge electrometric amplifier. Input resistance of this circuit is more than 20 TOhm. Input current is less than 7×10^{-13} Amps. Measurement range is from 0 to 20 V for input #1. This device is able to measure not only electrostatic potentials but also usual DC voltage. Probe is connected to plate of EL1.1 with RG-58 coax cable. R1 potentiometer sets zero. Microammeter PA1 shows static potential. This field meter is able to measure also static charge.

Capacitive divider [4] (coax cable stubs L1 and L2) is used to extend measurement range.

ADC interface may be connected instead of microammeter. ADC may be connected to PC and this static potential meter may be used for measurement results writing to PC. For example, you can see charging and charge decay curves, obtained by our field meter on figure 2.

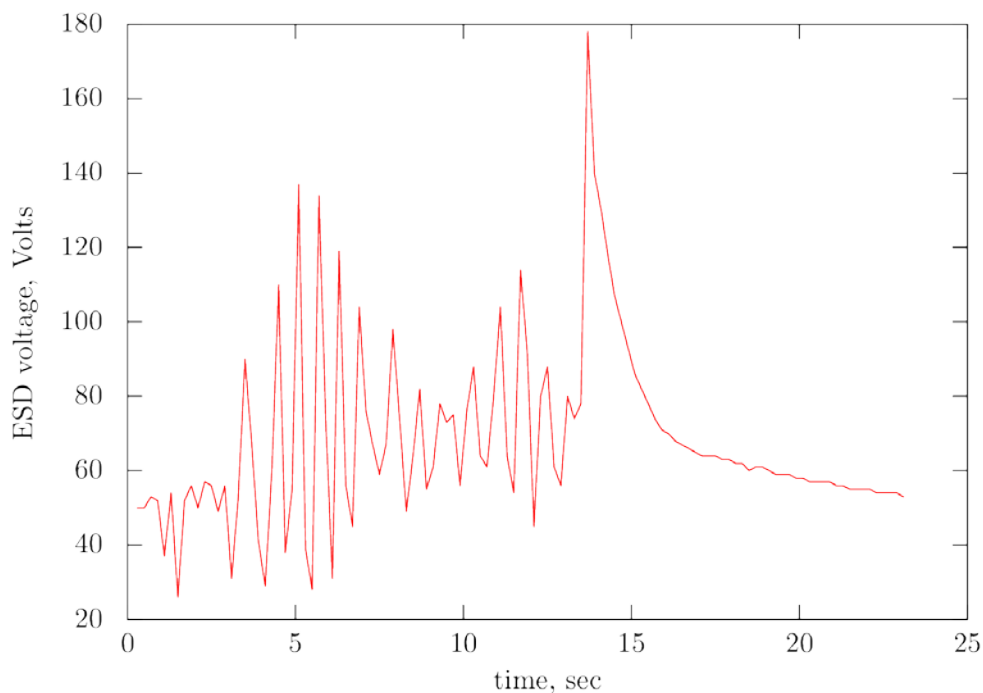


Figure 2 . Charging and discharging of PCB in contact with packing paper.

This electrostatic potential meter has some disadvantages. Preheat is needing for proper functionality and probe grounding is needing before each measurement.

This electrostatic potential meter circuitry was patented [5] in Russia and this device is used for static charge personal and equipment monitoring at electronic manufacturing company.

References

1. Miles R., Bond T., Meyer G. Report on non-contact DC electric field sensors. Lawrence Livermore National Laboratory, 2003.
2. Methods for measurement in Electrostatics. British Standart BS7506: Part2., 1996.
3. Inverted tube operation — A practical SE OTL amlifier topology. <http://greygum.net/sbench/sbench102/inverted.html>.
4. Lucas J. R. High voltage engineering. Department of electrical engineering University of Moratuwa, 2001. 211 pp.
5. Kuznetsov V. V. Elektrometer na elektronnykh lampakh v obraschemmom reahime // Patent №118066 10 July 2012. Federalnaya sluzhba po intellektualnoj sobstvennosti patentam i tovarnym znakam.

EQUIVALNCE OF INHIBITORY AND NON-INHIBITORY SAFE PETRI NETS

Pashchenko D.V., Trokoz D.A.
Penza State University

This article considers a problem of transformation of an inhibitory safe Petri net into a non-inhibitory safe Petri net, equivalent to it, by means of the inverse positions addition.

Keywords: inhibitory safe Petri nets, non-inhibitory safe Petri nets, inverse positions, equivalence of Petri nets.

1. Introduction

At the present time it is considered that inhibitory safe Petri nets, i.e. Petri nets with inverse links are more powerful than Petri nets without the said feature [1]. However, the present statement generally is not true [2]. We are to demonstrate that any inhibitory safe Petri net may be presented by a similar non-inhibitory Petri net.

To prove the present suggestion we shall consider all possible position-transition links for an inhibitory safe Petri net. In total there are 5 options of such links:

1. output non-inhibitory link;
2. output inhibitory link;
3. reverse non-inhibitory link;
4. reverse inhibitory link;
5. input link.

We shall consider each above stated link type in detail and describe the process of replacement of an inhibitory Petri net section, containing the given position-transition link, with an equivalent section of non-inhibitory Petri net. Then we are to demonstrate the possibility of similar transformation for a Petri net section, containing a position, present in all 5 above stated types of links simultaneously.

2. Output non-inhibitory link

The link of the said type includes one non-inhibitory arc that appears to be an output one for the position and an input one for the transition (Fig. 1).



Fig. 1 - Output non-inhibitory link

If the position, participating in the present link, has no inhibitory arcs connected with it, the present inhibitory net section requires no modification and may be transferred into an equivalent non-inhibitory net without any alterations. Otherwise, it is necessary to build an equivalent non-inhibitory net section. Thereto it is necessary to include an additional position (hereinafter referred to as an inverse position), which contains a token, while there is no token in the main position. The modified output non-inhibitory link realizing such action in the non-inhibitory net is presented in fig. 2.

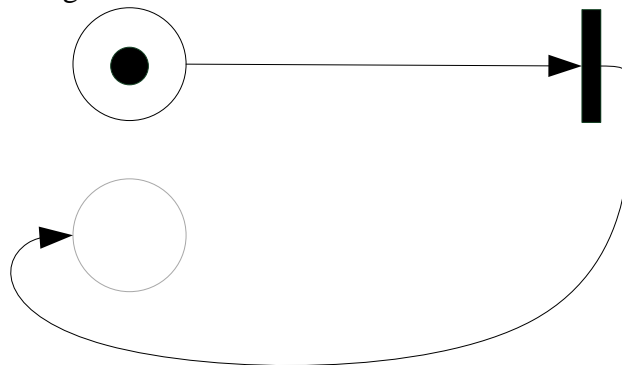


Fig. 2 - Modified output non-inhibitory link

The introduced inverse position, illustrated in grey in fig. 2, enables to avoid usage of inverse arcs irrespective of the number and complexity of links with participation of the initial positions, which will be demonstrated further in the article as a generalized Petri net section, embracing all variants of links, will be presented.

3. Output inhibitory link

The link of the given type includes one inhibitory arc that appears to be an output one for the position and an input one for the transition (fig. 3).



Fig. 3 – Output inhibitory link

The position participating in the given link includes an inhibitory arc, which means that such position-transition link requires certain conversions that would result in obtainment of an equivalent non-inhibitory Petri net section. Similarly to the previous case, it is necessary to introduce an inverse position, which contains a token, while there is no token in the main position. Herewith, the function of the input position for the transition will be performed by the inverse position, but not the main one. The modified output inhibitory link realizing such action in the non-inhibitory Petri net is presented in fig. 4.

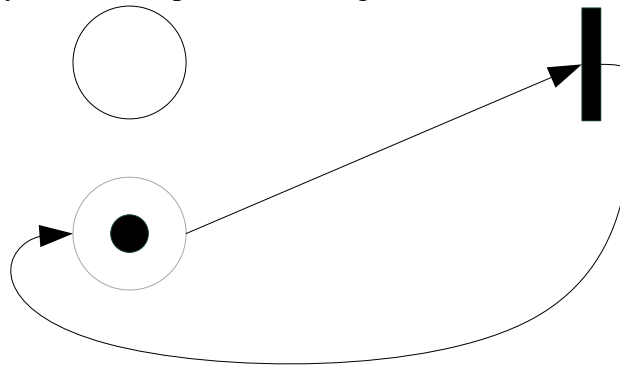


Fig. 4 – Modified output inhibitory link

The introduced inverse position (illustrated in grey in fig. 4) provides transition actuation, while there is no token in the main position, i.e. it provides the equivalent action of the non-inhibitory Petri net section similar to the inhibitory Petri net section.

4. Reverse non-inhibitory link

The link of the given type includes two non-inhibitory arcs. First arc appears to be an output one for the position and an input one for the transition, the second appears to be an output one for the transition and an input one for the position (fig. 5).

Similarly to the variant of the output non-inhibitory link: if the position participating in the given link has no inhibitory arcs connected to it, the present inhibitory net section requires no modification and may be transferred into an equivalent non-inhibitory net without any alterations.

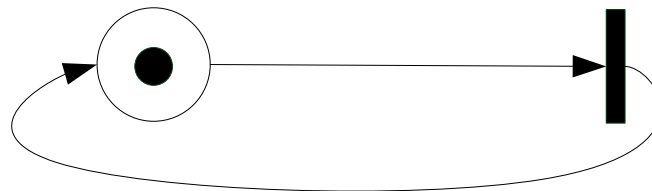


Fig. 5 – Reverse non-inhibitory link

Otherwise, it is necessary to build an equivalent non-inhibitory net section. Thereto it is necessary to include an inverse position. The modified reverse non-inhibitory link realizing such action in the non-inhibitory Petri net is presented in fig. 6.

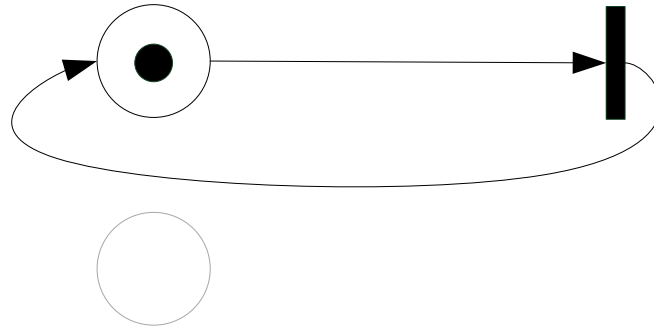


Fig. 6 – Modified reverse non-inhibitory link

Despite the fact that the inverse position, illustrated in grey in fig. 6, practically does not participate in the transaction in the present type of link, it is required in order to connect the present position with other transitions via inhibitory arcs. The necessity of the inverse link addition will be demonstrated further as we consider the generalized Petri net section embracing all possible variants of links.

5. Reverse inhibitory link

The link of the given type includes two arcs. The first arc appears to be an inhibitory output one for the position and an input one for the transition, the second appears to be an output one for the transition and an input one for the position (fig. 7).

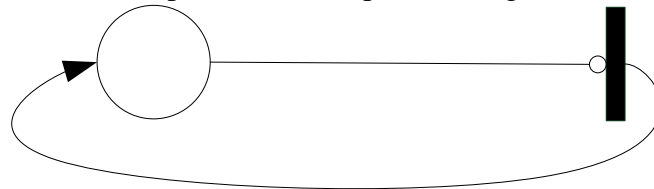


Fig. 7 – Reverse inhibitory link

Similarly to the previous cases, it is necessary to introduce an inverse position, which contains a token, while there is no token in the main position. Herewith, the function of the input position for the transition will be performed by the inverse position, and the main position will perform the function of an output position for the transaction. The described modification of the reverse inhibitory link for the non-inhibitory Petri net is presented in fig. 8.

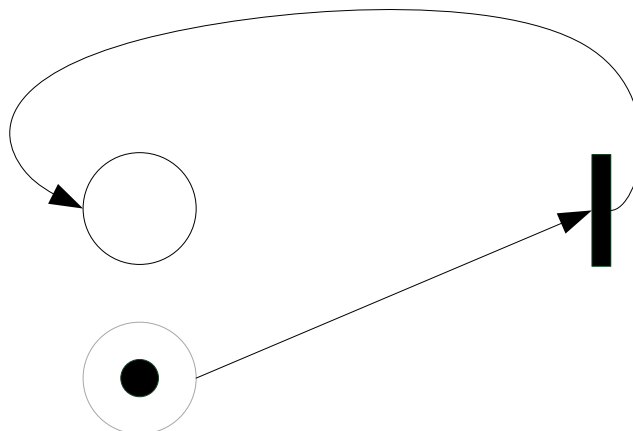


Fig. 8 – Modified reverse inhibitory link

The introduced inverse position (illustrated in grey in fig. 8) provides transition actuation, while there is no token in the main position. Herewith, a token goes from the inverse position into the main one, i.e. the equivalent action of the Petri net non-inhibitory section similar to the inhibitory Petri net section is provided.

6. Input link

The link of the given type includes one arc, which appears to be an output one for the transition and an input one for the position (fig. 9).



Fig. 9 – Input link

Similarly to the previous two types of links without inhibitory arcs, if the position participating in the present link has no inhibitory arcs connected to it, the present inhibitory net section requires no modification and may be transferred into an equivalent non-inhibitory net without any alterations. However, if the case does not meet these conditions, it is necessary to add an inverse position, from which a token will be extracted, while the main position will be taken by a token in the process of transition actuation. The modified input link realizing such action in the non-inhibitory Petri net is presented in fig. 10.

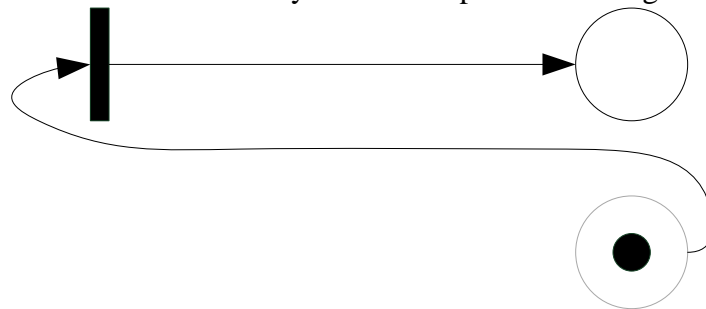


Fig. 10 – Modified input link

The introduced inverse position (illustrated in grey in fig. 8) provides transition actuation, while there is no token in the main position. Herewith, a token goes from the inverse position into the main one, i.e. the equivalent action of the Petri net non-inhibitory section similar to the inhibitory Petri net section is provided.

7. Generalized variant of conversion

Previously considered variants of the transition-position link in the inhibitory Petri net and respective conversions thereof into the equivalent non-inhibitory Petri net section appear to be particular, as there has been no demonstration that such conversion is eligible for an aggregate of the said variants.

We are to demonstrate that such conversions are eligible for a position that is simultaneously connected with transitions by all the above mentioned variants. The described inhibitory Petri net section is presented in fig. 11, where a figure next to a transition designates a number of a link type.

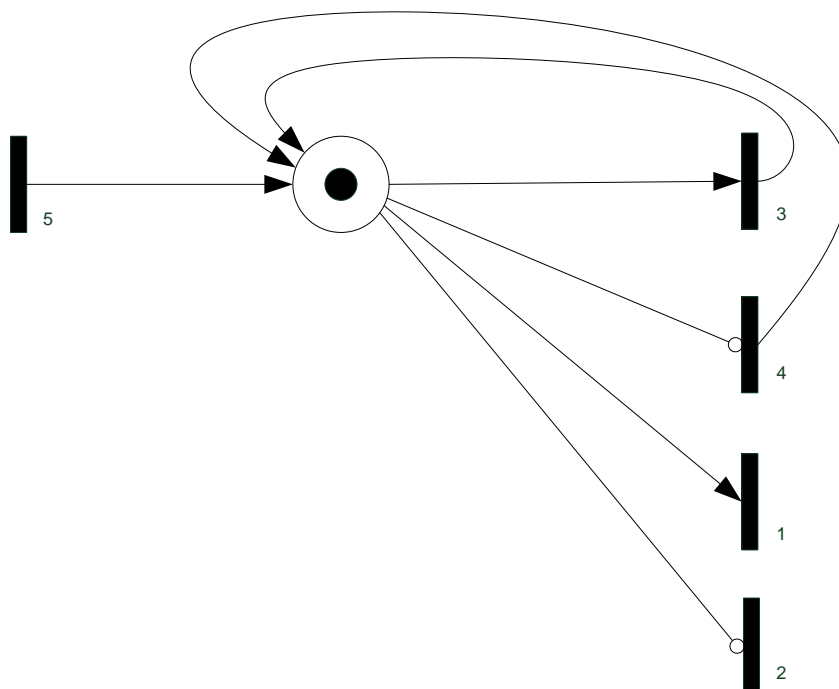


Fig. 11 – Generalized variant of the inhibitory Petri net section

The above presented generalized variant of the inhibitory Petri net section includes 5 different position-transition relations for one position. We shall carry out the conversion for each type of position-transition link separately, as performed in previous paragraphs of the article. As a result of such conversions we will obtain the non-inhibitory Petri net, presented in fig. 12.

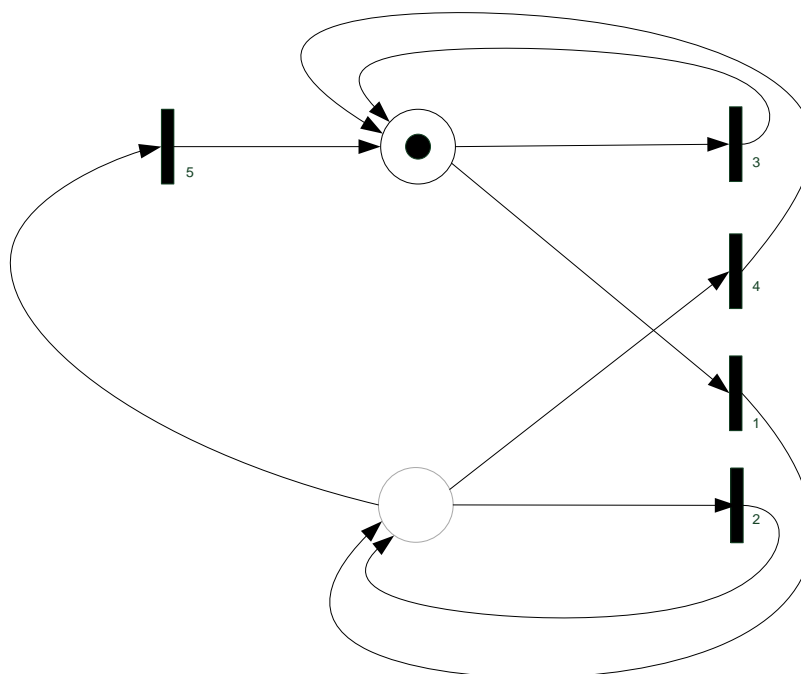


Fig. 12 – Equivalent non-inhibitory Petri net section

The non-inhibitory Petri net, depicted in fig. 12, performs the action similar to the inhibitory Petri net, presented in fig. 11. Hereof it is possible to conclude that the non-inhibitory Petri net obtained via conversions is equivalent to the initial inhibitory Petri net.

Moreover, the adduced illustrations demonstrate admissibility of superposition of separate conversions, i.e. it is eligible to perform a series of conversion for one position and it requires no additional modifications of the non-inhibitory Petri net, obtained as a result of a series of such conversions.

8. Conclusion

The present article proves the possibility of the inhibitory safe Petri net conversion into the equivalent non-inhibitory safe Petri net, and suggests a method of such conversion for all possible position-transition link types and the aggregate thereof.

On the basis of the carried out analysis we may conclude that the inhibitory safe Petri nets and the non-inhibitory safe Petri nets are equipollent, and all the problems solved by means of the former may be solved by the latter.

The present approach may be implemented for solution of particular problems of information protection systems that successfully exploit the mathematical apparatus of the theory of the inhibitory safe Petri nets [3], as well as for modeling diagnostic computation systems [4].

The results of the study may be applied in modeling of large data arrays [5] and in modeling of relational databases [6].

References

1. Pashchenko D.V. Problems in building multithreading models of software for the expert system of aircraft radar facilities / D.V. Pashchenko, D.A. Trokoz//University proceedings. Volga region. Engineering sciences. -2011. -№ 2 (18). -P. 21-29.
2. Volchikhin V.I. Modeling of a data upload subsystem of the ground control system for aircraft radar facilities using the Petri net apparatus / V.I. Volchikhin, D.V. Pashchenko, D.A. Trokoz// University proceedings. Volga region. Engineering sciences. - 2010. № 3. P. 37-48.
3. Pashchenko D.V. Development of a multithreading model of software for the expert system of aircraft radar facilities / D.V. Pashchenko, D.A. Trokoz// University proceedings. Volga region. Engineering sciences. - 2011. № 3. P. 56-64.
4. Pashchenko D.V., Trokoz D.A. Modeling principles of multithreading data processing using Petri nets for aircraft radar facilities diagnostics. -B collected articles: New information technologies and systems. Part 2. Proceedings of the 9th International scientific and technical conference, Penza, 2010, p. 89-94
5. Trokoz D.A. Strategy of parallel processing of large data arrays in the system of objective control of the radio-technical complex of radar patrol and guidance /V.A. Machalin, D.V. Pashchenko, D.A. Trokoz, M.N. Sinev //Problems of radio electronics problems. -2009. -Issue. 4. -P. 139-144. -(Series: Computer technology).
6. Pashchenko D.V. Tabular processing of data registered by aircraft radar facilities /D.V. Pashchenko, D.A. Trokoz//Problems of radio electronics. -2009. -Issue. 4. -2009. -P. 139-144. -(Series: Computer technology).

ABOUT THE MICROSCOPIC PICTURE OF THE HOLE TRANSPORT IN DEH-DOPED POLYCARBONATE

Pozhidaev Evgenii D., Smirnov Dmitrii D. and Pozhidaeva Natalia V.
National Research University Higher School of Economics,

This paper concerns the problem of charge carrier transport in homogeneous polymers.

Keywords: Charge transport, molecularly doped polymers, time of flight, radiation induced conductivity.

Our approach to the problem of charge carrier transport in homogeneous polymers assumes carrier hopping on a densely packed manifold of transport (hopping) centers retaining the short-range order of the respective single crystal [1,2]. The central idea, which distinguishes it from the Bassler's disorder theory [3], is that the energy scatter concerns only a small fraction ($\leq 1\%$) of hopping centers, which begin to act as traps. The majority of isoenergetic centers build up a transfer band (analogue of the conduction band or extended states) with microscopic mobility μ_0 equal to that in the respective single crystal. The origin of the energy scatter (and traps themselves) is ascribed to the elementary voids of the fluctuation free volume [4] forming an association with the normal hopping centers. Trap release rate (or frequency factor V_0) have been found to be modulated by molecular relaxations (specifically, hindered rotations) at elevated temperatures. To insure the dispersion parameter $\alpha \approx const$ over a wide range of time trap energy distribution is taken to be exponential.

These considerations allow one to reconcile hopping transport of charge carriers with the multiple trapping formalism (and the Rose-Fowler-Vaisberg model based on it) which describes the radiation induced conductivity of polymers so well [5]. Close analogy of the radiation induced conductivity response of DEH-doped polycarbonate and that of poly-N-vinylcarbazole and polystyrene suggests that the above considerations are possibly applicable to it.

Indeed, in this case the short-range order in the packing of dopant molecules may be lacking. Nevertheless, if the real reason for their energy scatter is the fluctuation free volume then we again come to the concept of the transfer band this time in the form of the diffusion cluster in the bond disordered system. The low value of the frequency factor ($\sim 10^6 \text{ s}^{-1}$) is rather surprising but in line with most common polymers including poly-N-vinylcarbazole. To understand this one needs information about relaxation dynamics (translational as well as rotational) of small guest molecules (DEH, TFA etc.) in rigid polymer matrices. The case of lightly doped Molecularly doped polymers is even more complex and merits special consideration. Effects of spatial correlation due to charge-dipole interactions are to be properly accounted for as well [6-9].

Molecularly doped polymers are disordered polymer systems if only because of positional disorder of the dopant molecules. By analogy with common polymers (photoconductive poly-N-vinylcarbazole included) charge carrier transport in Molecularly doped polymers is expected to be dispersive rather than Gaussian. To prove this assertion we performed extensive studies in DEH-doped polycarbonate using both the radiation induced conductivity and time-of-flight techniques. Except plateau region of the time-of-flight

transients excited by electron beam all observations could be consistently explained in terms of the multiple trapping model incorporating the multiple trapping formalism.

So, time-of-flight excited by electron beam and the radiation induced conductivity lead to contradictory results regarding hole transport in Molecularly doped polymers. We believe that only parallel measurements of time-of-flight and bulk conductivity generated by light and electron beam will help to understand the nature of this effect.

References

1. A.P.Tyutnev, D.N.Sadovnichii, V.S.Saenko, and E.D. Pozhidaev, Chem. Phys. Reports 19, №7 (2000)
2. A.P.Tyutnev, D.N.Sadovnichii, V.S.Saenko, and E.D. Pozhidaev, Polymer Science A 42, 6 (2000)
3. H.Bassler, Physica Status Solidi (b) 107, 9 (1981)
4. J.Lin, Q.Deng, and Y.C.Jean, Macromolecules 26, 7149 (1993)
5. A.P.Tyutnev, High Energy Chem. 30, 1 (1996)
6. A.V.Vannikov, A.D.Grishina, and S.V. Novikov, Russian Chem. Rev. 63, 103 (1994)
7. S.V. Novikov, D.H. Dunlap, V.M. Kenkre, P.E.Parris, and A.V. Vannikov, Phys. Rev. Lett. 81, 4472 (1998)
8. Tyutnev A.P., Ikhsanov R. Sh., Saenko V.S., Pozhidaev E.D. Analysis of the time-of-flight transients in molecularly doped polymers using the Gaussian disorder model // J. Phys.: Condens. Matter. 2011. V. 23. P. 325105(6 pages).
9. Tyutnev A.P., Saenko V.S., Pozhidaev E.D. Dipolar disorder formalism revisited // Chem. Phys. 2011. V. 389. N. 1-3. P. 75-80.

METHOD CONCEPTUALIZATION OF SUBJECT DOMAIN AS A BASIS OF TECHNOLOGY OF ACQUISITION KNOWLEDGE FOR INTELLIGENCE SYSTEMS

Bolotova L.S.
Moscow, MIEM SRI HSE

In the report methodological principles of designing of intelligence systems are considered and bases of a method of the conceptual analysis and designing of model of the subject domain, based on ideas of situational management and semiotics modelling are stated.

Keywords: decision-making, conceptualization, subject domain model.

Intelligence information systems as knowledge based systems

Today the term *INTELLIGENCE*, became adjective for concepts named systems, models, organizations, corporations, companies, etc. Thus, authors of these terms try to underline the knowledge significance, as most important resource of any organization. Our main point is that knowledge-based (KB) systems should be addressed with engineering approach, *i.e. as to the objects of engineering design*. Thus, there is a need for methodology, technology, tools supporting all stages of this process. The above analysis demonstrates that while the tools for KB designing and maintaining their integrity at all stages of the life cycle

are not available, there will be only variety of isolated approaches, methods, models, software [1, 2].

When we create some artificial system (AS), we always make a goal for which we are going to create AS. Knowledge should answer the question:

- how it is possible to achieve the desired goals through this AS;
- knowledge is to show how much the object is adequate for the goal achievement;
- what we have to do with this knowledge and how, to achieve our goals;
- a list of actions to be taken towards such objects is a starting point for designing any AS, as a facility for achievement of desired goals;
- these actions, may be not fully, but should be determined;
- complex solutions are represented by combinations of selected actions;

This elementary unit of activities is called *an act of activity*.

It arouses a question. What means for description of actions and knowledge can ensure achievement of the desired goals? As G.P. Schedrovitsky is saying it can be done by already assimilated means, i. e. the tools we have mastered (learnt how to understand them and use in practice) [3]. Such means are, for example, natural language (NL) or some formal languages, for example, a language of mathematical logics, algebra etc., if we learnt how to represent situations in these languages and to do the respective transformations. This situation should be equally fair for decisions taken by people, as well as those generated by intellectual information system (IIS) simulating these acts. It means that human knowledge required for goal achievement should be acquired with his help and then they are to become assimilated tools for IIS, i.e. its own tools. As *initial material* processed by us, there may be description of current situations and goals, and as *a product*, i.e. a result, *there should be decisions in the form of the necessary actions sequence, which are the transformation algorithms synthesized by AS*.

The one thing is clear. We need the systematic analysis of activities in the object domain and the technology of its realization. So let us decide what definition of the system we will take for further deliberations.

The principle of systematic activities in designing of AS

In the theory of systems and system analysis there are many definitions of the concept «System» and its main elements [3]. But, if to proceed from understanding that the system approach is the method to organize our activities, then this method is most fully described in the methodology and definition of G.P Schedrovitsky [4].

From the definition point of view, to represent something as a simple system means to describe it in terms of:

- processes (1);
- functional structure (2);
- organized material, i.e. a structure (3);
- material or morphology (4).

In other words, if there is some object, then to represent it in the form of simple system or monosystem means: describe it once as a process, the second time as a functional structure, for the third time, as an organized structure of the material or morphology, for the fourth time, as just a material. And these four descriptions should be attributed to one object and interrelated.

Then, to represent an object as a polysystem or a complex system, it should be described in such a way many times and links should be established between these four standard representations. This definition of the system includes descriptions: in terms of processes, functional structure and morphology.

To realize this structural and system approach, it is necessary:

- to specify a sequence of actions (operations or procedures), which will create the system;
- based upon these actions, to record the object properties as the object of these actions - (a), (b), (c)...
- to assign to the object symbolic forms, in which these properties will be recorded.

Thus, if the sequence of actions is known, we will be able to determine operational (procedural) content of the selected objects. Only now, and it is the most important thing, the question **about where natural boundaries of the object lie** can be answered. Every time they are outlined by where some process was able to propagate to. That is the scheme (**and the principle**) of the activity act.

So **the activity act** indicates the following:

- initial material – an object, tools and instruments;
- product- the result of transformation due to certain actions;
- certain goals;
- required knowledge.

So, knowledge is brought into activities «from outside» through communication. It absorbs the past experience and ensures the experience transfer, i.e. all components of the activity act. Thus, knowledge is always systematic in terms of its content, since it supports all elements of the activity act, but does not correlate with the object directly. This principle can be elaborated into two more:

- The first principle (one part of the activity act scheme: initial material, partially tools and product) – regards the totality of actions one has to implement: split the single whole, link the elements, identify properties, etc., correlate the latter with operations and actions.
- The second principle (the second part plays the role of the object in symbolic form) - regards symbolic form of the object.

This is a manifest of dual principle of any knowledge and any **symbolic form**.

A very important fundamental conclusion comes out of here: symbolic form, is what ensures correlation between actions and their object. If there is an indication to the object, there is also an indication to its arrangement. The object arrangement and our actions already correlated by the symbols arrangement. **In other words, a symbol is nothing, but what connects the operational aspect and the object design.**

It means that knowledge always carries four characteristic contents:

- indicates the object;
- indicates actions or operations;
- is expressed in certain symbolic form (linguistic, graphic etc.);
- indicates concepts, where it exists.

At the next step it is necessary to understand what ties are there between processes, functional structures, design and material. For each content there should be its own language, its own repertory of concepts, to get a four-plane image of our object. Then the system concept will be obtained. All four different contents are expressed in the symbolic form, which pulls them into a single one, but they are different, i.e. not isomorphic. It means that connectivity as all ties between the object elements gets reflected in its structure, which is an expression of its organized nature.

Methodological and technological grounds for designing a model of the object domain and knowledge bases in the decision taking and control systems

Following definition of the concept «System», for its realization it is necessary to answer the following questions:

How and in what structural unit can all forms (process, functional, organizational and morphologic) of representing the simulated and controlled object be connected together?

Based upon what concepts they should be selected?

How to determine the necessary and sufficient depth of the object description and all its elements, in which expressions and forms?

What language is required to describe all object facets (properties)? Etc.

In principle, the above definition gives answers to the questions asked, but it is necessary to find a clue to their constructive solution.

We believe that answers to these questions, can be rather efficiently given based upon a method and technology of the situation analysis and designing the object domain model developed in the works [5]. In addition to Schedrovitsky's ideas, an important role is attached to the following basic ideas:

- Gradual forming a situation model of the object domain in human brains as people gain experience (V.N. Pushkin [6]).
- Semiotic approach to description of complex and big control systems developed in the works of soviet linguists – Y.A. Shreider etc. [8].
- Application of the method of conceptual analysis and designing of systems for coordinated control developed by S.P.Nikanorov [9].

Application of the method of situation control of large systems, as the basis for description of semantics and dynamics of the object domain, suggested by D.A. Pospelov, Y.I. Klykov, L. S. Bolotova [5, 7, 8, 10].

Let us briefly review the main content of the mentioned above ideas.

1. Research of the human decision taking processes carried out by methods of psychology, neurophysiology and other scientific disciplines has demonstrated that psychological mechanism for regulation of human behavior and activities is closely associated with generating in the human brain the information model of the environment, where a body lives, including also data about the goal condition and feasible methods of influencing the environment required for this or that task solution. Goal condition is some desirable condition of the environment, i.e. the condition into which the environment should transform as a result of the object or system influence. Environmental objects are always related to each other somehow. Revealing their relations, as well as creation of information analogues of objects along with their inherent properties, allows to make the environmental model and, in particular, the model of the control object. Thus, the process of making situational abstractions shows that this process is substantially identification of the system of elements composing the problematic situation, establishing links between them and laws of their behavior [6].

2. As the main method for description of an object domain a semiotic approach has been suggested, i.e. the approach from symbols and symbolic systems point of view [8]. When researching symbolic models of activities, objects, their properties and relations between them, with the certain approach to their selection, the knowledge is found for description of processes, functions, arrangement of the system elements and its morphology.

3. The basis of conceptual analysis methodology and designing is the idea of analysis and designing of the object domain structure models and knowledge bases in the form of the invariant constructs (models) system and setting the method of their integration into some single conceptual structure [9]. All work with experts is implemented according to these models. The key idea of the conceptual analysis and designing (CA&D) is that the condition of solving the problem of this complexity is precise, producible, efficient brainwork of this problem subjects is ensured by conscious building it up, but not by noting the existing stereotypes. Its creation is a form of controlled self-consciousness reflexion. Scope of the object domains and depth of their research are not the limitation for such way of thinking The

output product of such technological brainwork is the standard, in terms of its form, model of object domains, which justification and conclusions can be controlled. All elements of the system are value-oriented by making the system goals, which can be obviously formulated. That is why the whole system language in a natural way comes out of concepts in use, but not vice versa, when concepts come out of the utilized language. As a result, the model of object domains can be represented in the form of constructs related in a special way, their descriptions and relations between them. With such approach there will be opportunities to compare constructs and to build more complex entities out of simple ones by means of formal logics and artificial intelligence, which is given an operational form.

4. The method of situation modeling is interconnecting all above ideas [5, 7, 10]

Three main principles make foundation of the method.

The first one emphasizes the language role in solving control tasks and confirms that there is a need in a language ensuring such formalization of the problem, which guarantees adequate, from human point of view, description of the information model of the object itself, its functioning processes and the environment defining conditions for taking decisions in particular situations.

The second concept of the method is based upon the principle of situation classification. The essence of it is that, when generating a control model, all possible situations should be subdivided into classes for each class to be possible to match with either a control decision or a model ensuring generation of acceptable rational decisions. Selection of the best decision out of this multitude can be done based upon either heuristic procedures, or the known precise mathematical models.

In this case it is assumed that the power of all situations multitude is considerably higher than the multitude of all tools for generation of rational decisions.

The third principle of the method supposes availability of apparatus for constructing the object control model based upon these modes training of how to take decisions. The training should be implemented either by experts, or on the basis of experience in solving the control tasks accumulated by the situation control model as it functions. Here the training means generation of the object model itself, and then the model for taking control decisions. The method of situation control has been developed specially for the case, when number of potential situations in the object domain of the control object is essentially higher than number of decisions, i.e. $S \gg U$. Thus, it is supposed that all decisions of multitude U are completed solutions not requiring additional interpretation, specification and finishing. However, the practice shows that such control systems are rare. So we can speak about instances, when number of possible situations is comparable with number of decisions, or there are sufficiently many solutions, to enumerate them in advance, i.e. $S \approx U$, or the multitude U is large enough and open. These are the cases for which the method of situation analysis and designing the model of the arbitrary nature object domain has been offered [5].

Conceptual structure of a single act of activities

Activities «cutting out» will be done in accordance with the solutions, which are the results of their implementation. In this context, any solution by its nature is an indication to one or several actions to be performed, to enable the action leading to respective changes in the environment or in the studied object domain.

Hence, further we will equate a decision with an action.

Correspondingly, let us introduce an action and its elements: *decision* – d is considered as an action with the following structure: *an action subject* – *an action* – *an action object* – *action components influencing the decision*. So, we have generated a metastructure for the concerned decision (See Fig.1), where X_{as} is an action subject (*action subject* – *as*); X_a is an action (*action* – *a*); X_{ao} is an action object (*action object* – *ao*); $X_{ac_1}, X_{ac_2}, \dots, X_{ac_n}$

are action components (*action components – ac*). The action subject, the action object and all action components are linked with the action X_a by binary structural relations R_{str} of three possible types: $r_{as}(X_{as}, X_a)$ are relations between the action subject and the action; $r_{ao}(X_a, X_{ao})$ are relations between the action and the action object; $r_{ac_1}(X_a, X_{ac_1}), r_{ac_2}(X_a, X_{ac_2}), \dots, r_{ac_n}(X_a, X_{ac_n})$ are relations between the action and the action components.

The long-term research has demonstrated that decisions for any other object domains may be represented by the same structures, which vertices are names of the action subject, the action itself, the action object and its components. In the decision there are two clear parts: functional and goal-oriented (subject – action-object – functional and goal-oriented (FGO) part) and securing (subject – action-(component 1, component 2, ..., component n) – S part). These parts form the single structure. Here it is natural to call the functional and goal-oriented part as the control task Z , and S part should be designated as Q . Then the whole structure will be their merge:

$$D = Z \cup Q,$$

where: $Z = r_{as}(X_{as}, X_a) \cup r_{ao}(X_a, X_{ao})$,

$$Q = r_{as}(X_{as}, X_a) \cup r_{ac_1}(X_a, X_{ac_1}) \cup r_{ac_2}(X_a, X_{ac_2}) \cup \dots \cup r_{ac_n}(X_a, X_{ac_n})$$

Following the CA&D method, the decision structure (Fig. 1.) is an artificial metasstructure convenient for arrangement of a dedicated designing process, i.e. a construct, and a complex construct consisting of simple (terminal) constructs like: *an action subject – an action (as-a)*, *action – action object (a-ao)*; *an action – an action component (a-ac)*). Let us call this construct *a conceptual structure of single decisions (CSSD)*. The multitude of CSSD will be designated as: $D = \{d_1, d_2, \dots, d_m\}$,

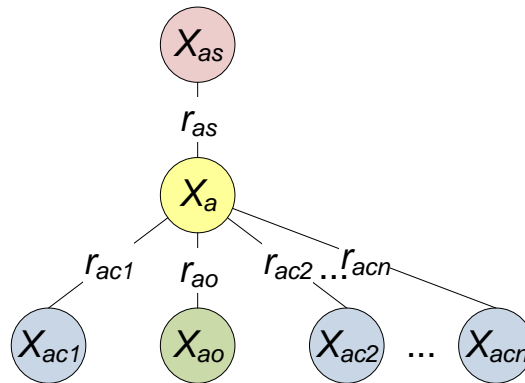


Fig. 1. Structural diagram of the single act of activities

$$d_i = z_i \cup q_i, i = \overline{1, m}.$$

Thus, vertices d_i outline boundaries of each action and the object domain as systems define operational (procedural) content of the selected objects of elements.

Evidently, all vertices of CSSD, except a vertex-action, may be interconnected by spatial, logic and other types of bonds (vertical, as well as horizontal), making, in their turn, simple constructs like: *as-ao*, *as-ac*, *ao-ac*, *ac-ac* with their two-directional, binary semantic

relations R_{som} between their vertices. Then CSSD is turning into the structure shown in Fig.

2. Now CSSD can formally be expressed as:

$$d_i = \{X(d_i), R_{str}(d_i), R_{sem}(d_i)\}.$$

It is known that any relation (bond) can be the *truth* (T), or a lie (L), i.e. to be or not to be. It is the *truth*, if certain conditions are met (one or several simultaneously). The conditions themselves, as we know, are formed on the basis of relations between values of CSSD vertices properties (for example, relations $=, \leq, \geq, \approx, \equiv, \neq$ and others), usually represented in the form of left part of the condition-action rule, as well as trueness of other relations in this structure. After identification of the required properties (*property* – p) CSSD vertices $X(d_i)$, a single decision becomes a structure shown in Fig. 3.

All elements of CSSD d_i possess their own set of properties $P(d_i)$ forming the multitude of its concepts $C(d_i)$. But between properties of CSSD vertices $X(d_i)$ there may be specific relations $R_p(d_i)$, for example, relations $=, \leq, \geq, \approx, \equiv, \neq$ and others. And the trueness of these relations is the condition of true relations between vertices.

Respectively, a model of the object domain fragment of a single decision is broadened due to addition of the multitude of properties and relations between them, i.e.:

$$C(d_i) = \{X(d_i), R_{str}(d_i), R_{sem}(d_i), P(d_i), R_p(d_i)\}, \quad i = \overline{1, m}, \text{ where:}$$

$P(d_i)$ is properties of all CSSD vertices d_i ; $R_p(d_i)$ is relations between properties of CSSD vertices d_i .

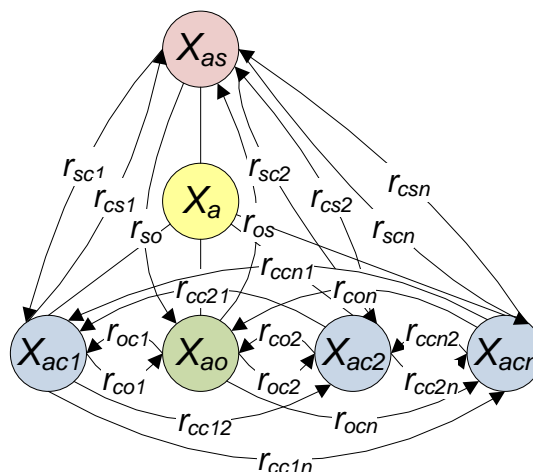


Fig. 2. Semantic structure of a single act of activities

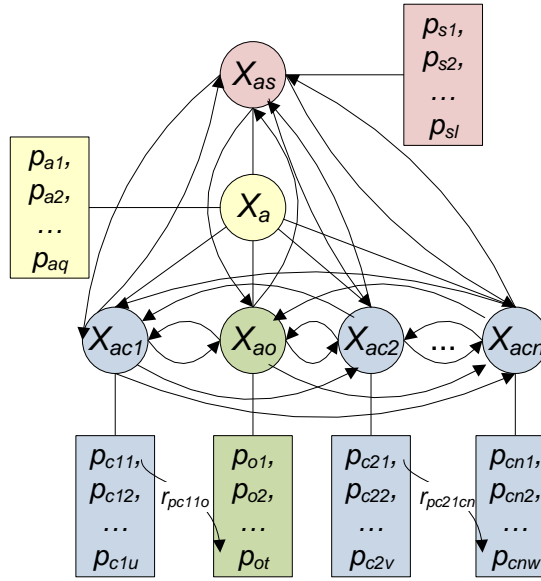


Fig. 3. Conceptual structure of a single act of activities

Object domain conceptual model

For designing of holistic system ODCM, CSSDs are generated for all elements of the multitude $D = \{d_1, d_2, \dots, d_m\}$. The final conceptual model of an object domain is the

result of their logic merge into a single ODCM: $C(D) = \bigcup_{i=1}^n C(d_i)$. However, this merge is not a

mechanical one, since all decisions (d_i) undergo some operations similar to multiple theoretical operations, such as: overlapping, inclusion, supplementing, deduction, fusing, etc. Besides this, there may be hierarchic relations between different CSSD, for example, between the whole and its part. In this cases a single decision can be transformed into a tree of actions (decisions) similar to the tree of a problem division into subproblems. Graphically such decision is described in the form of a reduction graph (AND/OR-graph), which vertices are equated with decision names – X_{a_i} ($i = \overline{1, n}$), and arcs – with the ratio of a part to the whole – r_{pow} .

Apart from this, one or several components of the decision d_i can themselves be objects of one or several actions in other CSSD, it means that the objects - components can play several roles simultaneously in this object domain, and different properties and relations will be important for each role, i.e. they should have different concepts. But the action X_{a_j} , obviously cannot be fulfilled until the required action is performed with the component $X_{ac_{2i}}$ of action X_{a_i} . It means that implicit relation «action – subaction» automatically emerges between actions of structures d_i, d_j . If there are several components like this, then vertices-actions of structures d_j, d_k ($j, k = \overline{1, m}$) will be related by a reduction bond AND/OR. For OR case it is necessary to establish priority of alternative actions implementation.

A chain of enclosed CSSD, which is formed as per relations action - subaction, subject – superaction, object – subobject, can last until the level of terminal actions-decisions is

reached, i.e. elementary acts of activities. As a result, another conceptual model is generated for the whole decision space of the object domain (OD DSCM):

$$D = \bigcup_{i=1}^m d_i \cup G(X_{as}, R_{pow}) \cup G(X_a, R_{pow}) \cup G(X_{ao}, R_{pow}),$$

where $G(X_{as}, R_{pow})$, $G(X_a, R_{pow})$, $G(X_{ao}, R_{pow})$ are hierarchy tree graphs for: action subjects (functional level of description); actions themselves (process or operational level of description); objects (structural or morphologic level of description), respectively.

In summary, a conceptual model of the object domain (ODCM) is represented in the form of a three layer graph: the first – hierarchy of functional subjects (functional level of description); the second – hierarchy of actions (process or operational level of description), the third - level of interaction between objects, action components and their relations (structural or morphologic level of description) connecting the operational aspect and the object design. It has been constructed and consists of many concepts of all entities, which appeared in the conceptual model of the object domains combined in common description.

Therefore, the conceptual model of the whole object domain (ODCM) can be described by the expression:

$$G(D) = \bigcup_{i=1}^m C(d_i) \cup G(X_{as}, R_{pow}) \cup G(X_a, R_{pow}) \cup G(X_{ao}, R_{pow}),$$

where $\bigcup_{i=1}^m C(d_i)$ is image of $F_D : S_{d_i} \rightarrow U_{X_{a_j}}$ ($i, j = \overline{1, m}$) or the knowledge

base of this object domain, others items are hierarchies of action subjects, actions and action objects.

Graph $G(D)$ formed as a result of matching actions with respective CSSD consisting of a control task (a functional part) ensuring the parts and their bonding through hierarchy relations, establishes all plurality of ways (or scenarios) for the multistep solution. Vertices of third type at their level are bonded by hierarchy relations, as well as semantic relations like: a place, a tool, a method etc. Each out of three layers is described by its graph: the first and second levels look the same – as a tree and differ only by their vertices interpretation; the third is the oriented graph, where every arc has its own name. The operational graph gives a full idea about the action hierarchy, their list at every level of decision taking, their objectives and boundaries. The number of action levels depends upon the depth of specialization required for the goal achievement defined by the tree root and extent of understanding and knowledge achieved in the researched object domain.

The structural graph (the 3 – d morphological level) is a semantic network with structural bonds and semantic relations. Judging by relations between the network vertices, it is always possible to establish roles to be played by each object. Evidently, each vertex (top) of the action tree X_{a_k} has its own subgraph $G_k(d_k)$, ($k = \overline{1, m}$), which actually gives the scenario of arriving at the decision containing CSSD of all actions lying on the way to the goal vertex. Thus, graph $G(D)$ can be considered as a totality of all possible scenarios for developing algorithms of decisions $G_k(d_k)$ corresponding to d_k -th vertex of ODCM $G(D)$. Location as per the OD structure development model can be from top to bottom (the

strategy reverse to development «from the goal – to the situation»), as well as from bottom to top (direct strategy of development «from the situation – to the goal»).

Conclusion

The suggested approach has the rich history, practical results, which allow to conclude about its high efficiency [5, 11, 12]. It was laid into the foundation of the situational analysis and designing method for OD models of arbitrary nature and knowledge bases of the systems based on various types of knowledge: decision taking and control systems, ontology, multi-agent systems. The practice has shown that skills and experience gained during the work according to the procedures of this method remain with a person forever giving him a capability of systematic and conceptual brainwork, and vivid imagination. The method has been developed into the technology, and is supported by software tools. All this makes it an invaluable instrument in hand of a knowledge engineer. The working procedure ensures a throughout designing of the knowledge bases on «turn-key» basis with minimum expenses and returns. Along the way it also solves a lot of problems of the knowledge representation, its formalization, and knowledge bases implementation for expert systems, ontology and many other systems. The existing experimental instrumental software package already allows to computerize the processes of knowledge bases formalization and implementation. There is a successful experience in designing and realization of applied systems for information technologies for control and decision taking, etc.

References

1. Gavrilova T.A., Horoshevskij V.F. Bazy znaniy intellektual'nyh sistem – SPb Piter, 2000;
2. Gavrilova T.A., Chervinskaja K.R. Izvlechenie i strukturirovanie znaniy dlja jekspertnyh sistem. – M.: Radio i svjaz', 1992, 200 s.
3. Barinov V.A., Bolotova L.S., Volkova V.M. i dr. Teorija sistem i sistemnogo analiza v upravlenii organizaciej. Spravochnik. // M.: Finansy i statistika, 2009, 846 s. (Vtoroe izdanie)
4. Putevoditel' po metodologii Organizacii, Rukovodstva i Upravlenija // Hrestomatija po rabotam Shhedrovickogo G.P.// Izd. «Delo», 2003, 159 s.
5. Bolotova L.S. uchebnik «Sistemy iskusstvennogo intellekta: modeli i tehnologii, osnovannye na znaniyah». M.: Finansy i statistika, 2012- S. 664;
6. Pospelov D.A., Pushkin V.N. Myshlenie i avtomaty. – M.: Sov. radio, 1972, 224 s.
7. Pospelov D.A. Situacionnoe upravlenie: teorija i praktika. – M.: Nauka, 1986, 284 s.
8. Shrejder Ju.A. Logika znakovyh sistem: Jelementy semiotiki. – M.: Editorial URSS, 2010, 64 s.
9. Nikanorov S.P. Teoretiko-sistemnye konstrukty dlja konceptual'nogo analiza i proektirovanija. – Ser.: Konceptual'nyj analiz i proektirovanie. Istorija napravlenija. – M.: Koncept, 2006.
10. Klykov Ju.I. Situacionnoe upravlenie bol'shimi sistemami. – M.: Jenergija, 1974, 135 s.
11. Bolotova L.S., Staryh V.A. Proektirovanie ontologij na osnove modeli predmetnoj oblasti, Zh-l «Informatizacij obrazovanij I nauki», M., INFORMIKA, 1(9), 2011, 88-106 s..
12. Bolotova L.S., Moroz Ju.V.// Igrovye podhody k obucheniju inzhenera po znaniyam , Zh-l «Upravlenie bol'shimi sistemami», vyp. 26, M., IPU RAN, 2009, s 5-20.

EFFECT OF ACCOUNTING INTERMITTENCY DEPENDENCE ON THE TIME OF LONGITUDINAL CORRELATION COEFFICIENT THIRD ORDER

Pyrkova O.A.

Moscow Institute of Physics and Technology (MIPT)

In this work, the following model is used: flow is considered as a mixture of turbulent (τ) and viscous (ν) regimes. Turbulent flow is taken with a weight equal to the intermittency coefficient $\gamma = \rho_\tau / \rho$, viscous - with a weight ($1 - \gamma$). A model dependence obtained for the longitudinal correlation is in good agreement with the experimental data of Batchelor-Townsend-Stewart.

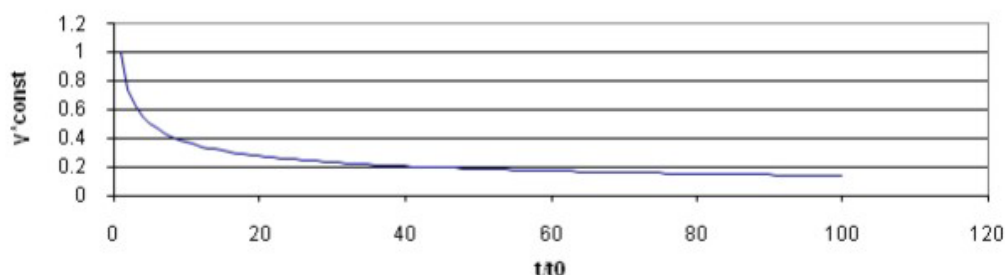
Keywords: intermittency coefficient, turbulent flow, Loitsyansky invariants.

Hinze J.O. clearly expressed opinion of the authors [1], [3], [7] that turbulence is a simple self-similar regime only partially. There are similarities and Loitsyansky invariants for each mode separately: $u_\nu^2 \lambda^5 = \text{const}$ and $u_\tau^2 \Lambda^5 = \text{const}$ [5].

The flow is assumed as a mixture of two regimes:

- the purely turbulent Kolmogorov regime (τ), taken with a weight equal to the value of the coefficient of intermittency (fraction of the turbulent regime) $\gamma = \rho_\tau / \rho$,
- and the purely viscous regime (ν), taken with the weight ($1 - \gamma$).

Assumed that the coefficient of intermittency is of the form $\gamma = 1 - e^{-c_1 K_T^+}$, like Loitsyansky [5].



Pic. 1. Time dependence of the coefficient of intermittency.

In this model the mixing of patterns characteristic of these regimes is the following:

$$\varphi = \gamma \cdot \varphi_\tau + (1 - \gamma) \cdot \varphi_\nu$$

where by the value of φ one should imply

$\langle u \rangle$ – the average scale of the pulsating part of flow velocity,

$\langle u^2 \rangle$,

$\langle P \rangle$ – the probability density of fluctuations, etc.

Since the coefficient of intermittency γ tends to zero as time increases [8], then φ tends φ_ν .

Hypothetical relationship is adopted in the model for the Loitsyansky integral

$$\text{Loi} = \int_0^\infty r^4 B_{LL} dr,$$

used in this study

$$\text{Loi}(t) = \gamma \cdot \text{Loi}_\tau + (1 - \gamma) \cdot \text{Loi}_\nu.$$

Here we use the notation:

r - the distance between the points,

t - the time,

$B_{LL} = u^2 f$ - the second-order correlation moment,

$f(r, t)$ - the second-order longitudinal correlation coefficient,

$u = \langle (u')^2 \rangle^{1/2}$ - the scale of the pulsating part of the flow velocity.

This is consistent with the conclusion made by Sedov [11] that the value of the Loitsyansky integral changes over time, and therefore, generally speaking, one cannot regard it as a characteristic constant.

The Loitsyansky integral is invariant only at the final stage of turbulent field decays, when it takes the value of (Loi)

Fundamental Karman-Howarth equation relates the magnitude of the two-point second-order and third-order longitudinal correlation moments:

$$\frac{\partial B_{LL}}{\partial t} = \frac{1}{r^4} \cdot \frac{\partial}{\partial r} \left(r^4 \left(B_{LL,L} + 2\nu \frac{\partial B_{LL}}{\partial r} \right) \right), \quad (1)$$

where ν - the kinematic coefficient of viscosity,

$B_{LL,L} = u^3 \mathbf{k}$ - and third-order longitudinal correlation moment,

$\mathbf{k}(r, t)$ - third-order longitudinal correlation coefficient.

Accounting intermittency amends value of the function $B_{LL,L}$

$$B_{LL,L} = \gamma \cdot (B_{LL,L})_T + (1 - \gamma) \cdot (B_{LL,L})_\nu.$$

We have

$$B_{LL,L} = \gamma \cdot (B_{LL,L})_T$$

in the hypothesis that the third-order longitudinal correlation moments are negligible in a purely viscous regime.

In the absence of viscosity ($\nu = 0$) Karman-Howarth equation (1) takes the following form in the purely turbulent Kolmogorov regime

$$\frac{\partial B_{LL}}{\partial t} = \frac{1}{r^4} \cdot \frac{\partial}{\partial r} (r^4 B_{LL,L}). \quad (2)$$

Equation (2) is initially not closed, because it contains two unknown functions.

Gradient hypothesis of Lytkin and Chernykh [6] is used to make it closed by the expression of the two-point third-order correlation moment $B_{LL,L}$ through the two-point second-order correlation moment B_{LL} in the regime of Kolmogorov turbulence in the inertial range:

$$(B_{LL,L})_\tau = 2K_T \frac{\partial B_{LL}}{\partial r}, \quad (3)$$

where K_T is the turbulent diffusion (viscosity) coefficient.

This provides a self-similar solution for purely turbulent motion.

Value of K_T is determined by the model expression, chosen in accordance with a number of limiting relations: the transition to a one-point description, the behavior in the inertial range, where it coincides with the expression in the works [4], [6], [9].

$$2K_T^+ = \frac{D_{LL} \tau_2^T}{\nu 3a_1} = \frac{1}{\nu 3a_1 \bar{\alpha}} \cdot \frac{D_{LL}^{1/2}}{\left(\frac{D_{LL}}{D_{LL}} \frac{1}{6} \right)^{1/2}} \frac{1}{\left(\frac{1}{\Lambda^2} + \frac{\psi_1^2}{r^2} \right)^{1/2}} = \frac{u_T \Lambda \varphi_1(r_*)}{\nu} \sim \frac{2\varphi(r_*)}{\bar{t}^{3/7}}.$$

Here $D_{LL} = 2u_T^2(1 - f_T)$ - the longitudinal structure function,

$D_{LL} = D_{LL} + 2D_{NN}$, N - normal to the r ,

τ_2^T - relaxation time in the two-point description,

$$r_* = \frac{r}{(\nu t)^{1/2}}, \quad \bar{a}_1 = \frac{a_1}{a_0} = 5.25, \quad \bar{\alpha} = \alpha a_0 = 0.255, \quad a_0 = 0.5, \quad \psi_1 = 2.09 \text{ - empirical constants,}$$

chosen to correspond to the limit regime.

Considering von Karman self-similarity $(B_{LL})_\tau = u_\tau^2 f_\tau(\xi_1)$ equation (2) takes the form

$$-B f_\tau = \sqrt{1 - f_\tau} \frac{\partial f_\tau}{\partial \xi_1}. \quad (4)$$

Here $\xi_1 = \frac{r}{\Lambda}$,

$$\text{Re}_\lambda = \frac{u \lambda}{\nu},$$

Λ - an integral correlation scale,

λ - the Taylor dissipation-length parameter,

$$B = \frac{13.2}{\text{Re}_\lambda} \frac{\Lambda}{\lambda} \text{ [8].}$$

One can find a solution of (2)

$$B \xi_1 = -2 \sqrt{1 - f_\tau} + \ln(1 + \sqrt{1 - f_\tau}) - \ln(1 - \sqrt{1 - f_\tau})$$

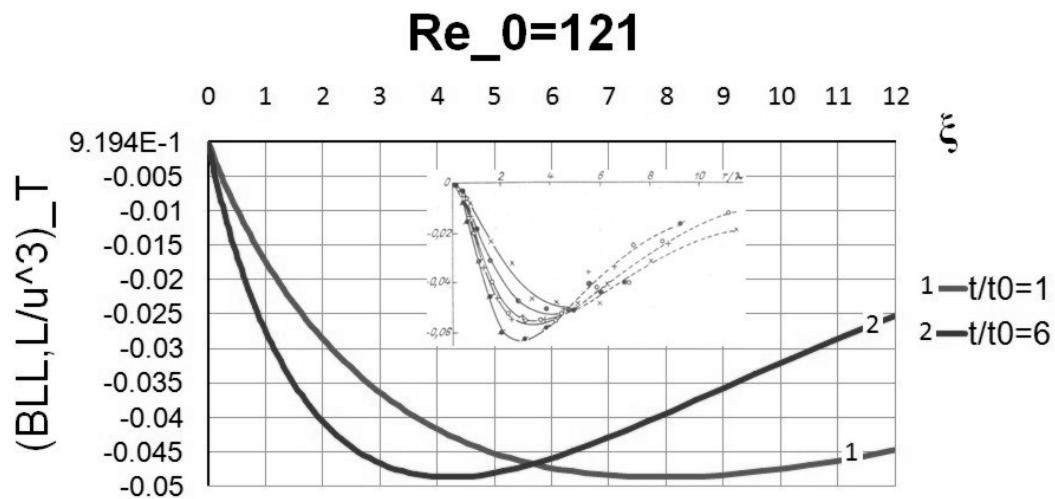
by integrating (4) with the boundary conditions $f_\tau|_{\xi_1=0} = 1$, $f_\tau|_{\xi_1=\infty} = 0$ [6], [10].

The value of Λ/λ is defined by the interpolation function of the generalized von Karman model for the spectrum [2]

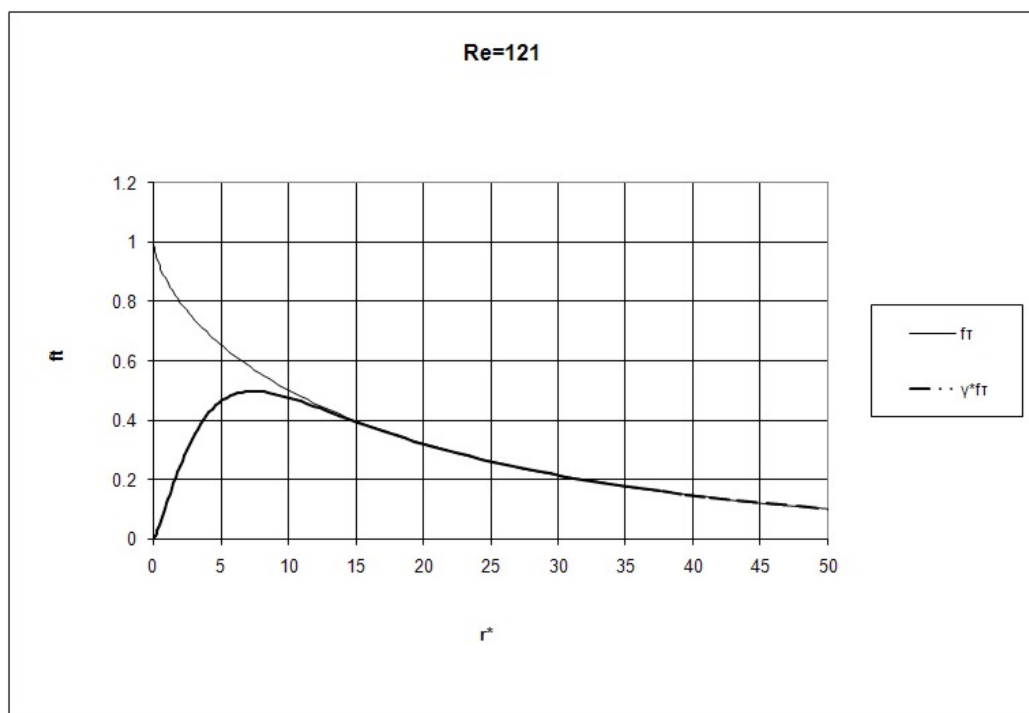
$$\frac{\Lambda}{\lambda} = 1.23 + 0.0351 \sqrt{\text{Re}_\lambda} (\sqrt{\text{Re}_\lambda} - 1).$$

Thus we have found that the value of B depends on the Reynolds number:

$$B = B(\text{Re}_\lambda).$$

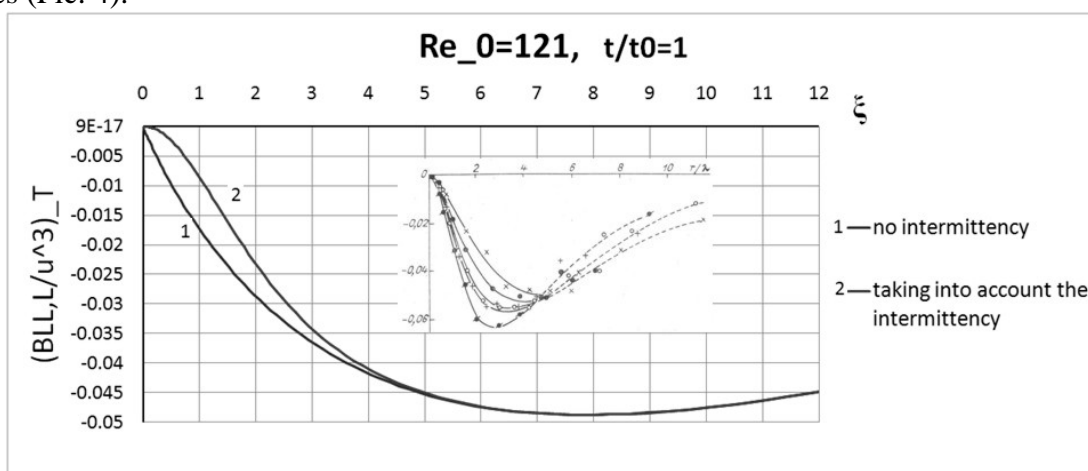


Pic. 2. The time dependence behavior of the third-order longitudinal correlation coefficient at short distances.



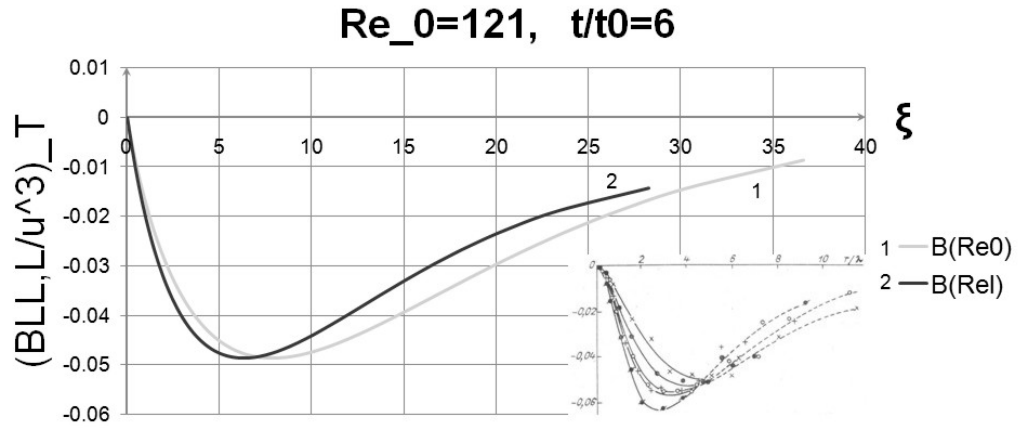
Pic. 3. The behavior of the longitudinal correlation coefficient [8]

Accounting for intermittency in a purely turbulent (Kolmogorov) mode leads to a decrease in its contribution to the third-order longitudinal correlation coefficient at short distances (Pic. 4).



Pic. 4. The behavior of the of the third-order longitudinal correlation coefficient without and with regard the intermittency.

Consideration depending on the time value B leads to a greater coincidence the behavior of the curves with the experimental data (Pic. 5).



Pic. 5. The behavior of the of the third-order longitudinal correlation coefficient taking into account depending on the time constant B

Since there is a

$$\left(\frac{B_{LL,L}}{u^3} \right)_\tau = 2\sqrt{2}\omega\sqrt{1-f_\tau} \frac{\partial f_\tau}{\partial \xi_1} = 2\sqrt{2}\omega\xi_1 B f_\tau,$$

then we have

$$\left(\frac{B_{LL,L}}{u^3} \right)_\tau = F(\xi_1).$$

It was found that the curves of the variables $\mathbf{k}(\xi_1, t) = \frac{B_{LL,L}}{u^3}(\xi_1, t)$ and $\xi_1 = \frac{r}{\Lambda}$ are the same at different time (Pic. 6).



Pic. 6. The behavior of the of the third-order longitudinal correlation coefficient according to ξ_1 .

Thus it can be concluded that

□ The model provides answers to questions that arise in connection with the behavior depends $\mathbf{k}(r, t)$.

□ A model dependence obtained for the third-order longitudinal correlation coefficient has asymptotically form of decay and is in good agreement with the experimental data of Batchelor—Tawnsend—Stewart.

□ Accounting for intrmittency effect at short distances: behavior of the curves more consistent with the experimental data.

□ It was found that the curves of the variables $\mathbf{k}(\xi_1, t)$ and ξ_1 are the same at different time. This fact confirms the hypothesis about the similarity of the generated turbulence from grid.

References

1. Batchelor G.K. The theory of homogeneous turbulence. - Cambridge.1953.
2. Driscoll R.J., Kennedy L.A.,\A model for the turbulent energy spectrum", Phys. Fluids, 26, No. 5, 1228-1233 (1983).
3. Hinze J.O. Turbulence. — N.Y. —Toronto— London. Mc Graw Hill. 1959.
4. Z.L. Korobitsina, G.G. Chernykh. Numerical simulation of the final periodavrozhdeniya homogeneous isotropic turbulence [in Russian] Novosibirsk: : Modelling in mechanics, SO AN SSSR 1992, vol. 6(23), no. 3, pp. 77–85.
5. Loitsyansky L.G., "Semiempirical theory of the interaction of molecular and molar exchange in turbulent flow," *Proceedings of the All-Union. Congress on Theor. and Appl. Mechanics* [in Russian], Leningrad: Academy of Sciences , 143-166 (1962).
6. Yu.M. Lytkin and G.G. Chernykh,\One method of closing the Karman-Howarth equation", [in Russian] In: Dynamics of Continuous Media, Inst. Hydrodynamics, Sib. Div., Acad. of Sci. of the USSR, 27, 124{130 (1976).
7. Monin A.S. and Yaglom A. M., *Statistical Fluid Mechanics: Mechanics of Turbulence*, Dover Publications, (2007).
8. A.A. Onufriev, A.T. Onufriev and O.A. Pyrkova,\The problem of the decay of homogeneous isotropic turbulence, taking into account the phenomenon of intermittency", [in Russian] In: Actual problems of fundamental and applied mathematics, MIPT, Moscow, 124-135 (2009).
9. Onufriev A. T. Description of turbulent transfer. Non-equilibrium models// M.:MPTI, 1995.
10. O.A. Pyrkova, A.A. Onufriev and A.T. Onufriev, \Initial time behavior of the velocity in a homogeneous and isotropic turbulent ow", [in Russian] Proceedings of MIPT, 3, No. 1, 127-131 (2011).
11. Sedov L., Similarity and dimensional methods in mechanics, 10th ed., CRC, (1993).

ANALYSIS AND FEATURES PARAMETERS NORMALIZATION EMC COSMIC DEVICES AND SYSTEMS

Grachev N.N.

Moscow, MIEM NRU HSE

This paper analyzes the problem of EMC spacecraft. Complexity of the problems of EMC is directly related to the main trends of design space RES. The results of analysis parameters EMC and rationing in developing RES spacecraft.

RES, space, EMC interference rationing

History of the development of space technology and space exploration contains many facts failures, malfunction of equipment and upland unexplained phenomena occurring on board the spacecraft (SC), has successfully passed all the ground tests.

These phenomena - this is the reason that the development of RES SC faced with the need to address one of the key problems of modern electronics - the problem of ensuring EMC on board a spacecraft. Numerous investigations of work equipment in the space allowed to draw conclusions about the specific conditions of work in a wide range of influencing factors of outer space. The fact that the exterior design elements SC, irradiated by UV radiation of the sun and flow of energetic charged particles may be at different electrical potentials and become sources of discharge currents and interference, significantly distorting characteristics of the surrounding plasma. For each type of interference and noise immunity (in chains, on the field, pulsed, narrowband) rule should be the same for all elements of RES SC, allowing corrective action to the layout of the complex without risking EMC conditions. The presence of common standards does not preclude the submission of individual additional requirements for individual elements and standards, if necessary.

Aggravation of the problem of EMC is directly related to the main trends of design space RES: microminiaturization leading to convergence in the space of transmission paths and work at lower signal levels, increased sensitivity control devices and scientific instruments, and multi-purpose implementation of complex scientific experiments covering related or common frequency band, saturation SC pretreatment devices for scientific information.

In the EMC space devices and systems are currently far from all, especially engineering and design, EMC characteristics are reflected in the existing documentation and they are not always specified in the TOR and specifications for products that speaks of the difficulties encountered in the creation of high quality on the basis of EMC production. With limited distribution area are departmental standards - OSTs, technical guidance materials (RTM) and Interagency requirements that are directly or indirectly related to the EMC space RES.

Among foreign standards in the founding document EMC area space RES is the U.S. standard MIL STD- 1541 including requirements for electronic equipment space RES [3]. The standard includes design requirements, adapted to the conditions of space, as well as precise guidelines to ensure the effectiveness of EMC. The standard is designed for selective application to shared space systems with particular emphasis on the design phase of the analysis. The standard provides requirements for EMC level systems, subsystems and equipment. Scope MIL STD- 1541 space systems, missile carriers, spacecraft, ground tracking stations. Accompanying document MIL STD- 1542 includes the requirements for EMC and grounding. Requirements MIL STD- 1541 contains requirements for electronic equipment exposed to the energy of electrons and protons of the solar wind plasma space on the dark side of the earth, which charges the satellite to levels 10 ... 20 kV. To describe the source of interference concerns arc peak current up to 1000 A and a pulse width of up to 1 μ s, forming a high-frequency field with a peak strength of 1000 V / m or more. The standard contains requirements for common ground and metallization (conductive coating) of the satellite. (There is a limit of 109 ohms resistance D insulative coating to limit the charge accumulated on the surface of the object. Standard provides multipoint grounding for secondary sources of secondary power supply as well as for discrete systems. Mixed grounding provides compatibility of saving cost and weight. The standard limits considered inrush current at power tires with simultaneous operation of onboard systems. Standardized physical quantities, their parameters, and the control scheme rules should maximize conform to the values and parameters of the equivalent circuits used in the numerical evaluation of the EMC. In this case it is possible to minimize the uncertainty intervals arising from the

translation of the monitored parameters to the parameters used in the numerical evaluation of EMC. Contents numerical evaluation methods EMC points to the desirability of establishing standards for the following physical quantities characterizing electromagnetic interference [1]: Phase current in obshchobortovoy mains, common mode current in all connecting cables, including power cables, magnetic field component interference RES; electric field component interference RES. The choice of the normalized current value of the main interferences, and no stress associated with the predominantly airborne communications conditions in the magnetic field between the contours of noise sources and receptors and relatively more complex struggle with magnetic interference compared to electric. It is advisable to separate the task rules on continuous narrowband and impulse noise. For narrowband interference norm is set to effective measured values in the regulated bandwidths measuring circuits. Obviously, it should be possible to establish a more narrow strips measuring circuits, given the need to control each harmonic component of the process noise. The latter is due to the presence of a significant number of RECs comprising digital circuits isochronous and narrowband measuring circuits responsive to the individual frequency components of the spectra of continuous interference. In establishing standards for transients necessary for opportunities to get closer to regulate levels of spectral components of individual pulses recorded by a temporary Released in fractions of a microsecond. In this case, be achieved the greatest certainty in assessing noise and lowest risk unnecessarily inflate the requirements for interference incorrectly calculating the peak reaction scheme receptor. For instance [1], the maximum possible input voltage amplitude discriminator in the case of a linear detector circuit

$$U_{l.d.max} = \int_{\Omega_n}^{\Omega_B} [G_c(\omega) + G_n(\omega)] R(\omega) d\omega \quad (1)$$

wherein $G_c(\omega)$, $G_n(\omega)$ - the spectral density of the signal voltage and interference calculated by integration of the corresponding process in a time interval equal to the time constant of path τ_p receptor to enter the amplitude discriminator:

$$G_n(\omega) = \left[\int_{-\tau_p/2}^{\tau_p/2} U(t) e^{-j\omega t} dt \right] \quad (2)$$

where $R(\omega)$ - frequency response plot tract receptor from its entrance to the amplitude discriminator; Ω_n , Ω_B - lower and upper frequency limits being perceived receptor interference. It uses the frequency characteristics of the modules. EMC assessment, excluding the phase relations is upper bound is generally overestimated. If necessary, it can be adjusted by appropriate directed factors determined experimentally statistical methods. Reaction path of the receptor with square-law detector is according to [4]

$$U_{k.d.max} = \int_{\Omega_n}^{\Omega_B} F \Sigma(\omega) d\omega \quad (3)$$

$$F \Sigma(\omega) = \frac{2}{\tau_p} |[G(\omega) + G(\omega)] R(\omega)|^2 \quad (4)$$

The main characteristics of noise, defining indicators quality of functioning of receptors (eg, the probability failure) are values of the spectral noise density at the inlet receptor in the frequency band of its susceptibility, as well as temporary flow characteristics interference pulses. Accordingly, as the characteristics of immunity with respect to continuous narrowband interference using frequency response minimum interference Supplementary U at which

$$U_{l.d.} > U_0 \quad \text{or} \quad U_{k.d.} > U_0 \quad (5)$$

where: U_0 - specified input voltage level.

Immunity Surge receptors characterized by one of two things: either the minimum value of the amplitude of the interference pulse with a given spectral composition, in which the condition (5) or the minimum value of a static parameter - the expectation of pulse amplitude - at fixed time parameters of pulsed flow and spectral composition pulses, in which the condition

$$P_{m.f.} > P_{m.f.доп.} \quad (6)$$

where: $R_{m.f.}$ - average frequency (probability) of false positives.

Fig. 1 shows examples of gain-frequency characteristics immunity with respect to the harmonic interference signal inputs superheterodyne receiver type and the onboard computer. Here ω_s , $\omega_{i.f.}$, ω_m - respectively the tuning frequency of the receiver intermediate frequency and mirror; Ω_n , Ω_v - frequency limits analysis of the receptor and susceptibility to interference.

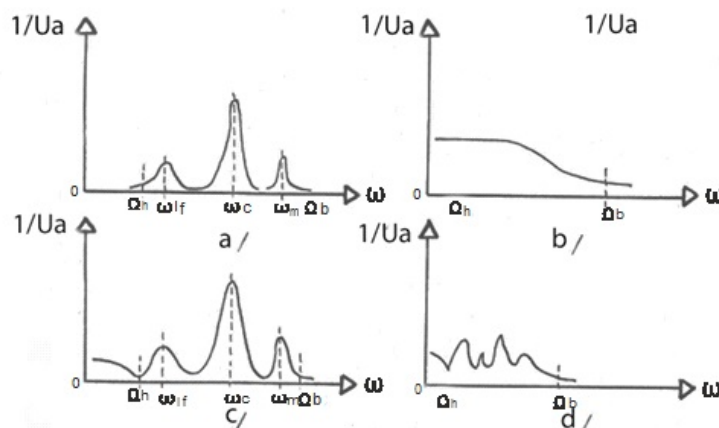


Fig. 1. Frequency characteristics of noise immunity receptors to harmonic interference and / - superheterodyne crystal receiver, the signal input; b / - -, the food chain; c / - on-board computer, the signal input; d / - -, the power supply circuit

Apart from the main reception channel, most receptors has one or more parasitic channels receiving formed due to the presence of non-linearity, spurious coupling or

resonances in the paths of the receptor. In this case, the integration in (1) and (3) is performed in a frequency band covering the reception channels and parasitic.

Norms on the interference environment settings (parameters coupling impedances and attenuation fields) currently would be inappropriate , since there is no satisfactory methods of control these parameters for avionics . Lack of standards on the parameters of the propagation medium can not talk about the fact that the system of norms fully fixed conditions ensuring EMC SC miscellanea layout change compartment with scientific equipment , changing design parameters of the cable network leads each time to assess the need for the control EMC . Experience of working on a number of SC [1] says that advisable to establish standards for noise immunity with respect to conducted disturbances, falling into elements and nodes SC board from the mains , the interference to the magnetic field to electric field interference (separately for harmonic and impulse noise) . With respect to the harmonic noise should be regulated frequency response of the permissible interference level at specified characteristics of the quality of functioning of the test site or block. With respect to impulse noise should be guided during the reproduction test immunity temporal and spectral characteristics of the actual pulse stream . The norm is defined as the value of the pulse height or level of the simulated noise in the readings of the standard meter interference with operation of the unit where the quality is not worse than the specified value. This is the most " direct reading " rules . Steps in the development of standards can be reduced to following. Initial treatment for tabular data each type of interference and noise immunity are their envelopes characteristics as the aggregate interference and maximum values. Immunity minimum values in each frequency discharge. Envelopes are assigned to all noise sources and receptors. Using egih characteristics produced numerical estimate EMC SC . If the assessment is positive, the

envelopes are accepted as norms on the parameters EMC . In case of a negative result is analyzed causes interferences.

EMC control parameters is carried out at all stages of development and manufacturing of RES, SC, as well as during the tests as part of the process and flight patterns. Methods should be possible uniform for devices differ in their functionality, schematic and design implementation, placing on board a spacecraft. When testing should play some "average" operating conditions. Methods should provide repeatability (Reproducibility) of the measurement, ie, the result obtained should not depend on the location of measurement, the measuring device instance, minor deviations in the actions of the equipment. Methods of control parameters EMC booth largely conventional. However, the measurement results should be correlated with the degree of disturbance of perception or interference source receptor. When working on board RES are near a metal SC hull surface, so if it becomes necessary to control interference simulation Case SC, which is used for the metal plane. Significant impact on the result of the measurement noise has a reciprocal arrangement of blocks. One of the factors limiting the accuracy of the measurements is the level of foreign interference. Especially essential when it gains control parameters EMC at the factory, where the level of extraneous noise can be very significant. Condition to obtain reliable test results is also saving for real high loads bearing noise immunity circuits contours.

References

1. Electromagnetic compatibility Space Science complex ARKAD-Z/Galperin YI, VA Gladyshev , Kozlov AI and Dr. M. : Nauka, 1984 , 190 p.
2. Mikhailov, VF Space Communication Systems: Proc. Benefit / VF Mikhailov, Moshkin VI, IV Bragin; SAC. St. Petersburg. 2006. 174 p.: Il.
- 3 . Pearlston SV The genesis and implication of MIL-STD- 1541 , electromagnetic requirements for space system. JEEE Electromagnetic Compatibility Symposium. San Antonio, 1975 , P. 213Ial-2BIa4, NewJork, 1975 , pp. 1-5..
- 4 . Jergensen D.E. and O.Advanced avionics system for an aerospace. - IEEE, AIAA, Digital Avionics Systems Conference, S, Proceedings of the USA, 1983 , p. 251-257 .
5. Adams W.J. SCemp induced., Magnetic field coupling to buried circuits. - IEEE, International Symposium on electromagnetic compatibility, Boston, 1985 , p. 385-389 .
6. Rich W.F. Potentials and Irradiation. 2 IEEE Transaction, 1975 , NS- 22 , N6, p. 2386-2391 .
7. Stevens N.J. Space environmental interaction with biased spacecraft surface. 2 AIAA Paper, 1980 , N 853 , 11pp.

QUESTIONS ANALYSIS EMC SPACE RES

Grachev N.N.

Moscow, MIEM NRU HSE

The article examines the EMC analysis of cosmic RES. The analysis of sources of electromagnetic interference. The main focus was on the prediction of electromagnetic interference of space objects RES. Analyzes the impact of accounting space factors on parameters EMC spacecraft.

Keywords: forecasting EMC, space RES, formation mechanisms of interference.

Numerical analysis of EMC components and systems RES is an important part of works to ensure EMC. Its values are vividly confirmed by the goals that he pursues at various

stages of design, construction, testing, commissioning and operation of the spacecraft: the definition of regular functions on the basis of the fundamental possibility of ensuring their EMC, develop the basic principles of layout airborne RES based EMC, the development requirements EMC parameters of individual staff RES and scientific instruments, checking the adequacy of the proposed circuit and design solutions for EMC, EMC refined estimate based on experimental data obtained during the test samples RES and complex as a whole; identification and selection of ways to eliminate the causes of harmful electromagnetic interference during operation of spacecraft.

The ultimate goal of the numerical evaluation of EMC EMC is the calculation of parameters of individual elements of the RECs and SC as a whole. The complexity of this problem lies in the variety of RES, their functionality. The new concept of quick blocks used in this project allows you to put more electronic equipment in one unit may whole subsystem.

The main function of the data processing subsystem is to manage the flow of data between the subsystem and a mass storage device for the data that will be used during the flight. Data transfer will be carried out through the optical data bus for a high level of noise immunity and memory usage on optical disks mass memory. To supply uses a lithium-thionyl chloride or bipolar nickel-hydrogen batteries. Modern information bus with their immunity and electromagnetic pulse can escape from the single-point grounding scheme, where all power rails are connected with a single point on the object. By chance the many factors affecting the EMC EMC indicators are statistical in nature. Typically, this set of probabilities unacceptable decline in the quality or operation of RES (as total score) will likely decline to an unacceptable level share reliable information on board the spacecraft . When calculating the final figure may be an additional factor to consider the relative importance of the information obtained from one or another subsystem. A source of electromagnetic interference can be any

Electrical and electronic devices on board a spacecraft , wherein the amplification is the generation and transformation of electromagnetic energy. Generated electromagnetic waves can thus carry information load (analog and digital signals oscillations with different types of modulation) , the functional load (the process of supplying power to the actuator or a scientific instrument) and, finally , be parasitic oscillations (noise , power supply ripple , overvoltage circuit switched pulses intercontact breakdown periods , etc.). A significant effect on airborne RES are external factors affecting space , not only electrification , leading to the formation of a wide range of interference , but also the impact of X-rays and high-energy particles , leading to the formation of impulse noise . The basis of the description and prediction of noise were used educational background noise in functional units of airborne RES. Later in the test prototypes RES form of distributions and the numerical values of the time parameters were refined interference . For a number of cases , mainly to predict interference from secondary sources of supply raw data obtained using " circuit simulation " noise sources, the development of the circuit model of the source of interference - the equivalent lumped circuit elements corresponding to the elements of the real circuit , conductors and parasitic coupling between the elements and conductors. Interference calculations at given points of the equivalent circuit is made using the apparatus of circuit theory . When this is necessary , of course, keeping high-frequency properties and parasitic elements such as thyristors , rectifier diodes , power transistors , etc. For impulse noise rather complex primary data structure are precisely the amplitude and timing noise. To calculate the spectral components using different approximating functions . As a more suitable function to approximate interference pulses can be offered function view

$$u(t) = Ume^{-\frac{t}{\tau}} \sin[\omega_0(t - t_1) + \varphi_0] \quad (1)$$

Choice of parameters U_m , τ , ω_0 , φ_0 achieved satisfactory approximation of the spectral characteristics of almost all actually observed interference pulses. Some parameters have a relatively small spread its values and similar projects for SC can be taken as constant coefficients determined experimentally. These include τ , ω_0 , φ_0 . EMC analysis of scientific instruments is to calculate the performance parameters of each functional unit under the influence of electromagnetic interference from other assemblies, subassemblies. In some cases, then calculates a final parameter functional reliability of the scientific complex in general. A significant level of non-uniformity of electrical and Magnetic noise components in terms of spacecraft, and also in time Depending on the mode of scientific complex forces go on individual assessment of ECMO for each block separately. There are two possible approaches: statistical, when the introduction of a number of statistical parameters considered accidental interference levels generated by individual units, noise attenuation in the propagation medium moments on and off individual units, etc.; deterministic when all accounted for in the calculation of the quantities received not random, such limits are assigned to them, the worst value. In a particular case, or evaluates the total impact of all complex spacecraft equipment for each unit, or regarded dual situation - in turn verified the absence of unacceptable interfering effect of each block to any other. Typically, separately analyzes the impact of the flow conducted disturbances, magnetic and electrical and statistical quasi-static fields and possible subsequent summation induced interference directly at the inputs receptors. It is also advisable separately, to some degree as independent tasks, consider the effect of continuous narrowband and wideband impulse noise, because the analog paths are the main disturbance is narrowband interference to digital - Switching broadband interference. Of particular importance is the analysis of space- RES at EMC effects of secondary electron emission. Photons colliding with the shell SC, cause the occurrence of electron emission from the surface and electromagnetic fields associated with the emergence of so-called. " currents of substitution ", the cause of which is the emission of electrons from the surface of the shell; currents occur in the material substitution spacecraft design and within blocks of REA [2]. Since these currents are induced by means of an electromagnetic pulse can have a negative impact on the functioning of the onboard electronic systems are interesting ways in which it is possible convenient and accurate calculation of the current values of substitution. The requirement for military and space technology provides resistance blocks CEA space to the phenomenon observed with action X-rays knock electrons out of which SC structure and cable shields. These " broken" electrons create cable conductors for the current pulses, which in turn will induce a high voltage on the interface circuit blocks. This effect is attenuated before administration interface circuit protection devices (terminal devices) that shunt current to the unit, and hence the voltage limit contacts. Protection device can be adjusted to adequate protection unit interfaces, but in this case problem of induction exposure of current elements unit circuits which are not connected to the interface circuits, and therefore are not protected against interference, which will induce a current within the block. Fig. 1 shows a protection device interface that can generate field sensing element circuit blocks. In an actual system the number of side loops of sources may be in the range of five to a few hundred.

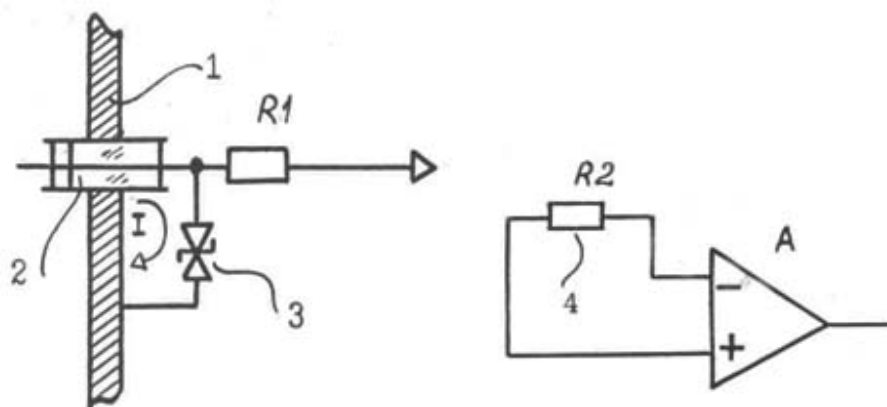


Fig.1. The mechanism of formation of a pulsed magnetic field.

1 - wall unit, 2 - block connector 3 - radiation source 4 - radiation detector

Methods of analysis and evaluation of the impact of this effect involves the following steps: 1) Parameter Description current source, 2) Defining a single power circuit, and 3) Determining the single receiver circuit 4) Determination of communication between source and receiver 5) calculating an open circuit voltage of the receiver; 6) Tests for checking the results of analysis, and 7) Perform energy in the load receiver. 8) Comparison of the calculated energy levels with the requirements specifications for a block. The amount of current in a circuit depends upon the type of cable, the level of X-radiation and an impedance circuit. The field strength depends linearly on the current source, and to a much greater extent on the geometric dimensions of the real circuit. Since the protection device functions operate shunt current, the paramount magnetic field. The magnetic field produced by the current that flows through the basic contour is defined by the following formula [3]

$$H = \frac{Ia^2}{r} \left(\frac{1}{r} + j \frac{2\pi}{\lambda} - \frac{2\pi}{\lambda} \right) e^{j2\pi r/\lambda} \quad (2)$$

where I - loop current in amperes; λ - wavelength in meters; a - loop radius in meters, d - distance from the center of the path in meters. It is assumed that $a \ll d$. Since the effect is close to a decaying sinusoid, a current source circuit I is determined by the following relation:

$$I = A \sin(2\pi t/T) e^{-bt} \quad (3)$$

wherein A - amplitude of the current (A); t - time (sec) T - current period (s); b - attenuation coefficient (sec⁻¹). Circuit receiver as defined in the radially connected arcs (Fig. 2) arranged concentrically in the plane of the ring receiver. Determining the receiver circuit in such a way facilitates the calculation of the current density, reducing solution double integral over the loop area of the receiver to a single integral, multiplied by, where θ -angle tightening extreme path segments receiver. Magnetic flux through the circuit of the receiver can be calculated by the formula.

$$\Phi = \mu \theta \int_{r_1}^{r_2} |H| r dr \quad (4)$$

where μ - magnetic permeability of free space; θ -width receiver circuit in radians; r - the radius drawn from the center of the source circuit, in meters; r_1 is the inner radius of the receiver circuit in the meter; r_2 - outside radius in meters of the receiver circuit.

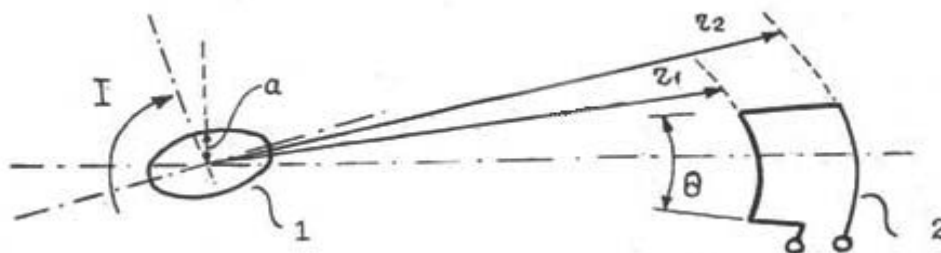


Figure 2 Model for circuit analysis 1 - Source 2 - receiver; a - radius of the loop; I - current in the circuit

Using the expression for the flux F to determine the voltage induced in a single-turn loop receiver can be used Faraday's law. The result is the following expression:

$$U_{oc} = \left[-A \sqrt{B^2 + \frac{4\pi^2}{T}} a^{-\beta t} \cos \left(\frac{2\sigma}{T} t + t g^{-1} \frac{bt}{2\pi} \right) \right] \left[\frac{a^2 \theta}{4} \mu \int_{r1}^{r2} \left[\left(\frac{1}{r^3} - \frac{4\pi^2}{\lambda^2 r} \right) + \right]^{1/2} r dr \right] \quad (5)$$

wherein A - amplitude of the peak current (A); a - radius source circuit (meters); b - attenuation coefficient (1 / s); r - distance from the center of the path; $r1$ - distance from the inner edge of the receiver to the center con-travel source (m); $r2$ - the distance from the outer edge to the center of the receiver circuit of the source (m) θ - the width of the receiver circuit (rad); T - current period (s); t - time (sec); μ - the permeability of free space; λ - wavelength (m).

The above-described equation can be solved by computer, taking into account changes all input parameters related to the physical geometry of the source and the receiver circuit, as well as setting the current signal source. Results of calculation - the voltage as a function of time $H(t)$. Test Data [3] confirm the results of the calculations. This algorithm can be used to assess the sensitivity of the different types of circuits. Using the coupling coefficient, we can determine the energy E in the circuit of the receiver using a simple model. In determining the energy in the circuit are important factors receiver input impedance of the device and loop impedance source. Comparison of the energy values of energies, leading to malfunction of the circuit elements, gives an indication of possible failures.

References

1. Mikhailov, VF Space Communication Systems: Proc. Benefit / VF Mikhailov, Moshkin VI, IV Bragin; SAC. St. Petersburg. 2006. 174 p.: Il.
2. Kursk VI Space telemetry. - Moscow: Nauka, 1970.
3. Adams W.J. SCemp induced., Magnetic field coupling to buried circuits. - IEEE, International Symposium on electromagnetic compatibility, Boston, 1985, p. 385-389.

CALCULATION LEASE PAYMENTS CURRENT ECONOMIC CONDITIONS

Tihonov G.V.,*Grachev N.N.

Moscow, MATI; *Moscow, MIEM-HSE

A method for calculating the lease payments in modern enterprises operating conditions to determine the reliability of repayment of lease payments taking into account the real possibilities of the lessee. Methodology approach to the calculation of the lease payments based on the level of financial enterprises lessees author suggests using not only private figures for lower limits of the recommended financial indicators but also composite index

obtained by calculation and selection of companies lessees of the number of small and medium enterprises through their ranking . Proposed leasing mechanism will improve the efficiency of leasing transactions and to broaden the technical re-equipment of small and medium enterprises of mechanical engineering .

Keywords: leasing, technical re-equipment, the lessor, Ranjit, financials

One of the major problems of the leasing business is to determine the size, dynamics lease payments and the total cost of the lease based on the real possibilities of the lessee. Calculation economically reasonable amount of payments to the lessor provides a certain level of profitability, and the lessee - acceptable in specific circumstances, the level of costs. For the lessor is important to consider and reflect leasing payments all expenses incurred by leasing transaction: - Firstly, related to the execution of the contract of sale (acquisition costs of credit, to pay the cost of the property seller, transportation property, payment of taxes, duties, etc.); - Secondly, related to the execution of the leasing contract the lessee (the cost of preparation and holding of the transaction: staff salaries, rent, depreciation of office equipment, travel, travel costs, office supplies, the cost of control over the property, insurance costs, etc . etc.). It must be emphasized that the calculation of the size of the lease payments can be made by different methods depending on the type of lease, forms and methods of payment as well as the conditions of the economy, ie with a steady development or subject to inflation. Experience of Western countries shows that the conditions for a well-functioning economy developed and tested numerous models for calculating lease payments. The Russian economy periodic lease payments or the value of the current lease payment leasing company generally has the following structure:

$$LP_i = AO_i + PK_i + B_i + NI_i + DU_i + NDS_i \quad (1)$$

where AO_i - depreciation (value settlement of the carrying value of the leased asset); PK_i - fee for credit resources; NI_i - property tax; B_i - reward the lessor; DU_i -additional services; NDS_i - deduction of VAT; i - number of the current payment.

If we examine all the structural components of the lease payments in the general formula (1), we can conclude that they are dependent on several factors. Highlighted in Figure 1, these basic factors.

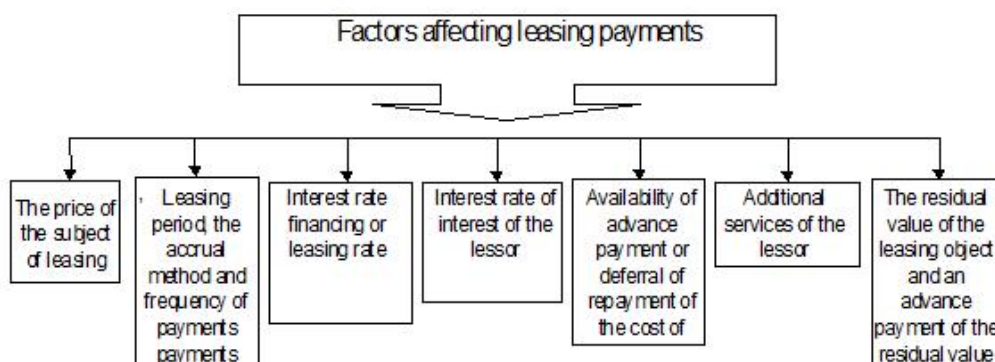


Fig. 1. The main factors affecting the lease payments

Analysis of components of the lease payment, showed that the main factors that have a significant impact on the structure of the lease payments are as follows: the frequency leasing payments; leasing rate, interest rate remuneration lessor a residual value; advance on the residual value, the presence of an advance payment or delay repayment of the value of the object leasing. These factors increase the cost lease transaction as compared to the original

cost of the leased asset. Calculations show that the lease payments, the faster will be repaid the cost of the leased asset, for example, by paying an advance or higher initial payments (dependence 1), the lower the amount of interest will be charged for the use of credit resources, as the interest charges accrued lease payments with the principal balance debt. This decreases the amount of remuneration of the lessor, if the rate is set as a percentage of the residual value of the leased asset. Conversely, if the lessee transfers the payment of the first payment to a later date (the dependence 3), increasing the total cost of the leased asset at the expense of large interest accrued on the principal balance of the loan and using the accrual of interest. The lower interest rate financing, the higher, ultimately, the effect achieved when using the lessee leasing transaction. Leasing rate is an objective value, the size of which is determined individually in each case and depends on factors such as risk assessment leasing transaction cost involved financial resources. It displays the actual leasing companies accruing interest rate on its rate of funding. At the same time, reducing the price of the contract due to the advance payment occurs distraction equity lessee. Therefore, the advance payment is appropriate only in the case of the special requirements of the lessor.

If the lease agreement stipulated redemption leasing subject to expiration, the lessee may transfer the amount of the advance paid to the lessor equal installments over the lease term on account of costs or production costs [2]. Provided rescheduling carrying value of the leased allows the lessee to establish production with minimum cost and pay the lease payments of revenue coming from the use of the leased asset. However, during the deferment fee is increased use of credit resources. Appreciation leasing increased if taken into account when calculating the value of additional services. However, the rate of rise in price of the leasing transaction is not always the main criteria that the lessee determines your choice. In practice, leasing transactions include obtaining maximum value added services and with the agreement of the parties, include the cost in the lease payments. Despite the fact that the lease payments are initially seem more expensive for the end user, but they are more attractive as a result reduce the price of leasing transaction by reducing the taxable base of the lessee.

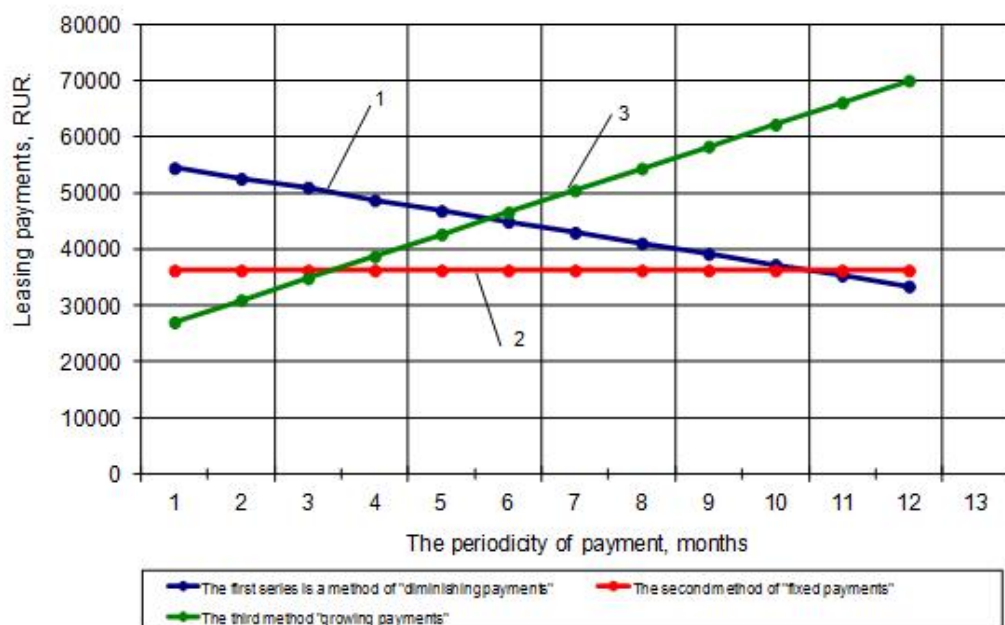


Fig.2. Proposed methods of lease payments

The residual value of the leased asset - the value of the leased asset is equal to its original cost less depreciation on it during the lease term. The main objective of the residual

value of the subject in the leasing transaction is to reduce the monthly payments under the lease agreement. During the term of the lease residual value will not be reimbursed to the lessor. This means that the leasing company has granted a reprieve to the lessee by the amount of the residual value. This kind of service is paid to the nature and the end of the contract the lessee shall pay the residual value and accrued interest thereon. By agreement of the parties the lessee may make equal or unequal installments residual value leasing object in the lease payments as an advance on the residual value. This approach allows the lessee to reduce the financial burden at the end of the lease agreement. In the linear depreciation method, if the contract provides early termination of a leasing deal, the leasing object has zero residual value. In nonlinear residual value depreciation method in the calculation of the leased asset leasing payments should not be below 20% [1]. The magnitude of the residual value of the leased asset for any depreciation method depends on the lease term and accelerated depreciation rate.

It is understood that the early redemption of the leased asset at its residual value is not always economically viable operation for the lessee. Early redemption of the leased asset leads to the fact that the lessee the value of the residual value of the leased asset is extinguished through the company's own funds. This means to reduce the working capital of the enterprise and reduce profits. To ensure the proper functioning of companies in the current economic conditions in Russia and according to their financial condition and taking into account the expected risk for the lessor offered rational schemes lease payments on the example of three small and medium enterprises of mechanical engineering. Repayment schemes lease payments businesses lessees on the financial performance and taking into account the anticipated risks are illustrated in Fig. 2. 1 Dependence of the lease payments for the first rank lessees quite acceptable and workable, firms have higher financial strength compared to others, and particularly the financial burden he bears no lessees. Applications such lessees are considered primarily as a consequence they provide reliable lease payments. The remaining applications are included in the next selection for anticipated risks to ensure the maximum load of the leasing company and they receive an acceptable profit. 2 dependence of the lease payments for the second rank lessees of the number of small and medium enterprises do not allow them to accumulate funds for one-time refund of the lease payment or withdraw them in large amounts of turnover before paying. Amount of the lease payment is the same, and only at the end of the lease period the equipment is transferred to the lessee at the residual value. In addition, payment of lease payments generated from the sale of products manufactured by leasing equipment. In such a scheme of repayment, the company can develop normally, its owners can lead normal life and is relatively easy to implement without much difficulty leasing payments.

Lessor is advantageous in that it reduces the risk of default of the lease payment and provides a certain level of profitability. Eliminate the risks associated with the implementation of the leasing project with lessees allows third rank dependence 3 serving lease payments smaller amounts. In the case of timely repayment of the lease payments the company can provide the following deal that meets his or her abilities. Leasing company without risking large amounts of credit history can trace lessees (and bank lending) and ensure their integrity. In case of default of the lessee losses will be relatively small. This approach has obvious advantages for lessees who have an opportunity to get the next object of lease, and possibly the best credit conditions upon prompt return of the lease payments.

References

1. Tax Code (Part Two).
2. RF Government Decree of 17 July 2002 № 983-p "On approval of recommendations for the development organization that engages in transactions with funds or

other assets of internal controls in order to counteract the legalization (laundering) of proceeds from crime and financing of terrorism" 2.

3. Position of the Central Bank of the Russian Federation "On the non-cash payments in the Russian Federation" dated 09/07/92.

4. Russian Federation Government Resolution № 409 "On Measures of State Support of Small Business in the Russian Federation for 1994-1995" dated April 29, 1994 / / Rossiyskaya Gazeta. - 1994. - May 31. - № 101.

5. Abraham YS, MI Leshenko Leshchenko AV Leasing in engineering. Textbook. - M.: GINFO 2001. - 64c.

6. E. Gavrilova, Pogorelov Yu Experience supporting small and medium enterprises // Latin America. - 1999. - № 7-8. - P. 29-40.

7. Tikhonov GV, Development of leasing of the technical re-equipment of small and medium enterprises. Dissertatsiya.-M.: 2005, P.64-67.

CURRENT ISSUES IN IMPROVING INFORMATION SECURITY SUBSYSTEM

Ustselemov V.N.

MESI

One of the approaches to building adaptive subsystem protection of information systems based on a hybrid model to overcome the risk level of the information system security subsystem infringer, including the procedure of case and neuro-fuzzy inference.

Keywords: information security, information security risk assessment, case, the protection system, threat, neuro-fuzzy inference.

Protection level of information resources is one of the main indicators of the effective functioning of the enterprise. At present, enterprises are forced to spend large sums on building a system to protect their information resources. This is due to the fact that every day around the world carried out a huge number of attacks on information systems to inflict maximum damage to their owners. Studies in the field of construction of information security systems, showed that today widely applied methods based on the concept of acceptable risk [1]. This is because the first is irresistible protection system can not be built, and secondly, many business leaders are not able to spend excessive financial and computing resources to improve security systems and are willing to take reasonable risks. Information Risk Management enables companies to find a balance between the cost of construction of information system protection and the resulting effect.

Currently in Russia in the construction of security subsystems based on the concept of acceptable risk, management standards ISO/IEC 17799 - 2005 "Information Technology. Practical information security management" and ISO/IEC 27001 - 2006 "Information Technology. Methods and means of security. Information Security Management System. Requirements". Among the existing methodologies for assessing risk information widely applied techniques such as: CRAMM, FRAP, OCTAVE, RiskWatch, GRIF, Microsoft and other technique [2, 3]. The analysis algorithms, the application of these techniques has revealed a number of significant drawbacks: the lack of an adaptive response to emerging threats, a limited set of templates that significant error assessments, etc.

One of the possible approaches that overcome these drawbacks is to build a hybrid model of the security subsystem of the information system on the basis of risk assessment to overcome her violator.

Analysis of available statistics showed that many types of attacks and their variations are performed on typical scenarios, with the change in the parameters of an information system in the period of destructive influences is typical (template) character.

Given these patterns authors developed a model, a generalized structure shown in fig.1. A key component of the model is a hybrid module level risk assessment, consisting of a block of precedential conclusion (BPC) and block neuro-fuzzy inference (BNI). Hybrid module level risk assessment allows us to calculate the value of the risk level to overcome the security subsystem information system (SSIS) based on the current values of its parameters. This gives you the opportunity to develop informed recommendations for the security administrator to configure SSIS.

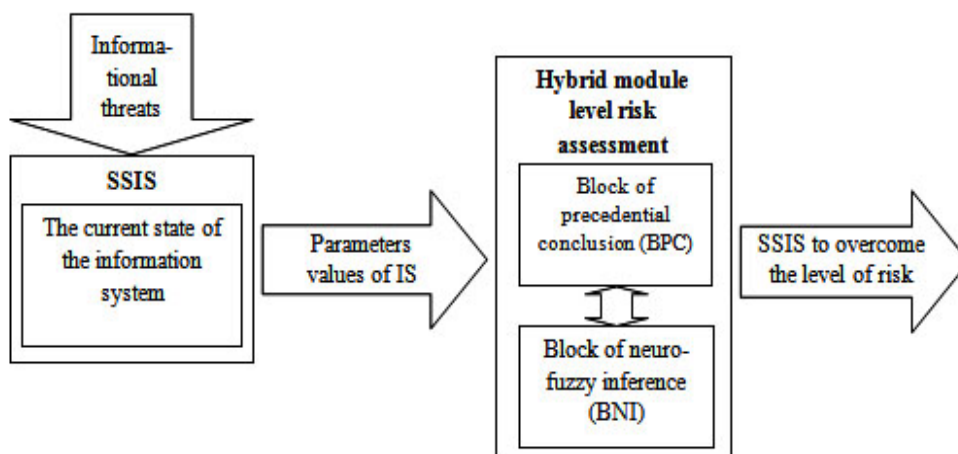


Fig.1 Model settings SSIS using hybrid module level risk assessment.

Determining the risk level to overcome the security subsystem offender information system, is based on the distribution of possible threats to the classes. Classes include the totality of threats precedent setting security subsystem for this type of threat. Classes are divided into two groups: a set of classes from the allowed states of the system in which the parameters of the system change occurs obviously familiar scenario (no exposure to threats), and classes of unresolved states (threats affect the system).

BPC is based on modernized CBR- cycle [4]. BPC accumulates available statistics about the threats and protective measures taken by the behavior of the system during the destructive effects of the offender. In line with the model specified block provides decisions on setting SSIS for a given time no more at sufficiently low cost computing resource.

Block neuro-fuzzy inference is based on fuzzy neural network Sugeno [5]. Application of an additional unit due to the need to determine the risk level in situations that do not have descriptions based precedent that allows for a more fine-tuning mechanisms of protection. Results functioning BNI involved in the formation of a new precedent for upload BPC.

Algorithm interaction of functional blocks module hybrid risk assessment of the offender overcome SSIS is presented in fig. 2.

On the basis of the model was developed with the help of software package which was a computational experiment, whose results are presented in fig. 3.1 and fig. 3.2.

The results obtained led to the conclusion that the application of the developed model to reduce production time control action for setting SSIS by 15-20%, and reduce the cost of computing resources on its production by 10-15%.

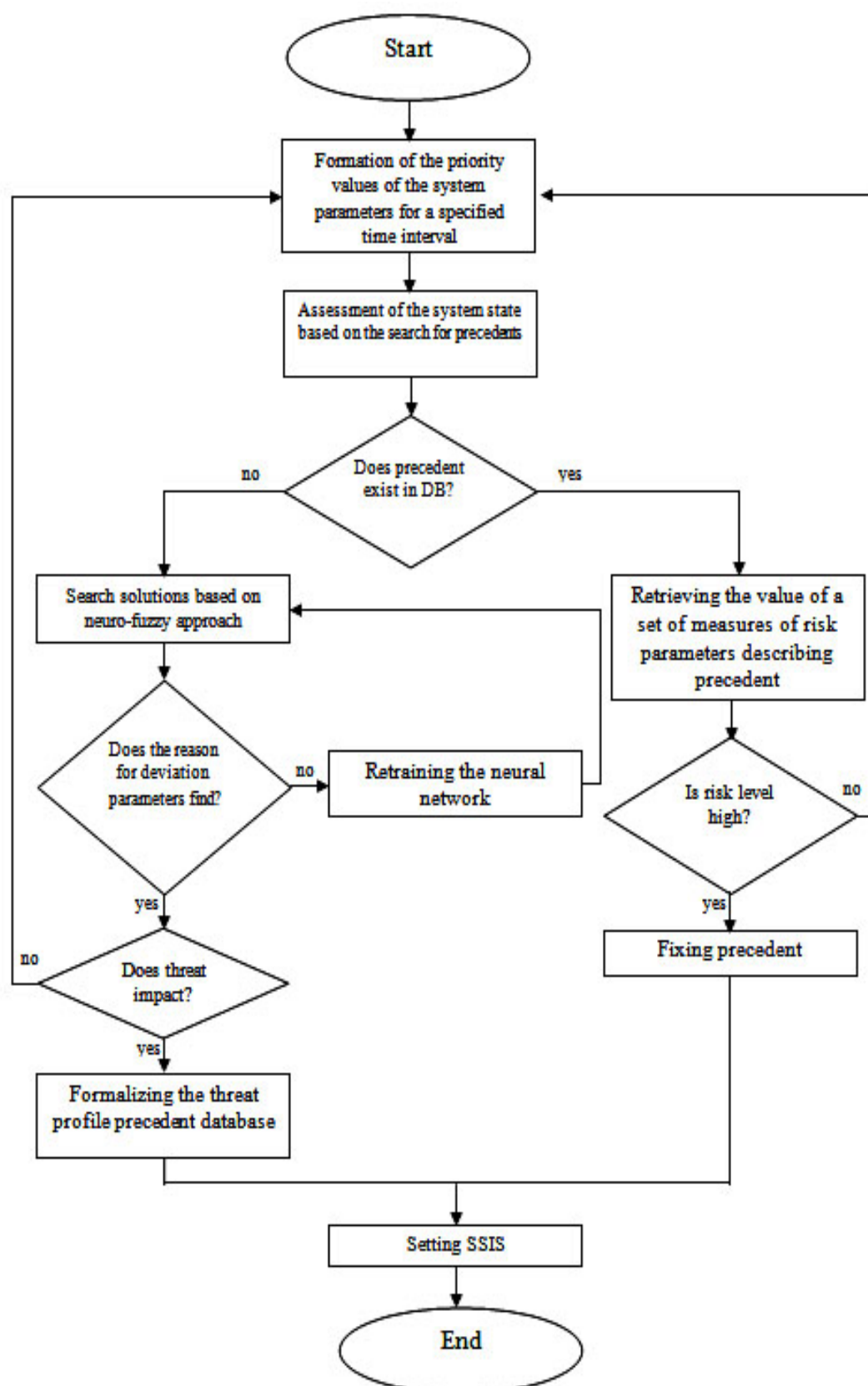


Fig. 2. Algorithm blocks interaction module hybrid risk assessment of the offender overcome SSIS.

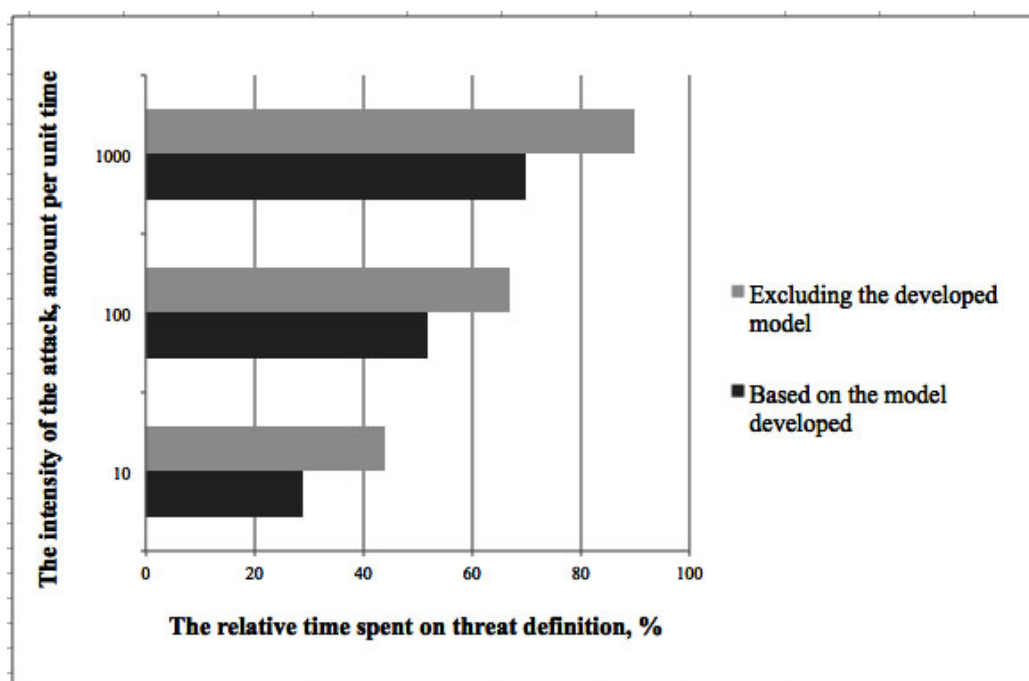


Fig. 3.1. Comparative diagram of the time spent on threat detection.

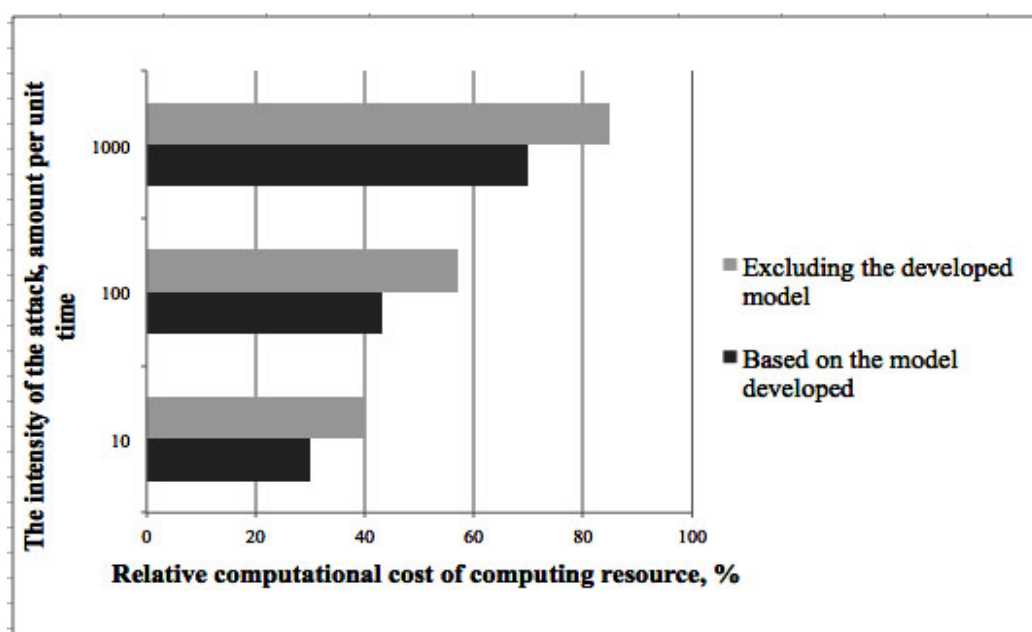


Fig. 3.2. Graph comparing the cost of computing resources on the development of measures to counter threats affecting.

The article describes a hybrid model to overcome the risk assessment of information system security subsystem infringer. It is shown that the use of a combination unit neuro-fuzzy inference and machine theory precedents allowed to solve the problem of improving the functioning of SSIS in terms of destructive influences attacks violators.

References

1. Berketov G.A., Mikrjukov A.A., Fedoseev S.V. Optimizacija sistemy obespechenija bezopasnosti informacii v avtomatizirovannyh informacionnyh sistemah. Sbornik trudov Mezhdunarodnoj nauchno-prakticheskoj konferencii «Innovacii na osnove informacionnyh i kommunikacionnyh tehnologij», Sochi, 2010, str. 329-332.

2. ISO/IEC 17799 - 2005 "Information Technology. Practical information security management".

3. ISO/IEC 27001 - 2006 "Information Technology. Methods and means of security. Information Security Management System. Requirements".

4. Varshavskij P.R., Ereemeev A.P. Metody pravdopodobnyh rassuzhdenij na osnove analogij i precedentov dlja intellektual'nyh sistem podderzhki prinjatija reshenij //Novosti iskusstvennogo intellekta, No 3, 2006. – S. 39 – 62.

5. M.G. Matveev, A.S. Sviridov, N.A. Alejnikova Modeli i metody iskusstvennogo intellekta – Moscow: Finansy i statistika; INFRA-M, 2008 – 448 s.

METHODS OF OPERATIONAL STATE MONITORING FOR INTERFACE AND COMPUTER PATHS OF AVIONICS SYSTEMS

Avakyan A., Kopnjonkova M.

JSC "Institute of Aircraft Equipment", Zhukovsky

Monitoring of an operational state is the substantial component of fault-tolerant systems with controlled redundancy. The paper considers such monitoring issues as check methods which provide required check confidence and check reliability, and sufficient check thoroughness to reconfigure a system to correct detected failures and malfunctions, as well as the limit check duration for any devices which implement critical functions.

Keywords: monitoring, check, redundancy, failure, malfunction, system reconfiguration.

The purpose of operational state monitoring is to check correct system functioning to isolate a failed area for which there is a redundant component. In this case the redundant component means not only a redundant component of automatic recovery, but also spare components for system restoration resulted from system repair.

Let us define the characteristics of a system state check component, such as check thoroughness, reliability and confidence:

- check thoroughness should be such that a failure is isolated to an area for which there is a redundant component (built-in or contained in the spares kit);
- check reliability;
- check confidence should be such that the probability of an undetectable failure does not exceed the standard probability of an undetectable failure specified in the airworthiness regulations and the standards for regularity of flight operations.

We shall deduce a formula which relates the probability of an undetectable failure of any device to the coefficient of device check confidence, to determine the coefficient of check confidence which provides the specified probability of the undetectable device failure. At the same time we shall propose that the following two check modes are available:

- test check;
 - check with additional methods which provide the probability of an undetectable failure specified in the airworthiness regulations [1, p. 14]. Let us introduce some conventions:
1. Test check confidence coefficient, η_T , equal to the ratio of the number of failures, n_T , detected during test check, to the total number of failures, N , i.e.:

$$\eta_T = \frac{n_T}{N} \quad 0 \leq \eta_T \leq 1. \quad (1)$$

Test check confidence coefficient for check with additional methods, η_d , equal to the ratio of the number of failures detected with additional check methods, n_d , to the total number of failures, N , i.e.:

$$\eta_d = \frac{n_d}{N} \quad 0 \leq \eta_d \leq 1. \quad (2)$$

False test check coefficient, η_{LT} , equal to the ratio of the number of false failures detected during test check, n_{LT} , to the total number of failures, N , i.e.:

$$\eta_{LT} = \frac{n_{LT}}{N} \quad 0 \leq \eta_{LT} \leq 1. \quad (3)$$

2. False tolerance check coefficient, η_{Ld} , equal to the ratio of false failures detected during tolerance check, n_{Ld} , to the total number of failures, N , i.e.:

$$\eta_{Ld} = \frac{n_{Ld}}{N} \quad 0 \leq \eta_{Ld} \leq 1. \quad (4)$$

Since the flow of failures for electronic devices is a Poisson one, then the failure probability for any device during the period t is:

$$P = 1 - e^{-\lambda t}, \quad (5)$$

where λ is the failure rate.

When λ has small values (less than 10^{-2} failures per hour), formula (3) can be transformed as follows:

$$P = \lambda t. \quad (6)$$

When t equals one hour, the failure probability (6) is equal to the number of failures per hour, since the failure rate is the number of product failures per time unit.

Based on expression (6), expression (1) can be transformed as follows:

$$\eta_T = \frac{P_T}{P_N} = \frac{P_T}{P_T + P_{nT}}, \quad (7)$$

where:

- P_T is the probability of a device failure detectable with the test check;
- P_N is the probability of a detectable and undetectable device failure;
- P_{nT} is the probability of a device failure undetectable with the test check.

Let us transform expression (7) relative to the probability of a failure undetectable with the test check, P_{nT} .

$$P_{nT} \cdot \eta_T = P_T - P_T \cdot \eta_T = P_T (1 - \eta_T).$$

Hence,

$$P_{nT} = \frac{P_T (1 - \eta_T)}{\eta_T}.$$

Since $\eta_T = \frac{P_T}{P_N}$, then P_{nT} will be equal to:

$$P_{nT} = P_N (1 - \eta_T). \quad (8)$$

Based on expression (7), expression (4) can be transformed as follows:

$$\eta_{LT} = \frac{P_{LT}}{P_N} = \frac{P_{LT}}{P_{NLT} - P_{LT}}, \quad (9)$$

where:

- P_{LT} is the probability of a false device failure detectable with the test check;
- P_{NLT} is the probability of a device failure detectable, undetectable and false detectable with the test check;
- P_{NT} is the probability of a device failure undetectable with the test check.

Let us transform expression (9) relative to the probability of a false failure detectable with the test check, P_{LT} .

$$P_{NLT} \cdot \eta_{LT} = P_{LT} + P_{LT} \cdot \eta_{LT} = P_{LT} (1 + \eta_{LT}) .$$

Hence, taking into account (54), we shall obtain:

$$P_{NLT} = P_N (1 + \eta_{LT}) \quad P_N = \frac{P_{NLT}}{(1 + \eta_{LT})} . \quad (10)$$

By substituting P_N from (10) into (8), we shall obtain an expression for a failure undetectable with the test check, with due account of false failures:

$$P_{NT} = P_{NLT} \frac{(1 - \eta_T)}{(1 + \eta_{LT})} = P_N \frac{(1 - \eta_T)}{(1 + \eta_{LT})} + P_{LT} \frac{(1 - \eta_T)}{(1 + \eta_{LT})} . \quad (11)$$

Formula (11) enables test check capabilities to be evaluated. In particular, it enables an answer to the question, whether it is possible to reach the undetectable failure probability of 10^{-9} and satisfy the airworthiness requirements [1, p.14], using test check methods. For this purpose we shall find a pessimistic, maximum possible lower estimated probability of an undetectable failure during the test check only. The practice shows that:

- the maximum test check coefficient can reach $\eta_T < 0.98$;
- the probability of a detectable and undetectable failure for a complicated electronic device is $P_N < 10^{-4}$;
- the false test check confidence coefficient is $\eta_{LT} < 0.2$;
- with the lowest check reliability, the false failure probability cannot exceed $P_{LT} = P_N \cdot \eta_{LT} < 2 \cdot 10^{-5}$.

By substituting these values in formula (56), we shall obtain the undetectable failure probability equal to $P_{NT} = 2 \cdot 10^{-6}$. As seen from this estimate, the test check does not allow the undetectable failure probability to be reached to satisfy the airworthiness requirements. Therefore, additional check methods are needed which allow the check confidence to be brought to values required to obtain the undetectable failure probability less than 10^{-9} .

Let us denote the additional check confidence coefficient with η_d and estimate the confidence value, η_d , required to obtain the undetectable failure probability less than $P_{nd} < 10^{-9}$.

Similarly to (8), the additional check confidence coefficient, η_d , will be equal to the ratio of the probability of a failure detectable with an additional check method to the probability of a failure undetectable with a test check method:

$$\eta_d = \frac{P_d}{P_N} = \frac{P_d}{P_d + P_{nd}}, \quad (12)$$

where:

- P_d is the probability of a device failure detectable with the additional check;
- P_{nd} is the probability of a device failure undetectable with the additional check.

By making the derivation similar to that for the probability of a failure undetectable with the test check relative to the probability of a failure undetectable with the additional check method, we shall obtain the following expression for P_{nd} :

$$P_{nd} = P_{Nld} \frac{(1-\eta_d)}{(1+\eta_{Ld})} = P_N \frac{(1-\eta_d)}{(1+\eta_{Ld})} + P_{Ld} \frac{(1-\eta_d)}{(1+\eta_{Ld})}, \quad (13)$$

where:

- P_{Nld} is the probability of a failure detectable, undetectable and false detectable with an additional check method;
- P_{Ld} is the probability of a false failure detectable with an additional check method;
- η_d is the confidence coefficient for an additional check method;
- η_{Ld} is the confidence coefficient for a false additional check method.

We shall find an expression for the additional check confidence coefficient, η_d , from (13).

$$\eta_d = 1 - \frac{P_{nd}}{P_{Nld}} (1 - \eta_{Ld}) = 1 - \frac{P_{nd}}{P_N + P_{Ld}} (1 - \eta_{Ld}). \quad (14)$$

Similarly to (9), η_{Ld} is equal to:

$$\eta_{Ld} = \frac{P_{Ld}}{P_N} = \frac{P_{Ld}}{P_{Nld} - P_{Ld}}.$$

Hence,

$$P_{Ld} = \eta_{Ld} P_N. \quad (15)$$

By substituting (7) into (6), we shall obtain:

$$\eta_d = 1 - \frac{P_{nd}}{P_N} \frac{(1-\eta_{Ld})}{(1+\eta_{Ld})}. \quad (16)$$

Let us substitute the following values into formula (16):

- the probability of a device failure undetectable with the additional check, $P_{nd} < 10^{-9}$ (airworthiness requirement for a catastrophic situation [1, p. 14]);
- the probability of a detectable and undetectable failure for a complicated electronic device, $P_N < 10^{-4}$;
- the false check confidence coefficient for an additional check method, $\eta_{LT} < 0.2$.

As a result of the calculation, we shall obtain the value of the check confidence coefficient for additional check methods equal to $\eta_d = 0.9999975$, which provides the undetectable failure probability of 10^{-9} . Such a check value close to one means that practically all components of the devices which implement critical functions, have to be checked to satisfy the airworthiness requirements.

It is shown above that the check confidence with a coefficient not greater than $\eta_T < 0.98$ can be reached with the test check. At the same time the undetectable failure probability will be $P_{nt} > 2 \cdot 10^{-6}$. Since such an undetectable failure probability does not satisfy the airworthiness requirements imposed upon the devices which implement critical functions and whose failures can result in a catastrophic situation, the check methods should be applied that provide the check confidence with a coefficient close to one.

Let us consider such a check method as applied to the most complicated typical device, such as an interface computer path. This is the majority control method for signals which carry parameter information and pass over the entire interface computer path (echo signal), by comparing values of a critical parameter, for example, a parameter which defines

an aircraft attitude. The check confidence close to one can be ensured by comparing echo signals of two paths via all interfaces implemented in a given device. After such a check has been performed with the majority control, i.e. with the pairwise comparison of three and more interface computer paths, a faulty path can be detected.

The selection of a signal comparison criterion is the main problem for this check method. With no claim to be exhaustive, let us consider a number of the most frequently used comparison criteria for information comparison.

Bit-by-Bit Comparison

For this method, words are compared with each bit at the output of the interface computer paths.

Advantages of the bit-by-bit comparison:

- the comparison procedure takes place continuously for each word and immediately and does not require any computing process interruptions;
- the procedure is more sensitive to any information corruptions on one of the compared paths;
- since the information of each bit can have only one of two numerical values, 0 or 1, the pairwise comparison of three interface computer path outputs will yield a single result with the information about a faulty path.

Disadvantages of the bit-by-bit comparison:

- **high sensitivity to insignificant information corruptions which do not affect information accuracy;**
- **the bit-by-bit majority control is possible, if the bits of identical words are compared, i.e. the information at the compared path outputs must be synchronized.**

Tolerance Comparison

For this method, the comparison criterion is a tolerance for parameter value accuracy.

Advantages of tolerance comparison:

- the comparison procedure takes place continuously for each word and immediately and does not require any computing process interruptions;
- the procedure is not sensitive to insignificant information corruptions within the tolerance limits.

The dependence of check efficiency on a tolerance is the disadvantage of the tolerance comparison. If this tolerance is large, some failures cannot be detected due to errors of first kind, and if the tolerance is small, false failures can occur (errors of second kind).

Moreover, this check method is not sensitive to such failures as “parameter freeze”, when a parameter value on a path does not change after a failure. If at the same time an actual parameter value varies within the tolerance limits, the failure will not be detected.

If the coincidence of all bits in compared messages about a parameter value is selected as a check criterion, multiple errors of first and second kind appear from inevitable fluctuations in the paths. Furthermore, this check method requires the strict synchronization of message sequences on the compared paths.

The methods, which do not compare parameter values in individual messages, but compare the parameter characteristics of message statistics, i.e. an integral parameter, are not subject to the drawbacks of the above methods.

A method of comparing confidence intervals for the residual variance of regression [3, p. 336] of a random process of compared parameter variation is the most efficient as shown below. The residual variance of regression is independent of parameter variations, and the confidence interval for this residual variance is independent of random fluctuations and sensitive to failures only.

Check with a Regression Filter

Let us describe the mathematics of building a regression filter with which we can obtain a confidence interval for the residual variance of a random process of compared parameter variation.

We shall add the following restrictions on the random process under consideration, which take place in real processes:

- a) The values of a random process are known only for parameter measurement moments, $\mathbf{t(i)}$ (where $\mathbf{i} = 1, 2, 3 \dots$), i.e. this is not a random continuous process, but a discrete one.
- b) Random processes feature an ergodic property in the areas where no transients are present [1, p. 339-343].

Let us denote a random process of parameter variation with $\mathbf{W(t)}$, and introduce a term “ergodicity interval”, $\mathbf{T_{\Theta}}$, an interval which can lie in any time domain and contain process characteristics equal to that defined in another interval greater than $\mathbf{T_{\Theta}}$. Then, the ergodicity conditions for the random process $\mathbf{W(t)}$ can be written as follows:

$\mathbf{W(t)}$ – the process is ergodic in the intervals:

$$\mathbf{t(i+N) - t(i) \geq T_{\Theta}}, \quad (17)$$

where \mathbf{N} is the number of ergodicity interval points.

We shall use condition (17) to build an ensemble of realizations for a synthesized random process (called conditional) which is adequate to a real process consisting of a single implementation. We shall take as the first realization of the new process any interval of the real process greater than $\mathbf{T_{\Theta}}$, which has the following time restrictions in the real process:

$$(\mathbf{t_1(n) - t_1(1)}) \bullet \mathbf{C \geq T_{\Theta}(2)}, \quad (18)$$

where

- $\mathbf{t_1(1)}$ is the time when the formation of the first realization and the entire ensemble begins;
- $\mathbf{t_1(n)}$ is the time, when the formation of the first realization and the entire ensemble terminates;
- \mathbf{n} is the number of points (measurements for one realization);
- \mathbf{c} is the number of realizations.

If the ensemble consists of \mathbf{C} realizations, the intervals for the entire ensemble can be written as follows:

$$\begin{aligned} &\mathbf{t_1(n) - t_1(1)}, \\ &\mathbf{t_2(n) - t_2(1)}, \\ &\dots\dots\dots \\ &\mathbf{t_c(n) - t_c(1)}. \end{aligned} \quad (19)$$

For the conditional random process that we have defined, we shall form a matrix with the values at the above described points:

It is seen from this ensemble of the intervals that the last point, $\mathbf{t_c(n)}$, of the conditional process corresponds to the point (measurement time), $\mathbf{t(N=c \bullet n)}$, of the real process. Let us introduce the term of a integration period for a random process, $\mathbf{T_{in}}$, which is equal to the period between the time of the first point of matrix (20), $\mathbf{t_1(1)}$, and the time of the last point of this matrix, $\mathbf{t_c(n)}$. Since the estimate of the confidence interval for residual variance will be calculated using matrix (20), the length of this interval must be such that the estimate be reliable. This interval must be greater than the ergodicity interval, $\mathbf{T_{\Theta}}$, (condition (18), so that the reliable estimate be obtained.

$$\mathbf{W(t)} = \begin{pmatrix} \mathbf{W_1(t_1), W_1(t_2) \dots W_1(t_j) \dots W_1(t_n)} \\ \mathbf{W_2(t_1), W_2(t_2) \dots W_2(t_j) \dots W_2(t_n)} \\ \dots\dots\dots \\ \mathbf{W_i(t_1), W_i(t_2) \dots W_i(t_j) \dots W_i(t_n)} \\ \dots\dots\dots \\ \mathbf{W_c(t_1), W_c(t_2) \dots W_c(t_j) \dots W_c(t_n)} \end{pmatrix} \quad (20)$$

Moreover, the integration interval must not exceed one second (a catastrophic situation evolves during one second as a minimum), so that a failure which can have catastrophic consequences be corrected. Therefore, in order to obtain efficient estimates for the ensemble of realizations, in particular the confidence interval for the residual variance, it is necessary to fulfill the condition:

$$1\text{sec} \geq T_{in} \geq (t_1(n) - t_1(1)) * C \geq T_3(5). \quad (21)$$

Let us introduce an additional restriction on the conditional random process. Random numbers (measured parameter values) contained in matrix (20) are subject to any multidimensional distribution where all moments above the second one are equal to zero. A multidimensional normal distribution is the most typical distribution of this type [3, p. 341].

Let us consider some operations with the values of matrix (20) to obtain the estimates of intermediate values, which are the arguments of regression functions for a random process, a residual variance and a confidence interval.

Let us determine a covariance matrix (22) and a correlation matrix (23), using this matrix (20):

[illegible]

[illegible]

where $\mathbf{k}_{j,j}$ and $\mathbf{r}_{j,j}$ are a covariance moment and a correlation moment between the random numbers of time sections, \mathbf{i} and \mathbf{j} , respectively.

While taking into account the introduced restrictions on the random distribution law, we shall determine:

- the estimate of a mathematical expectation for the random values of the conditional process at the section t_j , which will be equal to [3, p. 379]:

$$MW(t_j) = \frac{1}{C} \sum_{i=1}^C W_i(t_j) = a_c(t_j) , \quad (24)$$

- the estimate of a standard (rms) deviation for the random values of the conditional process at the section t_j , which will be equal [3, p. 379]:

$$GW(t_j) = \sqrt{\frac{\sum_{i=1}^C (W_i(t_j) - a_c(t_j))^2}{C-1}} = G_c(t_j), \quad (25)$$

- the estimates of elements in the covariance matrix and the correlation matrix, respectively, between the sections, j and l , which are determined with the following formulas [3, p. 441]:

$$k_{JI} = \frac{\sum_{i=1}^C (W_i(t_j) - a_c(t_j)) * (W_i(t_l) - a_c(t_l))}{C-1}, \quad (26)$$

- we shall obtain an estimate for a correlation coefficient by normalizing the covariance estimates with the standard deviation estimates for the sections, **j** and **l**:

$$r_{jl} = \frac{k_{jl}}{G_c(t_j) G_c(t_l)} . \quad (27)$$

The operation of estimating a linear regression coefficient, β_j , for each **j**-th column of matrix (22) is determined from the following formula [3, p. 447]:

$$\beta_i(t_j) = \frac{1}{|k_{i,j}|} \sum_{l=1}^{n-1} k_{0,l} K_{i,l} , \quad (28)$$

where:

- $\beta_i(t_j)$ is the estimate of the i-th linear regression coefficient at the section t_j of the matrix;
- $|k_{i,j}|$ is the determinant of the covariance matrix;
- $k_{0,l}$ is the estimate of a covariance element between the sections **0** and **l** of the matrix;
- $K_{i,l}$ is the algebraic complement of the element $k_{i,l}$ ($l=1,2,\dots,n-1$) of the covariance matrix.

The operation of estimating the residual variance, $(\sigma_{oa}(\mathbf{c}, \mathbf{n}))^2$, for the regression of the Π_1 parameter from the data of matrix (22) is determined from the following formula [3, p. 602]:

$$\begin{aligned} (\sigma_{oa}(\mathbf{c}, \mathbf{n}))^2 = & \frac{1}{C} \sum_{i=1}^C (W_i(t_0) - a_c(t_0) - \beta_1(t_1) * (W_i(t_1) - a_c(t_1)) - \dots - \\ & - \beta_k(t_j) * (W_i(t_j) - a_c(t_j)) - \dots - \beta_{n-1}(W_i(t_n) - a_c(t_n)))^2, \end{aligned} \quad (29)$$

where:

- $(\sigma_{oa}(\mathbf{c}, \mathbf{n}))^2$ is the estimate of the residual variance for the regression of the Π_1 parameter;
- $\mathbf{j} = 1, 2, \dots, n-1$.

Harold Cramer [3, p. 602] has proven that the statistics, Ψ , for the ratio of residual sum of squares to its estimate multiplied by the number of the realizations, **C**, is distributed to the χ^2 law with degrees of freedom of $V = C - n - 1$, i.e.

$$\psi = \frac{(\sigma_o)^2 C}{(\sigma_{oa}(\mathbf{c}, \mathbf{n}))^2}, \quad (30)$$

where:

- $(\sigma_o)^2$ is the value of the parameter residual variance;
- $(\sigma_{oa}(\mathbf{c}, \mathbf{n}))^2$ is the estimate of the parameter residual variance.

The probability density for the χ^2 distribution is defined by the formula [2, p. 150]:

$$K_V(x) = \begin{cases} P_V(\chi^2 \leq t) & \text{at } t > 0, \\ 0 & \text{at } t \leq 0. \end{cases} \quad (31)$$

The expression for $P_V(\chi^2 \leq x)$ is as follows:

$$P_V(\chi^2 \leq t) = \frac{1}{2^{\frac{V}{2}} \Gamma(\frac{V}{2})} t^{\frac{V}{2}-1} e^{-\frac{t}{2}}, \quad (32)$$

where $\Gamma(\frac{V}{2})$ is the gamma function, whose integral representation (Euler formula) for the continuous values, z , takes the following form [3, p. 143]:

$$\Gamma(z) = \int_0^{\infty} x^{z-1} e^{-x} dx. \quad (33)$$

For the integer values $z > 0$ the following correlations take place:

$$\Gamma(z+1) = z!, \quad 0! = \Gamma(1) = 1.$$

Let us introduce the designation $\frac{V}{2} = z + 1$, then the equality is true:

$$\Gamma\left(\frac{V}{2}\right) = \left(\frac{V}{2} - 1\right)!. \quad (34)$$

By substituting (34) into (32), we shall obtain the following, easy for calculations formula:

$$P_V(\chi^2 \leq t) = \frac{1}{2^{\frac{V}{2}} \left(\frac{V}{2} - 1\right)!} t^{\frac{V}{2}-1} e^{-\frac{t}{2}}. \quad (35)$$

Relying on the above stated, we can write the following inequality:

$$t_{\min}(V, P_{\min}) \leq \frac{(\sigma_o)^2 * C}{(\sigma_{od}(c, n))^2} \prec t_{\max}(V, P_{\max}) \quad (36)$$

where t_{\min} and t_{\max} are the reciprocal distribution of (34) for the probabilities, P_{\min} and P_{\max} , respectively, with V degrees of freedom.

Then the confidence interval for the standard deviation estimate, with the confidence probability of $P_d = P_{\max} - P_{\min}$, will take the form of the following inequality:

$$\sigma_{od}(c, n) \sqrt{\frac{t_{\min}(V, P_{\min})}{C}} \leq \sigma_o \prec \sigma_{od}(c, n) \sqrt{\frac{t_{\max}(V, P_{\max})}{C}}. \quad (37)$$

Since the majority comparison of residual variances is performed for the same parameter which has passed over at least three paths, we shall introduce an index, T , designating the path number, into the residual variance estimate identifier. With regard to this index, the residual variance estimate identifier will be as follows: $\sigma_{od}(c, n)T$.

Based on (37), the lower bound and the upper bound of the confidence interval for the standard deviation of the residual variance have the following values, respectively:

$$\sigma_{od}(c, n)_H T = \sigma_{od}(c, n) \sqrt{\frac{t_{\min}(V, P_{\min})}{C}}, \quad \sigma_{od}(c, n)_B T = \sigma_{od}(c, n) \sqrt{\frac{t_{\max}(V, P_{\max})}{C}}. \quad (38)$$

The confidence interval for the standard deviation of the residual variance is determined with the following formula:

$$D_{od}T = \sigma_{od}(c, n) * \left(\sqrt{\frac{t_{\max}(V, P_{\max})}{C}} - \sqrt{\frac{t_{\min}(V, P_{\min})}{C}} \right) = \sigma_{od}(c, n) * \Delta, \quad (39)$$

where Δ is the coefficient defining a fraction in the standard deviation of the residual variance which is equal to the confidence interval for the standard deviation of the residual variance.

Then the comparability and incomparability conditions for the confidence intervals of the standard deviation of the residual variance for a parameter which passes over the 1st path and the 2nd path, respectively, will be written as the following inequalities:

$$|D_{od1} - D_{od2}| \leq A - \text{comparable}, \quad |D_{od1} - D_{od2}| \geq A - \text{incomparable}, \quad (40)$$

where A is the comparability parameter which is chosen experimentally.

Let us estimate a necessary parameter measurement rate to obtain reliable estimates of the residual variance and a confidence interval of the residual variance. It is seen from formulas (29) and (39) that the reliability of estimates for the residual variance and the confidence interval for the standard deviation of the residual variance are dependent on the statistics, with which matrix (20) is built. Since the relationship between the residual variance and its estimate is defined with the expression (87), which is distributed as the Pearson distribution law, χ^2 [3, p. 258].

It is seen from expressions (36) and (39) that the confidence interval for the residual variance is dependent on the χ^2 reciprocal distribution, which is defined by the number of realizations for a random process of parameter variations, C , the number of points in each realization, n , and the confidence probability, with which we wish to obtain the confidence interval for the estimate.

The number of realizations, C , and the number of points in the realization define the number of degrees of freedom, V , with the following relationship:

$$V = c - n - 1 \quad (41)$$

It is seen from matrix (20) that the number of measurements, N , necessary for matrix formation, is $N = c \cdot n$. The practice shows that the minimum time of catastrophic situation progress is equal to one second. Therefore, the period of formation and processing for matrix (20), designated as $T_{\phi 0}$, should be less than one second. The period of formation for matrix (20), T_{ϕ} , will be equal to the period of one measurement, T_n , multiplied by the number of matrix elements, i.e. $T_{\phi} = T_n \cdot N$. Let us designate the period of matrix processing with T_0 .

Then $T_{\phi 0} = T_n \cdot N + T_0$.

From the other hand, N should be not less than the value which is enough to provide the reliability characteristics of matrix (20). Let us designate this magnitude with N_d . The above description yields the following inequality which defines requirements for the period of parameter measurement, T_n :

$$T_n \cdot N_d + T_0 \leq 1 \text{ sec.} \quad (42)$$

Inequality (42) cannot be always performed. For these cases the following procedure may be offered:

- After the period of formation, $T_{\phi} = T_n \cdot N$, for matrix (20) ends, the matrix data are not processed, but stored in a computer memory. From this point the second cycle of matrix (20) formation and processing begins.
- The third and subsequent cycles of matrix (20) formation begin not at the moment when during the previous cycle the period of formation and matrix data processing ends, but within a period equal to $1 \text{ sec} - T_0$.

With such a procedure of matrix (20) formation and processing, the result of matrix (20) processing, i.e. the result of comparison of confidence intervals for residual variances using formula (40), will appear each period less than a second. The implementation of the procedure is feasible since the speed of present-day computers is several orders greater than the parameter measurement rate.

In order to determine N_d , i.e. the number of random process realizations, C , and the number of measurements in each realization, n , the calculations of χ^2 distribution characteristics are performed. They are given in Table 5. The calculations are performed with the confidence probability:

$$P_d = P_{\min} - P_{\max} = 0.996,$$

where:

- P_{\min} is the lower bound of the confidence probability equal to the integral of the χ^2 distribution density; formula (35) defines the lower bound of the confidence interval for the standard deviation of residual variance;

- P_{\max} is the probability equal to the integral of the χ^2 distribution density; formula (80) defines the upper bound of the confidence interval for the standard deviation of residual variance.

The expression used to determine P_{\min} and P_{\max} is as follows:

$$P_{\min} = \frac{1}{2^{\frac{V}{2}} (\frac{V}{2} - 1)!} \int_{-\infty}^{t_{\min}} t^{\frac{V}{2}-1} e^{-\frac{t}{2}} dt \quad (43)$$

$$P_{\max} = \frac{1}{2^{\frac{V}{2}} (\frac{V}{2} - 1)!} \int_{-\infty}^{t_{\max}} t^{\frac{V}{2}-1} e^{-\frac{t}{2}} dt, \quad (44)$$

where:

- t_{\min} is the quantile of the lower estimate of the confidence probability which defines the lower bound of the confidence interval for the standard deviation of residual variance determined with formula (84);
- t_{\max} is the quantile of the upper estimate of the confidence probability which defines the upper bound of the confidence interval for the standard deviation of residual variance determined with formula (84).

Table 5 χ^2 Distribution Characteristics with Confidence Probability $P_d = 0.996$

n	C	V	P_{\min}	t_{\min}	P_{\max}	t_{\max} x	$\sqrt{\frac{t_{\min}(V, P_{\min})}{C}}$	$\sqrt{\frac{t_{\max}(V, P_{\max})}{C}}$	Δ	m=v -2	$\sigma = \sqrt{2 \cdot V}$
5	41	35	0.001 62	14. 5	0.997 8	62. 5	0.595	1.240	0.64 5	33	8.37
10	10 0	89	0.001 43	55	0.997 7	13 1	0.742	1.145	0.40 3	87	13.34
30	27 0	239	0.001 53	17 9	0.997 7	30 4	0.814	1.061	0.24 7	237	21.87

Columns 11 and 12 show the values of the mathematical expectation and the standard deviation of variance, respectively.

The table is formed for three measurements: $N=C*n=205, 1000, 8100$.

It is seen from the table that:

- When $N=205$, the number of realizations $c=41$ and the number of points in each realizations $n=5$, the confidence interval for the standard deviation of residual variance is 0.645 of the estimate for the standard deviation of residual variance

$$D_{od}T = \sigma_{od}(c, n) * 0.645;$$

- When $N=1000$, the number of realizations $c=100$ and the number of points in each realizations $n=10$, the confidence interval for the standard deviation of residual variance is 0.403 of the estimate for the standard deviation of residual variance

$$D_{od}T = \sigma_{od}(c, n) * 0.403;$$

- When $N=8100$, the number of realizations $c=270$ and the number of points in each realizations $n=10$, the confidence interval for the standard deviation of residual

variance is 0.247 of the estimate for the standard deviation of residual variance

$$D_{od}T = \sigma_{od}(c,n)*0.247.$$

The method of comparing information which has passed over different interface computer paths, has the following advantages:

- the method is slightly correlated with both the characteristics of compared information and the characteristics of devices which generate and process information. At the same time it is greatly correlated with the characteristics of a device state;
- the method requires no information synchronization.

References

1. Aviacyonnye pravila (chast' 25), Normy lyotnoj godnosti samolyotov transportnoj kategorii, izdaniye Mezhgosudarstvennogo aviacionnogo komiteta, Moskva, 2009
2. B.V.Gnedenko "Kurs teorii veroyatnostey", Gosudarstvennoye izdalel'stvo fiziko-matematicheskoy literatury, 3-e izd., pererab., Moskva, 1962
3. Harald Cramer "Matematicheskiye metody statistiki", izdatel'stvo "Mir", Moskva, 1973

USING FCA BASIS THEOREM ON CONCEPT LATTICES IN ANALYZING SCIENTIFIC MONOLOGIC TEXT ONTOLOGY

Dambaeva, S.V., Merdygeev B.D.

Russia, Ulan-Ude, East-Siberian State University of Technology and Management (ESSUTM)

Abstract. This article describes the features of the application of the basis theorem on concept lattices of FCA for analyzing ontologies. It is shown that the mathematical apparatus FCA can be successfully applied to the development of systems for automatic analysis and evaluation of automatically generated ontologies.

Keywords: Ontology, Formal Concept Analysis (FCA), concept lattice, basis theorem on concept lattice.

Introduction. To date, there are more than a dozen methods of evaluation of ontologies that put themselves one of the following purposes: completeness and accuracy of vocabulary domain, the adequacy of the structure in terms of taxonomy, relationships, etc. (best known in this regard, formal ontology Metaproperties OntoClean), acceptance (from a cognitive point of view). Gestalt approach, the performance with applications, choosing the best of several available ontology. All of these methods can be divided into manual, semiautomatic and automatic [1].

The conceptual basis of scientific monologic text ontology is created based on the automatic extraction knowledge from sources (encyclopedias, dictionaries, terminology and textbooks, research papers, etc.) [2]. This means that the scientific monologic text ontology generated automatically by extracting knowledge from the above sources and their treatment - ever-growing system. Therefore, for its analysis and evaluation necessary to develop methods to make this work without the involvement of experts, i.e. automatic ontology analysis and evaluation methods.

The technique, called Formal Concept Analysis (FCA), designed for the analysis of explicit knowledge. It can be used for ontology analysis and evaluation. Ontology analysis by FCA assumes conversion of ontology in the formal context, formal context concepts in the

concept lattice, and then ontology analysis on the concept lattice. The task of converting the ontology into a formal context described in earlier papers [4, 5]. In this paper, we describe two problems that were solved in converting formal context of ontology to concept lattice and applying FCA theorems to ontology analysis on the generated concepts lattice.

Application FCA in ontology analysis. FCA method can be used to analyze completeness and consistency on in-categorical relations set between different concepts (terms) of ontology, and these relations should be binary, so they can be converted into formal context.

All entries of the scientific monologic text ontology contain information of terms set having quantitative relationship with the term, described in the entry (convertible terms and correlates) [2].

Entry "Concept" also contains information of terms set, having in-categorical qualitative relations with the term, such as the "genus - species" relations (hierarchy), "whole - part" relations (aggregation). Analysis of these two types of relationships produced separately, i.e. for each type of relationship built its concept lattice.

Entries "Action", "State", "Event", "Property" and "Values" do not contain information about in-categorical relations. If viewed from this side concept lattices can be built only on the basis of the top-level hierarchy of entries "Concept."

Hierarchy and aggregation relationship types within the meaning suitable for presenting their concepts lattices. In-categorical relations also suggest a certain order, but direct analysis of their structure is not possible. To analyze these relations requires introduction of new agreements, so at the stage of studying FCA applied to the analysis of ontologies, it was decided to focus on two types of relationships - respect "genus - species" (hierarchy) and against "whole - part" (aggregation). Thus, there are two types of relationships that can be explored using concept lattices.

Quantitative relations of identity and correlation are not about order relationships. They are symmetric, non-hierarchical. Quantitative relations are horizontal, i.e. concepts are synonymous, would be located on a lattice of concepts at the same level. As a result of constructing lattices for the relations of identity and correlations we have to get extended lattice containing the upper and lower special nodes and just one level of nodes.

Quantitative relationships are the relationships between the interchangeable concepts (terms) – between objects of concepts lattice or its attributes, but it is impossible extract information about what the concept is an attribute and what the object from these relations. However, the method of Formal Concept Analysis can define the concepts that should be in the quantitative relationship.

Thus, the solution of the problem analysis of the ontology by FCA consists of three stages:

1. Convert relations "genus - species" and "whole - part" described in the entries of ontology in the formal context table;
2. The transformation the table formal context in the concept lattice;
3. Extraction from concept lattice one level terms that are synonymous or correlates as concepts that have the same attributes (for synonyms) or with some of the same attributes (perhaps similar meaning concepts or correlates) and not having a single common attribute (unrelated concepts). It will check not only the correctness of identity and correlation relations in the ontology entries, but also to supplement the missing relationship or bring new information about the relationship between concepts.

Features of using the basic theorem on concept lattices in constructing concept lattice of ontology. In the description of the basic theorem on concept lattices refer [3].

Let consider the features of the application the basic theorem on concept lattices to the analysis of concept lattices, formal contexts and ontologies in general. According to the basic

theorem of lattice concepts $\mathfrak{R}\langle G, M, I \rangle$ - complete lattice in which infimum and supremum are given by:

$$\begin{aligned}\wedge(A_t, B_t) &= \left(\bigcap_{t \in T} A_t, \left(\bigcup_{t \in T} B_t \right)'' \right) \\ \vee(A_t, B_t) &= \left(\left(\bigcup_{t \in T} A_t \right)'', \bigcap_{t \in T} B_t \right)\end{aligned}$$

Theorem describes a mechanism for constructing a concept lattices, namely, formed as the lattice nodes and the links between them. The theorem implies that lattice should contain the most common attribute (the supremum of the lattice) and the most common node (infimum of the lattice). If they are not, it is necessary add them as a nameless nodes of the lattice. Built concept lattice from the formal context table checked for compliance basic theorem. Ontology analysis by FCA assumes conversion of ontology in the formal context, formal context in the concept lattice, and then - the analysis of concept lattice. Therefore it is very important correct construction a concepts lattice.

Concept lattices can be depicted by the usual lattice diagrams. It would however be too messy to label each concept by its extent and its intent. A much simpler reduced labelling is achieved if each object and each attribute is entered only once in the diagram. The name of object g is attached to the lower half of the corresponding object concept $\gamma g := (\{g\}'', \{g\}')$, while the name of attribute m is located at the upper half of the attribute concept $\mu m := (\{m\}', \{m\}''')$. It is then still possible to read of all extents and all intents from the diagram for any concept (A, B) , we have

$$g \in A \Leftrightarrow \gamma g \leq (A, B) \text{ и } m \in B \Leftrightarrow (A, B) \leq \mu m.$$

In other words, extent and intent of an arbitrary concept can be found as the set of objects in the principal ideal and the set of attributes in the principal filter generated by that concept.

One of the problems in converting the formal context to concept lattice is the ability to represent the same formal context by different concept lattices. Figure 1 shows the different features of the lattice representation of the same formal context.

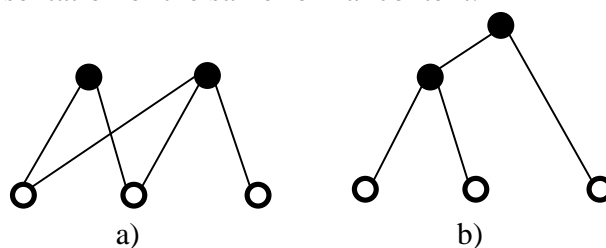


Figure 1: Representation elements of the lattice (a fragment of the lattice).
White elements - objects, black – attributes.

The figure shows that the two objects on the left have the same attributes. However, the third object has one of the attributes too. Representation of the lattice bonds between attributes can be in a form a) or as a variant b). Links between attributes in the embodiment b) said that the top attribute is present in all objects of the lower attribute. This version of the image is more logical links, but more difficult to implement.

Another problem is the low degree of visibility constructed concept lattices. Figure 2a shows the three objects and two attributes, all of these objects have all the attributes. Such representation of the lattice reduces the visibility of the lattice due to the large number of links. One way to increase the visibility of the lattice is adding additional nodes, which are not described in a formal context to combine the top attributes available to all objects, as shown

in Figure 2b. This improves the visibility of the lattice, but it also increases the complexity. These additional nodes should not affect in the analysis of the lattice. Such additional lattice nodes can be confused with a simple lattice intersection arc, so it is necessary to somehow labeled them and formally defined.

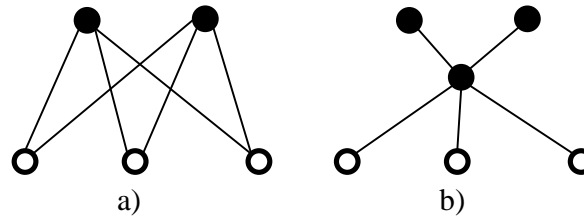


Figure 2: Adding additional node.
White elements - objects, black – attributes

Thus, a well-formed concept lattice has a supremum and infimum, it is a multilevel structure (Figure 1b) and has additional unnamed nodes added to increase its visibility.

Abridged subcontext. Relations on the arcs context $\langle G, M, I \rangle$ determined using the arrow relations defined as follows: for $h \in G, m \in M$, say:

$$\begin{aligned} g \swarrow m &: \Leftrightarrow \begin{cases} (g, m) \notin I \text{ and} \\ \text{if } g' \subseteq h' \text{ and } g' \neq h', \text{ then } hIm, \end{cases} \\ g \nearrow m &: \Leftrightarrow \begin{cases} (g, m) \notin I \text{ and} \\ \text{if } m' \subseteq n' \text{ and } m' \neq n', \text{ then } gIn, \end{cases} \\ g \nearrow m &: \Leftrightarrow g \swarrow m \text{ and } g \nearrow m. \end{aligned}$$

These relationships are rather specific, as are the relationships between objects and attributes that are not linked by the relation I . They needed to determine some of the following theorems. In the future they will be used in the allocation of subcontexts from the ontology.

As shown in Figure 3 the relationship defines the relationship between objects and attributes, and the attribute m does not link with the object g (m is not an attribute of g), but it links with the object h having all the attributes of g (which in this case can be considered as a special case of the object g).

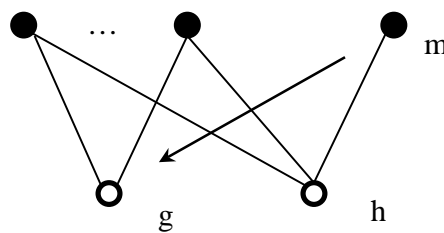
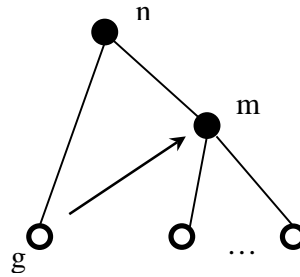


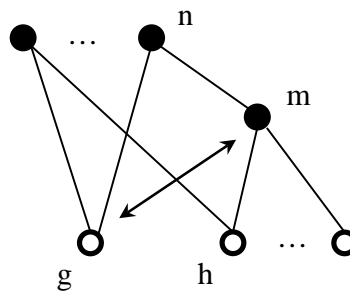
Figure 3: Arrow relation $g \swarrow m$

This relationship exists between the object and attributes links with specific instance of this object, and with the help of this relationship may be distinguished dial a specific instance of a shared object.

As shown in Figure 4 the relationship $g \nearrow m$ defines the relationship between object and attributes, and the attribute m is subattribute of more common attribute n , which links with object g (m is not an attribute g). In this case, n and m can bind relationship relatives or form part of an integer, with n - genus or whole, and m - view or part of, respectively, for each of the relations. This relationship exists between an object and an attribute that is subattributes any attribute of the object.


 Figure 4: Arrow relation $g \nearrow m$

As shown in Figure 5 the relationship includes the signs of the two previous relationship. This relationship exists between an object and an attribute that is subattribute any attribute of the object, and in this case the attribute has an object, which is a specific instance of the object.


 Figure 4: Arrow relation $g \searrow m$

For given $g \in G$ there exists an attribute $m \in M$ with $g \nearrow m$ if and only if g is \vee -irreducible (minimal, supremum-irreducible). Dually, $g \nearrow m$ holds for some $g \in G$ if and only if m is \wedge -irreducible (infimum-irreducible). Therefore if we define a formal context to be doubly founded if

$$(g, m) \notin I \Rightarrow \exists n \in M \ g \nearrow n \text{ and } m' \subseteq n'$$

$$(g, m) \notin I \Rightarrow \exists h \in G \ h \searrow m \text{ and } g' \subseteq h'$$

Concept lattices such context will contain many irreducibly. It can actually be shown that: if L - a lattice, then the set $J(L)$ \vee -irreducible is \vee -dense and set $M(L)$ \wedge -irreducible is \wedge -dense as it takes place in finite lattices. In accordance with the basis theorem of L is isomorphic to the concept lattice its standard context $(J(L), M(L), \leq)$.

A sufficient condition for $\langle G, M, I \rangle$, to be doubly founded is that its concept lattice $\mathfrak{R}\langle G, M, I \rangle$ - doubly founded lattice, i.e. that for any two elements $x < y$ are elements s and t such that s is minimal with respect to $s \leq y$, $s \not\leq x$ and t is maximal with respect to $t \geq x$, $t \not\geq y$. We can say s - the minimum element of the lattice, t - max.

In general, the definition of double-founded context suggests that this context has its own special object g , such that $g \leq x$, for any $x \in G$, and attribute m , such that $m \geq y$, for any $y \in M$.

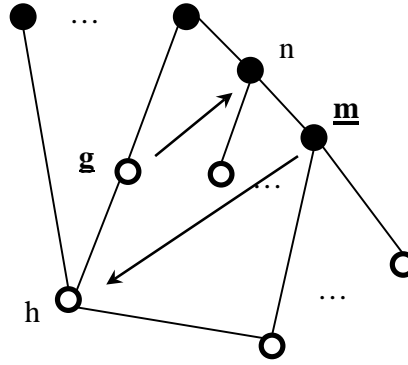


Figure 6: Example of relations describing the double-founded context

Each double-founded context contains subcontext isomorphic to the standard context. Such a subcontext is called reduced.

In order to create all the concepts of finite formal context we will make sample extensional (sets of objects of formal concept) formed in a closure system. The corresponding closure operator $A \mapsto A''$ can be easily calculated from the formal context. Assuming $G = \{1, \dots, n\}$, the linear strict order $<$ on subsets of G defined by:

$$A < B \Leftrightarrow A <_i B$$

for some $i \in G$, where

$$A <_i B \Leftrightarrow i \in B \setminus A \text{ и } A \cap \{1, \dots, i-1\} = B \cap \{1, \dots, i-1\}.$$

Moreover, let

$$A \oplus i := (A \cap \{1, \dots, i-1\}) \cup \{i\} - \text{addition to } i.$$

Concept lattice L of reduced subcontext can be constructed on the basis of subcontext $(J(L), M(L), \leq)$. $J(L)$ is set \vee -irreducible elements, wherein the set is \vee -dense. $M(L)$ is set \wedge -irreducible elements, wherein the set is \wedge -dense. This subcontext eliminates all the elements that are common in relation to other elements.

A reduced subcontext includes only specific objects. If in the construction concept lattice used unnamed nodes for combine attributes, they also eliminated. Therefore taped the connections between objects and combine attributes. For example, if any two attributes have all objects of some other attribute, then this another attribute to respect them will be common attribute and not enter into the reduced subcontext. This method reduces the context by removing more general information (objects and attributes) and the more specific the information is not lost.

Also, using the reduce subcontext helps to detect errors in the distribution of the concepts in sets of objects and attributes. When forming subcontext, a set of objects $J(L)$ and a set of attributes $M(L)$ is automatically generated from the lattice elements. Their formation is not considered main context sets G and M .

Reduce subcontext allocation algorithm has no mechanism for removing repeated links, but in the concept lattice of full context the due to general or more nodes this reconnection may look correct. In the reduction of context repeated links become apparent in most cases.

Reduce subcontext allocation is more formal mechanism for analyzing the structure of the context. One method of application reduce subcontext mechanism may be checking correctness ontology concepts separation into objects and attributes.

Conclusion. This article describes the features of the application of the basis theorem of concept lattices from mathematical apparatus FCA, which can be used for analyzing ontologies. In our description we was based on the materials described in [3].

Before the analyzing task stand the task of building the most comfortable concept lattice. The basis theorem on concept lattices is a rule of construction concept lattices for analysis. It was found that the structure of double founded formal context most convenient for analysis. Were studied reduced contexts and their applicability to examine the structure of formal context and of the concept lattice. The theorem applicant mechanism is based on the definition of the arrow relations on the concept lattice.

Besides the basis theorem on concept lattices mathematical apparatus FCA has search engines all the concepts from the formal context, through the definition of closure sets, install semantic interpretation concept lattice by identifying implications, identifying many valued contexts that may be useful for constructing ontology or data analysis when considering the same field of study from several points of view.

References

1. Gavrilova T.A., Gorovoi V.A., Bolotnikova E.S., Gorelov V. V. Sub"ektivnye metriki otsenki ontologii. ZONT-2009. [Subjective evaluation metrics of ontologies].
2. Naikhanova L.V. Tekhnologiya sozdaniya metodov avtomaticheskogo postroeniya ontologii s primeneniem geneticheskogo i avtomatnogo programmirovaniya: Monografiya. – Ulan-Ude: Izd-vo BNTs SO RAN, 2008. – 244 p. [Technology for creating methods of automatic construction ontologies using genetic programming and automata].
3. Ganter Bernhard, Wille Rudolf. Applied Lattice Theory: Formal Concept Analysis. – url: <http://www.math.tu-resden.de/~ganter/psfiles/concept.ps>.
4. Naikhanova L.V., Dambaeva S.V. Analiz struktury avtomaticheskoi generiruemoi ontologii i postanovka zadachi ee preobrazovaniya v reshetku formal'nykh kontekstov.: Matematika, ee prilozheniya i matematicheskoe obrazovanie (MPMO'11): Materialy IV Mezhdunarodnoi konferentsii. – Ch.2. – Ulan-Ude: Izd-vo VSGTU, 2011. S. 58-62. [Analysis of the structure automatically generated ontology and task of its transformation into a lattice of formal contexts].
5. Dambaeva S.V., Chulkov Ya.A., Busovikov P.A. Modul' generatsii tablits formal'nykh kontekstov iz ontologii zadannoi struktury. Teoreticheskie i prikladnye voprosy sovremennykh informatsionnykh tekhnologii: Materialy XI Vserossiiskoi nauchnoi konferentsii. – Ulan-Ude: Izd-vo VSGUTU, 2012. S.243-251. [Formal context table generation module from a given structure ontology].

MULTIWORD EXPRESSION DESCRIPTION IN LEXICAL DATABASES

Burukina I. P., *Burukina I. S.

*Penza State University, *Saint Petersburg State University, *Russian State University for the Humanities*

In this article we analyzed the problem of collocations (Multiword Expressions) extraction and their further introduction in lexical databases such as WordNet. We made several conclusions about the inner structure of Multiword Expressions in Russian and present the developed XML pattern for collocation description that can be implemented in RussNet lexical database and other systems.

Keywords: collocations, Multiword Expressions, XML description, lexical database, WordNet, RussNet.

Introduction

The present paper is based on the research conducted as part of the RussNet project (2011-2012) developed by the Department of Applied and Mathematical Linguistics, Faculty of Philology, Saint-Petersburg State University and lead by Irina Azarova.

Lexical semantic database RussNet is a database for Russian and its structure is similar to that of WordNet (WordNet project, Princeton University, New Jersey, USA). In such databases synonymous words are grouped in synsets according to their meanings and synsets are represented as nodes of graphs with hyponymy relations arcs. For each of four main parts of speech (verbs, nouns, adjectives and adverbs) new graph is built. However collocations (multiword expressions) are often left out despite their high frequency and their importance.

The RussNet synsets also do not include collocations. So far no successful method to represent multiword expressions in RussNet system has been proposed. Thus the main goal of the present research is to investigate the inner structure of multiword expressions in Russian and to develop XML pattern for collocation description that can be implemented in lexical databases. During the investigations Russian corpus Bokryonok (21 mln lexemes) was used as the main source of text material.

The term “multiword expressions” was first introduced by the researches of the Multiword Expression Project (Stanford University, California, USA) that was launched in 2001 and is lead by Dan Flickinger. Multiword expressions are “idiosyncratic interpretations that cross word boundaries (or spaces” [Sag et al. 2001]. In the present paper the term “multiword expression” is used as a synonym to the term “collocation” in its broad sense - combination of lexemes used together with high frequency that gets some “special” meaning non-definable as a simple combination of the meanings of its parts.

The article will start with brief discussion of multiword expressions extraction procedure and several interesting puzzles concerning unique properties of the Russian language will be mentioned. Then the developed practical classification of collocation will be introduced. Finally the article presents the XML pattern for collocation description in the RussNet.

Multiword expression extraction in Russian

The first step of the present research was to collect the data. 245 multiword expressions were manually extracted from the Russian corpus Bokryonok using combined linguistic and statistic approaches.

Firstly, 10 nouns, 7 verbs and 6 adverbs were selected as key words for further collocation extraction. The key words were chosen from the top-200 most frequent Russian words; their high frequency increase frequency of collocations and their usual polysemanticism affords an opportunity to derive more collocations with partially idiomatic meanings. Secondly, all the sentences containing key words were extracted from the Bokryonok corpus. Left and right contexts of the key words in these sentences were examined to find “candidate” collocations. Several rules were followed: 1) collocations can be discontinuous, 2) collocations should contain at least two content words, 3) collocations can contain auxiliary words (conjunctions, particles, etc.). Thirdly, candidate collocations were tested using Mutual information score and t-score.

The present research discovered several interesting puzzles for collocation extraction in Russian.

Russian is inflexional language and one can search for a language unit according to either its lemma or precise lexeme. Lemma based search increases rates of non-fixed collocations (for example, *белая ворона*, *lit. white crow*, “*black sheep*”). However for semi-fixed or fixed multiword expressions lexeme based search is preferable. For example, (1) is a

collocation with idiomatic meaning while (2) is a phrase and its meaning is simply a combination of the meanings of its parts.

(1) *Носить на руках*

lit. carry in one's arms

“make much of smb.”

(2) *Носить на руке*

lit. carry on one's arm

Two options appear concerning different parts of speech. Auxiliary words such as prepositions, conjunctions, particles and negations can be treated either as necessary or as optional parts of collocations. For example, (3) and (4) have two different meanings and (4) shouldn't be treated simply as “negative form” of (3); in the RussNet they should be assigned to different synsets. However (5) has the same meaning as (1) and negative particle serves only as a general sentential negation.

(3) *Дай бог*

lit. God, give (imperative form)

“God willing”

(4) *Не дай бог*

lit. God, do not give (imperative form)

“Heaven forbid”

(5) *Не носить на руках*

lit. not to carry in one's arms

(not to) “make much of smb.”

The choice between these options should be made according to the specific aims of a research. Thus in the present research the lexeme based auxiliary words included extraction is used.

Multiword expression classification

The developed classification of multiword expressions in Russian concerns three characteristics of collocations: 1) fixedness of word order, 2) discontinuity and 3) fixedness of unit forms. We distinguish five types of collocations:

11. Adj + Noun: non-fixed word order, discontinuous, non-fixed forms

Example: *молодой человек*, lit. young man, “boyfriend”, also is used to address to any male

12. Noun + Noun with preposition: fixed word order, usually continuous, semi-fixed forms

Example: *человек в футляре*, lit. man in a case, “the man who lives in a shell”

13. Noun + Noun in oblique case: fixed word order, usually continuous, semi-fixed forms

Example: *человек слова*, lit. man of a word, “man who keeps his word”

14. Verb + Noun (with or without preposition) or Infinitive: usually discontinuous, semi-fixed form

Example: *тянуть время*, lit. pull the time, “play for time”

15. Free continuous combinations of parts of speech with fixed word order and forms

Example: *все время*, lit. all the time, “always”

Multiword expression description pattern

The proposed XML-pattern for collocation description was developed on the base of XML-description pattern for single words in the RussNet. The main difference is the invented module PHRASE that includes the component-by-component description of the collocation structure. Key word or core word of the collocation is treated as main lexeme. There is an opportunity to describe the individual valency frames (potential dependent elements) of the components and type of relations between them (agreement, government, contiguity, collocation for expressions with fixed forms).

The pattern can be used to describe collocations of all five types. Fixed contiguous combinations are described as single units in [].

Below main sub-modules of the module PHRASE are presented.

1. module for the description of the structure:

<!ATTLIST ORDER order_type (fixed | non_fixed) #REQUIRED > - word order type description

<!ATTLIST CONTINUITY_TYPE cont_type (cont | discont) #REQUIRED > - continuity type description

<!ATTLIST FORM_TYPE type_of_form (non_fixed | semi_fixed | fixed) #REQUIRED > - unit forms type description

2. module for the description of each of the components:

<!ATTLIST COMPONENT_UNIT NUM (0 | 1) #REQUIRED POS CDATA #REQUIRED ID CDATA #REQUIRED > - grammar values

<!ELEMENT VALENCY_FRAME (VALENCY+)> - valency frame

3. module for the description of relations between the components:

<!ATTLIST COMPONENTS_RELATIONS components_rel_type (agreement | government | contiguity | collocation) #REQUIRED > - relations type description.

References

1. Amaro R., Chaves R.P., Marrafa P., Mendes S. Enriching Wordnets with New Relations and with Event and Argument Structures. 2003.
2. Atserias J., Climent S., Farreres X., Rigau G., Rodriguez H. Combining Multiple Methods for the Automatic Construction of Multilingual WordNets. 1997
3. Baldwin T., Bond F. Multiword Expression: some problems of Japanese NLP. - 2002.
4. Baldwin T. Multiword expressions. - 2004.
5. Fellbaum C. WordNet: An Electronical Lexical Database. 1998.
6. Smadja F. Retrieving collocations from text: Xtract. Computational Linguistics 19. 1993.
7. WordNet 3.0 Reference Manual.
8. <http://wordnet.princeton.edu/wordnet/documentation/>

COMBINING STATISTICAL AND SEMANTIC FEATURES FOR PATENTS PRIOR-ART RETRIEVAL

Dykov, M.A., Kravets, A.G., Korobkin, D.M., Ukustov, S.S., * Strelkov, O.I.
*Volgograd State Technical University, Volgograd, Russia, * Federal Institute of Industrial Property, Moscow, Russia*

In this paper we proposed a method for patents prior-art retrieval, which combines both statistical and semantic features. As statistical features we used patent documents topic distributions, obtained using multiple pre-trained LDA models. As semantic features we used modified semantic trees built from patent claims simplified texts. Performed experiments showed that proposed method significantly outperforms the baseline.

Keywords: Natural Language Processing, Semantic analysis, Topic modeling, LDA, patents prior-art search

Introduction

Every year more and more companies want to patent their inventions. That is why from year to year the number of patent applications is increasing. In 2012 there were more than 2300 thousands new patent applications, which is more than 9% increasing since the previous year. Intellectual capital, especially patent process, researches are fulfilled by international and governmental organizations as well as by enterprises at the corporative level. [1, 2] The escalating applications flow and more than 70 million set of granted patents increase the time that patent examiners have to spend to examine all incoming applications. Sometimes incoming applications wait for examination up to several years. Sometimes examiner has to make hundreds of search queries and to process thousands of existing patents manually during the examination procedure to make a decision: to approve the application or to reject it. This process can take him more than 20 hours [3]. The increasing workload of patent offices led to need for developing of automated decision support systems to help examiners in the examination process.

The task of patent applications examination can be divided into two main subtasks: the task of search for relevant granted patents – prior-art search and the task of the automated decision making about the application patentability. In this paper we consider the solution of the first subtask.

Related work

Many scientists tried to solve patent prior-art search task. The main research in patent retrieval started after the third NTCIR workshop [4]. There is an annual track CLEF-IP, which was created to compare different approaches in different tasks related to patent applications examination process, including prior-art search task. Xue proposed a method based on machine learning [5], D'hondt tried to use syntactic relations [6], Verma approach is based on citations and patent classes [7], Robertson created search query from patent's text and tried to extract granted patents using this query and to rank them using BM25 [8], Mahdabi used patent's summary as a query to search for relevant patents [9], Magdy used an approach based on unigrams and bigrams [10], Graf tried to use external knowledge bases [11]. Different researches used different parts of the patent to solve this task. Mahdabi used only description [12], Verma used all text fields [7], D'hondt used title, abstract and first 400 words of description [6] But, all these approached didn't show significantly improving compare to the baseline. Analyzing the work of D'hondt we found out that adding syntactic relations didn't show increasing of the accuracy. It was strange, because usually in different natural language processing tasks adding syntactic or semantic relations as features leads to increasing of the accuracy compare to the baseline [13, 14]. There are some reasons of this: patent claims contain a lot of complex and very long sentences, patent's texts contain many specific terms. That is why in this paper we decided to investigate the way how to simplify patent's texts to get advantages from applying semantic relations.

In this paper we propose a novel approach, in which we tried to combine both statistical and semantic features to increase the accuracy of prior-art search.

Methodology

We took existing patents from opens sources: USA patent office (USPTO) and Russian patent office. There are total 10 million American granted patents and 2 million Russian. We perform preprocessing for all existing granted patents.

On the first step of preprocessing we convert patents from all existing specification to one common specification. During this process we perform a conversion from the USPTO to IPC classification. On the next step we perform POS tagging. After, based on patents' classes, we slit the existing set of patents into subsets to train multiple independent LDA models. During LDA models training we built topic per document distribution for each patent. In conclusion, we apply a complex sentences splitting method for each sentence in patents claims and then we built simplified semantic trees for each sentence.

For the new patent application on the first step we perform its preprocessing the same way as we did with the existing corpus.

On the second step we apply a special algorithm to select a subset of pre-trained LDA models and after we calculate topics per document distribution for the application based on each of selected models. After that, we calculate a similarity between the application and existing patents based on the similarity between topics per document distributions. We select a subset of the most relevant patents for the third step.

On the third step we perform a semantic trees construction for application claims and then we compare these trees with trees from selected subset. After that we re-rank relevant patents from selected subset according to similarities between semantic trees.

Preprocessing

During the preprocessing of the existing patents set we selected following patent fields for the further processing: patent number, patent classes, publication date, citations, title, abstract, description. Existing corpuses of USA and Russian patents were presented in three different specifications. Everything was converted to the new specification. During the investigation of existing corpuses we found out that all American patents that were published after 1980 and all Russian patents that were published after 1990 have significant amount of grammatical mistakes. It happened because they were automatically converted to the digital representation using automatic texts from images recognition software. A large amount of grammatical mistakes significantly decreases the accuracy of statistical and semantic methods. To solve this problem we made some investigations to find out if it is really necessary to search possible relevant patents within old patents for prior-art search task. Using existing patents corpuses we built directed graph of citations:

$$G = (V, A)$$

where, V – is a set of vertices. The vertex of the graph is patent. A – is a set of edges. The existence of the edge that connects V_i and V_j means that the patent j is cited by the patent i .

Using this graph we performed an analysis of the difference between publication dates of patents and their citations. We took patents that were published during the last three years (Table 1).

Table 1. The average difference between publications dates of patents and their citations

The maximum difference between publication dates of the patent and its citation.	The percentage of all citations
10	59
15	77
20	86
25	91
30	94
35	96

Thus, taking only Russian patents published after 1990 and American patents published after 1990 we lose only 9% and 4% of possible relevant to the application patents respectively.

During the preprocessing step for statistical analysis we excluded from patents' texts the top 100 of the most frequent words and all words that appeared in the corpus only 1 time. In the most cases words that appeared only 1 time were mistaken words. Such words make up 90% of all words in the vocabulary. Sometimes there were also specific terms among these words. But the increasing of the accuracy and of the performance of statistical algorithms after the dropping of 90% of the vocabulary compensates the losing of these specific terms.

During the preprocessing we performed a morphological analysis for all patents in the corpus. This was necessary for the semantic analysis and for the terms selection for statistical analysis. We used existing open source frameworks for this task: Stanford POS tagger for English and TreeTagger for Russian [15,16]. These frameworks show some of the best performance in the morphological analysis. During the morphological analysis we replace original words with their base forms.

Using multiple LDA models for prior-art retrieval

We decided to use Latent Dirichlet Allocation (LDA) for the first step of prior-art retrieval [17]. This is one of topic modeling approaches which allows to represent a document as a topics distribution:

$$D = (P_1, P_2, P_3 \dots P_k)$$

$$\sum_{i=1}^k P_i = 1$$

where, D – is a document, P_i – shows the relevance of the topic i to the document, k – the amount of topics.

Applying of LDA for the similarity calculation between text documents showed its efficiency. But the drawback of this approach is its $O(mnk)$ complexity and its $O(mn)$ memory requirement. where, m – is a number of documents, n – the average number of words in the document [!!!]. Such complexity doesn't allow to effectively use LDA for the entire patents corpus. To solve this problem we decided to split the entire set of patents in subsets according to patents classes:

$$S = (S_{c1}, S_{c2}, S_{c3} \dots S_{cnc})$$

where, S – the entire patents set, S_{ci} – patents subset that belongs to the i class, nc – the number of patent classes.

For the Russian corpus $nc = 141$, for the US corpus $nc = 984$. Thus, the average size of the class is 10.000 patents, which allows to train LDA models effectively. During experiments we found out that the following parameters are the best for LDA models: the number of topics is 500, the number of iterations is 2000. We trained LDA models using the entire patents corpus. We used Mallet as a framework to train LDA models [18]. This framework was selected because of its performance and its ability to use distributed training of the LDA model on big texts sets.

For the new patent application we use the following steps to obtain relevant patents:

- 1) Select cc patent classes, which could be possible cited by the application. These classes contain application classes and classes, which could be possible cited by patents from the same classes as the application. We perform this selection using citations graph G .
- 2) Calculate multiple topics per document distributions using pre-trained LDA models belong to selected classes. So, the application can be represented as follows:
- 3) $App = \{(P_{11}, P_{12} \dots P_{1k}), (P_{21}, P_{22} \dots P_{2k}) \dots (P_{cc1}, P_{cc2} \dots P_{cck})\}$ Calculate similarities between topic per document distributions of application and existing patents using Kullback-leibler distance.
- 4) Rank the final list of relevant patents according to distributions similarities.

Semantic similarity calculation for the retrieved relevant patents reordering

We developed an additional algorithm for prior-art search, based on the semantic similarity calculation between application and patents. But, building semantic trees and searching their intersections requires much more resources than statistical methods, which is a

problem for the corpus of millions of patents. That is why we decided to apply this method as a second step to reorder a subset of patents retrieved using LDA models.

We build semantic trees using only patent claims, because this part of the patent contains its main points and its average size is 5 times smaller than the size of description. Patent claims have one feature, which makes it difficult to apply dependency and semantic parsers on claims sentences: the most of claims are written using one very long complex sentence. To solve this problem we developed a special complex sentence simplification algorithm. We split a complex sentence into simple sentences by special “marker” words. For English texts we selected the following “markers”: “thereby”, “such that”, “so that”, “where”, “whereby”, “wherein”, “when”, “while”, “but” e.t.c. For Russian language: “чей”, “который”, “причем”, “при этом”, “так, что”, “кроме того”, e.t.c.

Each patent claim can be represented as a set of semantic trees, a single tree for each sentence.

$$SN = (ST_1, ST_2, \dots, ST_{ns})$$

where, ST_i – is a semantic tree related to the i sentence in the patent claim, ns – the number of sentences. The semantic tree is built according to the predicate-argument structure of the natural language, so the tree can be represented as a set of vertices (predicates), nodes (arguments) and relations between them (semantic roles).

We used MaltParser to perform semantic parsing [19]. This solution allows to reach a moderate accuracy. But its main advantages are: it is an open-source software and it has pre-trained models for many languages, including Russian and English.

We performed a deep semantic analysis for all semantic trees (Figure 1).

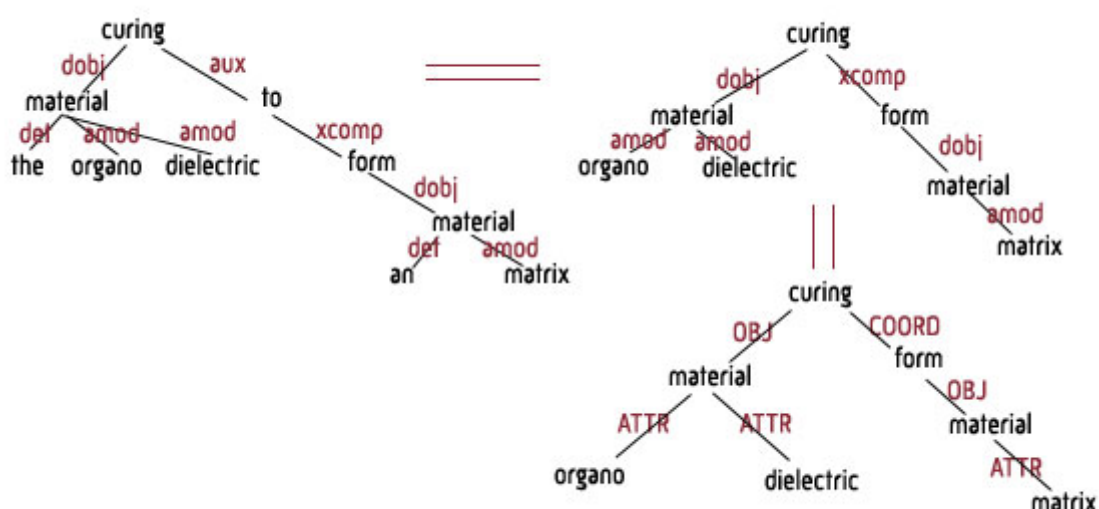


Figure 1. Semantic tree transformation during deep semantic analysis

We merge semantic roles into 5 classes: Subj, Obj, ATTR, APPEND, COORD. For example, for Russian language we merge the following roles into class Subj: “агент”, “квазиагент”, “несобст-агент”, “аппоз”, “дат-субъект”. For English language we merge the following roles into class ATTR: “arg”, “acop”, “mod”, “amod”, “nn”, “neg”, “expl”, “poss”, “possessive”, “attr”. We also removed from semantic trees roles, which are not important for similarity calculation: “aux”, “auxpass”, “cop”, “punct”, “det”, “predet” for English and “PUNC”, “вводн”, “изъясн” for Russian. All these roles are described by XXXX [20,21].

The semantic trees intersection can be calculated as follows:

$$Intersection(ST_k, ST_l) = \sum_{ij=1}^{nr} IsCommon(Words_i, Relations_{ij}, Words_j)$$

$$IsCommon(Words_i, Relations_{ij}, Words_j) = \begin{cases} 1, & Relations_{ij}(Words_i, Words_j) \in ST_k \\ & Relations_{ij}(Words_i, Words_j) \in ST_l \\ 0, & otherwise \end{cases}$$

where, *IsCommon* – is a function which determines if the triple, which consists of two words and relation between them, is common for both trees, *nr* – is a number of semantic relations in the tree.

Thus, the semantic similarity between two patents can be calculated with the following formula:

$$Similarity = \sum_{i=1}^{ns} \max_j intersection(ST_i, ST_j) / nr_i$$

Finally, we reorder the set of relevant patents according to their semantic similarity.

Experiments and Results

We test our methods using two separated test sets: for English and for Russian applications. To test Russian applications we took 200 granted patents belong to the H01 IPC class, which were published last year. We took 650 of these patents' citations which were published after 1990. For English we took 200 granted patents belong to the 174 USPC class with total number of 1100 citations. We performed prior-art search within all patents, which belong to the same class as test patents. The total number of patent that we used in this experiment is about 15000 for Russian and for English. We evaluated the quality of our method using the same metric that is used during CLEF-IP track: the recall for the top 1000, 500, 300, 200, 100, 50 retrieved patents. We compared our method with the baseline based on TF*IDF similarity. The results are presented in Table 2 for Russian test set and in Table 3 for English test set.

Table 2. Results of experiments for Russian test set

Recall/%	R50	R100	R200	R300	R500	R1000	R2000
TF*IDF	34	46	51	53.5	59	68	78
LDA	45	55	64	68	75	85	93
LDA+Semantic	51	61	69	74	78	88	93

Table 3. Results of experiments for English test set

Recall/%	R50	R100	R200	R300	R500	R1000	R2000
TF*IDF	36	48	52	55	61	70	81
LDA	46	56	66	69.5	76	86	94
LDA+Semantic	54	65	73	77	82	90	94

We used a top 2000 retrieved patents after LDA step for semantic analysis.

Discussion and Conclusion

As we can see from Table 2 and Table 3, proposed method, based on LDA, significantly outperforms baseline. Adding re-ranking, based on semantic similarity between application and patent, improved the independent implementation of LDA.

As we can see results obtained using English test set are better than results for Russian test set. It happened because used frameworks for morphological analysis and semantic parsing perform better on English corpus. But, still semantic parsers show not very good results, especially for patents claims.

In conclusion, we proposed a two-steps approach for patents prior-art retrieval. On the first step we applied a method, based on multiple LDA models. By using LDA we

outperformed the baseline accuracy. Multiple models allowed us to implement LDA for the entire patents set.

On the second step we used the similarity between semantic trees to re-rank top relevant patents from the first step. Semantic trees were built after applying of simplification algorithms on patent claims and then were modified using deep semantic analysis. These additional methods for semantic analysis allowed us to increase the accuracy of LDA on the second step.

In the future we are going to increase the accuracy by creating a training set based on patent claims and training a model for semantic parser using this set.

Acknowledgments

World Intellectual Property Organization, Russian Patent Office (Rospatent)

References

1. Alla G. Kravets, Alexandr S. Gurtjakov and Anatoliy P. Darmanian. Enterprise Intellectual Capital Management by Social Learning Environment Implementation. World Applied Sciences Journal 23 (7): pp. 956-964, 2013
2. Alla G. Kravets, Alexandr Gurtjakov and Andrey Kravets. Corporate intellectual capital management: learning environment method. PROCEEDINGS OF THE IADIS INTERNATIONAL CONFERENCE ICT, SOCIETY AND HUMAN BEINGS 2013, pp. 3-10
3. WIPO Economics & Statistics Series. 2013 World Intellectual Property Indicators, 2013
http://www.wipo.int/export/sites/www/freepublications/en/intproperty/941/wipo_pub_941_2013.pdf
4. Iwayama M., Fujii A., Kando N. and A. Takano. Overview of patent retrieval task at NTCIR-3. In Proceedings of NTCIR Workshop, 2002.
5. Xiaobing Xue and W. Bruce Croft. Automatic query generation for patent search. Proceedings of the 18th ACM conference on Information and knowledge management: pp. 2037-2040, New York, NY, USA 2009
6. Eva D'hondt, Suzan Verberne, Wouter Alink, and Roberto Cornacchia. Combining Document Representations for Prior-art Retrieval. CLEF Notebook Papers/Labs/Workshop, (2011), 2011
7. Manisha Verma, and Vasudeva Varma. Exploring Keyphrase Extraction and IPC Classification Vectors for Prior Art Search. CLEF Notebook Papers/Labs/Workshop, (2011), 2011
8. Robertson, S. E., Walker, S., Beaulieu, M. M., Gatford, M., & Payne, A. Okapi at TREC-4. In Proceedings of the 4th Text REtrieval Conference (TREC-4): pp. 73-96, 1996
9. Parvaz Mahdabi, Linda Andersson, Allan Hanbury, and Fabio Crestani. Report on the CLEF-IP 2011 Experiments: Exploring Patent Summarization. CLEF Notebook Papers/Labs/Workshop, (2011), 2011
10. W. Magdy and G. J. F. Jones. Applying the KISS Principle for the CLEF-IP 2010 Prior Art Candidate Patent Search Task. Workshop of the Cross-Language Evaluation Forum, LABs and Workshops, Notebook Papers, 2010
11. E. Graf, I. Frommholz, M. Lalmas, and K. van Rijsbergen. Knowledge modeling in prior art search. Advances in Multidisciplinary Retrieval, First Information Retrieval Facility Conference: pp. 31–46, 2010
12. Parvaz Mahdabi, Mostafa Keikha, Shima Gerani, Monica Landoni and Fabio Crestani. Building queries for prior-art search. Proceedings of the Second international conference on Multidisciplinary information retrieval facility: pp. 3-15, Berlin, 2011

13. Mikhail A. Dykov and Pavel N. Vorobkalov. “How-to” Questions Answering Using Relations-based Summarization. *World Applied Sciences Journal* 24: pp. 231-237, 2013
14. Mikhail A. Dykov and Pavel N. Vorobkalov. Twitter Trends Detection by Identifying Grammatical Relations. *Proceedings of the Twenty-Sixth International Florida Artificial Intelligence Research Society Conference*: pp. 259-262, 2013
15. Helmut Schmid. Improvements In Part-of-Speech Tagging With an Application To German. *Proceedings of the ACL SIGDAT-Workshop*, 1995
16. Kristina Toutanova and Christopher D. Manning. Enriching the knowledge sources used in a maximum entropy part-of-speech tagger. *Proceedings of the 2000 Joint SIGDAT conference on Empirical methods in natural language processing and very large corpora: held in conjunction with the 38th Annual Meeting of the Association for Computational Linguistics - Volume 13*: pp. 63-70, Stroudsburg, PA, USA, 2000
17. David M. Blei, Andrew Y. Ng and Michael I. Jordan. *The Journal of Machine Learning Research - Volume 3*: pp. 993-1022, 2003
18. David Blei. The computational complexity of LDA - <https://lists.cs.princeton.edu/pipermail/topic-models/2008-April/000211.html>
19. Johan Hall. MaltParser: An Architecture for Labeled Inductive Dependency Parsing. *Licentiate thesis*, Växjö University, 2006
20. Marie-Catherine de Marneffe and Christopher D. Manning. *Stanford typed dependencies manual* - http://nlp.stanford.edu/downloads/dependencies_manual.pdf
21. Sintakicheski razmechenniy korpus russkogo yazika: instryktsiya pol'zovatelya - <http://www.ruscorpora.ru/instruction-syntax.html>

METHOD OF COMPUTER MODELLING ACCURACY INCREASE FOR ELECTRONIC MEANS BASED ON INTERCONNECTION OF DIFFERENT PHYSICAL PROCESSES PROCEEDING

Kofanov Y.N., Sotnikova S.Y., *Lemanskiy D.A.
*Moscow, MIEM NRU HSE, *OAO «GSKB «ALMAZ – ANTEY»*

The paper is devoted to the development of a new method for computer modelling accuracy increase in case of the circuit and designer project decisions making. The original idea of joint consideration of electric, thermal and mechanical processes mathematical models with the physical model presented in the form of the representative fragment design of electronic means construction in which these processes proceed at the same time is offered. The paper proved the availability of new ideas use of mathematical and physical models integration for the accelerated identification of internal parameters of electronic means electronic components and constructive materials at the expense of the problem reducing dimension by the offered method. The values of the identified parameters provide a significant accuracy increase of physical processes computer modelling in.

Keywords: mathematical modelling accuracy, parameters identification, electronic means, physical model, electric processes, thermal processes, mechanical processes.

One of the most important tasks in the development of electronic means (EM) is the task of providing the required reliability rates. It, in turn, is the task of providing electrical, thermal and mechanical operation modes of electroradioproducts (ERP) and construction materials. These processes are the most influencing at reliability characteristics EM, thus protection of their negative influence on equipment is the most difficult. Support of operation

modes of ERP is understood as support of reasonable reserves for the above mentioned physical processes in the computer-aided design. On the currents, voltages, thermal emissions capacities, elements temperature, vibration acceleration and shock of ERP in the technical specifications (TS) are set the maximum permissible values. Also in constructional materials TS limits of their durability and the maximum allowable temperature are set.

Now thanks to broad development of a CAD at the enterprises by development of electronic equipment aim to receive their characteristics at early design stages, yet without having laboratory models and pre-production model. Powerful programs of mathematical modelling allow carrying out detailed calculations of electrical, thermal and mechanical operating modes of each radioelement. However due to the input data error the calculations of ERP operating modes in circuits and constructions materials are carried out without the required accuracy support. This cause the calculation reliability rates don't reflect the actual situation.

Test results of pre-production models at the final stages of EM design also often disagree from the results of electrical, thermal and mechanical processes. Now developers have to intuitively assign reserve coefficients to loadings of radioelements and materials, as is EM cause of failures because of exceeding of the actual values of currents, tension, temperatures and mechanical stresses over maximum permissible reference values.

One of the ways to provide reasonable reserves - increase of accuracy computer modelling of EM.

Modelling as any process due to its features, its specificity has errors. Modelling error - the difference between the true value of some quantity (received in the experiment) with the value received in modelling.

The analysis showed that in most cases the Modelling error has three elements.

1. Error of mathematical models. It is related with the detailing level of construction and is defined by the accounting level of physical process features in the circuit and construction and the accepted simplifications.

2. The error introduced by the computer use. It is related with the features of digital computing machines, i.e. with the dimension of the numbers representation and arithmetic algorithms perform the rounding numbers

3. Error of input data. It is related to that automatically in case of calculations values of physical parameters of elements models which contain in databases of modelling programs without dispersions are used.

As it was established, the third component of error makes the greatest contribution. The reason is that usually in the ERP and materials models are set nominal values of parameters. They are average statistical values for a variety of suppliers and are given in the database. However, the parameters are variations due to the technological specifics of each supplier, i.e. actual values of parameters ERP and materials differ from the nominal specified in database (see figure).

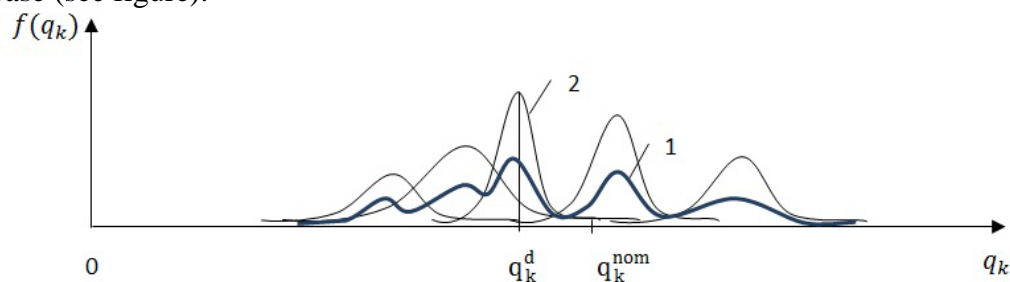


Figure. Location of parameter q_k for real ERP or the construction material of EM:
 q_k^{nom} – the nominal database value of k -th internal parameter as average multitude of ERP

suppliers (1); q_k^d – the real value of k -th internal parameter for the law of its distribution of specific ERP supplier (2)

In this paper it is offered to receive the real values of parameters by identification. Then if in case of modelling of the EM printing node to use them instead of nominal values, it is possible to receive the considerable lowering of modelling errors.

To identify the geometrical and physical parameters of ERP and the construction materials in this paper is offered to combine mathematical modelling with physical modelling [1]. Physical modelling involves the manufacture and testing of specially-made construction fragment model. The fragment is a printed circuit board. Its size is much smaller than the original circuit board. The fragment has radioelements, parameters of which are need to identification. Can be added other elements so that the fragment has some circuit, which was a small functional unit, which could be in the experiment to start the work. The elements fastening on a fragment is the same as the fastening of these elements in the projected printed circuit board. In this case, the allocated heat flows in the functioning of this schemes will be identical flows in the original scheme. The same applies to mechanical physical processes arising when exposed to vibration.

Thus, we will have the representative fragments specially selected from all printing circuit board reflecting flow of the main physical processes. In this paper it is offered to realize identification on the basis of complexification of supposed construction fragment physical model of EM with mathematical models of electrical, thermal and mechanical processes proceeding in this fragment.

To identify the real values of the parameters q_k^d of ERP and the construction materials of the designed printed circuit board created its mathematical model (electrical, thermal and mechanical), based on the created fragment model of construction EM (physical model). The defining characteristics y^d , received in the result of optimization should come as close as possible to defining characteristics y^{isp} , obtained in the result of measurements in the same control points.

It is offered the following sequence of parameters identification.

1. Preparation input data for identification, which includes electric circuit and design drawings of the projected electronic mean, the modelling program of electrical, thermal and mechanical processes.

2. Compiling models parameters list of the mentioned above processes, are to be identified. The list includes parameters, the values of which are not in the technical conditions issued by the manufacturer (for example, the internal thermal resistance), or depending on the type of installation (for example, stray capacitance mounting, heat resistance mounting, cylindrical rigidity of the printed circuit board with regard located on the printed circuit board ERP). Frequently the list is great. This is because when modelling EM mathematical models tend to have a higher dimension.

3. The choice of significant values from pre-compiled list (in p. 2) to identify by using the sensitivity function. I.e. the designer to reduce the dimension of the optimization problem can reduce the number of identifiable parameters, leaving only the most significant. Then in the process of identification will be determined only real values for only these parameters and the values of the remaining internal parameters will be equal to the nominal.

The selection of significant parameters is suggested by the values of the relative functions of parametric sensitivity [2] output characteristics EM included in the optimization criterion, to change each internal parameter printed circuit board:

$$S_{q_k}^{y_j} = A_{q_k}^{y_j} \times \frac{q_k^{nom}}{y_j^{nom}} = \frac{\partial y_j}{\partial q_k} \frac{q_k^{nom}}{y_j^{nom}},$$

where $A_{q_k}^{y_j}$ – absolute function of parametric sensitivity of the j-th output characteristics to a change in the k-th parameter;

q_k^{nom} – nominal value of the k-th parameter;

y_j^{nom} – nominal value of the j-th output characteristics;

∂y_j – differential (or a very small increment) the values of the j-th output characteristics;

∂q_k – differential (or a very small increment) the value of the k-th parameter.

4. The choice of optimization method, which depends on the properties of modelling programs for electrical, thermal and mechanical processes [3]. These programs in the process of optimization are used several times, and they should not delay the optimization process

5. The creation of a physical model, namely making the required number of fragments of printed circuit boards. Fragment is made of the same material as the board of the projected printed circuit board. For placement is taken one element for which you want to identify parameters. The simplest functional circuit make of them. The electrical signals (power and functional signals) connect the derived part of the construction of EM printed circuit board. This causes a flowing of interrelated electrical and thermal processes in it. Fragment can also be fixed on a shaker, in case of need, the identification of mechanical parameters. Measured define (output) features in a pre-selected control points that are available for installation of the sensors

6. At the same time the mathematical modelling of the circuit fragment and construction on a computer for obtaining the same defining characteristics. It is important to notice that a natural connection between the electrical, thermal and mechanical processes in the physical model of a fragment played when modelling simultaneously three programs electrical, thermal and mechanical modelling, related front-end programs-converters [4]

7. Measured and calculated defining characteristics are transmitted to the optimization program. The goal of the program: by automatic change of the identifiable parameters in the mathematical model on a computer achieve the minimum deviations of the calculated values from the defining characteristics of their measured values. On the range of changes of the identifiable parameters in the program is subject to restrictions, definite by physical meaning of the tasks. In the basis of the optimization criterion is used quadratic minimum criterion:

$$\min_{q^{mod}} H_i = \left(\frac{y_i^{mod} - y_i^{isp}}{y_i^{isp}} \right)^2, \quad \forall H_i < \varepsilon,$$

where $y^{isp} = f(q^{isp})$ – vector of measured defining characteristics;

$y^{mod} = f(q^{mod})$ – vector of defining characteristics obtained in the result of the modelling;

i – number of the defining characteristics;

q^{mod} – vector of identifiable parameters of the fragment model of the printed circuit board;

ε – small number set by designer, depends on the required degree of characteristics coincidence.

8. The obtained values of the parameters at the end of the optimization process are accepted as the final values of the identifiable parameters.

For practical realization of the identification in this paper offers a special program complex of identifying parameters of EM, the development of which was carried out by the author with the orientation to application of automated system for reliability and quality equipment ensuring ASONIKA developed in the Scientific school «ASONIKA» MIEM NRU HSE. [5].

In conclusion, proposed in this paper combined using of physical model with mathematical (interconnected electricity, thermal and mechanical models) allows to identify coefficients of temperature influence on electric parameters of ERP and the mechanical parameters of the board material. This helps you more accurately determine the load ERP and materials and, accordingly, more accurately calculate necessary parameters of reliability in mathematical modelling of projected EM.

The developed identification algorithm with the subsystems included in the system ASONIKA, form a holistic approach to the modelling accuracy increase and make more informed project decisions.

References

1. Kofanov Y.N., Sotnikova S.Y., Uvaysov S.U. Kompleksirovanie fizicheskogo i matematicheskogo modelirovaniya pri avtomatizacii proektirovaniya bortovyh jelektronnyh sredstv. – M.: Jenergoatomizdat, 2011.
2. Kofanov Y.N. Sistemnaya teoriya parametriceskoy chuvstvitelnosti. – M.: ANO «Academiya nadezhnosti», 2010.
3. Kofanov Y.N., Sotnikova S.Y., Uvaysov S.U. Dinamika optimizacionnogo processa pri identifikacii parametrov jelektronnyh sredstv. // Dinamika slozhnyh sistem – XXI vek – 2012. – №3. – s. 80-84.
4. Sotnikova S.Y. Kompleksnoe issledovanie harakteristik vysokonadezhnyh telekommunikacionnyh ustrojstv na rannih jetapah proektirovaniya s uchetom ih vzaimosvjazi. // Sistemnye problemy nadezhnosti, kachestva, informacionno-telekommunikacionnyh i jelektronnyh tehnologij v innovacionnyh proektah (INNOVATIKA – 2011). / Materialy Mezhdunarodnoj konferencii i Rossijskoj nauchnoj shkoly. Chast' 2. – M.: Jenergoatomizdat, 2011. – s. 37-39.
5. Sotnikova S.Y. Programmnyj kompleks modelirovaniya fizicheskikh processov pri avtomatizirovannom proektirovanii istochnikov vtorichnogo jelektropitanija dlja slozhnyh bortovyh sistem. // Dinamika slozhnyh sistem – XXI vek – 2012. – №3. – s. 84-87.

INFORMATIONAL SAFETY SUBSYSTEMS IMPROVEMENT AT RISK CORRUPTED OR LOST DATA

Berketov G., Mikryukov A., Fedoseev S.
Moscow, MESI

An approach to the definition of a rational set of information security protection subsystem mechanisms is developed in the risk of distortion or loss of data circulating in the system. A mathematical model is built to evaluate the rational construction costs for protection subsystem in keeping with information security risk assessment for different types of information threats.

Keywords: information security protection subsystem, the technique of estimating safety subsystem considering risks of information distortion, the security subsystem mathematical model, rational set of protection mechanisms.

Protection of information resources in the enterprise information systems is definitely an important task nowadays. Illegal distortion, destruction, or disclosure of information, disorganization of processing and transmission of information can be cause of serious material and moral states, businesses and individuals damages. It should be noted that the current trend is to increase the frequency of such events.

In this context, it is urgent that seek to improve information security management system (ISMS) on the risk of distortion data or loss data [1].

One of the most important tasks of constructing the optimal ISMS is the choice of the best mechanisms and tools. Such mechanisms should counteract (remove) threats and minimize the information system resources to security mechanisms work.

The authors have developed mathematical model, which allows you to build the rational construction costs subsystem protection in keeping with information security risk assessment for different types of information threats. The model generalizes the approaches outlined in [2,3]. Model-based estimation technique and recommendations developed for improving information security subsystem.

Following inputs are used for developed mathematical model:

$M = \{1, 2, \dots, m\}$ - the set of possible threats of unauthorized access;

$N = \{1, 2, \dots, n\}$ - a variety of ways to block channels unauthorized access, which may be included in the ISMS.

$R = \{1, 2, \dots, L\}$ - the set of protected objects (information resources);

$\mathbf{P} = (p_{ik}^j)$ - probability matrix neutralize threats by protection mechanisms, where p_{ik}^j - the probability of the i -th prevent threats for k -th mechanism in protecting the j -th resource;

- vector of remedies costs, where c_k - given the costs

associated with the development and maintenance of k -th protection mechanism;

$\gamma = (\gamma_i^j)$ - matrix of required probabilities distortionless in the realization of the i -th threat in relation to the realization of the j -th resource.

We introduce the set of Boolean variables:

$\mathbf{X} = \{x_k\}$, where $x_k = 1$, if the k -th data protection tool included in the ISMS,

$x_k = 0$ - otherwise.

Then the mathematical model problem of the choose the optimal composition of mechanisms of protection can be represented as follows:

$$\min: F(X) = \sum_{k=1}^n c_k x_k + \sum_{k=1}^L \sum_{i=1}^m r_i^j \left(1 - \prod_{k \in N_j(X)} p_{ik}^j \right), \quad (1)$$

$$f_i^j(X, P) = \prod_{k \in N_j(X)} p_{ik}^j \geq \gamma_i^j; \quad i = \overline{1, m}; \quad j = \overline{1, L}, \quad (2)$$

$$x_k \in \{0, 1\}, k = \overline{1, n} \quad (3)$$

where: $F(X)$ - the objective function ;

(X, P) - the probability of undistorted information in the j -th

information object (resource) as a result of the i -th threat at the selected protection mechanisms X ;

$N_j(X)$ - the set of indices of protections to prevent unauthorized access to the j -th resource at a given X ;

r_i^j - average damage in the realization of the i -th threat regarding the j -th object. Presented problem belongs to a class of discrete programming problems with Boolean variables.

Problem is solved by the method of vector recession. This method is an analogue of the gradient method. It is used to solve discrete optimization problems.

A metric space M with Hamming metric $\rho(X, X')$ is introduced on the set of bivalent vectors $X = (x_1, x_2, \dots, x_k)$, where $x_i \in \{0, 1\}$, defined by the number of components of the vectors X and X' for which $x_i \neq x'_i$. Closed vicinity with radius μ point X^0 is defined by

$$U_\mu(X^0) = \{X / \rho(X, X^0) \leq \mu\}. \quad (4)$$

Point X^* is called the minimum point of $F(x)$ regarding to the radius of the vicinity of μ , if for all points $X \in U_\mu(x^*)$ the inequality $F(x^*) \leq F(x)$ and $U_\mu(x^*) \setminus \{x^*\} \neq \emptyset$. As the Hamming distance is an integer number, as the radius μ is the positive integer. Downturn vector of $F(X)$ function in regard to the vicinity of the radius μ is defined on X^n vector - function of the form

$$\Delta_\mu(X) = \{, \quad (5)$$

$$\text{where: } \Delta_k = \Delta(X, X^k) = F(X^k) - F(X); k = \dots, \\ \{X^k / X^k = (x_1^{1^k}, \dots, x_n^{1^k}), k = (1, S)^- \} = U_\mu(X).$$

Some real numbers are means of the components of the downturn-vector. The following properties are for downturn vector: Point X is a local minimum of F if and only if $\Delta_i \geq 0$ for all $i = \dots$.

If X is not a local minimum of the function F relatively $U_\mu(X)$, then using the downturn vector we can to determine the point $X' \in U_\mu(X)$, such that $F(X') < F(X)$. Set of solutions which satisfy the constraints (2), denoted by D .

Algorithm to solve this problem is presented in Figure 1. Steps of the algorithm include:

Step 1. Randomly select some initial approximation X^0 and set the maximum size of the radius μ .

Step 2. Ask a sequence of radii $\{\mu_h\}$, satisfying the relations $0 < \mu_1 < \mu_2 < \dots < \mu_h = \mu_{\max}$. Step 3. Put $h = 0$.

Step 4. The algorithm does the following steps on each $(h + 1)$ -th step.

4.1. Put $k = 1$.

4.2. Consider a neighborhood $U_{\mu_k}(X^\top \mathbf{h})$ and define the set $G_k = U_{\mu_k}(X^\top \mathbf{h}) \cap \mathcal{D}$.

4.3. The means of the components of the downturn vector $\Delta_{\mu_k}(X^T h)$ let to determine whether the $F(X^T h)$ a minimum F relatively G. If yes, when $k < t$, replacing k by $k + 1$, go to step 4.2, when $k = t$ go to step 5. Otherwise, go to step 4.4.

The means of the components of downturn vector lets to find in point G (decision) X^{h+1} , for which $F(X^{h+1}) < f(X^h)$. Replace n by $h + 1$ and go to step 4.

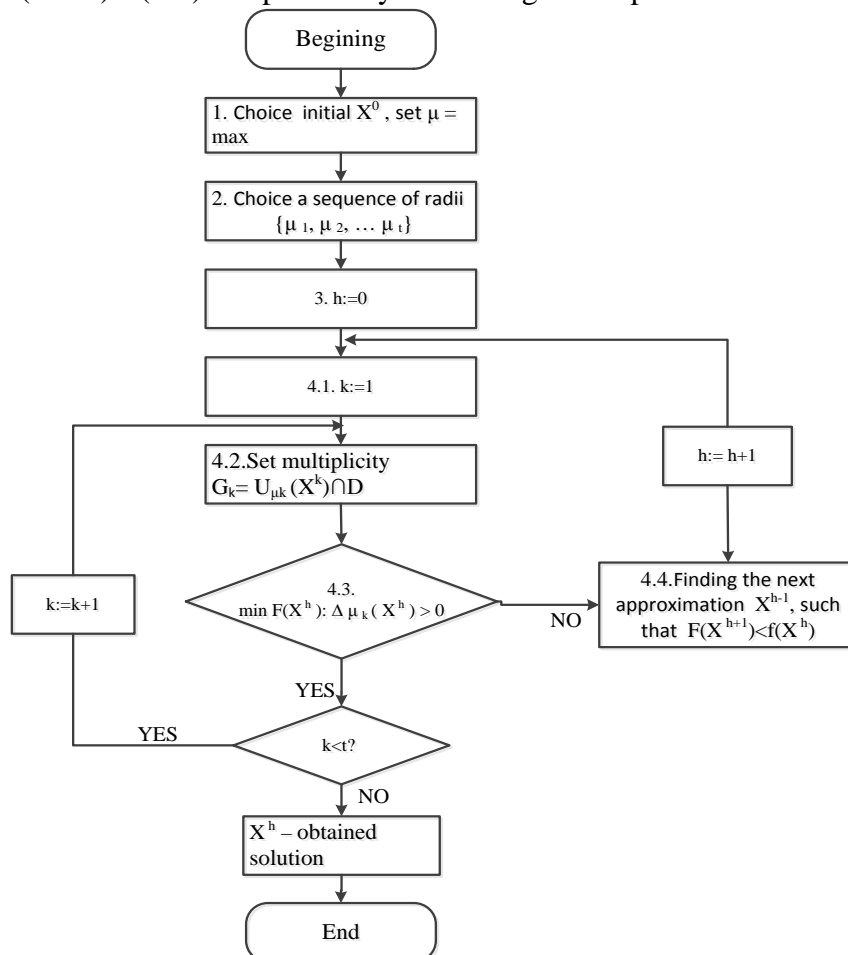


Figure 14. An algorithm for solving the problem of constructing a rational set of protection mechanisms.

Step 5. The end of algorithm.

When we are finding the global extremum problem as the maximum radius μ , we have to use a sufficiently large integer that can lead to an unacceptable amount of computation for the large-scale problems. In this case, we can restrict the approximate solution, or realize a rerun of the algorithm with different initial approximations X^0 at small μ .

The results of computer experiment confirmed the efficiency of the algorithm. Getting the solution is provided in a relatively small number of steps and does not require time-consuming and computing resources. The results of the simulation have shown that the performance of the ISMS is increased by 10-15%.

References

1. Shheglov A.Ju. Zashhita komp'yuternoj informacii ot nesankcionirovannogo dostupa. – Spb: Nauka i tehnika, 2004. – 384 s.
2. Berketov G.A., Mikrjukov A.A., Fedoseev S.V. Optimizacija sistemy obespechenija bezopasnosti informacii v avtomatizirovannyh informacionnyh sistemah. Sbornik trudov

Mezhdunarodnoj nauchno-prakticheskoy konferencii «Innovacii na osnove informacionnyh i kommunikacionnyh tehnologij», Sochi, 2010, str. 329-332.

3. Berketov G.A., Mikrjukov A.A., Fedoseev S.V. Metod reshenija zadachi sinteza sistemy obespechenija informacii v AIS. Sbornik trudov Nauchno-prakticheskoy konferencii «Innovacii v uslovijah razvitija informacionno-kommunikacionnyh tehnologij» Info-2012, g. Sochi, 2012g. str. 139-142.

COMPARATIVE ANALYSIS OF SOLUTIONS FOR FULL-TEXT SEARCH IN DIGITAL LIBRARIES

Savin G.I., Sotnikov A.N., Suleymanov R.S.
Moscow, JSCC of RAS

The aim of this paper is to explore current methods of full-text search in digital libraries. We focused on different types of materials storage paradigms, and on this basis we will compare various search mechanisms. We will also do a benchmark test of the most popular full-text search engines.

Keywords: full-text search, digital library, digital materials.

Introduction

Currently finding and materials exchange in digital library, often limited by documents bibliographic descriptions loaded into the system. Bibliographic descriptions fields (title, authors, etc.) do not always allow the reader to find the proper source. Publication title, as a rule, can not quite fully and fairly reflect the entire contents of the document. Words of the user-defined search query may be missing the title of the document when the document itself partially or fully satisfies the request.

To resolve this problem, the document placed in the funds of the system, is supplied with a text description - an abstract or keywords list. The abstract, of course, more than title reflects the content of the document, but to use this text for searching requires special tools to highlight the part of words and phrases that reflects the theme of the document. Traditionally, the procedure of obtaining a set of words provide by library staff manually. This introduces an element of subjectivity in this procedure and as a result the lists of words obtained for similar documents in different institutions, can vary greatly. To avoid this problem requires automatic search tools, independently analyzing the text of the abstract.

The second traditional way for documents search in libraries based on the using of different classification (hierarchical thematic rubricators BBK, UDC), which allows to distribute information groups. Automated search in the space of classified documents is reduced to a comparison with the description of the query text classifier columns and subsequent submission of all documents the user selected title, which differs little from the search for the title of publication or in the text of the abstract.

With increasing computing capacity of information resources has become possibility to store library information system together with a bibliographic description of the document itself. Documents stored in electronic storage, together with their descriptions, called electronic documents (ED). ED - an immutable object in time, stored on a computer readable format and linked with text description. Such a document can be a text file (a set of text files), and any other type of information (graphics, audio), stored as files. Library, which storage both ED and their descriptions is called a Digital Library (DL). In this kind of library user can search not only a bibliographic description of the document, but the document

content itself. To construct the index of an arbitrary text documents stored graphics or audio information, editors use a text description of the contents of this document (full-text search).

Let us consider the situation when it may be necessary: imagine that the database stores a lot of materials that integrate different areas of science and the library visitor, is studying the chaos theory. In case of full-text search for keywords "chaos theory", the result will be shown as all the materials from various sources and areas of sciences (mathematics, physics, information theory, etc.) that contain these keywords. At the same time they will be sorted by relevance, ie accordingly search semantically.

The article describes how to organize of full text search in digital libraries, and also shows the results of a comparative performance analysis of the most well-known programs and software libraries for full-text search with open-source code.

1. Storage options of full texts in digital libraries

Before describing methods for full-text search, we need to consider ways of storing the full texts in digital libraries. There are two storage options of full text:

1. Storage full texts in the database;
2. Storage full texts in text or binary files within the file system.

It is required to note that the information in the databases is also stored inside the file with a special structure, which is understandable database. Databases can store texts without markup (eg format plaintext), and texts with a special marking (HTML (HyperText Markup Language), XML (eXtensible Markup Language), etc.).

Full texts are stored within the file system. Files can be stored in different formats:

1. Text without markup – TXT format;
 2. Text Format - HTML, XHTML, XML, and others;
 3. Special book formats - EPUB (Electronic Publication), FB2 (FictionBook) and others;
 4. Binaries - PDF, DJVU, DOC, DOCX, etc.
- #### 2. Methods of organization of full-text search in digital libraries..

Depending on the method of storing the full texts in the electronic library is necessary to use various tools for full-text search. In total there are 3 options::

1. Using widgets of search engines;
2. Using the built-in database tools for full-text search;
3. Using a separate / external system (server) for full-text search

Consider all the above options, as well as the pros and cons of each.

2.1 The use of widgets from search engines for full-text search in digital libraries.

Modern Internet search engines such as Yandex, Google and Bing, allow us to embed their own search widget on any site indexed by them.

Widget - this primitive graphical user interface with a standard appearance and performing standard actions.

Тип формы: форма со стрелкой



Дизайн поисковой формы



#ffc000

— цвет фона поисковой формы

Example of search widget from Yandex.

Pros of using widgets from the search engines are:

- Easy implementation - to integrate the widget from search engine in your own e-library you have to insert in a certain location on the page code to display the widget, as well as create a new page, which will display the search results;

- Familiar user;
- Support of the morphology and lexicon;
- Correction of typographical errors;
- Search suggestions.

However, they have some serious disadvantages:

- Limited ability to customize the appearance;
- The extremely low rate of indexation - new materials from your digital library will be available to search only after the external search engine index them. It may take from a few days to five weeks;

- All materials and their source code should be in the public domain (ie available without authorization and restrictions), otherwise the crawler does not get to them and not to index.

Due to these disadvantages, we recommend using this method only if your library is rarely updated and you do not need to index new materials instantly.

Proceed to a more advanced tools.

2.2 Using the built-in DBMS tools for full-text search in digital libraries

In some modern DBMS (such as MySQL, PostgreSQL, etc.) there are built-in tools for full-text search. Consider the pros and cons for the example of MySQL Fulltext.

Pros of using built-in DBMS tools are::

- Ease of implementation - if your database has a built-in tools for full-text search, you need to activate them and configure, and then you can configure your own scripts to work with these tools;

- Timeless search index - new materials are automatically indexed;
- Full control over the configuration and appearance.

As disadvantages there are:

- Low velocity of search for large amounts of data;
- Failure to account for the morphology;
- Large load on the database.

If the fund of your digital library is updated frequently, but by itself it is not very large (in the range of 5-10 thousand records), you can use tools like MySQL Fulltext. If you have more materials, then to increase search speed it is better to switch to a separate search engine.

2.3 Using a separate / external system (server) for full-text search in the digital library

If there are more than 10,000 materials in the fund of your digital library or it is not possible to allow public search system to index them - then you should install and configure an external search engine. Currently, the three most popular systems for full-text search are:

- Sphinx;
- Apache Solr;
- Xapian.

All three systems are open source and can be used without restriction in any digital library. Let us consider each of them.

2.3.1 Sphinx search engine

Sphinx (SQL Phrase Index) — full-text search system developed by Andrei Aksenov and distributed under the GNU GPL. A distinctive feature is the high speed indexing and retrieval, as well as integration with existing DBMS (MySQL, PostgreSQL) and API for common web programming languages.

Key features:

- High indexing speed (10-15 MB / sec per processor core);

- High speed search (up to 150-250 requests per second per processor core, with one million documents);
- High scalability (biggest known cluster indexes to 3 billion documents and supports more than 50 million search queries per day);
- Support for distributed search;
- Support for full-text search multiple fields in the document (up to 32 by default);
- Support for several additional attributes for each document (ie, the group timestamps, etc.);
- Support of stop words;
- Support byte encodings and UTF-8;
- Support stemming - have built modules for English, Russian and Czech languages, modules are available for French, Spanish, Portuguese, Italian, Romanian, German, Dutch, Swedish, Norwegian, Danish, Finnish, Hungarian languages;
- Native support for MySQL (all types of tables, including MyISAM, InnoDB, NDB, archive , etc.) ;
- Native support for PostgreSQL;
- Support for ODBC compliant database (MS SQL, Oracle , etc.).
- The cons of Sphinx:
- Requires a separate server (virtual or physical);
- The search is available only on a database or specialized XML file;
- Sphinx returns only the link to the document and not a fragment of text in which you found the desired section.

2.3.2 Apache Solr search engine

Apache Solr — an extensible search platform from the Apache. The system is based on the Apache Lucene library and developed in Java. Features of it is that it is a not just a technical solution for the search platform namely, the behavior of which can easily extend / change / customize to fit any need - from conventional full-text search on the site to a distributed storage system / receive / text analytics and other data with a powerful query language.

Key features:

- Enhanced text search;
- Optimized for Web systems with a heavy load;
- Standard interfaces protocol - XML, JSON, HTTP;
- Web administration panel (interface for test queries , server status and component debugging and optimization analyzer ...);
- JMX statistics;
- Scaling - replication and sharding as part of the platform;
- Huge flexibility with powerful configuration system ;
- Extensibility through support plug-ins;
- Indexation in real time;
- Text analysis (multiple text filters);
- Caching ;
- Powerful query language (filters, sorting , working with date / time , feature requests , and more) ;
- Prepared clients for a variety of development languages (including PHP);
- Approximate search (inexact matching) and request validation errors (hint options);
- Indexing of text and binary files.

The cons of Apache Solr:

- Difficulty settings;

- Higher system requirements;
- A larger index than the Sphinx.

2.3.3 Xapian search engine

Xapian - is an open (GPL) cross-platform library written in C ++, there are modules for Python, PHP, Ruby, Perl, Java, Tcl, and C #.

Key features:

- Unicode support;
- Boolean search, search with rankings, mask, synonyms, there is support for sorting the results;
- Stemming support for 15 languages (including Russian);
- Support request correction dictionary (eg xapain inquiry will be replaced by xapian)
- search for documents in the image;
- Support for indexing documents in different formats out of the box (PDF, HTML, RTF, Microsoft Office, OpenDocument, even RPM packages and Debian), easy to add filters to support the new format.

The cons of Xapian:

- Extra large size of the index;
- Low velocity of indexation;
- Surface documentation;
- Failure to account for additional fields documents.

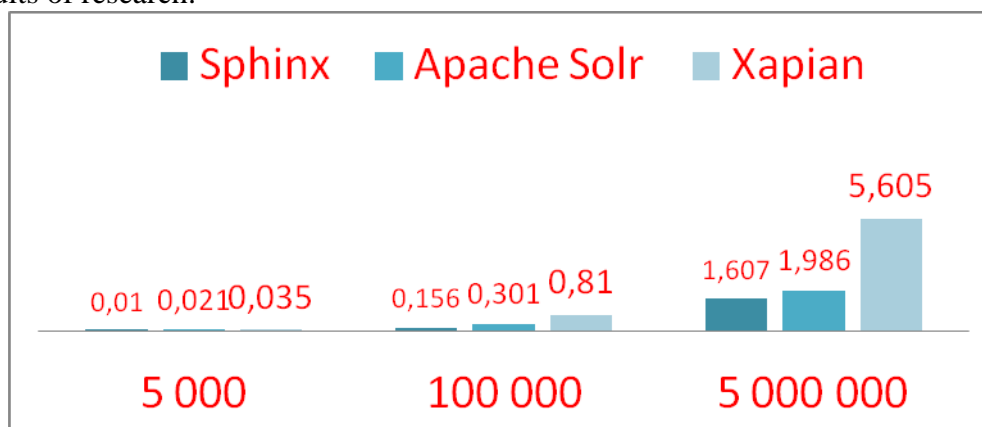
3. Search engines benchmark

The research was conducted on three tests for each of the engines:

1. 5000 records in the database, 30MB index;
2. 100,000 records in the database, 550MB index;
3. 5 million records in the database, 27.5 GB index.

Test includes 3 request for a search engine: 2 keywords, 2 keywords + 1 word with the prefix 2 keywords + 1 word with the prefix + 1 negative keyword. After receiving the results were calculated arithmetic mean value of three times in seconds.

Results of research:



The graph shows that the fastest search performs Sphinx, slightly lags Apache Solr. Xapian lags behind on orders. By increasing the amount of materials - the gap between Xapian and other systems increases.

Conclusions

In this article various means for the organization of a full text search methods in digital libraries. Has been discussed Based on the research of all possible options, as well as through the results of a comparative analysis of popular search services, following conclusions were made.

The widgets of search engines are effective in case if you do not have the resources for running other systems of full-text search. However, this method is the easiest to implement and if the library is rarely updated - it is quite possible to use.

In case of digital library is updated frequently, but it's volume is not large (in the range of 5-10 thousand records), it would be more effective to use full-text search tools which are build into DBMS. If the library fund has more materials, then to increase search speed it is better to switch to a separate search engine.

When it is necessary to index large number of binary and text files to the full text, Apache Solr would be the best one. If it is possible to extract text and upload them to the database - it is better to use the Sphinx.

If you can not install a separate server or a digital library application is written in C++ or other not oriented on WEB language - it's best to use the Xapian libraries.

The Sphinx can provide maximum search speed, ease of configuratiton and indexation.

References

1. S.R.Kruk, A.Westerki, E.Kruk, Architecture of Semantic Digital Libraries. Semantic Digital Libraries 2009, pp 77-85.
2. David W. Archer, Lois M. L. Delcambre, Fabio Corubolo, Lillian Cassel, Susan Price, Superimposed Information Architecture for Digital Libraries. Portland State University, 2008.
3. N. Lossau, B. Wilson, Search Engine Technology and Digital Libraries. Bielefeld University Library, Germany. D-Lib Magazine, June 2004.

INSTRUMENTATION AND METHODOLOGY SUPPORT FOR THE MOBILE LABORATORIES IN THE ENVIRONMENTAL CONTROL AND MONITORING OF RAIL TRANSPORT.

Borisova, A.V., Finochenko, V.A.
Rostov State Railway Universitet

The methodology of selecting unstrumentation and methodological solutions for environmental equipment wagon-lab. A functional diagram of a mobile measuring and computing complex (MMCEC) wagon-lab examined the measuring units, methods of analysis, implemented the specified measuring instruments.

Keywords: Measuring and computing complex, methodology for the optimal choice instrumentation and methodical decisions, environmental equipment of wagon-labs.

An essential component of effective environmental management is a system of environmental control and monitoring, directed on reception multi-dimensional information about the state of the environment and its possible negative developments. Railway transport compared with other types of transport is one of the most environmentally type of transport, but its contribution to environmental pollution remains high.

In recent years, environmental safety by "Russian Railways" has received increased attention. Collection of primary information about the state of the environment is performed by stationary and mobile environmental labs. In this case one of the factors affecting the efficiency, reliability and economic feasibility of producing ecoinformation is the optimal selection of instrumentation.

Considering specificity of the railway industry, the improvement of environmental control and monitoring was mainly directed at building the capacity of mobile labs based on passenger coaches.

Quality of mobile wagon labs is a big usable area, autonomous energy system and a significant supply of water, provide all the necessary conditions for the staff [1]. Now the entire length of Russian railways are 9 environmental wagon labs, with equipment devices which were selected in a portable version, focused mainly on the rapid analysis of the sample. But without of an integrated approach to the choice of instrumentation and methodological support when completing laboratory appear costs of unreasonable financial costs and possibly incomplete functionality of the equipment purchased.

It should be noted that resolution of this issue is not devoted too much work. Some discussed a comparison of different methods for two or three parameters, other criteria apply generalized recommendations, wearing a very general nature. For the choice of optimum device-methodical decisions under specified conditions developed a methodology, which builds on the system volume study of diverse data: status of natural objects, analyzed the possibilities of measuring instruments, including scientific and technical theories, concepts and methods [2].

Methodology for the optimal choice of equipment Eco analytical summarizes and complements the existing provisions of the universal theory of chemical analysis [3], method of choice of analytical equipment for the given parameters [4], presented in the theory of rational choice of instruments to equip labs within the application of qualimetry [5]. According to the proposed of methodology in the early stages of research goal is formed and is carried out setting eco-analytical laboratory tasks, and then analyzes the existing instrumentation and methodical decisions.

The next step is the formulation of a list of criteria for evaluating the devices from which to select the most significant for the given conditions of their operation. In which connection criteria should be defined so that they can anyway described mathematically formalized and allowing quantitative evaluation devices at their entirety. These are:

1. Functional and technical specifications of the devices;
2. Performance;
3. The degree of perfection of eco analytical equipment;
4. Reliability;
5. Cost parameters;
6. Compatibility with computers.

This list of criteria limiting indicator is the presence in the register of measuring instruments for use in Russia.

For define a list of criteria used subjective and objective methods. Objective methods this:

- the measuring, based on the use of technical means of measuring;
- estimated, based on the calculated numbers using characteristic values obtained by other analytical functions.

Subjective methods is the method of expert estimates, based on the opinions of analysts, instrument makers, technologists. List of criteria for the selection of analytical equipment is determined by the polled survey of experts. Information is provided by experts, included in base of knowledge which is a formal empirical knowledge of highly qualified specialists in the subject matter area. A correlation is established through the ranks of the weight of each parameter. Results obtained ranking criteria in order of importance are the basis for the final stage of the work - to develop recommendations for instrumentation and methodology support for environmental wagon laboratory.

According to proposed methodology developed functional scheme mobile measuring and computing complex environmental laboratory car (MMCEC) [6]. Figure 1 shows a functional block diagram of an improved MMCEC with the latest developments in the field of instrument-making.

This function scheme has the flexibility to change the configuration of the analytical equipment and includes:

- unit of instrumentation, designed to assess physical environmental factors (noise, vibration, meteorological parameters, electromagnetic radiation of a wide range of frequencies).
- unit of measurement and accessory equipment intended for performing chemical analysis of contaminants protection, preservation, storage and transport of trial.

When the chemical composition analysis of the pollution MMCEC allows the determination of the concentrations of two ways:

- by express analysis of directly on the inspected object;
- by sampling with further transportation them to the devices located on MMCEC (instrumental and laboratory method).

In the absence of the possibility of chemical analysis in conditions of expedition, some trial preserved and delivered to the regional road environmental laboratory. In MMCEC systemically combined ecoanalytical devices, mathematical software, tools and methods of metrological provision analysis.

Environmental wagon-lab created with the purpose assess the quality of the operational environment, including in the case of an emergency. The refore constitute the main instrument functional devices for express-analysis of indicators.

Environmental equipment MMCEC produced by leading domestic Instrumentation Company and is based on the following methods: spectroluminescent, spectrophotometric, IR- spectrometry, potentiometric, indicating, analog-to-digital conversion and digital filtering of the electrical signal.

Object of study	Sample preparation	Analitical pant	Results processing
-----------------	--------------------	-----------------	--------------------

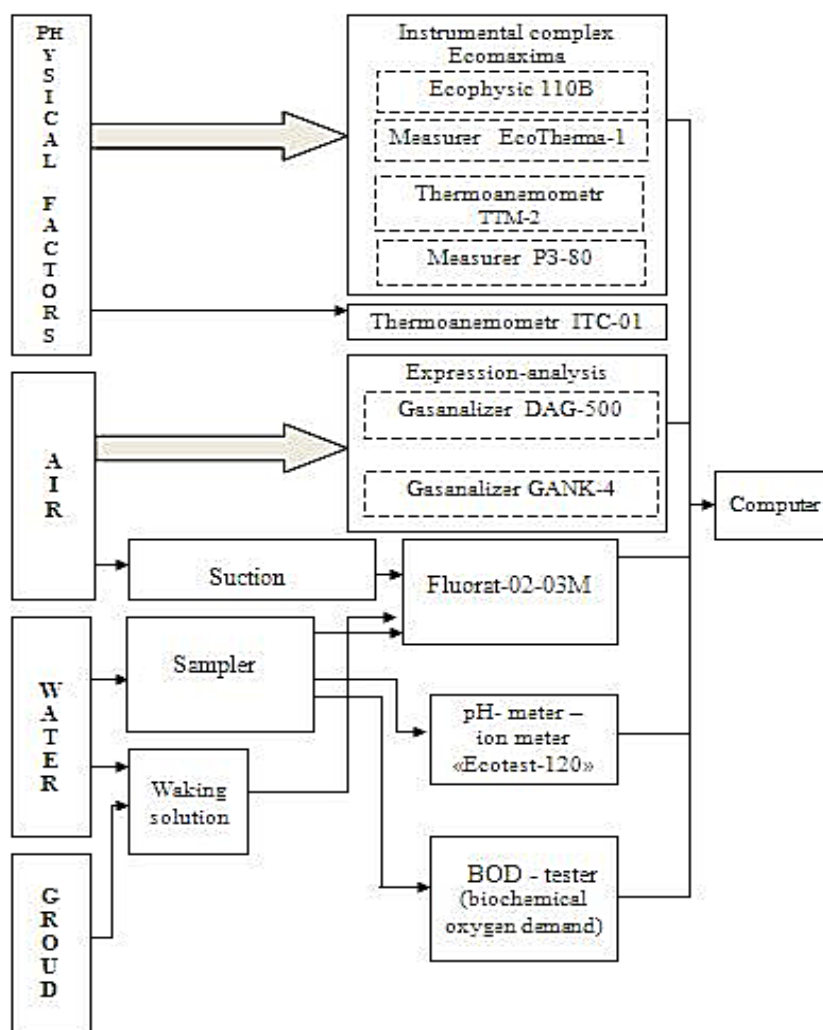


Figure 1. Functional scheme of MMCEC

Instrumentation and methodical complex presented at Figure 1, includes modern measuring instruments and accessories that meet high scientific and technical level and fully covers the list of environmental indicators be controlled under the environmental monitoring. Presented MMCEC grade, allows on-site to carry out complex analyzes, greatly facilitates sampling activity on the most remote parts of the railway.

Certainly technical development Instrumentation directly related to the ever-increasing development pressure on the environment, and as a result, expanding the range of eco-analytical tasks. Over the years the company "Russian Railways" was delivered to more than 750 environmental laboratories and pieces of laboratory instrumentation. View of the wide range of products offered by the instrument-making firms, close to technical performance indicators, topical task of measuring the right choice based on purpose and actually performed tasks laboratory.

Thus, the implementation methodology of optimal choice to acquire methodological solutions in industrial environmental control and monitoring of rail transport equipment will perform a mobile laboratory, significantly minimizing the time and cost.

References

1. Finochenko V.A. Sovremennye ecoanaliticheskie komplekсы na zheleznodorozhnom transporte/ Ecologicheskie sistemy i pribory, 2002. №3. – С.3-6.
2. Finochenko V.A. Metodologicheskie podkhody k vyboru ecoanaliticheskogo oborudovaniya dlya provedeniya monitoringa okrugayushchei sredy/ V.A. Finochenko, A.V. Borisova/ Ecologicheskie sistemy i pribory, 2011, №11. – С.47-49.
3. Gribov L.A. Universal'naya sistema khimicheskogo analiza/ L.A. Gribov, Yu.A. Zolotov, V.I. Kalmanovskii, L.L. Kunin, Yu.M. Luzhkov, A.A. Popov, V.S. Toroptsev/ Zhurnal analiticheskoi khimii, t.XXXVII, 1982. №6. – С. 1104 - 1121.
4. Shaevich A.B. Analiticheskaya sluzhba kak sistema/ Shaevich A.B. – Moskva: Izdatel'stvo «Khimiya», 1981 - 264 s.
5. Fedorovich G.V. Vybor apparatury dlya ispytatel'nykh laboratorii/ Mir izmerenii, 2009. №9. - С.32 – 40.
6. Finochenko V.A. Ekozashchitnye tekhnologii na zheleznodorozhnom transporte/ Finochenko V.A. – Rostov-na-Donu: Rostovskii gosudarstvennyi universitet putei soobshcheniya, 2009. – 111 s.

DEVELOPMENT REDUCED COMPUTATIONAL SCHEME IS BASED ON USING NUMERICAL METHODS FOR CALCULATION OF DYNAMIC CHARACTERISTICS MATHEMATICAL MODEL

Vostrikov A.V., Borisov N.I.
Moscow, MIEM HSE

In this paper, a new approach to the construction of a new computational scheme for calculating the reduced system of linear differential equations based on Euler's method. The idea of development is based on the reduction of mathematical expressions that define explicit and implicit Euler methods. New computational scheme provides benefits on time calculating unknown quantities in the local area, designated by the user, 2-3 orders of magnitude compared with the calculation of the unknown complete model with traditional methods.

Keywords: reduction, computational scheme, Euler methods.

One of the major problems of long-term operation of spacecraft (SC) and electrification is associated with the process of electrostatic discharge (ESD). In 30% of cases the loss of the spacecraft is due to electrification. ESD generate currents on the surface of the spacecraft, which induce in the onboard cabling crosstalk of up to 10 V. The interference of this magnitude can lead to failures of the onboard avionics. To minimize the possible failures of spacecraft electronics need to be modeled on the current spreading painting surface spacecraft. Further calculation is carried out interference in cables and recommendations for their screening or optimal route gaskets. For this purpose was developed MIEM electrophysical structural model (SEM) SC [1] and Software «Satellite-MIEM» for its implementation.

ON «Satellite-MIEM» synthesizes structural Electrophysical model (SEM) based on a predetermined polygonal 3D-model of the spacecraft (Fig. 1). Polygonal model consists of a set of elementary shapes - triangles or rectangles that can be transformed by means of the program in the surface mesh: a collection of linked nodes. The grid is uniform, that is, steps in all the coordinates are equal. Grid cell represents a rectangle or triangle. SEM number of nodes will be bulky SC $(1..2) \times 10^5$. Each link (branch) is represented as circuit elements (R, L,

C), the whole forming an equivalent circuit diagram surface spacecraft. When this component values of the same type are identical.

With the help of software «Satellite-MIEM», knowing the place of electrical discharge, you can get a picture of current spreading. To calculate the transient currents used in the most productive program for calculating electrical circuits LTSpice, but for circuit analysis of 150,000 nodes requires 83 hours (experiment was done on a computer with a dual-core processor clocked at 1.8 GHz on each core, RAM is 2 GB) [2], which is unacceptable for the space industry. Software used in numerical methods well show themselves only when calculating the smaller models [3]. Therefore there is a need for new methods of calculation large electrical circuits. Earlier in [4, 5] proposed a new approach of reduction of the linear circuit model based on the exclusion of sub-vectors model, which contain the state variables whose values do not exceed 1-2 % of the amount applied to the site of the discharge current. This paper proposes a new approach to the calculation of the reduced computational scheme of the system of linear differential equations on the basis of mathematical expressions that define the explicit and implicit Euler methods.

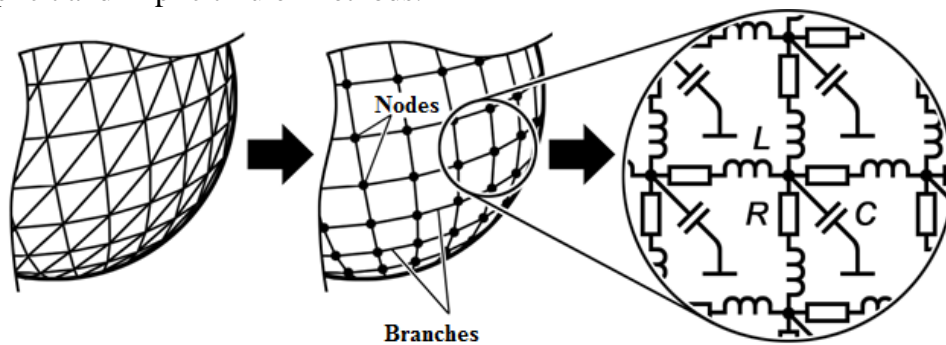


Fig. 1. Converting aggregate quadrilaterals in SEM

1. Statement of the Problem

Model circuits formed in the extended homogeneous coordinate basis can be written as a system of linear ordinary differential equations

$$C(\bar{Q}) \frac{d}{dt} \bar{X}(t) + G(\bar{Q}) \bar{X}(t) = \bar{Y}(t), \quad \bar{X}(0) = \bar{X}_0, \quad (1.1)$$

where $C(\bar{Q}), G(\bar{Q}) - (n \times n)$ are matrixes, $\bar{Q}^T = (q_1, \dots, q_r)$ is the vector of variable parameters of the model, $\bar{X}(t)$ is the unknown vector of phase variables (voltages in all nodes of the circuit and the currents flowing through the inductive elements), $\bar{Y}(t)$ is the vector of input signals.

Note the specificity of the model scheme.

1). Matrix C is nonsingular.

2). Variable parameters of the model are located in a small amount of equations $n_q, n_q \ll n$.

3). Number of output characteristics of the circuit to which the requirements are formulated optimization problem as well n_y и $n_y \ll n$.

4). Given that $m \leq n_q + n_y$, the original problem (1.1) can be written in block form:

$$\begin{bmatrix} C_{11} & C_{12} \\ C_{21} & C_{22}(\bar{Q}) \end{bmatrix} \frac{d}{dt} \begin{bmatrix} \bar{X}_1(t) \\ \bar{X}_2(t) \end{bmatrix} + \begin{bmatrix} G_{11} & G_{12} \\ G_{21} & G_{22}(\bar{Q}) \end{bmatrix} \begin{bmatrix} \bar{X}_1(t) \\ \bar{X}_2(t) \end{bmatrix} = \begin{bmatrix} \bar{Y}_1(t) \\ \bar{Y}_2(t) \end{bmatrix}, \quad (1.2)$$

$$\overline{X}(0) = \overline{X}_0,$$

where $C_{22}(\overline{Q}), G_{22}(\overline{Q}) - (m \times m)$ are matrixes, $\overline{X}_2(t) - (m \times 1)$ is the vector containing the desired output characteristics of the model.

It is necessary to convert the problem (1.2) in such a way that the resulting expression for the calculation of the output characteristics only contain the vector $\overline{X}_2(t)$ and kept a simple dependence of the output characteristics of the variable parameters. Since the transformed task will consist of m equations in $m \ll n$ should be a significant reduction in the complexity of computing the dynamic characteristics of the scheme at each step of its parametric optimization.

2. Discussion of ways to solve the problem

The approach is based on the use to calculate the dynamic characteristics of the numerical methods. This should not be subject to reduction of the original model as a system of linear ordinary differential equations and mathematical expressions for the one or the other numerical method.

When using numerical methods of solution process consists in calculating the decision vector at time points $t_0, t_1, t_2, \dots, t^*$, i. e. $\overline{X}(t_0), \overline{X}(t_1), \dots, \overline{X}(t^*)$. The solution at the point t_i calculated by solving the point t_{i-1} (one-step method) or by decisions in several previous points (multi-step method). Thus, one-step method at each step connects the vectors $\overline{X}(t_{i-1})$ and $\overline{X}(t_i)$, that is, in the general case there is an expression $F[\overline{X}(t_{i-1}), \overline{X}(t_i)] = \overline{0}$. When writing such expressions in block form we obtain

$$\begin{cases} F_1[\overline{X}_1(t_{i-1}), \overline{X}_2(t_{i-1}), \overline{X}_1(t_i), \overline{X}_2(t_i)] = \overline{0} \\ F_2[\overline{X}_1(t_{i-1}), \overline{X}_2(t_{i-1}), \overline{X}_1(t_i), \overline{X}_2(t_i)] = \overline{0} \end{cases} \quad (2.1)$$

(2.3) can not be obtained depending on the desired

$$\Phi[\overline{X}_2(t_{i-1}), \overline{X}_2(t_i)] = \overline{0}, \quad (2.2)$$

uses only two resolution subvector $m \ll n$, because as the initial data, we have two subsystems of equations with 4 unknowns. To solve the problem of reduction proposed use both explicit and implicit form of writing one-step method, resulting in an initial data we obtain the following system of equations

$$\begin{cases} F_{1\text{ЯBH}}[\overline{X}_1(t_{i-1}), \overline{X}_2(t_{i-1}), \overline{X}_1(t_i), \overline{X}_2(t_i)] = \overline{0} \\ F_{2\text{ЯBH}}[\overline{X}_1(t_{i-1}), \overline{X}_2(t_{i-1}), \overline{X}_1(t_i), \overline{X}_2(t_i)] = \overline{0} \\ F_{1\text{HEЯBH}}[\overline{X}_1(t_{i-1}), \overline{X}_2(t_{i-1}), \overline{X}_1(t_i), \overline{X}_2(t_i)] = \overline{0} \\ F_{2\text{HEЯBH}}[\overline{X}_1(t_{i-1}), \overline{X}_2(t_{i-1}), \overline{X}_1(t_i), \overline{X}_2(t_i)] = \overline{0} \end{cases} \quad (2.3)$$

The next section discusses how to retrieve the dependence (2.2) (2.3) applied to the problem (1.2) using the explicit and implicit Euler methods.

3. Development of reduced computational scheme

Explicit Euler method is given by

$$\overline{X}(t_i + h) = \overline{X}(t_i) + h \frac{d}{dt} \overline{X}(t_i),$$

that is

$$\frac{d}{dt} \bar{X}(t_i) = \frac{\bar{X}(t_i + h) - \bar{X}(t_i)}{h} = \frac{\bar{X}(t_{i+1}) - \bar{X}(t_i)}{h}.$$

Implicit Euler method is defined by:

$$\bar{X}(t_i - h) = \bar{X}(t_i) - h \frac{d}{dt} \bar{X}(t_i),$$

or

$$\frac{d}{dt} \bar{X}(t_i) = \frac{\bar{X}(t_i) - \bar{X}(t_i - h)}{h} = \frac{\bar{X}(t_i) - \bar{X}(t_{i-1})}{h}.$$

Therefore, for the initial system of equations (1.1), we obtain the following expressions

$$\frac{1}{h} C \bar{X}(t_{i+1}) - [C \frac{1}{h} - G] \bar{X}(t_i) = \bar{Y}(t_i), \quad (3.1)$$

$$[C \frac{1}{h} + G] \bar{X}(t_i) - \frac{1}{h} C \bar{X}(t_{i-1}) = \bar{Y}(t_i). \quad (3.2)$$

Moving the formula explicit method (3.1) one step back and using the notation $\bar{X}(t_i) = \bar{X}_i$, write the expression (3.1), (3.2), as follows:

$$C \bar{X}_i - [C - hG] \bar{X}_{i-1} = h \bar{Y}_{i-1}, \quad (3.3)$$

$$[C + hG] \bar{X}_i - C \bar{X}_{i-1} = h \bar{Y}_i. \quad (3.4)$$

In block form the system of equations of the two methods will be as follows:

$$\begin{bmatrix} C_{11} & C_{12} \\ C_{21} & C_{22} \end{bmatrix} \begin{bmatrix} \bar{U}_1 \\ \bar{U}_2 \end{bmatrix} - \begin{bmatrix} C_{11} - hG_{11} & C_{12} - hG_{12} \\ C_{21} - hG_{21} & C_{22} - hG_{22} \end{bmatrix} \begin{bmatrix} \bar{V}_1 \\ \bar{V}_2 \end{bmatrix} = h \begin{bmatrix} \bar{Y}_{(i-1)1} \\ \bar{Y}_{(i-1)2} \end{bmatrix}, \quad (3.5)$$

$$\begin{bmatrix} C_{11} + hG_{11} & C_{12} + hG_{12} \\ C_{21} + hG_{21} & C_{22} + hG_{22} \end{bmatrix} \begin{bmatrix} \bar{U}_1 \\ \bar{U}_2 \end{bmatrix} - \begin{bmatrix} C_{11} & C_{12} \\ C_{21} & C_{22} \end{bmatrix} \begin{bmatrix} \bar{V}_1 \\ \bar{V}_2 \end{bmatrix} = h \begin{bmatrix} \bar{Y}_{(i)1} \\ \bar{Y}_{(i)2} \end{bmatrix}, \quad (3.6)$$

where the vectors \bar{U} and \bar{V} - denote vectors \bar{X}_i и \bar{X}_{i-1} respectively.

To simplify subsequent expressions, we write the system (3.5), (3.6) as follows:

$$\begin{bmatrix} C_{11} & C_{12} \\ C_{21} & C_{22} \end{bmatrix} \begin{bmatrix} \bar{U}_1 \\ \bar{U}_2 \end{bmatrix} - \begin{bmatrix} A_{11} & A_{12} \\ A_{21} & A_{22} \end{bmatrix} \begin{bmatrix} \bar{V}_1 \\ \bar{V}_2 \end{bmatrix} = \begin{bmatrix} \bar{X}_1 \\ \bar{X}_2 \end{bmatrix},$$

$$\begin{bmatrix} B_{11} & B_{12} \\ B_{21} & B_{22} \end{bmatrix} \begin{bmatrix} \bar{U}_1 \\ \bar{U}_2 \end{bmatrix} - \begin{bmatrix} C_{11} & C_{12} \\ C_{21} & C_{22} \end{bmatrix} \begin{bmatrix} \bar{V}_1 \\ \bar{V}_2 \end{bmatrix} = \begin{bmatrix} \bar{Y}_1 \\ \bar{Y}_2 \end{bmatrix},$$

or

$$C_{11} \bar{U}_1 + C_{12} \bar{U}_2 - A_{11} \bar{V}_1 - A_{12} \bar{V}_2 = \bar{X}_1, \quad (3.7)$$

$$C_{21} \bar{U}_1 + C_{22} \bar{U}_2 - A_{21} \bar{V}_1 - A_{22} \bar{V}_2 = \bar{X}_2, \quad (3.8)$$

$$B_{11} \bar{U}_1 + B_{12} \bar{U}_2 - C_{11} \bar{V}_1 - C_{12} \bar{V}_2 = \bar{Y}_1, \quad (3.9)$$

$$B_{21} \bar{U}_1 + B_{22} \bar{U}_2 - C_{21} \bar{V}_1 - C_{22} \bar{V}_2 = \bar{Y}_2. \quad (3.10)$$

The system of equations (3.7) - (3.10) we obtain expressions that contain only unknown \bar{U}_2 and \bar{V}_2 .

By assumption $\det C_{11} \neq 0$, so

$$\bar{U}_1 = C_{11}^{-1}[\bar{X}_1 - C_{12}\bar{U}_2 + A_{11}\bar{V}_1 + A_{12}\bar{V}_2]. \quad (3.11)$$

Substitute the value found \bar{U}_1 in (3.9).

$$B_{11}C_{11}^{-1}[\bar{X}_1 - C_{12}\bar{U}_2 + A_{11}\bar{V}_1 + A_{12}\bar{V}_2] + B_{12}\bar{U}_2 - C_{11}\bar{V}_1 - C_{12}\bar{V}_2 = \bar{Y}_1,$$

or

$$\begin{aligned} &(-B_{11}C_{11}^{-1}C_{12} + B_{12})\bar{U}_2 + (B_{11}C_{11}^{-1}A_{11} - C_{11})\bar{V}_1 + (B_{11}C_{11}^{-1}A_{12} - C_{12})\bar{V}_2 = \\ &= \bar{Y}_1 - B_{11}C_{11}^{-1}\bar{X}_1. \end{aligned}$$

whence

$$\begin{aligned} \bar{V}_1 = &(B_{11}C_{11}^{-1}A_{11} - C_{11})^{-1}[\bar{Y}_1 - B_{11}C_{11}^{-1}\bar{X}_1 - (-B_{11}C_{11}^{-1}C_{12} + B_{12})\bar{U}_2 - \\ &- (B_{11}C_{11}^{-1}A_{12} - C_{12})\bar{V}_2]. \end{aligned} \quad (3.12)$$

So, we obtain the expression (3.11) of the form $\bar{U}_1(\bar{U}_2, \bar{V}_1, \bar{V}_2)$ and expression (3.12) $\bar{V}_1(\bar{U}_2, \bar{V}_2)$. They can be substituted in (3.8) or (3.10) and get that or any other formula for calculation of the reduced solution of a system of differential equations.

3.1. Option 1 (substitution of the expressions obtained in (3.8))

1). In (3.8) the value obtained for the subvector \bar{U}_1 .

$$C_{21}C_{11}^{-1}[\bar{X}_1 - C_{12}\bar{U}_2 + A_{11}\bar{V}_1 + A_{12}\bar{V}_2] + C_{22}\bar{U}_2 - A_{21}\bar{V}_1 - A_{22}\bar{V}_2 = \bar{X}_2.$$

After the unification of the matrix coefficients of the relevant variables, we obtain:

$$\begin{aligned} &[-C_{21}C_{11}^{-1}C_{12} + C_{22}]\bar{U}_2 + [C_{21}C_{11}^{-1}A_{11} - A_{21}]\bar{V}_1 + [C_{21}C_{11}^{-1}A_{12} - A_{22}]\bar{V}_2 = \\ &= \bar{X}_2 - C_{21}C_{11}^{-1}\bar{X}_1. \end{aligned}$$

2). Substitute in the resulting expression value (3.12) subvector \bar{V}_1 .

$$\begin{aligned} &[-C_{21}C_{11}^{-1}C_{12} + C_{22}]\bar{U}_2 + [C_{21}C_{11}^{-1}A_{11} - A_{21}](B_{11}C_{11}^{-1}A_{11} - C_{11})^{-1}[\bar{Y}_1 - \\ &- B_{11}C_{11}^{-1}\bar{X}_1 - (-B_{11}C_{11}^{-1}C_{12} + B_{12})\bar{U}_2 - (B_{11}C_{11}^{-1}A_{12} - C_{12})\bar{V}_2] + \\ &+ [C_{21}C_{11}^{-1}A_{12} - A_{22}]\bar{V}_2 = \bar{X}_2 - C_{21}C_{11}^{-1}\bar{X}_1. \end{aligned}$$

After similar terms, the latter expression takes the following form:

$$\begin{aligned} &[(-C_{21}C_{11}^{-1}C_{12} + C_{22}) - (C_{21}C_{11}^{-1}A_{11} - A_{21})(B_{11}C_{11}^{-1}A_{11} - C_{11})^{-1}(-B_{11}C_{11}^{-1}C_{12} + B_{12})]\bar{U}_2 + \\ &+ [(C_{21}C_{11}^{-1}A_{12} - A_{22}) - (C_{21}C_{11}^{-1}A_{11} - A_{21})(B_{11}C_{11}^{-1}A_{11} - C_{11})^{-1}(B_{11}C_{11}^{-1}A_{12} - C_{12})]\bar{V}_2 = \\ &= \bar{X}_2 - C_{21}C_{11}^{-1}\bar{X}_1 - (C_{21}C_{11}^{-1}A_{11} - A_{21})(B_{11}C_{11}^{-1}A_{11} - C_{11})^{-1}(\bar{Y}_1 - B_{11}C_{11}^{-1}\bar{X}_1). \end{aligned} \quad (3.1.1)$$

So, we obtain the desired reduced formula containing only subvectors \bar{U}_2 and \bar{V}_2 .

After a suitable change of variables, the system of equations (3.1.1) will have the form:

$$[C_{22}(\bar{Q}) + (G_{21}G_{11}^{-1}C_{11} - C_{21})G_{11}^{-1}G_{12} - G_{21}G_{11}^{-1}C_{12}]\bar{U}_2 +$$

$$+ \{-C_{22}(\bar{Q}) + (C_{21} - G_{21}G_{11}^{-1}C_{11})G_{11}^{-1}G_{12} + G_{21}G_{11}^{-1}C_{12} + h[G_{22}(\bar{Q}) - G_{21}G_{11}^{-1}G_{12}]\}\bar{V}_2 = \\ = \bar{X}_2 - C_{21}C_{11}^{-1}\bar{X}_1 - h^{-1}(C_{21} - G_{21}G_{11}^{-1}C_{11})G_{11}^{-1}[\bar{Y}_1 - (C_{11} + hG_{11})C_{11}^{-1}\bar{X}_1].$$

3.2. Option 2 (substitution of the expressions obtained in (3.10))

1). In (3.10) the value obtained for the subvector \bar{U}_1 .

$$B_{21}C_{11}^{-1}[\bar{X}_1 - C_{12}\bar{U}_2 + A_{11}\bar{V}_1 + A_{12}\bar{V}_2] + B_{22}\bar{U}_2 - C_{21}\bar{V}_1 - C_{22}\bar{V}_2 = \bar{Y}_2$$

After the unification of the matrix coefficients of the relevant variables, we obtain:

$$(-B_{21}C_{11}^{-1}C_{12} + B_{22})\bar{U}_2 + (B_{21}C_{11}^{-1}A_{11} - C_{21})\bar{V}_1 + (B_{21}C_{11}^{-1}A_{12} - C_{22})\bar{V}_2 = \\ = \bar{Y}_2 - B_{21}C_{11}^{-1}\bar{X}_1.$$

2). Substitute in the resulting expression value (3.12) subvector \bar{V}_1 .

$$(-B_{21}C_{11}^{-1}C_{12} + B_{22})\bar{U}_2 + (B_{21}C_{11}^{-1}A_{11} - C_{21})(B_{11}C_{11}^{-1}A_{11} - C_{11})^{-1}[\bar{Y}_1 - \\ - B_{11}C_{11}^{-1}\bar{X}_1 - (-B_{11}C_{11}^{-1}C_{12} + B_{12})\bar{U}_2 - (B_{11}C_{11}^{-1}A_{12} - C_{12})\bar{V}_2] + \\ + (B_{21}C_{11}^{-1}A_{12} - C_{22})\bar{V}_2 = \bar{Y}_2 - B_{21}C_{11}^{-1}\bar{X}_1$$

As a result, the expression takes the form

$$[(-B_{21}C_{11}^{-1}C_{12} + B_{22}) - (B_{21}C_{11}^{-1}A_{11} - C_{21})(B_{11}C_{11}^{-1}A_{11} - C_{11})^{-1}(-B_{11}C_{11}^{-1}C_{12} + B_{12})]\bar{U}_2 + \\ + [(B_{21}C_{11}^{-1}A_{12} - C_{22}) - (B_{21}C_{11}^{-1}A_{11} - C_{21})(B_{11}C_{11}^{-1}A_{11} - C_{11})^{-1}(B_{11}C_{11}^{-1}A_{12} - C_{12})]\bar{V}_2 = \\ = \bar{Y}_2 - B_{21}C_{11}^{-1}\bar{X}_1 - (B_{21}C_{11}^{-1}A_{11} - C_{21})(B_{11}C_{11}^{-1}A_{11} - C_{11})^{-1}[\bar{Y}_1 - B_{11}C_{11}^{-1}\bar{X}_1].$$

(3.2.1)

The system of equations (3.2.1) will have the form

$$[(-C_{21}C_{11}^{-1}C_{12} - hG_{21}C_{11}^{-1}C_{12} + C_{22} + hG_{22}) + [G_{21}G_{11}^{-1}(C_{11}G_{11}^{-1}G_{12} - C_{12}) - \\ - (C_{21} + hG_{21})G_{11}^{-1}G_{12} + (C_{21} + hG_{21})C_{11}^{-1}C_{12}]] = [(C_{22} + hG_{22}) + \\ + G_{21}G_{11}^{-1}(C_{11}G_{11}^{-1}G_{12} - C_{12}) - (C_{21} + hG_{21})G_{11}^{-1}G_{12}]\bar{U}_2 + [(C_{11}^{-1}C_{21}C_{12} - hC_{21}G_{12}C_{11}^{-1} + \\ + hG_{21}C_{12}C_{11}^{-1} - h^2G_{12}G_{21}C_{11}^{-1} - C_{22}) - (-hC_{21}G_{11}C_{11}^{-1} + hG_{21} - h^2G_{11}G_{21}C_{11}^{-1}) * \\ * (-hG_{11} + hG_{11} - h^2G_{11})^{-1}(-hC_{12}G_{11}C_{11}^{-1} + hG_{11}C_{12}C_{11}^{-1} - h^2G_{11}G_{12}C_{11}^{-1})]\bar{V}_2 = \\ = \bar{Y}_2 - (C_{21} + hG_{21})C_{11}^{-1}\bar{X}_1 - (-C_{21}C_{11}^{-1}hG_{11} + hG_{21} - h^2G_{21}G_{11}C_{11}^{-1})(-h^2G_{11})^{-1} * \\ * [\bar{Y}_1 - (\bar{X}_1 + hG_{11}C_{11}^{-1}\bar{X}_1)]$$

As a result of the acquisition of new computational schemes, based on the reduction of mathematical expressions Euler methods. With the help of the developed computational schemes calculation time painting current spreading over the surface of the spacecraft takes much less time spent in the traditional numerical methods. The complexity of the calculations in accordance with (3.1.1) and (3.2.1) in the modified step will be $3m^2$ operations, and at a constant step is m^2 operations. If $n=150000$ and $m=400$ for dense matrices computing speed compared with the implicit Euler method will increase approximately 52734375 times, and compared with the explicit Euler method to 140625 times.

This work is an output of a research project implemented as part of the Basic Research Program at the National Research University Higher School of Economics (HSE). The study

was implemented in the framework of the Basic Research Program at the National Research University Higher School of Economics (HSE) in 2014.

References

1. Azmy S. Ackleh, Edward James Allen, R. Baker Kearfott, Padmanabhan Seshaiyer // *Classical and Modern Numerical Analysis: Theory, Methods and Practice*/ 2009 by Chapman and Hall/CRC, 628 p.
2. Vostrikov A. V., Abrameshin A. E. Testirovanie kommercheskogo programmnogo obespecheniya dlya modelirovaniya i analiza ekvivalentnykh elektricheskikh skhem kosmicheskikh apparatov // *Tekhnologii elektromagnitnoi sovmestimosti*. 2012. № 1. S. 25-28.
3. Vostrikov A. V., Abrameshin A. E., Borisov N. I. Raschet navodok v bortovoi kabel'noi seti kosmicheskikh apparatov s pomoshch'yu makromodelirovaniya na osnove metodov Eilera // *Tekhnologii elektromagnitnoi sovmestimosti*. 2012. № 1 (40). S. 19-24.
4. Vostrikov A. V., Abrameshin A. E. Vychislitel'naya skhema uskorennoogo metoda rascheta navodok v bortovoi kabel'noi seti kosmicheskikh apparatov // *Tekhnologii elektromagnitnoi sovmestimosti*. 2012. № 3. S. 22-28.

ANALYSIS THE TRENDS OF EMPLOYMENT IN THE INFORMAL SECTOR OF THE ECONOMY

Stepanova E. G.

Stavropol, North-Caucasus Federal University

The approaches used to analyze the shadow component of economic activities in a context of main manpower's indicators have been considered in the given paper.

Keywords: shadow economy, informal economy, labor market, manpower, unemployment rate

The informal sector of the Russian economy was formed as a result of the implementation of reform processes of existing till 1990 administrative-command management system. Mistakes made by privatization of state property have caused a high degree of people's income polarization. People possessing considerably greater capitals, as a rule, do not want to be socially responsible and carry out their business in full compliance with current tax legislation. They try to hide the real income of their business that leads to deficiency of budgetary funds and further reduction of government's ability to finance social obligations.

The shadow sector of the economy is a significant and obvious phenomenon in any part of the world, yet especially in the developing and transition economies. As can be seen from the research carried out by F. Schneider shadow economy accounts for an average of 41% of the GDP in the developing countries, 38% - in the transition economies, and 17% - in the countries belonging to the Organization for Economic Co-operation and Development (OECD) [2]. According to the data from the World Bank, the International Consulting Group of A. T. Kearney this figure in Russia is 44% of the GDP.

Shadow economy may be viewed as citizens' attempt to avoid excessive tax burden and official regulations. A simple increase of taxes and the social security burden without analyzing the implication it may have for SE can result in a situation where such measures taken by the Government will urge people to move towards the shadow sector thus undermining the economy [3].

Is there a connection between the data estimating the scale of shadow economy and the official unemployment level? These two developments “may be linked in the sense that some of those reported as unemployed are actually busy working underground” [5].

For many years the EU-countries with a high level of unemployment have demonstrated growth in the shadow economy level. At the same time part of the products manufactured in the shadow sector is created by those who are on the officially unemployed list and who are being paid their unemployment benefits. This poses a question related to the accuracy of the unemployment statistics and its relation to shadow economy, the official statistics of the national accounts, and the unemployment figures. Mention to be made that nowadays the EU-countries are using the figures on the employment to have a more complete picture when checking the national accounts and evaluating the GNP (Decision 94/168/E.U., of 22.02.1994) [2].

The current demographic situation in the Russian Federation can be described with a maintained tendency towards a decrease in the nation’s population, its economically active part and the employment ratio despite the obvious migration flows.

An analysis of the number of the permanent population shows an average 2,3 mln decrease in the country within the period. The economically active population needs special attention if taken against the population on the whole as this particular part is directly involved into developing the social product. The major ratio in the total of the labor resources belongs to the working-age population. In 2011 this group suffered a 1,2% (1,1 mln) decrease if compared to 2003.

As is seen from the data above the share of the population in its working-age is constantly growing, and this index grew 8,5% within the period in question, reaching 69,8%. The change in this index is proportionate to the change in the level of the economically active working-age population (Figure 1).

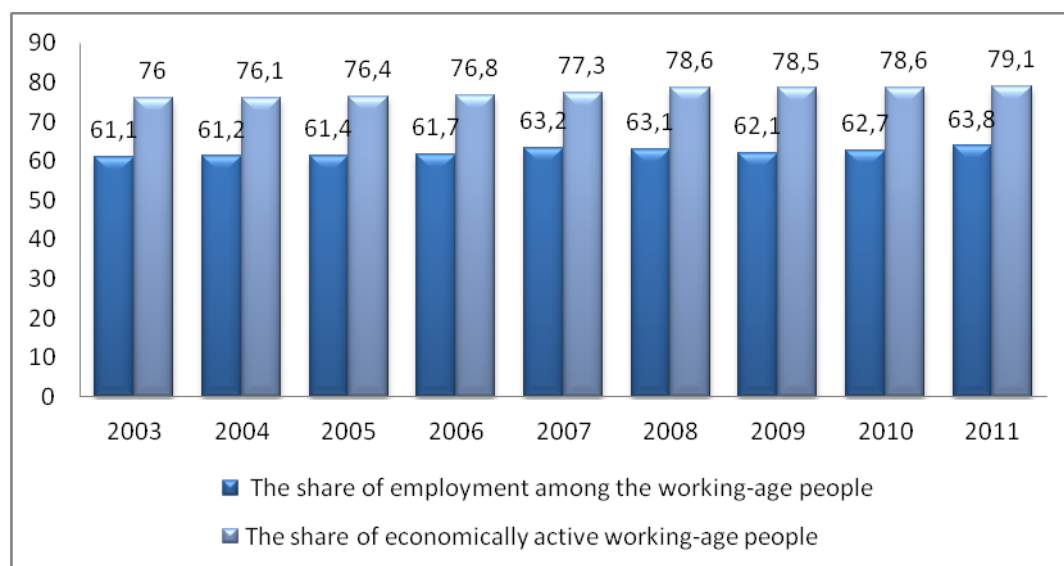


Figure 1. The dynamics of a manpower in the Russian Federation, %

The level of the economically active population, in turn, grew by 3,1% if compared to 2003 (61,1%) and reached 63,8 % in 2011.

The major impact on the number of the economically active population (calculated based on the number of those employed in the economy added to the unemployed number) was due to a change in the number of those employed in the economy. The number of the economically active population in Russia (2011) was 75,7 mln people including those employed in the economy – 70,7 mln, and the unemployed – 5,0 mln.

Most of the employed in 2011 году (65,6 mln) worked as hired employees (92,8% of all the employed); this figure grew 1,0% compared to 2003.

The share of the Russian people involved in the economy and not hired went down from 8,2 % in 2003 to 7,2% in 2011 making down to up 5,1 mln people.

Among those not hired most people are self-employed (3,9 mln) and only 0,8 mln are employers, which makes 1,2 % of the total employed population in 2011.

Looking at the change dynamics in the informal employment in Russia it is necessary to have a look at the labor market as a whole. The statistics says that the number of the population in 2003-2011 was decreasing.

However, the population's involvement in the economic activity was growing, people becoming more active and motivated, which is a positive sign at the labor market. The number of the employed (permanently) in companies officially registered as legal entities (according to the results of the population survey) has gone since 2008 by 0,8 mln people (1,4%).

An analysis of the employed population's structure by the types of employment and its dynamics shows that the employment growth was due to the informal sector of the economy where the number of people employed grew by 1,4 mln people (13,7%) within 2010-2011.

Looking at the data from the Russian Statistics Agency (Rosstat) we can see the following trend in the informal sector: the total number of the informally employed within 2003-2011 was growing while it reached its peak in 2008 – 13, 9 mln people (Figure 2).

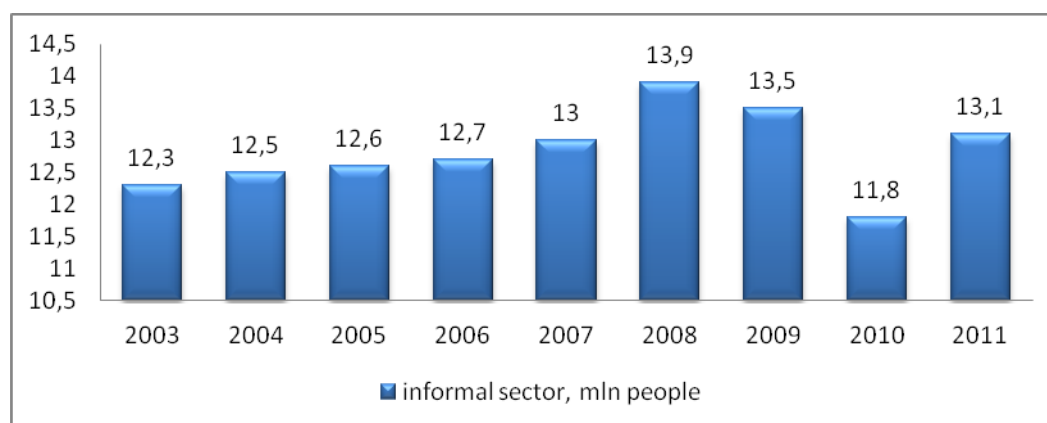


Figure 2. The dynamics of those inofficially employed 2003-2011

The sharp increase can be explained by the global financial crisis resulting in staff reduction in all the economic areas in the country. This made people look for some extra jobs. Employment in the informal sector ensured economic growth during the crisis compensating for the loss of workplaces at enterprises in the official sector of the economy. After 2009 even a slight employment reduction came along with reduced intensity in labor use and its efficiency. The reduction of those inofficially involved in the economy is due to the reduced number of workplaces in the country.

The growth of employment in the informal sector can have both negative and positive effects on the economy in general. On the one hand there is reduced efficiency in employing the labor force which results in slower economic development of the official sector; on the other hand this entails increased consumption and allows resolving social tension issues.

Drawing a conclusion to the above-mentioned it is necessary to say that understanding the processes underway in shadow economy as well as the mechanisms of its interrelation with, and effect on legal economy will result to making better founded decisions in the taxation, monetary, and social policy.

References

1. State Statistics Federal Agency official site [electronic resource] // access mode: <http://www.gks.ru/>.
2. 94/168/EC, Euratom: Commission Decision of 22 February 1994 on measures to be taken for the implementation of Council Directive 89/130/EEC, Euratom on the harmonization of the compilation of gross national product at market prices.
3. Kaufmann, D. Integrating the unofficial economy into the dynamics of post socialist economies: a framework of analyses and evidence/ D. Kaufmann, A. Kaliberda // Worldbank Policy Research Working Paper. 1996.
4. Schneider, F Shadow economies around the world: what do we really know? / F. Schneider / European Journal of Political Economy. September 2005. Volume 21, Issue 3. P. 598–642.
5. Tanzi, V. Uses and abuses of estimates of the underground economy / V. Tanzi // The Economic Journal. 1999. № 109 (June). P. 335–347.

PROBLEMS OF ASTEROID AND COMET HAZARD. ROLE OF MODERN INFORMATION TECHNOLOGY.

Kulagin(1) V., Dunham(2) D., Shustov(3) B., (2) KinetX,

(1) *Moscow Institute of Electronics and Mathematics of National Research University*
“Higher School of Economics”, Russia; (2) USA; (3) *Institute of Astronomy, Russia*

Development of a system for monitoring hazardous celestial bodies as well as assessment of risks and effects of impacts of such objects on the Earth are discussed. It is indicated that such a system should be based on an information analysis system for hazardous near-Earth objects, which should perform collection and processing of data on space bodies, provide the users with active and specialized information, and model disaster scenarios and provide choices for possible technologies of civil protection.

Persistence of modern civilization is subject to a number of threats of social and natural origins. Asteroid and comet hazard (ACH) is of notable significance in this list, which represents the threat of collision of the Earth with celestial objects, such as asteroids or comets. There is no doubt in the reality of this hazard. Chelyabinsk meteor of 2013 has demonstrated that such events are not infrequent.

Scientific focus on ACH for the Earth and human civilization emerged rather recently, not more than 30 years ago (before that time, perception of the threat lacked facts and unifying theory). Presently, studies of origins of bodies colliding with the Earth have been initiated, along with their orbital distribution in the space surrounding the Sun and collision rates with the Earth for bodies with various sizes and energies.

Currently, the orbits of the majority of near-Earth asteroids more than one kilometer in size are well known. It is considered that more than 80% of such objects are known (1096 objects discovered by February 1, 2014). However, the major threat to the Earth is not represented by these objects. Estimates of the number of undiscovered potentially hazardous asteroids with sizes ranging from 140 m to 1 km give the value of 20000 objects. Population of potentially hazardous objects with sizes from 50 to 140 m is estimated to be more than 200000 objects. These objects are continuously being discovered, but orbits of only few percent of them are known.

Addressing the issue of ACH is undoubtedly closely connected to the tasks of maintaining high levels of national security and implementation of a unified state system for

warning and mitigation of emergencies, as declared in the Strategy of national security of Russian Federation until 2020 and the Concept of long-term social and economic development of Russian Federation until 2020 among the most important tasks for development of our country.

The purpose of the presented research area is development of a system for monitoring hazardous celestial objects and estimating risks and outcomes for impacts of these objects on the Earth. It is proposed that the monitoring system should be based on a unified information analysis system, which provides an integrated informational support for situational risk analysis on the problem of ACH, as well as for devising the necessary activities for mitigation of the prospective damages in cases of emergency.

The development of the system for monitoring hazardous celestial bodies, risk assessment and mitigation of the ACH is of prime importance to Russian Federation – a country with a large territory, where an impact of a hazardous celestial body is more probable. The implementation of the information analysis system addresses national interests. Information provided by this system will play important role in establishing a justified and independent position of Russian in international cooperation on the issue of ACH. Further development in this area will provide for establishment of a center in Russia that stands on one level with the other international centers (Minor Planet Center (USA), NASA Jet Propulsion Laboratory (USA) and Spaceguard Central Node (European Union)) where potentially hazardous objects have been monitored for a number of years.

The problem of development of a Russian system for addressing space hazards has multiple components. The presented task of development of a system for monitoring hazardous celestial bodies, risk assessment and mitigation of the ACH includes solutions of several large scientific problems. The first problem for assessment of threat level from the hazardous objects is insufficient information on the parameters of motion of near-Earth asteroids and comets. In order to solve this problem, it is proposed to implement an information analysis center which would process all data on the near-Earth objects. The primary criterion for the efficiency of the center operations should be the accuracy of trajectory determination for hazardous celestial bodies. Any progress in this direction will require both high-precision tools for observing minor bodies of the Solar System and efficient methods and algorithms for calculation of these objects' orbits. Presently, methods, algorithms and programs for orbit calculation and prediction for asteroids and comets, which have been developed so far, while demonstrating their capacity and effectiveness require enhancements, increases in accuracy and reliability, inclusion of new perturbation sources which influence predictions of collisions.

The other problem is determination of effects caused by the hazardous celestial object's atmospheric entry and impact on the surface of our planet. The primary parameters of a space object that always determine the damaging effects of an impact are the speed and angle of impact, mass and type of the object. The effects are also influenced by physical and chemical characteristics of the surface at the impact site (impact on water can cause tsunamis, ground impact can cause earthquake, etc.). Therefore, there is evidently a severe necessity for devising mathematical models for impacts of celestial bodies on the Earth, which will comprise one of the main components of the information analysis system for monitoring of approaches by hazardous celestial bodies.

The information system for analysis of hazardous near-Earth objects will be closely connected with the system monitoring these objects. The main result of the conducted research is projected to be a unified information analysis system for monitoring of hazardous celestial bodies, risk assessment and mitigation of ACH, which will include:

1. A system for automatic collection of coordinate and non-coordinate data on near-Earth asteroids.

2. A hardware and software complex, which enables:
 - Exploring evolution of orbits of hazardous celestial objects at long time scales and visualizing the orbital changes with time;
 - Estimating probabilities of hazardous approaches of asteroids with the Earth;
 - Estimating probabilities of asteroid impacts in a given area on the Earth.
3. A hardware and software complex for providing the system users with real-time, general and specific information on the ACH.
4. A hardware and software complex for modeling disaster scenarios, which will enable considering all stages of impact by a space object (from atmospheric entry to crater formation and ejection of dangerous materials) for a wide selection of the impactor parameters based on the developed methods and corresponding models.
5. A software unit for support of decision-making in selection of civil defense technologies in cases of air blasts or ground impacts of celestial objects.
6. A database of possible effects of an asteroid impact on a given territory.

The projected results can be of interest to such Russian agencies as Roscosmos, EMERCOM, and other organizations providing security of special sites, property and population in Russia. The results generated during performance of the work can be utilized for creation of the information analysis center of the System for warning of space threats or for the Federal space program of Russia.

References

1. Asteroid and comet hazard: past, present and future. Ed. B.M.Shustov, L.V.Rykhlova. FIZMATLIT, Moscow, 2010. 294p.
2. Space missions and planetary defense. FIZMATLIT, Moscow, 2013. 276p.
3. Kulagin V.P., Dunham D. W., Tsvetkov V. Y. *Near-earth space as a habitat*. International Journal of Astrophysics and Space Science, Vol. 1, No. 3, 2013, pp. 12-15. Available: <http://publications.hse.ru/articles/112854145>
4. Kulagin V.P., Tsvetkov V.Y., Maksimova M.V. *The Convergence in Spatial Tasks*. European Researcher, Vol. 58, No. 9-1, 2013, pp. 2179-2184.
5. Kulagin V.P., Tsvetkov V., Barmin I., Savinykh I. *Near-Earth space as a target of global monitoring*. Vestnik FGUP NPO Lavochkina, No. 4, 2013, pp. 4-9.

RESEARCH OF FAILURE MECHANISMS OF SOLENOIDS AND CONTACTORS

Fokin V. M.

Moscow, National Research University "Higher School of Economics"

This work presents the results of failure mechanisms of solenoids and contactors and their failure rates presented in the American standard NSWC-11.

Keywords: reliability, radio electronics, contactors, solenoids, failure rate.

This study (research grant № 14-05-0038) supported by The National Research University - Higher School of Economics' Academic Fund Program in 2014. In modern radio-electronic equipment and means of automatics the various actuating, program, switch, brake, fix, block and other electromagnetic units construct on the basis of such executive elements, as electromagnets, solenoids, electromagnetic coupling, etc. [1]. In addition, the operation of high-power microwave devices that use extended electron beams (klystrons, TWT, BWO, etc.), can be achieved only by using systems that limit the electron flow. As such a means of limiting the power microwave generators and amplifiers, mainly used as

various forming apparatus based on magnetic fields of solenoids [2]. Thus, the failure of such components can not only lead to a decrease in the efficiency of the equipment, but also to the complete loss of functionality.

Solenoids – are electromechanical devices that convert electrical energy into mechanical motion. Usually this movement is used to move the load at a specified distance or the angle for the required time. Linear magnetic solenoids usually produce retracting movement of the plunger in the coil. They can also be equipped with a pusher attached to one end of the plunger providing thrusting movement. The plunger of the solenoid assembly, also known as armature (rotor) is made of nonferrous metal to increase the magnetism or the magnetic permeability. Rotary solenoid transforms the axial movement in the rotary move.

The simplest solenoid is able to perform movement only between the extreme positions. More advanced models of solenoids are allowed to adjust the force, velocity, acceleration and position. Special type of solenoids are linear rotary actuators. In them coil moves not rod and the motor, solenoid adequate accuracy and other characteristics (stepper or servo).

Typical designs of linear and rotary solenoids are shown in Figure 1.

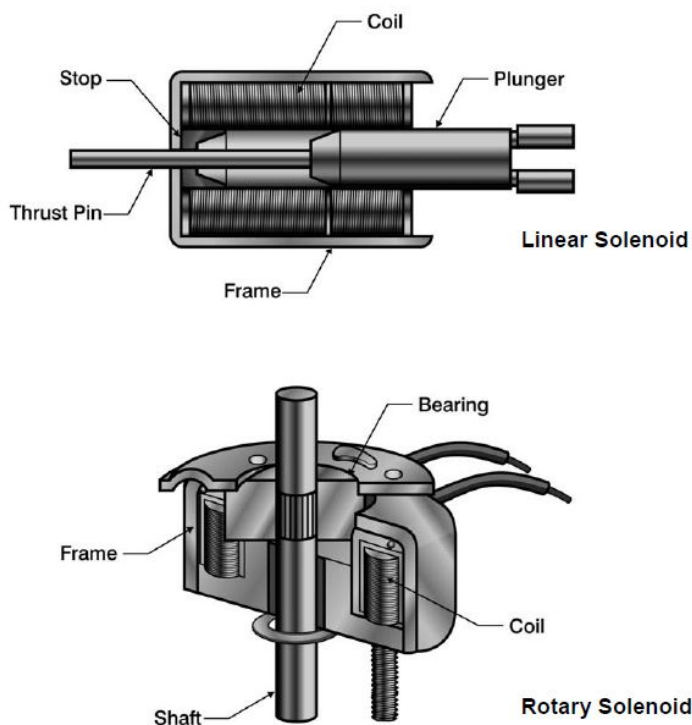


Fig. 1. Components of the linear and rotary solenoids

When voltage is applied to the coil, plunger is retracted into the solenoid, which causes the opening or closing of the valve. The backward movement of the plunger is provided with de-energized or the load itself, or spring return.

In mounting solenoid it's necessary to ensure good heat dissipation, so the surface area is significantly larger than the area of installation of the solenoid. Furthermore, solenoids have a time limit of use depending on the number of switching and the power of the input current. For example, if the operation time of the solenoid is greater than 5 minutes during one cycle, it should be seen in the continuous load (100% duty cycle).

The main failure modes of the electromagnetic solenoid are circuit at one or more coil windings, or breaking coil, usually caused by overheating. Thermal Dissipation in solenoid depends on the power consumption and operating time.

Contactors - are devices remote actions designed to enable and disable electrical power circuits apparatus. Engagement or disengagement contacts of the contactor carried out by means an electromagnetic actuator [3].

Contactor consists of the following main components: the main contacts, arc chute system, electromagnetic system and auxiliary contacts.

Main contacts carried closing and opening of the power circuit. They should be designed as a long passage of current and ON / OFF, including at high frequency. Considered normal contact position when the contactor coil is de-energized and released all the mechanical latch. Main contacts can be performed lever and bridge type. Lever contacts suggest moving the rotary system, bridging – straight suspension [4]. Typical design of contactor is shown in Figure 2.

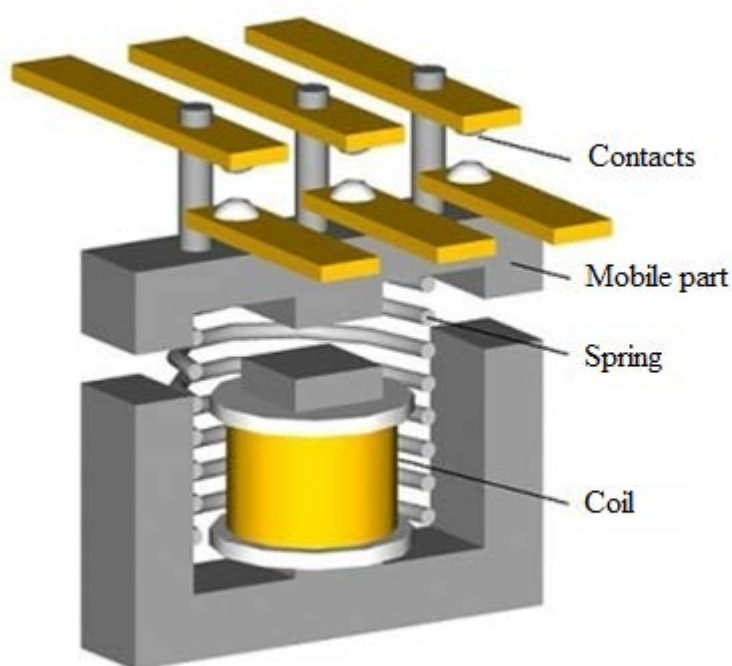


Fig. 2. Components of the contactor

Lifetime of the contactor contacts is usually limited, depending on the physical, chemical and electrical facts. Failure of the electrical contact is usually determined by increasing contact resistance by an amount exceeding the initial value of approximately twice.

Methods of calculating the reliability of mechanical and electromechanical devices, which include solenoids and contactors are considered in [5, 6], where it is shown that the most acceptable standard is methodology NSWC-11 [7]. The standard NSWC-11 considers typical failure mechanisms of solenoids and contactors, which are described in Table 1.

Table 1. Typical failure modes of a solenoids and contactors

FAILURE MODE	FAILURE MECHANISM	FAILURE CAUSE
Coil burnout	Inrush current causes coil overheating and burnout	Mechanical jamming of plunger

		Insufficient heat sink area for solenoid
		Supply voltage interruption resulting in inductive surge
	Heat builds up faster than it can be dissipated	Excessive cycling rate
Failure to operate	Increase in coil resistance preventing solenoid closure	Excessive ambient temperature
	Shorted coil at lead wires	Excessive moisture
Open inductor winding	Open lead at termination	Coil voltage over load, vibration
Armature (plunger) failure	Mismatch of solenoid force and load	Excessive plunger force creating hammering
Poor response time (pull-in time)	Insufficient solenoid force with respect to load	Jammed return spring
Poor release time (drop-out time)	Insufficient load or spring force to release plunger	Damaged/jammed spring or loss of load force
Damaged contactor	Contactor arcing	Excessive load voltage

The failure rate of the solenoid can be estimated from the following equation [7]:

$$\lambda_{SO} = \lambda_{SO,B} \cdot C_T \cdot C_K \cdot C_S$$

where: $\lambda_{SO,B}$ - base failure; C_T - temperature multiplying factor; C_K - application service factor; C_S - use rate.

The failure rate of the contactor (λ_C) can be written as [7]:

$$\lambda_C = \lambda_{C,B} \cdot v^m \cdot I^n$$

where: $\lambda_{C,B}$ - base failure rate of contactor assembly; v - voltage across contactor assembly; I - current; m - voltage constant; n - current constant.

A more general equation can be written for AC resistive loads [7]:

$$\lambda_C = \lambda_{C,B} \cdot C_v \cdot C_I$$

where: C_v - multiplying factor considering contactor voltage; C_I - multiplying factor considering contactor current.

For AC inductive loads, the power factor must be considered, modifying Equation as follows [7]:

$$\lambda_C = \lambda_{C,B} \cdot C_v \cdot C_I \cdot C_{PF}$$

где: $\lambda_{C,B}$ - base failure rate of contactor assembly; C_{PF} - multiplying factor considering the power factor.

DC loads generate greater arcing across the contacts than do AC loads. The failure rate equation for a contactor with DC loads is written as follows [7]:

$$\lambda_C = \lambda_{C,B} \cdot C_v \cdot C_I$$

где: $\lambda_{C,B}$ - base failure rate of contactor assembly; C_v - multiplying factor considering contactor voltage; C_I - multiplying factor considering contactor current.

Thus, the above failure mechanisms and corresponding failure rates models that take into account the influence of application modes coils and contactors can be used not only for evaluating the reliability problems of these elements, but also, if necessary, to ensure the reliability of equipment problems in general.

References

1. Savelyev I.V. Kurs obschej fiziki, t. 2. Elektrichestvo i magnetizm. Volni. Optika: Uchebnoe posobie. - 2-e izd., pererab. / I.V. Savelyev. - M.: Nauka, Gl. red. fiz-mat. lit., 1982. - 496 s.
2. Movshevich, B.Z. Impulsno-periodicheskii generator silnikh magnitnikh polei. / B.Z. Movshevich, E.A. Kopelovich, U.A. Kuznetsov. // PTE. - № 6. - 1989. - s.130-136.
3. GOST R 51731-2001 (MEK 61095-92) Kontaktory elektromechanicheskie bitovogo i analogichnogo naznachenia.
4. Sibikin, U.D. Montazh, ekspluatatsia i remont elektrooborudovania promishlennikh predpriyatii i ustanovok. / U.D. Sibikin, M.U. Sibikin. - M.: Visshaya shkola, 2001. - 462 s.
5. Zhadnov, V.V. Metody i sredstva ocenki pokazatelej nadezhnosti mekhanicheskikh i e'lektromekhanicheskikh e'lementov priborov i sistem. / V.V. Zhadnov. // Datchiki i sistemy. - 2013. - № 4. - s. 15-20.
6. Zhadnov, V. Methods and means of the estimation of indicators of reliability of mechanical and electromechanical elements of devices and systems. / V. Zhadnov. // Reliability: Theory & Applications: e-journal. - 2011. - Vol. 2, No 4. - p. 94-102.
7. NSWC-11 Handbook of reliability prediction procedures for mechanical equipment.

BUILDING KNOWLEDGE SPACE FOR SYNTHESIS OF TECHNICAL SYSTEMS WITH ENERGY-CIRCUIT METHOD

Khomenko T. V., Petrova I.Yu, Lezhnina Yu. A., Veselova Yu. A.
Astrakhan civil engineering institute

The method of constructing the knowledge space is consider. Received ontology physico-technical effects, allowing solving the problem of synthesis of technical systems using energy-information method chains.

Keywords: knowledge space, ontology, physical and technical effect, energy-information method chains, the synthesis of technical systems

Operation of technical systems is a complex interaction of many different physical effects. The principle of operation of technical systems is present as a structured set of different physical effects, which provides the system to a given function. At the same processes in the physical chains of different origin related through a lot of the physical nature of interchain PTE.

Catalogs of physical and technical effects compiled for tentative classification and application in chemical engineering, biotech and others areas. Many researchers attempted to systematize the description technically significant effects. Recently, developer use base of physical effects in information systems support the activities of the engineer -inventor, which based on a knowledge base on physical effects, which presented special physical knowledge in a structured manner, providing more convenient to find and use them. In [1] proposed to use the energy- model of different physical chains based on phenomenological equations of no equilibrium thermodynamics. In [2] proposed a generalized theory of transducers, which based on the principle of conservation of energy and the principle of reciprocity. In [3] attempted to develop a universal system-wide device simulation based on the similarity of mathematical descriptions of various physical processes: optical, acoustic, thermal, mathematical, electrical, etc.

It is necessary to have for all analogues not just similar, but a unified description equally reflects the essence of the different processes to analyze the different physical

processes. This requires structuring of data and knowledge about the objects of design [4, 5]. Structuring description of the effect and the presence of a formal part are the implementation conditions of the principles of synthesis algorithms, as well as information retrieval mechanisms that have fundamentally more features compared to traditional treatments search by name and keywords. This work is devoted to the development and research of knowledge representation in solving the problem of energy-synthesis models chains (ESMC) different physical nature. As a means of formalizing the selected domain ontology construction. Formal ontology can be seen as a set of vertices that represent scientific and technical characteristics associated hierarchical relationships. Building a complete and detailed ontology is a tedious task. The solution to this problem is largely determine by how the developer will be equipped with an ontology methods and technologies of its formation [6]. It is propose to use the apparatus for general topology structuring ontology ESMC. In this paper, to create an ontology was decided to limit the possibility of solving the problem of software synthesis based on the resultant structure.

To systematize the knowledge and build the knowledge space of energy-method design of technical systems to the information environment immersed content model of a topological space (Π, τ) . Identifying similar model elements is perform according to the developed technique.

Step 1. Transformation of knowledge MP in the knowledge space P by the proposed operational definitions: $InfMP \xrightarrow{oo} P$.

- basic concepts of MP are considered as elements of a finite set M;
- partition of M into classes [7]: $K := \langle \text{basic objects: minimal system of generators of initial concepts} \rangle$, $K' := \langle \text{objects Action: Extended system of concepts, reflecting the relationship between the basic objects} \rangle$, $K'' := \langle \text{objects -constructs: the resulting system of concepts, reflecting the relationship between objects, actions} \rangle$, $\Lambda := \langle \text{basic operations, the minimum system necessary operations on the concepts} \rangle$, discrete metric ρ introduce on M:

$$\rho = \begin{cases} 0, & \text{если } x = y \\ 1, & \text{если } x \neq y \end{cases},$$

which is considered in the context of semantic metrics [8] ρ : = «semantically close" and characterizes the strength of the associative link between thematic concepts analyzed, and has properties that are characteristic for the metric.

Result of the introduction of the metric is a partition $\sigma : (l = \overline{1, L})$ of the set of elements on L knowledge class [9]. Knowledge space - a set of discrete (isolated) points, each of which represents a specific set of concepts for the implementation of knowledge.

Simplify the analysis of options combinations (collectively concepts) can be due to research of knowledge space's local areas having certain structural property.

Step 2. Application of the operational apparatus topology as translation operator of the semantic foundations of different methods unity for designing technical systems in knowledge space with the topological structure: $P \xrightarrow{OT} T(P^\Phi, \tau_{P^\Phi})$.

Step 3. Informal presentation of a topological space pseudo cell complex $T_G(P^\Phi, \tau_{\Pi^\Phi})$.

Building a knowledge space to solve the problem of synthesis of technical systems. We apply the above steps for the construction of the knowledge space. The task of constructing a complete and exhaustive ontology of energy- method chains in this article is not solve. We confine ourselves to the problem of synthesizing chains certain physical nature. In the first phase, we solve the problem of classification. In the dialogue with the expert conducted content analysis domain, its elements and the relationships between them. Based on expertise in the space of elements of different physical nature determined attitude semantic

proximity elements. It is necessary to further form a plurality of base sites, base operations, objects, actions and objects constructs.

In the next step we obtain a set of basic concepts of momentum $K=\{ \text{impulse } P, \text{ voltage } U, \text{ charge } Q, \text{ current } I, \text{ resistance } R, \text{ conductance } G, \text{ stiffness } W, \text{ capacitance } C, \text{ inductance } L, \text{ deductive } D, \text{ factor physico-technical effects } \}$; a set of operations objects $K'=\{ I \cdot L = P, U \cdot C = Q, I \cdot R = U, Q \cdot R = P, I' \cdot R = U', K_{in} \cdot B_{in} = B_{out}, K_{in} \cdot B_{in} = P_{out}, K_{in} \cdot B_{in1} \cdot B_{in2} = B_{out} \}$, which is a set of energy-information method chains criteria and inter chain physico-technical effects; a set of objects-builder $K''=\{\text{chain, inter chain physico-technical effects}\}$; a set of basic operations $\Lambda=\{ \cdot, ', = \}$ (Table 1). In the next step we spend a grouping of basic concepts. On this way we obtain a set of influence variables, a set of reaction variables, a set of parameters, and a set of physico-technical effects coefficients.

Table1.

Partitioning elements of knowledge into classes K, K', K'', Λ .

a set of objects-builder K''	a set of operations objects K'	a set of basic concepts of momentum K	a set of basic operations Λ
A set of different physical chain	6 energy-information method chains criteria:	impulse P , voltage U , charge Q , current I , resistance R , conductance G , stiffness W , capacitance C , inductance L , deductive D	$\Lambda=\{ \cdot, ', = \}$
	1 Power $U \cdot I = N$		
	2 Static $I \cdot L = P$		
	Derivative criteria $P \cdot D = I$		
	3 Static $U \cdot C = Q$		
	Derivative criteria $Q \cdot W = U$		
	4 Static $I \cdot R = U$		
	Derivative criteria $U \cdot G = I$		
	5 Dynamic $dP/dt = U$		
	Derivative criteria $\int U dt = P$		
A set of inter chain physico-technical effects	6 Dynamic $dQ/dt = I$	U, I, N, P, L, D, C, Q, W, R, K_{in} – coefficients of physico-technical effects	$\Lambda=\{ \cdot, = \}$
	Derivative criteria $\int I dt = Q$		
	Structure of physico-technical effects: $K_{in} \cdot B_{in} = B_{out}$, $K_{in} \cdot B_{in} = P_{out}$, $K_{in} \cdot B_{in1} \cdot B_{in2} = B_{out}$		

Note that the union of values and parameters using basic operations can get energy-information method chains criteria. Blocking input and output variables by a factor physical and technical effects allows forming inter chain effects. Magnitude of the impact and magnitude of the reaction can act as inputs physical and technical effects. Set of basic operations is generated by analyzing the mathematical representation energy-information method chains criteria. Analysis of existing physical and technical effects shows that parameters defining the physical principle of the system can be observed as the output.

This structuring allows formally describe the principle of union of chains of different physical nature through physical and technical effects that transform the value of one of the physical nature to another physical nature value (Figure 3).

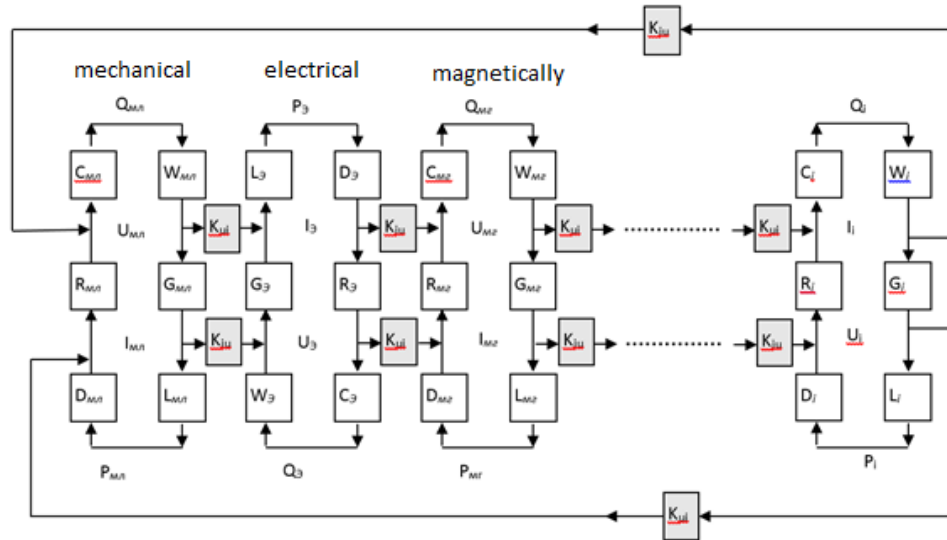


Figure 3. Count links for n chains of different physical nature

Converting the output values of i -th circuit in the input values of $i+1$ -th chain is also performed used selected basic operations (Table 1). Structuring the knowledge space of energy-chain method allowed us to obtain a three-level class hierarchy of the ontology. Ontology describes itself between the elements of the knowledge space. Filling ontology facts shown in Figure 4.

Obviously, a significant difference of the physical nature intra chain and inter chain dependency becomes significant when determining the structure of the ontology using a general topology. The resulting ontology is reflected in the informal representation of a topological knowledge space of energy-chain method as a pseudo cell complex.

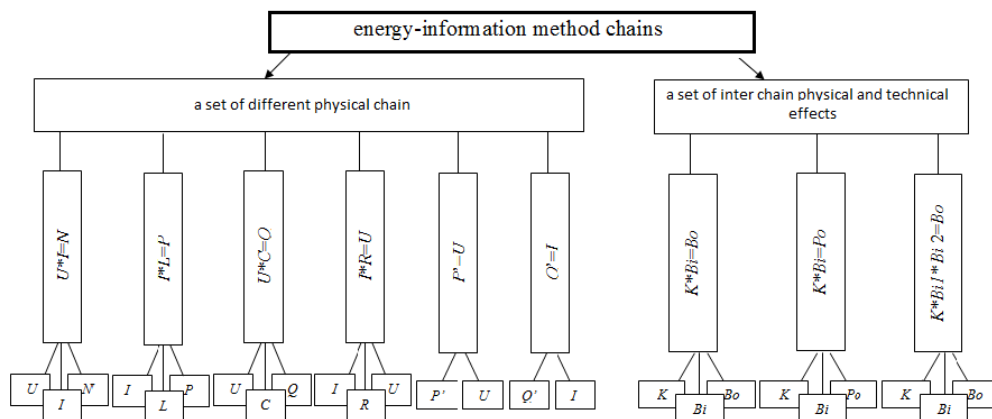


Figure 4. Ontology of energy-information method chains

Conclusion. The difference intra chain and inter chain dependency in terms of the physical nature is known. An application stage of formalization, in particular non-formal representation of a topological space pseudo cell complex, allows us to consider these differences as insignificant and determine the boundary of solved problems, distinguish the class of tasks. It is the use of the proposed method allows to get rid of detail which complicates the perception of ontology.

References

1. Irina Petrova, Viktoriya Zaripova, Systems of teaching engineering work on base of internet technologies. International Journal "Information Technologies and Knowledge" Vol.1, 2007, p.37-43
2. Kharkevich A.A. Izbrannye trudy. V 3-kh t.: M., «Nauka», 1973. T.1 - «Teoriya elektroakusticheskikh preobrazovatelei. Volnovye protsessy». 399 s.
3. Teoriya sistem i metody sistemnogo analiza v upravlenii i svyazi / V.N. Volkova, V.A. Voronkov, A.A. Denisov i dr. – M. : Radio i svyaz', 1983. – s.74-146.
4. Zaripova V.M., Petrova I.Yu. Model' razvitiya sredstv avtomatizatsii innovatsionnykh protsessov (Computer Aided Innovation - CAI) // Prikaspiiskii zhurnal: upravlenie i vysokie tekhnologii. 2012. № 3. S. 111–130.
5. Khomenko T.V. Sistemnye podkhody k analizu izmeritel'nykh ustroystv // Vestnik Astrakhanskogo gosudarstvennogo tekhnicheskogo universiteta. Seriya: Upravlenie, vychislitel'naya tekhnika i informatika. 2009. № 1. S. 88-93
6. Irina Yurievna Kvyatkovskaya, Valery Fedorovich Shurshev, Gennady Viktorovich Berezhnov and Yulia Arkadievna Lezhnina, Modified Algorithm of Information Retrieval Based on Graph Model and Latent Semantic Analysis. World Applied Sciences Journal 24 (Information Technologies in Modern Industry, Education & Society): (2013), p.250-255,
7. Vasil'ev Yu.S., Kozlov V.N., Maslennikov A.S. Kompetentnostnye modeli znaniy i soderzhaniya vysshego obrazovaniya// Nauchno-tekhnicheskie vedomosti SPbGPU. 2008. № 66. S. 7-9.
8. <http://www.digsolab.ru>
9. Fomenko A.T. Differentsial'naya geometriya i topologiya. Dopolnitel'nye glavy – Izhevsk: Izhevskaya tipografiya, 1999. – 252 s.

ANALYSIS OF BASIC MECHANISMS AND REASONS OF BREAKDOWN OF COOLING SYSTEMS' PUMPS

Tsyganov P.

Moscow, National Research University "Higher School of Economics"

The most popular constructions of cooling system pumps and the main mechanisms and reasons of pumps failures considered.

Keywords: pump, breakdown, cavitation

This study (research grant № 14-05-0038) supported by The National Research University - Higher School of Economics' Academic Fund Program in 2014. Liquid cooling systems are increasingly used in modern radio-electronic equipments. Pumps are the main components of these systems. Two types of pumps are mainly used in liquid cooling systems:

- reciprocating piston pumps
- radial flow pumps.

Reciprocating piston pump (Figure 1) consists of piston, working chamber, admission and discharge valves.



Figure 1 - Reciprocating piston pump

When the piston moves down, low pressure zone is created in the working chamber, admission valve opens and the fluid absorption occurs. When the piston moves upward the overpressure arises and the discharge valve opens, wherein the admission valve is closed. The fluid injection occurs.

Pulsation of pressure, which causes imbalance is the disadvantage of reciprocating piston pump. For all that valve shaft experiences heavy loads because of the irregularity of the torsion torque [1].

The fluid motion and the necessary pressure in radial flow pump (Figure 2) is created by the centrifugal force generated by the impact of blades of the impeller on the liquid. The impeller is fixed on the shaft inside the pump.

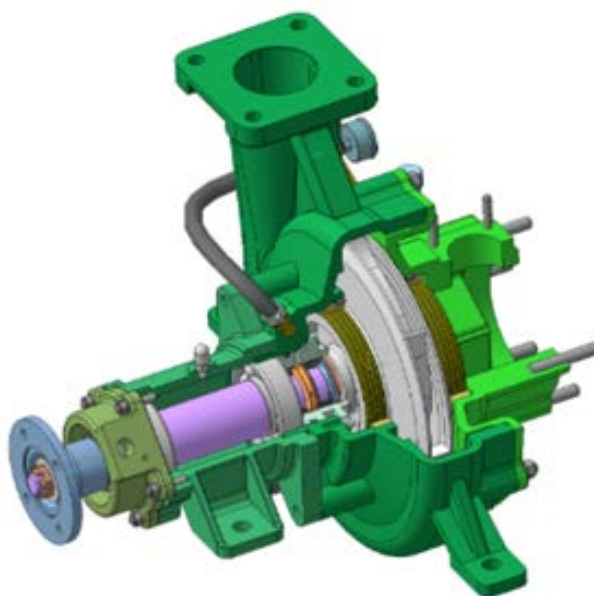


Figure 2 - Radial flow pumps

It has a helical shape and consists of two discs, which are bent in opposite direction of impeller rotation. When pump body is filled with liquid and impeller starts to rotate, the liquid in impeller channel will be shifted from the center. Underpressure arises in the central part. Fluid from inlet will flow into the central part, and fluid at the periphery will flow into the outlet pipeline [1].

Failures of both types of pumps can be classified as sudden and gradual[2-4]. The pump immediately stops working in case of sudden failure. The pump can continue to work in case of gradual failure, but its output pressure is significantly reduced.

For example, sudden failures include the destruction of thrust bearing of wheel of radial flow pump. Bearing damage may occur due to heavy load on the shaft, which may be due to damage, displacement or unbalancing of the shaft. Also these failures can lead to destruction of pump rotor [5].

Gradual failures include decline of the outlet pressure of the pump, which can be caused by the imbalance of pump wheel and cavitation effect during operation. Cavitation is disruption of the continuity of fluid flow due to lower pressure.

A large amount of bubbles, which consist of liquid and gas vapour, exuded from the solution, are generated in cavitation zone. When the pump operates, cavitation zone bubbles combine and form large bubbles, which in liquid form flow into the working zone of pump with high pressure.

The process of instant collapse of bubble is accompanied by water hammering. Cavitation phenomena in a radial flow pump reduce its efficiency, inlet and outlet pressure, lead to vibration and noise during operation. Cavitation in a centrifugal pump depends on the fluid flow rate and feed rate Q .

At the speed rate about 20 m/s the pressure drop in the pump is 0,8-2,5 kg/centimeter. As result the cavitation zone is formed in the pump. Then the feed rate is about $Q = (0,8-Q_{\text{optimum}})$ cavitation zone not formed. Then the feed rate is about $Q = (1,2-1,25) \cdot Q_{\text{optimum}}$ cavitation zone begin to forming. At the feed rate more than $Q = (1,40) \cdot Q_{\text{optimum}}$ the pump lose about 10 percents of performance [6].

All these factors may contribute to vibration during operation of the pump, which can cause damage of sealing ring and gasket. The damage causes the leak of a liquid. Causes of the leak depend on mode of use, environmental conditions and type of liquid. If the liquid is water, then it will not cause any consequences. If the liquid is Petroleum, Oils and Lubricants (POL), then the leak can lead to fire.

Failures of reciprocating piston pumps are similar to failures of radial flow pumps.

Pump failures can also be results of incorrect assembly of pump and improper maintenance. In case of improper maintenance, gaskets and seals may be installed improperly, that leads to a leak. Improper assembly of the pump can lead to the failure of mechanical components of the pump.

Thus, factors of impact of structural and technological performance, conditions and modes of operation, and also maintenance conditions must be entered into the mathematical model of the failure rate of the pump.

References

1. Zhabo, V.V. *Gidravlika i nasosy*. / V.V. Zhabo, V.V. Uvarov, M.: Energoatomizdat, 1984. - 328 s.
2. Zhadnov, V.V. *Metody i sredstva ocenki pokazatelej nadezhnosti mehanicheskikh i e'lektromehaniicheskikh e'lementov priborov i sistem*. / V.V. Zhadnov. // *Datchiki i sistemy*. - 2013. - № 4. - s. 15-20.

3. Zhadnov, V. Methods and means of the estimation of indicators of reliability of mechanical and electromechanical elements of devices and systems. / V. Zhadnov. // Reliability: Theory & Applications: e-journal. - 2011. - Vol. 2, No 4. - p. 94-102.
4. Markin, A.V. Metody ocenki nadyozhnosti elementov mexaniki i elektromexaniki elektronnyx sredstv na rannix etapax proektirovaniya. / A.V. Markin, S.N. Polesskij, V.V. Zhadnov. // Nadyozhnost'. - 2010. - № 2. - s. 63-70.
5. NSWC-11 Handbook of reliability prediction procedures for mechanical equipment.
6. Karelin, V.Ya. Kavitatsionnye yavleniya v tsentrobezhnyh i osevyh nasosah. / V.Ya. Karelin. - M.: Mashinostroenie, 1975. - 330 s.

INTERNAL EARTH STRUCTURE RENEWAL BY MEANS OF CORE IN INCLINED BOREHOLES ANALYSIS.

Lytvyn O. O., Shtepa N. I., Denisova O. I., Chorna O. S.
Ukraine, Kharkiv, Ukrainian engineering pedagogical academy

In the work minerals distribution three-dimensional model construction methods on the basis of the data about minerals distribution in each point of the set boreholes system and three variables interlineation functions methods are stated. The construction methods of three variables interlineation functions polinomial formulae in the inclined boreholes system, spline-interlineation functions on inclined boreholes system, placed both in the same plane and in an arbitrary way, as well as three variables interlineation functions formulae with the use of global interpolation formulae by Donald Shepard and Oleg N. Lytvyn generalizations are given. The properties of the constructed mathematical models, as well as the prospects of their use for the exploration of mineral resources are explored.

Keywords: mathematical model, interlineation, cores, inclined boreholes.

Introduction

Directional drilling is gradually becoming the main type of drilling both overland and at sea with the penetration of boreholes from stationary platforms. At the same time there is a tendency to the increase of requirements to accuracy of bottom boreholes hitting in the given point and on the compliance of project profile boreholes drillings. Therefore, it is necessary to ensure an effective control of the boreholes spatial position [1].

Mineral exploration is a well-known method, which is based on the analysis of the boreholes cores content, drilled in different points of the regions surface. In the works [2-5] the general method of constructing the spatial mathematical models of minerals distribution on the basis of the vertical boreholes cores content data and interlineation functions of three variables $f(x, y, z)$ - the distribution of minerals in each point (x, y, z) - is proposed and studied. In these works the assumption that all the boreholes are vertical is essentially used.

It should be noted that the research methodology of mineral resources and the adoption of the appropriate recommendations on the basis of cores drilling data are studied in details in O. N. Lytvyn, N. I. Shtepa, O. O. Lytvyn's monograph [7] (see bibliography to it). But the cases of the data use of mathematical modeling from the inclined boreholes cores were not studied in the monograph and relevant sources. In this work we believe that the information on the distribution of mineral resources is set on a system of both vertical and inclined special geometric shape boreholes.

The boreholes, for which the project presumes a certain deviation of the axis from the vertical to a certain curve, are called inclined. The inclined drilling is widely used in the drilling of boreholes for the exploration of oil, gas and solid minerals [6].

The authors believe that the only spatial mathematical model of minerals distribution in the crust of the planet, can serve as a basis for the establishment of an optimal method of mineral exploration.

Thus, the actual problem is constructing the spatial mathematical models of minerals distribution for the case when the information about minerals distribution function $f(x, y, z)$ is specified in the M inclined boreholes (vertical boreholes are also acceptable). To build the mathematical model for this case, we give first a mathematical definition of an inclined borehole.

The definition. We consider the inclined borehole as a set of points of this kind $\Gamma_k = \{(x, y, z): x = X_k(z), y = Y_k(z), -H \leq z \leq 0\}, k = \overline{1, M}$, where the functions $X_k(z), Y_k(z)$ satisfy the conditions $r'_k(z) < 0$ where $r_k = \sqrt{(X_k(z) - X_k(0))^2 + (Y_k(z) - Y_k(0))^2}$.

Thus, in this borehole definition we consciously believe, that the diameter of the one is equal to zero, i.e. is a certain line in aggregate. We note, moreover, that in this work the case of horizontal boreholes, in which at a fixed value $z = -H_1$, the system of points in the hole lies in the horizontal plane is excluded.

1. Interlineation on a system of inclined boreholes placed in the same plane.

Suppose that the system of boreholes is placed in such a way that each of them may be inclined only in the plane $y = Y_l = \text{const}, l = \overline{1, n}, x = X_k(z), k = \overline{1, m}$.

Let $s_{1k}(x, z), k = \overline{1, m}, s_{2l}(y), l = \overline{1, n}$ be the basic functions, which are defined by the formulae

$$s_{1k}(x, z) = \prod_{\substack{j=1 \\ j \neq k}}^m \frac{x - X_j}{X_k - X_j};$$

$$s_{2l}(y) = \prod_{\substack{i=1 \\ i \neq l}}^n \frac{y - Y_i}{Y_l - Y_i}.$$

Lemma 1. Basic functions $s_{1k}(x, z), s_{2l}(y), k = \overline{1, m}, l = \overline{1, n}$ have such a property

$$s_{1k}(X_p(z), z) = \delta_{k,p}, k, p = \overline{1, m}; s_{2l}(Y_q) = \delta_{l,q}, l, q = \overline{1, n}; G = [X_1(z), X_m(z)] \times [Y_1, Y_n] \quad (1)$$

Theorem 1. Operator $O_{mn}f(x, y, z) = \sum_{k=1}^m \sum_{l=1}^n s_{1k}(x, z) s_{2l}(y) f_{k,l}(z)$

is the operator of interlineation function $f(x, y, z)$ on a system of inclined boreholes

$\Gamma_k = \{(x, y, z): x = X_k(z), y = Y_l = \text{const}, -H \leq z \leq 0\}, k = \overline{1, m}; l = \overline{1, n}$, which has properties:

1. $O_{mn}f(X_p(z), Y_q, z) = f(X_p(z), Y_q, z) = f_{p,q}(z), p = \overline{1, M}; q = \overline{1, N}$.

2. For each fixed z operator $O_{mn}f(x, y, z)$ is an operator of the polynomial interpolation of functions on variables x and y .

Theorem 2. Let $f(x, y, z) \in C^{\mu, \nu, 0}(D)$, where $D \subset R^3$ is the area which all the boreholes belong to. Then the remainder of the interlineation $R_{mn}f(x, y, z) = f(x, y, z) - O_{mn}f(x, y, z)$ can be represented as

$$\begin{aligned}
 R_n f(x, y, z) = & \sum_{k=1}^n s_{1,k}(x, z) \int_{X_k(z)}^x \frac{\partial^\mu}{\partial \xi^\mu} f(\xi, y, z) \frac{(X_k(z) - \xi)^{\mu-1}}{(\mu-1)!} d\xi + \sum_{l=1}^n s_{2,l}(y) \int_{Y_l}^y \frac{\partial^\nu}{\partial \eta^\nu} f(x, \eta, z) \frac{(Y_l - \eta)^{\nu-1}}{(\nu-1)!} d\eta - \\
 & - \sum_{k=1}^n \sum_{l=1}^m s_{1,k}(x, z) s_{2,l}(y) \int_{X_k(z)}^x \int_{Y_l}^y f^{(\mu, \nu, 0)}(\xi, \eta, z) \frac{(X_k(z) - \xi)^{\mu-1}}{(\mu-1)!} \frac{(Y_l - \eta)^{\nu-1}}{(\nu-1)!} d\xi d\eta, \\
 & 1 \leq \mu \leq m, 1 \leq \nu \leq n.
 \end{aligned}$$

2. Mathematical minerals distribution model with the help of data from inclined boreholes cores placed in an arbitrary way.

We believe that for an arbitrary function $f(x, y, z) \in C(R^3)$ (generally speaking unknown), which is the distribution of minerals in the planet crust, its traces are known $f(X_k(z), Y_k(z), z) = \gamma_k(z)$, $k = \overline{1, M}$ in the points M of the inclined boreholes Γ_k , $k = \overline{1, M}$.

We input the signs $X(z)_k = X_k(z)$; $Y(z)_k = Y_k(z)$, $k = \overline{1, M}$

$$O_{M, \lambda} f(x, y, z; X(z), Y(z)) = \sum_{k=1}^M \gamma_k(z) \ell_{M, k, \lambda}(x, y; X(z), Y(z)), \lambda \geq 1, M = 2, 3, \dots,$$

$$\begin{aligned}
 \ell_{M, k, \lambda}(x, y, z; X(z), Y(z)) &= \prod_{i=1, i \neq k}^M \frac{d_i(x, y, z; X(z), Y(z))^\lambda}{d_{i, k}^\lambda} = \\
 &= \prod_{i=1, i \neq k}^M \left(\frac{d_i(x, y, z; X(z), Y(z))}{d_{i, k}} \right)^\lambda,
 \end{aligned}$$

$$d_i(x, y, z; X(z), Y(z)) = \sqrt{(X_i(z) - x)^2 + (Y_i(z) - y)^2}; d_{i, k} = \sqrt{(X_i(z) - X_k(z))^2 + (Y_i(z) - Y_k(z))^2}$$

which are interpolating operators on an irregular grid of nodes, proposed by O. N. Lytvyn [8]

in 1990, for the case $\gamma_k(z) = \gamma_k = \text{const}, k = \overline{1, M}$.

Theorem 3. If in the formula we put

$$\ell_{M, k, \lambda}(x, y; X(z), Y(z)) = \frac{\prod_{i=1, i \neq k}^M [(x - X_i(z))(X_k(z) - X_i(z)) + (y - Y_i(z))(Y_k(z) - Y_i(z))]^\lambda}{\prod_{i=1, i \neq k}^M [(X_k(z) - X_i(z))^2 + (Y_k(z) - Y_i(z))^2]^\lambda}$$

then the operator $O_{M, \lambda} f(x, y, z; X(z), Y(z))$ has the properties:

1. For $\frac{\lambda}{2} \in \mathbb{N}$ auxiliary functions $\ell_{M, k, \lambda}(x, y; X(z), Y(z))$ are polynomials of two variables x, y degree $(M-1)\lambda$, $\forall z \in [-H; 0]$.

2. $O_{M, \lambda} f(X_p(z), Y_p(z), z; X(z), Y(z)) = \gamma_p(z)$, $p = \overline{1, M}$.

We use at constructing operators $O_{M, \lambda} f(x, y, z; X(z), Y(z))$ such support functions, which are the generalization of D. Shepard:

$$h_{p, \lambda}(x, y) = \frac{\ell_{M, p, \lambda}(x, y, X(z), Y(z))}{\sum_{q=1}^M \ell_{M, p, \lambda}(x, y, X(z), Y(z))}.$$

Theorem 4. Such ratios are just:

if $\gamma_k(z) \in C[-H, 0]$, $k = \overline{1, M}$, then

$$O_{M,\lambda} f(x, y, z; X(z), Y(z)) \in C(R^3);$$

$$O_{M,\lambda}(X_p(z), Y_p(z), z; X(z), Y(z)) = \gamma_p(z), p = \overline{1, M}, \forall z \in [-H, 0].$$

3. Mathematical minerals distribution model between the system of irregularly placed inclined boreholes by the spline-interlineation functions methods.

We outline the steps of the algorithm for constructing spline-interlineation operators.

Step 1. We perform surface triangulation: introduce the notation $\mu = (\mu_1, \mu_2, \mu_3)$, $T_\mu = T_\mu(z)$ - the triangle at the depth z with the vertices $P_k(X_k(z), Y_k(z), z), k = \mu_1, \mu_2, \mu_3; \mu_1, \mu_2, \mu_3 \in \{1, 2, \dots, M\}$, that is $\overline{T_\mu(z)} = \{(x, y, z): (x, y, z) \in T_\mu(z)\}$ is a curvilinear prism.

Step 2. We build operator interlineations $O_\mu(x, y, z)$ for each triangle $T_\mu(z)$ in the form of

$$O_\mu(x, y, z) = f_{\mu_1}(z) \left(\frac{\varphi_{\mu_2, \mu_3}(x, y, z)}{\Delta_{\mu_1, \mu_2, \mu_3}(z)} \right) + f_{\mu_2}(z) \left(\frac{\varphi_{\mu_1, \mu_3}(x, y, z)}{\Delta_{\mu_1, \mu_2, \mu_3}(z)} \right) + f_{\mu_3}(z) \left(\frac{\varphi_{\mu_1, \mu_2}(x, y, z)}{\Delta_{\mu_1, \mu_2, \mu_3}(z)} \right),$$

$$\varphi_{p,q}(x, y, z) = \begin{vmatrix} x & y & 1 \\ X_p(z) & Y_p(z) & 1 \\ X_q(z) & Y_q(z) & 1 \end{vmatrix}.$$

$$\Delta_{\mu_1, \mu_2, \mu_3}(z) = \begin{vmatrix} X_{\mu_1}(z) & Y_{\mu_1}(z) & 1 \\ X_{\mu_2}(z) & Y_{\mu_2}(z) & 1 \\ X_{\mu_3}(z) & Y_{\mu_3}(z) & 1 \end{vmatrix} = \varphi_{\mu_2, \mu_3}(X_{\mu_1}(z), Y_{\mu_1}(z), z).$$

We introduce the operator to the examination

$$O_M F(x, y, z) = O_\mu f(x, y, z), (x, y, z) \in T_\mu(z) \times [-H, 0], T_\mu(z) \subset D = \bigcup_{\mu} T_\mu(z).$$

Let Q be the number of curved triangular prisms corresponding the triangulation.

Theorem 5. The operator $O_M(x, y, z)$ has the following properties:

a) it is the operator of three variables $f(x, y, z)$ functions interlineation on the system inclined boreholes $\Gamma_k, k = \overline{1, M}$, that is

$$O_M f(X_p(z), Y_p(z), z) = f(X_p(z), Y_p(z), z) = f_p(z), -H \leq z \leq 0, p = \overline{1, M};$$

b) to each continuous function $f(x, y, z) \in C(D)$ this operator puts also into compliance a continuous function $O_M f(x, y, z) \in C(D)$:

$$f(x, y, z) \in C\left(\bigcup_{\mu} T_\mu \times [-H, 0]\right), T_\mu(z) \subset D \Rightarrow O_M f(x, y, z) \in C\left(\bigcup_{\mu} T_\mu \times [-H, 0]\right).$$

We also introduce and investigate the operators spline-interlineation functions of three variables in the system of inclined boreholes $\Gamma_k(z) = \{(x, y, z): x = X_k(z), y = Y_k(z), -H \leq z \leq 0\}$, which are irregularly placed on the surface $z = 0$, using a piecewise quadratic approximation in the variables x, y in each of the triangular prisms.

We enter M auxiliary functions $h_k(t) \in C[0, 1], k = \overline{1, M}$, with the properties $h_k(0) = 0, h_k(1) = 1, k = \overline{1, M}$ and operators

$$\begin{aligned} \tilde{O}_M f(x, y, z) = O_\mu f(x, y, z) = f_{\mu_1}(z) h_{\mu_1} \left(\frac{\varphi_{\mu_2, \mu_3}(x, y, z)}{\Delta_{\mu_1, \mu_2, \mu_3}(z)} \right) + f_{\mu_2}(z) h_{\mu_2} \left(\frac{\varphi_{\mu_1, \mu_3}(x, y, z)}{\Delta_{\mu_1, \mu_2, \mu_3}(z)} \right) + \\ + f_{\mu_3}(z) h_{\mu_3} \left(\frac{\varphi_{\mu_1, \mu_2}(x, y, z)}{\Delta_{\mu_1, \mu_2, \mu_3}(z)} \right), \end{aligned}$$

$$(x, y, z) \in T_\mu \subset D, z \in [-H, 0].$$

We describe a method for constructing operators of three variables functions interlineation, which generalizes a well-known Zlamal method - functions of two variables approximation by the piecewise-polynomial (in particular, the piecewise-quadratic) functions on partitioning triangles.

Let $p(x, y, z)$ be an arbitrary polynomial of the second degree of two variables x, y with coefficients that depend on a third variable z : $p(x, y, z) = \alpha_1(z) + \alpha_2(z)x + \alpha_3(z)y + \alpha_4(z)x^2 + \alpha_5(z)xy + \alpha_6(z)y^2$ and $\Gamma_k(z) = \{(x, y, z) : x = X_k(z), y = Y_k(z), -H \leq z \leq 0\}$ - are the boreholes, which are the edges of triangular prisms $T(z)$, and $Q_i(z), 1 \leq i \leq 3$ - are the boreholes, which are going for $z \in [-H; 0]$ through the middle of the curved triangular prism faces parallel to the edges of the prism (Fig. 1).

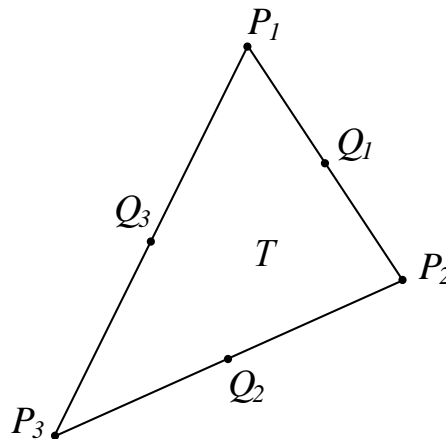


Fig 1. The view from the top of curved trihedral prisms $T(z)$ with fixed z with the boreholes on the edges and in the middle of the faces.

Generalization of the corresponding Zlamal approval in the case of functions approximation of three variables have the following theorem.

Theorem 6. Let an arbitrary breakdown of the region $D \times [-H, 0], D \subset R^2$ be set on the triangular area - prisms with curved, generally speaking, ribs

$$\bigcup_{i=1}^N T_i \times [-H, 0] = D \times [-H, 0].$$

Denote $h = \max_k \max_{-H \leq z \leq 0} \{h_k(z)\}$, $k = 1, 2, 3$; by the greatest length of the sides of the triangles $T_i(z) \subset D \times [-H, 0]$ and θ_0 is the smallest of the corners of the triangles T_i . Then, if $f \in C^3(D \times [-H, 0])$ and $s(x, y, z)$ is a unified piecewise polynomial function (variables x, y), then

$$\exists K > 0 : \|f - s\|_{W_2^1(D)} \leq K \frac{h^2}{\sin \theta_0} \left\{ \sup \left\{ \|D^\alpha f\|_{L_\infty(D)} : |\alpha| = 3 \right\} \right\} \forall z \in [-H, 0],$$

for a random triangulation angle, which satisfies the condition $\theta \geq \theta_0 > 0$, where the constant K does not depend on $f(x, y, z)$ and the geometry of the region D .

Here

$$\|f - s\|_{W_2^1(D)}^2 = \iint_D (f(x, y, z) - s(x, y, z))^2 dx dy + \iint_D \left[\left(\frac{\partial}{\partial x} (f(x, y, z) - s(x, y, z)) \right)^2 + \left(\frac{\partial}{\partial y} (f(x, y, z) - s(x, y, z)) \right)^2 \right] dx dy.$$

Note that in addition, that this method also allows the generalization for the case, when two and more inclined boreholes are placed between the ribs of a triangular prism. In this case, we obtain a piecewise-polynomial (in the variables x, y) interlineation of the functions of three variables of a more general type.

Similar piecewise-polynomial (variables x, y) of the interlineation formula may be also built for a partition of the set of points on the Earth's surface on the quads, i.e. to break the near-surface layer of the Earth's crust on the tetrahedral prisms. For example, for arbitrary four points $P_k(X_k(z), Y_k(z), z), k = \overline{1, 4}$, which are the vertices of a convex quadrangle $G_{1234} = P_1 P_2 P_3 P_4$, the three variables $f(x, y, z)$ functions interlineation operator on a system of four inclined boreholes $\Gamma_k = \{(x, y, z): x = X_k(z), y = Y_k(z), -H \leq z \leq 0\}, k = \overline{1, 4}$, may be written in the form of

$$\begin{aligned} O_{1234} f(x, y, z) &= \gamma_1(z) \frac{\varphi_{23}(x, y, z) \varphi_{34}(x, y, z)}{\varphi_{23}(X_1(z), Y_1(z), z) \varphi_{34}(X_1(z), Y_1(z), z)} + \\ &+ \gamma_2(z) \frac{\varphi_{14}(x, y, z) \varphi_{34}(x, y, z)}{\varphi_{14}(X_2(z), Y_2(z), z) \varphi_{34}(X_1(z), Y_1(z), z)} + \gamma_3(z) \frac{\varphi_{12}(x, y, z) \varphi_{14}(x, y, z)}{\varphi_{12}(X_3(z), Y_3(z), z) \varphi_{14}(X_3(z), Y_3(z), z)} + \\ &+ \gamma_4(z) \frac{\varphi_{12}(x, y, z) \varphi_{23}(x, y, z)}{\varphi_{12}(X_4(z), Y_4(z), z) \varphi_{23}(X_4(z), Y_4(z), z)}, \\ O_{1234} f(X_k(z), Y_k(z), z) &= \gamma_k(z), k = \overline{1, 4}. \end{aligned}$$

$$(x, y) \in G_{1234}, z \in [-H, 0], \quad \varphi_{p,q}(x, y, z) = \begin{vmatrix} x & y & 1 \\ X_p(z) & Y_p(z) & 1 \\ X_q(z) & Y_q(z) & 1 \end{vmatrix}.$$

4. Mathematical minerals distribution model between the irregularly placed inclined boreholes system by the methods of global functions interlineation.

4.1. The Generalized global Shepard's formula.

Generalized global Shepard's formula for the system of lines

$(X_k(z), Y_\ell(z), z), -H \leq z \leq 0, k = \overline{1, M}, \ell = \overline{1, N}$, may be represented as:

$$\begin{aligned} S_{M,N,\lambda}(f; x, y, z) &= \\ &= \begin{cases} \frac{\sum_{k=1}^M \sum_{\ell=1}^N f(X_k(z), Y_\ell(z), z) \left(\sqrt{(x - X_i(z))^2 + (y - Y_j(z))^2} \right)^{-\lambda}}{\sum_{i=1}^M \sum_{j=1}^N \left(\sqrt{(x - X_i(z))^2 + (y - Y_j(z))^2} \right)^{-\lambda}}, & (x - X_i(z))^2 + (y - Y_j(z))^2 \neq 0 \quad \forall \begin{matrix} i = \overline{1, M}, \\ j = \overline{1, N}, \end{matrix} \\ f(X_i(z), Y_j(z), z), & \text{if } (x - X_i(z))^2 + (y - Y_j(z))^2 = 0, i \in \{1, \dots, M\}, j \in \{1, \dots, N\}. \end{cases} \end{aligned}$$

Theorem 7. The operator $S_{M,N,\lambda}(f; x, y, z)$ has the properties:

- a) $f(x, y, z) \in C(R^3) \Rightarrow S_{M,N,\lambda}(f; x, y, z) \in C(R^3)$,
 б) $S_{M,N,\lambda}(f; X_i(z), Y_j(z), z) = f(X_i(z), Y_j(z), z), i = \overline{1, M}, j = \overline{1, N}$.

Differentiation $S_{M,N,\lambda}(f; x, y, z)$ by x or y on may convince that, in order to $S_{M,N,\lambda}(f; x, y, z) \in C^1(R^3)$, if $f(x, y, z) \in C^1(R^3)$ it is necessary that the measure of λ degree satisfy the ratio $\lambda > 1$. In addition, if $\lambda = 2$, then

$$\text{grad} S_{M,N,\lambda}(f; x, y, z) = 0, \forall (x, y, z) \in \{X_k(z), Y_l(z), z, k = \overline{1, M}, l = \overline{1, N}\},$$

since in this case the function

$$\ell_{k,l,2}(x, y, z) = \prod_{i=1, i \neq k}^M \prod_{j=1, j \neq l}^N (d_{i,j}(x, y, z))^2 = \prod_{i=1, i \neq k}^M \prod_{j=1, j \neq l}^N ((x - X_i(z))^2 + (y - Y_j(z))^2)$$

has a gradient, which is equal to zero at all points of the $(X_p(z), Y_q(z), z), p \neq k, q \neq l$.

Let us introduce to the examination the mathematical model of the spatial distribution of any of minerals in the form of:

$$S_{M,\lambda}(\{\gamma_p\}, x, y, z) = \frac{\sum_{k=1}^M \gamma_k(z) L_{k,\lambda}(x, y, z)}{\sum_{k=1}^M L_{k,\lambda}(x, y, z)}, L_{k,\lambda}(x, y, z) = \prod_{j=1, j \neq k}^M (d_j(x, y, z))^\lambda.$$

Theorem 8. The following ratios are just.

If $\gamma_k(z) \in C[-H, 0), k = \overline{1, M}$, then

$$S_{M,\lambda}(\{\gamma_p\}, x, y, z) \in C(R^3); S_{M,\lambda}(\{\gamma_p\}, X_k(z), Y_k(z), z) = \gamma_k(z), k = \overline{1, M}, \forall z \in [-H, 0).$$

4.2. Mathematical minerals distribution model by the global interpolation Lytvyn's formula generalization method.

We consider for arbitrary $f \in C(R^3)$, $f(X_k(z), Y_k(z), z) = \gamma_k(z), k = \overline{1, M}$, interlineation operators

$$O_{M,\lambda}(f; x, y, z) = \sum_{k=1}^M \gamma_k(z) \ell_{M,k,\lambda}(x, y, z), \lambda \geq 1, M = 2, 3, \dots,$$

$$\ell_{M,k,\lambda}(x, y, z) = \prod_{i=1, i \neq k}^M \frac{d_i(x, y, z)^\lambda}{d_{i,k}^\lambda} = \frac{\prod_{i=1, i \neq k}^M d_i(x, y, z)^\lambda}{\prod_{i=1, i \neq k}^M d_{i,k}^\lambda},$$

$$d_i(x, y, z) = \sqrt{(X_i(z) - x)^2 + (Y_i(z) - y)^2}; d_{i,k} = \sqrt{(X_i(z) - X_k(z))^2 + (Y_i(z) - Y_k(z))^2},$$

which for the case $\gamma_k(z) = \gamma_k = \text{const}, k = \overline{1, M}$ are interpolating operators on an irregular grid of nodes, proposed by O. N. Lytvyn in 1990. [9]

Theorem 9. For each $f(x, y, z) \in C(R^3)$ the ratios are

$$O_{M,\lambda}(f; x, y, z) \in C(R^3) \quad O_{M,\lambda}(f; X_p(z), Y_p(z), z) = \gamma_p(z), p = \overline{1, M}.$$

Taking into account that the denominators in the formula for $\ell_{M,k,\lambda}(x, y, z)$ are permanent numbers, we may come to the conclusion that $\ell_{M,k,\lambda}(x, y, z)$ is a polynomial of degree $(M-1)2r$ with the variables x, y , if $\lambda = 2r, r = 1, 2, \dots$

Note that the basis functions $\ell_{M,k,\lambda}(x, y, z)$ are also functions of the coordinates of points $D_k(X_k(z), Y_k(z), z), k = \overline{1, M} : \ell_{M,k,\lambda}(x, y, z) = \ell_{M,k,\lambda}(x, y, z; X(z), Y(z), z)$ and depend, of course, from the placement of these coordinates $D_k(X_k(z), Y_k(z), z), k = \overline{1, M}$.

Examples show that the behavior $O_{M,\lambda}(f; x, y, z)$, which helper functions of the form

$$\ell_{M,k,\lambda}(x, y, z) = \frac{\prod_{i=1, i \neq k}^M d_i(x, y, z)^\lambda}{\prod_{i=1, i \neq k}^M d_{i,k}^\lambda} \quad \text{use, can cause large fluctuations between points}$$

$D_k(X_k(z), Y_k(z), z), k = \overline{1, M}$ and, in addition, $\ell_{M,k,\lambda}(x, y, z) \rightarrow \infty$ because the numerator in them is an unlimited amount at $x^2 + y^2 \rightarrow \infty$. This statement is a consequence of the fact that the operators are obvious generalizations of Lagrange's polynomial interpolation operators of two variables in the case of irregularly placed nodes. On the Weierstrass's theorems, on a closed interval $[a, b]$ every continuous function can be closer with a given accuracy $\varepsilon > 0$ of the algebraic polynomial of some degree $n = n(\varepsilon)$. Nevertheless Lagrange's interpolation operators, as it is known, do not match to each of continuous functions in arbitrary points of interpolation. For example, it is proved that Lagrange's interpolating polynomial with uniformly distributed interpolation nodes on the interval $[-1, 1]$ for the function $f(x) = |x|$ does not coincide with this function. Therefore, below we will consider some other formulas for $\ell_{M,k,\lambda}(x, y, z)$.

Theorem 10. If in the formula $O_{M,\lambda}(f; x, y, z)$ we replace $\ell_{M,k,\lambda}(x, y, z)$ with $L_{M,k,\lambda}(x, y, z)$ with a rational support functions,

$$L_{M,k,\lambda}(x, y, z) = \frac{\ell_{M,k,\lambda}(x, y, z)}{\sum_{q=1}^M \prod_{p=1, p \neq q}^M \ell_{M,p,\lambda}(x, y, z)},$$

and if $\frac{\lambda}{2} \in N$, then $O_{M,\lambda}(f; x, y, z)$ is a positive interlineation operator $O_{M,\lambda}(f; X_p(z), Y_p(z), z) = \gamma_k(z), k = \overline{1, M}$.

Theorem 11. If in the formula $O_{M,\lambda}(f; x, y, z)$ we put

$$\ell_{M,k,\lambda}(x, y, z) = \prod_{i=1, i \neq k}^M \frac{(x - X_i(z))(X_k(z) - X_i(z)) + (y - Y_i(z))(Y_k(z) - Y_i(z))}{(X_k(z) - X_i(z))^2 + (Y_k(z) - Y_i(z))^2}, \quad (2)$$

the operator $O_{M,\lambda}(f; x, y, z)$ is an interlineation operator, if $\lambda > 0, \lambda = 2q, q \in N$, $O_{M,\lambda}(f; X_k(z), Y_k(z), z) = \gamma_k(z), k = \overline{1, M}$.

Conclusions

In this work authors show a brief overview of new minerals distribution mathematical models 3D construction methods by three variables interlineation functions on an inclined boreholes system methods. An assumption of functions $\gamma_k, k = \overline{1, M}$ system presence is used. In the work:

1. For the first time spatial mathematical models of minerals distribution between boreholes, regularly placed on the Earth's surface by spline - interlineation methods, polynomial interlineation functions $f(x, y, z)$, and also generalizations of D. Shepard and O. N. Lytvyn's global interlineation formulae are constructed and investigated.

2. Constructing method for MM mineral resources spatial distribution among inclined boreholes proposed in this paper, allows, after an appropriate generalization, to build MM structure of the Earth's crust with the use of all the inclined boreholes cores, which will lead to creating effective methods of mineral exploration and offshore fields development.

Therefore, one can note the following important and useful moments of mathematical modeling with the help of three variables interlineation functions with the use of information about the distribution in all points of inclined boreholes of the studied field. Firstly, the information used for this type of mathematical modeling is much more accessible and simple in comparison with the information obtained by the methods of seismic tomography. And at the same time, it allows to represent the mineral resources distribution in the field in the form of three variables function. This opens up opportunities for research and development of principally new mineral exploration methods. The authors of this article see at least two ways of the described mathematical models further use.

The first way involves the description of all the periodic table elements in each point of boreholes drilling. Thus, using three-dimensional mathematical models one can receive distribution of all the periodic table elements at any point among the inclined drilling boreholes. Then, taking into account all the available for today necessary and sufficient conditions (premises) of one or another mineral occurrence, we can make a conclusion about the probability of its occurrence in the relevant part of the studied field.

The second way foresees a considerable simplification of the first one. It consists of the following: only some of the periodic table elements and their compounds will be used for prospecting.

References

1. V. Kh. Isachenko. Inklinometriya skvazhin. / V. Kh. Isachenko // M.: Nedra, 1987. - 216 s.
2. O. M. Lytvyn. Matematychnye modelyuvannya rozpodilu korysnykh kopalyn za dopomogoyu interlinatsii funktsii tryokh zminnykh/ O. M. Lytvyn, N. I. Shtepa// Dop. NAN Ukrainy. № 1. 2009. – s. 25-29.
3. O. M. Lytvyn.. Metod otsinky zapasiv korysnykh kopalyn na osnovi analizu rezultativ sverdlovynnogo burinnya i uzagalnenoyi interlinatsii funktsii 3-kh zminnykh/ O. M. Lytvyn, N. I. Shtepa// Zbirnyk tez dopovidei XLII naukovo-praktychnoi konferentsii UIPA. 10-15 grudnya 2008 r. Chastuna 1. Kharkiv. 2008– s. 84.
4. O. M. Lytvyn. Pro matematychnye modelyuvannya struktury kory Zemli z vykorystanniam interlinatsii funktsii tryokh zminnykh / O. M. Lytvyn, N. I. Shtepa// Pratsi IV mizhnarodnoi shkoly-seminaru “Teoriya pryinyattya rishen”. Uzhgorod:YzhNU. 29 veresnya – 4 zhovtnya. 2008.– s.105.
5. O. M. Lytvyn. Matematychnye modelyuvannya rozpodilu korysnykh kopalyn za dopomogoyu interlinatsii funktsii tryokh zminnykh/ O. M. Lytvyn, N. I. Shtepa// Pratsi mizhnarodnogo sympoziumu Pytannya optymizatsii obchyslen (POO- XXXV): Krym, stm. Katsyveli, 24-29 veresnya 2009. T.2; Kyiv. 2009. – s. 20-24.
6. A. G. Kalinin. Bureniye naklonnykh skvazhin: Spravochnik/ N. A. Grigoryan, B. Z. Sultanov. // Pod.red. A. G. Kalinin/ - M.:Nedra. 1990. – 348s.
7. O. M. Lytvyn. Matematychnye modelyuvannya rozpodilu korysnykh kopalyn metodamy interlinatsii ta interfletatsii funktsii. / O. O. Lytvyn, N. I. Shtepa – Kyiv.:Naukova dumka. 2011. – 228s.
8. O. N. Litvin. Interpolirovanie funktsii: Ucheb.posobie. /O. N. Litvin// - Kiev: UMK VO. 1998. – 31s.
9. O. M. Lytvyn. Interlinatsiya funktsii ta deyaki yii zastosuvannya. – Kharkiv: Osnova. 2002. – 544 s.

METHOD OF THE COMPRESSION OF PHASE PORTRAITS OF GENERALIZED SPECTRAL DATA FOR SOLVING THEIR CLUSTERING AND RECOGNITION

Krasnov, A.E., Krasnikov, C.A., Chernov, E.A.
Moscow, MSUTM named K.G. Razumovsky

The method of presentation of generalized spectral data on the plane, based on the method phase portrait statistics is considered. The technique originally intended for the clustering and recognition of optical spectra is also applicable to any positive defined functions.

Keywords: phase portraits, spectral data, clustering, recognition.

Introduction

For the qualitative and quantitative reporting and subsequent analysis of multidimensional data (signals, spectra, a set of different parameters) in practice methods to display them on the plane are applied. Such methods in Russian literature are called «data visualization». In the foreign literature data visualization is understood in the narrow sense of the scientific field of system analysis «Data Meaning».

The main applications of imaging techniques, you can specify the trail-guides: compression of the information contained in the data; analysis of the databases content; pattern recognition; the support for expert systems; cartography; the recovery of data gaps; the of forecasting problems and the building of relationships between individual members of original sample data.

Formally, under the data visualization is usually understood the method of presentation of multidimensional data distribution on a plane, in which qualitatively the main regularities inherent the initial distribution is reflected - its cluster structure, topological features, internal dependencies between features, the information about the location of data in the original space, etc.

From the perspective of system analysis the multidimensional data visualization is to find this kind of mapping from the original space into two-dimensional plane in which some specified quality criteria (some functional of the coordinates of the data points before and after the projection procedure) will be optimized.

Various embodiments of solutions to the problem of projection are used : an orthogonal projection (the principal component analysis) with the property of the minimum sum of squared distances from the plane to the projection of the points of data, but effective only for normally distributed multivariate data; linear discriminant analysis (Fischer) , minimizing the ratio of "scatter " of the data within the classes to the "distance " between classes and effective for a small number of labeled classes; multidimensional scaling (Multiple Scale), which minimizes the distortion measure of the mutual distances between points in the source and output space mapping, but used only in when the initial information originally is presented not as a table type "object-sign", but in the form of a square table deleting objects from each other; the synthesis of curved surfaces (embedded in a multidimensional space) associated with significant topological problems; neural network, in which number of inputs is equal to the space dimension and the number of outputs equal to the dimension of the manifold - modeling; self-organizing cards (SOM – Self-Organizing Maps or SOFM – Self-Organizing Feature Maps), being representatives of neuronets,

connected in itself a clustering and visualization of multidimensional data, but rather difficult in control.

In recent works of authors the effective method of the spectral data compression, based on the modification Fischer's discriminant analysis, appeared extremely labor-consuming in realization was offered [1, 2].

In the real work the approach based on the compression of, so called, phase portraits or phase portraits statisticians is offered [3, 4].

The example of the comparison of an offered method with the method based on the modified discriminant analysis is given.

Basic provisions of the phase portrait method, its properties

Let F is the generalized spectrum (GS) – a set of positively certain data $F^T = (F_1, F_2, \dots, F_N)$, where $F_n \geq 0$ for $\forall n = 1, 2, \dots, N$. We will consider further only such GS which correspond to one-dimensional discrete signals or distributions – positively certain discrete F_n functions, as shown in the figure 1.

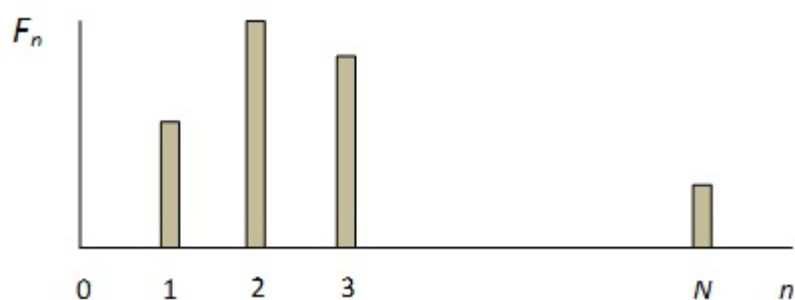


Fig.1. Positively certain discrete F_n function.

In compliance with the theory of the phase portraits (PP) to everyone GS F is put in compliance his Gilbert image G formed in the form of cyclic convolution

$$G_n = \sum_k g_{n-k} F_k, \quad g_n = (-1/5, 0, -1/3, 0, -1, 0, 1, 0, 1/3, 0, 1/5);$$

$$\sum_n G_n F_n = 0. \quad (1)$$

Discrete PP is formed as two-dimensional distribution of $w[F, G]$ – the distribution to the planes of joint F_n and G_k values (see fig. 2)

$$w[F_n, G_k] = \frac{N[F_n, G_k]}{N}, \quad \sum_n \sum_k w[F_n, G_k] = 1, \quad (2)$$

where $N[F_n, G_k]$ – quantity of points on the phase plane (F, G) , having coordinates (F_n, G_k) .

For descriptive reasons, in the figure (2) PP of a wavy signal (256 counting) are given in the absence and in the presence of Gaussian hindrances.

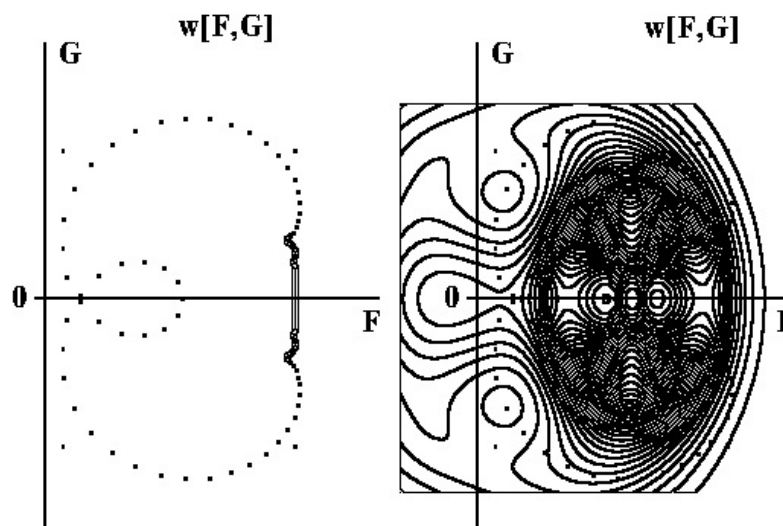


Fig. 2. The example of the PP of the wavy signal F (256 counting) in absence and in the presence of Gaussian hindrances.

PP of images of F_o and F_a of the printing letters (kirriliyets) constructed on the basis of the Fresnel's transformation are given in the figure (3).

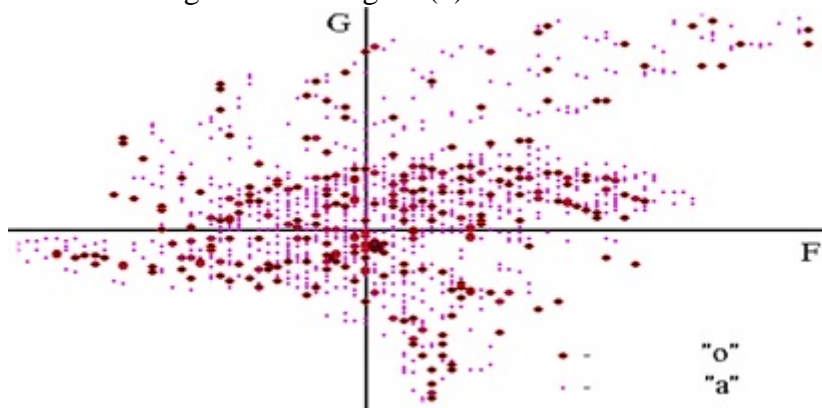


Fig. 3. The example of the PP of images F_o and F_a of the printing letters "o" and "a".

The PP remarkable properties is: their invariancy to shifts, turns (for images) and to changes of scales of signals and images; PP of relatives on correlation measures of similarity of signals and images considerably differ [4].

GS single-point display to the plane by the reduction of their PP

For the PP $w[F,G]$ display on the plane in the form of a point we will enter two functional transformations

$$\begin{aligned} X &= \sum_n \sum_k \Psi_X[F_n, G_k] w[F_n, G_k] = \frac{1}{N} \sum_n \sum_k \Psi_X[F_n, G_k] N[F_n, G_k], \\ Y &= \sum_n \sum_k \Psi_Y[F_n, G_k] w[F_n, G_k] = \frac{1}{N} \sum_n \sum_k \Psi_Y[F_n, G_k] N[F_n, G_k], \end{aligned} \quad (3)$$

where $\Psi_X[F_n, G_k]$ and $\Psi_Y[F_n, G_k]$ – two-dimensional discrete functions.

According to (1-3) the variation δ of any two-dimensional coordinate is expressed as function of a variation of GS

$$\begin{aligned}\delta X &= \frac{1}{N} \sum_n \sum_k \Psi_X[F_n, G_k] \delta N[F_n, G_k] \cong \frac{1}{N} \sum_n \sum_k \Psi_X[F_n, G_k] \frac{\Delta N}{\Delta F_n} \delta F_n, \\ \delta Y &= \frac{1}{N} \sum_n \sum_k \Psi_Y[F_n, G_k] \delta N[F_n, G_k] \cong \frac{1}{N} \sum_n \sum_k \Psi_Y[F_n, G_k] \frac{\Delta N}{\Delta F_n} \delta F_n,\end{aligned}\quad (4)$$

where $\Delta N/\Delta F$ – a discrete (differential) derivative.

For the maximizing at least one variation δX from (4) $\Psi_X[F_n, G_k]$ and $\Psi_Y[F_n, G_k]$ are entered in a look

$$\begin{aligned}\Psi_X[F_n, G_k] &= F_n \frac{\Delta N}{\Delta F_n} \delta F_n, \\ \Psi_Y[F_n, G_k] &= G_k \frac{\Delta N}{\Delta F_k} \delta F_k.\end{aligned}\quad (5)$$

Then transformation (3) will assume an air of the project of GS F and his Gilbert image G on the linear subspaces, defined by vectors x and y

$$\begin{aligned}X &= \sum_n x_n F_n, \quad x_n = \frac{\Delta N}{\Delta F_n} \delta F_n \left(\frac{1}{N} \sum_m N[F_n, G_m] \right); \\ Y &= \sum_k y_k G_k^+, \quad y_k = x_k.\end{aligned}\quad (6)$$

It is possible to simplify transformation (6), having used (1)

$$\begin{aligned}X &= \sum_n x_n F_n, \quad x_n = \frac{\Delta N}{\Delta F_n} \delta F_n \left(\frac{1}{N} \sum_m N[F_n, G_m] \right); \\ Y &= \sum_n y_n F_n, \quad y_n = \sum_k g_{n-k} x_k, \quad \sum_n y_n x_n = 0.\end{aligned}\quad (7)$$

Transformation (7) has simple algorithm – GS F is projected on two orthogonal linear subspaces, formed by a vector x and his Gilbert image by y .

The main complexity of a problem of the project in this case is transferred to a choice of a vector x which plays a role of a peculiar filter of basic spectral data of F_n

$$x_n = \alpha_n \delta F_n, \quad \alpha_n = \frac{\Delta N}{\Delta F_n} \left(\frac{1}{N} \sum_m N[F_n, G_m] \right), \quad (8)$$

and which coefficients x_n are proportional to a variation δF_n of counting of basic data.

Generally difficult to solve problem of a choice of such coefficients. However it is possible to enter restrictions:

- for a case of not marked data

$$x_n = \begin{cases} 1, & \text{if } \delta F_n \geq \delta F_{\text{thresh}}, \\ 0, & \text{in other cases;} \end{cases}$$

- for a case of the marked data a set of x_n gets out on the basis of a method of the linear Fischer's discriminant.

Threshold value δF_{thresh} for a rejection filtration is selected experimentally.

Visualization of generalized ranges

The visualization of GS of such hydrocarbonic connections, as gasolines was carried out. GS represented IR-Fourier ranges of average range (wave numbers of $450,30\text{ cm}^{-1}$ – $3999,64\text{ cm}^{-1}$).

Gasolines of different brands which are widely used in the Russian Federation were considered.

The algorithm of visualization of GS on the basis of Fischer's modified multiple discriminant was originally used [1, 2]: the 3-dimensional system of the Cartesian coordinates with z -coordinate coinciding with the center of mass of system was formed, Gilbert - an image of z -coordinate, and its rotation got out, search the plane the projection on which maximizes Fischer's criterion got out.

The result received in a MathCad package is given in the figure 4.

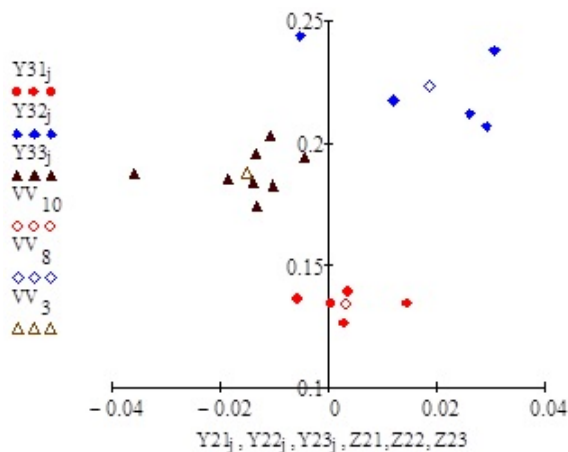


Fig. 4. The visualization of division of 18 gasoline's GS on three groups.

The decision yields acceptable results, but demands big (till several o'clock on the computer with a clock frequency of 2 gigahertz) account time.

For the reduction of time of the account only the pair clustering of GS was considered. The multiple clustering can be carried out by several dichotomies.

For a clustering of two groups Fischer's linear discriminant was used

$$J(w) = \frac{|\tilde{m}_1 - \tilde{m}_2|^2}{\sum_{i=1}^{n1} (\tilde{x}_{i,1} - \tilde{m}_1)(\tilde{x}_{i,1} - \tilde{m}_1)^T + \sum_{i=1}^{n2} (\tilde{x}_{i,2} - \tilde{m}_2)(\tilde{x}_{i,2} - \tilde{m}_2)^T}, \quad (9)$$

where the tilde over variables means their projection to an axis; \tilde{m}_1, \tilde{m}_2 – projections to an axis of the centers of mass of each of groups; $\tilde{x}_{i,1}, \tilde{x}_{i,2}$ – projections to an axis of separate vectors of the first and second groups; $n1, n2$ – quantity of vectors of the first and second groups, respectively.

The numerator of this expression characterizes dispersion between classes. The matrix in a denominator characterizes dispersion in a class.

In the figure 5 the example of the decision executed in a MathCad package is given.

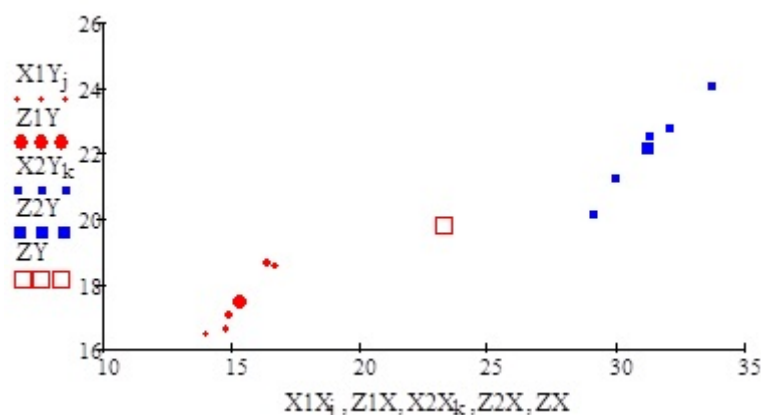


Fig. 5. The visualization of GS of A_80 gasolines (circles) and A_92 (small squares).

The solution of a task takes about an hour on the computer with a clock frequency of 2 gigahertz.

The use of an offered method allows to reduce considerably time for a clustering and identification of brands of gasolines (figure 6). Basic data in 4149 counting were exposed to a reject filtration, and on the remained 2000 counting visualization was carried out.

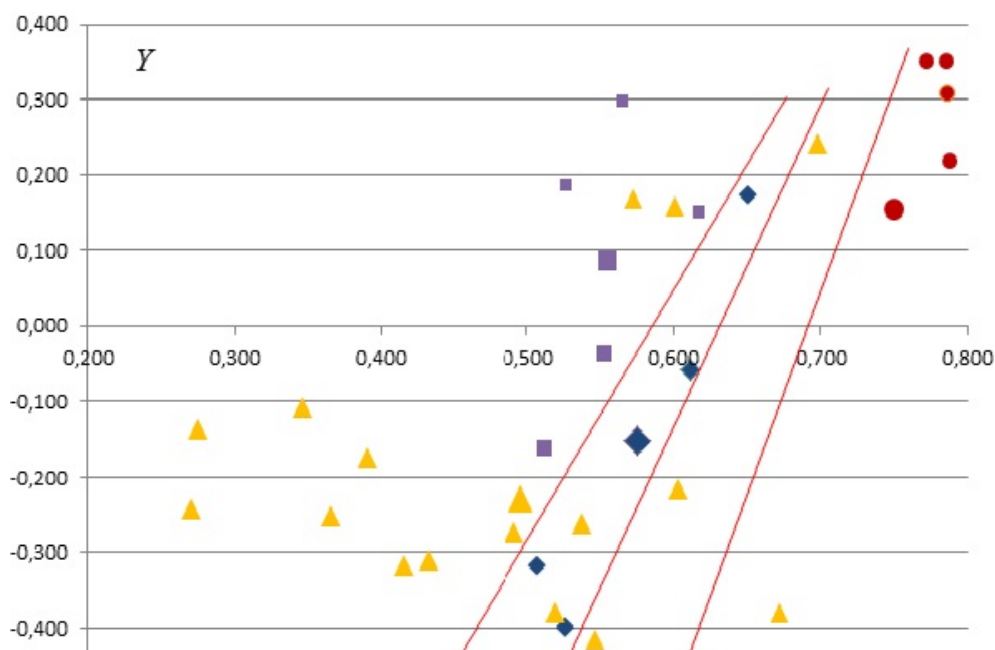


Fig. 6. The visualization of GS of gasolines (initial dimension of 4149 counting),
gasolines: 80_normal'– squares; 92_pegulyar – rhombuses;
95_premium– triangles; 98_super - circles).

The character of a clustering of representatives of gasolines is visually visible. So, for example, images of gasoline 95_premium are scattered on all clusters that speaks about existence of additives.

The gasoline of any unknown brand can be easily identified by means of the given visualization.

The machine time of the solution of a task (a clustering and identification) in an Excel package corresponds to real time of data input.

Conclusions

Received results can be recommended for use in various branches of science and technicians, educations, the industries, sociology and medicine where it is necessary to make visualization of various positively certain multidimensional data.

In too time, when using the multidimensional generalized ranges, along with considered above, the method stated in [5, 6] can be used.

References

1. Krasnov, V. Yan'kov, S. Krasnikov, E. Chernov. Optimal'naya klasterizatsiya mnogomernykh vectorov. Tekhnologii XXI veka v legkoi promyshlennosti (elektronnoe nauchnoe izdanie). № 6. Chast' II. 2012. Stat'ya № 24.
2. V. Yan'kov, E. Chernov. K optimal'noi klasterizatsii mnogomernykh vektorov. Tekhnologii XXI veka v legkoi promyshlennosti (elektronnoe nauchnoe izdanie). № 7. Chast' II. 2013. Stat'ya № 24.
3. Krasnov, I. Kompanets. Novyi sposob analiza obrazov na osnove statisticikh fazovykh portretov. Radiotekhnika, 2000, №1.
4. N. Evtikhiev, O. Evtikhieva, I. Kompanets, A. Krasnov i dr. Informatsionnaya optika. Rekomendovano Minobrazovaviem RF dlya izucheniya distsiplin po napravleniyu «Informatika i vychislitel'naya tekhnika». Pod red. N.N. Evtikhieva. – M.: Izdatel'stvo MEI, 2000. – 612c.
5. Krasnov, S. Krasnikov, S. Nikolaeva, A. Chernov. Agregirovannoe parametricheskoe opisanie sostoyanii slozhnykh sistem na raznykh urovnyakh ierarkhii. – M.: MIEM NIU VSHE, 2013. C. 278 – 285.
6. Krasnov, Yu. Saginov, N. Feoktistova, E. Chernov. Agregirovannoe opisanie sostoyanii slozhnykh sistem na osnove parnykh vzaimodeistvii ikh elementarnykh podsistem. Tekhnologii XXI veka v legkoi promyshlennosti (elektronnoe nauchnoe izdanie). № 7. Chast' II. 2013.

DEVELOPMENT OF HYBRID OBJECT-RELATIONAL DATABASE ON THE BASIS OF THE FRAME AND SLOT NORMAL FORM

Schelokov S.A., Sokolova I.M.
Orenburg State University

In this work the method of development of a hybrid object-relational database on the basis of the description of semantic networks with frames and slots in nodes is considered.

Keywords: conceptual modeling of systems of organizational management, semantic networks, frames, slots, infological and datalogical model of a database.

Modern ways of development and the creations of databases based on the traditional theory of relational databases, are limited for modern scales on the volume and a form of processed information. In relational databases storage and processing of arrays of information as requirements of normalization for the first normal form are violated isn't allowed. The offered method of development and creation of databases is based not on the traditional theory of relational databases [1], but on the theory of conceptual modeling of systems of organizational management [2,3].

The main idea of the method is description of a semantic network whose nodes are frames and slots.

One of novelty aspects of an offered method consists in new representation of datalogical and infological models of a database. In the theory of relational databases the

infological model is represented in the form of the ER chart (the chart essence - communication) or in the form of semantic object model. In the offered way the infological model is represented in the form of logical model of an object and relational database (fig. 1).

subclass (object) of presentation logic in a show-window of data

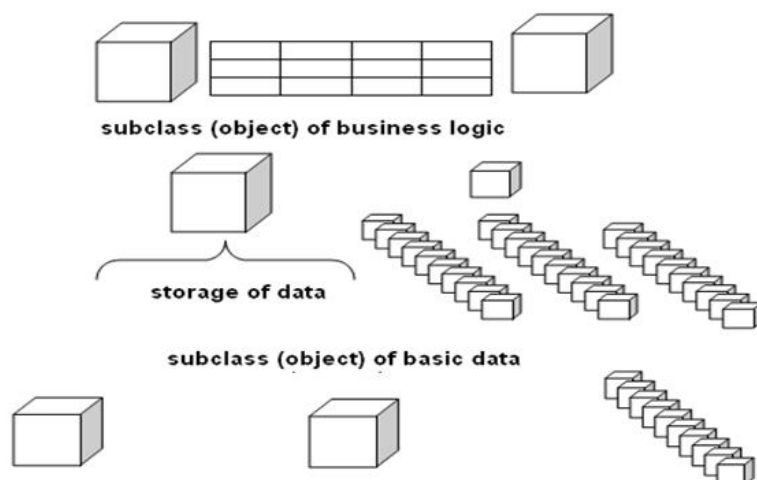
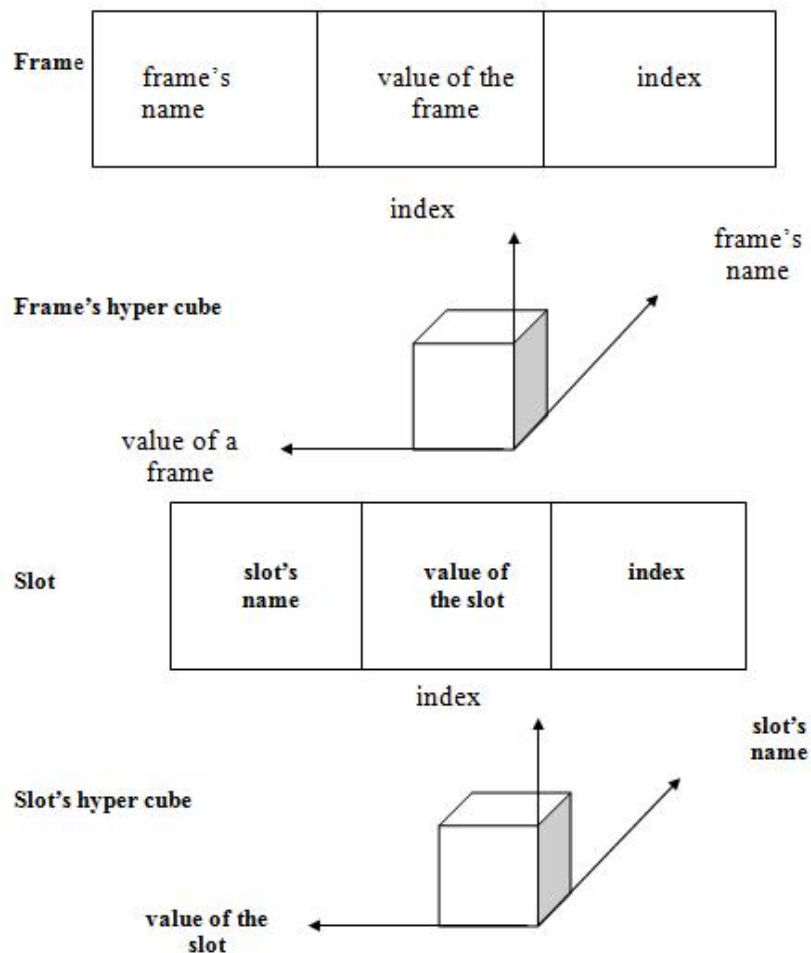


Fig. 1. It is a frame – slot model of a database

Frames and slots are interpreted in hyper cubes. In structure of hyper cubes there are arrays of information (fig. 2).



Array M: {2; $\pm \infty$ }

index	name										
	value										

Fig. 2. Interpretation of hyper cubes to tabular arrays

The basic element of novelty of a method consists in a binding of transactions of records to a vertical axis. The scheme of creation of objects (fig. 3) is made on the basis of object-oriented programming.

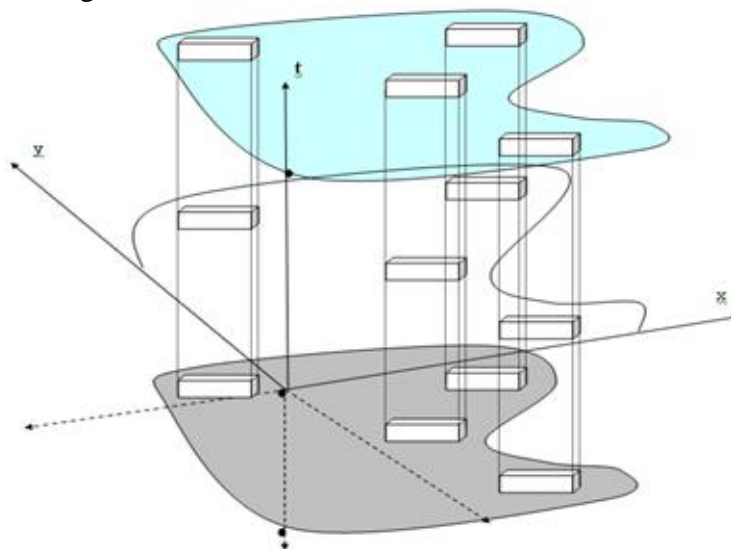


Fig. 3. The scheme of creation of objects in a database

On the initial (zero) level in a class of model of a database the programmer describes slots and frames in the form of arrays of information, describes modules of transactions between slots and frames, describes modules of analytical information processing and modules of presentation logic (the interaction interface with a database).

In the process of database usage the operator chooses from the class of objects slots necessary for recording on the level, fills in registration data and binds the level to the identifier of the index of the slot. The filled level is integrated on the server of the distributed database for analytical processing and presentation.

The considered method can be used when developing OLAP-products which are very actual now in systems of support of decision-making and are very various on structure. Analytical modules appeared as a part of packages of the financial and production software appendices SAP R/3, Oracle Applications and others. At the same time with leaders of the world market similar modules were included by Russian firms "Parus" and "IT" in their software.

The most popular is classification of OLAP-products by a way of data storage. Both initial, and modular data for cubes can be stored as in relational, and multidimensional databases. Therefore three ways of data storage are applied now: MOLAP (Multidimensional OLAP), ROLAP (Relational OLAP) and HOLAP (Hybrid OLAP). Respectively, OLAP-products as a way of data storage are divided by three similar categories.

The hybrid object-relational database on the basis of frames and slots allows to combine advantages and to minimize the shortcomings inherent in the previous classes: they unite analytical flexibility and speed of the response of MOLAP with continuous access to the real data peculiar to ROLAP. In case of use of hybrid architecture (HOLAP) source data remain in relational base, and modular data take place in the multidimensional base. Creation of an OLAP-cube is carried out at the request of OLAP-means on the basis of relational and

multidimensional data. Such approach allows to avoid the explosive growth of data. Thus it is possible to reach optimum time of execution of client requests.

The considered method will allow to develop methodical bases of creation of information systems. Object-oriented formalism, and also advantages of means of object-oriented design and programming allow not only successfully model organizational structures in the form of systems of objects (agents), but also to build dynamically developing structures. The agent system can formally be described as association of a set of types T , the alphabet of events X , sets of identifiers of objects I , classes (object models) C and objects O (the formalism is taken from materials of the European conferences on object-oriented programming of ECCOP):

$$S = (T, X, I, S, O).$$

For example, information system with self-organizing agent structure can be formalized as an concatenation of sets

$$S = (T; A; I, C = \{ \text{Input, OUTput, FUNction} \}; O; \Pi)$$

where T — a set of types of data of object system; A — the alphabet of events of object system; I — set of identifiers of objects; $C = \{ \text{Input, OUTput, FUNction} \}$ — a set of classes of structural elements (agents); $O = \{o_i\}$ — a set of elements of structure; Π — a set of rules of self-organization of this structure.

The direction of development of an offered method is research and practical implementation of links to frames and slots in a program code. For example, types of data in C# divide by the way of storage of elements into value types and reference types.

References

1. Sovetov, B.Ya. Databases: theory and practice: the textbook for bachelors / B.Ya.Sovetov, B.B. Tskhanovsky, V.D.Chertovskoy. – 2 – prod. – M: Publishing house of Yurayt. 2012. – 464 pages.
2. N.A.Solovyev, S.A.Schelokov. The concept of a frame and slot normal form of a database for control systems. Materials of the All-Russian scientific and practical conference – Orenburg, IPK Regional Public Institution Public Educational Institution, 2004.
3. A.A.Strogny, S. S. Azarov, Ya.I.Barsuk. Creation of conceptual model of control systems. USIM, 1988, No. 2.

A MODELING OF THE INFLUENCE OF VIBRATION ACTIONS ON THE RADIATION MIRROR ANTENNA BY USING ANSYS

Shishulin D.N., Yurkov N.K., Yakimov A.N.
Penza, Penza State University

By mathematical modeling methods it investigates the influence of vibration on design parabolic mirror antenna and its radiation pattern. Occurring deformations of antenna are estimated using three-dimensional models in the package ANSYS. A mathematical model is built and it allows to take into account the effect of deformation on the antenna radiation pattern.

Keywords: antenna, vibration, deformations, radiation pattern.

An antenna is the integral part of the radar system, it is serving as an intermediary between the transmitter and receiver. The antennas, that mounted on board of mobile

facilities, are being adversely affected. As a result of these external actions the antennas of the receiving and transmitting devices are deformed, that leads to changes in their phase fronts and radiation patterns. Thereby it is necessary to estimate not only the calculated characteristics of the designed antenna, but also how they are changed as a result of the emerging deformations [1, 2].

The estimation of results of external actions is a complex task, a rigorous analytic solution of which, due to the complexity of the antenna structure, is impossible, in most cases. So at the decision of such problems they often resort to the use of approximate methods, including approximate mathematical description of antenna's waveforms, that obtained experimentally [2].

The perspective direction of the study of such processes in the antennas is the use of computer technology. To investigate the antenna design they can be used, for example, the software packages ANSYS or SOLIDWORKS. They allow to perform calculations stress-strain state of the structure for stationary tasks. Packages ANSYS, SOLIDWORKS, like many others CAE, CAD – products for the mathematical modeling of various physical processes are using the method of finite elements, which combines the versatility of the algorithms for solving boundary value problems with the effectiveness of computer implementation calculations.

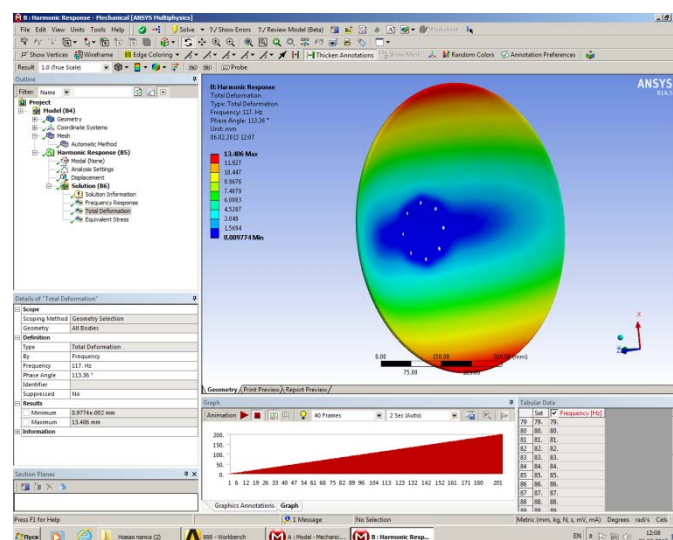


Fig. 1. The study of vibration actions on the parabolic antenna in the package ANSYS

Suppose that the object of study in the package ANSYS (Fig. 1) is a mirror of parabolic antenna with the diameter 0.71 m, 3 mm thick, fixed vertically with non-deformable disc "holder" in the center of the mirror at 8 points. The vibration with an amplitude of 3.1 mm and a resonant frequency of 48 Hz acts on the mirror. In this position of the mirror, under vibration load fluctuations, the main form of vibrations are asymmetric ones, and a holder design has a decisive influence on the shape fluctuations of the mirror [2].

Research on the influence of vibration actions on the parabolic antenna in the package ANSYS can get offset values of mirror along the normal to radiating surface in the analyzed points that required for calculate the effect of the deformation of antenna on the characteristics of its radiation by using the proposed method.

According to the proposed method, we represent the antenna reflector through its cross section in the principal planes. This is true that the radiation pattern (RP) of the antenna azimuth angles φ has the same shape for different fixed values of the elevation angle θ , and vice versa. This condition is usually performed the more accurate than the sharper the RP. Axisymmetrical mirror antennas are highly directional, so their spatial RP $F(\varphi, \theta)$ can be

approximately represented as [3]

$$F(\varphi, \theta) = F(\varphi) \cdot F(\theta), \quad (1)$$

where $F(\varphi)$ – RP in the horizontal plane; $F(\theta)$ – RP in the vertical plane .

Such two-dimensional $F(\varphi, \theta)$ $f(x, y)$ in the Cartesian system of the coordinates, represented as

Such two-dimensional divided RP $F(\varphi, \theta)$ there correspond also two-dimensional divided distributions of field $F(\varphi, \theta)$ in the Cartesian coordinate system, represented as [4]

$$f(x, y) = f(x) \cdot f(y), \quad (2)$$

where $f(x)$ – the field distribution in the antenna aperture along axis Ox horizontal plane; $f(y)$ – the field distribution in the antenna aperture along axis Oy vertical plane.

Since the mirror parabolic antenna is mounted vertically with the nondeformable disk "holder" in the center of the mirror, under vibration load fluctuations the main form of vibrations are the asymmetric ones (Fig. 2), and the holder design has a decisive influence on the shape of the mirror vibrations [2].

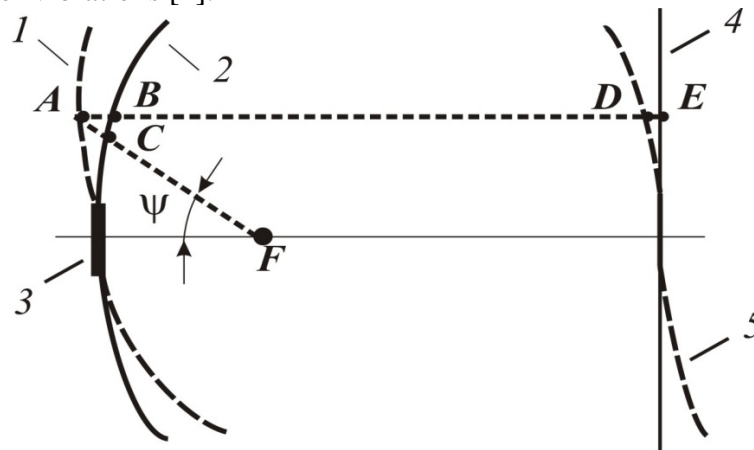


Fig. 2. Deformation mirror of antenna in vibration actions

Fig. 2 has the following meanings: 1 – distorted profile of mirror; 2 – undistorted of mirror profile; 3 – mirror holder; 4 – plane wave front; 5 – distorted wave front; F – focus of a parabolic mirror; ψ – partial beam direction of the electromagnetic wave; A , B , C , D , E – informative points describing path elongation of the top half of the wavelength and the shortening in the bottom half of mirror (A , B and C), and the distortion of the wave front (D and E).

As known [3], undistorted mirror of a parabolic antenna during its irradiation of focus creates a common-mode aperture field distribution in which with high accuracy by using lambda functions they can calculate RP formed by antenna. However, the phase distortion that created by the deformation of the mirror is not taken into account.

A discrete representation of the continuous radiating surface and, consequently, of its sections in the form of elementary radiators (Fig. 3) is perspective here. At the same time the search of the antenna field, that created by a system of elementary radiators at the observation point P is reduced, as a result, to the summation of the fields of all its constituent sources, considering the sources of amplitudes and phases

Here, the following notation: P – observation point; y_1, y_2, \dots, y_N – coordinates of phase centers of radiators located along an axis Oy ; r_1, r_2, \dots, r_N – distance from the phase centers of radiators to the observation point P ; r_0 – the distance from the geometric center of the radiating surface O to the observation point P ; $\theta_i = \theta_1, \theta_2, \dots, \theta_N$ – angle in the

direction of the observation point P relative to the symmetry axis of i -radiator; N – maximum sequence number of the elementary radiator relative to the axis of symmetry of the antenna.

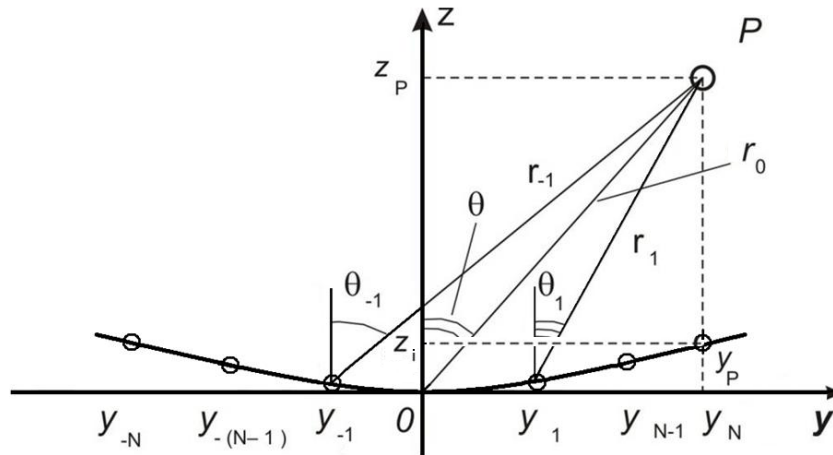


Fig. 3. Discrete representation of the cross section of a parabolic antenna reflector

According this intensity of the electric field E_Σ , produced such an antenna takes the form [1]:

$$E_\Sigma = \sum_{i=0}^n E_{\theta_i}, \quad (3)$$

where i – a number of radiator; E_{θ_i} – component of the electric field created by elementary radiator with the index i ; $n = 2N$ – even number of radiators.

The component of the electric field E_{θ_i} , that was created i -radiator in direction of the observation point P can be defined as

$$E_{\theta_i} = E_{0i} \cdot F(\theta_i) \cdot \frac{e^{-jk(r_i + \Delta r_i)}}{r_i + \Delta r_i}, \quad (4)$$

where E_{0i} – i -radiator's amplitude of intensity of the electric field at the surface of the antenna; $F(\theta_i)$ – level PR of i -radiator in direction to θ_i ; θ_i – angle of observation point P from the normal to a simple i -radiator in its centre; $j = \sqrt{-1}$ – imaginary unit; $k = \frac{2\pi}{\lambda}$ – wave number of the electromagnetic wave; λ – length of the electromagnetic wave; r_i – distance from the centre of the i -radiator to the observation point P ; Δr_i – changing the path of the partial beam of electromagnetic wave to the simple i -radiator because of the deformation of the mirror, leading to a phase shift of the field distribution in its aperture.

According to fig. 2, these deformations Δr_i can be found as the sum of the path segments wave AC and AB , by the way we can consider that $AC = AB \cdot \cos \psi$, where ψ – the angle of the observation point A from the mirror focus. Thus, by deviation of the informative point B undeformed mirror in position A on a distorted mirror (fig. 2) we can receive [5-7]

$$\Delta r_i = AB \cdot (1 + \cos \psi). \quad (5)$$

The amplitude of the electric field intensity of the i -radiator at the surface of the antenna E_{0i} can be defined from a distribution field $f(y)$ based on its position y_i along the axis Oy . The distribution field itself $f(y)$ is calculated by the traditional aperture method of

calculating for RP radiator [3].

As radiators it can be selected elementary sources of electromagnetic waves, such as Hertzian dipole, symmetrical half-wave vibrator, etc. For example, there may be used elemental linear radiators with a uniform excitation and with longitudinal dimensions equal to half the wavelength. The radiation pattern of such radiators $F(\theta_i)$ can be defined by the following formula [3]

$$F(\theta_i) = \frac{\sin u_i}{u_i}, \quad (6)$$

where $u = \frac{k l_i}{2} \sin \theta_i$; l_i — length of a simple i -radiator; θ_i — angle to the direction of the observation point P from the normal to the simple linear i -radiator.

In the proposed models we consider that radiators are identical, ignore their mutual influence, and we believe the current distribution are unchanged over time. On the fig. 3 the center of the antenna radiating surface O is combined with the center of a circle, that has a radius which equal to the distance r_0 from this centre to the observation point P . Such circle окружность is described by the radius vector of the distance r_0 when they turn the antenna relative to the direction P , that corresponds to the condition evaluation of its directional characteristics. Taking into account the adopted notation, the spatial distribution of radiators and the observation point P we can get the following calculated ratio.

The coordinations y_p and z_p of the observation point P have the following meanings (fig. 3):

$$y_p = r_0 \cdot \sin \theta, \quad (7)$$

$$z_p = r_0 \cdot \cos \theta. \quad (8)$$

In turn the distance from the random i -radiator r_i to the observation point P can be defined as

$$r_i = \sqrt{(y_p - y_i)^2 + (z_p - z_i)^2}, \quad (9)$$

where r_i — the distance from the observation point P relative to the phase center of the i -radiator.

The angle θ_i of the observation point P relative to the normal of the axis Oy from the phase center of the i -radiator can be defined as

$$\theta_i = \arccos [(z_p - z_i) / r_i]. \quad (10)$$

The radiation pattern of the antenna in a vertical plane $F(\theta)$ in view of the received expressions can be defined as

$$F(\theta) = E_{\Sigma}(\theta) / E_{\max}, \quad (11)$$

where $E_{\max} = E_{\Sigma}(0)$ — max level of the intensity of the electric field, that equal for symmetric antennas to its value in the direction of the axis of symmetry.

As a result of research of influence of vibration actions on mirror antenna in the package ANSYS there were obtained the values of displacement of a mirror along the normal to the surface in the analyzed points during vibration action and on the proposed method there was calculated RP of antenna $F(\theta)$ in vertical plane (fig. 4, graph 1), that is closed to the experimental one (fig. 4, graph 2), that is presented in the work [2].

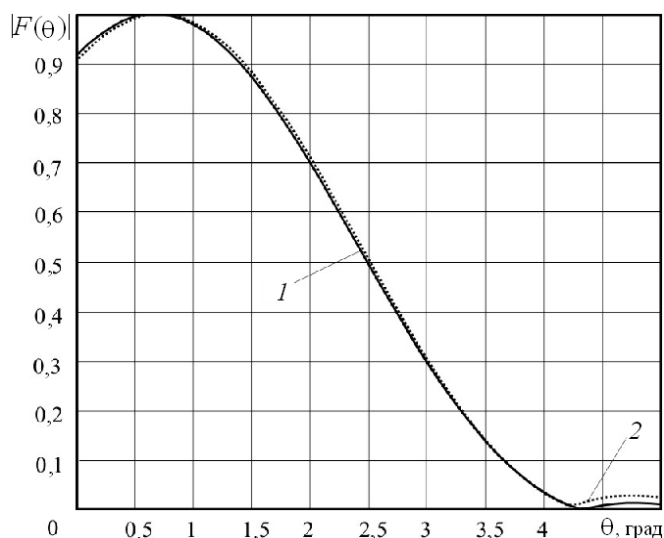


Fig. 4. The amplitude radiation pattern of a mirror antenna

So, the received results confirm the feasibility of using the package ANSYS to investigate the influence of vibration actions on the radiation of a parabolic antenna and the feasibility of the proposed method of calculation for vibration-resistant design mirror antennas.

References

1. A.N. Yakimov, Design of microwave antennas, taking into account external actions, a monograph, Penza State University Press, Penza, 2004, p. 206.
2. N.N. Abzhirko, Vibration effect on the characteristics of radar antennas, Sov. radio, Moscow, 1974, p. 168.
3. A.L. Drabkin, Antenna-feeder devices, Sov. radio, Moscow, 1974, p. 536.
4. E.A. Zasovin, A.B. Borzov, R.P. Bystrov, Radio engineering and radio-system, textbook for students, M.: Round, 2001, p. 752.
5. D.N. Shishulin, A.N. Yakimov, Methods of assessing the influence deformation on the mirror parabolic antenna the radiation characteristics, "Reliability and Quality," Proc. Sympos., Vol.1, Penza State University Press, Penza, 2010, pp. 398-399.
6. N.K. Yurkov, E.Yu. Maksimov, A.N. Yakimov, A finite-element model of the thermal influences on a microstrip antenna, Measurement Techniques. N.Y., Springer, Vol. 54, No. 2, May, 2011. P. 207-212.
7. N.K. Yurkov, A. N. Andreev, A. V. Blinov, A. N. Yakimov, Conceptual approach to introduction of information technology into the field of simulation, Measurement Techniques. N.Y., Springer, Vol. 42, No. 5, May, 1999. P. 421-426.

DATA PROCESSING METHODS FOR INFORMATION SYSTEM OF SUPPORT TOURISM BUSINESSES

Yarkin A. S., Popov F.A.

Biysk Technological Institute (branch) of the AltSTU, Biysk

The article is devoted to the solution of problems arising at creation of information system of support and development of travel business with application of the GIS technologies. The principle of a general analysis of large amounts of data is considered on the

basis of available algorithms also it is proved that at a certain approach, time for carrying out the analysis will be minimum.

Keywords: geographic information system, databases, tourism, analysis

For the last decades in Russia, tourism gained considerable development and turned into the mass phenomenon. Professionals and experts of the industry of tourism are in great need in the authentic and complex, cartographical provided information reflecting recreational resources and extent of development of tourist infrastructure of Russia and it is certain regions. It should be noted that such specialized comprehensive cartographic projects for governments, does not exist currently. The necessity to develop cartographic support the tourism industry is matured, which would fully reflect the recreational and tourist complex in the region and served as a source of reliable information to professionals in decision-making and organization of tourism.

Information system of support and development of travel business is intelligent information model based on actual performance and uniquely identifying the relationship and interaction of its components. The main purpose of the system is systematization and analysis of thematic data sets, forming the best offers for decision-makers and consumers. The system will cover the economic, organizational, managerial and entertainment area of tourism [1].

The developed information system is directed to the solution of the following tasks:

1) It is systematization of the information in the field of tourist activity. The computerized information system possesses opportunities of fast and reliable processing of large arrays of information.

2) It is data storage of different structure. One of main requirements to information system is continuous development, development of new functionality at which the saved-up data remain and supplemented with new values.

3) It is the analysis and forecasting of flows of information in the tourist sphere. Streams for the purpose of their minimization, standardization and the adaptation for adoption of adequate administrative decisions are studied.

4) It is the planning of development of travel business. Business Solutions have to be based on the forecast of tendencies of development of business as a whole and the analysis of milestones past.

5) It is providing intellectual functionality and minimum convenient interface for the operator and the user of system.

The fundamental principle of work of system consists in accumulation and systematization of data with the subsequent analysis and the user-friendly interface for access. Modern technologies are capable to provide creation of an uncountable set of communications between system data, providing intellectual selection of information. Geo information modeling as a basis of visual display of data in the best way will be entered in the concept of developed system [2].

Developing a support system for tourist business, it is necessary to construct the detailed model which is unmistakably describing real process of life cycle of one element of the tourist sphere.

When using OLAP-systems means of check of hypotheses in the analysis of data are provided to the analyst. Thus, the main objective of the analyst is generation of hypotheses. He solves it, based on the knowledge and experience. However, knowledge is not only at the person, but also in the saved-up data, which are exposed to the analysis. Such knowledge often calls “hidden” as they contain in gigabytes and terabytes information, which the person isn't able to investigate independently. In this regard, there is a high probability to miss hypotheses, which can bring considerable benefit [1].

Obviously, special methods of automatic analysis is necessary to use for the detection of hidden knowledge, by which are detected knowledge.

Possible problems during system development are:

1) The new data model requires practical application and has no analogues and steady parameters. Data model or database will be used experimentally and need time for testing performance.

2) Accumulation of irrelevant data – relevance of information lasts within one tourist season, and then comes the update cycle of information.

3) Forecasting on the basis of available data. Difficult process of analytics and forecasting at the first stages of life cycle of system will be completely abstract.

4) Collection of information. It is important preparing a user-friendly interface for managing information.

5) Total absence of the description of mechanisms of application of GIS's tools in similar information systems.

Key features of modern databases include mechanisms, the use of which greatly increases the speed of analytical processing, such as:

1) Preliminary shortchanging of data. Data, which are most often used for the analysis, are calculated in advance (for example, at night) and prepared for processing are stored on the DB server in the form of the multidimensional cubes, the materialized representations and special tables.

2) Caching tables in memory. Data that take up little space, but which often is addressed in the analysis (for example, reference books), are cached by database facilities in random access memory which is much reduced circulation to the slower disk subsystem.

3) Splitting tables into sections and tabular spaces. Data stored on separate disks. It will allow DBMS to read out and write down information in parallel.

It is obvious, not all data are exposed to the analysis. According to the laws of the information world - the simpler analysis mechanism, the quicker data is processed. It is possible scenario for building data so that data pass several cycles models. There is a simple idea - do not waste time processing for data that cannot be analyzed [3].

In the beginning, the simplest algorithms are used. The part of data which are processed by means of such algorithms and which are senseless for processing with use of more difficult methods is analyzed and excluded from further processing. The remained data are transferred to the following stage of processing where more difficult algorithms and so on a chain are used. On the last knot of the scenario of processing, the most difficult algorithms are applied, but the volume of analyzed data is many times less than initial selection. As a result, the general time necessary for processing of all data is decreases.

For example, at the solution of a problem of forecasting of demand originally recommended carrying out the XYZ analysis, which allows defining demand for various services. Services of group X steadily are on sale, application of algorithms of forecasting to them allows receiving the qualitative forecast. Services of group Y are on sale less steadily, for them it is necessary to build models not for each parameters, and for group that allows to decrease a time row and to ensure functioning of algorithm of forecasting. Services of Group Z chaotically are on sale therefore for them at all it isn't necessary building predictive models, the need for them must to be counted on the basis of simple formulas, for example, average monthly sales. According to statistic about 70% of demand is compose of services of group Z. About another 25% is compose services of group Y and only about 5% is services of group X. Thus, construction and application of difficult models actually at most for 30% of goods. Therefore, application described above approach will allow reducing time for the analysis and forecasting at 5-10 times.

Effective strategy of processing of large volumes of data is splitting data into segments and creation of models for each segment separately, with further association of results. Most often in large volumes of data, it is possible to allocate subsets some differing from each other. It can be, for example, groups of clients, goods, who behave similarly and for which it is expedient to build one model. In this case instead of creation of one difficult model for all it is possible to build by simple method for each segment. Similar approach allows increasing the speed of the analysis and to lower requirements to memory thanks to processing of smaller volumes of data in one pass. Besides, in this case analytical processing can be parallelized that positively affects spent time. Besides, for each segment various analysts can build different models.

In the presence of large volumes of data, it is possible to use for creation of model not all of information, and some subset. Correctly, the prepared selection of data set comprises information necessary for creation of qualitative model. Process of analytical processing is divided on 2 parts: creation of model and application of the constructed model to new data. Creation of difficult model is very spendy process. Depending on algorithm the data are cached and scanned, the set of auxiliary parameters is calculated. Application of already constructed model to new data demands resources tens times smaller. Very often, it is reduced to calculation of several simple functions.

Thus, if the model is under construction on rather small data sets and the model will be is applied to all data set, than time of receiving result will be reduced in tens times in comparison with attempt completely to process all available data set.

References

1. Buhalis, D., Law, R. Progress in information technology and tourism management: 20 years on and 10 years after the Internet—The state of eTourism research. *Tourism Management*, 29 (2008) 4, 609-623.
2. Popov F.A. Intellectualizatsiya pol'zovatelskih interfeisov informatsionnih sistem / F.A. Popov, N. Yu. Anufrieva // *Vestnik Tomskogo gosudarstvennogo universiteta*. – 2007.- №300(1). – С..130-133.
3. R. Chaiken, B. Jenkins, P.-A. Larson, B. Ramsey, D. Shakib, S. Weaver, and J. Zhou. SCOPE: Easy and Efficient Parallel Processing of Massive Data Sets. *VLDB*, 1(2008) 2.

INDIVIDUAL EDUCATIONAL COURSE SYNTHESIS METHOD USING EVOLUTIONARY METHODS OF EDUCATIONAL CONTENT SPACE FORMATION

Volosatova, T.M., Belomoytsev, D.E.
Moscow, BMSTU

Basic professional education problems are reviewed. Reasons for additional education are formulated. Method for solving existing educational courses redundancy problem is proposed. Individual educational courses synthesis process automation technique is presented. Educational content multidimensional representation features are mentioned.

Keywords: additional education, individual courses, educational content

The analysis of statistics of employment [1], and also selections of responses of graduates of the institutions shows that basic higher education at the present stage of

development of science and equipment often is insufficient further even for work in the specialty and doesn't satisfy requirements arising during professional activity.

The solution of arising problems with gaps in education on actual scientific and practical aspects is receiving missing knowledge within additional training and deepening in special courses passed earlier.

The sphere of educational services offers needing additional education people a wide range of various centers of training in which various educational programs, courses and other forms of expansion of an outlook of knowledge [2] are available.

However, the solution of the problem of insufficiency of basic education by receiving additional knowledge generates other problem – a problem of a choice of that additional course or an educational program which will allow necessary and sufficient volume to satisfy available scientific and practical requirements.

A solution to the problem of insufficiency of basic education "measure" observance in an extended education is important. Isn't a secret that many educational programs are initially organized with a certain degree of redundancy. Besides, even use of the programs, which contents very strictly corresponds to the declared direction, maybe, often, to lead to achievement of effect of redundancy at total illumination of target subject on the arisen question.

The reason of emergence of a similar situation consists in frequent impossibility to pick up ideally satisfying to a question which demanded additional training, an educational program that, in turn, results in need of drawing up wider, than it can be required, selections of programs or the courses which are partially taking up a target question.

It is expedient to solve a problem of redundancy of existing educational programs and courses by synthesis and use of their irredundant analogs under individual inquiries of target audience [3]. It is thus important to note that the greatest value of an indicator of compliance of the maintenance of a synthesizable course to a target question, and also a irredundancy is reached due to selection of an educational content in relation to practical statement of a target question.

In other words, if there is a need to get an additional education on a certain subject, for formation of an individual educational program it is necessary to find out in the beginning practical aspects of interesting subject [4], and then to create the related set of knowledge for construction on its basis of the program.

As practice shows, a certain complexity represents as a specification of practical aspects of a target question demanding an extended education, and understanding formation about the necessary depth of additional knowledge, an extended education volumes.

Often it leads to disclosure more new requirements already during training process. Possibly is to automate process of formation of individual educational programs by application of the developed technique which essence generally consists in comparison to the selected elements of space of scientific and practical achievements of elements of space of an educational content. These multidimensional spaces are formed on the basis of the analysis on the one hand theoretical aspects of existing educational programs, and on the other hand – scientific and practical achievements of mankind. During the analysis communications of achievements and theoretical aspects corresponding to them are defined.

Applied realization of the developed technique of synthesis of individual educational programs is applied within the project of a portal of distance learning of CADISS which gives opportunity to Internet users regardless of location to get access to educational services. Having defined a target scientific and practical question, the user has an opportunity to create the individual program of training in the theoretical aspects connected with a target question. Thus depth of consideration of the theory, volumes of

questions necessary for knowledge, and also aspects, acquaintance with which, probably is automatically offered, will be useful.

In addition to considered in [5] modular representation of materials within conducted research of efficiency of a technique of synthesis of individual educational programs it is offered to structure elements of space of an educational content from the point of view of evolutionary methods of creation of design decisions, in particular – genetic algorithms [6,7].

Representation of structure of educational courses by the description in the form of set of genes and chromosomes gives the chance to estimate effectively advantage of their perception being trained on the basis of specially developed criterion functions.

Application of specialized genetic operators [8] allows to carry out generation of various options of individual educational programs in total with the imposed restrictions on compatibility of some elements of space of an educational content.

Within test operation of applied realization of the developed technique of synthesis of individual educational programs within the project of a portal of distance learning of CADISS work of a technique on subject of the courses connected with information security, and also design automation is realized. Technique application for formation of individual programs of additional training allowed to reduce costs of time of passing of courses to 67% in comparison with similar indicators of expenses for passing of courses according to the fixed programs.

References

1. Serova L.M., Semenov A.A. Analiz razlichnyx istochnikov dannyx o monitoring trudoustroistva vypusknikov. Petrozavodsk. PGU, 2011.
2. Reiting tsentrov distantsionnogo obucheniya. 2013. <http://edu.jobsmarket.ru/company/rating/online/>.
3. Innovatsionnoe razvitie sovremennoi nauki: sbornik statei. Ufa: RIC BashGU, 2014.
4. Mkrtchan M.A. Organizatsiya obucheniya na osnove individualnyx obrazovatelnyx program. Krasnoyarsk, 2007.
5. Bondarchuk T.V. Proektirovanie individualnyx obrazovatelnyx program dlya uchashchixsya shkol. Sovremennye problem nauki i obrazovaniya. 2012. № 6
6. Norenkov I.P. Geneticheskie metody strukturnogo sinteza proektnykh resheniy. Informatsionnye tekhnologii. 1998. №1.
7. Norenkov I.P. Evristiki i ix kombinatsii v geneticheskix metodax diskretnoi optimizatsii. Informatsionnye tekhnologii. 1999. №1.
8. Belomoytsev D.E. Razrabotka metodiki avtomatizirovannogo proektirovaniya kanalov peredachi zashchishchennykh soobshcheniy v besprovodnykh soedineniyakh mobilnykh ustroystv. BMSTU. M., 2009.

USE OF EFFICIENCY PARAMETER OF REAL OPTIONS IN THE DECISION INNOVATIVE SOLUTIONS

Astafjev A.V., Fedoseev S.V., Mikrukov A.A., Berketov G.A.
Moscow, MESI

The possibility of using the optional approach to innovative decision-making is considered. Procedure to determine the efficiency of an option based on a comparison of the proceeds and expenses is proposed.

Keywords: real option, proceeds, expenses, required efficiency level of real option, option efficiency.

In practice, the task of making decisions on choosing the best course of action has specific differences in various subject areas. For example, in the innovation economy the problem of using of real options is often solved. This makes it feasible to develop special procedures for decision-making related to this problem. Under real option in this article we shall mean "any opportunity, right, or chance of getting the good in the future, to create that in the present you need to perform some action" [1].

To determine the effect of real options by decision maker (DM), there are different methods in practice. You can select two basic and most common of them: method of analysis of binary decision tree and method based on the use of Black-Scholes model.

Method of analysis of binary decision tree is to analyze the possible scenarios. Method makes it possible to obtain results in the case of several sources of uncertainty and a lot of steps. Determining the value of an option is to construct a binomial scheme, which is calculated at each point of the project cost, i.e. present value of all cash flows when the situation changes. [3]

The second method involves the use of Black-Scholes model, which was developed to assess premiums on European financial option type «call» [2]. Accordingly, the model characteristics used in real options was originally defined specifically for financial options. Application of the method, ultimately, boils down to finding the values of these characteristics for real options and substituting these values in the model

In applying two methods above you can not establish a relationship of potential cumulative income from the use of the option to the value of the total costs associated with the acquisition and execution of the option. This ratio, in turn, would estimate effectiveness of resource expenses.

To solve the above problem, we propose the following approach. Acting in the organization decision-making system is modified by the introduction of such a measure as a real option efficiency (E_O). In general, the expression of this indicator can be written as follows:

$$E_O = \frac{\text{Proceeds} - \text{Expenses}}{\text{Expenses}}. \quad (1)$$

Proceeds in (1) means a collection of material goods, which receipt is associated with the considered real options; *Expenses* - means a set of costs associated with the acquisition and use of real options.

In a situation when $E_O > 0$, the decision to invest resources in the acquisition and use of real options in general can be considered reasonable and leads (in the case of option execution) to obtain the organization income in one form or another. Depending on the the option, income, for example, can be expressed in savings on the situation without the option. The higher the E_O , the more proceeds accounted for 1 ruble expenses, the expenses is more effective.

Thus, the real option allows the decision maker to evaluate the ratio of the potential benefits to the value of investments.

There are various modifications of efficiency E_O to the particular decision support system, depending on DM specific objectives. For example, in the particular case of (1) the expression takes the following form:

$$E_O = \frac{\sum_{i=1}^n (VD_i * D_i) - \sum_{k=1}^m (VR_k * R_k)}{\sum_{k=1}^m (VR_k * R_k)}, \quad (2)$$

where, i - the type of proceeds. associated with the use of real option ($i = 1, 2, \dots, n$);

D_i - the value of the i -th proceed;

$V D_i$ - the probability of the i -th proceed;

k - type of expense, associated with the use of real options ($k = 1, 2, \dots, m$);

P_k - the value of the k -th expense;

$V R_k$ - the probability of the k -th expense.

In (2) proceeds and expenses are related based on the probability of their emergence.

The use of probability of proceeds and expenses in the calculation of efficiency is especially important when real options are using, as very often the probability of proceeds obtaining is significantly different from the probability of expenses incurring.

In practice, an additional tool is proposed in the decision -support systems. This is parameter $(E_0)_{\text{req}}$ - *required efficiency level of real option*, which will compared by DM with efficiency value of specific option . Comparison of these parameter is proposed to read as follows:

if $E_0 > (E_0)_{\text{req}}$ - real option is acceptable;

if $E_0 < (E_0)_{\text{req}}$ - real option is unacceptable or in need of processing in order to increase efficiency;

if $E_0 = (E_0)_{\text{req}}$ - you can make any decision on admissibility.

In case $E_0 < (E_0)_{\text{req}}$ there is a need to correct the evaluated option or to create a new real option that can replace the old option and having an efficiency above the standard level.

Correction of real option with unsatisfactory efficiency can be conducted by DM on the following main areas : reducing the expenses of the purchase and exercise of the option , an increase proceeds related to the exercise of options, consideration of possible ways to increase the probability of proceeds and to reduce the probability of expenses.

Consequently, the application of the proposed approach based on assessing the effectiveness of real option , enables to decision-makers :

evaluate the effectiveness of investments in the purchase and exercise of real options ;

compare the level of effectiveness of a particular option with a standard efficiency level;

ranking of real options by efficiency investments.

Measuring the effectiveness of real option is a localization of method DEA (Data Envelopment Analysis) for real options to take account of their specific economic and managerial properties.

Exploring the possibilities of method localization, we conclude that performance evaluation which is based not on the total amount of resources, but on one particular type of expended resources or based on a set of resources belonging to the vector of used resources may be is very important for the decision-maker.

DM can also be very interested not in the final, but in the intermediate result, which assumes no summation of all resource values derived from the vector resource, but only part of these resources (Table 1).

Table 1. Option efficiency, considering the set of resources

Vector of expended resources	Vector of derived resources
x_1	y_1
x_2	y_2
x_3	y_3
x_4	y_4
\dots	\dots
x_n	y_m
Option efficiency:	$\frac{\sum_{k=1}^3 [\beta_k M(Y_k)]}{\sum_{i=1}^2 [\gamma_i M(X_i)]}$

Formula for evaluating the efficiency, localized for real options:

$$E_0 = \frac{\sum_{k=1}^s [\beta_k M(Y_k)] - \sum_{i=1}^r [\gamma_i M(X_i)]}{\sum_{i=1}^r [\gamma_i M(X_i)]} * 100\% , \quad (3)$$

where X_i - set of expended resources by real options, which efficiency is required to estimate, ($i = 1, 2, \dots, r$);

Y_k - set of derived resources by real option, which are taken into account in the calculation of the efficiency, ($k = 1, 2, \dots, s$);

γ_i - the coefficient of the relative importance of i -th type of expended resource ($i = 1, 2, \dots, r$);

β_k - the coefficient of the relative importance of k -th type of derived resource ($k = 1, 2, \dots, s$).

It is assumed that the application of decision-making procedures, based on the real options concept, on the DEA method localization and on the using of required efficiency level of real option, will enhance the effective use of financial resources and, as a result, improve the quality of decision-makers decisions.

References

1. Astafjev A.V. The concept of real options / Scientific and technical statements SPbSPU N3(121), 2011.
2. Limitovskiy M.A. Investment projects and real options in emerging markets: Training and practical guide / - M.: Publishing Yurait, 2011.
3. Ziyatdinov A.S. Real options method for evaluating investment projects / Economics № 3 (64) "Economics and Management", 2010.
4. Astafjev A.V., Fedoseev S.V. Management decision-making scheme using optional approach Scientific and Practical Journal of Economics, Statistics and Information teak. Herald UMO. № 6 (2), 2012, p. 81-85.
5. Fedoseev S.V., Astafjev A.V. The procedure of multi-choice problem in investment management. Innovative information technology: Proceedings of the international scientific-practical Conference. Volume 2. - M.: MIEM HSE, 2013. Pp. 420-425.
6. Zavgorodniy V.I. Information risk management companies. Monograph. - M.: INION, 2009. p.174.

TRENDS AND PROSPECTS OF AIRCRAFT ELECTRICAL EQUIPMENT

Khalyutin S.P., Levin A.V., Kharkov V.P., Zhmurov B.V.
Moscow, Experimental Studio "NaukaSoft"

The report examines trends in the development of aviation electric equipment and shows the potential ways of its development.

Keywords: aircraft electrical equipment, more electrical aircraft, all electrical aircraft, electrical power plant.

The development of aircraft equipment in the modern world is determined mainly by strengthening the social orientation of the activities of States. On the one hand it is connected with the increasing requirements for environmental friendliness of aircraft (reduction of hazardous waste and noise), and on the other, with increased passenger comfort level (use on Board the aircraft, broadband Internet, individual systems of climatic parameters, the showers

and the like). At the same time, there is still a requirement to ensure the required level of safety.

Studies [1-4, 7-10] showed that the most prospective way to improve environmental performance, is the transition to a more electric and, at the limit and to the all-electric aircraft, which are absent pneumatic and hydraulic systems, and all the functions of the Executive power of the elements perform actuators. The interest to the increased electrification equipment aircraft by the substantial level of financing of the programs on this subject. [5] Known programs such as More Electric Aircraft (MEA), the implementation of which was allocated 400 million euros, POA (Power Optimized Aircraft) with a budget of approximately EUR 100 million, MOET (More Open Electrical Technologies). In the Russian Federation the concept of AEA (all-electric aircraft) developed under the supervision of TsAGI, and it involved more than 100 industrial enterprises, scientific research institutes and Universities. In electrification appeared passenger aircraft A380 and the Boeing 787, the F-35, the unmanned aerial vehicle «Barracuda» and other.

As for the power plant, then only a single type of energy (electric) leads to a significant increase its effectiveness and improvement of the working regimes, which in turn reduces the amount of harmful emissions into the atmosphere. However, in the power plants operating on the burning of hydrocarbons natural fuels (internal combustion engines and gas turbine engines), impossible to completely get rid of harmful emissions. Therefore, one of the directions in the development of the aircraft industry is the establishment of power plants to electric traction [6]. Intermediate stage of such a transition can become a hybrid power-plant. Possibility of wide application of electric power installations on the aircraft is primarily determined by their purpose, conditions and modes of flight. So, at high aerodynamic quality of the fuselage, the required capacity of power installation can be low, and consequently the lower the total cost of the trip, however, may require more power take-off stage. For example, for small aircraft and unmanned aviation generally flight is operated with minimal dynamics of maneuver simulation and does not require costly capacity of the power unit. Limitation of time of flight of aircraft is connected to electric traction with the total energy intensity of energy storage. Increase the level of passenger comfort is always connected with increase of volume of consumed electric energy (EE), and, consequently, a need to increase the installed capacity of the primary sources of EE. So on the Boeing 787 total installed capacity of the power sources [3] 1450 kVA, and on aircraft A-380 - 840 kVA (see figure 1).

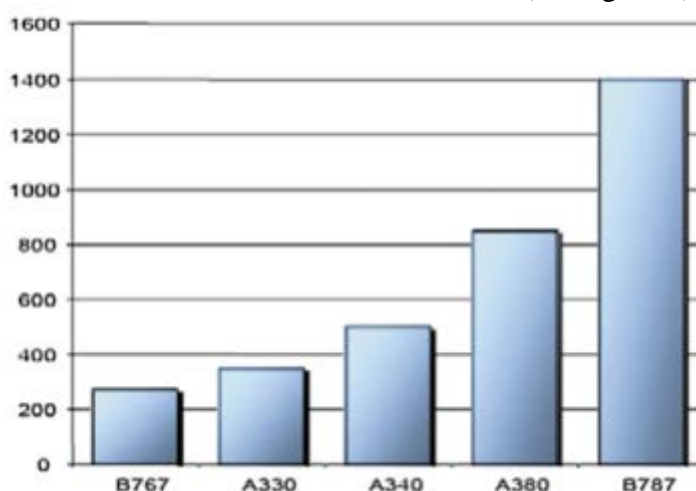


Figure 1. Trends installed capacity of electricity sources (kVA)

The increased power sources EE, demands search for new solutions as at designing traditional Electromechanical generators, and the creation of sources, working on different physical principles (electrochemical generators, photochemical generators and other).

Summarizing the above mentioned features, we can formulate the basic tendencies of development of aviation power industry:

- significant increase in both established and a single power sources on Board the aircraft;
- increase the number of electricity consumers, among which all major part is taken by the receivers of EE with pulse-periodic pattern of consumption, which worsens the conditions to ensure the required quality of EE on Board the aircraft;
- the possibility of hybrid and electric power plants that provide flight of an aircraft;
- increasing the necessary types of EE for separate groups of receivers and, as a consequence, the need for new types of electrical energy converters.

Given formulated trends and the need of choosing the most effective design solutions, you must determine the ways and prospects of development of aviation equipment that is based on a number of optimization problems for a generalized criterion of efficiency.

In General, the efficiency of the electrical power system (EPS) is determined by many parameters, which can be conditionally grouped (operational, economic, technical, technological and other). The definition of specific requirements of the EPS is the task of the chief designer of the plane.

The efficiency of the electricity system as physical energy system can be determined on the basis of structural-functional principle [11] - the effectiveness of each element of the system with optimal (from the point of view of reduction of losses) structure. The EPS elements - the essence of power converters, for which one of the main targets is the power density and efficiency. So Electromechanical converters (generators and motors) in the limit have the specific power to 0,25-0,3 kg/kW, static converters (rectifier devices, inverters and other) - up to 1 kg/kW. The ratio of the specific power and energy density batteries are shown in figure 2 [9].

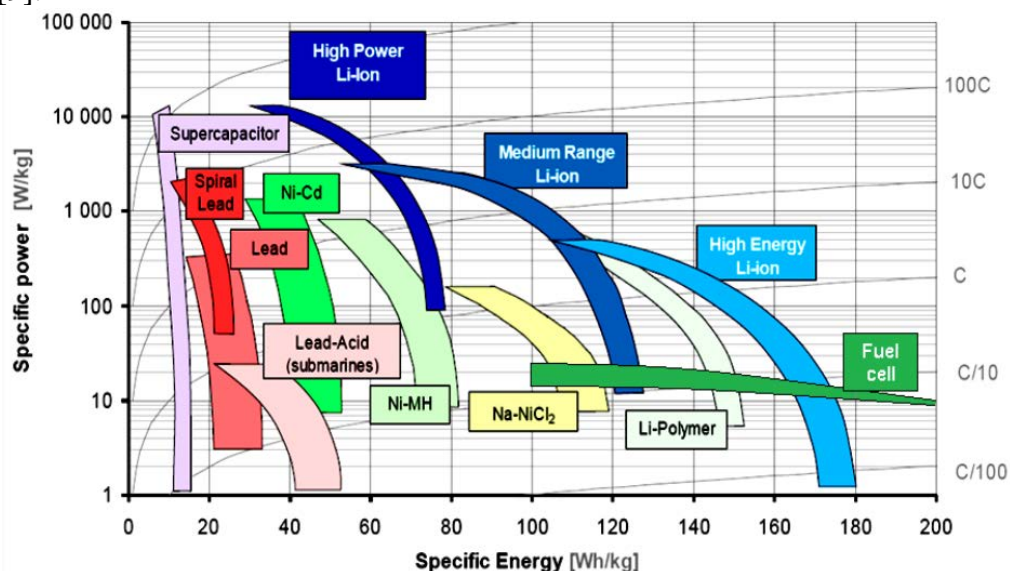


Figure 2. The ratio of the energy density and power density of batteries

An important criterion to assess the potential efficiency of the designed aircraft is the total energy intensity is stored on Board the energy. The main competition when this occurs between hydrocarbon fuel and electrochemical energy sources. Of electrochemical systems is the greatest theoretical energy content [14], in descending order, have the following:

- lithium-air=13000 W h/kg (without weight oxidant);

- aluminum air=8100 W h/kg (without weight oxidant);
- lithium fluoride=6300 W h/kg;
- lithium-sulfur (room temperature)=2600 W h/kg;
- sodium-sulfur (room temperature)=1500 W h/kg;
- iron-air (without weight oxidant)=900 W h/kg;
- sodium-iron-chloric=760 W h/kg;
- lithium-ion=500-800 W h/kg;
- lead-acid=160 W / h/kg.

Thus the heat of combustion of gasoline-11600 W h/kg.

However, efforts to create a more efficient electrochemical drives continue. So, a group of researchers from the University of Massachusetts in Boston (University of Massachusetts, Boston), headed by Dr. Stuart Licht (Stuart Licht) has developed a new type of renewable electrochemical power source of air-zinc elements, in which electricity is produced by the oxidation of zinc [13]. According to calculations, he will be able to surpass specific capacity tank of gas, as well as all other electrochemical generators and all types of rechargeable batteries. A new type of electrochemical cell can exceed (see figure 3) «calories» and gasoline (and almost twice), and liquid hydrogen (in two times), and zinc-air cells (almost three times), and lithium-ion batteries (ten times).

Thus, when creating a fully electric plane with electric propulsion systems is theoretically possible to keep the same, and in some cases, and to improve overall dimensions of the power system.

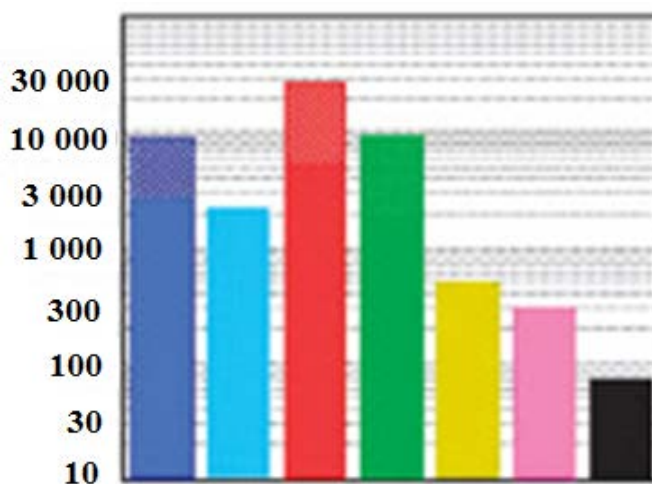


Figure 3. The comparison of experimental type - air-vanadium boride cells (red bar) with gasoline (blue), liquid hydrogen (blue), zinc (green), lithium-ion battery (yellow), Nickel-metal hydride battery (pink) and battery lead-acid (black). Left - density energy (watt-hours per liter). Scale - nonlinear (figure Licht et.al.)

Integration of the energy system in the complex, aircraft equipment requirements for unification and standardization system of power distribution at overlapping functions of control and protection. An example of implementation of these principles can serve as intelligent switchgear [15] (figure 4).

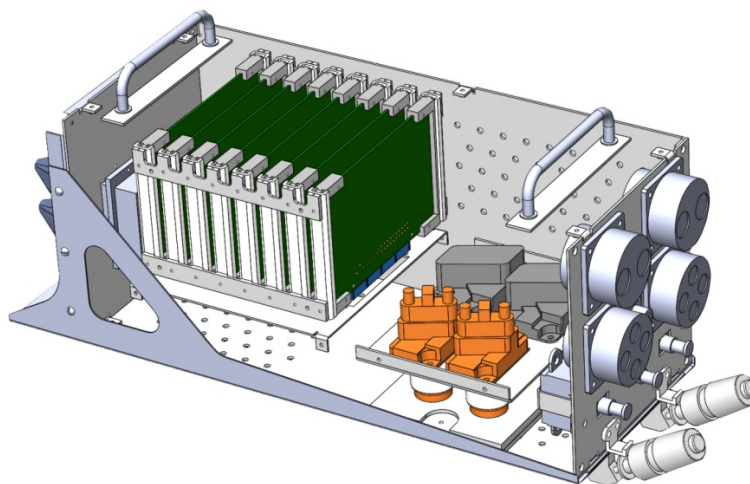


Figure 4. Intelligent switchgear

Seems promising directions of development of electric power complexes of flying machines will be:

- significant increase integration EACH with the power plant until its replacement by electric;
- decentralization of power generation and consumption (by type and location of secondary centers load management);
- optimization of multiple sources and energy storage devices for weight and dimensions by choosing the most energy-intensive;
- the application of a single intelligent control systems for power supply and consumption of electricity and, as the consequence, unification and scalability distribution modules and protection of electrical networks.

References

1. Bruskin D.E. Samoljeti s polnostju elektrifitsirovannim oborudovaniem. Ser. Electrooborudovanie transporta. – T. 6 / D.E. Bruskin, S.I. Zubatkin. – M.: VINITI, 1986. – 108 s.
2. Zlochevskiy V.S. Sistemi electosnabzheniya passazhirskih samoljotov. – M.: Mashinostroenie, 1971. – 376 s.
3. Moir I. Aircraft Systems: Mechanical, electrical, and avionics subsystems integration, Third Edition / I. Moir, A.Seabridge. – John Wiley & Sons, Ltd., 2008. – 504 p.
4. Moir I. Military Avionics Systems/ I. Moir, A. Seabridge. – John Wiley & Sons Ltd.: 2006. – 520 p.
5. Garganeev A. G. Techniko-economicheskije otsenki sozdaniya samoljota s polnostju elektrifitsirovannim oborudovaniem / A.G. Garganeev, S.A. Kharitonov // Docl. Tom. gos. universiteta system upravleniya i radioelektroniki. – 2009. – № 2 (20). – s. 179–184.
6. Jason Paur. Being Electric Doesn't Keep This Plane From Serious Aerobatics [Electronic resource]. URL: <http://www.wired.com/autopia/2013/06/e-fan-electric-airplane>
- 7 Garganeev A. G. Perspektivnie sistemi electosnabzheniya samoljota s polnostju elektrifitsirovannim oborudovaniem / A.G. Garganeev, S.A. Kharitonov // Docl. Tom. gos. universiteta system upravleniya i radioelektroniki. – 2009. – № 2 (20). – s. 185–192.
8. Voronovich S.A. Polnostju electriceskii samoljet/ S. Voronoich, V. Kargopol'tsev, V. Kutahov //Aviapanorama. – 2009. – № 2. – s. 23–27.
9. Khalutin S. P., Tulaev M.L., Zhmurov B.V., Starostin I.E. Modeling of complex electric power systems of aircrafts. M: Izd-vo VUNTZ air force «VVA them. Professor N.E. Zhukovsky and Y.A. Gagarin, 2010, 188 S.

10. Sistemi electrosnabzhenija letatel'nykh apparatov. [Text]: ucheb'nik / Tjul'jaev M.L.; Khalyutin S.P.; Ivanov V.V.; Zhmurov B.V.; Savenko V.A.; pod. red. S. P. Khalyutina. - M.: Izd-vo VUNTS VVS "VVA im. N. E. Zhukovskogo i Yu. A. Gagarina", 2010. - 428 s.
11. Khalutin S. P., Zhmurov B.V. Strukturno-funktsionalnoe modelirovanije electroenergeticheskikh system samoljota. Problemi bezopasnosti poljotov. 2009. № 6. s. 45-53.
12. Levin A.V., Alekseev I.I., Polnostju electrifitsirovannii samoljot – ot koncepcii k realizacii // Aviacionnaja promishlennost. - 2006. - №2. – s. 24-31.
13. Electrohimicheskaja yacheika v pervie prevzoidet po energoemkosti benzin [Electronic resource]. URL: <http://www.membrana.ru/particle/12833>
14. Beljaev S.S., Rikovanov A.S. Razrabotka universalnogo visokovolt'nogo batareinogo modulja dlja energoustanovok transportnogo i stacionarnogo naznacheniya na baze litii-ionnykh akkumuljatorov [Electronic resource]. URL: <http://cert-energy.ru/itog2012/belyaev.pdf>
15. Intellectualnoe raspredelitel'noe ustroistvo. [Electronic resource]. URL: <http://xlab-ns.ru/products/iru-3500.php>

METHOD OF SIGNALS INTERFERENCE IMMUNITY ESTIMATION USED IN MULTICHANNEL COMMUNICATION SYSTEMS

Eremina V.
Moscow, MNIRTI

The possibility of channels separation for the information transmission on communication lines at different types of carrier frequency modulation was shown. The analysis of modulation parameters for channels with the different data rates was performed.

Keywords: spread spectrum signal, frequency hopping, pseudo-random sequence, linear frequency modulation, discrete frequency modulation, the Euclidean distance.

Introduction. Improvment of the quality of the transmission channel or the throughput may be achieved by spreading of the channel frequency band of information transmission. [1] Using wideband signals with spreading spectrum allow to improve both parameters. For implementation of the spread spectrum signal carrier is modulated by special function, which spreads the spectrum, at that the chip duration of the transmitted message does not change.

The choice of spreading spectrum technique, which provides maximum interference immunity for a given channel bandwidth, is very relevant issue, since channel interference is a significant limitation of the users number of particular link. Thus, the objective of the research is to find the type of signal carrier modulation using the mathematical formalism of general algebra by the criterion of maximum interference immunity.

Description of communication system. Let us consider division multiplexing system, which implements various types of spreading spectrum. In particular, principles of communication channels separation with frequency hopping and code division multiple access (FH-CDMA) were researched in [2].

CDMA is based on the correlation properties of the signals. Frequency channel is divided into several tens logical subchannels, at that transmission and reception of these subchannels are carried out in the same frequency band simultaneously. Signals from different sources are encoded by individual pseudorandom sequence (PRS) and combined into a broadband signal (NLS) with dispersed energy. At the receiver signals are separated by

similar individual codes. Thus, in the same frequency band signals are formed, which do not affect each other.

FH-CDMA is implemented as follows: at the transmission side pseudo-random sequence (PRS) is formed, which controls the hopping frequency synthesizer (FS) by a given law. Since the control codes of frequency hopping (FH) are interconnected at transmission and reception, they are clearly identified by the receiver. Thus, if the code generator is synchronized with the input signal, it automatically synchronizes FS, whose algorithm corresponds exactly to the one that was used at the transmission. The FH is used in CDMA systems as follows. Any bit is transmitted as a combination of N frequencies, at that each frequency generates its own pseudorandom sequence (PRS). During a specified time interval carrier remains unchanged, and, thereafter, it stepwise changes. Algorithm of carrier frequency hopping is different for each user and it provides the simultaneous work of a large number of users in a common frequency band.

High interference immunity of this method is combined with the complexity of creating frequency synthesizer.

Linear frequency modulation (chirp) of carrier within the duration of signal element τ_{cdma} can be regarded as a particular case of frequency hopping. While spectrum is spreading on the value of chirp deviation it increases the number of channels in as many times as many values of deviation are used, while not below the given level of interference immunity [3].

Solution of the problem. Let us consider the combined utilization of address and spreading functions (continuous or discrete) for the problem of increasing number of information channels, taking into account that the chirp spread spectrum is easier to implement than using FH.

The method of signal modulation is need to define for reaching its greatest difference from any other used to transmit information to other users in order to provide minimal risk of entanglement really transmitted signal with another.

Model of information system is represented as follows. Suppose we have a message source generating one of the $S_k \{k = i, j\}$ possible messages for a specific user in each concrete moment of time. Second user utilizes the second of the rest of the messages. It needs to select the type of messages signal modulation, which prove the lowest probability of entanglement messages between users.

The source selects some specific signal $s_i(t) \in S$ and gives it to the channel input. At the receiving side (channel output) received oscillation $y(t)$ is observed, which is not an exact copy of the transmitted signal $s_i(t)$, but it is the result of signal transformation caused by the influence of channel noise [4].

Structural difference of signals must be sufficiently large enough according to the level of channel noise. Then on the receiving side, the decision about which of the possible signals from the set S was transmitted will be determined by the specified difference. To increase throughput the number of possible signals should be big enough and the difference of signals should be at the level of the receiver noise. We take the maximum likelihood method as optimal strategy of observation to estimate the separation of signals that provides the correct reception of all signals from the set S with equal probabilities. In accordance with this method to obtain the highest possible number of channels it is necessary to reduce the distance between the $s_j(t)$ and $s_i(t)$ to a value, at which the transformation of signal $s_j(t)$ into the observation $y_i(t)$ by the channel does not exceed a predetermined probability at a certain noise level of the receiver. Thus, the probability of transformation of any other signal in $y_i(t)$ is the least likely.

In a channel with additive white Gaussian noise (AWGN) transition probability between the transmitted signal and the output observation $p[y_i(t)|s_i(t)]$, that characterize the

transformation probability of channel any other input signal $s_j(t)$ (other than the real $s_i(t)$) in the output oscillation $y_i(t)$, exponentially decreases with Euclidean distance:

$$p[y_i(t)|s_j(t)] = k \exp\left(-\frac{1}{N_0} d^2(s, y)\right) \quad (1)$$

At the same time, the probability of transformation, presented above, decreases with increasing Euclidean distance between signals from the set S

$$d(s_i, s_j) = \sqrt{\int_0^T [s_j(t) - s_i(t)]^2 dt} \quad (2)$$

Let us consider the Euclidean distance to a discrete signal. Perform time discretization of continuous signal, i.e. represent the signal $s_i(t)$ by the samples $s_i = (iT)$, $i = 0, 1, \dots$, taken in a fixed interval T_s . If the whole signal energy is concentrated within a band W , and $T_s \leq 1/2W$, then samples s_i determine completely the continuous original signal $s_i(t)$. When the signal duration T has a total $n = T/T_s$ such samples and hence, n -dimensional vector $s_i = (s_0, s_1, \dots, s_{n-1})$ describes fully the signal. After such an operation with signal $s_j(t)$, we come to its n -dimensional vector equivalent $s_j(t) = (y_0, y_1, \dots, y_{n-1})$, which allows to find the Euclidean distance between the vectors s_i and s_j according to the Pythagorean theorem for n -dimensional vector space:

$$d(s_i, s_j) = \sqrt{\sum_{i=0}^{n-1} [s_j - s_i]^2} \quad (3)$$

If T_s is sent to zero, the vectors s_i, s_j , that are discrete equivalents of signals $s_i(t), s_j(t)$, will become vectors of infinite dimension, and hence reduced $s_i(t), s_j(t)$ since virtually there is no sampling time. At the same time, the above mentioned sum on the right side of equation (3) is replaced by integral (excluding multiplier), and we come to the definition of the Euclidean distance for time-continuous oscillation.

According to expression (1) - (2), the similarity of signals decreases with the increase of the Euclidean distance between these signals. Consequently, a decision about observation $y(t)$ compliance of any signal from set S can be transformed to a minimum distance rule:

$$d(s_i, y) = \min_k d(s_k, y) \quad (4),$$

i.e. the decision is made in favor of the signal that is closest in meaning to the Euclidean distance to the observation y .

Finally, the rule is as follows:

$$\min d(s_i, s_j) \text{ at } \min p[y_i(t)|s_j(t)], \quad (5)$$

From the above mentioned one can make a conclusion about the possibility of applying the concept of Euclidean distance in the construction field of signals separated by a minimum, but enough distance so that the receiver with the specified input noise level can identify the true signal with a given probability. This algorithm allows to obtain the best rate for noise immunity of communication system with a given number of channels. That is, to minimize the risk of reversal signals when deciding on the receiving side, the signals must be separated at the greatest possible distance. However, assigning a valid probability of reversal, we optimize communication system throughput by the presented algorithm.

Consider the signals with linear frequency modulation (chirp) and signals with discrete frequency modulation (DFM) with relation to the Euclidean distance. The calculation of Euclidean distance was performed for couples of chirp and DFM signal on the carrier frequency $f_0 = 5$ GHz with different slope of frequency deviation. Calculation of Euclidean distance for the chirp was performed for signals with frequency deviations $fd_2 = 8$ MHz, $fd_2 = 6$ MHz relatively the signal with frequency deviation $fd_1 = 10$ MHz. For DFM signals the total frequency change is also amounts 8 MHz, 6 MHz, calculation was performed relatively the

signal with frequency change of 10 MHz. For DFM the calculation was made at 8 and 16 frequency positions. The calculation results are shown in table 1.

Table 1. Results of Euclidean distance calculation

Frequency deviation of second signal, MHz	Chirp signal	DFM signal, 8 frequency position	DFM signal, 16 frequency position
8	1,663	2,874	2,906
6	2,690	3,193	3,043

Thus, DFM signals with the least frequency position have the largest Euclidean distance at the same frequency deviation.

Conclusion. Interchannel interference limits bandwidth of communication lines with a large number of users. The possibility of increasing the throughput of communication lines by selecting a modulation method for each carrier frequency and signal separation of the communication channel is shown. This paper gives the specific characteristics of communication channels with the different kind of modulation.

References

1. Pomehozashchishchennost' radiosistem so slozhnymi signalami/ G. I. Tuzov, V. A. Sivov, V. I. Prytkov et al. ; Ed. G. I. Tuzova. - Moscow: Radio i svyaz', 1985. - p. 264
2. Gribanov A. S., Eremina V. E., Nevzorov Y. V. Issledovanie napravlenii povysheniya propusknoi sposobnosti sistem svyazi s kodovym razdeleniem kanalov. *Elektrosvyaz'*, 2013, No. 5, pp. 24-26.
3. Garanin M. V., Zhuravlev V.I., Kunegin S. V. Sistemy i seti peredachi informatsii: Uchebnoe posobie dlya vuzov. Moscow.: Radio i svyaz', 2001. -p. 336.: pic. 4
4. Ipatov V. P. Shirokopolosnye sistemy i kodovoe razdelenie signalov. Printsypy i prilozheniya. Trans./Ed. V. P. Ipatova. Moscow.: Tehnocfera, 2007. - p. 488.

EVALUATION OF MODIFIED CLUSTERING ALGORITHM CLOPE

Bilgaeva L.P., Sambyalov Z.G.

Ulan-Ude, East Siberia State University of Technology and Management (ESSUTM)

This paper studies the problem of clustering quality evaluation of modified algorithm CLOPE. As a criterion of evaluation we proposed optimal match index. The result of clustering evaluation of the method shows that modified algorithm has a higher refractive quality index in compared with the standard algorithm CLOPE.

Keywords: semi-supervised clustering, quality evaluation of clustering, categorical data, optimal matching index.

Introduction. The classical approach to the problem of clustering suggests a fully automatic process without any a priori ability to set rules for solving the problem. Thus, we can't control the clustering process. This causes that affect the result of clustering does not, i.e. the final result depends on the chosen clustering algorithm. However, there are occasions when it is necessary to influence the result of clustering. That is the final partition into clusters must conform to certain rules, which sets the analyst. This problem can be solved by the semi-supervised approach of clustering [1].

Evaluation of the quality of the resultant structure of clusters is one of the important stages in the process of clustering. Most methods of evaluation the clustering quality using quantitative indicators called indexes or metrics. The most common clustering quality indices are the following: Rand index, Jaccard index, Fowlkes-Mallows index and the purity index of clusters. Typically, the quality evaluation is performed on the previously prepared data. Test data are generated by a prearranged scheme, each object of the original set is marked number or name of the original class. Clustering result is compared with a reference partition, and then the quality index is computed.

In this paper we propose a clustering quality evaluation method of semi-supervised clustering algorithm [2] based on an algorithm CLOPE [3].

Distinctive feature of modified CLOPE is computing of the following additional characteristics of cluster:

- number of attributes that belong to i – $a(i)$;
- unique set of attribute values in the cluster C – $A(C)$;
- the weight coefficient ω_i (Each attribute a_i is characterized by a positive real number ω_i).

In addition, we propose to change the computing method of the following characteristics of cluster:

- 1) $S(C) = |C| \times \sum_{i=1}^m \omega_i$ – area of a cluster;
- 2) $W(C) = \sum_{i \in A(C)} \omega_{a(i)}$ – width of a cluster.

Evaluation of the clustering. In this paper we propose a method of clustering quality evaluation based on a computing optimal match index. Computing of the index consist of searching an injective mapping of a set of reference clusters in the final set of clusters of the partition. In that injectivity mapping intersections sum of reference clusters and final clusters is maximized. Consider the procedure for computing the index of optimal matching.

Let, A_1, \dots, A_k – a priori clusters resulting from the generation of source data array;

k – a priori the number of clusters;

n_i – number of objects in the i -th cluster;

$R_1, \dots, R_{k'}$ – clusters obtained during the execution of the algorithm;

k' – number of clusters, which was defined clustering algorithm.

To evaluate the clustering quality should compare the obtained clusters $R_1, \dots, R_{k'}$ with a priori clusters A_1, \dots, A_k . For comparison, we should get one correspondence priori cluster A_i to resulting cluster R_{p_i} . A set of indexes $\{p_1, \dots, p_k\}$ should be selected up so as to maximize the sum c_i – amount of correct defined certain objects in the a priori cluster A_i . On this basis, c_i determined by the following formula:

$$c_i = |A_i \cap R_{p_i}| : \bigcap_i p_i = \emptyset, \bigcup_i p_i = \text{argmax} \sum_i c_i \quad (1)$$

After estimating the number of correctly identified objects c_i , we compute quality clustering index by formula:

$$I = \frac{\sum_{i=1}^k \frac{c_i}{n_i}}{k} \quad (2)$$

In formula 2 the numerator is the sum of the degrees of well-defined clusters. Let define the range of the quality clustering index. The lowest value of clustering quality index possible if the algorithm identifies each object in a separate cluster. Then the value of the index is equal to:

$$I_{min} = \frac{\frac{1}{n_1} + \frac{1}{n_2} + \dots + \frac{1}{n_k}}{k} = \frac{\sum_{i=1}^k \frac{1}{n_i}}{k} \quad (3)$$

The highest value of clustering quality index possible if the algorithm accurately determine the number of clusters, and correctly determined the composition of clusters.

Determine correctness degree of each cluster is equal to unity. Then, the index value is also equal to unity:

$$I_{max} = \frac{n_1 + n_2 + \dots + n_k}{n_1 + n_2 + \dots + n_k} = \frac{k}{k} = 1 \quad (4)$$

Thus, the range of the clustering quality index is defined on the interval $[\frac{\sum_{i=1}^k \frac{1}{n_i}}{k}; 1]$, where k - number of clusters a priori. A feature of this method of estimation is that the degree of correctness of the definition of clusters has an equal contribution to the index value is determined depending on the size of clusters. This can have the effect that, if the reference partition has a large number of small-sized clusters.

To illustrate the last statement we give one more example. Suppose we have the original set, the reference partition which consists of eight clusters with the four elements and one large cluster with hundreds of elements. Assume that there are 2 working partition of the original set (Figure 1). The first partition correctly identified all small clusters, but incorrectly identified a large cluster, breaking it in half. A second partition worked the opposite way. Tables 1 and 2 present the evaluation of the two partitions by quality indices.

Table 1 – Quality evaluation of clustering 1

Index of optimal match	Rand Index	Jaccard Index	FM Index	Purity index
0,94	0,62	0,49	0,7	1

Table 2 – Quality evaluation of clustering 2

Index of optimal match	Rand Index	Jaccard Index	FM Index	Purity index
0,55	0,98	0,97	0,98	1

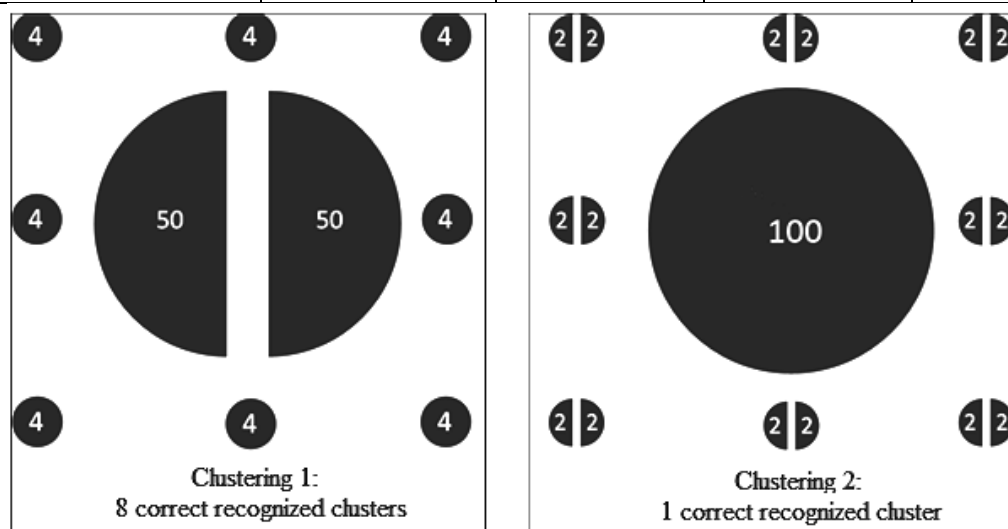


Figure 1 – Clustering samples

The tables show that the index of optimal match prefers the first partition of the second, because first case has more correctly identified clusters. Indices Rand, Jaccard and FM, the second partition on the contrary prefer the first, because these indices consider the total number of correctly identified objects into clusters without considering the correctness of the definition of each individual cluster. According to the purity index both partitions have the highest score, as each of these partitions cluster consists of the elements belonging to the same reference cluster.

The proposed method in this paper is preferable to assess the quality of clustering used in the case where the reference partition clusters are small size, and thus it is necessary to evaluate well defined clusters of. If necessary, correct estimation of the overall share of the

associated clusters reference methods should be used with indexes Rand, Jaccard or FM. For a small number of reference clusters use the method with the purity index. Thus, each quality index has its own point of view of clustering quality and in different situations is more or less applicability. In general, for a more complete evaluation of the quality of clustering is advisable to use several different methods to evaluate quality.

Analyze. For a comparative analysis of CLOPE and modified CLOPE we have made experiments of these algorithms on data sets from the open UCI Machine Learning Repository [4]. UCI Machine Learning Repository is the largest open repository of real and model data mining tasks. We have chosen the Zoo dataset for experiments. The dataset contains 101 transaction with information about animals. Each transaction contains 18 attributes describing the characteristics of the animal: the animal's name, 15 different logical attributes, one integer attribute number of limbs of an animal and the animal's biology class attribute.

A series of tests at different values of the coefficient of repulsion. All results are evaluated by quality indices Rand, Jaccard, FM, optimal matching and purity by attribute "animal biology class." The results are presented in Figure 2.

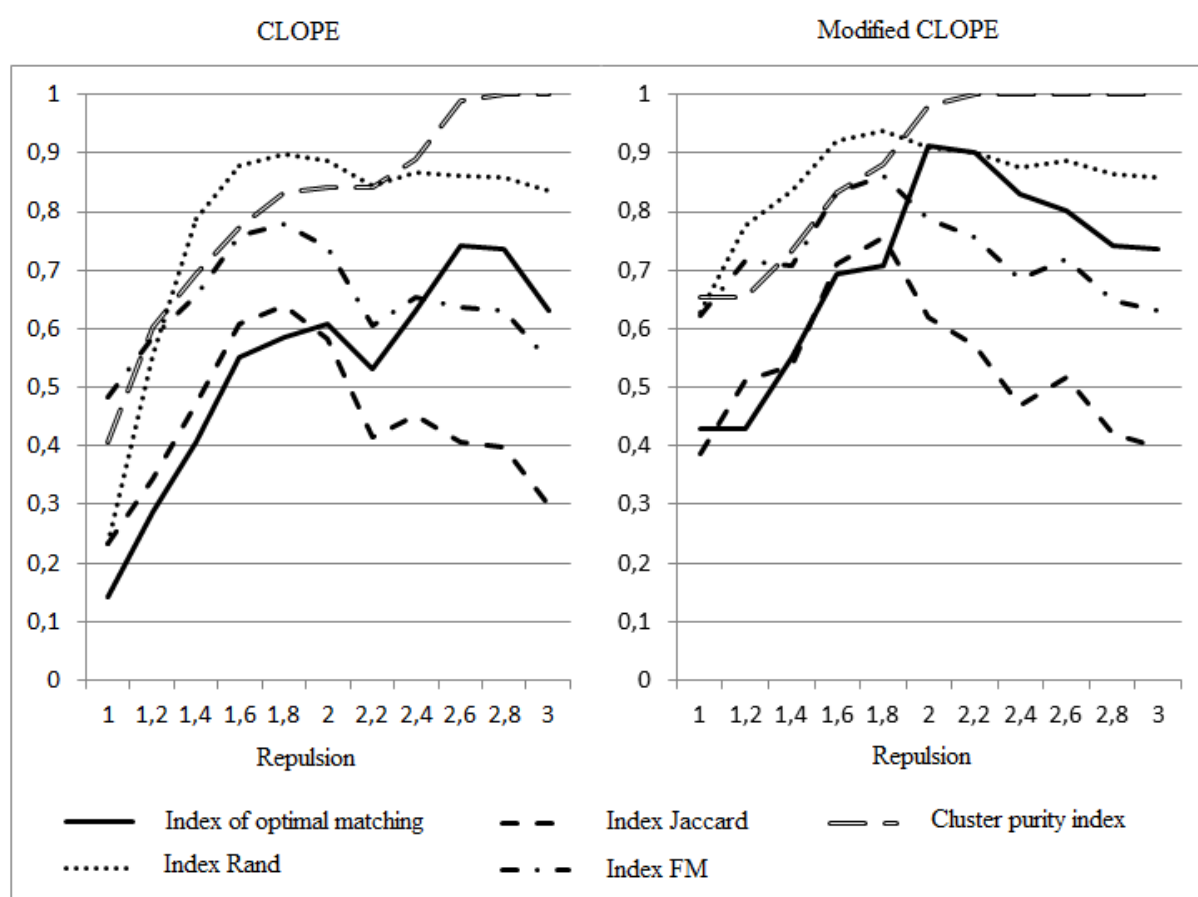


Figure 2 – Evaluation of the modified algorithm CLOPE

Clustering algorithm was modified weighting factor set to the value 2 in the attribute "animal biology class." The weighting coefficients in this attribute has been increased, since the values of this attribute are the most significant in the formation of clusters. All other attributes have a weighting factor of one.

Conclusion. Test results shows that the modified algorithm CLOPE has higher quality indices. The proposed approach allows to manage the process of clustering and obtain the

structure of clusters with different purity values on attributes. However, CLOPE modification makes algorithm more flexible and allows to solve the clustering task with the given conditions.

References

1. Nizar Grira, Michel Crucianu, Nozha Boujemaa. Unsupervised and Semi-supervised Clustering: a Brief Survey. In Proc. Of 7th ACM SIGMM international workshop on Multimedia information retrieval, 2004.
2. Yang, Y., Guan, H., You. J. CLOPE: A fast and Effective Clustering Algorithm for Transactional Data In Proc. of SIGKDD'02, 2002.
3. Bil'gaeva L.P., Sambyalov Z.G. Modifikatsiya algoritma klasterizatsii CLOPE //Fundamental'naya nauka i tekhnologii – perspektivnye razrabotki: sb. st. II mezhdunar. nauch.-prakt. konf. T.2. – Moskva: Izdatel'stvo NITs «Akademicheskii», 2013. – S. 86-90.
4. Paklin N.B. Klasterizatsiya kategoriinykh dannykh: masshtabiruemyi algoritim SLOPE [Elektronnyi resurs] //Nauchnaya biblioteka BaseGroup Labs. URL: <http://www.basegroup.ru/library/analysis/clusterization/clope>.

THE DEFINITION OF WELL-FORMED FORMULA ALGORITHM

Bazon S.A.

Ulan-Ude, East Siberia State University of Technology and Management (ESSUTM)

Abstract. This work is devoted to evaluating the results of a test tasks such as "typical problem" in automated testing systems. This work proposes methods to identify and evaluate the responses to tasks that require writing a sequences of formulas for solving the problem. This article discusses an algorithm for definition well-formed formula.

Keywords. test tasks, well-formed formula, test task “typical problem”

Introduction. In today's information society automated testing is a tool for monitoring the quality of teaching. Modern automated testing systems use different types of questions. In particular, questions allowing evaluating the ability to solving skills typical problems by entering results of the task. However, for the same class of problems, there are various methods for solving this class problem. Therefore there is a need evaluate ability to apply particular methods of solution, ie evaluate steps of solving the problem.

To solve this problem it is necessary develop a methods of recognition and evaluate answers to the tasks. This paper examines the tasks that require writing sequences of formulas for solving the problem.

The problem formulation. We introduce the following notation:

TT – test task “typical problem”;

R – answer to the task TT;

T – theory that created the test task;

$A = \{a_i \mid a_i - \text{symbol}, i = 1..k\}$ – alphabet theory T;

f_i – word in the alphabet A, $f_i \in A^*$

A^* – formulas set to answer of the test, $A^* \subseteq R$;

A_p^* – well-formed formulas set;

A_v^* – derivable formulas set;

$\overline{A_v^*}$ – not derivable formulas set;

θ_1 – quantitative indicator of the degree of correctness of the answer R;

θ_2 – qualitative indicator of the degree of correctness of the answer R.

We have a formulas set to answer of the test $A^* \subseteq R$.

Necessary to analyze a formulas set A^* , define values of θ_1 and θ_2 , for assessing the degree of correctness of the answer R .

Consider the general solution to the problem.

Methods of solving. We assume that the steps for solving the problem are represented as sequences of formulas $A^* \subseteq R$. Using the theory of ontology T [1], analyze the answer by the following algorithm.

Determine whether the formulas to answer $f_i \in A^* (i = 2..n)$ well-formed formulas, using a “*Definition of well-formed formula*”. If the formula f_i well-formed formula, it is included in the set $A_p^* (f_i \in A_p^*)$. Next formulas set A_p^* input to the algorithm “*Building a decision tree*”.

Using the algorithm “*Building a decision tree*” derive the formulas $f_{i+1} \in A_p^*$ from $f_i \in A_p^* (i = 1..n-1)$. If the formula f_i is deducible, it is included in the set A_p^* . As a result of this algorithm calculated numerical indicators that are input to the algorithm “*Determining the degree of correctness of the answer*”.

Using the algorithm “*Determining the degree of correctness of the answer*” define the values of θ_1 and θ_2 . These indicators will assess the degree of correctness of the answer R .

Consider the description of the algorithm “*Definition of well-formed formula*”.

The algorithm “*Definition of well-formed formula*”. We describe the rules for constructing formulas of the theory T , ie elements of the set $\Omega = \{\tau_1, \tau_2, \tau_3, \tau_4, \tau_5, \tau_6\}$, where:

τ_1 = “if c – constant and $c \in C$, a – variable and $a \in P$, z – operation sign and $z \in Z$, $(,)$ – delimiters and $(,) \in S$, then (cza) – formula”;

τ_2 = “if a, b – variables and $a, b \in P$, z – operation sign and $z \in Z$ и $(,)$ – delimiters and $(,) \in S$, then (azb) – formula”;

τ_3 = “if a – variable and $a \in P$, z – sign unary operation and $z \in Z$, то za – formula”;

τ_4 = “if f – formula, z – sign unary operation and $z \in Z$ и $(,)$ – delimiters and $(,) \in S$, then $z(f)$ – formula”;

τ_5 = “if f – formula, h – constant or variable and $h \in P \cup C$, z – operation sign and $z \in Z$ and $(,)$ – delimiters and $(,) \in S$, then (fzh) – formula”;

τ_6 = “if f, g – formula, z – operation sign and $z \in Z$ и $(,)$ – delimiters and $(,) \in S$, then (fzg) – formula”.

The rules $\tau_1, \tau_2, \tau_3, \tau_4$ construction rules are simple formulas, and τ_5, τ_6 – rules for constructing complex formulas [3]. This takes into account the priority of operations.

Using the rules for constructing formulas Ω , construct a binary directed tree consisting of nodes (vertices) – records of the form $G = (data, left, right)$, where $data$ – signs of operation and the atoms in the formula, $left, right$ – links to nodes that are children this node. Node $left$ is called the left child and node $right$ – right child. The tree G is constructed relatively youngest priority operation or relatively delimiter (for example, the sign “=”), part of the formula. If the formula $f_i \in A^*$ well-formed, then we construct a tree $G = (data, left, right)$ of this formula. If the formula f_i well-formed, it is included in the set A_p^* .

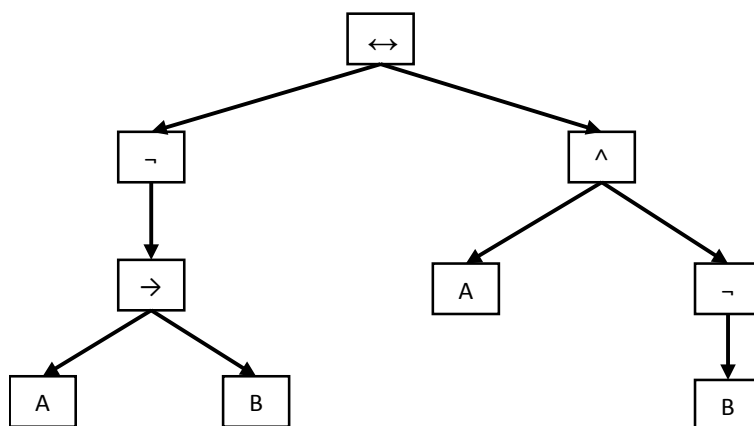


Figure 1 – Tree formulas $(A \rightarrow B) \leftrightarrow A \wedge \neg B$

Formulas $f_i \in A^*$ on which it is impossible to build a binary tree are considered ill-constructed.

Thus, analyzes formulas. Then formulas are well-formed, is input to the algorithm “Building a decision tree”.

Computational experiments. To test the algorithm was developed Java-plugin that allows you to enter formulas. In the future we plan to integrate it into Moodle LMS. Discipline "Logic" was selected for this experiment. Therefore Java-plugin allows you to enter formulas of this discipline.

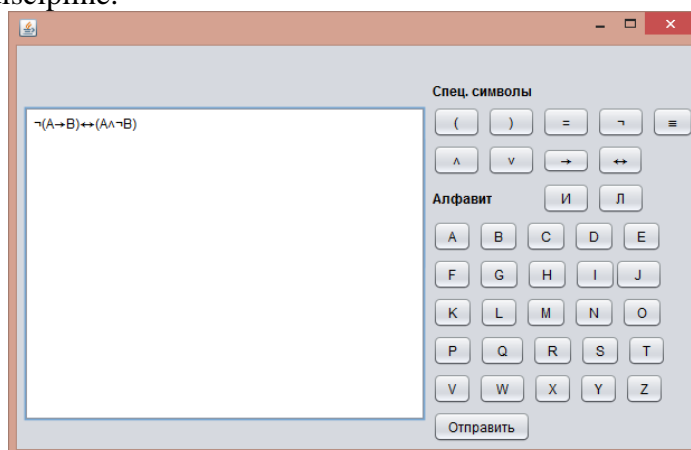


Figure 2 – Interface input formulas

By clicking on the “Send” button the program builds a binary tree $G = (data, left, right)$ for each formulas entered and saves in XML-frame. XML-frame structure corresponds to the structure of the tree $G=(data, left, right)$. After saving the XML-frame check it for compliance with the structure using DTD-validation file [2].

DTD-file for the frame formulas:

```
<! ELEMENT FRAME (FORMULA) >
<! ELEMENT FORMULA (SYMBOL+) >
<! ELEMENT SYMBOL (SYMBOL*) >
<! ATTLIST FRAME NAME CDATA #REQUIRED >
<! ATTLIST SYMBOL
TYPE CDATA #REQUIRED
VALUE CDATA #IMPLIED >
```

We describe the elements of the file:

1. FRAME – root document must have a child FORMULA.

2. FORMULA – formulas description must have one or more a child SYMBOL.
3. SYMBOL – each symbol description in the formula must have one or more a child SYMBOL.
4. Attributes:
 - a) NAME – filename binding site FRAME;
 - b) TYPE – symbol type, binding site SYMBOL;
 - c) VALUE – symbol value for an optional node SYMBOL.

Used types (TYPE) symbols:

- 1) x – left operand of binary operations;
- 2) y – right operand of binary operations, or the operand unary operation;
- 3) z – operation;
- 4) f – indicates the description of the subformula;
- 5) variable – indicates that the symbol – variable;
- 6) operation – indicates that the symbol – the operation;
- 7) sign – indicates a symbol value;
- 8) i – points to the left and right side of the formula using the attribute VALUE=1|2

Example of a valid XML-frame (formula $\neg(A \rightarrow B) \leftrightarrow A \wedge \neg B$)

```
<? xml version="1.0"?>
<! DOCTYPE FRAME SYSTEM "formula.dtd" > // Указывает на DTD-файл
<FRAME NAME="formulal.xml">
<FORMULA>
  <SYMBOL TYPE="i" VALUE="1"/>
  <SYMBOL TYPE="y">
    <SYMBOL TYPE="f">
      <SYMBOL TYPE="x">
        <SYMBOL TYPE="variable" VALUE="Переменная"/>
        <SYMBOL TYPE="sign" VALUE="A"/>
      </SYMBOL>
      <SYMBOL TYPE="y">
        <SYMBOL TYPE="variable" VALUE="Переменная"/>
        <SYMBOL TYPE="sign" VALUE="B"/>
      </SYMBOL>
      <SYMBOL TYPE="z">
        <SYMBOL TYPE="operation" VALUE="Импликация"/>
        <SYMBOL TYPE="sign" VALUE="→"/>
      </SYMBOL>
    </SYMBOL>
    <SYMBOL TYPE="z">
      <SYMBOL TYPE="operation" VALUE="Отрицание"/>
      <SYMBOL TYPE="sign" VALUE="¬"/>
    </SYMBOL>
  </SYMBOL>
  <SYMBOL TYPE="i" VALUE="2"/>
    <SYMBOL TYPE="x">
      <SYMBOL TYPE="variable" VALUE="Переменная"/>
      <SYMBOL TYPE="sign" VALUE="A"/>
    </SYMBOL>
    <SYMBOL TYPE="y">
      <SYMBOL TYPE="f">
        <SYMBOL TYPE="y">
          <SYMBOL TYPE="variable" VALUE="Переменная"/>
          <SYMBOL TYPE="sign" VALUE="B"/>
        </SYMBOL>
        <SYMBOL TYPE="z">
          <SYMBOL TYPE="operation" VALUE="Отрицание"/>
          <SYMBOL TYPE="sign" VALUE="¬"/>
        </SYMBOL>
      </SYMBOL>
    </SYMBOL>
    <SYMBOL TYPE="z">
      <SYMBOL TYPE="operation" VALUE="Конъюнкция"/>
      <SYMBOL TYPE="sign" VALUE="∧"/>
    </SYMBOL>
  </SYMBOL>
</FORMULA>
```

</FRAME>

Thus, by applying this algorithm, we obtain XML-frames for well-formed formulas in the student answer. Then XML-frames input to the algorithm “*Building a decision tree*”.

Conclusion. The developed algorithm allows to reveal well-formed formulas to answer of the test. Improperly formed formulas in the future we plan to analyze the syntax errors in the formula. The next step is to develop an algorithm “Building a decision tree”. The basis of this algorithm is planned to lay a method of automated theorem proving.

References

1. Naikhanova L.V. Tekhnologiya sozdaniya metodov avtomaticheskogo postroeniya ontologii s primeneniem geneticheskogo i avtomatnogo programmirovaniya: Monografiya. – Ulan-Ude: Izd-vo BNTs SORAN, 2008. – 244 s.
2. G.E. Berman. DOCUMENT TYPE DEFINITION [Elektronnyi resurs]. URL: - <http://gberman.narod.ru/xmllections/dtd/dtd/dtd.htm>.
3. Chen' Ch., R. Li Matematicheskaya logika i avtomaticheskoe dokazatel'stvo teorem / Pod red. S.Yu. Maslova. M.: Nauka, 1983. 360 s.
4. Bazaron S.A., Rukavichnikov A.V. Sposob raspoznavaniya i otsenivaniya otvetov na testovye zadaniya «Tipovaya zadacha» – Sbornik izdannykh trudov VII Mezhdunarodnoi nauchno-prakticheskoi konferentsii «Sovremennye informatsionnye tekhnologii i IT-obrazovanie» – Moskva, 2012. S. 619-631

INVESTIGATION OF THE THERMAL PROCESSES INFLUENCE IN ELECTORADIOPRODUCTS ON THE RELIABILITY INDICATORS OF ELECTRONIC RADIO EQUIPMENT BY USING ANALYSIS PROGRAMS OF THERMAL REGIMES

Manohin A.I., Aminev D.A., Sotnikova S.Yu., Ivanov I.A., Uvaysov S.U.
Moscow, HSE

Maintenance of reliability of radio-electronic equipment taking into account thermal modes for various classes of electroradioproducts (ERP) within the limits of system ASONIKA is considered.

This work was supported by the Russian Foundation for Basic Research (project 14-07-00422).

The reliability of the created electronic radio equipment (ERE), which determines its competitiveness on the internal and external market, largely depends on the effectiveness and quality of design. Constant complication ERE, the growth of requirements to and reduction of terms of designing causes necessity of wide use of methods of complex mathematical modeling of physical processes in the equipment. Leader of this direction is the automated system for ensuring of reliability and quality of the equipment, ASONIKA. It is a single tool that allows you to make complete calculation of parameters of reliability of electronic equipment [1-5].

Reliability is a property of the object to save time and within the established values of all parameters, characterizing the ability to perform the required functions in the given modes and conditions of use, maintenance, storage and transportation [1]. Quantitatively, the reliability of the equipment is the reciprocal of the failure rate for a specified interval of time. Reliability quantitatively characterizes the extent to which this object has certain properties, may influence the reliability. Indicators are single and comprehensive. Single indicators are:

reliability, durability, maintainability, persistence. Comprehensive reliability factors: for example, availability and more.

Availability indicators: the probability $P(t)$; average time to failure T_{cp} ; mean time between failure T_o ; gamma-percent time to failure T_γ ; failure rate $\lambda(t)$; the parameter failure rate $\omega(t)$; the average share of non-failure operating time $I(t)$; the density of the distribution system uptime $f(t)$; parameters: reliability, durability, for example, the average resource, etc.

For a basic model of dependence of one of the main indicators of reliability failure rate on temperature and accepted the equation Swedish chemist Svante Arrhenius equation (Arrhenius equation). It approximates the dependence of the rate constants of chemical reactions k on temperature many slow the processes of destruction and failures, including the ion drift, diffusion of impurities, formation of intermetallic compounds, creep, crystallographic microelectronic structural materials.

$$k = Ae^{\left(-\frac{E_A}{RT}\right)},$$

where A - a factor of frequency (for bimolecular (two-component) reactions $A \approx 10^{11}$), characterizes the frequency of collisions of reacting molecules, $R=8.31441$ - universal gas constant, E_A - the activation energy, T - the temperature in degrees Kelvin, K.

The factor of frequency A weakly depends on temperature $A = const\sqrt{T}$, the temperature from 200 °C to 300 °C leads to changes in the frequency of collisions at 10 % and is usually not considered. Activation energy is the minimum amount of energy required to tell the system (in chemistry is expressed in joules per mole) that have a reaction. The activation energy for some of radioelements fits into the range from 0.1 to 0.7 eV (9600...67500 j/mol) and is presented in the following table [5].

Table 1. The activation energy of radioelements

Type of radioelement	Activation energy	
	EV	j/mol
ICS bipolar, digital	0.4	38600
MOS, digital	0.7	67500
Transistor	0.4	38600
Diodes	0.15	14500
Stabilizer	0.12	11600
Capacitors: - electrolytic	0.17	16400
- not electrolytic	0.25	24100
Resistors: - carbon	0.36	34700
- film	0.12	11600
- wire	0.1	9600

If necessary the activation energy is determined on the basis of identification. Take two samples of a product that has worked specified time at temperatures T_1 and T_2 . Obtained failure rate is λ_1 and λ_2 allow identifying the activation energy, using a mathematical model of the form:

$$Ea = 8,617 \times 10^{-5} \frac{T_1 T_2}{T_2 - T_1} \ln \frac{\lambda_2}{\lambda_1}, \text{ EV}$$

For the first approach, the assessment of dependency failure rate on temperature can be used Vant Hoff's rule, which states that a temperature increase of 10 oC increases the rate

$$\frac{k_2}{k_1} = \gamma^{\left(\frac{T_2 - T_1}{10}\right)}$$

of reaction from 2 to 4 times: $\frac{k_2}{k_1}$, where k_1, k_2 - speed reactions at temperatures T_1 and T_2 , γ - temperature reaction coefficient.

Substituting in this equation expressions for the reaction rates from Arrhenius equation, after elementary transformations and by taking a logarithm, obtain expressions for the activation energy $E_a = R \ln(\gamma) (T(T + 10))/10 = 0,83 \ln(\gamma) T(T + 10)$, which will display graphically for $\gamma = 2$ and $\gamma = 4$ (fig. 1a).

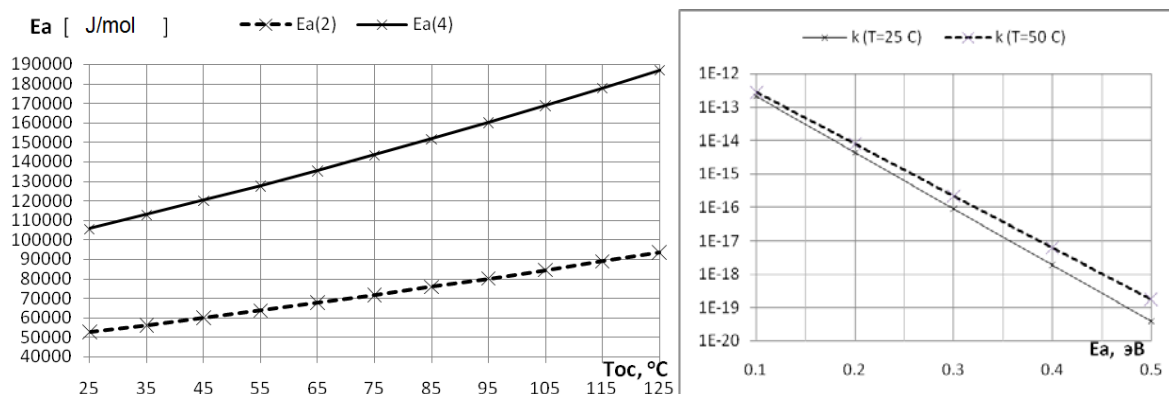


Fig. 1. The dependence of the boundary of activation energy E_a for $\gamma = 2$ and $\gamma = 4$ (a) and the dependence of the chemical reaction rate k (logarithmic scale) of activation energy at temperatures of 25 and 50 °C (b)

It is obvious (see previous table), for most real radioelements activation energy below 50,000 j/mol and the increase in the reaction rate is less than 2. Therefore, to ERP, Guy - Guff rule, consider $\gamma = 2$ and this value is often overestimated. Therefore, for a more accurate calculation of the reaction rate is better to use the Arrhenius equation. We estimate the rate of the reaction on it for two temperatures of 25 and 50 °C (fig. 1b).

Obviously, the reaction rate k decreases with increasing energy of activation and increases with increasing temperature. And the higher the energy of activation, the stronger the temperature dependence of the reaction rate. Build graphics (fig. 2) relative to the speed of reaction (referred to 25 °C) for resistors ($E_a = 0.1$ eV), bipolar transistors and ICS ($E_a = 0.4$ eV), MOS IP ($E_a = 0.7$ eV).

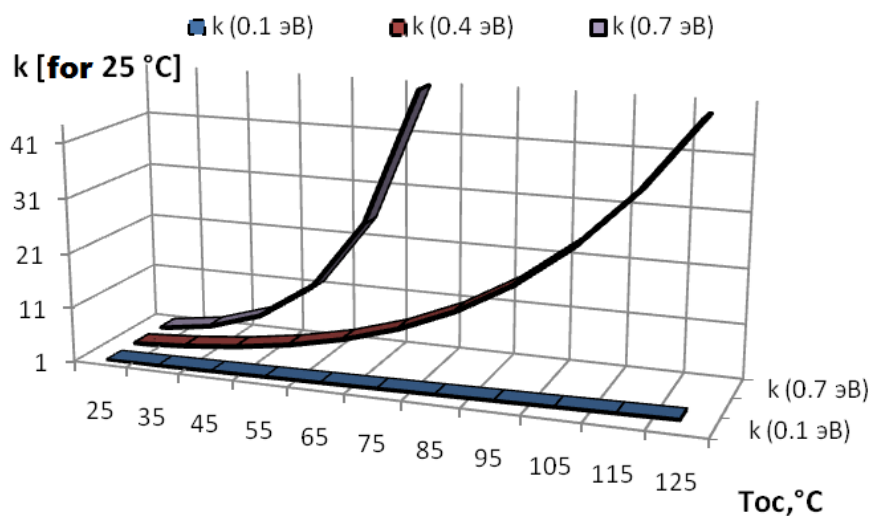


Fig. 2. The dependence of the relative velocity of chemical reaction k (reduced to 25 °C) on temperature for the activation energy of 0.1, 0.4, 0.7 eV

The higher activation energy the greater the dependence of reaction rate on temperature. All the above refers to the theoretical estimates of the rate of a chemical reaction formula Arrhenius equation. In practice, the use of experimental data collected in the reference books on reliability. According to the Handbook for domestic products [1] the mathematical model (MM) of the calculation of the failure rate of electroradioproducts (FR ERP) has the following form:

$$\lambda_{\sigma} = \lambda'_{\sigma} \times Kp \times \prod_{i=1}^n K_i$$

where λ'_{σ} - the original (the so-called basic) rate of failure (1/h) type (group) ERP given to the conditions of electrical rated load at ambient temperature $t_a = 25$ oC; K_i - the factors, taking into account changes in operating FR, depending on various factors, including temperature; n - number of significant factors.

The coefficient mode Kr (Kt, Kst) is determined by the value of the electric load and (or) ambient temperature (housing products) and is used to recalculate the initial failure rate to the actual application modes ERP equipment. These values are given in the guide in analytical form. Interesting, but these dependencies are only for ERP, and for connections brazing, metallized through holes and other such dependencies is not given. In the future, consider the dependence of the Kr on temperature as determining the dependence of the intensity of failures on temperature for ERP.

All of ERP, you split, from the point of heat view, into two categories: active (transistors, diodes, IP and etc) and passive (without internal heat sources) capacitors etc. Temperature of passive elements mainly determined by the ambient temperature and the heat from other active elements. Active ERP have overheated from its own heat dissipation on environment and for more urgent carrying out modeling of thermal regime. The main heat restriction for passive ERP are T_a - the maximum permissible ambient temperature, active possible variants: or T_a or T_c - body or T_{pnmax} - temperature p-n junction (active area).

Evaluate the change of temperature dependent Kr typical species ERP: active - ICS, transistor, resistor and passive - condenser. The calculation formulas for the regime coefficient will take from the Handbook of reliability ERP [1], and bring them to the table.

Table 2. Mathematical models of regime coefficients Kr for typical ERP

Mathematical model	Describing variables (t – the ambient temperature, oC)
Integrated micro circuits (ICS)	
$K_{D^*} = Ae^{B(t+273)}$	where A and B – constants tabulated coefficients that depend on the type of ICS
Ceramic, with inorganic thin-film, dielectric condensers	
$K_{D^*} = A \left[\left(\frac{U / U_t}{N_s} \right)^H + 1 \right] e^{B \left(\frac{t+273}{N_t} \right)^G}$	where A, B, Nt, G, H, Ns – constant coefficients; U - operating voltage, V; Un - rated voltage.
Permanent no wire resistor: metal-dielectric, metallic	
$K_{D^*} = Ae^{B \left(\frac{t+273}{N_t} \right)^G} e^{\left[\frac{P / P_t}{N_s} \left(\frac{t+273}{273} \right)^J \right]^H}$	where A, B, Nt, G, Ns, J, H – constant coefficients; P – working power dissipation resistors, W; Pn – rated dissipation power resistors, W.
The silicon medium-power transistor 2T504A	

$K_p = A \cdot e^{\left(\frac{N_t}{273+t+(175-ti \cdot \ddot{a} \ddot{o} . i \cdot \hat{a} \hat{e} \hat{n} .) + \square t \cdot \hat{E} \cdot \hat{y} \hat{e} \left(\frac{ti \cdot \ddot{a} \ddot{o} . i \cdot \hat{a} \hat{e} \hat{n} - t \hat{n} i \cdot \hat{e} \alpha}{150} \right)} \right)} \times$ $\cdot e^{\left(\frac{273+t+(175-ti \cdot \ddot{a} \ddot{o} . i \cdot \hat{a} \hat{e} \hat{n} .) + \square t \cdot \hat{E} \cdot \hat{y} \hat{e} \left(\frac{ti \cdot \ddot{a} \ddot{o} . i \cdot \hat{a} \hat{e} \hat{n} - t \hat{n} i \cdot \hat{e} \alpha}{150} \right)}{T_i} \right)^L}$	where A, N _t , T _M , L, Δt – tabular permanent models [1]
Microwave transistor-based AsGa	
$K\delta = A \cdot e^{\left(\frac{N_t}{273+t+\square t + \hat{E} \cdot \hat{y} \hat{e}} \right)}$	see above

Now let's build the graphics for the relevant ERP (fig. 3).

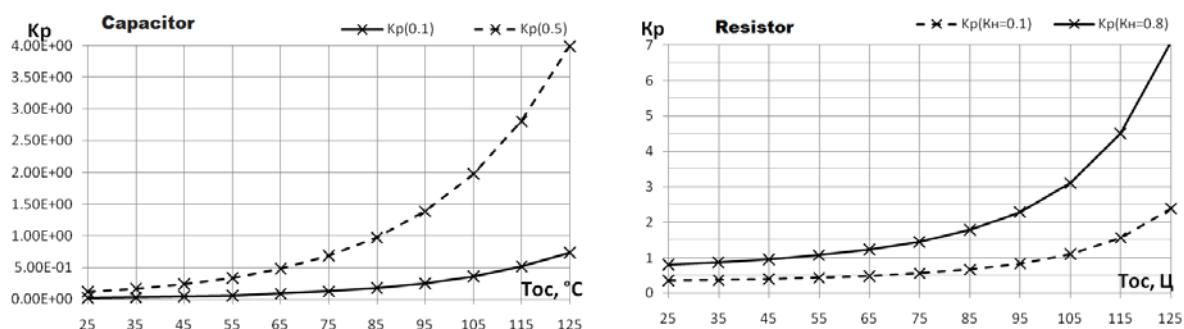


Fig. 3. The dependence of the regime coefficient Kr from Ta for condensers and resistors at a load factor for condensers KN = 0.1 and 0.5 (a), and resistors for KN = 0.1 and 0.8 (b)

Thus, when the ambient temperature of 10 C from 25 to 35 degrees failure rate condensers increased by 42 % for both coefficients load (KN = 0.1 and for KN = 0.5). For resistors FR increase of 5 % for KN = 0.1 and 8 % for KN = 0.8.

Consider the dependence of the Kr on the ambient temperature for logical circuits with different degree of complexity: 10-100 elements (A = 20-3 and B = 20.7-3), and 1000-5000 (A = 16-3 and B = 20.7-3) elements (fig. 4).

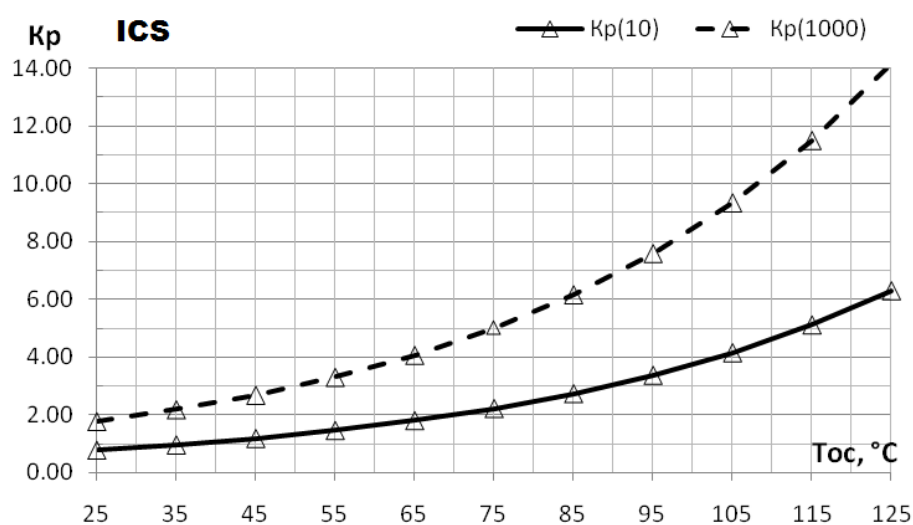


Fig. 4. The dependence of the regime coefficient from the ambient temperature for integrated circuits with different degree of complexity

Now we give the results of calculations presented above in the form of graphs in a tabular form (table 3). In column Kst10(norm) and Kst1000(norm) shows the values Kst10 and Kst1000 normalized to a temperature of 25 °C, i.e. up to this temperature $Kst10(norm) = Kst1000(norm) = 1.0$.

Table 3. The dependence of the regime coefficient Kst and Kst normalized to 25 degrees from the ambient temperature for ICS to a different degree of complexity (for 10 elements and for 1000 items).

Ta	Kst10	Kst1000	Kst10(norm)	Kst1000(norm)
25	0.78714	1.77106	1.00	1.00
35	0.96913	2.18055	1.23	1.23
45	1.19321	2.68473	1.52	1.52
55	1.46910	3.30547	1.87	1.87
65	1.80877	4.06974	2.30	2.30
75	2.22698	5.01071	2.83	2.83
85	2.74189	6.16926	3.48	3.48
95	3.37585	7.59567	4.29	4.29
105	4.15640	9.35189	5.28	5.28
115	5.11741	11.51417	6.50	6.50
125	6.30062	14.17640	8.00	8.00

Thus, when the temperature of the environment from 25 °C to 35 °C failure rate increased by 23 % for both types of chips.

We will consider the medium-transistor silicon 2T504A (fig. 5). If the ambient temperature exceeds the value of t , electric load on the device must be reduced, because otherwise the transition temperature exceeds the maximum allowed.

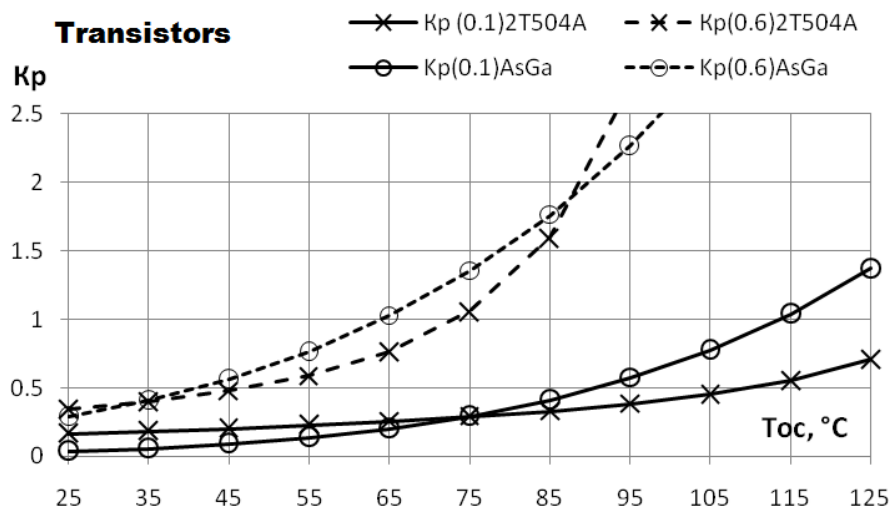


Fig. 5. The dependence of the regime coefficient of the ambient temperature for 2T504A and AsGa microwave transistors at a load factor $KN = 0.1$ and $KN = 0.6$

Thus, when the temperature of the environment from 25 °C to 35 °C failure rate increased 12 % for $KN = 0.1$ % and 16% for $KN = 0.6$. I.e. for heat-loaded dependency element of reliability from the temperature is a little higher.

Evidently for transitory 2T504A when the load ratio is 0.6 the ambient temperature more than 85 °C is invalid and for the work it is necessary to reduce the load ratio.

RF transistor change of ambient temperature from 25 to 35 degrees Cu 58 % for KN=0.1 % and 43% for KN=0.5. I.e. for heat-loaded dependency element of reliability from the temperature a little below.

For microwave transitory if KN = 0.1 a maximum ambient temperature is 115 °C, for KN = 0.5 a maximum ambient temperature is 75 °C.

Table 4. The increase in the estimated failure rate (%) at elevated ambient temperature from 25 °C to 35 °C for different ERP at different KN

	Transistor	UHF transistor	Resistor	Capacitor	ICS
KN(min)	12 %	58 %	5 %	42 %	23 %
KN(max)	16 %	43 %	8 %	42 %	23 %

The most heat-dependent proved microwave transistors of gallium arsenide. Unfortunately for semiconductor ERP - transistors, diodes in specifications there is inconsistency in the indication of the maximum permissible temperature – it is or the ambient T_a or the body T_b or crystal (active area) T_{pmax} . Although it is obvious that the main constraint is the temperature of the transition, as the crystal is the most heated and the temperature - sensitive element ERP (Fig. 4.):

$$T_{per} = T_a + \Delta t_{per-body} + \Delta t_{body-a} = T_a + P \cdot R_{int} + \Delta t_{body-a}$$

As an example consider the thermal regime of the transistor [4]. In the beginning let us consider the thermal regime of the transistor, without respect to its installation on the printed circuit Board (PCB) (hanging in the air 4, 6, and in the second case the transistor will be installed on PCB.

Graphically the model of a thermal mode (MTP) of the transistor executed is given in a subsystem of thermal calculation of ASONIKA-T [3] below (fig. 6), and behind it decryption of the reference designations of this MTP is provided also.

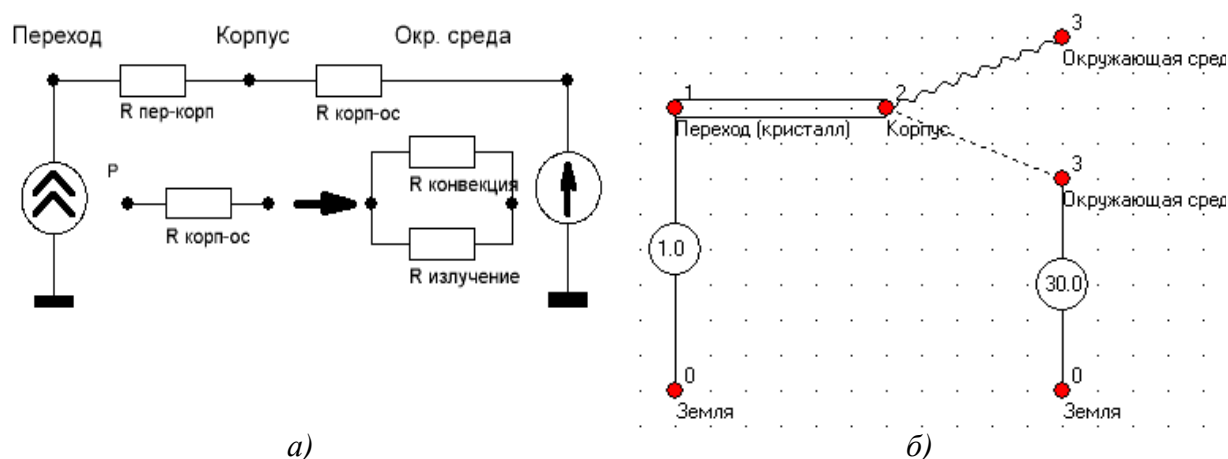


Fig. 6. The topological model of thermal process (MTP) of the isolated transistor as a) in the form of the equivalent electrical circuit, b) model in the form of the undirected graph in a subsystem of ASONIKA-T

Nodes of topological MTP: 1 - crystal of the transistor, 2 - the transistor body, 3 – environment.

The branch 1-2 of MTP simulates thermal resistance transition – body and is usually set in specifications for ERP. The source of heat release in 1 W - describes heat release in semiconductor transition of the transistor. Branches 2-3 describe the radiation and convection in environment from a surface of the transistor body.

After creations of MTP it is possible to calculate in a subsystem ASONIKA-T the temperatures of these elements. In this specific case it was temperatures transition $T_{per} = 51$ °C, the body $T_k = 41$ °C, in case of environment of $T_a = 30$ °C i.e. temperature difference between transition and environment is about 20 °C. It is obvious that the greatest temperature will be on a transistor crystal, slightly less on the body and the lowest – ambient temperature.

We will construct MTP of the transistor and the resistor set on the printed circuit board (PCB). The part of MTP from a crystal before the body is similar. The Nodes of MTP 2-19 simulate PCB. Nodes 18 and 19 - the body of ERP on PCB. Node 20 – a transistor crystal. The node 1 – environment. The heat flow from the body shares on two parts – the part of a flow is sent by convection and radiation to environment, and the part through outputs (thermal resistance of fixing) refluxs on the printed circuit board (PCB). On PCB heat spreads and by a heat emission is transferred in the environment.

As it was already spoken, in reality ERP usually set on a printing node therefore it is necessary to carry out calculation of the thermal ERP mode as a part of a printing node (see fig. 7). As the printing node is the main constructive node of ERP, for its calculation there is subsystem ASONIKA-TM intended for calculation thermal and mechanical modes of printing nodes. Though MTP in this case even is more difficult, than in the previous case, but for a printing node as a standard node, MTP is built automatically and therefore here isn't provided.

Calculation of a thermal mode of a printing node with different elements set on it showed that temperature of the transistor decreases. That says that PCB executes a role of an element of additional cooling.

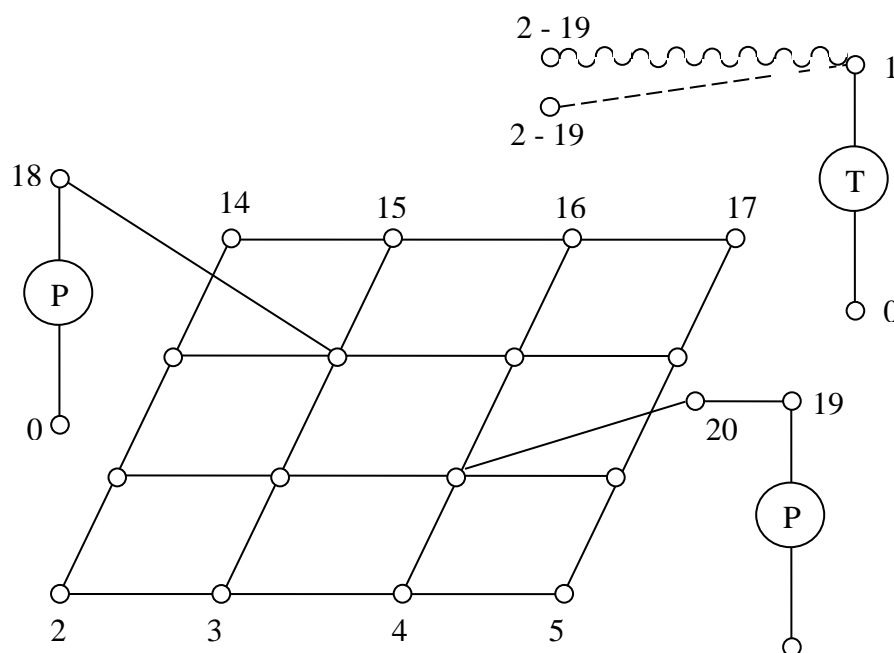


Fig. 7. The model of thermal process (MTP) of transistor with a printed circuit board

Powerful transistors at the big capacities require use of the radiator and MTP becomes even more difficult. As not always there is an opportunity to carry out thermal calculation, in the reference manual on reliability recommendations about count of these temperatures each other are made.

Conclusions

For medium - performance transistor by the increase of the load coefficient sharply decreases the maximum operating temperature of the environment.

The limitation of the working temperature ERP must be made before the calculation of reliability, as in the model of reliability they can't be tracked. Widely used Vant Hoff's rule that the failure rate ERE rising twice when the temperature by 10 degrees gives depend assessment.

To clarify the temperature conditions may be advisable to use a subsystem of thermal processes analysis ASONIKA-T, TM [2]. For the automated calculation of reliability, you can use a subsystem of reliability and quality ASONIKA-K [2].

References

1. Nadezhnost' yelektroradioizdelii: Spravochnik. - M.: MO RF, 2004. – 620 s.
2. Shalumov A., Malyutin N., Kofanov YU. Avtomatizirovannaja sistema ASONIKA dlja proektirovanija vysokonadezhnyh radioelektronnyh sredstv na principah CALS-tehnologii. Tom 1 Izdatel'stvo: Yenergoatomizdat, 2007. – 368 s.
3. Kofanov Y.N., Manohin A.I., Uvaisov S.U. Modelirovanie teplovyh processov pri proektirovanii, ispytaniyah i kontrole kachestva radioelektronnyh sredstv: Ucheb. posobie. / MGIYeM., M., 1998. – 140 s.
4. Manohin A.I. Issledovanie teplovyh rezhimov radioapparatury s pomosh'yu vychislitel'nogo yeksperimenta.// Sovremennye problemy radioelektroniki. //Sb. nauchnyh trudov. Pod redakciei A. V. Sarafanova. – Krasnojarsk: IPC KGTU, 2003. – s. 505-511.
5. Starostin A.K., Okshevskii L.L. Yelementy osnov nadezhnosti avtomobil'noi yelektroniki. M.: NPO «Avtoelektronika», 1995. – 137s.

DIRECT AND REVERSE PROJECTION PROCEDURES IN PROBLEMS OF 3D OBJECTS RECONSTRUCTION FROM IMAGES

Veselov E.A., Uvaysov S.U., Furman, Ya. A., Lvov B.G.
Moscow, HSE

This article presents a research of direct and reverse projection procedures. Presents Mathematical calculations of spatial situated point projection are presented as particular case for obtaining the expressions which describe this process. The application of these processes in problems of three-dimensional object reconstruction from images is demonstrated by a simple 3D object.

The fundamental problem of three-dimensional object reconstruction from images based on its projections on the surface is the determination of the coordinates of points on its surface. This problem can be solved by using the methods of direct and reverse projection [4].

As an example, we provide a special case where only one surface point is taken as research object (Fig. 1). Thus, there are two questions of fundamental importance are connected with the process of projection: to determine the location of their projection for a given an arbitrary point of the object and to determine where the straight line, which should be an appropriate point on the subject for this arbitrary point of the projection [1].

The process of the point **B** projection on the plane XOY is illustrated for the two watchpoint are set the guide vectors **d₁** and **d₂** on Fig. 1. We assume that:

- 1) $\mathbf{B} = \{x; y; z\}$ – the coordinates of the intersection of two straight \mathbf{L}_1 and \mathbf{L}_2 point;
- 2) The straight \mathbf{L}_1 has the direction vector $\mathbf{d}_1 = d_{11}\mathbf{i} + d_{12}\mathbf{j} + d_{13}\mathbf{k}$ and passes through the point $\mathbf{C}_1 = C_{11}\mathbf{i} + C_{12}\mathbf{j}$ on plane \mathbf{XOY} .
- 3) The straight \mathbf{L}_2 has the direction vector $\mathbf{d}_2 = d_{21}\mathbf{i} + d_{22}\mathbf{j} + d_{23}\mathbf{k}$ and passes through the point $\mathbf{C}_2 = C_{21}\mathbf{i} + C_{22}\mathbf{j}$ on plane \mathbf{XOY} .

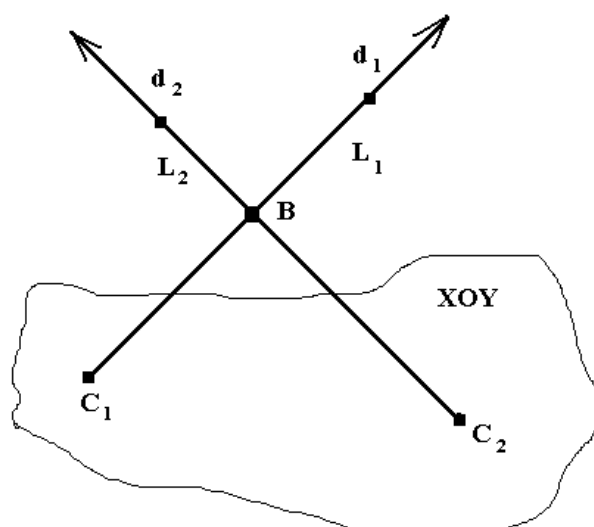


Fig. 1. Intersection of two straight point \mathbf{L}_1 and \mathbf{L}_2 its projection on the plane \mathbf{XOY} .

We calculate the formulas to determining the coordinates of the projection of a point, which characterized the process forward projection [3]. Recorded for straight \mathbf{L}_1 and \mathbf{L}_2 the

following relations based on the principles equation of the straight line passing through point:

$$\frac{x - C_{11}}{d_{11}} = \frac{y - C_{12}}{d_{12}} = \frac{z}{d_{13}} \quad (1)$$

$$\frac{x - C_{21}}{d_{21}} = \frac{y - C_{22}}{d_{22}} = \frac{z}{d_{23}} \quad (2)$$

After the transformation we have expressions to define the coordinates of the point projection on the surface for watchpoint \mathbf{d}_1 :

$$C_{11} = x - \frac{d_{11} \cdot z}{d_{13}} \quad (3)$$

$$C_{12} = y - \frac{d_{12} \cdot z}{d_{13}} \quad (4)$$

We have the same results for watchpoint d_2 :

$$C_{21} = x - \frac{d_{21} \cdot z}{d_{23}} \quad (5)$$

$$C_{22} = y - \frac{d_{22} \cdot z}{d_{23}} \quad (6)$$

Reverse projection problem is the need to calculate the coordinates of the object, in particular, point B on available projections of the point onto the plane XOY [4].

We calculate the variable x from the expressions for the process forward projection (3)

and (4) which is the coordinate of point B on the axis OX for both projection (for L_1 and L_2

respectively):

$$x = \frac{d_{11} \cdot z}{d_{13}} + C_{11} \quad (7)$$

$$x = \frac{d_{21} \cdot z}{d_{23}} + C_{21} \quad (8)$$

If expression (7) to be equal to expression (8) we obtain the following results:

$$(y - C_{12}) \frac{d_{11}}{d_{12}} = z \frac{d_{11}}{d_{13}} \quad (9)$$

$$(y - C_{22}) \frac{d_{21}}{d_{22}} = z \frac{d_{21}}{d_{23}} \quad (10)$$

In order to find an expressions for all three coordinates of point B , it is necessary to formulate and solve a system of equations (9) and (10):

$$\begin{cases} (y - C_{12}) \frac{d_{11}}{d_{12}} = z \frac{d_{11}}{d_{13}} \\ (y - C_{22}) \frac{d_{21}}{d_{22}} = z \frac{d_{21}}{d_{23}} \end{cases} \Rightarrow \begin{cases} y \frac{d_{11}}{d_{12}} - z \frac{d_{11}}{d_{13}} = C_{12} \frac{d_{11}}{d_{12}} \\ y \frac{d_{21}}{d_{22}} - z \frac{d_{21}}{d_{23}} = C_{22} \frac{d_{21}}{d_{22}} \end{cases} \quad (11)$$

This system of equations is solved by the method of Kramer [2]. We obtain the following keys as a result of preliminary transformations on the chosen method:

$$\Delta = \begin{vmatrix} \frac{d_{11}}{d_{12}} & -\frac{d_{11}}{d_{13}} \\ \frac{d_{21}}{d_{22}} & -\frac{d_{21}}{d_{23}} \end{vmatrix}, \quad \Delta_1 = \begin{vmatrix} C_{12} \frac{d_{11}}{d_{12}} & -\frac{d_{11}}{d_{13}} \\ C_{22} \frac{d_{21}}{d_{22}} & -\frac{d_{21}}{d_{23}} \end{vmatrix}, \quad \Delta_2 = \begin{vmatrix} \frac{d_{11}}{d_{12}} & C_{12} \frac{d_{11}}{d_{12}} \\ \frac{d_{21}}{d_{22}} & C_{22} \frac{d_{21}}{d_{22}} \end{vmatrix}.$$

This qualifiers are calculated:

$$\Delta = -\frac{d_{11}}{d_{12}} \frac{d_{21}}{d_{23}} - \left(-\frac{d_{11}}{d_{13}} \frac{d_{21}}{d_{22}} \right) = \frac{d_{11}}{d_{13}} \frac{d_{21}}{d_{22}} - \frac{d_{11}}{d_{12}} \frac{d_{21}}{d_{23}},$$

$$\Delta_1 = -C_{12} \frac{d_{11}}{d_{12}} \frac{d_{21}}{d_{23}} - \left(-C_{22} \frac{d_{11}}{d_{13}} \frac{d_{21}}{d_{22}} \right) = C_{22} \frac{d_{11}}{d_{13}} \frac{d_{21}}{d_{22}} - C_{12} \frac{d_{11}}{d_{12}} \frac{d_{21}}{d_{23}},$$

$$\Delta_2 = C_{22} \frac{d_{11}}{d_{12}} \frac{d_{21}}{d_{22}} - C_{12} \frac{d_{11}}{d_{12}} \frac{d_{21}}{d_{22}} = (C_{22} - C_{12}) \frac{d_{11}}{d_{12}} \frac{d_{21}}{d_{22}}.$$

The coordinates y and z are calculated from the received data:

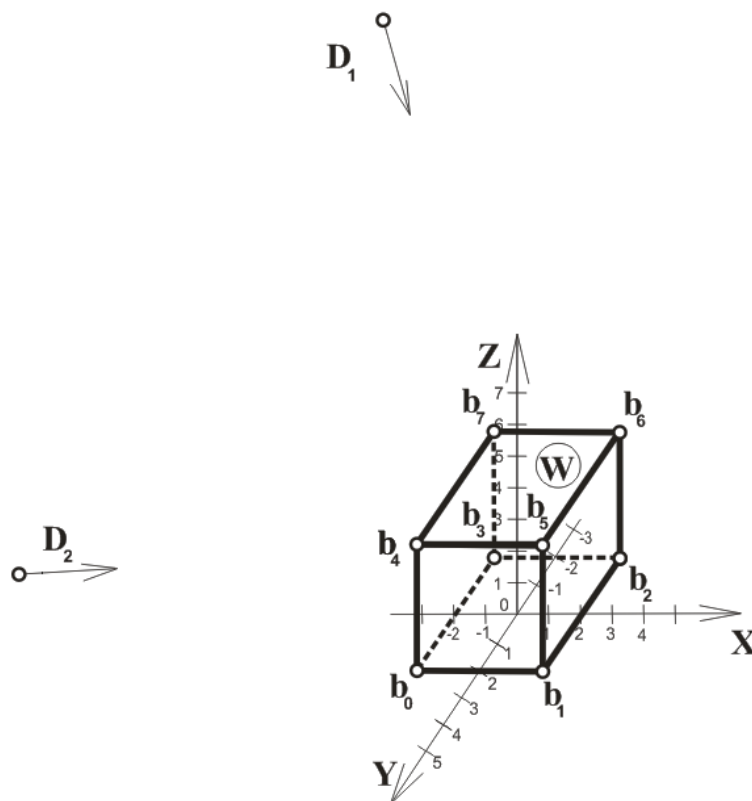
$$y = \frac{\Delta_1}{\Delta} = \frac{C_{22} \frac{d_{11}}{d_{13}} \frac{d_{21}}{d_{22}} - C_{12} \frac{d_{11}}{d_{12}} \frac{d_{21}}{d_{23}}}{\frac{d_{11}}{d_{13}} \frac{d_{21}}{d_{22}} - \frac{d_{11}}{d_{12}} \frac{d_{21}}{d_{23}}} \quad (12)$$

$$z = \frac{\Delta_2}{\Delta} = \frac{(C_{22} - C_{12}) \frac{d_{11}}{d_{12}} \frac{d_{21}}{d_{22}}}{\frac{d_{11}}{d_{13}} \frac{d_{21}}{d_{22}} - \frac{d_{11}}{d_{12}} \frac{d_{21}}{d_{23}}} \Rightarrow z = \frac{C_{22} - C_{12}}{\frac{d_{12}}{d_{13}} - \frac{d_{22}}{d_{23}}} \quad (13)$$

Accordingly, the x coordinate is calculated:

$$x = \frac{d_{21} \cdot (y - C_{22})}{d_{22}} + C_{21} \quad (14)$$

As a consequence basic mathematical relationships for the description of direct and reverse projection procedures are obtained. In such way, it is possible to reconstruct the coordinates of points on the surface of the 3D object from coordinates of the points of its projections on the surface. For example, a simple polytope in the form of a rectangular parallelepiped is taken and made the procedures of direct and reverse parallel projection (the direction vector of watchpoint to each point of the projected object are parallel) (fig. 2).

Fig. 2. Object **W**

Object **W** is projected on the underlying surface with two watchpoints ($\mathbf{D}_1 = -10\mathbf{i} + 10\mathbf{j} + 10\mathbf{k}$ и $\mathbf{D}_2 = -10\mathbf{i} - 10\mathbf{j} + 10\mathbf{k}$) to obtaining the necessary two projections for subsequent recovery. The underlying surface is ground plane of the object ($\mathbf{b}_0, \mathbf{b}_1, \mathbf{b}_2, \mathbf{b}_3$). Coordinates of the projected object are next ($\mathbf{b}_n = b_1\mathbf{i} + b_2\mathbf{j} + b_3\mathbf{k}$):

$$\mathbf{b}_0 = -2\mathbf{i} + 2\mathbf{j};$$

$$\mathbf{b}_4 = -2\mathbf{i} + 2\mathbf{j} + 4\mathbf{k};$$

$$\mathbf{b}_1 = 2\mathbf{i} + 2\mathbf{j};$$

$$\mathbf{b}_5 = 2\mathbf{i} + 2\mathbf{j} + 4\mathbf{k};$$

$$\mathbf{b}_2 = 2\mathbf{i} - 2\mathbf{j};$$

$$\mathbf{b}_6 = 2\mathbf{i} - 2\mathbf{j} + 4\mathbf{k};$$

$$\mathbf{b}_3 = -2\mathbf{i} - 2\mathbf{j};$$

$$\mathbf{b}_7 = -2\mathbf{i} - 2\mathbf{j} + 4\mathbf{k}.$$

Using expression (3) and (4) coordinates of the projections of points $\mathbf{b}_4, \mathbf{b}_5, \mathbf{b}_6$ and \mathbf{b}_7

are calculated. After transformations we obtain the following data:

- projections of points \mathbf{b}_4 : $\mathbf{C}_1 = 2\mathbf{i} - 2\mathbf{j}$ и $\mathbf{C}_2 = 2\mathbf{i} + 6\mathbf{j}$;

- projections of points \mathbf{b}_5 : $\mathbf{K}_1 = 6\mathbf{i} - 2\mathbf{j}$ и $\mathbf{K}_2 = 6\mathbf{i} + 6\mathbf{j}$;

- projections of points \mathbf{b}_6 : $\mathbf{M}_1 = 6\mathbf{i} - 6\mathbf{j}$ и $\mathbf{M}_2 = 6\mathbf{i} + 2\mathbf{j}$;

- projections of points \mathbf{b}_7 : $\mathbf{N}_1 = 2\mathbf{i} - 6\mathbf{j}$ и $\mathbf{N}_2 = 2\mathbf{i} + 2\mathbf{j}$.

Projections of the object \mathbf{W} on the surface looks like this after conducting a direct parallel projection (Fig. 3):

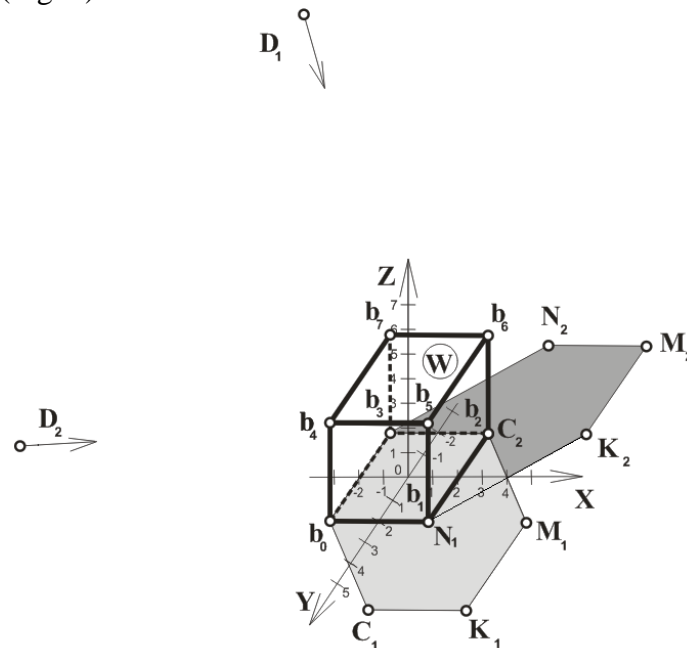


Fig. 3. The projection of the object points to \mathbf{W} on the plane \mathbf{XOY}

To conduct reverse parallel projection setting only the coordinates of the projection of points on the surface (Fig. 4). In fact, this process is the reconstruction of a three-dimensional object from a two-dimensional image, because all point projections are in one plane [4].

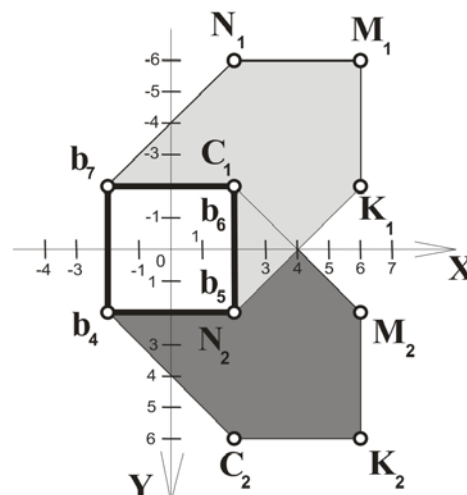


Fig. 4. The projection of the object \mathbf{W} relative to watchpoint \mathbf{D}_1 и \mathbf{D}_2

Using the previously derived expressions of reverse projection we can find the point coordinates of the object $\mathbf{b}_4, \mathbf{b}_5, \mathbf{b}_6$ and \mathbf{b}_7 (the coordinates of the points of the base object \mathbf{W} are known). For example, let us consider finding of one of the points, and others are calculated in the same way.

Using formulas (12), (13) and (14) point coordinates are reconstructed from points projections $\mathbf{c}_1 = 2\mathbf{i} - 2\mathbf{j}$ и $\mathbf{c}_2 = 2\mathbf{i} + 6\mathbf{j}$:

$$y = \frac{\Delta_1}{\Delta} = \frac{c_{22} \frac{d_{11}}{d_{13}} \frac{d_{21}}{d_{22}} - c_{12} \frac{d_{11}}{d_{12}} \frac{d_{21}}{d_{23}}}{\frac{d_{11}}{d_{13}} \frac{d_{21}}{d_{22}} - \frac{d_{11}}{d_{12}} \frac{d_{21}}{d_{23}}} = \frac{6 \frac{(-10)}{10} \frac{(-10)}{(-10)} - (-2) \frac{(-10)}{10} \frac{(-10)}{10}}{\frac{(-10)}{10} \frac{(-10)}{(-10)} - \frac{(-10)}{10} \frac{(-10)}{10}} = 2;$$

$$z = \frac{c_{22} - c_{12}}{\frac{d_{12}}{d_{13}} - \frac{d_{22}}{d_{23}}} = \frac{6 - (-2)}{\frac{10}{10} - \frac{(-10)}{10}} = 4;$$

$$x = \frac{d_{21} \cdot (y - c_{22})}{d_{22}} + c_{21} = \frac{(-10) \cdot (2 - 6)}{(-10)} + 2 = -2;$$

$$\mathbf{b}_4 = -2\mathbf{i} + 2\mathbf{j} + 4\mathbf{k}.$$

Similarly the remaining points are reconstructed:

$$\mathbf{b}_5 = 2\mathbf{i} + 2\mathbf{j} + 4\mathbf{k}, \mathbf{b}_6 = 2\mathbf{i} - 2\mathbf{j} + 4\mathbf{k} \text{ и } \mathbf{b}_7 = -2\mathbf{i} - 2\mathbf{j} + 4\mathbf{k}.$$

Based on the data obtained in the process of review direct and reverse projection procedures the following conclusions can be make:

- as one of the methods in the problems of reconstruction of three-dimensional objects you can use the reverse projection in the analysis of two-dimensional images;
- this method is quite effective and simple, do not demands the complex mathematical operations;
- for reconstruction the coordinates of a point object you must have not less than two projections on the surface.

References

1. Barbash, Yu. L. Static pattern recognition theory questions. / Yu. L. Barbash, B. V. Varskiy, V. S. Zinov'ev; Pod red. Varskogo B.V. – M.: Sov. radio, 1977.
2. Efimov, N. V. Linear algebra and multidimensional geometry. / N. V. Efimov, E. R. Rozendorn. – M.: Main edition of physical and mathematical literature "Science"1974.
3. Furman, Ya. A. Introduction to the contour analysis and its position to the image processing and signal processing./ Ya. A. Furman, A. V. Krevetskiy, A. K. Peredreev, A. A. Rozhentsov, R. G. Khafizov, I. L. Egoshina, A. N. Leukhin; pod red. Ya. A. Furmana. – M.: FIZMATLIT, 2002. – 592 s.
4. Furman, Ya. A. Recovering 3D image object from its perspective projection on a flat surface./ Ya. A. Furman, E. A. Popov, R. V. Eruslanov // Vestnik MarGTU. – 2010. - №2(9). – S. 53-66.

INDEX

Abalov N.V.	514	Chernov P.S.	528
Abed O.A.	67	Chorna O. S.	655
Abrameshin A.E.	319	Dambaeva S.V.	600
Afanasyeva M. A.	417	Denisova O. I.	655
Al-Saadi H.A.	79	Dianov V.N.	14, 519, 523
Alsova O.K.	207	Djudjun D.E.	281
Americanov A.A.	216	Dmitriev A.V.	161
Aminev D.A.	702	Dobroserdov O.G.	290
Andronik A.V.	112, 121, 107	Domnin A.L.	26
Aniskov R.V.	144	Dunham D.	642
Anop M.	3	Dunin V. O.	294
Aringazin A. K.	389	Dykov M.A.	609
Artemov I. I.	490	Egorov V. A.	294
Artyukh S.V.	84	Egunov V.A.	67, 79, 81, 84
Astafjev A.V.	683	Elizarov A.A.	380
Atabaeva V.D.	321	Elizarov V.N.	535
Avakyan A.	589	Enatskaya N.Yu.	282
Avdeuk O.A.	52, 55, 97, 157, 163, 165	Eremin D.V.	398
Avilova E.D.	195	Eremina V.	691
Ayusheeva N.N.	502	Fedin N. A.	18
Bagmutov V. P.	184	Fedorenko J.V.	311
Balakina E.V.	101	Fedorov E.I.	514
Barilla J.	337	Fedoseev S.V.	620, 683
Baulina O. V.	226	Fedotov V.N.	195
Baydachenko V.A.	167	Fedyanov E.A.	133
Bazaron S.A.	698	Finochenko V.A.	629
Belomoytsev D.E.	681	Fokin V. M.	644
Berketov G.A.	620, 683	Furman Ya. A.	710
Bilgaeva L.P.	694	Gazizov T.R.	452
Bogachev K.A.	216	Gevondian T.A.	519
Bogdanov E. P.	184	Girich V. S.	59, 62, 65
Bolotova L.S.	558	Gluhova O.E.	314
Bondarev A.	89	Goldovskii Y. M.	474
Borisov N.I.	633	Golev D.M.	345
Borisova A.V.	629	Golushko D.A.	512
Borodin A.K.	101	Gorobcov A.S.	121
Botvinkin P.	351	Gorodov E.Y.	514
Brodsky Yu. I.	234	Gorunov A. I.	129
Bublík T.	244	Goryachev N.V.	443
Bulgakova N.V.	514	Grab I.D.	443
Burukina I. P.	606	Grachev N.N.	573, 577, 581
Chernodarov A.	261	Gretsov M. V.	155
Chernov E.A.	664	Gretsova N. V.	140, 169

Gretsova H. V.	155	Krokhalev A. V.	97, 160, 163, 165
Gromkov N.V.	306	Kropotov Y.A.	324
Gubarev V.V.	514	Kulagin V.	642
Ingemansson A.	89	Kulikova O. A.	363
Ipatova V. M.	541	Kuptsov S.M.	467
Istomina T.V.	230	Kuragin A.V.	514
Istratov A. Yu.	18	Kurakina N. I.	24
Itkis E.M.	133	Kusheeva T.N.	502
Ivanov F.F.	398	Kusnetsov V.V.	545, 548
Ivanov I.A.	702	Kuts A.V.	358
Ivanov V.K.	34	Kuz'min S. V.	160, 163, 165
Ivo Lazar	69	Kuzmin V.N.	133
Joao A.J.	306	Kuznetsova O.N.	406
Kagan M. Yu.	319	Lebskiy S. L.	126, 147
Kalmykova M.A.	528	Lemanskiy D.A.	616
Kamaev V.	351	Levin A.V.	686
Karpov A.V.	495	Lezhnina Yu. A.	648
Karpov I.V.	499	Lezhnyov E.V.	216
Kechiev L.N.	545	Linetskiy B.L.	219
Kelina N.Y.	535	Luminarskaya E.S.	14
Khakimullin E.R.	282	Luppov V.V.	203
Khalyutin S.P.	686	Lushpa I.L.	483
Khalyutina O.S.	41	Lvov B.G.	710
Kharkov V.P.	254, 686	Lysak V. I.	160, 163, 165
Kharlamov V. O.	160, 163, 165	Lysenko A.V.	329
Khomenko T. V.	648	Lytvyn O. O.	655
Khritkin S.A.	370	Manohin A.I.	702
Kinet X.	642	Mashkov V.	337
Klochkov U.S.	270	Matlin M. M.	126, 147, 148
Kofanov Y.N.	616	Medennikov V.I.	203
Kolesnikova A.S.	314	Mekhanov V.B.	26
Kolganov A.	333, 422	Melnikov G.A.	514
Kopnjonkova M.	589	Merdygeev B.D.	600
Korobkin D.M.	609	Merkulev A. Yu.	301
Korobov A. V.	129, 172	Merkulov A.A.	144
Korobova K.V.	216	Mihailov A. A.	408
Korsakov I.N.	321, 438	Mikhalichuk V.	3
Kosenok N.Y.	230	Mikitchuk A.	300
Krainev D.	89	Mikrukov A.A.	683
Krashenninnikov A.V.	161	Mikryukov A.	620
Krasnikov C.A.	664	Mikshina V.S.	270
Krasnov A.E.	664	Mironova A.S.	355
Kravchuk A.A.	142	Miroshkin V.M.	357
Kravets A.G.	609	Miroshnichenko S. Yu.	290
Krevchik P. V.	389	Mityakov A. V.	457
Krevchik V. D.	389, 490	Mixeev M. Yu.	358

Monakhov M.A.	366	Savin G.I.	624
Mozgovoi Yu.D.	370	Savkin A. N.	107, 112, 121, 163, 165
Murashkina E.N.	378	Savochkina M.M.	274
Nasonov A.A.	81, 86	Savostyanov G.V.	314
Nazarov D.	385	Schelokov S.A.	670
Nikitin A. A.	140	Sedov A.A.	107, 112
Nikitina O.A.	452	Sedova T.L.	219
Nikolaev A.D.	533	Sekashev V.A.	52, 55
Nikolaev P.A.	533	Semenov A.	461
Novokshchonov A.A.	81, 86	Semenov M. B.	389
Orlova Yu.A.	446	Semenova L.	463
Palyukh B.V.	34	Shalkovsky A.G.	467
Panasik D.S.	216	Shandybina I.M.	126, 147, 148
Parpula S. A.	59, 62, 65	Shaymardanov R.V.	380
Pashchenko D.V.	550	Shepeleva Yu. V.	406, 408
Pecherskaya E. A.	406, 408	Shilin A.A.	176, 177
Pecherskaya R.M.	406, 408	Shilin A.N.	176, 177, 197
Perelyaev D.S.	414	Shipilov E.S.	161
Perelyayev S. E.	414	Shiryaev S.A.	161, 195
Petrenko A.R.	176, 177	Shishulin D.N.	673
Petrov S.A.	197	Shtepa N. I.	655
Petrova I.Yu.	648	Shumskij S.N.	97
Pilkov A. V.	411	Shustov B.	642
Piskaev K.Yu.	358	Simonov N.P.	490
Polezhaev D.V.	126	Simr P.	337
Popov A.V.	148	Sivagina U.A.	443
Popov F.A.	678	Skakunov V.N.	142, 144
Posevkin R.	420	Slepchenkov M.M.	314
Pozhidaev E. D.	557	Smirnov D. D.	557
Pozhidaeva N. V.	557	Sokolova I.M.	670
Prikhod'kov K. V.	97, 163, 165	Solovyev A.S.	147
Prikhodkova I. V.	97	Sotnikov A.N.	34, 624
Pustovalova N.	426	Sotnikova S.Y.	616, 702
Puzino Y.A.	432	Starostin I.E.	41
Pyrkova O.A.	568	Stepanova E. G.	639
Radomsky A. N.	411	Stolyarchuk A. S.	129, 172
Rayushkina A.A.	161, 195	Strelkov O.I.	609
Raznometov D. A.	438	Sudorgin S.A.	50
Rozaliev V.L.	446	Sukhanov M.A.	121
Ryabov D.V.	406	Suleymanov R.S.	624
Rybakova N. O.	408	Sviridov A.	333, 422
Safonova I. E.	474	Tankov G.V.	512
Salnikov S.G.	203	Tarantsev K. V.	477
Salov V.K.	452	Tatarinov U. S.	457
Sambyalov Z.G.	694	Terehov R.V.	514

Tetyushev A.A.	148
Tihonov G.V.	581
Tikhonov A.N.	219
Tishenko P.O.	172
Toporkova O.V.	148
Trokoz D.A.	550
Trubochkina N.K.	219
Trusov V.A.	301
Tsyganov P.	652
Tsyganova N. A.	474
Tubol O.A.	167
Ukustov S.S.	609
Uskova K.S.	207
Ustselemov V.N.	585
Uvaysov S.U.	702, 710
Vaganova T.V.	195
Valyukhov D.P.	281
Vasich K.N.,	169
Vasil`ev V.A.	528
Vdovenko A.V.	129, 172
Veselov E.A.	710
Veselova Yu. A.	648
Viter A. V.	7
Volodin K.I.	358
Volosatova T.M.	681
Vorobyeva E.E.	321
Vostrikov A.V.	633
Yakimov A.N.	673
Yamamoto K.	389
Yarkin A. S.	678
Yurkov N.K.	301, 329, 443, 673
Yurmanov V.A.	358
Zaitsev R. V.	389
Zakhariev I. Yu.	507
Zatylkin A.V.	329, 519
Zavyalov D.V.	86
Zayarniy V. P.	59, 62, 65
Zemlyakov A.V.	167
Zhelenkov B. V.	474
Zhmurov B.V.	686
Zhoga V.V.	142, 144
Zotov N.M.	101
Zubrilov V.G.	281

Section 2

INNOVATION INFORMATION TECHNOLOGIES IN SCIENCE

Anop M., Mikhailichuk V.

APPLICATION OF PARTICLE SWARM OPTIMIZATION ALGORITHM FOR
PARAMETRIC RELIABILITY OPTIMIZATION PROBLEM..... 3

Viter A.V.

TERRESTRIAL BIOTIC CARBON SEQUESTRATION: THE EXPERT SYSTEM FOR
THE TECHNIFICATION OF THIS PROCESS 7

Dianov V.N., Luminarskaya E.S.

INTEGRATED APPROACH FOR THE DIAGNOSTICS OF LATENT DEFECTS IN
MODERN EQUIPMENT 14

Istratov A.Yu., Fedin N. A.

TO THE PROBLEM OF THE HANDWRITING CHARACTERS RECOGNITION 18

Kurakina N. I.

GEOINFORMATION TECHNOLOGIES IN COMPLEX MONITORING OF WATER
AREAS..... 24

Mekhanov V.B., Domnin A.L.

MODELING IN CPNTOOLS BITRATE MEASUREMENT ALGORITHMS IN THE
PACKET-SWITCHED NETWORKS 26

Ivanov V.K., Palyukh B.V., Sotnikov A.N.

INTELLIGENT SUBJECT SEARCH SUPPORT IN SCIENCE AND EDUCATION..... 34

Starostin I.E., Khalyutina O.S.

MATHEMATICAL MODELING OF THE HEMISPHERICAL RESONATOR
GYROSCOPE 41

Sudorgin S.A.

NUMERICAL SIMULATION OF THE ELECTRICAL TRANSPORT PROPERTIES OF
SEMICONDUCTING ZIGZAG CARBON NANOTUBES 50

Sekashev V.A., Avdeuk O.A.

ALGEBRAIC DESCRIPTION SENSOR FOR MEASUREMENTS OF LARGE MASSES 52

Sekashev V.A., Avdeuk O.A.

DEVELOPMENT OF AN ALGORITHM FOR AUTOMATIC LAYOUT AT THE
LOCATION OF FRAGMENTS OF SCHEMATICS..... 55

Parpula S. A., Girich V. S., Zayarniy V. P.

THE MODELING OF SHEET SYMMETRIC ANTENNA WITH A LINEAR EXTENDING
APERTURE FOR THE ARRAY..... 59

Parpula S. A., Girich V. S., Zayarniy V. P.

EXPERIMENTAL STUDY OF SHEET SYMMETRIC ANTENNA WITH LINEAR
EXPENDING APERTURE FOR ARRAYS 62

Parpula S. A., Girich V. S., Zayarniy V. P.

DISK ALL-ROUND LOOKING ANTENNA BASED ON LINEAR EXPANDING SLOT
LINES..... 65

Egunov V.A., Abed O.A.

MOBILE ROBOT CONTROL BY VOICE COMMANDS..... 67

Ivo Lazar 69

PARAMETER MEASURING OF CONSTELLATION DIAGRAMS IN PARTICULAR
DVB-T SIGNALS..... 69

Egunov V.A., Al-Saadi H.A.

“SMART HOUSE” CONTROL USING WIRELESS COMMUNICATION CHANNEL..... 79

Novokshchonov A.A., Nasonov A.A., Egunov V.A.

BLOCK IMPLEMENTATION OF ALGORITHMS FOR SOLVING SPARSE SYSTEMS
OF LINEAR EQUATIONS WITH THE HIGH-PERFORMANCE COMPUTING TOOLS 81

Egunov V.A., Artyukh S.V.

FPGA AS COPROCESSORS IN SOLVING PROBLEMS OF LINEAR ALGEBRA 84

Nasonov A.A., Novokshchonov A.A., Zavyalov D.V.

OPTIMIZATION OF BLOCK REALIZATION OF ALGORITHMS OF LINEAR
ALGEBRA USING SIMD-INSTRUCTIONS OF THE PROCESSOR ON THE EXAMPLE
OF INTEL® MIC SIMD..... 86

Bondarev A., Ingemansson A., Krainev D.

MATHEMATICAL MODEL AND pc PROGRAM FOR THE CALCULATION OF THE
MACHINED FINISHED SURFACE ROUGHNESS IN TURNING THE STAINLESS
STEELS WITH ADVANCE PLASTIC DEFORMATION 89

Avdeuk O.A., Krokhalev A. V., Prikhodkova I. V., Prikhodkov K. V., Shumskij S.N. MODELING OF FORMATION AND GROWTH OF FLAME KERNEL IN SPARK IGNITION ENGINES (SIE)	97
Balakina E.V., Borodin A.K., Zotov N.M. φ - s – DIAGRAM MODELLING TECHNIQUES FOR TIRES	101
Savkin A.N., Sedov A.A., Andronik A.V. COMPARISON OF CUMULATIVE DAMAGE FATIGUE LIFE MODELS UNDER AUTOMOBILE SERVICE LOADING BY THE EXAMPLE OF MEDIUM CARBON STEEL AISI 5140	107
Savkin A.N., Sedov A.A., Andronik A.V. ON THE STEEL DAMAGE SIMULATION UNDER VARIABLE AMPLITUDE LOADING BY THE POWER, ENERGY AND STRAIN FAILURE CRITERIONS.....	112
Savkin A.N., Gorobcov A.S., Andronik A.V., Sukhanov M.A. FATIGUE ANALYSIS OF THE AUTOMOBILE SUSPENSION ARM UNDER VARIABLE AMPLITUDE LOADING	121
Matlin M.M., Shandybina I.M., Lebskiy S.L., Polezhaev D.V. RESEARCH WORK SLIPCLUTCH IN A VIRTUAL ENVIRONMENT.....	126
Stolyarchuk A. S., Korobov A. V., Vdovenko A. V., Gorunov A. I. EVALUATION OF CYCLIC DAMAGE OF STRUCTURAL MATERIALS ON THE BASIS OF THE INTERACTIONS OF LOCAL DAMAGES	129
Itkis E.M., Kuzmin V.N., Fedyanov E.A. THE SIMULATION OF HCCI ENGINE PERFORMANCE BY THE SINGLE-ZONE NUMERICAL MODEL COMPLETED BY PHYSICALLY REASONABLE ADJUSTING FUNCTIONS	133
Nikitin A. A., Gretsova N. V. THE MODEL OF IONIC TRANSPORT IN A CELL WITH TWO MEMBRANES	140
Zhoga V.V., Kravchuk A.A., Skakunov V.N. NAVIGATION ALGORITHM FOR MOBILE ROBOT USING COMPUTER VISION SYSTEM WITH STRUCTURED-LIGHT CAMERA	142

Zhoga V.V., Aniskov R.V., Merkulov A.A., Skakunov V.N. STRUCTURE MULTIPROCESSOR DISTRIBUTED CONTROL SYSTEM OF THE MOBILE ROBOT	144
Matlin M. M., Shandybina I.M., Lebskiy S. L., Solovyev A.S. USE THE VIRTUAL ENVIRONMENT FOR RESEARCH WELDED SEAMS WHEN STUDYING SUBJECT «ELEMENTS OF MACHINE »	147
Matlin M.M., Shandybina I.M., Popov A.V., Tetyushev A.A., Toporkova O.V. THE USE OF THE INFORMATION SYSTEM OF DISTANCE LEARNING FOR RATING STUDENT ACADEMIC PERFORMANCE IN THE COURSE “MACHINE ELEMENTS AND DESIGN PRINCIPLES”	148
Gretsova H. V., Gretsov M. V. THE SELF-OSCILLATORY PROCESSES IN BIOLOGICAL SYSTEM OF THE BOUND TRIGGERS	155
Avdeuk O.A. SYNTHESIS OF THE SYSTEM INTERFACE OF MULTICOHERENT MEASURING SYSTEMS ON THE BASIS OF NEURAL NETWORKS	157
Kharlamov V. O., Krokhaliev A. V., Kuz'min S. V., Lysak V. I. OBTAINING OF Cr ₃ C ₂ -Ti HARD ALLOYS USING EXPLOSIVE PRESSING	160
Dmitriev A.V., Rayushkina A.A., Shiryaev S.A., Shipilov E.S., Krashennnikov A.V. MANAGEMENT INFORMATION SYSTEMS - THROUGH IMPROVED FUNCTIONING OF URBAN PASSENGER TRANSPORT, AND QUALITY OF TRANSPORT SERVICES POPULATION.....	161
Krokhaliev A. V., Kharlamov V. O., Avdeyuk O. A., Prihod'kov K. V., Savkin A. N., Kuz'min S. V., Lysak V. I. OPTIMIZATION OF Cr ₃ C ₂ -Ti HARD ALLOYS USED IN SLIP BEARINGS	163
Krokhaliev A. V., Kharlamov V. O., Avdeyuk., O. A., Prihod'kov K. V., Savkin A. N., Kuz'min S. V., Lysak V. I. FRICTIONAL PROPERTIES OF HARD POWDER ALLOYS USING EXPLOSIVE PRESSING	165
Baydachenko V.A., Zemlyakov A.V., Tubol O.A. SPATIAL MODEL OF ANKLE.....	167

Vasich K.N., Gretsova N.V.

THE "REACTION - DIFFUSION" MODEL TAKING INTO CONSIDERATION THE
ARBITRARY EXTERNAL MICROWAVE RADIATION 169

Stolyarchuk A.S., Vdovenko A.V., Korobov A.V., Tishenko P.O.

SOME REGULARITIES OF SUMMATION OF FATIGUE DAMAGES UNDER CYCLIC
CREEP OF MATERIALS 172

Shilin A.N., Shilin A.A., Petrenko A.R.

SYSTEMS FOR DIAGNOSING AND PREDICTION OF EMERGENCY OPERATION
MODES OF OVERHEAD POWER LINES 176

Shilin A.N., Shilin A.A., Petrenko A.R.

NEUROCOMPUTING SYSTEM FOR DIAGNOSING AND PREDICTION OF
EMERGENCY OPERATION MODES OF OVERHEAD POWER LINES 177

Bagmutov V. P., Bogdanov E. P.

FEM SIMULATION OF PROCESSES OF ELASTIC-PLASTIC DEFORMATION OF
MULTIPHASE POLYCRYSTALLINE MATERIALS 184

Avilova E.D, Rayushkina A.A., Vaganova T.V, Shiryaev S.A., Fedotov V.N.

FORMATION OF A SINGLE MEDIUM, AS ASPECTS OF IMPROVING FOREIGN
TRADE MARKET WORK FREIGHT TRANSPORTATION..... 195

Petrov S.A., Shilin A.N.

SIMULATION OF GEOMETRIC TRANSFORMATION IN OPTOELECTRONIC
SYSTEMS WITH THE USE OF QUATERNION THEORY..... 197

Medennikov V.I., Salnikov S.G., Luppov V.V.

PERSPECTIVES OF DEVELOPMENT OF INTERNET TECHNOLOGIES FOR
AGRICULTURAL ENTERPRISES BASED ON TYPIFICATION IN UNIFIED WEB
SPACE OF AGRARIAN KNOWLEDGE..... 203

Alsova O.K., Uskova K.S.

MEDICAL MIXED-TYPE DATA CLUSTERING WITH MIXDC SOFTWARE..... 207

Americanov A.A., Bogachev K.A., Korobova K.V., Lezhnyov E.V., Panasik D.S.

USING THE UPGRADED PYROELECTRIC SENSOR IN ROBOTIC DEVICES. 216

Linetskiy B.L., Sedova T.L., Tikhonov A.N., Trubochkina N.K.

SPATIAL TECHNOLOGY ENVIRONMENT FOR THE IMPLEMENTATION OF
INNOVATIVE SCIENTIFIC AND EDUCATIONAL PROJECTS 219

Baulina O. V.

TECHNIQUE OF APPLICATION OF BIOLOGICAL FEEDBACK ON THE BASIS OF STABILOGRAFIYA IN GYMNASTICS 226

Istomina T.V., Kosenok N.Y.

BIOTECHNICAL LIFE SUPPORT SYSTEM..... 230

Brodsky Yu. I.

BOURBAKI'S STRUCTURE THEORY IN THE PROBLEM OF MULTI-COMPONENT SIMULATION MODELS SYNTHESIS 234

Bublík T.

PERFORMANCE TOOL FOR FAST DETECTION OF JAVA STRUCTURES..... 244

Kharkov V.P.

SYNTHESIS OF ADAPTIVE CONTROL FOR NONLINEAR SYSTEMS 254

Chernodarov A.

MONITORING AND DIAGNOSIS OF OBSERVABLE DYNAMICAL SYSTEMS BY THE USE OF COMBINED GOODNESS-OF-FIT TESTS 261

Klochkov U.S., Mikshina V.S.

COMPUTER USAGE IN THE ANALYSIS OF VALIDITY OF DECISION MAKING CRITERIA. 270

Savochkina M.M.

DEVELOPMENT OF NEW DESIGN OF FIBER-OPTIC DIFFERENTIAL PRESSURE SENSOR..... 274

Valyukhov D.P., Djudjun D.E., Zubrilov V.G.

DISTRIBUTED COMPUTER CONTROL SYSTEM FOR ELECTRON SPECTROMETER, GATHERING AND MATHEMATICAL PROCESSING OF ELECTRON SPECTRA 281

Enatskaya N.Yu., Khakimullin E.R.

DIVISION OF A POPULATION OF ELEMENTS INTO A GIVEN NUMBER OF DISCERNIBLE PARTS 282

Dobroserdov O.G., Miroshnichenko S.Yu.

AUTOMATIC DIGITAL ELEVATION MODELS CREATION FROM RASTER TOPOGRAPHIC MAPS 290

Dunin V. O., Egorov V. A.

DESIGNING AND DEVELOPING INTELLIGENT INFORMATION SYSTEMS TO
SUPPORT MEDICAL FACILITIES 294

Mikitchuk A.

EXPERIENCE IN THE USE OF THE WCF SERVICE IN A GAME APPLICATION FOR
WINDOWS PHONE..... 300

Merkulev A.Yu., Trusov V.A., Yurkov N.K.

GRAPHENE AS A MATERIAL FOR A NEW GENERATION OF HEAT SINKS 301

Joao A.J., Gromkov N.V.

HISTORY OF DEVELOPMENT OF ELECTRO-MUSICAL INSTRUMENTS IN RUSSIA .. 306

Fedorenko J.V.

INVESTIGATION LISSAJOUS ORBITS AROUND THE L2 LIBRATION POINT OF THE
EARTH-MOON SYSTEM 311

Gluhova O.E., Kolesnikova A.S., Slepchenkov M.M., Savostyanov G.V.

NEW IT-SOLUTIONS FOR BREAKTHROUGH RESEARCH IN NANO- AND
BIOELECTRONICS 314

Kagan M.Yu. , Abrameshin A.E.

PHYSICAL GROUNDS OF THE INFORMATION STORAGE AND REORDERING IN
MAGNETIC NANOCLOUDS 319

Korsakov I.N. , Atabaeva V.D., Vorobyeva E.E.

THE PATIENT-PHYSICIAN RELATIONSHIP IN REMOTE HEALTHCARE
MONITORING 321

Kropotov Y.A.

MULTI-CHANNEL ALGORITHM COMPENSATION ECHO SIGNALS IN
TELECOMMUNICATION HANDSFREE SYSTEMS..... 324

Lysenko A.V., Zatylnik A.V., Yurkov N.K.

ACTIVE PROTECTION SYSTEM OF RADIO-ELECTRONIC FACILITIES 329

Kolganov A., Sviridov A.

GSM MODULES IN ENERGY EFFICIENT M2M-SYSTEMS 333

Mashkov V., Barilla J., Simr P.

ILLUSTRATIVE MODELING OF COALITION FORMATION 337

Golev D.M.

MEASURING DEVICE FOR CALIBRATION OF MECHANICAL CONVERTING
SYSTEM OF FIBER-OPTIC DIFFERENTIAL PRESSURE SENSOR 345

Botvinkin P., Kamaev V.

METHODS OF PROTECTION FROM ADVERSE FACTORS THAT MAY AFFECT
AUTOMATED INFORMATION AND MEASUREMENT SYSTEMS 351

Mironova A.S.

MEDICAL ASPECTS OF RESEARCH GUNNER'S HEALTH 355

Miroshkin V.M.

CREATE A CLOUD DATABASE IN A PRIVATE DATA CENTER USING WINDOWS
AZURE PACK..... 357

Mixeev M.Yu., Yurmanov V.A., Kuts A.V., Piskaev K.Yu., Volodin K.I.

INCREASING THE PRECISION OF METROLOGICAL CHARACTERISTICS OF
SMART SENSORS IN LARGE SCALE MONITORING SYSTEMS..... 358

Kulikova O. A.

MODERN STATE OF THE PROBLEM OF THE DEFINITION OF THE DISEASE AS A
RESULT OF THE VIOLATIONS OF ADAPTATION..... 363

Monakhov M.A.

PROCEDURE FOR CREATING DATABASE PARTITIONON THE CHARACTERISTICS
OF RELIABILITY OF MECHANICAL ELEMENTS 366

Mozgovoi Yu.D, Khritkin S.A.

PHYSICAL EFFECTS AND PROBLEMS IN GAMMA-ELECTRONICS 370

Murashkina E.N.

DEVELOPMENT SEQUENCE DIAGRAM OF NEURAL NETWORK IDENTIFICATION OF
A COMPLEX SIGNAL USING THE UNIFIED MODELING LANGUAGE UML 2.0..... 378

Shaymardanov R.V., Elizarov A.A.

MICROWAVE MEDICAL ELECTROD BASED ON SLOW-WAVE SYSTEM 380

Nazarov D.

AN APPROACH TO COMPLEX SYSTEMS SENSITIVITY ESTIMATION ON THE
BASIS OF REGIONS OF ACCEPTABILITY 385

Krevchik V. D., Semenov M. B., Zaitsev R. V., Krevchik P. V., Aringazin A. K., Yamamoto K.	
NONLINEAR TRANSPORT AND OPTICAL PROPERTIES OF QUANTUM DOTS FOR NANOMEDICINE.....	389
Eremin D.V., Ivanov F.F.	
NUMERICAL SIMULATION OF THE NATURAL GAS FLOW IN THE SECTION OF THE GAS PIPELINE.....	398
Pecherskaya E. A., Pecherskaya R.M., Shepeleva .Yu.V., Kuznetsova O.N., Ryabov D.V.	
METHODICAL ERRORS OF DIELECTRIC PARAMETERS OF FERROELECTRICS MEASUREMENT	406
Pecherskaya E. A., Pecherskaya R.M. Shepeleva, Yu. V., Mihailov A. A., Rybakova N. O.	
PARAMETERS INTERDEPENDENCY ANALYSIS OF UNIVERSITIES INTERNATIONAL RATINGS BASED ON QUALITY CONTROL TOOLS.....	408
Pilkov A. V. Radomsky A. N.	
THIRD ORDER INTERMODULATION DISTORTION REQUIREMENTS FEAUTERES FORMULTI-CHANNEL RADIO RECIEVER	411
Perelyayev S. E., Perelyaev D.S.	
ON THE THEORY PARAMETRIZATION OF THE THREE-DIMENSIONAL ROTATIONS GROUP ABSOLUTE RIGID BODY. METHODS AND APPENDICES	414
Afanasyeva M. A.	
POLYIMIDES FOR THE PROTECTION OF SPACECRAFT EQUIPMENT.....	417
Posevkin R.	
SENTIMENT ANALYSIS AS THE METHOD OF INFORMATION EXTRACTION.....	420
Sviridov A., Kolganov A.	
PRESELECTOR OF WIRELESS SIGNALS OF SATELLITE NAVIGATION SYSTEMS.....	422
Pustovalova N.	
USING COMMON ONTOLOGY OF SOFTWARE REQUIREMENTS FOR AUTOMATED REQUIREMENTS FORMALISATION TOOL'S DEVELOPMENT.....	426
Puzino Y.A.	
SIMULATION OF A CYLINDRICAL ROD STRETCHING PROCESS DURING HOT DEFORMATION.....	432

Raznometov D. A., Korsakov I.N.

ALGORITHMS FOR GATHERING WIRELESS WEARABLE SENSORS INFORMATION
IN REMOTE HEALTHCARE MONITORING..... 438

Grab I.D., Sivagina U.A., Goryachev N.V., Yurkov N.K.

RESEARCH METHODS OF COOLING SYSTEMS..... 443

Rozaliev V.L., Orlova Yu.A.

APPLYING THE AUTOMATED SYSTEM FOR THE DETERMINATION OF EMOTIONS
IN THE EDUCATION'S TASKS FOR PEOPLE WITH DISABILITIES 446

Salov V.K., Gazizov T.R., Nikitina O.A.

CONVERGENCE OF MULTIPLE ITERATIVE SOLUTION OF LINEAR ALGEBRAIC
SYSTEMS WITH A FULLY VARYING MATRIX USING A SINGLE CALCULATED
INITIAL PRECONDITIONER..... 452

Mityakov A. V, Tatarinov U. S.

SAMPLING DATA PROCESSING – APPROACH TO SPEEDING UP ITERATIVE
ALGORITHMS ON MAPREDUCE MODEL 457

Semenov A.

MULTIAGENT APPROACH FOR DEVELOPING HYBRID INTELLECTUAL SYSTEM .. 461

Semenova L.

DOUBLE-LEVEL EXPERT SUPPORT SYSTEM OF MAKING DECISION IN THE
CHOICE OF ELECTRIC SYSTEMS DEVELOPMENT MODEL 463

Shalkovsky A.G., Kuptsov S.M.

INFORMATION MODEL OF REMOTE HEALTHCARE MONITORING SYSTEM..... 467

Safonova I. E., Zhelenkov B. V., Goldovskii Y. M., Tsyganova N. A.

TO THE QUESTION OF EVALUATING THE RELIABILITY OF FUNCTIONING OF THE
ELEMENTS OF THE TELECOMMUNICATION ENTERPRISE-WIDE NETWORKS 474

Tarantsev K. V.

NUMERICAL MODELING OF THE PROCESSES OF COAGULATION AND
DISPERSION OF DROPS IN ELECTRIC FIELD 477

Lushpa I.L.

THE CALCULATION OF THE VIBROINSULATORS' FAILURE RATE..... 483

Artemov I. I., Krevchik V. D., Simonov N.P. THE FORMATION PROCESS OF NANOCLOUDS IN THE METAL SURFACE LAYER, INITIATED BY NONLINEAR TUNNELING DYNAMICS IN THE ELECTROSTATIC FIELD.....	490
Karpov A.V. INFORMATION PROCESSING METHODS IN VISUAL SENSOR NETWORKS.....	495
Karpov I.V. ISSUES OF LONG-HOP AND SHORT-HOP ROUTING IN WIRELESS AUDIO SENSOR NETWORKS.....	499
Ayusheeva N.N., Kusheeva T.N. IDENTIFYING SEMANTIC CONTENT-BLOCK OF TERMS AND RELATIONS IN SCIENTIFIC TEXTS.....	502
Zakhariev I. Yu. THE DETERMINATION OF AMg6 ALLOY SUPERPLASTIC CHARACTERISTICS BASED ON THE FREE BULGING TEST	507
Zatylnik A.V., Tankov G.V., Golushko D.A. MODELING THE INTRODUCTION OF MECHANICAL INFLUENCES IN THE DESIGN OF RADIO-ELECTRONIC FACILITIES.....	512
Gubarev V.V., Abalov N.V., Bulgakova N.V., Gorodov E.Y., Kuragin A.V., Melnikov G.A., Terehov R.V., Fedorov E.I. INTELLIGENT SYSTEM “OBJECT-MODEL-APPLICATION RESULT”	514
Dianov V.N., Gevorgyan T.A. PARKING SYSTEM OF HIGH RELIABILITY	519
Dianov V.N. INTEGRO-DIFFERENTIAL DIAGNOSIS OF FAILURES COMBINATIONAL CIRCUITS.	523
Vasil`ev V.A., Kalmykova M.A., Chernov P.S. COMPUTER SIMULATIONS OF ELASTIC COMPONENTS OF NANO- AND MICROELECTROMECHANICAL SYSTEMS	528
Nikolaev P.A., Nikolaev A.D. THE TASK OF DETERMINING THE NUMBER OF TEST PULSES TO EVALUATE THE RESISTANCE OF ENGINE CONTROL SYSTEM OF A VEHICLE TO ELECTROMAGNETIC RADIATION OF LIGHTNING	533

Elizarov V.N., Kelina N.Y.

THE METHODS OF STATISTICAL ANALYSIS AND DATA MINING IN
INFORMATION SYSTEM FOR IMMUNE-BIOCHEMICAL TESTS 535

Ipatova V. M.

AN ATTRACTOR OF THE DIFFERENTIAL INCLUSION FOR THE MULTILAYER
OCEANIC GENERAL CIRCULATION MODEL 541

Kusnetsov V.V., Kechiev L.N.

CHARGED BOARD EVENT ANALYSIS USING CIRCUIT SIMULATOR FOR PCB
MOUNTED MOSFET 545

Kusnetsov V.V.

ELECTROSTATIC POTENTIAL METER WITH HIGH INPUT OVERSHOOTS
ROBUSTNESS 548

Pashchenko D.V., Trokoz D.A.

EQUIVALNCE OF INHIBITORY AND NON-INHIBITORY SAFE PETRI NETS 550

Pozhidaev E. D., Smirnov D. D., Pozhidaeva N. V.

ABOUT THE MICROSCOPIC PICTURE OF THE HOLE TRANSPORT IN DEH-DOPED
POLYCARBONATE 557

Bolotova L.S.

METHOD CONCEPTUALIZATION OF SUBJECT DOMAIN AS A BASIS OF
TECHNOLOGY OF ACQUISITION KNOWLEDGE FOR INTELLIGENCE SYSTEMS 558

Pyrkova O.A.

EFFECT OF ACCOUNTING INTERMITTENCY DEPENDENCE ON THE TIME OF
LONGITUDINAL CORRELATION COEFFICIENT THIRD ORDER 568

Grachev N.N.

ANALYSIS AND FEATURES PARAMETERS NORMALIZATION EMC COSMIC
DEVICES AND SYSTEMS 573

Grachev N.N.

QUESTIONS ANALYSIS EMC SPACE RES 577

Tihonov G.V., Grachev N.N.

CALCULATION LEASE PAYMENTS CURRENT ECONOMIC CONDITIONS 581

Ustselemov V.N.

CURRENT ISSUES IN IMPROVING INFORMATION SECURITY SUBSYSTEM..... 585

Avakyan A., Kopnjonkova M.

METHODS OF OPERATIONAL STATE MONITORING FOR INTERFACE AND
COMPUTER PATHS OF AVIONICS SYSTEMS 589

Dambaeva S.V., Merdygeev B.D.

USING FCA BASIS THEOREM ON CONCEPT LATTICES IN ANALYZING
SCIENTIFIC MONOLOGIC TEXT ONTOLOGY 600

Burukina I. P., Burukina I. S.

MULTIWORD EXPRESSION DESCRIPTION IN LEXICAL DATABASES..... 606

Dykov M.A., Kravets A.G., Korobkin D.M., Ukustov S.S., Strelkov O.I.

COMBINING STATISTICAL AND SEMANTIC FEATURES FOR PATENTS PRIOR-
ART RETRIEVAL..... 609

Kofanov Y.N., Sotnikova S.Y., Lemanskiy D.A.

METHOD OF COMPUTER MODELLING ACCURACY INCREASE FOR ELECTRONIC
MEANS BASED ON INTERCONNECTION OF DIFFERENT PHYSICAL PROCESSES
PROCEEDING..... 616

Berketov G., Mikryukov A., Fedoseev S.

INFORMATIONAL SAFETY SUBSYSTEMS IMPROVEMENT AT RISK CORRUPTED
OR LOST DATA 620

Savin G.I., Sotnikov A.N., Suleymanov R.S.

COMPARATIVE ANALYSIS OF SOLUTIONS FOR FULL-TEXT SEARCH IN DIGITAL
LIBRARIES 624

Borisova A.V., Finochenko V.A.

INSTRUMENTATION AND METHODOLOGY SUPPORT FOR THE MOBILE
LABORATORIES IN THE ENVIRONMENTAL CONTROL AND MONITORING OF
RAIL TRANSPORT. 629

Vostrikov A.V., Borisov N.I.

DEVELOPMENT REDUCED COMPUTATIONAL SCHEME IS BASED ON USING
NUMERICAL METHODS FOR CALCULATION OF DYNAMIC CHARACTERISTICS
MATHEMATICAL MODEL 633

Stepanova E. G.

ANALYSIS THE TRENDS OF EMPLOYMENT IN THE INFORMAL SECTOR OF THE ECONOMY 639

Kulagin V., Dunham D., Shustov B., Kinet X.

PROBLEMS OF ASTEROID AND COMET HAZARD. ROLE OF MODERN INFORMATION TECHNOLOGY..... 642

Fokin V. M.

RESEARCH OF FAILURE MECHANISMS OF SOLENOIDS AND CONTACTORS..... 644

Khomenko T. V., Petrova I. Yu, Lezhnina Yu. A., Veselova Yu. A.

BUILDING KNOWLEDGE SPACE FOR SYNTHESIS OF TECHNICAL SYSTEMS WITH ENERGY-CIRCUIT METHOD 648

Tsyganov P.

ANALYSIS OF BASIC MECHANISMS AND REASONS OF BREAKDOWN OF COOLING SYSTEMS' PUMPS 652

Lytvyn O. O., Shtepa N. I., Denisova O. I., Chorna O. S.

INTERNAL EARTH STRUCTURE RENEWAL BY MEANS OF CORE IN INCLINED BOREHOLES ANALYSIS..... 655

Krasnov A.E., Krasnikov C.A., Chernov E.A.

METHOD OF THE COMPRESSION OF PHASE PORTRAITS OF GENERALIZED SPECTRAL DATA FOR SOLVING THEIR CLUSTERING AND RECOGNITION..... 664

Schelokov S.A., Sokolova I.M.

DEVELOPMENT OF HYBRID OBJECT-RELATIONAL DATABASE ON THE BASIS OF THE FRAME AND SLOT NORMAL FORM 670

Shishulin D.N., Yurkov N.K., Yakimov A.N.

A MODELING OF THE INFLUENCE OF VIBRATION ACTIONS ON THE RADIATION MIRROR ANTENNA BY USING ANSYS 673

Yarkin A. S., Popov F.A.

DATA PROCESSING METHODS FOR INFORMATION SYSTEM OF SUPPORT TOURISM BUSINESSES 678

Volosatova, T.M., Belomoytsev, D.E.

INDIVIDUAL EDUCATIONAL COURSE SYNTHESIS METHOD USING EVOLUTIONARY
METHODS OF EDUCATIONAL CONTENT SPACE FORMATION 681

Astafjev A.V., Fedoseev S.V., Mikrukov A.A., Berketov G.A.

USE OF EFFICIENCY PARAMETER OF REAL OPTIONS IN THE DECISION
INNOVATIVE SOLUTIONS 683

Khalyutin S.P., Levin A.V., Kharkov V.P., Zhmurov B.V.

TRENDS AND PROSPECTS OF AIRCRAFT ELECTRICAL EQUIPMENT 686

Eremina V.

METHOD OF SIGNALS INTERFERENCE IMMUNITY ESTIMATION USED IN
MULTICHANNEL COMMUNICATION SYSTEMS 691

Bilgaeva L.P., Sambyalov Z.G.

EVALUATION OF MODIFIED CLUSTERING ALGORITHM CLOPE..... 694

Bazaron S.A.

THE DEFINITION OF WELL-FORMED FORMULA ALGORITHM..... 698

Manohin A.I., Aminev D.A, Sotnikova S.Yu., Ivanov I.A., Uvaysov S.U.

INVESTIGATION OF THE THERMAL PROCESSES INFLUENCE IN
ELECTRORADIOPRODUCTS ON THE RELIABILITY INDICATORS OF ELECTRONIC
RADIO EQUIPMENT BY USING ANALYSIS PROGRAMS OF THERMAL REGIMES..... 702

Veselov E.A., Uvaysov S.U., Furman, Ya. A., Lvov B.G.

DIRECT AND REVERSE PROJECTION PROCEDURES IN PROBLEMS OF 3D
OBJECTS RECONSTRUCTION FROM IMAGES 710

Materials of
the International Scientific - Practical Conference
INNOVATIVE INFORMATION TECHNOLOGIES
Part 2

Edited by S.U. Uvaysov;
Executive editor I.A. Ivanov

Printed in author's redaction

Computer layout:
S.S. Uvaysova, A.S. Uvaysova,
S.M.Lishov, R.Yu.Pashev, D.S.Panasik
Cover design: R.Yu.Pashev

Signed to print 08.04.1014
Format 60x84/16. Paper «Pioneer»
Conventional quires 2.3 Print run 500 copies Order № 51
HSE
109028, Moscow, B.Trehsvyatitsky lane, 3.